# HIC 2024

# 15th International Conference on Hydroinformatics

## From Nature to Digital Water: Challenges and Opportunities

May 27-30, 2024 Beijing, China

# ABSTRACT BOOK

Editors:
**Hao Wang, Philippe Gourbesville, Jianyun Zhang**

Hosted by:

Organized by:

ISBN: 978-90-834302-0-1
ISSN: 3007-2174

# HIC 2024

# 15th International Conference on Hydroinformatics

## From Nature to Digital Water: Challenges and Opportunities

May 27-30, 2024 Beijing, China

Editors:

**Hao Wang**
**Philippe Gourbesville**
**Jianyun Zhang**

**ISBN: 978-90-834302-0-1**

**ISSN: 3007-2174**

Abstracts included in this book are part of the 15th International Conference on Hydroinformatics (2024) cited on the cover and title page, and the book has been published under the IAHR Publications Ethics and Malpractice Statement.

The views expressed in the abstracts are those of the authors and do not necessarily reflect the views of the editors, publishers, or sponsoring organizations. While every effort has been made to ensure the accuracy and reliability of the information within this publication, neither the editors nor the publishers assume any responsibility for errors or omissions, or for any consequences resulting from the use of the information contained herein.

**Abstract Book of the 15th International Conference on Hydroinformatics**
"From Nature to Digital Water: Challenges and Opportunities"
May 27-30, 2024, Beijing, China

**Editors:** Hao Wang, Philippe Gourbesville, Jianyun Zhang

**Published by:**

**IAHR – International Association for Hydro-Environment Engineering and Research**
IAHR Madrid Office: Paseo Bajo Virgen del Puerto, 3 28005 Madrid, Spain
IAHR Beijing Office: A-1 Fuxing Road, Haidian District 100038 Beijing, China

**IWHR – China Institute of Water Resources and Hydropower Research**
A-1 Fuxing Road, Haidian District 100038 Beijing, China

**Published in:** May 2024

ISBN: 978-90-834302-0-1
ISSN: 3007-2174

# Preface

Welcome to the **15th International Conference on Hydroinformatics** - **HIC 2024**, a gathering dedicated exploring challenges and opportunities on the path from nature to digital water.

Within the following pages, you will discover 362 extended abstracts selected among the 437 submitted and that represent the forefront of Hydroinformatics, each one aiming at stimulating innovations and insights.

This conference, hosted with enthusiasm by the Ministry of Water Resources of the People's Republic of China, in collaboration with the International Association for Hydro-Environment Engineering and Research (IAHR) and the International Water Association (IWA), stands as a testament to the power of collaboration and collective expertise. Jointly organized by leading institutions including the China Institute of Water Resources and Hydropower Research (IWHR), the State Key Laboratory of Simulation and Regulation of Water Cycle in River Basin, the Key Laboratory of Digital Twin for River Basins of the Ministry of Water Resources, and the Yinshanbeilu Grassland Eco-Hydrology National Observation and Research Station, HIC 2024 serves as a nexus for the world's foremost minds in Hydroinformatics.

As we convene under the theme "**From Nature to Digital Water: Challenges and Opportunities**," the abstracts presented traverse six key topics and sixteen special sessions, each delving into critical aspects of Hydroinformatics. The breadth of subjects covered reflects the multifaceted nature of our discipline.

Key topics:

1. Space-Air-Ground Integrated Monitoring
2. Hydrological and Hydraulic Modeling and Solutions
3. Big Data Acquisition and Data Management
4. Multi-Scenario Applications of Digital Twins
5. Climate Change and Adaptation
6. Digital Empowerment in Water Management and Education

Special sessions:

1. From Models to Decision Support Systems
2. Digital Twins for Watersheds: Challenges and Advanced Hydroinformatic Solutions
3. Water Knowledge Platforms and Applications
4. Flash Flood Program: Advanced Hydroinformatic Approaches for Flash Flood Defence and Prevention
5. Urban Flooding and Waterlogging
6. Extreme Drought and Its Impacts in a Changing Environment
7. New Remote Sensing Methods and New Products for Hydroinformatics Solutions
8. Modelling and Machine Learning for Understanding Flash Floods and Mitigating Their Impact on Society

9. Climate Change Impacts on Urban Flooding: Challenges and Innovative Solutions
10. Marine and Coastal Hydroinformatics
11. Data-Driven Risk Management of Water-Related Disasters
12. High-Performance Computing in Hydrodynamics, Hydrology and Hydroinformatics
13. River and Lake Protection and Intelligent Management
14. Smart Water Management and Technology in the Era of Climate Change
15. Hydroinformatics of Deep Tunnel Drainage Systems
16. Return on Experience: Operational Benefits of Hydroinformatics for Water Utilities and Cities

HIC 2024 celebrates the 30th anniversary of the conference initiated in 1994. Over the past three decades, with the work of the IAHR/IWA Joint Committee on Hydroinformatics and of several International Water Association Specialist Groups, a community has been created and has continuously questioned and advanced the key concepts of hydroinformatics through numerous activities.

Since the 1980s, over the last 40 years, the hydroinformatics paradigm formulated in 1991 by Michael B. Abbott has emerged with the technical development of computer resources associated with scientific improvement for numerical simulations. If the initial stage was very much related to computational hydraulics, hydroinformatics has gradually integrated and encompassed social and technological dimensions to provide efficient solutions to water-related problems. With the exponential development of digital solutions, the hydroinformatics paradigm, concepts and methods, based on a wise combination of scientific hydraulic knowledge and technological abilities/methods, have matured and are now seen as the needed innovations for addressing complex water systems and tackling significant challenges. Water systems can be segmented into three primary domains, each corresponding to distinct activities and business operations:

- Protection of natural water-related environments and ecosystems.
- Natural hazard mitigation and disaster prevention.
- Water uses.

The first domain encompasses actions required to assess and guide the environmental impacts of development proposals and projects related to specific water uses.

The second domain is focused on water-related natural hazard mitigation actions. Floods, droughts, water-borne and vector disease outbreaks, famines, landslides and avalanches are the processes covered by this domain.

The last domain addresses the added influence of human activity on the water cycle. Generally, “water uses” encompasses the consumption by agriculture, industry, energy production and households. This also includes instream uses such as fishing, recreation, transportation and waste disposal. Urban areas are of prominent importance in this domain considering the increasing economic migration processes towards smart cities (a challenging target for large cities), in the context of climate change impact and ageing urban water infrastructures.

Inherited from the previous editions, HIC2024 was the opportunity for the community to meet and share the latest challenges and solutions. Water uses represent the largest field where digital solutions can be developed and implemented. In the coming years, new approaches

for water management will emerge accompanied by the deployment of solutions and their gradual integration into a global Information System (IS). This will ensure interoperability and minimize redundancy. Realizing this approach will necessitate close collaboration among professionals from various fields to achieve the needed holistic approach. Obviously, the introduction of technological solutions will impact massively on water services and will induce a drastic transformation of business processes. The digital transformation of the water sector is still in its early stages. It must encompass numerous dimensions before reaching the expected holistic paradigm able to tackle water challenges efficiently. Over the last few years, with the massive development of computational resources and the deployment of affordable sensors, Digital Water has emerged as a pivotal concept. Many water professionals now recognize the value of digital twins as a means to synthesise data, provide a comprehensive overview and ultimately control physical devices through their digital representation.

In March 2024, IAHR released its Strategic Plan for 2024-2027, marking a new era for this 89-year-old association that aims at becoming the global hub of knowledge and innovation for holistic water engineering. Four Thematic Priority Areas have been identified in this strategic plan to show and demonstrate the solutions produced by members to address some the major challenges faced by our modern societies:

- Climate Change Adaptation and Mitigation
- Water for the Energy Transition, Food Security and Nature
- Improving Resilience against Water Hazards and Disasters
- Digital Transformation (as a transversal and crosscutting process)

In this proceeding volume, articles are grouped into one of these four Thematic Priority Areas to get aligned with the new IAHR Strategic Plan and so better inform the community about the concrete contributions this conference tries to make to foster a vibrant exchange of ideas, share cutting-edge technologies and successful practices in the field of Hydroinformatics, and pave the way for the best solutions and strategies to ensure global water security and achieve the water-related goals of the United Nations 2030 Agenda for Sustainable Development.

Hoping the read of this volume will contribute to stimulate your creativity and innovation within HydroinforImatics field!

Hao Wang, Chair of the International Scientific Committee

Philippe Gourbesville, Vice Chair of the International Scientific Committee

Jianyun Zhang, Vice Chair of the International Scientific Committee

# HIC 2024: Hosts, Organizers and Co-Organizers

## Hosts

- Ministry of Water Resources of the People's Republic of China (MWR)
- International Association for Hydro-Environment Engineering and Research (IAHR)
- International Water Association (IWA)

## Organizers

- China Institute of Water Resources and Hydropower Research (IWHR)
- State Key Laboratory of Simulation and Regulation of Water Cycle in River Basin
- Key Laboratory of Digital Twin for River Basins of the Ministry of Water Resources
- Yinshanbeilu Grassland Eco-Hydrology National Observation and Research Station

## Co-Organizers

- China Three Gorges Corporation (CTG)
- China South-to-North Water Diversion Corporation Limited
- Danish Hydraulic Institute (DHI)
- International Economic & Technical Cooperation and Exchange Center, Ministry of Water Resources of the People's Republic of China (INTCE)
- Nanjing Hydraulic Research Institute (NHRI)
- Xiaolangdi Multipurpose Dam Project Management Center
- Changjiang River Scientific Research Institute (CRSRI)
- Yellow River Institute of Hydraulic Research (YRIHR)
- Pearl River Water Resources Research Institute (PRWRI)
- International Research and Training Center on Erosion and Sedimentation (IRTCES)
- Beijing Water Authority
- Macau University of Science and Technology (MUST)
- Tsinghua University
- Tianjin University
- Sichuan University
- Hohai University
- Xi'an University of Technology (XUT)
- North China University of Water Resources and Electric Power (NCWU)
- Power China Huadong Engineering Corporation Limited
- Power China Chengdu Engineering Corporation Limited
- China Gezhouba Group Municipal Engineering Co., Ltd.
- Shanghai Investigation, Design & Research Institute Co., Ltd.
- Dayu Huitu Technology Group

- CETC Digital Technology Co. Ltd.
- Shandong Survey and Design Institute of Water Conservancy Co., Ltd.
- Henan Water & Power Engineering Consulting Co., Ltd.
- China Siwei Surveying and Mapping Technology Co., Ltd.
- Beijing Guoxinhuayuan Technology Co., Ltd.
- PIESAT Information Technology Co., Ltd.
- Beijing GiStack Information Technology Co., Ltd.
- China South-to-North Water Diversion Group Water Networks Intelligent Technology Co., Ltd.

# HIC 2024: Committees

## Organizing Committee

**Chair:**

- **Daoxi Wang** (Vice Minister of Water Resources of the People's Republic of China)

**Vice Chairs:**

- **Wenguang Yao** (Director General, Department of Flood and Drought Disaster Prevention, MWR)
- **Hai Jin** (Director General, Department of International Cooperation, Science and Technology, MWR)
- **Feng Qian** (Deputy Director, Information Center, MWR)
- **Jing Peng** (President, China Institute of Water Resources and Hydropower Research)

**Members:**

- **Xiaolin Li** (Deputy Director General, General Office, MWR)
- **Qian Yang** (Deputy Director General, Department of Water Resources Management, MWR)
- **Dezhi Xu** (Deputy Director General, Department of Rural Water and Hydropower, MWR)
- **Ping Wang** (Deputy Director General, Department of Water Diversion Management, MWR)
- **Hong Duan** (Vice President, Secretary General, Chinese Hydraulic Engineering Society)
- **Zhao Hao** (Director, International Economic & Technical Cooperation and Exchange Center of Ministry of Water Resources)
- **Jiqun Dai** (President, Nanjing Hydraulic Research Institute)
- **Xiuli Ding** (Vice President, Changjiang River Scientific Research Institute of Changjiang Water Resources Commission)
- **Xin Yu** (President, Yellow River Institute of Hydraulic Research)
- **Jianli Zhang** (Deputy Director, International Research and Training Center on Erosion and Sedimentation)
- **Chao Ma** (Professor, Tianjin University)
- **Hong Xiao** (Professor, Sichuan University)
- **Xuemei Liu** (Vice President, North China University of Water Resources and Electric Power)
- **Joseph Hun-Wei Lee** (President, Macau University of Science and Technology)
- **Gabriele Freni** (Università Di Enna Kore, Italy)
- **Sanda-Carmen Georgescu** (University Politehnica of Bucharest, Romania)
- **Philippe Gourbesville** (President, International Association for Hydro-Environment Engineering and Research)

**Secretary General:**

- **Liuqian Ding** (Vice President, China Institute of Water Resources and Hydropower Research)

## International Scientific Committee

**Chair:**

- **Hao Wang** (Academician, Chinese Academy of Engineering; Professor, China Institute of Water Resources and Hydropower Research)

**Vice Chairs:**

- **Philippe Gourbesville** (President, International Association for Hydro-Environment Engineering and Research)
- **Jianyun Zhang** (Academician, Chinese Academy of Engineering; Professor, Nanjing Hydraulic Research Institute)

**Members:**

- **Andrei-Mugur Georgescu** (Technical University of Civil Engineering of Bucharest)
- **Anton Anton** (Technical University of Civil Engineering of Bucharest)
- **Branko Kerkez** (University of Michigan)
- **Bruno Brunone** (University of Bologna)
- **Dan Niculae Robescu** (Technical University of Civil Engineering of Bucharest)
- **Daniele Biagio Laucelli** (Polytechnic University of Bari)
- **Duan Chen** (Director, Department of Hydraulics, Changjiang River Scientific Research Institute of Changjiang Water Resources Commission)
- **Dusan Prodanovic** (University of Belgrade)
- **Emmanouil Varouchakis** (Technical University of Crete)
- **Epsica Chiru** (Romanian Water Association)
- **Fang Yang** (Vice President, Pearl River Hydraulic Research Institute)
- **Florentina Moatar** (French National Institute for Agricultural Research)
- **Frank Molkenthin** (Brandenburg University of Technology Cottbus-Senftenberg)
- **Gabriel Racoviteanu** (Technical University of Civil Engineering of Bucharest)
- **Gyewoon Choi** (Environment Cooperation of Incheon)
- **Hui Liang** (Chief Engineer, Intelligent Institute, Shanghai Investigation, Design & Research Institute Co., Ltd.)
- **Ilinca Nastase** (Technical University of Civil Engineering of Bucharest)
- **Ioana Fagarasan** (Politehnica University of Bucharest)
- **Jean-Luc Achard** (Institut National Polytechnique de Grenoble)
- **Jijian Lian** (President, Tianjin University of Technology)
- **Joseph Hun-Wei Lee** (President, Macau University of Science and Technology)
- **Juan Lyu** (Director, Research Center on Flood and Drought Disaster Reduction, China Institute of Water Resources and Hydropower Research; Former Deputy Director, Center of Flood and Drought Disaster Prevention, Ministry of Water Resources of the People’s Republic of China)
- **Jun Feng** (Professor, Hohai University)
- **Ken Thomas** (Waterford Institute of Technology)
- **Konstantinos Papatheodorou** (International Hellenic University Serres Branch)

- **Leiming Shi** (President, PowerChina Huadong Engineering Corporation Limited)
- **Luigi Berardi** (University of Chieti-Pescara)
- **Lydia Vamvakeridou-Lyroudia** (KWR Watercycle Research Institute)
- **Maurizio Righetti** (Free University of Bozen-Bolzano)
- **Nicolaos Theodossiou** (Aristotle University of Thessaloniki)
- **Nicolas Riviere** (National Institute of Applied Sciences, Lyon)
- **Olivier Piller** (French National Institute for Agricultural Research)
- **Qing Liu** (President, China South-to-North Water Diversion Group Water Networks Intelligent Technology Co., Ltd.)
- **Qiuhua Liang** (Loughborough University)
- **Quanxi Xu** (President, Changjiang River Scientific Research Institute of Changjiang Water Resources Commission)
- **Romeo Susan-Resiga** (Politehnica University of Timișoara)
- **Sandor Ianos Bernad** (Romanian Academy)
- **Sandra Soares-Frazao** (KU Leuven Engineering Group)
- **Sebastian Muntean** (Romanian Society)
- **Shiqiang Wu** (Vice President, Nanjing Hydraulic Research Institute)
- **Wenqi Peng** (Chief Engineer, China Institute of Water Resources and Hydropower Research)
- **Xiangdong Qiu** (Deputy General Manager, Intelligent Engineering Corporation, PowerChina Chengdu Engineering Corporation Limited)
- **Xiao Ma** (Vice President, Yellow River Institute of Hydraulic Research)
- **Xindai An** (President, Yellow River Engineering Consulting Co., Ltd.)
- **Xudong Fu** (Head, School of Civil Engineering, Tsinghua University)
- **Yang Cai** (Past Director, Information Center, Ministry of Water Resources of the People’s Republic of China)
- **Ying Gao** (Deputy General Manager, Henan Water & Power Engineering Consulting Co., Ltd.)
- **Yunzhong Jiang** (Director, Department of Water Resources, China Institute of Water Resources and Hydropower Research)
- **Zoran Kapelan** (Delft University of Technology)

## IAHR/IWA Joint Committee on Hydroinformatics

**Chair:**

- **Gabriele Freni** (Università Di Enna Kore)

**Vice Chair:**

- **Ibrahim Demir** (University of Iowa)

**Past Chair:**

- **Orazio Giustolisi** (Technical University of Bari)

**Member:**

- **Duan Chen** (Changjiang River Scientific Research Institute)
- **Qiuhua Liang** (Loughborough University)
- **Frank Molkenthin** (Braundenburg University of Technolgy Cottbus- Senftenberg)
- **Dimitri Solomatine** (IHE Delft Institute for Water Education)

# Table of Contents

## Technologies for water management and monitoring

## Hydraulic and hydrological modeling

## Water – Energy – Food nexus



## Climate change impacts

## Complex water systems, remote sensing and control

## Big-data, knowledge, and water data management

## Environmental, Marine and Coastal Hydroinformatics

## Hydroinfomatics for extreme hydrological events and resilience improvement

## Digital transformation of urban water systems

**Theme:** Technologies for water management and monitoring
**IAHR Thematic Priority Area:** [TPA-4] Digital Transformation
https://doi.org/10.3850/iahr-hic2483430201-1

# Integrating Digital City Model for Sustainable Stormwater Management under Climate Change: A Case Study of Nature-Based Solutions in Udonthani City, Thailand

**Fahad Ahmed[1], Lars Backhaus[2], Ho Huu Loc[3], Mukand Singh Babel[1], Juergen Stamm[2]**

[1] Asian Institute of Technology, Thailand
[2] TUD Dresden University of Technology, Dresden, Germany
[3] Wageningen University & Research, The Netherlands

*Corresponding author: josh.ho@wur.nl*

## 1 Introduction

The rapid urbanization has led to sudden alterations in land use, impacting natural hydrological processes and altering flood patterns within cities [1]. The reduction of green spaces and the increase of impermeable surfaces have resulted in a detrimental rise in both runoff volumes and peak discharges [2]. Climate change is not expected to alter the nature of intense rainfalls directly, it is projected to impact their severity, frequency, and potentially their geographical range [3]. Past studies have stressed the importance of studying Nature based Solutions (NBS) which are strategies relying on and imitating natural processes to mitigate problems like flooding. These strategies are known by many terms such as best management practices, green infrastructure, low impact development (LID) techniques, and sustainable urban drainage systems (SUDS) [4]. NBS have gained significant attention as urban flood risk management strategies since they attempt to replicate the natural predevelopment drainage conditions. “Green infrastructure” or NBS reduces runoff but cannot fully replace “grey infrastructure” due to safety concerns in extreme events. Also, ecological factors necessitate controlled construction scales for “grey infrastructure”. Hence, coupling “grey-green infrastructures” is crucial for optimal urban runoff control and enhancing water security. Assessing integrated flood management before construction is challenging, but numerical modeling and computational technologies provide a sustainable strategy. Digital city models offer streamlined management, communication, and consensus-building, efficiently showcasing the crucial role of NBS in flood mitigation to public authorities, stakeholders, and citizens.

Thailand has faced numerous flood disasters in the past, and the 2011 Thailand flood stands out as one of the most catastrophic floods in modern history [5, 6]. Udonthani city with dynamic land use and high socioeconomic significance, faces recurrent flooding, particularly in low-lying urban areas highlighting the necessity to evaluate the performance of NBS for mitigating urban flooding. The study presents a digital web app utilizing free and open-source software and data to promote NBS awareness in urban stormwater management under climate change.

## 2 Material and Methods

The methodology employed in this study involved several key steps to incorporate digital city models for sustainable stormwater management. A stormwater management model (SWMM) was constructed to simulate the impacts of various NBS measures, namely green roofs (GR), permeable pavements (PP), and bioretention cells (BC) in response to a prior rainfall event in the city. Five scenarios were devised for SWMM modelling: Scenario 1 served as the basecase (without NBS), Scenario 2 introduced GR on 50% of buildings across all sub-catchments, Scenario 3 incorporated PP on 50% of roads/pavements in all sub-catchments, Scenario 4 implemented BC covering 20% of all impervious areas, and Scenario 5 combined 50% GR, 50% PP, and 20% BC. These scenarios were analysed to assess their respective effects on stormwater management. Then, a 3D digital city model was constructed using CesiumJS, to provide 3D-Web-GIS functionality. Google Open Buildings v3 and Open Street Map, including Open Street Map Buildings (OSM), were extensively utilized to enhance the model's accuracy and detail. Geospatial analysis was performed using core data of the city, such as building information, land cover, sewage systems, and groundwater tables. The NBS measures were integrated and structurally organized within the 3D digital city model to facilitate cross-referencing and further analysis. The performance of different NBS measures was evaluated within each scenario, and the best-performing measures were suggested based on their effectiveness in mitigating stormwater issues. The selected NBS measures and their corresponding results were implemented within the 3D digital city model. Various techniques, such as color-coding measures, highlighting objects or computational assessments were employed to enhance understanding and promote awareness among public authorities, stakeholders, and citizen altogether.

## 3 Results and Discussion

The combined NBS scenario demonstrated the most substantial reductions in both junction flooding and total system inflow at the outfall. There was maximum flood reduction at a junction of 65% and a mean flood reduction at a junction of 74%. Whereas the maximum total inflow at the outfall was decreased by 59%, and the mean total inflow was reduced by 60%.

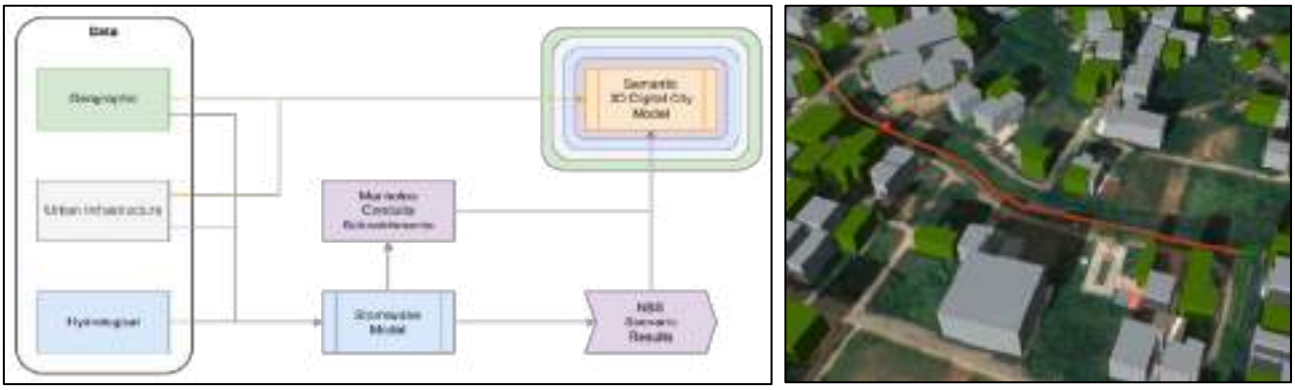


Figure 1 Conceptual Framework - Current Phase (Left); SWMM integrated with 3D digital city model (Right)

On the contrary, the standalone NBS scenario featuring 50% GR exhibited insignificant reductions in both instances. The maximum flood reduction at a junction was only 4%, and the mean flood reduction at a junction was 7%. Similarly, the maximum total inflow at the outfall was reduced by only 7%, with a mean total inflow reduction of 7%. This impact can be attributed to the fact that only half of the buildings were installed with green roofs in this specific scenario.
Moreover, the standalone NBS scenario incorporating 20% BC showcased greater reductions compared to both the 50% GR and 50% PP scenarios. The maximum flood reduction at a junction reached 32%, with a mean flood reduction at a junction of 48%. Additionally, the maximum total inflow at the outfall experienced a notable reduction of 45%, while the mean total inflow was decreased by 42%. This performance can be attributed to the larger area converted into permeable green surfaces, enhancing the capacity for stormwater retention and infiltration.

## 4 Conclusions

Udonthani case study showcased the usage of Google Open Buildings v3 for building semantic digital city model and combine it with stormwater management assessment. The integration of combination NBS demonstrated significant reductions, with mean total inflow and maximum total inflow decreasing by 60% and 59% respectively. However, the aim of achieving such a high reduction through extreme NBS measures is unlikely and can be considered as a hypothetical showcase. Overall, the study showcases effects of grey-green infrastructure and raise the awareness of NBS potential among varying target audiences. The current work is still in its early stages, utilizing Open Data sources with limited quality and spatial resolution hence, calibration and validation of the SWMM model is required. Future steps include assessing NBS performance under future climate change projections and integrating a 2D model to improve model accuracy and depict the effects on city infrastructure using semantic attributes.

## Reference

[1] Akhter M, Hewa G. The Use of PCSWMM for Assessing the Impacts of Land Use Changes on Hydrological Responses and Performance of WSUD in Managing the Impacts at Myponga Catchment, South Australia. Water (Basel) 2016; 8: 511.
[2] Qin Y. Urban Flooding Mitigation Techniques: A Systematic Review and Future Studies. Water (Basel) 2020; 12: 3579.
[3] Howard G; BJ. The Resilience of Water Supply and Sanitation in the Face of Climate Change, Vision 2030. Geneva, Switzerland, 2010.
[4] Vogel JR, Moore TL, Coffman RR, et al. Critical Review of Technical Questions Facing Low Impact Development and Green Infrastructure: A Perspective from the Great Plains. Water Environment Research 2015; 87: 849–862.
[5] Loc HH, Park E, Chitwatkulsiri D, et al. Local rainfall or river overflow? Re-evaluating the cause of the Great 2011 Thailand flood. J Hydrol (Amst) 2020; 589: 125368.
[6] Loc HH, Park E, Chitwatkulsiri D, et al. Local rainfall or river overflow? Re-evaluating the cause of the Great 2011 Thailand flood. J Hydrol (Amst) 2020; 589: 125368.

**Theme:** Technologies for water management and monitoring
**IAHR Thematic Priority Area:** [TPA-4] Digital Transformation
https://doi.org/10.3850/iahr-hic2483430201-3

# GIS-Based Machine Learning Applications as Decision Support Systems to Enhance Groundwater Monitoring Networks

**Gómez-Escalonilla V[1], Martínez-Santos P[1*], Díaz-Alcaide S[1], Montero González E[1], Martín-Loeches M[2]**

[1] Universidad Complutense de Madrid. C/Jose Antonio Novais 2, 28040 Madrid, Spain
[2] Universidad de Alcalá. Av. de León, 4A, 28805 Alcalá de Henares, Madrid

** Corresponding author: pemartin@ucm.es*

**Abstract.** Machine learning approaches are currently being explored as tools to underpin water management. Applications range from the prediction of groundwater levels to the improvement of classic numerical models. We present an approach to underpin the design of groundwater quality monitoring networks based on the application of multiple supervised classification algorithms. The method is illustrated through its application to a series of aquifer systems in central Spain. Classifiers were trained on a sample of borehole data to identify which spatially-distributed variables explain the presence of selected contaminants in groundwater. Spatially-distributed explanatory variables included slope, thickness of the unsaturated zone, lithology, and land use, among others. The best performing algorithms as per AUC, test score, precision and recall metrics, were used subsequently to identify unmonitored locations where contamination is likely to occur. This results in the identification of those spatially-distributed factors that seemingly explain the presence of contamination in groundwater. Furthermore, it allowed us to identify the unmonitored areas of potential concern where new observation points would be needed. This method provides an alternative to expert-based criteria as to where to site new groundwater monitoring stations and can be readily exported to other settings. Tree-based classifiers such as random forest and extra trees proved the most accurate predictors of groundwater contamination, rendering predictive and AUC scores in excess of 0.8.

**Keywords:** groundwater monitoring, nitrate, machine learning, observation wells, supervised classification, Spain

## 1 Introduction

Agrochemicals are common pollutants in aquifer systems. Widespread presence of nitrate and pesticides is often associated with cultivated surfaces, and poses a major challenge to groundwater management worldwide. The first step towards managing groundwater contamination consists of adequately monitoring and mapping. While theoretically simple, this often presents important difficulties associated with hydrogeological considerations, monitoring well siting and construction, all of which hamper data interpretation. Because drilling is expensive, and because networks often rely on preexisting infrastructures, networks are frequently less than optimal in terms of spatial resolution.

Machine learning is seen as a potentially major breakthrough in improving groundwater monitoring networks. In particular, predictive contaminant mapping can help decision-makers identify where to drill new monitoring points based on the likelihood of finding contaminants.

## 2 Methods

This research illustrates a predictive mapping approach based on the application of machine learning algorithms to determine which spatially distributed variables are linked to the presence of nitrate in a series of aquifers of central Spain. Spatially-distributed explanatory variables included slope, thickness of the unsaturated zone, lithology, and land use, among others, whereas contaminant data

was obtained from a sample of 213 boreholes. Predictive maps were built by means of tree-based algorithms. Five different models were used to predict the nitrate concentrations from groundwater samples and the above-mentioned explanatory variables. In this work, the Decision Tree classifier, the Random Forest classifier, the AdaBoost classifier, the Gradient Boosting classifier and the ExtraTrees classifier were used. These supervised classification algorithms are included in MLMapper version 2.0 [1]. All models integrated in the MLMapper code derive from the SciKit-Learn toolbox [2].

## 3 Results

All models showed test scores or accuracy values higher than 0.73. Random forest and AdaBoost were the worst performing models. Gradient Boosting and simple decision tree showed 0.75 and 0.77, respectively, for the test score metric. Finally, the ExtraTrees model outperformed the previous algorithms by achieving 0.83 on this metric. As previously mentioned, there is a ratio of 45:55 between negative (nitrate concentration below 37.5 mg/l) and positive (nitrate concentration above 37.5 mg/l) points. Therefore, the predictive performance of each class must be analyzed separately. This was addressed by the F1 score for both classes. The F1 scores for the negative class were higher than for the positive one, with the former ranging from 0.77-0.86 and the positive class ranging from 0.67-0.78 for the entire set of algorithms. The ExtraTrees classifier showed high performance in both the negative and positive classes, with F1 scores of 0.86 and 0.78, respectively. Regarding the area under curve (AUC), the values range from 0.79 for the Adaboost algorithm to 0.88 for the ExtraTrees classifier. Based on the predictive performance, the ExtraTrees classifier will be used to develop the following analysis of the feature importance and the spatial prediction of the nitrate concentrations.
The most important variable for the ExtraTrees classifier to predict nitrate concentrations was the unsaturated zone thickness, followed by latitude, lithology, distance to rivers and longitude. This was followed in order of importance by distance to livestock farms, climatic factors such as temperature and precipitation, and surface and subsurface factors such as soil type and sand content. The remaining variables such as elevation, slope, geomorphology, land cover and NDVI showed similar and low values of importance.

## 4 Conclusions

Algorithm outcomes suggests that supervised classification provides an adequate means to identify physical and chemical variables linked to groundwater contamination. Futhermore, the results imply that the official delineation of areas vulnerable to nitrate underestimates the extent of the problem. While additional monitoring boreholes would be required to confirm this, it is also concluded that predictive maps can be used as a tool to drive the enhancement of groundwater monitoring networks.

## References

[1] V. Gómez-Escalonilla, P. Martínez-Santos, M. Martín-Loeches (2022). Preprocessing approaches in machine-learning-based groundwater potential mapping: an application to the Koulikoro and Bamako regions, Mali. Hydrology and Earth System Sciences, 26(2), 221-243

[2] F. Pedregosa, G. Varoquaux, A. Gramfort, V. Michel, B. Thirion, O. Grisel, M. Blondel, P. Prettenhofer, R. Weiss, V. Dubourg, J. Vanderplas, A. Passos, D. Cournapeau, M. Brucher, M. Perrot, E. Duchesnay (2011). Scikit-learn: Machine learning in Python. Mach Learn Python. 12:2825–2830.

**Theme:** Technologies for water management and monitoring
**IAHR Thematic Priority Area:** [TPA-4] Digital Transformation
https://doi.org/10.3850/iahr-hic2483430201-5

# GIS for Water Utilities Web Center

**Panyawat Sirithum [1], Wariyanan Marwan [2]**

[1] Department of Engineering Standard and Geographic Information,
Metropolitan Waterworks Authority of Thailand (MWA) 400 Prachacheun Road,
Tungsonghong, Laksi, Bangkok 10210, Thailand
[2] Department of Risk Management,
Metropolitan Waterworks Authority of Thailand (MWA) 400 Prachacheun Road,
Tungsonghong, Laksi, Bangkok 10210, Thailand

*Corresponding author*: *torbackfour@gmail.com*

**Abstract.** Metropolitan Waterworks Authority (MWA), Thailand has developed Geographic Information System (GIS), "GIS WEB CENTER" to support engineering and service work for MWA in the area of 3,195 km2 with 2.5 million customers and a combined water supply production capacity of 5.0 million cubic meters per day. According to the Enterprise GIS project, MWA's develop GIS applications to be linked with 5 core water utilities systems, namely WLMA, SCADA, CIS, SAP, Water Quality Online respond to the requirements of users to the system efficiently, which can be integrated GIS data to be support related users to be more efficient ,forward to providing GIS data to be accurate, complete, up-to-date. The result of web application can be used to make a decision for water pressure management, sufficiently and water pipe asset management for maximum benefits to the organization and distribute good quality water to customers covers all community and sustainable.

**Keywords:** CIS; DMA; GIS; SCADA; WLMA

## 1 Introduction

The Metropolitan Waterworks Authority (MWA), Thailand is a state enterprise under the supervision of the Ministry of Interior that has been operating since 16 August 1967. The enterprise's primary mission is to provide raw water for use in supply, production, delivery and distribution of water in Bangkok, Nonthaburi and Samut Prakan provinces, as well as to operate other business related to or beneficial to the waterworks.

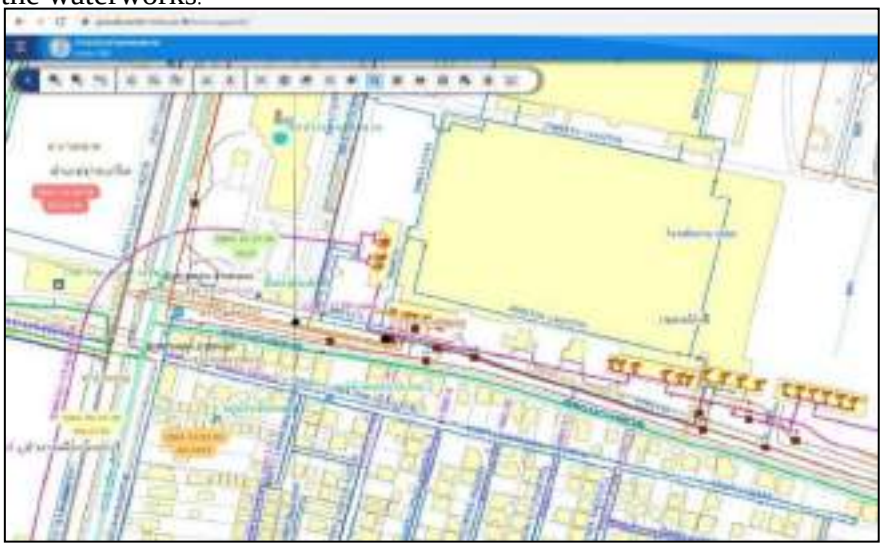

Figure 1 GIS Web Center

Furthermore, the MWA's actively works to manage wastewater and manage water pressure while supporting for reduction in water wastage by administrating surveillance areas to effectively reduce water loss in the DMA, and we have a GIS database system to aid us in analysis and decision-making, in addition to making use of new technologies to minimize activities that waste water.

## 2 Methods

According to the Enterprise GIS project, MWA's develop GIS applications to be linked with 5 core water utilities systems, namely WLMA, SCADA, CIS, SAP and Water Quality Online to respond to the requirements of users to the system efficiently. GIS WEB CENTER can be integrated GIS data to be support related users to be more efficient ,forward to providing GIS data to be accurate, complete, up-to-date and can apply to pipe asset management In order to the GIS for Water Utilities Data Recording functions, There are 4 main functions to input the information in GIS WEB CENTER

- Implementation of pipe and equipment information functions (Job Management)
- Shutting off water supply distribution in the trunk main system and the water distribution pipelines
- Meter data recording
- Creating CAD file based on each DMA.

## 3 Results and Discussion

The advantages of this web application, Users can be export the information directly. Ex. Job Management report, Meter data recording report, Notification report of water stoppage area, CAD file. This project's outcomes can be summarizing and export data to a document reports, namely pipe length and equipment report, service area report.

## 4 Conclusion

The result of GIS WEB CENTER with complete as well as updated data can be used to make a decision for water pressure management, sufficiently and water pipe asset management, budget plan and Pipeline maintenance work plan, pipeline declination risk assessment for maximum benefits to the organization and distribute good quality water to customers covers all community and sustainable.

Table 1 Length of Pipe

| Pipe Length (km) Classified by pipe type | | | | | | | | | | | | | |
|---|---|---|---|---|---|---|---|---|---|---|---|---|---|
| | ST | SCP | RCP (ST) | CI | PC-ST | PC | AC | DI | PVC | GI | HDPE | PB | Total |
| Tunnel | 143.1 | 0.0 | 0.0 | 0.0 | 47.8 | 0.0 | 0.0 | 0.0 | 0.0 | 0.0 | 0.0 | 0.0 | 190.9 |
| | | | | | | | | | | | | | |
| Trunk Main | 1,579.6 | 44.4 | 61.2 | 100.0 | 0.0 | 36.3 | 6.6 | 3.1 | 0.0 | 0.0 | 6.5 | 0.0 | 1,837.7 |
| | | | | | | | | | | | | | |
| Distribution Pipe | 678.4 | 0.0 | 0.0 | 11.9 | 0.0 | 0.0 | 2,626.6 | 1.1 | 33,135.3 | 218.1 | 364.7 | 1,751.6 | 38,787.0 |
| | | | | | | | | | | | | | |
| (Total in Distribution System) | 2,401.01 | 44.4 | 61.2 | 111.2 | 47.8 | 36.3 | 2,633.2 | 4.2 | 33,135.3 | 218.1 | 371.2 | 1,751.6 | 40,815.6 |

## Reference

[1]Bailey, Trevor C., and Anthony C. Gatrell. 1995. *Interactive Spatial Data Analysis.* England: Prentice Hall.

[2]O'Sullivan, David, and David Unwin. 2010. *Geographic Information Analysis.* New Jersey, USA: Wiley.

**Theme:** Technologies for water management and monitoring
**AHR Thematic Priority Area:** [TPA-4] Digital Transformation
https://doi.org/10.3850/iahr-hic2483430201-7

# Strategy of Water Transfer Efficiency Improvement in Central Route of South-To-North Water Diversion Project

**Xinlei Guo, Jiajia Pan, Hui Fu, Tao Wang, Jiazhen Li, Yuzhuang Chen**

State Key Laboratory of Simulation and Regulation of Water Cycle in River Basin, China Institute of Water Resources and Hydropower Research, Beijing 100038, China

*Corresponding author: guoxinlei@iwhr.com*

**Abstract.** The efficiency and safety management of the Central Route of the South-to-North Water Diversion Project (CRSNWD) during winter are significantly impacted by ice. The study aims to illustrate the spatial and temporal variability of water temperature and ice distribution, understand the driving factors behind ice propagation in the system, and propose ice-prevention plans for wintertime water transfer. The results of field observations reveal that the ice-affected region is smaller and has a shorter duration than anticipated. The study identified air temperature, water diversion discharge, solar radiation, and wind speed as the most dominant factors influencing ice processes in the system. Severe ice jams that occurred in January 2016 resulted from a combination of lower accumulated freezing degree days, larger flow discharge, and a short-term cold wave. A high wind speed in the Caohe duct causes a rapid decrease in water temperature and significant ice formation. Based on these findings, the study proposes shortening operation periods, reducing ice-affected regions, optimizing hydraulic control parameters, and developing ice-prevention techniques to enhance the wintertime operation of the CRSNWD.

**Keywords:** water temperature and ice distribution; South-to-North Water Diversion; wintertime safety

## 1 Introduction and method

The significant latitudinal difference and the special meteorological conditions of freezing and thawing in the north and south make the winter operation of the Central Route trunk canal experience complicated conditions such as water transfer by ice floes and ice cover [1][2]. From December 2011 to February 2023, relevant departments carried out field observations for 12 consecutive winters in the 480 km section of the Anyanghe siphon to the Beijuma culverts. The purpose of this study is to find out the air temperature, water temperature and ice processes of the trunk canal from December to February based on the above data, analyze the spatial and temporal variability of water temperature and ice distribution, and clarify the water temperature conditions formed by the Central Route border ice, ice floes and ice cover, and then propose ice-prevention plans for wintertime water transfer.

## 2 Results and discussion

### 2.1 Characteristics of water temperature and ice distribution in the CRSNWD

Fig. 1 gives the three-month average winter temperatures in December-February, the January average temperature and the 7-day average temperature of the lowest cold wave at the Baoding meteorological station from 1956-2021, with Baoding corresponding to a stake of about 1,100 km in the Central Route trunk canal. The average winter temperature at the Baoding meteorological station in the last 65 years has shown an overall upward trend, from -4.0°C to -1.5°C, which is in line with the general trend of climate warming in the CRSNWD. Comparison shows that the average winter temperature corresponding to the ice jam in 2015-16 is once in two years, while the negative accumulated temperature in January is lower than that in 2020-21, which is once in seven years, and the recurrence interval is longer. In winter, the water of the CRSNWD continued to lose heat, such as the low negative cumulative temperature in January, the extreme sudden cold wave is prone to lead to cooling and massive ice formation, superimposed on the large flow discharge and high Froude number conditions are prone to trigger a situation similar to the localized ice jam in 2015-16. This suggests

that the negative cumulative temperature in January in the CRSNWD has a greater impact on the attenuation of water temperature than the average winter temperature, and can be used as an indication of the occurrence or non-occurrence of ice jams. Fig. 2 analyzes the water temperature, air temperature, and water discharge processes of the Hutuohe siphon for two winters, 2017-18 and 2019-20. The results show that under the similar temperature conditions in the two winters before mid-January, the water diversion discharge in 2017-18 is 49.2 $m^3$ / s, which is 10.8 % lower than that in 2019-20, and the water temperature of the former is 1.5 °C lower than that of the latter. From February to March, the water temperature in 2017-18 was lower than that in 2019-20, exceeding 2.5 °C, mainly because the former had lower temperature and smaller water diversion discharge.

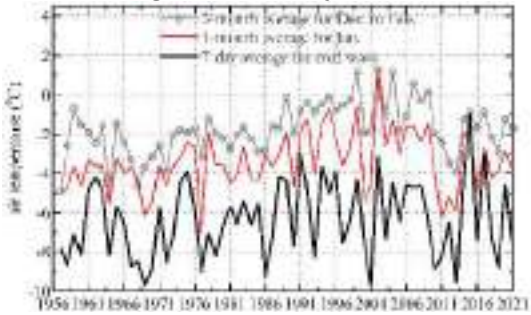

Figure 1 The monthly average temperature and the 7-day average temperature of the lowest cold wave in winter of Baoding Meteorological Station from 1956 to 2021.

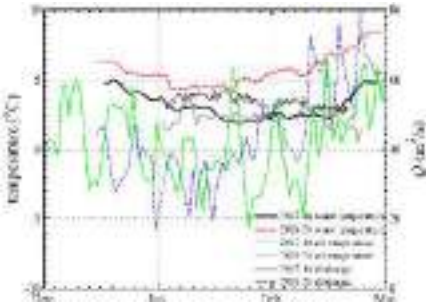

Figure 2 The water temperature, air temperature, and flow discharge of the Hutuohe siphon for two winters.

## 2.2 Strategy of water transfer efficiency improvement in the CRSNWD

(1) The study shows that increasing the flow discharge can reduce the decline rate of water temperature, increase the turbulence mixing intensity of water flow, the heat capacity of the water and the critical length of the water temperature from positive to negative. It is necessary to explore a new mode of non-ice cover large flow discharge transfer in winter, that is, meet the water demand from the water quantity, delay the formation of the ice cover from the water temperature, control the ice processes from the hydraulic, reduce the length of the affected canal section and the number of water outlets, and then extend the water transfer time and increase the water transfer volume.

(2) Dynamic optimal scheduling and mode switching of water transfer in winter. After the forecast and early warning in the actual dispatching, the flow discharge can be reduced to the safe range within 2-3 days. Therefore, it is necessary to optimize the judgment threshold of the ice period, dynamic scheduling mode and fast switching method of large flow discharge to existing mode during ice period according to online monitoring and short-term meteorological forecast, so as to improve the water transfer capacity in winter through scientific dynamic scheduling.

(3) Auxiliary enhancement after the application of new equipment, new models, new technologies and new materials. New stations should be added to study the new monitoring and intelligent ensemble early warning and forecasting technology of water temperature and ice distribution within the CRSNWD to support high-precision monitoring and forecasting of water temperature, ice distribution and ice disaster. It is necessary to study the fine simulation technology of water temperature and ice distribution in combination with the control threshold range of water temperature and ice distribution. On the basis of improving the simulation accuracy, the hydraulic control index is optimized to support the improvement of water transfer efficiency.

## 3 Conclusions

This study analyzes the evolution and influence mechanism of winter water temperature and ice distribution in the CRSNWD. Under the premise of ensuring the safe operation of the CRSNWD, the countermeasures for improving the water transfer efficiency of the CRSNWD in winter are put forward from three aspects.

## Reference

[1] Xinlei Guo, Kailin Yang, Hui Fu, et al. Ice processes modeling during reverse transfer of open canals: a case study. J. Hydro-environ Res., 2017, 17: 56-67.

[2] Jiajia Pan, Xinlei Guo, Tao Wang, et al. A detailed energy budget model for the Central Route of the South-to-North Water Diversion Project in China. J. Hydraul Eng., 2024, 55(2): 179-189.

**Theme:** Technologies for water management and monitoring
**IAHR Thematic Priority Area:** [TPA-4] Digital Transformation
https://doi.org/10.3850/iahr-hic2483430201-9

# Leak Detection through Acoustic Signal Clustering with Gaussian Mixture Modelling

**Y. Yu[1], S. Rabab[1], R. Collins[1], T. Alps[2], E. Hampton[3], J. Boxall[1]**

[1]Department of Civil and Structural Engineering, University of Sheffield, Sheffield, S1 3JD, United Kingdom
[2] HWM-Water Ltd, Ty Coch House, Llantarnam Park Way, Cwmbran, NP44 3AW, United Kingdom
[3]Dwr Cymru Welsh Water, St Mellons, Cardiff, CF3 0LT, United Kingdom

*Corresponding author: Yicheng.yu@sheffield.ac.uk*

**Abstract.** This study introduces a new data analysis methodology for the detection and location of leakage from water distribution infrastructure. A short-time Hanning windowing technique has been used as a low-pass filter for data segmentation and preprocessing. Our methodology capitalizes on the short-time zero-crossing rate and the short-time energy analysis of acoustic signals to effectively identify leakage. Additionally, Gaussian Mixture Modelling has been employed to cluster acoustic data, thereby improving the precision of leakage detection. We have conducted analysis and classification of leakage signals from both plastic and iron pipes, demonstrating advance over previous acoustic based detection method overcoming some issues wave attenuation in plastic pipes and enhance detection accuracy across different materials. Such advances are vital for both economic and environmental reasons.

**Keywords:** Acoustic sensing, clustering, GMM, leakage, pipe material, water pipe,

## 1 Introduction

Acoustic methods have been at the forefront of detecting, characterizing and localising leaks [1, 2]. These methods have undergone significant research and development, showcasing their potential in various contexts. However, challenges remain due to how the material composition of pipes influences the efficacy of leak noise detection by acoustic loggers as evidenced by the research presented in [3]. One of the primary difficulties arises in the context of plastic pipes, where the attenuation of acoustic waves is considerably higher than in pipe made from other materials [1]. This phenomenon makes the detection of leaks in plastic pipes more challenging.

## 2 Methodology

This paper presents a novel approach to identifying leaks within water piping systems, leveraging the acoustic properties of leak-induced signals and machine learning based analysis. Specifically, we focus on two fundamental acoustic signal characteristics: the zero-crossing rate (ZCR) and the signal energy. These features have been widely recognized for their effectiveness in various audio analysis applications but have seen limited exploration in the context of leak detection.

The zero-crossing rate (ZCR, defined in Eq. (1) as ), which measures the rate at which the signal changes from positive to negative or vice versa, is indicative of the frequency content of the signal. In the context of water leak detection, a higher ZCR is hypothesized to correlate with the presence of a leak, due to the turbulent flow noise generated by escaping water. On the other hand, the energy of the signal (defined in Eq. (2)), representing the average power of the acoustic emission, is expected to increase with the severity of the leak.

$$Z_n = \frac{1}{2}\sum_{m=0}^{M-1}\left|\mathrm{sgn}\left(x_n(m)\right) - \mathrm{sgn}\left(x_n(m-1)\right)\right| \quad (1)$$

$$E_n = \sum_{m=0}^{M-1} x^2(m) \quad (2)$$

where  and  are the short time ZCR and energy, respectively. sgn is the sign function, *M* is the number of sample points in the short time segment. To accurately extract the zero-crossing rate and energy features from the time-domain leakage noise, our methodology incorporates the use of short-time Fourier transform (STFT) with Hanning windowing. The segmentation of the acoustic signal is achieved by applying a Hanning window of 300 points, reflecting a strategic balance between resolution and computational efficiency. The acoustic logger, pivotal to our data acquisition process, operates at a sampling frequency of 4096 Hz, capturing 10-second recordings that are rich in detail and conducive to precise analysis. The choice of the Hanning window serves a dual purpose: it segments the signal and acts as an effective low-pass filter, thereby preconditioning the data by mitigating the impact of high-frequency noise components. The extracted features are subsequently integrated into a Gaussian Mixture Modelling (GMM) framework. This statistical approach allows for the clustering of acoustic data based on similarities in feature space, enabling the predictive modelling of leakage presence with heightened accuracy.

## 3 Results

Due to the considerable diminution of the energy in leak signals in plastic pipes, employing the signal amplitude for leak detection presents substantial challenges (see Figure 1 (left)). Nevertheless, our analysis shows that alternative characteristics, such as the zero-crossing rate, may offer viable avenues for identifying leaks. This is exemplified in Figure 1 (right), wherein, despite the absence of a notable augmentation in leak noise, an escalation in the zero-crossing rate could potentially facilitate the identification of a leak in a plastic pipe.

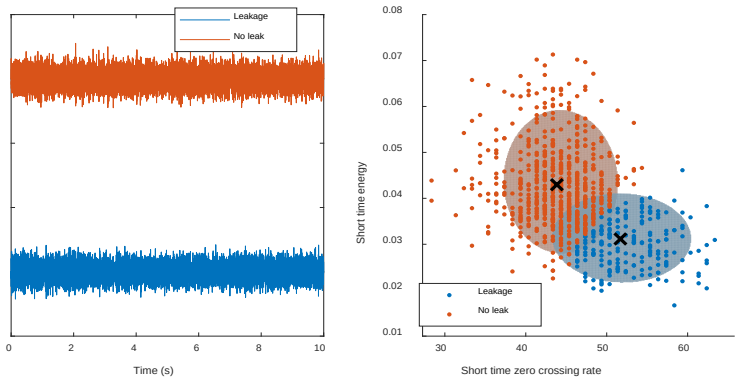


Figure 1. comparison of leakage noise and background noise from a plastic pipe (left) one sample of time domain data, (right) GMM clustering using ZCR and energy.

## 4 Conclusions

A novel method based on analysis of the zero cross rate and signal energy, using Hanning window and Gaussian Mixture Model are shown effective for leak detection in plastic pipes.

## Reference

[1] Y. Yu, A. Safari, X. Niu, B. Drinkwater and K. V. Horoshenkov, “Acoustic and ultrasonic techniques for defect detection and condition monitoring in water and sewerage pipes: A review,” Applied Acoustics, vol. 183, p. 108282, 2021.

[2] H. Fan and T. Z. Salman Tariq, “Acoustic leak detection approaches for water pipelines.,” Automation in Construction, vol. 138 , p. 104226, 2022.

[3] J. D. Butterfield, R. P. Collins and S. B. Beck, “Influence of pipe material on the transmission of vibroacoustic leak signals in real complex water distribution systems: case study,” Journal of Pipeline Systems Engineering and Practice, vol. 9, no. 3, p. 05018003, 2018.

**Theme:** Technologies for water management and monitoring
**IAHR Thematic Priority Area:** [TPA-4] Digital Transformation
https://doi.org/10.3850/iahr-hic2483430201-11

# Leak Localization in Long Water Conveyance Pipes by Transient Wave-Based Method

**Asiedu R. Sarpong[1], Ling Zhou[2], Tongchuan Che[1]**

[1] College of Water Conservancy and Hydropower Engineering, Hohai University, Nanjing, China
[2] Department of Civil and Environmental Engineering, The Hong Kong Polytechnic University, Hong Kong SAR, China

*Corresponding author: zhhlu@hhu.edu.cn*

**Abstract.** Transient wave-based leak detection methods have been extensively developed for urban water supply pipes. However, they might become inaccurate in long pipes due to their large diameters and long lengths. In this paper, the transient wave reflection (TWR) method is used in long water conveyance pipes to specifically localize a leak anomaly both numerically and experimentally, with wavelet transform used to identify the reflected wave in noisy environment, and to determine the leak detection range. As a results, the TWR produced accurate localization estimations.

**Keywords:** Conveyance pipe; detection; leak; localization; transient wave; wavelet transform.

## 1 Introduction

Transient wave-based leak detection methods have been extensively developed for urban water supply pipes. However, these methods may become inaccurate in long pipes based on their large diameters and lengths, and fast wave damping, whose mechanisms are still unclear. This paper aims to clarify this problem by using transient wave reflection (TWR) method in long water conveyance pipes to specifically localize a leak anomaly, with wavelet transform used to identify the reflected wave in noisy environment, and to determine the leak detection range based on the critical signal-to-noise-ratio (SNR).

## 2 Leak localization method and model

The 1-D water hammer of dynamic and continuity equations are solved by the method of characteristics with finite difference technique [1], and Brunone's model for unsteady friction [2]. A reservoir-pipe-valve (RPV) system in both intact and leaking pipe cases are analysed to determine the transient wave behaviour both numerically and experimentally.

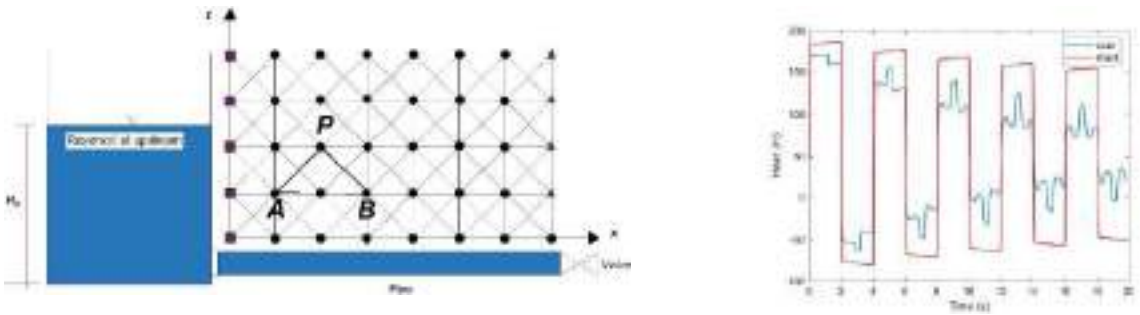


Figure 1 Schematic of an RPV system with discrete grids and Transient wave behaviour in an intact and leaking pipes.

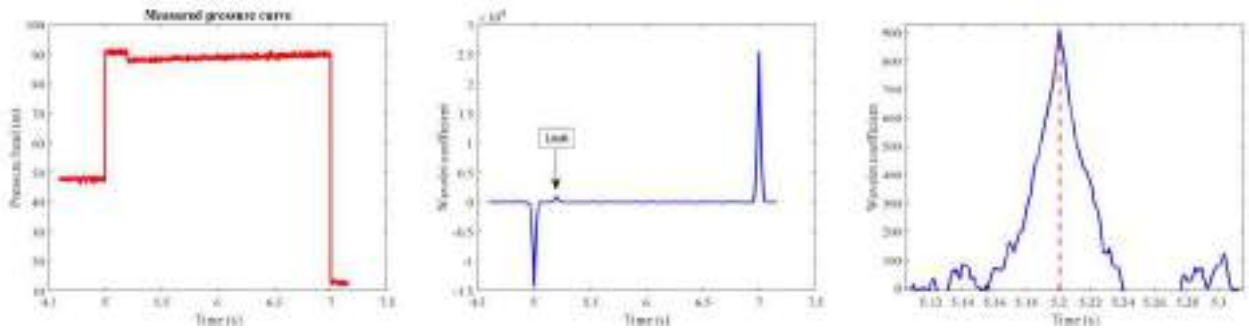

Figure 2 Pressure signal with additive white noise analysed by wavelet transform; left: first pressure head cycle; middle: identification of leak located at $X_L$ = 900 m from upstream; right: enlarged part showing leak reflected wave.

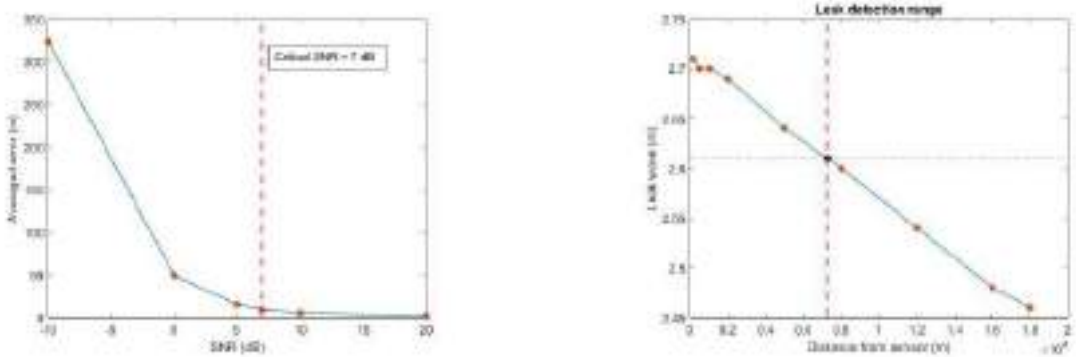

Figure 3 A 2km long pipe; left: critical SNR = 7 dB which allows for leak localization in target pipe; right: leak detection range for TWR in target long pipe is determined at 7255 m, shown in red short-dashed line.

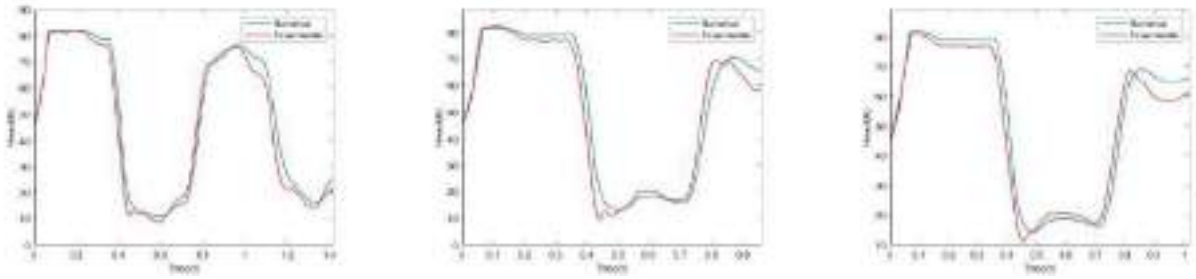

Figure 4 Validation of numerical and experimental data having same parameters and a pipe length L = 241.52 m, when actual leak locations; left: $X_L$ = 84.71 m; middle: $X_L$ = 152.3 m; right: $X_L$ = 173.03 m.

## 3 Results analysis and Conclusions

The TWR method has proven to be a reliable method for localizing a leak in long water conveyance pipes. In Figure 4 the estimated $X_L$ for (*left, middle, right)* leak cases are 83.4 m, 153.4 m, and 173.4 m respectively. The wavelet transform of db1 is capable of identifying leak singularity in noisy environment. The magnitude of the leak wave amplitude decreases as the distance from sensor to leak location increases. It is worth mentioning that the leak detection range is affected by the leak size, its distance from the measurement section, and the standard deviation in the reflected signal.

## Reference

[1] E. B. Wylie, V. L. Streeter, and L. Suo, *Fluid transients in systems*, vol. 1. Prentice Hall Englewood Cliffs, NJ, 1993.

[2] B. Brunone, U. M. Golia, and M. Greco, “Effects of two-dimensionality on pipe transients modeling,” Journal of Hydraulic Engineering, vol. 121, no. 12, pp. 906–912, 1995.

**Theme:** Technologies for water management and monitoring
**IAHR Thematic Priority Area:** [TPA-4] Digital Transformation
https://doi.org/10.3850/iahr-hic2483430201-13

# Identification and Localization of Background Leakage Using Customer Consumption Data

**S. Rabab[1], R. Collins1, Y. Yu[1], A. Taliana[2], S. Trow[3], J. Boxall[1]**

[1] Department of Civil and Structural Engineering, University of Sheffield, Sheffield, UK
[2] Welsh Water, St Mellons, Cardiff, UK
[3] HWM-Water Ltd, Llantarnam Park Way, Cwmbran, UK

*Corresponding author: s.rabab@sheffield.ac.uk*

**Abstract.** The paper describes the application of an 'all connections' (i.e. every household connection simulated as a node) hydraulic model for a case study DMA. Stopwatch loggers were deployed to obtain household demand data as well as pressure sensors for network conditions. Comparison of measured and modelled inlet flow provided an estimation of network side leakage, with analysis of head loss pairs used to identify the location of network side leakage. Modelling also revealed information about the network configuration. Key unique aspects are the use of real-world, intensive, customer water consumption data and all connections model to facilitate the accurate detection of previously hidden leakage.

**Keywords:** All connections model, Background leakage, Intensive customer demand data

## 1 Introduction

Identifying and locating leakage from water distribution systems presents a significant challenge for the water industry. Approximately half of reported leakage in the UK is attributed to Background Leakage, which may be determined from the minimum achieved night flows identified during a leakage survey of an area. Without tackling Background Leakage, it is very challenging to reduce leakage to a level acceptable under a truly sustainable assessment. In the UK the target has been set to half leakage by 2050 [1]. Data on individual customer water consumption has the potential to improve the estimation of background leakage. However, high-resolution datasets of the water consumption for each property along with the pressure data at numerous key locations in a DMA are not commonly available.

## 2 Material and Methods

The DMA studied and reported here was deemed of good performance with acceptable, non-actionable levels of leakage, under traditional leakage assessment methods. Individual property water consumption data (one minute resolution) was collected in a case study District Meter Area (DMA) for a one-week period using Invenio Stopwatch loggers. These provided high spatial and temporal resolution consumption data and allowed identification of customer side leakage. Pressure data at one-minute intervals was also collected at every accessible hydrant and at the DMA inlet. DMA inlet flow was also recorded at 1 minute for the same period. An all-connections hydraulic model was built by using the high-resolution measurements of water consumption for each property in the DMA. The missing demands, where Stopwatch loggers could not be deployed, was infilled using nearby customer demand data. Thus, all demand was accounted for or estimated. Figure 1(a) shows the all-connection model for the case study DMA. It should be noted that the DMA was anonymised, with its layout disguised to maintain confidentiality of the data which is GDPR sensitive [2]. Calibration of the hydraulic model was performed to identify the correct network configuration and any discrepancies to other data, DMA inlet flow and pressure measurements. Through hydraulic

modelling and head loss analysis network side leakage was identified and localised, that were previously hidden.

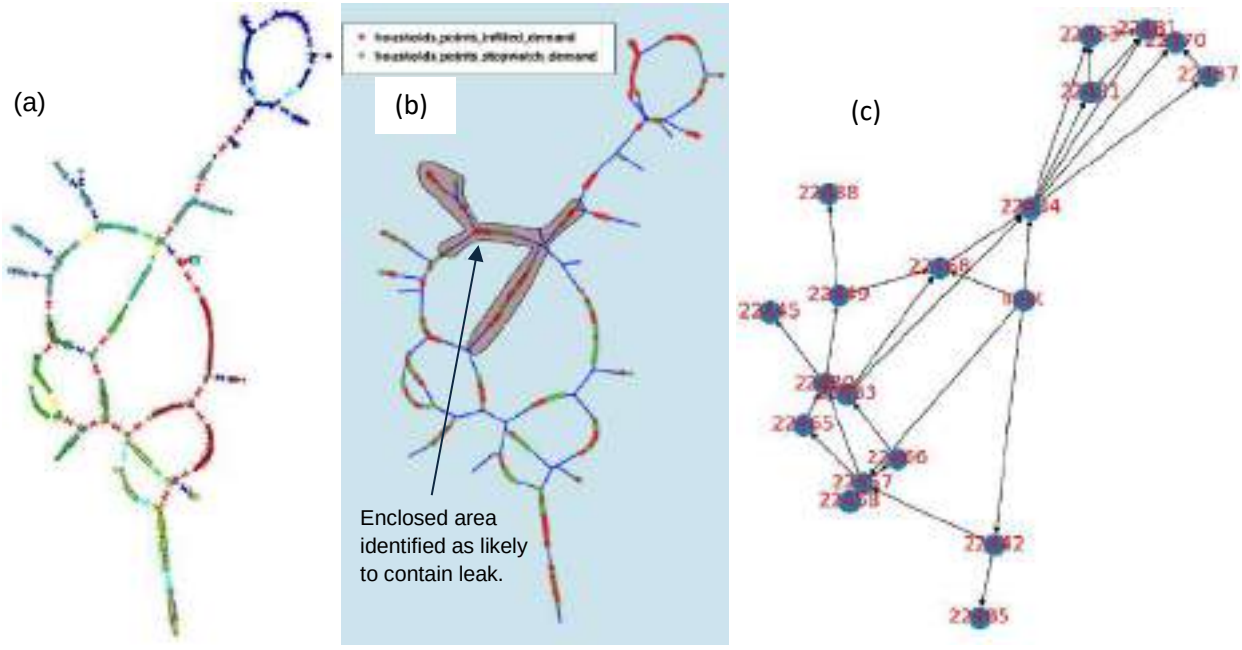


Figure 1 (a) Anonymised Network (b) area of identified leak (c) head loss pairs

## 3 Results and Discussion

Stopwatch coverage was good with more than 70% of property consumption data available. A total of 0.08 l/s customer side leakage was found by the Stopwatch continuous profiles in 23 properties. In Figure 1 (b) the green dots show properties with stopwatch data and the red dots ones that were missing and had to be estimated. Comparison of the measured and modelled DMA inlet flow showed the unaccounted flow in the DMA due to the leakage and uncertainty in infilling unmeasured consumer demands, with the nightline level providing a more accurate estimation of network side leakage. In addition to leakage detection, the modelling approach also identified and located network operations during the monitoring period that reduced the unaccounted flow by 0.5 l/s. The later data logging showed a remaining 0.5 l/s unaccounted flow in the DMA. Head loss pairs were created from all connected pressure measurement points in the DMA, Figure 1 (c). This revealed an issue with the network configuration, as imported from GIS records. The correct behaviour could only be modelled by closing a valve in the inlet chamber. This valve status was confirmed by an operational team. Differences in modelled and measured head losses were then able to identify the location of the 0.5 l/s unaccounted flow as highlighted in Figure 1 (b). An operational team found three leakages in the area identified.

## 4 Conclusion

Background leakage was estimated using property water consumption data and the anomalies in measured and modelled head loss identified the location of leakage in a case study DMA. The method proposed and demonstrated here for an operational DMA has the potential to help us reduce leakage and hence make our water distribution systems resilient to future challenges from climate change and increasing populations.

## Reference

[1] R. Collins, J. Boxall, S. Trow, S. Tooms, and E. Hampton, “Managing Background Leakage: Stage A Report” Feb. 2023.
[2] R. Collins, E. Hampton, S. Rabab, S. Trow, S. Tooms, and J. Boxall, “Managing Background Leakage: Project Introduction,” in Proc. Computing and Control Water Industry Conference, Leicester, UK: 2023.

**Theme:** Technologies for water management and monitoring
**IAHR Thematic Priority Area:** [TPA-4] Digital Transformation
https://doi.org/10.3850/iahr-hic2483430201-15

# Urban Environment and Sustainable Drainage Approach in The Mediterranean Climate Context: Toward Guideline for Pre-Project Assessment

**Erika Llerena Ona[1], Morgan Abily[2], Olivier Delestre[3], Jeremy Targosz[4], Beniamino Russo[5], Jackson Tellez[5], Yannick Mamindy-Pajany[4], Félix Billaud[4]**

[1] CNRS, Université Côte d'Azur, Observatoire de la Côte d'Azur, IRD, Géoazur, Nice, France
[2] Université Côte d'Azur, CNRS, Observatoire de la Côte d'Azur, IRD, Géoazur, Nice, France
[3] Université Côte d'Azur, CNRS, LJAD & Polytech'Lab, Nice, France
[4] Régie Eau d'Azur, Nice, France
[5] Flumen Research Institute, Civil and Environmental Engineering Department, Universitat Politècnica de Catalunya, Barcelona, Spain

*Corresponding author: evllerena.o@gmail.com*

**Abstract.** The growth of urban areas, by stressing water resources and infrastructure management, has promoted the development and spreading of different techniques under the label of sustainable drainage systems approach. These techniques aim to improve infiltration and reduce runoff. The Nice Metropolis (France) has decided to conduct a study to test good practices before implementing such a drainage-favouring approach. An urban pilot area has been selected with the specific challenges of being located within an industrial zone close to an exploited alluvial aquifer. Here, the first stage of this ongoing study is presented where best practices and recommendations assessment has been performed. The review focuses on guidelines and experiences from already implemented solutions under the specifics of Mediterranean climate conditions. In the presented pilot case study, test will be performed with high-resolution runoff and hydrogeological numerical modelling, where the runoff quality and its effect on the underlying water table is of special interest. Based on the pilot study, a methodology is proposed to draw up applied recommendations for municipalities at the pre-project stages on how to (i) have a critical relative comparison of the different categories of drainage favouring solutions, (ii) guide for assessment and proposal of a set of tailored numerical modelling approaches, and (iii) provide recommendations for short, mid and long-term monitoring of the drainage solutions impact. The strategy for the numerical modelling approach selection is also discussed.

**Keywords:** Groundwater, Numerical modelling, Permeable pavements, Runoff, Runoff quality, Sustainable Urban Drainage Systems.

## 1 Context for the study

The 14th Street in the Carros municipality, to the north of Nice city, in the South of France has been chosen as the pilot site to enhance this fully impervious area by implementing techniques that favour runoff drainage. The site poses challenges in two main aspects due to its location: its proximity to the distant protection perimeter of a currently exploited alluvial aquifer and the fact that it is situated within an industrial zone. The study focuses on permeable pavements as the main system to implement in this specific case study. Based on this pilot study, a methodology is proposed for municipalities to evaluate and select drainage solutions at initial project stages, including a comparative analysis of the drainage solutions, guidance for the numerical modelling process and impact monitoring recommendations for different timeframes.

Sustainable drainage alternatives to handle runoff are widely used nowadays. Nevertheless, questions arise regarding how the quality of the infiltrated runoff will affect the underlying groundwater, what

measures can be taken to avoid a negative effect, and how their impact can be monitored once its operation has started.

## 2 Relative Comparison of categories of drainage solutions

A multidimensional matrix has been elaborated to establish a relative comparison between several categories of drainage solutions. The comparison starts by evaluating their physical requirements in terms of surface and depth, bearing in mind the limitations of urban areas. The following assessment regards the ability of the system to improve runoff quality and its potential to recharge groundwater through its treatment capabilities and retention time. Lastly, the next stage takes into account the system operation concerning maintenance needs and monitoring. As a specific for this pilot, the suitability for the Mediterranean climate was also included in the comparison criteria based on already implemented cases [1]. As a result of the solutions screening through the matrix, a selection of the most suitable drainage solutions allows us to consider numerical modelling approach implementation.

## 3 Numerical Modelling Strategies

A catalogue of modelling approaches that could be used to test the different drainage solutions is proposed. The goals for the numerical modelling are, once the selection process has concluded, to evaluate i) runoff quantity and ii) its infiltration impact into the soil due to the implementation of the drainage solution. Regarding the former, a first decision is needed for the type of model to be set. It goes in hand with the input requirements of the future project digital elevation model, rainfall design scenario, and hydraulic parameters described briefly in Table 1. As for the latter, a one-dimensional hydrogeological model is preferred as it has been the most commonly used [2]. The required input data consists of soil and pollutant characterisations, and drainage material properties (Table 1). In both cases, establishing the geometry, boundary and initial conditions is necessary to represent the scenarios aimed to be modelled.

Table 1 Numerical Models Overview.

| | Runoff Model | Hydrogeological Model |
|---|---|---|
| Inputs | Digital Elevation Model (DEM), rainfall design scenarios, future project plans, hydraulic characteristics. | Soil layer characteristics and hydrogeological properties, water table level variation scenarios, categories of pollutants. |
| Modelling approach | Conceptual hydrological model, Diffusive wave approximation, 2D Shallow Water Equations. | Unsaturated zone (Richards Equation, Simplified gravity flow …); Saturated Zone (Darcy Equation); Combination of both. |
| Typical Modelling software | HEC-HMS, MIKE SHE, Iber, MIKE 21, TELEMAC. | MODFLOW, FEFLOW. |

The generalization of this approach aims to produce guidelines for practical modelling strategies for the different categories of drainage solutions.

## Reference

[1] A. I. Abellán García, N. Cruz Pérez, and J. C. Santamarta, ‘Sustainable Urban Drainage Systems in Spain: Analysis of the Research on SUDS Based on Climatology’, *Sustainability*, vol. 13, no. 13, p. 7258, Jun. 2021, doi: 10.3390/su13137258.

[2] D. Tedoldi, G. Chebbo, D. Pierlot, Y. Kovacs, and M.-C. Gromaire, ‘Impact of runoff infiltration on contaminant accumulation and transport in the soil/filter media of Sustainable Urban Drainage Systems: A literature review’, *Science of The Total Environment*, vol. 569–570, pp. 904–926, Nov. 2016, doi: 10.1016/j.scitotenv.2016.04.215.

**Theme:** Technologies for water management and monitoring
**IAHR Thematic Priority Area:** [TPA-4] Digital Transformation
https://doi.org/10.3850/iahr-hic2483430201-17

# Utilizing AQUARIUS as Water Resource Management Software: A Decision Support Tool in the Operational Area of Jasa Tirta I State-Owned Enterprise, Indonesia

**Rasyid Muhammad Amirul Muttaqin[1], Astria Nugrahany[1], Heddy Bramantya[1]**

[1] Jasa Tirta [1] State-Owned Enterprise, Malang 65145, Indonesia

*Corresponding author: rasyid@jasatirta1.net, astria@jasatirta1.net, heddybramantya@jasatirta1.net*

**Abstract.** Perusahaan Umum Jasa Tirta I (PJT-I) is a State-Owned Enterprise in Indonesia that focuses on Water Resources Management. In conducting its business processes, PJT-I is highly influenced by hydroclimatic conditions, water availability, river basin conditions, and water quality. Therefore, the operational activities of PJT-I heavily rely on accurate data and information related to water resources. PJT I has implemented the AQUARIUS software modules (Connect, Time-Series, Forecast, and WebPortal) as a decision support tool to provide timely and reliable data for decision-makers. AQ Connect module is responsible for managing the automatic extraction of time-series data from external sources. AQ Time-Series system is the core of AQUARIUS, serving as the primary platform for managing water resource data. AQUARIUS Forecast, as a flexible modelling environment, is specifically designed for river system modelling, processing, and time-series simulation. Finally, AQUARIUS WebPortal is a browser-based information and data presentation system. The implementation of AQUARIUS currently provides real-time information on 16 parameters of water resource from a total of 324 sensors and observations managed by PJT-I. Thus, the implementation of AQUARIUS has improved the effectiveness and efficiency of water resource management by PJT-I overall.

**Keywords:** AQUARIUS Software, Decision Support Tool, Real-Time Information, Water Resource Management

## 1 Introduction

PJT-I currently manages and utilizes water resources in five river basins under the jurisdiction of the Public Works and Housing Ministry. In conducting its business processes, PJT-I is highly influenced by hydroclimatic conditions, water availability, river basin conditions, and water quality. Therefore, the operational activities of PJT-I heavily rely on accurate data and information related to water resources. It is crucial for PJT-I to have the capability to access, analyze, and manage accurate and timely information to enhance the efficiency of water resource management. Hence, the company has implemented the AQUARIUS software as a decision support tool. The four main modules of AQUARIUS—Connect, Time-Series, Forecast, and WebPortal—are integrated into PJT-I to provide timely and reliable data for decision-makers.

## 2 AQUARIUS Software Modules

Aquarius is a comprehensive water resource management software designed to enhance the value of water-related data [1]. With Aquarius, users can easily acquire, process, model, and publish information in real-time. One of its main features is the ability to access data from various sources in real-time. Additionally, Aquarius facilitates analysis tasks by providing tools to visualize, scan, and ensure quality assurance/control (QA/QC) of data using rating curves, automated error detection, and intuitive correction tools. This ensures a maintainable audit trail and enables users to efficiently

compare time-series or discrete data. Furthermore, Aquarius offers graphical information and contextual visualization functions, allowing users to forecast and convey technical and non-technical information in real-time. These features empower users to make faster and more accurate decisions regarding water resource management.

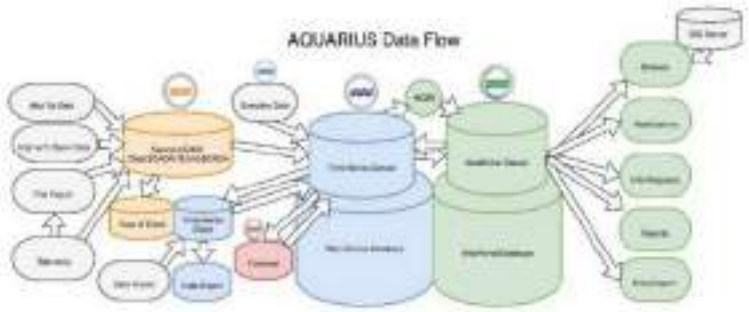


Figure 2 AQUARIUS data flow to acquire, process, model, and publish water information in real time.

### 2.1 AQUARIUS Connect

The AQ Connect module is responsible for managing the automatic extraction of time-series data from external sources.

### 2.2 AQUARIUS Time-Series

Meanwhile, the AQ Time-Series system is the core of AQUARIUS, serving as the primary platform for managing water resource data, including quantity and quality data, as well as meteorological information and other sensors. This system includes components such as the Time-Series Server, Database, Springboard, and Tools that work together to handle time-series data corrections without affecting raw data, the development of rating curves, derivation, and automatic data computation, as well as the production workflow and data publication from various data sources.

### 2.3 AQUARIUS Forecast

AQUARIUS Forecast, as a flexible modeling environment, is specifically designed for river system modeling, processing, and time-series simulation. This module can incorporate complex operational rules into the model, replicating specific operational requirements such as reservoir rules, environmental releases, and water allocation.

### 2.4 AQUARIUS WebPortal

Finally, AQUARIUS WebPortal is a browser-based information and data presentation system that integrates various aspects of data collection, data storage, reporting, data computation, and data management, providing an efficient real-time information display. With this implementation, PJT-I can be more effective and efficient in managing water resources, enhancing the overall performance of the company.

## 3 Summary and Conclusion

The implementation of AQUARIUS currently provides real-time information on 16 parameters of water resource from a total of 324 sensors and observations managed by PJT-I. Graphical customization of all observation data and its derivatives serves as a decision support tool. Real-time alert notifications from forecasts and monitoring of parameter conditions prepare PJT-I to handle disaster actions. Thus, the implementation of AQUARIUS has improved the effectiveness and efficiency of water resource management by PJT-I overall.

## Reference

[1] Aquatic Informatics Inc., 2009. Aquarius HydrologicWorkstation Software. 200–322 Water St., Vancouver, B.C. V6B 1B6, Canada. info@aquaticinformatics.com.

**Theme:** Technologies for water management and monitoring
**IAHR Thematic Priority Area:** [TPA-4] Digital Transformation
https://doi.org/10.3850/iahr-hic2483430201-19

# A Hybrid Approach Integrating CE-QUAL-W2 with Neural Network-Based Boundary Condition Prediction in Soyang Reservoir, Republic of Korea

**Sungjin Kim[1], Sewoong Chung[1]**

[1] Chungbuk national university [1], Chungdae-ro, Seowon-gu, Cheongju-si, Chungcheongbuk-do, Republic of Korea

*Corresponding author: schung@chungbuk.ac.kr*

**Abstract.** Mechanical models (MM), like CE-QUAL-W2 (W2), are pivotal for addressing water pollution issues and informing water management policies [1]. However, uncertainties, such as model parameters and input data, challenge their reliability [2]. This study introduces a novel hybrid model integrating W2 with various boundary condition prediction models to enhance turbidity predictions in Soyang Reservoir. W2 was calibrated using real-time turbidity data collected at the Soyang Dam from January to December 2020. Nine machine learning models, hydrological simulation program Fortran (HSPF), and load estimator (LOADEST) were employed for boundary condition prediction. Korea Water Resources Corporation (K-water) provided field data for training and testing, with flow rate and rainfall data used to predict inflow turbidity. Among the models, the neural network demonstrated superior performance compared to HSPF, linear regression, and decision tree models. The Long short-term memory (LSTM) model emerged as the most effective in predicting inflow turbidity. When applied as boundary condition data for W2, the LSTM model significantly improved turbidity predictions compared to existing linear regression equations.This study underscores the potential of neural network-based deep learning models to enhance MM performance in cases of insufficient boundary condition data, ultimately improving the accuracy of predictions and model reliability.

**Keywords:** CE-QUAL-W2, Data driven model, Hybrid model, Soyang Reservoir, Turbidity

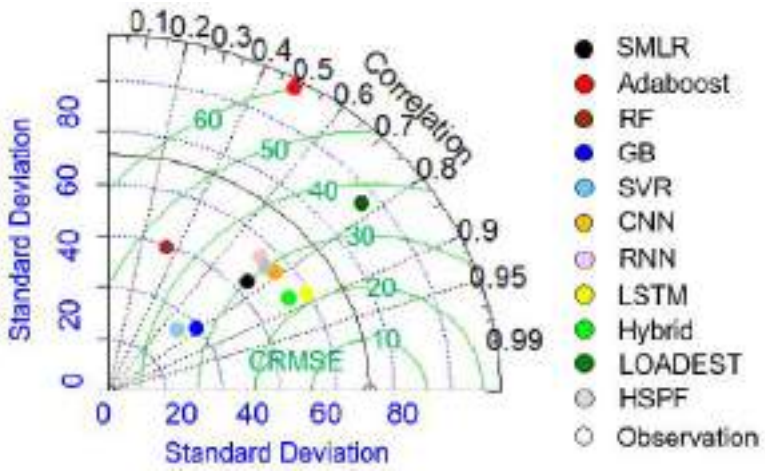


Figure 3 Comparison of turbidity simulation performance of each model using Taylor diagram (CRMSE : centered root mean square error)

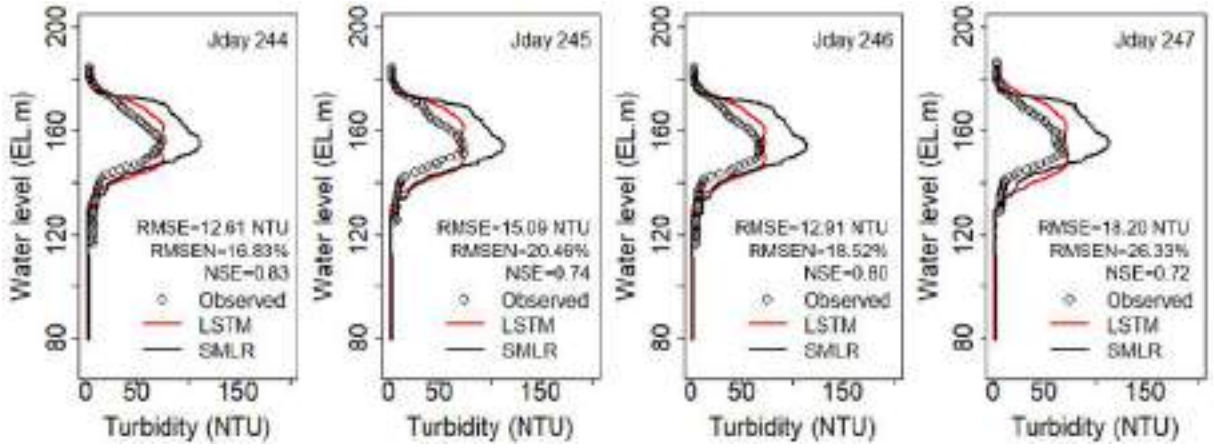


Figure 2 Comparison of observed turbidity profiles with simulated results using CE-QUAL-W2 at monitoring station

Table 2 Comparison of water temperature prediction performance of single point based inflow SS boundary conditions data production models during training and testing period

| Model | Training (2016~2019) | | | Testing (2020) | | |
|---|---|---|---|---|---|---|
| | RMSE (NTU) | NSE | Adj.$R^2$ | RMSE (NTU) | NSE | Adj.$R^2$ |
| SMLR | 30.131 | 0.115 | 0.580 | 33.118 | 0.128 | 0.555 |
| Adaboost | 75.225 | 0.128 | 0.285 | 74.265 | 0.167 | 0.228 |
| RF | 53.324 | 0.119 | 0.287 | 47.119 | 0.375 | 0.105 |
| GB | 41.112 | 0.296 | 0.714 | 35.343 | 0.058 | 0.521 |
| SVR | 42.071 | 0.295 | 0.346 | 38.369 | 0.395 | 0.336 |
| CNN | 30.375 | 0.488 | 0.773 | 30.186 | 0.294 | 0.566 |
| RNN | 32.841 | 0.471 | 0.748 | 33.348 | 0.235 | 0.502 |
| LSTM | 26.248 | 0.716 | 0.865 | 24.732 | 0.558 | 0.710 |
| Hybrid | 24.118 | 0.753 | 0.853 | 26.013 | 0.491 | 0.689 |
| LOADEST | - | - | - | 37.325 | 0.568 | 0.600 |
| HSPF | - | - | - | 30.577 | 0.282 | 0.563 |

**Acknowledgement:** This work was supported by the Korea Environmental Industry & Technology Institute (KEITI) through the Aquatic Ecosystem Conservation Research Program, funded by Korea Ministry of Environment (MOE) (Grant number 2021003030004).

**Reference**

[1] Schuwirth, N., Borgwardt, F., Domisch, S., Friedrichs-Manthely, M., Kattwinkel, M., Kneis, D., Kuemmerlen, M., Langhans, S. D., Marinez-Lopez, J., Vermeiren, P, How to make ecological models use ful for environemental management, Ecological Modelling, 2019, 411, pp. 1-11.

[2] Arhonditsis, G. B., Neumann, A., Shimoda, Y., Kim, D. K., Dong, F., Onandia, G., Yang, C., Javed A., Brady, M., Vish, A., Ni, F., Cheng, V, Castles built on sand or predictive limnology in action? Part A: Evaluation of an integrated modelling framework to guided adaptive management implementation in Lake Erie, Ecological Informatics, 2019, 53, pp. 1-26.

**Theme:** Technologies for water management and monitoring
**IAHR Thematic Priority Area:** [TPA-4] Digital Transformation
https://doi.org/10.3850/iahr-hic2483430201-21

# A Field Study of Pipe Condition Assessment Using Hydro-Acoustic Noise

**Wei Zeng[1]*, Si Tran Nguyen Nguyen[1], Martin Lambert[1] and Jinzhe Gong[2]**

[1] School of Architecture and Civil Engineering, University of Adelaide, SA 5005, Australia
[2] School of Engineering, Deakin University, Geelong Waurn Ponds Campus, VIC 3216, Australia

*Corresponding author: w.zeng@adelaide.edu.au*

**Abstract.** Condition assessment of water transmission pipelines is of important necessity for prioritizing rehabilitation. This paper outlines a pilot field study of the non-invasive and non-destructive condition assessment using hydroacoustic noise. The hydroacoustic noise was generated at a discharge valve due to the turbulence of the discharge, and it was measured by pressure transducers at some access points (e.g., air valves) along the field pipe. A signal deconvolution process was then applied to transfer the hydroacoustic noise to a compositional impulse response function (IRF) which is composed of IRFs of different pipe sections. From the field study, it shows hydroacoustic noise can replace traditional hydraulic transient waves for pipe condition assessment.

**Keywords:** Pipe condition assessment, hydroacoustic waves, impulse response, hydraulic transient.

## 1 Introduction

Hydraulic transient based methods have been developed for condition assessment of water transmission pipelines. Typically, hydraulic transient pressure waves can be generated by sharply operating a side discharge valve. The transient pressure including the incident wave and the transient reflections will be collected and analysed to identify anomalies, such as leaks [1], pipe wall deterioration and corrosion [2]. However, the sensitivity and spatial resolution of transient-based techniques are limited. To address this issue, hydroacoustic wave was used in this paper to replace hydraulic transient waves. The research reported a field study using hydroacoustic noise and a signal deconvolution process to identify some impedance changes in a transmission pipe.

## 2 Field experiments

Field work has been undertaken on a regional AC transmission main as shown in Figure 1. The pipeline runs for over 9 km from a T-junction with a 375 DICL pipe. The water storage tank at the other end was isolated from the system by closing the inline valve at the entrance of the tank. The pipeline has several material and diameter changes with details shown in the schematic. GPS coordinates were gathered during the tests and were used to determine the chainages of the testing points as shown in Figure 1.

Hydroacoustic noise was generated at the generation point (G) and was measured at the measurement points (M1 and M2) as shown in Figure 1. At the generation point, a check valve based transient generator and a pressure transducer were installed on the standpipe that is connected with the pipe main. At the measurement point, a single pressure transducer was installed. The sampling frequency of the DAQ system for measuring pressure data was 2kHz. Each DAQ system contains a GPS unit for time synchronization.

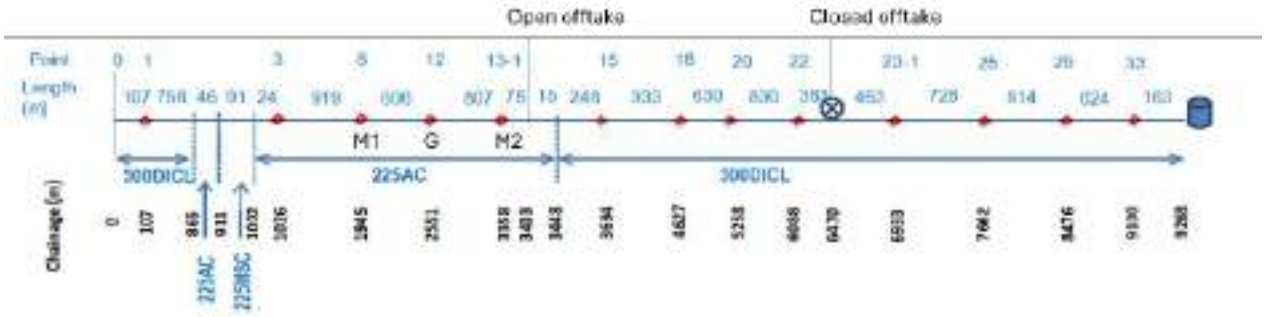


Figure 1. Layout of the field pipe system.

## 3 Methodology and results

The pressure measurements (in the frequency domain) at the generation point and the measurement points are defined as , and . The deconvolution between the pressure at the measurement points and the pressure at the generation point will lead to a combination of IRFs of the pipe system at different regions. By taking the deconvolution between and as an example, the deconvolution can be written as

$$\frac{P_2}{P_G} = H_2(1 - R_R + R_{R2}) \quad (1)$$

where where $H_2$ is the transfer function between G and M2, $R_R$ is the IRF (in the frequency domain) of the pipe at the right side of G, and $R_{R2}$ is the IRF of the pipe at the right side of M2.

The signal deconvolution between $P_1$ and $P_G$ (defined as $IRF_1$) and the pressure deconvolution between $P_2$ and $P_G$ (defined as $IRF_2$) can be then obtained as shown in Figure 2.

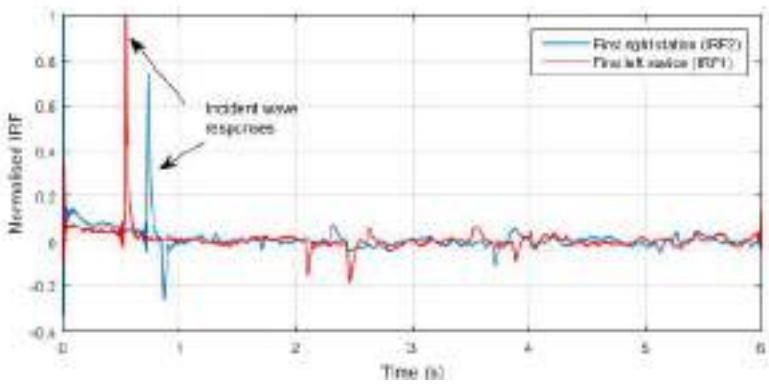


Figure 2. Normalised IRFs obtained from signal deconvolution.

The peak responses in IRF1 and IRF2 indicate the incident waves that propagate from the generation point to the measurement points. The occurring times of these spikes, = 0.528 s and = 0.714 s, correspond to the time take for the wave to travel from PG to P1 and P2, respectively. Other spikes in the IRF trace as shown in Figure 2 are associated with some impedance changes as shown in Figure 1. Thus, the results show that the IRFs obtained from the hydroacoustic noise can successfully identify the changes in this field water pipe.

## Reference

[1] X. Wang, J. Lin, A. Keramat, M. S. Ghidaoui, S. Meniconi, and B. Brunone, "Matched-field processing for leak localization in a viscoelastic pipe: An experimental study," *Mechanical Systems and Signal Processing*, vol. 124, no. 6, pp. 459-478, 2019/06/01/ 2019.

[2] W. Zeng, J. Z. Gong, A. C. Zecchin, M. F. Lambert, A. R. Simpson, and B. S. Cazzolato, "Condition Assessment of Water Pipelines Using a Modified Layer-Peeling Method," (in English), *J. Hydraulic Eng.*, vol. 144, no. 12, p. 04018076, Dec 2018, doi: 04018076.

**Theme:** Technologies for water management and monitoring
**IAHR Thematic Priority Area:** [TPA-4] Digital Transformation
https://doi.org/10.3850/iahr-hic2483430201-23

# Increasing The Performance of The Water Meter Test for Reducing Apparent Loss and Gaining High Productivity with Less Time

**Teepagorn Chaladtanyakij[1], Chayanon Choongpon[2], Peerapong Choopum[3], Phongphanu Srisomsong[4], Jittawat Kunanusont[5], A-phiwat Kaeophaithun[6], Pisit Kitnarumit[7]**

[1-7] Water Meter Department, Metropolitan Waterworks Authority,
72 Latyao Chatuchak, Bangkok 10900, Thailand

*Corresponding author: teepagorn.ck@gmail.com*

**Abstract.** Metropolitan Waterworks Authority (MWA) in Thailand has faced water loss termed apparent loss owing to inaccuracy of the mechanical water meter. Hence, the MWA's master plan is indicated to solve this problem leading to reducing apparent loss approximately 2.4 and 3.7 million cubic meters in year 2020 and 2021 respectively by employing the electronic water meter and meter size reduction. However, this project focuses on the electronic water meter. Then, the accuracy test for the electronic water meter needs providing. From the past to present, this test for the mechanical water meter has been operated by the volumetric method. By using this method, the electronic water meter takes a long time in the accuracy test. Accordingly, two new test systems, employed the weighing (DN15-40) and master meter [Coriolis-mass-flow meter] (DN50-300) methods, can save time 49.4 to 63.8% leading to at least two times productivities. In doing so, as a standard service laboratory of the government sector, revenue around 45,000 USD per year can be received. In summary, the weighing and master-meter methods for the accuracy test can save time 49.4 to 63.8%, gaining at least two times productivities, indirectly reducing apparent loss and earning revenue around 45,000 USD a year.

**Keywords:** Apparent Loss, Electronic Water Meter, Master Meter Method, Weighing Method

## 1 Introduction

In accordance with the water loss termed apparent loss due to the inaccuracy of the mechanical water meter, Metropolitan Waterworks Authority (MWA) in Thailand has a plan roadmap to continuously solve this obstacle by both reducing the oversized meter and utilizing the electronic water meter instead of some mechanical water meters. As a consequence, the result of reducing apparent loss was approximately 2.4 and 3.7 million cubic meters in year 2020 and 2021 respectively. Nonetheless, this work focuses on the usage of the electronic water meter. Accordingly, the new accuracy test system needs providing for the electronic water meter because the old test system, employed the volumetric method, spends a long time when being utilized with the electronic water meter.

## 2 Material and Methods

In accordance with OIML R49 and ISO 4064, prior to installing any water meter, all water meters need to be passed the accuracy test as indicated in the initial verification by varying at least three flow rates comprising minimum flow rate ($Q_1$), transitional flow rate ($Q_2$) and permanent flow rate ($Q_3$). Moreover, from the standard mentioned above of the water meter having class 2, the maximum permissible error (MPE) is limited within ± 5% in the lower flow rate ($Q_1 \leq Q < Q_2$) and ± 2% in the upper flow rate ($Q_2 \leq Q \leq Q_3$). Then, there is a formula to calculate the percentage of relative error of the tested water meter comparing to the reference as presented in the equation (1).

$$\text{Relative Error (\%)} = \frac{Vi - Va}{Va} \quad (1)$$

**Relative Error (%)** = error of the tested water meter (or unit under test) comparing to the reference

$\mathbf{V_i}$ = indicated volume reading from the display of the tested water meter (or unit under test)
$\mathbf{V_a}$ = actual volume coming from the reference
At MWA's flow measurement laboratory, the accuracy test system having been operated employs the volumetric method (the prover tank). In case of the mechanical water meter having a short measuring range or a high value of minimum flow rate ($Q_1$), the accuracy test by the volumetric method takes a normal time. However, the drawback of this method is to spend very long time for the electronic water meter. Consequently, the entire productivities are certainly decreased. To solve this obstacle, two new test systems for the electronic water meter are utilized by virtue of the weighing (DN15 - 40) and master meter [Coriolis mass flow meter] (DN50 - 300) methods. In detail, ISO 4185 is employed for the weighing method.

## 3 Results and Discussion

The data is obviously plotted in form of graph represented in Figure 1 below.

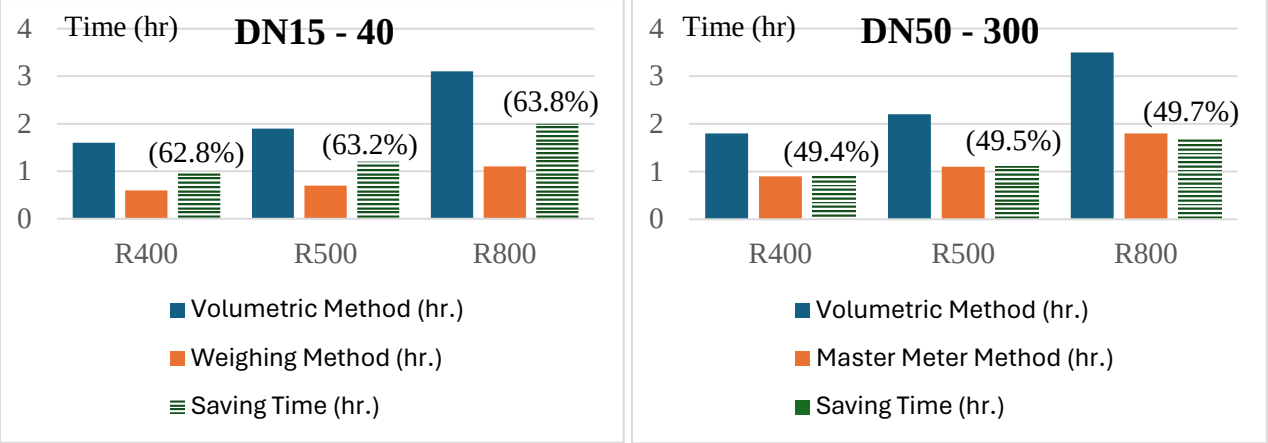


Figure 1. The comparison of tested time

It can be clearly explained form Figure 1 that when operating the accuracy test of the electronic water meter sized DN15 – 300 with low to high measuring ranges (R400 - 800) by virtue of volumetric method, the average tested time is 2.4 hours. In contrast, the average tested time of two new test systems comprising the weighing and master meter method is reduced to 1 hour. Therefore, the processed change in MWA can save time averagely 1.4 hour or 56.0%. In doing so, at least two times productivities can be earned.

As a result of doing this, it can be stated that when the electronic water meter has been widely and abruptly used because of the rapidity of the accuracy test, the apparent loss in MWA has been meaningfully declined. Additionally, both new methods of the accuracy test can be efficiently performed with the MWA's meter and the meter of the other sectors hiring MWA to do the accuracy test. In doing so, as a standard laboratory of the government sector, revenue around 45,000 USD per year can be received.

## 4 Conclusions

In summary, thanks to the weighing (DN15 - 40) and master meter (DN50 - 300) methods for the accuracy test of the electronic water meter mentioned above, it can save working time approximately 49.4 to 63.8%, gain at least two times productivities, reduce indirectly the apparent loss and earn revenue around 45,000 USD a year.

## 5 Acknowledgments

This work is completely subsidized by Metropolitan Waterworks Authority (MWA) in Thailand.

## References

[1] ISO 4064-1:2014, Water meters for cold potable water and hot water - Part 1: Metrological and technical requirements
[2] ISO 4064-1:2014, Water meters for cold potable water and hot water - Part 2: Test methods
[3] OIML R49-1:2013, Water meters for cold potable water and hot water - Part 1: Metrological and technical requirements
[4] OIML R49-2, Water meters for cold potable water and hot water - Part 2: Test methods
[5] ISO 4185, Measurement of liquid flow in closed conduits - Weighing method
[6] Metropolitan Waterworks Authority Enterprise Plan Roadmap

**Theme:** Technologies for water management and monitoring
**IAHR Thematic Priority Area:** [TPA-4] Digital Transformation
https://doi.org/10.3850/iahr-hic2483430201-26

# Experimental Evaluation of a Pressure Transient Source Localization Method in An Operational Water Distribution Network

**Carlos Jara-Arriagada[1] and Ivan Stoianov[1]**

[1] InfraSense Labs, Department of Civil and Environmental Engineering, Imperial College London, London, SW7 2AZ, UK

*Corresponding author: cij18@imperial.ac.uk*

**Abstract.** The increasing implementation of pressure control schemes in water distribution networks requires a continuous monitoring and localization of hydraulic instabilities or pressure transients. To locate these sources, we previously introduced a new method that considers the uncertainty in network connectivity. The method was formulated and tested with simulated transient data but it did not undergo empirical validation. In this study, our objective is to validate the effectiveness of the proposed method using a distinct dataset of hydraulic data from an operational network. We have tested the performance of the method under multiple recurring transient events generated by an industrial user. Our analysis showed that, despite the multiple uncertainties typical of operational networks, the method produced consistent results, with an average error of approximately 45 m. We also examined how the removal of sensors impacted the accuracy of the results. Our findings indicate that, in the current case study, the method remains reliable with as few as five pressure sensors. These results reconfirm the method's suitability for operational networks, enabling continuous and autonomous localization of sources of pressure transients, and improving the accuracy of hydraulic models' connectivity.

**Keywords:** High-resolution pressure sensing, pressure transients, source localization, urban water systems management, water network monitoring, water supply networks

## 1 Introduction

Accurately localizing the sources of pressure transients is essential for managing and mitigating their damaging impact in water distribution networks (WDNs). Recently, we introduced a novel pressure transient source localization method in [1]. The method includes a novel optimization problem formulation that accounts for uncertainties in network connectivity such as pipe blockages by analysing multiple wave propagation paths using the k-shortest path routing problem [1]. Additionally, a heuristic to handle uncertainties in wave arrival times was also implemented [1]. The method has been evaluated using simulated data from hydraulic pressure transient models [1]. However, to confirm its application and practical effectiveness, an evaluation with real experimental data is needed. This manuscript fills this gap by evaluating the method with high-resolution pressure data acquired from a WDN in the UK where a recurrent presence of pressure transients is observed.

## 2 Material and Methods

The acquired data included high-resolution water pressure time series from a total of six time-synchronised pressure sensors installed in a WDN. The method was firstly applied to a well-defined transient pressure event recorded after midnight as a first trial. We then utilized multiple pressure transients observed during the monitoring period to assess the consistency of the results and distribution of errors. Finally, the effect of removing sensors in the network was examined.

## 3 Results

The results showed that the method accurately identified the transient source in the initial trial test. We also observed that the method consistently produced reliable results for different times of the day

when pressure transients occurred. The distribution of errors in the results showed a mean error of 44.7 m, with a standard deviation of 19.98 m, from a total of 93 transient events analysed. The analysis for the number of sensors has indicated that the method can still be reliable in locating close solutions to the true transient source if a minimum number of 5 sensors is used.

## 4 Discussion

The method for pressure transient source localization have shown to be reliable for locating transient pressure, and to detect irregularities in hydraulic connectivity. The maximum errors in localization are within an acceptable range, so that a water utility can determine a search area to look for a typical transient source in water distribution networks.

The method for pressure transient source localization involves using the k-shortest path routing algorithm to identify potential paths for pressure waves to reach sensors. Deviations from the shortest path indicate discrepancies in the hydraulic model. In this case study, the method mostly selected the shortest path for all sensors except one, suggesting uncertainty. An analysis of potential errors in the determination of wave travel times and in the hydraulic model suggested two potential main reasons for the selection of an alternative shortest path by the method. One reason suggests potential wrong allocation of material properties in the pipes. Alternatively, closed valves could divert the pressure wave. This uncertainty underscores the need for accurate data on pipe materials and valve statuses for effective pressure transient source localization.

## 5 Conclusions

This manuscript has sought to validate the performance of the pressure transient source localization method presented in [1] using a unique dataset from a real operational WDN. The results of this work showed that the method can reliably locate a transient source solution close to the true source of transient events. We performed a series of tests using multiple real transient events to confirm the consistency of the results. We observed that even under uncertainties in wave arrival times, the distribution of errors in results show reasonable distances from the true source. In addition, a preliminary analysis for the influence of the number of sensors has shown that the method for this case study was able to perform well even with 5 sensors. It is still possible to use 4 and 3 sensors, but the spread of errors increases considerable. A current limitation of the method is that it only locates a unique point in the network to be a transient source. This limitation can be addressed by using the information of the shortest paths selected by the algorithm in combination with a scoring algorithm such as the one proposed in [2]. By implementing this combination of methods, a search area can be obtained. Accurate and updated information of pipe materials can be critical for the performance of this method. Further research should look into the implementation of this method within a global framework for monitoring and condition assessment of water distribution networks. Additionally, improvements in the formulation and speed of computation of the method should be sought.

## 6 Acknowledgements

This work was funded by the National Agency for Research and Development (ANID)/Scholarship Program/DOCTORADO BECAS CHILE/2020–72210314; and the Royal Academy of Engineering Senior Research Fellow in Dynamically Adaptive Water Supply Networks (RCSRF2324-17-41)

## Reference

[1] C. Jara-Arriagada, A.-J. Ulusoy, and I. Stoianov, “Localization of Transient Pressure Sources in Water Supply Networks with Connectivity Uncertainty,” J Water Resour Plan Manag, vol. 150, no. 4, Apr. 2024, doi003A 10.1061/JWRMD5.WRENG-6235.

[2] S. Srirangarajan, M. Allen, A. Preis, M. Iqbal, H. B. Lim, and A. J. Whittle, “Wavelet-based burst event detection and localization in water distribution systems,” J Signal Process Syst, vol. 72, no. 1, pp. 1–16, Jul. 2013, doi: 10.1007/s11265-012-0690-6.

**Theme:** Technologies for water management and monitoring
**IAHR Thematic Priority Area:** [TPA-4] Digital Transformation
https://doi.org/10.3850/iahr-hic2483430201-28

# Prediction of Residual Chlorine Concentration using Machine Learning Algorithms for Water Quality Control in AI Water Treatment Plant

**Juhwan Kim[1*], Jinwoo Song[2], Seungmin Lee[3] and Soojin Kim[4]**

[1] Department of Civil Engr., Inha University, Incheon, 22212, South Korea
[2] Jemulpo Renaissance Planning Div., Incheon City, Incheon, 21554, South Korea
[3] Program in Smart City Engr., Inha University, Incheon, 22212, South Korea
[4] Department of Civil Engr., Inha University, Incheon, 22212, South Korea

*Corresponding author: juhwan Kim@juhwan@inha.ac.kr*

**Abstract.** Machine learning models are developed to stabilize the residual chlorine concentration of the outflow section from the sedimentation basin for the purpose of real-time monitoring of water quantity and quality data and intelligent control of the chlorination process in water treatment plant (WTP). Multiple regression model, artificial neural network, and random forest among artificial intelligence algorithms were used to predict the residual chlorine concentration in the outflow section of the sedimentation pond of the B Water purification plant, and the results were compared and analyzed. Residual chlorine concentration in the sedimentation basin, water temperature, turbidity, pH, electrical conductivity, inflow volume, and alkalinity data are collected and used as input variables, and residual chlorine concentration in settling basin as output variable. These results showed that the random forest model made the most accurate predictions for the B WTP. The mathematical model, multiple regression, performed the worst in terms of goodness of fit. The results can be shown due to the difference in scale and dimensionality of water quantity and quality data and the variability of chlorine input due to seasonal water quality changes. As results, it is concluded that a decision tree-based model such as a random forest is suitable for the application of artificial intelligence algorithms in the B WTP. Based on the results from this study, it is expected that the residual chlorine concentration in the outflow section of the sedimentation basin can be maintained consistently by adjusting the chlorine injection in real time in the B WTP.

**Keywords:** Machine learning, Residual chlorine concentration, Water treatment plant

## 1 Introduction

In the process of water treatment facilities for water supply, control technology is needed to improve efficiency, such as injection of chemicals necessary for water quality management and operation. Water quality management technology for treatment plants is being promoted to develop artificial intelligence (AI) based control technology for some unit processes such as coagulation and filtration processes or ozone, but the intelligence of the entire process is still in the introductory stage. Due to the recent occurrence of rust or chironomus larva in tap water, the government aims to establish a smart system that can identify all processes from water intake to water facilities in real time and automatically respond to the accidents.

## 2 Methods

The AI based prediction model has a simple input and output of water quality data and can predict water quality using collected data without considering physical, chemical, and biological processes. Based on these preceding studies, this study aims to improve the operation and management of existing water treatment processes by developing a methodology that predicts residual chlorine and automatically controls the amount of chemicals input, through various AI algorithms. In this study,

among them, RF, LSTM and multiple regression model were used and analysed and compared. The structure of the AI algorithm performed in the previous study was specified and supplemented, and an optimal residual chlorine prediction model was developed by applying a genetic algorithm as an optimization methodology for parameters. AI based models such as RF and LSTM and mathematical Multi-Regression (MR) methods were applied, and the performance was compared and evaluated as shown in Figure 1.

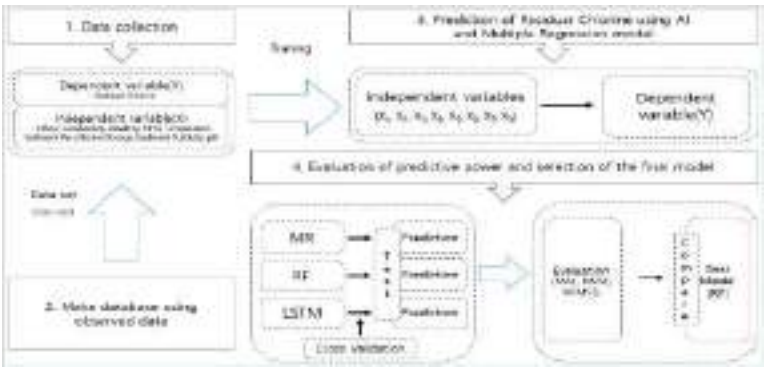


Figure 1. Conceptual diagram of the study.

## 3 Results

As a result of comparison, the random forest-based prediction model showed the best performance. Surprisingly, it was confirmed that the performance of LSTM was the lowest, which is judged to be due to the characteristics of the data. Evaluated performance can be seen in Table 1 and Figure 2.

Table 1. Performance evaluation of application models

| Model | MAE | R-Squard | RMSE | NRMSE | Rank |
|---|---|---|---|---|---|
| Multiple Regression | 0.0966 | 0.6712 | 0.1228 | 0.1224 | 2 |
| Random Forest | 0.0474 | 0.9147 | 0.0629 | 0.0630 | 1 |
| LSTM | 0.1019 | 0.8416 | 0.1230 | 0.1296 | 3 |

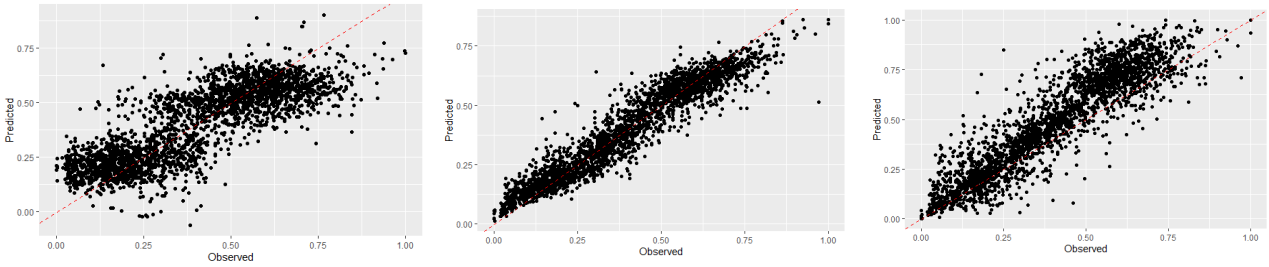


Figure 2. Results comparison between observed and estimated values

## 4 Conclusions

As results of comparing and analyzing several artificial intelligence-based predictive models and multiple regression models in this study, it was presented that the application of RF as like a decision tree structure is the most appropriate when the data distribution is large and the difference in dimension and scale is large, such as water quality data.

## References

[1] Breiman, L. (2001). Random forests. Machine learning, Vol. 45, No. 1, pp. 5-32.

[2] Kim, J.H., Lee, K.H., Kim, S.J., Kim, K.H. (2022). “Machine learning model for residual chlorine prediction in sediment basin to control pre-chlorination in water treatment plant” Journal of Korea Water Resources Association, Vol. 55, No. S-1, pp. 1283-1293.

**Theme:** Technologies for water management and monitoring
**IAHR Thematic Priority Area:** [TPA-4] Digital Transformation
https://doi.org/10.3850/iahr-hic2483430201-30

# Development and Application of an Evaluation Index for Risk Management in Water Distribution Systems

**Dongwoo Jang**[1]

[1] Incheon National University, Academy-ro 119 Yeonsu-gu, Incheon, 22012, Rep. of Korea

*Corresponding author: jdw@inu.ac.kr*

**Abstract.** Recent efforts to maintain efficient water distribution networks have led to the installation of measuring devices for real-time monitoring of flow, water pressure, and water quality factors. Research is being conducted to use this data for accident prediction and efficient maintenance. In this study, water supply factors that influence pipeline risk were identified, and an index for risk assessment was developed by determining the weight of each factor. Through literature review, both domestic and international, key factors included in the risk index calculation were identified, such as pipeline aging assessment, real-time hydraulic and water quality measurements, soil corrosivity, asset management, and water treatment plant quality factors. Within five classification systems, specific sub-factors were selected, and the weight of each factor was determined through a survey of water supply experts. The Analytic Hierarchy Process (AHP) analysis showed that pipeline aging assessment factors, real-time measurement data, water supply asset management, soil corrosivity, and water treatment plant quality factors were the most significant. The water distribution network risk assessment index derived from this study can be used for individual evaluations of each pipeline, district metered area, and administrative region, aiding in prioritizing pipeline replacements and network operations.

**Keywords:** Water distribution network, risk assessment, Analytic Hierarchy Process (AHP), maintenance efficiency

## 1 Introduction

Efficient management of water distribution networks is crucial for ensuring reliable water supply and minimizing service interruptions. Recent advancements in sensor technology have enabled the installation of measuring devices for real-time monitoring of flow, water pressure, and water quality factors within water distribution systems [1,2]. Leveraging this wealth of data presents an opportunity to improve maintenance practices and anticipate potential accidents. This study aims to develop a robust risk assessment index for water distribution networks by identifying key factors influencing pipeline risk and assigning weights to each factor based on expert opinions.

## 2 Methodology

### 2.1 Literature Review

A comprehensive review of existing literature, both domestic and international, was conducted to identify key factors influencing pipeline risk in water distribution networks. Factors included pipeline aging assessment, real-time hydraulic and water quality measurements, soil corrosivity, asset management practices, and water treatment plant quality factors.

### 2.2 Factor Selection

From the literature review, key factors were selected for inclusion in the risk assessment index. These factors were categorized into five classification systems: pipeline aging assessment, real-time measurement data, asset management, soil corrosivity, and water treatment plant quality.

### 2.3 Weight

Determination: A survey was conducted among water supply experts to determine the relative importance of each factor. Experts were asked to assign weights to each factor using the Analytic Hierarchy Process (AHP), considering their expertise and experience in the field.

### 2.4 Index Development

The assigned weights were used to develop a comprehensive risk assessment index for water distribution networks. The index allows for individual evaluations of each pipeline, district metered area, and administrative region, providing insights into prioritizing maintenance activities and optimizing network operations.

## 3 Results and Discussion

The AHP analysis revealed that pipeline aging assessment, real-time measurement data, asset management practices, soil corrosivity, and water treatment plant quality were the most significant factors influencing pipeline risk. These findings emphasize the importance of considering various aspects of network operation and maintenance in risk assessment.

### 3.1 Quantitative Analysis via AHP and Arithmetic Mean Calculation

Using the Analytic Hierarchy Process (AHP), we initially categorized and assessed multiple risk factors based on expert surveys. Subsequently, to refine these assessments, we calculated the arithmetic mean of the weights assigned by individual practitioners to derive the final weights for five main risk assessment categories. These final weights were presented in Table 8.

### 3.2 Final Weight Distribution

The calculated final weights for each risk category are as follows:

Pipeline Aging Assessment: Received the highest weight of 40.5%. This significant weight reflects the consensus among experts regarding the critical impact of aging infrastructure on the overall risk profile of water distribution systems.

Real-time Measurement Data: This category, which includes the real-time monitoring of flow, pressure, and water quality, was assigned a weight of 18.6%. The relatively high weight underscores the importance of timely data in managing and mitigating risks in water distribution.

Water Supply Asset Management: Close in weight to real-time data, asset management practices received a weight of 18.5%. This highlights the critical role of effective asset management in risk reduction, focusing on maintenance schedules and lifecycle management of water distribution assets.

Soil Corrosivity: With a weight of 12.1%, soil corrosivity was identified as a less dominant but still significant factor that affects the integrity and longevity of water pipelines.

Water Treatment Plant Quality Factors: The quality output from water treatment plants was assigned the lowest weight of 10.4%, indicating that while important, it has a lesser immediate impact on pipeline risk compared to other factors.

## 4 Conclusion

This study presents a novel approach to developing a comprehensive risk assessment index for water distribution networks. By integrating key factors and expert opinions, the index provides a valuable tool for water utilities to prioritize maintenance activities, optimize network operations, and enhance overall system reliability. Future research could focus on refining the index through additional data collection and validation studies.

## Reference

[1] Nunes, R., Arraut, E., & Pimentel, M. Risk Assessment Model for the Renewal of Water Distribution Networks: A Practical Approach. Water. 15 (2023) 1–20.

[2] Christodoulou, S., Agathokleous, A., Charalambous, B., & Adamou, A. Proactive, risk-based approach to monitoring the integrity of urban water distribution networks using artificial neural networks and statistical models Water Resources Management.24 (2010) 3715-3730

**Theme:** Technologies for water management and monitoring
**IAHR Thematic Priority Area:** [TPA-4] Digital Transformation
https://doi.org/10.3850/iahr-hic2483430201-33

# Nodes Dominating the Spread of Contaminants in Sewer Networks: A Different Approach to Monitoring

**Antonietta Simone[1], Mariacrocetta Sambito[2]**

[1]Department of Engineering and Geology, University "G. D'Annunzio" of Chieti Pescara, Pescara (Italy)
[2]School of Engineering and Architecture, University of Enna "Kore", Cittadella Universitaria, Enna (Italy)

*[1] 0000-0001-8400-5201, antonietta.simone@unich.it, [2] 0000-0003-4277-8622, mariacrocetta.sambito@unikore.it*

**Abstract.** The release and spread of contaminants into sewer networks are critical topics based on a complex process, whose management is sometimes very complicated due to the connective structure of these systems, which present a high number of potential entry points, thus requiring many analyses to identify the most probable emission areas. The need of defining computationally advantageous sampling designs that carries out the localization of contamination sources and allows the definition of intervention priorities is increasingly pressing.
In order to manage such a situation, it is essential to understand and model dilution and dispersion phenomena of pollutants within the system in light of their connective structure. In this context, the present study proposes a strategy aimed at identifying nodes in sewer networks that have a high diffusion capacity, i.e. those nodes that, once contaminated, are able to propagate the contamination in a significant way due to their topological characteristics. These nodes, due to their strategic position in the network and their proximity to relevant nodes, dominate the contaminant diffusion processes. In fact, although they do not represent the most crossed nodes among all the paths towards the receptor, they represent points from which each contaminant has a greater probability of propagating in the network, and in this sense, they should be constantly monitored.

The strategy is characterized by a two-step procedure which involves to: (i) evaluate the impact that the release of pollutants into a node has on the entire network using the depth-first search method algorithm. This information leads to the creation of a network contamination map; (ii) use a topological approach to define a ranking of importance of the network nodes with respect to their ability to spread information, and therefore pollutants. The contamination area of each node, defined in the previous step, is used as starting information in this analysis phase.

Implementing information on the contamination capacity of each node makes the results of the analysis more effective compared to the selection of topological (e.g., Horton hierarchy) or hydraulic (e.g., lateral inflow) ones. Finally, to validate the performance of the strategy, it is applied to a literature sewer system used as benchmark.

**Theme:** Technologies for water management and monitoring
**IAHR Thematic Priority Area:** [TPA-4] Digital Transformation
https://doi.org/10.3850/iahr-hic2483430201-34

# What Happened on the Water-Sediment Interface for the Microbial-Mediated Cycling of Biogenic Elements under Different HP

**Chai Beibei[1], Li Yumei[1], Zhuo Tianyu[2], Lei Xiaohui[3], Chen Bin[4]**

[1] Hebei University of Engineering
[2] Tianjin University
[3] China Institute of Water Resources and Hydropower Research
[4] Beijing Normal University

*Corresponding author: cbb21@163.com*

**Abstract.** Microorganisms are closely linked to collectively drive the biogeochemical cycles of the Earth. Hydrostatic pressure is an important factor affecting the structure of microbial communities in deep-water reservoir sediments. Simulated microcosm experiments with static hydrostatic pressure as the only variable were conducted. We investigated the impact of four different pressure gradients (0.1 MPa (atmospheric pressure), 0.2 MPa, 0.5 MPa, and 0.7 MPa) on the species composition of microorganisms related to carbon, nitrogen, phosphorus, and sulfur cycling, as well as the abundance of functional genes and metabolic pathways. Results showed that high hydrostatic pressure regulates the expression of *phoD*, *phoA*, *ppk*, *ppx-gppA*, and *pqqC* in bacteria, promoting the transformation of Fe/Al-P into Ca-P and the release of phosphorus in reservoir sediment. Furthermore, high hydrostatic pressure increases the abundance of sulfate reduction genes (*cysD*, *cysC*), while decreasing the abundance of sulfur oxidation genes (*soxB*), leading to an increase in $H_2S$ production from S metabolism. High pressure also increases the participation of microbial carbon cycle species in sediment samples, enhances the abundance of functional genes such as *ALDO*, *ACO*, *sdhA*, and *sdhC*, promoting carbon fixation through the Calvin cycle and the citrate cycle, and inhibiting methane production. In conclusion, the increase in pressure has a significant impact on the Earth's biogeochemical cycles by altering the microbial species and associated functional genes involved in the carbon, nitrogen, phosphorus, and sulfur cycles. The study results offer new insights into the microbial-driven biogeochemical cycles at the sediment-water interface of deep-water reservoirs.

**Keywords:** Reservoir, Hydrostatic pressure, Microorganisms, Biogenic Elements, Functional Genes, In Situ Monitoring and Simulating in Lab

## 1 Introduction

Dam construction can lead to increased retention of nutrient and organic loads in reservoir sediments, which may exhibit more active potential of phosphorous (P) mineralisation and exchange at the sediment–water interface (SWI)[1].Unlike shallow-water ecosystems, deep reservoirs (water depth >50 m) have unique P sources, cycling processes and eco-environmental effects owing to artificial control of water levels and associated changes in hydrostatic pressure [2].An in situ study showed that among various environmental factors (e.g., dissolved oxygen, pressure, pH, total nitrogen), hydrostatic pressure was the primary factor shaping the structure of sediment microbial communities in deep-water reservoirs [3]. The study aimed to investigate how hydrostatic pressure influences microbial biogenic element pathways at the sediment-water interface (SWI) in large-scale deep-water reservoirs. It hypothesized that pressure affects microbial communities, functional genes, and metabolic pathways, thus driving organic matter conversion. To test this, a microcosm experiment simulated four pressure levels at the SWI using sediment and water from a large drinking water reservoir. Changes in microbial species composition, functional gene abundance, and carbon cycling metabolic pathways were analyzed under varying pressure levels.

## 2 Materials and methods

The study conducted field and laboratory experiments to investigate microbial activities and nutrient dynamics in sediment and water samples collected from Jinpen Reservoir in Shaanxi Province, China. Sediment and water samples were analyzed for physicochemical properties, and a subset of sediment samples was treated with NaN3 to inhibit microbial activity, serving as a control. The hydrostatic pressure simulation experiment involved four pressure levels, including atmospheric pressure, mimicking different depths in the reservoir. Various analyses, including DGT measurements of labile Fe, P, and S in sediments, DNA extraction and metagenomic shotgun sequencing, and non-targeted metabolomic analysis, were conducted.

## 3 Results and discussion

Results showed that high hydrostatic pressure regulates the expression of phoD, phoA, ppk, ppx-gppA, and pqqC in bacteria, promoting the transformation of Fe/Al-P into Ca-P and the release of phosphorus in reservoir sediment. Furthermore, high hydrostatic pressure increases the abundance of sulfate reduction genes (cysD, cysC), while decreasing the abundance of sulfur oxidation genes (soxB), leading to an increase in H2S production from S metabolism. High pressure also increases the participation of microbial carbon cycle species in sediment samples, enhances the abundance of functional genes such as ALDO, ACO, sdhA, and sdhC, promoting carbon fixation through the Calvin cycle and the citrate cycle, and inhibiting methane production. High hydrostatic pressure initially increases and then decreases the number of species involved in the nitrogen cycle, enhancing the abundance of functional genes, and the abundance of microorganisms involved in this pathway. In addition, high hydrostatic pressure affects the distribution of microplastics in sediments, driving the microbial degradation of plastics at the functional gene level, leading to a reduction in the size of microplastics and their transformation from fragmented pieces into smaller particles.

## 4 Conclusions

This study found that micro-pressure accelerated phosphate (Po) mineralization to phosphate (Pi) in deep reservoir surface sediments, enhancing microbial functions associated with phosphorus (P) mineralization, P solubilization, and sulfate reduction while inhibiting sulfur oxidation. Increased hydrogen sulfide ($H_2S$) production from microbial sulfur metabolism led to FeS precipitation, reducing P binding sites and releasing P. High pressure stabilized sediment microbial communities, promoting carbon-fixing bacteria like Proteobacteria, Chloroflexi, and Actinobacteria, along with piezophilic taxa mainly in Proteobacteria. Elevated pressure increased functional gene abundances related to carbon fixation and methane metabolism. Different pressure conditions showed similar microbial community composition but significant differences in connectivity and piezotolerant genes, primarily within Proteobacteria. High pressure promoted denitrification-related functional genes and certain microbial taxa, reducing nitrogen pollution in reservoirs. However, further research is needed to explore gene expression and transformation mechanisms at this interface.

## Reference

[1] T. Maavara, R. Lauerwald, P. Regnier, et al, Global perturbation of organic carbon cycling by river damming, J. Nat. Commun. 8 (2017) 5347.

[2] J.F. Wang, J.G. Chen, S.M. Ding, et al. Effects of seasonal hypoxia on the release of phosphorus from sediments in deep-water ecosystem: a case study in Hongfeng Reservoir, Southwest China, J. Environ. Pollut. 219 (2016) 858-865.

[3] B.B. Chai, T.L. Huang, X.G. Zhao, Y.J. Li, Phospholipids fatty acids of drinking water reservoir sedimentary microbial community: Structure and function responses to hydrostatic pressure and other physico-chemical properties, J. Journal of Environmental Biology.36 (2015) 845-855.

**Theme:** Technologies for water management and monitoring
**IAHR Thematic Priority Area:** [TPA-4] Digital Transformation
https://doi.org/10.3850/iahr-hic2483430201-36

# Enhancing Safety and Stability in Real-time Optimization Control for Bioreactors in Wastewater Treatment: A TransLSTM-Net-Based Model Predictive Control with Rationality Verification

**Weihao Chen[1], Wenchong Tian[1], Yuting Liu[1] and Kunlun Xin[1†]**

[1] College of Environmental Science and Engineering, Tongji University, Shanghai 200092, China;

*Corresponding author: xkl@tongji.edu.cn*

**Abstract.** Anaerobic-anoxic-aerobic (AAO) is acknowledged as a fundamental biological treatment process in urban wastewater treatment plants (WWTPs). Presently, data-driven deep learning models are increasingly utilized for constructing AAO process simulation and optimization control methods; nevertheless, the challenge of poor interpretability persists. The stability and security of the data-driven AAO optimization control system remain elusive, resulting in a lack of reliability in practical applications. In this study, we designed a deep learning network structure called TransLSTM-Net and developed a model predictive control method (TransLSTM-Net-MPC) with rationality verification. By optimizing the aeration volume, internal recirculation, and sludge internal recycle processes, safe and effective real-time control of AAO is achieved. Additionally, the SHAP method was utilized to analyze the interpretability of the deep learning model, thereby further enhancing the credibility of TransLSTM-Net-MPC. These methods underwent validation using data from a real-world WWTP in eastern China. The results demonstrate that the TransLSTM-Net-MPC model accurately predicts the effluent quality variables of the AAO system. Furthermore, the explanations provided by the model have verified its credibility to a certain extent, thereby enhancing the confidence of operators and stakeholders. The integration of TransLSTM-Net-MPC with rationality verification not only reduces the aeration volume by nearly 8% compared to traditional controllers but also establishes a stable control trajectory, thereby proving to be a robust real-time control method for WWTPs.

**Keywords:** AAO process; deep learning; interpretability; model predictive control; wastewater treatment plants

## 1 Methodology

TransLSTM-Net description: In this study, the Encoder structure from the Transformer was extracted and combined with established CNN and LSTM architectures to jointly design a TransLSTM-Net. The aim of the TransLSTM-Net is to predict the state of the bioreactor (specifically DO and MLSS) at the next time point by learning the intricate relationships among influent data, state data, and control variables within the bioreactor at the current time point. Following multiple parameter adjustments and testing, a suitable network structure and training parameters were determined to achieve satisfactory predictive performance.

**SHapley Additive exPlanations (SHAP):** SHAP is a model interpretation package developed in Python that can explain the output of any machine learning model. This study conducted interpretability analysis on the test data using the SHAP method. From the time dimension, the impact of the preceding and succeeding 20 timesteps in the training data on the output results was compared. From the input feature dimension, the study listed the different input dimensions in descending order of their importance to the overall model.

**The Rationality Verification for TransLSTM-Net-MPC:** Leveraging the previously described deep learning prediction model, this study employed the particle swarm optimization (PSO) algorithm to construct a dynamic optimization model within the framework of the standard MPC architecture. This study optimized three control variables: aeration volume, internal recirculation, and internal

sludge circulation. Following the construction of TransLSTM-Net-MPC, it is imperative to initially evaluate the rationality of its output control variables and the effectiveness of the control to ensure the safety and efficacy of the strategy. The proposed rationality verification in this study primarily focuses on three aspects: whether the current optimized control variables fall within the specified range set by engineers, whether they align with similar historical situations, and whether the control effect of the current optimized control variables is considered acceptable.

## 2 Results

In this study, the TransLSTM-Net utilized state, influent, and control variables from the previous 20 timesteps (equivalent to 600 minutes) as input to predict the bioreactor's state variables at the next timestep. To bolster credibility, the model underwent training and testing using two datasets: one from December 26 to 31, 2019, and another from April 27 to May 1, 2020. The monitoring frequency was set at 5-minute intervals, with each dataset containing 10,000 data points. Table 1 compares the proposed model's performance to the baseline, demonstrating its superior ability to predict unknown datasets effectively.

Table 1 MSE and NSE of the prediction results for different proposed models on the test dataset

| Model | Training Dataset | MSE on the Test Dataset | NSE on the Test Dataset |
|---|---|---|---|
| LSTM | 1 | 0.1306 | 0.9048 |
| TransLSTM-Net | 1 | 0.0984 | 0.9414 |
| LSTM | 2 | 0.1826 | 0.8035 |
| TransLSTM-Net | 2 | 0.0587 | 0.9594 |

Given SHAP's focus on local interpretability, this study selected the feature DO4 as an exemplar to elucidate the deep model. The results revealed a partial dependency among the four DO variables, confirming the influence of aeration on DO. From a temporal standpoint, the study illustrated the varying degrees of influence of input variables at different time steps in historical data on the subsequent system state. This demonstrates the TransLSTM-Net's ability to capture temporal dependencies in time series data, affirming its potential in predicting wastewater quality.

The optimized control led to an 8% reduction in average aeration over a 24-hour period compared to historical controls, while $Q_r$ remained stable and $Q_{sr}$ increased. This increase in $Q_{sr}$ may be attributed to the wider threshold range established by historical data. The optimized control variables exhibited stable changes primarily within the upper and lower limits established during the safety verification process. Given that aeration is the primary energy-consuming process, this reduction will result in an overall decrease in energy consumption for the biological reactor.

Table 2 Control results of TransLSTM-Net-MPC-Rationality Verification

| | Average aeration volume in 48h（$m^3$/min） | Average $Q_r$ （$m^3$/s） | Average $Q_{sr}$ （$m^3$/s） | Aeration optimization ratio |
|---|---|---|---|---|
| LSTM-MPC-Rationality Verification | 60.833 | 1.197 | 3.297 | 8.0% |
| historical control | 66.104 | 1.196 | 2.692 | / |

## 3 Conclusion

In summary, the TransLSTM-Net-MPC model, with rationality verification, exhibits a certain level of interpretability. It can suggest reasonable and safe optimization control strategies based on historical operational experience, thereby achieving energy savings in practical WWTPs. However, despite these advantages, further exploration of the model's interpretability and the selection of appropriate strategies to balance safety and optimization performance in the TransLSTM-Net-MPC model with rationality verification remain significant challenges for the future.

**Theme:** Technologies for water management and monitoring
**IAHR Thematic Priority Area:** [TPA-4] Digital Transformation
https://doi.org/10.3850/iahr-hic2483430201-38

# Chlorophyll Distribution Dynamics in Urban Reservoirs Based on High Temporal-Spatial Resolution Data

**Peng Xiao [1], Yu Tao [1], Tiefu Xu [2], Aijie Wang [1]**

[1] Harbin Institute of Technology (Shenzhen), Shenzhen 518000, China
[2] Heilongjiang University, Heilongjiang 150000, China

*Corresponding author: Yu Tao, taoyu@hit.edu.cn*

**Abstract.** Algal blooms impact water quality and are unpredictable, challenging water safety management. Despite existing research having made progress in understanding their mechanisms, the complex environmental interactions and their dynamic nature hinder accurate prediction of algal bloom evolution. Current monitoring methods lack a satisfying resolution to track blooms, which underscores the need for better approaches. Here, we introduce a high-resolution monitoring method using underwater robots to map algal bloom dynamics in detail, revealing significant shifts in chlorophyll concentration from sediment to water surface post-rainfall.

**Keywords:** Algal Bloom, High Spatiotemporal Resolution， monitor， Source Tracing

## 1 Introduction

The complexity of algal blooms, influenced by factors like nutrient availability, climate, and biological interactions, challenges research and management[1]. The limitations of current monitoring systems hinder capturing blooms' dynamics[2]. Recent advances in intelligent monitoring technologies promise better understanding by collecting detailed, continuous data, potentially leading to breakthroughs in predicting and managing algal blooms through integrating these tools with ecological theories[3-4].

## 2 Material and methods

Here, we developed and deployed a monitoring method characterized by high spatiotemporal resolution, employing a customized multi-channel, multi-parameter underwater robot for data and sample collection. Based on the remotely operated vehicle (ROV), the robot integrates YSI EXO2 7-in-1 sensors (total algae, pH, fDOM, dissolved oxygen, conductivity, temperature and turbidity) and an octuple water sampler. The equipped QPS underwater positioning system enabled precise location positioning and data acquisition underwater. Using this method, high spatial and temporal resolution monitoring of algal bloom dynamics was carried out in a reservoir in Shenzhen, a South China city, from March to July 2023.

## 3 Results

We utilized high spatiotemporal resolution data to trace the outbreak of an intense algal bloom following a significant rainfall event from May 7 to May 10. The chlorophyll concentrations at 1m depth revealed the bloom's initiation in the reservoir's northwest on May 8 at 9:00. Chlorophyll concentrations increased rapidly throughout the reservoir over the next two days (Fig. 1a). Three-dimensional high-resolution data further detailed the three-dimensional distribution of chlorophyll concentrations before and after the rainfall, highlighting the bloom's spread across the reservoir. Surface chlorophyll was diluted post-rainfall, with increases at different depths suggesting the

influence of rainwater impact and sediment resuspension. The bloom's rapid expansion happened with concentrations peaking at 42.36 μg/L (Fig. 1b).

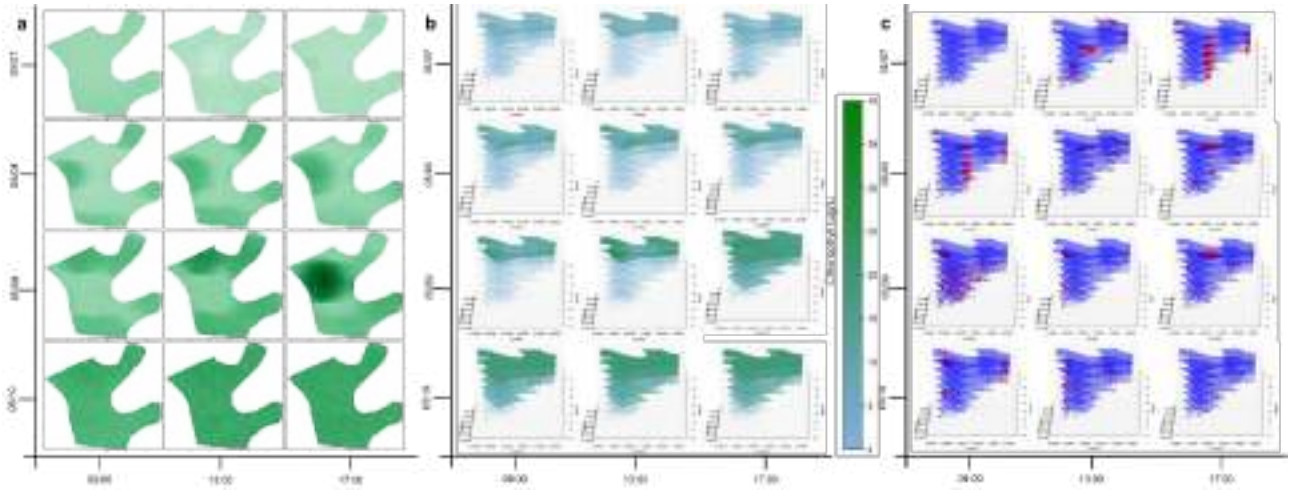

Figure 1 Chlorophyll Concentration and Anomaly Distribution from May 7 to May 10. a) Distribution map of chlorophyll concentration at 1m depth. b) Three-dimensional distribution map of chlorophyll concentration. c) Three-dimensional distribution map of chlorophyll concentration anomaly, with red indicating anomalous points and blue indicating normal points.

## 4 Discussion

We developed a method called Layered Anomaly Detection Analysis (LADA) to manage the complexity of high spatiotemporal resolution data on chlorophyll-a concentrations, with a particular focus on its varied distribution across different depths. This method independently processes chlorophyll data at each depth, utilizing normalization for statistical analysis to identify anomalies exceeding twice the standard deviation. Data processed by LADA revealed signs of chlorophyll being released during sediment resuspension (Fig. 1c). This aligns with existing research on dormant algal spores in sediments, suggesting that sediment resuspension could lead to widespread algal proliferation, thereby initiating comprehensive bloom outbreaks. However, given the uncertainties associated with these observations, further research is necessary to solidify these conclusions.

## 5 Conclusions

In this study, we leveraged high spatiotemporal resolution data by using intelligent underwater robots to elucidate the dynamics of chlorophyll distribution in urban reservoirs, uncovering substantial shifts from sediment to water surface post-rainfall. This endeavor challenges traditional monitoring paradigms by providing detailed insights into algal bloom progression and paves the way for more accurate and predictive environmental management strategies. Future directions will focus on refining these methodologies and expanding their application to broader aquatic systems to enhance our predictive capabilities and develop preemptive measures against algal proliferation, considering the complex interplay between various environmental factors and the aquatic ecosystem.

## Reference

[1] Huisman, J., et al., Cyanobacterial blooms. Nat Rev Microbiol, 2018. 16(8): p. 471-483.
[2] Guan, W., et al., Monitoring, modeling and projection of harmful algal blooms in China. Harmful Algae, 2022. 111: p. 102164.
[3] Yanwu, Z., et al.A system of coordinated autonomous robots for Lagrangian studies of microbes in the oceanic deep chlorophyll maximum.[J].Science robotics,2021,6(50).
[4] Ostrovsky, I., et al., Bloom-forming toxic cyanobacterium Microcystis: Quantification and monitoring with a high-frequency echosounder. Water Res, 2020. 183: p. 116091.

**Theme:** Technologies for water management and monitoring
**IAHR Thematic Priority Area:** [TPA-4] Digital Transformation
https://doi.org/10.3850/iahr-hic2483430201-40

# Development of an A-Priori Numerical Indicator for the Evaluation of the Impact of Diffusion and Dispersion in Water Distribution Systems

**Stefania Piazza[1], Mariacrocetta Sambito[1] and Gabriele Freni[1]**

[1] Department of Engineering and Architecture, University of Enna "Kore", Cittadella Universitaria, 94100 Enna, Italy

*Corresponding author: stefania.piazza@unikore.it*

**Abstract.** Modelling water quality in distribution networks is essential for detecting contamination, but currently simplified models are used that neglect diffusion and dispersion. The Péclet number, previously used to evaluate the suitability of one-dimensional advective transport without compromising model accuracy, has been shown to be ineffective for two-dimensional advective-dispersive modelling in real systems. The present study aims to determine a new indicator: to discriminate the dominance of the advective-dispersive process, to have a rapid decision-making tool capable of establishing a priori the behaviour of the distribution network, to use the numerical model more for water quality modelling.

**Keywords:** advective-dispersive-diffusive model, EPANET model, numerical indicator, water distribution network.

## 1 Structure

Water quality modelling plays a significant role for detecting contamination in distribution networks [1]. Current models [2] ignore diffusion and dispersion, critical in low Reynolds number scenarios [3]. These simplifications work for turbulent flows in short pipes but fail in laminar and transitional flows, common in low-flow situations, dead-end pipes, or service connections. Despite turbulent flows in main pipelines, diffusive-dispersive processes become significant due to laminar flows in complex network areas, particularly at night. Advective simplification offers computational efficiency for large networks, yet a method to discern when this approach suffices or when diffusion is necessary is needed. The Péclet number has been widely used to determine when one-dimensional advective transport is reliable without compromising model accuracy [4]. A recent analysis conducted by the authors [5] extended the use of the Péclet number to two-dimensional advective-dispersive modelling, highlighting that it could not be used as a parameter to identify the dominance of the advective or dispersive process in real systems, as the latter cannot be neglected for long pipes, in any flow regime. For this reason, the present study aims to determine a new indicator that can effectively discriminate the dominance of the advective or dispersive process, to have a rapid decision-making tool capable of establishing a priori the behaviour of the distribution network, to use the numerical model more for water quality modelling.

## 2 Material and Methods

Starting from the definition of the dimensionless Taylor time, the new indicator was determined as the ratio between the product of the longitudinal dispersion coefficient E and the time with the travel time , and the radius of the pipe a, as reported in equation (1).

$$M^i(\theta_1, \theta_2) = \begin{cases} 1, & if\ P\left(X^i > X^i_{\theta_1}\right) \geq \theta_2 \\ 0, & otherwise. \end{cases} \quad (1)$$

The EPANET model [2], the one-dimensional (1D) advective-diffusive model [6] and the new dynamic model proposed by the authors EPANET-DD (Dynamic-Dispersion) [7] were applied to a

district of the Palermo water distribution network (Oreto-Stazione), contaminated with a soluble contaminant, and the Nash-Sutcliffe efficiency (NSE) coefficient was evaluated in order to measure how well a simulation model predicts an outcome variable.

## 3 Results and Discussion

Figure 1 highlights a threshold for an efficiency of NSE=0.9 equal to =5.40, below which the two dispersive models reproduce similar results in modelling the contaminant. Considering the same NSE efficiency value, the  value reduces to 3.98 (EPANET – 2D advective-dispersive model) or expands to 35 (EPANET – 1D advective-dispersive model).

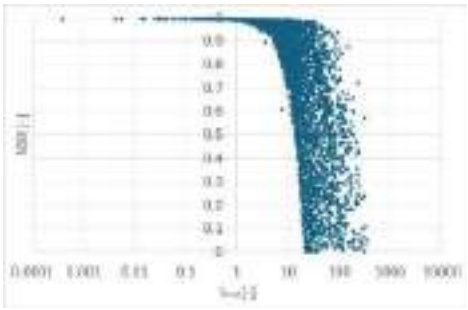

**Figure 1.** Nash-Sutcliffe efficiency relative to dimensionless time , evaluated by comparing 1D and 2D advective-dispersive models.

## 4 Conclusions

This study allowed us to determine a parameter to discriminate the advective or dispersive behaviour of a water distribution network. In fact, if we assume a priori the efficiency / error that we wish to obtain in modelling the contaminants within a water distribution network, it is possible to discriminate values of this new indicator which allow us to distinguish the dominance of dispersive processes compared to the advective ones.

## Reference

[1] Piazza S., Sambito M. and Freni G., 2023, Analysis of Optimal Sensor Placement in Looped Water Distribution Networks Using Different Water Quality Models, Water, 15(3), pp 1-11.
[2] Rossman L., 2000, EPANET 2 Users Manual, Environmental Protection Agency.
[3] Piazza S., Blokker E. J. M., Freni G., Puleo V. and Sambito M., 2020, Impact of diffusion and dispersion of contaminants in water distribution networks modelling and monitoring, Water Supply, 20(1), pp 46-58.
[4] Abokifa A. A., Xing L. and Sela L., 2020, Investigating the Impacts of Water Conservation on Water Quality in Distribution Networks Using an Advection-Dispersion Transport Model, Water, 12(4), pp 1-18.
[5] Piazza S., Sambito M. and Freni G., 2024, Definition and application of the Péclet number threshold for water quality analysis in water distribution networks, Journal of Hydroinformatics.
[6] Shang F., Burkhardt J. B. and Murray R., 2023, Random Walk Particle Tracking to Model Dispersion in Steady Laminar and Turbulent Pipe Flow, Journal of Hydraulic Engineering, 149(7), pp 1-9.
[7] Piazza S., Sambito M. and Freni G., 2022, A Novel EPANET Integration for the Diffusive–Dispersive Transport of Contaminants., Water, 14(17).

**Theme:** Technologies for water management and monitoring
**IAHR Thematic Priority Area:** [TPA-4] Digital Transformation
https://doi.org/10.3850/iahr-hic2483430201-42

# Optimizing Intake Layer Selection for Drinking Water Treatment using a Long Short-Term Memory (LSTM) Network

**Minhyeok Lee[1], Seoeun Kwak[2], Yunhwan Kim[1], Moon Jeong[1], Meeyoung Park[2*], Yong-Gyun Park[1**]**

[1] Department of Environmental and Energy Engineering, Chonnam National University, 77 Yongbong-ro, Buk-gu Gwangju, 61186, Republic of Korea
[2] Department of Computer Engineering, Kyungnam University, 7, Gyeongnamdaehak-ro, Masanhap-po-gu, Changwon-si, Gyeongsangnam-do, 51767, Republic of Korea

*Corresponding author. Tel: +82-62-530-1856, E-mail: ygpark7@jnu.ac.kr*

**Abstract.** Managing the quality of drinking water sources is essential to ensure the high operational and treatment efficiency of water treatment plants. Poor water quality in drinking water sources can lead to overloading of water treatment plants and high treatment costs. In this study, we utilized LSTM (Long Short-Term Memory), a deep learning algorithm suitable for analyzing and predicting time series data, to predict the seasonal and annual water quality of Juam Lake in South Korea and select the optimal water intake point. To ensure the high performance of the deep learning model, we used water quality network data from Lake Juam, South Korea, collected between January 2013 and June 2023. Statistical techniques were applied to the water quality measurement network data to more accurately analyze the influence of water quality factors. The results of this study suggest that deep learning-based algorithms can improve the treatment and operational efficiency of water treatment plants and can be used to monitor the performance of water intake and treatment facilities.

**Keywords:** optimal water intake layer; drinking water treatment; water quality; deep learning; LSTM

## 1 Introduction & Significance

This study highlights the escalating challenges to water quality, driven by factors like urbanization, industrialization, and climate change, particularly in regions with distinct seasons. Seasonal variations lead to issues such as thermal stratification in lakes and reservoirs, causing oxygen depletion, ion release, and harmful algal blooms. Reservoirs used for drinking water face water quality degradation, impacting the treatment process and increasing costs. To mitigate these problems, selective water intake adjusts depth based on water quality, necessitating an understanding of seasonal variations. Advanced monitoring systems and the LSTM model aid in forecasting water quality. The study employs data from Juam Lake, South Korea, using LSTM for predictions and proposing a method for optimal intake layer selection.

## 2 Material and Methods

In this study, we collected water quality data from Juam Lake spanning from January 2013 to June 2023 using the national automatic water quality monitoring system. We applied the LSTM model, a deep learning technique, to predict the best water intake layer for one year. Our analysis considered key water quality parameters to identify the optimal intake layers.

## 3 Results and Discussion

The LSTM deep learning model had two layers with 50 nodes each and used the tanh activation function. Data was split into training and test sets (7:3 ratio) to prevent overfitting, and Min-Max normalization was applied for faster training. We optimized the model through hyperparameter tuning (time steps: 168 hours, prediction periods: 24 hours, epochs: 200, 300, 500, 700, batch sizes: 32, 64).

Model performance was assessed using root mean squared error (RMSE), and results were visualized in time-series graphs. Table 1 shows the best LSTM models with their respective epochs and batch sizes for each water quality parameter.

Table 1 The RMSE results of the optimal LSTM model for each parameter.

| | Chl-a | DO | EC | Turbidity | pH | TOC | T-N | T-P | WT |
|---|---|---|---|---|---|---|---|---|---|
| Epoch | 700 | 700 | 700 | 700 | 700 | 700 | 700 | 700 | 700 |
| Batch size | 32 | 32 | 32 | 32 | 32 | 32 | 32 | 32 | 32 |
| **RMSE** | **1.619** | **0.359** | **1.811** | **0.386** | **0.145** | **0.103** | **0.013** | **0.001** | **0.559** |

We used a priority-based approach to assess water source contamination for different water quality factors. If contamination was detected, we selected the appropriate intake layer to minimize its impact on water treatment. Weekly average values of predicted water quality data allowed us to track how the recommended intake layer changed each week. Withdrawals were mostly from the upper layer, followed by the middle layer. Chl-a influenced middle layer intake, while T-N affected upper layer intake. During the year, the middle layer was used for 17 weeks, primarily in early spring and summer, while the upper layer was preferred for the remaining 35 weeks due to elevated T-N levels.

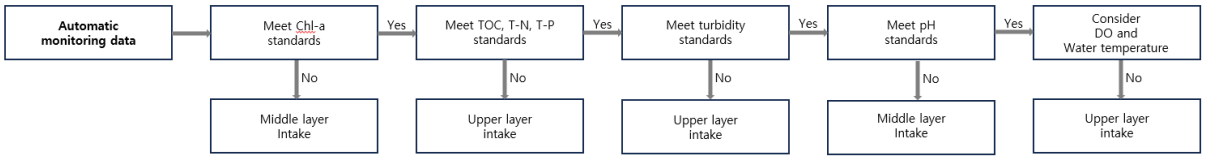


Figure 1 The process for the selection of the source water intake layer.

## 4 Conclusions

This study focused on managing water sources effectively for drinking water treatment plants. It monitored and predicted water quality changes in Juam Lake. T-N and chl-a were key factors affecting water quality. Seasonal variations included pH and EC increases in summer, nutrient rise in spring, and DO peak in spring. Summer had frequent turbidity outliers due to heavy rainfall. An intake layer selection mechanism based on LSTM predictions preferred the top layer for 35 weeks and the middle layer for 17 weeks in early spring and summer. This research aims to improve water treatment plant efficiency.

## Reference

[1] Kim Y. H., Kwak S. E., Lee M. H., Moon J., Park M. Y. and Park Y. G. (2023). Determination of optimal water intake layer using deep learn-ing-based water quality monitoring and prediction. Water, 16(1), 1-16.

[2] Yang W. M. (2023). Development of rule-based operation method for selecting optimal water quality when taking raw water from lakes. Chonnam National University, Gwangju, Republic of Korea.

**Theme:** Technologies for water management and monitoring
**IAHR Thematic Priority Area:** [TPA-4] Digital Transformation
https://doi.org/10.3850/iahr-hic2483430201-44

# Development of Efficient Two-Stage Transient-Based Leak Detection Method in Water Pipe Networks

**Manli Wang[1]; Bin Pan[1]; Alireza Keramat[1]; Tong-Chuan Che[1]; Huan-Feng Duan[1]**

[1] Department of Civil and Environmental Engineering, The Hong Kong Polytechnic University, Hong Kong SAR, China

*Corresponding author: Huan-Feng Duan (hf.duan@connect.polyu.hk)*

**Abstract.** Urban water safety including water shortage and water quality issues have received increasing attention through global urbanization. Urban water pipe networks (UWPNs), as transporters of freshwater, its long-time operation and underground construction make it challenging to timely identify and repair the leaky parts in the networks. Currently, the global average water leakage rate in the UWPNs is still around 30%. Therefore, more efficient leak investigation and water loss management technologies are urgently demanded. The transient-based method (TBM) has garnered increased focus for its notable attributes of precision, effectiveness, and easy operation in pipe systems in past few decades. Nevertheless, the applications of existing TBMs are largely confined to simple pipe systems for unrealistic computational efficiency or implementational complexity. This study aims to develop an efficient strategy for leak detection in complex pipe networks based on the separability of leak location and size in the time domain and simplify the 2D optimization problem into two 1D estimations to first identify the leak location followed by size calculation. Both numerical and experimental applications confirm its validity and effectiveness. The achievement of this study helps to further improve the applicability of the transient-based method for effective water resources management in UWPNs.

**Keywords:** Leak detection; Transient-based method (TBM); Variable separation; Water pipe networks.

## 1 Introduction

Achieving fast, robust, and accurate leak detection in UWPNs is crucial for maintaining urban water security. The transient-based methods that fulfill the criteria have gained more attention in the past few decades [1]. Among these methods, the time domain inverse transient analysis method provides robust and accurate detection by utilizing complete transient signal and optimizing the coupled leak location and size simultaneously by matching the measured and modeled signals [2]. Nevertheless, as the pipe system complexity grows, the involved model data invocations increase exponentially, causing computational cumbersome. This study proposes a two-stage 1D estimation that simplifies the simultaneous optimization by separating the leak variables, significantly enhances the computational efficiency of current time-domain transient-based methods for leak detection.

## 2 Methodology

Let $h^{obs}$ represent the measured transient signal from the pipe system that contains system noise $n$ following Gaussian distribution. Traditional 2D optimization estimates leak location and size simultaneously by matching the measured and modeled transient signals. By applying Taylor expansion to modeled signal and neglecting the higher-order terms, it can be written as

$$\{\hat{z}_L, \hat{\alpha}_L\} = \arg\min_{z_L, \alpha_L} \left\| \mathbf{h}^{obs} - \mathbf{h}^{NL} - \mathbf{f}(z_L)\alpha_L \right\|_2^2 = \arg\min_{z_L, \alpha_L} \left\| \Delta\mathbf{h} - \mathbf{f}(z_L)\alpha_L \right\|_2^2 \quad (1)$$

where the estimated leak location and size are denoted as $\hat{z}_L$ and $\hat{\alpha}_L$, and $z_L$, $\alpha_L$ are the potential leak variables. $\mathbf{h}^{\mathrm{NL}}$ represents the intact pipe (no leak in the system), $\Delta\mathbf{h}$ is the leak-related transient signal containing system noise $\mathbf{n}$. They are written in vector form in the equations. The maximum likelihood estimation for leak size is a least square solution of Eq. (1), it gives

$$\hat{\alpha}_L = \frac{\mathbf{f}(z_L)^T \Delta\mathbf{h}}{\mathbf{f}(z_L)^T \mathbf{f}(z_L)} \tag{2}$$

Substituting Eq. (2) back to Eq. (1), gives the objective function regarding the leak location

$$\{\hat{z}_L\} = \arg\max_{z_L} \left( \Delta\mathbf{h}^T \mathbf{f}(z_L) \frac{\mathbf{f}(z_L)^T \Delta\mathbf{h}}{\mathbf{f}(z_L)^T \mathbf{f}(z_L)} \right) = \arg\max_{z_L} \left( B^2 \right) \tag{3}$$

in which $B$ is the objective function. By applying the proposed method, one can first find the global maximum for the estimated leak location with Eq. (3), followed by solving Eq. (2) for leak size estimation.

## 3 Numerical validation in pipe networks

A 5-loop pipe network is utilized for primary verification of the applicability and accuracy of the proposed method. The configuration and settings of the system are shown in Figure 1(a). The transient signals are simulated using the Method of Characteristics (MOC), with each pipe comprising 30 nodes. The leak is located at the 20th node in pipe no. 5, and its size is 25% of the pipe flowrate.

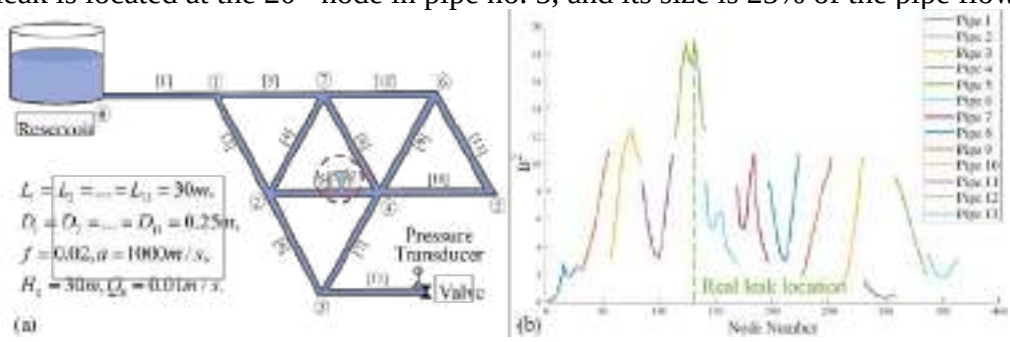


**Figure 4.** Case study and results: (a) pipe network configuration and settings; (b) $B^2$ for leak localization.

Following the proposed method, $B^2$ from Eq. (3) is plotted in Figure 1 (b) to localize the leak. The global maximum point corresponding to the estimated leak location matches with the actual location indicated by the green dashed line, indicating the accurate localization. Consequently, the leak size is determined with Eq. (2) to be 24.87% of the pipe flowrate, with a minimal error of 0.52%. Nevertheless, the proposed method is about 15 times faster than traditional 2D optimization. The results demonstrate the high accuracy and efficiency of the proposed method for leak detection in complex pipe networks.

## 4 Conclusion

This paper proposes a novel two-stage leak detection method based on the factorized transient model. It simplifies the 2D optimization of leak variables into two 1D estimation problems, reducing the number of transient model invocations. This approach enhances the computational efficiency for transient-based leak detection and further improves its applicability for effective water resources management in UWPNs.

## 5 Acknowledgment

This study was supported by the Hong Kong Research Grants Council (RGC) under GRF projects no. 15201523 and no. 15202122; and the Science and Technology Department of Guangdong Province under project no. 2023A0505030007.

## Reference

[1]. Duan, H.F., et al., State-of-the-art review on the transient flow modeling and utilization for urban water supply system (UWSS) management. Journal of Water Supply: Research and Technology-Aqua, 2020. 69(8): p. 858-893.

[2]. Liggett, J., A. and L.C. Chen, Inverse transient analysis in pipe networks. Journal of Hydraulic Engineering, 1994. 120(8): p. 934-955.

**Theme:** Technologies for water management and monitoring
**IAHR Thematic Priority Area:** [TPA-4] Digital Transformation
https://doi.org/10.3850/iahr-hic2483430201-46

# Research and Design of Maintenance Information Platform for Sewage Treatment in Highway Service Area

**Dong Ni*, Jian Wang, Shegang Shao**

Research institute of Highway, MOT, Beijing, 100088, China

*Corresponding author: d.ni@rioh.cn*

**Abstract.** In order to solve the problem of information management of sewage treatment in highway service area, considering the design framework of environmental monitoring and energy consumption management, an overall scheme based on three-tier structure is established. Combined with the corresponding process operation monitoring, business process informatization and system management and control refinement model, the system requirements analysis is carried out by using object-oriented analysis and design method to determine the system requirements of the single service area management platform. Around the formulated requirements analysis, the modules in the functional architecture are divided according to the modular idea, and the edge layer, IAAs layer, platform layer Function application of application layer and display layer. The informatization construction of highway service area puts forward the informatization management function of service area to realize the real-time supervision of highway service area.

**Keywords:** service area, informatization, network structure, operation and maintenance

## 1 Introduction

Scholars at home and abroad have done a lot of research on the technical application of information construction in highway service areas, and obtained many practical results [1-3]. The purpose is to improve the information level and service level through the application of new technologies [4]. At present, there are some problems in the sewage treatment station in the expressway service area, such as difficult maintenance, unstable operation, and unstable effluent, many faults, high maintenance cost, common shutdown, single point management and inadequate service. In view of these problems, integrate and apply various resources and technologies to develop the on-line monitoring system and remote centralized control platform of water quality and quantity of sewage treatment station in expressway service area, so as to realize the on-line real-time monitoring and early warning analysis of water quality and quantity of sewage treatment station in expressway service area, process operation status monitoring.

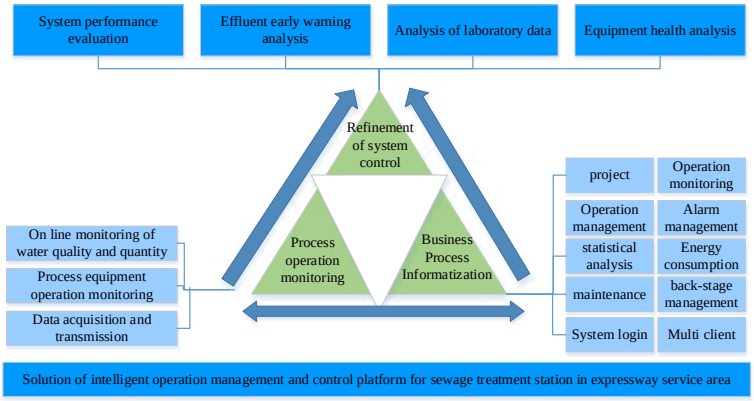


Figure 1. Structure design of operation and maintenance information platform

## 2 Construction of information platform

The process operation monitoring function includes the online monitoring ability of water quality and quantity of sewage treatment station in expressway service area, the operation monitoring ability of on-site equipment and the ability to capture video image data of on-site conditions through camera.

### 2.1 structural stratification

Realize the remote real-time control of the operation status of sewage treatment process equipment, require the sewage treatment process equipment to open the external communication interface, and meet the communication protocol access requirements of the database server of the intelligent operation control platform.

### 2.2 energy consumption management

The intelligent operation control platform in the service area can monitor the real-time energy consumption data of the on-site sewage treatment equipment, store the historical data for query, monitor the operation and use of the equipment, generate various energy consumption management reports, analyze the energy consumption, energy consumption cost evaluation, etc., so as to meet the daily production management needs of each sewage treatment system.

## 3 system performance evaluation

On the basis of process operation monitoring and business process informatization, through in-depth learning and knowledge mining of sewage treatment station data on the platform, provide in-depth optimization and fine control for the whole process of various types of sewage treatment systems.

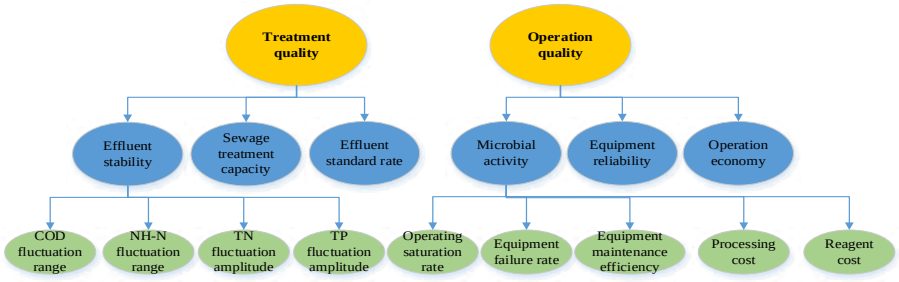


Figure 2. Relationship between operation performance evaluation indexes of sewage treatment system

## 4 Conclusion

Taking the highway service area of Gansu Province as the research background, combined with the sewage treatment situation of highway service area of Gansu Province, this paper carries out information construction, realizes the "three unification" of long-term operation and maintenance of sewage treatment in the service area (unified management system, unified management policy and unified data analysis), and establishes the sewage treatment information management system of highway service area.

## References

[1]WANG Y,TIAN S .Database System of Chemical Waste Statistic Based on Browse/Server Mode of Web. Research and Exp loration in Laboratory, 2009, 1(026.

[2]Banihabib, S.M.R. Research on service efficiency evaluation of expressway service area based on DEA [J]. Transportation research,201 7,13(04):35-41.

[3]Valipour, M., M.E., Banihabib, S.M.R., Behbahani. Monthly inflow forecasting using auto-regressive artificial neural network. Journal of Applied Sciences, 2012,12(20): 2139-2147.

[4]Xiaoyan Shen, Lihua Wang, Jingshuai Yang. Estimation of the Percentage of Mainline Traffic Entering Rest Area Based on BP Neural Network [J]. Journal of applied sciences, 2013, 13( 14):2632-2638.

**Theme:** Technologies for water management and monitoring
**IAHR Thematic Priority Area:** [TPA-4] Digital Transformation
https://doi.org/10.3850/iahr-hic2483430201-48

# Enhanced Green Hydrogen Production Potential at Reservoir Sediment-Water Interface under Elevated Hydrostatic Pressure

**Yuemei Li[1], Lixin He[2,3], Beibei Chai[2,4*], Tianyu Zhuo[5], Kehong Yu[6], Zhixuan Zhou[1], Xiaohui Lei[7], Bin Chen[8]**

[1] School of Water Conservancy and Hydroelectric Power, Hebei University of Engineering, Handan 056038, China.
[2] Collaborative innovation center for intelligent regulation and comprehensive management of water resources, School of Water Conservancy and Hydroelectric, Hebei University of Engineering, Handan 056038, China.
[3] Hebei Provincial Key Laboratory of Intelligent Water Conservancy, Handan, Hebei 056038, China.
[4] Handan Key Laboratory of Low-carbon Energy, Handan, Hebei 056038, China.
5Tianjin University,Tianjin 300072, China.
[6] School of Energy and Environmental Engineering, Hebei University of Engineering, Handan 056038, China.
[7] State Key Laboratory of Simulation and Regulation of Water Cycle in River Basin, China Institute of Water Resources and Hydropower Research, Beijing 100038, China
[8] Tianjin Water Group Binhai Water Co., Ltd., Tianjin 300308, China.

*Corresponding author: cbb21@163.com*

**Abstract.** This study utilizes microcosm simulation experiments combined with metagenomic technology to investigate the impact mechanisms of four static water pressure conditions (atmospheric pressure, 0.2 MPa, 0.5 MPa, and 0.7 MPa) on hydrogen production from reservoir sediment at the microbial community structure, functional gene, and metabolic pathway levels. The results indicate that compared to atmospheric pressure, an increase in static water pressure leads to an initial increase and subsequent decrease in the total number of hydrogen-producing bacterial species in the sediment. The relative abundance of bacteria and fungi decreases by an average of 0.17% and 0.02%, respectively, while the proportion of archaea increases by an average of 0.19%. Furthermore, high pressure tightens microbial community ecological network connections, enhancing system stability. High static water pressure increases the relative abundance of functional genes related to glycolysis pathways and acetate metabolism, such as glK, ppgK, fadJ, atoA, and gene-enzyme synthesis related to butyric acid metabolism, promoting glycolysis pathways, acetate metabolism, and butyric acid metabolism pathways, thus unlocking more hydrogen release potential. These findings indicate the hydrogen production potential of reservoir sediment via anaerobic fermentation.

**Keywords:** Metagenomics; Hydrostatic pressure; Microbial community structure; Anaerobic hydrogen production; Sediment

## 1 Introduction

Biohydrogen production, particularly through anaerobic fermentation using organic waste like sewage sludge, offers a green energy solution while mitigating waste management issues[1]. The composition of microbial communities significantly affects anaerobic fermentation performance[2]. Past studies have revealed trace amounts of $H_2$ at the water-sediment interface in reservoirs[3], indicating the potential for hydrogen production from sediment organic substrates. However, research in this area is limited. Thus, investigating the influence of static water pressure on microbial pathways and mechanisms of hydrogen production at the water-sediment interface in large, deep reservoirs is crucial.In this study, we varied static water pressure at the sediment-water interface of reservoirs to

understand its impact on microbial communities, functional genes, and metabolic pathways related to hydrogen production. Using metagenomic techniques, we investigated how different pressure conditions affect microbial processes involved in hydrogen production.

## 2 Materials and methods

The study collected sediment and water from Jinpen Reservoir in Xi'an, China. Sediment and water were subjected to hydrostatic pressure simulation in the lab to mimic different depths in the reservoir. Metagenomic sequencing and non-targeted metabolomic analysis were conducted to assess microbial community and metabolite composition.

## 3 Results

A total of 2,178 microorganisms with hydrogen production potential were identified, spanning 90 phyla, 158 classes, 275 orders, and 468 families. The number of species initially increased and then decreased with rising static water pressure. Bacteria dominated the community, with decreasing proportions relative to archaea and fungi as hydrostatic pressure increased. Proteobacteria, Candidatus_Rokubacteria, Actinobacteria, and Acidobacteria were prominent phyla, with varying abundance patterns under different pressures. Candidatus_Rokubacteria_bacterium and Betaproteobacteria_bacterium were dominant species, decreasing with increasing pressure. Functional pathway analysis revealed glycolysis as the predominant pathway across all conditions. Candidatus_Rokubacteria, Betaproteobacteria, and Deltaproteobacteria were significant contributors to hydrogen production pathways. Sixty-one functional groups were identified, with slight differences between pressure conditions. Comparative analysis with the KEGG gene database identified functionally divergent genes associated with glycolysis, gluconeogenesis, pyruvate metabolism, and butanoate metabolism. Notably, *GAPDH* and *pfkA* were prominent glycolysis genes, while *DLAT* was significant in pyruvate metabolism.

## 4 Conclusions

For deepwater reservoirs, changes in water depth leading to variations in hydrostatic pressure are critical factors affecting the microbial community structure in sediments. This study conducted simulation experiments to investigate the mechanism by which hydrostatic pressure affects the hydrogen-producing microorganisms at the sediment-water interface at different water depths, using metagenomic approaches. The results indicate slight differences in microbial community composition and shared functional groups under different hydrostatic pressure conditions. Under high-pressure conditions, the microbial community exhibits a more stable collaborative relationship. High hydrostatic pressure enhances hydrogen release potential by altering the microbial community structure and promoting the abundance of genes related to glycolytic and acetogenic pathways, such as *glK*, *ppgK*, *pfkB*, *ALDO*, *GAPDH*, *fadJ*, *atoA*, as well as genes associated with butyric acid metabolism (fadJ, atoA), and the enzymatic generation related to these pathways. However, further in-depth investigations are needed regarding the gene expression and detailed metabolic mechanisms reflected by the transcriptome results at this interface and the related influencing factors.

## Reference

[1] J.H. Wang, L. Liu, C.Z. Zhang, Y.F. Chen, Z. Guo, Advancements in process simulation of anaerobic fermentation hydrogen production from slugde, J/OL. Environmental Engineering. (2024) 1–9.

[2] Y. Maspolim, Y. Zhou, C. Guo, Determination of the archaeal and bacterial communities in two-phase and single-stage anaerobic systems by 454pyrosequencing, J. Journal of Environmental Science.36 (2015) 121–129.

[3] B.B. Chai, Pollutants Flux on the Sediments Multi-Phase Inter face in Drinking Water Reservoir and Pollution Controlling Technology, D. Xi ‘ an University of Architecture and Technology, 2012.

**Theme:** Technologies for water management and monitoring
**IAHR Thematic Priority Area:** [TPA-4] Digital Transformation
https://doi.org/10.3850/iahr-hic2483430201-50

# Microplastics Increase the Risk of Greenhouse Gas Emissions and Water Pollution in a Freshwater Lake by Affecting Microbial Function in Biogenic Element Cycling: A Metagenomic Study

**Chai Beibei[1], Zhuo Tianyu[2], Li Yumei[1], Yu Kehong[1], Chen Bin[3]**

[1]Hebei university of Engineering, Handan, 056038, China
[2]Tianjin University, Tianjin 300072, China.
[3]Beijing Normal University, Beijing 100875, China

*Corresponding author: cbb21@163.com (B. Chai); chenb@bnu.edu.cn (B. Chen)*

**Abstract.** Microplastics (MPs) are recalcitrant to degradation in the environment, causing combined and persistent organic pollution. Aquatic ecosystems are being increasingly polluted by microplastics (MPs), which calls for an understanding of how MPs affect microbially driven biogenic element cycling in water environments. However, the effects of various MPs on microbially driven biogenic element cycling in water environments have been insufficiently investigated at the gene level. In the present study, natural water samples were collected from a freshwater lake in northern China and incubated with three popular types of MPs in a simulated experimental device. The following questions were raised and solved based on metagenomics: (1) How did various MPs affect microbial species abundance, community composition, and potential function in carbon, nitrogen, phosphorus, and sulfur cycling? (2) Which MP type had the greatest effect on microbial community structure and specific functions in biogenic element transformation? (3) What effects could various MPs have on microbially driven biogenic element cycling at the functional gene level? A 28-day incubation experiment was conducted using freshwater lake water added with three polymer types of MPs (i.e., polyethylene, polypropylene, polystyrene) separately or in combination at a concentration of 1 items/$m^3$. Metagenome DNA extraction and shotgun sequencing (metagenomics) were used to study the effects of various MPs on microbial communities and functional genes related to carbon, nitrogen, phosphorus, and sulfur cycling. Results showed that Sphingomonas and Novosphingobium, which were indicator taxa (genus level) in the polyethylene treatment group, made the largest functional contribution to biogenic element cycling. Following the addition of MPs, the relative abundances of genes related to methane oxidation (e.g., *hdrD*, *frhB*, *accAB*) and denitrification (*napABC*, *nirK*, *norB*) increased. These changes were accompanied by increased relative abundances of genes involved in organic phosphorus mineralization (e.g., *phoAD*) and sulfate reduction (*cysHIJ*), as well as decreased relative abundances of genes involved in phosphate transport (*phnCDE*) and the SOX system. Findings of this study underscore that MPs, especially polyethylene, increase the risk of greenhouse gas emissions ($CO_2$, $N_2O$) and water pollution ($PO_4^{3-}$, $H_2S$) in freshwater lakes at the functional gene level.

**Keywords:** microplastics, metagenomics, microbial community structure, functional genes, freshwater environment, elemental cycling

## 1 Introduction

Microplastics (MPs) persist in the environment, accumulating organic pollutants and acting as carriers for particulate matter and trace metals in water[1]. Their impact on water ecology and microbial-driven biogeochemical cycling remains a concern[2]. Research indicates MPs alter microbial communities and metabolic processes, affecting carbon, nitrogen, phosphorus, and sulfur cycling[3]. They influence greenhouse gas emissions and microbial functional genes, with different types of MPs exerting varying effects. This study investigates how MPs affect microbial communities and biogenic element cycling in a freshwater lake, aiming to provide insights for managing water pollution risks.

## 2 Materials and methods

The study collected natural water samples from a wetland area in northern China and examined the presence and effects of microplastics (MPs) on microbial communities. Three types of MPs commonly found in freshwater environments were chosen for the experiment. These MPs were transformed into fibrous particles resembling those typically found in water bodies. The experiment involved incubating water samples with different MP treatments for 28 days and then analyzing microbial communities through metagenomic sequencing. The sequencing data underwent various processing steps, including quality filtering, taxonomical classification, assembly, gene prediction, and functional annotation. Microbial diversity and composition were analyzed using several statistical methods. The study aimed to understand how MP pollution affects microbial communities in aquatic environments, with implications for ecosystem health and water quality management.

## 3 Results

Research findings indicate that a total of 1,962,023,888 reads were generated from 14 samples, with an average of 140,144,563.4 reads per sample. Before analysis, short reads (<50 bp) and reads containing ambiguous bases were removed. The composition and dominant species abundance of microbial communities in water samples varied with microplastic (MP) type and incubation time. Following MP addition, the dominance of key species also changed. Significant differences in microbial community composition were observed between each MP treatment group and the RAW group. *Sphingomonas sp. 32-66-10* and *Clavibacter sp.* were identified as dominant species across all samples. Relative abundance of *Sphingomonas sp. 32-66-10* increased significantly with MP addition compared to the RAW group. Additionally, MP addition led to a significant decrease in the relative abundance of *Clavibacter sp.* and some other microbial species. Indicator species analysis identified representative microbial communities in each treatment group, indicating a significant impact of MP pollution on the diversity and functional contribution of lake water microbial communities. According to α-diversity analysis and PCoA, the addition and type of MPs significantly altered the diversity and composition of lake water microbial communities. Quantitative analysis of carbon, nitrogen, phosphorus, and sulfur cycles showed that polyethylene (PE) had the greatest impact on microbial-driven biogeochemical cycles of carbon, nitrogen, phosphorus, and sulfur in lake water. Finally, MP pollution enhanced the biogeochemical cycling functions of certain microbes but reduced the functional contribution of others, indicating the impact of MP pollution on lake ecosystem.

## 4 Conclusions

This study found that different types of microplastics (MPs) affect microbial communities and nutrient cycling in lakes. MP addition promoted certain carbon pathways, increasing $CO_2$ and $N_2O$ emissions. MPs influenced phosphate and sulfate processes, potentially increasing phosphate and $H_2S$ production. Polyethylene had the strongest impact on nutrient cycling. Overall, MPs alter lake ecosystems, posing pollution risks. Understanding these effects is crucial for managing MP pollution. Future research should focus on long-term effects and quantifying pollutants affected by MPs.

## Reference

[1] L. Hildebrandt, F.L. Nack, T. Zimmermann, et al, Microplastics as a Trojan horse for trace metals, J. Hazard Mater Lett, 2 (2021) 100035.
[2] G.Y. Peng, R. Bellerby, F. Zhang, et al, The ocean's ultimate trashcan: Hadal trenches as major depositories for plastic pollution, J. Water Res, 168 (2020) 115121.
[3] S. Sridharan, M. Kumar, N.S. Bola, et al, Are microplastics destabilizing the global network of terrestrial and aquatic ecosystem services, J. Environ. Res. 198 (2021) 111243.

**Theme:** Technologies for water management and monitoring
**IAHR Thematic Priority Area:** [TPA-4] Digital Transformation
https://doi.org/10.3850/iahr-hic2483430201-52

# Water Quality Monitoring of Inland Waters Using Remote Sensing Based on GEE and Sentinel-2 Imagery

**Wei Jiang [1], Fanping Kong [2], Xiaohui Ding [3], Gan Luo[1], Zhiguo Pang[1]**

[1] China Institute of Water Resources and Hydropower Research, A-1 Fuxing Road, Haidian District, Beijing 100038, China
[2] Beijing Capital Air Environmental Science & Technology Co., Ltd., Beijing 100176, China
[3]School of Software and Internet of Things Engineering, Jiangxi University of Finance and Economics, 665 Yuping Road, Nanchang 330013, China

*Corresponding author: Wei Jiang. jiangwei@iwhr.com*

**Abstract.** Accurate determination of spatiotemporal distribution characteristics of water quality parameters holds pivotal importance in monitoring water environments and aquatic ecosystems. This study is centered on the rivers and lakes within Jiujiang city, aiming to address the increasing need for more efficient, comprehensive, and continuous water quality remote sensing monitoring. Leveraging the Google Earth Engine (GEE) cloud platform and Sentinel-2 satellite data, three crucial water quality parameters—Total Nitrogen (TN), Total Phosphorus (TP), and Chlorophyll-a (Chla) concentration—are chosen for investigation. Through amalgamating field water quality sampling data, statistical regression models were formulated to enable remote sensing monitoring of water quality parameters. This advancement significantly enhances the efficiency of routine water quality monitoring and assessment, offering a scientific basis for decision-making in water environmental management.

**Keywords:** Water quality monitoring, remote sensing, Google Earth Engine, Sentinel-2,

## 1 Introduction

Currently, water quality remote sensing monitoring primarily focuses on optical parameters with distinct optical characteristics, such as chlorophyll-a concentration (Chla), suspended particulate matter (SPM), and colored dissolved organic matter (CDOM)[1-2]. Some studies have utilized empirical models based on remote sensing data to establish TP and TN inversion models for Lake Taihu with relatively high accuracy regarding the waters of Jiujiang City [3-4]. Based on the GEE cloud platform and Sentinel-2 satellite data, combined with traditional water quality monitoring station data, the spectral response characteristics of total nitrogen (TN), total phosphorus (TP), and chlorophyll-a (Chla) concentrations are comprehensively analysed. We have employed an empirical algorithm to construct a water quality parameter inversion model. By applying this model to Sentinel-2 satellite imagery data from the past three years, we have studied the spatiotemporal variations of water quality parameters in the rivers and lakes of Jiujiang City. The results could provide decision support for comprehensive water environment management in Jiujiang City.

## 2 Methodology and results

The research method is to achieve remote sensing quantitative inversion of TN, TP and Chla by analyzing the spectral response mechanism of water quality, carrying out water body extraction of rivers and lakes, building a remote sensing sample library of water quality parameters through the GEE platform. Based on the flowchart, the water quality parameter mappings, including TN, TP and Chla, are generated in Figure1.

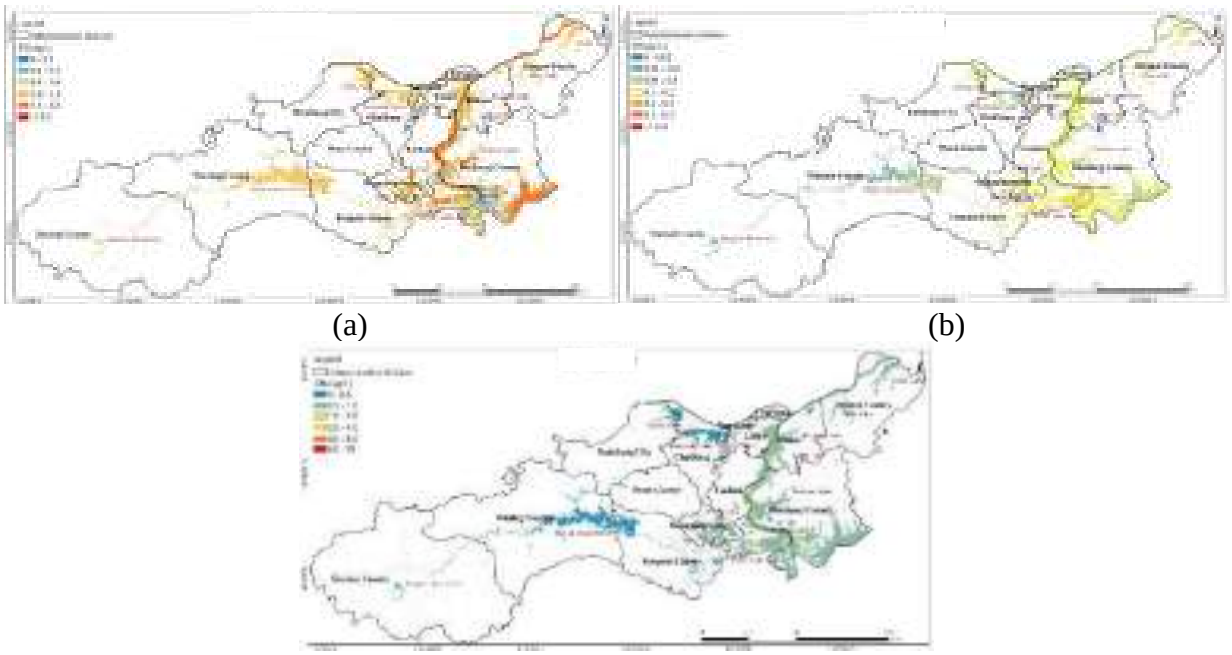

(a) (b)

(c)

Figure 1 Water quality parameters inversion result based on remote sensing ((a) is TN, (b) is TP, (c) is Chla)

## 3 Conclusion

This paper utilizes the GEE cloud platform to generate three water quality parameter mapping, namely TN, TP, and Chla concentrations, based on conventional empirical models. This advancement significantly enhances the efficiency of routine water quality monitoring and assessment, offering a scientific basis for decision-making in water environmental management.

## 4 Acknowledgements

This research was financially supported by the National Natural Science Foundation of China (42301450), the National Key Research and Development Program of China (2022YFC3301600 and 2023YFE0110300) and Scientific and Technological Innovation Talent Project of the Disaster Reduction Center of IWHR (WH0166B012023).

## Reference

[1] Palmer S C J, Kutser T and Hunter P D. Remote sensing of in-land waters: challenges, progress and future directions. RemoteSensing of Environment, 2015, 157: 1-8

[2] Li S, Song K, Wang S, et al. Quantification of chlorophyll-a in typical lakes across China using Sentinel-2 MSI imagery with machine learning algorithm[J]. Science of the Total Environment, 2021, 778: 146271.

[3] Pahlevan N, Smith B, Alikas K, et al . Simultaneous retrieval of selected optical water quality indicators from Landsat-8, Sentinel-2, and Sentinel-3[J].Remote Sensing of Environment,2022, 270.

[4] Jiang W , Ni Y , Pang Z ,et al.An Effective Water Body Extraction Method with New Water Index for Sentinel-2 Imagery[J].Water, 2021, 13(12):1647.

**Theme:** Technologies for water management and monitoring
**IAHR Thematic Priority Area:** [TPA-4] Digital Transformation
https://doi.org/10.3850/iahr-hic2483430201-54

# Channel Flow Field Recognition Method and Application Based on Eagle-eye Bionic Vision

**Hairong Gao [1], Zihan Liu[1], Yu Han[*,1]**

[1] College of Water Resources and Civil Engineering, China Agricultural University, Beijing 100083, China

*Corresponding author: yhan@cau.edu.cn*

**Abstract.** This manuscript establishes a cloud-edge integrated platform for intelligent perception of hydrological information. It constructs an Eagle-eye bionic vision intelligent flow measurement model and equipment suitable for multi-level canal networks, achieving real-time perception of water information and quantified representation of the entire flow field. The Eagle-eye bionic vision intelligent flow measurement equipment integrates a monocular camera and a binocular camera. The monocular camera is utilized to capture surface flow images of the channel. The binocular camera recognizes the waterline based on the deep learning algorithm, constructs the triangular model of water level, measuring point and distance measurement, and senses the depth of parallax in binocular stereo sense, and monitors the water level information of the canal system in real time. Further integration of monocular flow measurement and binocular water depth recognition technologies, combined with logarithmic laws, allows for the derivation of cross-sectional average flow velocity.

**Keywords:** Eagle-eye bionic ision,Channel flow field identification,Intelligent flow measurement equipment

## 1 Introduction

Irrigation stands as one of the principal factors enhancing crop yield, with irrigation districts constituting vital public infrastructure projects in China, crucial for national food security. Moreover, the most substantial water-saving potential lies within these irrigation districts. Monitoring water flow serves the primary purpose of understanding the state of water resources, encompassing parameters such as flow rate, velocity, and water level, facilitating improved planning, management, and conservation of water resources.

## 2 Material and methods

In July 2023, the Eagle-Eye bionic vision intelligent flow measurement equipment test was carried out in the Xiwu Canal of Jin 'an Irrigation District in Xinjiang. The length of the test section of the Xiwu Canal is about 80 m and the width is about 4.2 m. During the experiment, the monocular camera and binocular camera were taken in video mode, and the image resolution was 3840 × 2160 pixels. The shooting time is about 10 minutes once, 100 s video is selected, 1200 frames are extracted for analysis, and the interval between adjacent images is 0.4 s.

In this study, the logarithmic law is used for calculating the mean flow velocity across sections, with the calculation formula as follows:

$$\mathrm{u} = A\ln y + B \tag{3}$$

Where, A represents $Au_*$, B represents $\mathrm{u}_* A\ln\left(\frac{u_*}{\nu}\right) + Bu_*$, B represents the correlation coefficient, u* represents the local shear velocity, ν represents the kinematic viscosity of water, y represents the distance from each point on the vertical line in the channel to the sidewall.

## 3 Results

To calculate the flow rate across the channel section, it is necessary to obtain the velocity distribution across the entire section. This involves integrating the water level values calculated using the YOLO algorithm based on deep learning and the surface flow velocities calculated using the dense optical flow method. Once the values of A and B in the formula for calculating the velocity distribution across the section are determined, the velocity across the entire section can be calculated using these values.As shown in Figure 1, the distribution of velocity across the section can be obtained by analyzing the velocity distribution pattern across different zones of the section. The velocity distribution across the entire section of the channel exhibits a roughly symmetrical pattern. Analyzing the flow velocity in the normal direction, it is observed that the velocity increases when moving away from the sidewalls, with the maximum velocity occurring at the water surface. This is because the sidewall resistance is high, resulting in a lower velocity along the sidewalls of the channel section.

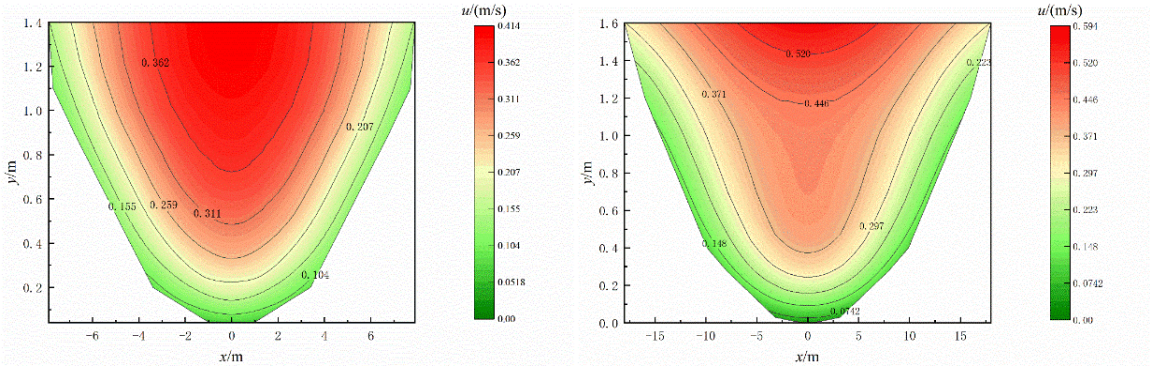


Figure 1 Distribution of Flow Velocity Across Channel Section

## 4 Conclusion

The application of the optical flow method and YOLO algorithm to channel flow field recognition indicates that the calculated flow velocity and water level values are close to the actual flow velocity measured by the portable flowmeter and the water level values measured by the staff gauge, with a model accuracy of over 90%.

The combination of monocular flow measurement and binocular water level recognition technology, along with the logarithmic law, allows for the accurate calculation of mean flow velocity across sections.

## References

[1]Zhiyu, L., Yuhuan, L. & Xiangyi, K. 2021 Problems, strategies and key technology research of flood forecasting and early warning for small and medium-sized rivers. Journal of Hohai University (Natural Sciences) 49 (1), 1–6.

[2]Fu, M., Luo, Z., Feng, L. & Que, X. 2023 Water productivity maximization and ecosystem monitoring to estimate tourism economic value. Water Supply 23 (11), 4672–4681.

[3]Letessier, C., Cardi, J., Dussel, A., Ebtehaj, I. & Bonakdari, H. 2023 Enhancing flood prediction accuracy through integration of meteorological parameters in river flow observations: A case study Ottawa river. Hydrology 10 (8), 164.

[4]Maranzoni, A., D'Oria, M. & Rizzo, C. 2023 Quantitative flood hazard assessment methods: A review. Journal of Flood Risk Management 16 (1), e12855.

[5]Ichiro, F. 2017 Discharge measurements of snowmelt flood by space-time image velocimetry during the night using far-infrared camera. Water 9 (4), 269.

**Theme:** Technologies for water management and monitoring
**IAHR Thematic Priority Area:** [TPA-4] Digital Transformation
https://doi.org/10.3850/iahr-hic2483430201-56

# The impact of the Three Gorges Reservoir on Nitrogen and Phosphorus Concentrations in the Middle Reach of the Yangtze River

**PENG Lian, ZHAO Min, QIAN Bao***

Bureau of Hydrology, Changjiang Water Resources Commission，Wuhan，Hubei 430010，China

*Corresponding author: jacber@163.com*

**Abstract.** In order to explore the impact of the operation of the Three Gorges Project on the nitrogen and phosphorus nutrient levels in the middle reaches of the Yangtze River over the past decade, based on the monitoring data of NH3-N and TP concentrations in the main stream of the Yangtze River from 2013 to 2022 at Yichang, Jianli, Luoshan, No. 37 Dock, Huangshi，Jiujiang, Chenglingji and Xiantao sections, the inter-annual variation trend of nitrogen and phosphorus concentrations in the main stream of the Yangtze River was explored by using the spearman rank correlation coefficient method. The results showed that the concentration of NH3-N in the middle reaches of the Yangtze River was at a relatively low level during the study period. Except for Jianli and Jiujiang sections, the other sections could meet the Class I water standard. The TP concentration in the middle reaches of the Yangtze River is basically in the Class III water standard, while the TP content in the section from Chenglingji and Xiantao is relatively low, reaching the Class II water standard. During the study period, the concentrations of $NH_3$-N and TP in the middle reaches of the Yangtze River showed an overall significant downward trend.

**Keywords:** the Three Gorges Reservoir；nitrogen and phosphorus concentration；spearman rank correlation coefficient method；inter-annual variation；intra-annual variation

## 1 Introduction

Nutrient enrichment in water bodies has become a global environmental issue. Elevated concentrations of nutrients such as nitrogen and phosphorus in water are the primary factors triggering eutrophication. After the formal operation of the Three Gorges Dam, it may have an intercepting effect on nutrient salts in the water. Eutrophication of water bodies leads to the excessive growth of planktonic organisms and algae, rapid depletion of dissolved oxygen, and a significant deterioration in water quality. This study examines the overall levels and interannual trends of NH3-N and TP concentrations in the middle reaches of the Yangtze River, exploring the impact of the Three Gorges Dam operation on nitrogen and phosphorus in the water, providing important data for water quality management in the middle reaches of the Yangtze River, and serving as a reference for the prevention and control of water body eutrophication.

## 2 Methods

We employed the Spearman rank correlation coefficient method to perform significance tests on the interannual trends of NH3-N and TP concentrations in the water at various monitoring sections. The formula for calculating the Spearman rank correlation coefficient is as follows:

$$d_i=X_i-Y_i$$

## 3 Results

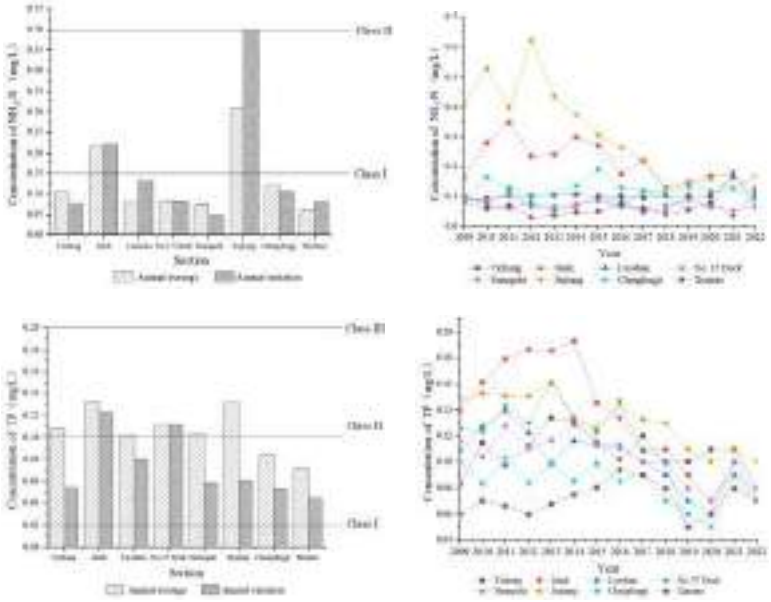

Figure 1 Annual mean value 、 inter-annual amplitude and Inter-annual change curve of ammonia nitrogen and total phosphorus concentration in the middle reaches of Yangtze River

The results of the Spearman rank correlation coefficient test indicate that at α=0.05 significance level, the Jianli section shows statistical significance, indicating an overall decrease in water $NH_3$-N concentrations. At α=0.01 significance level, the Jiujiang section shows statistical significance, further confirming an overall decreasing trend in water $NH_3$-N concentrations.The results of the Spearman rank correlation coefficient test show that at α=0.05 significance level, the No.37 Dock and Chenglingji sections exhibit statistical significance, indicating an overall decrease in water TP concentrations. At α=0.01 significance level, the Jianli, Luoshan, Huangshi, and Jiujiang sections show statistical significance, further confirming an overall decreasing trend in water TP concentrations.

## 4 Conclusion

During the study period, there was significant spatial variation in $NH_3$-N concentrations in the water of the middle reaches of the Yangtze River. $NH_3$-N concentrations were higher in the upper reaches of the Yangtze River and at the confluence of the middle and lower reaches, exceeding Class II water quality standards, while the main stream of the middle reaches, Dongting Lake, and the Han River met Class I water quality standards.The spatial variation in TP (total phosphorus) concentrations in the water of the middle reaches of the Yangtze River was relatively small. The annual mean and interannual variations in TP concentrations in the main stream of the middle reaches of the Yangtze River were slightly higher than those in Dongting Lake and the Han River.The years 2012 to 2013 marked an important turning point in water quality changes in the middle reaches of the Yangtze River.

## References

[1]ZHANG X G, CHEN M L, LIU P R, et al. Spatial Variability of Soil Organic Matter in Typical Area of the Yellow River Delta[J]. Journal of Yangtze River Scientific Research Institute,2017,34(5): 27-30.

[2]YANG J J. The Historical Analysis on the Evolution of the relationship Between Economy and Ecology in the Yangtze River Economic Zone (from 1979 to 2015) -Taking Water Environment as the Center[D]. Wuhan: Zhongnan University of Economics and Law,2018.

[3]TANG D L, DI B P, WEI G F, et al. Spatial, seasonal and species variations of harmful algal blooms in the South Yellow Sea and East China Sea[J]. Hydrobiologia, 2006, 568: 245-253.

**Theme:** Technologies for water management and monitoring
**IAHR Thematic Priority Area:** [TPA-4] Digital Transformation
https://doi.org/10.3850/iahr-hic2483430201-58

# Numerical Study of The Dam Break of A Rock-Filled Porous Media Structure

**Behrad Tarami[1], Bahman Ehteshami[1] and Yee-chung Jin[1,*]**

[1] Faculty of Engineering and Applied Science, University of Regina, Regina, Saskatchewan, S4S0A2, CANADA

** Corresponding author: yee-chung.jin@uregina.ca*

**Abstract.** The Lagrangian method describes fluid motion by tracking individual fluid parcels and monitoring their properties as they move. In this study, the Moving Particle Semi-implicit method, a mesh-free numerical approach, is utilized to simulate the dam break of a rock-filled porous media structure. Due to the creation of shocks during the dam break, conventional treatment methods are inadequate, necessitating further refinements. Numerical simulations employing MPS demonstrate reasonable agreement with experimental data.

**Keywords:** dam break, MPS, particle method, rock fill dam.

## 1 Introduction

Flow or wave motion passing through porous media carries significant implications across various engineering fields, including harbor engineering, geotechnical engineering, hydrology, and coastal engineering. Porous media, characterized by randomly distributed pores within a rigid body, pose challenges for analytical modeling but are amenable to study through complex numerical simulations [1]. The Lagrangian approach, utilizing moving particles to discretize the problem domain, offers advantages such as simplified mesh generation, handling of large deformations, and easy tracking of interfaces and boundaries. Over the past decades, the Moving Particle Semi-implicit (MPS) [2] method has been successfully applied in numerous scientific disciplines in Civil, Environmental Engineering, Materials, and ocean Engineering. In these domains, the MPS method has demonstrated its efficacy in accurately reproducing the behavior of free-surface viscous flows.

The MPS method involves dividing the fluid into numerous particles, each carrying data on position, pressure, and velocity. Developed to analyze incompressible flows, the MPS method represents all components of the Navier-Stokes equations using particle interaction models, where each particle's motion is governed by its interactions with neighboring particles. Key advantages of the MPS method include its adaptability to complex topographies and its ability to capture discontinuities in solutions. Moreover, the MPS method can incorporate physical effects such as turbulence, non-linearities in equations, and moving boundaries and interfaces.

Notably, MPS is the method for spatial integration of partial differential equations and MPS extends the finite volume method to a mesh-free approach and utilizes particle number density to satisfy flow incompressibility, unlike the finite volume method, which relies on velocity divergence.

Dam break scenarios induce shocks upstream and downstream, presenting challenges for numerical solutions due to high hydraulic gradients. In this study, a one-dimensional MPS discretization is employed to model free-surface flow near a porous dam, effectively addressing these challenges.

## 2 Method

The MPS method characterizes the development of a physical system by modeling interactions between discrete particles. Each particle influences its neighbors, with the extent of influence determined by a specialized weighted function (kernel function). This influence is inversely

proportional to the distance between the particle and its neighbor. Employing a prediction-correction algorithm, the MPS method analyzes incompressible flows. Interaction between particles and neighboring particles is calculated using weight functions. Mesh-free solvers for Shallow Water Equations (SWE) automatically conserve mass, simplifying computation while maintaining accuracy [3].

## 3 Results

Simulations are conducted in a tank with specified dimensions and a block structure placed centrally. Fine glass balls with defined porosity form the porous structure. Comparisons between MPS results, experimental data, and other numerical models demonstrate the method's efficacy, particularly in simulating flow through the porous structure.

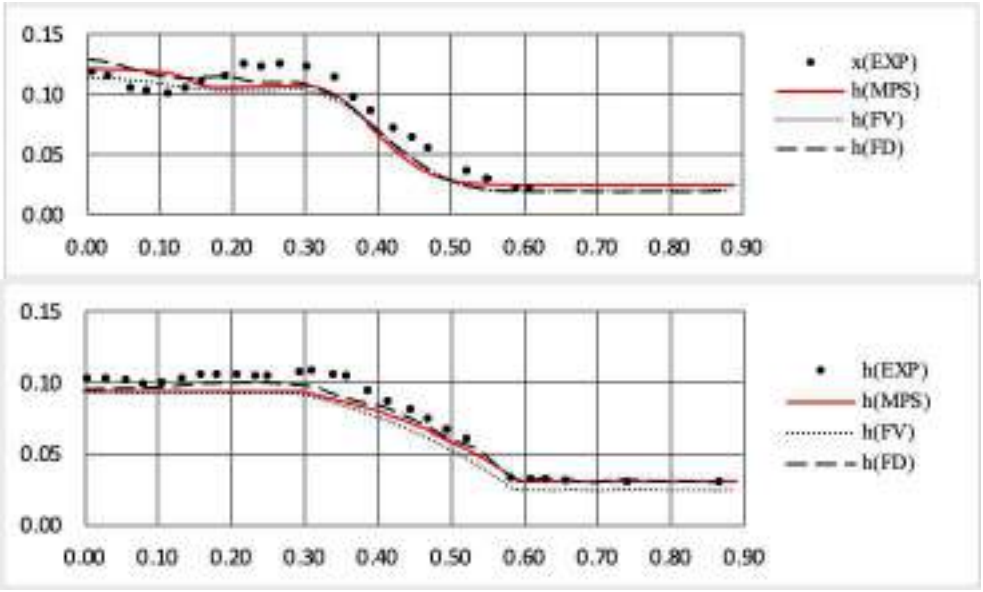


**Figure 1** Comparison between free surface height at: $t$=1.2s and $t$=4.0s.

The MPS results are compared with experimental data and different numerical models. As can be seen, MPS method has good results through the porous structure.

## 4 Conclusion

Investigations into particle size effects on water flow simulation accuracy reveal that a particle size of 0.001m balances accuracy and computational efficiency best. Smaller sizes yield less accurate results while incurring higher computational costs. Therefore, for the current problem, a particle size of 0.001m is deemed optimal.

## References

[1] Chwang A. and Chan A., 1998, Interaction between porous media and wave motion, Annual Review of Fluid Mechanics, 30, pp. 53-84. https://thermopedia.com/content/10120/.

[2] Koshizuka S. and Oka Y., 1996, Moving-particle semi-implicit method for fragmentation of incompressible fluid, Nuclear Science and Engineering, 123, pp.421-434.

[3] Sarkhosh P. and Jin Y.C., 2021, MPS-Based Model to Solve One-Dimensional Shallow Water Equations, Water Resources Research, 57, e2020WR028742.

**Theme:** Technologies for water management and monitoring
**IAHR Thematic Priority Area:** [TPA-4] Digital Transformation
https://doi.org/10.3850/iahr-hic2483430201-60

# Simulation of Winter Wheat Yields in North China Plain Based on DSSAT Model and Its Influencing Factors

**Yuan Shi[1], Yijun Guo[1], Yifan Li[1] , Meijian Bai[1], Yanan Liu[1]**

[1] China Institute of Water Resources and Hydropower Research, Beijing 100038, China

*Corresponding author: Yuan Shi. 86091263@qq.com*

**Abstract.** In this study, a wheat growth simulation model in the DSSAT software, was investigated for its ability to simulate the growth and yield of winter wheat in the region and to find the optimal plan for the estimation of genetic parameters and the model verification. The CERES-Wheat model was tested during a period of 2 years' field experiments under 11 different irrigation treatments . The experimental data were used to run the model. A total of 4 different plans for model calibration and verification were designed and the DSSAT-GLUE, a program package for parameter estimation in DSSAT, was used to estimate the relevant genetic coefficients. The CERES-Wheat model has certain limitations when simulating the agro-ecological processes of winter wheat in North China. If the CERES-Wheat model is expected to be applied more ubiquitously in the management and research of winter wheat in this area, then it is necessary to further investigate the water-stress response mechanisms of winter wheat and the simulation methods.

**Keywords:** Winter wheat; CERES-Wheat; DSSAT; Model calibration; Model validation; Irrigation

## 1 Introduction

In this study, the CERES-Wheat model was run using field experimental data for winter wheat grown under water stress at different growth stages in two consecutive growing seasons. Different plans for model parameter estimation and verification were analyzed and compared. The objectives of this study were: (1) to evaluate the reliability of the CERES-Wheat model for simulating the growth, development, and yield formation of wheat under water stress; and (2) to test four different plans for model calibration and validation, and select the optimal plan for simulating the agro-ecological processes of winter wheat under water stress. Our results provide evidence for the formulation of deficit irrigation regimes for winter wheat based on the CERES-Wheat model, and support further extensive applications of this model in simulation studies on agro-ecological systems in the arid and semi-arid areas of China.

## 2 Material and methods

The field experiment was conducted at the Water-Saving Irrigation Experimental Station (39°37.25′ N, 116°25.21′ E, 31.3m a.s.l.) in Daxing District, Beijing. The minimum weather data consists in solar radiation, daily maximum and minimum temperatures, and precipitation. Management data and crop parameters were gained from experimental data. Soil parameters were gained from experimental data.DSSAT-GLUE, a program package for parameter estimation, was used to calibrate the genetic coefficients of the winter wheat cultivar 'JM-22'.The evaluation of model calculation and validation was based on relative root mean square error (RRMSE) and absolute relative error (ARE) between simulated and measured values. The RRMSE and ARE indicate the relative difference between simulated and measured values, and both are dimensionless statistics that can be compared among different variables. Lower RRMSE and ARE values indicate higher simulation accuracy of the model.

## 3 Results and discussion

Comparing the results of model calibration and validation among the four different plans, all seven crop coefficients of winter wheat were within the parameter range of the DSSAT model.

The modulated precision of soil layers indicates that modulated precision and soil layers depth have positive correlation, the ARE and RRMSE of simulated and observed values are 18.1% and 21.3% , 13.8% and 16.5%, 10.9% and 12.7%, 5.1% and 6.1% respectively at different soil layers of depth 0-10cm,10-20cm, 20-40cm, 40-80cm.This is because the closer the distance of measured point to soil surface is, the more obvious the impact of climate changes, tillage and other factors to the soil-water content is, the greater the error of simulated and observed values is.

Based on the above analyses and related studies, the DSSAT model has high simulation accuracy for the growth, development, and yield formation of winter wheat under sufficient water and nutrient supply. However, for drought and staged water stress treatments, the simulation accuracy for crop grain quality and yield components varies depending on the stage at which water stress occurs. Our results showed that the simulation accuracy of the model is low under water stress, especially when water stress occurs after the jointing stage.

## 4 Conclusions

Parameter sensitivity analysis and suitability evaluation of the DSSAT-CERES-Wheat model is a key step in the estimation of winter wheat yield using the model. The results of this study can provide a scientific theoretical basis for parameter optimization and regional application of the DSSAT-CERES-Wheat model in Beijing area of North China.

## Acknowledgements

This study was financially supported by the National Key Research and Development Program (No. 2016YFC040140306) and Key Research and Development Program of Xinjiang Production and Construction Corps (No. 2019AB035)

## Reference

[1] Jones, J.W., G. Hoogenboom, C.H. Porter, K.J. Boote, W.D. Batchelor, L.A. Hunt, P.W. Wilkens, U. Singh, A. J. Gijsman, J.T. Ritchie, and 2003. "The Dssat Cropping System Model." *European Journal Agronomy* 18, no. 3-4 (2003): 235-65.doi:10.1016/s1161-0301(02)00107-7.

[2] Bannayan, M., H. Mansoori, and E. E. Rezaei. "Estimating Climate Change, $Co_2$ and Technology Development Effects on Wheat Yield in Northeast Iran." *International Journal of Biometeorology* 58, no. 3 (2014): 405-15.doi:10.1007/s00484-013-0635-1.

[3] Dettori, M., C. Cesaraccio, A. Motroni, D. Spano, and P. Duce. "Using Ceres-Wheat to Simulate Durum Wheat Production and Phenology in Southern Sardinia, Italy." *Field Crops Research* 120, no. 1 (2011): 1-188.doi:10.1016/j.fcr.2010.09.008.

[4] Thorp, K. R., D. J. Hunsaker, A. N. French, J. W. White, T. R. Clarke, and P. J. Pinter. "Evaluation of the Csm-Cropsim-Ceres-Wheat Model as a Tool for Crop Water Management." *Transactions of the ASABE* 53, no. 1 (2010): 87-101.doi:10.13031/2013.29505.

[5] He, J., M. Dukes, and J. Jones. "Applying Glue for Estimating Ceres-Maize Genetic and Soil Parameters for Sweet Corn Production." *Transactions of the ASABE* 52, no. 6 (2009): 1907-20

[6] He, J., J. W. Jones, and W. D. Graham. "Influence of Likelihood Function Choice for Estimating Crop Model Parameters Using the Generalized Likelihood Uncertainty Estimation Method." *Agricultural Systems* 103, no. 5 (2010): 256-64.doi:10.1016/j.agsy.2010.01.006.

**Theme:** Technologies for water management and monitoring
**IAHR Thematic Priority Area:** [TPA-4] Digital Transformation
https://doi.org/10.3850/iahr-hic2483430201-62

# Enhancing Water Quality Through Flood Control Reservoir Operations: An EFDC Modeling Approach for the Yeongsan River

**Seungjin Sim[1], Kwangduk Song[2], Wonmo Yang[2], Jaebeom Kwon[2], Yong-Gyun Park[1]**

[1] Department of Environmental and Energy Engineering, Chonnam National University, 77 Yongbong-ro, Buk-gu, Gwangju, 61186, Republic of Korea
[2] Gaon S&T, 1-6, Suwan-ro 52beon-gil, Gwangsan-gu, Gwangju, 62305, Republic of Korea

*Corresponding author: cherries1228@nate.com*

**Keywords:** environmental fluid dynamics code; flood control reservoir; monitoring and modeling; water quality improvement; Yeongsan River

**Abstract.**The Yeongsan River in South Korea faces significant water quality challenges despite its status as one of the country's major rivers. This study employs the Environmental Fluid Dynamics Code (EFDC) model to investigate the impact of freshwater and flood control reservoir discharge on the river's water quality. Utilizing data from the Yeongsan River Basic Plan Revision, the study conducted simulations and pilot operations at two flood control reservoirs to analyze water quality changes under various operational scenarios. Results indicated water quality improvements in parameters like COD, T-N, and T-P during discharge, while other parameters likes TOC and Chl-a exhibited varied water quality improvement effects depending on conditions. The study underscores the influence of flood control reservoir water quality and external factors on water quality improvements. However, the analysis was limited to a few discharge events, necessitating further research to comprehensively assess water quality improvements considering additional flood control reservoirs, diverse scenarios, and seasonal variations. This study aims to identify the optimal operation strategy for improving water quality and stable water supply in the Yeongsan River and thereby contribute to improving the river's ecosystem.

## 1 Introduction

The Yeongsan River in South Korea is recognized as one of the four major rivers in the country, yet it encounters significant water quality challenges. Despite having a relatively small watershed area, the river encompasses urban and densely populated regions. Unfortunately, the water quality in the Yeongsan River is compromised, primarily due to the release of water from agricultural dams and a structural vulnerability that leads to water shortages. This study employs the Environmental Fluid Dynamics Code (EFDC) model to comprehensively investigate the repercussions of freshwater and flood control reservoir discharge on the river's water quality. The primary objective is to gain a deeper understanding of these effects and to identify the most efficient operational strategies for enhancing water quality. Additionally, the study aims to ensure a stable water supply for various purposes and to contribute to the overall improvement of the river's ecosystem through rigorous testing and verification processes.

## 2 Methodology

The study used the EFDC model and depth data from the Yeongsan River Basic Plan Revision. The grid system had a calculation area of 36.6×49.4 km (16.141 km2), with grid spacing ranging from 6 to 330 meters, and a total of 3,176 grids. Three vertical layers were considered with elevation values from -6.4 to 71.8 meters. Experimental conditions included monitoring water levels at Jooksanbo and collecting meteorological data, such as wind direction and speed, from an Automatic Weather Station.

## 3 Result and conclusion

This study analyzed the water quality impact of flood control reservoirs' freshwater discharges. It simulated various operational scenarios for these facilities using the EFDC model to find optimal methods. Pilot operations were conducted at two reservoirs, monitoring water quality inside the reservoir and in the river during discharges. Analysis results showed water quality changes due to facility discharges. Various scenarios were created considering rainfall, discharge rates, and water quality standards, resulting in 48 scenarios. The EFDC model simulated water quality scenarios for parameters including COD, TOC, T-N, T-P, and Chl-a.

This study examined the effectiveness of flood control reservoirs in improving water quality under various conditions. It was observed that certain parameters, including COD, T-N, and T-P, exhibited water quality improvements meeting the favorable conditions during discharge. However, other parameters like TOC and Chl-a showed varying water quality improvement effects depending on the conditions. This variability appears to be influenced by the water quality status of flood control reservoirs and external factors such as inflow from the Yeongsan River. It is essential to note that the model used data from a limited number of freshwater releases. Therefore, further research considering more flood control reservoirs, diverse scenarios, and seasonal variations is necessary to assess water quality improvement effects comprehensively.

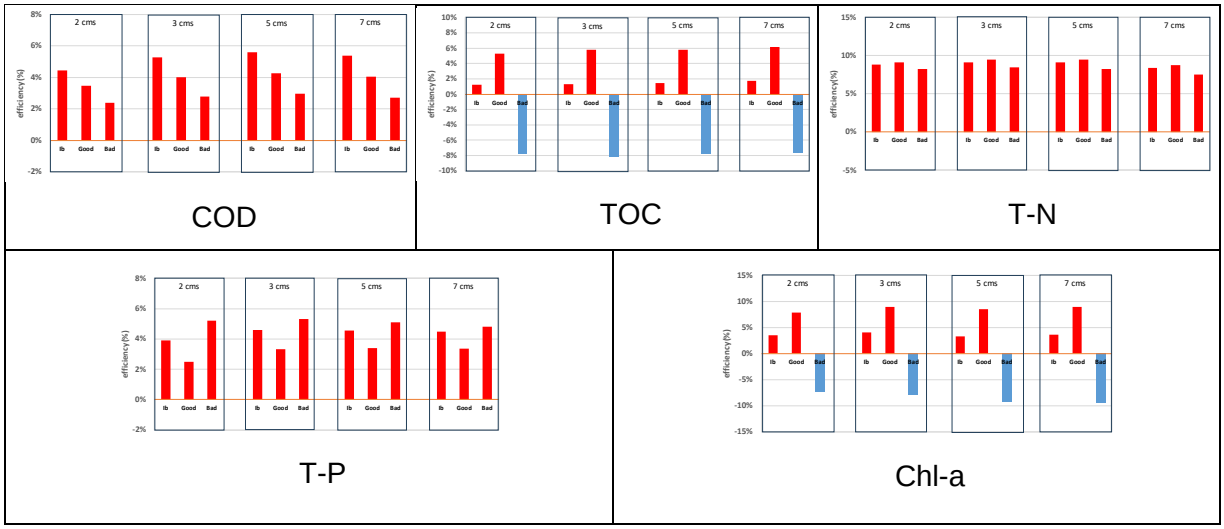


Figure 5 The analysis results of water quality improvement efficiency at the Naju Bridge

## Reference

[1] Kim J. S., Park S. C., Park S. H., Lee W. B., Water quality improvement effect of Yeongsan River in non-flooding season using detention reservoir, *Korean Society of Water Science and Technology*, **29**(4) (2021), 47-59.

[2] Ministry of Environment (Republic of Korea), Final report on survey research for the establishment of comprehensive water quality improvement measures for the Yeongsan River. 2021.

[3] Ministry of Environment (Republic of Korea), Final report on verification of optimal utilization of flood control areas for Yeongsan River water quality improvement and establishment of an implementation plan, 2023.

**Theme:** Technologies for water management and monitoring
**IAHR Thematic Priority Area:** [TPA-4] Digital Transformation
https://doi.org/10.3850/iahr-hic2483430201-64

# The Application of Smart Water Management System in Improving Urban Water Supply Efficiency

**Li Ziming[1],Song Xiaoying[2],Jing Ming[1],Chen Xiuhong[3],Chang Buhui[1]**

[1]Yellow River Conservancy Commission Yellow River Water Conservancy Research Institute,ZhengZhou 450000,China
[2]Luohe Water Resources Comprehensive Security Center,LuoHe 462000,China
[3]Yellow River Conservancy Commission Hydrological and Water Resources Survey Bureau,ZhengZhou 450000,China

*Corresponding author: Li Ziming.E-mail addresses:lzm7512523@163.com*

**Abstract.**Urban residents are densely populated, and the scale of water supply enterprises varies. The management situation is uneven, and the low efficiency of urban water supply is a common problem in the management of water supply enterprises. In the context of national carbon peak and carbon neutrality, water supply enterprises need to take more proactive measures to achieve industry goals of carbon compliance and carbon neutrality, and the improvement of efficiency management is an important link. The smart water management system optimizes network planning and water allocation by establishing a hydraulic model of the water supply and drainage network. The integration of GIS technology and traditional technology realizes three-dimensional visualization management of the network. DMA partition leakage management can monitor the leakage of each block at any time. In terms of operation management and later maintenance, the above technical measures can provide great convenience and save costs for water supply enterprises, Continuously improving the comprehensive management capacity and resource utilization level of urban water affairs.

**Keywords:** Smart Water management system Efficiency Management GIS DMA Zoning Hydraulic Model

## 1 Introduction

As an important carrier for transporting water resources, urban water supply networks are the lifeline of urban development. However, factors such as pipeline over service, severe corrosion, unreasonable layout, and low management level have caused significant waste of resources, and there is an urgent need for scientific and reasonable urban water supply management. Energy conservation and emission reduction are important means to achieve carbon peak and carbon neutrality. In the context of rapid development of information technology, the application of smart water management is of great significance for the development of urban water management and the improvement of efficiency management [1].

## 2 Method

### 2.1 Hydraulic optimization scheduling of water supply network

At present, there are problems such as lack of unified planning for urban water supply networks, high operating costs, serious pipeline leakage and explosion, lower transmission and distribution capacity than water supply demand, and outdated water supply management level.These problems can be solved through hydraulic optimization scheduling models for water supply networks[2].

### 2.2 GIS 3D visualization management of pipeline network

At present,the management of underground water supply pipelines has the characteristics of single means,high manpower and material resources consumption,long feedback time intervals,and inconvenient data storage,which make it unable to effectively protect the underground water supply

pipeline network,resulting in repeated damage to the pipeline network during construction[3].At the same time,it is difficult to accurately judge during emergency repairs,leading to the inability to effectively deal with the occurrence of fault events.Therefore, it is necessary to use GIS three-dimensional visualization of pipeline networks to achieve effective management of urban water supply networks.

### 2.3 DMA Partition Leakage Management System

At present, the leakage rate of various water supply enterprises in China remains high,and it is difficult for them to effectively solve it by adopting an empirical control leakage model.But the Partition Measurement (DMA) management mode is one of the good management modes[4]. Drawing on the management experience of the foreign water supply industry, the Zone Measurement (DMA) management model is one of the good management models[5].

## 3 Results

In the process of improving the efficiency management of the smart water management system in the urban area of Zhengzhou,China,hydraulic optimization scheduling of the water supply network,GIS three-dimensional visualization management of the network,and DMA zoning leakage management system were adopted,and good results were achieved.

## 4 Conclusion and suggestions

### 4.1 Conclusion

Through the hydraulic optimization and scheduling of the water supply network in the smart water management system,the three-dimensional visualization management of the network GIS,and the DMA zoning leakage management system,significant improvements have been made in urban water supply efficiency management.This will play a better role in achieving the industry goals of carbon compliance and carbon neutrality in the future.

### 4.2 Suggestions

There are some difficulties that need to be explored in improving the efficiency of urban water supply through smart water management.

(1) In the future, it is expected to optimize the scheduling of water supply quality with the water supply quality as the objective function. And combining water quality regulation with energy regulation is also a new challenge that needs to be solved in the future.

(2) Combining with smart cities requires a greater emphasis on analysis and the integration of IoT technology to create a smart pipeline network.

(3) In terms of automatic partitioning of pipeline networks, we look forward to exploring a fully automated algorithm that is not affected by human intervention in the future.

## References

[1] Yu Liu.Discussion on the construction of a unified remote data collection platform for the Internet of Things in smart water management[J].Environmental engineering,2023,11(3):31-40.

[2] Robak Anna.Perceived measured water supply service:evidence from New Zealand[J].International Journal of Water Resources Development,2022,38(6).19-23.

[3] Na Zhou,Shu Li,Peng Chen,et al.Beijing Water Resources Dispatching Business System for Smart Water Management[J].China Water Resources,2023,14(05):55-58.

[4] Nasiha H J, Shanmugam P. Estimation of settling velocity of sediment particles in estuarine and coastal waters[J]. Estuarine, Coastal and Shelf Science, 2018, 203: 59-71.

[5] Selim Ahmed M..A newera for public-private partnership (PPPs) in Egypts urban water supplyprojects:risk assessment and operating model[J].HBRC Joumal,2022,18(1).12-16.

**Theme:** Technologies for water management and monitoring
**IAHR Thematic Priority Area:** [TPA-4] Digital Transformation
https://doi.org/10.3850/iahr-hic2483430201-66

# Sediment Discharge Prediction for the Xiaolangdi Reservoir Based on Machine Learning Algorithms

**Junchao Shi[1,2], Xinjie Li[2], Hailong Wang[1],Xiaofei Yan[2],Qiang Wang[2],Jie Liu[3]**

[1] Zhongyuan University of Technology, Zhengzhou 45007, China
[2] Yellow River Institute of Hydraulic Research, YRCC,Zhengzhou,45003, China
[3] Huanghe Science and Technology University, Zhengzhou,450063,China

*Corresponding author: Li.xin_wd@163.com*

**Abstract.** In response to the limited capability of one-dimensional flow and sediment models to represent complex hydrological conditions, this research incorporates two machine learning algorithms, namely K-Nearest Neighbors (KNN) and Gradient Boosting Regression (GBR), to predict sediment discharge in reservoirs. The simulation utilizes flow and sediment data from the Xiaolangdi Reservoir spanning the years 2000 to 2019. The simulation results indicate that among the various machine learning algorithms employed for constructing sediment discharge prediction models, the Gradient Boosting Regression (GBR) exhibits the best performance. The experimental findings demonstrate that the algorithmic simulation results can serve as references for sediment discharge prediction in reservoirs and subsequent scheduling strategies.

**Keywords:** machine learning algorithm; reservoir sediment discharge; prediction model

## 1 Introduction and method

In recent years, many outstanding researchers and professionals have made remarkable progress in water flow and sediment transport studies through unremitting exploration and innovation, and they have successfully improved water flow and sediment transport prediction models and enhanced the prediction accuracy. For example, Li et al.[4] established a random forest-support vector machine (RF-SVM) model to predict runoff of the Longjiang Reservoir. The experimental results show that the overall accuracy of the model is high enough to meet the requirements, but there is still room for improvement regarding local extreme flow prediction. Liu et al.[5] applies the long short-term memory (LSTM) neural network to the prediction of monthly precipitation, and the authors experimentally proved that the prediction accuracy of the LSTM model is higher than that of other models, which is more accurate than other models. The prediction accuracy of the LSTM model is higher than other models. Similarly, Tong[6] adopted the LSTM algorithm to improve the accuracy of river flow and sediment transport prediction by utilizing the temporal nature of hydrological data. In the aforementioned study, several researchers employed various algorithms to predict water-sediment dynamics, aiming to identify an optimal model combination with minimal errors and the capability to provide relatively accurate forecasted data. The Xiaolangdi Reservoir was examined in this research, in which two types of predication models, namely k-nearest neighbors regression (KNN) and gradient boosting regression (GBR), were used. Their prediction results were compared to determine the optimal model for sediment discharge prediction.

## 2 Model performances and comparisons

Machine learning algorithms were introduced to establish KNN and BGR prediction models. After that, selected data was input to obtain the reservoir sediment discharge predicted by different models. The correlation analysis graph for predicted and actual values using GBR and KNN algorithms is shown in Figure 1.

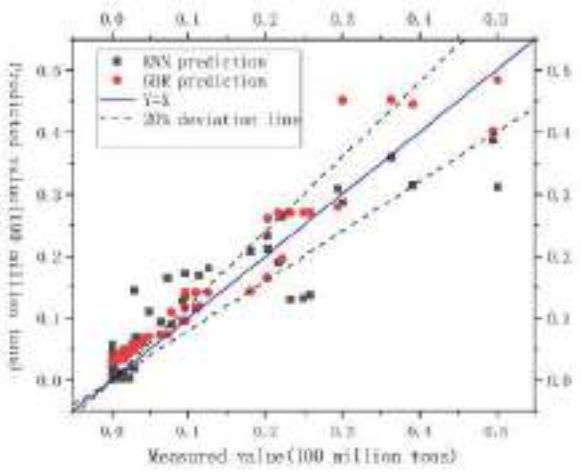


Figure 6 Correlation analysis between predicted and true values

## 3 Conclusions

In this research, a GBR-based model was used to predict the reservoir sediment discharge under the influence of multiple factors. Relevant datasets were created by data preprocessing, such as removing null values and outliers. A reservoir sediment discharge prediction model was then established by carefully selecting features according to the processed data. The results suggest that the model is reasonably accurate and precise in predicting the reservoir sediment discharge. However, it is worth noting that few model-predicted values differ considerably from the true values. The problem may be caused by special circumstances or unusual events, and this has to be addressed and solved in future practical applications. Overall, most model-predicted values are close to the true values, confirming the robustness and reliability of machine learning in reservoir sediment discharge prediction. These findings provide useful references for further application and optimization of the algorithm.

## Reference

[1] Longfei Sun,Xiujie Guo,Ting Wang, et al. Study on the estimation of sediment composition in the released sediment during the water diversion and sediment release period of the Xiaolangdi Reservoir ［J］. Yellow River of China, 2022, 44(8): 47-51.

[2] Li Wu,Zuheng Wang,Liang Wang, et al. Water Quality Monitoring and Evaluation of Xiaolangdi Reservoir in the Yellow River Based on Principal Component Analysis and Fuzzy Mathematics[J]. Bulletin of Soil and Water Conservation, 2020, 40(05): 118-124.

[3] Zhixiang You,Xiaoyang Hu. A Brief Discussion on the Safety Production Supervision of Xiaolangdi Water Conservancy Hub[J]. Yellow River of China, 2023, 45(S2): 118-119.

[4] Lingjie Li, Yintang Wang, Hu Qingfang, et al. Long-Term Reservoir Runoff Forecast Based on Random Forest and Support Vector Machine[J]. Journal of Water Resources and Water Transport Engineering, 2020, (4): 33-40.

[5] Xin Liu,Ning Zhao,Jinyun Guo, et al. Monthly Precipitation Forecast on the Qinghai-Tibet Plateau Based on LSTM Neural Network[J]. Journal of Geo-Information Science, 2020, 22(8): 1617-1629.

[6] Taowen Tong. Research on River Runoff and Sediment Concentration Prediction Method Based on LSTM Deep Learning [J]. Journal of Irrigation and Drainage, 2021,40(S1):1-4.

[7] Wenxing Li,Tiancheng Wang,Huawei Li. Method of Automatic Test Vector Generation for Digital Circuits Based on K-Nearest Neighbor[J]. Journal of Computer-Aided Design & Computer Graphics, 2023, 35(11): 1802-1810.

[8] Karthikeya H K, Sudarshan K, Shetty D S. Prediction of agricultural crops using KNN algorithm[J]. Int. J. Innov. Sci. Res. Technol, 2020, 5(5): 1422-1424.

[9] Xiaofei Yan,Xiujie Guo,Longfei Sun. Research on Sand Discharge Prediction of Wanjiazhai Reservoir Based on Machine Learning Algorithms[J]. Water Resources and Power, 2023, 41(03): 79-82.

**Theme:** Technologies for water management and monitoring
**IAHR Thematic Priority Area:** [TPA-4] Digital Transformation
https://doi.org/10.3850/iahr-hic2483430201-68

# Analysis of Influencing Factors and Water Conservation Potential of Household Water Consumption in China

**Liwei Zhan [1], Yongnan Zhu [1], Mengyuan You [1], Yong Zhao [1], Haihong Li [1]**

[1] China Institute of Water Resources and Hydropower Research, Beijing 100038, China

*Corresponding author: zhyn@iwhr.com*

**Abstract.** Domestic water consumption is currently the fastest growing sector in China's socio-economic water demand, and there is an urgent need for detailed and systematic analysis. To address this issue, a questionnaire was designed to collect relevant information on water use by Chinese residents, including dining, bathing, laundry, toilet flushing, household cleaning, as well as personal hygiene. The study analyzed factors influencing residents' domestic water use, and various water-saving scenarios were set to explore water-saving potential. The study found a 21% difference in per capita domestic water use among residents in different regions of China. Bathing, with an average water consumption of 38L/person·day, was identified as the primary water behavior causing this difference and a key area for future fine water monitoring and conservation efforts. Simulating scenarios to enhance residents' water-saving awareness, implementing water-saving measures, and replacing high-efficiency water appliances could save 32% of per capita domestic water use in China. It is recommended to continuously promote water-saving efforts according to the characteristics of domestic water use in different regions of China.

**Keywords:** influence factor, residential water consumption, water conservation potential

## 1 Introduction

In recent years, there has been a continuous increase in residential water consumption in China. As urbanization quality continues to improve in China, residential water consumption will become the main growth point of China's economic and social water use, as well as a key focus of water conservation efforts. Domestic water consumption is currently the fastest growing sector in China's socio-economic water demand, and there is an urgent need for detailed and systematic analysis. To address this issue, this study designs a survey questionnaire on residents' water consumption habits. The aim is to collect relevant information on fine-grained water use among residents, accounting for six categories of behaviors: dining, bathing, laundry, flushing, household cleaning, and personal hygiene. The study analyzes the characteristics of water consumption among residents in different regions of China and examines the differences. It constructs a model of influencing factors on residential water consumption, identifying key factors affecting water use. The study creates water-saving scenarios to explore the potential for saving water in residential consumption. This study aims to provide technical and practical support for the fine-grained monitoring and management of residential water consumption and to promote water conservation efforts.

## 2 Data sources

The data were collected through a survey questionnaire, which primarily included 37 items of detailed water-related information such as residents' personal and household basic information, water usage behaviors, water conservation awareness, and the water efficiency status of appliances. The research team distributed the survey questionnaires nationwide using a combination of offline visits and online distribution methods from October 2020 to November 2022. A total of 18,438 questionnaires were collected, and after preprocessing the questionnaire data, 18,180 were deemed valid, with an effective rate of 98.6%.

## 3 Results and discussion

The results indicate that the average per capita daily residential water consumption in China is 113 L/(person·day). Across different regions, there is a 21% difference in the total per capita daily residential water consumption. Overall, gender, age, household size, and income level have significant effects on water usage. Under the comprehensive water-saving scenario involving increasing residents' water conservation awareness, replacing higher water efficiency grade appliances, and utilizing household wastewater, the average per capita daily residential water consumption in China can decrease to 77 L/(person·day), reducing the current water consumption by approximately 32%. In all regions, the per capita daily residential water consumption will decrease by over 30%, indicating a significant and positive water-saving effect.

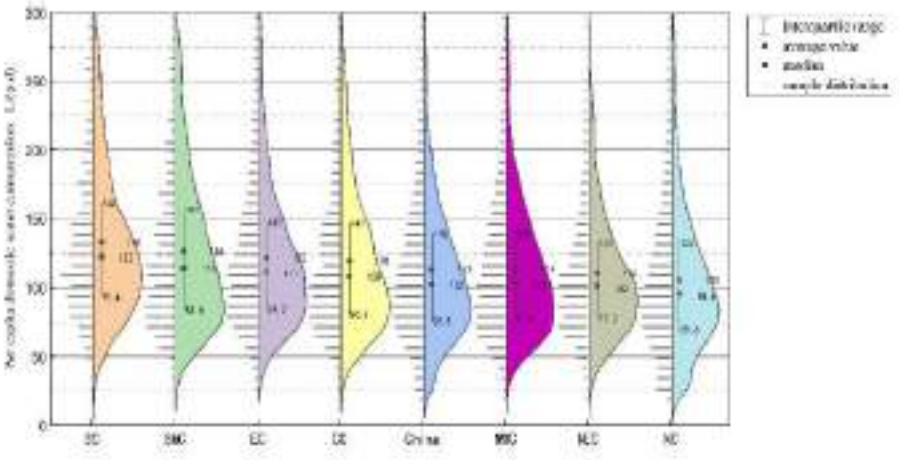

Figure 7 Frequency histogram of per capita domestic water use

## 4 Conclusion

In the future, focusing on reducing water consumption in bathing and personal hygiene will be crucial for water conservation efforts in China. This involves further analyzing water usage patterns, understanding the driving mechanisms behind them, and tailoring strategies to the water usage characteristics and habits of different user groups.

There is still untapped potential for water conservation in different regions of China. It is essential to continue promoting water conservation efforts tailored to the specific characteristics of each region. By thoroughly exploring the potential for water conservation in daily life, we can enhance the efficient utilization of water resources in different regions, which is crucial for ensuring water security and sustaining economic and social development in China.

## Reference

[1] Shi L R, Wang L Z, Li H H, et al. Impact of residential water saving devices on urban water security: the case of Beijing, China[J]. Environmental Science: Water Research & Technology,2022,8:326-342.

[2] Makki, A. , Stewart, R. , Panuwatwanich, K. , & Beal, C. Revealing the determinants of shower water end use consumption: enabling better targeted urban water conservation strategies. Journal of Cleaner Production, 2013, 60: 129-146.

[3] Gregory, G.D., Di Leo, M.. Repeated behavior and environmental psychology: the role of personal involvement and habit formation in explaining water consumption [J]. Journal of Applied Social Psychology, 2003, 33: 1261-1296.

**Theme:** Technologies for water management and monitoring
**IAHR Thematic Priority Area:** [TPA-4] Digital Transformation
https://doi.org/10.3850/iahr-hic2483430201-70

# River Flow Monitoring: The Influence of Graphical Enhancement Techniques on Image Velocimetry Performances

**Francesco Alongi[1], Silvano Dal Sasso[2], Robert Ljubičić[3], Dario Pumo[1], Leonardo V. Noto[1]**

[1] University of Palermo, Palermo, 90145, Italy
[2] University of Basilicata, Matera, 75100, Italy
[3] University of Belgrade, Belgrade, 11120, Serbia

*Corresponding author: francesco.alongi01@unipa.it*

**Abstract.** Image velocimetry techniques for river flow monitoring have progressively spread due to the advantages of such methods with respect to traditional approaches. Image-based techniques can non-intrusively provide river discharge, with accuracy depending on several factors (e.g., environmental and hydraulic conditions, processing software, etc.). A key stage of image-based techniques workflow is frames pre-processing. In particular, graphical enhancement is often needed to maximize contrast between tracer and background, improving software capability to detect and track the tracer motion. This work aims to investigate the influence of graphical enhancement methods on the results of image-based analyses, comparing traditional and less common algorithms. Analyses were conducted on videos acquired during a measurement campaign on two rivers in Sicily (Italy), where simultaneous ADCP reference measurements were also collected. Different graphic filters were applied to frames and the enhanced sequences were then processed using two optical software programs (i.e., PIVlab and SSIMS-Flow). Performances are evaluated in terms of errors in surface velocity and discharge assessment, using ADCP measurements as benchmark. Results confirm the overall high potential of image-based techniques and provide insights on the importance of using the appropriate enhancement filters based on the selected processing software and environmental conditions at recording time.

**Keywords:** flow velocity measurement, image velocimetry, optical preprocessing techniques, discharge

## 1 Introduction

Velocity measurements are traditionally gathered using mechanical or electromagnetic current meters, and recently by ADCPs. These techniques require a direct contact with the water flow, posing a risk for instruments and personnel, especially under high flow conditions. Recent technological advancements are supporting the development of innovative approaches, including remote sensing methods like the optical techniques, using radars, terrestrial, or satellite detectors. Image-based methods and their application to large-scale cases, thus, offer a promising new frontier in river monitoring, not only for their non-intrusiveness, but also for the simple implementation, the rapidity of measurements, and the cost-effective instrumentation employed. Image-based techniques are often performed using the following workflow: (i) artificial introduction of tracer on the river surface (if it is not already present), (ii) video recording of tracer motion, (iii) pre-processing, (iv) processing, and (v) post-processing of image sequences. Images' pre-processing is a crucial stage [1], and consists of stabilization (i.e., removal of camera movements), orthorectification (i.e., correction of lens distortions and application of real reference system), and often graphic enhancement of the frames that will be processed in the following stages. Graphic enhancement aims to maximize the contrast between the tracer materials floating on the water surface and the water surface itself (background). This can favour the processing software for the frame-by-frame detection of the tracer particles and the tracking of tracer motion. Graphic enhancement is indeed a complex process, as it should account for several environmental and hydraulic disturbances in the sequences (e.g., lighting changes, sun glares, rain, wind, turbulence, etc.). Several existing algorithms with different complexity can be used

for graphically filtering the recorded sequences, and it is important to carefully choose the appropriate algorithms depending not only on the adopted optical technique, but also on the environmental and hydraulic conditions under which the sequences were recorded.
The aim of this work is to investigate the influence of the choice of specific image enhancement algorithms on the results arising from image-based methods, through the comparison of both commonly used and new enhancement algorithms. In the present work, the enhancement algorithms were first applied separately and then in a combined manner, analysing the response of two optical software packages, PIVlab [2] and SSIMS-Flow [3].

## 2 Materials and Methods

Analyses were conducted using a dataset of videos acquired in two rivers in Sicily (Italy), i.e., the Oreto and Platani rivers. A total of six independent measurements were acquired on different days during the period 2020-2021. Case studies are representative of different river characteristics, environmental and hydraulic conditions, as well as different video acquisition modalities. Optical measurements at the Oreto river were performed from bridge with a HD camera mounted on a tripod, while videos at the Platani river were collected by drone. Seeding phase was preliminary performed due to the absence of natural tracer. Simultaneous benchmark measurements in a cross-section transect within the video recording areas were obtained for all the cases using an ADCP. After a proper stabilization and orthorectification of the recorded sequences, six different graphic enhancement algorithms, shown in Table 1, were applied.

Table 3 Graphic filters combinations considered for the analyses.

| | Filters | | Filters | | Filters |
|---|---|---|---|---|---|
| #1 | Grayscale | #3 | Grayscale+H.pass | #5 | Backg.rem.+RGB channel |
| #2 | Grayscale+Int.Cap. | #4 | Backg.rem. | #6 | Grayscale+CLAHE |

Some algorithms are simple and common (e.g., Grayscale) (Figure 1), while others are combination of more filters aimed, for example, to return binary results (e.g., Canny detector).

(a) 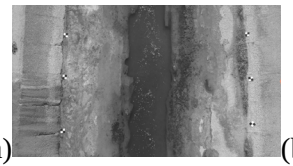 (b)  (c) 

Figure 8 Platani river case: application of (a) grayscale, adding (b) CLAHE, or (c) intensity capping filters.

## 3 Results and Discussion

Implications in using a proper graphic enhancement algorithm or a combination of filters, have been evaluated in terms of error in the surface velocity and discharge estimation over six case studies, considering benchmark discharges collected by ADCP. It is worth noting that unfiltered video sequences processing can lead to errors in the evaluation of discharge up to 50%, due to an inaccurate surface velocity field reconstruction affected by environmental disturbances and different sources of noise. The application of enhancing filters can reduce errors in estimating discharge of 30% and 35% using PIVlab and SSIMS-Flow software, respectively. These findings are in agreement with results shown in [4,5].

## 4 Conclusion

The aim of this work was to investigate the influence of applying different graphics enhancement algorithms by evaluating the performance obtainable by two different processing software. A clear improvement in the estimation of surface velocities and discharge was found in all cases, with different best filters combinations depending on the two used software. Results confirm the high potential of image-based techniques and the crucial role of the graphic enhancement phase in improving the results from image-based analyses. The selection of the enhancement algorithm should

be done carefully, choosing appropriate filters or combination of filters, based on software used and environmental and hydraulic conditions in which videos are recorded.

**Reference**

[1] Alongi, F., Pumo, D., Nasello, C., Nizza, S., Ciraolo, G., Noto, L.V., 2023. An automatic ANN-based procedure for detecting optimal image sequences supporting LS-PIV applications for rivers monitoring. Journal of Hydrology 626, 130233. https://doi.org/10.1016/j.jhydrol.2023.130233

[2] Thielicke, W., Stamhuis, E.J., 2014. PIVlab – Towards User-friendly, Affordable and Accurate Digital Particle Image Velocimetry in MATLAB. Journal of Open Research Software 2. https://doi.org/10.5334/jors.bl

[3] Ljubičić, R., Dal Sasso, S.F., Zindović, B., 2024. SSIMS-Flow: Image velocimetry workbench for open-channel flow rate estimation. Environmental Modelling & Software 173, 105938. https://doi.org/10.1016/j.envsoft.2023.105938

[4] Koutalakis, P., Zaimes, G.N., 2022. River flow measurements utilizing UAV-based surface velocimetry and bathymetry coupled with sonar. Hydrology 9, 148. https://doi.org/10.3390/hydrology9080148

[5] Ljubičić, R., 2022b. Jupyter Notebooks on Image Enhancement for UAV Velocimetry Purposes. https://github.com/ljubicicrobert/Image-enhancement-for-UAV-velocimetry

**Theme:** Technologies for water management and monitoring
**IAHR Thematic Priority Area:** [TPA-4] Digital Transformation
https://doi.org/10.3850/iahr-hic2483430201-73

# Research on Integrated Emergency Management Mechanism and Risk Management Guarantee System for the Whole Process of Exceeding-Design Flood of River Basin

**Yang Liting[1,2], Li Changwen[1,2*], Huang Yan[3], Zhou Rui[1,2], Lin Sujing[1,2], Huang Jiale[1,2]**

[1] College of Hydraulic and Environmental Engineering, China Three Gorges University, Yichang 443002, China
[2] Hubei Key Laboratory of hydropower engineering construction and management, China Three Gorges University, Yichang 443002, China
[3] Changjiang Water Resources Commission of the Ministry of Water Resources, Wuhan 430010, China

*Corresponding author: Li Changwen, lichangwen@alumni.hust.edu.cn*

**Abstract.** The problem of coping with river basin exceeding-design flood in China is prominent, and emergency and risk management are facing complex and severe situations and challenges under the influence of multiple changing environments, such as global climate change, human activities and engineering scheduling. Applying the theories of catastrophology, informatics, management science and other disciplines, the characteristics and management ideas of river basin exceeding-design flood risk are analysed by means of system analysis and theoretical derivation. The international advanced risk management experience and successful practice of emergency management are summarized. The sufficient, necessary and constraint conditions of river basin exceeding-design flood emergency management are analysed. The whole process risk management guarantee system of pre-disaster risk zoning, risk regulation and control in disaster and post-disaster risk compensation is constructed. The response mechanism of five-span coordination and the whole process integration of prevention, resistance and rescue, and the construction scheme of "flood control command sand table" are put forward, which realizes the quantification and visualization of response measures, risks and potential under different water conditions and the trade-off between "protection and abandonment" decision-making relationship. The research results provide theoretical support for the management and control of river basin exceeding-design flood.

**Keywords:** catastrophe insurance and cross-regional compensation; flood control command sand table; river basin exceeding-design flood; risk regulation, control and avoidance; risk zoning and management

## 1 Introduction

Under the influence of global warming and high-intensity human activities, the frequency and intensity of extreme rainstorms have increased significantly [1-3]. The incidence of floods is expected to increase [7-8] and the risk of floods will increase [4-6]. Although relevant studies have been carried out on exceeding-design flood at home and abroad [9], there is still a lack of systematic review of the formation mechanism and propagation path of exceeding-design flood risks from the perspective of river basin. In view of this, this paper proposes the integrated emergency management mechanism and risk management guarantee system for the whole process of the super-standard flood in the basin, so as to minimize the risk of rare floods.

## 2 Method

According to the internationally accepted definition of flood risk, from the perspective of measures to reduce the loss of exceeding-design flood disaster, the exceeding-design flood risk can be described by the following formula:

$$DR = H / C_1 \times E / C_2 \times V / C_3 \quad (4)$$

## 3 Results

The risk of flood is eternal. Only by moderately bearing a certain limit of risk and reasonably sharing risks in different forms can it possible to seek a coordinated development road. Therefore, flood risk management is a moderate risk-taking management idea. Aiming at rationally regulating flood control behaviour and enhancing the self-adaptive ability of the whole society, the construction idea of the whole process and integrated river basin exceeding-design flood prevention emergency management mechanism and the construction scheme of the river basin exceeding-design flood risk management guarantee system are put forward.

## 4 Conclusion

The characteristics of river basin exceeding-design flood risk are sorted out, and it is proposed that the basic feature of risk management is to pursue the objectives of moderation and limitation.

The dominant idea of river basin exceeding-design flood risk management is put forward, that is, the fact that flood risk exists objectively. Therefore, it is necessary to rationally regulate flood control behaviour and enhance the adaptive ability of the whole society.

Summarised the research results of international flood risk management, and put forward the construction idea of the integrated management of five-span coordination of river basin exceeding-design flood and the emergency management mechanism of the whole process of prevention, resistance and rescue. Based on the theory of military command, the sufficient conditions of "knowing the sky", "knowing the land" and the necessary conditions of "knowing oneself" and "knowing others" and the related constraints are analysed, and the construction scheme of "flood control command sand table" is put forward to improve the emergency management mechanism of river basin exceeding-design flood.

Systematically constructed a risk management system for the whole process of pre-disaster risk zoning and management, risk regulation, control and avoidance when disaster occurs and post-disaster catastrophe insurance and cross-area compensation for river basin exceeding-design flood. The research shows that the spatial differentiation of exceeding-design flood risk is obvious, and the management needs to coordinate engineering and non-engineering measures according to local conditions.

## Reference

[1] Ayat H., Evans J. P., Sherwood S. C., et al. Intensification of subhourly heavy rainfall. Science, 2022, 378(6620): 655-659.

[2] Boers N., Goswami B., Rheinwalt A., et al. Complex networks reveal global pattern of extreme-rainfall teleconnections. Nature, 2019, 566(7744): 373–377.

[3] Taylor C. M., Belušić D., Guichard F., et al. Frequency of extreme Sahelian storms tripled since 1982 in satellite observations. Nature, 2017, 544(7651): 475–478.

[4] Yin J., Gentine P., Zhou S., et al. Large increase in global storm runoff extremes driven by climate and anthropogenic changes. Nature Communications, 2018, 9: 4389.

[5] Dottori F., Szewczyk W., Ciscar J. C., et al. Increased human and economic losses from river flooding with anthropogenic warming. Nature Climate Change, 2018, 8(9): 781–786.

[6] Paprotny D., Sebastian A., Morales-Nápoles O., et al. Trends in flood losses in Europe over the past 150 years. Nature Communications, 2018(9): 1985.

[7] Loreti S., Ser-Giacomi E., Zischg A., et al. Local impacts on road networks and access to critical locations during extreme floods. Scientific reports, 2022, 12: 1552.

[8] Winsemius H. C., Aerts J., van Beek, L. P. H., et al. Global drivers of future river flood risk. Nature Climate Change, 2016, 6(4): 381–385.

[9] Wang Z., Sun Y., Li C., et al. Analysis of Small and Medium–Scale River Flood Risk in Case of Exceeding Control Standard Floods Using Hydraulic Model. Water. 2022, 14(1): 57.

**Theme:** Technologies for water management and monitoring
**IAHR Thematic Priority Area:** [TPA-4] Digital Transformation
https://doi.org/10.3850/iahr-hic2483430201-75

# Numerical Study of The Dam Break of a Rock-Filled Porous Media Structure

**Behrad Tarami[1], Bahman Ehteshami[1] and Yee-chung Jin[1,*]**

[1] Faculty of Engineering and Applied Science, University of Regina, Regina, Saskatchewan, S4S0A2, CANADA

** Corresponding author: yee-chung.jin@uregina.ca*

**Abstract**. The Lagrangian method describes fluid motion by tracking individual fluid parcels and monitoring their properties as they move. In this study, the Moving Particle Semi-implicit method, a mesh-free numerical approach, is utilized to simulate the dam break of a rock-filled porous media structure. Due to the creation of shocks during the dam break, conventional treatment methods are inadequate, necessitating further refinements. Numerical simulations employing MPS demonstrate reasonable agreement with experimental data.

**Keywords:** dam break, MPS, particle method, rock fill dam.

## 1 Introduction

Flow or wave motion passing through porous media carries significant implications across various engineering fields, including harbor engineering, geotechnical engineering, hydrology, and coastal engineering. Porous media, characterized by randomly distributed pores within a rigid body, pose challenges for analytical modeling but are amenable to study through complex numerical simulations [1]. The Lagrangian approach, utilizing moving particles to discretize the problem domain, offers advantages such as simplified mesh generation, handling of large deformations, and easy tracking of interfaces and boundaries. Over the past decades, the Moving Particle Semi-implicit (MPS) [2] method has been successfully applied in numerous scientific disciplines in Civil, Environmental Engineering, Materials, and ocean Engineering. In these domains, the MPS method has demonstrated its efficacy in accurately reproducing the behavior of free-surface viscous flows.

The MPS method involves dividing the fluid into numerous particles, each carrying data on position, pressure, and velocity. Developed to analyze incompressible flows, the MPS method represents all components of the Navier-Stokes equations using particle interaction models, where each particle's motion is governed by its interactions with neighboring particles. Key advantages of the MPS method include its adaptability to complex topographies and its ability to capture discontinuities in solutions. Moreover, the MPS method can incorporate physical effects such as turbulence, non-linearities in equations, and moving boundaries and interfaces.

Notably, MPS is the method for spatial integration of partial differential equations and MPS extends the finite volume method to a mesh-free approach and utilizes particle number density to satisfy flow incompressibility, unlike the finite volume method, which relies on velocity divergence.

Dam break scenarios induce shocks upstream and downstream, presenting challenges for numerical solutions due to high hydraulic gradients. In this study, a one-dimensional MPS discretization is employed to model free-surface flow near a porous dam, effectively addressing these challenges.

## 2 Method

The MPS method characterizes the development of a physical system by modeling interactions between discrete particles. Each particle influences its neighbors, with the extent of influence determined by a specialized weighted function (kernel function). This influence is inversely

proportional to the distance between the particle and its neighbor. Employing a prediction-correction algorithm, the MPS method analyzes incompressible flows. Interaction between particles and neighboring particles is calculated using weight functions. Mesh-free solvers for Shallow Water Equations (SWE) automatically conserve mass, simplifying computation while maintaining accuracy [3].

## 3 Results

Simulations are conducted in a tank with specified dimensions and a block structure placed centrally. Fine glass balls with defined porosity form the porous structure. Comparisons between MPS results, experimental data, and other numerical models demonstrate the method's efficacy, particularly in simulating flow through the porous structure.

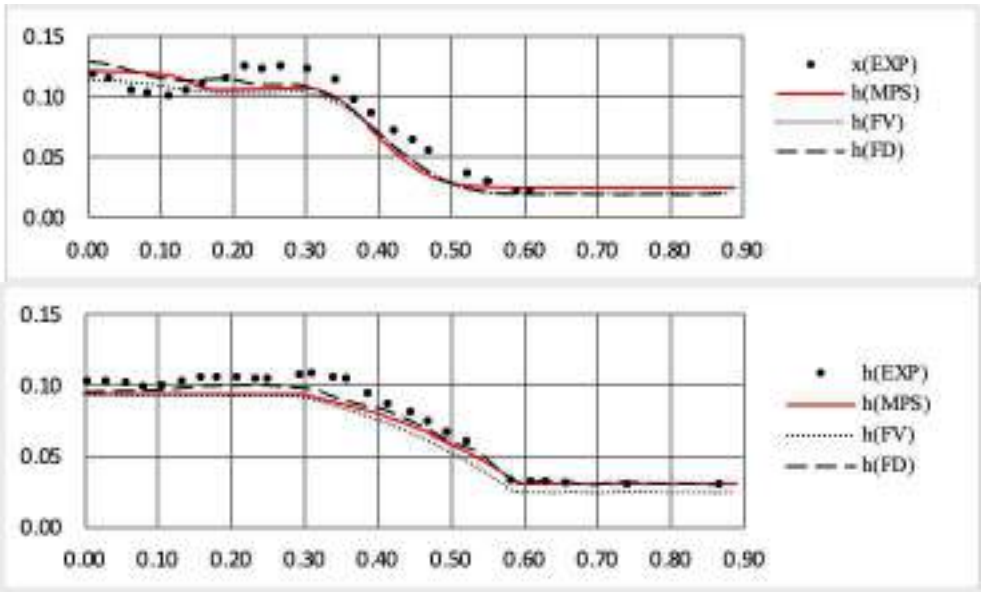


**Figure 1** Comparison between free surface height at: $t$=1.2s and $t$=4.0s.

The MPS results are compared with experimental data and different numerical models. As can be seen, MPS method has good results through the porous structure.

## 4 Conclusion

Investigations into particle size effects on water flow simulation accuracy reveal that a particle size of 0.001m balances accuracy and computational efficiency best. Smaller sizes yield less accurate results while incurring higher computational costs. Therefore, for the current problem, a particle size of 0.001m is deemed optimal.

## References

[1] Chwang A. and Chan A., 1998, Interaction between porous media and wave motion, Annual Review of Fluid Mechanics, 30, pp. 53-84. https://thermopedia.com/content/10120/.

[2] Koshizuka S. and Oka Y., 1996, Moving-particle semi-implicit method for fragmentation of incompressible fluid, Nuclear Science and Engineering, 123, pp.421-434.

[3] Sarkhosh P. and Jin Y.C., 2021, MPS-Based Model to Solve One-Dimensional Shallow Water Equations, Water Resources Research, 57, e2020WR028742.

**Theme:** Technologies for water management and monitoring
**IAHR Thematic Priority Area:** [TPA-4] Digital Transformation
https://doi.org/10.3850/iahr-hic2483430201-77

# Future Water Management Vision and Direction of ECO-I

**Park, Cheolhyun1***

ECO-I 484 Neungheodae-ro Yeonsu-gu, Incheon 21978, Republic of Korea

**Abstract.** The Yellow Sea, a vital yet highly vulnerable marine region, faces significant environmental threats primarily due to human activities such as industrial discharge, coastal reclamation, and pollution. In response to these challenges, the Incheon Environmental Corporation, ECOI, operates eleven sewage treatment facilities employing advanced technologies to mitigate these effects by effectively treating and removing pollutants like total nitrogen (T-N) and total phosphorus (T-P). In an effort to further strengthen marine ecosystem restoration and pollution control, the YES Initiative has been established, advocating a collaborative governance model that includes a diverse array of stakeholders.

**Keywords:** YES Initiative, Apex Board, Marine ecosystem restoration, Pollution control strategies, Colleges (governance groups), Microplastics

## 1 Introduction

The ecological integrity of the Yellow Sea has been increasingly compromised due to a range of human activities coupled with environmental mismanagement. This study aims to explore the role of ECOI in addressing these environmental challenges through the utilization of sophisticated sewage treatment technologies such as Modified Ludzack-Ettinger (MLE), A20, Bio sac, Korea Membrane Bio-Reactor (KSMBR), and Oxidation ditch. Additionally, the study delves into the structural and operational impact of the YES Initiative, a comprehensive effort designed to restore and preserve the marine environment of the Yellow Sea.

## 2 Method

Employing a qualitative analysis approach, this research scrutinizes the sewage treatment methodologies deployed by ECOI. These methods are pivotal in reducing harmful effluent before it reaches the Yellow Sea, crucial for maintaining the ecological balance. Furthermore, the governance mechanisms of the YES Initiative are critically examined. The Initiative is organized into six specialized 'Colleges,' each focusing on a different aspect of environmental concern. These Colleges facilitate targeted problem-solving strategies, contributing significantly to the overarching governance framework led by the Apex Board—a democratic body that makes key strategic decisions.

## 3 Results

Analysis of the data reveals that the technologies implemented by ECOI significantly reduce the levels of T-N and T-P in the treated water. Moreover, the governance model of the YES Initiative, with its specialized Colleges and democratic Apex Board, has been instrumental in formulating and implementing inclusive and effective environmental strategies. These strategies are not only aimed at mitigating pollution at its source but also extend to the adoption of advanced filtering technologies that are particularly effective against microplastics, a growing concern in marine conservation.

## 4 Conclusion

ECOI's advanced treatment facilities, when combined with the YES Initiative's robust governance model, play a crucial role in addressing the complex ecological challenges facing the Yellow Sea. By harnessing diverse expertise and resources, these initiatives not only enhance marine biodiversity but

also establish a benchmark for international collaboration in the field of marine ecosystem restoration. The collective efforts of ECOI and the YES Initiative are setting a precedent for effective environmental management, with the potential to influence similar initiatives globally.

**References**

[1] Han Nam University Institute of Science and Technology Law (2015), A Study on Marine Governance and Marine Management Systems, Implications for International Maritime Law and Northeast Asian Maritime Order
[2] Yeosijae Institute for Sustainable Studies (2020), Northeast Asia Governance for Solving the Yellow Sea Pollution
[3] Korea Environmental Corporation under the Ministry of Environment (2018), Study on Effective Sewage Treatment Plans During Rainfall
[4] Ministry of Oceans and Fisheries (2021), The 3rd Basic Plan for Marine and Fisheries Development
[5] Inter-ministerial Coordination of the Republic of Korea (2020), The 5th National Environmental Master Plan
[6] Korea Ocean Research & Development Institute (2009), Establishment of a National Strategic Plan for the Yellow Sea Large Marine Ecosystem
[7] Incheon Research Institute (2024), Study on the Characteristics of Microplastics in Incheon Coastal Waters

**Theme:** Technologies for water management and monitoring
**IAHR Thematic Priority Area:** [TPA-4] Digital Transformation
https://doi.org/10.3850/iahr-hic2483430201-79

# Intergrated Smart Sewerage Pipe Network System for Preventing Urban Flooding

**Yoo, Junyoung[1*]**

ECO-I 484 Neungheodae-ro Yeonsu-gu, Incheon 21978, Republic of Korea

**Abstract.** The Smart Water Grid concept has emerged as a transformative approach to tackle the growing challenges posed by climate change and increasing urban population densities. By integrating advanced technologies into sewage systems, this innovative strategy aims to enhance the sustainable management of water resources and significantly mitigate the risks associated with urban flooding. Employing real-time data monitoring and leveraging cutting-edge Information and Communication Technology (ICT), the system optimizes sewage transport, treatment, and discharge processes. This optimization is crucial in improving water circulation efficiency and reducing urban flood risks.

**Keywords:** Smart Water Grid, Sustainable Water Management, Urban Flooding Prevention, Real-time Data Monitoring, Big Data Analysis, GIS Database Enhancement

## 1 Introduction

In the face of increasingly frequent and severe urban flooding incidents, prompted by climate change and rapid urbanization, cities around the globe are compelled to rethink their water management strategies. The Smart Sewage Project in Incheon, South Korea, represents a pioneering initiative that leverages cutting-edge technologies to enhance the resilience and efficiency of urban sewage systems. This project integrates advanced monitoring tools such as flow meters and rain gauges within a unified network of sewage facilities, establishing a sophisticated real-time monitoring system. The data derived from this system play a crucial role in formulating proactive flood response strategies, thus significantly mitigating potential flood damages. This paper delves into the operational aspects and successes of the Smart Water Grid, underscoring its impact on urban flood prevention and the broader implications for sustainable urban development and environmental protection. Through an analysis of empirical data and specific case studies, this study illustrates the transformative potential of integrating information and communication technology (ICT) with traditional water management practices, setting a precedent for future advancements in urban water systems management

## 2 Method

The Smart Sewage Project encompasses a broad integration and management effort, connecting all sewage treatment plants and network facilities in Incheon into a single, unified network. This integration facilitates the systematization of collected operational data for big data analysis, which is instrumental in deriving optimal operational strategies. Moreover, enhancements to the existing sewage pipeline GIS database have enabled more precise flood analysis in 30 flood-prone areas, providing a robust foundation for preventive measures and rapid response.

## 3 Results

This study illustrates how the establishment and operation of the Smart Water Grid create synergies that contribute significantly to effective urban flood prevention and water resource management. Through specific examples and empirical data, it is evident that this systematic approach not only bolsters sustainable urban development but also plays a critical role in environmental protection. The

successes documented in this study lay a solid groundwork for potential replication and application in other regions, promising wide-reaching benefits in the realms of flood prevention and sustainable city planning.

## 4 Conclusion

This comprehensive approach to managing urban water systems and preventing floods through smart technologies represents a key advancement in how cities can protect themselves against the adverse effects of climate change while ensuring sustainable growth and environmental stewardship. The integration of ICT with traditional water management practices paves the way for more resilient urban environments.

## References

[1] Choi Gye-Woon, Jung Yeon-Joong, Jo Hyung-Geun, Gu Bon-Jin, Kim Ki-Hyung (2021), Smart Water Grid Technology and the Future of Water Supply

[2] Jeong Seung-Kwon, Jeon Gye-Won (2020), A Study on the Development of Smart Water Grid Key Performance Index for the Implementation of Smart City

**Theme:** Hydraulic and hydrological modeling
**IAHR Thematic Priority Area:** [TPA-4] Digital Transformation
https://doi.org/10.3850/iahr-hic2483430201-81

# Simulation of Precipitation-Generated Debris Flow in The Laval Basin, France

**M. Abily[1], G. Antoine[2], O. Delestre[3,4,5], L. Girolami[6,7], N. Goutal[8,4], F. Taccone[8]**

[1] Université Côte d'Azur, CNRS, Observatoire de la Côte d'Azur, IRD, Géoazur, Nice, France
[2] EDF – R&D, Electrical Engineering and Structural Mechanics Department, France
[3] LJAD, Université Côte d'Azur, CNRS, Nice, France
[4] Laboratoire d'Hydraulique Saint-Venant, Ecole des Ponts ParisTech – EDF R&D, Chatou, France
[5] Polytech'Lab, Université Côte d'Azur, Sophia-Antipolis, UPR UniCA 7494, France
[6] GéHCO, Université de Tours, Campus Grandmont, Tours, France
[7] RECOVER, INRAE-Aix-Marseille Université, 3275 Route de Cézanne, Aix-en-Provence, France
[8] EDF R&D LNHE-Laboratoire National d'Hydraulique et Environnement, Chatou, France

*Corresponding author: florent.taccone@edf.fr*

**Abstract.** This study aims to model hydraulic transfers and erosion sources in steep mountain watersheds using a physically-based hydraulic model. Immature debris flows and shallow landslides are significant sediment sources in such environments. These phenomena are here simulated thanks to a gravity-driven erosion model and a 1D vertical infiltration model integrated into TELEMAC-2D numerical code. The new erosion model employs a fully dynamic system and Coulomb-like bottom friction to better represent debris flow properties. Evaluation against field data (on the Laval catchment, Southern French Alps) demonstrates the ability to reproduce the hydrological response of the basin and also the realistic erosion and deposition patterns.

**Keywords:** debris flow, rainfall runoff, shallow water model, TELEMAC-2D

## 1 Introduction

With the combination of steep slopes and highly erodible soil, mountain watersheds are susceptible to export a large amount of sediment at their outlets. Dam reservoirs might be filled by these sediments. This might impact both the hydro-electricity production and safety. Our purpose is to build a model representative of the watershed's hydrology and of the upstream gravity-driven erosion sources. These sources supply a classical erosion and sedimentation model in the hydraulic network. In this paper, the modelling of all the above-mentioned processes and the coupling method are presented. Then, the modelling approach will be validated on the Laval catchment.

## 2 Modelling strategy

The modelling of rainfall runoff and debris flow processes is achieved thanks to a coupling between several models into TELEMAC-2D code. On one time step, we first evaluate the infiltration rate using a two-layer Green-Ampt model [1]. Then the runoff modelling is achieved thanks to the shallow water equations (with rainfall and infiltration source terms for the mass conservation equation and Darcy-Weisbach's friction law with Lawrence's friction coefficient [2] for the momentum equation). It is solved on an unstructured mesh thanks to an explicit well-balanced finite volume scheme (HLLC numerical flux and Chen and Noelle's hydrostatic reconstruction [3]), the friction is treated semi-implicitly. Then, the erosion term (E) is calculated thanks to the evaluation of a detachment criterion. This criterion depends on the slope and the water depth. And the deposition term (D) is evaluated with a formula similar to the one used for the cohesive sediment deposition [4]. It depends on the debris flow velocity, the critical deposition velocity, the sediment concentration and the settling

velocity. The debris flow is then modelled thanks to another shallow water model, with E and D as source terms and a Coulomb friction term. Finally, the bottom elevation is modified by taking into account erosion (E) and deposition (D). The available eroded layer is limited by the wetting front calculated with the infiltration model. Thus, only the saturated part of the soil is considered available for debris flow and deposition terms are calculated.

## 3 The domain

The Laval catchment covers an area of 86.4 ha, with a medium slope. 68% of its surface area is bare, and the subsoil consists mainly of black marl. This basin (located in the southern French Alps) is monitored by the Draix-Bleone observatory [5], which allows to test our approach.

## 4 Results

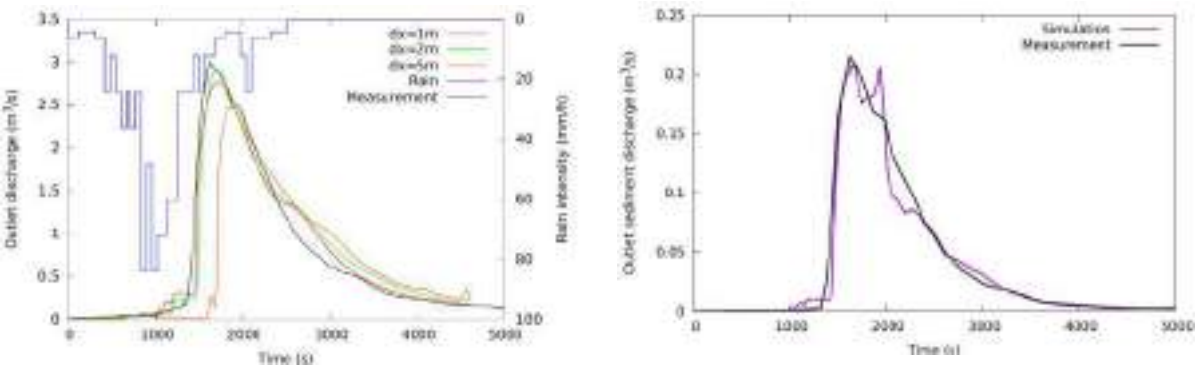


Figure 9 Discharge (left) and flux of sediment (right) at the outlet - 29th may

We have considered three mesh resolutions (1, 2 and 5 m). The 1 m mesh has around 2 millions elements. The mesh is forced to follow the lowest point of the river, for hydraulic network continuity. We tried out different scenarios for different seasons, which implies differences in rainfall and soil water content. The event considered here is the 29th of May 2012 succeeding six rainy events from the 21st to the 27th of May. The maximal value of the rain intensity is 84 mm/h and the peak discharge is 3 $m^3$ /s. We notice that both the discharge and the flux of sediments at the outlet are well calculated for this event.

## 5 Conclusion

We have obtained a model that reproduces the hydrological and sedimentary behaviour of a mountainous basin such as the Laval. This needs to be verified for other events and the behaviour within the basin needs to be studied by analysing changes in topography.

## Reference

[1] M. Esteves, X. Faucher, S. Galle, M. Vauclin, Overland flow and infiltration modelling for small plots during unsteady rain: numerical results versus observed values, Journal of Hydrology, 228(3-4), (2000), 265-282, https://doi.org/10.1016/S0022-1694(00)00155-4.

[2] D. S. L., Lawrence, Macroscale surface roughness and frictional resistance in overland flow, Earth Surface Processes and Landforms, 22(4), (1997), 365–382.

[3] G. Chen, S. Noelle, A new hydrostatic reconstruction scheme based on subcell reconstructions, SIAM Journal on Numerical Analysis, 55(2), (2017), 758-784, https://doi.org/10.1137/15M1053074.

[4] Takahashi, T. (2007). Debris -ow: Mechanics, Prediction and Countermeasures. Taylor & Francis.

[5] Draix-Bleone Observatory. (2015). Observatoire hydrosédimentaire de montagne Draix-Bléone [Data set]. Irstea. https://dx.doi.org/10.17180/obs.draix

**Theme:** Hydraulic and hydrological modeling
**IAHR Thematic Priority Area:** [TPA-4] Digital Transformation
https://doi.org/10.3850/iahr-hic2483430201-83

# Coastal Urban Flooding and Risk Analysis under Extreme Weather Conditions: A Case Study in Hong Kong

**Zhi-Yong LONG[1], Huan-Feng Duan[1,2,*]**

[1] Department of Civil and Environmental Engineering, The Hong Kong Polytechnic University, Hong Kong, 999077, China
[2] Research Institute for Land and Space, The Hong Kong Polytechnic University, Hong Kong, 999077, China

*Corresponding author: hf.duan@polyu.edu.hk*

**Abstract.** This paper presents a study on the coastal urban flooding risk assessment through numerical modelling and analysis. The urban area of Kowloon in Hong Kong is taken for case study, with aim to examine the influences of different factors including rainfall, storm surge, and sea level rise under extreme weather conditions. To this end, a coupled model framework of one-dimensional (1D) drainage networks and two-dimensional (2D) overland flows is developed based on the open-source codes, which is then validated and applied for the investigation. For analysis, different scenarios of rainfalls and storm surges with 50-year, 100-year, and 200-year return periods respectively, coupled with SLR scenarios of 0.5 meter and 1 meter, are examined for the consequences of coastal urban flooding including flooding area and depth. The findings highlight the significant differences in the induced flood risk distribution and intensity across different scenarios. Based on the various numerical cases and results, the dynamic evolution of flooding risks in this studied area is also inspected in both temporal and spatial domains. These models, results and findings are not only pivotal for enhancing flood risk management in Hong Kong but also valuable for other coastal urban areas with similar challenges under climate change.

**Keywords:** Coastal flooding, Climate change, Rainfall, Storm Surge, Sea Level Rise

## 1 Introduction

Coastal cities worldwide face increasing flood risks due to rapid urbanization, climate change, and rising sea levels [1]. The compound effects of extreme rainfall, storm surges, and sea level rise (SLR) can lead to severe flooding, causing damage to infrastructure and disrupting urban life [2]. Hong Kong, a densely populated coastal city in southern China, is particularly vulnerable to these flood risks [3]. To effectively manage flood risks in coastal cities like Hong Kong, it is essential to understand and quantify the compound effects of multiple flood drivers. Previous studies have primarily focused on individual flood drivers [4], but there is a growing need to consider the interactions between rainfall, storm surge, and SLR in flood risk assessments [5]. This study aims to assess the coastal urban flooding risk in Hong Kong under extreme weather conditions using a coupled 1D-2D hydrodynamic model. The objectives are to:

- Develop and validate a coupled 1D-2D model for simulating urban flooding in Hong Kong.
- Quantify the relative contributions of rainfall and storm surge to flood extent and volume.
- Investigate the nonlinear effects of SLR on compound flooding in Hong Kong.

## 2 Study area and Methodology

This study employs a coupled model approach, combining LISFLOOD for 2D overland flow modeling and SWMM for 1D drainage network modeling, to assess the flood risk in Kowloon, Hong Kong. A coupling program facilitates the exchange of water flow between the two modules, accurately representing the interactions between the overland flow and the drainage network.

## 3 Results and Conclusion

This study assesses the coastal urban flooding risk in Hong Kong under extreme weather conditions using a validated coupled 1D-2D model. The analysis reveals that increasing storm surge and rainfall return periods lead to higher flood risks, with rainfall playing a dominant role compared to storm surge. A combination of a 200-year storm surge and a 200-year rainfall return period results in a 24% increase in flood area.

The impact of sea level rise (SLR) on coastal flooding is not linear, with flood volume increasing by 28.7% under a scenario with a 200-year return period for both rainfall and storm surge and a 1-meter SLR (Fig. 1). Seawater directly inundates coastal areas by overtopping seawalls at higher water levels.

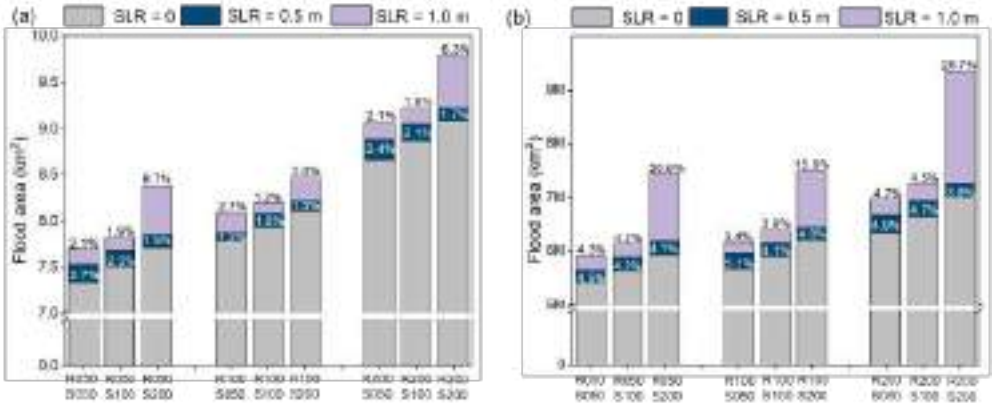


Figure 1 (a) Areas and (b) Volume affected by flooding and inundation with SLR, progressive storm surge heights and rainfall (cumulative). Note: The height of the bar chart is the relative increase.

The findings emphasize the importance of considering the complex interactions between rainfall, storm surge, and SLR in assessing and managing coastal urban flood risks. The coupled 1D-2D model is a valuable tool for simulating and analyzing compound flood scenarios, enabling decision-makers to develop effective flood mitigation strategies. This study contributes to the growing knowledge on coastal urban flood risk assessment and underscores the need for proactive and adaptive flood risk management strategies to enhance the resilience of coastal cities facing increasing flood risks due to climate change.

## Acknowledgments

This study was supported by the Hong Kong Research Grants Council (RGC) under CRF-YCRG project no. C5002-22Y and NSFC/RGC JRS project no. N_PolyU599/22.

## Reference

[1] Nicholls, R.J., Lincke, D., Hinkel, J., Brown, S., Vafeidis, A.T., Meyssignac, B., Hanson, S.E., Merkens, J.L. and Fang, J., 2021. A global analysis of subsidence, relative sea-level change and coastal flood exposure. Nature Climate Change, 11(4), pp.338-342.

[2] Bevacqua, E., Maraun, D., Vousdoukas, M.I., Voukouvalas, E., Vrac, M., Mentaschi, L. and Widmann, M., 2019. Higher probability of compound flooding from precipitation and storm surge in Europe under anthropogenic climate change. Science advances, 5(9), p.eaaw5531.

[3] Huang, W., Ye, F., Zhang, Y.J., Park, K., Du, J., Moghimi, S., Myers, E., Pe'eri, S., Calzada, J.R., Yu, H.C. and Nunez, K., 2021. Compounding factors for extreme flooding around Galveston Bay during Hurricane Harvey. Ocean Modelling, 158, p.101735.

[4] Yin, J., Jonkman, S., Lin, N., Yu, D., Aerts, J., Wilby, R., Pan, M., Wood, E., Bricker, J., Ke, Q. and Zeng, Z., 2020. Flood risks in sinking delta cities: time for a reevaluation?. Earth's Future, 8(8), p.e2020EF001614.

[5] Zscheischler, J., Westra, S., Van Den Hurk, B.J., Seneviratne, S.I., Ward, P.J., Pitman, A., AghaKouchak, A., Bresch, D.N., Leonard, M., Wahl, T. and Zhang, X., 2018. Future climate risk from compound events. Nature climate change, 8(6), pp.469-477.

**Theme:** Hydraulic and hydrological modeling
**IAHR Thematic Priority Area:** [TPA-4] Digital Transformation
https://doi.org/10.3850/iahr-hic2483430201-85

# Coupling of SWMM With 2D Hydrodynamic Model for Simulation of Urban Flooding

**ZHANG Yue[1], DAI Tingyu[1], HE Lemin[1], WANG Guomiao[1], ZHOU Lu[1], BOURBAN Sébastien E.[2], MIN Jiesheng[1]**

[1] Zhejiang Yuansuan Technology Co., Ltd., Hangzhou, China
[2] EDF R&D National Laboratory for Hydraulics and Environment (LNHE)

*Corresponding author: celine.zhang@yuansuan.com*

**Abstract.** Urban waterlogging often causes significant economic losses and even threatens the safety of people's lives. Digital platforms which could provide forecast and for-alert regarding the city's water levels and submerged areas under heavy or continuous rainfall help in preventing and mitigating such risks and losses. To facilitate the development of an urban flooding risk management digital platform, a waterlogging prediction model was constructed by integrating the 2D hydrodynamics module of the open TELEMAC system and SWMM (Storm Water Management Model). This coupled model enables the simulation of surface water level changes, considering digital elevation model (DEM) and surface friction, through the 2D hydrodynamic model. Similarly, the underground drainage systems, considering wells and pipelines, are simulated with SWMM. The exchange of variables between the two model is achieved at each time step, ensuing synchronization between the simulation results of surface inundation and underground drainage.

**Keywords:** Open TELEMAC system, risks management, SWMM, Urban Waterlogging

## 1 Introduction

From 2012 to 2023, a total of 503 heavy rain weather processes occurred in China[1]. Some of these heavy rains have caused serious disaster events, such as the "7.20" event in Zhengzhou, Henan Province, which led to serious urban waterlogging and river floods[2].

The causes of urban waterlogging can be divided into natural factors and man-made factors[3], and urban waterlogging is prone to occur when heavy precipitation exceeds the drainage capacity of the city. For the study of urban waterlogging, the simulation can be achieved from different angles. Lyu J H et al. used the SWMM model to evaluate the city's drainage capacity and waterlogging risk from the perspective of the underground pipe network[4]. Liu J H et al. used TELEMAC-2D to analyze the surface water accumulation on Xiamen Island under different rainstorm scenarios[5].

As a 1D pipeline model, SWMM (Storm Water Management Model) can simulate urban drainage systems, but cannot provide information such as inundation range and flow velocity, while the 2D fluid dynamics module of the open TELEMAC system can simulate processes such as submerged water accumulation on the ground surface. In order to promote the development of a digital platform for urban flood risk management, TELEMAC-2D and SWMM were coupled to construct a prediction model that could consider both underground drainage and surface inundation.

## 2 Material and method

### 2.1 TELEMAC-2D model

Geographic information such as digital elevation model (DEM) and surface friction are considered in TELEMAC-2D. Precipitation data will also be provided to TELEMAC-2D to simulate the change of water level and the flow on the ground.

### 2.2 SWMM model

Pipe network facilities such as manholes, pipelines, and outlets are considered in SWMM to simulate the underground drainage system.

### 2.3 Coupling between two model

At every time step, the water depth on the ground at each position of manhole calculated by TELEMAC-2D will be sent to SWMM. Then, the drainage capacity is calculated according to the current state of the pipe network by SWMM. Water on the ground will drain through the manhole using source term in TELEMAC-2D when the pipe network has not reached its maximum capacity, otherwise water accumulates due to overload of drainage capacity. The net discharge of each manhole will be calculated, whether in or out, and provide to TELEMAC-2D as the discharge of sources. The exchange of variables between the two models is implemented at each time step, allowing for synchronization between the results of the surface inundation and subsurface drainage simulations.


Figure 10 Coupling processes

## 3 Results and discussion

We started by building a model of a flat area which has 1 m of standing water, and with a manhole and an outlet connected to it by pipe underground. This model is used to verify the coupling. The results show that the model realizes the real-time water exchange between the ground and the underground, and the water on the surface is discharged through the manhole according to its capability.

A second model includes the underground simplified pipe network of an urban area, and the corresponding DEM surface elevation data is built to simulate the coupled model under rainfall scenarios. The model can obtain the spatial and temporal distribution information under the condition of considering the urban drainage system at the same time, such as the inundation process of the urban area, the water depth, water level and flow velocity of each location.

## 4 Conclusions

The waterlogging prediction model based on the coupling of TELEMAC-2D model and SWMM model can provide more practical support for the development of urban flooding risk management digital platform. On the basis of the current work, the calculation speed and parallel computing capability of the model can be further developed and optimized, and the calculation efficiency can be improved to meet the needs of the timeliness of urban waterlogging prediction.

## Reference

[1] https://www.cma.gov.cn
[2] https://www.gov.cn/xinwen/2022-01/21/content_5669723.htm
[3] Wang J B, Zhang Q, Wu L P, Gou A P, Review on Researches about Urban Waterlogging in China, Journal of Anhui Agricultural Sciences, 2013, 41 (30): 12072-12078+12097.
[4] Lyu J Y, Shen X, Hao M Y. Evaluation of drainage capacity and waterlogging risk based on SWMM [J]. Journal of municipal technology,2022,40(7):237-241.
[5] Liu J H, Li Z J, Mei C, et al. Urban flood analysis for different design storm hyetographs in Xiamen Island based on TELEMAC-2D. Chin Sci Bull, 2019, 64: 2055–2066, doi: 10.1360/N972018-01180.

**Theme:** Hydraulic and hydrological modeling
**IAHR Thematic Priority Area:** [TPA-4] Digital Transformation
https://doi.org/10.3850/iahr-hic2483430201-87

# Dynamics and Mechanisms of Urban Flash Flooding Induced by Training Rainstorms: Case Study in Hong Kong

**Kaihua Guo[1], Haochen Yan[1], Mingfu Guan[1*]**

[1] Department of Civil Engineering, the University of Hong Kong, Hong Kong SAR, China

*Mingfu Guan: mfguan@hku.hk*

**Abstract.** This study examines the phenomenon of "training rainstorms" and their implications for urban flooding. By utilizing a spatially distributed hydrodynamic model and validating the results with crowd-sourced data, the dynamic process of the "9.7" storm in the Sha Tin and Wong Tai Sin districts was successfully simulated. The study reveals that under different design rainfall scenarios, the central urban area, where residents are concentrated, is particularly susceptible to inundation. The severity of internal flooding and inundation increases with higher peak intensities and longer durations of rainfall. Risk areas within the study region were categorized into low, medium, and high, with the differences diminishing as the risk level rises. Additionally, the impact of storm paths on risk areas is minimal compared to the influence of the storm's return period. Furthermore, the study highlights the significant role of rainstorm development paths and land use in determining the risk of urban flooding. This information holds valuable insights for urban planning and the implementation of effective warning systems in areas prone to training rainstorms. Ultimately, it contributes to the proactive management and mitigation of internal flooding risks.

**Keywords:** Training rainstorms, Hydrodynamic model, Urban flood, Storm spatiotemporal design

## 1 Introduction

In meteorology, "training rainstorms" denote a meteorological phenomenon wherein successive convective cells or thunderstorms traverse a fixed region, following one another like cars on a train track[1]. These storms assume a linear configuration, generating new ones over prior locations, establishing a recurring rainfall pattern over an extended duration. Substantial rainfall in areas with specific conditions[2], such as saturated antecedent soil moisture or local topographical valleys, may result in flash floods, leading to severe casualties and substantial property losses[3]. Against the backdrop of the summer monsoon in China, the manifestation of "training rainstorms" is frequent, exemplified by the unprecedented rainfall in Shenzhen and Hong Kong on September 7, 2023. During this extraordinary rainfall event, multiple air currents conveyed abundant moisture, fostering intense raincloud clusters and delineating a distinctive "training rainstorm" in the Pearl River Delta. The peak hourly precipitation reached 150 millimetres, causing widespread urban flooding in Shenzhen and Hong Kong. It is imperative to comprehend the mechanisms governing urban flash flood generation during training rainstorms.

## 2 Methodology

The Sha Tin and Wong Tai Sin districts were significantly affected by the calamity, making them the selected research areas. The full shallow water equation based 2D hydrodynamic model are applied. The "training rainstorms" are designed as elliptical rain cells that enter the study area from the top right corner along the diagonal and exit from the bottom left corner. This process is repeated twice, with a total rainfall duration of 8 hours. The difference lies in the angle between the major axis of the rain cell and the x-axis, which is set at 45 degrees (a), 0 degrees (b), and 135 degrees (c). The peak intensity of the rain cells is designed based on the Hong Kong rainstorm formula, representing a return period of 2-years, 10-years, and 100-years respectively.

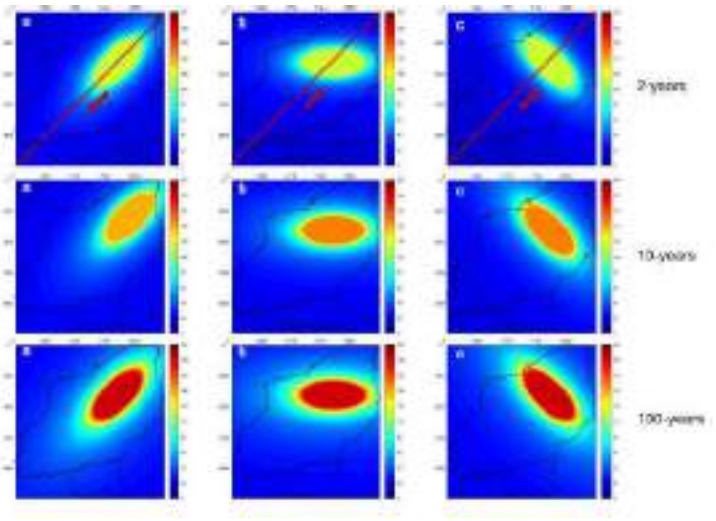

Figure 1 Design of "training rainstorms" with different return periods

## 3 Results and discussion

Model is validated with crowd sourced data collected from news. The Grid-level hazard mapping method[4] is applied in this section. The differences in risk areas among various design storms diminish as we move from L to M and H risk categories, with disparities of around 2% for both L and M risks and less than 1% for H risk. As the return period of storm increases, the disparities in risk areas diminish, albeit to a small extent. By comparison, the influence of the storm's path on the risk area is far greater than the impact of the recurrence interval. Regarding the development paths of different rainstorms, (a)Storm yields the largest risk area, followed by (b)Storm, and (c)Storm yields the smallest. This trend holds true for various recurrence intervals as well. Statistical analysis reveals that (a)Storm's development path results in the highest rainfall in the research area, consequently leading to a larger risk area. Moreover, the centre of the rain cluster during (a)Storm predominantly falls within urban areas, which are more susceptible to urban flooding, thus contributing to a larger risk area. Consequently, a combination of rainstorm development paths and land use increases the risk of urban flooding.

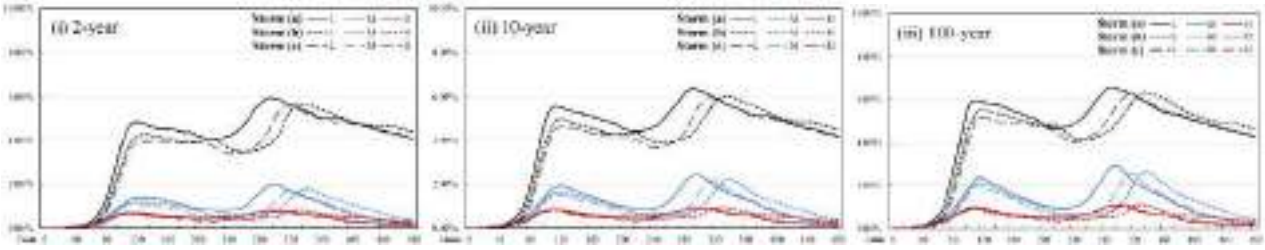

Figure 5. Risk area percentage with different design storms

## Reference

[1] Peters, J. M. and Roebber, P. J.: Synoptic control of heavy-rain-producing convective training episodes, Monthly Weather Review, 142, 2464-2482, 2014.

[2] Peters, J. M. and Schumacher, R. S.: Dynamics governing a simulated mesoscale convective system with a training convective line, Journal of the Atmospheric Sciences, 73, 2643-2664, 2016.

[3] Peters, J. M. and Schumacher, R. S.: Mechanisms for organization and echo training in a flash-flood-producing mesoscale convective system, Monthly Weather Review, 143, 1058-1085, 2015.

[4] Guan, M., Guo, K., Yan, H., and Wright, N.: Bottom-up multilevel flood hazard mapping by integrated inundation modelling in data scarce cities, Journal of Hydrology, 129114, https://doi.org/10.1016/j.jhydrol.2023.129114, 2023.

**Theme:** Hydraulic and hydrological modeling
**IAHR Thematic Priority Area:** [TPA-4] Digital Transformation
https://doi.org/10.3850/iahr-hic2483430201-89

# Flood Risk Modelling of Metro Systems in Coastal Megacities: Case Study of the "9.7" Black Rainstorm in Hong Kong

**Chen Liang[1], Kaihua Guo[2], Mingfu Guan[3]**

[1] Department of Civil Engineering, University of Hong Kong, Hong Kong SAR

*Corresponding author: Dr. Mingfu Guan, email: mfguan@hku.hk*

## 1 Introduction

During severe flood events, surface floodwater often infiltrates underground spaces, rendering these structures vulnerable to rapid and direct impacts. While existing studies indicate that multi-criteria decision-making methods excel in calculating and weighting the contribution of numerous factors in flood risk assessment, they tend to lack in dynamic evaluations of flood risk. Scenario-based approaches emphasize assessing floodwater performance as a reflection of hazard factors, but they often fail to adequately consider multiple factors of vulnerability and exposure, which are integral and necessary components of the flood risk assessment triangle. This study addresses a significant gap in existing research by developing a comprehensive approach to assess the flood risk of metro systems. It overcomes spatial and temporal limitations while considering multiple factors. Initially, the study quantifies the flood hazard of metro systems through two-dimensional modelling of rainfall-induced flooding. Subsequently, vulnerability and exposure factors are integrated with the hazard map to provide a comprehensive assessment of flood risk for metro systems during flood events.

## 2. Methodology

The study area selected for this research is Hong Kong. To analyze surface water flood dynamics in detail, a flood hydrodynamic model employing 2D shallow water equations (2D SWEs) is utilized. The flood risk assessment of metro systems during flooding is quantified using Eq. (1) as follows:

The hazard index is determined as the standardized area where floodwater depth exceeds the standard height of water-proof structures. The floor area surrounded by all entrances of a station serves as a representative measure of exposure. The vulnerability index, selected as the number of connected metro lines of a station, reflects both ridership flow density and station significance.

## 3. Preliminary results

Using the reported inundated locations during the black rainstorm event, we conducted calibration and validation of the 2D SWEs model, as depicted in Fig. 1. Figures 2a and 2b illustrate the temporally sensitive nature of the flood hazard level of the metro system, which varies with rainfall intensity, as inundation is a direct consequence of rainfall. Figures 2c and 2d depict the spatial distribution of the exposure and vulnerability levels of the metro system. By applying Eq. (1), the flood risk of metro systems at 0:00 and 11:00 on Sep 8th are depicted in Figures 2e and 2f. The number of metro stations beyond medium flood risk at peak rainfall intensity is 6% more than the stations at low rainfall intensity. It can be concluded that the comprehensive flood risk of the metro system is temporally sensitive to the time history of rainfall.

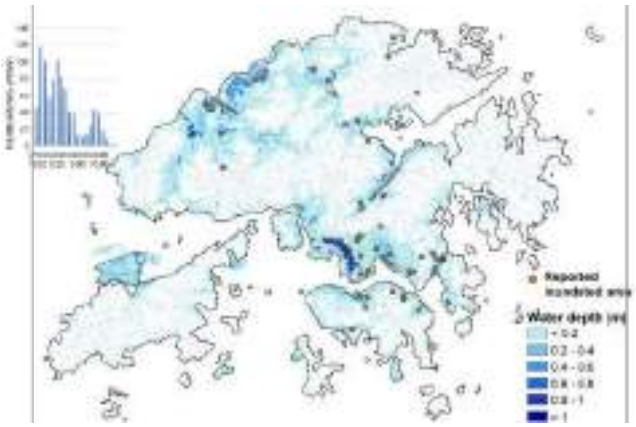

Figure 1 Reported inundated area of 9.7 black rainstorm event and the corresponding simulated floodwater depth at 08/09 0:00 in Hong Kong.

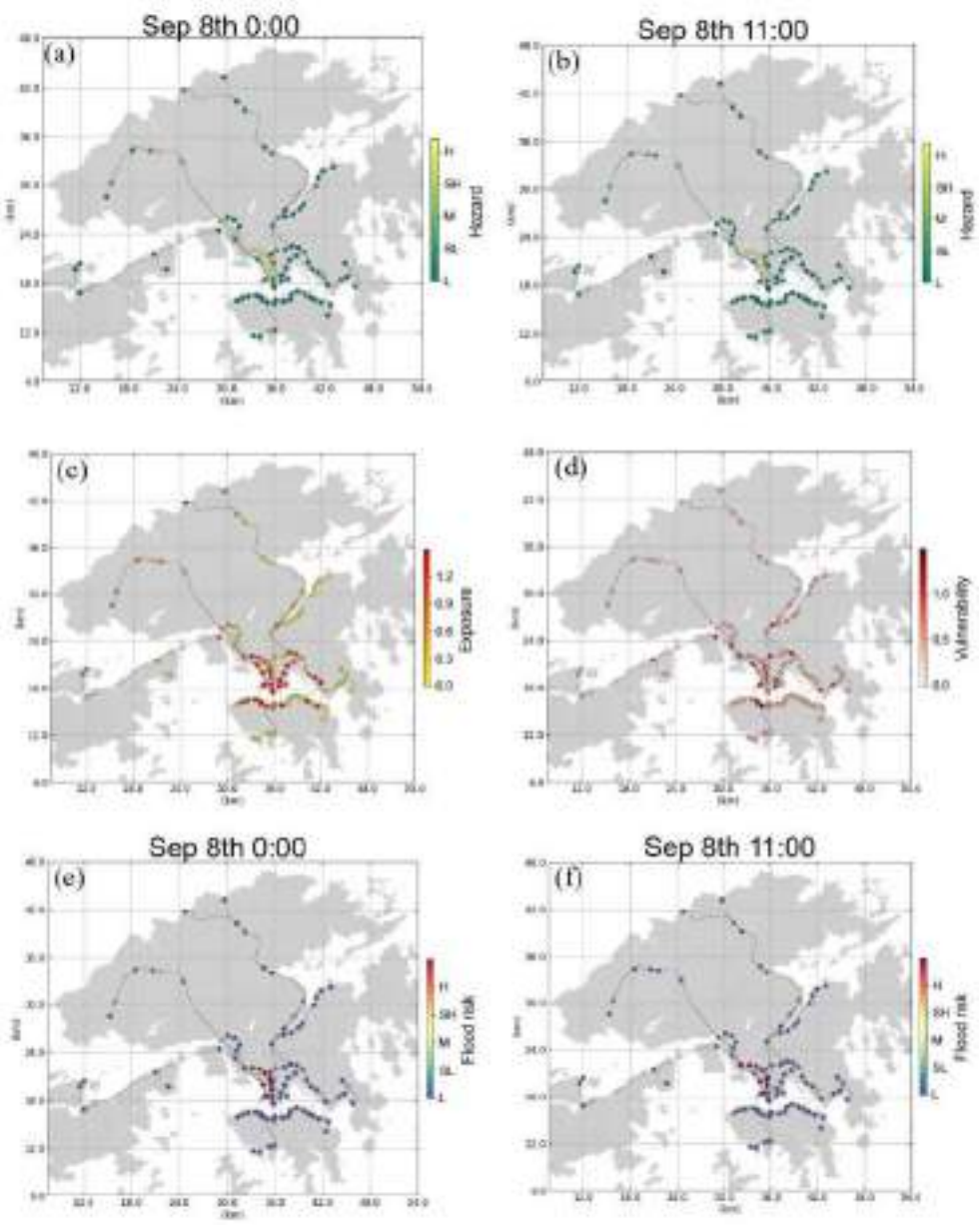


Figure 2 The (a), (b) hazard, (c) exposure, (d) vulnerability, and (e), (f) flood risk level of the metro system in Hong Kong.

**Theme:** Hydraulic and hydrological modeling
**IAHR Thematic Priority Area:** [TPA-4] Digital Transformation
https://doi.org/10.3850/iahr-hic2483430201-91

# Modelling of Turbulent Flow Over a Submerged Boulder in Open Channels

**Penghua Teng[1], J. Gunnar I. Hellström [1], Dan Nilsson[1]**

[1] Division of Fluid and Experimental Mechanics, Department of Engineering Sciences and Mathematics, Luleå University of Technology, SE-971 87 Luleå, Sweden

*Corresponding author: teng.penghua@ltu.se*

**Abstract.** Large boulders on a roughness streambed can influence local flow fields, turbulent structures, sediment transport rates, and aquatic habitats. In this paper, based on a previously conducted physical experiment, a resolved Computational Fluid Dynamics (CFD)-Discrete Element Method (DEM) approach is employed to represent turbulence flow over a submerged boulder in a rough surface channel. Simulation results illustrate flow dynamics over the boulder. The flow velocity profiles in numerical results show a good agreement with the experimental data. The results show that the presence of the boulder alters the flow field in their vicinity. Additionally, by comparing simulations of a boulder in both rough and smooth channel conditions, surface roughness influences the near-bed flow velocity and local turbulence around the submerged boulder.

**Keywords:** Immobile boulders, CFD-DEM, Bed roughness, Turbulent flow

## 1 Introduction

Large, immobile boulders, often found in steep mountain streams, play a crucial role in shaping the local flow dynamics, turbulence, sediment transport rates, and aquatic habitats, as evidenced by previous studies. The presence of these boulders introduces a significant degree of roughness to the streambed, which can be categorized based on the flow regime around them—namely, isolated, wake interference, or skimming flow regimes. The classification into these regimes is typically determined by the spacing between boulders or the concentration of boulders, providing a framework for understanding their influence on flow dynamics. An isolated flow regime is usually defined as a boulder spacing more than 6 times the boulder diameter. In this study, based on a previous flume experiment, a resolved CFD-DEM approach is employed to represent the isolated flow regime around a submerged boulder in a rough surface channel. Additionally, a comparison of a boulder in both rough and smooth channels is performed to study the effects of the bed roughness on the flow regime behand a boulder.

## 2 Methodology

A resolved CFD-DEM approach has emerged as a promising tool for modelling fluid-particle flows. The core idea of this method is to add a force term to the Navier-Stokes equations, in order to take under consideration the presence of the solid particles.

Based on a previously flume experiment [1], this study adopts the approach to represent the flow over a submerged boulder in a rough channel. The large eddy simulation (LES) is employed to model the turbulent features, and the multiple-sphere (MS) method is used to represent a boulder by a cluster of particles. Figure 1 shows the computational domain for simulations and a represented boulder. Table 1 shows the conditions of the simulations and flume experiment of Papanicolaou et al. [1].

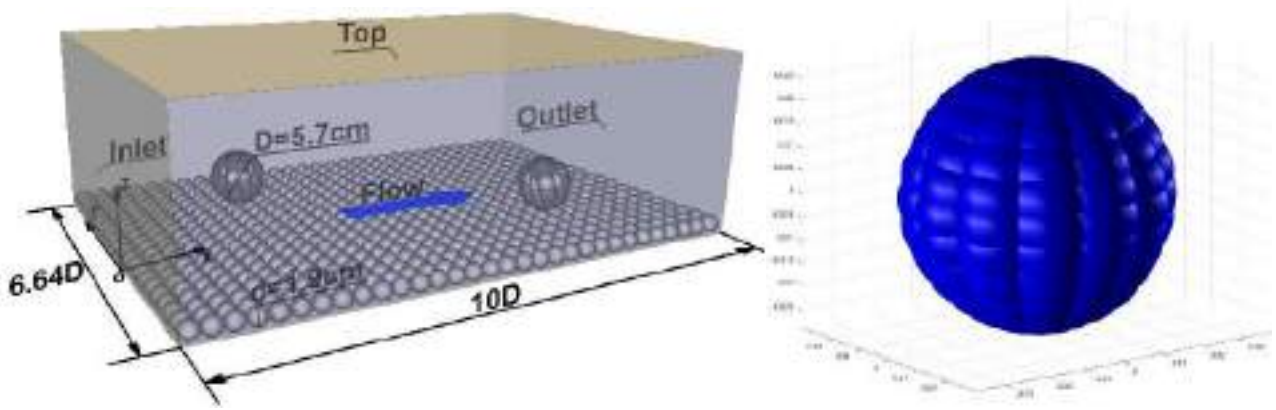


(a) (b)

Figure 1 (a) Computational domain and (b) represented boulder.

Table 1 Conditions of the numerical simulation and the experimental test of Papanicolaou et al. [1].

| | Water depth (m) | $U_{bulk}$ (m/s) | $D$ (m) | $d$ (m) | $Re$ |
|---|---|---|---|---|---|
| Simulation | 0.193 | 0.78 | 0.057 | 0.019 | 150, 500 |
| Experiment | 0.193 | 0.78 | 0.055 | 0.019 | 150, 500 |

*$Re$ is calculated based on water depth.

## 3 Results

Figure 2 shows the time-averaged streamwise velocity profiles obtained from the experiment and simulation, and Figure 3 shows turbulent intensity both rough bed surface and smooth bed surface models.

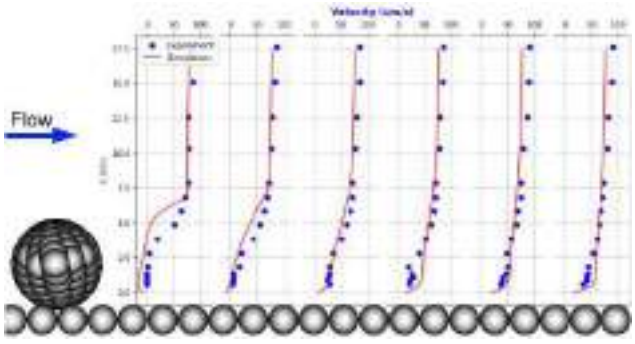


Figure 2 Time-averaged streamwise velocity profiles

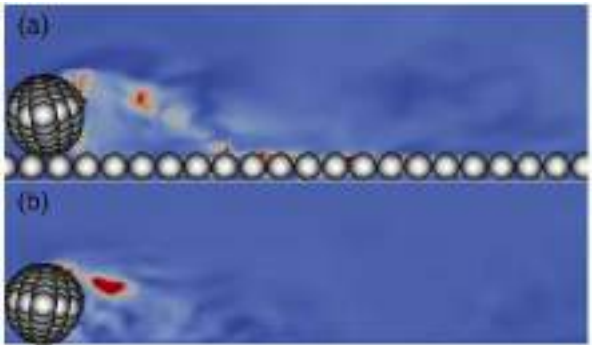


Figure 3 Turbulent intensity: (a) rough bed surface, (b) smooth bed surface

## 4 Conclusions

In this study, the resolved Computational Fluid Dynamics-Discrete Element Method (CFD-DEM) approach was utilized to simulate turbulent flow over a submerged boulder in a rough surface channel. Validation of the numerical model was achieved through comparison with flume experiments, confirming its capability in modelling flow characteristics around a boulder. The comparison between models with rough and smooth channel beds emphasizes the significance of considering bed roughness in predicting flow dynamics around a boulder.

## Reference

[1] Papanicolaou, A. N., Kramer, C. M., Tsakiris, A. G., Stoesser, T., Bomminayuni, S., Chen, Z., Effects of a fully submerged boulder within a boulder array on the mean and turbulent flow fields: Implications to bedload transport, Acta Geophysica. 60(6), 2012, pp. 1502–1546.

**Theme:** Hydraulic and hydrological modeling
**IAHR Thematic Priority Area:** [TPA-4] Digital Transformation
https://doi.org/10.3850/iahr-hic2483430201-93

# A Complementary Approach of Air Supply to Spillway Aerator

**James Yang[1,2], Shicheng Li[2]**

[1] R&D Hydraulic Laboratory, Vattenfall AB, Älvkarleby 81426, Sweden
[2] Civil & Architectural Engineering, KTH Royal Institute of Technology, Stockholm 10044, Sweden

*Corresponding author: shicheng@kth.se*

**Abstract.** Some spillway aerators suffer from insufficient air supply. As a complementary measure, an aerator splitter is conceived, with an ogival form in cross-section. CFD modeling is performed to assess its behaviors in terms of flow pattern, air supply, cavity pressure, etc. The results show that the chute flow is pierced, and a stable elongated opening is created downstream, thus allowing effective suction of air into the air cavity.

**Keywords:** aerator, air-flow behavior, air supply, cavitation, spillway, splitter

## 1 Background

Some spillways are entangled by cavitation damages, even if aerators are installed. Part of the reasons is ascribed to insufficient air supply to the flow. Additional air supply is thus necessary, especially if the design discharge becomes higher (Yang et al. 2019a). A nappe splitter, vertically placed at an existing aerator, is designed for additional air supply to the aerator flows. The study aims to illustrate the splitter as an option for complementary air supply for both existing and new spillways,

## 2 Splitter configuration

With a splitter in a high velocity flow, the following should be considered. (1) Little disturbance is imposed on the flow; (2) Harmful negative pressures are avoided; and (3) The splitter opening should be stable to avoid air-pressure fluctuations in the aerator. One configuration is shown in Figure 1, with the splitter formed by two arcs in cross-section ($R$ = 8 m, $W$ = 1 m, $L$ = 2.78 m).

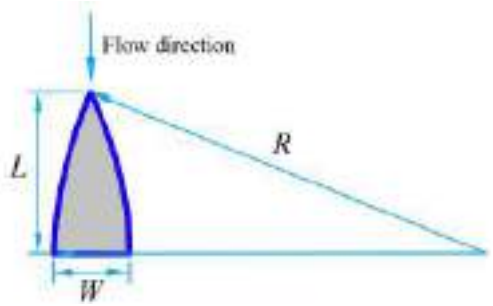


Figure 1 Splitter formed by two arcs

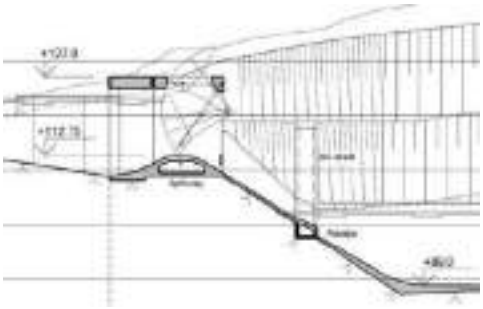

Figure 2 A prototype spillway with an aerator

## 3 Prototype spillway

A prototype spillway is adopted in the study (Yang et al. 2019b). Figure 2 illustrates its profile with an aerator. The crest elevation is +112.75 m; the chute width is 25.0 m. The duct is designed with 13 rectangular air vents of the same size. Each vent measures 1.0 m in width and 1.0 m in height; the total vent area is thus 13.0 m$^2$. The vents are not placed equidistantly but symmetrically to the chute axis.

## 4 Results

The splitter is placed on an existing aerator, with its downstream edge coinciding with the aerator offset. CFD is performed in Fluent, with the RNG k-ε and the Two-Fluid models. Four layouts are modelled: Case 1 – layout without splitter; Case 2 – splitter at the center; Case 3 – two splitters placed at a one-third chute width from the sidewalls and Case 4 – as in Case 3, with both air shafts sealed. The flow pattern (Case 2) is shown in Figure 3. With the $L/W$ = 2.40 splitter, the flow pattern is acceptable in terms of local splash. At the splitter, the flow is divided, creating an opening behind it. For the chosen shape, the opening is stable and does not fluctuate sidewards. Due to the air pressure difference across the flow, this opening allows air to enter the cavity. The use of one splitter or two leads to relatively uniform air pressure across the aerator. The low cavity pressure is improved in the middle of the chute and the air supply into the flow becomes enhanced.

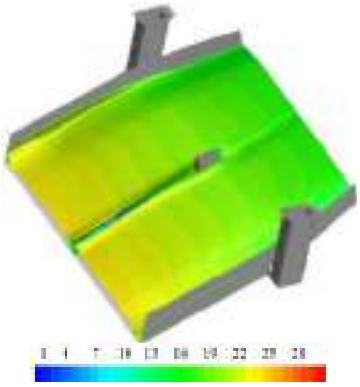

Figure 3 Water-surface profile (case 2) colored by velocity magnitude

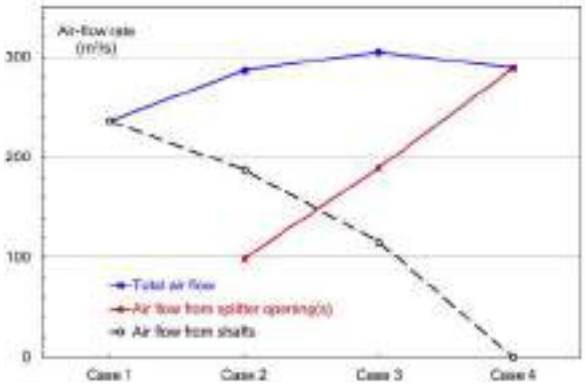


Figure 4 Air-flow rate through the air shafts and the splitter opening(s)

Figure 4 compares the air-flow rates of the four cases. From Case 1 to 4, the air flow from both shafts is 236.2, 187.4, 115.7 and 0 $m^3/s$. From Case 2 to 4, the air flow through the splitter opening is 99.1, 189.5 and 288.9 $m^3/s$. Compared with the original aerator (Case 1), the introduction of one splitter (Case 2) elevates the air flow by 21%. Two splitters (Case 3) are more effective than one, with air flow enhancement by 29%. Even if both shafts are sealed, e.g. by snow cover (Case 4), the air flow from the splitter openings is larger than in Case 1, thus satisfactorily accommodating the air demand. Owing to the short path from the atmosphere to the air cavity, the use of the splitter(s) is undoubtedly a complementary method for air supply to the aerator flow.

## 5 Conclusions

The use of a splitter one two on an aerator is an effective method for air supply. It improves the air pressure distribution in the air cavity and enhances the air-flow rate into the lower edge of the trajectory flow. With respect to chute slope, approach flow velocity and other contributing factors, the splitter configuration should be optimized within the range of operation discharges.

## Acknowledgments

Being part of research project “Spillway discharge safety – quality and assurance in CFD for air-water flow pre-dictions (VKU32011)”, this study is funded by the Swedish Center for Sustainable Hydropower (SVC).

## Reference

[1] Yang, J.; Andreasson, P.; Teng, P.H.; Xie, Q.C., 2019a. The past and present of discharge capacity modelling for spillways – a Swedish perspective. Fluids, 4, 10.

[2] Yang, J.; Teng, P.H.; Lin, C., 2019b. Air-vent layouts and water-air flow behaviors of a wide spillway aerator. Theoretical and Applied Mechanics Letters, 9, 130–143.

**Theme:** Hydraulic and hydrological modeling
**IAHR Thematic Priority Area:** [TPA-4] Digital Transformation
https://doi.org/10.3850/iahr-hic2483430201-95

# Physical and Numerical Modeling of Flow Behaviors of Piano Key Weirs

**Shicheng Li[1], James Yang[1,2]**

[1] Civil & Architectural Engineering, KTH Royal Institute of Technology, Stockholm 10044, Sweden
[2] R&D Hydraulic Laboratory, Vattenfall AB, Älvkarleby 81426, Sweden

*Corresponding author: shicheng@kth.se*

**Abstract.** Many hydropower dams in Sweden have insufficient discharge capacity. As an effective flood discharge structure, the piano key weir has gradually become an alternative in the refurbishment of the existing dams. Along with investigating its structural performance in cold climates, laboratory and CFD studies are conducted to examine its discharge capacity and hydraulic behaviors and compare the two approaches. This study confirms CFD's accuracy in predicting PK weirs' hydraulic behaviors, with a maximum relative error of 11.6% observed at higher heads. It also highlights PK weirs' comparative effectiveness and provides insights into optimizing their design for improved flood management in existing and new hydraulic facilities.

**Keywords:** Piano key weir, discharge capacity, physical modeling, CFD

## 1 Introduction

As in other countries, a significant number of the original dam spillways in Sweden have insufficient discharge capacity. Many of them have already been rebuilt to satisfy the new design flood guidelines. The others undergo an upgrade process from design to reconstruction. As an effective discharge structure, the PKW has gradually become an alternative in refurbishments. Model tests of a PKW are made in the laboratory. The model, with a 0.375 m height and a 1.14 m width (three weir cycles), is examined in a 2.00 m wide flume, and the flow rate is up to ~320 liter/s. In parallel with the model studies, CFD simulations are also performed. The main purpose is to benchmark the physical and numerical results and to gain confidence in CFD modeling for practical design purposes.

## 2 Experimental layout

In terms of flow discharge capacity, Lempérière and Ouamane [1] proposed a near-optimal weir configuration. The weir geometry is shown in Figure 1, in which $B_i = B_o = 0.9P_m$, $B_b = 1.8P_m$, $P_i = P_o = 1.5P_m$, $B - 2T_s = 3.6P_m$, $\alpha_i = \alpha_o = \alpha = 29.05°$, and $P_m$ = distance between the crest elevation and the virtual intersection point of the two keys. The optimal $W_i/W_o$ range is within $W_i/W_o = 1.25–1.50$. In this study, $W_i = 1.33P_m$ and $W_o = P_m$ are chosen, thus $W_i/W_o = 1.33$. The width and the developed crest length of a weir cycle are $W = 38.0$ cm and $L = 146.0$ cm.

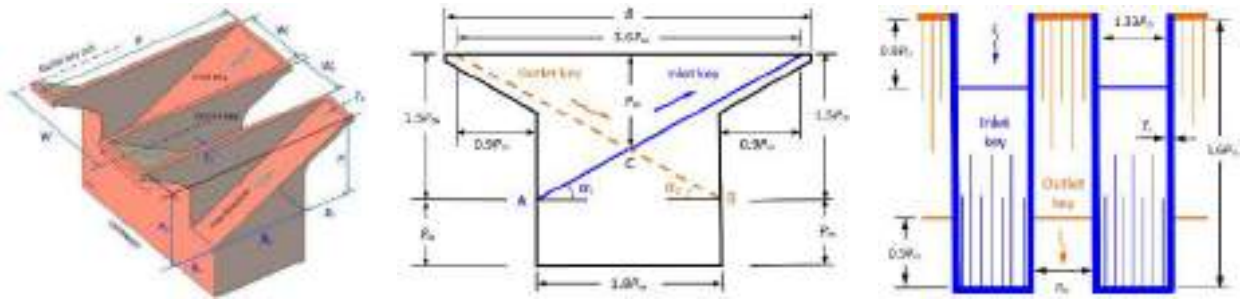

Figure 1 Parameter definition of the type-A PK weir.

## 3 CFD setup

The RNG $k$-$\varepsilon$ turbulence model combined with the VOF method is adopted to reproduce the flow behaviors. The entire domain is discretized using a structured mesh, comprising a total of ~600,000 cells. The cell sizes range from a minimum of 1.5 cm to a maximum of 7.0 cm.

## 4 Flow discharge

The unique design of PK weirs is mainly for improving the flow rate over the weir compared to conventional linear weirs. Based on the developed crest length $L$ of a single weir cycle, the flow rate $Q$ over a PK weir is expressed using an empirical equation:

$$Q = \frac{2}{3} CL\sqrt{2gH^3} \tag{1}$$

where $C$ = discharge coefficient, and $H$ = total head over the weir. Figure 2(a) compares the CFD and experimental discharge coefficient. The discharge coefficient exhibits a characteristic behavior where it rises and then drops with an increase in the water head. The excellent agreement between the CFD simulations and experimental measurements underscores the accuracy of the numerical approach. The maximum relative error is 11.6%, and a higher head seems to lead to a more significant error. Figures 2(b,c) show the experimental and simulated water surface, which is consistent.


(a) (b) (c)

Figure 2 Discharge coefficient (a), experimental (b), and simulated water surface (c).

## 5 Conclusion

The combination of experimental and CFD modeling has enabled a detailed examination of the flow dynamics. This study verifies CFD's accuracy in forecasting PK weirs' hydraulic performance, noting a maximum relative discrepancy of 11.6% at high flow conditions. This validation supports the use of CFD as a reliable tool for designing and optimizing PK weirs.

## Reference

[1] Lempérière, F and Ouamane, A. 2003. The piano keys weir: a new cost-effective solution for spillways. International Journal of Hydropower and Dams, 10(5), pp 144–149.

**Theme:** Hydraulic and hydrological modeling
**IAHR Thematic Priority Area:** [TPA-4] Digital Transformation
https://doi.org/10.3850/iahr-hic2483430201-97

# Numerical Simulation of Confluence Flow with Various Discharge Ratios and Junction Angles

**Van Thinh Nguyen[1] and Jihwan Kim[1]**

[1] Department of Civil and Environmental Engineering, Seoul National University, Seoul 08826, South Korea

*Corresponding author: vnguyen@snu.ac.kr*

**Abstract.** This study aims to conduct a three-dimensional numerical investigation of the effect of various discharge ratios and junction angles of confluent flow on flow patterns, shapes of separation zones and water levels. The flow calculation is based on the Reynolds-Averaged Navier-Stokes (RANS) equations for the mean flow field together with two-equation SST k-ω turbulence closure model. In addition, the free surface level is tracking by the volume of fluid (VOF) method. The numerical simulations are carried out for different discharge ratios and junction angles. The results are validated against the observation data obtained from various experiments. It shows that an increase in the discharge ratio and junction angle is resulting in enlarging the separation zone; and an increase in discharge ratio leads to strong variation of the water level near the separation zone.

**Keywords:** Confluent flow, discharge ratio, junction angle, separation zone, turbulence

## 1 Introduction

Confluent flow has been studied by various authors; however, most previous studies are limited to a specific flow configuration, such as for a single-angle junction, a discharge ratio or Froude number. There are still few studies that examine the combined influences of different junction angles and discharge ratios (the ratio of the upstream main channel discharge to the total discharges of the branch and main channels) on flow patterns. This study aims to conduct a three-dimensional numerical simulation to investigate the effect of discharge ratios and junction angles on the flow patterns at confluences, including shapes of separation zones and water depths, using the open source CFD package OpenFOAM (http://www.openfoam.com). The flow calculation is based on the Reynolds-averaged Navier–Stokes (RANS) equations for the mean flow field together with the SST k-ω turbulence closure model. The numerical results with different discharge ratios have been validated against the observational data obtained from Weber et al.'s experiments [1], while the numerical results with different angles were validated against the observation obtained from Gurram et al.'s experiments [2].

## 2 Validations

### 2.1 Validation against Weber et al.'s experimental data [1]

In this experiment, the junction angle is 90 degree, the water depth at inlets (of main and branch channels) is 0.33m, Froude number is around 0.37, and discharge ratios q* (the ratio of the branch channel flow rate to the total flowrate at downstream of the confluence) are 0.25 and 0.75. All distances were normalized by the channel width, W = 0.914 m. The nondimensionalized coordinates are called x*, y*, and z* for x/W, y/W, and z/W, respectively.

Figure 1 shows the comparisons of velocity distribution between the experiments and simulation results at the free surface and at z*=0.278, respectively. In general, the flow patterns were similar, and the separation zones were observed to be increased as the discharge ratio is increased.

Furthermore, a comparison between the experiment and simulation of water depth profiles along different longitudinal sections shows very good agreement, and it also reveals that the fluctuation of the water surface is getting stronger as the discharge ratio is increased.

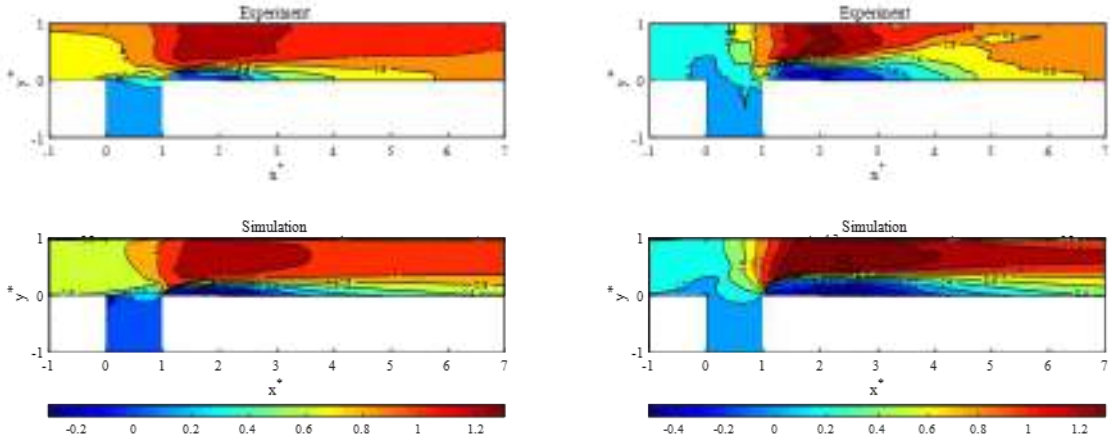


Figure 1 Velocity distribution at free surface with q*=0.25 (left) and q*=0.75 (right).

## 2.2 Validation against Gurram et al.'s experimental data [2]

In this experiment the junction angles are 30, 60, and 90-degree, water depth at both inlets is 0.1m, and Froude number of 0.5. The discharge ratios are 0.25, 0.5, and 0.75. A comparison of the maximum thickness $b_s$ and length $L_s$ of the separation zone between the experiment and simulation reveals that the simulation results exhibit good agreement with the observations in general. It was also reveals that the maximum thickness $b_s$ and length $L_s$ increase when the junction angle, as well as the discharge ratio, are increased, as shown in Table 1.

Table 1. Comparison of the size of separation zones for q*=0.75.

| Angle | Maximum thickness, $b_s$ | | | Length, $L_s$ | | |
|---|---|---|---|---|---|---|
| (deg) | Exp. (m) | Sim. (m) | Error (%) | Exp. (m) | Sim. (m) | Error (%) |
| 30 | 0.057 | 0.053 | 7.01 | 0.23 | 0.17 | 26.1 |
| 60 | 0.140 | 0.132 | 5.71 | 1.18 | 1.21 | 2.54 |
| 90 | 0.207 | 0.195 | 5.79 | 1.93 | 1.82 | 5.69 |

## 3 Conclusion

The effect of discharge ratios and junction angles on the flow at confluences were investigated using an open source CFD package OpenFOAM. The numerical results were validated against the experiments conducted by Weber et al. [1] and Gurram et al. [2]. It shows that the separation zone is enlarged as the discharge ratio and junction angle increase, and the water depth varies stronger near the separation zone as the discharge ratio increases.

## References

[1] Weber, L. J., Schumate, E. D., & Mawer, N. (2001). Experiments on flow at a 90 open-channel junction. Journal of Hydraulic Engineering, 127(5), 340-350.

[2] Gurram, S. K., Karki, K. S., & Hager, W. H. (1997). Subcritical junction flow. Journal of Hydraulic Engineering, 123(5), 447-455.

**Theme:** Hydraulic and hydrological modeling
**IAHR Thematic Priority Area:** [TPA-4] Digital Transformation
https://doi.org/10.3850/iahr-hic2483430201-99

# Investigation of the Effect of Air Injection on Scour Mitigation behind Apron

**Jeonghu Lee[1], Van Thinh Nguyen[1]**

[1] Department of Civil and Environmental Engineering, Seoul National University, Seoul 08826, South Korea

*Corresponding author: vnguyen@snu.ac.kr*

**Abstract.** This study investigates the effect of air injection on scour mitigation behind an apron under a wall jet flow condition. We employed a combined large eddy simulation (LES) and discrete element method (DEM) technique within the OpenFOAM framework, further incorporating the volume of fluid (VOF) method to reproduce air flow and free surface. The dimensions of the simulated scour were in good agreement with those obtained from empirical formulas derived from a well-known laboratory experiment, indicating a reliable model. Our research focused on analyzing the flow structures and sediment behaviors when air was injected at the end of apron at various flow rates. The air injection was found to significantly decrease the bedload transport rate and the maximum scour depth by reducing the near-wall streamwise mean velocity. Moreover, as the rate of air injection increased, there was a further reduction in the maximum scour depth, accompanied by a greater increase in the near-wall streamwise turbulence intensity. The simulation results clearly demonstrate the potential of air injection in mitigating scour behind an apron, presenting it as a viable alternative approach to diminishing scouring effects.

**Keywords:** Air injection, bedload transport, LES-DEM coupling, scour mitigation, wall jet flow

## 1 Introduction

The effectiveness of air injection has been demonstrated in practice, which reduces the strength of the flow by redirecting the flow upward and thereby significantly reducing scouring [1, 2]. However, detailed examinations of the effects of air injection on flow structures and sediment fluxes have not been conducted until recently. In this context, this study focuses on investigating the flow structures and sediment behaviors with air injected at the end of apron at various flow rates to find out the physical mechanism of scour mitigation by air injection. A coupled model of large eddy simulation (LES) and discrete element method (DEM) is employed to reproduce the bed turbulent flow structures and sediment behaviors. The three-dimensional hydrodynamics are simulated using LES approach to capture the instantaneous flow behaviors by means of time-dependent, 3D Navier-Stokes equations. The universal behaviors of smaller eddies (subgrid-scale) are solved by Smagorinsky model [3]. The numerical model used in this study is validated against well-known experimental formulas to ensure its reliability. The outcomes of the present study are anticipated to provide valuable insights for the management of scour problem behind aprons, contributing to their long-term sustainability and resilience.

## 2. Computational setup

In this study, an experimental case from [4], addressing the local scouring process caused by submerged wall jet flows, is selected to construct a computational domain. The computational domain for the wall jet flow induced by the opening of a sluice gate is illustrated in Figure 1. The length scale of the computational domain is detailed in Table 1. The number of air slots consist of four depending on the air injection flow rates. The air slots are positioned along the apron boundary, and the ratio of

air injection flow rate $Q_a$ to the inflow water flow rate $Q_w$ is determined as $q_r = Q_a/Q_w$ = 0.25, 0.5, and 1.

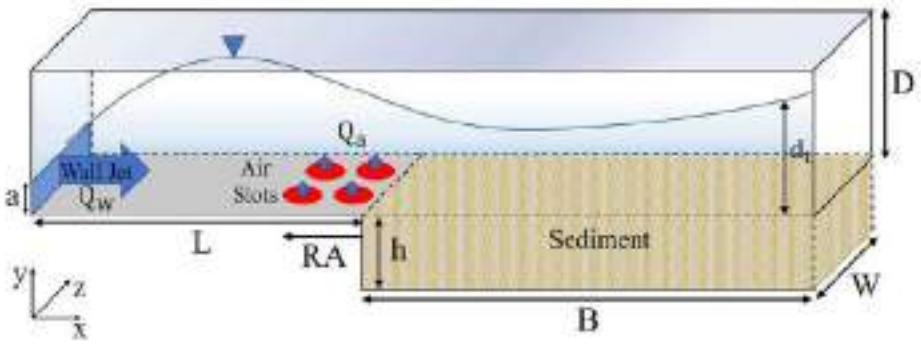


Figure 1 Schematic diagram of the computational domain for wall jet flow behind a sluice gate (diagram is not to the scale).

Table 1. Length scale of the computational domain.

| a (m) | L (m) | h (m) | B (m) | D (m) | W (m) | $d_t$ (m) |
|---|---|---|---|---|---|---|
| 0.02 | 0.66 | 0.11 | 3.0 | 0.61 | 0.02 | 0.31 |

## 2 Conclusion

The two-phase (water-sediment) LES-DEM coupling was expanded to incorporate air phase by introducing VOF concept to implement free surface and air injection. The altered bed profile without air injection exhibited good agreement with laboratory experiment results. The mean velocity, turbulence intensity, and bedload transport rate downstream of the apron were numerically quantified. Based on the simulation results, the following conclusions and observations can be summarized:

When air was injected, the bedload transport rate in the sediment zone significantly decreased throughout the entire simulation, resulting in minimal changes to the bed profile. By the end of the simulation, the maximum scour depth was found to decrease by 51.85% to 90.74%, depending on the air injection flow rate. In summary, it is demonstrated that an increase in the air injection flow rate leads to a significant mitigation of scour.

To analyze the cause of the decrease in sediment flux due to air injection, we examined the flow and turbulence structures for both cases with and without air injection. The near-bed streamwise mean velocity at the end of the apron decreased significantly, depending on the air injection flow rate. Based on the simulation results, the reduction in near-bed streamwise velocity primarily contributes to the mitigation of scour behind the apron.

## References

[1] Champagne, T. M., Barkdoll, B. D., Gonzalez-Castro, J. A., & Deaton, L. Scour reduction by air injection: Flow patterns and turbulence. Journal of Hydraulic Engineering. 2016;142(3), Art. no. 06015023.

[2] Tipireddy, R. T., & Barkdoll, B. D. Scour reduction by air injection at a cylindrical bridge pier: Experimental determination of optimal configuration. Journal of Hydraulic Engineering. 2019;145(1), Art. no. 06018016.

[3] Smagorinsky, J. General circulation experiments with the primitive equations: I. The basic experiment. Monthly weather review. 1963;91(3):99-164.

[4] Chatterjee, S. S., Ghosh, S. N., & Chatterjee, M. Local scour due to submerged horizontal jet. Journal of Hydraulic Engineering. 1994;120(8):973-992.

**Theme:** Hydraulic and hydrological modeling
**IAHR Thematic Priority Area:** [TPA-4] Digital Transformation
https://doi.org/10.3850/iahr-hic2483430201-101

# The Lattice Boltzmann Wetting and Drying Technique with Added Flow Turbulence

**Elysia Grace Barker[1], Jian Guo Zhou[1]**

[1] Manchester Metropolitan University, Manchester, M15 6BH, United Kingdom

*Corresponding author: Elysia.G.Barker@stu.mmu.ac.uk*

**Abstract.** In this paper, a wetting and drying technique for the enhanced lattice Boltzmann method for shallow water equations (eLABSWE) was improved by utilising the lattice Boltzmann turbulence (LABSWETM) model, which considers flow turbulence naturally by incorporating the standard subgrid-scale stress model into the lattice Boltzmann equation within the collision and streaming steps. To remain consistent, a version of the LABSWETM is incorporated into the wet-dry interface calculations. The eLABSWE is a promising model with its simplicity and flexibility which responds well to improvements, adaptations, and different complex flow cases. This method is excellent at accurately simulating flow around objects, particularly in areas where flow is strongly three-dimensional, and, with the use of the LABSWETM, turbulent flow is accurately simulated. As a result of this, it stands to reason that the eLABSWE would be ideal to model urban flash flooding. However, there are limitations arising from the eLABSWE, such as its heavy reliance on equilibrium distributions, and stability issues are easy to encounter with this type of flow. To overcome some of these issues, the incorporation of turbulence into the wet-dry interface calculations has improved the accuracy of more complex flows around the wet-dry boundary.

**Keywords:** Drying, Lattice Boltzmann, Modelling, Shallow Water, Turbulence, Wetting

## 1 Introduction

The wetting and drying process is an important aspect to consider when modelling shallow water flows due to their ability to be greatly and easily influenced by small adjustments in external forces affecting the wet-dry front [2]. This is of particular interest in flood modelling given the topography of the affected area will not be completely saturated before a flood or flash flood event, resulting, usually, in the formation of a shockwave which then propagates forwards [5]. Additionally, turbulence is particularly complex and challenging phenomenon to model. Turbulent flows usually have unsteady numerical wave speeds and involve extensive complex and spatial domain evolution resulting in the need for fine numerical meshes and computationally heavy simulations [4]. Several techniques using the lattice Boltzmann method have been brought together to improve the wet-dry interface calculations of turbulent flow cases, as it is necessary to deal with turbulent flows with a wet-dry front in most environmental hydraulic studies, though it is rarely found in literature [1].

## 2 Methodology

The lattice Boltzmann approach to simulating the wet-dry front in shallow flows is implemented using method described in [2]. Given this method utilises the eLABSWE, the LABSWETM is applied to the eLABSWE in the same manner as described in [3] which defines a new relaxation time, , as a result of the eddy viscosity appearing in the momentum equations when using the subgrid-scale stress model. Additionally, the new relaxation time along with its method of calculation is integrated into the wet-dry interface calculations using a condition mentioned in [4]. This condition alters the value of  depending on the behaviour of the particles at neighbouring lattice nodes to remain consistent with the interactions between particles at the wet-dry interface.

## 3 Results and Discussion

Strong changes in the direction of a channel can produce 3D flow patterns, which often cause issues with results obtained by the 2D shallow water equations. To test the capabilities of this method in such a way, a test case describing flow in a 90˚ bend was taken from [1] and the results were compared.

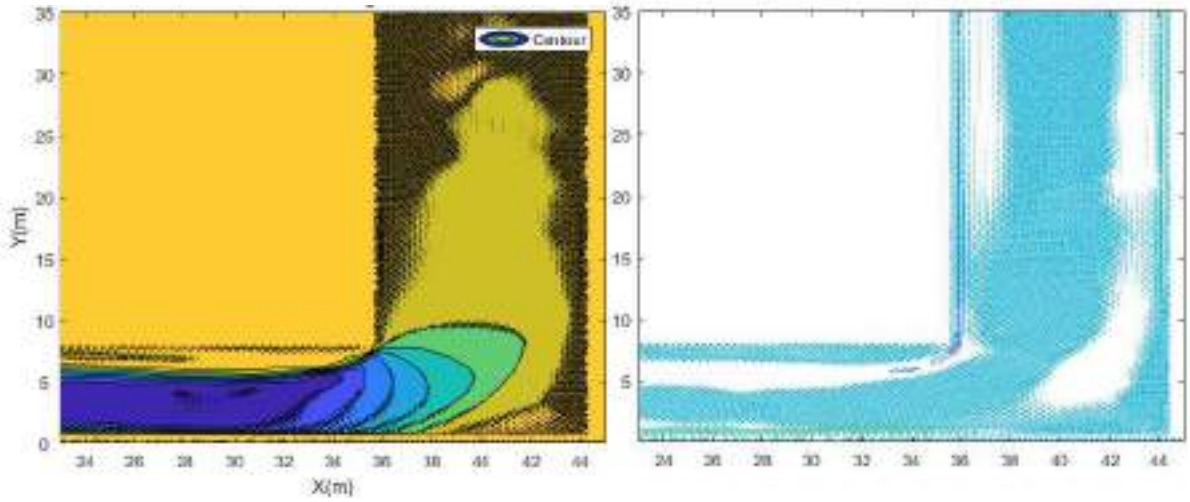


Figure 11 Turbulent flow in a 90˚ bend after 100 seconds (Velocity field (m/s), left, Vortices, right)

Overall, the results obtained using the eLABSWE turbulence model with a wetting and drying front show promise. The results, when compared to those outlined in [1], have a strong resemblance to both the experimental data and the numerical results available. Further testing and investigation will be carried out to make improvements to the model with the aim of adapting further to include many other physical characteristics such as sediment transport, rainfall, variation of land use, objects and obstacles, and more.

The method has efficiently and accurately simulated the flow of water in a 90˚ bend, highlighting its usefulness in modelling such cases with 3D flow patterns, which is a well-established feature of the LABSWE. Expanding the capabilities of this model should lead to an efficient and accurate method for modelling flash floods, particularly in areas where other methods struggle such as around buildings in urban areas.

## Reference

[1] Cea, L., Puertas, J. & Vázquez-Cendón, ME. Depth Averaged Modelling of Turbulent Shallow Water Flow with Wet-Dry Fronts. Arch Computat Methods Eng 14, 303–341 (2007). https://doi.org/10.1007/s11831-007-9009-3

[2] J.G. Zhou, Lattice Boltzmann Methods for Shallow Water Flows, Springer, 2004, DOI: 10.1007/978-3-662-08276-9

[3] J.H. Pu. Turbulence modelling of shallow water flows using Kolmogorov approach. Computers & Fluids, 2015, 115, p.66-74.

[4] J.Q. Xia, R.A. Falconer , B.L. Lin & G.M. Tan, Modelling flood routing on initially dry beds with the refined treatment of wetting and drying, International Journal of River Basin Management, 2010, 8:3-4, 225-243, DOI: 10.1080/15715124.2010.502121

[5] H. Liu, J.G. Zhou. "Lattice Boltzmann approach to simulating a wetting─drying front in shallow flows". Journal of Fluid Mechanics 743. (2014).

**Theme:** Hydraulic and hydrological modeling
**IAHR Thematic Priority Area:** [TPA-4] Digital Transformation
https://doi.org/10.3850/iahr-hic2483430201-103

# SPH Simulation of Transient Flow with Unsteady Friction in Pipelines with Entrapped Air Pocket at Dead End

**Huaicheng Fan[1], Qingzhi Hou[1,2], Xuliang Yang[2]**

[1] State Key Laboratory of Hydraulic Engineering Intelligent Construction and Operation, Tianjin University, Tianjin 300350, China
[2] School of Civil and Transportation Engineering, Qinghai Minzu University, Xining 810007, China

*Corresponding author: Qingzhi Hou, qhou@tju.edu.cn*

**Abstract.** Urban flooding has caught lots of attentions around the world. It has been verified that the water flow regime transition and impact pressure can be affected by entrapped air pocket in urban drainage pipeline system. Traditional rigid column model cannot capture the pressure oscillation due to water hammer effect for neglecting water compressibility. As a particle method, smoothed particle hydrodynamics (SPH) provides an effective way to introduce the water compressibility into simulation. In this paper, an elastic model with unsteady friction is developed to simulate the transient flow in pipelines with entrapped air pocket at the dead end. In this model, the steady Darcy-Weisbach friction model is replaced by the Brunone unsteady friction model in classical water hammer equation. Two different cases are studied to verify the proposed model. The results show that the SPH-based elastic model can effectively predict the pressure oscillation in the system due to compression of entrapped air pocket. The unsteady friction model has no significant effect on the entrapped air in pipeline with a dead end.

**Keywords:** Elastic model, entrapped air pocket, smoothed particle hydrodynamics, unsteady friction model

## 1 Introduction

This paper proposes an SPH-based elastic model with Brunone unsteady friction model for simulating a compressed entrapped air pocket in a pipeline with a dead end to predict the pressure oscillation in the system. Two different governing equations for entrapped air pocket were used. The results demonstrates that the proposed particle model is an effective tool to simulate the transient flow with an entrapped air pocket in the pipeline.

## 2 Methodology

Smoothed particle hydrodynamics (SPH) is used this study. The kernel approximation is given as:

$$\left\langle \nabla f\left(x\right)\right\rangle =-\int_{\Omega} f\left(x'\right)\cdot\nabla W\left(x-x',h\right)dx' \tag{1}$$

where $\left\langle \cdot \right\rangle$ is the kernel approximation operator, $W\left(x-x',h\right)$ is the kernel function, which is cubic-spline in this study, and $h$ is the smoothing length. Therefore, the classic water hammer equation can be written as:

$$\frac{\mathrm{d}p_a}{\mathrm{d}t}=-c^2\sum\nolimits_b m_b\left(u_a-u_b\right)\frac{\mathrm{d}W_{ab}}{\mathrm{d}x_a} \tag{2}$$

$$\frac{\mathrm{d}u_a}{\mathrm{d}t}=-\frac{1}{\rho^2}\sum\nolimits_b m_b\left(p_a-p_b+\Pi_{ab}\right)\frac{\mathrm{d}W_{ab}}{\mathrm{d}x_a}+g\sin\theta-f\frac{u_a\left|u_a\right|}{2D} \tag{3}$$

where $\Pi_{ab}$ is the artificial viscosity term.

In this study, Brunone unsteady friction model is used [1], and the air pocket governing equations are polytropic process and Martin's model [2].

## 3 Result and discussion

The experiments of Zhou *et al*. [3] and Zhou *et al*. [4]. are simulated to verify the proposed model. And the results are shown below.

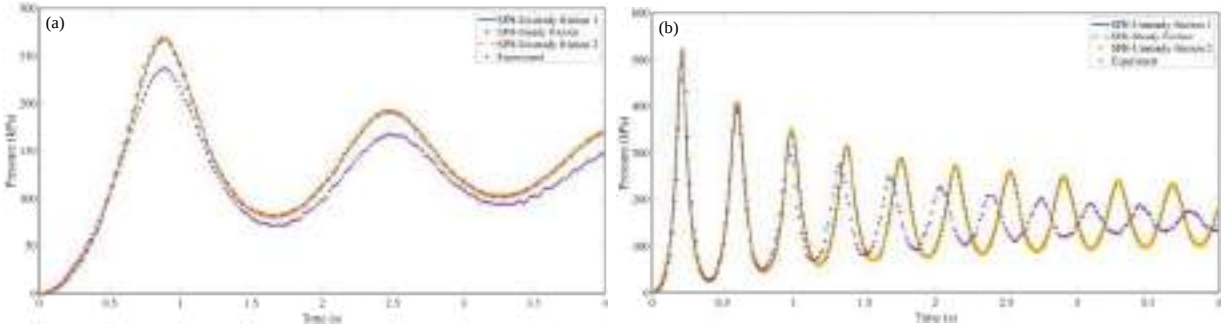


**Figure 1.** Comparison between numerical results of SPH with steady friction, SPH with unsteady friction and experiment, air pocket governing equations are polytropic process equation used in SPH-Unsteady friction 1 and Martin's model [2] used in SPH-Unsteady friction 2, respectively: (a) Zhou *et al*. [3], (b) Zhou *et al*. [4]

The results in figure 1 (a) show that the numerical results can only reproduce the occurrence time of the maximum pressure and frequency of the pressure oscillation, but the calculated peaks are all higher than measured data. In figure 1 (b), the numerical result basically overlaps with measured data in the first three peak (first 1 s). However, with the increasing of the simulation time the amplitude becomes higher than the measured data, and the phase becomes faster than the measured data.

During the motion of water column, the well-defined air-water interface will gradually tilt or even be completely replaced by the air-water mixture. In a horizontal pipeline, the air-water interface will tilt very quickly due to gravity as observed by Zhou *et al.* [3], resulting in a large difference between the calculation and the measurement. In a vertical pipeline, the air-water interface can remain the shape for some time, resulting in good agreement between the calculation and measurement. That is, the stratification of the air-water interface can alleviate the pressure fluctuation to some extent.

## 4 Conclusion

Unsteady friction model has no significant effect on the numerical results in such cases in which there is an entrapped air pocket compressed in a pipeline with a dead end. For modeling the entrapped air pocket, the polytropic process is equivalent to Martin's model. During the actual motion of the water column, there is a break occurring in the well-defined air-water interface in varying degrees, which is mild in horizontal pipelines but drastic in vertical pipelines. And their occurrences do not meet the basic assumptions of the proposed model. Such break is the main reason for the inconsistence of the calculated results by the model in two different cases. The attenuation mechanisms of pressure oscillation during rapid filling of pipeline with an air pocket entrapped at the dead end are different for the horizontal and vertical cases. It is the stratification of the air-water interface for the horizontal case, and it is air-water mixture for the vertical case.

## Reference

[1] B. Brunone, U. M. Golia, M. Greco, Some remarks on the momentum equation for fast transients, Proc. 9th and Last Round Table Int. Meeting on Hydraul. Trans. Column Separation − IAHR Group, (4-6 Sep. Valencia, ES), pp. 140-148. 1991.

[2] C. S. Martin, Entrapped air in pipelines, Proc. 2nd Int. Conf. Press. Surges − BHR Group, (27-29 Sep. London, UK), ed H. S. Stephens, A. L. King and C. Stapleton, pp. 15-28. 1976.

[3] F. Zhou, F. E. Hicks, P. M. Steffler, Observations of air-water interaction in a rapidly filling horizontal pipe, J. Hydraul. Eng. 128(6) (2002) 635–639.

[4] L. Zhou, T. Pan, H. Wang, D. Liu, P. Wang, Rapid air expulsion through an orifice in a vertical water pipe, J. Hydraul. Res. 57(3) (2019) 307–317.

**Theme:** Hydraulic and hydrological modeling
**IAHR Thematic Priority Area:** [TPA-4] Digital Transformation
https://doi.org/10.3850/iahr-hic2483430201-105

# River-Aquifer Interaction - Where Is the Problem in Calculating Volumetric Exchange? Hupsel Case Study

**Maria Grodzka-Łukaszewska*[1], Joachim Rozemeijer[2], Ype van der Velde[3], Grzegorz Sinicyn[1]**

[1] Faculty of Building Services, Hydro and Environmental Engineering, Warsaw University of Technology, 00-653 Warsaw, Poland
[2] Deltares: Utrecht, NL
[3]Vrije Universiteit Amsterdam: Amsterdam, NL

** Corresponding author: maria.grodzka@pw.edu.pl*

**Abstract**. The purpose of the research was to compare two conceptually different physi-cal-mathematical models of groundwater flow, the HOA and the Velocity-Oriented Approach (VOA), by creating two corresponding numerical models and calculating the water flow in the subsoil for the same real hydrogeological situation (Hupsel, The Netherlands). For this comparison, the measurement results from the DYNAQUAL project were used. The results of this experiment served as a comparative measure of the compliance of VOA and HOA numerical models with real measurements.

**Keywords:** river-aquifer interaction, Velocity Oriented Approach, Head-Oriented Approach, groundwater flow model, water exchange measurement, water exchange modelling

## 1 Introduction

In this article, the authors compared two conceptually different mathematical and physical models of groundwater flow - HOA and VOA, by performing calculations for the same real hydrogeological situation (Hupsel catchment, the Netherlands). The comparison of these theoretical models consisted of (1) reconstructing the water exchange situation between the aquifer and the canal on the basis of data obtained from the DYNAQUAL field experiment (2) creating two numerical models VOA and HOA, (3) comparing the exchange rates between the river and the two models and the aquifer, and (4) comparing the results of the field measurements with the results of both numerical models. Comparing the results of the model with the measurement results allowed the authors to conclude which of the models calculates the amount of water exchange between the river and the adjacent aquifer.

## 2 Results

The model was calibrated using the "trial and error" method and by the automatic calibration method using the PEST optimization package. The measure used to compare the HOA and VOA models were the volumes of water that the aquifer supplied to the channel calculated by these models in the period from 1.11.2007 to 16.12.2007 with the measured values from the DYNAQUAL field experiment. The graph in Figure 1 shows the channel-aquifer exchange calculated with the HOA and VOA model.

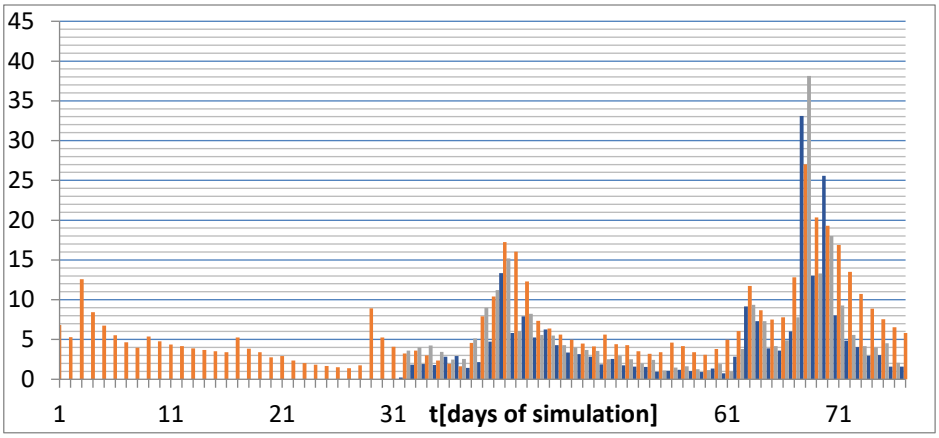


**Figure 1.** Results of the HOA (orange) and VOA (grey) model - calculated water exchange between the channel and the aquifer compared with measurements (blue).

## 3 Conclusion

The basic premise of the research undertaken was the observation that in issues such as calculating the interaction of surface waters with groundwater, it is necessary to use a groundwater flow model that guarantees a very accurate numerical estimation of all three components of the specific flow field (or the field of filtration velocity $v_p$).

The formal similarity of each of the three Velocity Oriented Approach equations to the Head Oriented Approach equation enables the implementation of Visual MODFLOW (software commonly used to solve HOA model equations) to solve VOA model equations.

As a result of the comparison of the HOA and VOA models on the example of the same selected real hydrogeological situation (DYNAQUAL field experiment, Hupsel river catchment, the Netherlands), where there is an interaction of surface and groundwater, it was found that the VOA model gives results more similar to the measurement results - error the exchange water volume of the channel in a given time interval determined by the VOA model is on the order of 19%, while the HOA model exchange water volume error is on the order of 63%.

Comparison of the results of the HOA and VOA models in the Hupsel catchment and their comparison with the data from the DYNAQUAL field experiment shows that the VOA model gives results closer to the measurement results in most of the modeled time steps. In the period from 1.11.2007 to 16.12.2007, the error in the volume of water fed to the channel determined by the VOA model is of the order of 19%, while the error of the volume of water supplied to the channel in the HOA model is of the order of 63%.In conclusion, it can be stated that the theoretical model of the velocity-oriented approach (VOA) is an approach that enables the determination of the water exchange flux between surface and groundwater with satisfactory accuracy. Due to the lack of numerical differentiation (typical for the HOA model), the numerical implementation of the VOA gives better estimates of the water exchange flux between the river bed / channel and more accurate approximations of the water-bearing trajectory in the immediate vicinity of the river / channel.

**Theme:** Hydraulic and hydrological modeling
**IAHR Thematic Priority Area:** [TPA-4] Digital Transformation
https://doi.org/10.3850/iahr-hic2483430201-107

# Flow Velocity Distribution in Rivers through Image-Based Technique Calibrated by ADCP Measurements

**Donatella Termini[1], Peyman Peykani[1]**

[1] University of Palermo, Department of Engineering, 90128, Palermo, Italy

*Corresponding author: donatella.termini@unipa.it*

**Keywords:** ADCP measurements, Flow velocity distribution, Image-based technique, River monitoring

## 1 Introduction

In the context of climate change, the knowledge of flow discharge is of crucial importance. Flow discharge is not a direct measurement but is estimated on the basis of information of flow velocity and cross-sectional flow area. Thus, accurate flow velocity measurements are critical for defining early warning systems for flood management and for quick decision-making for emergency actions. In recent years, the acoustic Doppler current profiler (ADCP) has been especially used to measure flow velocity profiles and the flow discharge, in natural and man-made waterways[1]. During flood events, because of continuously changing in flow velocities, water depths, and high sediment concentrations, conditions is not safe for measurement operator. As consequence, in high flow conditions, measurement equipment's like current meters and/or more advanced instruments such as ADCP cannot be used. For this reason, especially in the last decade, alternative approach based on image processing techniques has been increasingly used to obtain the distribution of the surface velocity, from which the flow discharge might be estimated. Several software tools have been also implemented for the image-based technique application, enabling researchers and practitioners to derive flow velocity data with high spatial and temporal resolution [2,3]. In comparison to the traditional measurement methods, the image-based technique presents the advantage to be non-intrusive allowing the safe estimation of surface velocity distribution also during floods. One of challenges in the application of image techniques is determining the error in estimating surface velocity, whose quantification depends on many factors characterizing not only the measurement conditions but also the processing method used.

## 2 Material and methods

In this study, the efficiency of the digital image-technique for remote monitoring of surface velocity in river is analysed. The analysis conducted by using accurate ADCP flow velocity measurements in selected reaches of rivers in Palermo's (Sicily-Italy) territory (Figure 1). For implementation of image-based technique, Camera Nikon D5300, with high-resolution images (1920x1080 pixels) and of 30 fps acquisition frequency, was used. In this study on the contrary to classical LSPIV procedures, the image-based technique is applied only by using moving grains and natural tracers. The calibration of the procedure was operated by comparing the values of the free surface velocity estimated by usign the acquired images with the ADCP's stationary measurements.

Figure 1 Overview of the study area

## 3 Results and Concluding Remarks

Figure 2 reports the comparison between the velocity distribution obtained in a selected cross section of the Oreto River and the local ADCP measure. Figure 2 shows that the velocity values compare well, thus demonstrating that the use of natural tracer or sediments on the free surface allows user to accurately apply the image-based technique. Further applications have been also conducted performing sensitivity analysis of the estimated surface velocity to integration area and the image resolution.

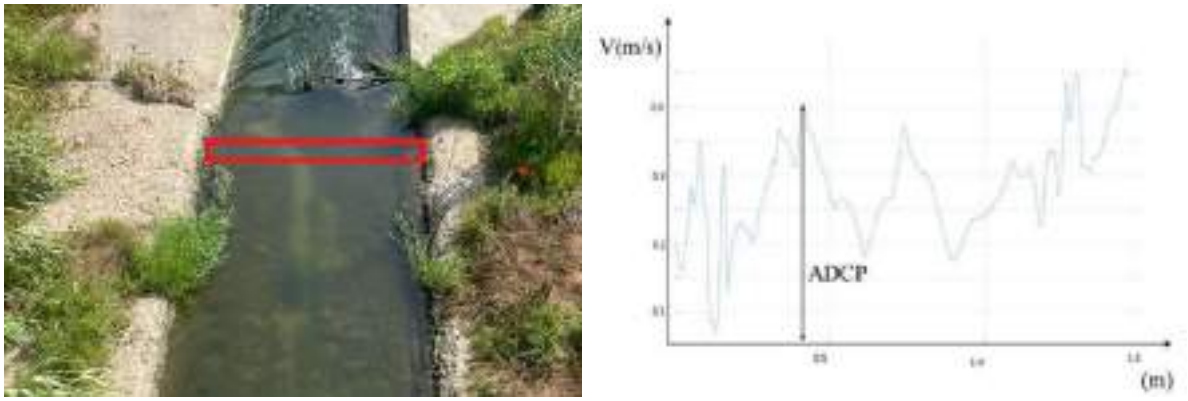


Figure 2 Comparison of velocity determined by image analysis with ADCP measure

Our study underscores the importance of using accurate measurement technologies for calibrating image-based techniques used for monitoring surface velocity distribution also during flood events. This information is especially important for flood management practices.

## Acknowledgements

This study was carried out within the RETURN Extended Partnership and received funding from the European Union Next-GenerationEU (National Recovery and Resilience Plan – NRRP, Mission 4, Component 2, Investment 1.3 – D.D. 1243 2/8/2022, PE0000005). Part of this study has been supported by project PRIN2017 " ENTERPRISING".

## Reference

[1] Muste M, Yu K, Pratt TC, Abraham D. ADCP measurements at fixed river locations. InHydraulic Measurements and Experimental Methods 2002 2002 (pp. 1-12).

[2] Fujita I, Muste M, Kruger A. Large-scale particle image velocimetry for flow analysis in hydraulic engineering applications. Journal of hydraulic Research. 1998 May 1;36(3):397-414.

[3] Termini D, Di Leonardo A. Efficiency of a digital particle image velocimetry (DPIV) method for monitoring the surface velocity of hyper-concentrated flows. Geosciences. 2018 Oct 19;8(10):383.

**Theme:** Hydraulic and hydrological modeling
**IAHR Thematic Priority Area:** [TPA-4] Digital Transformation
https://doi.org/10.3850/iahr-hic2483430201-109

# One-Dimensional Mathematical Modeling of Water Flow and Sediment Transport in the Haibowan Reservoir

**Jingyi Guo[1,2],Xinjie Li[2], Xiaoying Li[1], Fei Yang[2], Qiang Wang[2]**

[1] College of Water Resources and Hydropower, Hohai University, Nanjing, 210098, China
[2] Yellow River Institute of Hydraulic Research , Zhengzhou, 450003, China

*Corresponding author: xin_wd@163.com*

**Abstract.** Physical models are not able to fully characterize changes in boundary conditions of sedimentation patterns in reservoirs across rivers with high sand content. To address this issue, a one-dimensional mathematical model of water flow and sediment transport in the Haibowan Reservoir was constructed based on the basic equations for turbid open-channel flows, the mass balance equation for suspended sediment transport, and the measured data of the Haibowan Reservoir on the Yellow River. Finally, the model was validated using the measured data of the Haibowan Reservoir in 2019. According to the long-term simulation of the flow rate, sand content and thalweg, high simulation accuracy was observed. This indicates that the model can provide a scientific basis and technical support for formulating sediment discharge plans and making management decisions for the Haibowan Reservoir in future.

**Keywords:** reservoir sedimentation, Haibowan Reservoir, one-dimensional water flow and sediment transport mathematical modeling

## 1 Introduction

Since the early 1980s, one-dimensional mathematical models have been successfully applied in research and engineering practice[1]. As the understanding of water flow and sediment transport increases, related one-dimensional mathematical models have gradually developed into classical models and are widely used in reservoir sediment transport calculation. For example, Chen et al.[2] used a one-dimensional mathematical unsteady non-uniform sediment transport model to deduce the riverbed elevation changes in the Sanmenxia Reservoir area. This paper utilized the basic equations for turbid open-channel flows and the mass balance equation for suspended sediment transport to construct a one-dimensional mathematical model of the water flow and sediment transport in the Haibowan Reservoir. The model results were validated and analyzed, with a view to providing a scientific basis and technical support for the future planning and decision-making of sediment discharge plans for the Haibowan Reservoir.

## 2 Method

### 2.1 Basic equations

In the Haibowan Reservoir area, the water depth is shallow and the longitudinal gradient in front of the dam is small. Therefore, when floodwater with a large amount of sediments enters into the backwater area, it is unlikely to create significant density differences between the floodwater and the clear reservoir water, resulting in a small chance for hyperpycnal flow formation[3]. Hence, basic equations for turbid open-channel flows were adopted in constructing the one-dimensional mathematical model of water flow and sediment transport.
Continuity equation for water flow:

$$\frac{\partial A}{\partial t}+\frac{\partial Q}{\partial x}=0 \tag{5}$$

Equation of water motion:

$$\frac{\partial Q}{\partial t}+\frac{\partial\left(\frac{Q^2}{A}\right)}{\partial x}+gA\frac{\partial Z}{\partial x}+\frac{gn^2Q^2}{AR^{\frac{4}{3}}}=0 \tag{6}$$

Non-equilibrium transport of suspended load:

$$\frac{\partial(AS)}{\partial t}+\frac{\partial(QS)}{\partial x}+\alpha\omega B(S-S_*)=0 \tag{7}$$

Riverbed deformation:

$$\rho_0\frac{\partial A_0}{\partial t}=\alpha\omega B(S-S_*) \tag{8}$$

### 2.2 Model solution methods

This paper adopted HLL to discretize and solve governing equations numerically. The numerical solution of the water flow and sediment transport process is performed separately.

### 2.3 Parameter selection

The model parameters were determined according to the water flow and sediment transport data of the Haibowan Reservoir in 2018. After trial and error, the parameters of the one-dimensional mathematical model of water flow and sediment transport are selected as follows: (1) calculation time interval: the time step of the water flow is 1s; (2) riverbed resistance: the resistance coefficient equals 0.035; (3) saturation recovery coefficient: 0.8 during erosion and 0.2 for deposition; (4) grid division: 200 grids in the transverse direction and 150 grids in the longitudinal direction.

### 2.4 Model validation

The water flow, sediment transport and topographic data in 2019 were used to validate the model.

## 3 Results

The simulated outflow rate, outflow sand content, and reservoir thalweg elevation are consistent with the measured values. The corresponding $R^2$ values equal 0.914, 0.715, and 0.850, respectively.

## 4 Conclusion

The model can provide a scientific basis and technical support for formulating sediment discharge plans and making management decisions for the Haibowan Reservoir in future.

## References

[1] N. Papanicolaou A, Elhakeem M, Krallis G, et al. Review of sediment transport simulation - current status and future trends[J]. Mechanics Progress, 2010, 40(03): 323-339.

[2] Qianhai Chen, Hongwei Fang, Guangqian Wang. One-dimensional unsteady and nonuniform sediment transport mathematical model for the Three Gorges Reservoir area[J]. Advances in Water Science, 2004, 15(2): 160-164.

[3] Kezhi Wang, Xiaomin Liu, Tingxi Liu et al. Sediment discharge effect and influencing factors of Haibo Bay Reservoir[J]. Journal of Desert Research, 2023, 43(5): 9-17.

**Theme:** Hydraulic and hydrological modeling
**IAHR Thematic Priority Area:** [TPA-4] Digital Transformation
https://doi.org/10.3850/iahr-hic2483430201-111

# Redetermination of Environmental Flow After Hydropower Decommission Using Hydraulic and Habitation Models: A Case Study in The Chishui River Basin, China

**Zhenhua Cui[1,2,3], Shuai Niu[2], Ni Xiao[1,2,3], Liang Wang[1,2,3], Wenlin Zhai[1,2,3]**

[1] National Research Institute for Rural Electrification, 122 Xueyuan Road, Hangzhou, 310012, China
[2] Nanjing Hydraulic Research Institute, 223 Guangzhou Road, Nanjing, 210029, China
[3] Research Center on Rural Hydropower, MWR, 122 Xueyuan Road, Hangzhou, 310012, China

*Corresponding author: zhenhuacui1225@qq.com*

**Keywords:** Chishui River, Environmental Flow, Hydraulic Analysis, Weighted Usable Area (WUA)

## 1 Introduction

The National Nature Reserve for the Rare and Endemic fishes of the Upper Reaches of the Yangtze River is located in the Chishui River Basin, and some small hydropower stations have been decommissioned in recent years. The main functions of the reserved reservoirs have changed from hydropower generation to water supply, flood control, irrigation, and even ecological operation for the protected fishes downstream of the dam. Therefore, determining the sensitive environmental flow to restore the suitability of fish habitats has become increasingly urgent and necessary.

Considering the hydraulic models and suitable habitat model, this study employs the Instream Flow Incremental Methodology (IFIM) to conduct two-dimensional hydrodynamic simulations and fish habitat simulations of the river reach below the reservoir dam in the Chishui River Basin, thereby establishing a quantitative response model between the environmental flow and the suitable physical habitat area for target fishes. By analyzing the Weighted Usable Area (WUA), the changes in suitable physical habitats under various environmental flow conditions during sensitive periods are examined to determine the optimal range of environmental flow for the target fish species. The outcome of this research can serve as a scientific basis for environmental flow operation of the reserved reservoir after hydropower removal.

## 2 Material and methods

### 2.1 Introduction of the case

The Baini River is a minor tributary of the Chishui River, with a main stream length of 37 km and a drainage area of 273 $km^2$. The Hydropower Station is a seasonal regulating diversion-type power station located downstream on the main stream of the Baini River. The dam is around 5.4km from the confluence of the Baini River and the Chishui River. The total reservoir capacity is 43.38 million $m^3$. After the removal of the small hydropower station, the environmental flow of the reservoir should be adjusted based on the water demand of the target rare and endemic fishes downstream.

### 2.2 Hydrodynamic Model

Combining with the topographical characteristics of the downstream section of the reservoir dam and the basic data of the river system, the length of the simulated river reach is determined to be about 5.4 km, and the simulation area is 201800 $km^2$.

Employing an unstructured irregular mesh, this model could delineate the shoreline conditions of the simulated region. The average area of each mesh element is 0.8 $m^2$. The mesh density meets the requirements of river flows simulation under small environmental flow conditions in this case study. Referring to the roughness coefficient table, the river roughness coefficient was adopted as 0.040.

### 2.3 Habitat Model

The habitat model establishes the habitat suitability curves for the target species, determining habitat suitability indexes based on the distribution of water velocities and depths under different flow conditions. Then, WUA was used to evaluate the suitability of the fish habitat. The Instream Flow Incremental Methodology (IFIM) was proposed by the U.S. Fish and Wildlife Service, which establishes a relationship between various flow regimes and the effective habitats for characteristic species through the integration of hydrodynamic models and biological information models, thereby providing a basis for flow regulation.

### 2.4 Target Fish and the Suitability Curves

Based on the fish samples collected in the study area, a total of 546 fish specimens were collected from the Baini River, which have been identified as belonging to 3 orders, 6 families, 22 genera and 22 species. Among them, two fish species are endemic to the upper reaches of the Yangtze River: *Sinogastromyzon sichangensis* and *Acrossocheilus monticolus* (Günther), both of which are small-sized, fast-flowing fish species. Therefore, these two endemic fish species are selected as the target species for river habitat simulation. Based on the 111 sample data of the target fishes in the Chishui River Basin, the suitability curves of water velocity and depth for the target fishes have been acquired.

## 3 Results and discussion

In order to explore the correspondence between the different environmental flows and the suitable habitat area downstream of the dam, a total of 28 environmental flow conditions were set up for simulation, and the suitable habitat area and proportion downstream of the dam under different environmental flow conditions were statistically analyzed. Four simulation conditions with environmental flow rates of 1, 5, 10 and 20 were selected, and the spatial distribution results of suitable habitat area were calculated to obtain the Weighted Usable Area (WUA) distribution figure. Based on the simulation results of suitable habitat area in the downstream reach of the dam under various environmental flow conditions, a relationship curve was established between the flow rate and the Weighted Usable Area (WUA) downstream of the dam.

The results shows that the WUA reaches its maximum at 9 $m^3/s$, with an area of 56307.3 $m^2$, accounting for 27.9% of the total river reach area. The optimal flow range is between 2 to 20 $m^3/s$. In this flow range, the WUA for river fish survival consistently accounts for more than 20% of the total river reach area. When the flow rate exceeds 9 $m^3/s$, the WUA decreases as the flow increases.The lower limit of the optimal flow range is 2 $m^3/s$, and the habitat area accounts for 20% of the total river reach area. Therefore, it is recommended to adopt a target environmental flow of 2 $m^3/s$ as the optimal environmental flow for the target fish species.

## 4 Conclusions

(1) *Sinogastromyzon sichangensis* and *Acrossocheilus monticolus* (Günther) are selected as target species for habitat simulation in the watershed.

(2) This article employs a habitat simulation method based on the principles of IFIM. The optimal flow range is between 2 to 20 $m^3/s$, in which the area of river habitat suitable for fish survival accounts for over 20% of the total river reach area.

(3) The research findings provide technical support for calculation of reservoir environmental flow during sensitive periods of rare fishes and optimal reservoir regulation.

**Theme:** Hydraulic and hydrological modeling
**IAHR Thematic Priority Area:** [TPA-4] Digital Transformation
https://doi.org/10.3850/iahr-hic2483430201-113

# Riverway Flow Simulation for the Yellow River Estuary

**Bojun Liu[1,2], Yun Zhao[1], Shuntian Liang[1], Kefei Li[1]**

[1] Yellow River Engineering Consulting Co., Ltd, Zhengzhou 450003, China
[2] Key Laboratory of Water Management and Water Security for Yellow River Basin, Ministry of Water Resources, Zhengzhou 450003, China

**Abstract.** The Yellow River is called "the Mother River" in China. The Yellow River Estuary is the closest area to the Bohai Sea, in which the Yellow River delta and its related land are included. The broadest and most complete native wetland ecosystem in the warm temperate zone of China is dynamically generated by unique water and sediment conditions and the weak tidal dynamic environment in the Yellow River Estuary. There are few researches, in the current, on the hydrodynamic simulation of the Yellow River Estuary, and the effective river flow simulation of the Yellow River Estuary is important for the control of water and sediment in the lower Yellow River. Therefore, hydrologic and hydrodynamic methods are employed to simulate the riverway flow process and calculate the flow propagation time in different sections in this paper. The study can provide scientific basis for ecological protection and water resources management in the Yellow River Estuary area.

**Keywords:** Flow process, hydrodynamic simulation, modeling, water level, Yellow River Estuary

## 1 Introduction

There are few studies on the hydrodynamic simulation of the Yellow River Estuary, and the simulation of the estuary streamflow is difficult to be accurate as well[1]; the existing studies mostly focus on the simulations of sediment transport process and riverway topography change[2-3]. In this paper, the flow process and flow duration of the Qingshuigou riverway and the Diaokouhe riverway at the Yellow River Estuary were simulated. The generalized riverways are shown in Figure 1.

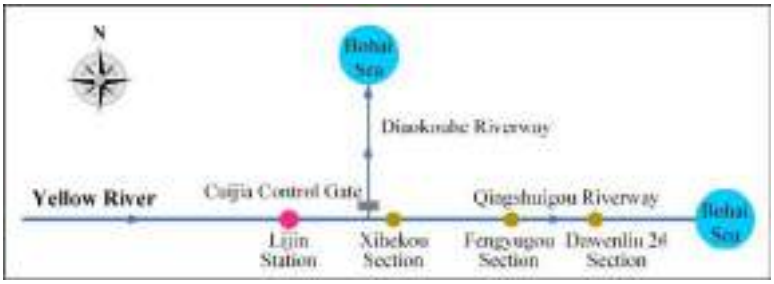


Figure 12 Generalized seagoing riverways in the Yellow River Estuary

According to the measured runoff data of the Lijin Station, the runoff showed a decreasing trend from 1956 to 2020. The annual distribution of Lijin runoff showed a single-peak variation, and the runoff mainly concentrated in July to October, accounting for 60.26% of the annual runoff amount (seen in Figure 2).

## 2 Modeling and Simulation results

One-dimensional hydrodynamic model was employed to simulate the runoff of the riverway between the Lijin Station and Xihekou Section, and the Hydrologic Simulation Method was used to calculate the runoff of the riverway between the Xihekou Section and the Yellow River Estuary[4-5]. The results of parameter calibration and model validation for the Lijin Station-Xihekou Section riverway are shown in Figure 3.

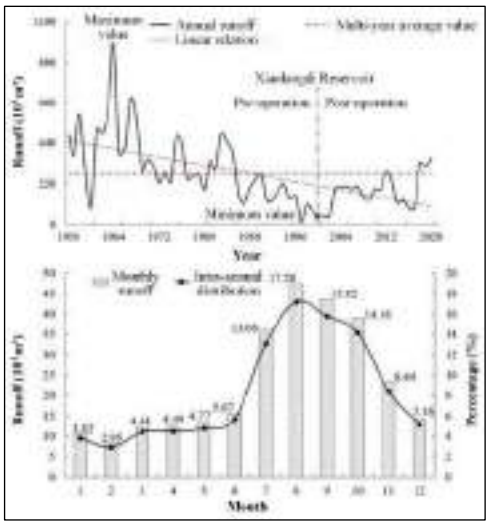

Figure 2 Runoff variation

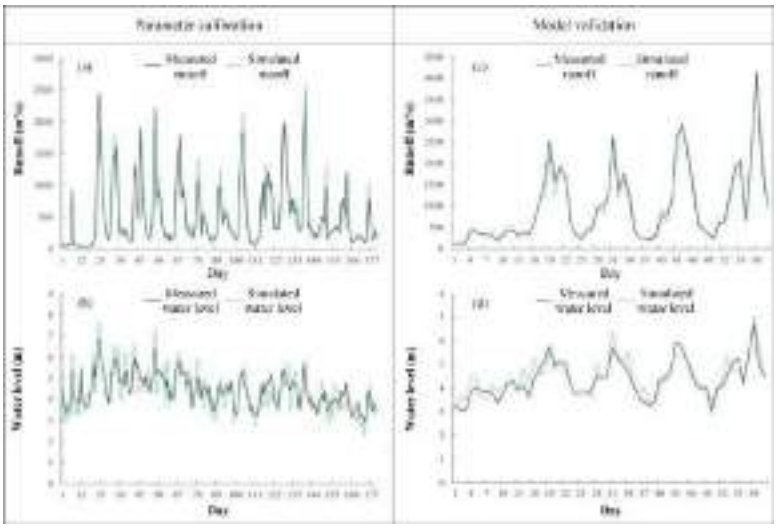

Figure 3 Model calibration and validation

Table 1 shows that when the flowrate of the Lijin Station is 500m³/s, the runoff takes 19.2h to reach to the Cuijia Control Gate of the Diaokouhe River, and then it takes another 11.8h to reach to the Fengyugou Section. Besides, the runoff from the Lijin Station takes 64.8h to flow into the mouth of the sea when the incoming flowrate is 100m³/s at the Lijin Station, and it takes 39.1h when the incoming flowrate is 500m³/s, and it takes 28.8h when the incoming flowrate is 1000m³/s. In other words, runoff only takes one day and 4.8h from the Lijin Station flow into the Bohai Bay when the flowrate at the Lijin Station was over 1000m³/s.

Table 4 Calculation results of the interval water flow time under different runoff conditions

| | Section | Runoff of the Lijin Station (m³/s) | | | | | |
|---|---|---|---|---|---|---|---|
| | | 100 | 300 | 500 | 700 | 900 | 1100 |
| Water flow time (h) | Lijin Station-Xihekou Section | 31.8 | 20.0 | 19.2 | 18.5 | 14.5 | 14.1 |
| | Cuijia Control Gate-Diaokouhe Estuary | 38.4 | 24.2 | 23.2 | 22.3 | 17.5 | 17.1 |
| | Xihekou Section-Fengyugou Section | 19.5 | 12.3 | 11.8 | 11.3 | 8.9 | 8.7 |
| | Xihekou Section-Dawenliu 2# Section | 26.6 | 16.8 | 16.1 | 15.5 | 12.2 | 11.8 |
| | Xihekou Section-Yellow River Estuary | 33.0 | 20.8 | 19.9 | 19.1 | 15.1 | 14.7 |
| | Lijin Station-Yellow River Estuary | 64.8 | 40.8 | 39.1 | 37.6 | 29.6 | 28.8 |

**Acknowledgments:** The research would not have been possible without the interest and cooperation of the Yellow River Conservancy Commission of the Ministry of Water Resources.
**Funding**: This work was supported by the National Key R&D Program of China (2022YFC3202405-04) and the Development Funding Project by Water Youth Talent from Beijing Jianghe Water Development Foundation (2022-05).

## Reference

[1] Xia J, Liu B. J, Cheng D. D, Discussion on water security and high-quality development of Yellow River Basin, Yellow. River. 43, 10(2021) 11-16. (in Chinese)
[2] Ma R, Han K. Y, Zhang H. W, et al, Numerical simulations of Yellow River estuary evolution in different governance modes, J. Hydroelectric. Eng. 4(2018) 68-78. (in Chinese)
[3]Li D. F, Zhang H. W, Zhong D. Y, et al, Preliminary impact analysis of the Yellow River Estuary sediment on the lower reaches based on 2D numerical simulation, Yellow. River. 43, 5(2021) 17-23+29. (in Chinese)
[4] Rodrigo C. D. P, Walter C, Diogo C. B, Validation of a full hydrodynamic model for large-scale hydrologic modelling in the Amazon, Hydrol. Process. 27, 3(2013) 333-346.
[5] Zhang Z. P, Zhang Z. X, Liu S. Y, et al, Study on ecological flow of Changxinggang Rvier based on one-dimensional hydrodynamic-water environment coupling model, Water. Resour. Hydrop. Eng. 54, 10(2023) 160-169. (in Chinese)

**Theme:** Hydraulic and hydrological modeling
**IAHR Thematic Priority Area:** [TPA-4] Digital Transformation
https://doi.org/10.3850/iahr-hic2483430201-115

# Urban Flooding Risk Analysis and Rapid Identification Based on 1D/2D Coupled Modeling

**Wei Zhang[1,2,3*], Xuan Wan[1], Peizhen Qu[1], Zimeng Zhuang[1], Junqi Li[1,2,3]**

[1] Key Laboratory of Urban Stormwater System and Water Environment, Ministry of Education, Beijing University of Civil Engineering and Architecture, Beijing 100044, China
[2] Beijing Engineering Research Center of Sustainable Urban Sewage System Construction and Risk Control, Beijing University of Civil Engineering and Architecture, Beijing 100044, China
[3] Beijing Energy Conservation & Sustainable Urban and Rural Development Provincial and Ministry Co-construction Collaboration Innovation Center, Beijing 100044, China

*Corresponding author: zhangwei@bucea.edu.cn*

**Abstract.** Urban flooding risk identification is one of prerequisites for urban flooding control, and 1D/2D coupled modeling provide an alternative approach. Based on the classic hydraulics method, the hydraulic performance of the sewer in the drainage sewer system was analyzed, and the main influencing factors of sewer hydraulic surcharge and manhole overflow were clarified and quantified. In this study, a quick identification method of manhole overflow based on the diameter and slope of upstream and downstream sewer of manhole was proposed, which can provide a feasible method for the rapid identification of urban flooding. The case verification under a variety of scenarios show that the recognition accuracy of the method was higher than 75% under the design rainfall conditions. Moreover, the coupling method of one-dimensional sewer model and two-dimensional surface overflow model based on manhole and inlet as coupling nodes was explored. Through laboratory experiments, the key parameter values of the two coupling modes were proposed. Furthermore, generalized processing methods for key elements in two-dimensional surface overflow models was analyzed, including buildings, roads and community fences.

**Keywords:** 1D/2D coupled modeling; rapid identification; risk analysis; urban flooding

## 1 Introduction

Urban flooding risk identification is one of prerequisites for urban flooding control, and a large number of studies have focused on the study of identification methods [1]. 1D/2D coupled modelling is one of these methods that have been studied, which provide an alternative approach for precise risk identification. However, 1D/2D coupled modelling implementation requires a significant cost in model building, and it also requires a lot of data that may not be available for most cases [2]. Hence, quick identification method for urban flooding risk is a great demand, especially in engineering practice. Even for the coupled model based on the hydrological and hydrodynamic mode, there are still several issues that need to be further studied [3], such as the 1D/2D coupling method, key elements conceptualization in 2D surface overflow models, etc. Urban flooding risk rapid identification method and key issues about 1D/2D coupling modelling for flooding risk analysis will be further explored.

## 2 Method

Based on the classic hydraulics method, the diameter and slope of upstream and downstream sewer of manhole was analysed compensatively to identify the possibility of manhole overflow, which include three types connection relationship (Fig.1 a). InfoWorks ICM was adopted to establish 1D/2D coupled model for a typical urban drainage basin to explore the 1D/2D coupling related issues (Fig. 1 b).

(a) Sewer connections (b) 1D/2D model (c) Laboratory experiments

Figure 1 Typical storm sewer connections and 1D/2D coupled model

## 3 Results

### 3.1 Quick identification method of manhole overflow

A quick identification method of manhole overflow based on the diameter and slope of upstream and downstream sewer of manhole was proposed. Based on this method, a quick reference map of the possibility of manhole overflow was established, which can provide a feasible method for the rapid identification of urban flooding. The case verification under a variety of scenarios show that the recognition accuracy of the method was higher than 75% under the design rainfall conditions.

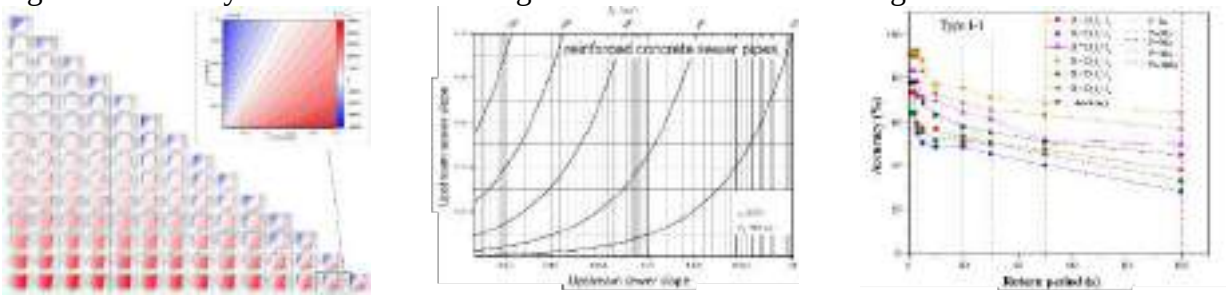

(a) Hydraulics analysis (b) Quick reference map (c) Accuracy verification

Figure 2 Quick identification method and verification

### 3.2 Coupling method of 1D/2D model

The coupling method of one-dimensional sewer model and two-dimensional surface overflow model based on manhole and inlet as coupling nodes was explored. Through laboratory experiments, the key parameter values of the two coupling modes were proposed.

### 3.3 Key elements in 2D surface overflow models

Generalized processing methods for key elements in two-dimensional surface overflow models was analysed, including buildings, roads and community fences.

## 4 Conclusion

Urban flooding risk rapid identification method and key issues about 1D/2D coupling modelling for flooding risk analysis may provide an important basis for the accurate identification of urban flooding based on 1D/2D coupled modelling.

## Reference

[1] F. Jalayer, R. De Risi, F. De Paola, et al. Probabilistic GIS-based method for delineation of urban flooding risk hotspots. Nat Hazards 73, (2014) 975–1001.

[2] A. Singh,, D. Dawson,, M. Trigg, et al. A review of modelling methodologies for flood source area (FSA) identification. Nat Hazards 107, (2021) 1047–1068.

[3] J. Leandro, R. Martins. A methodology for linking 2D overland flow models with the sewer network model SWMM 5.1 based on dynamic link libraries. Water Sci Technol 73 (12), (2016) 3017–3026.

**Theme:** Hydraulic and hydrological modeling
**IAHR Thematic Priority Area:** [TPA-4] Digital Transformation
https://doi.org/10.3850/iahr-hic2483430201-117

# Performance Assessment of Machine Learning and Statistical Models for Wet-Period Rainfall Forecasting

**Rashid Farooq[1], Monzur Alam Imteaz[1]**

[1] Department of Civil and Construction Engineering, Swinburne University of Technology, Melbourne, Australia

*Corresponding author: rfarooq@swin.edu.au*

**Abstract.** Accurately predicting seasonal rainfall variations in the Northern Territory (NT) is critical for water resource management. These variations are complex, influenced by several influential climatic anomalies. In this study, a supervised machine learning (ML) and statistical model were employed to delineate seasonal rainfall in two distinct stations within the Northern Territory, Australia, utilizing monthly dataset from 1900 to 2023. This research attempts to find a nonlinear relationship between the NT wet-period rainfall and the lagged climate indices, using seasonal autoregressive integrated moving average (SARIMA) and CatBoost model, incorporating input datasets featuring various climate indices. Comparative assessments, utilizing metrics such as root mean square error (RMSE), Mean Absolute Error (MAE) and correlation coefficient (R), indicated a substantial enhancement in model performance with the statistical approach. It was observed that SARIMA model can provide higher correlations using the lagged indices for forecasting wet-period period rainfall in compared to ML method. Using these indices in SARIMA, the model correlation in the testing phase increased up to 83%, and 77% for the two case study stations of Alexandria and Anthony Lagoon in NT, respectively.

**Keywords:** Climate indices, CatBoost, Machine learning, Rainfall, SARIMA

## 1 Introduction

Accurate long-term precipitation prediction remains a significant and enduring challenge. The complexity of rainfall regimes stems from the interplay of diverse physical variables influenced by both global climate change and localized urbanization. These factors induce significant spatiotemporal variability, rendering long-term precipitation forecasting highly challenging. This has enhanced ongoing research efforts by hydrologists and atmospheric scientists worldwide, particularly in Australia.

## 2 Methodology

The wet-period rainfall data from 1900 to 2023, encompassing the months of December to February, was sourced from the BoM Australian for two Northern Territory stations: Alexandria and Anthony Lagoon. Time series data of rainfall for both stations are presented in Figure 1.

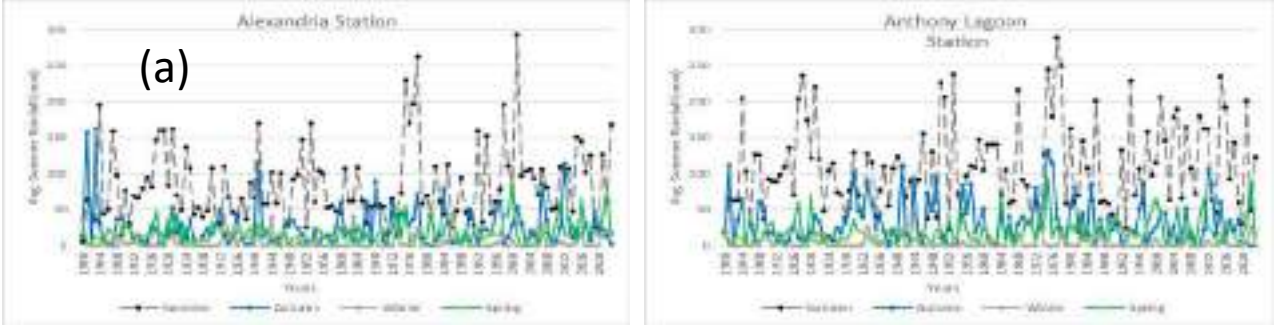


Figure 13 Time series pattern of the observed stations (a) Alexandria and (b) Anthony Lagoon

## 3 Results and Discussion

Figure 2 visualizes the time series predictions made by the chosen models (SARIMA and CatBoost) against the actual rainfall observed at the Alexandria station. Both models display a capability to capture the major fluctuations such as peaks and dips in rainfall patterns, suggesting some level of effectiveness. However, the CatBoost model exhibits a closer agreement with the observed rainfall compared to the SARIMA model, indicating potentially better performance in predicting rainfall patterns for Alexandria.

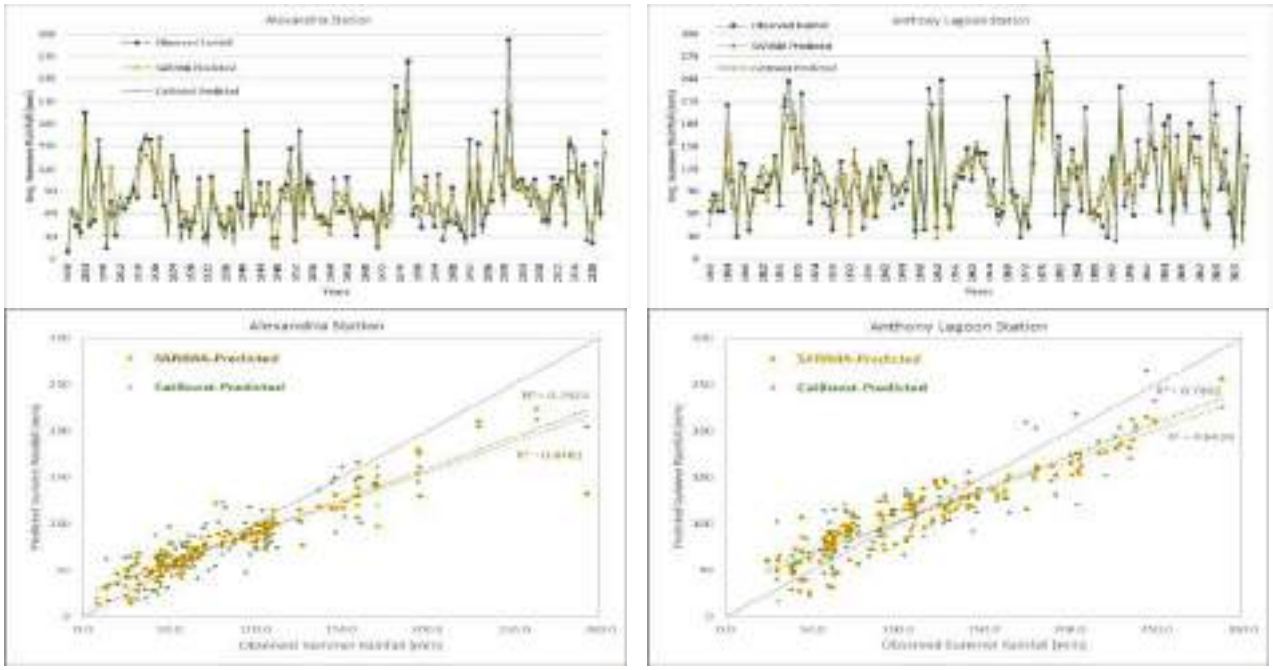


Figure 2: Comparison of time series and scatter plots analyses between observed and predicted seasonal rainfall using CatBoost and SARIMA models at Alexandria and Anthony Lagoon stations

The scatter plot interestingly suggests that SARIMA model achieved superior accuracy compared to CatBoost models in predicting rainfall at the Alexandria station as shown in Figure 3. This is evidenced by the SARIMA model's lower Root Mean Squared Error (RMSE) of 1.26 and Mean Absolute Error (MAE) of 0.91, compared to the CatBoost model's values of 3.47 and 2.63, respectively. Additionally, the SARIMA model exhibited a stronger correlation with observed rainfall, with a correlation coefficient of 0.82 compared to the CatBoost model's 0.77 in the testing phase. Moreover, a similar trend is observed for the Anthony Lagoon station. These findings suggest that the SARIMA model is better suited for capturing the complexities of rainfall patterns at both the stations.

## 4 Conclusion

Previous studies have not focused on finding the effect of various indices separately on NT rainfall and could not develop a good correlation to predict seasonal rainfall. Current study concludes that combined lagged climate indices have more effect on rainfall predictability than the single climate indices. Our results revealed that the SARIMA model outperformed the CatBoost model to predict the wet-period rainfall at the selected station. In addition to past rainfall data, these indices combinations increased the model correlation in the testing phase up to 83% and 77% for the two case study stations, respectively.

The selected models are capable of forecasting wet-period rainfall, allowing water stakeholders, particularly agriculturalists, to make low-risk decisions earlier in the crop cycle. In future research, we will examine the prediction of various machine learning algorithms on seasonal rainfall in other parts of Northern Territory.

**Theme:** Hydraulic and hydrological modeling
**IAHR Thematic Priority Area:** [TPA-4] Digital Transformation
https://doi.org/10.3850/iahr-hic2483430201-119

# Unprecedented Compound Drought and Hot Extremes Events in Sichuan: An Angle from Copula Analysis

**Lilingjun Liu[1], Xiaosheng Qin[1]**

[1] School of Civil and Environmental Engineering, Nanyang Technological University, 50 Nanyang Ave., 639798, Singapore

*Corresponding author: xsqin@ntu.edu.sg*

**Abstract.** This study comprehensively investigates the extreme conditions of compound drought and hot extremes (CDHE, or CHD) that occurred in the summer of 2022 over Sichuan province with the utilization of copula analysis. The concurrence of compound events is analyzed over the last 60 years (1963-2022), with surface runoff and daily maximum temperature used as indicators to measure drought and hot extremes, respectively. The JRP (joint return period) and LMF (likelihood multiplication factor) are computed to measure the extreme conditions and correlation strength of CDHE, followed by the assessment of CDHE occurred in 2022 summer. The results show that the year 2022 is marked by its exceptionally high return period of hot extremes as well as the third largest return period of drought. The concurrence of these two extreme events collectively contribute to the unprecedented JRP of CDHE up to 538 years in 2022, which is significantly larger than the 86 years in 2006, which is the 2nd severe CDHE in the past 60 years. The increase of LMF of compound events in year 2022 over 5 different LULC types are analyzed. It is shown that compared with non-urban area, where the LMF increase by 1.4 times in 2022, the LMF over urban area experience a surge to 13.63, with a drastic increase of 10.3 times. This research provides a quantitative analysis of the severity and dynamics of compound climate extremes in Sichuan, highlighting the increasing risk, particularly in urban regions. It offers valuable insights for future risk assessment and planning to mitigate the impact of such climate events.

**Keywords:** compound hot droughts (CHD), compound drought and hot extremes (CDHE), copula analysis

## 1 Introduction

The increasing prevalence of compound drought and hot extremes (CDHE) presents significant challenges to populated cities under the climate change. The conventional climate extremes analysis based on return period may not be able to comprehensively reflect the extreme conditions of these compound events. The copula analysis is adopted in this study, to conduct a meticulous investigation on the extraordinary climate conditions of summer 2022 in Sichuan, to decipher the severity and interrelation of these extremes. By examining historical data from 1963 to 2022, the research aims to quantify the distinctiveness of the 2022 events and understand their broader implications, especially in urban settings, thereby informing future risk management and planning strategies.

## 2 Material and Methods

The daily total surface runoff and maximum temperature data are obtained from ERA5 dataset [1], provided by ECMWF. To avoid the occurrence of hot extremes occurring in winter, only the warm season (JJA) are considered in this study. As the copula analysis is a tool to connect the marginal distribution of multiple variables to generate their joint distribution, the marginal distribution is fitted for surface runoff and temperature yearly data from 7 marginal distribution candidates with MLE. Then the BIC criterion is employed to select the best candidate for each grid point. Subsequently, the copula fitting, and best-fit member selection is conducted in a similar manner from 9 copula families. Once the copula functions are determined, the JRP and LMF can be obtained from the method proposed by Zscheischler and Seneviratne [2]. By specifying the 2 comparison categories, the long-

term and year 2022, the extreme conditions of compound events are conducted using JRP and LMF. The LULC and population density data are also used to investigate the correlation between the intensity of compound events and the development of area.

## 3 Results and Discussion

The study analyzed the extreme climate conditions of compound hot extremes in Sichuan Province during the summer of 2022, comparing the return periods and likelihood multiplication factor (LMF) of these events to historical data. While the drought intensity in 2022 had a return period of 6.68 years, less severe than in 2006, it was still above the long-term average. However, the hot extremes reached an unprecedented return period of 270.77 years, far exceeding any past records. This resulted in a joint return period for compound drought and hot extremes of 537.99 years, indicating the strongest concurrence in the last six decades. The LMF in 2022 peaked at 3.36, showing a significantly stronger correlation between these extremes compared to previous years. In Chengdu, Mianyang, and Nanchong, the joint return periods and LMF values dramatically increased, underscoring the exceptional severity of these events in 2022, with LMF increases of 1490%, 235%, and 86% respectively. Furthermore, the likelihood of concurrent drought and hot extremes across different LULC types in Sichuan Province are investigated. Grassland areas, primarily located in the high-altitude western Sichuan, showed the lowest long-term average LMF values, indicating fewer hot extremes. In contrast, urban areas in 2022 saw a dramatic increase in LMF, rising 10.3 times above the long-term median, the highest among all LULC types. This surge highlights the elevated risk and exposure of urban areas to compound climate extremes, with urban LMF reaching 13.63 compared to a much smaller increase in non-urban areas. This underscores the significance of joint return periods analysis of compound climate extremes, and also the importance of the rapid increase of CDHE over urban regions.

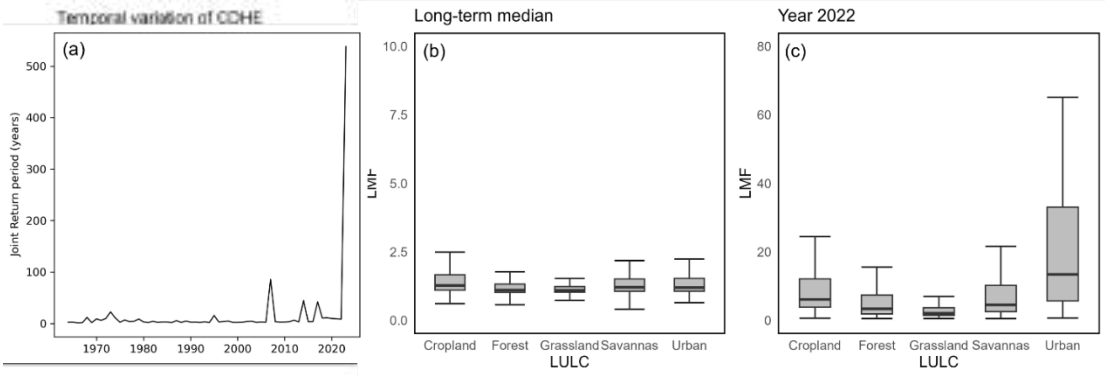


Figure 1. The temporal variation of CDHW in Sichuan Province.

## Acknowledgements

The authors would like to acknowledge the financial support from the Singapore MOE Academic Research Fund Tier 2 (MOE-T2EP50122-0003) for the completion of this research. The European Center for Medium-Range Weather Forecasting (ECMWF) is acknowledged for providing ERA5 reanalysis data.

## Reference

[1] Hersbach, H., Bell, B., Berrisford, P., Hirahara, S., Horányi, A., Muñoz-Sabater, J., ... and Thépaut, J. N. (2020). The ERA5 global reanalysis. Quarterly Journal of the Royal Meteorological Society, 146(730), 1999-2049.

[2] Zscheischler, J., and Seneviratne, S. I. (2017). Dependence of drivers affects risks associated with compound events. Science advances, 3(6), e1700263

**Theme:** Hydraulic and hydrological modeling
**IAHR Thematic Priority Area:** [TPA-4] Digital Transformation
https://doi.org/10.3850/iahr-hic2483430201-121

# NEOPRENE: Generating Stochastic Rainfall from Python

**Manuel del Jesus[1], Salvador Navas[1], Javier Diez-Sierra[2]**

[1] Instituto de Hidráulica Ambiental "IHCantabria", Universidad de Cantabria, Santander, Spain
[2] Instituto de Física de Cantabria (IFCA), Universidad de Cantabria-CSIC, Santander, Spain

*Corresponding author:manuel.deljesus@unican.es*

**Abstract.** Extensive time series data on precipitation at various temporal resolutions (typically daily or hourly) serve as fundamental input for studies pertaining to hydrology, hydraulics, and climatology. However, frequently, the available records lack the requisite length, completeness, temporal precision, or spatial extent to facilitate robust analysis. In this context, we present NEOPRENE, a Python library designed to generate synthetic precipitation time series. NEOPRENE facilitates the simulation of multisite synthetic precipitation, mirroring observed statistical characteristics across varying temporal scales. Through three illustrative case studies, we showcase the utility of this library, emphasizing its application in modeling extreme precipitation events and disaggregating daily rainfall observations into hourly increments. NEOPRENE is openly available on GitHub under the GPLv3 license, permitting unrestricted usage for both research and commercial endeavors. Additionally, we offer Jupyter notebooks featuring practical examples to encourage adoption among researchers and practitioners engaged in studies related to vulnerability, impact assessment, and adaptation.

**Keywords:** Extremes, Open-source, Python, Rainfall, Synthetic generation

## 1 Introduction

Extreme precipitation is essential to design infrastructures and to assess different water-induced risks. However, observational records may not be long or complete enough to provide accurate estimations for high return period events. Moreover, short observational records may contain biases that are difficult to explore with the observed value alone. In this work we present NEOPRENE (Diez-Sierra et al., 2023), an open-source Python rainfall generator that helps to analyze precipitation time series, improving our capabilities to characterize extreme events for any location, as well as to properly characterize other biases in the observational record.

NEOPRENE implements the Nyeman-Scott or Cox and Isham (Cox & Isham, 1988) model for precipitation. The model assumes that precipitation is organized in storms, that arrive following a Poisson process, with each storm constituted by rainfall cells, with some of their properties represented by statistical distributions. This decomposition allows rainfall events to be clustered and thus to better represent real precipitation statistics.

## 2 The NEOPRENE library

The NEOPRENE library employs the Neyman–Scott process to analyze spatiotemporal rainfall patterns, enabling the depiction or generation of rainfall distributions as they evolve over time. This model also allows for the replication of rainfall occurrences at specific locations without considering the broader rainfall dynamics in the vicinity.

Rainfall generation involves two main stages: calibration and simulation. During the calibration phase, parameters are adjusted to best match the statistical characteristics of the input series or provided rainfall data. Subsequently, in the simulation phase, these parameters are utilized to generate a time

series of the rainfall process, either at specific points or across spatial fields, in accordance with the specified parameters.

Furthermore, the NEOPRENE library offers various functionalities for validation purposes and facilitates the disaggregation of daily rainfall data into hourly intervals.

## 3 Use cases

In this work we present results for three study cases: one for a single site synthetic time series generation, another for rainfall decomposition and, finally, a multi-site synthetic time series generation. Different statistics and tests are carried out to show the capabilities of the model to reproduce the observed characteristics of real rainfall time series.

Rainfall decomposition is especially interesting, since it allows to generate plausible hourly rainfall time series from daily observations that respect the scaling laws for the study sites. This application is useful for forensic analysis of extreme events.

## 4 Results and Discusion

NEOPRENE offers a user-friendly interface for generating synthetic rainfall data across both space and time, leveraging the Neyman–Scott process. In comparison to alternative statistical methods like probability distribution models or Markov chain models (Wilks, 1998), point processes such as Neyman–Scott excel in capturing the interplay of rainfall patterns over time and space, particularly for extreme events. However, this method necessitates more computational resources and familiarity with its internal workings.

Relative to artificial neural networks (ANNs) (Welten et al., 2022), point processes may exhibit less adaptability in accommodating nonlinear relationships or external data. Despite this, ANNs remain less prevalent in synthetic rainfall generation, with their primary application centered around rainfall–runoff prediction.

NEOPRENE's effectiveness is underscored by its validation in replicating hourly and daily return periods across numerous gauges in Spain. Moreover, its implementation addresses the primary challenge associated with the model's practical use—namely, the complexity of parameter estimation.

It's worth noting that the spatial model has certain limitations, including the need for supervision during model adjustment and reliance on assumptions like homogeneity, rendering it unsuitable for locations where statistical characteristics deviate significantly from the mean.

## Reference

[1] Cox, D. R. & Isham, V., 1988. A Simple Spatial-Temporal Model of Rainfall. Proceedings of the royal society a: Mathematical, physical and engineering sciences, 415(1849), 317–328.

[2] Diez-Sierra, J., Navas, S. & Jesus, M. del., 2023. NEOPRENE v1.0.1: A Python library for generating spatial rainfall based on the NeymanScott process. Geoscientific model development, 16(17), 5035–5048.

[3] Wilks, D. S.: Multisite Generalization of a Daily Stochastic Precipitation Generation Model, J. Hydrol., 210, 178–191, https://doi.org/10.1016/S0022-1694(98)00186-3, 1998.

[4] Welten, S., Holt, A., Hofmann, J., Schelter, L., Klopries, E.-M., Wintgens, T., and Decker, S.: Synthetic Rainfall Data Generator Development through Decentralised Model Training, J. Hydrol., 612, 128210, https://doi.org/10.1016/j.jhydrol.2022.128210, 2022.

**Theme:** Hydraulic and hydrological modeling
**IAHR Thematic Priority Area:** [TPA-4] Digital Transformation
https://doi.org/10.3850/iahr-hic2483430201-123

# Assessment of Joint Probabilistic Behaviour of Fine-Resolution Rainfall and its Impact on Prediction of Urban Hydrological Peak Flows

**Xiaosheng Qin[1], Lilingjun Liu[1]**

[1] School of Civil and Environmental Engineering, Nanyang Technological University, 50 Nanyang Ave., 639798, Singapore

*Corresponding author: xsqin@ntu.edu.sg*

**Abstract.** This study meticulously assesses the interplay of fine-resolution rainfall and its subsequent impact on urban hydrological peak flows in a tropical urban catchment. To achieve this objective, a meticulous analysis of 5-minute rainfall series is undertaken, emphasizing the extraction of critical variables, including the 5-minute maximum intensity and the 30-minute rainfall intensity preceding the peak. These two variables undergo a thorough examination of their interconnections using copula, facilitating a nuanced understanding of their probabilistic relationships. Subsequently, a bivariate frequency assessment is employed to unravel the intricacies of joint return curves. The study proceeds to forecast peak urban hydrological flows within a typical catchment area by establishing connections among the identified variables, employing a linear regression model. The results underscore the notable impact of joint probabilistic rainfall behaviour on urban peak flows. The Bayesian-based Markov Chain Monte Carlo (MCMC) approach proves effective in addressing uncertainties arising from describing bivariate behaviours. The findings furnish valuable perspectives for urban water managers, empowering them with essential information for judicious decision-making in the realm of urban water management.

**Keywords:** copula analysis, extreme rainfall, MCMC, urban hydrology

## 1 Introduction

Urban areas are increasingly vulnerable to the adverse effects of extreme weather events, with rainfall patterns playing a crucial role in shaping hydrological dynamics within these environments. The intricate interplay between precipitation characteristics and urban hydrology necessitates a deep understanding of their joint probabilistic behaviour. This study aims to conduct a copula analysis using fine-resolution rainfall data collected at 5-minute and 30-minute intervals to evaluate the influence of rainfall characteristics on hydrological flows within a tropical catchment.

## 2 Material and Methods

The study framework focuses on a tropical urban catchment documented by Kim et al. [1], situated in the central region of Singapore, covering an area of approximately 100 km$^2$. Drawing from the findings from [1], we extracted specific data points comparing simulated runoff with rainfall data from typical events. Utilizing this information, we constructed a linear regression model to predict peak runoff based on rainfall, aiming to establish a streamlined method for projecting runoff. This serves as a benchmark for our subsequent frequency assessment. The copula analysis is implemented employing the Multivariate Copula Analysis Toolbox (MvCAT), advanced by Sadegh et al. [2], which facilitates the exploration of 26 parametric models from copula families. Rainfall data was gathered from three nearby stations, each providing a 10-year dataset of 5-minute rainfall records. By consolidating these datasets, we compiled a 30-year record suitable for conducting extreme value analysis. From this unified dataset, we identified and labelled the peak values of $I_5$ and $I_{30}$ for each

year as $I_{5max}$ and $I_{30max}$, respectively. Copula parameter is estimated through the MCMC process which facilitates efficient exploration of parameter spaces and estimation of properties of interest. Samples from MCMC representing posterior copula parameters will be utilized for subsequent uncertainty analysis via Monte Carlo simulation. Uncertainty stemming from copula parameter estimation will be probabilistically propagated to describe the range of variation in combinations of two variables under joint return periods.

## 3 Results and Discussion

The regression demonstrates that the model utilizing two variables achieves the highest accuracy, surpassing both the 5-minute and 30-minute models. The marginal distribution of $I_{5max}$ and $I_{30max}$ are modelled using normal and Birnbaum-Saunders distributions, respectively. For copula analysis, the Burr copula model is identified as the best model [2]. The posterior samples from MCMC were used to carry out uncertainty analysis using direct Monte Carlo simulation. Figure 1 illustrates the outcomes of the uncertainty analysis concerning copula fitting and discharge simulation using the regression model. Considering the uncertainty ranges of all design variables, we utilize the established regression model to forecast potential flows from the catchment. For a 200-year return period, the most probable flow is estimated to be 3118.7 $m^3/s$, with an ensemble range due to uncertainty spanning from 3089.2 to 3210.4 $m^3/s$. This range constitutes approximately 3.9% of the most probable flow. Overall, the influence of uncertainty stemming from the pair of design variables appears to be relatively minor. It is also observed that the 30-minute rainfall intensity yields higher flow estimations across various return periods, whereas the 5-minute one results in lower estimations. For instance, for the 200-year return period, $I_{5max}$ leads to a total flow of 2506.3 $m^3/s$, whereas $I_{30max}$ yields 3549.7 $m^3/s$. This underscores that the joint probabilistic consideration of both variables encompasses the effects of individual variables, offering a more reasonable estimation of extreme values.

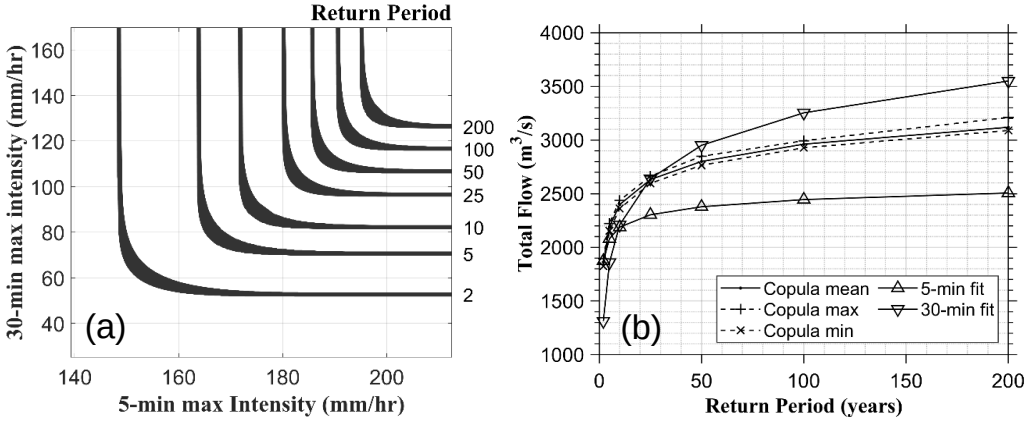


Figure 1. Projected flow results in consideration of copula fitting uncertainty.

## Acknowledgements

This research is supported by the Ministry of Education, Singapore, under its Academic Research Fund Tier 1 (Grant No. RG72/22). Any opinions, findings and conclusions or recommendations expressed in this material are those of the authors and do not reflect the views of the Ministry of Education, Singapore.

## Reference

[1] N. I. Kim, H.C.C. Lloyd, A. Mohammad, Loc H.H., Ha, L.S. Drivers of model uncertainty for urban runoff in a tropical climate: the effect of rainfall variability and subcatchment parameterization, Journal of Water Management Modelling, 31 (2023) C496.

[2] M. Sadegh, E. Ragno, A. AghaKouchak, Multivariate Copula Analysis Toolbox (MvCAT): Describing dependence and underlying uncertainty using a Bayesian framework, Water Resour. Res., 53 (2017) 5166–5183.

**Theme:** Hydraulic and hydrological modeling
**IAHR Thematic Priority Area:** [TPA-4] Digital Transformation
https://doi.org/10.3850/iahr-hic2483430201-125

# Use Of IHA's Sustainable Development Criteria to Evaluate Existing Permanent Reservoirs: Application to Romanian Case Studies

**Camelia Teau[1,2], Ioana Popescu[2,3]**

[1] Mures Water Administration, Romanian Waters, 540057 Tg. Mures, Romania
[2] Faculty of Civil Engineering, Politehnica University of Timisoara, 300223 Timisoara, Romania
[3] Department of Hydroinformatics and Socio-Technical Innovation, IHE Delft Institute for Water Education, 2601 DA Delft, The Netherlands

*Corresponding author: i.popescu@un-ihe.org*

**Abstract**. Present paper presents the ongoing research that aims to develop a framework to evaluate the sustainability of existing reservoirs, after several years of being in operation. The proposed framework starts from the coherent and internationally recognized method of International Hydropower Association (IHA), and adapts it for existing in-operation structures. As such, it highlights the opportunities for improvement and the development of a sustainability evaluation framework that is easy to understand and made available to Romanian water boards, and stakeholders as well. It proposes to adopt a transparent methodology to which all stakeholders can have access to. The research aims to adapt the protocol to the existing dams and dikes, keeping the relevant indicators for each study and creating a sustainability profile by evaluating the performance of the selected indicators. Each evaluation is tailor made for the case study under consideration. The scoring of the indicators is based on available data about the objective of the structure, and on the factual data regarding current performance.

**Keywords:** hydrotechnical infrastructures, SDGs, IHA protocol, Romania

## 1 Introduction

According to the UN SDG Index rankings ([1]), Romania's overall performance in monitoring SDGs ranked 39th out of 165 countries in 2021 and 35th in 2023. While Romania's overall global position is favorable, it has a relatively lower position at the European level. Therefore there is necessary to have ongoing monitoring of the SDG indicators, as well as clear defined methodologies to evaluate various SDG indicators, aiding in the identification of areas needing improvement.
One of the important SDGs for Romania is SDG 7, due to its hydropower potential. Moreover, the sustainable utilization of hydropower plays a crucial role in meeting the specified national climate objectives ([2]). Romania's progress in achieving SDG 7 for affordable and clean energy stands at 71.4%, showing improvement but with moderate challenges. This status affects SDG 13, climate action, which stands at just 50%, showing stagnation and significant challenges. Given the significance of maximizing Romania's hydropower capacity, there is an emphasis on improving the effectiveness of existing hydrotechnical structures, especially dams. This research looks into methodologies for evaluating the sustainability of present hydropower facilities, including dams and surrounding reservoir dikes.

## 2 Methods

The International Hydropower Association (IHA) released the Hydropower Sustainability Assessment Protocol (HSAP) in 2010 to evaluate the sustainability of dams during the critical design phase of infrastructure projects ([4]). Developed over two years from 2008 to 2010, the protocol was formulated in response to a recommendation from the World Commission on Dams. It involved a comprehensive approach considering policies and performance standards, with input from

stakeholders representing various sectors. Notably, the HSAP was updated in 2018 to address climate change resilience and mitigation. The evaluation covers over 20 criteria categorized into environmental, technical, economic, and social aspects, including human rights and gender-related issues. It addresses all stages of project design, from early stages to operation, with each stage having its own set of evaluation criteria.
In order to determine sustainability of dams this protocol was used to evaluate Romanian dams, in particular it was applied to Cincis dam, Hunedoara county, Romania

## 3. Results and discussion

The chosen case study to illustrate the concept of HSAP is the Cincis dam in Romania, situated at the confluence of the Cerna and Teliucu Superior rivers within the Mures basin. Built in the early sixties (1961-1964), the dam was intended to create a reservoir to supply water to the downstream industrialized city of Hunedoara and act as a flood protection measure. The reservoir has a catchment of 305 km$^2$. The dam is 48 meters tall, with a reservoir covering 867 hectares, characterized by sandy shores on nearly 50% of its perimeter ([3]). As its role has evolved over time, with decreased industrial activity and reduced demand for water supply, the dam now offers increased storage availability. Evaluating the functionality of this structure is essential given its changed role.

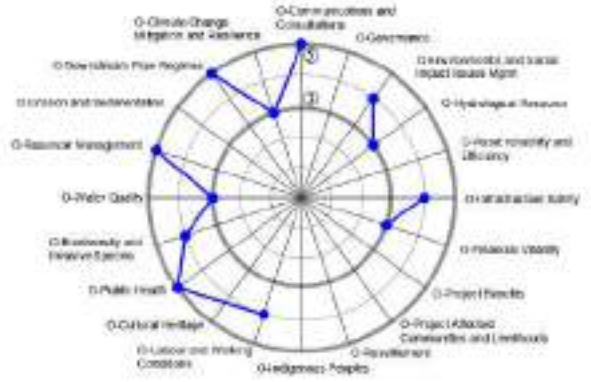

*Figure 14. HSAP protocol values for Cincis dam, Hunedoara, Romania*

Application of the HSAP protocol for a series of main criteria gives results as presented in Figure 1. Criteria are evaluated on 5 levels, with a minimum of 3 showing good practices, and 5 proven best practices. Any level bellow 3 needs special attention.

## 4. Conclusions and recommendations

While the periodic approvals for dam operations are essential, they may not adequately cover the various sustainability aspects that Romania seeks to enhance. Hence, the use of protocols such as the one of HSAP can be used to determine areas necessitating improvement ([5]). This tool would be of help to decision-makers and stakeholders. As a next step a study on how such a protocol needs to be adapted for existing structures is recommended. .

## References

[1] United Nations, (2023) Transforming our world: the 2030 Agenda for Sustainable Development. https://sdgs.un.org/2030agenda (last accesed January 2024)
[2] Teau C., Popescu I., Florescu C., Constantin A., Ciocan C.M., Vlaicu V. (2023) Implementation of water related Sustainable Development Goals in Romania: overview of current and future challenges, ) IOP Conference Series: Earth and Environmental Science, 1136 (1), art. no. 012013, DOI: 10.1088/1755-1315/1136/1/012013
[3] Gaftoi, D, Abdulamit, A., Aldea, A., Sarghiuta, R., Popescu, C. (2021) Assessing Structural Safety of an Arch Dam Using in Situ Vibration Tests, IOP Conference Series: Materials Science and Engineering 1203(1), art no 022122, doi:10.1088/1757-899X/1203/2/022122
[4]HSAP (2022) Hydropower Sustainability Assessment Protocol available from https://www.hydrosustainability.org/ (last accessed December 2023)
[5] LeRoy Poff, N., Olden, J. (2017) - Can dams be designed for sustainability?, Science, 358 (6368), 1252-1253. DOI: 10.1126/science.aaq1422

**Theme:** Hydraulic and hydrological modeling
**IAHR Thematic Priority Area:** [TPA-4] Digital Transformation
https://doi.org/10.3850/iahr-hic2483430201-127

# Exploration of the hydraulic functioning of the Malpasset Dam Wreckages Using Standard 1D-2D Numerical Codes

**Amillat Ali[1], Belliard Zian[1], Kanlinsou Fidèle[1], Mur Joanna[1], Nassiri Fatima Ezzahra[1], Remila Sara[1], Delestre Olivier[2,3], Cordier Florian[2], Olivares Gonzalo[4], Collange Luc[5] and Abily Morgan[6]**

[1] Université Côte d'Azur, EUR, SPECTRUM, France
[2] EDF R&D LNHE-Laboratoire National d'Hydraulique et Environnement, Chatou, France
[3] Université Côte d'Azur, CNRS, LJAD, France
[4] Institut Flumen, Universitat Politècnica de Catalunya – Centre Internacional de Mètodes Numèrics en Enginyeria, Barcelona, España
[5] Departement du Var, France
[6] Université Côte d'Azur, Observatoire de la Côte d'Azur, CNRS, IRD, Géoazur, France

**Abstract.** The Malpasset Dam, (France) experienced a catastrophic failure in December 1959 [1]. The remaining components of the dam (bottom outlet, breach cavity and partially destroyed crest), create a particular situation which in case of intense rainfall can potentially lead to a 9 m depth retention pond above the riverbed. The dam wreckages have been secured in 2022. Yet, no in-depth hydraulic study has been performed to characterize the hydraulic of the remaining system. This study focuses on the challenging task of understanding the hydraulic functioning of the dam wreckages by exploring their structural intricacies, using 1D and 2D free surface flow modeling approaches. The primary objective involves (i) creating a sufficiently precise representation of the dam's remnants, then (ii) performing a comparative analysis using standard modeling softwares solving the Shallow Water Equations system: HEC-RAS (1D-2D), IBER 2D, and TELEMAC-2D. High resolution LiDAR data and a specific topographic data gathering campaign allowed to capture the structure and the morphological characteristics within the study area. 2D meshes were created using the three software's recommended meshing tools and approaches, and similar scenarios were run with each model in order to conduct comparisons. The hydraulic behavior of dam's debris simulated by the three different approaches is compared and discussed. Numerical findings will help to design a 3D printed physical model dedicated to research on this specific configuration and educational purpose.

**Keywords: Comparative analysis, Hydrodynamics, Malpasset Dam, Numerical modeling, SWE**

## 1 Modeling approach

The modeling of the Malpasset dam wreckages in the Reyran (France) river is achieved using three codes solving the Shallow Water Equations: HEC-RAS, Iber and TELEMAC-2D [2]. Aerial born LiDAR cloud points of 1 m resolution was used to build the digital terrain model of the study area (12 km²). The Dam wreckage crest topography was gathered by field measurements. Soil occupation map was processed to extract spatialized roughness coefficients. A 2D computational domain with a mesh cell size ranging from 0.5 m (near the dam crest) to 10 m was build-up with each software to model the study area. The breach cavity's geometry led us to simplify it into a rectangular culvert with equivalent dimensions whereas the bottom outlet (1.5 m diameter) was also included in the computational codes using culvert insertion functions (discussed in the paper).

## 2 Simulation scenario

One scenario was proposed in order to study the hydraulic functioning of the dam wreckages and the flood dynamics along 24 hours from a flood event on December 1st, 2019. The hydrograph comes from the VIGICRUES database (https://www.vigicrues.gouv.fr) [3].

## 3 Preliminary results

The three models yeld comparable results, with a maximum water depth of 12.8 m, a maximum velocity of 11.3 $m.s^{-1}$ (figure 1), a dam wreckages spill duration of 2h15 min and a water retention volume of 532,653 $m^3$. The computational time (table 1) differs between the three softwares due to several factors including the computers characteristics and computing processes, which will be detailed in the presentation.


Figure 15 Maximum water depths (left, in m) and velocities computed with HEC-RAS (right, in m. $s^{-1}$)

The full paper will compare not only the hydraulic characteristics provided by hydraulic variables analysis (spill discharge, maximal depth, emptying time, etc.) from the three simulations but also discuss the assumptions and ease of inclusion of the culver structures to represent both (i) the bottom valve, and (ii) the cavity.

Table 5 Simulations computational characteristics for the three softwares

| Software | IBER | HEC-RAS | TELEMAC-2D |
|---|---|---|---|
| CPU architecture | Intel i5 11th Gen 4 CPU, 8 Go RAM | Intel i7 11thGen 8 CPU, 8 Go RAM | Azzura Cluster |
| Number of CPU | 4 | 8 | - |
| Simulation time (h) | 18,5 | 21 | 48 |
| Computing time (h) | 10,3 | 6 | 3 |
| Ratio | 1,8 | 3,5 | 16 |

## Reference

[1] AJ Rollet, S. Dufour et C. Morhange , (2012) « The rupture of the Malpasset dam 50 years later: a privileged observatory for the study of extreme events? » , Méditerranée , 118 | 2012.

[2] V. Thanh Tung (2018). Parallel and distributed algorithms for computational fluid flow simulations. Doctoral thesis, Nanyang Technological University, Singapore.

[3] Olivier Piotte, Thibaut Montmerle, Catherine Fouchier, Anne Belleudy, Lea Garandeau, Bruno Janet, Celine Jauffret, Julie Demargne & Didier Organde (2020) Les évolutions du service d'avertissement sur les pluies intenses et les crues soudaines en France, La Houille Blanche, 106:6, 75-84, DOI: 10.1051/lhb/2020055

**Theme:** Hydraulic and hydrological modeling
**IAHR Thematic Priority Area:** [TPA-4] Digital Transformation
https://doi.org/10.3850/iahr-hic2483430201-129

# The Auto Calibration of TELEMAC-2D Model with A Data Assimilation Algorithm

**HUANG Weihong[1], LIAO Tian[1], WEI Ronglian[1], ZHOU Lu[1], BOURBAN Sébastien E.[2], MIN Jiesheng[1]**

[1] Zhejiang Yuansuan Technology Co., Ltd., Hangzhou, China
[2] EDF R&D National Laboratory for Hydraulics and Environment (LNHE)

*Corresponding author: rlwei@yuansuan.com*

**Abstract.** Hydrodynamic models play an increasingly crucial role in digital twin basin systems, particularly in the context of flood risk forecasting and assessment. The accuracy of hydrodynamic model is of utmost importance as they are utilized for early warning and intervention measures to ensure civil protection. In this study, auto calibration of TELEMAC-2D model was carried out with in-situ water depth data using a 3DVAR-based assimilation algorithm. Prior to the auto calibration process, sensitivity analysis of TELEMAC-2D model and 3DVAR algorithm were performed to determine the optimal geometry mesh resolution and 3D-VAR parameters. The assimilation process was carried out with observation data from the flood event in July, 2023.

**Keywords:** Data Assimilation, Model Calibration, TELEMAC-2D

## 1 Introduction

Prewarning and intervention measures are vital for safeguarding lives and property during flood events. This study aims to automatically calibrate the TELEMAC-2D model0 to enhance its applicability in digital twin watershed systems, particularly in improving flood risk prediction and assessment.

### 1.1 TELEMAC-2D model

TELEMAC-2D is a 2D hydrodynamic model of open TELEMAC system, capable for applications in river hydraulics and free-surface maritime. TELEMAC-2D model was applied to simulate flash flood phenomena in an interested area, and 3DVAR algorithm0 was employed to auto calibrate the model parameter, namely bottom friction.

### 1.2 3DVAR algorithm

By normalizing the acquired monitoring water depth, this algorithm constrains auto calibration to a quadratic functional minimization problem involving deviations between the analysis field and the observation field, so as the analysis field and the background field.

$$J(x) = (x - x^b)^T B^{-1}(x - x^b) + \left(y^o - H(x)\right)^T R^{-1}(y^o - H(x)) \quad (1)$$

with the cost function, a quantification of the uncertainties on the a priori errors, a quantification of the uncertainties on the observation errors and the observation operator that selects in the calculation results00.

## 2 Methodology

Firstly, a series of sensitivity analysis on the mesh sizes and downstream boundary conditions were conducted of the TELEMAC-2D model.
Secondly, a river roughness field was assumed as true state, from which pseudo-observations00 were generated by TELEMAC-2D simulations. The 3DVAR algorithm would be used to recover the "true" state under a highly diverse background roughness field. The reliability of the 3DVAR algorithm shall be validated. During the experimental process, the quantification and sensitivity analysis of various uncertainties on the a priori errors and observation errors were conducted.
Based on the experiments described above, the fundamental parameters of 3DVAR algorithm were determined. Lastly, based on water depth series from 2 monitoring stations in a flood-prone watershed, segment-specific roughness values for river reaches of TELEMAC-2D model were calibrated.

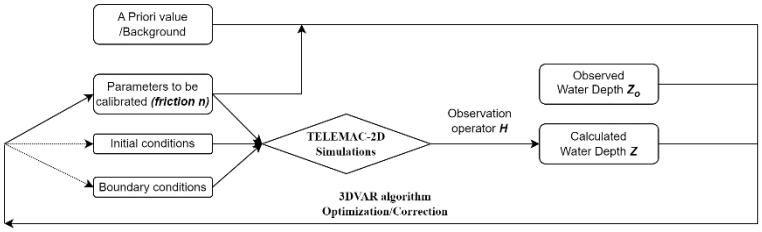


Figure 1 TELEMAC-2D-3DVAR coupling process

## 3 Model validation & Results discussion

### 3.1 TELEMAC-2D sensitivity analysis

The calculated water depth at the location of stage meters in TELEMAC-2D model was primarily sensitive to the roughness of the river channels, with minimal influence from grid size and downstream water level.

### 3.2 3DVAR algorithm verification

and are constant variances of a priori errors and observation errors. 3 different calculation tests were conducted with varying and values. The results indicate that overall, the 3DVAR algorithm could accurately reproduce the "true" roughness of the riverbed. Meanwhile, when the confidence in the background was very low compared to the one in the observations, i.e., when , it was verified that the roughness field computed by the 3DVAR algorithm was closer to the "true" state.

$$B = \sigma_B^2 I \quad (2)$$

$$R = \sigma_R^2 I \quad (3)$$

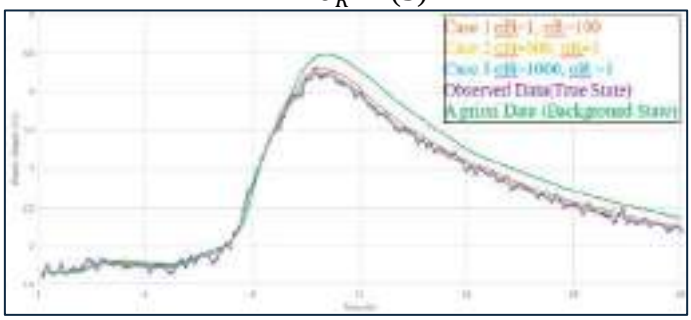

Figure 2 simulated and observed water depth at a monitoring station with different

### 3.3 Results discussion

Based on a real flood event in July 2023, auto-calibration and validation of the river roughness in TELEMAC-2D model were conducted by 3DVAR algorithm. The computed water depth of TELEMAC-2D model were compared with the observed water depth data at 2 monitoring stations, showing a satisfactory of data agreement, with NSE coefficients exceeding 0.85 for both stations.

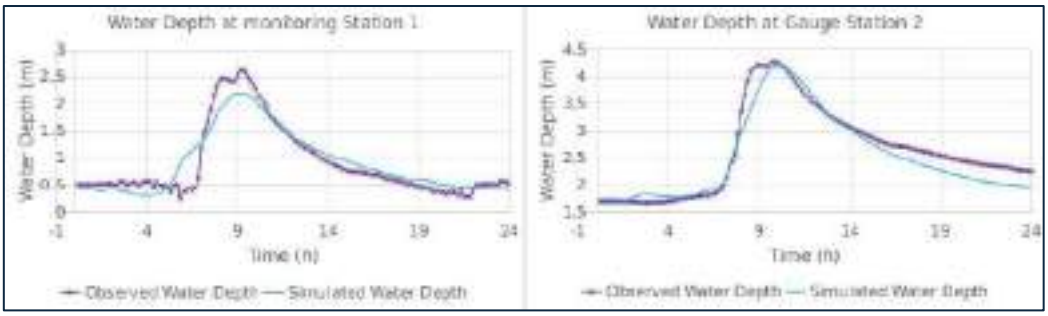


Figure 3 Comparison of simulated and observed water depths during July 2023 flood

## 4 Conclusion

This study demonstrates the implementation of an automatic calibration process for the TELEMAC-2D hydrodynamic model using 3DVAR algorithm. The method enhances model accuracy and assures more reliable flood warnings and risk assessments. The parameters ( and ) in the 3DVAR algorithm would affect data assimilation results, yet overall, the algorithm could effectively restore the real roughness values in the TELEMAC-2D model. By conducting sensitivity analysis, the optimal parameters of 3DVAR algorithm were determined, thereby helping to improve the data assimilation results.

## Reference

[1] https://www.opentelemac.org/

[2] Zhang Z P G P .Analysis and numerical study of a hybrid BGM-3DVAR data assimilation scheme using satellite radiance data for heavy rain forecasts[J].Journal of Hydrodynamics, Ser. B, 2013.DOI:10.1016/S1001-6058(11)60382-0.

[3]Lorenc A. C., Analysis methods for numerical weather prediction, Quarterly Journal of the Royal Meteorological Society, 112(474), pp.1177-1194, 1986.

[4]Talagrand O., Assimilation of Observations, an Introduction, Journal of the Meteorological Society of Japan, 75(1B), pp.191-209, 1997.https://docs.salome-platform.org/latest/gui/ADAO/en/methodology.html#to-test-a-data-assimilation-chain-the-twin-experiments

**Theme:** Hydraulic and hydrological modeling
**IAHR Thematic Priority Area:** [TPA-4] Digital Transformation
https://doi.org/10.3850/iahr-hic2483430201-132

# Study on Geometric Optimization of Vertical Shaft Swirl Spillway Based on Kriging Kurrogate Model

**Wen Wang[1,2], Tao Xue[1,2], Minghao Deng[1,2], Hunan Qiu[1,2], Shaobo Xue[1,2]**

[1] Xi`an University of Technology, NO.5 South Jinhua Road, Xi'an, 710048, Shaanxi, China
[2] State Key Laboratory of Eco-hydraulics in Northwest Arid Region, NO.5 South Jinhua Road, Xi'an, 710048, Shaanxi, China

*Corresponding author: wangwen1986@hotmail.com*

**Abstract.** This study investigates the design optimization of vertical shaft swirl spillways to improve flood discharge efficiency and energy dissipation in hydraulic systems. Using computational fluid dynamics (CFD) and Kriging surrogate modeling, it addresses the complex dynamics of swirling flows in spillways. The Realizable k-ε turbulence model and the Multi-Objective Genetic Algorithm (MOGA) are employed for the geometric optimization, leading to significant performance enhancements. The results show that the optimized design achieves an energy dissipation efficiency of up to 81.88%. This approach underlines the effectiveness of combining advanced computational tools and optimization techniques in hydraulic engineering, providing new design ideas for the safe and stable operation of spillways.

**Keywords:** Numerical simulation, Optimization algorithms, Realizable k-ε turbulence model, Response surfaces, Shape optimization, Vertical shaft swirl spillway

## 1 Introduction

The study contributes to the field of hydraulic engineering by exploring optimization approaches for vertical shaft swirl spillways, with the objective of enhancing flood discharge efficiency and energy dissipation in large-scale hydraulic systems[1]. These spillways are pivotal in dam operations, mitigating flood risks and conserving energy. However, their complex flow dynamics, characterized by three-dimensional, two-phase, and swirling flow patterns, pose design and optimization challenges[2]. Due to the complex control boundary conditions and the multitude of parameters involved in the structural design of vertical shaft spillways, traditional methods often fall short in predicting hydraulic behavior accurately[3]. The focus in the flow process is on enhancing the stability of the flow regime and improving the energy dissipation rate, which necessitates the use of advanced computational tools[4]. This research emphasizes the need for optimized spillway design, utilizing the Realizable k-ε turbulence model and Kriging surrogate modeling to address these challenges effectively. The methodological innovation allows for an efficient exploration of the design space, offering a substantial reduction in computational demand while maintaining high accuracy levels.

## 2 Materials and Methods

The methodological framework of this study is anchored in the synergistic use of computational fluid dynamics (CFD) and surrogate modeling, specifically the Kriging technique. The research employs FLUENT software for conducting detailed numerical simulations of the spillway's hydraulic dynamics, utilizing the Realizable k-ε turbulence model to account for the complex flow interactions within the spillway structure. This model is chosen for its proven capability in accurately simulating turbulent swirling flows, which are characteristic of vertical shaft spillways. The geometric optimization process is driven by a comprehensive analysis involving sensitivity studies, mesh optimization, and turbulence model comparison. Initial simulations provided insights into the flow behavior, guiding the selection of geometric parameters for subsequent optimization. The Kriging surrogate model, known for its efficiency in predicting unknown outputs from a given set of inputs, was then developed using simulation data. This model served as the basis for identifying the optimal spillway design, reducing the computational load significantly. To ensure the robustness of the simulations, a detailed mesh sensitivity analysis was conducted, leading to the selection of a mesh scheme that balances computational

efficiency with accuracy. The study also included a turbulence model adaptability study, where the Realizable k-ε model was compared against other models, confirming its superior capability in capturing the spillway's hydraulic characteristics. The optimization utilized advanced algorithms, including Genetic Algorithm (GA) and Multi-Objective Genetic Algorithm (MOGA), to explore the multi-dimensional design space. These algorithms facilitated the identification of design configurations that meet the predefined performance criteria, such as maximizing energy dissipation rate and optimizing flow uniformity.

## 3 Results and Discussion

The results from the comprehensive simulation and optimization exercises revealed a significant enhancement in the spillway's performance. The optimized design, determined through the Kriging surrogate model, demonstrated improved energy dissipation efficiency and reduced flow irregularities. Specifically, the study identified key geometric parameters, such as the depth of the stilling well and the contraction ratio, which critically influence the spillway's hydraulic performance. Comparative analyses between the original and optimized designs showed a notable increase in energy dissipation rates, with the optimized configuration achieving up to 81.88% efficiency, compared to 74.46% in the original design. This improvement underscores the effectiveness of the optimization process in enhancing the spillway's operational efficacy. The hydraulic model validation, conducted through numerical simulations, corroborated the experimental findings, affirming the reliability of the simulation results. The flow coefficient and velocity characteristics, integral to the spillway's design, matched closely with the experimental data, with discrepancies within the acceptable range of 5%, thereby validating the computational approach used in the study. Sensitivity analysis further illuminated the impact of various design parameters on the spillway's performance, guiding the optimization efforts. The interaction effects between parameters were also explored, providing insights into the complex relationships governing the spillway's hydraulic behavior and informing the decision-making process in the optimization strategy[5].

## 4 Conclusions

The research successfully optimized the vertical shaft swirl spillway using CFD simulations and Kriging surrogate modeling, marking a substantial advancement in hydraulic engineering. The optimized design, demonstrating improved energy dissipation and flow stability, offers a robust framework for similar hydraulic structures. This study underscores the effectiveness of advanced simulation and optimization techniques in enhancing hydraulic infrastructure design, contributing significantly to the field and fostering the development of more sustainable flood management systems. Looking forward, the research horizon for vertical shaft swirl spillways is broad, with potential for further advancements in design and optimization. Future work should extend the exploration of design parameters and performance metrics, including air entrainment rate and discharge capacity, to achieve a more holistic spillway assessment. Utilizing various surrogate models may enhance the optimization process by increasing the accuracy and reliability of design predictions. Extending the computational domain to cover the full spillway system could yield a more comprehensive understanding of its operational dynamics, potentially leading to better real-world performance. A focused approach that combines computational methods with practical insights and optimization techniques could improve the efficiency and sustainability of water management infrastructures.

## Reference

[1] Carty, A., O'Neill, C., Nash, S., Clifford, E., & Mulligan, S. (2019). Hydrodynamic modelling approaches to assess mechanisms affecting the structural performance and maintenance of vortex drops shaft structures. Journal of Structural Integrity and Maintenance, 4(3), 162-178.

[2] Rincón, M. J., Reclari, M., Yang, X. I., & Abkar, M. (2023). Validating the design optimisation of ultrasonic flow meters using computational fluid dynamics and surrogate modelling. International Journal of Heat and Fluid Flow, 100, 109112.

[3] Sun, X., Kim, S., Yang, S. D., Kim, H. S., & Yoon, J. Y. (2017). Multi-objective optimization of a Stairmand cyclone separator using response surface methodology and computational fluid dynamics. Powder Technology, 320, 51-65.

[4] Karimi, M., Akdogan, G., Dellimore, K. H., & Bradshaw, S. M. (2012). Quantification of numerical uncertainty in computational fluid dynamics modelling of hydrocyclones. Computers & chemical engineering, 43, 45-54.

[5] Ye, P., & Pan, G. (2017). Global optimization method using adaptive and parallel ensemble of surrogates for engineering design optimization. Optimization, 66(7), 1135-1155.

**Theme:** Hydraulic and hydrological modeling
**IAHR Thematic Priority Area:** [TPA-4] Digital Transformation
https://doi.org/10.3850/iahr-hic2483430201-134

# Modelling Sediment Transport in Key Reservoirs on Yellow River

**Yang Fei[1, 2], Wang Qiang[1, 2], Wang Yuanjian[1, 2]**

[1] Yellow River Institute of Hydraulic Research, Yellow River Conservancy Commission, Zhengzhou, 450003, China
[2] Key Laboratory of Lower Yellow River Channel and Estuary Regulation, Ministry of Water Resources, Zhengzhou, 450003, China

*Yang Fei: yangfeihaoyun@163.com*

**Abstract.** Sediment transport simulation is the technical foundation of the water and sediment regulation (WSR) which aims to alleviate the sedimentation problem on Yellow River. This paper introduces a hydrodynamic model for sediment transportation simulation in reservoirs. The generation and move process of turbidity currents and the open channel flow was coupled together. The incipient shear stress of consolidated deposition was considered as adjustable parameter adept to different conditions. The model enables to simulation flow and sediment transport in different reservoirs on Yellow River. The joint operation of key reservoirs in the upper and middle reaches of Yellow River was overviewed. Practical application has proven that it is capable of handling the joint WSR in reservoir groups. Water-sediment spatial matching between reservoirs would affect sediment discharge. Operations of adjacent reservoirs should be matched whereas the downstream reservoir low water level encounters with upstream discharge peak. The drawdown flushing duration should depend on the sediment available for scouring. Monotonous one-step drawdown process is desirable to ensure the full development of erosion.

**Keywords:** Reservoir, Water and Sediment Regulation, Water and Sediment Transport Model, Yellow River

## 1 Introduction

Yellow River is characterized by heavy sediment load with a naturally uncoordinated water and sediment relationship, although the past 60 years of runoff and sediment load observations show obvious changes in water and sediment relationship in the Yellow River. Water and sediment regulation (WSR) plays a crucial role on the balance of sediment transport in the Yellow River since 2002[1]. Sediment transport simulation is the technical foundation of the WSR. To optimize operation of key reservoirs on Yellow River, flow and sediment transport models based on reasonable mathematical description is reliable.

## 2 Method

The research method adopts a 1D mathematical model of water and sediment transport simulation. The numerical solution of the governing equations is solved in an asynchronous way. The bed brinkpoint plays a critical role as step in retrogressive erosion. Numerical calculations have a large scale for dividing the longitudinal grid of the reservoir, making it difficult to accurately distinguish the bed brinkpoint. That might results in the numerically smoothed bed and the supercritical flow to be assimilated as subcritical flow. Consequently, local associated depth-averaged streamwise velocity and corresponding sediment transport capacity are inhibited. To eliminate this negative impact, the model determines the location of the step/brinkpoint on the grid Fr and improve local sediment transport capacity by adding a certain coefficient through calibration. The deposition in the reservoirs on Yellow River is composed of fine particles and has significant cohesive. The deposited sediment gradually drains and consolidates tightly after long-term gravity sedimentation, greatly decreasing its

erodibility. Critical bed shear stress $\tau_c$ is considered for the deposited sediment and its value is verified by trial and error. Erosion occurs when the flow shear stress on bed exceeds $\tau_c$.

## 3 Results

Pre-flood-season WSR is launched mainly based on Xiaolangdi Reservoir from June 21 to July 11 in 2023. The calculated sediment discharge is basically consistent with the measured ones(Figure 1a). In 2023, the upper Yellow River has experienced a shortage of incoming runoff. Jointly operation was applied to four reservoirs including Liujiaxia, Qingtongxia, Haibowan, and Wanjiazhai for WSR. The scheduling scheme for each reservoir was worked out after several design plans comparisons by numerical results. The joint sediment discharge of these three reservoirs, was effectively flushed under efficient utilization of water resources(Figure 1b).

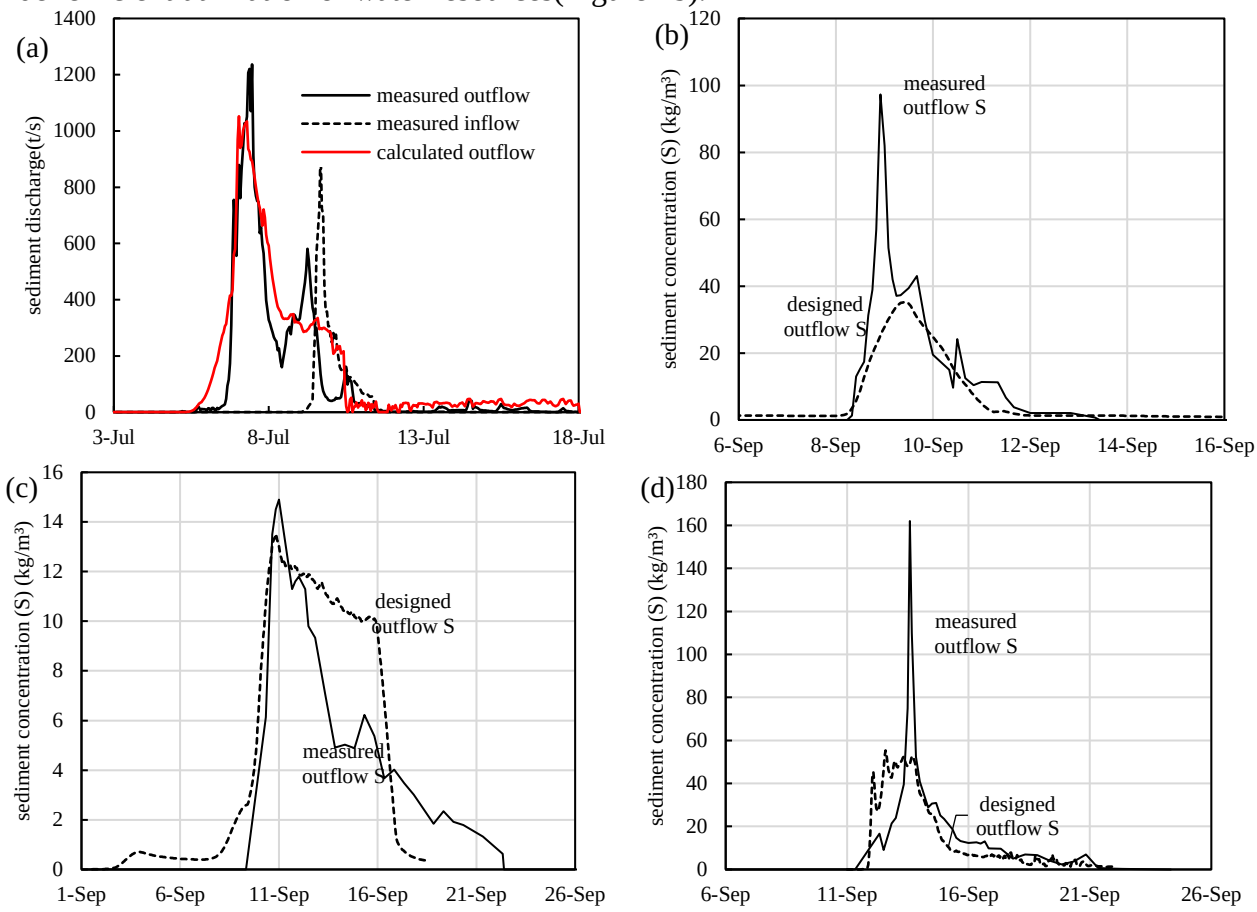


Figure 3 (a)Sediment discharge for Xiaolangdi Reservoir. Designed and measured outflow sediment concentration for (b) Qingtongxia Reservoir, (c) Haibowan Reservoir, and (d) Wanjiazhai Reservoir.

## 4 Conclusion

Sediment transport simulation is the technical foundation of the water and sediment regulation. The model enables to simulation flow and sediment transport in different reservoirs on Yellow River. A few suggestions for operation schedules to maximize flushing can be provided here: Matching of inflow peak with w.s.e. can increase erosion in reservoir, reasonable duration for minimum w.s.e. should be set to achieve efficient flushing, and monotonous one-step drawdown process is desirable to ensure the full development of erosion.

## Reference

[1] D. Kong, C. Miao, J. Wu, et al. The hydro environmental response on the lowerYellow River tothewater–sediment regulation scheme. Ecol. Eng. 79(2015): 69–79.

**Theme:** Hydraulic and hydrological modeling
**IAHR Thematic Priority Area:** [TPA-4] Digital Transformation
https://doi.org/10.3850/iahr-hic2483430201-136

# Enhancing Flash Flood Warning Using a Frequentist Approach: A Case Study of Ba Catchment in Fiji

**Swastika Devi[1], Ziyi Wu[2], Leonardo Alfonso[3] and Biswa Bhattacharya[3*]**

[1] Fiji Meteorological Service, Fiji
[2]Eco-Environmental Monitoring and Research Center, Pearl River Valley and South China Sea Ecology and Environment Administration, Ministry of Ecology and Environment, Guangzhou, China Guangzhou, China
[3]IHE Delft Institute for Water Education, Delft, Netherlands, Delft, 2611 AX, Netherlands.

* *Corresponding author: B.Bhattacharya@un-ihe.org*

**Abstract**. The current Fiji Flash Flood Guidance System utilized by the Fiji Meteorological Service provides binary flood alerts (flood/ no-flood), leading to uncertainties in decision-making. This study introduces a probabilistic Flash Flood Guidance (FFG) approach using a frequentist methodology to address this limitation. The focus is on the Ba Catchment in Fiji, aiming to establish risk classes under varying rainfall and antecedent soil moisture (AMC) conditions. The research pursues three main objectives: a) investigating historical rainfall and flash flood data under different AMC; b) evaluating flash flood occurrence probability, leading to the establishment of risk classes for effective decision-making; c) validating the approach with a case study in the Ba catchment. The study employs analysis of 43 flash flood events during January 2018 to March 2023, emphasizing the Frequentist FFG risk probabilities and their implications. Flood risk is grouped into four levels based on the likelihood of occurrence. Performance is evaluated for 17 events, and results indicate a higher Probability of Detection (93%) for the Frequentist FFG compared to existing FFG system (67%).

**Keywords:** Flash floods, FFG, Frequentist, forecasting, Fiji.

## 1 Introduction

Flash Floods poses significant threat and causes extensive devastation worldwide. They pose immense destructive forces which are capable to alter river paths, inundate homes and carry away anything unfortunate to stand in their way (Rentschler et al., 2022). Regardless of the rare major floods or frequent small floods, both events have the tendency to set back years of economic development and hinder poverty reduction measures (Rentschler et al., 2022). The Frequentist approach entails examining the occurrence frequency of empirical conditions, such as rainfall, that have previously led to observed events like flooding (Brunetti et al., 2015; Wu et al., 2022). The probability of an event is measured by its relative frequency of occurrence in a series of repeated experiments. Frequentist is a well-established and readily applicable method, which demonstrate strong performance and is computationally inexpensive leading to its wide usage in the field of meteorology (Wu et al., 2022). The essence of frequentist method is that it considers the uncertainties associated with forecasting flash flood which can lead to minimizing false alarms and missed events while reducing disaster risks. This research pursues three main objectives: a) investigating historical rainfall and flash flood data under different AMC; b) evaluating flash flood occurrence probability, leading to the establishment of risk classes for effective decision-making; c) validating the approach with a case study in the Ba catchment in Fiji.

## 2 Methods

The study area, Ba Catchment is situated on the western part of Viti Levu covering a drainage area of 957km2. The primary river, known as Ba River, originates from the mountainous regions in the

central part of Viti Levu approximately 83 km from sea and at an elevation of around 1068m. Hourly rainfall data from 1st January 2018 to 31st March 2023, has been sourced from the climate data archives of the Fiji Meteorological Service (FMS) for 6-hourly rainfall events. A quantitative methodology is employed, utilizing rainfall and flash flood occurrence data. Log-transformed 6-hourly rainfall events leading to flash floods are analysed using Kernel Density Estimation (KDE) and a Gaussian weighting function. Probability thresholds are established, grouping flood risk into four levels based on the likelihood of occurrence: very low (<10% probability), low (≥10 to <20% probability), significant (≥20 to <60% probability), and high (≥60% probability), each associated with tailored decision support measures and colour coding.

## 3 Results

The study employs analysis of 43 flash flood events during January 2018 to March 2023. Performance is evaluated for 17 events, demonstrating its proactive risk assessment capabilities. The results indicate a higher Probability of Detection (93%) for the Frequentist FFG method compared to the existing FFG system (67%). In this way, very low risk signified no flood warning while low risk (yellow), significant risk (orange) and high-risk (red) classes were considered as warning signifying flooding with varying degree of uncertainty (Table 1).

**Table 1:** Contingency table for frequentist FFG

| Frequentist FFG Approach | Flash flood Occurrence | |
|---|---|---|
| | Yes | No |
| Very low risk: (<10% probability) - Decision: no action | 1 (Miss) | 0 |
| Low risk (≥10% probability <20%) - Decision: Advisory | 1 (hit) | 0 |
| Significant risk: (≥20% probability <60%) - Decision: Alert | 3 (hit) | 1 (false alarm) |
| High risk: (≥60% probability) - Decision: Warning | 10 (hit) | 1 (false alarm) |

## 4 Conclusions

The Frequentist FFG approach offers a valuable enhancement to the existing FFG. By establishing risk classes under varying conditions, the approach improves decision-making accuracy and communication.

## References

[1] Rentschler, J., Salhab, M., & Jafino, B. A. (2022). Flood exposure and poverty in 188 countries. *Nat Commun*, 13(1), 3527. doi:10.1038/s41467-022-30727-4.

[2] Brunetti, M. T., Peruccacci, S., Antronico, L., Bartolini, D., Deganutti, A. M., Gariano, S. L., & Guzzetti, F. (2015). Catalogue of Rainfall Events with Shallow Landslides and New Rainfall Thresholds in Italy. In (Vol 2, pp. 1575-1579): *Engg. Geology for Society and Territory*.

[3] Wu, Z., Bhattacharya, B., Xie, P., & Zevenbergen, C. (2022). Improving flash flood forecasting using a frequentist approach to identify rainfall thresholds for flash flood occurrence. *Stochastic Environ. Res. and Risk Assessment*. https://doi.org/10.1007/s00477-022-02303-1

**Theme:** Hydraulic and hydrological modeling
**IAHR Thematic Priority Area:** [TPA-4] Digital Transformation
https://doi.org/10.3850/iahr-hic2483430201-138

# The Optimal Algorithm for Urban Surface Runoff Based on Cellular Automata

**Mengnan He[1], Cheng Chen[1], Donghao Wu[2]**

[1] Nanjing Hydraulic Research Institute, Nanjing 210029, China;
[2] Taihu Basin Monitoring Center of Hydrology and Water Resources, Wuxi 214024, China

*Corresponding author: mnhe@nhri.cn*

**Abstract.** Accurately characterizing urban surface runoff process is essential for reducing the uncertainty of urban hydrological model. Based on the quantification of flow pattern urban surface runoff flow characteristics, this study proposed an optimal urban flow direction algorithm based on cellular automata (UCA), and the UCA algorithm was verified by the the numerical simulation and physical experiments under different rainfall events. Results showed that the optimal water distribution weights of UCA algorithm for converge flow and diverge flow are 2.0 and 1.1 respectively. The relative error and root mean square error between the UCA's simulation and theoretical values of specific catchment area are the smallest on ellipsoid, inversed ellipsoid, saddle and plane slopes. The Nash Efficiency (NSE) coefficient of UCA algorithm is significantly higher than that of the classical 4+4N algorithm (with an increase of NSE by 0.12~0.69). In particular, the misjudgment of the initial runoff flow pattern by the 4+4N algorithm can be effectively corrected under the light rain event, which can provide a better solution for urban waterlogging and non-point source pollution modeling in the future.

**Keywords:** flow pattern, cellular automata, converge flow, diverge flow, water distribution weight

## 1 Introduction

Rapid urbanization not only alters surface infiltration processes but also introduces various steep and gentle terrains, complicating the composition of urban surface water hydraulic gradients.[1] As an important part in urban hydrological models, the **flow direction** describes the route of water flow from higher to lower elevations among various surface geomorphological units,[2] which would be crucial for calculating parameters like catchment area and topographic index. However, the **existing flow direction algorithms** ignore the real flow pattern of water itself in the grid. Actually, the real flow pattern is a coexistence of diverge flow and converge flow, and water does not always flow according to elevation differences among the surrounding grids. Therefore, we proposed an optimal urban flow direction algorithm based on cellular automata (UCA), and conducted numerical and physical experiments to calibrate and validate the proposed UCA algorithm. The main objectives are (i) to quantitatively distinguish the real flow pattern (diverge flow or converge flow) under the complex hydraulic gradients characteristic of urban environments, and (ii) to improve the modeling performance of urban rainfall-runoff process.

## 2 Urban flow direction algorithm based on cellular automata

The proposed UCA algorithm implements a flow pattern judgement rule is to quantitatively distinguish the real flow pattern (diverge flow or converge flow).

## 3 CA-based rainfall-runoff simulation

The optimal water distribution weights ($p_c$ and $p_d$) for urban areas under flow patterns of steep slope (converge flow) and gentle slope (diverge flow) are 2.0 and 1.1, respectively. The 4+4N algorithm can predict the runoff process for moderate and heavy rainfall events well ($NSE \geq 0.76$, $R \geq 0.88$), but the simulation results for light rain event were not that ideal ($NSE = 0.24$). While the UCA algorithm

achieves better prediction for the early confluence period. In particular, the *NSE* of the light rain event was significantly improved from 0.24 to 0.93, because the flow pattern can be judged in real-time during the early confluence period.

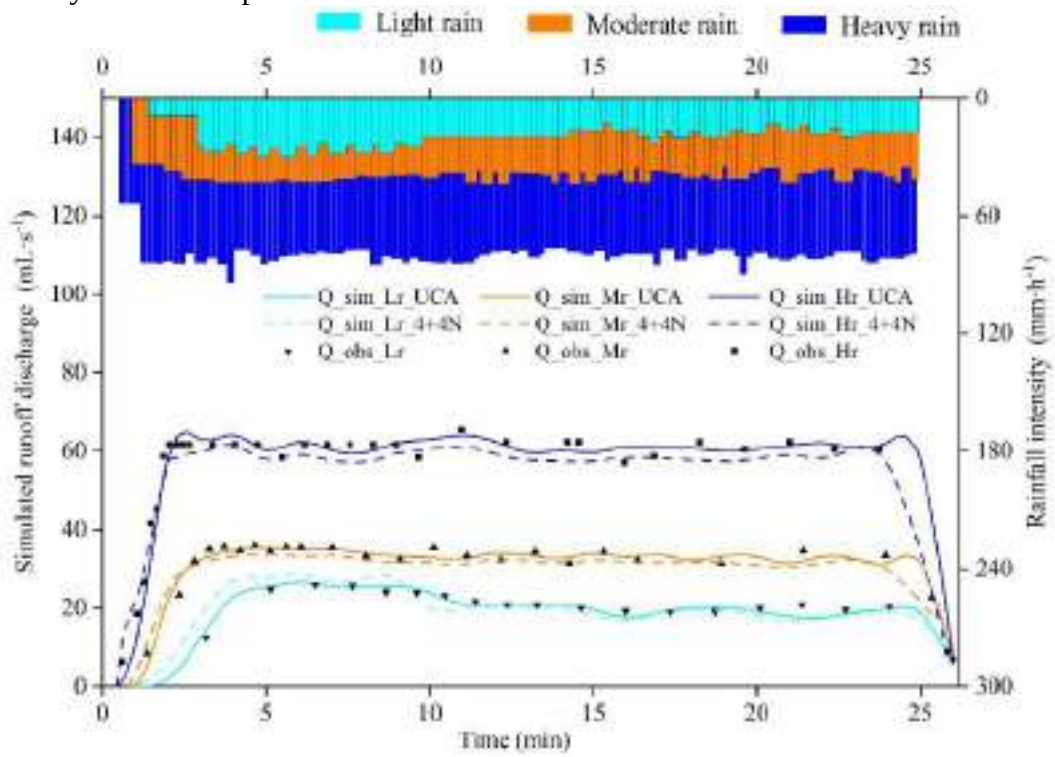


**Figure 1**. Time series of observed and simulated runoff discharge by 4+4N and UCA algorithm.

**Table 1.** Statistical metrics of the simulated runoff against the observed runoff.

| Rain type | *NSE* | | *R* | |
|---|---|---|---|---|
| | 4+4N | UCA | 4+4N | UCA |
| Light rain | 0.24 | 0.93 | 0.71 | 0.97 |
| Moderate rain | 0.76 | 0.94 | 0.88 | 0.97 |
| Heavy rain | 0.83 | 0.95 | 0.95 | 0.98 |

## 4 Conclusions

- An optimal urban flow direction algorithm based on cellular automata (UCA) was proposed to improve the modeling performance of urban rainfall-runoff process.
- The optimal water distribution weights for converge flow and diverge flow are 2.0 and 1.1 respectively.
- The misjudgment of the initial runoff flow pattern by the 4+4N algorithm can be effectively corrected under the light rain event, which can provide a better solution for urban water logging and non-point source pollution modeling in the future.

## Reference

[1] Song X., Zhang J., Wang G., et al. Development and challenges of urban hydrology in a changing environment:II: Urban stormwater modeling and management, Advances in Water Science, 2014, 25(5): 752–764. (in Chinese)

[2] Dai Y., Chen L., Zhang P., et al. Construction of a cellular automata-based model for rainfall-runoff and NPS pollution simulation in an urban catchment, Journal of Hydrology, 2019, 568: 929-942.

**Theme:** Hydraulic and hydrological modeling
**IAHR Thematic Priority Area:** [TPA-4] Digital Transformation
https://doi.org/10.3850/iahr-hic2483430201-140

# Impact of Culvert Representation in the Brague River Flood Model Using TELEMAC-2D

**Emmanuel Ah-woane[1], Zied Amama[2,3], Florian Cordier[2], Thibaut Davarend[1], Jenna Lotfi[1], Mohammed Assaba[4], Arkadii Sochinskii[1], Samer Majdalani[5], Roger Moussa[6], Morgan Abily[7] and Olivier Delestre[8,3,1]**

[1] Polytech'Lab, Université Côte d'Azur, Sophia-Antipolis, UPR UniCA 7494, France
[2] EDF R&D LNHE-Laboratoire National d'Hydraulique et Environnement, Chatou, 78400, France
[3] Laboratoire d'Hydraulique Saint-Venant, Ecole des Ponts ParisTech – EDF R&D, Chatou, 78400, France
[4] Hydrologist and Expert for the Aix-en-Provence Court of Appeal, BET ELMA CONSEIL, Nice, 06100, France
[5] HSM, CNRS, IRD, Univ Montpellier, Montpellier, 34093, France
[6] LISAH, INRAE, IRD, Montpellier SupAgro, Univ Montpellier, Montpellier, 34060, France
[7] Université Côte d'Azur, CNRS, Observatoire de la Côte d'Azur, IRD, Géoazur, Nice, 06000, France
[8] LJAD, Université Côte d'Azur, CNRS, Nice, 06000, France

*Corresponding author: olivier.delestre@univ-cotedazur.fr*

**Abstract.** The Brague river (South-east France) has been historically subjected to significant flooding events. This research primarily focuses on October 3, 2015 flood event. Our analysis includes one of the main tributaries of the Brague river, namely the Valmasque. In the study domain, several hydraulic structures cross the river, which can hinder the river flow during extreme flood events. Our objective in this work is to assess the influence of culvert representation, within the domain on hydraulic discharge, and to examine the resultant variations in flood extents and water depth. In order to reach this goal, we propose to use the TELEMAC-2D modelling flood software to simulate a range of modelling approaches that accounts differently for the flow in the culverts area such as opened or closed topography or using culvert discharge equations.

**Keywords:** Culverts, Flash Flood Event, Hydraulic Structures, TELEMAC-2D

## 1 The Brague floodplain

The Brague catchment is located in Mediterranean region, in Alpes-Maritimes department. Due to its location, the catchment is subjected to extreme events, especially intense rainfall and flash-flood, with the most recent ones occurring in 2015 and 2019 [1]. The study area (figure 1a), which corresponds to the Brague floodplain, corresponds to the downstream part of the catchment. Its lower part collects water from four main tributaries. Hydraulic structures, notably culverts, are located all along these watercourses (e.g., under the A8 highway, see figure 1b).

## 2 Simulation scenarios

Five scenarios (Open, Close, Culvert, Logjam – Fullbank, Logjam – Peak) were proposed in order to study the impact of culvert and its representation on the flood dynamics of October 3, 2015. These scenarios are based on a digital terrain model modified at culverts locations. The "Close" scenario seals topography at culvert locations, aiming to assess the highway's influence on hydraulic continuity. The "Open" scenario (baseline) reproduces culvert conditions with equivalent-width openings in topography at the culverts location, to provide a simple representation of the hydraulic structure. The

three other scenarios consider culvert as a sink-source pair modelled with TELEMAC-2D. Two of the scenarios considering culverts modelled with TELEMAC-2D focus on logjam phenomena.

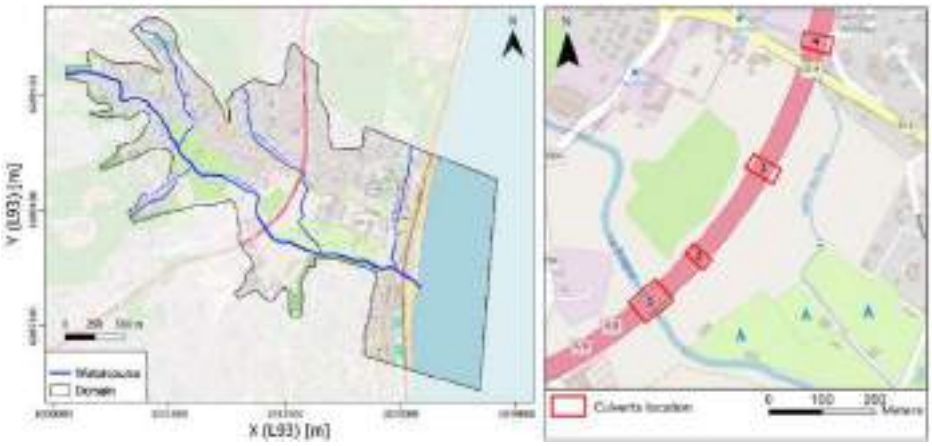


Figure 1 (a) The study area with the Brague river and its tributaries, (b) culvert location below the highway.

## 3 Results

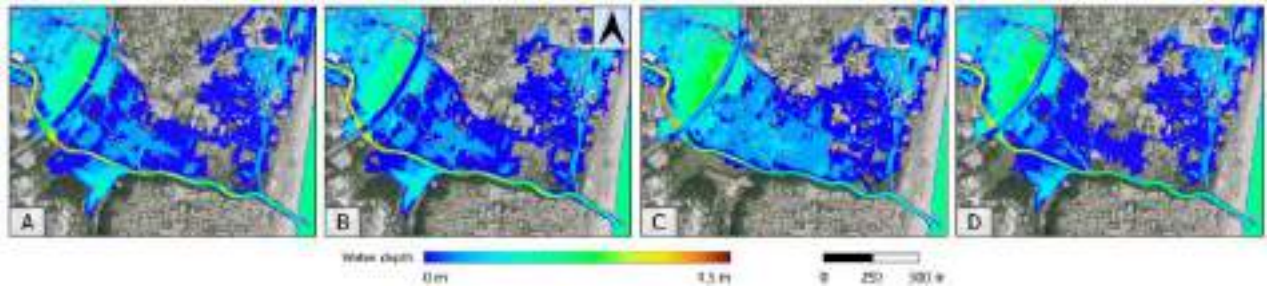


Figure 2 Flood dynamics at t = 7,000 s. between Open, Culvert, Close and Logjam – Fullbank (respectively A, B, C, D) scenarios.

The simulation results show similar flood dynamic between the Open and Culvert scenarios, indicating effective representation of culverts with TELEMAC-2D. Flow dynamics vary notably between scenarios (figure 2). In the “Logjam – Fullbank” scenario, downstream flooding due to highway overflow occurs at the slower rate. The area downstream of the highway experiences flooding from both highway overflow and the Maïre stream overflow. Despite variations in flow dynamics, overall flood extents remain similar across scenarios. The impact of culverts on high water levels (HWLs) is hidden by the magnitude of the event, highlighting the limitations of solely considering HWLs and flood extent in flood dynamics comprehension. Further insights into the results, particularly concerning logjams, highway overflow, HWLs, and flood dynamics, are detailed in the full paper.

### Acknowledgements

The authors are grateful to the OPAL infrastructure and the Université Côte d’Azur’s Center for High-Performance Computing for providing resources and support, financed by the UCAJEDI Investments in the Future project (ANR-15-IDEX-01) managed by the National Research Agency.

### Reference

[1] Brigode, P., Vigoureux, S., Delestre, O., Nicolle, P., Payrastre, O., Dreyfus, R., Nomis, S., Salvan, L. & l’équipe « post-event surveys » d’HyMeX (2021). Inondations sur la Côte d’Azur : bilan hydro-météorologique des épisodes de 2015 et 2019, LHB, 107:1, 1-14 (in French) https://doi.org/10.1080/27678490.2021.1976600

**Theme:** Hydraulic and hydrological modeling
**IAHR Thematic Priority Area:** [TPA-4] Digital Transformation
https://doi.org/10.3850/iahr-hic2483430201-142

# Numerical Simulation of Sudden Siltation in Yangtze Estuary under Extreme Weather

**Lu Chuanteng[1], Han Yufang[1], Luo Xiaofeng[1], Zhu Xianbo[1]**

[1] Nanjing Hydraulic Research Institute, Nanjing 210029, China

*Lu Chuanteng: ct/u@nhri.cn*

**Abstract.** Under the extreme weather condition, the sediment-water mixture with high concentration that is caused by the wave would give rise to the sudden silting of the channel, and then increases the channel silting volume. Based on the field hydrological data during typhoon “Malakas”, it establishes the three-dimensional tidal current and sediment mathematical model of the Yangtze River estuary under the wave-current interaction, which is used to study the problem of sudden silting in North Channel. The mathematical model verifies the process of North Channel’s water sediment during typhoon “Malakas”, and the result shows that its similarity is better. By separating the wave, the writer discusses the different of sediment concentration and channel siltation under the combined action of both tide and wave flow and studies the influence of the typhoon wave on the silt of channel. The studied results show that the wave of typhoon has a great influence on the sediment concentration with the depth of -15m in shallow water area. Meanwhile, the sediment concentration of North Channel increases gradually from the upstream to the outside and as a result it changes the distribution trend of sediment concentration as High in the middle and low in both ends of North Channel under the normal weather. The wave of typhoon has less influence to the back silting distribution of inner waterway of North Channel entrance, and the sediment deposition increases dramatically at the outer waterway of North Channel entrance. That is to say that the sudden silting of channel mainly takes place outside the North Channel, and the sediment source is the surrounding shoals.

**Keywords:** CJK3D; Deep water channel; Sudden silting; Typhoon wave; Yangtze River estuary

## 1 Introduction

Typhoon wave is one of the inevitable natural disasters in estuarine and coastal areas. In the Yangtze estuary, typhoon wave usually occurs in flood season, which is easy to form the "triple collision"[1] of typhoon, flood and spring tide, increasing the damage of typhoon wave.With the development of numerical simulation technology, the flow movement, sediment changes and seabed topography changes under typhoon wave conditions can be well simulated by mathematical models[2-9]. The problem of sudden sedimentation in the deep water channel of the North Channel of the Yangtze Estuary is very complicated[10-12], and there are few research results at present. On the basis of previous studies, this paper uses mathematical models to simulate the changes of seabed topography in the Yangtze Estuary area under typical typhoons, and analyzes the characteristics of channel sudden silting under typhoon conditions, so as to provide technical support for the maintenance of the Yangtze Estuary channel.

## 2 Method

Based on the field hydrological data during typhoon “Malakas”, it establishes the three-dimensional tidal current and sediment mathematical model of the Yangtze River estuary under the wave-current interaction, which is used to study the problem of sudden silting in North Channel.The upper boundary of the mathematical model is Nanjing, the offshore is near the -30m isobath, the south side is Zhapu in Hangzhou Bay, and the north side is Rudong. The grid of the mathematical model adopts triangular grid, with a total number of 76127 grid units, and the minimum grid unit side length is

about 17m.The mathematical model verifies the process of North Channel's water sediment during typhoon "Malakas", and the result shows that its similarity is better.

## 3 Results & conclusion

(1) Under the condition of typhoon waves, the sediment concentration in the shallow waters of the -15m isobath from the middle of the North Passage to the mouth of the North Passage increases sharply, and the sediment concentration in the deep waters of the -15m isobath changes relatively little.
(2) In the middle and upper part of the North Passage, the impact of typhoon waves on sediment concentration is relatively small. In the middle and lower part of the North Passage, under the condition of typhoon waves, the sediment concentration gradually increases to the mouth of the North Passage, changing the sediment concentration distribution trend of "high in the middle and low at both ends" when there is no wave in the North Passage.
(3) Under the condition of no typhoon waves, the sedimentation of the North Passage shows a trend of "large in the middle and small at both ends". Under the action of typhoon waves, the sedimentation characteristics of the channel inside the North Passage are basically unchanged, and the sedimentation amount of the channel outside the North Passage increases sharply, indicating that the sudden sedimentation of the channel mainly occurs outside the North Passage, and the sediment source is the surrounding shoal.

**The paper is supported by the National Key Research and Development Program (2023YFC3208501).**

## Reference

[1] Xia Mingyan, Xu Fumin, Wen Yuncheng. Study on storm water increase distribution along the lower Yangtze River under different typhoon paths [J]. Ocean Engineering, 2022, 40 (03): 115-122.
[2] BAI Y C, ZHANG B, ZHANG Y Q, et al.) et al.Sediment-carrying capacity of wave and mechanism of sudden silting in navigation channel [J]. Journal of Hydraulic Engineering, 2007 (6) : 646-653. (in Chinese)
[3] LI SQ, LU Y J, ZUO L Q, et al.) et al. Incipient motion of sediment in wave and combined wave-current boundary layers[J]. Advances in Water Science, et al. Incipient motion of sediment in wave and combined wave-current boundary layers[J]. Advances in water Science, 2014, 25 (1): 106-114. (in Chinese)
[4] LIU C, LIANG Y, WANG Q, et al. [LIU C, LIANG Y, WANG QS, et al. Hongji wave flow and its impact on flood discharge in Modaomen Estuary [J]. Advances in Water Science, 2017, 28(5):770-779. (in Chinese)
[5] KUANG C, MAO X, LIU P, et al. Influence of wind force on a silt-muddy coast: Huanghua Harbor Coast, China[J]. Journal of Waterway Port Coastal & Ocean Engineering, 2015, 141(6): 1-15.
[6] KUANG C P, CHEN S Y, ZHANG Y, et al. A two-dimensional morphological model based on next generation circulation solver II: Application to Caofeidian, Bohai Bay, China[J]. Coastal Engineering, 2012, 59(1):14-27.
[7] NAM P T, LARSON M, HANSON H, et al. A numerical model of nearshore waves, currents, and sediment transport[J]. Coastal Engineering, 2009, 56(11):1084-1096.
[8] HAO P Z, FENG X X, LI J T, et al. Forecast method of progressive distribution for sudden sedimentation under heavy storm conditions in out channel of Binzhou port [J]. Chinese Harbor Engineering, 2007(6): 24-27. (in Chinese)
[9] DONG S, CONG J S, KONG L S. Stochastic analysis of sudden siltation of silty sand in open channels[J]. Journal of Ocean University of China 2007, 37 (1): 147-150. (in Chinese)
[10] ZHAO D Z, LIU J, WU H L. Preliminary analysis of typhoon-induced sudden sedimentation in navigation channel in Yangtze estuary over last decade [J]. Journal of Sediment Research, 2012(2): 54-60. (in Chinese)
[11] KONG L S, GU F F, WANG W, et al. et al. Statistics and analysis of typhoon-induced sudden siltation for Yangtze estuary deepwater channel[J]. Port & Waterway Engineering, 2015(5): 150-152+173. (in Chinese)
[12] XU M, ZHANG C K. Study of the effect of storm waves on the rapid deposition of the Yangtze River estuary channel[J]. Journal of Hydrodynamics, 2004(2): 137-143. (in Chinese)

**Theme:** Hydraulic and hydrological modeling
**IAHR Thematic Priority Area:** [TPA-4] Digital Transformation
https://doi.org/10.3850/iahr-hic2483430201-144

# Prediction of Chlorophyll-a in Algae in the Yangtze River Basin Based on Structural Equation Modeling and Artificial Neural Network

**Xiaxia Li1,2,3, Minghao Ji4, Chao Wang5, Yao Cheng4, Hongtao Li6, Yong Wu6, Lixin He2,3, Xiaohui Lei5, Bin Chen7, Beibei Chai2,3**

[1] School of Water Conservancy and Hydroelectric Power, Hebei University of Engineering, Handan 056038, China
[2] Collaborative Immovation Center for Intelligent Regulation and Comprehensive Management of Water Resources, School of Water Conservancy and Hydroelectric，Hebei University of Engineering, Handan 056038, China
[3] Hebei Key Laboratory of Intelligent Water Conservancy, Hebei University of Engineering, Handan 056038, China
[4] School of Water Conservancy and Hydroelectric Power
[5] State Key Laboratory of Simulation and Regulation of Water Cycle in River Basin, China Institute of Water Resources and Hydropower Research, Beijing 100038, China
[6] Chengdu University of Technology, Chengdu, 610059, China
[7] State Key Joint Laboratory of Environment Simulation and Pollution Control, School of Environment, Beijing Normal University, Beijing 100875, China

*Corresponding author: cbb21@163.com (B. Chai)*

## 1 Introduction

Lakes, critical freshwater reservoirs, are essential for human sustenance and flood control, with over 100 million worldwide storing the majority of Earth's liquid surface freshwater. In the Yangtze River Basin, a key economic region in China, approximately 60% of large freshwater lakes are located. However, water quality assessments reveal a concerning trend: oligotrophic and mesotrophic lakes have declined, while eutrophic lakes persist, posing ecological challenges.

Eutrophication, a global ecological issue, fosters toxic algae proliferation in lakes, threatening aquatic ecosystems and human health by impairing water quality and biodiversity. Total phosphorus emerges as the primary nutrient pollutant driving algae growth, particularly in the Yangtze River Basin where its concentration varies across river reaches.

Big data analysis offers a promising avenue for understanding and addressing water quality issues. Techniques like decision trees and neural networks enable accurate prediction of water quality changes, crucial for timely intervention measures. Structural equation modeling (SEM) reveals phosphorus as the primary factor influencing algae growth, enhancing our understanding of ecological dynamics.

To improve algae growth prediction, this study employs enhanced neural network models and SEM analysis. Through comprehensive monitoring and data collection across the Yangtze River Basin, targeted strategies for water management and algae control are proposed, aiming to mitigate pollution and enhance water quality. This research contributes robust methods for algae growth prediction and informs effective water quality management practices in the study area.

## 2 Materials and methods

The study focuses on the Yangtze River Basin, a vital region spanning 15 provinces and accommodating a significant portion of China's population. Field sampling and monitoring data

collection were conducted to analyze water quality indicators and chlorophyll-a (Chla) concentrations in the basin's lakes. Structural equation modeling (SEM) was employed to identify factors influencing algae growth, while three neural network models (LSTM, CNN-LSTM, and CNN-BiLSTM) were utilized for Chla prediction. Model performance was evaluated using metrics such as mean squared error (MSE), root mean squared error (RMSE), mean absolute error (MAE), and mean absolute percentage error (MAPE)[1]. These methods offer insights into water quality dynamics and enable accurate prediction of algae growth in the Yangtze River Basin.

## 3 Results

The results and discussion section presents comprehensive findings regarding variations in lake water quality, factors influencing algae growth, and the prediction of chlorophyll-a (Chla) concentrations in the Yangtze River Basin.

Evaluation of physicochemical parameters across nine monitoring points revealed seasonal variations in water temperature (WT) and consistent pH and dissolved oxygen (DO) levels meeting Class I water quality standards. However, varying levels of chemical oxygen demand (CODMn), ammonia-nitrogen (NH3-N), total nitrogen (TN), and total phosphorus (TP) were observed, with some points exceeding Class III or IV standards due to industrial discharge and agricultural pollution. Notably, TN and TP levels were often elevated, indicating nutrient enrichment and potential eutrophication, particularly in areas affected by urbanization and tourism.

Structural equation modeling (SEM) identified key factors affecting algae growth, emphasizing phosphorus limitation and the significance of the nitrogen-to-phosphorus (N/P) ratio. Direct influences of physical indicators on nutrient levels were observed, with WT, TP, N/P, and DO significantly impacting Chla concentrations. Phosphorus emerged as a primary limiting factor, with implications for pollution control strategies in phosphorus-rich regions of the basin.

Three machine learning models (LSTM, CNN-LSTM, CNN-BiLSTM) were employed to predict Chla concentrations, demonstrating varying performance across monitoring points. The CNN-BiLSTM model generally outperformed others, highlighting its potential for accurate Chla predictions and eutrophication management. Prediction results suggested decreasing Chla concentrations over time, indicative of potential mitigation of eutrophication in the lakes. Comparison with previous studies underscored the superior performance of the proposed models, offering valuable insights for algae research and water quality management in the basin.

The developed models offer promising applications for predicting algae growth and other water quality indicators in the complex landscape of the Yangtze River Basin. By leveraging minimal yet significant factors influencing algae growth, these models can enhance prediction accuracy and inform proactive measures for preventing algal blooms. Future research directions may involve integrating prediction models with complementary methodologies and expanding their scope to address broader ecological challenges in the basin and beyond..

## 4 Conclusions

This study modeled chlorophyll-a concentration as a proxy for algae in lakes across the Yangtze River Basin based on national monitoring data of water quality and aquatic environmental indicators. Despite the overall improvement of water quality in recent years, there were still pollution issues in some areas of the basin, as indicated by high levels of chemical oxygen demand, total nitrogen, and total phosphorus. Structural equation modeling revealed water temperature, total phosphorus, dissolved oxygen, nitrogen-to-phosphorus ratio, and total nitrogen as major factors determining algae growth. Three neutral network models were developed with the five influencing factors as input variables, and all models performed well in predicting chlorophyll-a concentration. The CNN-LSTM model yielded superior prediction performance for the Tuojiang River and lower Yangtze River, the LSTM model was the best option for Hanjiang River, and the CNN-BiLSTM model was suitable for other water bodies. This study provides optional models for large-scale prediction of algal blooms in the Yangtze River Basin. It is recommended to increase the monitoring points in water bodies across

the basin as much as possible. Different spatial data with statistical correlations can be integrated to overcome the limitation of online monitoring in depicting spatial variations of algal blooms and enhance the robustness of deep neural networks in training and testing.

**Reference**

[1] Dagdougui, H.; Bagheri, F.; Le, H.; Energy, L. D. J.; Buildings, 2019. Neural Network Model for Short-term and Very-short-term Load forecasting in District Buildings. J. 203. https://doi.org/10.1016/j.enbuild.2019.109408

[2] Jin, T.; Cai, S.; Jiang, D.; Liu, J. J. E. S.; Research, P., 2019. A data-driven model for real-time water quality prediction and early warning by an integration method. J. 26, 30374 - 30385.

[3] Yang, Y.; Xiong, Q.; Wu, C.; Zou, Q.; Yu, Y.; Yi, H., et al., 2021. A Study On Water Quality Prediction By A Hybrid Cnn-Lstm Model With Attention Mechanism. J. Environmental science

[4] Zhang, W.; Li, J.; Liu, T.; Leng, S.; Yang, L.; Peng, H., et al., 2021. Machine Learning Prediction And Optimization Of Bio-Oil Production From Hydrothermal Liquefaction Of Algae. J. 342, 126011. https://doi.org/10.1016/j.biortech.2021.126011

**Theme:** Hydraulic and hydrological modeling
**IAHR Thematic Priority Area:** [TPA-4] Digital Transformation
https://doi.org/10.3850/iahr-hic2483430201-147

# Flipped Classroom for Teaching Pressure Pipe Flow (Steady State Conditions and Flow Transients)

**Vesipa Riccardo***

Department of Environment, Land and Infrastructure Engineering, Politecnico di Torino, C.so Duca degli Abruzzi 24, 10129 Torino, Italy

** Corresponding author: riccardo.vesipa@polito.it*

**Abstract**. Pressure pipe flow -and in particular flow transients- is a complex topic to be taught with classical teaching methods. In this manuscript, I report my experience of a flipped classroom for teaching pressure pipe flow. The course was organized in 14 modules. Each module consisted in 4.5 hours self-study (theory) and 4.5 hours classroom (programming and applications). With this approach, students were motivated to study and understand day-by-day theory. At the end of the course, students successfully master to write scripts to solve (with the method of the characteristics) flow transient problems of real-world engineering case studies.

**Keywords**. Flipped classroom, Flow transients, Pressure pipe flow

## 1 Overview

Pressure pipe flow -and in particular flow transients- is a complex topic to be taught with classical teaching methods such as the traditional classroom (frontal lessons). The main difficulty stems from the audience. Such topics are typical in programs of civil engineering. However, students of civil engineering usually receive little formation about partial differential equations and the numerical methods required for their solution. In addition, due to time limitations, it is a challenge to consistently develop (during classroom) the theoretical, practical and numerical aspects. The result is that pressure pipe flow -and in particular flow transients are either developed from a theoretical perspective (but students lack the ability to apply the knowledge) or from a more practical perspective (but students don't understand the underlying physics and numerical aspects). In this manuscript, I report my experience of a flipped classroom [1] for teaching pressure pipe flow, that overcomes some of this limitations, and provides a sounder understanding and ability to apply the topic.

## 2 Methodology

The course (total 60 hours frontal lessons, 150 hours total student effort) was organized in 14 modules. Each module consisted in 4.5 hours classroom, and 4.5 hours self-study. 24 hours were intended to additional study for preparation for the final exam. Seven modules were focused on pressure pipe flow in steady state. Seven modules were instead focused of flow transients. The main -ambitious- learning objective for student was to be able to apply the method of the characteristics (implemented in MATLAB) to solve real world problem involving flow transients.

## 3 Results and Conclusions

The key novelty of my experience was to implement the concept of the "flipped classroom". During the 4.5 hours self-study, students watched recorded lecture of theory and studied additional material (for a duration of about 4 hours) Each module was completed with a test of duration 30 minutes. During the 4.5 hours classroom, 30 minutes were dedicated to review the key-points of the underlying theory. 4 hours were dedicated to develop practical exercise under the supervision of the

lecturer. It is worth mentioning the 4 hours of supervised work were the key added value of this approach. With this availability of time it was possible to go into deep details of both script coding and analysis of the results. It was possible to transfer the sound theoretical knowledge developed during the self-study into practical and analytical skills.

## References

[1] Abeysekera, L., Dawson, P., 2015, Motivation and cognitive load in the flipped classroom: definition, rationale and a call for research. Higher Education Research & Development, vol 34 (1), pp 1–14

**Theme:** Hydraulic and hydrological modeling
**IAHR Thematic Priority Area:** [TPA-4] Digital Transformation
https://doi.org/10.3850/iahr-hic2483430201-149

# Optimizing Mobile Sensor Movement and Trajectory to Improve Water Distribution Network Calibration

**Alemtsehay G. Seyoum [1], Simon Tait[1], Alma N.A. Schellart[1], Will Shepherd[1], Joby Boxall[1]**

[1] Department of Civil and Structural Engineering, University of Sheffield, Sheffield, S1 3JD, UK

*Corresponding author:a.g.seyoum@sheffield.ac.uk*

**Abstract.** This study introduces a novel approach for network calibration, optimizing mobile sensor movement and trajectory to enhance the quality of collected data. By randomly selecting initial deployment locations and fine-tuning sensor speed and path, network coverage, ranging from 44% to 59% can be achieved. This contributes to network calibration enhancement, achieved with the use of a single mobile sensor.

**Keywords:** Calibration, mobile sensor, sensor trajectory, optimization, water distribution network

## 1 Introduction

Effective management and optimization of performance and reliability of water distribution networks requires accurate calibration of hydraulic models. This involves adjusting parameter values to minimize discrepancies between predicted and accurate observations of actual behaviour [1]. Traditional calibration methods rely on fixed sensors placed at specific locations, resulting in limited spatial coverage and data gaps [2]. Mobile sensor technology, like autonomous robots, offers improved flexibility and mobility in data collection, potentially providing a more comprehensive assessment of pipe networks' performance [3]. This study aims to introduce a new method for optimizing mobile sensor placement, movement and trajectory in water distribution networks to enhance hydraulic model calibration accuracy and therefore network performance and management.

## 2 Material and methods

A new software functionality to simulate mobile sensing has been developed to inform strategic deployment a mobile sensor, to inform factors such as initial location, speed and trajectory. The approach integrates sensor strategy and network calibration, treating them as dual optimization objectives. The primary objective is to minimize the calibration performance residual, reflecting disparities between measured and computed pressure head. The secondary objective aims to maximize knowledge derived from sensor measurements and sensor coverage within the network. The decision variables include the initial location, sensor's path and speed along with pipe roughness. The method employs NSGA II for optimization and EPANET for performance evaluation.

## 3 Results and Discussions

The approach's effectiveness was tested using the network described in [4] (Figure 1), with the original configuration of the model serving as the 'ground truth' for comparing simulated values during calibration. Optimization runs involved randomly selecting initial sensor release locations (e.g. Node1, Node8, Node12, Node19, Node21, Node24) representing physically diverse network positions. In each run, a single mobile sensor is employed, considering 16 candidate pipe roughness values ranging from 0.045 to 6.77 mm, 16 sensor speeds spanning from 0.3 to 1.8 m/s, along with 32 randomly generated paths. The mobile sensor simulation, covering 24 hours with 1-hour time steps, capturing relevant hydraulic data at points throughout the network. The optimization process iterates through 5000 generations with a population size of 100. Figure 2 illustrates the optimization progress,

while Table 1 summarizes coverage as a function of sensor speeds (ranging from 0.3 to 1.4 m/s), with coverage ranging from 44% to 59%, and the unique ID for each link visited for each optimal solution given. Coverage refers to the ratio of unique links visited by the sensor to the total number of links. Optimal solutions exhibit varying pipe roughness error metrics, with mean, standard deviation, skewness, and mean absolute error (MAE) ranging from -0.25 to 0.22mm, 2.27 to 2.60mm, -0.82 to -1.05, and 1.24 to 1.48mm, respectively. While the optimal solutions display varying degrees of pipe roughness error metrics, the range of values remains relatively narrow. It is important to highlight that achieving equivalent accuracy would require fixed sensor with 90% nodal coverage.

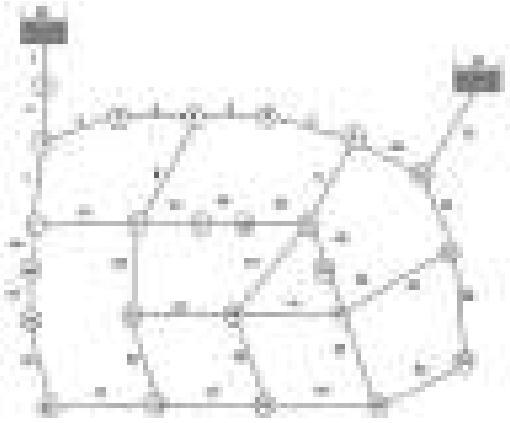

Figure 1 Network layout

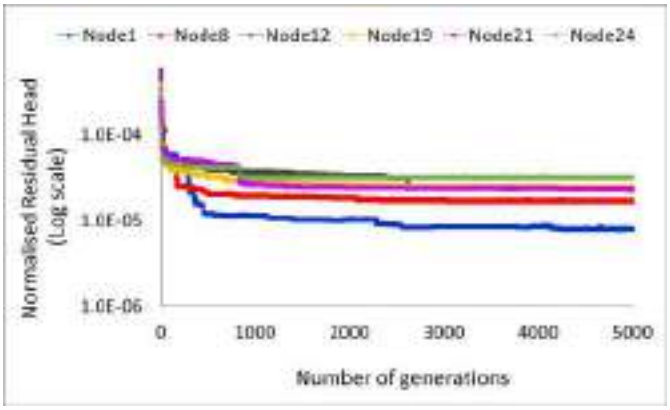


Figure 2 Progression of the optimization runs

Table 1 Optimal sensor parameters

| Initial node | Speed (m/s) | Coverage (%) | Unique links visited along the optimal sensor path |
|---|---|---|---|
| 1 | 0.5 | 44 | 1,2,3,4,8,18,22,28,32,31,26,17,16,12,27 |
| 8 | 1.4 | 50 | 8,5,6,10,11,21,25,23,28,32,31,26,17,16,7,2,1 |
| 12 | 0.3 | 44 | 11,10,6,5,4,3,2,1,7,16,17,26,31,27,22 |
| 19 | 1.0 | 47 | 23,22,18,8,4,3,7,16,17,26,31,32,33,29,2,1 |
| 21 | 0.5 | 59 | 26,17,16,12,8,4,3,2,1,7,18,22,28,33,34,30,25,23,32,27 |
| 24 | 0.6 | 59 | 33,32,31,26,17,16,7,2,1,3,4,5,6,10,11,21,25,29,34,30 |

## 4 Conclusion

Our study presents a novel mobile sensing approach for optimized deployment strategy, ensuring substantial coverage for efficient data collection for network calibration. The research provides clear evidence that mobile sensors offer the potential to transform the accuracy of our understanding, representation and hence management and operation of ageing drinking water distribution systems.

**Acknowledgement:**

This work is supported by the UK's Engineering and Physical Sciences Research Council (EPSRC) Programme Grant EP/S016813/1.

## Reference

[1] L. E. Ormsbee, Implicit network calibration, J. Water Resour. Plann. Manage. 115(1989) 243-257.
[2] A. Shahmirnoori, M. Saadatpour, A. Rasekh, Using mobile and fixed sensors for optimal monitoring of water distribution network under dynamic water quality simulations, Sustainable Cities and Society 82(2022) 103875.
[3] S. R. Mounce, W. J. Shepherd, J. B. Boxall, K.V. Horoshenkov, J.H. Boyle, Autonomous robotics for water and sewer networks, IAHR Hydrolink 2(2021) 55-62.
[4] M.S. Kadu, R. Gupta, P.R. Bhave, Optimal design of water networks using a modified genetic algorithm. with reduction in search space, J. Water Resour. Plann. Manage.134(2008) 147-160.

**Theme:** Hydraulic and hydrological modeling
**IAHR Thematic Priority Area:** [TPA-4] Digital Transformation
https://doi.org/10.3850/iahr-hic2483430201-151

# Optimization of Effective Volume of Urban Sewage Pumping Station Based on Fuzzy Optimization Method

**Jiawei Chen, Jiachun Liu, Biao Huang**

School of Civil & Environmental Engineering and Geography Science, Ningbo University, Ningbo, Zhejiang, China

*Corresponding author: liujiachun@nbu.edu.cn.*

**Abstract.** This study selected a residential area in Ningbo City as the research area and modeled the sewage network using Infoworks software. By integrating single-day electricity price fluctuations, service area sewage discharge patterns, and drainage network topologies, the daily electricity cost of the pumping station, pump start-stop frequency, and flood depth are designated as preferred objectives, employing the fuzzy optimization method and multi-objective optimization methods to analyze and optimize the effective volume of sewage pumping stations. The optimal effective volume of the pumping station obtained by optimization can save 15.9% of the daily electricity cost and reduce 13.3% of the start-stop cycles of the pump when there is no overflow event in the drainage system, which significantly reduces the operating cost of the sewage pumping station. This study can provide theoretical support for the optimization of drainage pumping station volume as well as economical operation.

**Keywords:** Effective volume; Fuzzy optimization method; Operating cost; Sewage pumping station

## 1 Methodology

In this study, a residential community in Ningbo City was selected, which has a relatively independent drainage system that is hardly affected by the surrounding area. The total area of the zone is about 24000 $m^2$ and the population is about 1400. The per capita daily sewage discharge for this study was 215L (Chen et al. 2022). The drainage network of this area is connected to the sewage pumping station, the pump flow $Q$ = 0.118 $m^3/s$, the inlet pipe diameter of the pumping station is 500 mm, the bottom elevation of the outlet pipe is -1.20 m, the size of the reservoir upstream of the pumping station is 4.18×3.11×6.65 $m^3$, and the electricity cost of the area is taken as the charge of time-sharing tariffs of Ningbo city.

The fluctuation of pump station discharge and flood depth in the inspection manhole over a single day with an effective pump station volume of 42.17 $m^3$ is depicted in Fig.1. Notably, on that day, the pumps operated four times: the first and second pumps ran during off-peak hours, while the third pump operated during peak hours, and the fourth pump spanned both off-peak and peak hours. Therefore, the daily electricity costs of the pumping station and the associated pump operations are intricately linked to the periods corresponding to local electricity prices. Specifically, during off-peak hours, the pumping station utilized electricity at the lowest cost.

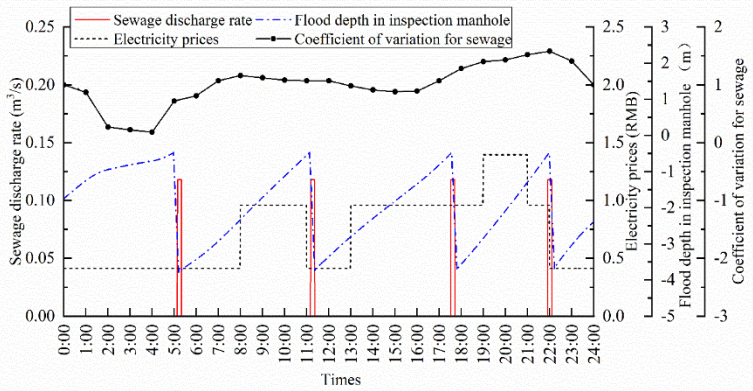


**Figure 1** Fluctuation of daily electricity price, coefficient of sewage change, discharge of pumping station and flood depth change.

Figure 2 illustrates the comparison of data for each preferred scenario under the condition of a pumping station reservoir effective volume of 42.17 $m^3$ over an operating cycle of 7 days. The daily electricity cost of the pumping station amounts to 160.03 RMB, marking the lowest among all scenarios and achieving a 15.9% cost savings at its maximum efficiency. The number of pump start-stop times totals 26, representing a 13.3% reduction from the maximum frequency. Moreover, the flood depth in the manhole is -0.409 m, falling below the levels observed in other scenarios and avoiding overflow incidents. Following the fuzzy optimization method, the optimal scenario is determined based on the largest relative superiority degree. Consequently, Scenario 7 emerges as the most superior option according to this principle, indicating that the sewage pumping station is optimized with an effective volume of 42.17 $m^3$.

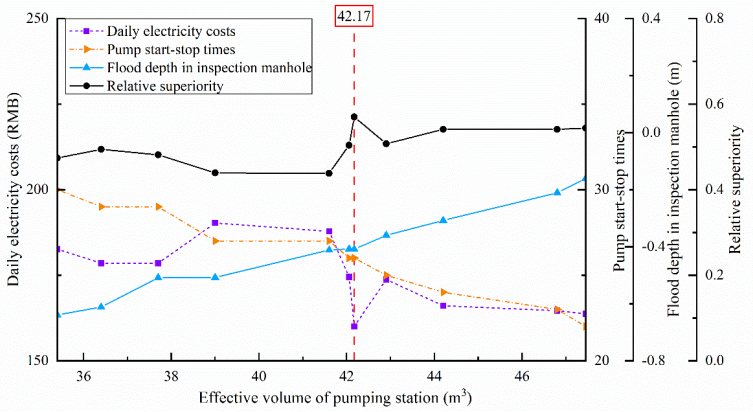


**Figure 2** Data comparison of optimal solution of sewage pumping station.

## Reference

[1] Barán, B., Von Lücken, C., & Sotelo, A. Multi-objective pump scheduling optimisation using evolutionary strategies. Advances in Engineering Software, 2005, 36(1), 39-47..

[2] Chen, X., Huang, B., Zhang, S., Liu, J., Qian, Y., Wang, C., & Zhu, D. Z. Performance evaluation of sewer system upgrade in an old residential area in Ningbo, China. Journal of Environmental Engineering, 2022, 148(8), 04022044.

[3] Wang, X., Ma, X., Liu, X., Zhang, L., Tian, Y., & Ye, C. Research on optimal operation of cascade pumping stations based on an improved sparrow search algorithm. Water Science & Technology, 2023, 88(8), 1982-2001.

**Theme:** Hydraulic and hydrological modeling
**IAHR Thematic Priority Area:** [TPA-4] Digital Transformation
https://doi.org/10.3850/iahr-hic2483430201-153

# Analyzing Organic Carbon Mass Balance in a Stratified Reservoir to Support Total Organic Carbon(TOC) Management in a Monsoon Climate

**Dongmin Kim[1], Sewoong Chung[2]**

[1] Chungbuk national university[1,1,] Chungdae-ro, Seowon-gu, Cheongju-si, Chungcheongbuk-do, Republic of Korea
[2] Chungbuk national university [2, 1,] Chungdae-ro, Seowon-gu, Cheongju-si, Chungcheongbuk-do, Republic of Korea

*Corresponding author: schung@chungbuk.ac.kr*

**Abstract.** This study focuses on Daecheong Reservoir, located in a monsoon climate region, facing persistent algae overgrowth and significant organic matter inflow during rainfall events from adjacent forests, farm fields, and rice paddies. This underscores the need for a nuanced approach to organic matter management, particularly addressing recalcitrant organic matter (ROC) and Total Organic Carbon (TOC) emerges as a crucial indicator in this context[1]. The objective of this research was to propose an efficient TOC management strategy by examining the organic matter load characteristics and organic carbon mass balance of Daecheong Reservoir, utilizing a 3D hydrodynamic and water quality model[4]. The analysis revealed higher contribution rates from internal sources during pre- and post-monsoon periods, contrasting with elevated external contributions during the concentrated rainfall of the monsoon period. Over the entire 2018 period, internal load accounted for 56%, surpassing external load at 44%. The study emphasized the predominant impact of internally generated organic carbon within the reservoir. Therefore, a targeted management plan addressing the primary production constituting 38% of the internal origin, is deemed effective for TOC management[2,3]. In addition, during the monsoon period, Sedimentation removal is efficient because a large amount of particulate organic matter flows in with rainfall.

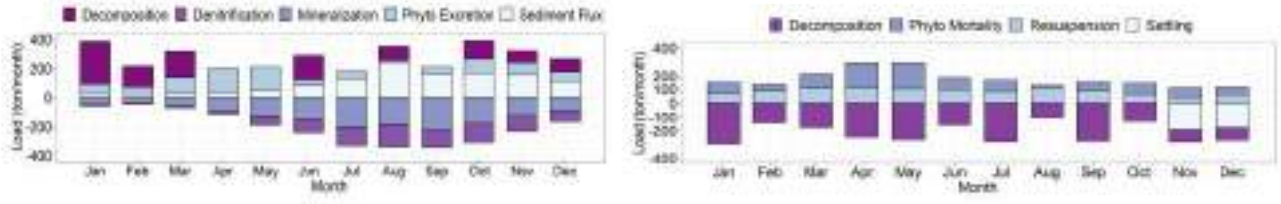


(a) DOC circular analysis (b) POC circular analysis

Figure 16 Analysis results of material circulation by organic matter properties

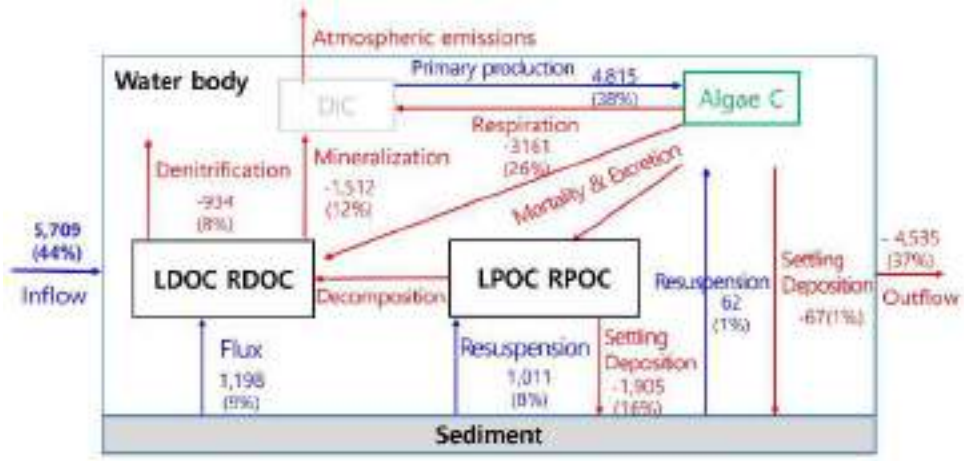


Figure 2 Reservoir Organic carbon Mass balance analysis results

Table 6 Organic carbon mass balance results by mechanism

| Type | Source/Sink | Loading(ton/yr) | Ratio(%) |
|---|---|---|---|
| Input | Inflow | 5,709 | 44 |
| | Primary production | 4,815 | 38 |
| | Sediment flux | 1,198 | 9 |
| | POC resuspension | 1,011 | 8 |
| | Algae Resuspension | 62 | 1 |
| | Total loading | 12,795 | 100 |
| Output | Outflow | 4,535 | 37 |
| | Mineralization | 1,512 | 12 |
| | POC Deposition | 1,905 | 16 |
| | Algae Deposition | 67 | 1 |
| | Algae Repiration | 3,161 | 26 |
| | Denitrification | 934 | 8 |
| | Total loading | 12,117 | 100 |

**Keywords:** management, mass balance, nutrification, numerical model, organic carbon, water quality

**Acknowledgement:**

This work was supported by Korea Environmental Industry & Technology Institute(KEITI) through Aquatic Ecosystem Conservation Research Program Program(or Project), funded by Korea Ministry of Environment(MOE)(2021003030004)

## Reference

[1] P.C. Hanson., M.L. Pace., S.R. Carpenter., J.J. Cole., E.H. stanley, Intergrating landscape carbon cycling: research needs for resolving organic carbon budgets of lakes, Ecosystems, 2015, 18(3), pp. 363-375.

[2] R. Mendonça., R.A. Müller., D. Clow., C. Verpoorter., P. Raymond., L.J. Tranvik., S. Sobek, Organic carbon burial in global lakes and reservoirs, Nature communications, 2017, 8(1), pp. 1-7.

[3] J. Chen., H. Yang., Y. Zeng., J. Guo., Y. Song., W. Ding, Combined use of radiocarbon and stable carbon isotope to constrain the sources and cycling of particulate organic carbon in a large freshwater lake, China, Science of the Total Environment, 2018, 625, pp. 27-38.

[4] B. Hodges., C. Dallimore, Aquatic Ecosystem Model : AEM3D v1.0 User Manual, Hydronumerics, Australia, 2019.

**Theme:** Hydraulic and hydrological modeling
**IAHR Thematic Priority Area:** [TPA-4] Digital Transformation
https://doi.org/10.3850/iahr-hic2483430201-155

# Effects of Land Use and Terrain Characteristics on Hydrological Signatures: A Comparative Study of Two Adjacent Subbasins

**Haifan Liu[1], Mingfu Guan[1]**

[1] Department of Civil Engineering, the University of Hong Kong, Hong Kong, China

*Corresponding author: Mingfu Guan (mfguan@hku.hk)*

**Abstract.** Land use/land cover change (LULCC) inevitably alters hydrological processes in a catchment. Catchment characteristics, including topography, are also crucial for predicting the impact of LULCC. However, studies examining the effects of LULCC and topography simultaneously and thoroughly across multiple catchments are limited. We applied an Integrated Surface-Subsurface Hydrological Model (ISSHM), the Simulator for Hydrologic Unstructured Domains (SHUD), in two subtropical basins within China's Great Bay Area (GBA) to assess the influence of urbanization-induced LULCC and terrain slope on four key hydrological processes: surface runoff, subsurface flow, evapotranspiration (ET), and infiltration, on a daily scale. Our findings reveal that the correlation between slope and subsurface flow is greater in different zones of the basin. LULUC has a strong influence on infiltration. In gently sloping basins, LULCC affects subsurface flow over a wider range of areas, whereas in more steeply sloping basins, the range of areas affecting subsurface flow is smaller and concentrated near the foothills. These findings provide insights into the different responses of daily-scale hydrologic processes in various basins.

**Keywords:** Hydrological Processes; ISSHM; Land Use/Land Cover Change; Topography

## 1 Introduction

Human activities such as urbanization and deforestation result in land use/land cover change (LULCC), impacting watershed hydrology and influenced by topography [1, 2]. Hydrological modeling, particularly Integrated Surface-Subsurface Hydrological Models (ISSHMs), provides a detailed assessment tool of these impacts across catchment scales [3]. However, existing research, often limited to single watershed due to data and calibration constraints, lacks a comprehensive understanding of the effects of LULCC and topography across multiple catchments. This study uses the Simulator for Hydrologic Unstructured Domains (SHUD), an ISSHM, to examine the collective effects of terrain slope and urbanization-driven LULCC on hydrological processes in two subtropical basins within China's Great Bay Area (GBA), aiming to enhance our understanding of the integrated hydrological impacts of LULCC and topography.

## 2 Methods

We compared and analyzed the effects of slope angle and urbanization-driven LULCC on four hydrological processes using an ISSHM. Our approach involved: (1) setting up a hydrological model for the study site with the collected dataset and calibrating it for localized representation; (2) using the calibrated model to run designed simulations; and (3) applying statistical methods to thoroughly analyze and compare the simulation results, highlighting the similarities and differences between the two subbasins on daily scale.

## 3 Results

Utilizing an ISSHM model, SHUD, we investigated the effects of topographical slope and urbanization-induced LULCC on surface runoff, subsurface flow, ET, and infiltration across different spatial conditions in two subtropical basins. We found that slope has a strong correlation with

subsurface flow in both two basins compared to other hydrological processes (Fig. 1). Considering the impact of LULCC, it markedly affects infiltration and surface runoff processes in the basin, with spatial variability in subsurface flow impact (Fig. 2).

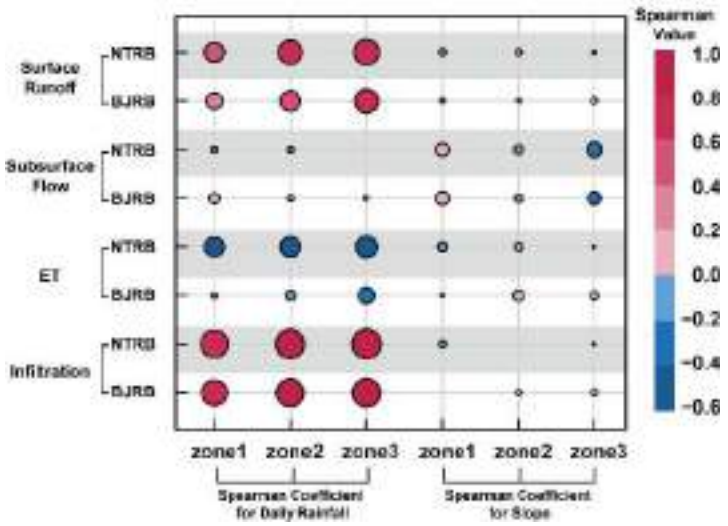


Figure 17 Effects of slope, with marker size illustrating the correlation level.

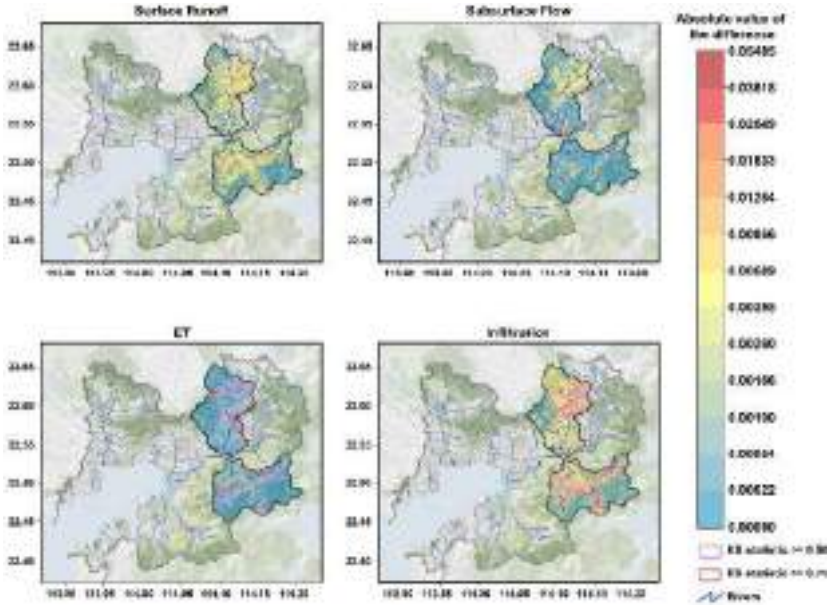


Figure 2 Map of absolute mean differences at each grid between HLU and CLU patterns, with significant variations in daily hydrologic output CDFs marked according to the KS statistic.

**Acknowledgements**

This work is financially supported by General Research Fund projects (No. 17210923).

**References**

[1] Brown, A.E., Zhang, L., McMahon, T.A., Western, A.W., Vertessy, R.A., A review of paired catchment studies for determining changes in water yield resulting from alterations in vegetation, J. Hydrol. 310 (2005) 28–61.

[2] Strahler, A. N., Quantitative analysis of watershed geomorphology, Eos Trans. AGU, 38 (1957) 913–920.

[3] Paniconi, C., Putti, M., Physically based modeling in catchment hydrology at 50: Survey and outlook, Water Resour. Res. 51 (2015) 7090–7129, https://doi.org/10.1002/2015WR017780.

**Theme:** Hydraulic and hydrological modeling
**IAHR Thematic Priority Area:** [TPA-4] Digital Transformation
https://doi.org/10.3850/iahr-hic2483430201-157

# Integrated Hydrological Modeling and Analysis Tool for Rainfall-Runoff and Flow Hydrograph Estimation in Sicilian Watersheds

**A. Francipane[1], G. Cipolla[1], D. Treppiedi[1], C. Mattina[1], L.V. Noto[1]**

[1] Dipartimento di Ingegneria, Università degli Studi di Palermo, Palermo, Italia

*Corresponding author: antonio.francipane@unipa.it*

**Abstract.** This work presents a Python-based tool aimed at better understanding the watershed response by overcoming some of the simplifications specially made in modelling flood hydrographs. By leveraging GIS capabilities, the tool uses spatially distributed data for a more accurate representation of basin characteristics and processes. The capability to analyze both synthetic and historical precipitation makes the tool useful to assess catchment responses under various scenarios. This is particularly valuable for studying phenomena like flood hydrographs, where accurate predictions are essential for risk assessment and management. The tool has been tested on Sicilian catchments with the aim of deriving the catchment response to both synthetic and historical precipitation and proving a promising step forward in hydrological modeling.

**Keywords:** Concentration time, GIS, Hydrological modeling, Python script for QGIS,

## 1 Introduction

Due to the strong heterogeneity of basin characteristics and the complexity of processes, lumped models have often been preferred or used contextually to the spatially distributed ones [1], especially in areas suffering by data scarcity, since they require less computational effort and parametrization. In the latest years, however, this limit has been partially overcome thanks to the development of Geographic Information Systems (GIS), which has made it possible to integrate spatially distributed data and advanced analysis tools. One of the most challenging goals for which the use of GIS may be the game-changing point for hydrological modelling is to achieve a reliable estimation of time of concentration. Indeed, despite its importance, a unique definition and approach to evaluating it are still missing and, most of the time, very old empirical formulations are used [2]. Moreover, they provide only the maximum time of concentration in the basin of interest, while in some hydrological applications, it would be convenient to derive the spatial distribution of the times of concentration.
In this work, we present a Python-based tool developed in QGIS that integrates GIS functionalities and hydrological modelling techniques to overcome some simplifying hypotheses usually made in hydrological studies and enable a comprehensive assessment of runoff response under various hydro-meteorological scenarios, especially for the estimation of design flood hydrographs. The tool has been applied and tested on three Sicilian catchments, with the aim of deriving their responses to both synthetic and historical precipitation.

## 2 Material and methods

The tool here proposed follows a two-phase approach. More in detail, the first phase consists of data import and pre-processing, in which spatial and temporal datasets, including digital elevation models (DEM), land cover maps, and rainfall gauge locations for all Sicily, are imported; the tool then derives the spatial distribution of flow velocity along the hillslopes and river network following [3]. The second phase follows a multistep framework, depending on the fact that the user wants to simulate an historical or synthetic event, in which the tool *i*) delineates the watershed, *ii*) derives its characteristics and calculates the basin's time of concentration and critical rainfall events, *iii*) generates the Depth-Duration Frequency (DDF) curves based on empirical relationships between rainfall duration,

intensity, and return periods for different time intervals (in the case of a synthetic event), *iv*) calculates the net rainfall by considering antecedent moisture conditions and the Curve Number (CN) method and, finally, *v*) the hydrograph at the watershed outlet.

## 3 Results and discussion

The tool has been applied to three Sicilian basins with different sizes and hydrological characteristics to test the capability of the model to correctly reproduce their responses to precipitation. Just to give an example, Figure 1 shows an excerpt of the interactive shell of the QGIS-Python console along with some of the results of the tool, such as the DDF curves for different return periods, total and net precipitation, time-area diagram, and discharge at the outlet of the basin.

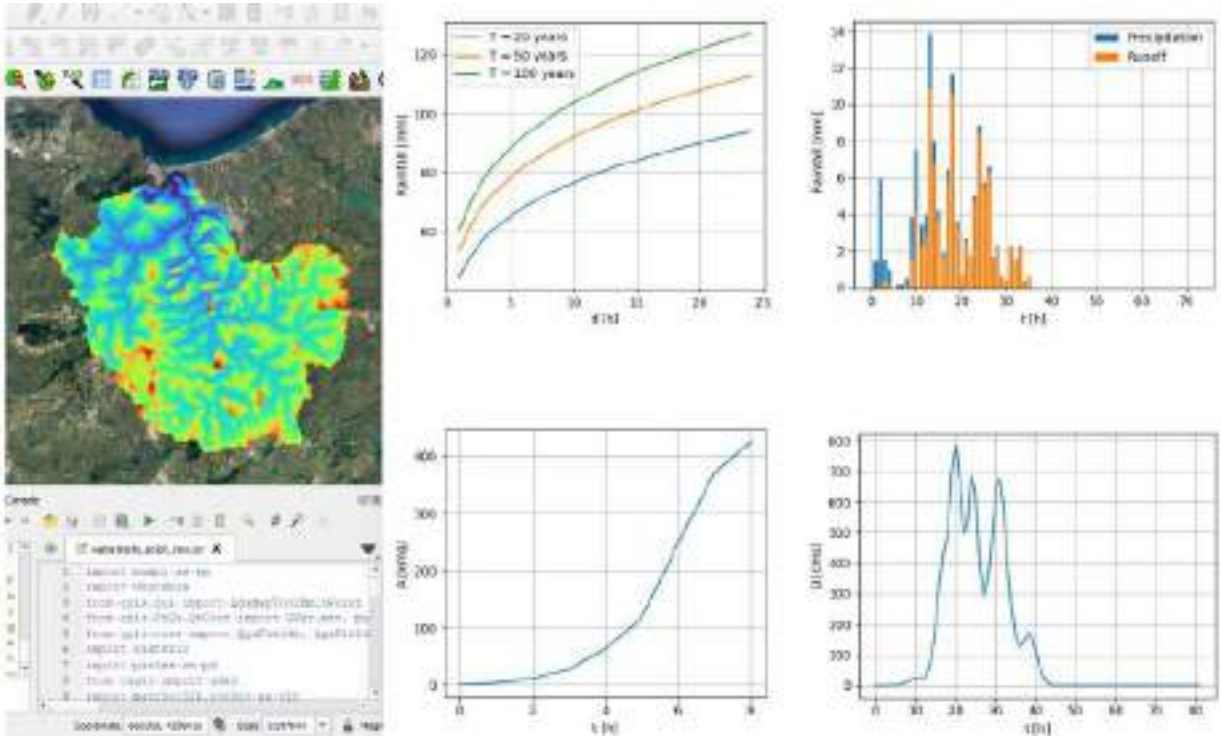

Figure 18 Excerpt of the interactive shell of the QGIS-Python console and some results.

## 4 Conclusions

The tool here developed showed important advancements with respect to the methodology so far applied in Sicily, especially in the assessment of a spatially distributed time of concentration map that makes it possible to derive a more realistic catchment response to precipitation. Moreover, by providing appropriate data, the tool is flexible enough to be adapted to other regions of the world.

## Reference

[1] Moghadam, S.H., Ashofteh, P.-S., Loáiciga, H.A., 2023. Investigating the performance of data mining, lumped, and distributed models in runoff projected under climate change. Journal of Hydrology 617, 128992. https://doi.org/10.1016/j.jhydrol.2022.128992.

[2] Salimi, E.T., Nohegar, A., Malekian, A., Hoseini, M., Holisaz, A., 2017. Estimating time of concentration in large watersheds. Paddy Water Environ 15, 123–132. https://doi.org/10.1007/s10333-016-0534-2.

[3] Cho, Y., Engel, B.A., Merwade, V.M., 2018. A spatially distributed Clark's unit hydrograph based hybrid hydrologic model (Distributed-Clark). Hydrological Sciences Journal 63, 1519–1539. https://doi.org/10.1080/02626667.2018.1516042.

**Theme:** Hydraulic and hydrological modeling
**IAHR Thematic Priority Area:** [TPA-4] Digital Transformation
https://doi.org/10.3850/iahr-hic2483430201-159

# Black Carbon Impact on Snow Albedo and Snowmelt by Coupling Radiative Transfer Model and Hydrological Modeling

**Diego Pacheco[1], Dayanne Perersen[1], Lina Castro[1]**

[1] Universidad Técnica Federico Santa María, Av. España 1680, Valparaíso, 2390123, Chile

*Corresponding author: lina.castro@usm.cl*

**Abstract.** Light absorbing particles (LAPs) deposition onto snow surface increases the shortwave radiation absorption and accelerates melting. In this study, Utha Energy Balance (UEB) snow model and OptiPar radiative transfer model have been coupled through an empirical approach to simulate the accumulation and depletion of snowpack and quantify the effect of LAPs deposition on snow albedo and melting on a time basis scale (2015-2019) in the Juncal River Basin, Chile. Here, snowpack was simulated using a one-layer scheme to reproduce snow metamorphism, while energy balance is focused on the snow surface. To account for LAPs, dry deposition rates onto snow were used as tuning parameters and constant for the period analyzed. LAPs mass accumulates in the upper layers, while also considering a fraction of BC agglomerates can scavenge based on melting magnitude. Albedo simulations were validated based on field measurements at 2800 m.a.s.l in the same catchment. Results here support that BC and dust emissions can alter the energy budget of the snowpack, reducing the maximum accumulation and inducing an early melt-out of the seasonal snowpack of less than a week early, comparing to a free LAP's scenario, depending on the year simulated, mostly attributable to BC deposition onto snow surface.

**Keywords:** Energy Balance, OptiPar, Light absorbing particles, snow model.

## 1 Introduction

Light-absorbing particles, known as LAPs, are recognized as contributors to Climate Change. When these particles, including Black Carbon (BC), Brown Carbon (BrC), Volcanic Ash, and/or Mineral Dust (MD), deposit onto snow or glaciers, they darken the surface and reduce the surface albedo [1,2]. LAPs directly influence the energy balance by enhancing the absorption of shortwave radiation, inducing snowmelt [3]. Given that the Central Andes has been affected by a mega-drought since 2010, with increasing temperature trends and annual precipitation deficit [4], glacier retreat [5] and snow cover and albedo decrease [6, 7], is necessary to understand the impact that LAPs induce in snow cover duration and accumulation. The following study aims to analyze the impacts con BC and MD deposition onto the snow surface, regarding the snowpack albedo and snowpack duration. The study area is Juncal river basin located at 32.9°S and 70.2°W in the Central Andes, less than 100 km away from Santiago, capital of Chile. It covers an area of 341 km2 and comprises a wide altitude range from 2200 to nearly 6000 m.a.s.l. To study the impacts of LAPs deposition onto the snow cover, the Utha Energy Balance (UEB) was coupled to the radiative transfer model OptiPar. UEB does not simulate the snow microstructure and LAPs accumulation through the snowpack layers, an empirical representation of the snow stratigraphy is used to estimate essential properties for the radiative transfer model such as grain size variation and LAPs concentration. Across the simulation, OptiPar takes the snow properties of the superficial layers at each time step to calculate the snow surface spectral albedo.

## 2 Results and discussion

For the calibration years of UEB, the model has shown a satisfactory performance, with KGE values ranging between 0.932 and 0.955, and NSE values between 0.864 and 0.909. In the case of validation years, the model showed an acceptable performance for 2014, 2016, and 2019 (KGE > 0.7). Regarding to LAPs impacts, the model was capable to simulate the accumulation of LAPs on the surface. Simulated daily BC concentrations onto snow surface ranged between nearly 0 to 0.30 $mg \cdot kg^{-1}$, with an average concentration of 0.10 $mg \cdot kg^{-1}$, values within the magnitude order of the samples collected around weather-atmospheric station.

Albedo was simulated with Optipar, the results show a good correlation between simulated and measured albedo values ($r = 0.688$). And, on the contrary, it underestimates the variability ($\gamma = 0.45$) and the range values of the snow surface albedo. To assess the impacts of LAPs on the snowpack dynamics, a simulation free of LAPs was performed. Results show that albedo difference due LAPs incorporation into the model varies depending on the year, with yearly mean values of daily albedo reduction ranging between 0.011 in 2018, and 0.023 in 2017. Maximum differences were observed at the end of the season, with albedo reduction higher than 0.1 (2016). This albedo reduction is on average 2.1% lower than the clean scenario, with maximum values over 15% at the end of the season.

Differences in maximum accumulation (SWEmax) and snowpack duration (SD) were observed while comparing clean and contaminated simulations. Small differences were observed in SWEmax values, with a maximum of 5.7 mmwe, and a maximum shortening of up to 3 days in the SD. To analyze the sensitivity of the model to changes in the average deposition rates, cases with different contamination scenarios were run, varying calibrated BC dry and wet deposition rates and MD deposition rates. In general, results show that the MD concentrations accumulated onto snow surface are low to produce a significant impact on the seasonal snowpack, and the impacts are considerably low against BC's. Only BC simulations show that snow duration can reduce on average 7 days the snowpack duration in most contaminated cases, with a maximum albedo decrease of 0.038, and an average decrease up to 20 mmwe of the SWEmax.

## 3 References

[1] Beres, N. D., Sengupta, D., Samburova, V., Khlystov, A. Y., & Moosmüller, H. (2020). Deposition of brown carbon onto snow: Changes in snow optical and radiative properties. Atmospheric Chemistry and Physics, 20, 6095–6114. https://doi.org/10.5194/acp-20-6095-2020

[2] Constantin, J. G., Ruiz, L., Villarosa, G., Outes, V., Bajano, F. N., He, C., Bajano, H., & Dawidowski, L. (2020). Measurements and modeling of snow albedo at Alerce Glacier, Argentina: Effects of volcanic ash, snow grain size, and cloudiness. Cryosphere, 14 (12), 4581–4601. https://doi.org/10.5194/tc-14-4581-2020

[5] Dussaillant, I., Berthier, E., Brun, F., Masiokas, M. H., Hugonnet, R., Favier, V., Rabatel, A., Pitte, P., & Ruiz, L. (2019). Two decades of glacier mass loss along the Andes. Nature Geoscience, 12 (10), 802–808. https://doi.org/10.1038/s41561-019-0432-5

[4] Garreaud, R. D., Boisier, J. P., Rondanelli, R., Montecinos, A., & Veloso-aguila, H. H. S. D. (2020). The Central Chile Mega Drought ( 2010 – 2018 ): A climate dynamics perspective. (January 2019), 421–439. https://doi.org/10.1002/joc.6219

[3] Li, X., Kang, S., Sprenger, M., Zhang, Y., He, X., Zhang, G., Tripathee, L., Li, C., & Cao, J. (2020). Black carbon and mineral dust on two glaciers on the central Tibetan Plateau: Sources and implications. Journal of Glaciology, 66 (256), 248–258. https://doi.org/10.1017/jog.2019.100

[6] Malmros, J. K., Mernild, S. H., Wilson, R., Tagesson, T., & Fensholt, R. (2018). Snow cover and snow albedo changes in the central Andes of Chile and Argentina from daily MODIS observations (2000–2016). Remote Sensing of Environment, 209 (February 2017), 240–252. https://doi.org/10.1016/j.rse.2018.02.072

[7] Shaw, T. E., Ulloa, G., Farías-Barahona, D., Fernandez, R., Lattus, J. M., & McPhee, J. (2021). Glacier albedo reduction and drought effects in the extratropical Andes, 1986-2020. Journal of Glaciology, 67 (261), 158–169. https://doi.org/10.1017/jog.2020.102

**Theme:** Hydraulic and hydrological modeling
**IAHR Thematic Priority Area:** [TPA-4] Digital Transformation
https://doi.org/10.3850/iahr-hic2483430201-161

# Development of a Digital Workflow for Layer Reduction Strategies and Visual-Analytical Outcome Analysis to Enhance Geo-Hydraulic Modeling Efficiency

**Erik Nixdorf[1], Mike Sips[2], Peter Morstein[2]**

[1] Federal Institute for Geosciences and Natural Resources, Cottbus 03048, Germany
[2] Helmholtz Centre Potsdam, Potsdam 14473, Germany

*Corresponding author: erik.nixdorf@bgr.de*

**Abstract.** Reducing hydrogeological complexity is a crucial step in the development process of many 3D groundwater models aiming to reduce computational costs and to keep the model parsimonious. This study presents a combined approach, leveraging expert knowledge to simplify stratigraphy and analyze changes in geohydraulic simulation outputs based on selected strategies. Hereby we develop and merge two open source tools: “Stratmerge” for calculating simplified stratigraphy extents and parameters as well as “Stacked Parameter Relation” for visual data exploration of geohydraulic ensemble simulations. We test the suitability of our approach by simulating groundwater flow in the sedimentary aquifer of the Selke River Basin in Germany using an underlying hydrogeological model of user-defined complexity. The groundwater flow is simulated by applying the finite element simulator OpenGeoSys 6.4. We demonstrate that our combined approach is feasible and generic, simplifies model construction as well as provides insight into the dependencies between the hydrogeological model setup and the simulation results. Our approach could be used by hydrogeological modelers for a wide variety of aquifers constituted of sedimentary granular material.

**Keywords:** Groundwater flow modeling, Hydrostratigraphic simplification, Modeling accuracy, OpenGeoSys, Open-Source

## 1 Introduction

Unconsolidated sand and gravel deposits overlying a bedrock form the most exploited aquifer systems on the globe [1]. 3D geohydraulic models describing the groundwater flow dynamics within these aquifer systems are a reliable tool to ensure efficient groundwater management and avoid overexploitation of resources. The sedimentary aquifers can be very heterogeneous regarding their granular composition and hydrogeological properties due to different diagenesis processes and may form a complex system of permeable zones separated by less permeable hydrogeological units [2].
The most common approach to deal with the hydrogeological complexity is to derive a stratigraphy of distinct individual layers that can each be described with a set of hydrogeological parameters [3]. The stratigraphic hydrogeological model often consists of a number of layers that are both larger than required for the purpose of the groundwater flow model and too large to be parameterized adequately by the given set of observation data [4]. Hence, simplification of the stratigraphic system by forming composite layers and deriving effective hydrogeological properties is a crucial but challenging step in developing a parsimonious geo-hydraulic model [5].
In this paper, we present an expert-based approach to assist the set-up and evaluation of geo-hydraulic models with different hydrostratigraphic simplification strategies by combining two self-developed open-source software tools.

Using a real-world scenario of simulating groundwater flow in a regional aquifer system with up to eight hydrostratigraphic layers as a test case, we illustrate that with our approach we are able to obtain satisfactory model performance while avoiding building, simulating, and calibrating a geo-hydraulic model with the maximum hydrostratigraphic complexity.

## 2 Material and Methods

To address the challenges mentioned above we introduce a combined workflow for the generation and visual evaluation of simplified groundwater flow models. We implement a toolchain solely based on open-source software (Fig. 1). First, the free and open-source Python module Stratmerge is developed to integrate functionality for reducing geological complexity and computing equivalent hydrogeological parameters into a standardized framework. A yaml [6] based interface allows the expert/user to define data i/o and to adjust processing parameters to achieve the intended geological simplification.

Second, we apply a visual analytics tool using the concept of Stacked Parameter Relation (SPR) to visually explore and compare the result of each geo-hydraulic simulation as a function of its underlying stratigraphic layer combinations. The advantage of SPR is that it shows all combinations of different layers in a compact overview visualization using hierarchical stacking [7]. The SPR can be accessed using the web browser, is platform-independent, and does not require further installation on the user's computational architecture.


Figure 1: General workflow of the toolchain. The yellow boxes comprise the tools that are provided by this study

## 3 Results and Discussion

The demonstration area for our approach covers 809 km² of a regional unconsolidated aquifer system in North-East Germany. The area is selected due to different water management targets, such as the design of infiltration wells along a former pit mine and the threat of waterlogging in lowland areas. Additionally, a complex stratigraphic model consisting of eight distinct layers, derived from 2382 drill logs, each characterized by a specified range for porosity and hydraulic conductivity estimates (Tab. 1), is available [8]. We apply Stratmerge initially to streamline the stratigraphy to six layers and subsequently to generate 96 realizations, each varying in the degree of stratigraphic complexity. Stationary geohydraulic simulations are conducted using OpenGeoSys 6.4 [9] and the results are evaluated by comparing with observations from 14 monitoring wells using the root mean square error (RMSE) and with the water flow across the interface to a former mining site which was observed to be on average 0.31 m³/s. In addition, we set up a geohydraulic model based on the complex full hydrostratigraphy and calibrated the eight hydraulic conductivity using PEST [10] which required in total 149 model calls.

Table1 Minimum and maximum values of hydraulic conductivity (kf) and effective porosity (Φ) for each stratigraphic layer provided by [8]

| Hydrogeological Unit | Abbreviation | Kf_min [m/s] | Kf_max [m/s] | Φ_min [%] | Φ_max[%] |
|---|---|---|---|---|---|
| Open pit dumps | mi | 1.0e-07 | 7.0e-04 | 8 | 26 |
| Lower Saale Terrace | ntgwl1 | 4.0e-04 | 3.0e-03 | 21 | 30 |
| Middle Saale Terrace | mtgwl3 | 5.0e-04 | 2.0e-03 | 24 | 32 |
| Elsterian Base Moraine | egm | 1.0e-08 | 8.0e-05 | 6 | 16 |
| High Elster Terrace | htgwl5 | 1.0e-04 | 2.0e-03 | 21 | 30 |
| Quaternary | q | 1.0e-08 | 7.0e-04 | 14 | 24 |

| | | | | | |
|---|---|---|---|---|---|
| Tertiary | t | 5.0e-09 | 3.0e-05 | 6 | 28 |
| Pre-tertiary | pt | 5.0e-12 | 6.0e-06 | 1 | 20 |

Exploring the simulation results in the SPR reveals non-linear relationships between the chosen layer combinations and the output metrics (Fig.2). For instance including the “egm” layer into the model decreases the model performance, resulting in a higher RMSE value, when most other layers are excluded from the stratigraphy as well. However, this effect varies for more complex stratigraphies. Similarly, some combinations (e.g., no “egm” but “htgwl5” layer) result in the simulation of considerably higher flow rates than the observed data when the hydrostratigraphic layer of the mining area ("mi") and the unstructured sediments are included in the stratigraphic model, too. In contrast, for more complex models, the influence of both layers on the flow rate becomes negligible.
The fully calibrated model results in an RMSE of 3.17 m and a flow rate to the mine of 1.52 m³/s which is about 5 times larger than the observation value. In contrast, visualizing different combinations of uncalibrated model combinations using the SPR a model can be found which describes both well, the distribution of hydraulic head and the flow rates to the mining area. For instance, the combinations I (RMSE = 5.35 m and flow = 0.83 m³/s) and II (RMSE = 8.98 m, and flow = 0.25 m³/s) offer a better performance trade-off between flow and head estimates. Subsequently, the key asset of our workflow is the incorporation and utilization of expert knowledge to prioritize relevant geological attributes and facilitate the selection of composite layers and stratigraphic models, ultimately leading to more accurate and resource-efficient geohydraulic simulations. Through their experience and understanding of the geological context, our workflow enables experts to identify implausible configurations, ensuring that the resulting model reflects the inherent geological complexities while maintaining physical plausibility and accuracy in the simulations.

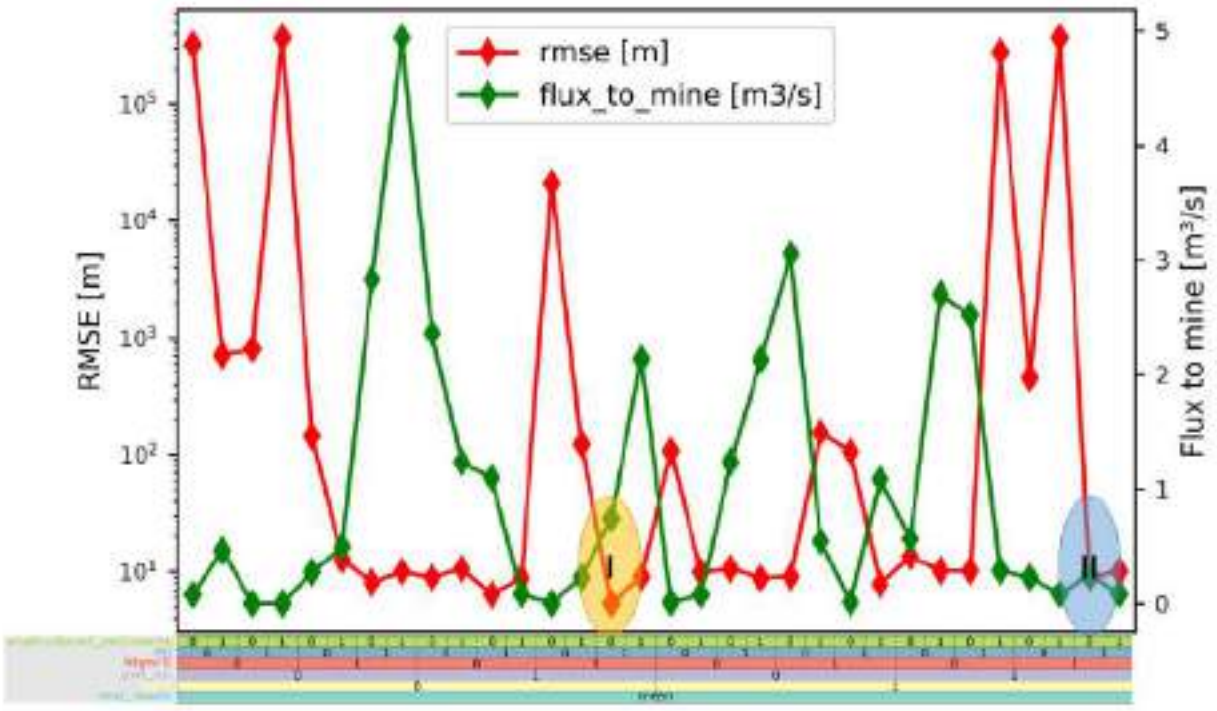


Figure 2: SPR scatter plot to depict the simulation results for each layer combination on top of the hierarchical stacking of the layer combinations. The combinations I and II mentioned in the text are visualized with colored ellipses

## 4 Conclusion

In conclusion, our study introduces a comprehensive workflow to assist the parameterization of geo-hydraulic models in complex aquifer systems. By integrating a hydrostratigraphy simplification tool informed by expert insights with a visual-analytical approach to hierarchically stack model outcomes, our methodology empowers hydrogeologists to reveal non-linear impacts of model complexity

reduction and to save computational resources by optimizing the selection of composite layers of the aquifer system. The open-source approach and the open standards for input and output data offer the flexibility to integrate a diverse range of geohydraulic simulators, including popular platforms such as MODFLOW and OpenGeoSys into our workflow. Further improvement may include the selection of a subset of promising combinations of hydrogeological models and their incorporation into a model calibration workflow using parameter calibration tools such as PEST.

**References**

[1]J. Margat and J. van der Gun, *Groundwater around the World: A Geographic Synopsis*. CRC Press, 2013.

[2]P. A. Witherspoon and R. A. Freeze, 'The role of aquitards in multiple-aquifer systems', *Eos, Transactions American Geophysical Union*, vol. 53, no. 7, pp. 743–746, 1972, doi: 10.1029/EO053i007p00743.

[3]S. C. Åberg, A. K. Åberg, and K. Korkka-Niemi, 'Three-dimensional hydrostratigraphy and groundwater flow models in complex Quaternary deposits and weathered/fractured bedrock: evaluating increasing model complexity', *Hydrogeol J*, vol. 29, no. 3, pp. 1043–1074, May 2021, doi: 10.1007/s10040-020-02299-4.

[4]H. Zhou, J. J. Gómez-Hernández, and L. Li, 'Inverse methods in hydrogeology: Evolution and recent trends', *Advances in Water Resources*, vol. 63, pp. 22–37, Jan. 2014, doi: 10.1016/j.advwatres.2013.10.014.

[5]M. C. Hill, 'The Practical Use of Simplicity in Developing Ground Water Models', *Groundwater*, vol. 44, no. 6, pp. 775–781, 2006, doi: 10.1111/j.1745-6584.2006.00227.x.

[6]O. Ben-Kiki and C. Evans, 'YAML Ain't Markup Language (YAML™) Version 1.2', 2009.

[7]T. Mihalisin, J. Timlin, and J. Schwegler, 'Visualization and analysis of multi-variate data: a technique for all fields', in *Proceeding Visualization '91*, San Diego, CA, USA: IEEE Comput. Soc. Press, 1991, pp. 171-178,. doi: 10.1109/VISUAL.1991.175796.

[8]A. Wollmann, 'Aufbau eines hydrogeologischen Strukturmodells für das Einzugsgebiet – Untere Selke – 2017', TERRAnotion GbR, Halle (Saale), Jun. 2018.

[9]L. Bilke *et al.*, 'OpenGeoSys'. Zenodo, Apr. 2022. doi: 10.5281/zenodo.7092676.

[10]J. Doherty, 'PEST: A Unique Computer Program for Model-independent Parameter Optimisation', *Water Down Under 94: Groundwater/Surface Hydrology Common Interest Papers; Preprints of Papers*, pp. 551–554, 1994, doi: 10.3316/informit.752715546665009.

**Theme:** Hydraulic and hydrological modeling
**IAHR Thematic Priority Area:** [TPA-4] Digital Transformation
https://doi.org/10.3850/iahr-hic2483430201-165

# Advancements and Challenges in Gridded Precipitation Datasets: Bias Correction and Downscaling Techniques for Enhanced Modeling in Sicily

**Niloufar Beikahmadi[1]*, Calogero Mattina[1], Dario Treppiedi[1], Antonio Francipane[1], Leonardo V. Noto[1]**

[1]Dipartimento di Ingegneria, Università degli Studi di Palermo, Palermo, Italy

**Corresponding author. Email: niloufar.beikahmadi@unipa.it*

**Keywords:** Bias-Adjustment, Convolutional Deep Network, Distribution-Based Methods, IMERG

## 1 Introduction

Spatial-temporal resolution advantages of Satellite Precipitation Products are limited by biases compared to ground observations. Various bias adjustment methods exist, from scaling methods to sophisticated techniques like Quantile Mapping (QM). However, many assume stationarity, leading to inaccuracies in variable climates. Alternative methods, instead, including Equidistant CDF Matching (ECDFM) [1], CDF transferring (CDFt)[2], Quantile Delta Mapping (QDM), aim to address non-stationarity. Also, recent advancements in deep learning offer new methods, such as Convolutional Neural Networks (CNNs) and Long Short-Term Memory (LSTM) networks, promising good performances in capturing spatial-temporal dependencies of climate phenomena [3]. Our study proposes a two-stage bias adjustment framework integrating multiple methodologies and advanced deep learning techniques to mitigate systematic bias in Global Precipitation Measurement (GPM) Integrated Multi-satellitE Retrievals for GPM (IMERG) satellite estimates for the Sicily, Italy. Also, to tackle one of the most important issues that affects semiarid regions as Sicily, i.e., precipitation datasets with zero-inflation, it exists different methods varying from Singularity Stochastic Removal (SSR) [4] to complex zero-truncated models [5].

## 2 Material

Study is focused on Sicily, the largest Mediterranean island, which spans approximately 25,700 km$^2$, having an average annual precipitation of about 715 mm. We used aggregated and interpolated precipitation data during 2013-2022 from the *Servizio Informativo Agrometeorologico Siciliano* (SIAS). Additionally, we included daily precipitation data from the IMERG product (IMERGDF-07 Final run, version 07), covering the same period and same spatial resolution of 0.1° × 0.1°.

## 3 Methods

Employing a two-step approach, firstly, we evaluated precipitation characteristics including magnitude, frequency, and trend to select suitable correction methods. We implemented four distribution-based methods: empirical / parametric Quantile Mapping, QDM, CDFt, and ECDFM. We addressed zero-inflation in datasets by using techniques such as the left tail censoring (_c), SSR, or truncated hurdle fit (_h). All these methods preserve multiplicative trends across all quantiles while accommodating seasonality. Therefore, four above mentioned bias-corrected precipitation datasets alongside raw IMERG data serve as input to the 2D Convolutional LSTM network, which excels in capturing both spatial and temporal dependencies of natural phenomena such as precipitation.

## 4 Results and Discussion

Figure 1 illustrates the percentage bias in daily precipitation before (raw IMERG) and after bias-correction using various methods. Raw IMERG data generally overestimates precipitation across statistical metrics, while correction methods reduce uncertainties, albeit with varying effectiveness depending on the metric. Moreover, methods that account for zero precipitation effectively reduce bias for dry days, with CDFt and QDM_c emerging as top performers overall.

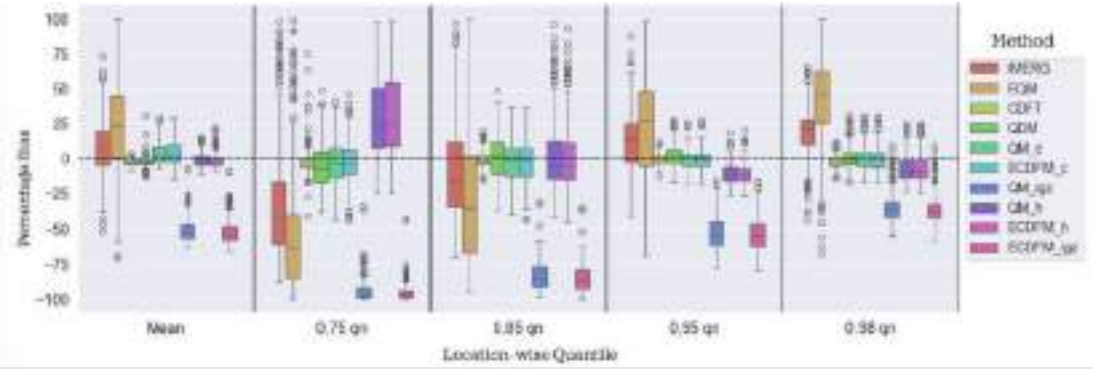


Figure 19- Boxplots comparing percentage bias in daily precipitation before (IMERG) and after bias adjustment using different methods (CDFt, QDM, ECDFM, QM) for selected quantiles.

Figure 2 displays the spatial distribution of percentage bias for leading correction methods applied to IMERG, showing significant reduction in spatial bias patterns post-correction. CDFt performs well in minimizing bias, followed by QDM, while QM and ECDFM introduce some new spatial patterns.

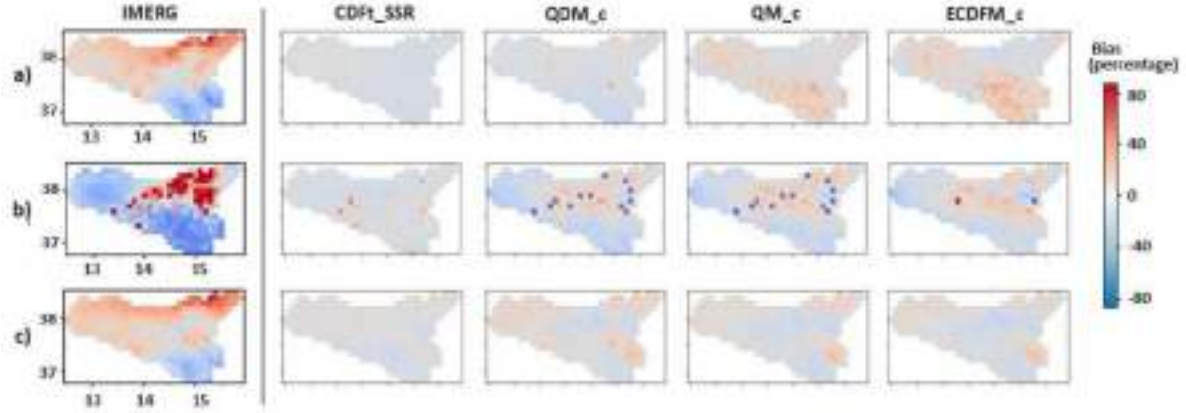


Figure 20- Spatial distribution of percentage bias for precipitation correction methods (CDFt_SSR, QDM_c, QM_c, and ECDFM_c) on IMERG data, calculated for the mean (a), 0.75th (b), and 0.95th (c) quantiles.

## References

1. Li, H., J. Sheffield, and E.F. Wood, Bias correction of monthly precipitation and temperature fields from Intergovernmental Panel on Climate Change AR4 models using equidistant quantile matching. Journal of Geophysical Research: Atmospheres, 2010. **115**(D10).
2. Michelangeli, P.A., M. Vrac, and H. Loukos, Probabilistic downscaling approaches: Application to wind cumulative distribution functions. Geophysical Research Letters, 2009. **36**(11).
3. Harilal, N., M. Singh, and U. Bhatia, Augmented convolutional LSTMs for generation of high-resolution climate change projections. IEEE Access, 2021. **9**: p. 25208-25218.
4. Vrac, M., T. Noël, and R. Vautard, Bias correction of precipitation through Singularity Stochastic Removal: Because occurrences matter. Journal of Geophysical Research: Atmospheres, 2016. **121**(10): p. 5237-5258.
5. Zuur, A.F., et al., Zero-truncated and zero-inflated models for count data. Mixed effects models and extensions in ecology with R, 2009: p. 261-293.

**Theme:** Hydraulic and hydrological modeling
**IAHR Thematic Priority Area:** [TPA-4] Digital Transformation
https://doi.org/10.3850/iahr-hic2483430201-167

# Reconstruction of Maximum and Minimum Temperature Time Series for the Mediterranean's Largest Island

**Calogero Mattina[1], Dario Treppiedi[1], Antonio Francipane[1], Leonardo Valerio Noto[1]**

[1] Dipartimento di Ingegneria, Università degli Studi di Palermo, Palermo, Italy

*Corresponding author: calogero.mattina01@unipa.it*

**Abstract.** Analyzing potential indicators of climate change necessitates access to extensive historical datasets. However, measurement gauges are subject to frequent replacement or upgrades, resulting in spatial and/or temporal inconsistencies that undermine the reliability of these datasets. This is the case of Sicily, the largest island in the Mediterranean Sea, which is characterized by the presence of two different monitoring networks, spanning partially different periods. By using a spatial interpolation method, we merge the information from these networks and obtain continuous daily maximum and minimum temperature series for the 1980-2023 period in a 2x2 km grid.

**Keywords:** climate characterization, temperature, time series reconstruction

## 1 Introduction

The analysis of possible signals of climate change requires historical datasets covering as long periods as possible. These datasets are essential not only to reconstruct past climate, but also to validate the results of climate models, so as to examine how future climate will evolve. Among all the climate variables, temperature is one of the most responsive to the impacts of climate change. Depending on the future greenhouse gasses emission scenarios, the global temperature change is projected to vary between +1°C (i.e., very low emissions) and +4°C (i.e., very high emissions) by the end of the 21st century [1]. Satellite or reanalysis datasets provide estimates of weather and climate variables that are continuous over time, but they are often characterized by significant biases [2]. On the other hand, measurement gauges are often replaced or upgraded, creating spatial and/or temporal discontinuities that do not allow for their straightforward use [3]. Hence, we apply here a methodology based on the spatial interpolation of temperature data from two different networks in Sicily Island (Italy). This allows us to obtain a spatially and temporally continuous dataset from observed temperature data (T-ATLAS), which is useful for reconstructing the Island's climatology, but also for searching for possible climate change signatures.

## 2 Data and Methods

We focus on Sicily Island, which is the largest island in the Mediterranean Sea and is located in the transition area between the arid climate of North Africa and the more temperate European climate [3]. Focusing on maximum and minimum daily temperatures, the island is characterized by two different monitoring networks: the first one provided by the Osservatorio delle Acque – Agenzia Regionale per i Rifiuti e le Acque (OA-ARRA), which covers the period 1980-2012, and the second one provided by the Servizio Informativo Agrometeorologico Siciliano (SIAS), which provides data from 2002 to the present. Since these two datasets cover partially different periods, we aim to use a spatial interpolation method to integrate data from these networks and to obtain continuous daily maximum and minimum temperature series for the 1980-2023 period. To do this, we combine the Ordinary Kriging (OK) with a daily environmental lapse rate (ELR), that it is useful to consider the role of the altitude in the interpolation process. We firstly use the observations from the OA-ARRA dataset to

reconstruct daily temperature values over the period 2002-2012 at the coordinates of SIAS stations. With a reasonably long period of overlap between the two networks (i.e., 2002–2012), we test the accuracy of the OK-ELR method in reconstructing the temperature signal through different performance indices. After this validation procedure, we interpolate the data with the UK-ED method by using a high-resolution grid (i.e., 2x2 km), covering the whole Sicilian territory.

## 3 Results

We firstly use the daily temperatures from the two datasets to compute a daily environmental lapse rate. Exploiting the relationship between air temperatures and altitude is necessary to i) refer the variable to see level before applying the OK, ii) re-enter the altitude information after the OK. This procedure has been preferred to using a constant value over the year, as it was found that it greatly varies seasonally, presenting a peak in winter and lower values in summer.

Hence, it has been tested the reliability of the OK-ELR procedure. As an example, Figure 1 shows the comparison of the re-constructed signal from the OA-ARRA and the recorded values from the SIAS network for Palermo station point for the year 2003. As it is possible to observe, the series overlap almost perfectly, confirming the reliability of the two datasets and the interpolation method.

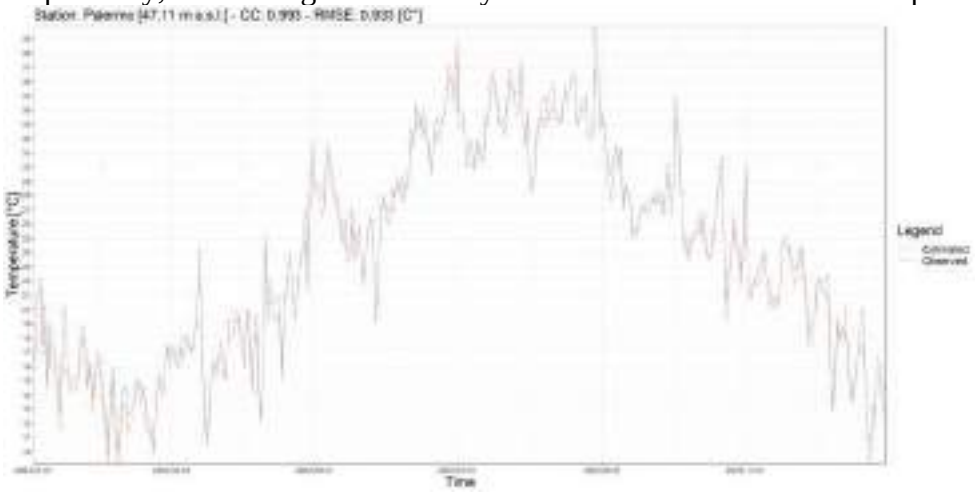


*Figure 21 – Comparison between the daily maximum temperatures in 2003 from the OA-ARRA interpolated network (orange) and the SIAS recorded values network (blue) for Palermo station.*

Therefore, we interpolate maximum and minimum temperature values from 1980 to 2023 using a 2x2 km grid, reconstructing a spatially and temporally continuous ATLAS for Sicily.

## 4 Conclusions

In recent years, Sicily has been often identified as a primary hotspot of climate change. Availability of datasets as extensive as possible is critical for recognizing any changes in weather-climate variables, and it is also useful for validating climate model outputs. Due to the presence of two different temperatures dataset, we reconstruct a gridded temperature ATLAS (T-ATLAS) for the period 1980-2023 by combining the Ordinary Kriging with the environmental lapse rate. We found that this procedure provides reliable results, providing remarkably accurate estimates for the interpolated variables.

## Reference

[1] IPCC, 2023: Climate Change 2023: Synthesis Report. Contribution of Working Groups I, II and III to the Sixth Assessment Report of the Intergovernmental Panel on Climate Change [Core Writing Team, H. Lee and J. Romero (eds.)]. IPCC, Geneva, Switzerland, pp. 35-115.

[2] Velikou, K.; Lazoglou, G.; Tolika, K.; Anagnostopoulou, C. Reliability of the ERA5 in Replicating Mean and Extreme Temperatures across Europe. Water 2022, 14, 543.

[3] Ducré-Robitaille, Jean-François, Lucie A. Vincent, and Gilles Boulet. "Comparison of techniques for detection of discontinuities in temperature series." International Journal of Climatology: A Journal of the Royal Meteorological Society 23.9 (2003): 1087-1101.

[4] Beck, H., Zimmermann, N., McVicar, T. et al. Present and future Köppen-Geiger climate classification maps at 1-km resolution. Sci Data 5, 180214 (2018).

**Theme:** Hydraulic and hydrological modeling
**IAHR Thematic Priority Area:** [TPA-4] Digital Transformation
https://doi.org/10.3850/iahr-hic2483430201-169

# Study On Water Quality Improvement Schemes and Benefits in Benxi Section of The Taizi River

**Mingwei Wang[1], Jianwei Liu[1], Bing Yang[1], Jun Wei[2], Fenfei Chen[2], Huabin Li[2]**

[1] Faculty of Infrastructure Engineering, Dalian University of Technology, Dalian 116024, China
[2] Power China Hua Dong Engineering Corporation Limited, Hangzhou 311122, China

*Corresponding author: jwliu@dlut.edu.cn*

**Abstract.** The construction of river wetlands is an important means to improve the water environment of rivers. However, how to determine the reasonable construction plan of river wetlands is a difficult problem at present. Taking Benxi Section of Taizi River as the research object, the MIKE 11 model was established to simulate the reduction effect of COD and $NH_3$-N concentration in Benxi section of Taizi River under four kinds of wetland construction schemes, so as to determine the most suitable scheme. Based on AHP method and fuzzy optimization principle, the utilization efficiency of river water resources before and after wetland construction was evaluated. The results show that the pollutant concentration in river can be effectively reduced after the construction of wetland, and the greater the daily treatment capacity of wetland, the greater the pollutant reduction rate in Benxi section of Taizi River, and the less excessive water body. After the construction of river wetlands to improve the water quality of the river, the water resource utilization efficiency of the Benxi section of the Taizi River can reach a good level. This study can provide scientific reference for the determination of channel wetland construction scheme in Taizi River and other similar rivers.

**Keywords:** Hydrodynamic water quality model, River channel wetland, Taizi River, Water resources utilization benefit evaluation

## 1 Introduction

Currently, research efforts primarily focus on the coordinated operation of reservoir groups and dams. Further investigation is needed on how to simulate the effect of river wetlands on water quality improvement.[1-5] In this study, the Benxi section of the Taizi River is selected as the research subject. A one-dimensional hydrodynamic water quality model is constructed to simulate the reduction of pollutants in the river under various wetland construction schemes. Through the integration of the Analytic Hierarchy Process (AHP) method with fuzzy evaluation techniques, the impact of constructing riverine wetlands on the utilization benefits of water resources is assessed. This study provides a scientific basis for river water quality improvement and the construction of riverine wetlands.

## 2 Material and methods

The Taizi River, located between 122°26′ to 124°53′ east longitude and 40°29′ to 41°39′ north latitude, spans a total length of 413 km with a drainage area of 13,883 $km^2$. It plays a crucial role in the agricultural, industrial, and urban development of Liaoning Province. However, the growing water demand and pollution pose threats to its economic development. This study utilizes data from 2017 and employs the MIKE11 model to simulate the water quality in the Benxi section[6]. Additionally, the fuzzy preference method (Formula 1 and Formula 2) is employed to evaluate the water resource utilization benefits before and after wetland construction.

## 3 Results and discussion

Artificial wetlands types: surface flow, horizontal subsurface flow, vertical subsurface flow, each with unique traits (Table 1). In Liaoning's cold climate, surface flow artificial wetlands are inefficient in winter. Despite high costs, vertical subsurface flow artificial wetlands excel in $NH_3$-N, COD, BOD5 removal, requiring less space. Hence, this study adopts vertical subsurface flow artificial wetlands. Given the climate and factors, cattail and reed are chosen as primary species, with iris, water celery, arrowhead, and water willow as secondary, resilient perennials. Taizi River's multiple tributaries significantly impact its water quality. Establishing artificial wetlands at tributaries reduces pollutant influxes into the river. Similarly, artificial wetlands can tackle severe pollution sections along the river. Treated effluent partially replenishes the Taizi River. Three artificial wetlands planned at Nansha River, Xing'an Village, and Xiaojia River (Figure 2). Focusing on May's non-flood season, targeting COD and $NH_3$-N. Simulated max COD and $NH_3$-N concentrations in wetland effluent are 30 mg/L and 1.5 mg/L. Four construction schemes proposed (Table 2), optimizing treatment capacity. HD module simulation spans Jan 1 - Dec 31, 2017, calibrated for accurate results (Figure 3). Pollutant diffusion and attenuation coefficients calibrated for COD and $NH_3$-N in AD module (Table 3). Simulation results show reliable performance (Figure 4). MIKE11 model used to simulate COD and $NH_3$-N concentrations downstream Xiaojia River in May 2016. Over 52% and 43% of water bodies violate COD and $NH_3$-N standards (Figure 5), revealing severe pollution. Four riverine wetland schemes assessed; scheme 4 chosen for optimal cost-effectiveness (Figure 6). AHP method employed to evaluate water resource benefits (Table 4). Post-construction, significant social, economic, and ecological benefits anticipated (Table 5), with water resources meeting industrial and agricultural needs, promoting regional development, and enhancing ecological quality.

## 4 Conclusions

The study utilized the MIKE11 model to simulate the effect of various wetland construction schemes on river water quality, determining the optimal construction plan. Furthermore, it evaluated the water resource utilization benefits before and after wetland construction using a fuzzy evaluation model.

As the daily processing capacity of artificial wetlands increases, the improvement rates of COD and $NH_3$-N in the Benxi section of the Taizi River also increase. Scheme 3 and Scheme 4 showed similar effects on improving river water quality, both of which could elevate the overall water quality to Class III. Considering that Scheme 3 has a larger construction scale than Scheme 4, Scheme 4 was selected as the optimal scheme.

In the constructed evaluation system for river water resource utilization, the weights of agricultural irrigation, industrial water use, and urban water supply accounted for more than half of the total weight, indicating that economic benefits dominate in river water resource utilization. After wetland construction, the economic benefits, ecological environmental benefits, and overall benefits changed from average to very good compared to before construction.

Therefore, constructing wetlands can effectively improve the water quality of the Benxi section of the Taizi River and consequently enhance water resource utilization benefits.

## Reference

[1] B.Q. Zheng, M. Dou, Q.T. Zuo, et al, Research on adjustability of water quality improvement from operation dispatch of sluiceand dam, J. Water Resources and Hydropower Engineering. 42 (2011) 28–31.

[2] M. Hijosa-Valsero, R. Sidrach-Cardona, E. Bécares, Comparison of interannual removal variation of various constructed wetland types, J. Science of the Total Environment. 430 (2012) 174–183.

[3] D.V. Erler, D. Tait, B.D. Eyre, et al, Observations of nitrogen and phosphorus biogeochemistry in a surface flow constructed wetland, J. Science of the Total Environment. 409 (2011) 5359–5367.

[4] H.L. Zhu, X.L. Shi, Y.C. Li, et al, Evaluation of runoff simulation using trmm precipitation data based on SWAT model, J. Research of Soil and Water Conservation. 24 (2017) 105–112.

[5] I. Boureima, V. Gyrya, J.A. Saenz, et al, Dynamic calibration of differential equations using machine learning, with application to turbulence models, J. Journal of Computational Physics. 457 (2022) 110924.

[6] Q.Q. Sun, Y.L. Chen, Carbon emission characteristics of an urban sewage treatment plant in a southern province, J. Chinese Journal of Environmental Engineering. 17 (2023) 3231–3244.

**Theme:** Hydraulic and hydrological modeling
**IAHR Thematic Priority Area:** [TPA-4] Digital Transformation
https://doi.org/10.3850/iahr-hic2483430201-171

# Underground Mining Impact on Groundwater in Kuye River Basin, China: A Coupling Model Study

**LI Shu[1, 2], ZHANG Fengran[1, 2], QI Qingsong[1, 2], LI Ningbo[1, 2], WU Junhua[1, 2]**

[1] Water Resources Department, Yellow River Institute of Hydraulic Research, YRCC, Zhengzhou 450003, China;
[2] Henan Key Laboratory of Ecological Environment Protection and Restoration of Yellow River Basin, Zhengzhou 450003, China;

*Corresponding author: lididshu30@163.com*

**Abstract.** The Kuye River Basin has experienced a rapid depletion of groundwater due to the increased coal production. In this study, by introducing the empirical equations derived from the three zone theory in the coal mining industry in China as a boundary condition, a calculation model was developed by coupling the soil and water assessment tool and visual modular three-dimensional finite-difference ground-water flow model (SWAT-VISUAL MODFLOW). The model was applied to several coal mines in the basin to quantify the groundwater impact of underground mining. For illustration purposes, three underground mining observation stations were selected for groundwater change simulation in 2009, producing the results that agreed well with the observed data. We found that groundwater level was closely related to the height of the fractured water-conducting zone caused by underground mining and a higher height led to a lower groundwater level. This finding was further supported by the calculation that underground mining was responsible for 23.20mm aquifer breakages in 2009. Thus, preventing surface subsidence due to underground mining can help protecting the basin's groundwater.

**Keywords:** coupled SWAT-VISUAL MODFLOW; groundwater; Kuye River Basin; underground mining for coal;

## 1 Introduction

The intensified coal mining in the Kuye River Basin since launching the Western Development Strategy in China in 2000 has increased the coal yield from $0.2174\times10^8$ tons in 1998 to $2.03 \times 10^8$ tons in 2009. Underground mining can directly alter runoff generation mechanisms [1,2], and both water quantity and quality at local to basin scales, and have variable effects on groundwater. To the best of our knowledge, no study has been reported about the application of the empirical equations of the three zone theory as a boundary condition for modeling the dynamic change of groundwater caused by underground mining in several coal mines at the basin scale.

## 2 Materials and Methods

The Kuye River, situated in the transitional zone between Inner Mongolia and Shaanxi Province (38°22'—39°50' N and 109°28'—110°45' E) is one of the major tributaries of the middle Yellow River, extending 242 km in length and covering a drainage area of 8706 $km^2$. The coupled SWAT-VISUAL MODFLOW model was used to simulate the groundwater response to underground mining in the basin. The data used include digital elevation model (DEM), geological and hydro-meteorological data from rainfall gauges, hydrological and meteorological stations. With respect to the hydrologic cycle processes impacted by underground mining, the three zone theory widely used in the coalfields of China was introduced as the criterion for set-up of the scenarios. Scenario A assumes each of three fissures are 5 km long and 1 km wide. One-way compressive strength of the overlying strata is usually 20–40 Mpa, whereas the intersection angle between coal seams and

horizontal plane is less than 54º. Equations (1) and (2) were chosen for calculating the constant head of the groundwater in the fractured zone:

$$H_1 = \frac{100\sum M}{4.7\sum M + 19} + 2.2 \quad (1)$$

$$H_\eta = 20\sqrt{\sum M} + 10 \quad (2)$$

where $H_1$ is the height of the caving zone, $H_\eta$ is the height of the fractured water-conducting zone, and $M$ is the depth of coal seams, equivalent to the height of the goaf area in meters.

## 3 Results and Discussion

The groundwater storage disrupted by underground mining in 2009 was calculated to be 23.20 mm. The groundwater storage consists of static storage (within aquifer in the upper part of goafs) and dynamic storage (mine discharge). The coal output in 2009 was $2.03\times10^8$ t with mine discharge of 0.31 $m^3$/t, resulting in a dynamic storage change of 7.23 mm and the static storage by 15.97 mm. 0 illustrates the headwater regime of the first aquifer in December 2009 for both scenarios, where the white area represents the portion of depleted aquifer. Compared with Scenario B, the depletion area of Scenario A is about four-fold larger.

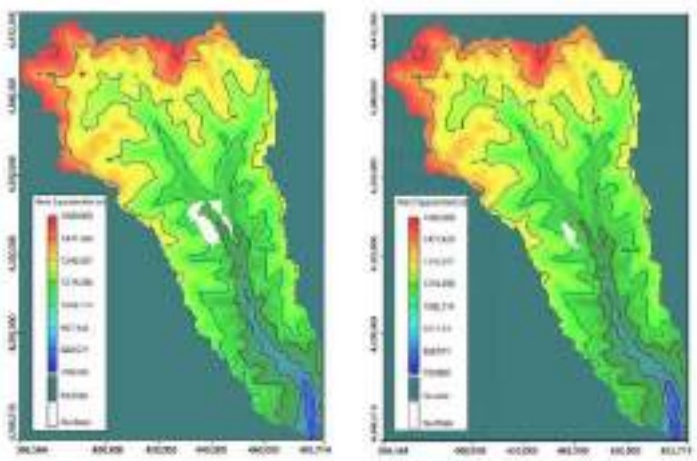

Scenario A Scenario B

Figure 1 Groundwater level simulated by the coupled S-VM model for December 2009, Scenario A (with underground mining) and Scenario B (without underground mining).

## 4 Conclusions

In this study, the S-VM model was applied to quantify the groundwater change in the Kuye River Basin in 2009, producing the reasonable results which were further confirmed by a comparison with the observed data. After locating three coal mine pits and defining the important parameters for the hydraulic conductivity of four aquifers, the fractured water-conducting zone induced by underground mining was found out to be one of major causes of the groundwater reduction in the Kuye River Basin in 2009. Therefore, the groundwater regime can be improved by means of lowering fractured water-conducting zone height. This study may provide a reference in water protection mining to other similar basins.

## Reference

[1]Álvarez, R.; Ordóñez, A.; García, R.; Loredo, J. An estimation of water resources in flooded, connected underground mines. Eng. Geol.2018,232,114-122.

[2]Xu, S.; Zhang, Y.; Shi, H.; Wang, K.; Geng, Y.; Chen, J. Physical Simulation of Strata Failure and Its Impact on Overlying Unconsolidated Aquifer at Various Mining Depths. Water 2018, 10, 650-668.

**Theme:** Hydraulic and hydrological modeling
**IAHR Thematic Priority Area:** [TPA-4] Digital Transformation
https://doi.org/10.3850/iahr-hic2483430201-173

# Interaction of Rainfall, Topography, Vegetation, and Soil Characteristics on Hydrological Behavior in Small and Medium-sized Catchments: A case study within the Yangtze River Basin, China

**Shiyun Lin[1,3], Jiali Guo[1,2,3], Shan-e-hyder Soomro[1,3], Yinghai Li[1,2,3]**

[1] College of Hydraulic & Environmental Engineering, China Three Gorges University, Yichang Hubei, 443002, China
[2] Hubei Key Laboratory of Construction and Management in Hydropower Engineering, China Three Gorges University, Yichang 443002, China
[3] Institute of Water Resources Informatics, China Three Gorges University, Yichang 443002, China

*Corresponding author: jiali.guo@ctgu.edu.cn*

**Abstract:** Due to the heterogeneity of climatic and underlying variables of different catchments and the limited description of present hydrological models for hydrological processes, it is of great importance to select an appropriate model for flooding simulation based on the actual conditions of the interested basins. In this research, three hydrological models with different structures were selected for different types of catchments within the Yangtze River Basin. Extracted multiple indicators to explore the influence of catchment characteristics on hydrological processes, and the response degree of hydrological processes to various characteristics in different typical small and medium-sized catchment was obtained.

**Keywords:** Catchment characteristics, Hydrological models, Hydrological processes, Yangtze River

## 1 Introduction

Conceptual hydrological models, which are not only based on a complete physical foundation but also scientifically reflect hydrological processes and water cycle mechanisms, have the characteristics of low cost, high efficiency, and easy to operate [1]. This study selected three different structured hydrological models for various types of catchments within the Yangtze River Basin. Rainfall, vegetation, soil type, and topography indicators were extracted and analyzed to investigate the relationship between hydrological effects in small and medium-sized catchment and catchment characteristics. This research aims to provide support for the selection and establishment of models for flood forecasting in small and medium-sized catchments.

## 2 Materials and methods

### 2.1 Study area

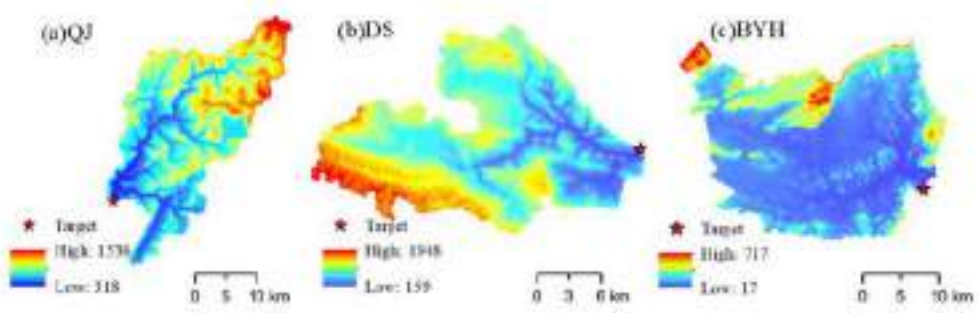


Figure 22 The three catchments in this study.

The geographical and elevation distributions of the catchment shown in Figure 1. They are the Boyang River catchment (BYH) in the mixed agricultural-plain catchment, the Qu River catchment (QJ) in the mixed farming-hilly catchmentmixed farming-hilly catchment, and the Danshui River catchment (DS) in the densely forested mountainous catchment.

### 2.2 Hydrologic Modeling

This study selected three storage-production runoff mechanism models, each with different structural characteristics, include the Xin'anjiang model [2], TOPMODEL [3], and MISDC [4]. The NSGA-II algorithm was selected as the model parameter optimization method [4][5]. The Nash-Sutcliffe efficiency coefficient and Mean Absolute Error were chosen as the two objective functions to construct the optimization algorithm's objective function model.

## 3 Results and Discussion

The main findings of the study are as follows:

- With a strong correlation between runoff coefficients and total rainfall amounts.
- The applicability ranking of the models in the BYH catchment is XAJ > MISDC > TOPMODEL; in the QJ catchment, the applicability ranking is TOPMODEL > MISDC > XAJ; and in the DS catchment, the applicability ranking is MISDC > XAJ > TOPMODEL. The MISDC model demonstrates the best general applicability.
- The storage-discharge models in each study catchment show differences.
- The runoff coefficient follows the sequence BYH > QJ > DS, whereas the peak flow modulus results are completely opposite, with BYH < QJ < DS.
- The average topographic index values for the catchments follow the pattern: BYH > QJ > DS.
- The channel slope and average catchment slope showing the trend: BYH < QJ < DS, while the catchment area and main channel length exhibit the trend: BYH > QJ > DS.

## 4 Conclusions

Multiple factors such as rainfall, topography, vegetation, and soil types play a crucial role in the hydrological processes of small to medium-sized catchments. When there are differences in climatic zones within the catchment, variations in rainfall patterns become most apparent, while in similar climatic zones, topography has a more pronounced impact on the catchment's flow characteristics. In catchments with significant topographic variations, the development of aquifers tends to be weaker, resulting in rapid fluctuations in water levels and quick responses to floods within the catchment. Vegetation retention in the catchment has a limited impact on smaller regions, and differences in soil composition contribute to variations in runoff components within the catchment. When selecting and constructing hydrological models for different watersheds, the watershed characteristics should be taken into consideration. When the model's adaptability is poor, the influence of watershed characteristics should be analyzed, and model structures should be improved, or pre/post-processing should be conducted in conjunction with the basin characteristics.

## Reference

[1] Liu Z., Wang Y., Xu Z., et al. Conceptual hydrological models[J]. Handbook of hydrometeorological ensemble forecasting, 2017: 1-23.
[2] Zhao R. J. The Xinanjiang model applied in China[J]. Journal of hydrology, 1992, 135(1-4): 371-381.
[3] Beven K. J., Kirkby M. J. A physically based, variable contributing area model of basin hydrology/Un modèle à base physique de zone d'appel variable de l'hydrologie du bassin versant[J]. Hydrological sciences journal, 1979, 24(1): 43-69.
[4] Brocca L., Melone F., Moramarco T. On the estimation of antecedent wetness conditions in rainfall–runoff modelling[J]. Hydrological Processes: An International Journal, 2008, 22(5): 629-642.
[5] Bekele E. G., Nicklow J. W. Multi-objective automatic calibration of SWAT using NSGA-II[J]. Journal of Hydrology, 2007, 341(3-4): 165-176.

**Theme:** Hydraulic and hydrological modeling
**IAHR Thematic Priority Area:** [TPA-4] Digital Transformation
https://doi.org/10.3850/iahr-hic2483430201-175

# Flood Risk Analysis of Zhongxin River in Lianping County Based on IFMS

**Haoran Zhu[1] Chao Dai[1]**

[1] School of Civil Engineering, Sun Yat-sen University, Guangzhou, 528478, China

*Corresponding author: Chao Dai daich8@mail.sysu.edu.cn*

**Abstract.** Located in the Zhongxin River Basin, the study focused on the Lianping County section, where a coupled 1D-2D hydrodynamic model was constructed using the IFMS. The observed flood data of Zhongxin station from July 4 to July 6, 2022 was used for parameter calibration, and the flood inundation extent for various return periods was simulated. The results indicate that the study area shows a good flood resilience with a recurrence interval of up to 20 years. However, for floods with a return period of 20 years or greater, the residential areas are likely to experience varying degrees of flooding. This suggests that enhanced flood control measures are necessary to strengthen the region's resilience to flooding.

**Keywords:** Coupled 1D-2D hydrodynamic model; Flood inundation analysis; IFMS

## 1 Overview

This paper presents a flood simulation study using the IFMS model, focusing on the Lianping County section of the Zhongxin River Basin in Guangdong Province. We conducted simulations across different recurrence periods using a calibrated model to analyse the impact of flooding on several key towns within the basin. The findings offer valuable decision support for flood control strategies.

## 2 Methods

Establishing a one-dimensional model of the river and a two-dimensional model of the inundation area respectively and coupled them into an 1D-2D hydrodynamic model to study the flood region.

## 3 Results

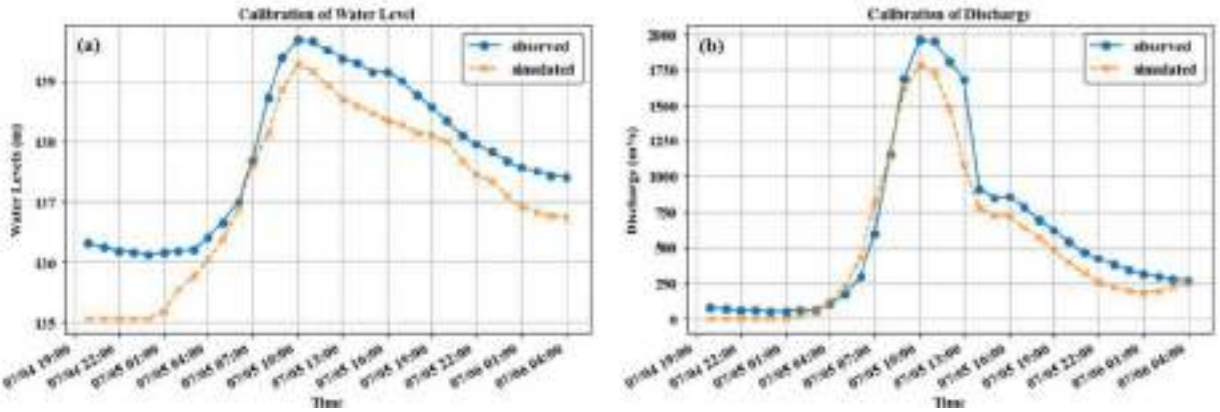


Figure 1. Hydrograph of simulated and observed flows for calibration: (a) water level and (b) discharge, hourly data.

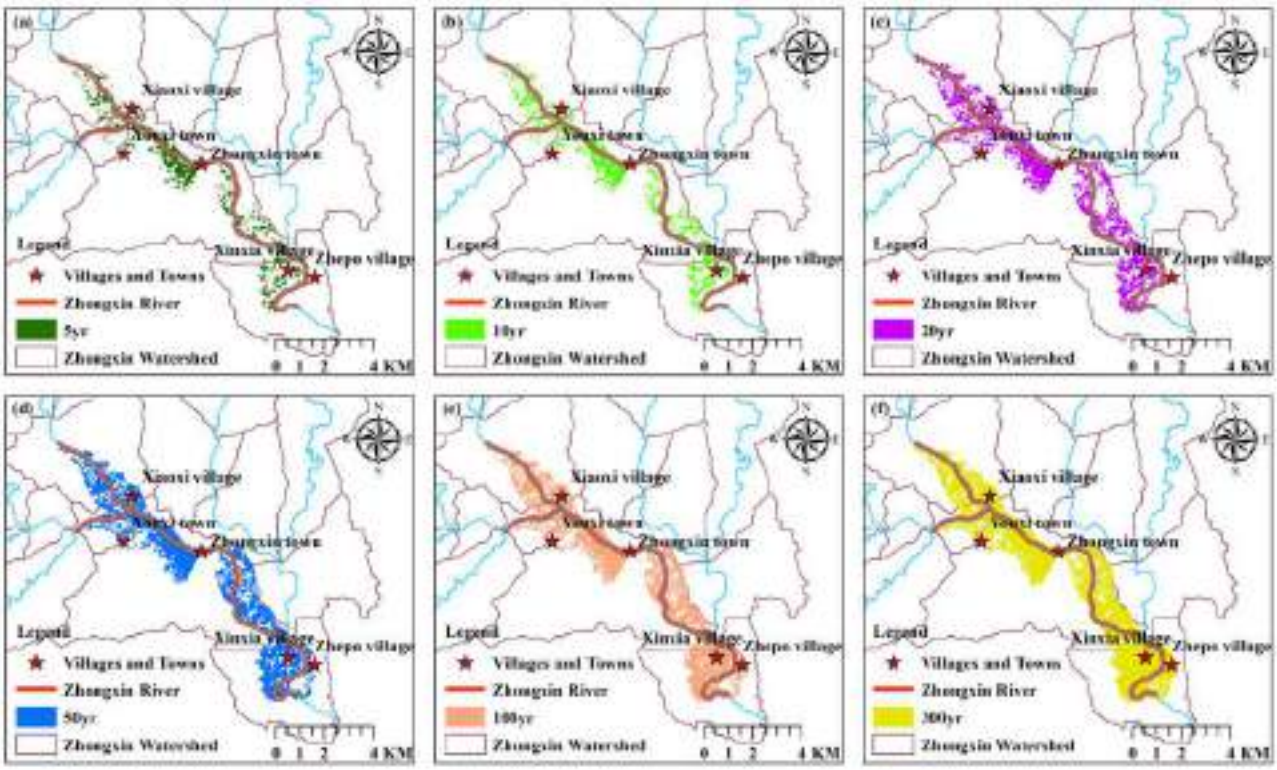


Figure 2. Map of flood inundation in the Zhongxin Town section for various recurrence intervals ranging from once in 5 to 300 years, depicted from (a) 5 years to (f) 300 years.

## 4 Conclusions

This paper develops a coupled one-dimensional and two-dimensional hydrodynamic model which has been validated for its reliability in simulating floods in the Zhongxin River Basin. Flood inundation maps across various recurrence intervals reveal that the region exhibits significant flood resilience for events with a recurrence period of less than 20 years. However, areas experience varying degrees of inundation when floods recur at intervals of 20 years or more. These findings indicate a need for enhanced flood control measures to further strengthen the region's resilience to flooding.

## Reference

[1] Wang, C. (2021). Rain and flood simulation and LID mitigation benefits assessment of sponge cities based on IFMS (Master's thesis). Ningxia University.
[2] Yang, B. (2021). Compilation and application of flood risk maps in the urban section of Jinxi Jiang-Le County. Fujian Hydropower, 1-3+11.
[3] Ma, J. et al. (2017). Application of flood analysis software in the compilation of flood risk maps. China Water Resources, 17-20.
[4] Li, K. et al. (2023). Flood risk analysis of the urban section of Qingyi River in Hongya County based on IFMS. Journal of Southwest Minzu University (Natural Science Edition), 49, 562-568.
[5] Zhai, X. et al. (2023). Rainstorm and mountain flood inundation risk analysis of small watersheds based on CNFF-IFMS. In Proceedings of the 2023 China Hydraulics Academic Conference (Vol. 1). China Hydraulic Engineering Society, p. 8.
[6] Zhong, H. et al. (2022). Flood scenario simulation based on the hydrological and hydrodynamic model in the Puyang River Catchment. Water, 14(23), 3873.
[7] Hu, Z. et al. (2023). Analysis of the 2022 storm and flood events in the Pearl River Basin. China Rural Water and Hydropower, 41-45.
[8] Wang, L. (2022). Lessons from the defense against the extraordinary flood in the Beijiang River on June 22. China Water Resources, 8-10.
[9] Liu, X. et al. (2021). Research on flood risk analysis based on hydrodynamic models. Shaanxi Water Resources, 78-82.

**Theme:** Hydraulic and hydrological modeling
**IAHR Thematic Priority Area:** [TPA-4] Digital Transformation
https://doi.org/10.3850/iahr-hic2483430201-177

# Study on the Improvement of Urban Flood Control Capacity Based on Hydrodynamic Model

**Binbin Wu[1,2], Haijun Yu[1,2,*], Jianming Ma [3], Geng Sun[4], Lingyun Zhao[4], Jie Mu[1,2] and Wangyang Yu[1,2]**

[1] China Institute of Water Resources and Hydropower Research, Beijing, 100038, China
[2] Research Center on Flood and Drought Disaster Reduction of the Ministry of Water Resources, Beijing, 100038, China
[3] National Institute of Natural Hazards, Beijing, 100085, China
[4] Beijing IWHR Corporation, Beijing, 10004, China

** Haijun Yu: yuhaijun@iwhr.com*

**Abstract**. Low-lying cities are usually built along rivers with greater risk of flooding, it is urgent to carry out research on improving flood control capacity. In this paper, taking Jintang County of Chengdu City, Sichuan Province as an example, a 1D-2D coupled hydrodynamic model was established to simulate flood inundation and evaluate the flood control effects of different engineering measures, including river regulation and flood diversion. The water level in the urban area could be reduced by 0.62~2.43m, urban inundated area decreased by 30%, and the urban flood control capacity improved effectively.

**Keywords:** Flood control capacity, flood control engineering measures, flood simulation, 1D-2D coupling

## 1 Introduction

Most cities are built along rivers, and in the process of urbanization, they continue to expand around and even occupy the rivers. Recent researches also indicate that urbanization is expanding into flood-prone areas around the world, including riverbeds and floodplains, and China is facing a more severe situation [1, 2]. This kind of rapid urbanization increases the flood exposure of cities. Especially under the influence of climate change, extreme weather has increased and the risk of inundation of cities has been multiplied, in particular for those low-lying cities.

A case study of the urban area of Jintang County, which is a typical low-lying city on the main Tuojiang River, was conducted. The urban area of Jintang County has been inundated several times in recent years, such as floods in July 2013, July 2018 and August 2020. Prolonged floods seriously threaten the safety of people's lives and property, and restrict the development of local economy and society. Consequently, it is urgent to carry out studies on understanding the inundation characteristics and improving flood control capacity.

## 2 Material and methods

The self-developed Integrated (IWHR) Flood Modeling System (IFMS) [3] was employed to simulate the 1D and 2D hydrodynamic processes of the urban area of Jintang County. The 1D model included the four rivers (Beihe river, Zhonghe river, Pihe river and Tuojiang river) flowing through the study area, with a total of 411 cross-sections. Quadrilateral unstructured grids were constructed to set up the 2D model, which contains 71708 active cells with an average grid size from 15m to 30m. The high-precision DEM data were then interpolated into the model grids. The 1D and 2D model were coupled by using lateral connections.

Two consecutive floods in August 2020 were simulated by the coupled hydrodynamic model. Water level and discharge at Sanhuangmiao Hydrological Station, and survey results of flood inundation

area and flood marks were used to calibrate the model. Measured or derived inflows were used for the upstream boundary. The downstream boundary of the model adopted the water level and flow rate relationship curve of Jiulongtan Power Station.

## 3 Results and discussion

### 3.1 Model Verification

Modeled and observed values at Sanhuangmiao Hydrological Station showed reasonable agreement in both floods. The Nash efficiency coefficients for water level and discharge were higher than 0.90, the relative errors of peak flow were less than 1%, the peak time errors were less than 1 h, and the maximum water level errors were less than 0.2m. The simulated inundation ranges of the two typical floods in August 2020 were basically consistent with the actual survey inundation range for the urban area (Fig 1). The simulated maximum inundation depth were also consistent with the investigated flood marks, and the absolute errors between the modeled and surveyed values at most points were within 0.2m. Those results demonstrated that the coupled hydrodynamic model has high accuracy.

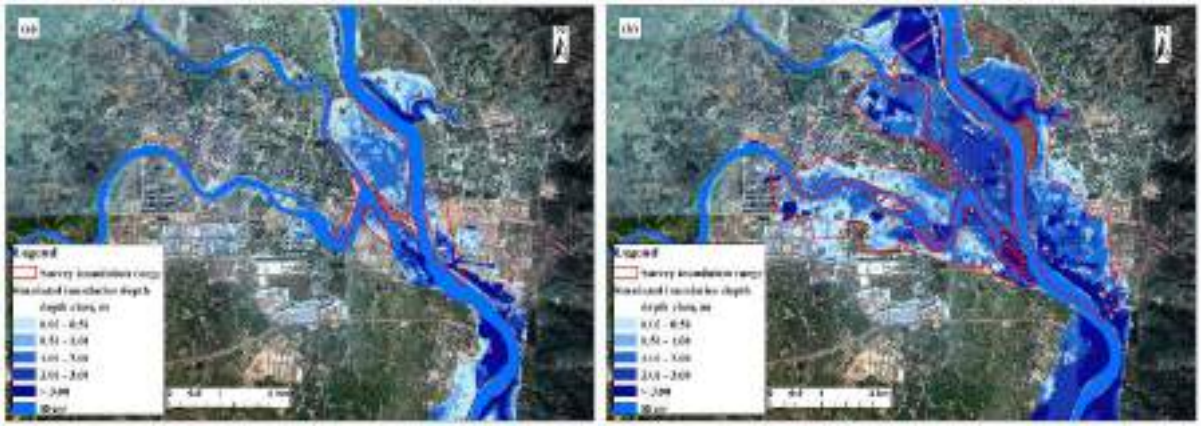

**Figure 1.** Investigation and simulation of two typical floods in the urban area of Jintang County: (a) Flood20200812 and (b) Flood20200817.

### 3.2 Effects of flood control engineering measures

Two major flood control engineering measures were proposed to improve the flood control capacity of the urban area of Jintang County: 1) River regulation project, including dredging and widening of channels in the urban area and Tuojiang River, and 2) Pihe River flood diversion project, including the surface open channel (including Qimu river, a tributary of Tuojiang river) and the tunnel through the mountain (Fig 2). Flood20200817 was used to assess the flood control effects of the two engineering measures. Results showed that the combined measures could effectively improve the urban flood control capacity (Table 1). The water level in the urban area could be reduced by 0.62~2.43m, in which the reduction of the urban section of Pihe River was 1.10~2.43m. The water level at the confluence of three rivers decreased by 1.10m, and the urban inundated area decreased by 30%.


**Figure 2.** Layout of flood control engineering measures.

**Table 1.** Effects of flood control engineering measures for Flood20200817.

| River reach | Reduction of water level or inundated area | | |
|---|---|---|---|
| | River regulation project | Pihe River flood diversion project | Combined measures |
| Urban section of Pihe river | 0.37~0.75m | 0.70~1.70m | 1.10~2.43m |
| Urban section of Zhonghe river | 0.37~0.53m | 0.40~0.70m | 1.03~1.21m |
| Urban section of Beihe river | 0.33~0.37m | 0.30~0.60m | 0.62~1.05m |
| Confluence of three rivers | 0.39m | 0.67m | 1.10m |
| Urban inundated area | 11.03% | 17.50% | 30.02% |

## 4 Conclusions

An integrated 1D-2D hydrodynamic model was established to simulate flood inundation and assess flood control effects of different engineering measures for the urban area of Jintang County. The coupled hydrodynamic model was verified using data from two consecutive floods in August 2020; the model adequately simulated the flow characteristics along the main river channels and the floodplain with a reasonable level of accuracy. The combination of river regulation project and Pihe River flood diversion project could effectively improve the urban flood control capacity with the water level reduction of 0.62~2.43m and inundated area reduction of 30% for the urban area of Jintang County.

## Acknowledgments

This study was supported by National Key Research and Development Program of China (Project No. 2023YFC3010704).

## References

[1] Rentschler J., Avner P., Marconcini M., Su R., Strano E., Vousdoukas M. and Hallegatte S., 2023, Global evidence of rapid urban growth in flood zones since 1985, *Nature*, 622, pp 87–92

[2] Tellman, B. Sullivan J.A., Kuhn C., Kettner A.J. and Slayback D.A., Satellite imaging reveals increased proportion of population exposed to floods, 2021, *Nature*, 596, pp 80–86
[3] Ma J.M., Yu H.J., Zhang D.W., Zhang H.B., Wu B.B. and Mu J., Adoption of evaluation software in flood risk map drawing, 2017, *China Water Resources*, 5, pp 17–20 (in Chinese)

**Theme:** Hydraulic and hydrological modeling
**IAHR Thematic Priority Area:** [TPA-4] Digital Transformation
https://doi.org/10.3850/iahr-hic2483430201-181

# Influence of the Mouth Bar on Saltwater Intrusion in Microtidal Estuary of Modaomen Estuary

**Wang Pu Gu Zhitong Ye Shengbo Liu Feng**

School of Ocean Engineering and Technology, Sun Yat-sen University

*Corresponding author: liuf53@mail.sysu.edu.cn*

**Abstract.** The estuary's topography, especially the mouth bar, is crucial for preventing saltwater intrusion. This study focuses on the mouth bar's impact on saltwater intrusion in the Modaomen Estuary. It employs the Delft3D numerical model to construct two estuary models—with and without the mouth bar—to explore its impact on saline intrusion during the dry season and reveal the mechanisms.The model results show that, under the effect of river flow and tide, the mouth bar has a significant effect on reducing the saltwater intrusion distance by 54.5% on spring tide and 25% on neap tide. The intensity of the mouth bar's weakening effect on the saltwater intrusion is different at different tides,which is mainly caused by the inconsistent changes of stable shear flux and tidal oscillation flux during spring and neap tides.During neaps, mouth bar will increase stable shear while weakening the tidal action intensity, resulting in a smaller weakening effect on salt water intrusion than that at spring tides. This study deepens the understanding of saltwater intrusion mechanisms in complex estuarine topography, with practical significance for water security and salt tide prevention in the estuarine area.

**Keywords:** microtidal estuary, saltwater intrusion, the mouth bar, numerical simulation ,mechanism analysis

## 1 Introduction

Saltwater intrusion is affected by a variety of factors, including external driving forces such as runoff, tide, wind, sea level and wave, and internal topographic changes [1]. Previous studies mostly focused on the response relationship of saltwater intrusion to external driving forces and its physical mechanism [2], and there were few studies on topographic changes, especially the influence of the mouth bar on the upwelling of saline tides. The mouth bar is a relatively important geomorphic unit in river delta system. Runoff, tide and wave jointly affect the formation and evolution of the mouth bar .Due to the shallow bar, it obstructs the water flow and produces strong bottom shear stress, which enhances the water mixing and energy dissipation, and affects the salt transport between the estuary and the ocean.The Modaomen Estuary in the Guangdong-Hong Kong-Macao Greater Bay Area is essential for runoff, but it is threatened by saltwater intrusion during the dry season. This paper establishes an ideal Modaomen Estuary to study the response mechanism of saltwater intrusion to the evolution of the mouth bar, aiming to provide reference and guidance for other estuarine areas.

## 2 Methods

### 2.1 Delft3D numerical model

This paper utilizes Delft3D to establish a three-dimensional numerical simulation model of an ideal estuary, based on the actual settings of the Modaomen Estuary. By setting ideal geometric shapes and modeling parameters, numerical simulation experiments are conducted to investigate the complex circulation and salinity structure of the Modaomen Estuary.

### 2.2 Salt flux decomposition mechanism

This paper employs the method provided by James A. Lerczak and W. Rockwell Geyer, which decomposes the tidal cycle average salt flux into three components based on different driving forces: the stable shear diffusion , the tidal oscillation salt flux , and the advective transport Qf * So. The specific formula is as follows:

$$F_S = \langle \int usdA \rangle \quad (1.1)$$

$$\varphi_0 = \frac{1}{A_0} \langle \int \varphi dA \rangle \quad (1.2)$$

$$\varphi_E = \langle \frac{h+\eta}{h} \varphi \rangle - \varphi_0 \quad (1.3)$$

$$\varphi_T = \varphi - \varphi_0 - \varphi_E \quad (1.4)$$

In the equations, φ can represent either the velocity u or the salinity s. denotes the cross-sectional area averaged over the tidal cycle. Thus, the salinity flux Fs can be expressed as

$$F_S = \langle \int (u_0+u_E+u_T)(S_0+S_E+S_T)dA \rangle = \langle \int \left(u_0S_0 + u_ES_E+u_TS_T\right)dA \rangle$$
$$= Q_fS_0 + F_E+F_T \quad (1.5)$$

## 3 Result

### 3.1 Saltwater Intrusion Distance

The model results show that under the influence of river flow and tides, the mouth bar of the estuary significantly reduces saltwater intrusion, reducing the invasion distance by 54.5% on spring tide days and by 25% on neap tide days.

### 3.2 Changes in Estuary Circulation

The presence of the estuary mouth bar significantly reduces estuary circulation and salinity stratification at the mouth cross-section, during both spring and neap tides. It induces reversing circulation during neap tides and strong upslope flow with eddies during spring tides, impacting the mixing and flow patterns of high- and low-salinity water.

### 3.3 Mechanism of the Mouth Bar's Impact on Saltwater Intrusion

The presence of an estuary mouth bar enhances tidal oscillation transport while reducing stable shear transport. During neap tides, the mouth bar strengthens stable shear by weakening landward tidal action. During spring tides, the mouth bar further weakens tidal oscillation.

## 4 Conclusion

The presence of a mouth bar in the Modaomen estuary alters the dynamic mechanism of saltwater intrusion. It enhances tidal oscillation transport while reducing stable shear transport. The mouth bar reduces tidal amplitude and promotes salinity stratification and estuarine circulation. During neap tides, the mouth bar increases stable shear to compensate for reduced salt input. During spring tides, the mouth bar further weakens tidal oscillation, reducing salt transport. Thus, the mouth bar plays a stronger role in reducing saltwater intrusion during spring tides.

## Reference

[1] GONG Wengping,ZHANG Guang,ZHANG Heng, et al. The effects of mouth bar on salt intrusion in a partially mixed estuary[J]. Journal of Hydrology, 2022, 612: 128261.

[2] GONG Wengping,SHEN Jian. The response of salt intrusion to changes in river discharge and tidal mixing during the dry season in the Modaomen Estuary, China[J]. Continental Shelf Research, 2011, 31(7): 769-788.

**Theme:** Hydraulic and hydrological modeling
**IAHR Thematic Priority Area:** [TPA-4] Digital Transformation
https://doi.org/10.3850/iahr-hic2483430201-183

# Streamflow Simulation in Baihe River Basin Based on SWAT Model

**Mengyan Shen[1,*], Miaomiao Ma[1], Zhicheng Su[1] and Xuejun Zhang[1]**

[1] Department of Drought Mitigation and Policy Research, Research Center on Flood and Drought Disaster Reduction of the Ministry of Water Resources, China Institute of Water Resources and Hydropower Resesarch, Beijing, 100038, China

** Corresponding author: Mengyan Shen@18351423980@163.com*

**Abstract**. To provide a reference for future streamflow forecast work in Baihe River, this paper applied the SWAT model to the Baihe River basin for streamflow simulation. It concludes that the SWAT model has good applicability in the streamflow simulation of the Baihe River basin. NSE, $R^2$, and PBIAS were 0.77, 0.79, and 19.5%, respectively, during the calibration period (2001~2004), and 0.63, 0.64, and 15.3%, respectively, during the validation period (2005~2008). Also, the low precision during the validation period could be due to the neglect of reservoir operations.

**Keywords:** Baihe River basin, streamflow simulation, SWAT model

## 1 Introduction

The Baihe River basin lies in the upper reaches of the Hanjiang River basin, and its hydrological control station is also the intake control station of Danjiangkou Reservoir, which is the water source of the Middle Route of South-to-North Water Diversion Project. Therefore, the Baihe River basin is not only directly related to the long-term operation of the Middle Route of the South-to-North Water Diversion Project, but also indirectly relates to the sustainable socioeconomic development in Northern China. However, in recent decades, due to the continuous intensification of global climate change and human activities, the hydrometeorological elements have changed, which has an impact on the hydrological cycle process. Thus, it is necessary to research the streamflow forecast in Baihe River in recent years.

## 2 Materials and methods

### 2.1 Study area and data

The Baihe hydrological station (110.1°E, 32.8°N) serves as the intake control station of Danjiangkou Reservoir, which is the water source of the Middle Route of South-to-North Water Diversion Project. The basin controlled by Baihe hydrological station is located between 31.6°-34.3°N latitude and 106.0°-110.4°E longitude with a catchment area of 59115 $km^2$ which constitutes 37.18% of the overall catchment area of Hanjiang River. The data used in this paper are: DEM, land use data, soil data, meteorological data, and observed streamflow data required for calibration.

### 2.2 SWAT model

The SWAT model for hydrological simulation consists of two main components: the land surface water cycle and the river confluence calculation [1]. The land surface water cycle operates based on the principle of water balance, which can be expressed by the following formula:

$$SW_t = SW_0 + \sum_{i=1}^{n}\left(P_{day} - R_{sur} - ET_a - W_{seep} - Q_{gw}\right) \quad (9)$$

where $SW_t$ represents the final moisture of the soil, mm; $SW_0$ is the initial moisture content of the soil, mm; $i$ represents the iteration or index number within the summation; n is the time, days; $P_{day}$ means

the total amount of precipitation, mm; $R_{sur}$ represents the surface runoff in the region, mm; $ET_a$ is the evapotranspiration, mm; $W_{seep}$ refers to the amount of water that infiltrates the vadose zone from the soil profile, mm; $Q_{gw}$ indicates the return flow, mm.

## 3 Results and discussion

In this study, 28 parameters affecting the streamflow process were selected for parameter sensitivity analysis, and global sensitivity analysis was used. Finally, 13 parameters that had a greater impact on streamflow were chosen and used as model parameter calibration based on the SUFI-2 optimization algorithm. Among them, ALPHA_BF, CN2, and EPCO were the three most sensitive parameters.
The results of the calibration and verification are shown in Figure 1 (a) and (b), respectively, and it is obvious that the simulated streamflow aligned well with the observed streamflow. Also, NSE and $R^2$ were above 0.75 during the calibration period, and both NSE and $R^2$ were above 0.60 during the verification period. During both the calibration and verification periods, PBIAS were within 20%. It can be considered that the SWAT model has good applicability in the Baihe River basin.
The exceptionally high peak flow in 2005 could be attributed to the influence of reservoir operations (e.g., Shiquan and Ankang Reservoirs, which are seasonal regulation reservoirs), which may have resulted in a relatively poorer simulation performance during the verification period.

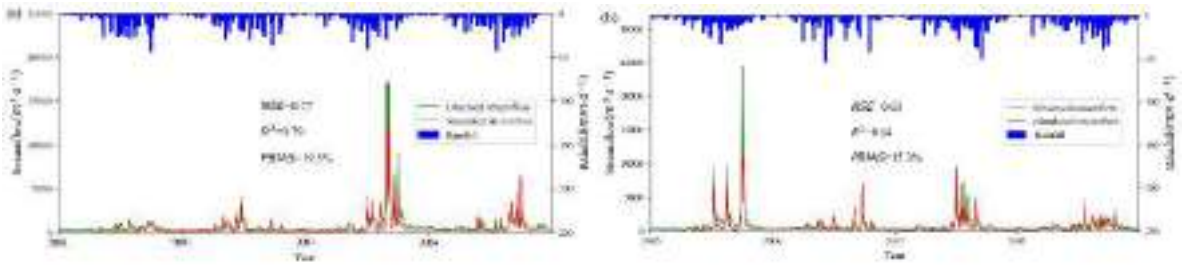

**Figure 1.** Simulated and observed streamflow for (a) the calibration period and (b) the verification period in Baihe hydrological station.

## 4 Conclusions

The SWAT model has good applicability in the streamflow simulation of the Baihe River basin, and ALPHA_BF, CN2, and EPCO were the three most sensitive parameters. Furthermore, the low precision during the verification period could be primarily attributed to the neglect of reservoir operations. In the future, we will further study the impact of reservoir operation on streamflow, in order to provide a baseline for streamflow forecast work in the Baihe River.

## 5 Acknowledgments

This research was funded by Five Talents of the China Institute of Water Resources and Hydropower Research – International Composite Talent Project (Y0203982012).

## References

[1] Li K., Wang Y.Q., Xu J.J., et al., 2020, Runoff simulation of Tangnaihai hydrological station in source area of Yellow River based on SWAT model, IOP Conference Series: Earth and Environmental Science, 612(1), pp 012047.

**Theme:** Hydraulic and hydrological modeling
**IAHR Thematic Priority Area:** [TPA-4] Digital Transformation
https://doi.org/10.3850/iahr-hic2483430201-185

# Enhancing the Storage Capacity of Coastal Plain River Networks Based on Flood Simulation

**Yao Liu [1], Shunli Chen [2], Yongzhi Liu [1], Rui Tian [3], Yanyun Ruan [3], Xiang Wang [3], Xiaoyang Liu [3], Jianhua Zhao [3], Wenting Zhang [4],**

[1] Nanjing Hydraulic Research Institute Hydrology and Water Resources Department 1 No.1 Guangzhou Road , Nanjing and 210017, China
[2] Linhai Water Conservancy Bureau 2 No. 219 Dongfang Avenue , Linhai and 317000, China
[3] China Yangtze Power Corporation, 3 No. 1 Xibajianshe Road , Yichang and 430014, China
[4] Department of Hydrology and Water Resource, Hohai University, 4 No.1 Xikang Road, Nanjing and 210098, China

*Corresponding author: yzliu@nhri.cn*

## 1 Introduction

Water is crucial for human survival and socio-economic development. In coastal areas, flooding disasters caused by storm surges coexist with issues such as seawater intrusion due to overexploitation of groundwater[1]. During the flood season, preventing river overflow caused by heavy rainfall is essential, while also considering groundwater recharge and mitigating seawater intrusion in coastal areas[2]. Maintaining low river levels reduces the risk of flooding in low-lying areas near rivers. However, this approach contradicts the concept of groundwater recharge and leads to problems such as insufficient water storage in river networks after heavy rainfall and restricted urban water supply[3]. Therefore, finding a balance between groundwater resource conservation and flood disaster prevention and enhancing the storage capacity of coastal plain river networks are critical issues in coastal plain areas.

## 2 Research method,

The flood control standard for outer embankments of the Datian Plain is set at a 20-year return period. By fully utilizing the drainage and tide-blocking gates within the study area, external flooding from the Lingjiang River can be resisted. This study is based on a hydrodynamic-hydraulic coupled model developed independently by Nanjing Hydraulic Research Institute Hydrology and Water Resources Department to construct a flood simulation model for the Datian Port basin.

## 3 Flood simulation results based on characteristic water levels

### 3.1 Calculation of Characteristic Water Levels

Section 80064 near the Datian Port Dam is selected as the representative section, with a warning water level of 3.3 meters. The wet perimeter method is used to calculate the ecological water level for the representative section. The ecological water level for section 80064 is calculated to be -1.35 meters.

### 3.2 Impact of Increasing the Warning Water Level on Flood Inundation

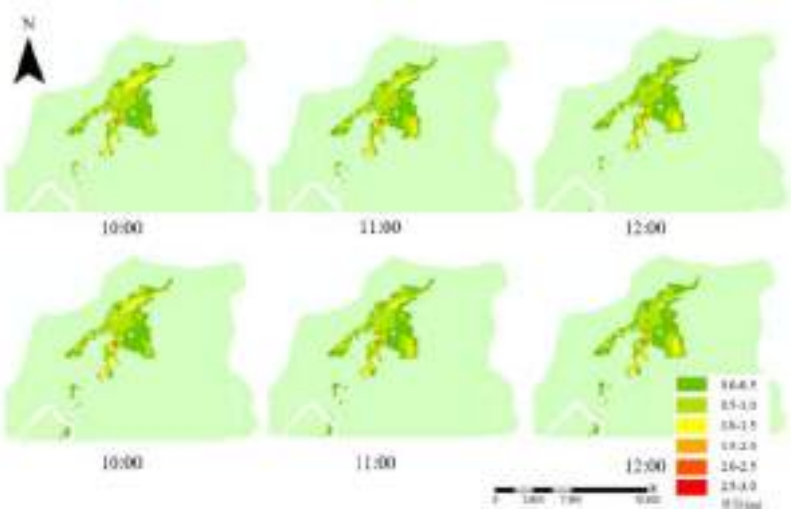


Figure 1 The flood inundation situation in the Datian Plain when raising the warning water level to 3.4m and 3.5m.

When the initial warning water level is raised to 3.4 meters, there is no significant difference in flood inundation compared to when it is 3.3 meters, except for a 0.6 $km^2$ inundation area near Ling Lake. When the initial warning water level is raised to 3.5 meters, significant flood inundation occurs on the right bank of the Ling River outside Datian Port Dam. The warning water level of the river network in Datian Plain is reasonable, and there is 0.1m room for raising.

### 3.3 Analysis of River Network Reservoir Capacity

The channel storage capacity is selected as the indicator to measure the river's reservoir capacity. When the warning water level is raised by 3.4m, the total safe water volume in the Datian Plain amounts to 3,278,000 cubic meters, an increase of 115,000 cubic meters compared to the initial warning water level of 3.3m, thus expanding the adjustable storage space.

## 4 Conclusion

Starting from the natural properties of different water levels in the river channels of the study area, the river flow is divided into ecological protection flow, safety flow, and disaster flow based on ecological and warning water levels. Combining river section data, characteristic water levels such as ecological flow and safety flow are calculated to measure the river network's reservoir capacity. Based on a hydrodynamic-hydraulic coupled model, flood situations under different warning water levels are simulated to verify the rationality of the current warning water level settings and explore potential improvements. Raising the warning water level to expand the reservoir capacity of the plain river network facilitates fine control of the river network space and provides a reference for adjusting river network water levels during the flood season.

## Reference

[1] Fauzie A K. Assessment and management of coastal hazards due to flooding, erosion and saltwater intrusion in Karawang, West Java, Indonesia[J]. Journal of Coastal Sciences, 2016, 3(2): 8–17.

[2] Kolathayar S, Sitharam T G, Yang S. Coastal reservoir strategy to enhance India’s freshwater storage by impounding river flood waters: a detailed overview[J]. Water Supply, IWA Publishing, 2019, 19(3): 703–717.

[3] Padowski J C, Jawitz J W. Water availability and vulnerability of 225 large cities in the United States[J]. Water Resources Research, 2012, 48(12): 2012WR012335..

**Theme:** Hydraulic and hydrological modeling
**IAHR Thematic Priority Area:** [TPA-4] Digital Transformation
https://doi.org/10.3850/iahr-hic2483430201-187

# Hydrodynamic Processes and Challenges in Flood Modeling

**Lidong Zhao, Ting Zhang, Jianzhu Li, Ping Feng**

State Key Laboratory of Hydraulic Engineering Intelligent Construction and Operation, Tianjin University, Tianjin 300072, China

*Corresponding author: zhangting_hydro@tju.edu.cn*

**Abstract.** Urban floods have become a trouble for sustainable urban development. Taking Beiyangyuan Campus of Tianjin University as the study area, a coupled SWMM and MIKE21 model was constructed to explore the urban hydrological effects and the flood risk under low impact development (LID). The results show that permeable pavement has the best runoff control effect, and even implementing a small percentage of LID practices can effectively control runoff. Duration time is an important influence on flood risk, and the impact of flow velocity on flood risk is very small in plain cities.

**Keywords:** Flood risk, inundation characteristics, low impact development, urban flood modeling

## 1 Introduction

Global climate change and rapid urbanization led to frequent extreme rainstorms and flooding. Urban flood modeling and risk assessment are the vital methods for the management of flood disaster. Meanwhile, Low impact development (LID) as an essential measure of urban stormwater control, it is necessary to explore the impacts of LID on urban flood. This work focuses on numerical modeling methods for urban floods, the impacts of LID on urban floods, and the urban flood risk assessment by combining multiple methods.

## 2 Methods

The Beiyangyuan Campus of Tianjin University was selected as the study area; it is located in the Jinnan District of Tianjin, China, with a total area of approximately 2.4 $km^2$. Many LID practices have been implemented in the study area, mainly including bio-retention cells (19.4 ha), sunken greenbelts (19.7 ha) and permeable pavement (9.5 ha), which is an exemplary case study for exploring the effect of LID practices on urban floods.

Design storm based on *Tianjin Sponge City Construction Technical Guidelines* [1], LID removal scenarios and LID density scenarios are set up to explore the impact of LID on urban floods. Referring to the relevant literature [2-4], the flood risk and its influencing factors in the study area were analyzed using combined multi-methods based on water depth (WD), water depth & duration time (WD&DT), and hazard rating (HR). The impact of duration time on flood risk was analyzed by risk level changes from WD to WD&DT, and the impact of flow velocity on flood risk was analyzed by risk level changes from WD to HR.

## 3 Results

As shown in Figure 1, permeable pavement performs best in the reduction of runoff volume, while the bio-retention cell takes the second place, and the sunken greenbelt has limited effect. Implementation of the 20% LID practice had the greatest runoff control effect, especially during frequent light rainfalls.

As shown in Figure 2, after adding consideration of duration time, the proportion of risk levels upgraded to moderate or high is more than 90%. Adding the consideration of flow velocity, the 27-

36% low-risk area changes to moderate risk; further multiple linear regression analysis shows that the contribution of flow velocity to the flood risk is minimal.

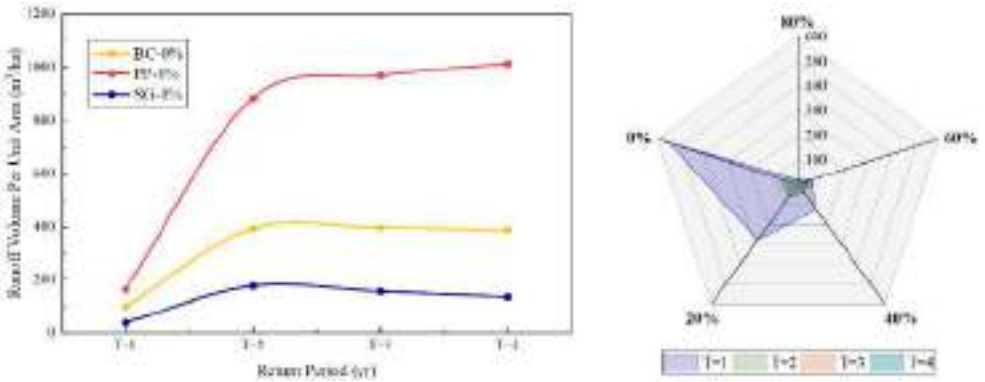

Figure 1 Runoff volume increase rate after LID removal and density reduction

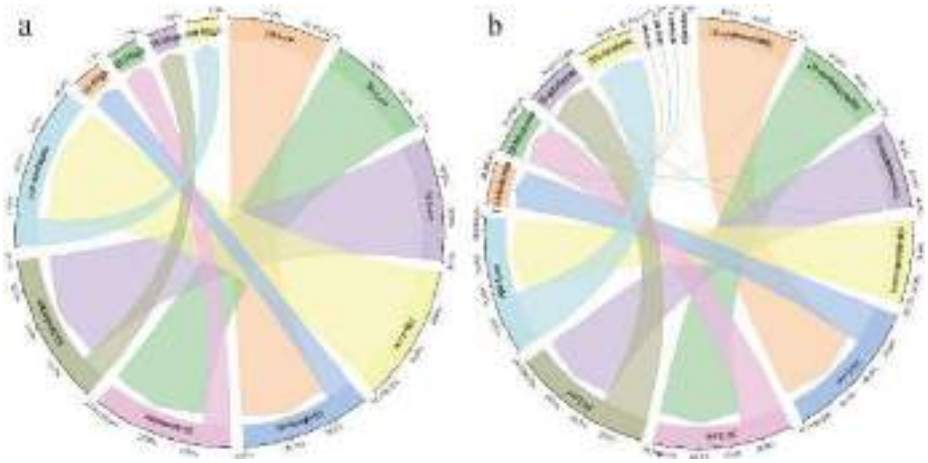


Figure 2 Risk level changes: (a) from WD to WD&DT; (b) from WD to HR

## 4 Conclusions

In this paper, based on the constructed SWMM and MIKE21 coupled model, we discussed the urban hydrological effects and the flood risk under LID. The main conclusions are as follows:

- Permeable pavement performs best in the reduction of runoff volume, inundation area, and inundation depth, and the implementation of even a tiny percentage (4% of the catchment area) of LID practices can be effective in controlling runoff.
- Duration time has an important influence on the flood risk in the study area. The possibility of flow impact hazards in the study area is minimal.

## Reference

[1] Tianjin Housing and Urban-Rural Construction Commission, 2016. The Tianjin Sponge City Construction Technical Guidelines. https://zfcxjs.tj.gov.cn/ztzl_70/bzgf/xxbz/xxbzgf/202010/t20201029_4031124.html.

[2] Xu, T., Xie, Z., Zhao, F., Li, M., Yang, S., Zhang, Y., Yin, S., Chen, S., Li, X., Zhao, S., Hou, Z., 2022. Permeability Control and Flood Risk Assessment of Urban Underlying Surface: A Case Study of Runcheng South Area, Kunming. Nat. Hazards, 111(1), 661-686.

[3] Huang, W., 2016. Risk assessment of Waterlogging and Hydraulic simulation of urban drainage network. Master's Thesis, South China University of Technology, Guangzhou, China.

[4] Defra, 2008. Flood and Coastal Defence Appraisal Guidance, Social Appraisal, Supplementary Note to O perating Authorities: Assessing and Valuing the Risk to Life from Flooding for Use in Appraisal of Risk Management Measures. https://assets.publishing.service.gov.uk/government/uploads/system/uploads/attachment_data/file/181441/risktopeople.pdf.

**Theme:** Water – Energy – Food nexus
**IAHR Thematic Priority Area:** [TPA-2] Water for the Energy Transition Food Security and Nature
https://doi.org/10.3850/iahr-hic2483430201-189

# Potential Energy Recovery Evaluation in Mountain Irrigation Distribution Networks

**Francesca Peretti[1], Andrea Menapace[1], Massimiliano Renzi[1] and Maurizio Righetti[1]**

[1] Faculty of Engineering, Free University of Bozen-Bolzano, Bolzano, 39100, Italy

*Corresponding author: francesca.peretti@student.unibz.it*

**Abstract.** Pressure regulation valves are commonly installed in water distribution networks to maintain optimal hydraulic conditions throughout the network. Research suggests that sustainable micro-turbines, such as pumps used as turbines, can replace pressure reducing valves to recover energy. Although urban water supply systems have been extensively studied, research on irrigation networks has been limited. The study aims to evaluate the potential energy recovery of a mountain irrigation network using hydraulic modelling and simulation combined with a methodology for optimal machine selection. The study was conducted on a real network located in a mountainous region of Northern Italy, with altitudes ranging from 790 to 1,397 meters above sea level. The results indicate that the network has the potential to recover 33.2% of the total energy available at all hydrants, which is a promising outcome for energy recovery. This energy assessment is crucial for identifying opportunities to efficiently use natural resources and reduce the environmental impact of irrigation practices.

**Keywords:** Irrigation, Potential Energy Recovery, Pressure Reducing Valves, Pump as Turbine, Water Distribution Network

## 1 Introduction

Pressure reducing valves (PRVs) are commonly used to control excess pressure in water distribution networks and maintain appropriate pressure levels. However, micro-hydropower, such as a pump operating in reverse mode as a turbine (PaT), is also a cost-effective solution for recovering excess pressure in the network. Urban water distribution systems have been extensively studied, but it is also important to evaluate irrigation systems as the agricultural sector is a major consumer of water [1]. Some methodologies have been developed to predict the flow and head in the network, taking into account the management of irrigation on-demand. However, irrigation scheduling, another widely used irrigation management technique in agriculture, results in different system configurations and behaviours. Furthermore, it is crucial to assess irrigation systems situated in elevated areas, such as mountainous regions, to determine their energy recovery capabilities. The objective of this study is to evaluate the potential energy recovery of a mountain irrigation network located in Northern Italy. The network is governed by a weekly irrigation schedule and will be evaluated using hydraulic modelling and simulation. Additionally, a methodology for optimal machine selection will be employed.

## 2 Material and methods

To evaluate the potential energy recovery of the network, two main steps were taken. The weekly irrigation water demand for crops was estimated using the FAO methodology [2,3]. Subsequently, irrigation time was calculated and assigned to each hydrant by developing a weekly schedule based on the plant's constraints. A hydraulic model of the network was conducted using QEpanet [4], and a hydraulic simulation was performed to determine the flow and pressure throughout the entire irrigation season. The available pressure to be recovered was calculated by considering all the points where pressure reducing valves (PRVs) are installed. A minimum irrigation pressure of 40 m for

sprinklers type was taken into account. The methodology implemented by M.K. Kostner et al. [5] for optimal PaT selection was used to select the best efficiency point (BEP) of the PaT which produces the highest energy recovery and predict the machine's behaviour in part load operation using the equations developed by M. Rossi et al. [6]. This methodology was applied to a real irrigation network located in Northern Italy, covering an area of 197 ha and consisting of 21 pressure reducing valves.

## 3 Results and discussion

The amount of energy that PaTs can recover depends on various factors, including the flow range, head, and average efficiency of the machine, as well as the total operating time. The system generates a total energy output of 292.1 MWh/year during the irrigation season. Sprinkler irrigation is estimated to consume 72.2 MWh/year, with distributed losses amounting to 44.3 MWh/year. This means that there is a potentially recoverable energy of 175.7 MWh/year at all hydrants. When considering only the hydrants connected to pressure reducing valves, the available energy is 166 MWh/year. PaTs can produce approximately 97 MWh/year, which represents 33.2% of the plant's total energy, as shown in Figure 3. The mountain plant has a very high energy recovery potential, as demonstrated by the recovery of 1.47 MWh/year/ha.

## 4 Conclusions

The results indicate that up to 33.2% of the total energy in the network can be recovered, corresponding to 1.47 MWh/year/ha. Mountain networks are particularly suitable for this kind of technology due to their altitude differences and high available head in the lowest points of the network. Additionally, the irrigation schedule allows for the prediction of plant behaviour since the schedule is strictly followed by the farmers. However, the accuracy of this result may vary depending on the demand scenario, which may depend on weather conditions. Therefore, it is necessary to consider different future scenarios to fully understand the solution's reliability. Further analysis could be conducted to evaluate the economic impact of this technology and determine whether it is more convenient to install PaT instead of PRV. Nevertheless, these results are promising in terms of energy recovery, which underscores the need for further analysis.

## Reference

[1] FAO AQUASTAT Dissemination System, (n.d.). https://data.apps.fao.org/aquastat/?lang=en (accessed March 27, 2024).

[2] G. Ravazzani, C. Corbari, S. Morella, P. Gianoli, M. Mancini, Modified Hargreaves-Samani Equation for the Assessment of Reference Evapotranspiration in Alpine River Basins, J. Irrig. Drain. Eng. 138 (2012) 592–599. https://doi.org/10.1061/(ASCE)IR.1943-4774.0000453.

[3] R. Allen, L. Pereira, D. Raes, M. Smith, FAO Irrigation and drainage paper No. 56, Rome Food Agric. Organ. U. N. 56 (1998) 26–40.

[4] A. Menapace, G.R. Pisaturo, A. De Luca, D. Gerola, M. Righetti, EPANET in QGIS framework: the QEPANET plugin, J. Water Supply Res. Technol.-Aqua 69 (2019) 1–5. https://doi.org/10.2166/aqua.2019.087.

[5] M.K. Kostner, A. Zanfei, J.C. Alberizzi, M. Renzi, M. Righetti, A. Menapace, Micro hydro power generation in water distribution networks through the optimal pumps-as-turbines sizing and control, Appl. Energy 351 (2023) 121802. https://doi.org/10.1016/j.apenergy.2023.121802.

[6] M. Rossi, A. Nigro, M. Renzi, Experimental and numerical assessment of a methodology for performance prediction of Pumps-as-Turbines (PaTs) operating in off-design conditions, Appl. Energy 248 (2019) 555–566. https://doi.org/10.1016/j.apenergy.2019.04.123.

**Theme:** Water – Energy – Food nexus
**IAHR Thematic Priority Area:** [TPA-2] Water for the Energy Transition Food Security and Nature
https://doi.org/10.3850/iahr-hic2483430201-191

# Coupling Causal-loop of System Dynamics and Centrality of Network Analysis to Identify Key Elements for Water-energy-food Nexus

**Duan Chen[1,2], Ze Fang[1]**

[1] Changjiang River Scientific Research Institute, Wuhan, China, 430010
[2] Hubei Key Laboratory of Water Resources & Eco-Environmental Sciences, Wuhan,China,430010

*Corresponding author: chenduan@mail.crsri.cn*

**Abstract.** Water-energy-food nexus can be considered as a complex network that is constituted by a large number of system elements (nodes) and their connections (edges). Identification of the hub nodes i.e., the key elements of the network is a critical step in simulating the water-energy-food nexus. This study coupled System Dynamics modeling and Network Analysis (NA) to identify the key elements of the water-energy-food nexus. Two cases concerning different scales of water-energy-food nexus are used for demonstrating the effectiveness of the proposed approach.

**Keywords:** Water-energy-food nexus; Key elements; System dynamics; Network analysis

## 1 Introduction

Water-food-energy nexus has been receiving extensive attention after it was officially introduced in Bonn Nexus Conference. The nexus is essentially a coupled system of water, food and energy systems, each of which generally involves a large number of system elements. Identifying the most important system elements, i.e., the key elements, may contribute towards a better and more accurate understanding of the behavior of the overall complex system of systems. As modelling the complete nexus often results in an unwieldy computational effort (Akhtar et al., 2013; Wa'el et al., 2017), identification of the key elements can help with prioritization of the entire variable list, and therefore, offer a chance to reduce the dimensions of the problem. Among all of the reported quantitative models of the water-food-energy nexus, the simplification of system elements is either not addressed or performed based on empirical judgement. None of them consider prioritizing the elements based on their importance in the complex system.

## 2 Method

System Dynamics（SD）is a system approach to understand the nonlinear behavior of complex systems over time by using stocks, flows, internal feedback loops, table functions and time delays. Network analysis (NA) or Network Theory (Anderson& Vongpanitlerd, 2013) is the study of graphs as a representation of relations between discrete objects and has applications in many disciplines including computer science, biology, economics, finance, operations research, and sociology. A network can be defined as a graph in which nodes and/or edges have attributes (e.g. names). Centrality is an important indicator in network analysis, and is used to measure the degree to which network structure contributes to the importance of a node in a network. Since the word "importance" has wide number of meanings, many different definitions of centrality are proposed. Commonly used three centralities – specifically, degree centrality, betweeness centrality and closeness centrality – were considered in this study.

## 3 Cases

Two cases concerning different scales of water-energy-food nexus are used in this study. Wa'el et al (2017) conducted a research of water-energy-food nexus using system dynamics and focus on household scale. Akhtar et al (2013) develop a system dynamics model called ANEMI_2 for society-biosphere-climate-economy-energy nexus and focus on global scale. These two cases involved 47 and 214 elements, respectively.

## 4 Results

The causal-loop diagrams of the two cases are firstly transformed as two networks by treating the system elements as nodes and the relations between nodes as edges of which. The adjacent matrix of the networks is then established and the corresponding network is formulated. The three centrality index (normalized) are calculated for each node of the network and are shown in Fig.4. As can be seen from Fig.1, some nodes has greater values on one centrality index while smaller values on the others. In order to judge the importance of the nodes, a non-dominated sorting is applied on the nodes and sorts the nodes in accordance with the Pareto dominance. The nodes are categorized into different levels. According to the non-dominated concept, nodes within the same level are considered as equal i.e. the same important. The important elements of the two nexus are identified based on the network centrality index. Those elements are either have more connections i.e. greater degree centrality or locate on more strategic positions i.e. greater betweeness centrality or more independent i.e., greater closeness centrality.

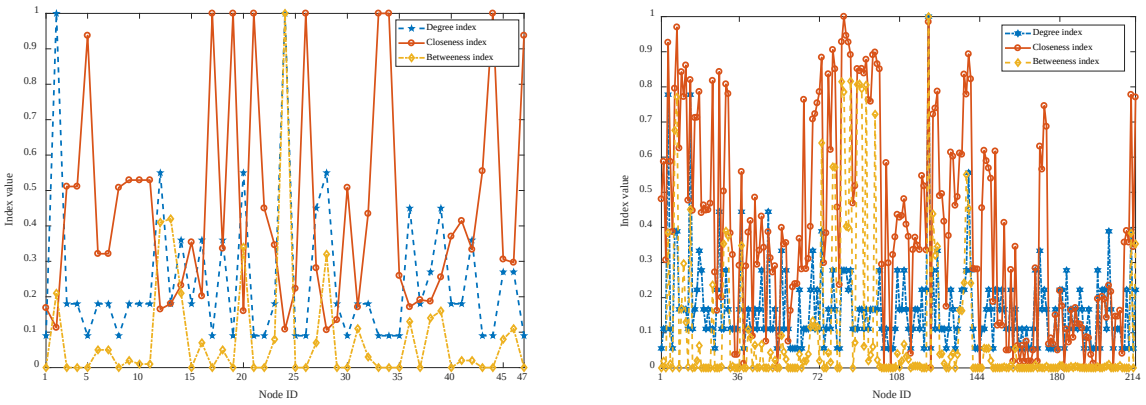


Fig.1 Three centrality index for each node of (a) Water-energy-food nexus at household and (b) Society-biosphere-climate-economy-energy at global

## 5 Conclusions

The study proposed an approach which couples causal-loop of system dynamics and centrality of network analysis. The proposed approach used three network centrality indices to identify the key system elements of complex water-energy-food nexus, rather than empirical judgement. The importance of the nodes in two nexus i.e., water-energy-food at house hold scale and society-biosphere-climate-economy-energy nexus at global scale are ranked base on non-dominance sorting. The resultant prioritized variable list not only provides insight of the complex nexus but also offers a chance for dimension reduction of the problem.

## Reference

[1] Akhtar, M. K., Wibe, J., Simonovic, S. P., & MacGee, J. (2013). Integrated assessment model of society-biosphere-climate-economy-energy system. Environmental modelling & software, 49, 1-21.

[2] Wa'el A, H., Memon, F. A., & Savic, D. A. (2017). An integrated model to evaluate water-energy-food nexus at a household scale. Environmental Modelling & Software, 93, 366-380.

**Theme:** Water – Energy – Food nexus
**IAHR Thematic Priority Area:** [TPA-2] Water for the Energy Transition Food Security and Nature
https://doi.org/10.3850/iahr-hic2483430201-193

# An Integrative Analytical Framework of Water-Energy-Food Security for Sustainable Development at the Country Scale: A Case Study of Five Central Asian Countries

**Lingang Hao [1,2,3], Ping Wang [2,3], Jingjie Yu [2,3], Hongwei Ruan [3]**

[1] Yellow River Institute of Hydraulic Research, Zhengzhou, Henan, China
[2] Key Laboratory of Water Cycle and Related Land Surface Processes, Institute of Geographic Sciences and Natural Resources Research, Chinese Academy of Sciences, Beijing, China
[3] University of Chinese Academy of Sciences, Beijing, China

*Corresponding author: Jingjie Yu (yujj@igsnrr.ac.cn)*

**Abstract.** Thoroughly understanding the security of water, energy and food (WEF) and the factors that influence them is essential for sustainable development management in any region. This study proposed a new analytical framework for WEF security evaluation in both individual sectors and the whole system, using the technique for order preference by similarity to an ideal solution (TOPSIS) and four dimensions of security indicators: availability, self-sufficiency, productivity and accessibility. The internal relationships among the three sectors and the main factors influencing WEF security were analysed by Spearman's rank correlation and radar graphs, respectively. The five countries in Central Asia (CA), which are experiencing WEF crises and facing great challenges in achieving their sustainable development goals (SDGs), were chosen as a case study in this paper. Our results showed that Kazakhstan attained the highest WEF security level, followed by Kyrgyzstan, Turkmenistan and Uzbekistan; Tajikistan exhibited the lowest security level from 2000-2014. Three types of internal relationships among the three sectors were identified: synergies, trade-offs and unclassified. The unclassified relationship type accounted for the largest share of 54% in CA, suggesting great potential for synergetic improvement among the three sectors. Approaches for improving the country WEF security based on our research are as follows: Kazakhstan should prioritize food allocation and supply, Kyrgyzstan and Tajikistan should increase energy and food production and raise the supply level and usage efficiency of water and food, Turkmenistan should increase the available water resources and food production and improve the supply level and usage efficiency of water and energy, and Uzbekistan should both increase the available amount and enhance the WEF management performance.

**Keywords:** Central Asian countries, Integrated method, Resource security, Sustainable development, Water-energy-food nexus

## 1 Introduction

However, there is still no sufficient integrative analysis of WEF security and the relationships among the three sectors globally, and studies related to factors that reduce WEF security and methods to improve WEF security are lacking (Albrecht et al., 2018; Putra et al., 2020). These limitations hinder the management and improvement of the WEF security nexus and associated SDGs at the country scale in data limited regions. To fill the research gaps, this study develops an assessment indicator system for WEF security and a hybrid framework that integrates the technique for order preference by similarity to an ideal solution (TOPSIS), Spearman's rank correlation and radar graphs to systematically analyse WEF security at the country scale.

## 2 Methods

The proposed evaluation framework of WEF security comprises three main phases.

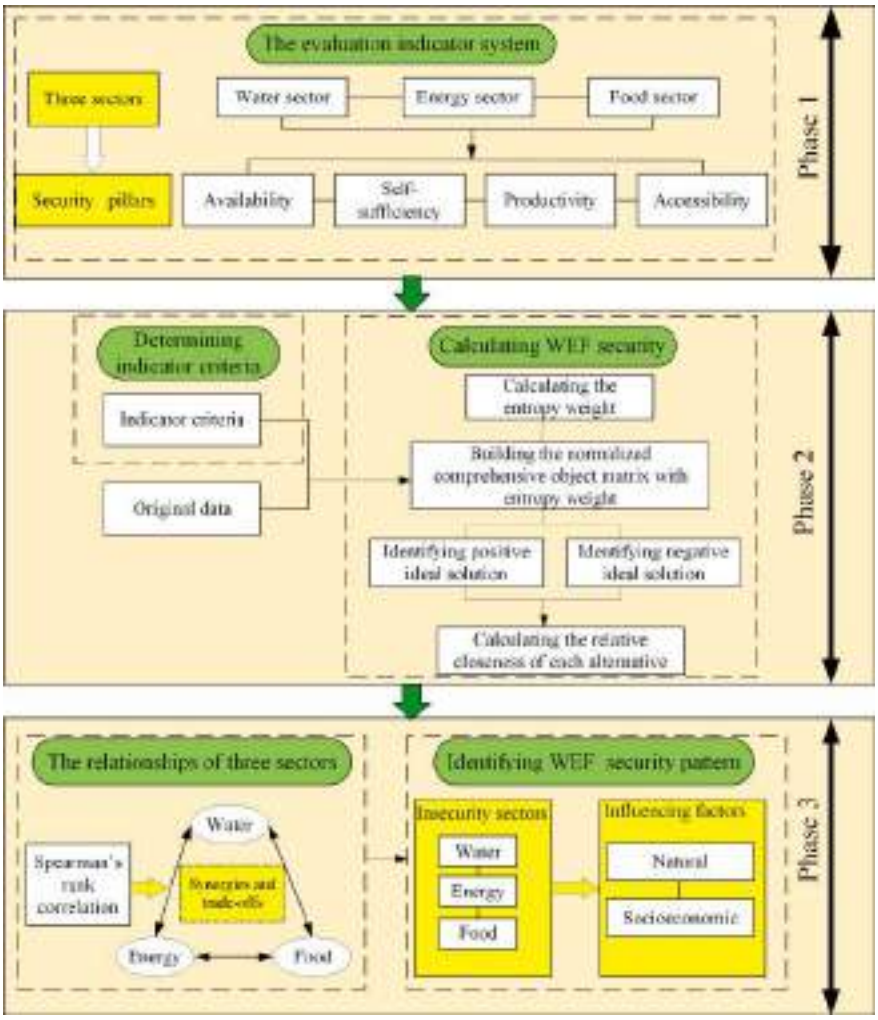


Figure 23 Flowchart for integrative analysis of WEF security.

## 3 Results

Regarding the water sector, the security degree in the five CA countries revealed a steady or slight increase, except for Kazakhstan. In the energy sector, Kazakhstan and Turkmenistan attained significantly higher security degrees than Tajikistan, Turkmenistan, and Uzbekistan. In the food sector, the change trends varied significantly among the five CA countries. Food security fluctuated significantly more than water and energy security. We observed the same shares of synergies and trade-offs among the three sectors in CA and the largest share of unclassified relationships, accounting for 54% of all relationships.

## 4 Conclusion

Our results indicated that WEF security and the degree of security in the three sectors exhibited steady trends, continuous increasing and decreasing trends, and fluctuating increasing and decreasing trends within the five CA countries. Moreover, the water sector was the most critical variable regarding WEF security in CA, which was verified by the fact that water insecurity poses a threat not only to upstream water resource-rich countries (Tajikistan and Kyrgyzstan) but also to downstream water resource-poor countries (Turkmenistan, Uzbekistan and Kazakhstan).

## 5 References

[1] Albrecht, T.R., Crootof, A., Scott, C.A., 2018. The Water-Energy-Food Nexus: A systematic review of methods for nexus assessment. Environ. Res. Lett. 13 (4), 043002.

[2] Putra, M.P.I.F., Pradhan, P., Kropp, J.P., 2020. A systematic analysis of Water-EnergyFood security nexus: A South Asian case study. Science of The Total Environment 728, 138451.

**Theme:** Water – Energy – Food nexus
**IAHR Thematic Priority Area:** [TPA-2] Water for the Energy Transition Food Security and Nature
https://doi.org/10.3850/iahr-hic2483430201-195

# Utilization Of Water Conserved by Renewable Substitution for Thermal Power: Adaptive Reservoir Operation and Incremental Benefits

**Haixing Gou[1, 2], Chao Ma[1, 2, *]**

[1] State Key Laboratory of Hydraulic Engineering Simulation and Safety, Tianjin University, Tianjin 300072, China
[2] School of Civil Engineering, Tianjin University, Tianjin 300072, China

*Corresponding author: mac_tju@tju.edu.cn*

**Abstract.** The interprovincial transmission of clean energy has replaced the traditional water intensive thermal power, resulting in water savings in the power-receiving areas. To further utilize the water savings to generate the incremental benefits, a general model framework is proposed to quantify the saved water and reallocate it to cope with emergency events and promote hydropower based on reservoir reoperation. The incremental benefits and optimal reallocation mode of the water savings have been revealed through a case study in Henan Province. The results indicate an annual water savings of 175.160 million $m^3$ in Henan Province due to renewable substitution, which contributes to an increase in hydropower generation and emergency water supply ranging from 14.584 GWh to 32.267 GWh and 0 to $1.724 \times 10^8$ $m^3$, respectively, under different hydrological scenarios. To boost the incremental benefits of water savings, the source reservoir is suggested to prioritize the emergency water supply in dry years and enhance hydropower generation in wet years. The general framework can be extended to other energy-water systems to assess incremental benefits and propose adaptive reservoir reoperation schemes, which provides new insights into water management from the perspective of renewable energy substitution.

**Keywords:** Emergency water supply, Incremental benefits, Renewable energy substitution, Water saving reallocation

## 1 Introduction

To address the mismatch between resource endowment and load centers in China, abundant renewable energy has been increasingly transmitted across geographical boundaries. This changes the energy structures in eastern power-receiving provinces in China, where thermal power dominates the power structure. Given that thermal power dependent on coal is water-intensive [1], renewable energy substitution for thermal power (RST) will create indirect benefits of water savings [2]. Despite a preliminary exploration with regard to the water conservation of renewable penetration [3], there has been little discussion about reallocation of the water savings through associated water conservancy projects. Therefore, a novel framework based on reservoir operation model is constructed to adaptively reallocate the water savings and provide new solutions for ensuring the emergency water supply and promoting hydropower.

## 2 Material and methods

The reservoir benefits will be enhanced when additional water is preserved and further reallocated by the reservoir. As shown in Fig. 1, a general model framework is proposed to incorporate the quantification of the water saved by RST into a reservoir operation model to realize optimal water saving reallocation, which is solved by nondominated sorting genetic algorithm II.

The thermal power-dominated Henan Province was chosen as the case study. A large amount of clean electricity is replacing thermal power in Henan Province. Water demand reduction in Henan Province resulted from RST would affect the operation of the source Danjiangkou (DJK) reservoir.

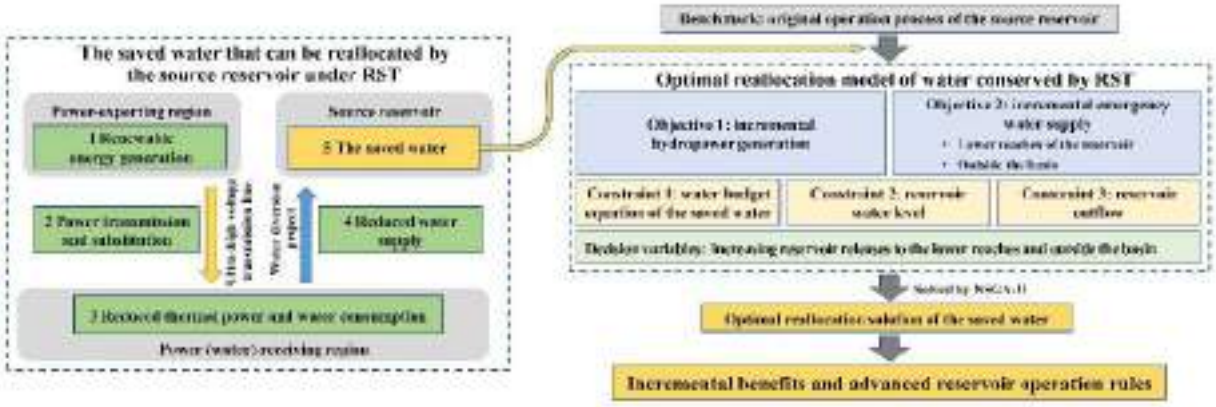


**Fig. 1.** General framework for optimal reallocation of water conserved from RST.

## 3 Results and discussion

An annual 175.160 million $m^3$ of water would be conserved by RST and further reallocated by the DJK reservoir. The reallocation of the water savings can simultaneously create the benefits of hydropower generation as well as emergency water supply. With optimal reallocation of the water savings under RST, the net increments of the emergency water supply under five different hydrological scenarios are $1.139 \times 10^8$ $m^3$, $1.711 \times 10^8$ $m^3$, $1.724 \times 10^8$ $m^3$, $0.515 \times 10^8$ $m^3$ and $0.445 \times 10^8$ $m^3$, respectively. The benefits of the emergency water supply are relatively large in scenarios with dry inflow and low initial water level, and almost all the saved water is used to meet the emergency demand. This is because the reservoir can maintain a lower water level, providing adequate capacity for preserving additional water. In addition, water conserved in reservoirs raises the water level and enhances hydropower generation. The net increments of hydropower generation are equivalent to 0.276%-0.329% of the annual average power generation of the DJK reservoir.

To maximize the incremental benefits, the source reservoir should adopt different operation schemes. In years with deficient inflow and reservoir storage, the source reservoir should discharge the water savings downstream to prioritize the emergency water demand during the summer flood season. After that, the reservoir can conserve the surplus water savings across years with low flood risk. In years with abundant inflow, downstream emergency water demands can be normally met. The water savings should be discharged for power generation before the autumn flood season to avoid water abandonment.

## 4 Conclusions

This paper proposed a novel framework for quantification and reallocation of water savings caused by RST. The method was applied to an energy-water system centred on Henan Province, China. The results show that by adaptively utilize the water savings caused by RST, the source reservoir can create incremental benefits of hydropower and emergency water supply. And the source reservoir is suggested to ensure emergency water supply in dry years and enhance hydropower in wet years. The conclusions guide the reservoir in making better use of the water savings under renewable penetration.

## Reference

[1] Feng, K., et al., The energy and water nexus in Chinese electricity production: A hybrid life cycle analysis. Renewable & Sustainable Energy Reviews, 2014. 39: p. 342-355.

[2] Li, M.Q., et al., Water conservation from power generation in China: A provincial level scenario towards 2030. Applied Energy, 2017. 208: p. 580-591.

[3] Johst, M. and B. Rothstein, Reduction of cooling water consumption due to photovoltaic and wind electricity feed-in. Renewable & Sustainable Energy Reviews, 2014. 35: p. 311-317.

**Theme:** Water – Energy – Food nexus
**IAHR Thematic Priority Area:** [TPA-2] Water for the Energy Transition Food Security and Nature
https://doi.org/10.3850/iahr-hic2483430201-197

# Integrated Assessment of Crop Planting Suitability: A Case Study in the Hetao Irrigation District of China Using HJ-1A/1B satellite data

**Bing Yu[1], Songhao Shang[2 *], Jiaye Li[1]**

[1] Guangdong Provincial Key Laboratory of Intelligent Disaster Prevention and Emergency Technology, Dongguan University of Technology, Dongguan, 523808, China
[2] State Key Laboratory of Hydroscience and Engineering, Tsinghua University, Beijing, 100084, China

*Corresponding author: Prof. Songhao Shang, shangsh@tsinghua.edu.cn*

**Abstract.** Addressing the challenges posed by land and water resource constraints, the attainment of the Sustainable Development Goal of zero hunger by 2030 remains a crucial challenge. A key aspect in achieving this goal is determining the appropriate planting pattern for various crops to enhance regional-scale crop water productivity with limited water available for irrigation. However, current researches on remote sensing-based assessments of regional crop water productivity and planting suitability are still limited. In this study, we present a satellite-based integrated approach to assess crop planting suitability, aiming to enhance regional crop water productivity. Focusing on the Hetao Irrigation District (HID), a representative irrigation district in arid region of China, we use remote sensing data (HJ-1A/1B) to estimate crop water productivity for maize and sunflower within the HID from evapotranspiration and yield estimates. Additionally, we introduce a novel crop planting suitability index based on the frequency distribution of crop water productivity. These indices can be used to determine appropriate crop planting distribution. The proposed method can be applied in irrigation district or regional scale, and the results offer valuable insights for local governments in decision-making to maximize regional crop water productivity.

**Keywords:** Crop distribution optimization; Crop planting suitability; Hetao Irrigation District; Remote sensing; Water productivity

## 1 Introduction

Climate change and population growth are contributing to a substantial surge in human demand for food. Projections suggest that by 2050, global food demand is expected to increase by at least 50% compared to the baseline level in 2005/2007 [1-2]. This escalating demand poses a great challenge in achieving the Sustainable Development Goal of zero hunger by 2030 (SDG 2) for on the whole globe. Thus, enhancing crop production with limited and decreasing water available for irrigation remains a pivotal scientific issue in the 21st century [3].

- Expanding cropland area and increasing crop yield per unit planting area are two approaches for enhancing crop production [4]. The former is often deemed unsustainable and the latter is an effective measure to boost crop yield.
- Prioritizing the cultivation of crops with higher water productivity in a specific grid cell can lead to improved water productivity across the entire district [5]. The accurate estimation of crop water productivity has become a crucial foundation for constructing the crop planting suitability index (CPSI).
- In recent years, remote sensing data has been extensively applied to the large-scale monitoring of agriculture due to its convenient acquisition and widespread coverage [6-7]. However, research on the estimation of crop water productivity (CWP, defined as the ratio of crop yield to water consumption during crop growing season) relying entirely on remote sensing data

remains relatively limited, especially in arid irrigated areas with the cross-cultivation of different crops.

The main objective of this study is to develop a CPSI from remote sensing-based CWP estimation, which is used to optimize the spatial distribution of major crops in the Hetao Irrigation District (HID), a representative irrigation district in arid region of the upper Yellow River Basin. Using HJ-1A/1B remote sensing data as our primary input, we conduct a comprehensive assessment of the planting suitability for major crops, including maize and sunflower, within the HID.

## 2 Results

In this study, we develop an integrated satellite-based approach to assess crop planting suitability, with the aim of enhancing regional-scale crop water productivity. Specifically, we construct planting suitability indices for two major crops, maize and sunflower, in the Hetao Irrigation District (HID). Initially, we estimate the water productivity of these crops by utilizing remotely sensed data to derive crop yield and water consumption during the growing season. Subsequently, we introduce an innovative method based on the frequency distribution of crop water productivity to construct crop planting suitability indices. Finally, the optimization of crop planting distribution (Figures 1 and 2), based on the planting suitability indices for both crops, facilitate the improvement of regional-scale crop water productivity.

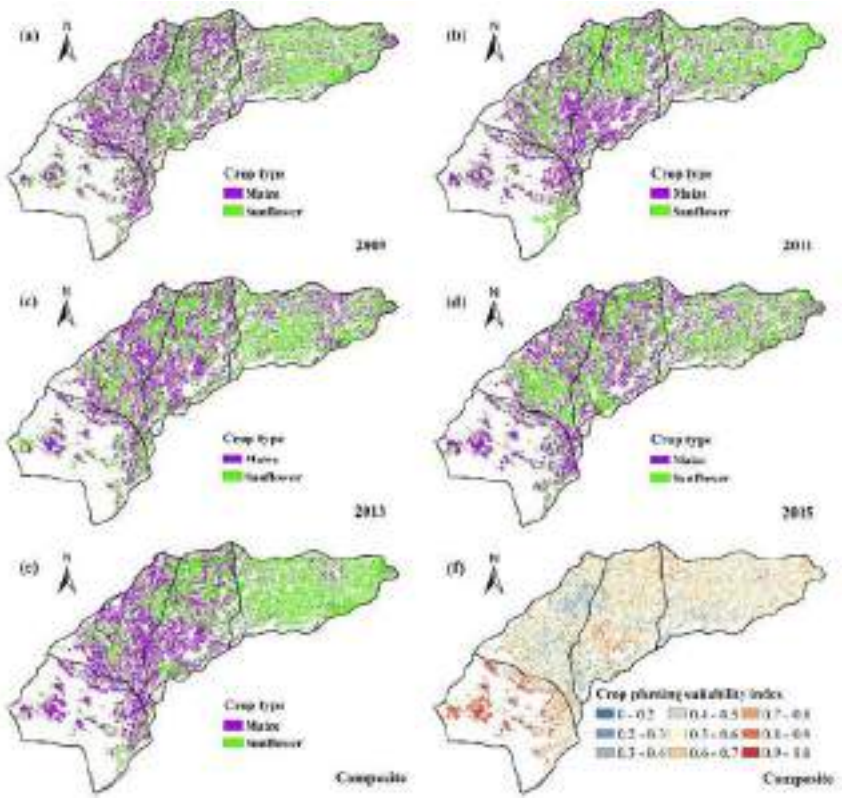

Figure 24 Suitability maps for maize and sunflower planting under the condition that all fields exclusively cultivate these crops. (a-d) Annual distribution maps (2009, 2011, 2013, 2015). (e) Composite planting distribution. (f) Corresponding composite planting suitability index.

Through a comparison of the distribution of suitable and unsuitable grid cells for maize and sunflower planting from 2009 to 2015, the suitable planting area for maize increases from 21% in 2009 to 43% in 2015, and for sunflower, it increases from 31% to 46%. The spatial distribution reveals a cross-distribution pattern for suitable and unsuitable crop planting. Following the optimization of crop planting distribution, the multi-year average growth percentages of water productivity for maize and sunflower at the regional scale are 7.6% and 5.0%, respectively.

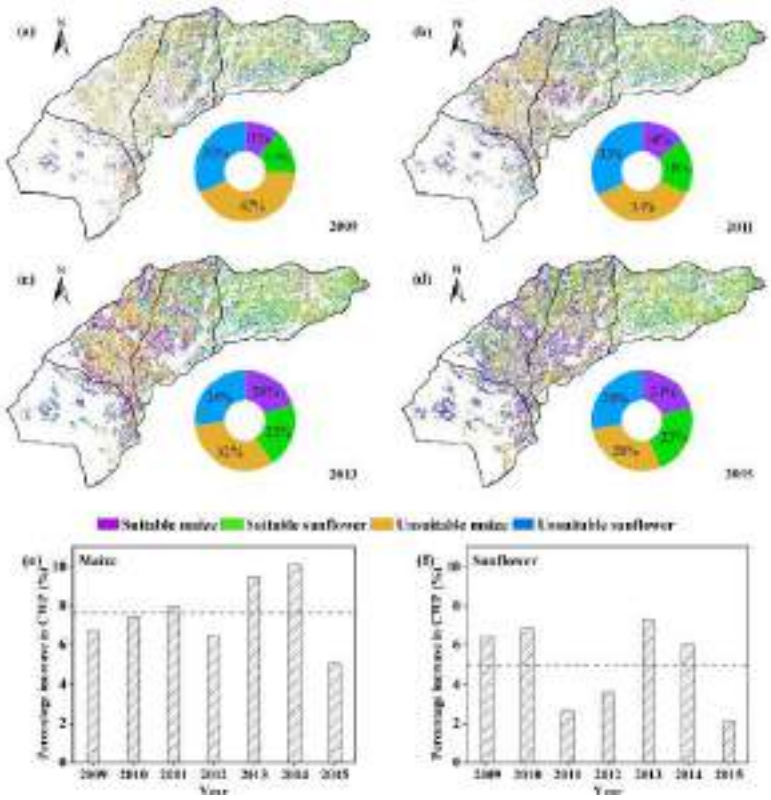

Figure 2 Comparisons between the actual distributions of crop planting and the optimal planting distributions in 2009, 2011, 2013, and 2015 (a-d), along with the resulted increments in crop water productivity (e-f).

This study assesses the planting suitability of major crops in a typical arid irrigation district in China from the perspective of crop water productivity. Diverging from existing studied [8], this study avoids delving into factors affecting crop water productivity, such as soil properties and groundwater levels, which are challenging to obtain. Employing a results-oriented approach, our study not only presents a distinctive perspective but also introduces a method with robust applicability.

## Reference

[1] Alexandratos, N. and Bruinsma, J., World Agriculture towards 2030/2050: The 2012 Revision, Food and Agriculture Organization of the United Nations (FAO), Rome, Italy, 2012.

[2] Beltran-Pena, A., Rosa, L. and D'Odorico, P., Global food self-sufficiency in the 21st century under sustainable intensification of agriculture. Environ Res Lett, 15 (2020) 095004.

[3] Kang, S., Hao, X., Du, T., Tong, L., Su, X., Lu, H., Li, X., Huo, Z., Li, S. and Ding, R., Improving agricultural water productivity to ensure food security in China under changing environment: From research to practice. Agr Water Manage, 179 (2017) 5-17.

[4] Rosa, L., Adapting agriculture to climate change via sustainable irrigation: biophysical potentials and feedbacks. Environ Res Lett, 17(2022) 063008.

[5] Xue, J. and Ren, L., Evaluation of crop water productivity under sprinkler irrigation regime using a distributed agro-hydrological model in an irrigation district of China. Agr Water Manage, 178 (2016) 350-365.

[6] Bandaru, V., Yaramasu, R., Pnvr, K., He, J., Fernando, S., Sahajpal, R., Wardlow, B., Suyker, A. and Justice, C., PhenoCrop: An integrated satellite-based framework to estimate physiological growth stages of corn and soybeans. Int J Appl Earth Obs, 92(2020) 102188.

[7] Weiss, M., Jacob, F. and Duveiller, G., Remote sensing for agricultural applications: A meta-review. Remote Sens Environ, 236 (2020) 111402.

[8] Ren, D., Xu, X., Engel, B., Huang, Q., Xiong, Y., Huo, Z. and Huang, G., A comprehensive analysis of water productivity in natural vegetation and various crops coexistent agro-ecosystems. Agr Water Manage, 243 (2021) 106481.

**Theme:** Climate change impacts
**IAHR Thematic Priority Area:** [TPA-1] Climate Change Adaptation and Mitigation
https://doi.org/10.3850/iahr-hic2483430201-200

# Historical Trends and Future Projections of Annual Rainfall from CMIP6 Models in Ho Chi Minh City, Vietnam

**Dang Nguyen Dong Phuong[1, 2]**

[1] Department of Civil and Environmental Engineering, Seoul National University, Seoul, 08826, Republic of Korea
[2] Research Center for Climate Change, Nong Lam University Ho Chi Minh City, Ho Chi Minh City, 700000, Vietnam

*Corresponding author: dangnguyendongphuong@gmail.com*

**Abstract.** Climate risks have posed a major threat to local communities settling in worldwide low-lying coastal megacities, including Ho Chi Minh City, Vietnam. Hence, this study first aimed to contribute towards a comprehensive understanding of temporal trend patterns of annual rainfall and absolute extremes through multi-temporal trend tests. This study further employed the quantile delta mapping method to develop daily bias-corrected rainfall data based on the outputs in the latest CMIP6 under eight shared socio-economic pathway (SSP) greenhouse gas emission scenarios. Evaluation of model performance was implemented by repeatedly leaving successive five years out in turn for estimating testing errors. The outcomes imply the high applicability of well-calibrated transfer functions, even for high quantiles, to the production of future rainfall scenarios. The projected changes in annual rainfall and absolute extremes were obtained by estimating multi-model medians from CMIP6 models for future periods with reference to the base period (1995-2014). Generally, annual rainfall in Ho Chi Minh City is projected to increase substantially, and Thu Duc station is consistently responsible for the highest increases in annual rainfall, with the projected changes being approximately 30.9% (8.3 - 77.8%) under the high-end scenario (i.e., SSP5-8.5) by the end of the twenty-first century.

**Keywords:** Ho Chi Minh City, Multiple trend tests, Quantile delta mapping, Rainfall projections, Temporal trend patterns, Trend-preserving bias correction

## 1 Introduction

Human-induced climate change has already caused substantial losses and damages to almost all bio-physical systems on the planet, and the extent of adverse impacts is documented disproportionately across all sectors and regions. Ho Chi Minh City, Vietnam's most developed urban area, is facing numerous complex and multifaceted issues due to climate-related risks. Thus, there is an urgent demand for a better understanding of historical and future changes in climatic variables in order to advance more viable countermeasures to mitigate the threat of climate extremes to the local community in Ho Chi Minh City.

## 2 Material and methods

The present study employed multiple non-parametric statistical trend tests [1, 2] to clarify the nature of temporal changes in annual rainfall and absolute extremes in Ho Chi Minh City.

The quantile delta mapping (QDM) algorithm [3], designed to explicitly preserve relative changes in all quantiles of the distribution of simulated rainfall from a considered climate model, was applied to construct future daily rainfall in Ho Chi Minh City under a wide range of SSP-based scenarios of CMIP6 GCMs.

## 3 Results and Discussion

The outcomes from multi-temporal trend analysis reveal that 12 rainfall sites in Ho Chi Minh City exhibited heterogeneous patterns of annual rainfall and absolute extremes, including a preponderance of either increases or decreases, a mixed pattern of alternating increases and decreases, or even an abrupt reversal in trend directions. The findings also underpin the superiority of the multiple trend tests over the traditional application of a single trend test for the sake of hydro-meteoro-climatological trend analysis.

Annual rainfall in Ho Chi Minh City is anticipated to increase under most greenhouse gas emissions scenarios for the near to far future periods. Moreover, the projections of annual rainfall in Thu Duc station consistently exhibit higher increases than those for the remaining rainfall stations. For example, under the high-end scenario (i.e., SSP5-8.5) for the long-term period (2081-2100), annual rainfall in Thu Duc station is projected to exhibit the highest increase, with the estimates of the multi-model median (uncertainty range) being approximately 30.9% (8.3% to 77.8%). Moreover, extreme rainfall events in Ho Chi Minh City are expected to become more intense under almost all future scenarios, and the climate change signals for the Rx5day are substantially higher than those for the Rx1day and annual rainfall. The highest increases in the multi-model median of Rx1day and Rx5day are estimated at around 40.1% for Thu Duc station and 80.4% for Cat Lai station, respectively, under the SSP5-8.5 scenario by the year 2100.

## 4 Conclusions

To shed light on temporal trend possibilities of annual rainfall and extreme rainfall absolute indices (i.e., Rx1day and Rx5day) in 12 rainfall stations evenly distributed over Ho Chi Minh City, the present study employed the multiple non-parametric statistical trend tests with various beginning and ending years for all possible periods of at least ten years in length during the entire analyzed period (1980-2022). In order to provide future rainfall projections in Ho Chi Minh City, the present study applied a trend-preserving bias correction technique, namely quantile delta mapping (QDM), to raw CMIP6 GCM models to generate bias-corrected rainfall time series for the near to far future periods under a wide range of potential worldwide greenhouse gas emissions, including five high-priority scenarios (i.e., SSP1-1.9, SSP1-2.6, SSP2-4.5, SSP3-7.0, and SSP5-8.5) and three additional ones (i.e., SSP4-3.4, SSP4-6.0, and SSP5-3.4).

It is acknowledged that urban flooding in Ho Chi Minh City is exacerbated by the combined impacts of sea level rise, heavy rainfall, and inadequate drainage capacity. This urgent issue gives rise to various adverse corollaries to the daily activities of the local community. Therefore, there is the expectation that the outcomes from this study could be directly fed into a wide range of impact models in order to quantify the potential impacts of climate change on diverse aspects of the local community in Ho Chi Minh City, e.g., urban flooding management, drainage system design, among other pressing urban planning activities reacting to climate-related risks.

## Reference

[1] G.J. McCabe, D.M. Wolock, A step increase in streamflow in the conterminous United States, Geophys. Res. Lett. 29 (2002) 38-31–38-34.

[2] Z. Zhang, A.D. Dehoff, R.D. Pody, New approach to identify trend pattern of streamflows, J. Hydrol. Eng. 15 (2010) 244–248

[3] A.J. Cannon, S.R. Sobie, T.Q. Murdock, Bias correction of GCM precipitation by quantile mapping: how well do methods preserve changes in quantiles and extremes?, J. Clim. 28 (2015) 6938–6959

**Theme:** Climate change impacts
**IAHR Thematic Priority Area:** [TPA-1] Climate Change Adaptation and Mitigation
https://doi.org/10.3850/iahr-hic2483430201-202

# Simpcce: A Software Tool to Analyze Reservoir Inputs Under Climate Change

**Salvador Navas[1], Manuel del Jesus[1]**

[1] Instituto de Hidráulica Ambiental "IHCantabria", Universidad de Cantabria, Santander, Spain

*Corresponding author:manuel.deljesus@unican.es*

**Abstract.** As a result of climate change and global warming, precipitation and temperature patterns are expected to be altered in many regions worldwide, leading to changes in the water cycle. These hydrological dynamics' disruption may decrease minimum reservoir inflows during low precipitation periods, significantly affecting reservoir operations and the demands they meet. Hence, conducting climate change studies becomes imperative to understand potential water resource evolution and devise adaptive strategies to mitigate climate change effects on reservoirs. Recent regional climate change studies in Spain underscore the importance of ensuring that all information derived from these studies is easily accessible. Consequently, the SIMPCCe tool (https://github.com/IHCantabria/SIMPCCe) has been developed and presented in this work as a supplement to the "Methodological Guide for Estimating Minimum Reservoir Inflows in the Context of Climate Change." This tool implements the methodology outlined in the guide, allowing for straightforward assessment of climate change effects on reservoir water availability.

**Keywords:** Climate Change, Artificial Neural Networks, Reservoir management, Water management

## 1 The SIMPCCe application

The SIMPCCe application is a tool developed in Python that serves as a complement to the guide to minimum contributions to reservoirs. With this application, from a given location on the river network, it is possible to make climate change forecasts of the contributions. The analysis is based on the download of information from official sources in order to build and train a regression model based on neural networks that allows the reproduction of the series of contributions at a point in the river network from climatic data on a monthly scale (precipitation and temperature). Once the neural network has been trained and through climate change data, it is possible to obtain forecasts of contributions in the future.

The application consists of 5 different modules:

1. Downloading information.
2. Configuration of the contributing basin to the given point.
3. Training a Neural Network for Flow Prediction
4. Correcting bias in climate change models
5. Simulation and analysis of climate change scenarios

Each of these modules is described below.

### 1.1 Downloading information

The first step that must be carried out in any study of the impact of climate change is to obtain the sources of information that allow the study to be carried out, both for the historical period (also called the control period), and to analyze future scenarios of climate change. The SIMPCCe application automatically downloads the following climatic and hydrological data for analysis:

- Database SPAIN02 v5 version, which provides monthly precipitation and temperature data for the period 1950 to 2015 in a regular grid of 0.1º (~10km) resolution (Herrera et al., 2012)
- Results of contributions in spatial format of the SIMPA hydrological model provided by the Center for (CEDEX 2019) Hydrographic Studies of CEDEX.
- Data from climate forecasts for the 21st century in Spain, carried out by AEMET of the CORDEX project at monthly temporary resolution for RCP45 and RCP85.

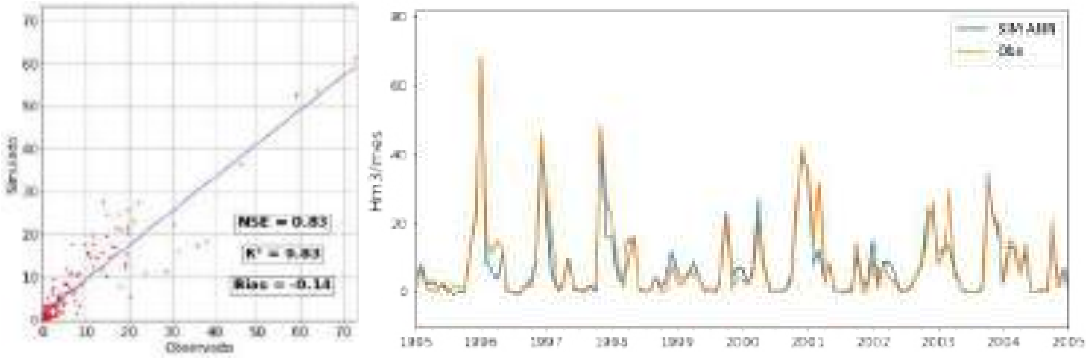


Figure 25 Validation of ANN produced results. Left-hand side, validation statistics. Right-hand side, time series comparison.

### 1.2 Configuration of the contributing basin to the given point

From the coordinates of the point where the study dam is located, the contributing basin is delimited through the geomorphological properties that can be obtained from a digital model of the terrain incorporated in the application. In addition to the definition of the contributing basin, the application establishes a mesh of distributed points where the climatic data (predictors - variables from which it is predicted) are extracted in order to train the neural network and at the drainage point of the basin defined by the user, the series of SIMPA inputs (predicting - variable that is predicted) is extracted. The application also allows the user to establish their own series of monthly contributions different from that of SIMPA in order to train the neural network.

### 1.3 Training a Neural Network for Flow Prediction

The SIMPCCe application uses a neural network-based regression algorithm (ANN) that feeds into data from the SIMPA model, allowing predictions to be made without using the hydrological model explicitly. This is possible due to the monthly time resolution that is established in the methodology. The use of regression algorithms facilitates the iterative calibration process, as this process is performed automatically and accurately. The choice of the ANN algorithm over those that appear in bibliographic sources is mainly due to the computational time needed to adjust the models and the high predictability achieved in the contributions. The way to train or calibrate a neural network model is through finding the best parameter settings to minimize or maximize the desired metric. The tools developed in this guide try to maximize the coefficient of determination ($R^2$), maximize the Nash-Sutcliffe coefficient (NSE) and minimize the percentage of bias (PBIAS). Figure 1 shows an example of the goodness-of-fit analysis of a neural network trained to reproduce the inputs in a reservoir.

### 1.4 Correcting bias in climate change models

One of the main drawbacks of GCMs/RCMs climate forecasts is that they cannot be used directly in hydrological applications in basins, as they have very significant biases. It is therefore important to reduce the scale of global or regional models through bias correction, using basin-distributed reference series. There are several methods of bias correction, however, the methodology followed

by the application uses the SDM quantile mapping method Scaled Distribution Mapping (Cannot et al. 2015). The choice of this method is due to the fact that it takes into account the frequency of rainy days (for precipitation) and the probability of events, and because it is not necessary to rely on the invalid assumption of stationarity.

### 1.5 Simulation and analysis of climate change scenarios

As mentioned above, the main objective of the application is to analyse the vulnerability of reservoirs, understanding the reduction of contributions to reservoirs as a threat. Once the series of inputs for the different climate change scenarios have been obtained, it is necessary to carry out a statistical analysis to assess the influence of climate change on the inputs in the study reservoirs.

The application allows us to obtain time series of inputs for each climate change model and scenario and, in addition, in graphical form provides an accurate statistical analysis to help the operator in decision-making.

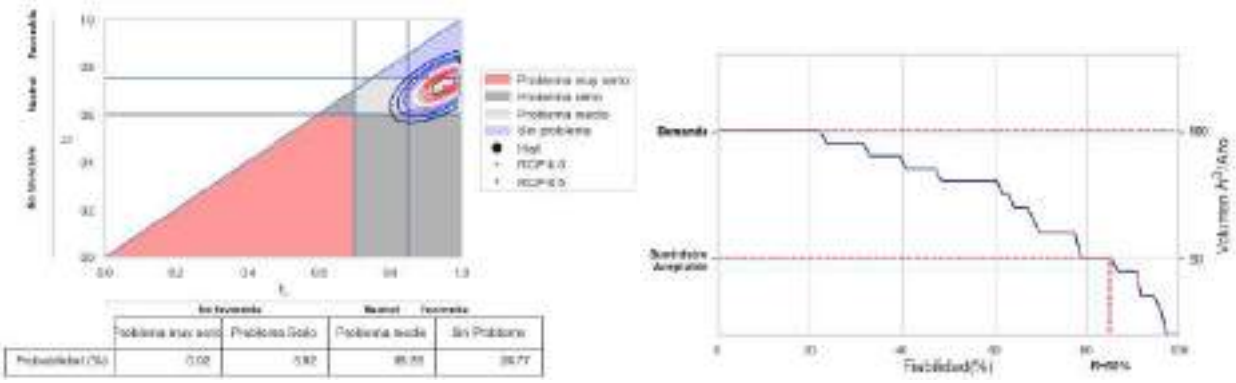

Figure 2 Example of a decision-making analysis based on the results provided by SIMPCCe.

## 2 Example use for decision-making

As mentioned above, the result of the analysis proposed in this guide allows us to obtain series of future contributions, and from the management models, to convert them into series of demand-dependent supplies for different climate change scenarios. With the series of supplies provided by a reservoir, it is possible to identify the reliability indices, and in turn, the associated risk for the climate change scenario and model considered. From these data, a probability envelope can be elaborated through the multivariate normal distribution associated with a set period of time, for example 2041-2070, and calculate the probability that the reservoir may have each of the defined problem types as shown in Figure 2.

This type of analysis, together with the reservoir management model that is available, makes it possible to propose adaptation measures that reduce the risk of presenting serious and very serious problems, simulating each of them together with the series of inputs obtained through the methodology proposed in this guide. In this case, the measures that can be proposed may be more "harsh", for example, carrying out reservoir increases, establishing new rules for the operation of reservoirs or carrying out a reordering of demands.

## 3 Conclusions

Data-based modelling, like the one presented in this work, based on the use of artificial neural networks (ANN), is an interesting approach for preliminary analysis for decision-makers in water

related problems. Data-based models are lightweight, once calibrated, and can be used to easily explore a plethora of scenarios, which may reinforce the robustness of the decisions made.

SIMPCCe is a very simple tool that allows to work with public databases or observed time series to generate future river discharges and water availability for different purposes. Combined with statistics, it allows to provide statistical responses to the most common management questions, which in turn, may serve to make risk-optimal decisions.

Although SIMPCCe has been originally developed for Spain, it can make use of data from anywhere. Moreover, as it is an open-source tool, it can be modified and adapted to work with the data structures of the national databases of any other country, so it is a small effort away from being used to tackle problems anywhere on the globe.

**Reference**

[1] Cannon, A. J., Sobie, S. R., & Murdock, T. Q. (2015). Bias correction of GCM precipitation by quantile mapping: How well do methods preserve changes in quantiles and extremes? Journal of Climate, 28(17), 6938–6959. https://doi.org/10.1175/JCLI-D-14-00754.1

[2] CEDEX. (2019). Evaluation of water resources in the natural regime in Spain (1940/41-2017/18). Article 157.

[3] Chávez-Jiménez, A., Lama, B., Garrote, L., Martín-Carrasco, F., Sordo-Ward, A., & Mediero, L. (2013). Characterisation of the Sensitivity of Water Resources Systems to Climate Change. Water Resources Management, 27(12), 4237–4258. https://doi.org/10.1007/s11269-013-0404-2

[4] Herrera, S., Gutiérrez, J. M., Ancell, R., Pons, M. R., Frías, M. D., & Fernández, J. (2012). Development and analysis of a 50-year high-resolution daily gridded precipitation dataset over Spain (Spain02). International Journal of Climatology, 32(1), 74–85. https://doi.org/10.1002/joc.2256

[5] Navas, S., del Jesus, M., & Gómez, D. V. (2022). Methodological guide for the estimation of minimum contributions to reservoirs in the context of climate change. Canal Foundation. https://www.fundacioncanal.com/docs/guia_embalses_cbio_climatico_FundCanal_2022.pdf

**Theme:** Climate change impacts
**IAHR Thematic Priority Area:** [TPA-1] Climate Change Adaptation and Mitigation
https://doi.org/10.3850/iahr-hic2483430201-206

# Future Hydrological Dynamics Under Climate Change in The Aa of Weerijs Catchment

**Muhammad Haris Ali[1,2], Claudia Bertini[1], Ioana Popescu[1,2], Andreja Jonoski[1] and Schalk Jan van Andel[1]**

[1] Department of Hydroinformatics and Socio-Technical Innovation, IHE Delft Institute for Water Education, 2601 DA Delft, The Netherlands
[2] Water Resources Section, Delft University of Technology, 2628 CD Delft, The Netherlands

*Corresponding author: h.ali@un-ihe.org*

**Abstract.** Catchments worldwide are experiencing hydrological changes due to the changing climate. Grasping the dynamics between climate change and catchment hydrology paves the way for better management practices. This research aimed to assess future water availability in the Aa of Weerijs catchment, in The Netherlands, by employing a hydrological model forced with meteorological projections for the 2050s. These meteorological projections are derived from the latest KNMI'23 climate scenarios and aligned with IPCC 2021's global projections. Results indicate a projected increase in average annual rainfall by 1.4% to 6.2% compared to the base period (2010-2019). However, owing to rising temperatures, projected increases in actual evapotranspiration (AET) are larger, ranging from 13.8% to 14.7%. As a result, hydrological components such as river discharge (Q), groundwater recharge (R) and baseflow (BF) are foreseen to experience negative effects. These projected changes exhibit seasonality and vary according to different climate scenarios. Overall, however, the negative impact of climate change on the hydrology of catchments is expected to be significant, particularly in terms of reduced average values of Q, R and BF during summer.

**Keywords:** Aa of Weerijs, climate change, hydrological modelling, KNMI'23 climate scenarios, MIKE-SHE

## 1 Introduction

Climate change is causing disruptions in spatio-temporal climatic patterns, resulting in shifts in the timing, frequency, and duration of hydrological extremes around the globe [1]. During the summer of 2018, a significant part of Europe experienced dry and hot weather conditions, primarily due to large-scale high-pressure climatic conditions. In the Netherlands, each month of the summer (June, July, August - JJA) was warmer and drier than usual, resulting in adverse effects on the hydrological cycle and elevated values of drought indicators [2]. Due to climate change, such weather incidents may happen in the future more often. In this study, we analysed the impact of projected climate change on the hydrology of the Aa of Weerijs catchment, situated in the South-East part of the Netherlands and shared with Belgium.

## 2 Material and methods

To achieve the objective, a fully distributed physically-based hydrological model coupled with hydrodynamic model was set up using MIKE-SHE and MIKE-11 modelling system of DHI, Denmark. The model has a grid size of 500 by 500 m and it is run both for the historical (base) period 2010-2019 and for future climate conditions. Future meteorological data was obtained from the recently released Koninklijk Nederlands Meteorologisch Instituut (KNMI'23) climate scenarios dataset that translates the IPCC 2021 global climate projections for the Netherlands [3]. The KNMI ran their in-house global climate model, aligning the simulation results with CMIP6-based target values. These simulations were then downscaled using a regional climate model and also bias-corrected using the Quantile Delta Mapping method. The KNMI'23 dataset comprises six projection scenarios,

determined by the combination of three $CO_2$ emissions (SSP5-8.5, SSP2-4.5, SSP1-2.6), each with either wetting or drying conditions (HN, HD, MN, MD, LN, LD, where H/M/L indicate high/medium/low emissions and N/D indicate wet ('nat' in Dutch)/dry conditions). The hydrological model of Aa of Weerijs was run with meteorological data from each scenario for a time horizon denoted '2050', where the 30-year period (2036-2065) represents the average condition of '2050'. The results were then compared with the base period. The outcomes of the comparison across all scenarios are presented in a range based on the highest and lowest values achieved overall.

## 3 Results

In the horizon 2050, the average annual rainfall is projected to increase by 1.4% to 6.2% compared to the base period. However, model results indicated that due to the rise in temperatures, the AET is projected to increase even more significantly, ranging from 13.8% to 14.7%. This higher increase in AET compared to rainfall resulted in a decrease of Q at the outlet of the catchment, BF, and R by -7% to -19.6%, -2.9% to -9.8%, and -8% to -20.7%, respectively (figure 1). Over summer (JJA), these average values are projected to further reduce to -27.3% to -32.3% for Q at the outlet of the catchment, -6.8% to -12.5% for BF, and -106% to -139% for R. Over winter (December, January, February - DJF), the trends vary based on the climate scenario, with the percentage change compared to the base period ranging between -14.4% to 2% for Q at the catchment outlet, -0.2% to -7.8% for BF, and -3% to 7.8% for R. The wider range of percentage changes in hydrological components under different scenarios may also include possible uncertainties in predicting the impact of future climate change, that stem from various sources, including model parameters, model structure, and inputs. However, the overall trends of these projections indicate a significant negative impact of climate change on the hydrology of the catchment, with decreases in water balance components during summer that are higher than any increases in winter.

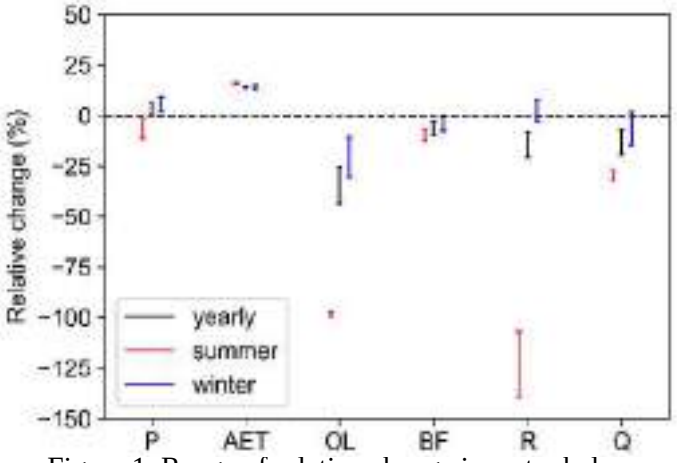


Figure 1. Range of relative change in water balance components under climate scenarios with reference to base period for summer, winter and whole year. P: precipitation, AET: actual ET, OL: overland flow, BF: baseflow, R: groundwater recharge, Q: discharge

## 4 Conclusions

We conclude that even the climate scenarios with lower emissions exhibit adverse effects on the catchment's hydrology. The catchment is likely to experience water shortages, particularly during the summer months. Therefore, it is imperative for decision- and policy- makers to consider and implement mitigation or adaptation strategies in response to these challenges.

## 5 Acknowledgments

The research presented here was supported by the European Union's Horizon 2020 research and innovation programme "EIFFEL project" (www.eiffel4climate.eu, Grant No.101003518).

## Reference

[1] M. Mazzoleni, F. Dottori, H.L. Cloke, G. Di Baldassarre, Deciphering human influence on annual maximum flood extent at the global level, Communications Earth & Environment 3(1), 2022.
[2] S.Y. Philip, S.F. Kew, K. Van Der Wiel, N. Wanders, G.J. Van Oldenborgh, Regional differentiation in climate change induced drought trends in the Netherlands, Environmental Research Letters 15(9), 2020.
[3] R. Van Dorland, J. Beersma, J. Bessembinder, N. Bloemendaal, KNMI National Climate Scenarios 2023 for the Netherlands, Royal Netherlands Meteorological Institute, WR-23-02, De Bilt, 2023.

**Theme:** Climate change impacts
**IAHR Thematic Priority Area:** [TPA-1] Climate Change Adaptation and Mitigation
https://doi.org/10.3850/iahr-hic2483430201-208

# Assessment of Terrestrial Water Storage Variations and Spatial Heterogeneity Across the Pearl River Basin：The Influences of Climate Change

**Weijin Pan [1], YuLei Xie [1]**

[1] Institute of Environmental and Ecological Engineering, Guangdong University of Technology, Guangzhou 510006, China

*Corresponding author: xieyulei@gdut.edu.cn*

**Abstract.** The spatial and temporal distribution of terrestrial water storage (TWS) can be influenced by climatic change. However, studies on Pearl River Basin (PRB) terrestrial water storage anomalies (TWSA)spatial and temporal heterogeneity and drivers are extremely lacking. Therefore, In this study, we investigated the variation of TWSA in the PRB during 2003-2017, subsequently analyzed the relationship between TWSA and climate change, and proposed the use of Geodetector Model(GDM) on a seasonal scale to reveal the role of different factors of climate change in driving the spatial variability of the PRB. The results show that (1) TWSA in the PRB increased significantly at a rate of 5.63 ± 0.77 mm/a over the fifteen years. The effects of precipitation(PRE), potential evapotranspiration(PET), Land Surface Temperature(LST), and NDVI, on the spatial variability of TWSA differed significantly in each season. For PRB, the relative contributions of PRE to TWSA or the interactions of PRE and other factors to TWSA always occupy a dominant position. These conclusions can provide beneficial guidance for managing and assessing local water resources.

**Keywords:** Climate change, TWSA, Pearl River Basin, Relative contributions, Interactions

## 1 Introduction

Terrestrial water storage (TWS) is defined as the total amount of water stored on land, and the related changes represent the dynamic of available freshwater resources under regional and national scales that have a stronger relationship with natural ecosystems and socioeconomic development[1].
This study will propose a seasonal perspective to analyze the impacts of climate change on TWSA to provide applicable assessment tools and scientific decision-support information for regional water resources management.

## 2 Material and Methods

The study area in PRB, and the actual terrestrial water storage is derived from GRACE TWS, using meteorological data including precipitation, potential evapotranspiration, land surface temperature, and NDVI. In this study, we will utilize Mann-Kendall[2] to understand the temporal patterns of change in the GRACE TWS, and Sen's slope[3] estimation to measure the extent of change in the TWS, followed by The Geodetector model[4] will be used to detect the relative contributions and interactions of each factor on TWSA.

## 3 Results

The results are organized in two ways: spatial and temporal variations in terrestrial water storage and analysis of impact factors.

- From 2003 to 2017, the average TWSA in the PRB exhibited a significant increasing trend, with a rate of 5.63 ± 0.77 mm/a, the spatial analysis shows a comprehensive growth of TWSA

in the PRB from of 2003 to 2017, ranging from 0.7 mm/a to 9.4 mm/a and showed similar growth trends in all seasons

- Precipitation dominated climate driver contributes relatively significantly to TWSA in DJF and MAM, and most factor pairs have enhanced effects with higher Q values than individual factor effects, i.e., the interactions between factor pairs have stronger relative importance for TWSA.

## 4 Discussion

- The results of the study were similar to previous studies[5] in that although there was a similar trend in the growth of TWSA in PRB in all seasons, there was still a difference in the magnitude of growth in each season.
- For the PRB, precipitation is the dominant cause only in some seasons, and it is more important to pay attention to the interactions between factors on TWSA.
- If the dominant factors causing changes in terrestrial water stocks are to be studied in depth, whether human activities under the influence of climate change will have an impact on changes in terrestrial water stocks is also a question worth exploring.

## 5 Conclusions

TWSA in PRB showed an increasing trend from 2003 to 2017, especially in the center of PRB, and showed similar trends in all four seasons. Precipitation remains the main contributor to terrestrial water storage, and the interaction of the factors increases the explanatory power of changes in terrestrial water storage compared to individual factors.

## Reference

[1] Humphrey V, Rodell M, Eicker A. Using satellite-based terrestrial water storage data: A review[J]. Surveys in Geophysics, 2023, 44(5): 1489-1517.

[2] Yue S, Pilon P, Cavadias G. Power of the Mann–Kendall and Spearman's rho tests for detecting monotonic trends in hydrological series[J]. Journal of hydrology, 2002, 259(1-4): 254-271.

[3] Sen P K. Estimates of the regression coefficient based on Kendall's tau[J]. Journal of the American statistical association, 1968, 63(324): 1379-1389.

[4] Song Y, Wang J, Ge Y, et al. An optimal parameters-based geographical detector model enhances geographic characteristics of explanatory variables for spatial heterogeneity analysis: Cases with different types of spatial data[J]. GIScience & Remote Sensing, 2020, 57(5): 593-610.

[5] Yang B, Li Y, Tao C, et al. Variations and drivers of terrestrial water storage in ten basins of China[J]. Journal of Hydrology: Regional Studies, 2023, 45: 101286.

**Theme:** Climate change impacts
**IAHR Thematic Priority Area:** [TPA-1] Climate Change Adaptation and Mitigation
https://doi.org/10.3850/iahr-hic2483430201-210

# Methodologies for uncertainty analysis in rainfall data assimilation aimed at urban drainage design storm identification

**Giulia Failla[1], Gabriele Freni[1], Mariacrocetta Sambito[1], Gaetano Beninati[2], Andrea Federico[2], Marcella Lo Bianco[2]**

[1] Università degli Studi di Enna "Kore" – Facoltà di Ingegneria ed Architettura, Via delle Olimpiadi 2, 94100 Enna
[2] Sering Ingegneria – Via Enrico Amari – 90128 Palermo

*Corresponding author: gabriele.freni@unikore.it*

**Abstract.** The accuracy of rainfall-runoff models is essential for understanding climate variability, managing water resources, and mitigating flood risks. Rainfall data, as a crucial input to hydrological processes, significantly contributes to the uncertainty of these models. Focusing on the Addis Ababa catchment, an approach for the assimilation of rainfall data has been studied, integrating satellite and ground observations to enhance urban drainage design through the precise identification of design storms. At the methodology's core is applying the bootstrap method for evaluating spatial uncertainty in Intensity-Duration-Frequency (IDF) curves within a comprehensive rain gauge network. Findings derived from a dataset encompassing 17 stations reveal variability in uncertainty ranging from 0.10% to 28%, highlighting areas within the urban core that necessitate targeted improvements for data accuracy and network consistency. By advancing precision in urban hydrological assessments, the research contributes to improved water resource management and the development of resilient and sustainable urban water systems

**Keywords:** Bootstrap Approach, Intensity-Duration-Frequency, Spatial Uncertainty

## 1 Introduction

An uncontrolled rainfall-runoff process can cause many problems, such as the degradation of public resources and flooding that endangers life and properties. Increased stormwater flows due to urbanization or changes in climatic conditions expand floodplains, bringing flooding to locations where it did not occur before and worsening flood problems in areas already prone to flood.

The dynamics of urban drainage systems are significantly influenced by the variability and uncertainty inherent in rainfall data. Hydrologic design of storm sewers, culverts, retention/detention basins and other components of stormwater management systems are typically performed based on specified design storms derived from the rainfall intensity-duration-frequency (IDF) estimates and an assumed temporal distribution of rainfall.

State-of-the-art applications require the availability of past rainfall data to obtain reliable design for a period that should be at least comparable with the return period of the hydraulic design. Often, rainfall data series are not continuous and need to contain information about short events and sub-hourly peaks that may be relevant for urban drainage systems.

Remote sensing and data assimilation techniques may help by integrating high-resolution satellite data (with sufficient temporal continuity) with piecemeal ground data. At the same time, ground data can reduce the inherent uncertainty due to the indirect estimation of rainfall volume using satellite radiation measurements.

Integrating satellite data with observations from ground stations has made uncertainty analysis of area rainfall estimates indispensable. This paper aims to analyze the spatial rainfall uncertainty of the IDF curves within the rain gauge network defined in Addis Ababa's hydrological catchment.

In this study, the regionalization and the assessment of uncertainty in terms of spatially averaged rainfall estimates were evaluated using the bootstrap method.

## 2 Methods

Situated between latitudes 8°46' N and 9°13' N, and longitudes 38°35' E and 39°00' E, the Addis Ababa catchment spans approximately 1,430 km². This area has been strategically selected for analysis due to its intricate hydrology and the profound effects of urbanization on its drainage systems, establishing it as an exemplary model for study.

The catchment area is distinguished by its complex topography and a dense network of water bodies, factors that contribute to the variability in rainfall distribution across the region. The terrain's gradient shifts markedly (2251-3097 m.a.s.l facilitating the identification of three distinct elevation zones: low, medium, and high. Moreover, the catchment is bifurcated into two principal sections, separated by the two main rivers: the Little and the Great Akaki. Central to this hydrological basin, the city of Addis Ababa experiences considerable urban growth, characterized by extensive urbanization and a high proportion of impervious areas.

The bootstrap technique evaluates uncertainty maps for all estimated rainfall depths at assigned return periods. This study adopts a bootstrap method to quantitatively assess the uncertainty of areal rainfall estimates and its effects on rainfall dataset (Uboldi et al., 2014).

The bootstrap method is a powerful statistical tool used to estimate the distribution of a statistic (like the mean or variance) by resampling with replacement from the data. It allows for estimating of the sampling distribution of almost any statistic, providing a simple way to calculate confidence intervals and significance tests for complex estimators. The bootstrap method has been widely applied in hydrological data analysis.

## 3 Results and discussion

In our study's conclusion, the uncertainty evaluation analysis reveals that the range of uncertainty spans from as low as 0.10% to as high as 28%. This spectrum of uncertainty underscores the inherent robustness of rainfall developed from integrating satellite-derived and terrestrial-measured datasets. The distribution of uncertainty across the study area is not uniform, with pronounced concentrations of higher uncertainty localized within the central urban matrix of the city.

This spatial patterning of uncertainty can be attributed to the sensitivity of these areas to the iterative processes and the different sample data sets generated via the bootstrap methodology. This insight suggests the need for targeted improvements in this area, such as enhancing data quality collected by adding rain gauges that records sub-hourly and improving the rain gauge network's consistency.

Addressing these areas of uncertainty is crucial for more accurate urban hydrological assessments, leading to better water resource management and reduced uncertainties in rainfall-runoff models. This approach not only supports the optimization of water resource management but also contributes to the broader goal of achieving resilient and sustainable urban water systems.

## Reference

[1]. Selle, B., & Hannah, M. (2010). A bootstrap approach to assess parameter uncertainty in simple catchment models. Environmental Modelling and Software, 25(8), 919–926. https://doi.org/10.1016/j.envsoft.2010.03.005

[2]. Uboldi, F., Sulis, A. N., Lussana, C., Cislaghi, M., & Russo, M. (2014). A spatial bootstrap technique for parameter estimation of rainfall annual maxima distribution. Hydrology and Earth System Sciences, 18(3), 981–995. https://doi.org/10.5194/hess-18-981-2014

**Theme:** Climate change impacts
**IAHR Thematic Priority Area:** [TPA-1] Climate Change Adaptation and Mitigation
https://doi.org/10.3850/iahr-hic2483430201-212

# The Non-Stationarity of Extreme Rainfalls in The Greater Bay Area Revealed by Multi-Source Merged Gridded Datasets

**Haochen Yan[1], Mingfu Guan[1]**

[1] Department of Civil Engineering, The University of Hong Kong, Hong Kong SAR, China

*Corresponding author: mfguan@hku.hk*

**Abstract.** Sub-daily rainfall extremes are increasingly posing threats to the society in the warming climate. The low resolution and accuracy of gridded rainfall datasets and very limited accessibility/availability of gauge observations hinder a reliable characterization of such changing extremes. Taking the Greater Bay Area of China as an example, we developed a long-term (1991-2020), high spatiotemporal-resolution (10 km, hourly) rainfall dataset using a Random Forest-based multi-source merging technique. The dataset is demonstrated to outperform than all the candidate gridded products and effectively fill the gap among the sparse gauge networks. Furthermore, non-stationary frequency based on the dataset shows greater increases in rainfall intensities over the north-central part of the region compared with the southern coastal region. Our results show, for the first time, that urbanization nonlinearly increases rainfall intensities at different durations and return periods.

**Keywords:** 3–6 keywords (in alphabetical order)

## 1 Introduction

Human-induced global warming has intensified extreme rainfalls (whose intensity is higher than the 2-year return level) for most land areas globally [1]. Such changes and significant regional variabilities may cause severe socioeconomic impacts through flash flooding, especially in urban areas. While continuous and rapid urbanization is placing more areas under rising flood risk, particularly in the economic growth hubs in the Asia-Pacific region, the lack of gauge stations with a long time span as well as temporal resolution is a common challenge for hydrologists to detect and characterize the potential non-stationarity of extreme rainfalls. Although many recent studies provide evidence for the non-stationarity of extreme rainfalls towards increasing intensities, scopes are usually limited to above-daily timescales based on sparse and nonuniform spatial gauge networks, or even single stations, as regional indicators. Our recent study (partially presented herein and also published in [2]) focused on the Greater Bay Area (GBA) of China, one of the most important megacity agglomerations and economic hubs around the world, demonstrating the necessity of utilizing high spatiotemporal-resolution gridded data to characterize of regional non-stationarity.

## 2 Materials and methods

Quality assessment of several gridded rainfall products for the GBA showed poor agreement with hourly gauge observations (Fig. 1). Then, MSWEP V2.8, Era5-Land and IMERG-V7 are selected as candidates of Random Forest-based multi-source merging (RF-Merge) [3] due to relatively better performance, with covariates of mean areal elevation derived from FAMDEM data. The merged data are then applied to conduct nonstationary frequency analysis from hourly to daily durations for each grid in the GBA [2]. Both physical covariates and time are selected as explanatory variables to obtain the best-fit model structure. Annual trend of the return levels of various durations are analysed.

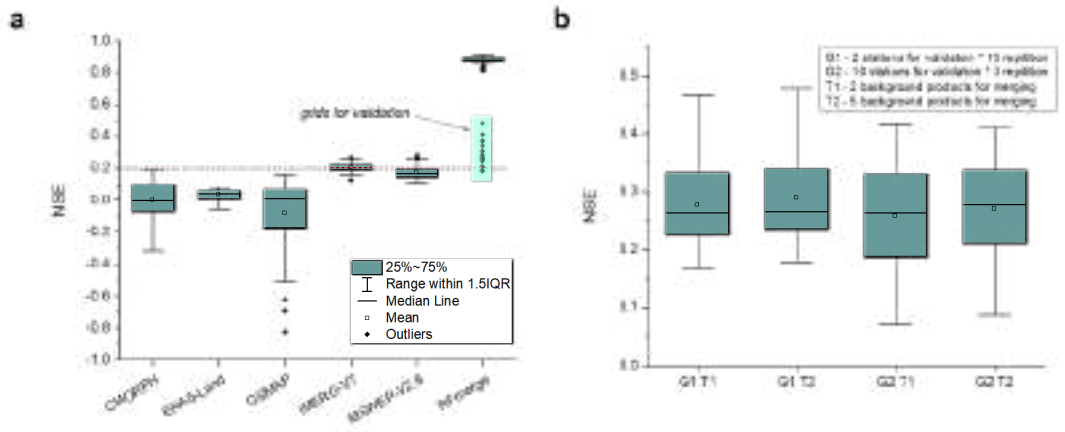


Fig. 1. Quality evaluation of gridded rainfall products with gauge stations in the GBA.

## 3 Results and discussions

The RF-MEP dataset significantly improved the original data in terms of the Nash–Sutcliffe efficiency (NSE) coefficient whilst also preserving spatial details beyond that of the gauge network (Fig. 1). Frequency analysis shows non-stationarity dominates most part of the GBA (Fig. 2). For the 10-year return period, the maximum trend (+12.2%/10yr) for hourly rainfall is in central Guangzhou; comparable positive trends also occur in northwestern Huizhou. Negative trends in daily extremes around the southern coastlines (Zhuhai, Shenzhen, and Hong Kong) reach -20%/10yr. In addition, the southwest and east show a low degree of non-stationarity. Over 1 h to 24 h durations, clusters of non-stationarity tend to shrink and retreat northwards; the proportion of the study area with stationary rainfall extremes also expands. As the event duration increases, fewer grids are detected with the nonstationary behaviour. North-central and eastern Guangzhou plus northwestern Huizhou have increasing intensities for all return periods and durations, whereas negative-trend clusters extend inland from the southern coastlines especially for longer durations (12- to 24-hour).

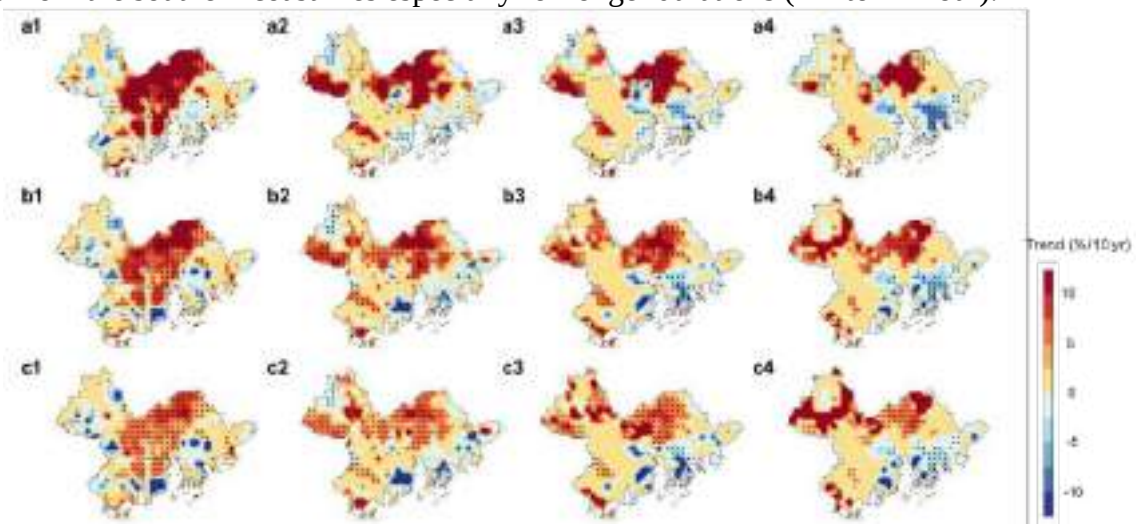


Fig. 2 Non-stationarity patterns (trend normalized by the stationary return levels) at 2- (a), 10- (b), and 100-year (c) return periods for 1-, 6-, 12- and 24 h durations (numbered 1-4). Dots mark $\alpha \leqslant 0.05$ significance.

## Reference

[1] Fowler, H. J. et al. Anthropogenic intensification of short-duration rainfall extremes. Nat Rev Earth Environ 2, 107–122 (2021).

[2] Yan, H et al. Urbanization further intensifies short-duration rainfall extremes in a warmer climate. Geophysical Research Letters 51, e2024GL108565 (2024).

[3] Baez-Villanueva, O. M. et al. RF-MEP: A novel Random Forest method for merging gridded precipitation products and ground-based measurements. Remote Sensing of Environment 239, 111606 (2020).

**Theme:** Climate change impacts
**IAHR Thematic Priority Area:** [TPA-1] Climate Change Adaptation and Mitigation
https://doi.org/10.3850/iahr-hic2483430201-214

# Green Infrastructures Performance Towards Stormwater Management under Climate Change

**Qian YU[1, 2, 3], Wenjing Lu[1], Jing Wang[1, 2, 3], Na Li[1, 2]**

[1] China Institute of Water Resources and Hydropower Research, Beijing, 100038, China
[2] Research Center on Flood & Drought Disaster Prevention and Reduction of the Ministry of Water Resources, Beijing, 100038, China
[3] Key Laboratory of Water Safety for Beijing-Tianjin-Hebei Region of Ministry of Water Resources, Beijing 100038, People's Republic of China

*Corresponding author: yqcherie@126.com*

**Abstract.** Modeling the effects of GIs on controlling stormwater runoff under different rainfall characteristics plays an important role in planning and designing Green Infrastructure (GI) to adapt to climate change. The Jinan Daminghu Sponge City Construction pilot area is selected as the study area in this paper. Based on the daily precipitation data of Jinan National Meteorological Station from 1951 to 2021, both the Mann-Kendall test and Sen's slope estimator are adopted to analyze the temporal variations of precipitations and extremes. On this basis, the Flood Risk Analysis Software (FRAS) is used to analyze the GIs' performance towards controlling rainfall runoff. The results indicate that the annual mean precipitation shows an insignificant growth trend. The interannual precipitations vary significantly. In addition, the extreme precipitation is projected to increase. Therefore, we set six rainfall scenarios to analyze the control effects of GIs on rainfall runoffs under different rainfall characteristics. The results show that the reduction ratios of inundation areas under 5-year, 10-year, and 20-year are 11.02%, 9.32%, and 8.02%, respectively. The reduction rates under different rainfall intensities are 20.14%, 14.37%, and 10.58%, respectively. GIs have good control effects on the inundation areas under rainfalls with small return periods and rainfall intensities.

**Keywords:** green infrastructure, Mann-Kendall test, rainfall characteristics, stormwater management

## 1 Introduction

In recent decades, China's rapid urbanization has been accompanied by an increase in the frequency of short-term heavy rainfall events, driven by climate change [1]. Consequently, urban flooding issues in China have become more severe due to the combined pressures of urban development and climate variability. To address these challenges and simultaneously tackle water-related environmental and ecological concerns, China introduced the concept of Sponge City Construction (SCC) in 2013. At the heart of the sponge city concept lies the principle of low impact development (LID), also known as green infrastructure (GI). Previous studies have demonstrated the effectiveness of GIs in managing water quantity during small to moderate rainfall events [2-3]. However, there has been limited research on the impact of GIs on water quantity under varying rainfall characteristics, such as intensity and duration.

In line with the latest report from the IPCC [4], which highlights an increase in the frequency and intensity of heavy precipitation events across most land areas since the 1950s, our study aims to analyze rainfall variations in Jinan over the past 70 years and assess trends in extreme precipitation events. Additionally, we have developed six scenarios with variations in return periods and intensities to evaluate the effectiveness of GIs in managing rainfall runoff.

## 2 Material and methods

Jinan, located in the temperate monsoon climate zone, experiences over 60% of its annual precipitation during the summer, with significant interannual variability. There are six national weather stations (Jinan, Jiyang, Shanghe, Zhangqiu, Changqing, and Pingyin) in the city. For this study, the Jinan station (representing the urban area of the piedmont plain), is selected as the reference station. Using the long-term daily precipitation data from 1951 to 2021, we apply the Mann-Kendall test and Sen's slope method to analyze the spatiotemporal evolution of multi-year rainfall characteristics in Jinan city. 7 extreme precipitation indicators are included, i.e., SDII, R95PTOT, R99pTOT, R10mm, R30mm, R50mm and Rx5day.

In addition, we set six rainfall scenarios with variations in rainfall frequencies and intensities to analyze the control effects of GIs' performances on stormwater management. The three rainfall return periods are rainfall events with a 5-year return period, 10-year return period and 20-year return period, respectively. The design rainstorm intensity with three return periods is calculated based on the short duration rainstorm intensity formula in Jinan. The independently developed software Flood Risk Analysis Software (FRAS) is then employed to simulate the inundations under different scenarios.

## 3 Results and discussion

### 3.1 Changes in rainfall characteristics

The annual precipitation in the main urban area of Jinan has shown a fluctuating growth trend over the past 71 years, but the growth trend is not significant, with an average annual precipitation of 696.8mm. The SDII in the main urban area of Jinan has shown a relatively clear increasing trend from 1998 to 2021, while R95pTOT and R99pTOT (both showing overall increasing trends) and R10mm have shown overall decreasing trends. In summary, the long-term precipitation changes in Jinan are not significant, but there is a certain degree of increasing trend in extreme precipitation events in the main urban area, especially in the past 20 years.

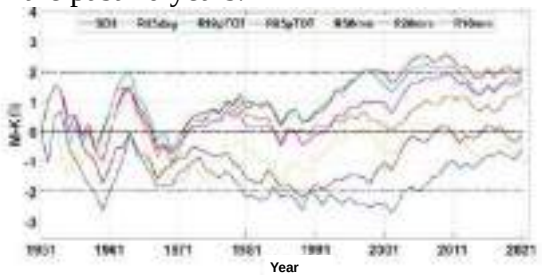


Figure 26 The Mann-Kendall trend of extreme precipitation indicators.

### 3.2 Effects on inundation areas under different rainfall characteristics

The findings indicate a reduction in inundation areas following the implementation of GIs across various rainfall frequencies and intensities, implying their effectiveness in mitigating inundation to some degree. Notably, GIs demonstrate the most pronounced efficacy during 5-year events, with reduction ratios of inundation areas at 11.02%, 9.32%, and 8.02% for 5-year, 10-year, and 20-year scenarios, respectively. As rainfall volumes increase with return periods, the control effects on inundation areas diminish. Similarly, higher rainfall intensities correspond to decreased reduction rates in controlling inundation areas, with rates of 20.14%, 14.37%, and 10.58% observed under different rainfall intensities, respectively.

These simulation outcomes align with field observations reported by Carpenter and Kaluvakolanu [5] and Lewellyn et al. [6], underscoring the significant role of grey infrastructures in urban pluvial flood control. While GIs offer less robust control compared to grey infrastructures, they offer broader benefits, including improvements in surface water quality and heightened public awareness of water security. These multifaceted advantages are especially crucial given the myriad water-related challenges confronting urban areas [7].

**Acknowledgements**

This research was funded by the Yangtze River Water Science Joint Fund Project [No. U2340225] and the National Natural Science Foundation of China [No. 51909273]. The support provided by the IWHR Talented International Expert Program is also acknowledged.

**Reference**

[1] Min S K, Zhang X, Zwiers F W, et al 2011 Human contribution to more-intense precipitation extremes. Nature, 470(7334) 378-381.
[2] ATKINS 2015 Flood loss avoidance benefits of green infrastructure for stormwater management. Maryland.
[3] Yu Q, Li N 2021 Research Progress and Perspective of Effects of Low Impact Development on Rainfall Runoff Reduction under Different Rainfall Characteristics. Water Resources and Power, 39(08), 18-21+9. (in Chinese)
[4] IPCC, 2021. Summary for Policymakers. In: Climate Change 2021: The Physical Science Basis. Contribution of Working Group I to the Sixth Assessment Report of the Intergovernmental Panel on Climate Change [Masson-Delmotte, V., P. et al (eds.)]. (Cambridge University Press. In Press)
[5] Carpenter D D, Kaluvakolanu P 2010 Effect of roof surface type on storm-water runoff from full-scale roofs in a temperate climate. J. Irrig. Drain. E-ASCE, 137(3) 161-169.
[6] Lewellyn C, Lyons C E, Traver R G, et al. 2015 Evaluation of seasonal and large storm runoff volume capture of an infiltration green infrastructure system. J. Hydrol. Eng., 21(1) 04015047.
[7] Yu Q, Li N, Wang S, et al. 2020 Study on comprehensive benefit assessment systems for low impact development practices. Journal of Hydroelectric Engineering. 39(12), 94-103. (in Chinese)

**Theme:** Climate change impacts
**IAHR Thematic Priority Area:** [TPA-1] Climate Change Adaptation and Mitigation
https://doi.org/10.3850/iahr-hic2483430201-217

# Estimation of Carbon Emissions Based on Remote Sensing and Neural Network in China

**Kaitong Qin[1], Songjie Wu[1], Chen Chen[1], Tiejian Li[2], Jiaye Li[1]**

[1] Dongguan University of Technology, Dongguan 523808, Guangdong, China
[2] Tsinghua University, Beijing 100084, China

*Corresponding author: chenchen@dgut.edu.cn*

**Abstract.** Global climate warming is advancing at a unprecedent pace, primarily fueled by the rapid increase in carbon emissions. Unlike traditional carbon emission inventories, the satellite-based observations of column carbon dioxide concentration ($XCO_2$) provide a new perspective for estimating carbon emissions. However, a key challenge lies in defining the $XCO_2$ background, essential for determining $XCO_2$ enhancement, and establishing relationship between $XCO_2$ (anomaly) and carbon emissions. This study comparatively analyzes various methods for defining $XCO_2$ background areas, including national, latitudinal ranges, or non-emission areas approaches. Then a novel method for carbon emission estimation is proposed, leveraging K-means clustering and Generalized Regression Neural Network (GRNN). Using $XCO_2$ (anomaly), net primary productivity (NPP), and population distribution as inputs, and the Open-source Data Inventory for Anthropogenic $CO_2$ (ODIAC) as output, the GRNN model is trained on data from 2014 to 2019 and then used to estimate the spatial distribution of national carbon emissions in 2020. A relatively well-performing model attains a determination coefficient ($R^2$) of 0.969 and Mean Absolute Error (MAE) of 0.186 $gC/m^2/day$, demonstrating a significant improvement compared to existing research. The findings can provide recommendations for $XCO_2$ enhancement and improve our understanding of satellite-based carbon estimation.

**Keywords:** Carbon emissions, GRNN, Remote sensing, $XCO_2$

## 1 Introduction

The climate change caused by greenhouse gas emissions is one of the key factors influencing global hydrological cycle changes, with $CO_2$ being a major component. To support China's strategic objectives of achieving carbon peak and carbon neutrality, accurate and effective estimation of carbon emission is indispensable. The satellite-based observations of $XCO_2$ offer valuable insights for this purpose. In this study, the datasets and models used for a new carbon emission estimation method are provided in Sect. 2, and the estimation results will be discussed in Sect. 3.

## 2 Material and methods

The datasets used in this study include the $XCO_2$ dataset Mapping-XCO2 [1], the NPP dataset MOD17A3HGF Version 6.1 [2], the population distribution dataset LandScan Global [3], and the fossil fuel $CO_2$ emissions dataset ODIAC [4], which serves as the model's dependent variable. Additionally, this study proposes a new method for enhancing $XCO_2$ and a new model for carbon emissions prediction based on K-means clustering [5] and GRNN [6].

## 3 Results and discussion

Figure 1 shows the scatter plot of the estimation effect of a well-performing model when the number of clusters is 7, showing good predictive accuracy and a linear distribution relationship. The $R^2$ reached 0.969, while the MAE was only 0.186 $gC/m^2/day$. For actual emissions between approximately 5 and 10 $gC/m^2/day$, some samples exhibit relatively large errors, which is due to the insufficient number of clusters, resulting in spatial heterogeneity not being mitigated effectively.

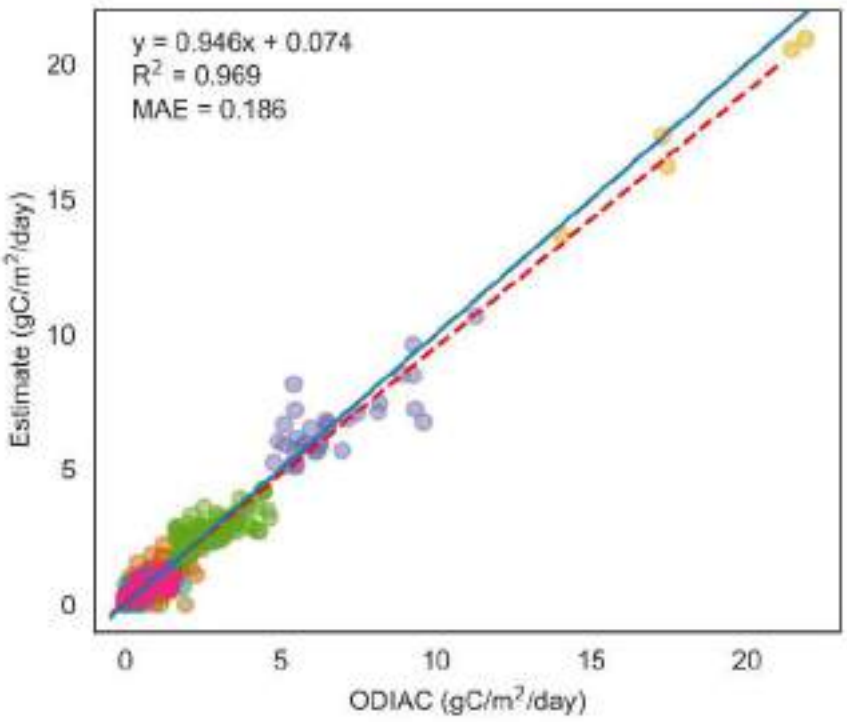


Figure 1 Scatterplot between ODIAC emissions and estimated emissions in 2020.

## 4 Conclusions

The new methods for enhancing $XCO_2$ and anthropogenic $CO_2$ emissions estimation proposed in this study have achieved better result compared to previous studies. The findings can not only provide recommendations for $XCO_2$ enhancement in similar research endeavours, but also enhance our understanding of carbon estimation through the utilization of satellite-based carbon observations.

## Reference

[1] M. Sheng, L. Lei, Z.-C. Zeng, W. Rao, H. Song, C. Wu, Global land 1° mapping XCO2 dataset using satellite observations of GOSAT and OCO-2 from 2009 to 2020, (2021). https://doi.org/10.7910/DVN/4WDTD8.

[2] S. Running, M. Zhao, MODIS/Terra Net Primary Production Gap-Filled Yearly L4 Global 500 m SIN Grid V061, (2021). https://doi.org/10.5067/MODIS/MOD17A3HGF.061.

[3] K. Sims, A. Reith, E. Bright, J. Kaufman, J. Pyle, J. Epting, J. Gonzales, D. Adams, E. Powell, M. Urban, A. Rose, LandScan Global 2022, (n.d.). https://doi.org/10.48690/1529167.

[4] T. Oda, ODIAC Fossil Fuel CO2 Emissions Dataset, (2015) 258GB. https://doi.org/10.17595/20170411.001.

[5] J. MacQueen, Some methods for classification and analysis of multivariate observations, in: 1967.

[6] D.F. Specht, A general regression neural network, IEEE Trans. Neural Netw. 2 (1991) 568–576. https://doi.org/10.1109/72.97934.

**Theme:** Climate change impacts
**IAHR Thematic Priority Area:** [TPA-1] Climate Change Adaptation and Mitigation
https://doi.org/10.3850/iahr-hic2483430201-219

# Increased Populations Will Enlarge Population Exposure to Extreme Snowfall over Eurasia before Middle-Term of the 21st Century

**Wenqing Lin[1,3,*], Huopo Chen[2], Dawei Zhang[1,3], Fan Wang[1,3], Wuxia Bi[1,3], Weiqi Wang[1,3]**

[1] State Key Laboratory of Simulation and Regulation of Water Cycle in River Basin, China Institute of Water Resources and Hydropower Research, Beijing, 100038, China
[2] Nansen-Zhu International Research Centre, Institute of Atmospheric Physics, Chinese Academy of Sciences, Beijing, 100029, China
[3] Research Center on Flood & Drought Disaster Prevention and Reduction of the Ministry of Water Resources, Beijing, 100038, China

*Corresponding author: linwq@iwhr.com*

**Abstract.** The frequent occurrences of extreme snowfall over part of Eurasia have caused substantial economic losses and severely impacted society. This study utilizes CMIP6 model datasets and future population projections to predict population risks from changes in extreme snowfall across Eurasia under SSP2-4.5 and SSP5-8.5 scenarios while also attributing the factors influencing future changes in population exposure. Our results show that snowstorm days and corresponding population risk continue to increase on averaged Eurasia during the mid-term (2041-2060) of the 21st century and before. In particular, population exposure to snowstorm days will increase by 4.1% and 1.8% in the near (2021-2040) and mid-term across Eurasia, especially significant over Central Asia, East Asia, and the Mediterranean. Population contribution is the main factor of changes in population exposure to snowstorm days over Eurasia, followed by climate and climate-population interaction. By the end of this century, as the snowstorm days and population decrease dramatically, the corresponding population exposure will further decrease. Therefore, the potential population risks associated with the increase in snowstorm events in Eurasia should be taken into consideration for climate adaptation policymaking until the mid-21st century.

**Keywords:** Climate Change, Contribution, Extreme Snowfall, Eurasia, Population Exposure

## 1 Introduction

Recently, some parts of Eurasia have also been frequently attacked by heavy snowfall events, which have caused severe impacts on the local economy, transportation, power grid, animal husbandry, and so on[1-2]. Therefore, in the context of further global warming, how extreme snowfall events in Eurasia will change and their impacts on the population is a scientific issue worthy of attention.

## 2 Data and Methods

This study utilizes observation (including the Rainfall Estimates on a Gridded Network (REGEN, https://researchdata.edu.au/rainfall-estimates-gridded-v1-2019/1408744) dataset and Climate Prediction Center dataset), 23 CMIP6 (Coupled Model Intercomparison Project Phase 6) model datasets and future population projections to predict population risks from changes in extreme snowfall across the Eurasian continent under SSP2-4.5 and SSP5-8.5 scenarios while also attributing the factors influencing future changes in population exposure. Specifically, we take into account intense_day (refers to the number of days for daily snowfall greater than 5mm per day), snowstorm_day (refers to the number of days for daily snowfall greater than 10mm per day) and their variations over Eurasia and its six subregions and analyze the main reasons for this change.

## 3 Results

Our results show that under the SSP2-4.5 (SSP5-8.5) scenario, snowstorm will increase by 0.3% (0.7%) and 0.5% (0.2%) during near-term (2021-2040) and mid-term (2041-2060), respectively. In North Asia, the increase in snowstrom still reached 1.3% and 2.8%. Therefore, the probability of snowstorm in most parts of Eurasia will increase further in the future, especially in North Asia. The total population of Eurasia is projected to peak around 2040 under the SSP2 scenario and then decline. Before the mid-term, compared with the current climate (1995-2014), the population in East Asia, Central Asia, the Mediterranean Sea, and some parts of Mongolia will increase.

Moreover, the large value centers of intense_day and snowstorm_day exposure are primarily located in eastern China and parts of Northern Europe. On the averaged Eurasia, population exposure to intense_day will decrease by 4.5% (4.8%), 8.9% (15.0%), and 29.2% (50.0%) in the following three periods under SSP2-4.5 (SSP5-8.5) scenario, respectively. It is worth noting that in the SSP2.4-5 scenario, the population exposure to snowstorm_day will increase by 4.1% and 1.8% in the near (2021-2040) and mid-term (2041-2060), respectively, while decreasing by 21.3% at the end of the 21st century. Under the SSP5-8.5 scenario, snowstorm_day exposure first increase was 3.5%, then the middle and the end term will decrease by 2.8% and 42.0%, respectively. At regional scales, snowstorm_day will increase by more than 5.0% during the near and mid-term over Central Asia, East Asia, and Northern Europe. Apart from the Tibet Plateau, the population exposure to snowstorm days in the other five regions will further increase in the near and middle term, especially significant over Central Asia, East Asia, and the Mediterranean.

Regarding the whole of Eurasia, population exposure risk causes show that intense_day exposure will decrease is affected by following the climate factor > population factor > climate-population cofactor. Moreover, population contribution is the main factor of changes in population exposure to snowstorm days over Eurasia, followed by climate and climate-population interaction. In terms of snowstorm_day exposure variation under the SSP2-4.5 scenario during the near and mid-term, which was mainly affected by the change of population (86.5% and 98.9%), followed by climate factors (14.3% and 9.6%) and climate-population cofactors (-0.8% and -8.5%). Under the SSP5-8.5 scenario, the contribution factors to the increase of snowstorm_day exposure in Eurasia in the near and middle of the 21st century and the decrease in end-term exposure are consistent with those under the SSP2-4.5 scenario (population factor > climate factor > population-climate cofactors). By the end of this century, as the snowstorm days and population decrease dramatically, the corresponding population exposure will further decrease.

## 4 Conclusions

Snowstorm days and corresponding population risk continue to increase on averaged Eurasia during the mid-term of the 21st century and before. Population exposure to snowstorm days will increase by 4.1% and 1.8% in the near and mid-term across Eurasia, especially significant over Central Asia, East Asia, and the Mediterranean. Population contribution is the main factor of changes in population exposure to snowstorm days over Eurasia, followed by climate and climate-population interaction. By the end of this century, as the snowstorm days and population decrease dramatically, the corresponding population exposure will further decrease. Therefore, the potential population risks associated with the increase in snowstorm events in Eurasia should be taken into consideration for climate adaptation policymaking until the mid-21st century.

## Reference

[1] Krasting JP, Broccoli AJ, Dixon KW, et al. Future changes in Northern Hemisphere snowfall[J]. Journal of Climate, 2013, 26: 7813-7828.

[2]Lin WQ and Chen HP. (2022) Daily snowfall events on the Eurasian continent: CMIP6 models evaluation and projection[J]. International Journal of Climatology, 42: 6890-6907.

**Theme:** Climate change impacts
**IAHR Thematic Priority Area:** [TPA-1] Climate Change Adaptation and Mitigation
https://doi.org/10.3850/iahr-hic2483430201-221

# Determination of Rainfall Wet and Dry Stages and Analysis of Sediment Reduction by Soil and Water Conservation Measures in Typical Basin of Fen River

**Chunjing Zhao[1,2], Xiangbing Kong[1,2,*], Kai Guo[1,2], Yinan Wang[1,2], Peng Jiao[1,2], Jintao Zhao[1,2]**

[1] Yellow River Institute of Hydraulic Research, Zhengzhou, 450003, China
[2] Key Laboratory of Water and Soil Conservation in the Loess Plateau, MWR, Zhengzhou, 450003, China

*Corresponding author: kongxb@foxmail.com*

**Abstract:** The study of the characteristics of rainfall periods with wet-normal-dry and the contribution of soil and water conservation measures to sediment reduction at different stages in a long-term sequence is of great significance for coping with extreme environmental changes and rational allocation of soil and water conservation measures. The small basins of Jian and Tunlanchuan, the primary tributaries of the Fen River Basin, were selected as the typical basins. The precipitation data from 1962 to 2014 were normalized and smoothed. Results suggest that: the precipitation in typical basin showed a fluctuating trend of decreasing first and then increasing; The sediment reduction of terrace and forest in different stages showed: wet year> normal year> dry year, while sediment reduction in grassland is wet year> dry year> normal year; The proportion of sediment reduction of forest, terrace and grassland in Jianhe Basin in wet, normal and dry years is : 1:3.1:0.5, 1:2.5:0.4, 1:2.5:0.4, and the proportion in Tunlanchuan Basin is 1:6:0.2, 1:4.9:0.2, 1:4.9:0.2, respectively. In the same wet, normal and dry years, the measures of sediment reduction from large to small are : forest, terrace, grassland. forest measures play an important role in sediment reduction, accounting for more than 80 % of the total sediment reduction of soil and water conservation measures on the slope.

**Keywords:** Fen River, precipitation, sediment reduction, soil and water conservation measures

## 1 Introduction and method

The Loess Plateau is the most serious soil erosion area in the world, the area where ecological problems are concentrated in China, and the key area for soil and water conservation and ecological construction in China[1]. The study of long time series precipitation abundance, flatness and dryness stage characteristics, scientific understanding of slope management measures in different stages, is conducive to dealing with extreme environmental changes and the rational allocation of soil and water conservation measures system, to improve the effectiveness of soil and water conservation management; the Tyson polygon method is used to calculate the surface rainfall in the basin; the long time series trend of rainfall in the Fen River Basin is analysed by using the methods of sliding average and cumulative distance level; The calculation of the sediment reduction index of the basin slope measures adopts the "sediment modulus reduction method".

## 2 Results

### 2.1 Characteristics of precipitation in the Fen River Basin

The annual rainfall in the Fen River Basin showed an overall trend of decreasing and then increasing, the rainfall of the main flood season fluctuated continuously over time, and there was no obvious trend of change; the precipitation in general shows three wet-normal-dry processes, in which the precipitation from 1979 to 2009 is on the dry side, and the precipitation from 1960 to 1978 and since 2010 is on the wet side.

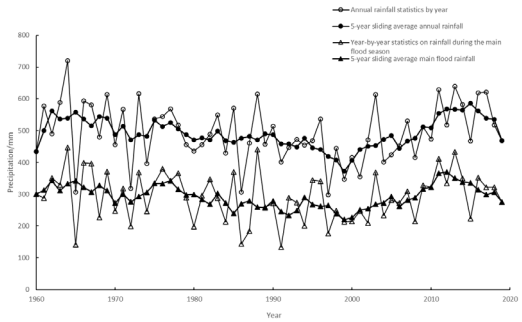


Figure 27 Multi-year rainfall in the Fen River Basin

## 2.2 Sediment reduction of soil and water conservation measures in typical basins

The sediment reduction of soil and water conservation measures in typical basins are, in descending order: forest, terrace and grassland; compared with terrace measures, the relative sediment reduction contribution of forest is higher in the year of wet water, and the sediment reduction of forest measures accounts for more than 80% of the sediment reduction of soil and water conservation measures on the total slope, and the role of sediment reduction of forest in the year of wet water is especially obvious

Tabel 1 Sediment reduction by soil and water conservation measures in typical basins

Unit:10kt

| Year of precipitation | Terrace | | Forest | | Grassland | | Total | |
|---|---|---|---|---|---|---|---|---|
| | Jianhe | Tunlan chuan | Jianhe | Tunlan chuan | Jianhe | Tunlan chuan | Jianhe | Tunlan chuan |
| Wet year | 65.91 | 20.94 | 201.04 | 125.97 | 32.16 | 4.10 | 299.11 | 151.01 |
| Normal year | 54.43 | 17.30 | 136.32 | 85.42 | 21.78 | 2.78 | 212.53 | 105.49 |
| Dry year | 52.05 | 16.54 | 130.43 | 81.72 | 21.70 | 2.77 | 204.18 | 101.03 |

## 3 Conclusion

The change of precipitation can directly change the recharge source of runoff, which causes the change of runoff and surface, the Fen River's precipitation is consistent with the overall rainfall trend in the middle reaches of the Yellow River[2], the sediment reduction of soil and water conservation measures in typical basins are, in descending order: forest, terrace and grassland; compared with terrace measures, the relative sediment reduction contribution of forest is higher in the year of wet water, and the sediment reduction of forest measures accounts for more than 80% of the sediment reduction of soil and water conservation measures on the total slope, and the role of sediment reduction of forest in the year of wet water is especially obvious, which indicates that the typical basins within the the sediment reduction effect of forest is especially obvious in the year of wet water, indicating that the forest in the typical basin can achieve better sediment reduction benefits when the rainfall is large.

## References

[1] Guobin Liu, Zhouping Shangguan, Wenyi Yao,et al. Ecological effects of soil conservation in Loess Plateau[J].Joumal of Chinese Academy of Sciences,2017.32(1)11.

[2] YuanjianWang, Xudong Fu , Guangqian Wang.Spatial and temporal distribution characterstics of rainfal in the Yelow River Basin[J]. Joumal of Tsinghua Uniersity(Natural Science Edition, 2018,58(11):972-978.

**Theme:** Climate change impacts
**IAHR Thematic Priority Area:** [TPA-1] Climate Change Adaptation and Mitigation
https://doi.org/10.3850/iahr-hic2483430201-223

# Streamflow Modelling in Karst Regions using Soil and Water Assessment Tool SWAT Under Socio-Economic Pathways (SSPs): (A Case Study of Hongshui River Basin HRB, China)

**Touseef Muhammad[1], Lihua Chen[1*], and Yiyi Zhang[2]**

[1]College of Civil Engineering and Architecture, Guangxi University, Nanning 530004, China;
[1*] College of Civil Engineering and Architecture, Guangxi University, Nanning 530004, China;
[2]Guangxi Power Transmission and Distribution Network Lightning Protection Engineering Technology Research Center, Guangxi University, Nanning 530004, China

*Corresponding author: xdslclh@gxu.edu.cn*

**Abstract.** Climatic variability and quantification of climate change impacts on hydrological parameters are persistently uncertain. This study examined how climate change affects hydroclimate-focused changes in hydrological parameter means and streamflow based on the multi-model ensemble mean of earth system models in the sixth phase of the Coupled Model Intercomparison Project (CMIP6). A Remote Sensed Evapotranspiration (RSET) using (Gravity Recovery and Climate Experiment) GRACE data was incorporated into the Soil and Water Assessment Tool (SWAT) model across the Hongshui River Basin (HRB) to anticipate hydrologic responses to future climatic conditions. The second half of the twentieth century (1960–2020) and twenty-first century (2021–2100) SSPs (Shared Socioeconomic Paths) conducted for CMIP6 models projected precipitation (5–16%) for the entire HRB. The ensemble of GCMs predicted a 2 °C increase in HRB annual mean temperature. The average changes in long-term future scenarios suggest that streamflow will rise by 4.2% under SSP-126, 6.2% under SSP-245, 8.45% under SSP-370, and 9.5% under SSP-585. The relative contribution of climate change in streamflow variability is 11% using the climate elasticity approach over the HRB. Most modelling ensemble members provide promising findings for future water resources management techniques, despite the huge uncertainty in hydrological variable projections.

**Keywords:** Climate Change, CMIP6, SSP's, SWAT

## 1 Introduction

Human activities and physical characteristics of watersheds (such as topography, soil, and vegetation), affect hydrological processes on a large scale. Investigating changes in hydrological processes is significant due to global warming and other water-related issues [1]. A significant challenge is global warming, and it is the leading cause of this problem. The average temperature of the Earth's climate system changes because of climate change, and that affects the hydrological cycle [2]. Recent increases in temperatures and precipitation patterns have altered the hydrological cycle, and that may have a significant impact on local precipitation patterns. The impact of these changes on the hydrological cycle will have either a positive or negative impact on stream flows [3]. In southern China, the Hongshui River basin is the largest tributary of the Xijiang River basin and an important ecological construction target. Human activities substantially impact the Hongshui River basin's complex climate. This research is vital to understanding how climate influences streamflow evolution in the HRB. This study's findings may also help us better understand how reservoirs affect hydrological processes and provide promising findings for future water resources management techniques.

## 2 Materials and Methods

The Hongshui River is the main tributary of the Xijiang River in the Pearl River basin, which is endowed with immense waterpower resources. The Hongshui River Basin (HRB) is located in southwest China as shown in Figure 1. This study used Integrated data of GRACE and CMIP6 data including DEM, LULC, and Soil FAO data as input for SWAT simulation to enhance streamflow modeling. We also used the climate elasticity approach to estimate climate change's contribution to streamflow. Incorporating remotely sensed evapotranspiration pre-processed GRACE data, precipitation, and temperature data derived from CMIP6-developed SSPs and reservoir data improved the accuracy of the hydrological models.

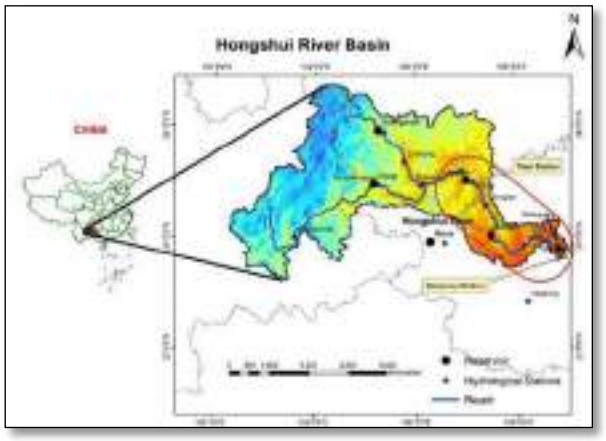


Figure 28 Location Map of Hongshui River Basin (HRB)

## 3 Results

The following results were summarized. (a) The analysis of SSPs run for CMIP6 models for the second half of the twentieth century (1960–2020 of historical run) and twenty-first century (2021–2100) concluded that the BCC-CSM2 and MPI GCMs showed increasing annual precipitation (by 5–16%) for the entire Hongshui River basin (HRB). (b) The anticipated increases in the annual mean temperature throughout the entire HRB were examined, and an ensemble of GCMs showed an increase of nearly 2 °C. (c) The scenarios suggest that the future streamflow will rise by 4.2% under SSP-1.26, 6.2% under SSP-2.45, 8.45% under SSP-3.70, and 9.5% under SSP-5.85. (d) Using the climate elasticity technique, the relative contribution of climate change in the streamflow for the Hongshui River basin (HRB) is 10.8% and 12.5%.

## 4 Conclusion

The use of satellite-based observations may aid in improving model findings. In light of this purpose, a framework is proposed to assist in the use of remotely sensed observations to enhance hydrological modelling in basins. Despite the substantial uncertainty in forecasting hydrological variables, the majority of modelling ensemble members produce acceptable findings that may be used to guide future water resource management plans.

## Reference

[1] Scanlon, B.R., et al., Global impacts of agricultural land-use changes on water resources: quantity versus quality. Water Resources Research, 2006.

[2] Ahmadaali, J., et al., Analysis of the Effects of Water Management Strategies and Climate Change on the Environmental and Agricultural Sustainability of Urmia Lake Basin, Iran. Water, 2018. 10(2).

[3] Chen, Y., et al., Regional climate change and its effects on river runoff in the Tarim Basin, China. Hydrological Processes, 2006. 20(10): p. 2207-2216.

**Theme:** Climate change impacts
**IAHR Thematic Priority Area:** [TPA-1] Climate Change Adaptation and Mitigation
https://doi.org/10.3850/iahr-hic2483430201-225

# Analysis on Flood Control Situation of Huaihe River under Extreme Rainstorm Event

**Lu Zhijie[1], Wang Kai[1], Feng Zhigang[1]**

[1]Hydrological Bureau of Huaihe River Water Resources Commission (Information Center),Bengbu, Anhui233001, China

**Abstract.** In recent years, extreme weather has occurred frequently in China, and records of short-term heavy rainfall have been constantly broken.In view of flood and drought disaster prevention, adhere to problem oriented and goal oriented, enhance risk awareness and sense of hardship, and relocate the "21 · 7" rainstorm in Zhengzhou to the middle and upper reaches of the Huaihe River.Based on the existing flood control engineering system and physical geographical status of the main stream of the Huaihe River, relying on the integrated system of flood forecasting and dispatching of the Huaihe River, the impact of this round of rainstorm on the flood control situation in the middle and upper reaches of the Huaihe River is analyzed, and the flood process of major river control sections, large reservoirs, and the use of detention areas are analyzed to provide reference for the prevention of non-standard floods.

**Keywords:** Rainstorm relocation;Huaihe River;simulation analysis;Over standard flood

## 1 Introduction

From July 14, 2021, rainstorm to heavy rainstorm will fall in most parts of the Huaihe River basin due to the combined influence of the North China continental high pressure and the southwest vortex shear[1].The heavy rainfall is mainly concentrated from July 19 to 22, when rainstorm falls to heavy rainstorm in the upper reaches of Hongru River, the middle and upper reaches of Shaying River, and the upper reaches of Wohe River. The local extremely heavy rainstorm in the upper reaches of Shaying River has a rainfall of 250mm above the mouth of Shaying River.Several large and medium-sized reservoirs in the rainstorm area exceed the flood limit water level, and some medium-sized reservoirs exceed the highest water level in history. The highest water level and maximum flow rate at Zhongmu Station and Fugou Station, both tributaries of the Shaying River, are ranked first in the historical series[2-3].

## 2 Method

The "21·7" rainstorm in Zhengzhou is located in the new county seat at the upstream of Huanghe River, the main stream of the Huaihe River, with the center of the rainstorm, and the distribution of the "21·7" rainstorm is translated to the main stream of the Huaihe River, with the rainfall magnitude and time history unchanged. For the "21·7" rainstorm, the rainfall period is from 8:00 on July 17 to 8:00 on July 21, a total of 4 days[4].

Based on the Huaihe River flood forecasting and dispatching system, rainstorm relocation operation is carried out. Step 1 selects typical historical rainstorm events, and here selects the "21 · 7" extremely heavy rainstorm in Zhengzhou; Step 2: Select the rainfall level for translation, where 25mm or more is selected; Step 3 to step 5 start to frame select the original data range of rainfall translation, where step 3 is the start, step 4 is the frame selection operation, and step 5 is the end of the frame selection.

After step 5 is completed, the system will automatically translate the rainstorm event values on the national base map to the base map center of the main business system.
This time, most of the rainstorm center is set above Wangjiaba on the Huaihe River. After the rainstorm area has been translated, check the Confirm Position check box on the function option panel, and the system will pop up the rainstorm relocation event information input box. In the input box, the user can enter the name of the relocation event, the start time of the relocation rainstorm (the default is the set forecast basis time), and the covered basin range. After selecting and clicking OK, the system will automatically complete the rainfall conversion calculation and enter the database.

## 3 Result

The calculation of the production and concentration of each unit in the watershed is carried out using three model methods: API model, short-term API model, and three water source Xin'anjiang model. The river convergence is calculated using the segmented continuous routing of the Maskingen River convergence.
Through model simulation calculation, after the above-mentioned heavy rain in the Huaihe River system, the whole line from Xixian County to Wujiadu above the main stream of the Huaihe River will be over insured, and the southern tributaries of Huanghe River and Bailu River will be over insured.

## 4 Conclusion

Based on the "21 · 7" rainstorm process, through displacement simulation analysis and calculation, under the scenario of not enabling flood control works, the whole line from the main stream of the Huaihe River below Xixian County to Wujiadu above will be over insured, and the southern tributaries of Huanghe River and Bailu River will be over insured.Through joint scheduling of reservoirs and the use of flood storage areas, the water level of the section from Runhe River to Wujiadu River can be reduced by 1.5-2.7m, the over protection range of the Runhe River section can be reduced to 0.6m, the Zhengyangguan River section can be lowered to near the warning water level, and the section below Zhengyangguan will not exceed the warning level. However, due to the short-term surge in incoming water from the Xixian Wangjiaba section, the incoming water from the river significantly exceeds the current flood discharge capacity, and the Wangjiaba section will experience overflow.

## Reference

[1] Jin Bingling, Lu Ami, Zhang Pu, etc.Analysis on the Causes of "21.7" Extreme rainstorm Weather in North Henan[J].Meteorology and Environmental Science,2022,245(2):65-74.
[2] Yang Changqing, Jiao Yingle, Yu Changchang, etc.Investigation on "21 · 7" rainstorm Flood and River Embankment Danger in Jiaozuo[J].Yellow River,2023,45(07):58-61.
[3] Wang Zili, Song Xiuchang, He Xianfeng, etc.Investigation and Analysis of River Embankment Danger in "7.20" extremely heavy rainstorm in Zhengzhou[J].Yellow River,2022,44(7):44-47.
[4] Liu Changjun, Lv Juan, Zhai Xiaoyan, etc.Flood risk simulation and comparative analysis of "21 · 7" rainstorm in Henan[J].Water Resources and Hydropower Express,2021,42(09):8-14.

**Theme:** Climate change impacts
**IAHR Thematic Priority Area:** [TPA-1] Climate Change Adaptation and Mitigation
https://doi.org/10.3850/iahr-hic2483430201-227

# Transboundary Precipitation and Flood Response in the China-Nepal Region: A Case Study of the Strong ENSO Event-2015 in the Karnali River Basin, Nepal

**Tirtha Raj Adhikari [1, 2, 3], Qiuhong Tang[1,4], Binod Baniya [1,5], Li HE [1,4], Ram Prasad Awasthi[6] , Suraj Shrestha[3, 7] Paul P.J. Gaffney[1]**

[1]Key Laboratory of Water Cycle and Related Land Surface Processes, Institute of Geographic Sciences and Natural Resources Research, Chinese Academy of Sciences, Beijing, China,
[2]College of Applied Sciences-Nepal, Environmental Science, Kathmandu, Affiliated to: Tribhuvan University
[3]Central Department of Hydrology and Meteorology, Tribhuvan University, Kirtipur, Kathmandu, Nepal
[4]University of Chinese Academy of Sciences, Beijing, 100049, China
[5]Central Department of Environmental Science, Tribhuvan University, Kirtipur, Kathmandu
[6]China Department of Hydrology and Meteorology, Government of Nepal
[7]Kathmandu Center for Research and Education, Chinese Academy of Sciences-Tribhuvan University, Kirtipur, Kathmandu, Nepal.

*Corresponding author: tirtha43@gmail.com Or tirtharajadhikari63@gmail.com*

**Abstract.** This study examined the flooding of the Karnali River Basin (KRB) linked to El Niño and La Niña effects. It has been analyzed precipitation patterns and major floods from China to Nepal and India (1964-2020). Using the HEC HMS and HEC RAS models in the transboundary KRB with ENSO events. The ENSO's impact found a connection with hydrometeorological parameters on the flood response downstream of KRB. This research will help in future planning and managing the water resources during strong El Niño or La Niña events

## 1 Introduction

This study explores the combined effects of El Niño/La Niña (ENSO) events and local factors on flooding in Nepal's Karnali River Basin (KRB). While previous research explored using ENSO for short-term streamflow prediction ([1,2]), the link between ENSO and flooding in transboundary rivers like the KRB remains unclear. This research addresses this gap. Flooding is a major threat in the KRB, with high discharge events posing significant risks. To safeguard downstream communities, accurate flood prediction models are essential. This study emphasizes the value of combining hydrological and hydrodynamic models with recent data for improved flood prediction. The research highlights the importance of considering both global (ENSO) and local factors, as referenced in prior studies ([2,3]). The Indo-Gangetic Plain (IGP) downstream of the KRB is particularly vulnerable due to land-use practices and infrastructure development. Understanding these dynamics is crucial for flood preparedness, especially in high-risk zones. The study reveals a significant impact of ENSO events on flood discharge variations in the KRB, with discharge ranging from 3354 $m^3/s$ to 23295 $m^3/s$ between 1964 and 2020. This research sheds light on this influence, providing valuable insights for improving flood response strategies. Effective flood preparedness in the KRB requires a holistic understanding of both global climate phenomena and local vulnerabilities to floods.

## 2 Methods:

- Historical data analysis like rainfall, river flow, and topography for 56 years and considered the basin area as a physical characteristic according depicted Figure 1.
- Using the established flood simulation models (HEC-HMS and HEC-RAS) with daily data to analyze the connection between ENSO events, precipitation patterns, and flood occurrences based upon passed study [3, 4].
- Model calibration and validation according [5] to validated the accuracy of the flood models by comparing the observed and model peak discharge.

## 3 Results

The study investigated the impact of El Niño (ENSO) on precipitation and floods in the Kelani River Basin (KRB) over a 56-year period. The findings emphasize the importance of improved water management strategies during El Niño events flood response given in Figure 1. Modeling also suggests that frequent channel changes occur on the right bank of the Karnali River, affecting water flow dynamics.

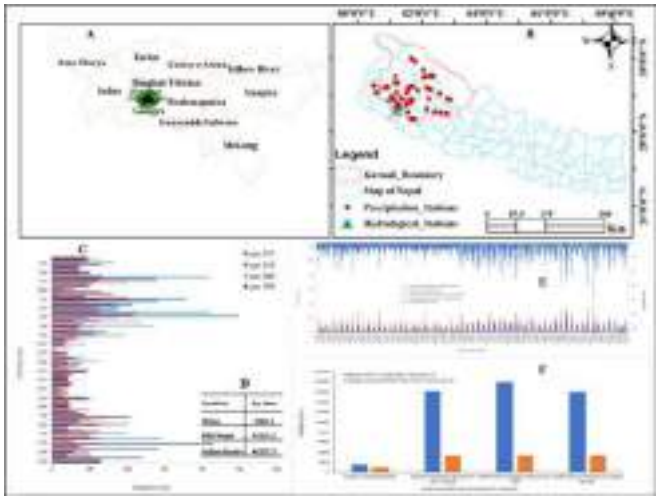

Figure 1: Indicates (A) HKH region (B) Red line indicates the transboundary KRB (C) Elevation wise transboundary maximum precipitation (D) Location wise transboundary basin area (E) is the flood response of ENSO-event & non-ENSO-events (F) Blue bars indicate La Niña flood discharge and orange red bar indicate the El Niño effect flood response of the KRB.

## 4 Conclusion

This study determined the discharge increases from China-Nepal border (3060 $m^3/s$) to 43117 $m^3/s$ at KRB station and 46177.3 $m^3/s$ at Indian border. Also, highlights the correlation between transboundary precipitation and flood response during the El Niño years monsoon season 2015 to emphasizes the importance of understanding ENSO for water management in this region.

## References

[1] H. J. Simpson, M. A. Cane, A. L. Herczeg, S. E. Zebiak, and J. H. Simpson, “Annual River Discharge in Southeastern Australia Related to E1 Nino-Southern Oscillation Forecasts of Sea Surface Temperatures Comparison of seasonal precipitation (P) variations,” 1993.

[2] E. Kahya and J. A. Dracup, “The influences of Type 1 El Nino and La Nina events on stream flows in the Pacific southwest of the United States,” J Clim, vol. 7, no. 6, 1994.

[3] T. R. Adhikari et al., “Evaluation of Post Extreme Floods in High Mountain Region: A Case Study of the Melamchi Flood 2021 at the Koshi River Basin in Nepal 2023.

[4] T. Raj Adhikari and S. Panthee, “Application of Hydrodynamic (HEC-RAS) Model for Extreme. Flood Analysis in Far-West Province: A Case Study of Chamelia River Basin, Darchula District, Nepal,” 2020

[5] M. Rashid, S. Faruque, M. M. Rashid, S. B. Faruque, and J. B. Alam, “Modeling of Short Duration Rainfall Intensity Duration Frequency (SDR-IDF) Equation for Sylhet City in Bangladesh 2012.

**Theme:** Climate change impacts
**IAHR Thematic Priority Area:** [TPA-1] Climate Change Adaptation and Mitigation
https://doi.org/10.3850/iahr-hic2483430201-229

# Monitoring Water Transparency, Total Suspended Matter and the Beam Attenuation Coefficient in Inland Water Using Innovative Ground-Based Proximal Sensing Technology

**Na Li[1],Yunlin Zhang[2], Kun Shi[1]**

[1] State Key Laboratory of Lake Science and Environment, Nanjing Institute of Geography and Limnology, Chinese Academy of Sciences, Nanjing, 210008, China
[2] State Key Laboratory of Lake Science and Environment, Nanjing Institute of Geography and Limnology, Chinese Academy of Sciences, Nanjing, 210008, China

*Corresponding author: ylzhang@niglas.ac.cn (Y. Zhang).*

**Abstract:** The GBPS was equipped with a hyperspectral imager placed 4–5 m above the water surface to minimize the impacts of the atmosphere and clouds. In this study, combined with 583 water samples obtained from four field samplings, GBPS datasets were first applied to estimate the total suspended matter (TSM), Secchi disk depth (SDD) and beam attenuation coefficient at 550 nm (C(550)) in Taihu Lake (TL), Liangxi River (LR) and Funchunjiang Reservoir (FR).

**Keywords:** Complex weather conditions; Ground-based proximal sensing; High-frequency observation

## 1 Introduction

At present, a range of water environmental concerns, including eutrophication[1], harmful algal blooms[2], and decreasing water clarity[3], pose a serious threat to the growth and reproduction of aquatic animals and vegetation and even to human health[4]. Therefore, it is necessary to establish an accurate, high-frequency continuous water quality monitoring system for capturing the short-term rapid dynamic process and the long-term trend of water quality, which is also of great significance in elucidating the response of water quality to meteorological change and artificial disturbance.

## 2 Methods

### 2.1 2.1 Field data

TL, Fuchunjiang Reservoir (FR), Liangxi River (LR) and Nanjing urban rivers (NUR) were selected to characterize the complexity and regional differences of the optical active substances of water bodies. A total of 164, 100, 109 and 210 water samples were collected from TL, LR, FR and NUR from October 28 to November 3, 2020; November 7-9, 2020; November 10-13, 2020; and March to May 2021, respectivel.

### 2.2 2.2 GBPS dataset acquisition and preprocessing

R is calculated through the measurement of the upwards and downwards irradiance on the water surface obtained from the hyperspectral imager according to the following equation:

$$R = E_u / E_d \quad (10)$$

where $E_u$ and $E_d$ represent the upwards irradiance and the downwards irradiance obtained on the water surface by the ground-based hyperspectral imager, respectively.

## 3 Results

### 3.1 3.1 Model development and validation

The calibration dataset of SDD varied from 0.2 m to 1.12 m with a mean value of 0.45 ±0.2 m when TSM ranged from 2.87 mg/L to 89.53 mg/L with a mean value of 29.95 ±16.61 mg/L and C(550) ranged from 0.58 m-1 to 35.93 m-1 with a mean value of 13.20 ±8.35 m-1. Mean while, the validation dataset of SDD varied from 0.2 m to 1.13 m with a mean value of 0.45 ±0.2 m when the TSM ranged from 4.32 mg/L to 77.76 mg/L with a mean value of 29.80 ±16.37 mg/L and C(550) ranged from 0.67 m-1 to 31.55 m-1 with a mean value of 13.19 ±8.33 m- 1.

### 3.2 3.2 Time series of the optical-related parameter variation

Overall, there were significant differences in SDD and C(550) among the three water bodies (nonparametric test, p 0.05). Specifically, the TSM (13.13 ±2.46 mg/L) and C(550) (6.10 ± 1.63 m-1) of FR were markedly lower than those of TL (TSM: 65.37 ± 64.86 mg/L, C(550): 21.93 ±10.80 m-1) and LR (TSM: 41.86 ±12.19 mg/L, C(550): 20.12 ±3.93 m-1), which was the opposite of the SDD in FR (0.63 ±0.06 m), TL (0.30 ±0.09 m) and LR (0.28 ±0.05 m). The results were consistent with field observations, meaning that the un derwater light field of FR was the brightest among the three water bodies.

## 4 Conclusion

In this study, three empirical models of water optical-related parameters (SDD, TSM and C(550)) with high R2 and low error were developed and validated based on 583 water samples collected from four field samplings and GBPS data with a spectral resolution of 1 nm and a minimal interval of 30 seconds. The empirical models based on GBPS data yielded high accuracy in estimating TSM, SDD and C(550) ($R2 \geq 0.79$). Subsequently, the time-series data of SDD, TSM and C(550) derived from GBPS data recorded two accidental water events in TL(November 1 and 3), significant linear trends in LR (November 7 to 9), and a periodic diurnal variation characteristic in FR (November 11 to 13). The GBPS, with the advantages of high temporal and spectral resolution and the applicability of complex weather conditions, compensates for in situ aircraft and satellite observation deficiencies, allowing us to capture more detailed water quality information and episodic events. Therefore, GBPS is a cost-effective and important part of an integrated water quality air-space-ground monitoring system in the future, exhibiting wide application prospects.

## References

[1] Qin, B., Deng, J., Shi, K., Wang, J., Brookes, J., Zhou, J., Zhang, Y., Zhu, G., Paerl, H.W., Wu, L., 2021. Extreme climate anomalies enhancing cyanobacterial blooms in eutrophic Lake Taihu, China. Water Resources Research 57, e2020WR029371.

[2] Qin, B., Li, W., Zhu, G., Zhang, Y., Wu, T., Gao, G., 2015. Cyanobacterial bloom management through integrated monitoring and forecasting in large shallow eutrophic Lake Taihu (China). Journal of Hazardous Materials 287, 356-363.

[3] Shi, K., Zhang, Y., Zhu, G., Qin, B., Pan, D., 2018. Deteriorating water clarity in shallow waters: evidence from long term MODIS and in-situ observations. International Journal of Applied Earth Observation and Geoinformation 68, 287-297.

[4] Zhang, Y., Jeppesen, E., Liu, X., Qin, B., Shi, K., Zhou, Y., Thomaz, S.M., Deng, J., 2017. Global loss of aquatic vegetation in lakes. Earth-Science Reviews 173, 259-265.

**Theme:** Climate change impacts
**IAHR Thematic Priority Area:** [TPA-1] Climate Change Adaptation and Mitigation
https://doi.org/10.3850/iahr-hic2483430201-231

# Long-Term Prediction of Water Temperature and Stratification Changes in the Soyang Reservoir Due to the Impact of Climate Change

**Yeojeong Yun**[1], **Sewoong Chung**[1,*]

[1] Department of Environmental Engineering, Chungbuk National University, Cheongju, 28644, Republic of Korea

** Corresponding author: schung@chungbuk.ac.kr*

**Abstract.** This study examines the impact of climate change on water temperature in Soyang Reservoir, South Korea, crucial for effective water management. Through simulations spanning 2016 to 2070, diverse climate scenarios are integrated, revealing rising temperatures and variability. Notable observations include differing temperature increases between RCP 4.5 and 8.5 scenarios, influencing water temperature stratification. Stratification strength projections highlight potential impacts on aquatic ecosystems. These findings emphasize the importance of accurate temperature predictions amidst uncertainty, particularly regarding water quality and ecosystem dynamics in the face of climate change.

**Keywords:** Impact of Climate Change, Long-Term Prediction, Stratification strength, Water temperature

## 1 Introduction

The anticipated rise in temperature attributed to climate change holds profound implications for environmental factors, encompassing water temperature, algal bloom occurrences, and hypoxia[1, 2, 3, 4, 5]. Accurate prediction and comprehension of the ensuing effects on water quality are imperative for sustainable water management.[6, 7, 8]. This study focuses on assessing the impact of climate change on water temperature in the Soyang Reservoir, South Korea, with the aim of contributing to effective water resource management.

## 2 Methods

Through the simulation of water temperature and stratification strength under diverse climate scenarios spanning from 2016 to 2070, this research integrates climate change models, water quality prediction models, and water quality scenarios. A total of 42 scenarios, including two RCP models (RCP 4.5, RCP 8.5), seven downscaled GCM models, a daily inflow generation model (SWAT) and a hydro-water quality model (CE-QUAL-W2) were employed.

## 3 Results & conclusion

The results reveal a general trend of increased water temperature and variability within the Soyang Reservoir due to projected future temperature elevations. Notable observations include the highest water temperature increase in the RCP 8.5 upper layer at 0.062℃/year and the lowest in the RCP 4.5 lower layer at 0.011℃/year(table 1). Differences in temperature rise rates between upper and lower layers significantly influence the strength of water temperature stratification. Stratification strength, calculated using rLakeAnalyzer in R language, spans from 1,777.56 to 4,026.32 J/m2 at RCP 4.5 and 2,318.72 to 4,446.29 J/m2 at RCP 8.5. Although the range difference between RCP scenarios is subtle, higher values are observed in RCP 8.5. Comparison with stratification strength calculated from historical water temperature data (2005-2015) indicates an expected increase in simulated stratification strength during future periods. These findings underscore the need for accurate

predictions of water temperature and quality amid heightened uncertainty, particularly in the context of potential impacts on aquatic ecosystems and reservoir mixing characteristics resulting from increased temperatures driven by climate change.

Table 1 Annual rising of upper and lower layer water temperature by scenario and ratio of upper and lower layer water temperature to air temperature.

| RCP | Scenario | Upper temperature | | Lower temperature | |
|---|---|---|---|---|---|
| | | ℃/year | % | ℃/year | % |
| 4.5 | CCSM4 | 0.029 | 94.8 | 0.02 | 63.1 |
| | CMCC-CM | 0.023 | 57.7 | 0.011 | 28.6 |
| | FGOALS-s2 | 0.018 | 95.6 | 0.014 | 74.1 |
| | HadGEM-ES | 0.031 | 79.4 | 0.016 | 41.3 |
| | INM-CM4 | 0.052 | 119.7 | 0.033 | 76.9 |
| | MIROC- | 0.016 | 86.7 | 0.003 | 17.3 |
| | ESM-CHEM | 0.036 | 82.7 | 0.017 | 39.2 |
| | Average | 0.029(±0.012) | 88.1 | 0.016(±0.009) | 48.6 |
| 8.5 | CCSM4 | 0.036 | 80 | 0.03 | 67.8 |
| | CMCC-CM | 0.053 | 78.2 | 0.031 | 46.1 |
| | FGOALS-s2 | 0.047 | 104.6 | 0.025 | 56.2 |
| | HadGEM-ES | 0.062 | 81.1 | 0.03 | 39.7 |
| | INM-CM4 | 0.051 | 70.5 | 0.026 | 36 |
| | MIROC- | 0.025 | 97.8 | 0.006 | 24.4 |
| | ESM-CHEM | 0.062 | 88 | 0.038 | 53.7 |
| | Average | 0.048(±0.014) | 85.8 | 0.027(±0.010) | 46.3 |

**Acknowledgments**

This work was supported by the Korea Environmental Industry & Technology Institute (KEITI) through the Aquatic Ecosystem Conservation Research Program, funded by Korea Ministry of Environment (MOE) (Grant number 2021003030004).

**Reference**

[1] Noh, S., Park, H., Choi, H., and Lee, J. (2014). Effect of climate change for cyanobacteria growth pattern in Chudong station of lake Daechung, Journal of Korean Society on Water Environment, 30(4), 377-385. [Korean Literature]

[2] Wagner, C. and Adrian, R. (2009). Cyanobacteria dominance: quantifying the effects of climate change, Limnology and Oceanography, 54(6part2), 2460-2468.

[3] Paerl, H. W. and Huisman, J. (2009). Climate change: a catalyst for global expansion of harmful cyanobacterial blooms, Environmental microbiology reports, 1(1), 27-37

[4] Intergovernmental Panel on Climate Change (IPCC). (2014). Mitigation of climate change, Contribution of working group III to the fifth assessment report of the intergovernmental panel on climate change, 1454.

[5] International Steategy for Disaster Reduction (ISDR). (2007). Risk Reduction: 2007 Global Review, International Steategy for Disaster Reduction

[6] Fang, X. and Stefan, H. G. (2009). Simulations of climate effects on water temperature, dissolved oxygen, and ice and snow covers in lakes of the contiguous US under past and future climate scenarios, Limnology and Oceanography, 54(6part2), 2359-2370

[7] Jung, I. W., Bae, D. H., and Kim, G. (2011). Recent trends of mean and extreme precipitation in Korea, International journal of climatology, 31(3), 359-370. [Korean Literature]

[8] Shin, Y. and Jung, H. (2015). Assessing uncertainty in future climate change in Northeast Asia using multiple CMIP5 GCMs with four RCP scenarios, Journal of Environmental Impact Assessment, 24(3), 205-216.

**Theme:** Climate change impacts
**IAHR Thematic Priority Area:** [TPA-1] Climate Change Adaptation and Mitigation
https://doi.org/10.3850/iahr-hic2483430201-233

# Impact of Extreme Climate and Land-Use Change on Inducing Floods and Droughts in The Upper Luanhe River Basin

**Ge Gao [1,2], Jia Liu [2], Jianzhu Li [1], Ping Feng [1], Yicheng Wang [2]**

1. State Key Laboratory of Hydraulic Engineering Intelligent Construction and Operation, Tianjin University, Tianjin 300072, China
2. State Key Laboratory of Simulation and Regulation of Water Cycle in River Basin, China Institute of Water Resources and Hydropower Research, Beijing 100038, China

*Corresponding author: gaoge1998@tju.edu.cn*

**Abstract**: In recent years, extreme hydrological events have been more frequent in the Luanhe River Basin. Studying the response mechanism of extreme hydrological events in the Luanhe River Basin to climate change and land-use variations is of significant scientific and practical value for disaster prevention and mitigation under new circumstances. This study focuses on the control area of Sandaohezi Hydrological Stations as the study area. Twelve extreme climate indices are selected to analyze the trends in extreme climate changes, and calculations are conducted to determine their correlation with extreme hydrological events. A SWAT hydrological model is constructed to explore the response patterns of extreme hydrological events to climate and land-use variations. The results indicate a notable warming and drying trend, with rising extreme temperatures, decreasing precipitation, and more concentrated extreme rainfall. Extreme hydrological events are mainly influenced by climate change, with climate change having a greater impact on extreme dry events than extreme flood events.

## 1 Introduction

Climate change and land-use change has intensified the occurrence of hydrological events like severe floods and droughts, posing serious threats to public safety and socio-economic stability [1]. This study focuses on the Sandaohezi hydrological station control basin in the upper Luanhe River basin, to explore the response patterns of extreme hydrological events to climate and land-use variations.

## 2 Study area and methods

This study focuses on the control area of Sandaohezi hydrological stations as the study area. Six extreme temperature indices including TNn, TNx, TXn, TXx, SU, Tx90p and six precipitation indices including Rx1day, Rx5day, PRCPTOT, SDII, R10, R20 are selected to analyze the trends in extreme climate changes [2]. The POT method is used to recognize extreme hydrological events, including extreme flood events and extreme dry events [3], and the 96% and 4% percentiles of the multi-year runoff series are selected as thresholds, respectively. Pearson correlation analysis is conducted to determine the strength of the correlation between extreme climate indices and extreme hydrological events [4]. A SWAT hydrological model is constructed, and the response patterns of extreme hydrological events to climate and land-use variations are explored by altering climate or land-use inputs [5].

## 3 Results and discussion

TNn, TNx, TXn, TXx, SU, and Tx90p all exhibit an increasing trend, indicating a warming trend. Rx1day, Rx5day, R10, R20, and PRCPTOT all demonstrate varying degrees of decline, indicating a decrease in precipitation in the study area. The decline rate of SDII is relatively small, suggesting concentrated extreme rainfall. Correlation analysis between extreme hydrological events and twelve extreme climate indices shows significant correlations. Extreme flood events are notably correlated

with all precipitation indices and high-temperature indices. Extreme dry events correlate with extreme temperature indices. Simulated runoff from the SWAT model indicates that extreme hydrological events are primarily influenced by climate change, with a more pronounced impact on extreme dry events than on extreme flood events. Between 1980 and 1999, the climate positively impacted extreme flood events, primarily due to increased precipitation. Between 2000 and 2018, the increase in extreme high-temperature events has led to a higher frequency of extreme dry events and a decrease in extreme flood events. The influence of land-use change on extreme hydrological events is minimal, with a greater impact on extreme dry events than on extreme flood events.

## 4 Conclusions

The results indicate a warming and drying trend in the study area, with a decrease in total precipitation but a concentration of extreme rainfall. Extreme flood events are mainly caused by extreme precipitation events and climate warming, while extreme dry events are mainly caused by extreme high temperatures. Extreme hydrological events are primarily influenced by climate change compared to land-use change, with climate change exerting a greater impact on extreme dry events than extreme flood events.

## References

[1] S. Lu, X. Bai, W. Li, N. Wang, Impacts of climate change on water resources and grain production, Technol. Forecast. Soc. Change. 143 (2019) 76-84.

[2] T. Ozturk, F. S. Saygili-Araci, M. L. Kurnaz, Projected Changes in Extreme Temperature and Precipitation Indices Over CORDEX-MENA Domain, Atmos. 12 (2021).

[3] X. Pan, A. Rahman, K. Haddad, T. B. M. J. Ouarda, Peaks-over-threshold model in flood frequency analysis: a scoping review, Stoch. Environ. Res. Risk Assess. 36 (2022) 2419-2435.

[4] E. Ghaderpour, P. Mazzanti, G. S. Mugnozza, F. Bozzano, Coherency and phase delay analyses between land cover and climate across Italy via the least-squares wavelet software, Int. J. Appl. Earth Obs. Geoinf. 118 (2023).

[5] M. L. Tan, P. W. Gassman, X. Yang, J. Haywood, A review of SWAT applications, performance and future needs for simulation of hydro-climatic extremes, Adv. Water Resour. 143 (2020).

**Theme:** Climate change impacts
**IAHR Thematic Priority Area:** [TPA-1] Climate Change Adaptation and Mitigation
https://doi.org/10.3850/iahr-hic2483430201-235

# Copula-based Hydrometeorology-Wildfire Relationship Analysis in United States

**Ke Shi[1], Yongsen Yang[1]**

[1] China Institute of Water Resources and Hydropower Research, 100038 Beijing, China

*Corresponding author: Ke Shi, ke.dlut@outlook.com*

**Abstract.** Wildfires are a natural part of the ecosystem in U.S.. It is vital to classify wildfires using a comprehensive approach that simultaneously considers wildfire activity and burned area. On this basis, the influence of hydrometeorological variables on wildfires can be further analyzed. Therefore, this study first classified wildfire types using a wildfire bivariate probability framework. Then, by considering six hydrometeorological variables, the dominant hydrometeorological variables for different wildfire types in 17 ecoregions of the United States were quantified. In addition, based on the results of this hydrometeorology-wildfire relationship analysis, we obtained new clusters that simultaneously considered wildfire characteristics and the impact of hydrometeorology on the wildfires. In particular, the results were as follows: (1) Through the probability of wildfire bivariate statistical characteristics, wildfires could be classified into five types in this paper; (2) The dominant hydrometeorological variables under different wildfire types were discussed in 17 ecoregions of the United States; and (3) In the four new cluster regions, intensifying droughts are a concern in clusters 1 and 4, while there are multiple concerns in cluster 3, namely, stronger winds, higher temperatures, and more drought.

**Keywords:** Wildfire; Hydrometeorology; Wildfire regime; Copula.

## 1 INTRODUCTION

Wildfires constitute an integral ecological process in the natural Earth system associated with regional and global biogeochemical cycles, human activities, and vegetation structure [1]. Subjectively, it appears that more wildfire activities could lead to more severe wildfires and larger burned areas. However, the reduction in wildfire activities (number of wildfires) driven by policy and wildfire management has resulted in changes in the vegetation structure and an increase in fuel accumulation in the western United States [2]. As a consequence, wildfire suppression and the subsequent increase in fuel loads have coincided with warmer and drier wildfire seasons, causing high-severity wildfire events yielding large burned areas [3]. These two seemingly contradictory situations are attributed to the unique structure of the relationship between the wildfire activity and burned area, posing challenges to comprehensively assess the wildfire characteristics.

Accordingly, in this study, we determine the univariate distribution of these two target wildfire characteristics. Second, we calculate the joint probability of the wildfire activity and burned area according to a copula-based joint distribution. Then, the average method is applied to balance the copula-based bivariate and univariate probability distributions to calculate the wildfire priority index. Finally, through this wildfire priority index, the spatiotemporal variability and return period trends of the wildfire risk can be explored.

## 2 MATERIALS AND METHODS

In this study, wildfire statistics data pertaining to the continental United States were obtained from the 5th edition of the Forest Service Fire Program Analysis-Fire Occurrence Database [4]. This comprehensive dataset includes 2.17 million wildfire records.

As described in the introduction, direct application of bivariate probability distributions in wildfire frequency analysis can result in neglect of single mega-wildfire events and numerous wildfire events with a normal-sized burned area. Accordingly, we adopted the average method to determine the wildfire priority index to balance bivariate joint probability and univariate probability.

## 3 RESULTS AND DISCUSSION

From the univariate probability and the joint bivariate probability of wildfire, we calculated the wildfire priority index. The wildfire priority index is the average of the three probability values of the wildfire univariate probability and the bivariate joint probability. Then, according to the return period trends of wildfire priority index, future wildfire risk changes can also be determined. In particular, the return period trends of wildfire priority index are shown in Fig. 1. The results indicated that the return period of log-burned-area exhibits a significant increasing trend in California, Texas, and Arkansas. Moreover, most of the southeastern continental United States exhibits significant decreasing trends.

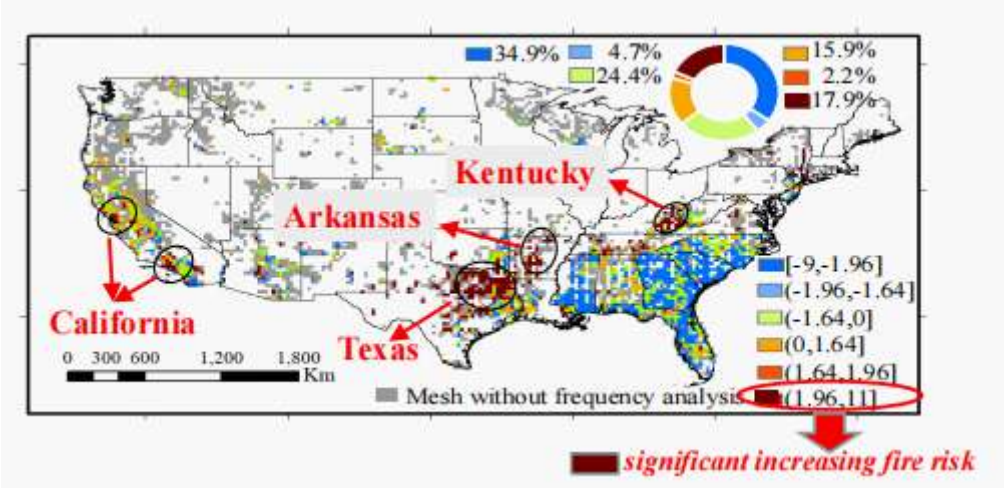


Figure 29 The trends of wildfire bivariate characteristic.

## 4 CONCLUSIONS

Overall, the framework of wildfire frequency analysis proposed in this study can provide a reference to better understand the spatiotemporal characteristics of wildfire statistics. This new approach of wildfire risk assessment will also facilitate the consideration of postfire effects.

## Reference

[1] Bowman, D.M., et al. 2009. Fire in the Earth system. Science 324(5926), 481-484.
[2] Hurteau, M.D., et al. 2014. Climate change, fire management, and ecological services in the southwestern US. Forest Ecology and Management 327, 280-289.
[3] Dennison, P.E., et al. 2014. Large wildfire trends in the western United States, 1984-2011. Geophysical Research Letters 41(8), 2928-2933.
[4] Short, K.C. 2021 Spatial wildfire occurrence data for the United States, 1992-2018. [FPA_FOD_20210617].

**Theme:** Climate change impacts
**IAHR Thematic Priority Area:** [TPA-1] Climate Change Adaptation and Mitigation
https://doi.org/10.3850/iahr-hic2483430201-237

# Analysis and Countermeasures for Typical Cascade Dam Break events in China

**Jie Mu [1,2,*] , Minghua Chu [1,2] , Fuxin Chai [1,2] ,Yesen Liu[1,2] , Hongbin Zhang [1,2] , Weihong Xu [1,2]**

[1]China Institute of Water Resources and Hydropower Research
[2]Research Center on Flood & Drought Disaster Prevention and Reduction of the Ministry of Water Resources

*Corresponding author: mujie@iwhr.com*

**Abstract**. The peak flow and velocity of dam break flood are much greater than that of rainstorm flood or snowmelt flood. If cascade dam break happens, it will induce a serious flood disaster and huge damage. Therefore, it is important to study the cause and process of cascade dam break floods. This paper carries out an analysis of the "75·8" dam break events of Banqiao reservoirs in Henan province, and the dam break events of Yongan and Xinfa reservoirs in Inner Mongolia in 2021. A refined two-dimensional hydrodynamic model, reservoir regulation model and dam break flow simulation model are constructed to explore the break process and mechanism of cascade dams. According to the analysis results, the countermeasures to prevent or reduce the impact of dam break are put forward, in order to provide decision support for the dam break defense of cascade reservoirs.

**Keywords:** dam break flood, cascade reservoirs, numerical model, countermeasures

## 1 Introduction

There are many cascade reservoirs on the main rivers in China. According to the collected data from 1954 to 2021, the average annual dam break rate in China was $5.3\times10^{-4}$, and from 2000 to 2021, this data dropped to $0.5\times10^{-4}$, far below the international level. Under the influence of climate change, the over-standard flood occurs frequently, which leads to occasional cascade dam break events, which has a great impact on the production and life of the downstream residents. Therefore, it is important to study the cause and process of cascade dam break floods.

## 2 Material and methods

The flood flow of dam break was calculated base on the method proposed by China Academy of Railway Sciences, which is stipulated in Hydraulic Calculation Manual. The self-developed Integrated (IWHR) Flood Modeling System (IFMS) was employed to simulate the 2D hydrodynamic processes of the flood evolution.

## 3 Analysis of historical cascade dam break events

### 3.1 Banqiao and the uptream reservoirs

In August 1975, the cascade dam break event were occurred in Banqiao and the 5 upstream reservoirs. The total storage capacity of the 5 small reservoirs accounts for 0.26% of Banqiao Reservoir. The total flood peak caused by the 5 upstream reservoirs is 7976$m^3$/s. Because the downstream channel of the 5 reservoirs were wide and far from Banqiao Reservoir, the flood peak to the dam site of Banqiao Reservoir was reduced to 328.7$m^3$/s. Therefore, the dam break of upstream reservoirs had little effect on Banqiao Reservoir in general. The main reason for the cascade dam break events were the over-standard flood.

The new Banqiao Reservoir was rebuilt at the original site. There are 2 medium-sized reservoirs and 17 small reservoirs in the upstream, with a total storage capacity of $34.77\times10^4$ $m^3$. The total storage capacity of the 19 upstream reservoirs accounts for 5.2% of the rebuilt Banqiao Reservoir. According to the numerical calculation of dam-break flow and the simulation of flood evolution, if all the dams of 19 upstream reservoirs break, under the worst scenarios of the combination of the basin flood peak and the dam break peak flow, the inflow of the Banqiao Reservoir will reaches 17126 $m^3/s$. The dam break flood of the upstream reservoirs will have a great impact on the safety of the Banqiao Reservoir. But due to the improvement of flood control standards and the increase of the discharge capacity after reconstruction, the Banqiao Reservoir can basically guarantee the dam safety. But the flood of the downstream Suiping hydrological station will be increase to 4650 $m^3/s$, which exceed the guaranteed flow(guaranteed flow is 2800$m^3/s$). The inspection and defense of dike should be taken.

### 3.2 Yongan and Xinfa Reservoirs

In July 2021, the cascade dam break events occurred in Yongan and Xinfa Reservoirs.The total storage capacity of Yongan Reservoir accounts for 21% of Xinfa Reservoir. The dam flood peak flow of Yongan Reservoir was 4500$m^3/s$ and accounts for 41.4% of the inflow of Xinfa Reservoir. The dam break flood of Yongan Reservoirs has great impact on the dam destruction of Xinfa Reservoir. The dam safety condition are as follows under the scenario of the measures of strengthening the wave wall, putting tarp over the dam slop and expanding spillway in Xinfa reservoir. (1) Strengthening the wave wall. The highest water level will reach 228.0m, 0.8m above the crest of the wave wall (227.20 meters) and 2.00 meters above the crest of the dam (226.00 meters). Therefore, in order to ensure the dam safety, it is necessary to raise the wave wall by more than 2.0 meters, and ti's very difficult. (2) Putting tarp over the dam slop. If this measure is adopted, the overflow time will be 6 hours and the maximum water level will be 227.82 meters (0.62 meters above the top of the wave wall). This measures is risky for dam safety. (3)Digging and expanding the spillway. When the excavation depth of the spillway is 6.1m and 3.0m respectively, the highest water level will not exceed the crest of the dam and the top of the wave wall. If the expansion measures are adopted, the above conditions can be achieved when the spillway expansion widths is 140m and 40m respectively.

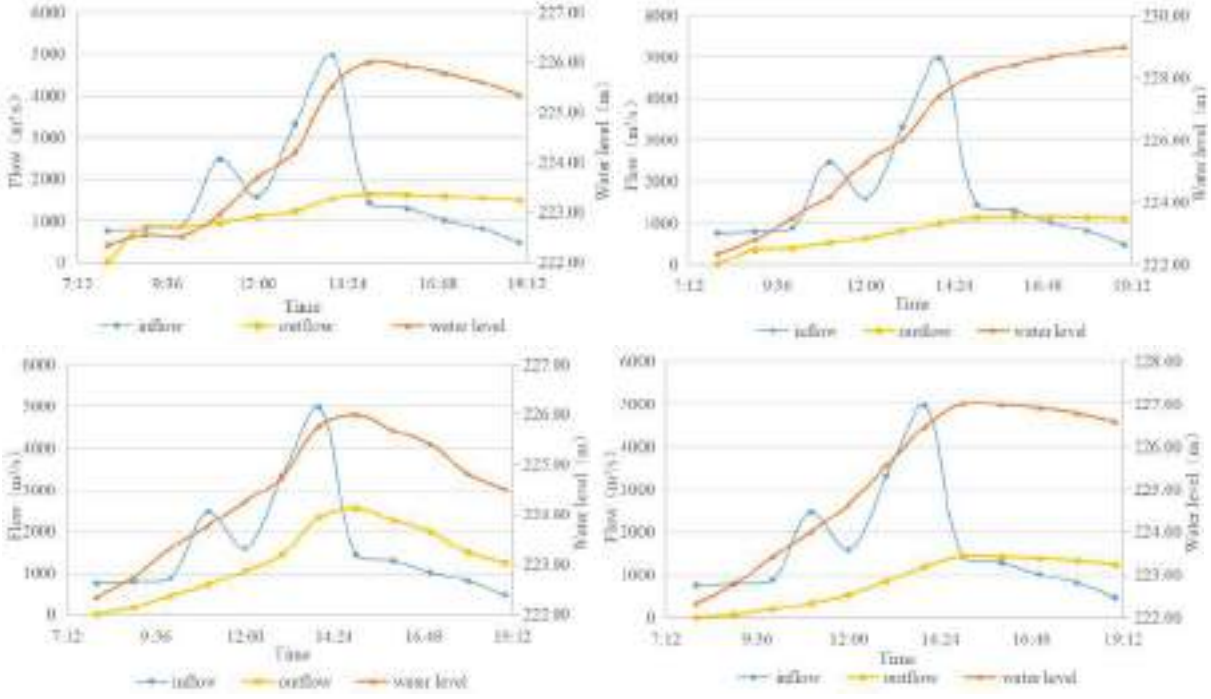


Figure 30 Calculation result of spillway expansion scheme of Xinfa Reservoir (a.excavation depth of the spillway is 6.1m; b.excavation depth of the spillway is 3.0m; c.the expansion widths of the spillway is 140m; d. the expansion widths of the spillway is 40m )

## 4 Cause analysis of dam break

The reasons for the cascade dam break events are summarized as, the reservoir managers lack of risk awareness and emergency response ability, the design standards of some reservoirs are relatively low, and the flood discharge capacity of the downstream river and the emergency capacity are insufficient.

## 5 Countermeasures and suggestions

(1) emergency measures. The upstream reservoir should send early warning information in time. The downstream reservoirs should lower the water level in advance, vacate the flood storage capacity, reserve emergency materials, and remind the downstream governments to transfer affected residents.
(2) conventional measures. The risk analysis of the cascade dam break events would be incorporated into reservoir planning, design and safety appraisal. We will improve the capacity of the "four preparations" for flood prevention and strengthen the emergency response ability. And risk assessments should be carried out, flood control standards, design flood flow, flood storage capacity, discharge capacity should be reviewed regularly. And operability of the reservoirs dispatching scheme and the emergency plan for over-standard flood should be checked.
It is worth mentioning that if reservoirs are close to each other, even if there are advanced forecasting and warning systems and sufficient emergency facilities, it is difficult to avoid accidents when encountering over-standard floods. Therefore, it is necessary to transfer affected residents as soon as possible.

## Acknowledgments

This study was supported by Major Project of National Natural Science Foundation of China (Project No.52394235 ).

## Reference

[1] Zhou X.B., Chen Z.Y., Huang Y.F., Wang L., Li X.N., Evaluations on the safety design standards for dams with extra height or cascade impacts[J]. Journal of hydraulic engineering. 2015(46)7:765-772.
[2] Zhang J.Y., Yang Z.H., Jiang J.P. A study on reservoir dam defects and breaches in China[M].Science Press.2014.
[3] Yang Z.Y., Guo H.M., Cao G.C., Inundation process of downstream cities by dam break flood form cascade reservoirs[J]. Journal of Yangtze River Scientific Research Institute.2017,34(9)47-51,78.

**Theme:** Climate change impacts
**IAHR Thematic Priority Area:** [TPA-1] Climate Change Adaptation and Mitigation
https://doi.org/10.3850/iahr-hic2483430201-240

# Response of Water Use Efficiency of Different Vegetation Types at Various Scales on the Tibetan Plateau to Climate Change

**Minglei Yao[1], Yanyan Cheng[2], Xiaogang He[2], Tao Yu[1]**

[1] Yangtze Eco-Environment Engineering Research Center, China Three Gorges Corporation; Wuhan, China
[2] Department of Civil and Environmental Engineering, National University of Singapore

*Corresponding author: yao_minglei@ctg.com.cn*

**Abstract.** Studying the relationship and coupling laws between carbon sequestration and water consumption in the vegetation of the Tibetan Plateau is crucial for addressing the potential conflicts between carbon sink and water yield functions on the plateau. By employing the Community Land Model version 5 (CLM5), adapted for the Tibetan Plateau, and a machine learning approach based on Boosted Regression Tree (BRT), this research simulated and analyzed the variations in water use efficiency (WUE) of different vegetation types at various scales under different climate change scenarios. The findings are as follows: (1) Precipitation is the primary control factor for the variation of Plant-scale Water Use Efficiency (PWUE) in woodlands and grasslands. Under the background of climate change, PWUE in woodlands mainly decreases with increasing precipitation, while in grasslands, it mainly increases. This leads to a positive impact of climate change on grassland PWUE (3.0% to 4.3%) and a negative impact on forest PWUE (-3.7% to -9.1%). (2) Climate change has a significant negative effect on Ecosystem-scale Water Use Efficiency (WUE) in woodlands (-0.050 to -0.054 gC $kg^{-1}$ $H_2O$), and a significant positive effect on grasslands (0.071 to 0.104 gC $kg^{-1}$ $H_2O$). The main reason is that climate change reduces carbon use efficiency in woodlands (29% to 30%) while significantly enhancing it in grasslands (102% to 256%). Overall, climate change increases the future WUE of overall vegetation (0.055 to 0.086 gC $kg^{-1}$ $H_2O$), mitigating the potential conflict between carbon sink and water yield functions on the Tibetan Plateau.

**Keywords:** Climate change, ecosystem-scale water use efficiency, plant-scale water use efficiency, Tibetan Plateau, vegetation carbon-water flux

## 1 Introduction

The Tibetan Plateau is famous as the "Asian Water Tower" and "Ecological Security Barrier". In addition to its important function of water conservation, the Tibetan Plateau has also provided an important boost for China to achieve the dual carbon goals of "carbon peak and carbon neutrality". However, the process of vegetation carbon sequestration usually consumes a certain amount of water, and there may be potential conflicts between water conservation and carbon sequestration. Studying the relationship and coupling pattern between carbon sequestration and water consumption of vegetation on the Tibetan Plateau is crucial to addressing the potential contradiction between the carbon sink and water production functions of the Tibetan Plateau. This study has important scientific significance and potential application prospects for the enrichment and development of theories and methods on the impact of climate change on carbon-water coupling of vegetation on the Tibetan Plateau.

## 2 Material and methods

CLM5 requires meteorological forcing and land cover data as input parameters. We use three-hour meteorological forcing obtained from the China Meteorological Forcing Dataset (CMFD) (Kun and Jie, 2019) at 0.1° to drive CLM5 simulations from 1979 to 2018. During the spin-up, the 40 years

CMFD was recycled for 800 years until all water, carbon, and nitrogen state variables reached equilibrium. The land use and land cover of TP is extracted from the 30m China's Land-Use/Cover Datasets obtained from Resource and Environment Science and Data Center. Through comprehensive analysis, a land surface process model CLM5 for the Tibetan Plateau was constructed; then, based on the machine learning method of Boosted Regression Tree, the carbon-water coupling change pattern and its main controlling factors of different scales and different vegetation on the Tibetan Plateau were simulated and analyzed.

## 3 Results and discussion

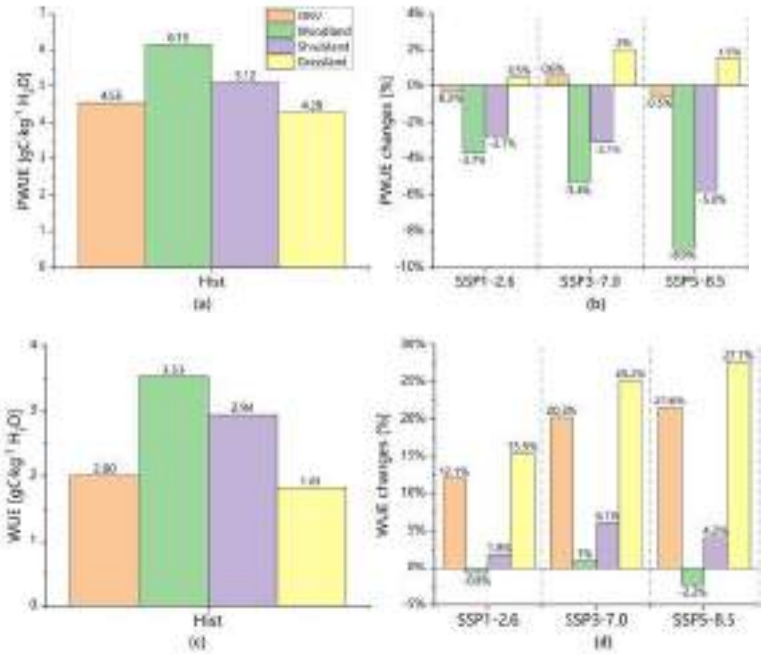


Figure 1 Different vegetation (a) PWUE and (c) WUE in the historical period (the value is 1985-2014 mean), and percent changes in (b) PWUE and (d) WUE at the end-of-the-century relative to the historical period under the SSP1-2.6, SSP3-7.0, SSP5-8.5 scenarios

## 4 Conclusions

Based on the machine learning method and feature importance analysis of Boosted Regression Tree, the variation pattern of plant canopy-scale water use efficiency PWUE and its influencing mechanism were explained. It was found that precipitation was the main controlling factor for future changes in PWUE in both woodlands and grasslands; in the context of climate change, both PWUE tended to increase and then decrease with increasing precipitation, but PWUE in woodlands was mainly in the range of decreasing with increasing precipitation, while grasslands was mainly in the range of increasing with increasing precipitation; resulting in a positive impact of climate change on PWUE in grasslands and a negative effect on woodland. Based on the transformational relationship between plant canopy and carbon-water coupling characteristics at the ecosystem scale, the change pattern of water use efficiency (WUE) at the ecosystem scale and its main controlling factors were analysed. It was found that climate change had a significant negative effect on the WUE of woodlands and a significant positive effect on the WUE of grasslands, mainly because climate change reduced the carbon use efficiency of woodlands; and significantly increased the carbon use efficiency of grasslands. Overall, climate change increased the future WUE of the overall vegetation, mitigating the potential conflict between carbon sink and water production functions on the Tibetan Plateau.

## Reference

[1] Kun, Y., Jie, H., 2019. China meteorological forcing dataset (1979-2018). In: National Tibetan Plateau Data, C. (Ed.). National Tibetan Plateau Data Center. DOI:10.11888/AtmosphericPhysics.tpe.249369.file

**Theme:** Climate change impacts
**IAHR Thematic Priority Area:** [TPA-1] Climate Change Adaptation and Mitigation
https://doi.org/10.3850/iahr-hic2483430201-242

# Fifteen-year statistical analysis of cloud characteristics over China using Terra and Aqua Moderate Resolution Imaging Spectroradiometer observations

**Yuyang Chen**[1]

[1] Yangtze Eco-Environment Engineering Research Center, China Three Gorges Corporation, Wuhan 430010, China

*Corresponding author:chen_yuyang@ctg.com.cn*

**Abstract.** This study utilizes 15 years of observations from the Moderate Resolution Imaging Spectroradiometer (MODIS) aboard NASA Terra and Aqua satellites (March 2003 to February 2018) to analyze spatio-temporal variations in macro- and micro-physical cloud properties across China. Parameters studied include cloud fraction (CF), cloud top pressure (CTP), cloud top temperature (CTT), cloud optical thickness (COT), and effective radius ($r_e$) of liquid water and ice clouds. The multiyear averaged CF is approximately 61% across China, with notable seasonal and regional variations. CF is higher in summer and winter (~64–65%) compared to spring and autumn (~58%). Regional classification reveals distinct CF distribution patterns, with more clouds in southern and southeastern regions than in northern and northwestern areas. Cloud properties also vary between land and ocean, with larger CF over ocean and significant differences between morning and afternoon CF over land. COT distribution mirrors CF patterns across seasons, while cloud $r_e$ values are influenced by aerosol pollution, exhibiting higher values in northwestern and Tibetan Plateau regions. These findings contribute to a better understanding of cloud dynamics and regional variations.

**Keywords:** China, cloud effective radius, cloud fraction, cloud optical thickness, cloud top pressure, MODIS

## 1 Introduction

Clouds are pivotal in the Earth's energy balance and hydrological cycle, influencing climate dynamics. Understanding their properties and processes is crucial, yet remains a challenge in climate modeling. Clouds' radiative effects significantly impact Earth's energy balance, with observed net cloud radiative forcing exceeding that of doubled CO2. Aerosols, acting as cloud condensation nuclei, alter cloud properties, affecting radiative forcing and cloud lifetime. Accurate representation of clouds in climate models is imperative, particularly over polluted regions like East Asia. In this paper, we present a detailed investigation of the spatio-temporal distribution of cloud properties over China using MODIS data. Our analysis includes histograms and joint histograms of selected cloud parameters to enhance understanding. The findings will contribute to advancing our knowledge of cloud characteristics and their implications for climate dynamics.

## 2 Material and methods

We utilized Collection 6.0 level-3 MODIS atmosphere monthly products (MOD08 for Terra, MYD08 for Aqua) to analyze cloud climatology over China (March 2003 to February 2018). Terra MODIS captures morning clouds (~10:30 a.m. LST), while Aqua MODIS senses afternoon clouds (~1:30 p.m. LST), enabling morning-afternoon cloud property comparisons. These products, sorted into 1° cells on a global grid, employ a cloud product algorithm integrating infrared and visible techniques (King et al., 2003; Platnick et al., 2003). Our study focuses on China's latitudes (15°N–55°N) and longitudes (70°E–140°E), emphasizing cloud characteristics. Seasonal mean properties are computed for winter, spring, summer, and autumn. We examine temporal changes in cloud amount, Terra-Aqua cloud

fraction disparities, and frequency of occurrence and joint histograms for liquid water and ice clouds. China is divided into N, NE, S, NW, and TP regions for spatial and temporal analysis, aiding in comprehensive understanding of China's cloud climatology.

## 3 Results and discussion

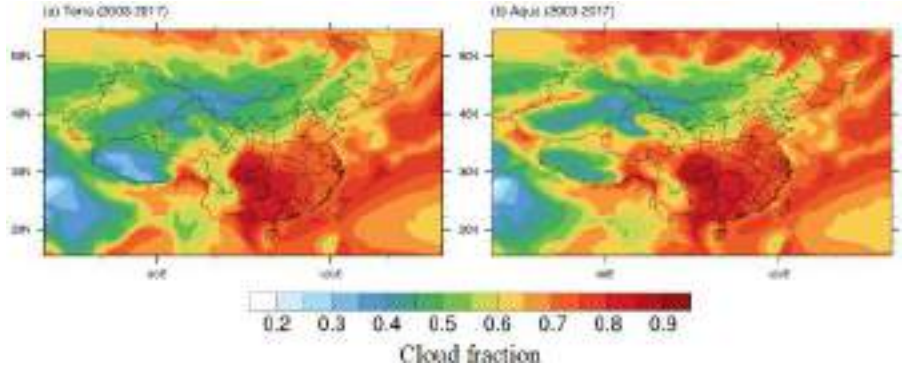


Figure 1 Temporal variation of seasonal mean and year-round mean daytime cloud fraction over the region with latitudes of 15°–55°N and longitudes of 70°–140°E from March 2003 to February 2018 based on MODIS observation cloud data product

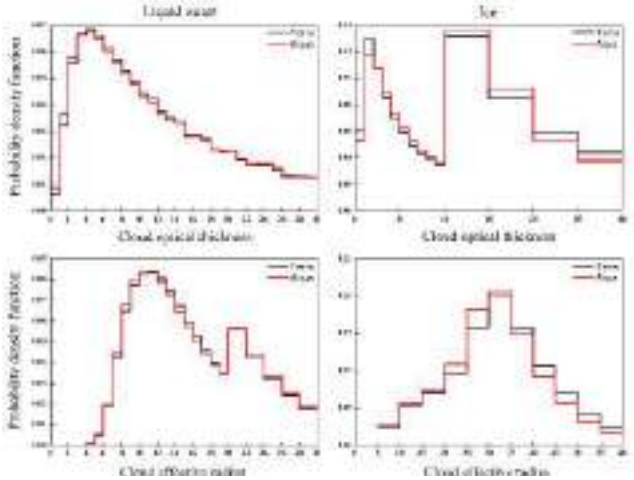

Figure 2 The probability density function of COT (upper panels) and the corresponding cloud $r_e$ (bottom panels) of liquid water (left column) and ice (right column) from both Terra (black lines) and Aqua (red lines) in July 2010 over the study area

## 4 Conclusions

Utilizing MODIS level-3 cloud products from Terra and Aqua (Collection 6.0), our 15-year analysis (March 2003 - February 2018) unveils significant spatio-temporal variations in cloud properties over China. Key findings include:

Seasonal variations in cloud fraction (CF), with higher values in summer and winter (~64–65%) compared to spring and autumn (~58%). Trends in CF reveal an annual increase of 1.7% per decade till 2012, with a pronounced rise in autumn. Regional disparities in CF, notably higher in southern and southeastern regions. Differences between morning and afternoon CF, particularly pronounced over the Tibetan Plateau. Cloud top pressure (CTP) patterns vary by region and season, with lowest values over the Tibetan Plateau and highest over northeastern China. Similar spatial patterns observed in cloud top temperature (CTT), with coldest cloud tops over the Tibetan Plateau. Cloud optical thickness (COT) highest in southern China across all seasons, attributed to water vapor availability. Distinct spatial distribution patterns for liquid water and ice cloud effective radius ($r_e$), with smaller values over southern China. Non-Gaussian probability density functions (PDFs) for COT and cloud $r_e$, with varying vertical distributions among seasons.

**Theme:** Climate change impacts
**IAHR Thematic Priority Area:** [TPA-1] Climate Change Adaptation and Mitigation
https://doi.org/10.3850/iahr-hic2483430201-244

# Quantifying the Influence of Atmospheric Factors on Rainstorm Extremes Using ERA5: Implications for Flood Early Warning in Henan, China

**Yu Lang[1], Ze Jiang[2], Xia Wu[3]**

[1] Institute of Natural Resource Owner's Equity, Chinese Academy of Natural Resources Economics, Beijing 101149, China

[2] School of Civil and Environmental Engineering, University of New South Wales, Sydney, NSW 2052, Australia

[3] College of Hydrology and Water Resources, Hohai University, Nanjing 210098, China

*Corresponding author: ze.jiang@unsw.edu.au*

**Abstract.** This study investigates heavy rainstorm-induced floods to enhance flood forecasting and mitigation strategies. We address challenges in identifying dominant meteorological factors influencing extreme rainfall events due to limited atmospheric observations. Leveraging high-resolution ERA5 reanalysis data, we examine the relationship between extreme rainstorms and synoptic features. We propose a cumulative distribution function based metric to assess six potential meteorological drivers. Our analysis highlights in Henan, China, vertical wind velocity (Wind) and precipitable water (PW) as dominant factors in summer events, while CAPE and Wind play significant roles in winter . These findings offer insights for regional flood management amid extreme rainfall events.

**Keywords:** Extreme rainstorms; Dominant factor; ERA5; Cumulative distribution function

## 1 Introduction

Understanding the causative processes behind heavy rainstorm floods is crucial for improving flood forecasting and mitigation strategies. However, identifying the dominant meteorological factors influencing extreme rainfall events at specific locations remains a challenge due to limited data availability and sparse atmospheric observations. This study utilizes high spatiotemporal resolution ERA5 reanalysis data to explore the relationship between extreme rainstorms and their associated synoptic features at various pressure levels. By investigating the causative processes of heavy rainstorm-induced floods, this research aims to contribute to the advancement of flood forecasting and mitigation efforts.

## 2 Materials and Methods

Take advantage of the latest generation of ERA reanalysis data, with its high spatiotemporal resolution, we are able to investigate the relationship between extreme rainstorms and its synoptic features across different levels of atmosphere. A novel metric is introduced for identifying the dominant factor based on the cumulative distribution function (CDF) [1]. The concurrence among extreme events is quantified by of the percentage of the extreme condition over a given duration for all the events in the entire historical period. The proposed metric, M, can be defined as follows [2]:

$$M^i(\theta_1, \theta_2) = \begin{cases} 1, & if\ P\left(X^i > X^i_{\theta_1}\right) \geq \theta_2 \\ 0, & otherwise. \end{cases} \quad (1)$$

where  is the hourly value of atmospheric variable *i* during the given event duration, for instance, 72 hours, since the storm event began,  is the value of the atmospheric variable *i* corresponding to the CDF of  (e.g., 0.95), which can be regarded as the threshold of extreme conditions. For each specific event, the percentage of the atmospheric variable *i* reaching the extreme condition () can be calculated. If the percentage exceeds  (e.g., 15%), representing that the extreme condition maintains over a given

duration, then the atmospheric variable *i* can be identified as the driver of this extreme event, and its value of metric M is 1.

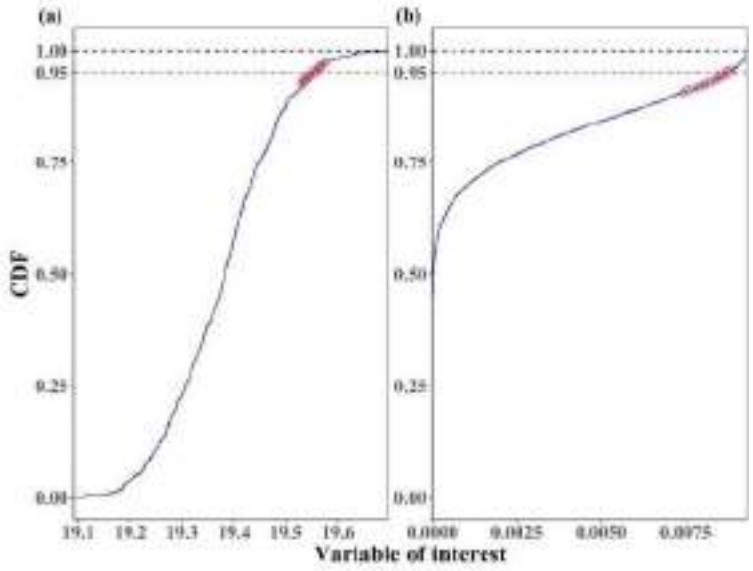


Figure 1. Illustration of the method used to identify drivers of extreme events through the demonstration of two synthetic time series cases. Subplot (a) represents a case where the variable shown is identified as the driver of the extreme event, while subplot (b) depicts a case where the variable is not considered a driver, i.e. not exceeding 15% of event duration. The blue line presents the CDF of all values in the entire period. The red circles present the cumulative probabilities of the hourly values during the 72 hours after the extreme event began. The CDF of 95% (horizontal red dashed line) is defined as the threshold of the extreme condition.

## 3 Results

The results demonstrate that extreme precipitation events predominantly occur during the summer months (June to August) over the entire Henan province. Throughout the year, PW, Wind, and relative humidity (RH) are the most common drivers for extreme precipitation events in Henan province. From a seasonal perspective, Wind and PW are the dominant factors influencing summer extreme events, whereas convective available potential energy (CAPE) and Wind are more significant during winter. High levels of PW indicate abundant moisture supply, while strong vertical wind, representative of the large-scale horizontal convergence, draws moisture from the surrounding area to supply the moisture needed for the extreme event. In contrast, CAPE signifies atmospheric instability in winter. Specifically, for Zhengzhou city, Wind is the primary driver of summer extreme rainstorms, but CAPE is more influential in winter extreme rainfall events. Zhengzhou witnessed peak hourly rainfall exceeding 200 mm during the July 2021 floods [3].

## 4 Conclusions

The analysis of dominant factors can provide insights for further flood estimations and forecasts in the study region in the future. Among six potential factors considered in this study, including precipitable water (PW), the average temperature (Tavg) and the temperature difference (Tdiff) between the pressure level at 850 hPa and 500 hPa, relative humidity (RH), convective available potential energy (CAPE), and vertical wind velocity (Wind), it shows that in the region, Wind and PW are dominant factors in summer, while CAPE and Wind are highly related factors in winter. For Zhengzhou city particularly, Wind is the key driver for summer extreme rainstorms, while CAPE plays a key role in winter extreme precipitation events. The insights from this methodology are vital for regional flood management and mitigation strategies, especially in the context of climate change-induced extreme rainstorms.

## Reference

[1] Chen, X. and F. Hossain, Understanding Model-Based Probable Maximum Precipitation Estimation as a Function of Location and Season from Atmospheric Reanalysis. Journal of Hydrometeorology, 2018. 19(2): p. 459-475.

[2] Lang Y, Jiang Z, Wu X. (2022). Investigating the Linkage between Extreme Rainstorms and Concurrent Synoptic Features: A Case Study in Henan, Central China. Water, 14(7), 1065.

[3] Wang, H., et al., Urban flood forecasting based on the coupling of numerical weather model and stormwater model: A case study of Zhengzhou city. Journal of Hydrology: Regional Studies, 2022. 39: p. 100985.

**Theme:** Emerging concepts and solutions in modelling methods
**IAHR Thematic Priority Area:** [TPA-4] Digital Transformation
https://doi.org/10.3850/iahr-hic2483430201-246

# Decision Support Systems and Hydroinformatics Solutions: Needs and Gaps

**Philippe Gourbesville**[1,2]

[1] Institute of Water Resources and Hydropower Research, China
[2] Université Côte d'Azur, Polytech Lab, 930 route des Colles,06903 Sophia Antipolis, France
Corresponding author: philippe.gourbesville@unice.fr

**Abstract.** Over the recent years, the Decision Support Systems (DSSs) have appeared as target objective for multiple water professionals. This trend is supported by the emerging concept of Digital Twin that is a key component within DSSs. The availability of reliable affordable sensors, the improved performances of communications networks, the availability of cloud solutions and the access to massive computational resources have boosted the possibility to integrate data, to produce information and to produce forecasts with models running in a consistent digital environment. The growing demand for integration within the DSSs is an opportunity and a challenge for the Hydroinformatic community that should revise computational approach, data handling for real-time operation and integration within environments that are not only focused on water but integrate at least most of the utilities at the city scale. The analysis of various DSSs currently deployed mainly in Europe and in Asia has allowed to identify needed improvements to match the expectation of the water professionals and furthermore of the communities. Efforts should be focused on three key areas: simplification of orchestration tasks, optimization of computing tasks and improved rendering processes especially for spatial information. The too limited efforts engaged within those areas over the last two decades are negatively impacting the operational deployment of Hydroinformatics solutions and contribute to exclude them from the major platforms used for the DSSs.

**Keywords:** Computing, Decision Support Systems, Orchestration, Spatial information.

## 1 Context

Over the recent years, the Decision Support Systems (DSSs) have appeared as target objective for multiple water professionals. This trend is supported by the emerging concept of Digital Twin that is a key component within DSSs. The availability of reliable affordable sensors, the improved performances of communications networks, the availability of cloud solutions and the access to massive computational resources have boosted the possibility to integrate data, to produce information and to produce forecasts with models running in a consistent digital environment. The growing demand for integration within the DSSs is an opportunity and a challenge for the Hydroinformatic community. The integration process is slow due to various challenges that must identified and addressed in priority.

## 2 Methodology

Identification of needs was achieved by a review of major DSSs deployed in Europe and in Asia, mainly in the field of flood management and operating at various spatial scale

- Thailand water information system hosted by Hydro Informatic Institute (https://www.hii.or.th);
- Water Management System (WAMIS) from South Korea (http://wamis.go.kr);
- National Flash Flood disaster prevention platform used in China [1];
- VigieCrues - French national modelling architecture for flood forecasting (https://www.vigicrues.gouv.fr);

- Länderübergreifendes Hochwasser PortalLHP – German national center for flood monitoring (https://www.hochwasserzentralen.de);
- AquaVar – Decision Support System used by Nice Metropolis in France [2];
- Aquadvanced - Decision Support System used by Singapore and Marseille and Biarritz municipalities in France [3], [4].

## 3 Results and discussion

The analysis has identified three key areas: simplification of orchestration tasks, optimization of computing tasks and improved rendering processes especially for spatial information.

### 3.1 Orchestration

DSSs gather multiple components that request to be operated in a specific to deliver the expected results. This operational organization is a major aspect of DSSs and contribute greatly to their performances. This aspect is frequently underestimated during the architecture development and requests a significant workload. Orchestration of the various models and their sequential use must be defined within a specific module with the DSS environment. The orchestration module coordinates all the other modules and can be parameterized by the user through a web-based user interface most of the time. The module includes the following components:

- A simulation module defined as a wrapper around one or several specific simulation tools that have to be used. The wrapper offers the possibility to add a new simulation tool without modification of the global architecture of the DSS;
- Several configuration modules that rely on a corresponding module to automatically set up the simulation parameters for a specific model. Those modules can perform a data format update when necessary.
- A scheduler that allows running automatically the simulation engines in the background. The scheduler uses a table similar to a Unix crontab which can be set up by the user.
- A data acquisition module that is fetching the requested input data from a data storing environment that is itself collecting live data from various field sensors. The module implements a common interface that allows an easy connection to new data sources.
- A data delivery module that is pushing the results obtained from the simulation engines into the storing environment. As for the previous module, this component implements a common interface that allows delivering of results in different ways (database, plain file system, etc.).

The data acquisition and data delivery modules as well as the orchestrator communicate with external applications through RESTful (Representational State Transfer) interfaces (RESTful). RESTful Application Program Interfaces (APIs) rely on the HTTP protocol and provide an architecture style suitable for networked applications. This architecture allows to transparently access the engine through a web-based user interface or alternatively as a web-service [2].

Standard orchestration modules are currently lacking and should be proposed to facilitate integration of models with DSS platforms. Projects developing approaches like OpenMI initiative [5] would be obviously very welcome to federate the community and stimulate unified developments.

### 3.2 Computing optimization

Codes of numerous deterministic hydrological and hydraulic models have been produced more than 30 or even 40 years ago. Within the perspective of this period, the use of Hydroinformatic solutions was limited to design and assessment tasks, the integration within DSSs was not clearly anticipated. Due to those objectives, the efficiency of the computational methods was continuously challenging the available computational resources but without an in-depth revision of the produced codes. Today the computational resources – parallel computing, GPU and High Performance Computing – request optimized codes that fit with their characteristics: call to external files can deeply affect parallel procedures and reduce efficiency. Efforts have to be engaged in two concurrent directions: codes

optimized for new computational practices and use of fasted numerical methods with the deterministic models. In a similar way, but for a larger extend, the data driven models should follow a similar path.

### 3.3 Spatial information rendering

If efforts have been focused on the efficiency of the computational methods that are embedded with the core part of the models, the data management procedures involved within the preprocessing and the post processing processes are now frequently the most challenging bottlenecks for the implementation and deployment for real-time operation of the modelling systems. In fact, the constraint can be easily understood by the used data formats that are currently used by most of tools were not designed with the objective of real-time operation. For this reason, formats remain heavy and lengthy by mobilizing heavy computational power and writing process within the storing devices. A good example is given by most of the current systems used to handle and display spatial information. In a wide number of cases, the spatial information is addressed with GIS tools that are mobilizing databases and display routines that have been created for limited datasets and, in most case, with static elements. In such environments, representation of dynamic processes like inundation propagation requests to display attributes of pixels over time. The frequently used format netCDF (Network Common Data Form) allows to handle array-oriented scientific data and is mobilized to generate inundation maps in a pixel-based approach. The lack of efficient data format and the systematic use of pixel-based approach are two major constraints that are deeply affecting the development of real-time modelling and Decision Support Systems development. Innovative data formats able to handle large spatial datasets and dynamic processes are deeply needed. The current formats [6] such as GRIB (Gridded Binary), BUFR (Binary Universal Form for the Representation of meteorogical data), HDF5 (Hierarchical Data Format 5, [7]), netCDF4 (last evolution of the netCDF format, [8]) and Zarr (file format designed to store large arrays of data) are not providing the requested performance even if they are offering potential improvements such as HDF5. In addition, the needed formats must be compliant with the WaterML 2.0 OGC standard [9] that is the standard information model for water observations.

## 4 Conclusions

The performed analysis has identified three key areas where efforts must be concentrated. The lack of developments in those areas contributes to marginalize the Hydroinformatic solutions and delay their integration within DSSs. Efforts must be engaged to produce unified and consolidated approaches that can ensure the production of the needed tools in the water sector and integrated within the global framework of utilities from city to national scale.

## References

[1] Liu, C., Guo, L., Ye, L., Zhang, S., Zhao, Y. and Song, T., 2018. A review of advances in China's flash flood early-warning system. *Natural hazards*, *92*, pp.619-634.

[2] Ma, Q., Gourbesville, P. and Gaetano, M., 2020. Aquavar: decision support system for surface and groundwater management at the catchment scale. In *Advances in Hydroinformatics: SimHydro 2019-Models for Extreme Situations and Crisis Management* (pp. 19-28). Springer Singapore.

[3] Laplace, D., MERTZ, J., Schoorens, J., Jourdan, L., Pouyssegur, P., Gandouin, C., Ohayon, T., Tavernier, C. and Nègre, C., 2019. Aquadvanced, un outil numérique pour la gestion optimisée du système d'assainissement de Marseille. *MATÉRIEL de TRAITEMENT et d'ANALYSE des EAUX*, p.57.

[4] Sharifi, A., Beris, A.T., Javidi, A.S., Nouri, M.S., Lonbar, A.G. and Ahmadi, M., 2024. Application of artificial intelligence in digital twin models for stormwater infrastructure systems in smart cities. *Advanced Engineering Informatics*, *61*, p.102485.

[5] Harpham, Q.K., Hughes, A. and Moore, R.V., 2019. Introductory overview: The OpenMI 2.0 standard for integrating numerical models. *Environmental Modelling & Software*, *122*, p.104549.

[6] Ambatipudi, S., & Byna, S. (2022). A comparison of hdf5, zarr, and netcdf4 in performing common i/o operations. *arXiv preprint arXiv:2207.09503*.

[7] Folk, M., Heber, G., Koziol, Q., Pourmal, E., & Robinson, D. (2011, March). An overview of the HDF5 technology suite and its applications. In *Proceedings of the EDBT/ICDT 2011 workshop on array databases* (pp. 36-47).

[8] Lee, C., Yang, M., & Aydt, R. (2008). NetCDF-4 performance report. *URL: https://support. hdfgroup. org/pubs/papers/2008-06 netcdf4 perf report. pdf*.
[9] Harpham, Q.K., Hughes, A. and Moore, R.V., 2019. Introductory overview: The OpenMI 2.0 standard for integrating numerical models. *Environmental Modelling & Software*, *122*, p.104549.

**Theme:** Emerging concepts and solutions in modelling methods
**IAHR Thematic Priority Area:** [TPA-4] Digital Transformation
https://doi.org/10.3850/iahr-hic2483430201-250

# A Digital Twin Modelling Strategy in Basin Flood Prevention, Case Study Of "23·7" Catastrophic Flood Analysis in Yongding River Basin

**WANG Haowen[1,2], ZHANG Xiaoxiang[2,3], ZHANG Kejian[1,2], Xu Hao[1,2], MA Qiang[4], YANG Xuejun[5]**

[1] College of Hydrology and Water Resources, Hohai University, Nanjing 210098, China;
[2] Jiangsu Province Engineering Research Center of Watershed Geospatial Intelligence, Nanjing 211100, China
[3] College of Geography and Remote Sensing, Hohai University, Nanjing 211100, China
[4] China Institute of Water Resources and Hydropower Research, Beijing 100038, China
[5] Hydrology Bureau of Haihe River Water Conservancy Commission, Ministry of Water Resources, Tianjin 300170, China

*Corresponding author: maqiang@iwhr.com*

**Abstract.** The climate change and the increase of human activities had continuously improved the complicity of flood disaster. By setting up the digital twin flood prevention platform, local managers will have more chances to deeply understand the real-time disaster mechanism and its future process. Taking the "23·7" catastrophic flood of Yongding River Basin as an example, this paper uses the Chinese distributed hydrological model and IFMS 2D flood simulation software, different models with various spatial precision were constructed to simulate the flood in three parts of the basin. The modelling analysis indicates that the Guanting-Shanxia area is the main flow generation area during this flood event, with obviously higher rainfall-runoff coefficient than other areas of the catchment. The model applied in this study is able to represent the quantity of different flood components. And the modelling strategy applied in this study can efficiently represent the flood process in detail in time and space. All simulation run for 30 days' flood can been finished in 5mins. The hydroinformatics application presented in this study can be used as a technical reference to guide the implemented digital twin watershed in other river basins.

**Keywords:** "23•7" catastrophic flood, digital twin watershed, distributed hydrological model, modelling platform, modelling strategy

## 1 Introduction

Under the current situation, the extreme flood events in China show a relatively higher frequency than before[1]. In order to comprehensively improve the flood control capacity of China, the basin model platform has been considered as the core of the digital twin construction. Nowadays, many experts have proposed different strategies to create operational models for supporting flood decisions [2].Taking Yongding River Basin as an example, both distributed hydrological and hydrodynamic models is applied for producing detailed information about flow generation process and movement during "23·7" catastrophic flood. The modelling results can also provide references for supporting the future design of both engineering and Non-engineering measures in this river basin.

## 2 Methods

Separating the Yongding River Basin with different hydro-junctions, (1) the upstream is defined until the Guanting reservoir which covered by a deterministic distributed hydrological model with 10-30km$^2$ area sub-catchment as minimum computation unit; (2) the middle part of the basin named with Guanting-Shanxia area starts from Guanting reservoir until Lugou bridge covered by more precise model with 1-10km$^2$ area sub-catchment as minimum computation unit; (3) the downstream part is

defined from Lugou bridge until the Qujiadian station simulated by a 2D high resolution hydraulic model with more than 70,000 girds. In addition, the distributed hydrological model of Hydro-SAT and the hydraulic model of IMFS applied in this study are both developed by IWHR [3-4].

## 3 Results

The simulation results show higher accuracy with average difference of flood peak 17% and NSEs in the range from 0.5 to 0.81. The modelling analysis indicates that the Guanting-Shanxia area is the main flow generation area during this flood event, with obviously higher rainfall-runoff coefficient than other areas of the catchment. The model applied in this study is able to represent the quantity of different flood components. And the runoff generation mechanism of Guangting-Shanxia area is mainly consisted with Horton and Dunne flow mixed in time and space.

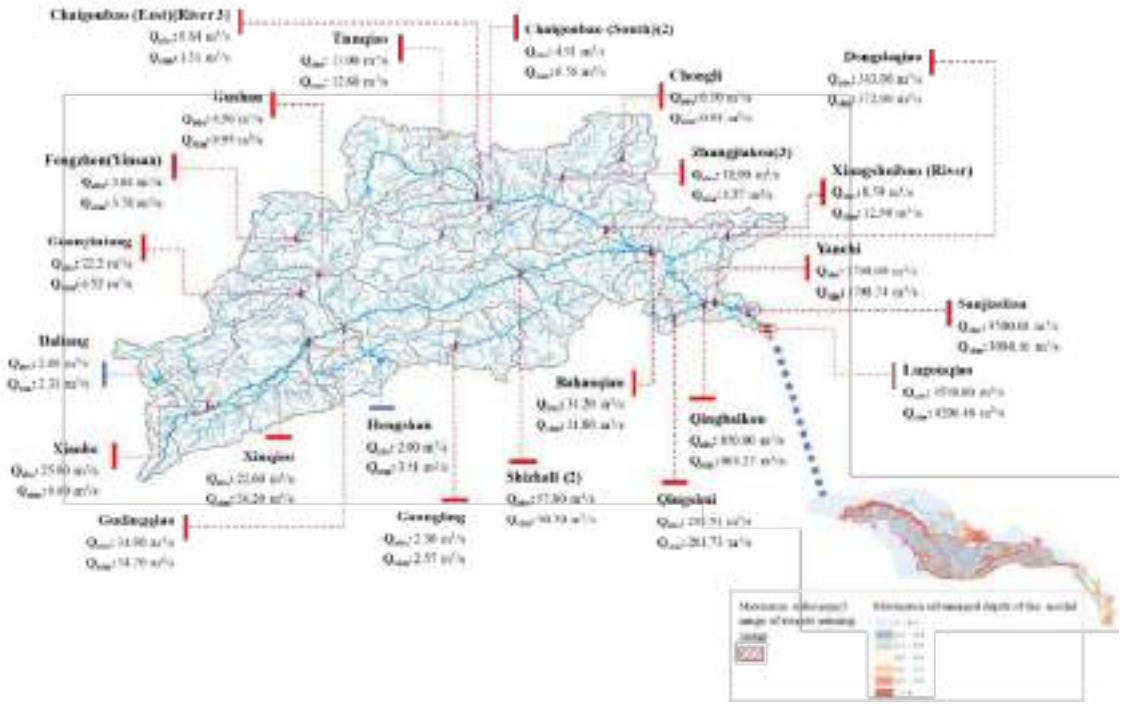


Fig.1. Comparison between observed and simulated flood peak of Yongding River Basin

## 4 Conslusions

This study produces a digital twin modelling strategy in basin flood prevention. The following conclusions are made based on the outcomes of this study:

- The applicability of both Hydro-SAT model for mechanism analysis and IFMS model for representing flood movement of flood disaster in Yongding River Basin has been validated.
- The modelling strategy applied in this study can efficiently represent the flood process in detail in time and space. All simulations run for 30 days' flood can been finished in 5mins.

## Reference

[1] Hu Pan, Chen Bo, Shi Peijun. Spatiotemporal. patterns and influencing factors of rainstorm-induced flood disasters in China. Acta Geographica Sinica. 76(2021)1148-1162.

[2] Mijic A, Liu L, O'Keeffe J.et al.A meta-model of socio-hydrological phenomena for sustainable water management.Nature Sustainability, 7(2024)7–14.

[3] Liu Changjun, Zhou Jian, Wen Lei, et al. Research on spatio temporally-mixed runoff model and parameter regionalization for small and medium-sized catchments. Journal of China Institute of Water Resources and Hydropower Research, 2021, 19(1): 99-114.

[4] Liu Changjun, Wen Lei, Zhou Jian, et al. Comparative analysis of hydrological and hydrodynamic calculation method for flash flood in small watershed. Journal of China Institute of Water Resources and Hydropower Research,17(2019)262-270.

**Theme:** Emerging concepts and solutions in modelling methods
**IAHR Thematic Priority Area:** [TPA-4] Digital Transformation
https://doi.org/10.3850/iahr-hic2483430201-252

# Flow Velocity Distribution in Rivers Through Image-Based Technique Calibrated by ADCP Measurements

**Donatella Termini[1], Peyman Peykani[1]**

[1] University of Palermo, Department of Engineering, 90128, Palermo, Italy

*Corresponding author: donatella.termini@unipa.it*

**Keywords:** ADCP measurements, Flow velocity distribution, Image-based technique, River monitoring

## 1 Introduction

In the context of climate change, the knowledge of flow discharge is of crucial importance. Flow discharge is not a direct measurement but is estimated on the basis of information of flow velocity and cross-sectional flow area. Thus, accurate flow velocity measurements are critical for defining early warning systems for flood management and for quick decision-making for emergency actions. In recent years, the acoustic Doppler current profiler (ADCP) has been especially used to measure flow velocity profiles and the flow discharge, in natural and man-made waterways[1]. During flood events, because of continuously changing in flow velocities, water depths, and high sediment concentrations, conditions is not safe for measurement operator. As consequence, in high flow conditions, measurement equipment's like current meters and/or more advanced instruments such as ADCP cannot be used. For this reason, especially in the last decade, alternative approach based on image processing techniques has been increasingly used to obtain the distribution of the surface velocity, from which the flow discharge might be estimated. Several software tools have been also implemented for the image-based technique application, enabling researchers and practitioners to derive flow velocity data with high spatial and temporal resolution [2,3]. In comparison to the traditional measurement methods, the image-based technique presents the advantage to be non-intrusive allowing the safe estimation of surface velocity distribution also during floods. One of challenges in the application of image techniques is determining the error in estimating surface velocity, whose quantification depends on many factors characterizing not only the measurement conditions but also the processing method used.

## 2 Material and methods

In this study, the efficiency of the digital image-technique for remote monitoring of surface velocity in river is analysed. The analysis conducted by using accurate ADCP flow velocity measurements in selected reaches of rivers in Palermo's (Sicily-Italy) territory (Figure 1). For implementation of image-based technique, Camera Nikon D5300, with high-resolution images (1920x1080 pixels) and of 30 fps acquisition frequency, was used. In this study on the contrary to classical LSPIV procedures, the image-based technique is applied only by using moving grains and natural tracers. The calibration of the procedure was operated by comparing the values of the free surface velocity estimated by usign the acquired images with the ADCP's stationary measurements.

Figure 1 Overview of the study area

## 3 Results and Concluding Remarks

Figure 2 reports the comparison between the velocity distribution obtained in a selected cross section of the Oreto River and the local ADCP measure. Figure 2 shows that the velocity values compare well, thus demonstrating that the use of natural tracer or sediments on the free surface allows user to accurately apply the image-based technique. Further applications have been also conducted performing sensitivity analysis of the estimated surface velocity to integration area and the image resolution.

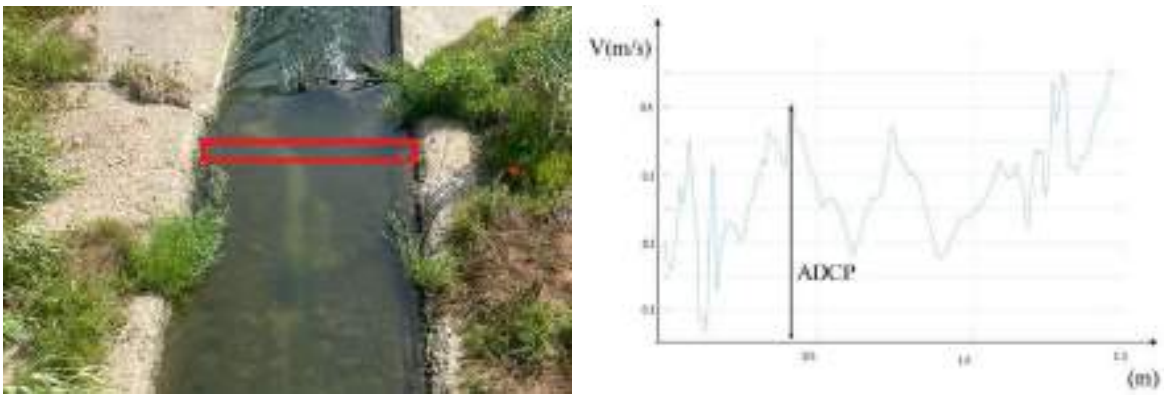


Figure 2 Comparison of velocity determined by image analysis with ADCP measure

Our study underscores the importance of using accurate measurement technologies for calibrating image-based techniques used for monitoring surface velocity distribution also during flood events. This information is especially important for flood management practices.

**Acknowledgements**

This study was carried out within the RETURN Extended Partnership and received funding from the European Union Next-GenerationEU (National Recovery and Resilience Plan – NRRP, Mission 4, Component 2, Investment 1.3 – D.D. 1243 2/8/2022, PE0000005). Part of this study has been supported by project PRIN2017 " ENTERPRISING".

**Reference**

[1] Muste M, Yu K, Pratt TC, Abraham D. ADCP measurements at fixed river locations. InHydraulic Measurements and Experimental Methods 2002 2002 (pp. 1-12).

[2] Fujita I, Muste M, Kruger A. Large-scale particle image velocimetry for flow analysis in hydraulic engineering applications. Journal of hydraulic Research. 1998 May 1;36(3):397-414.

[3] Termini D, Di Leonardo A. Efficiency of a digital particle image velocimetry (DPIV) method for monitoring the surface velocity of hyper-concentrated flows. Geosciences. 2018 Oct 19;8(10):383.

**Theme:** Emerging concepts and solutions in modelling methods
**IAHR Thematic Priority Area:** [TPA-4] Digital Transformation
https://doi.org/10.3850/iahr-hic2483430201-254

# Large-Size Convolutional Network and Flowattention Based Video Speed Measurement Algorithm for High Water Velocity Situations

**Xiaolong Wang[1], Guocheng An[1],Yanwei Zhang[1] and Fanli Xia[1]**

[1] the Artificial Intelligence Research Institute of Shanghai Huaxun Network System Co., LTD., Chengdu, Sichuan 610074, China

*Corresponding author: wangxiaolong@eccom.com.cn*

**Abstract.** Estimating river surface velocity is crucial for water resource allocation and flood prevention. Traditional intrusive flow measurement cannot monitor the whole river in real-time. In contrast, non-contact image processing technologies can access overall river flow distributions in real-time. However, current optical flow velocimetry methods have poor accuracy at high river speeds. To address this, we propose an improved optical flow velocimetry method. The proposed method consists of three independent modules: optical flow estimation, perspective transformation and flow field estimation. It uses a ReplKNet feature extractor with large convolutional kernels to enhance the receptive field and extract more global features, avoiding omitted extraction at high velocity. The optical flow optimization module incorporates FlowAttention, GRU, and position encoding for better temporal-spatial awareness. After multiple iterations, the model more accurately predicts optical flow. Experiments on the optical flow dataset and the real river dataset show that the method performs well for in large pixel displacements.

**Keywords:** Attention Mechanisms; Deep Learning; Optical Flow Estimation; Recurrent Neural Networks; Video Velocimetry

## 1 Introduction

This paper introduces an enhanced OFV method for high-flow river velocimetry, optimizing the RAFT[1] optical flow estimation model. The improvement involves replacing the feature extraction module with the ReplKNet[2] network, which uses large convolutional kernels to better capture global features at high velocities, preventing feature omission. Additionally, Flowattention[3] and GRU are incorporated into the optical flow optimization module, along with positional coding to integrate time and space domain information with the attention mechanism, enhancing feature correlation. The method outperforms RAFT and other traditional methods on both optical flow estimation and real river datasets.

## 2 Material and methods

The proposed method framework, depicted in Figure 1, comprises three modules for processing two consecutive frames to estimate river surface velocity (RSV). First, it calculates the optical flow map between the frames. Then, it transforms this map into a displacement map through perspective transformation. By accumulating displacement maps from consecutive frames, the framework estimates a two-dimensional flow field, representing RSV's magnitude and direction.

## 3 Results and discussion

**Table 1.** Different methods for estimating velocity in the Hurunui River for different ranges

| | MSE | |
|---|---|---|
| Method | All velocity | Fast velocity(faster than 2.5m/s) |
| RAFT[1] | 0.121 | 0.069 |
| GMA[4] | 0.09 | 0.049 |

| | | |
|---|---|---|
| FlowFormer[5] | 0.099 | 0.04 |
| Ours | 0.063 | 0.013 |

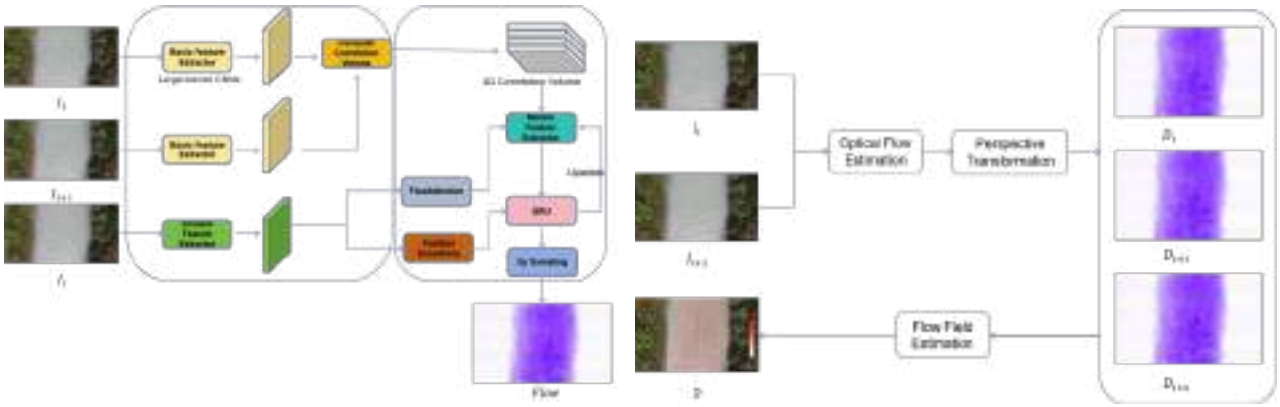


**Figure 1.** Overview of the proposed proposed method andoptical flow estimation model.

The experimental results on the real high-flow river dataset are shown in Table 1, and our proposed method gives one of the best results across the full flow range, and the error is smaller in the high-flow range.

## 4 Conclusions

We propose an improved optical flow estimation model based on neural network. By modifying the traditional CNN to a large convolutional size CNN based on the original RAFT and adding Flowattention attention mechanism and position coding, the proposed model can dynamically adjust the matching weight of each pixel using contextual features to improve the accuracy of the network in predicting large pixel displacements. The performance of the method is evaluated using an optical flow dataset and a real river dataset, and the results show that it outperforms previous methods in both datasets, especially in complex environments or high water velocity situations.

## References

[1] Teed Z, Deng J. Raft: Recurrent all-pairs field transforms for optical flow[C]//Computer Vision–ECCV 2020: 16th European Conference, Glasgow, UK, August 23–28, 2020, Proceedings, Part II 16. Springer International Publishing, 2020: 402-419.

[2] Ding X, Zhang X, Han J, et al. Scaling up your kernels to 31x31: Revisiting large kernel design in cnns[C]//Proceedings of the IEEE/CVF conference on computer vision and pattern recognition. 2022: 11963-11975.

[3] Wu H, Wu J, Xu J, et al. Flowformer: Linearizing transformers with conservation flows[J]. arXiv preprint arXiv:2202.06258, 2022.

[4] Jiang S, Campbell D, Lu Y, et al. Learning to estimate hidden motions with global motion aggregation[C]//Proceedings of the IEEE/CVF International Conference on Computer Vision. 2021: 9772-9781.

[5] Huang Z, Shi X, Zhang C, et al. Flowformer: A transformer architecture for optical flow[C]//European Conference on Computer Vision. Cham: Springer Nature Switzerland, 2022: 668-685

**Theme:** Emerging concepts and solutions in modelling methods
**IAHR Thematic Priority Area:** [TPA-4] Digital Transformation
https://doi.org/10.3850/iahr-hic2483430201-256

# Optical Flow-Based River Surface Velocity Measurement Algorithm Under Complex Illumination Conditions

**Guocheng An[1], Tiantian Du[2], Yanwei Zhang [1]**

[1] the Artificial Intelligence Research Institute of Shanghai Huaxun Network System Co., LTD., Chengdu, Sichuan 610074, China
[2] School of Electronic Information and Electrical Engineering, Shanghai Jiao Tong University, Shanghai 200240, China

*Corresponding author: anguocheng@eccom.com.cn dtt372@sjtu.edu.cn zhangyanwei@eccom.com.cn*

**Abstract.** In the field of hydrological monitoring, accurate assessment of river surface velocity (RSV) is crucial for flood control, disaster prevention, and soil erosion mitigation. RSV measurement techniques can be classified into contact and non-contact methods based on environmental conditions. This study proposes a deep learning-based optical flow computation method for RSV measurement, utilizing the VideoFlow optical flow estimation architecture to effectively track and identify particles in water flow. To enhance accuracy, we define the region of interest for optical flow estimation and perform image distortion correction. By simulating real river scenarios in the laboratory and collecting data, we validate the reliability of this method in complex environments. Results indicate that in river scenes with velocities not exceeding 2.5m/s, the relative error estimated by this method is below 15%. Compared to traditional methods, it offers lower cost and enables continuous real-time dynamic measurement of the entire flow field, providing a more effective solution for hydrological monitoring.

**Keywords:** river surface velocity, VideoFlow, optical flow, illumination conditions, attention mechanism

## 1 Introduction

This paper presents a multi-frame optical flow estimation method, termed VideoFlow-RSV, applied to river flow velocity estimation. The method exhibits stronger robustness and is suitable for river scenarios with noise such as reflections and shadows under natural illumination. Specifically, we adopt the VideoFlow [7] architecture, leveraging temporal cues in multi-frame optical flow estimation. The network not only resolves the ambiguity issue in two-frame optical flow estimation due to insufficient information but also enhances robustness against noise such as shadows through the introduction of attention mechanisms and positional encoding. Furthermore, to comprehensively validate the algorithm's robustness in complex river scenarios, we constructed a diversified water flow scene platform in the laboratory to simulate real river scenarios and collected rich and diverse water flow data. Experimental results demonstrate that the proposed method outperforms traditional optical flow estimation methods and the original RAFT model in river flow velocity measurement tasks.

## 2 Methods

We employ the VideoFlow [1] architecture to estimate the pixel-wise displacement field of the river surface images. VideoFlow is an innovative framework designed for optical flow estimation in video sequences. It efficiently computes bidirectional optical flows for multiple frames in videos by leveraging temporal cues. To achieve this, VideoFlow segments the input multi-frame video into overlapping sets of three frames. The Tri-frame Optical Flow (TROF) module processes each set, while the Motion Propagation (MOP) module combines the outputs for multi-frame optical flow

estimation. TROF framework is depicted in Figure 1. Furthermore, we performed distortion correction on the collected video data and constrained it to the watershed area as the region of interest. Finally, by converting pixel-level displacements into world coordinate displacements, we obtained the estimation of the river flow velocity.

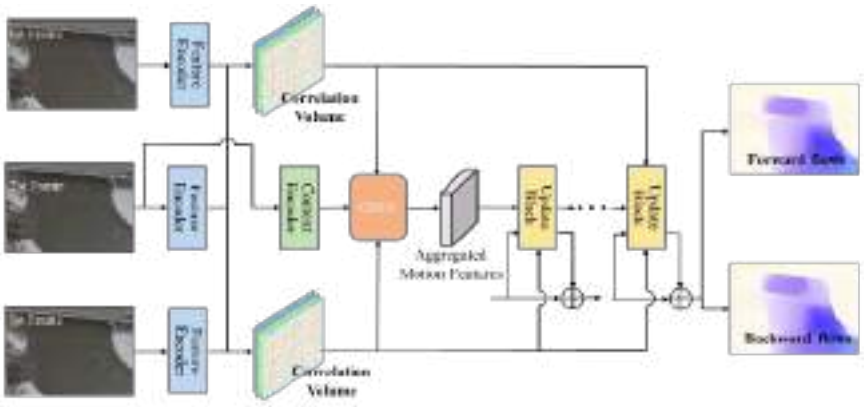

**Figure 1.** Tri-frame Optical Flow Framework of VideoFlow

## 3 Experiment data and their results analysis

**Table 1.** Datasets of various scenario in laboratory and their velocity measurement results

| Velocity-Range | Tracer | Light | Shadow | Resolution | RDV-Velocity | Mid-Velocity | Max-Velocity |
|---|---|---|---|---|---|---|---|
| 0~1m/s | √ | 1000W lamp | √ | 2k/1080p/720p | 0.98m/s | 0.700 m/s | 1.100 m/s |
| | √ | 1000W lamp | X | 2k/1080p/720p | 0.86m/s | 0.832 m/s | 0.982m/s |
| | √ | Dark | X | 2k/1080p/720p | 0.86m/s | - | - |
| | X | 1000W lamp | √ | 2k/1080p/720p | 0.98m/s | 0.912m/s | 1.131 m/s |
| | X | 1000W lamp | X | 2k/1080p/720p | 0.89m/s | 0.881m/s | 1.202 m/s |
| | X | Dark | X | 2k/1080p/720p | 0.86m/s | - | - |

We have constructed a river simulation platform in our laboratory capable of simulating various scenarios, aimed at collecting simulated river data from 144 different scenes or perspectives. Partial data and measurement results are listed in Table 1. Experimental results indicate that VideoFlow-RSV is capable of accurately estimating river flow speeds within the range of 2m/s, even in scenarios with shadows but without tracer particles, with errors remaining within 15%. However, the model's performance is less satisfactory for high flow rate scenarios. Therefore, our next research direction will focus on optimizing and improving flow speed estimation in high-flow and low-light scenarios.

## References

[1] Shi, X., Huang, Z., Bian, W., et al. "Videoflow: Exploiting temporal cues for multi-frame optical flow estimation." Proceedings of the IEEE/CVF International Conference on Computer Vision. 2023.

**Theme:** Emerging concepts and solutions in modelling methods
**IAHR Thematic Priority Area:** [TPA-4] Digital Transformation
https://doi.org/10.3850/iahr-hic2483430201-258

# A Distributed Modeling Strategy of Basin Flood Assessment, Application of "23·7" Catastrophic Flood in Haihe River Basin

**Qiang Ma[1], Changjun Liu[1], Philippe Gourbesville[1], Siyuan Chang[1], Wenjing Lu[1]**

[1] China Institute of Water Resources and Hydropower Research, Beijing 100081,

*Corresponding author: maqiang@iwhr.com*

**Abstract.** In order to comprehensively understand the hydrological processes in the whole water cycle of large river basin, this study proposed a distributed modeling strategy for setting up high performance numerical models over large area to analysis complicated catastrophic flood process. Taking the example of the "23.7" catastrophic flood in Haihe River Basin (320,600 km$^2$), 176 SKY-HydroSAT distributed hydrological models and 8 2D IFMS hydrodynamic models has been set up and used for representing the whole flood process during that disaster. The modelling results show that with the 5 days total rainfall of 49.4 billion m$^3$, the flood disaster happened in Haihe River Basin is mainly caused by the extreme rainfall landed on the Shanxia region in Yongding River (47,000 km$^2$) and the upstream of South branch of Daqing River (43,060 km$^2$). The rainfall-runoff coefficient of those areas almost reach 0.8 with the peak flow of Lugouqiao station (Yongding River) over 4540 m$^3$/s and Zhangfang station (Dqing River) over 7330 m$^3$/s. The fast flood flow produced by the upper stream area of the Haihe River Basin can be concluded as one of the main causes of this flood disaster characterized with relatively higher peak and normal water amount. The distributed hydrological and hydrodynamic models applied in this study show higher preference in shorter time consumption and higher accuracy which already be integrated into the digital twin platform of Haihe River Basin.

**Keywords:** Hydroinformatic application, distributed modeling strategy, "23·7" catastrophic flood, Haihe River Basin

## 1 Introduction

The new generation of Hydroinformatics technologies will deeply improve the digital capability of water industry. With the high preference computation technique, the real time distribution simulation over large basin becomes feasible which would strongly improve the water management. This study presents a distributed modelling strategy for the assessment of a catastrophic flood happened in Haihe River basin. With 49.4 billion m$^3$ of total rainfall in 5 days, the "23.7" catastrophic has led 22 branches in the Haihe River basin over the warming threshold value and 8 of them suffered the maximum flood peak in history [1]. One of the main challenges in this study is to deal with the big amount of hydro-data collected from thousand stations and reservoirs. And another is how to set up the distributed models over large basin area and to represent the whole flood progress of this catastrophic disaster.

## 2 Material and Methods

In order to comprehensively understand the whole progress of the "23.7" catastrophic flood disaster in Haihe River Basin (320,600 km$^2$), the hourly rainfall records in 5302 rain gauges, hourly water level and discharge observation from 1385 hydro-stations, and the in and out flow records from 1239 reservoirs are all collected and used to launch and validate the distributed hydrological models. Moreover, the high resolution DEM data over 8 flood detention areas has been collected and applied for setting up the hydrodynamic models to represent the flood evolution in those places. Considering the underlying surface and terrain characteristics of Haihe River Basin, the SKY-HydroSAT model developed by China Institute of Water Resources and Hydropower Research (IWHR) has been applied for setting up 176 distributed hydrological model over 23,000 km$^2$[2]. And the IFMS

hydrodynamic model is used in 8 active flood detention area for representing the flood evolution through villages [3].

## 3 Results and discussion

176 distributed hydrological model over the flood generation area of the Haihe River Basin has been set up in this study with averaged control area of 1121 km$^2$. With the observation data collected from 116 stations and reservoirs located in the modelling area, the calibrated model results show high accuracy of less than 15% of peak flood error and averaged NSE values over 0.7. In addition, comparing to the remote sensing monitoring data, the flood process simulated in the 8 flood detention area has been validated with less than 10% of maximum flooded area. Evaluating the effects of hydraulic structures during this flood, the ratio of flood peak reduction of 84 reservoirs is 77% which intercepted 2.85 billion m$^3$ and avoided around 5,000 km$^2$ farmland to be flooded.

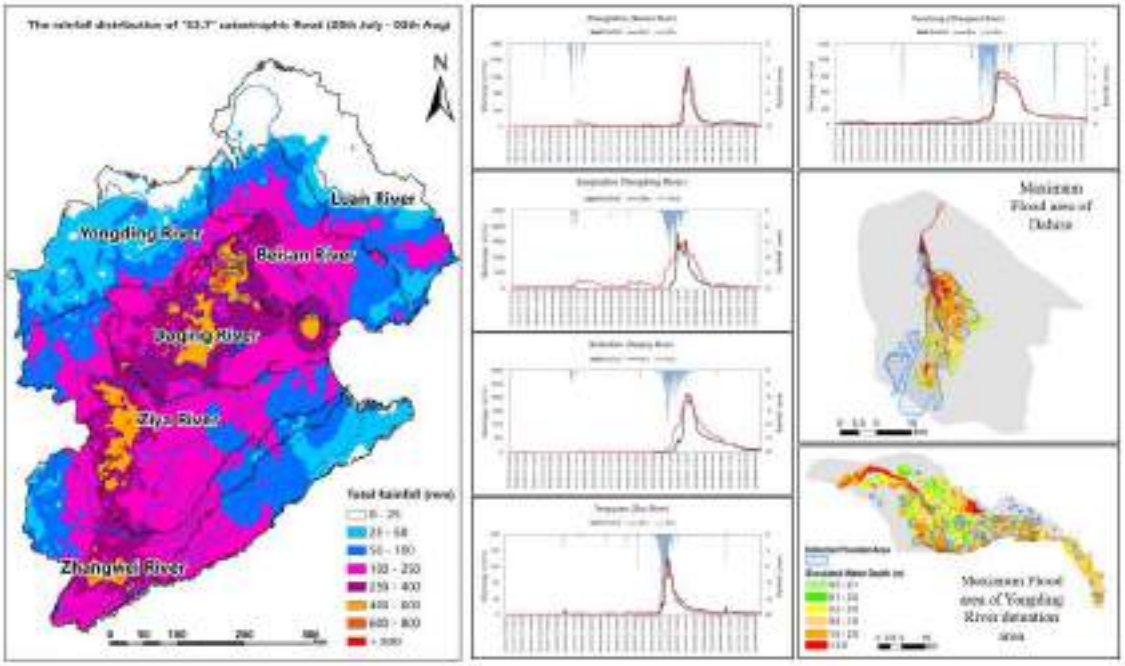


Fig.1: The modelling results of “23.7” catastrophic flood in Haihe River Basin

## 4 Conclusions

From the modelling simulation of “23.7” catastrophic flood in Haihe River Basin, the following conclusions have been achieved:

- The rainstorm is concentrated at certain parts of the Haihe River Basin and leads to the rainfall-runoff coefficient of those area reach 0.8 which causes high flood peak at the middle and downstream parts of the catchment.
- 84 large and medium-sized reservoirs in the basin have intercepted and stored over 2.85 billion m$^3$ of flood, with an average ratio of flood peak reduction 77%. They have reduced flooding in 24 towns and more than 5,000 km$^2$ of farmland, avoiding the relocation of 4.623 million people.

## Reference

[1] Haihe River Basin Commission of the Ministry of Water Resources. Investigation and Analysis Report on the "23.7" Basin-Wide Extreme Flood and Rainstorm in the Haihe River Basin [R].

[2] LIU C J, ZHOU J,WEN L, et al. Research on spatio temporally-mixed runoff model and parameter regionalization for small and medium-sized catchments [J]. Journal of China Institute of Water Resources and Hydropower Research, 2021, 19(1): 99-114.

[3] YU H J, MA J M, ZHANG D W, et al. Application of IFMS Urban software in urban flood risk mapping [J]. CHINA FLOOD & DROUGHT MANAGEMENT, 2018, 28(07):13-17.

**Theme:** Emerging concepts and solutions in modelling methods
**IAHR Thematic Priority Area:** [TPA-4] Digital Transformation
https://doi.org/10.3850/iahr-hic2483430201-260

# A Modelling-Based Mechanism Analysis of Flood Disaster, Application Of "23•7" Catastrophic Flood in Daqing River Basin

**Ying Wang[1,2], Zhaoxu Shi[1,2], Yongcheng Yang[2,3], Qiang Ma[4], Hui Fan[5], Xiaoxiang Zhang[2,3]**

[1] College of Hydrology and Water Resources, Hohai University, Nanjing 210098, China
[2] Jiangsu Province Engineering Research Center of Watershed Geospatial Intelligence, Nanjing 211100, China
[3] College of Geography and Remote Sensing, Hohai University, Nanjing 211100, China
[4] China Institute of Water Resources and Hydropower Research, Beijing 100038, China
[5] Hydrology Bureau of Haihe River Water Conservancy Commission, Ministry of Water Resources, Tianjin 300170, China

*Corresponding author: maqiang@iwhr.com*

**Abstract.** To clearly understand the mechanism of flood disaster at the mountainous area, a deterministic distributed hydrological model which could be able to separately represent the flood components such as surface flow, soil flow and base flow is currently requested by the local stakeholders. In this study, a distributed hydrological model (Hydro-SAT) development by IWHR has been applied in the modelling analysis of "23•7" catastrophic flood in Daqing River Basin. Calibrated with the data obtained from the gauging stations in different branches of Daqing River Basin, the simulation results show higher performance with average relative errors of 4.5% difference of peak flow and average NSE equals to 0.7. The main flood generation area in Daqing River Basin is located at the mountainous area in the northern part of the catchment with average rainfall-runoff coefficient around 0.7. The fast flood flow produced by the mountainous area of the river basin can be concluded as one of the main causes of this flood disaster characterized with relatively higher flood peak and normal flood amount. The study validates Hydro-SAT's suitability for flood disaster mechanism analysis and suggests its potential application in similar basin contexts.

**Keywords:** "23·7" catastrophic flood, Daqing River Basin, distributed hydrological model, flood mechanism

## 1 Introduction

According to the climate change, the occurrence of extreme rainfall events shows an obvious increasing trend, especially at the mountainous area with relatively larger terrain undulation and steep surface slope which often causes serious flood characterized with high flow velocity (Asadieh & Krakauer, 2015; Sillmann et al., 2017). Nowdays, the hydrological model has widely accepted as one of operational tools to represent the flood generation mechanism (Wagener, 2001; Zhang, 2010). Therefore, taking the example of "23·7" catastrophic flood disaster in Daqing River Basin, this study proposes a modelling-based approach to analysis the flood generation mechanism within sub-catchments scale. The model is able to separately describe the variation of different flow components during this extreme event that underscores its significance in understanding and mitigating flood hazards in complex terrains.

## 2 Material and Methods

The distributed hydrological model (Hydro-SAT) developed by IWHR has been applied in this study. The model has been set up with "3-layers" virtual reservoirs including the top soil layer, soil layer and groundwater layer which respectively calculates different flow components. The model has been well calibrated with observed data collected from gauging stations and evaluated by NSE coefficient and Peak flow difference

## 3 Results and discussion

Calibrated with the data obtained from the gauging stations in different branches of Daqing River Basin, the simulation results show higher performance with average relative errors of 4.5% difference of peak flow and average NSE equals to 0.7.The main flood generation area in Daqing River Basin is located at the mountainous area in the northern part of the catchment with average rainfall-runoff coefficient around 0.7. The total flood flow produced at the outlet of this area is consisted with different flow component including Horton and Dunne mixed surface flow at the steep slope area, soil flow and a certain amount of groundwater with few fluctuations.

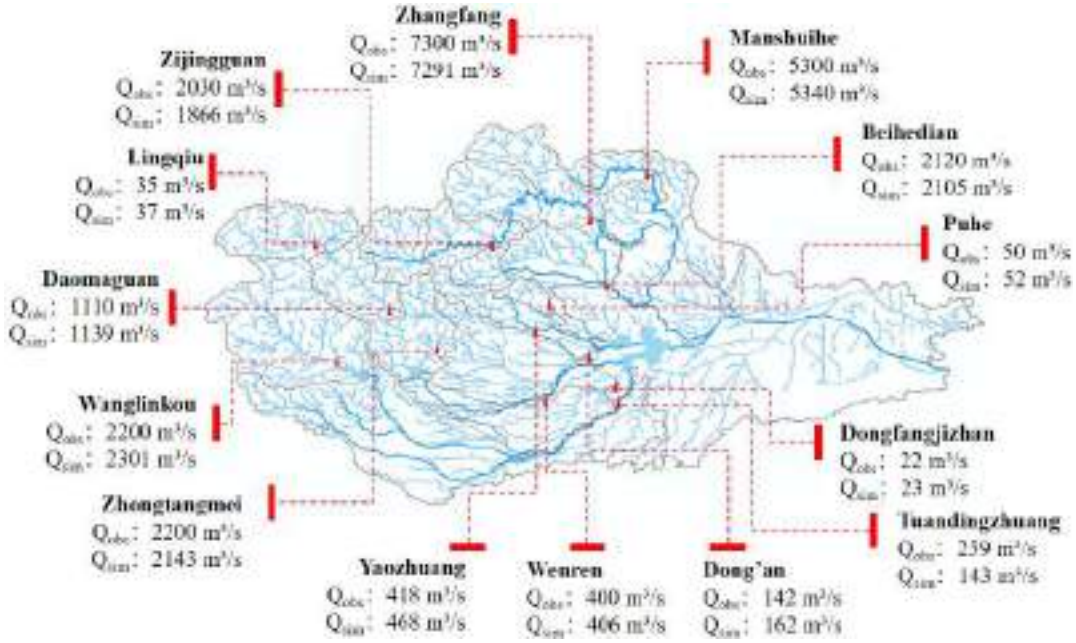


Fig.1: The modelling results of “23.7” catastrophic flood in Daqing River Basin

## 4 Conclusions

This study produced a modelling approach to analysing the spatiotemporal variation of flood generation mechanism of Daqing River Basin under “23 • 7” catastrophic flood. The following conclusions are made based on the outcomes of this study:

- The applicability of Hydro-SAT model for mechanism analysis of flood disaster has been indicated and validated.
- The fast flood flow produced by the mountainous area of the Daqing River Basin can be concluded as one of the main causes of this flood disaster characterized with relatively higher flood peak but normal flood amount.

## Reference

[1] B. Asadieh, N. Y. Krakauer, Global trends in extreme precipitation: climate models versus observations, Hydrology and Earth System Sciences. 2 (2015) 877-891.

[2] Jana Sillmann, Thordis Thorarinsdottir... & Francis W. Zwiers, Understanding, modeling and predicting weather and climate extremes: Challenges and opportunities, Weather and Climate Extremes. 18 (2017) 65-74.

[3] Jian-yun Zhang, Review and reflection on China’s hydrological forecasting techniques, Advances in Water Science. 21 (2010) 435-443.

[4] Wagener, T., et al., A framework for development and application of hydrological models, Hydrology & Earth System Sciences. 5 (2001) 13-26.

**Theme:** Emerging concepts and solutions in modelling methods
**IAHR Thematic Priority Area:** [TPA-4] Digital Transformation
https://doi.org/10.3850/iahr-hic2483430201-262

# Flood Modeling Strategy of Digital Twin Watershed: A Case Study of "23·7" Big Flood Assessment in Ziya River

**Fangrui Dong[1], Tao Sun[1*], Wenjing Lu[1], Xiaoxiang Zhang[2], Xuejun Yang[3], Qiang Ma[1]**

[1] China Institute of Water Resources and Hydropower Research, Beijing 100038, China
[2] College of Geography and Remote Sensing, Hohai University, Nanjing 211100, China
[3] Hydrology Bureau of Haihe River Water Conservancy Commission, Ministry of Water Resources, Tianjin 300170，China

*Corresponding author: sunt@iwhr.com*

**Abstract.** Affected by the global climate change, the challenges to flood management on catchment scale has increased. However, digital twin watershed is found effectively to improve its flood control capacity. In this study, taking the "23·7" big flood happened in Ziya River Basin, a digital twin flood modelling strategy has been presented with integration of hydrological and hydraulic models developed in China. The distributed hydrological models covered full catchment above Xianxian hydrojunction and three high resolution 2D hydraulic models over three flood storage areas has been set up and integrated into a modelling platform. The simulation results of 26 gauging stations shows higher accuracy with 7% difference of flood peak and averaged NSE 0.7. From this modelling assessment, the upper and middle parts of the Ziya River Basin showed an obvious Horton and Dunne mixed runoff generation mechanism during the whole flood period. Scientifically optimized the outflow of large reservoirs such as Huangbizhuang reservoir, the flooded area in Xianxian flood storage area has been reduced 68%. The modelling strategy proposed in this study is clear and operational for guiding the implement of digital twin watershed in other places and the models set up following the strategy shows high performance and efficiency.

**Keywords:** "23·7"catastrophic flood, digital twin watershed, distributed hydrological model, hydraulic simulation

## 1 Introduction

Climate change is exacerbating the formation and development of global ocean heatwaves, leading to more extreme climates in mid-high latitudes[1-2]. In recent years, China has frequently suffered extreme flood disasters, resulting in huge damages of social economic and casualties. In order to better deal with the challenges brought by extreme weather hazards, and to achieve the objective of scientific regulation of hydraulic constructions and efficient utilization of flood resources, more and more experts agreed with the construction of intelligent basin system for improving the ability of forecasting and the level of flood management.

## 2 Methods

The Ziya River Basin is the second largest sub-catchment and located in the central and southern part of the Haihe River Basin, with a total basin area of 47000 km2. The Ziya River Basin mainly includes two major river systems, the Hutuo River and the Fuyang River. Those two rivers are merged in front of the Xianxian junction, and then flows into the Bohai Sea through Tianjin city. In this study, the model is covered 97% of the Ziya River Basin ended at the Xianxian junction. According to the underlying characteristics and the topological structure of the catchment, the model of Ziya River Basin has been separated into 34 models with averaged control area around 1336km2. In addition, the distributed hydrological model of Hydro-SAT chosen in this study is developed by IWHR[3].

## 3 Results

The simulation results show higher accuracy with averaged difference of flood peak 7% and averaged NSE 0.7. The modelling analysis indicates that the middle stream of Hutuo River and the upstream of Fuyang River are the main flow generation area during this flood event, with obviously higher rainfall-runoff coefficient than other areas. The model applied in this study is able to represent the quantity of different flood components. 82.03% area of Ziya River Basin shows Horton and Dunne flow mixed runoff generation mechanism, while other areas are consisted with only Dunne runoff generation mechanism. The precipitation centre is mainly concentrated in the Yehe River at the middle part of the Hutuo River and the upper part of the Fuyang River. The rainfall path is from southeast to north of Ziya River, and the time duration is from July 28th to August 1st.

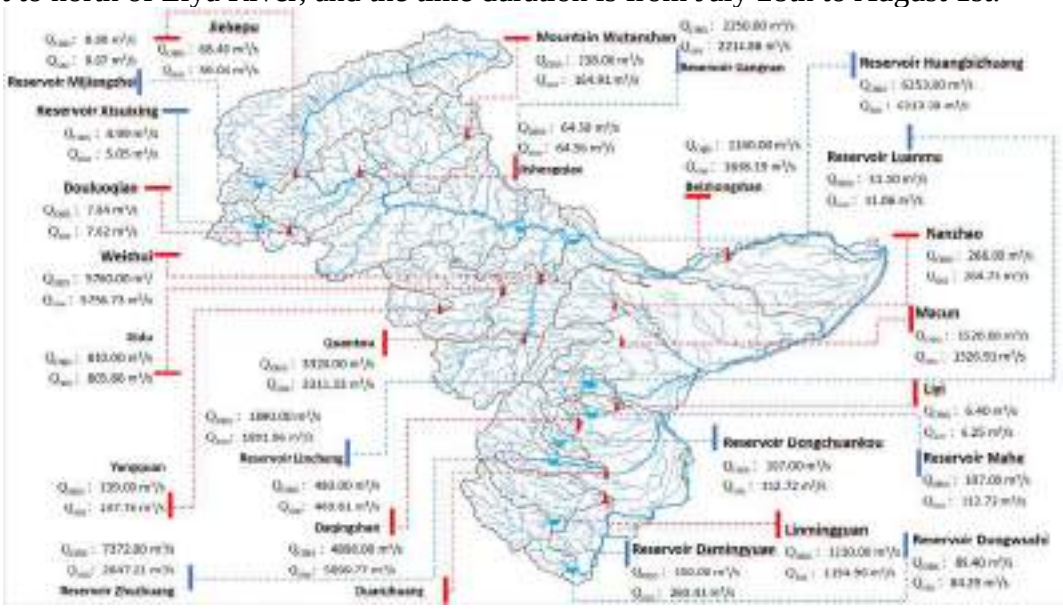


Fig1. The modelling results of “23.7” catastrophic flood in Ziya River Basin

## 4 Conclusions

This study produces a detailed assessment of the variation of flow generation mechanism during “23.7” catastrophic flood in Ziya River Basin. The following conclusions are made based on the outcomes of this study:

- The changes of runoff generation mechanism in this study are related to the distribution of precipitation. 82.03% area of Ziya River Basin shows the Horton and Dunne flow mixed runoff generation mechanism.
- This study conducts distributed simulation and review of extreme rainstorm floods in Ziya River Basin, which provides a scientific basis for clarifying the flood source and evaluating the effects of flood control projects.

## Reference

[1] Gu Wei,Chen Li-Juan,Wang Yong-Guang,Gao Hui,Wang Lin & Liu Yu-Yun.(2022).Extreme precipitation over northern China in autumn 2021 and joint contributions of tropical and mid-latitude factors.Advances in Climate Change Research(6),835-842.

[2] Masson-Delmotte V, Zhai P, Pirani A, et al. Climate change 2021: The physical science basis. Contribution of working group I to the sixth assessment report of the Intergovernmental Panel on Climate Change[M]. Cambridge, United Kingdom and New York, NY, USA: Cambridge University Press, 2021.

[3] Liu Changjun, Zhou Jian, Wen Lei, et al. Research on spatio temporally-mixed runoff model and parameter regionalization for small and medium-sized catchments. Journal of China Institute of Water Resources and Hydropower Research, 2021, 19(1): 99-114.

**Theme:** Emerging concepts and solutions in modelling methods
**IAHR Thematic Priority Area:** [TPA-4] Digital Transformation
https://doi.org/10.3850/iahr-hic2483430201-264

# Research And Practice on Integration Technology of Digital Twin Huaihe River Forecast and Rehearsal

**Youbing Hu[1], Shijin Xu[1], Kai Wang[1], Banghui Chen[1], Zhigang Feng[1], Jian Xu[2], Mengkai Qiang[2]**

[1] Hydrological bureau (Information Center) of Huaihe River Commission, Bengbu, Anhui 233001, China
[2] Anhui Huaihe Water Resources Technology Co., Ltd., Bengbu, Anhui 233000, China

*Corresponding author: Youbing Hu, ybhu@hrc.gov.cn*

**Abstract.** The construction of the digital twin Huai River serves as a crucial measure and starting point for achieving "unified planning, unified governance, unified scheduling, and unified management" as well as promoting high-quality development in the Huai River Basin during this new stage. "Forecasting, early warning systems, rehearsals, and preplanning" are essential means and measures for preventing flood and drought disasters. Building upon the pilot task practice of the digital twin Huai River project and following the link mechanism of "rainfall-flow generation-confluence-evolution," an integrated coupling computing technology is explored to enable accurate forecasting and efficient rehearsal of basin water engineering. This approach fully leverages hierarchical services and parallel computing advantages to provide technical support for effectively responding to demands related to basin flood forecasts and decisions regarding flood control projects.

**Keywords:** digital twin of Huaihe River, engineering simulation, flood forecasting, Huaihe River system, micro-services, parallel computing

The Huaihe River Basin is a highly overlapping area of national strategic importance, including the integration of the Yangtze River Delta and the ecological economic belt of the Huaihe River. Located in the transitional zone of north and south climates, the weather system is complex and changeable. The terrain is flat with poor water storage and drainage conditions, and floods and drought disasters occur frequently. It is urgent to use information technology to improve the digital and refined level of basin flood control management[1,2]. Smart water conservancy is the most significant symbol of high-quality development of water conservancy in the new stage, and digital twin basin is the core and key to promote the construction of smart water conservancy[3,4]. Flood control scheduling is the focus and difficulty of comprehensive scheduling of hydraulic engineering. Relying on the integrated technology of flood forecasting and pre-play under the flood "four-pre" system, it is an effective technical support means for the implementation of current flood control operation forecasting and scheduling[5,6]. Diao et al develop the reservoir group flood prevention and forecasting and scheduling system based on graph theory[7]. Chen et al design and develop a basin flood control forecasting and scheduling integrated system based on the networked service concept for the decision-making needs of flood control forecasting and scheduling in the Yangtze River Basin[8]. Ren et al pointed out that flood control scheduling is the focus and difficulty of comprehensive scheduling of hydraulic engineering and analyzed in detail the current level and existing problems of flood control scheduling in the basin's hydraulic engineering[9]. Wang et al established a digital twin Huaihe River flood control "four-pre" platform through high-precision data baseboards, high-performance computing power, and high-precision algorithms[10].

Hydrological and meteorological data are of various types, increasing year by year. The business objects continue to expand and are becoming more complex. To meet the business needs of flood

forecasting and scheduling for modern big data, high concurrency, and efficient simulation analysis, this paper explores a set of key technologies that fully leverage the advantages of layered services and high concurrency, guided by business needs, and rely on the digital twin Huaihe River flood control "four-pre" platform construction practice to provide technical support for efficient operation of basin flood forecasting, flood control engineering scheduling decisions and other businesses.

A platform development overall hierarchical architecture and its functional module composition were proposed for the business process and application needs of the digital twin Huaihe River flood control "four-early warning," which provides a reference for the construction of system functions.

Hydrological forecasting model program category and hydraulic engineering group scheduling knowledge base parameters were aggregated and excavated to design the forecast solution information data type and scheduling rules knowledge of the data structure database. This was coupled with the system platform through the persistent layer data framework MyBatis.

In the hydrological forecasting on multiple nodes in the river system, the hydrological simulation process of the section "rainfall-runoff-accumulation-evolution" was split, a pipeline river system hierarchical concurrent computing mode was proposed, and the parallel calculation of the river node runoff forecast was achieved.

In the water conservancy engineering joint scheduling and verification, a producer-consumer concurrent computing model based on information interconnection was proposed, which realized the parallel operation of prediction and calculation of the impact of engineering scheduling.

## Reference

[1] Qian Min. Flood problems and countermeasures in the middle reaches of Huaihe River[M]. Beijing: China Water Resources and Hydropower Publishing Press, 2019: 1-17.

[2] Wang Kai, Qian MingKai, Xu Shijing, et al, Construction and application of flood forecasting and dispatching system in resisting large flood in Huaihe River Basin[J]. Water Resources Informatization, 2021(2):1-5, 9.

[3] Li Guoying. Build a digital twin basin to promote the high-quality development of water conservancy in the new stage[N]. Learning Times, 2022-06-29(001).

[4] Cai Yang, Chen Jianguo, Cao Miao, et al. Accelerate the construction of a intelligent water conservancy system with ' four pre ' functions[J]. China Water Conservancy, 2021(20): 2-5.

[5] Huang Qiyou, Hu Ke, Yu Siyang, et al. Research and application of integrated flood forecasting and dispatching of river systems[J]. Water Power, 2022,48(06):36-40,104.

[6] Yu Shan, Huang Yan, Wang Xuemin, et al. Discussion on construction of intelligent dispatching platform for water engineering in Changjiang River Basin[J]. Yangtze River, 2022,53(02):189-197.

[7] Diao Yanfang, Duan Zhen, Zhang Rong, et al. Risk Analysis of Cascade Reservoirs' Joint Flood Control Operation Mode with Forecast Information[J]. Water Power, 2018,44(08):82-86.

[8] Chen Yubin, Zou Bingyu, Niu Wenjing, et al. Research on several key technologies of flood control forecasting and integrated dispatching system in basin[J]. Yangtze River, 2019,50(07):223-227.

[9] Ren Minglei, He Xiaoyan. Understanding and Discussion on Reservoir Flood Control Operation[J]. Yangtze River, 2011,42(S2):58-60,103.

[10] Wang Kai, Xu Shijin, Liu Changjun, et al. Key technology of "four pre" system for fl ood control of digital twin Huaihe River[J]. Water Resources Informatization, 2023,(06):1-4+31.

[11] Hu Youbing, Chen Banghui, Xu Shijin, et al. Research on concurrent computing of river runoff forecast based on pipeline model[J]. Water Resources Informatization, 2023,(04):50-53.

[12] Hu Youbing, Qian Mingkai, Xu Shijin, et al. Study on Concurrent Joint Scheduling Method of Basin Water Engineering Groups[J]. Journal of China Hydrology. 2022,42(01):54-58.

**Theme:** Emerging concepts and solutions in modelling methods
**IAHR Thematic Priority Area:** [TPA-4] Digital Transformation
https://doi.org/10.3850/iahr-hic2483430201-266

# An Integrated Modelling Strategy of Digital Twin Watersheds, Application of Digital Watershed Platform of Dawen River Basin

**Siyuan Chang[1,2], Changjun Liu[1,2], Qiang Ma[1,2], Aiqing Kang[1] and Xixi Cui[1,2]**

[1] China Institute of Water Resources and Hydropower Research, Beijing, PR China
[2] Research Center on Flood & Drought Disaster Reduction of the Ministry of Water Resources, Beijing, PR China

*Corresponding author: Liucj@email.iwhr.com*

**Abstract.** The progress of hydroinformatics technologies creates both new challenges and opportunities for the flood management. How to integrate different kinds of hydro-models into a unified platform and make all modules to run properly and efficiently has become one of hot topics widely discussed in the many hydroinformatics committees. Taking the example of Dawen River Basin, an advanced modelling platform consisted with three kinds of hydro-models including distributed hydrological model, 1D and 2D coupling hydraulic model and reservoir operation model has been set up for supporting the decision-making process of flood management. The Dawen River Basin (8944km$^2$) has been characterized as one of the most complex catchment in Shandong province, China. With the Optimized computation process among three kinds of models in the catchment, the parallel computing technologies has been applied in the modelling platform of Dawen River Digital Twin System. With 42 distributed hydrological models covered full catchment area, 1D and 2D hydraulic models with 1616 cross sections and 69315 computation girds, and operation models of 23 reservoirs, all modelling accuracy and efficiency has been validated during "Dussuri" typhoon flood disaster period. The hourly simulation for 3 day was completed in less than 5 minutes. Moreover, the averaged flood peak difference is 10% with peak time difference less than 3h. The modelling strategy indicated in this study shows high applicability to be promoted to other medium and large catchments with strong human impacts for improving the flood defense and operate abilities.

**Keywords:** Modelling strategy, Digital twin watershed, modelling platform, flood management, Dawen River Basin

## 1 Introduction

Taking the advantages of new hydroinformatics technologies, more and more local flood manage demands to have a smart water conservancy system for supporting their real-time decision making process. In order to reach that objective, the power of the modelling platform plays significant role of the system. Many experts and scholars have done a lot of research on how to setup a efficient and operational digital twin model platform [1-3]. Taking Dawen River Basin in Shandong Province China as an example, this study developed an integrated modelling platform with 5 components including modelling management, scheme management, scheduling management, external service and other functions with standardized modelling packaging and unified registration management of various professional water models. Besides, this platform has achieved the coupling and integration of different models and algorithms which almost covered the full flood defense process from flow generation and convergence, flow evolution to reservoir regulation. Supported by the model standardization, construction of simulation schemes and computation parallelization, the hourly forecast model running in real time is able to produce 3 days forecast over whole catchment area. Now, the modelling platform has been used in operation and can considered as main reference for the design of digital twin basin model platform in other area.

## 2 Material and methods

The Dawen River Basin digital twin model platform mainly includes five functional modules: model management, calculation scheme management, scheduling management, model service and model assessment. According to the underlying surface conditions and river section morphology of the Dawen River Basin, the models integrated in the modelling platform follow natural process of "rainfall-production-confluence-evolution" and have 42 distributed hydrological model covering 607 small river basins, 18 one-dimensional hydrodynamic model covering 683km branches, 8 two-dimensional hydrodynamic model covering 1945km$^2$, and the dispatching model of 23 reservoirs. With the parallel computing framework, all those models with 3 days simulation can be finished in 2mins.

## 3 Results

During the "Dussuri" Typhoon period, 2023, the modelling platform has been running in operation and produce hourly real-time forecast for next 3 days. Comparing with the observed data, the forecast results of 72 sections in the Dawen River Basin have only 10% flood peak difference in average and peak time error less than 3h. On 29$^{th}$ July 2023 9:00am, the model is able to forecast the peak discharge of Qiaodian reservoir (6.39 m$^3$/s) which is almost as same as the observation (6.67 m$^3$/s) with only 1hours difference. Moreove at the downstream, the forecast flow of Dawenkou Station is 644 m$^3$/s, and the measured flow is 660m$^3$/s with only 2 hours difference.

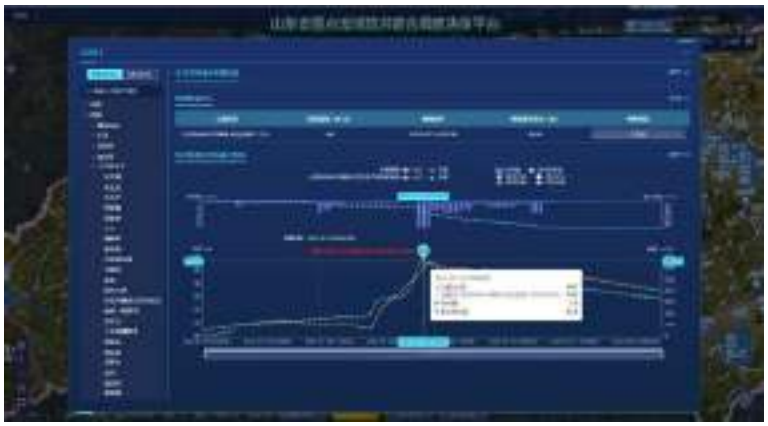

Figure 1 Forecast results for Dawen River Basin at 9 am on July 29, 2023

## 4 Conslusions

In this paper, an integrated modelling platform of Dawen River Basin with many kinds of models has been presented. The following conclusions can be drawn from the results of this study

- The multi-model integration and parallel computation framework presented in this study is able to reach to objective of having accurate and efficient real-time forecast.
- The construction of the model platform improves the reusability of the model and provides a good support for the standardized management and efficient business application of the model.

## Reference

[1] LI Zhe, XIANG Da-xiang, CHEN Zhe, CUI Chang-lu, Design and development of drought defense information platform for the Changjiang River Basin driven by digital twins, Journal of Yangtze River Scientific Research Institute[J], 1-11.

[2] Yang Fang, Song Lixiang, Li Xudong, et al. Development and application of "four pre-warning" system model for flood and drought disaster prevention in the Pearl River Basin [J]. China Water Resources, 2023(4): 10-14.

[3] Li Xupeng, Wang Ying. Thoughts on the Construction of digital twin system of the Yellow River in Shandong [A]. 2023 (11th) Proceedings of China Water Conservancy Information Technology Forum [C]. Hohai University, Wuhan University, Network and Information Center of Yangtze River Water Resources Commission, Hubei Water Resources and Hydropower Research Institute, 2023: 217-227.

**Theme:** Emerging concepts and solutions in modelling methods
**IAHR Thematic Priority Area:** [TPA-4] Digital Transformation
https://doi.org/10.3850/iahr-hic2483430201-268

# Discussion on the construction of the Integrated System for Water Engineering Forecasting and Scheduling in Taihu region

**Dongzhou Li [1,2], Guoqing Liu [1,2], Ziwu Fan [1,2], Guang Yang [1,2], Yipeng Liao [1,2], Jingxiu Wu[1,2], Xuan Huang[1,2], Fan Yang[1,2]**

[1] Nanjing Hydraulic Research Institute, Nanjing, China
[2] Key Laboratory of Taihu Basin Water Resources Research and Management of Ministry of Water Resources, Nanjing, China

*Corresponding author: Liu Guoqing, gqliu@nhri.cn*

**Abstract.** The Taihu Basin is one of the most complex river network, water conservancy projects. The integration of the forecast model and project operations is the key to solving the accurate control of water conservancy projects in the plain river network. Under the background of digital twin basin construction, the framework of the system has been formulated, and the work flow, core function module and critical path has been designed. The "Four pre" system for water conservancy project operations, which integrated the digital hall, digital twin display, "Four pre" operation, consultation assistance, has been established. The system has been developed and deployed. The results show that the whole solution based on digital twin basin framework is feasible. The system has been used in the cooperative projects operation of Yangtze river, Taihu and polder areas. At the present stage, the system realized the replaying of the past flood events, recreating the present and previewing the future. The research results has been applied effectively in the regional flood control and the operation of "water diversion from Yangtze River to Taihu Lake" project, which played an exemplary role in the first batch of digital twin projects of the Ministry of Water Resources.

**Keywords:** Digital twin, Forecasting and scheduling, Four pre, Taihu Lake region

## 1 Introduction

With the continuted development of digitalization and the construction of Digital China during the "14th Five-Year Plan" period, water conservancy development has entered a new stage. According to the spirit of the important speeches and instructions on building a strong cyber nation by General Secretary Xi Jinping, Minister Li Guoying pointed out that the construction of smart water conservancy is one of the six major implementation paths and the most significant indicator for promoting high-quality development in the new stage of water conservancy. He called for the accelerated construction of digital twin basin with "Four pre" functionality, to realize smart water conservancy scenarios featuring digitalized settings, intelligent simulation, and precise decision-making.

## 2 Method

The construction of the system is based on the physically existing basins, with models at its core, and the water conservancy intelligent exchange platform as the link. The overall architecture includes information infrastructure, data foundation, model platform, and knowledge platform. Among these, focusing on the construction of the digital twin water network, the information infrastructure provides "computational power" support, the data foundation offers "data basis" support, while the model platform and knowledge platform deliver "algorithm" services. The water conservancy intelligent exchange platform connects the data foundation, model platform, and knowledge platform, serving the co-construction and sharing, and supports the integrated "Four pre" business applications of water engineering forecasting and scheduling.

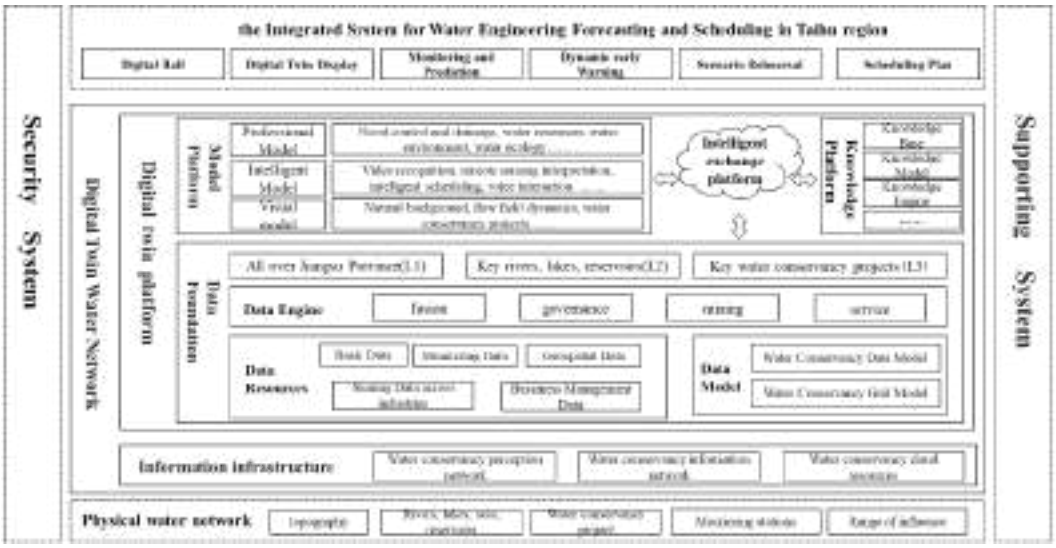


Figure 1 Overall architecture

The key Technologies used in this paper include: Multi-source Data Foundation Construction and Fusion Technology; River Network Multi-scale Hierarchical Intelligent Simulation Technology; Perception and Model Joint-Driven Forecasting Technology; Model Library Standardization, Packaging, and Interaction Technology.

## 3 Results

On the basis of constructing the data foundation for the Taihu Lake region in Jiangsu Province and integrating the water engineering forecasting and scheduling models for the Taihu Lake region of Jiangsu Province, the integrated platform for water engineering forecasting and scheduling in the Taihu Lake region of Jiangsu Province has been developed. This platform specifically includes functional modules such as the Digital Hall, Digital Twin Display, "Four pre" Scheduling, and Consultation Assistance.

## 4 Conclusion

The system construction is guided by the management needs of basin, regional, and city engineering scheduling taking into account the requirements for the construction of digital twin basins, and has formulated an integrated overall solution for forecasting and scheduling. It has constructed a data foundation, integrated river network models, and based on the intelligent exchange platform, implemented the "Four pre" function for regional flood control and water diversion.

## Reference

[1]Guoying LI. Accelerate the construction of digital twin river basins to enhance national water security[J]. Water Conservancy Construction and Management, 2022, 42(09): 1-2.

[2]Yan HUANG. Practices and thoughts on the intelligent dispatching of river basin water projects[J]. China Flood & Drought Management, 2019, 29(05): 8-9.

[3]Yang CAI,Zhiyu LIU,Chunpeng SUN,et al. Practice and thinking of scientific prevention in 2020 major flood[J]. Water Resources Informatization, 2021, (01): 1-5.

[4]Yan HUANG,San YU,Bin LUO, et al. Development of the digital twin Changjiang River with the pilot system of joint and intelligent regulation of water projects for flood management[J]. Journal of Hydraulic Engineering, 2022, 53(03): 253-269.

**Theme:** Emerging concepts and solutions in modelling methods
**IAHR Thematic Priority Area:** [TPA-4] Digital Transformation
https://doi.org/10.3850/iahr-hic2483430201-270

# Digital Twin Water Network Empowering Multi-Service Scenarios Applications and Practices

**Yang Guang[1,2], Fan Ziwu[1,2], Liu Guoqing[1,2], Li Dongzhou[1,2], Chao Yutian[1]**

[1] Nanjing Hydraulic Research Institute, Nanjing 210000, China
[2] Key Laboratory of Taihu Basin Water Resources Research and Management of Ministry of Water Resources, Nanjing 210000, China

*Corresponding author:Liu Guoqing, gqliu@nhri.cn*

**Abstract:** Currently, the pilot work of the digital twin basin by the Ministry of Water Resources is drawing to a close. The digital twin project for the typical water network in Taihu Lake region, as one of the four pioneering projects in Jiangsu Province, includes ten sub-projects. Each sub-project takes into account the comprehensive characteristics of the water network outline, the order and the knot in the Taihu Lake region, focusing on rivers, lakes, reservoirs, cities and polders as primary pilot sites. Centered around the concept of co-construction and sharing, this paper expounds on the ways in which the digital twin water network empowers the applications of multi-business scenarios from four aspects: new situations, new ideas, new standards, and new platforms. This includes the multi-level data foundation that integrates "points-lines-planes" in the Taihu Lake basin, the refined river network model and services for Taihu Lake region in Jiangsu Province, and the "2+N" multi-scenario "four-pre" business applications. The construction achievements can provide experiences for the construction of Jiangsu's digital twin water conservancy, effectively supporting the construction of China's future smart water conservancy system.

**Keywords:** Data Foundation, Digital Twin Water Network, "four-pre" System, Model Services, Taihu Lake Region

## 1 Introduction

In response to the Ministry of Water Resources' requirements for the construction of digital twin basin, Jiangsu Province actively applied for pilot projects. As one of the four pioneering projects in the province, the digital twin project for the typical water network in the Taihu Lake region involves 10 sub-projects, covering the river, lakes, reservoirs, cities, polders and other different objects. The pilot project explored solutions for building a large-scale data foundations through the integration of multi-source data, the online operation and customized service mode of integrated basin models, and the "2+N" multi-scenario "four pre" business application process. The achievements of this construction can provide experiences for the construction of digital twin water conservancy projects and effectively support the future construction of China's smart water conservancy system[5].

## 2 Materials and Methods

(1) Multi-Level Data Foundation

A data foundation covering the entire Taihu Lake area is constructed, by aggregating and integrating data from different regions, multiple levels and sources, providing shared services in the form of data services to all sub-projects to avoid redundant construction. Data types include basic data, perceptual data, business data, cross-industry shared data, and geospatial data.

(2) Refined river network model

Multi-scale hierarchical online model of the Taihu Lake area in Jiangsu Province

The total area of the Taihu Lake region in Jiangsu Province is 21,600 $km^2$. Based on the characteristics of the water system division, it can be divided into hydraulic districts such as HuXi, Wucheng Xiyu, Yangcheng Dian Mao, and Hangjiahu (Su), the administrative areas mainly include cities like Zhenjiang, Changzhou, Wuxi, and Suzhou.

(3) “four-pre” scheduling business fuction

It has created a multi-level user function architecture model of "high-level situational awareness-intermediate four “four-pre” scheduling-basic daily management", and developed general core functions such as situational awareness, forecasting, early warning, pre-act, pre-planning, and consultation support.

## 3 Results

(1) Integrated Forecasting and Scheduling System for the Taihu Lake Region

The integrated forecasting and scheduling system for the Taihu Lake region mainly includes four functional modules: Digital Hall, Twin Display, Four Predictions Scheduling, and Consultation Support.

(2) Digital Twin Gehu Lake System

The Digital Twin Gehu Lake System, by constructing an "atmospheric-hydrological-hydrodynamic-water environment-water ecology" comprehensive sensing system for both above and underwater elements, achieves flood forecasting for the Gehu Lake region, pre-action simulation for the Yangtze River to Taihu Lake water transfer, and early warning monitoring of the water ecological environment.

## 4 Conclusion

The construction of a digital twin water network in the Taihu Lake area involves multiple business applications such as flood and drainage warning dispatch, Yangtze River to Taihu Lake water allocation, water environment governance enhancement, ecological river and lake health diagnosis, river network joint control and coordination, and blue-green algae control. By reconstructing business processes and covering multi-scenario businesses for water security assurance, it explores common issues that may arise during the construction of digital twin water conservancy, providing practical value for future smart water conservancy project construction.

**Theme:** Emerging concepts and solutions in modelling methods
**IAHR Thematic Priority Area:** [TPA-4] Digital Transformation
https://doi.org/10.3850/iahr-hic2483430201-272

# Embedded Transient Hydraulic Simulations with Machine Learning Processing for Leak Detection In Water Distribution Networks

**Andrea Menapace[1], Maurizio Tavelli[1], Daniele Dalla Torre[1] and Maurizio Righetti[1]**

[1] Faculty of Engineering, Free University of Bozen-Bolzano, Bolzano, Piazza Domenicani 3, 39100, Italy

*Corresponding author: andrea.menapace@unibz.it*

**Abstract.** The digitalisation, along with the implementation of smart grids, is driving a new era of efficient and sustainable water distribution systems. Implementing smart sensors, transmission systems, and integrated support systems allows for the development of cutting-edge technologies in real-time monitoring and control, ensuring prompt detection and accurate localisation of anomalies and water losses par excellence. Transient test-based techniques consist of the generation and monitoring of small pressure waves in the pipelines with the final aim of identifying any anomalies through the analysis of the transient signals. To enable this technology to be suitable for real-world applications, it is necessary to develop techniques for processing transient pressure signals for real-time anomaly detection. Thus, a methodology embedding an unsteady hydraulic model for generating big training datasets with machine learning algorithms exploiting this synthetic transient data for automatically identifying leaks in pipes is proposed. The feasibility of this methodology is demonstrated by two different complexity tests, which ensure promising results in the case of both single conducts and simple networks.

**Keywords:** Artificial Neural Networks, Leaks Detection, Numerical Hydraulic Modelling, Sustainable Water Management, Transient Signal Processing, Water Distribution Networks

## 1 Introduction

A comprehensive understanding of the water distribution system's behaviour is achievable by Transient Test-Based Techniques (TTBT), which are based on a controlled generation of a small pressure transient and the consequent recording of the pressure signal over time in one or more strategic points of the pipeline network [1]. This non-intrusive test provides significant information about the anomalies due to the influence of the pressure signals on the size and shape of leaks, along with the hydraulic and physical characteristics of the distribution pipeline network [2]. For this purpose, transient signal processing has been done for many years by experts who are able to analyse the signal for each specific system and accurately identify abnormal behaviour [3]. However, recent literature has primarily concentrated on the analysis of single pipes, with only pioneering studies delving into network analysis [4]. Furthermore, there has been limited exploration into the automatic processing of transient signals with the assistance of deep learning methodologies [5]. Due to these reasons, this contribution proposes an automatic leak detection tool by coupling a numerical unsteady hydraulic solver with a machine learning (ML) processing algorithm.

## 2 Methodology

The methodology aims to achieve autonomous anomaly detection within TTBT, exploring ML techniques for continuous data analysis. However, acquiring a substantial dataset for ML algorithm advancement is challenging. Synthetic data from numerical simulations offers a viable solution. Key tasks include generating synthetic pressure transient signals and developing automatic anomaly detection methods. An accurate hydraulic solver is essential for simulating unsteady hydraulic behavior in pipeline systems. The generated datasets are crucial for training the ML detection

algorithm, which inputs simulated transient data to locate anomalies along the pipeline system. This integrated approach combines data generation through numerical simulations with ML anomaly detection development. Ad numerical solver, we adopt a one-dimensional semi-implicit scheme to solve compressible flows in compliant networks of elastic pipes. The scheme is based on the one proposed in [6] and is then extended to networks of pipes with local failures. Instead, a feed-forward neural network (FFNN) methodology is used for anomaly detection, consisting of an input layer of pressure transient signals, hidden layers, and an output layer returning the leak position to process pressure transient signals in hidden layers, efficiently identifying leak positions through its output layer.

## 3 Results

Two tests of different complexity are included to highlight the quality of the proposed methodology. *Test 1* represents a single long transmission water main, while *Test 2* is about a small distribution network, which makes the problem of leak detection with the TTBT considerably more complex. A pressure valve is responsible for the manoeuvre that generates the pressure transient that is measured in measurement points located in significant points of the networks. Both tests are not related to laboratory experiments or real cases but have the sole purpose of evidencing the suitability of the proposed methodology. The accuracy of the leak detection of *Test 1* is excellent, with a mean absolute error (MAE) of 0.3 m on a 1000 m pipeline., while the MAE in *Test 2* results of 0.59 m despite the greater complexity.

## 4 Conclusion

Proposing an embedded methodology for leak localisation tools utilising TTBT. It employs an unsteady hydraulic solver to generate synthetic pressure signals to train automatic ML anomaly detection methods. A deep-learning algorithm, FFNN-based, processes transient signals to pinpoint leak locations. Two tests demonstrate TTBT's suitability for real-world leak detection. This preliminary showcase highlights the potential of big data analysis and deep learning, marking a step towards integrated network diagnostic protocols for modern water smart grids. These advancements promise enhanced efficiency and resilience in water distribution systems, promoting sustainable water management practices.

## 5 Acknowledgement

This research was funded by funded by the European Union - Next Generation EU within the framework of the PRIN 2022 project Hybrid Transient-machine learning approach for "ANomaly DEtection and classification in water transmission Mains (TANDEM)", grant number 6477. M.T. is a member of the INdAM-GNCS group.

## Reference

[1] Brunone, B., & Ferrante, M., Detecting leaks in pressurised pipes by means of transients, Journal of hydraulic research, (2001), 39(5), 539-547.
[2] Covas, D., Ramos, H., Lopes, N., & Almeida, A. B., Water pipe system diagnosis by transient pressure signals, In Water Distribution Systems Analysis Symposium 2006, (2006), (pp. 1-19).
[3] Meniconi, S., Capponi, C., Frisinghelli, M., & Brunone, B., Leak detection in a real transmission main through transient tests: Deeds and misdeeds, Water Resources Research, (2021), 57(3), e2020WR027838.
[4] Manzi, D., Brentan, B., Meirelles, G., Izquierdo, J., & Luvizotto Jr, E., Pattern recognition and clustering of transient pressure signals for burst location, Water, (2019), 11(11), 2279.
[5] Ayati, A. H., Haghighi, A., & Ghafouri, H. R., Machine Learning–Assisted Model for Leak Detection in Water Distribution Networks Using Hydraulic Transient Flows, Journal of Water Resources Planning and Management, (2022), 148(2), 04021104.
[6] M. Dumbser, U. Iben, M. Ioriatti, An efficient semi-implicit finite volume method for axially symmetric compressible tubes, Applied Numerical Mathematics, (2015), 89, 24-44.

**Theme:** Emerging concepts and solutions in modelling methods
**IAHR Thematic Priority Area:** [TPA-4] Digital Transformation
https://doi.org/10.3850/iahr-hic2483430201-274

# Implementing Liquid Neural Networks for Enhanced Plant-Wide Control of A Wastewater Treatment Plant

**Cristian Camilo Gomez Cortes[1,*], Kimberly Solon[1], Ingmar Nopens[1], Elena Torfs[2]**

[1] BIOMATH, Department of Data Analysis and Mathematical Modelling, Faculty of Bioscience Engineering, Ghent University, Coupure links 653, 9000 Ghent, Belgium
[2] modelEAU, Département de génie civil et de génie des eaux, Université Laval, 1045, Avenue de la Médecine, Québec G1V 0A6, Canada

*Corresponding author: cristiancamilo.gomezcortes@ugent.be*

**Abstract.** Wastewater treatment plants (WWTPs) face operational challenges due to their resource-intensive nature, greenhouse gas emissions, and residual sludge production. PID-based control systems struggle with nonlinear disturbances like extreme weather. This study explores Liquid Neural Networks (LNN)-based agent Reinforcement Learning (RL) on a Benchmark Simulation Model No.2 plant under three scenarios: normal/dry-weather, storm, and winter conditions. The LNN-based agent achieves an average operational cost improvement compared to conventional PID approach, implementing a 70% less connected network than a full-connected approach. The control methodology presented is a promising solution to the complex nonlinear challenges associated with control in WWTPs.

**Keywords:** Global control system, Reinforcement Learning, Liquid Neural Networks, WWTP

## 1 Overview

Wastewater treatment plants (WWTPs), essential for reducing environmental pollution face multiple operational challenges given their resource-intensive nature, greenhouse gas emissions, and the production of residual sludge. Control and optimization within WWTPs are particularly complex due to the high nonlinearity inherent in the biological and dynamic processes involved.

Conventional Proportional-Integral-Derivative (PID)-based control systems, which are effective under normal operational conditions, struggle with nonlinear disturbances such as extreme weather [1]. Moreover, these controllers are mainly implemented locally making it challenging to simultaneously address the multiple operational challenges. Addressing these limitations necessitates a global control methodology under normal and extreme scenarios. Although machine learning methodologies such as Deep and Multi-agent Reinforcement Learning (RL) have been applied in this context, the large number of parameters required limit their interpretability and transferability [2]. In this study, Liquid Neural Networks (LNN) [3]-based agent Reinforcement Learning control is explored to address the multiple WWTP challenges and limitations of conventional control.

## 2 Methodology

In RL, an agent learns to make sequential decisions through interactions with an environment, aiming to maximize the accumulative reward function. The agent is created by implementing LNN, a variant of recurrent neural networks characterized by continuous differential equations governing spatiotemporal decision-making. Furthermore, a specialized set of neuron compartments was engineered encompassing sensory processing, control, and motor output to optimize the network's design for sparse efficiency.

This innovation significantly augments computational efficiency, facilitating scalability and transferability. The reward function incorporates crucial metrics such as operational cost, effluent quality, and operational stability.

The WWTP studied is represented by the Benchmark Simulation Model No.2 plant [4]. A RL control with a LNN-based agent is implemented on the WWTP under three scenarios: (i) normal/dry weather, (ii) storm, and (iii) winter conditions. The plant performance is compared with a PID-based controlled WWTP.

## 3 Results and Discussion

Through comprehensive analysis, including cost evaluation and assessment of operational scenarios, notable improvements have been observed. Operational costs, encompassing energy consumption, chemical usage, and process efficiency, showed a significant reduction of 15-20% under normal conditions and up to 30-40% during extreme events such as storm surges and influent quality spikes. Moreover, the LNN-based agent demonstrated remarkable adaptability and resilience, ensuring stability and reliability even in challenging conditions.

Furthermore, the neural network architecture of the LNN-based agent exhibited high sparsity levels exceeding 70%, indicating a reduced number of active connections between neurons. This inherent efficiency allowed for optimized memory utilization and faster computations without compromising performance accuracy. Leveraging sparsity in neural networks not only enhances computational efficiency but also facilitates scalability, making the LNN-based agent a promising solution for advanced control strategies in highly nonlinear large-scale wastewater treatment applications.

## 4 Conclusion

The control methodology presented is a promising solution to the complex nonlinear challenges associated with control in WWTPs. This method:

- significantly improved the operational cost in normal and extreme conditions, compared to conventional PID control.
- reduced the number of parameters and network size, thereby improving the transferability, scalability, and interpretability of the model.
- allows for global optimization of operational cost, effluent quality, and operational stability (result in full paper).

The full paper will include results for a real full-case plant (Tilburg WWTP, Netherlands).

## 5 Acknowledgments

We gratefully acknowledge the support and resources provided by the EU-funded project DARROW, which significantly contributed to the success of this endeavor.

## References

[1] Gernaey, K. V., Jeppsson, U., Vanrolleghem, P. A., & Copp, J. B. (2014). Scientific and Technical Report No. 23: Benchmarking of Control Strategies for Wastewater Treatment Plants. IWA Publishing: London, UK. https://doi.org/10.2166/9781780401171

[2] Hasani, R., Lechner, M., Amini, A., Rus, D., & Grosu, R. (2021). Liquid time-constant networks. In Proceedings of the AAAI Conference on Artificial Intelligence (Vol. 35, No. 9, pp. 7657-7666). https://doi.org/10.48550/arXiv.2006.04439

[3] Hernández-del-Olmo, F., Gaudioso, E., Duro, N., Dormido, R., & Gorrotxategi, M. (2023). Advanced Control by Reinforcement Learning for Wastewater Treatment Plants: A Comparison with Traditional Approaches. Applied Sciences, 13(8), 4752. https://doi.org/10.3390/app13084752

[4] Iratni, A., & Chang, N. B. (2019). Advances in control technologies for wastewater treatment processes: status, challenges, and perspectives. IEEE/CAA Journal of Automatica Sinica, 6(2), 337-363. https://doi.org/10.1109/JAS.2019.1911372

**Theme:** Emerging concepts and solutions in modelling methods
**IAHR Thematic Priority Area:** [TPA-4] Digital Transformation
https://doi.org/10.3850/iahr-hic2483430201-276

# New Data Augmentation Method for Rainfall-Runoff Calculation Using Machine Learning and Examining its Applicability

**Masayuki HITOKOTO[1], Takeru ARAKI[1]**

[1] Nippon Koei Co., Ltd, 2304 Tsukuba-shi Ibaraki-ken 300-1259, Japan

*Corresponding author: hitokoto-ms@n-koei.jp*

**Abstract.** There are many studies on dam inflow prediction and river water level prediction using machine learning. However, these methods have a major problem that they are less applicable to inexperienced large-scale floods. The authors have been proposed to improve the prediction accuracy of dam inflow prediction using machine learning by data augmentation based on the theory of rainfall-runoff. The proposed method improves the accuracy of the inflow prediction model by adding virtual large-scale floods asaugmented data to the learning data. Specifically, we assume a steady-state condition of constant rainfall, and use atheoretical dataset of virtual floods as the augmented data, such that the total amount of rainfall in the basin is equalto the dam inflow. In this study, we studied the applicability of the proposed method in seven dam basins in Japan. Case studies were conducted on several flood events, including these large-scale floods. We used a feed forward deep neural networkas the machine learning model. For all dams, it was confirmed that the prediction accuracy improved by applying the proposed method. We analyzed the hydrological characteristics of past flood events used for learning, and analyzed under what conditions the proposed method would be most effective.

**Keywords:** deep learning, dam inflow prediction, data augmentation, extreme floods

## 1 Introduction

In this study, we applied data augmentation to machine learning models and conducted case studies for seven basins in Japan. We also verified the applicability of the model to large-scale floods that significantly exceeded the training cases.

## 2 Material and methods

The location and the shape of target dams are shown in figure 1. Actual inflow and rainfall data from 2002 to 2021 were obtained for each target dam from the Water Information System. The major floods during these periods were extracted as target data. The model used in this study was a feed-forward neural network consisting of an input layer, two hidden layers, and an output layer. The data augmentation method proposed in this study, we assumed a steady state of constant rainfall and virtual flood data in which the total rainfall to the basin and the dam inflow were equal (runoff coefficient = 1.0). The augmentation method assumes that the surface soil of the basin is completely saturated.

## 3 Results and discussion

The calculation results for the five out of seven dams were considerably closer to the actual peak inflow, which greatly improves the accuracy of the prediction. For the other two dams, altough improved by the proposed method, the calculated results were still far below the actual results. The prediction model trained by the floods with large runoff coefficient has originally high applicability to large-scale floods, and the degree of improvement by the proposed method is also large. And the

proposed method is also effective even when there are few floods with large runoff coefficient, although the effect is small.

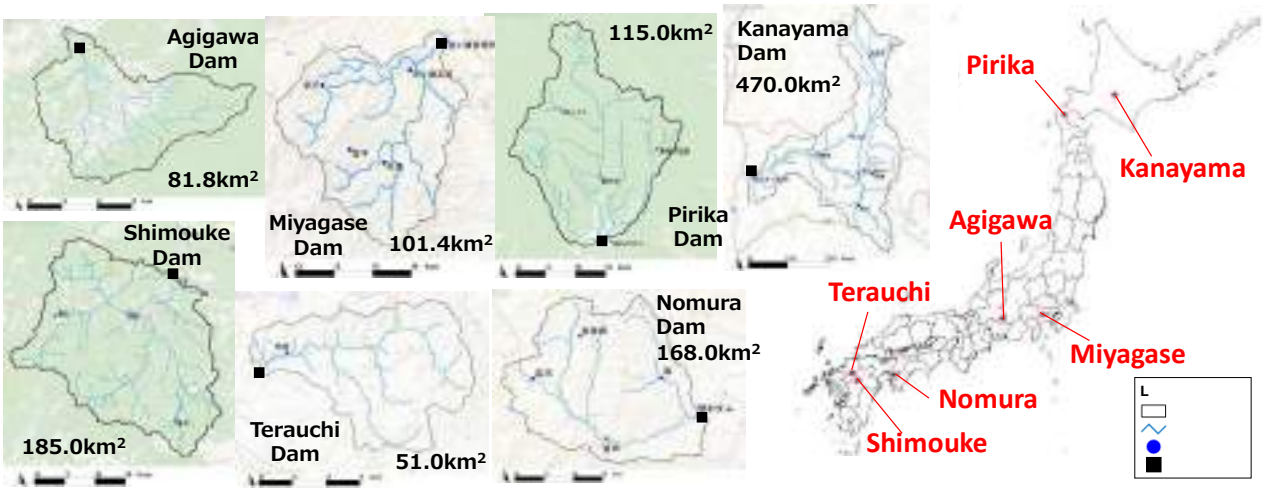


Figure 31 Location and shape of target dams

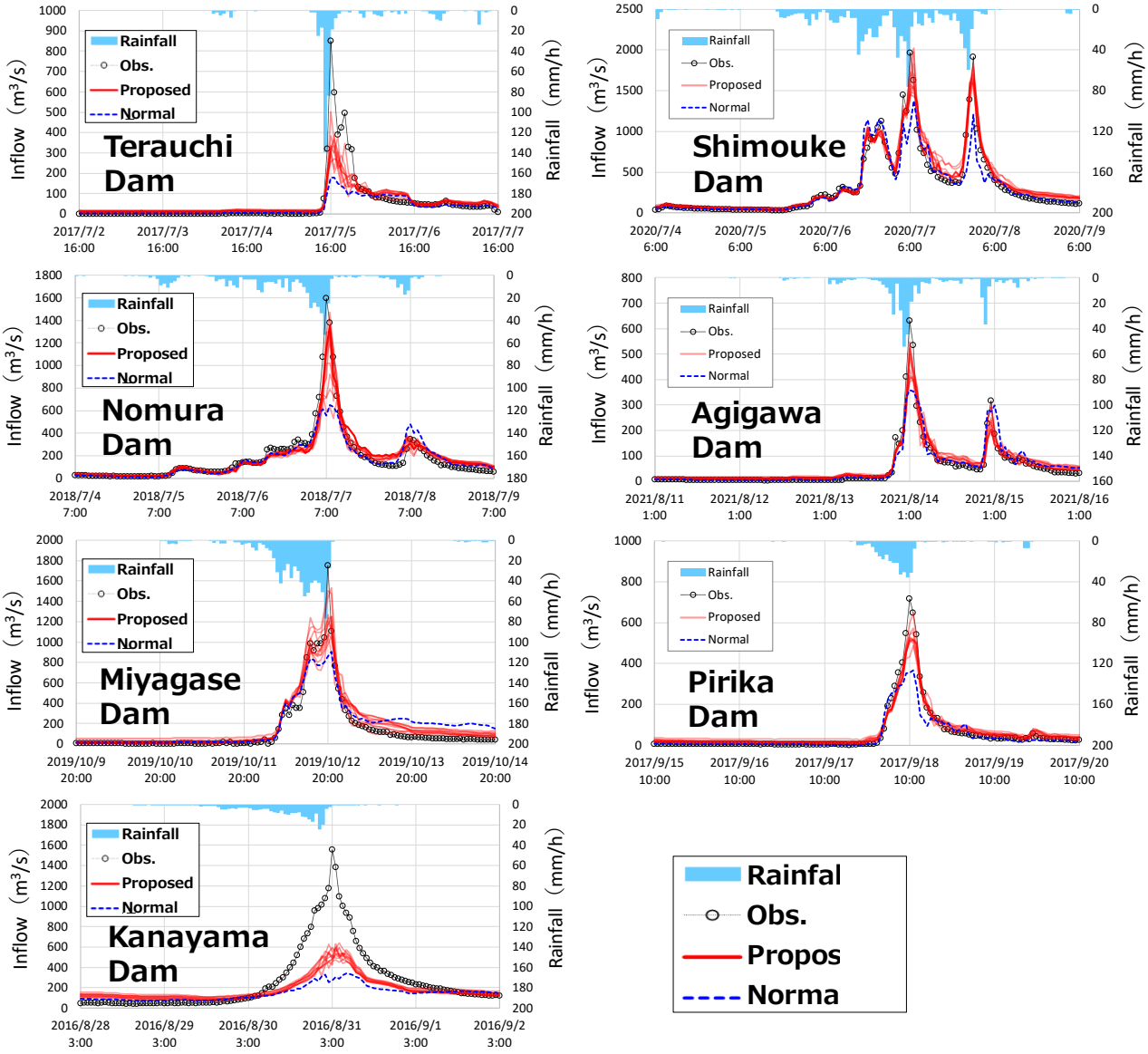


Figure 32 Results of test calculations for the largest floods in each dam

**Theme:** Emerging concepts and solutions in modelling methods
**IAHR Thematic Priority Area:** [TPA-4] Digital Transformation
https://doi.org/10.3850/iahr-hic2483430201-278

# Integrating Social Media, News and Machine Learning for Enhanced Hydrological Event Detection and Management

**Joao Pita Costa[1], Gerald A. Corzo Perez [2], Inna Novalija3, Luis Rei [3,4], Matej Senožetnik[1] and I. Casals del Busto[5]**

[1] International Research Centre for Artificial Intelligence under the auspices of UNESCO (IRCAI), 1000 Ljubljana, Slovenia
[2] UN IHE, 2611 Delft, The Netherlands
[3] Jožef Stefan Institute, 1000 Ljubljana, Slovenia
[4] Event Registry, 1000 Ljubljana, Slovenia
[5] Aguas de Alicante, 03008 Alicante, Spain

*Corresponding author: joao.pitacosta@quintelligence.com*

**Abstract.** Recent trends indicate a significant rise in hydrological extremes, challenging conventional management and forecasting methods. This study introduces an innovative approach leveraging machine learning and social media analytics, focusing on X (rebranded from Twitter), to improve the detection and management of hydrological events. By analysing geotagged tweets and incorporating news data, our machine-learning model identifies and categorises information related to hydrological extremes. This integration allows for enhanced real-time monitoring and sentiment analysis, providing insights into public perception and the effectiveness of response strategies. We employ Granger causality to establish predictive links between social media content and hydrological indicators, enabling preemptive measures and potentially reducing event impacts. Our comprehensive approach addresses the physical dimensions of extreme weather events and captures the public's emotional responses, offering a holistic view of disaster management. Significant findings from our research demonstrate the potential of combining machine learning with social media data to advance our understanding and management of water-related disasters. This strategy represents a significant step forward in environmental research and disaster response, harnessing the power of digital platforms and big data analytics. The study's outcomes suggest that this method can significantly contribute to hydrology and socio-hydrology, offering a novel perspective on integrating technology and social insights for better water management practices.

**Keywords:** Disaster Management, Hydrological Events, Machine Learning, Public Perception, Sentiment Analysis

## 1 Methodology.

Globally, there has been a noticeable increase in hydrometeorological extremes, necessitating innovative approaches to the analysis and management of these events [1]. Numerous researchers have underscored the need to leverage advancements in Artificial Intelligence (AI), and the vast amount of data available on the internet for this purpose. Online social media platforms, especially X (earlier named Twitter), have emerged as a valuable resource in this context. They offer real-time polling on specific topics, often labelled with geolocation, providing a particularly relevant and timely source of data. X's ongoing contribution to the research community has generated many research results, particularly in computing the sentiment of text-based posts, which this study aims to build upon in line with current research. These platforms not only facilitate the integration of hydrology and socio-hydrology but also provide a historical record of the public's perception of extreme events, their impacts, and consequences [2].

## 2 Results & Discussion.

While X data regarding urban water events such as water loss and leakage is often lacking, substantial data can be collected for larger-scale water events. This information can serve as an early warning to water resource providers monitoring these channels, enhancing their ability to respond effectively. However, this area of research presents several challenges, including managing large databases, handling complex data, and learning from this data using rapidly evolving machine learning algorithms including input from sentiment analysis (Fig 1).

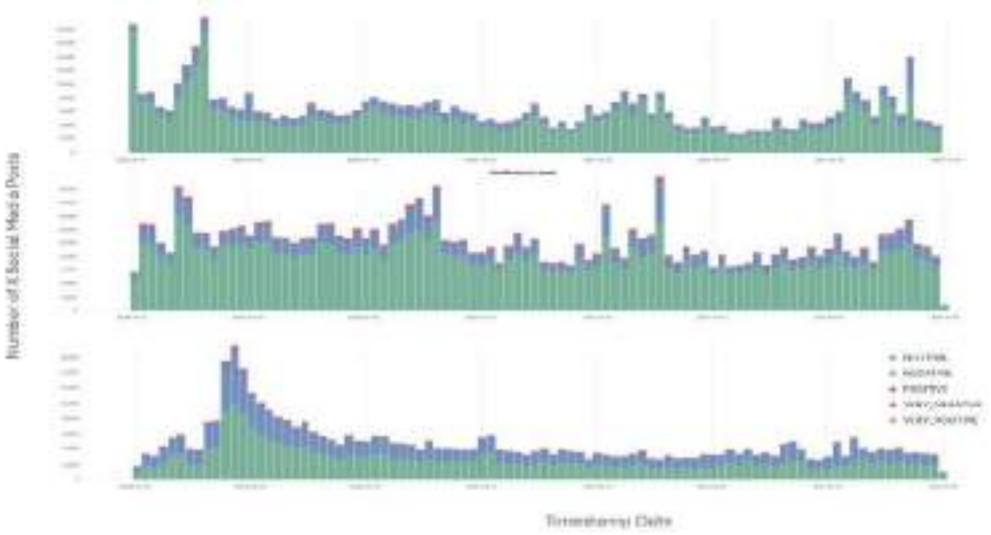

Figure 33 Sentiment of X social media posts on floods (above), storms (middle) and waterborne diseases (below), during 1.1.2020-20.9.2021, with noticeable different amount of neutrality.

Hence, the central research question we address in this paper is 3-fold and regards the following: (i) Can sentiment analysis provide us with a signal reflecting the impact and emergency of the extreme event; (ii) can we use knowledge extracted from news to inform the appropriate collection of social media data related to identified events and related concepts towards making the detection of extreme weather events more efficient; and (iii) can we access causality in relating the information collected in social media with weather parameters to improve the application of social media forecasting and analysis to this type of events.

## 3 Conclusion.

With the approach considered in this paper we were able to capture from the events depicted in the news, where we can rely on more context for better text mining efficiency, the main concepts to search on X social media posts in order to have a news-informed nowcasting of extreme weather events. Moreover, we show how sentiment analysis can help in identifying the different levels of intensity of such an event, also taking into consideration potential bias reflecting high levels. This is extended with the application of novel methods of emotion detection to news and social media posts showing synchrony between emotions present in both sources. Finally, we explore Granger causality and relevance of complementary data sources such as that of weather parameters.

## References.

[1] Pita Costa J., Rei L., Bezak N., Mikoš M., Massri M. B., Novalija I. and Leban G. (2024). Towards improved knowledge about water-related extremes based on news media information captured using artificial intelligence." International Journal of Disaster Risk Reduction 100: 104172.

[2] Mikoš, M., Bezak, N., Costa, J.P., Massri, M.B., Novalija, I., Jermol, M., Grobelnik, M. (2022) Natural-Hazard-Related Web Observatory as a Sustainable Development Tool. In: Progress in Landslide Research and Technology, 1(1).

**Theme:** Emerging concepts and solutions in modelling methods
**IAHR Thematic Priority Area:** [TPA-4] Digital Transformation
https://doi.org/10.3850/iahr-hic2483430201-280

# Sediment Discharge Prediction for the Xiaolangdi Reservoir Based on Machine Learning Algorithms

**Junchao Shi[1,2], Xinjie Li[2], Hailong Wang[1],Xiaofei Yan[2],Qiang Wang[2],Jie Liu[3]**

[1] Zhongyuan University of Technology, Zhengzhou 45007, China
[2] Yellow River Institute of Hydraulic Research, YRCC,Zhengzhou,45003, China
[3] Huanghe Science and Technology University, Zhengzhou,450063,China

*Corresponding author: Li.xin_wd@163.com*

**Abstract.** In response to the limited capability of one-dimensional flow and sediment models to represent complex hydrological conditions, this research incorporates two machine learning algorithms, namely K-Nearest Neighbors (KNN) and Gradient Boosting Regression (GBR), to predict sediment discharge in reservoirs. The simulation utilizes flow and sediment data from the Xiaolangdi Reservoir spanning the years 2000 to 2019. The simulation results indicate that among the various machine learning algorithms employed for constructing sediment discharge prediction models, the Gradient Boosting Regression (GBR) exhibits the best performance. The experimental findings demonstrate that the algorithmic simulation results can serve as references for sediment discharge prediction in reservoirs and subsequent scheduling strategies.

**Keywords:** machine learning algorithm; reservoir sediment discharge; prediction model

## 1 Introduction and method

In recent years, many outstanding researchers and professionals have made remarkable progress in water flow and sediment transport studies through unremitting exploration and innovation, and they have successfully improved water flow and sediment transport prediction models and enhanced the prediction accuracy. For example, Li et al.[4] established a random forest-support vector machine (RF-SVM) model to predict runoff of the Longjiang Reservoir. The experimental results show that the overall accuracy of the model is high enough to meet the requirements, but there is still room for improvement regarding local extreme flow prediction. Liu et al.[5] applies the long short-term memory (LSTM) neural network to the prediction of monthly precipitation, and the authors experimentally proved that the prediction accuracy of the LSTM model is higher than that of other models, which is more accurate than other models. The prediction accuracy of the LSTM model is higher than other models. Similarly, Tong[6] adopted the LSTM algorithm to improve the accuracy of river flow and sediment transport prediction by utilizing the temporal nature of hydrological data. In the aforementioned study, several researchers employed various algorithms to predict water-sediment dynamics, aiming to identify an optimal model combination with minimal errors and the capability to provide relatively accurate forecasted data. The Xiaolangdi Reservoir was examined in this research, in which two types of predication models, namely k-nearest neighbors regression (KNN) and gradient boosting regression (GBR), were used. Their prediction results were compared to determine the optimal model for sediment discharge prediction.

## 2 Model performances and comparisons

Machine learning algorithms were introduced to establish KNN and BGR prediction models. After that, selected data was input to obtain the reservoir sediment discharge predicted by different models. The correlation analysis graph for predicted and actual values using GBR and KNN algorithms is shown in Figure 1.

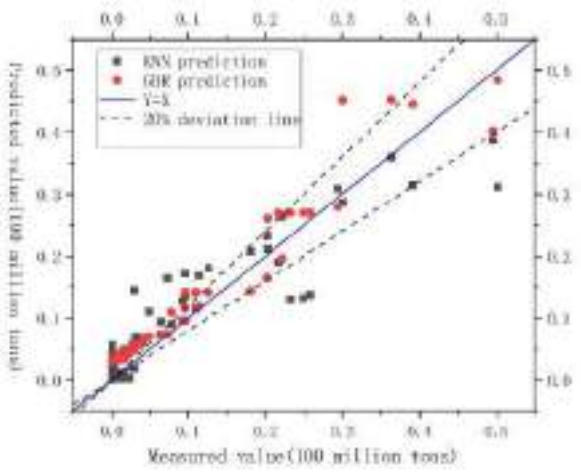


Figure 34 Correlation analysis between predicted and true values

## 3 Conclusions

In this research, a GBR-based model was used to predict the reservoir sediment discharge under the influence of multiple factors. Relevant datasets were created by data preprocessing, such as removing null values and outliers. A reservoir sediment discharge prediction model was then established by carefully selecting features according to the processed data. The results suggest that the model is reasonably accurate and precise in predicting the reservoir sediment discharge. However, it is worth noting that few model-predicted values differ considerably from the true values. The problem may be caused by special circumstances or unusual events, and this has to be addressed and solved in future practical applications. Overall, most model-predicted values are close to the true values, confirming the robustness and reliability of machine learning in reservoir sediment discharge prediction. These findings provide useful references for further application and optimization of the algorithm.

## Reference

[1] Longfei Sun,Xiujie Guo,Ting Wang, et al. Study on the estimation of sediment composition in the released sediment during the water diversion and sediment release period of the Xiaolangdi Reservoir ［J］. Yellow River of China, 2022, 44(8): 47-51.

[2] Li Wu,Zuheng Wang,Liang Wang, et al. Water Quality Monitoring and Evaluation of Xiaolangdi Reservoir in the Yellow River Based on Principal Component Analysis and Fuzzy Mathematics[J]. Bulletin of Soil and Water Conservation, 2020, 40(05): 118-124.

[3] Zhixiang You,Xiaoyang Hu. A Brief Discussion on the Safety Production Supervision of Xiaolangdi Water Conservancy Hub[J]. Yellow River of China, 2023, 45(S2): 118-119.

[4] Lingjie Li, Yintang Wang, Hu Qingfang, et al. Long-Term Reservoir Runoff Forecast Based on Random Forest and Support Vector Machine[J]. Journal of Water Resources and Water Transport Engineering, 2020, (4): 33-40.

[5] Xin Liu,Ning Zhao,Jinyun Guo, et al. Monthly Precipitation Forecast on the Qinghai-Tibet Plateau Based on LSTM Neural Network[J]. Journal of Geo-Information Science, 2020, 22(8): 1617-1629.

[6] Taowen Tong. Research on River Runoff and Sediment Concentration Prediction Method Based on LSTM Deep Learning [J]. Journal of Irrigation and Drainage, 2021,40(S1):1-4.

[7] Wenxing Li,Tiancheng Wang,Huawei Li. Method of Automatic Test Vector Generation for Digital Circuits Based on K-Nearest Neighbor[J]. Journal of Computer-Aided Design & Computer Graphics, 2023, 35(11): 1802-1810.

[8] Karthikeya H K, Sudarshan K, Shetty D S. Prediction of agricultural crops using KNN algorithm[J]. Int. J. Innov. Sci. Res. Technol, 2020, 5(5): 1422-1424.

[9] Xiaofei Yan,Xiujie Guo,Longfei Sun. Research on Sand Discharge Prediction of Wanjiazhai Reservoir Based on Machine Learning Algorithms[J]. Water Resources and Power, 2023, 41(03): 79-82.

**Theme:** Emerging concepts and solutions in modelling methods
**IAHR Thematic Priority Area:** [TPA-4] Digital Transformation
https://doi.org/10.3850/iahr-hic2483430201-282

# Near Real Time Flood Detection Technique using SAR Data and Deep Learning Methods

**Gopi P[1], Manjula R[1], Chandrasekar K[2]**

National Institute of Technology near BHEL, Trichy - 620015, India
[2] National Remote Sensing Centre, Balanagar, Hyderabad and 500037, India

*Corresponding author: gopisri25588@gmail.com*

**Abstract.** Due to the unpredictable nature of flood occurrences, prompt and accurate flood detection was critical for disaster management. Recent advancements in deep learning offered immense potential for flood detection, yet the scarcity of high-quality flood datasets posed a challenge. The Godavari River Basin was selected for flood modeling due to its diverse communities often affected by floods, making it essential to study the socio-economic impacts and develop strategies to protect these populations. The 2019 flood incident in the Godavari River Basin was categorized into training, testing, and application sets. Assessment of various convolutional neural network models using these datasets had demonstrated significantly higher efficiency. The study was examined the impact of VH polarization, VV polarization, and auxiliary DEM involvement on flood detection. VH polarization emerged as more favorable for flood detection, while the addition of DEM showed limited influence within the Godavari River Basin. Leveraging the strongly labeled datasets, a convolutional neural network was applied to real-time flood detection for the 2019 flood event. The results from these experiments aligned with earlier findings from the robust datasets, affirming the efficacy of the approach. The higher accuracy of F1 Score 0.91 and 0.92 were achieved particularly on 06th August 2019 and 18th August 2019 post flood events respectively.

**Keywords:** Flood Detection, Synthetic Aperture Radar, Digital Elevation Model, Vertical Transmitter and Horizontal Receiver, Vertical Transmitter and Vertical Receiver, Convolutional Neural Network.

## 1 Structure

Please use only the styles of this template (Title, Authors, Affiliations, Corresponding author, Main for your text, Headings 1–3). Bulleted lists may be included and should look like this:

- First point
- Secondo point
- And so on

### 1.1 Figures

All figures should be numbered with Arabic numerals (1, 2, 3,….). Every figure should have a caption. All photographs, schemas, graphs and diagrams are to be referred to as figures. Line drawings should be good quality scans or true electronic output. Low-quality scans are not acceptable. Figures must be embedded into the text and not supplied separately. Lettering and symbols should be clearly defined either in the caption or in a legend provided as part of the figure.

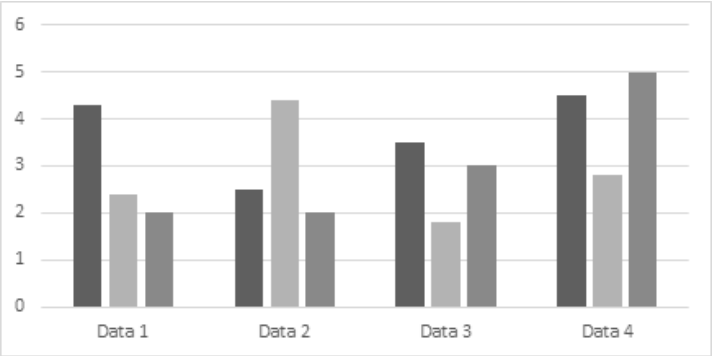


Figure 35 Figure caption [Times New Roman, 11pt, centred]

### 1.1.1 Tables

All tables should be numbered with Arabic numerals. Every table should have a caption. Headings should be placed above tables, centred. Only horizontal lines should be used within a table, to distinguish the column headings from the body of the table, and immediately above and below the table. Tables must be embedded into the text and not supplied separately. Below is an example which the authors may find useful.

Table 7 Table caption [Times New Roman, 11pt, centred]

| Text | Text | Text |
|---|---|---|
| Text 1 | 5 | 5 |
| Text 2 | 6 | 2 |
| Text 3 | 2 | 1 |

## 2 References

References must be listed at the end of the paper. Authors should ensure that every reference in the text appears in the list of references and vice versa. Indicate references by [1] or [2,3] in the text.
Some examples of how your references should be listed are given at the end of this template in the ‘References’ section, which will allow you to assemble your reference list according to the correct format and font size.

### 2.1 Equations

Equations and formulae should be typed in Mathtype, and numbered consecutively with Arabic numerals in parentheses on the right hand side of the page (if referred to explicitly in the text). They should also be separated from the surrounding text by one space.

$$\rho = \frac{\vec{E}}{J_C\left(T = \text{const.}\right) \cdot \left( P \cdot \left( \frac{\vec{E}}{E_C} \right)^m + \left(1 - P\right) \right)} \tag{1}$$

## Reference

[1] J. Van der Geer, J.A.J. Hanraads, R.A. Lupton, The art of writing a scientific article, J. Sci. Commun. 163 (2000) 51–59.
[2] W. Strunk Jr., E.B. White, The Elements of Style, third ed., Macmillan, New York, 1979.
[3] G.R. Mettam, L.B. Adams, How to prepare an electronic version of your article, in: B.S. Jones, R.Z. Smith (Eds.), Introduction to the Electronic Age, E-Publishing Inc., New York, 1999, pp. 281–304.

**Theme:** Emerging concepts and solutions in modelling methods
**IAHR Thematic Priority Area:** [TPA-4] Digital Transformation
https://doi.org/10.3850/iahr-hic2483430201-284

# Computer Vision-Based Method for Rainfall Estimation Using CCTV Cameras and Smartphone Videos

**Manuel Fiallos-Salguero[1], Soon-Thiam Khu[1], Jingyu Guan[2], Tianzhi Wang[1], Mingna Wang[2,*]**

[1] School of Environmental Science & Engineering, Tianjin University, Tianjin, 300350, China
[2] School of Civil Engineering, Tianjin University, Tianjin, 300072, China

*Corresponding author: mingna.wang@tju.edu.cn*

**Abstract.** Rainfall has been considered a crucial resource for effective management and control in various fields (e.g., flood control); however, the rainfall data recorded by traditional monitoring methods shows deficient accuracy and reflects low spatiotemporal resolution. Based on that, suitable rainfall measurement methods need to be developed to enhance the extreme rainfall track and reduce the vulnerability of considerable damage that might occur in urban areas. This study develops a new approach based on computer vision algorithms and enhanced geometrical optics analyses to improve rain streak detection and rainfall estimation from videos with complex backgrounds. Thus, the proposed approach revealed a satisfactory reduction in the error rate for the rainfall estimation with the enhancement of data collection, extraction, and measuring, showing promising results for rainfall monitoring applied to complex-real rain event scenarios at different times.

**Keywords:** Computer vision algorithms, Image and video processing, Rainfall estimation, Rainfall monitoring, Spatial-temporal resolution.

## 1 Introduction

The estimation and measurement of rainfall are required for many scientific, social, and commercial activities; however, difficulties in rainfall measurement could lead to a worsening fraction of rainfall generated by direct runoff and hydrological response [1]. Therefore, adequate techniques for measuring rainfall have received considerable attention from different investigations, analyzing the applicability of new approaches in order to improve the existing rainfall measurement.

Various studies have described crowdsourcing as a promising approach to addressing the data collection from many involved public resources (e.g., smartphones and closed-circuit television (CCTV) cameras) as data contributors [2], becoming a potential tool as a complementary source of information in situations with limited data, providing valuable and continued observations [3]. However, this system has still shown various uncertainties (e.g., lighting and camera settings) in the image processing and measurement results. This study focuses on developing a computational model to estimate the rainfall intensity in videos taped by surveillance cameras and smartphones, which lie on complex and hybridized algorithms to analyze the background of digital sources and decompose the images based on their main features (i.e., brightness and contrast).

## 2 Material and methods

This study is based on two main stages: (1) the pre-processing stage and (2) the processing stage. In order to establish correct patterns for further analysis, various short videos were randomly selected to define the most suitable region of interest (*ROI*) and calculate the image quality signature (*IQS*) values from each frame. Moreover, to reduce the time processing of our proposed model, a CNN model was trained to classify the video frames and extract the main features of the image. Then, the data analysis is carried out by extracting and classifying frames of the video input to select the most suitable scenario for its *IQS* data comparison, applying the precise filters for the rain layer detection and *ROI*

election. Afterward, the rainfall intensity estimation was conducted, extracting the rain streaks and calculating their size and terminal speed using the geometrical optics algorithms. In addition, to verify the magnification and blur effects in the rain layer, a control point was designed to filter the raindrop sizes, solely analyzing the raindrops' diameters ($D$) in a specific interval (0.5 mm $\leq D \leq$ 6 mm). Finally, the raindrop size distribution and rainfall intensity were estimated based on rainfall intervals and analyses conducted.

## 3 Results and discussion

Our proposed model has shown good performance in analyzing different rain events with complex backgrounds, improving raindrop detection and easy adaption to the plane conditions in frames of various video resolutions. Comparing the rainy events captured by devices, this study registered a mean absolute percentage error (MAPE) ranging between 3.9 % to 12.7 % for videos captured using ordinary cameras and 6.7 % to 11.2 % in videos filmed by smartphones (Table 1). Therefore, our results have shown a slight error level evaluated using the MAPE, and by comparing these findings with the other studies, our proposed model reached a lower error rate than those obtained by their approaches [1, 4-6].

Table 1 Evaluation of the model's performance under different scenarios and rain events.

| Rain event | Video ID | Duration | Cumulative rainfall recorded (mm) | | MAPE | MAE | RMSE |
|---|---|---|---|---|---|---|---|
| | | | Model + Video | Rain gauge | | | |
| August 4 | BC_1 | 46 min | 15.18 | 14.8 | 7.5 | 0.22 | 0.28 |
| | SC_1 | | 14.95 | | 12.7 | 0.36 | 0.50 |
| August 12 | BC_2 | 175 min | 29.58 | 30.4 | 4.6 | 0.38 | 0.47 |
| | SC_2 | | 29.5 | | 3.9 | 0.54 | 0.65 |
| September 9 | SP_1 | 4 min | 0.22 | 0.2 | 11.2 | 0.02 | 0.02 |
| | SP_2 | 2 min | 0.2 | | 6.7 | 0.01 | 0.02 |

Note: BC and SC are the low- and high quality camera, respectively. SP is the smartphone.

## 4 Conclusions

In this study, we developed a hybrid model to increase rainfall detection in digital sources from various devices to measure the rainfall intensity based on computer vision algorithms. The approach conducts a subtraction-based method to identify the rain streak layer using the main features of rain images. Based on that, the rain streaks were extracted using geometric optical analysis, increasing the data quality and accuracy retrieved from the images analyzed and enhancing the rainfall rate and depth estimation for a single frame that induces a continued analysis for further studies.

## Reference

[1] X. Wang, M. Wang, A novel quality control model of rainfall estimation with videos–A survey based on multi-surveillance cameras, J. Hydrol., 605, (2022), 127312.

[2] A.B. Chen, J.L. Goodall, Flood resilience through crowdsourced rainfall data collection: Growing engagement faces non-uniform spatial adoption, Water Resour. Res., 609, (2022), 127724.

[3] F. Zheng, R. Tao, Crowdsourcing methods for data collection in geophysics: State of the art, issues, and future directions, Rev. Geophys., 56, (2018), 698-740.

[4] S. Jiang, V. Babovic, Advancing opportunistic sensing in hydrology: A novel approach to measuring rainfall with ordinary surveillance cameras, Water Resour. Res., 55, (2019), 3004-27.

[5] F. Zheng, H. Yin, Toward Improved Real‐Time Rainfall Intensity Estimation Using Video Surveillance Cameras, Water Resour. Res., 59, (2023), e2023WR034831.
[6] H. Yin, F. Zheng, Estimating rainfall intensity using an image-based deep learning model, Engineering, 21, (2023), 162-74.

**Theme:** Emerging concepts and solutions in modelling methods
**IAHR Thematic Priority Area:** [TPA-4] Digital Transformation
https://doi.org/10.3850/iahr-hic2483430201-287

# Flow Data and Water Level Prediction Using Ann

**Shivaanand V[1], Priyanga S A[1], Dr. Manjula R[1]**

[1] National Institute of Technology Tiruchirappalli, Tanjore Main Road, National Highway 67, Tiruchirappalli - 620015, India

*Corresponding author: 103122093@nitt.edu*

**Abstract.** ANN is a versatile tool which can be used in many applications. This study uses ANN for prediction of water level and flow data for Musiri by taking daily data from 1 Jan 2006 till 31 Dec 2011. Comparative study is performed by taking daily data from 4 other stations and predicted the flow data and water level at Musiri. Flow data prediction for Musiri using 4 other stations gives  = 0.917, while water level prediction for Musiri using 3 other stations gives  = 0.9562. This paper provides a study for using distant stations for prediction during the unavailability of data for the required station.

**Keywords:** ANN, Flow data prediction, Water level prediction.

## 1 Introduction

Flow and water level data is an important factor as it is used for many applications, such as flood simulations and other modelling purposes. But in many cases flow data is not available in many stations and in some cases, there are lots of missing data, due to which this information cannot be used for accurate simulations. For non-perennial rivers as the flow is highly variable, if there is missing or unavailability of data, it leads to wrong simulated data.
Application of ANN is demonstrated in this paper which shows great accuracy in prediction of data, with relatively low computation.

## 2 Methodology

### 2.1 ANN for forecasting

ANN used in this study is a Backpropagation network with one hidden layer linked to immediately previous layers. The input for flow are using 4 other stations from the middle Cauvery Sub-basin, Urachikotti Station U, Thevur Station T, Elunuthimangalam Station E, Kodumudi Station K and output flow stations is, Musiri station M.The input for Water level prediction are using 3 stations E, K, U and the output is M. Similar input and output parameters are taken for predicting M in both cases. Data from 2006 to 2011 was used in the input to train and for verification of the trained forecaster.

Table 1 Input and Output data parameters

| Input station data for time t | Training set for prediction of M | Validation set for prediction of M | Output for station for time | Model |
|---|---|---|---|---|
| K<br>U<br>E<br>T | 70% of each month from 2006 to 2011, i.e., 21 days of each month taken for training | 30% of each month from 2006 to 2011, i.e., 7 days of each month taken for training | M | MUKET |

1-day prediction is taken as  and the actual data is at time . MUKET model (4 stations) for flow prediction and MUKE model (3 stations) for water level prediction.

## 3 Results and Discussion

### 3.1 Flow data prediction

MUKET model was used, which produced M, with  and a Mean absolute error (MAE) of 36.485. (Figure 1)

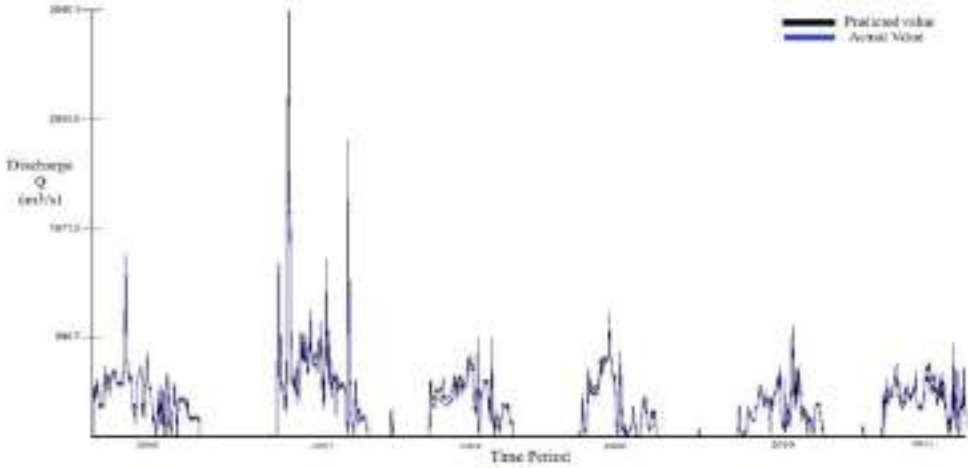


Figure 1 Validation set for 1 – day prediction of flow data using all 4 stations

### 3.2 Water level data prediction

MUKE model was used, which produced M, with  and MAE of 0.052. (Figure 2)

Figure 2 Validation set for 1 - day prediction of water level data using all 3 stations

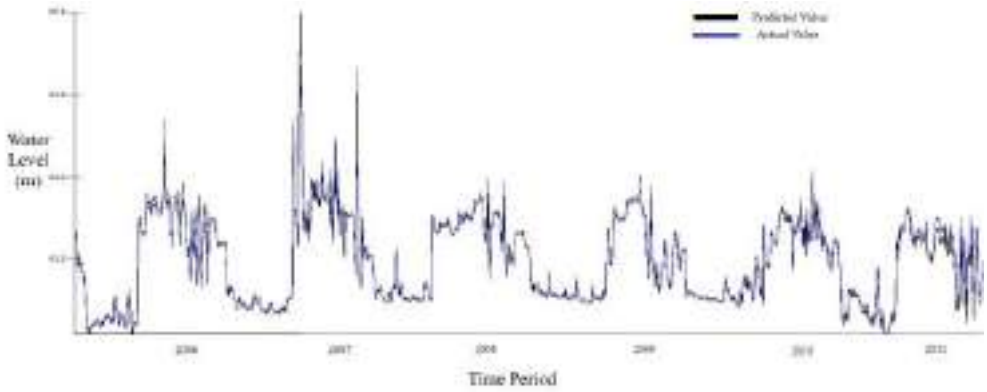


## 4 Conclusion

As flow data is highly variable compared to the water level data, M predicted by MUKET model with values range from 0.8 to 0.92 and is good as river Cauvery is a non-perennial river. Water level predicted by MUKE model for M is more accurate than flow data prediction, with  values ranging from 0.93 to 0.97, which are excellent results since we have given the inputs of only water level data from other stations. Thus, flow and water level can also be predicted for non-perennial rivers with fairly accurate results.

## Reference

[1] Liong SY, Lim WH, Paudyal GN (2000), River stage forecasting in Bangladesh: Neural network approach. J Comput Civil Eng ASCE 14(1):1-8

[2] Islam MN, Liong SY, Phoon KK, Liaw CY, Forecasting of river flow data with a general regression neural network, 272:285-290.

[3] Kim D E, Gourbesville P, Liong SY (2019), Overcoming data scarcity in flood assessment using remote sensing and artificial neural network. Smart Water 4(1): 1-15

**Theme:** Emerging concepts and solutions in modelling methods
**IAHR Thematic Priority Area:** [TPA-4] Digital Transformation
https://doi.org/10.3850/iahr-hic2483430201-289

# Study Of Flood Forecasting Based on Recurrent Neural Network for Urban River in The Piedmont Plain

**Wang Fan[1], Chen Chang[2]**

[1] China Institute of Water Resources and Hydropower Research, Beijing 100038, China
[2] Research Center on Flood & Drought Disaster Reduction of the Ministry of Water Resources, Beijing 100038, China

*Corresponding author: Chen Chang 2234104368@qq.com*

**Abstract.** The flood in the piedmont plain city exhibits characteristics of both mountain and urban floods, posing challenges for hydrological simulation and flood forecasting. This study utilizes two different modelling approaches to make flood forecasting and evaluate the performance of models in Xiaoqing River and Futuan River basins in China. The findings demonstrate that: 1) the integrated model, based on BiGRU, exhibits flexible capabilities in predicting discharge and water level processes. It is suitable for forecasting both single flood events and providing continuous predictions for long series of processes, while maintaining a high level of prediction accuracy within a specific forecast step. 2) the hybrid model, combining the LSTM and the two-dimensional hydrodynamic model, demonstrates remarkable accuracy in predicting the water level process of the target section. In this model, the LSTM is employed to simulate flood processes in hilly areas and provide boundary conditions for the two-dimensional hydrodynamic model. Through comprehensive case assessment and analysis, we contend that both modeling methods can be effectively utilized as innovative approaches for predicting river floods in piedmont plain cities.

**Keywords:** Flood forecasting; Neural networks; Piedmont plain cities; Urban rivers

## 1 Introduction

The issue of urban flooding has become increasingly prominent in the context of climate change and rapid urbanization expansion. The runoff and confluence processes in urban areas are more intricate and challenging to predict compared to those in natural river basins. In recent years, the recurrent neural (RNN) network has garnered significant attention due to its exceptional performance in flood prediction[1-3]. In this study, we conduct some further application and exploration of RNN-based models in flood prediction in urban rivers in piedmont plains.

## 2 Study basins

Both of the two study basins are situated within Shandong Province, China, as shown in Figure 36. Specifically, the Huangtaiqiao Hydrology station of Xiaoqing River is located in Jinan City, encompassing a control basin area of 321 $km^2$. Additionally, the Futuan River is situated in Rizhao City with a basin area spanning 1,063 $km^2$.

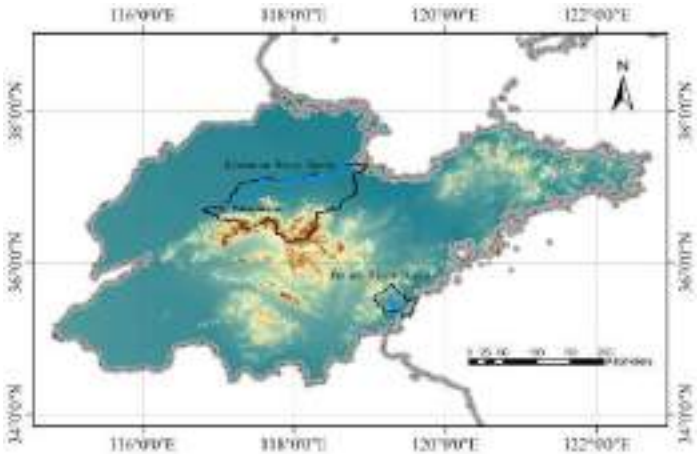

Figure 36 Location of study basins

## 3 Approaches

In the Xiaoqing River Basin, we attempt to develop a flood forecasting model based on Bidirectional Gate Recurrent Unit (BiGRU) network, specifically for predicting the discharge and water level process at Huangtaiqiao hydrological station. In the Futuan River basin, different technical approaches are employed. For the hilly area upstream, a Long Short-Term Memory (LSTM) network is utilized to construct a discharge prediction model, and the predicted process serves as the boundary condition for the two-dimensional hydrodynamic model, which is employed to forecast water levels in the urban area of piedmont plain.

## 4 Results and Conclusion

The prediction results, see Figure 37, demonstrate that the RNN-based models can accurately forecast flood processes, encompassing the dynamics of floods, as well as crucial information such as the peak discharge and occurrence time, irrespective of whether it pertains to hilly areas or regions comprising urban plains. Moreover, the data-driven model enables flexible outputting of flow and water level processes, which makes it highly suitable for flood forecasting of urban river.

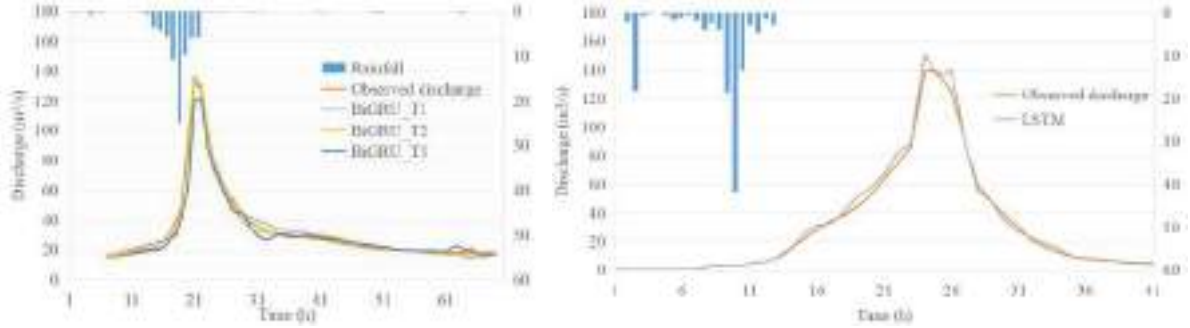


Figure 37 Illustration of flood forecasting results

## Reference

[1] Gude V, Corns S, Long S Z N. Flood Prediction and Uncertainty Estimation Using Deep Learning[J]. Water, 2020, 12(3).

[2] Ahmed A A M, Deo R C, Feng Q, et al. Deep learning hybrid model with Boruta-Random forest optimiser algorithm for streamflow forecasting with climate mode indices, rainfall, and periodicity[J]. Journal of Hydrology, 2021, 599.

[3] Liu Y, Wang H, Feng W W, et al. Short Term Real-Time Rolling Forecast of Urban River Water Levels Based on LSTM: A Case Study in Fuzhou City, China[J]. International Journal of Environmental Research and Public Health, 2021, 18(17).

**Theme:** Emerging concepts and solutions in modelling methods
**IAHR Thematic Priority Area:** [TPA-4] Digital Transformation
https://doi.org/10.3850/iahr-hic2483430201-291

# Flood Emergency Remote Sensing Monitoring by Drone Swarm based on Deep Reinforcement Learning

**Yu Zhe[1], Lu Wenjing[2]**

[1] Tsinghua University, 30 Shuangqing Road, Haidian District, Beijing, 100084, China
[2] China Institute of Water Resources and Hydropower Research, A-1 Fuxing Road, Haidian District, Beijing, 100038,China

*Yu Zhe: yz20@tsinghua.org.cn*

*Lu Wenjing: luwj@iwhr.com*

**Abstract.** In recent years,drone remote sensing technology has been widely employed in flood prevention and mitigation. The critical point of flood emergency monitoring lies in obtaining timely the leakage warning information of dams. Flood emergency monitoring is often confronted with a multitude of challenges, encompassing severe climatic conditions, intricate terrain, restricted monitoring timeframes, and stringent data accuracy requisites. Current mainstream drone remote sensing monitoring methodologies, characterized by their reliance on predetermined flight trajectories, encounter a plethora of challenges, including incomplete dam image shooting, insufficient image resolution, delayed emergency response, and lengthy data acquisition times. To address these challenges, we propose an drone swarm remote sensing monitoring method based on deep reinforcement learning. Drone swarm can autonomously adjust the drones' shooting positions in order to improve the integrity and resolution of dam images, while reducing the shooting time in challenging climatic conditions and complex environments. The versatility, low cost, and high robustness of drone swarms offer significant advantages in addressing time-sensitive flood emergency monitoring, and represent a key area for future development.

**Keywords:** deep reinforcement learning, drone swarm, flood emergency monitoring

## 1 Introduction

With the development of artificial intelligence technology, low-cost, highly efficient, and strongly autonomous drones have played an important role in the field of flood emergency monitoring as a new type of remote sensing platform[1]-[3]. However, challenges concerning the clarity of dike leakage details and the timely capture of images still persist. The primary objective of flood emergency monitoring is to promptly gather critical information regarding dike leakage warnings.
In this paper, we propose an intelligent remote sensing monitoring method for drone swarms based on deep reinforcement learning. Our main contributions are threefold:

- Developed a drone swarm comprising cooperative multi-level UAVs (high and low altitude). The high-altitude drones provide a global view for task allocation and enable adaptive aerial photography by low-altitude drones.
- Built an autonomous cooperative decision model using deep neural networks, which leverages environmental prediction information and flight path inference to enhance the state input of the policy model[4],[5].
- Established a reward function based on the distinctiveness of jointly captured images, encouraging agents to explore aerial photography paths that generate images markedly different from previous ones, thereby enhancing image clarity and completeness.

Our method enhances the learning efficiency of agents through enhanced state input and utilizes a non-repetitive exploration reward mechanism[6], reducing the difficulty of setting reward values and improving the feasibility of autonomous aerial photography by drone swarm.

## 2 Material and Methods

Emergency monitoring of flood disasters can provide intelligence information for pre-disaster prediction and post-disaster rescue. In particular, real-time information such as river water level and dam leakage before the flood can greatly improve the timeliness and effectiveness of flood response. Currently, methods such as image processing, Internet of Things (IoT), and machine learning are mainly used for flood prediction[7],[8]. The main multi-agent machine learning methods used in drone swarms include genetic algorithms, ant colony algorithms, and deep reinforcement learning. Deep reinforcement learning methods have a notable advantage in handling dynamic environments. The key to deep reinforcement learning methods lies in reward design.

We incorporate the method of dynamic reward scaling proposed by Li et al.[6] and designs a reward mechanism based on the familiarity of jointly-taken images. This approach motivates drone agents to focus on increasing the disparity between images captured before and after acquisition. Furthermore, to mitigate potential strategy biases that could arise during the exploration process and affect both exploration efficiency and flight safety, our method incorporates historically successful strategies as augmented state inputs[5].

## 3 Conclusions

Remote sensing monitoring has found extensive applications in real-world environments, with drones playing a crucial role in augmenting the timeliness and quality of such monitoring activities. Nevertheless, in real-world environments, adverse weather conditions and uncertainties are inevitable prior to the occurrence of a flood. Deep reinforcement learning methods have shown promising capabilities in tackling challenges posed by dynamic environmental conditions. This article highlights that the use of drone swarms based on deep reinforcement learning for emergency flood remote sensing monitoring holds significant potential and represents a crucial direction for future technological advancements.

## Reference

[1] Sun Yayong, Huang Shifeng, Ma Jianwei, et al.Research on application of UAV network remote sensing observation technology in flood disaster emergency monitoring[J]. China Flood & Drought Management, 2022, 32 (1) : 90-95.

[2] Kucharczyk M, Hugenholtz C H. Remote sensing of natural hazardrelated disasters with small drones: Global trends, biases, and research opportunities[J].Remote Sensing of Environment, 2021, 264: 112577.

[3] Huang Shifeng, Ma Jianwei, et al. Situation and prospect of flood disaster monitoring by remote sensing in China. Water Resources in China (2021).

[4] Schaul, Tom, et al. Universal value function approximators. International conference on machine learning(ICML). PMLR, 2015.

[5] Yu Zhe, Sun Kailai, et al. A Goal-Conditioned Reinforcement Learning Algorithm with Environment Modeling. 2023 42nd Chinese Control Conference (CCC) (2023): 8763-8768.

[6] Li Chenghao, et al. Never Explore Repeatedly in Multi-Agent Reinforcement Learning. ArXiv abs/2308.09909 (2023): n. pag.

[7] Munawar, Hafiz Suliman , A. W. A. Hammad , and S. T. Waller. A review on flood management technologies related to image processing and machine learning. Automation in Construction 132.8(2021):103916.

[8] Arshad B, Ogie R, Barthelemy J, Pradhan B, Verstaevel N, Perez P. Computer Vision and IoT-Based Sensors in Flood Monitoring and Mapping: A Systematic Review. Sensors. 2019; 19(22):5012.

**Theme:** Emerging concepts and solutions in modelling methods
**IAHR Thematic Priority Area:** [TPA-4] Digital Transformation
https://doi.org/10.3850/iahr-hic2483430201-293

# Application of Bayesian Optimisation to Water Quality Monitoring in Urban Drainage Systems

**Mariacrocetta Sambito[1], Gabriele Freni[1,*], Stefania Piazza[1]**

[1] Università degli Studi di Enna "Kore" – Facoltà di Ingegneria ed Architettura, Via delle Olimpiadi 2, 94100 Enna

*Corresponding author: gabriele.freni@unikore.it*

**Abstract.** In the water sector, the problem of polluting source identification was mainly investigated regarding pressurized distribution networks respect to sewers even if the Water Framework Directive 2000/60/EC and equivalent laws in many countries introduce the principle that the polluter pays so asking the water manager to detect the most pollutant discharges in sewers. In previous studies, a probabilistic approach to positioning water quality sensors in urban drainage networks shows the progressive increase in identification probability obtained through the Bayesian approach. Following the past literature, the present work aims to improve it, inserting new information beyond network topology, i.e. a piece of grey information from commercial/industrial activities inventory. The methodology is applied on the real test-case represented by the sub-catchment of sewer system Palermo (Italy).

**Keywords:** modelling, pollution detection, sensors, urban drainage

## 1 Introduction

The problem of water quality has always aroused considerable interest within the scientific community, as it is closely connected with the risks associated with public health ( [1] - [2] - [3]) and environmental problems [4]. For this reason, many researchers have applied different methodologies to monitor the water quality parameters (chemicals and biologicals) of water distribution networks (WDN) and urban drainage systems (UDS) ( [5] - [6] - [7]). The latter can be a valuable tool to check the input values to the sewage treatment plants to monitor the processes' removal efficiency.

IoT has evolved so much that its definition has changed compared to the original one. For IoT we mean all the technologies develop on the "things". This technology aims to improve the classical use of things providing internet connection. In fact, with this technology, we can enhance the potential of any object, instrument or sensor connected to a telecommunications network. Therefore, this approach aims to simplify every object, from the simple ordinary life tool to the most complex sensor. This approach has been demonstrated to help the company reach the concept of Industry 4.0, an industry specialising in digital systems that can be easily controlled via computers, tablets, and smartphones.

Such new monitoring possibilities require optimization algorithms to get the highest potential from combining novel technology and water engineering knowledge.

The present study will investigate integrating such engineering optimisation methods in urban drainage monitoring. Considering the complexity of the solution space (mainly consistent with all the possible sensor combinations for a provided urban drainage system) and the high computational costs of modelling instances, using usual Bayesian methods may need exceptional resources to search for the optimum preserving information on solution reliability. On the other side, using standard optimisation techniques may provide efficient solutions with reasonable computational costs but loose details on the solution's reliability, preventing any possibility of upgrading the solution every time new information is provided.

## 2 Application

Using the Bayesian approach, new information, coming from the analysis, is incorporated in the approach allowing the operator to gain insight on the system once new contamination events are detected and identified. In this way, the approach is suitable for solving problems in which data are initially piecemeal and the operator plans to improve the monitoring strategy. For the solution of this problem, two main components are required: a calibrated model for hydraulic and water quality simulations in sewer systems and a Bayesian Artificial Intelligence (AI) solver for likelihood estimation and probability update. The EPA SWMM model was used to perform the hydraulic and water quality simulations in this case.

The sensor location problem for identifying the illicit intrusion for the case study has already been investigated in [8] but using genetic algorithms. In particular, different single- and multi-objective optimization procedures have been compared to locate sensors in the sewer optimally. In [7] without pre-conditioning, initially, all nodes had equal probability to be the candidate nodes for sensor placement and all nodes had equal probability to be an illicit contamination source. Therefore, the contamination events are randomly simulated to evaluate each sensor's probability to identify the contamination source.

## 3 Results and conclusions

Applying the BN approach allowed to identify 16 network nodes that may be used to locate salinity sensors. The number of selected nodes is less than 1% of the total number of nodes (manholes) of the network. Eight sensors are located in the red zone of the network (where urban drainage is under groundwater level), six are in the capillary fringe, and two are located in the other parts of the network (correspondent to more than 80% of the network). The proposed approach effectively integrates experimental campaigns, mathematical modelling and AI to solve an urban drainage management problem: seawater infiltration in sewers. The model and AI were combined to analyse the system and propose possible locations of a limited number of sensors (based on external constraints). The main objective of the AI applications was the maximization of overall probability to locate contaminant sources (seawater infiltration points). After the deployment of the monitoring network, the AI system and the model were again used to predict the most probable location of sources and to guide an experimental campaign to validate the prediction. The application to Mondello network successfully identified two source areas containing two infiltration locations.

## Reference

[1] M. Sambito and G. Freni, “Optimal positioning of water quality sensors in sewer during dry and wet weather,” in AIP Conference Proceedings, 2020.
[2] S. Piazza, M. Sambito and G. Freni, “Experimental evidence of diffusion and dispersion impact on optimal positioning of water quality sensors in distribution networks,” in AIP Conference Proceedings, 2021.
[3] M. Sambito and G. Freni, “Strategies for improving optimal positioning of quality sensors in urban drainage systems for non-conservative contaminants,” Water (Switzerland), vol. 13, no. 7, 2021.
[4] M. Sambito, A. Severino , G. Freni and L. Neduzha, “A systematic review of the hydrological, environmental and durability performance of permeable pavement systems,” Sustainability (Switzerland), vol. 13, no. 8, 2021.
[5] N. Oliker and A. Ostfeld, “Inclusion of Mobile Sensors in Water Distribution System Monitoring Operations,” Journal of Water Resources Planning and Management, vol. 142, 2016.
[6] M. Weickgenannt, Z. Kapelan, M. Blokker and D. A. Savic, “Optimal Sensor Placement for the Efficient Contaminat Detection in Water Distribution Systems,” Water Distribution Systems Analysis, 2008.
[7] M. Sambito, C. Di Cristo, G. Freni and A. Leopardi, “Optimal water quality sensor positioning in urban drainage systems for illicit intrusion identification,” Journal of Hydroinformatics, vol. 22, no. 1, pp. 46-60, 1 January 2020.
[8] Korb K. B. & Nicholson A. E. (2010). Bayesian Artificial Intelligence. Second Edition. CRC Press.

**Theme:** Emerging concepts and solutions in modelling methods
**IAHR Thematic Priority Area:** [TPA-4] Digital Transformation
https://doi.org/10.3850/iahr-hic2483430201-295

# An Enhanced Deep Learning Model Based on CNN-GRU-Attention for Rainfall Retrieval Using Microwave Links

**Zhongcheng Wei[1,2], Tong Li[1,2], Luming Song[1,2]**

[1] School of Information and Electrical Engineering, Hebei University of Engineering, Handan, 056038, China
[2] Hebei Key Laboratory of Security and Protection Information Sensing and Processing, Handan, 056038, China

*Corresponding author: Zhongcheng Wei.weizhongcheng@hebeu.edu.cn*

**Abstract.** With the development of 5G and Integrated Sensing and Communication (ISAC) technology, Microwave Links (MLs) have been proven useful for providing accurate rainfall information close to the ground surface. Traditional empirical models are less adequate to address the non-linear relationship between the ML attenuation and rainfall intensity data, thus leading to low accuracy of rainfall retrieval. Therefore, this paper proposes a cascaded hybrid model combining convolutional neural network (CNN) and gate recurrent units (GRU), while incorporating an attention mechanism, named as CNN-GRU-Attention, to learn the correlation between ML attenuation and rainfall intensity data, and then to predict the rainfall intensity by inputting ML attenuation data into the CNN-GRU-Attention model. We compared the experimental results of our model with traditional ITU power-law model. The results demonstrate that the CNN-GRU-Attention model outperforms the power-law model in the consistency between predicted and actual rainfall intensities, our model achieved the correlation coefficient values of 0.97 in April and 0.92 in July, representing improvements of 7.76% and 2.22% respectively compared to the best-performing existing model.

**Keywords:** convolutional neural network (CNN), gate recurrent units (GRU), microwave link (ML), rainfall retrieval

## 1 Introduction

With the emergence of Integrated Sensing and Communication (ISAC) technology [1] , it has become possible to measure rainfall using microwave links (MLs) between communication base stations. Rainfall retrieval studies often rely on a widely used model called the power-law model. With the advancement of deep learning, ANN has been used to retrieved rainfall intensity based on ML[2] , Then, a lot of research focused on the performance evaluation of RNN in ML-based rainfall retrieval [3]. Due to the varying duration and intensity of rainfall events, there are key pieces of information present in rainfall data. Therefore, this paper proposes a hybrid model combining CNN and GRU, while incorporating an attention mechanism.

## 2 Model Construction

We utilize the standard scaler, hample filter and sliding window for processing. Then we combine CNN and GRU, while incorporating an attention mechanism, aims to improve the accuracy and reliability of rainfall intensity estimation by effectively establishing the temporal relationship in rainfall processes and focusing more on rainfall-related information. Figure 1 illustrates the overall architecture.

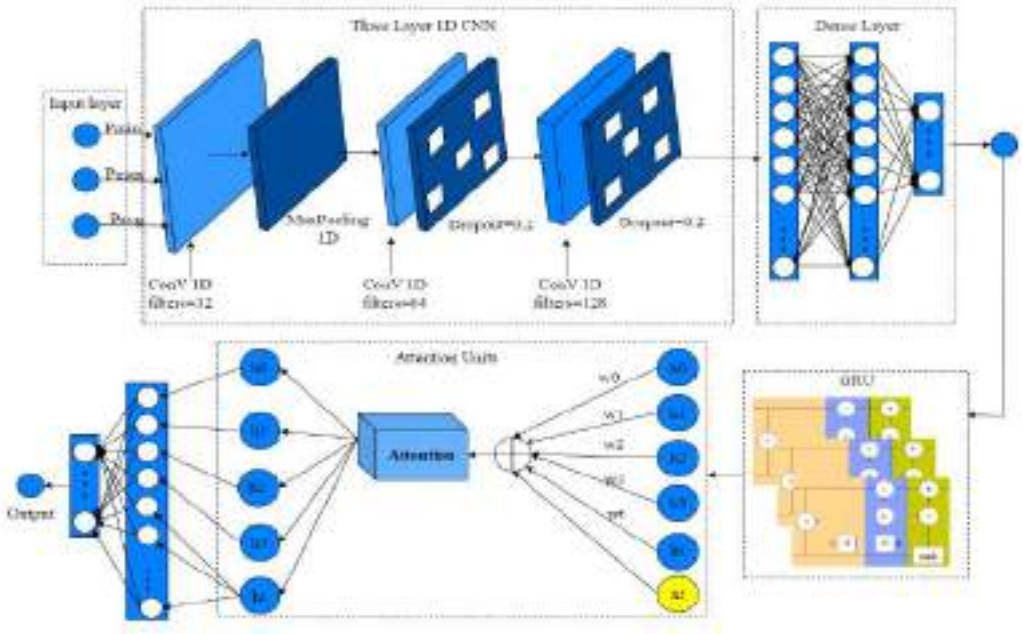


Figure 1 Overall architecture

## 3 Results and Discussion

In this paper, we proposed a novel CNN-GRU-Attention model that combines temporal and spatial feature extraction for rainfall inversion tasks. Compared to the power-law models, our model exhibited higher stability and accuracy, making it a promising alternative. Experimental results demonstrated significant improvements achieved by the enhanced CNN-GRU-Attention model in handling the non-linear relationship between ML attenuation and rainfall intensity data. The experimental results showed that our model achieved the correlation coefficient values of 0.97 in April and 0.92 in July, representing improvements of 7.76% and 2.22% respectively compared to the best-performing existing model. The model exhibits superior accuracy and generalization capabilities in rainfall inversion tasks, enabling more precise predictions of future rainfall conditions. Table 1 shows the comparison of rainfall inversion results from multiple models in April and July.

Table 1 Comparison of rainfall inversion results from multiple models in April and July

| Month | Model | MSE | CC | RMSE | EVS |
|---|---|---|---|---|---|
| April | Power Law | 0.38 | 0.49 | 2.03 | 0.049 |
| | CNN-GRU | 0.29 | 0.90 | 0.54 | 0.90 |
| | Our Model | 0.05 | 0.97 | 0.04 | 0.94 |
| July | Power Law | 0.28 | 0.86 | 1.05 | 0.023 |
| | CNN-GRU | 0.14 | 0.90 | 0.42 | 0.80 |
| | Our Model | 0.05 | 0.92 | 0.24 | 0.83 |

## Reference

[1] IMT-2030 (6G) Promotion Group. Research Report on Communication-Aware Integrated Technology Release Version (2021).

[2] Ahuna M N, Afullo T J, Alonge A A, et al. Rain attenuation prediction using artificial neural network for dynamic rain fade mitigation. SAIEE Africa Research Journal, 110 (2019) 11–18.

[3] Habi H V, Messer H. Uncertainties in short commercial microwave links fading due to rain, IEEE Speech and Signal Processing (ICASSP), (2020) 9006–9010.

**Theme:** Emerging concepts and solutions in modelling methods
**IAHR Thematic Priority Area:** [TPA-4] Digital Transformation
https://doi.org/10.3850/iahr-hic2483430201-297

# A Hybrid LSTM and RF Model for Rainfall Inversion Using Commercial Microwave Link

**Luming Song[1,2], Bin Lian[3], Lili Huang[3], Tong Li[1,2] , Jijun Zhao[1,2]**

[1] School of Information and Electrical Engineering, Hebei University of Engineering, Handan, 056038, China
[2] Hebei Key Laboratory of Security and Protection Information Sensing and Processing, Handan, 056038, China
[3]School of Water Conservancy and Hydroelectric Power, Hebei University of Engineering, Handan, 056038, China

*Corresponding author: Jijun Zhao.zjijun@hebeu.edu.cn*

**Abstract.** Accurate rainfall intensity estimation is of paramount importance for water resource management and flood disaster mitigation. Commercial microwave link (CML)-based rainfall inversion has been recognized as an effective method to provide more detailed rainfall information. Our research presents a hybrid model for CML-based rainfall measurement that employs long short-term memory (LSTM) with regularization and dropout, expressed as LSTM-RD, and random forest (RF). This model aims at probing into the correlation between CML attenuation and rainfall intensity and consequently improving the precision of rainfall intensity estimation. Regarding the estimation of medium-term and short-term rainfall events, our hybrid model yields a correlation coefficient of 0.84, 0.96, and a mean squared error of 0.07, 0.09. These results exhibited notable superiority over performance indices presented by the standalone LSTM-RD and RF models. The results obtained from our model indicated a tremendous potential in the overall accuracy and stability of rainfall intensity estimates based on CML.

**Keywords:** rainfall intensity, CML, RF, LSTM

## 1 Introduction

To address the limitations of traditional methods of measuring rainfall, the commercial microwave link (CML)-based rainfall inversion method exploits the rainfall-induced attenuation properties of microwave signals and infers rainfall intensity by analyzing the changes in the attenuation strength of the CML.

Since the first use of CML for rainfall measurement in 2006 [1], researchers around the world have joined the race to enhance the technique. In recent years, with the development of deep learning, these techniques have been widely applied to CML-based rainfall inversion. In 2023, Janco et al. [2] compared RNN and empirical models in estimating rainfall intensity, and it was found that the most significant improvement was observed in predicting light rain events.

Although CML-based rainfall measurement performances have been improved by deep learning methods, the application of feature extraction has some limitations, as the nonlinear relationship between features was not fully explored. In response to this issue, this research uses the rolling window and polynomial features to solve this problem. By combining long short-term memory with regularization and dropout, expressed as LSTM-RD, and random forest (RF), we have extracted CML attenuation data of different time scales. It has enabled the ability to capture rainfall patterns and changes, which enhances the ability to extract and understand non-linear patterns in CML attenuation data.

## 2 Material and Methods

We propose a feature engineering technique that combines rolling window and polynomial features for data preprocessing to enhance the ability to capture the intrinsic temporal attributes and nonlinear relationships in the data. In addition, we develop a new hybrid model combining LSTM-RD and RF to not only capture the features of time-series data but also improve the accuracy of rainfall intensity inversion based on CML. The framework of the model is shown in Figure 1.

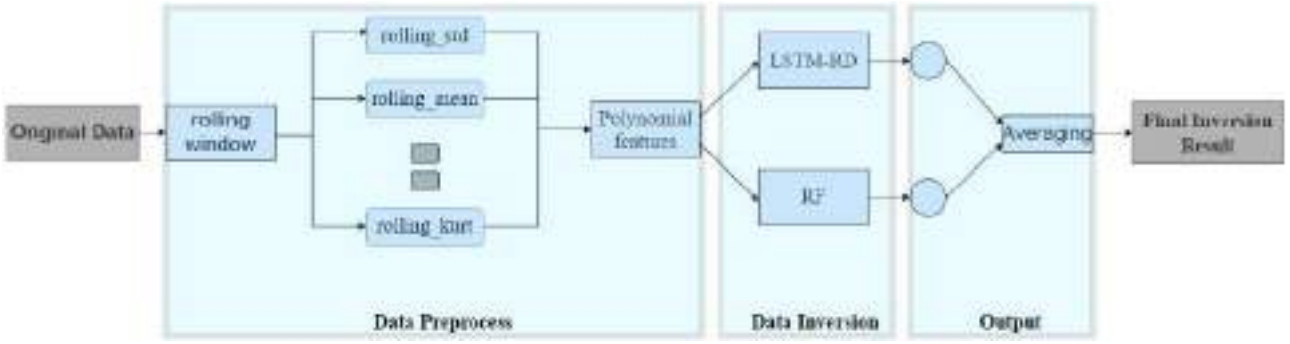


Figure 1 The framework of our proposed integrated method

## 3 Results and Discussion

The open-source dataset in Prague [3] is used to validate our hybrid LSTM-RD and RF model. Table 1 is the comparison of different performance evaluation indices for the three models, from which, we can draw the following conclusions: the hybrid model performs well in all the evaluation indexes, with CC and $R^2$ being the highest and MSE and RMSE being the lowest, which indicates that the hybrid model is not only accurately inverts the rainfall intensity, but also has good explanatory ability. The results underscore the potential of such hybrid modeling approaches in enriching our understanding of rainfall patterns and intensity.

Table 1 Comparison of rainfall intensity inversion model performance

| Models | CC | MSE | RMSE | MAE | $R^2$ |
|---|---|---|---|---|---|
| LSTM-RD | 0.95 | 0.14 | 0.38 | 0.16 | 0.87 |
| RF | 0.93 | 0.15 | 0.39 | 0.09 | 0.86 |
| Our hybrid model | 0.96 | 0.09 | 0.29 | 0.11 | 0.92 |

## 4 Conclusions

In this research, we introduce a hybrid model combining LSTM-RD and RF for rainfall intensity inversion using Commercial Microwave Link data. This model leverages the temporal processing capabilities of LSTM and the complex pattern recognition prowess of RF, aiming to enhance feature extraction and pattern identification in rainfall inversion tasks, particularly when analyzing the Prague dataset. The experimental findings reveal that this hybrid approach significantly outperforms the individual models in terms of stability, accuracy, and explanatory power.

## Reference

[1] H. Messer, A. Zinevich, and P. Alpert, Environmental Monitoring by Wireless Communication Networks. Science 312 (2006) 713.

[2] R. Janco, J. Ostrometzky, and H. Messer, In-City Rain Map from Commercial Microwave Links—Challenges and Opportunities. Sensors 23, 10 (2023) 4653.

[3] M. Fencl, M. Dohnal, P. Valtr, et al., Atmospheric observations with E-band microwave links–challenges and opportunities. Atmospheric Measurement Techniques 13, 12 (2020) 6559–6578.

**Theme:** Emerging concepts and solutions in modelling methods
**IAHR Thematic Priority Area:** [TPA-4] Digital Transformation
https://doi.org/10.3850/iahr-hic2483430201-299

# On Runoff and Sediment Reduction Effect and Critical Threshold of Soil and Water Conservation in Sanchuan River Basin

**Xiaoying Liu[1], Qunfang Zheng[2]**

[1] China Institute of Water Resources and Hydropower Research, 20 Chegongzhuang Road West, Beijing 100048, China;
[2] Beijing Forestry University, Qinghua Road East, 100038, China

*Corresponding author: liuxy@iwhr.com*

**Abstract.** Located in the middle reaches of the Yellow River from Hekouzhen to Longmen, the Sanchuan River watershed in Shanxi Province spans 176.4 kilometers in length and covers an area of 4,161 square kilometers. Since the 1970s, this watershed has conducted extensive and integrated soil conservation practices, including afforestation, terrace construction, and grassland establishment, and thus have significantly expanded. Analysis based on the observed data indicate that these measures have substantially reduced runoff and sediment loads within the watershed. Warping dam constructions have proven to be the most effective at reducing, followed by afforested areas and terraced fields, with grasslands showing the least impact. Furthermore, research has identified a threshold effect in the efficiency of these conservation practices; Specifically, when the proportion of terraced land within the basin exceeds 35% to 40%, the sediment reduction stabilizes at approximately 90%.

**Keywords:** Soil conservation measures; Sediment reduction; Sanchuan River basin

## 1 Introduction

the Sanchuan River basin has carried out large-scale comprehensive management of water and soil conservation since the 1970s, and has been listed as one of the eight national key water and soil conservation control areas since 1982. The amount of new water and soil conservation measures in each decade increased significantly compared with that in the 1960s, and the area of water and soil conservation forest was the largest, with an increase of more than 100 times; The second is beach land and grass planting, which increased significantly each in the 1980s and 1990s compared with the 1960s; Although the area of newly increased terraces decreased in the 1980s compared with that in the 1970s, it increased significantly in the 1990s. Although the number of warping dams cannot be compared with that in the 1960s, the new number increased by 23.8% and 38.8% respectively in terms of the changes in the 1980s and 1990s, 2000 s,which is enough to show the obvious changes(Fig.1). Based on observed data of the watershed, the Figure 2 indicate the role of single water and soil conservation measures in flood and sediment reduction in the Sanchuan River basin. Forest and grass measures are more obvious than terraces, grassland measures are the smallest t in flood and sediment reduction, and the warping dam and reservoir measures play the largest role.

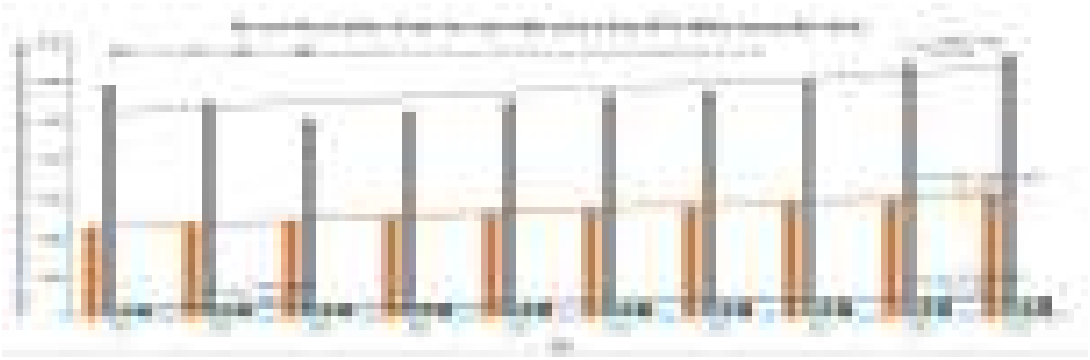

Figure 1 Reserved area of water and soil conservation measures from 1997-2006 in Sanchuan River basin

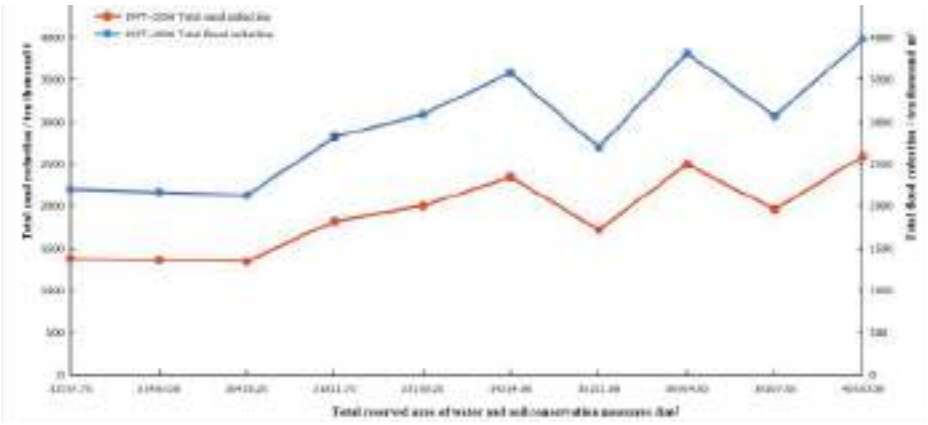

Figure 2 Relationship between the reserved area of water and soil conservation measures and flood and sediment reduction in the Sanchuan River basin

## 2 Conclusion

From the perspective of Sanchuan River basin, water and soil conservation measures have an obvious effect on flood and sediment reduction. From the perspective of single measures, the flood and sediment reduction effect of dam land is greater, followed by woodland and terrace, and grassland is relatively least and the effect of water and soil conservation measures on flood and sediment reduction has a certain threshold, not an infinite relationship.

## 3 Acknowledgments

This research was financially supported by the National Nature Science Foundation of China -Yellow River Joint Fund (U2243210).

## Reference

[1] Yao Wenyi, Analysis and evaluation of water and sediment change in the Yellow River basin [M] Zhengzhou: Yellow River Water Conservancy Press, 2011.
[2] Liu Xiaoyan, Cause study of sharp decrease of water and sediment in the Yellow River in recent years [M] Beijing: Science Press, 2017.

**Theme:** Emerging concepts and solutions in modelling methods
**IAHR Thematic Priority Area:** [TPA-4] Digital Transformation
https://doi.org/10.3850/iahr-hic2483430201-301

# Physics-Informed Neural Networks as Surrogate Models of Transient Mixed Flow Simulator

**Shixun Li[1], Wenchong Tian[1], Hexiang Yan[1†]**

[1] College of Environment Science and Engineering, Tongji University, Shanghai, People's Republic of China.

[†]*Corresponding author: hxyan@tongji.edu.cn*

**Abstract.** The current research explores the application of physics-informed neural networks (PINN) in solving the Saint-Venant equations (SVE) for transient mixed flow in urban drainage network systems. This paper firstly defines a coefficient to unify water hammer and open channel equations into SVE , and then embedded it into the loss function in the neural networks. Meanwhile, the water height, velocity, and this coefficient can be outputted in three sub-networks separately with different network-architecture and hyperparameters. And the training dataset is obtained from physical experiments, while the test dataset is based on a numerical solution using finite volume Harten-Lax-van Leer (HLL) solver. By embedding governing equations as the loss function, setting the initial conditions, boundary conditions, and data from experimental monitoring gauges, this surrogate model can directly solve for water depth (or pressure) and velocity within the corresponding computational domain by inputting temporal and spatial information. Ultimately, a sensitivity analysis was undertaken concerning hyperparameter selection, with subsequent discourse on the limitations inherent to PINN.

**Keywords:** Approximate Riemann solver, Hydrodynamic simulator, Physics-based deep learning, Saint Venant Equations, Transient mixed flow

## 1 Introduction

Urban flooding is an inevitable problem in the context of climate change and current rapid urbanization process. In order to improve risk assessment and evacuation management, urban stormwater model is an important tool for predicting urban flooding. As a vital part of flood risk management and climate resilience enhancement schemes, urban drainage system and its numerical model are the key support of solving urban flooding problem. Existing numerical methods, such as Finite Difference Method (FDM), Finite Volume Method (FVM), etc., struggle a balance between numerical accuracy and high computational costs. Currently, there is extensive research on calculating hydrodynamic problems through data-driven methods, which can effectively address the above issues.

Physics-Informed Neural Networks (PINN) is a semi-supervised learning method that couples measurement data with physics laws and applies deep neural networks (DNN) to solve PDE. Because of its great potential in solving PDEs to describe the unrepresented physics, PINN has appeared in the fields of hydrodynamics and hydrology. This work proposed a novel PINN-based surrogate model for transient mixed flow analysis in closed conduit.

## 2 Methodology

Consider an experimental test case. The experimental apparatus comprises a 30 m-long horizontal rectangular open channel with a 10 m-long roof to produce transitions between free-surface and pressurized flows. Before the experiment, the channel is filled with stationary water up to a height of 0.128 m, then a wave is generated by opening the gate to induce mixed flows in the partially covered channel. PINN adopts AD to derive the variables and embeds the residual values of PDE into the loss

function. Based on this principle, for the complex rectangular cross-section transient mixed flow, this paper defines a novel factor to formally unify the water hammer and the open-channel equations and embeds it into the PDE-Loss of PINN. Obviously, water depth , velocity , and control factor are outputted by different neural networks with different hyperparameters. The neural network- has 6 layers and 128 neurons; the neural network- has 6 layers and 64 neurons; the neural network- has 4 layers and 32 neurons; with a total of 100,000 iterations. To optimize the model parameters, two optimization algorithms are used: (1) Adam with mini-batches, and (2) L-BFGS algorithm with full-batch.

## 3 Results (more details are shown in full paper)

The proposed model is validated by comparison with experimental and numerical results for Wiggert benchmark, in which the flow inside the rectangular pipe gradually transitions from open-channel flow to pressurized flow. Additionally, the numerical results is based on finite-volume method using HLL solver, which also is regarded as the test dataset of PINN. The mesh number is 200 in this case, i.e., m, and the . The strickler coefficient is 0.0015 and the pressure wave celerity is 25 m/s. In this paper, the time series of the upstream and downstream depths given by Wiggert were digitized and subjected to linear interpolation for boundary condition definition, while transmissive boundary conditions were employed for velocity specification.

However, PINN does not require mesh and CFL number settings, and the friction coefficient is also set to 0.0015, but the pressure wave speed can be set to 1200m/s. The results are shown in Table 1, where is the of pressure and is the of velocity, and

where φ is the head pressure (water depth) h or the velocity u.

Table **1.** Errors in the PINN with different hyperparameters

| ID | h, u & [layers-neurons] | iterations | L2:h(%) | L2:u(%) |
|---|---|---|---|---|
| I | [6-128][6-128][4-32] | 10,000 | 2.56 | 4.78 |
| II | [10-128][6-128][4-32] | 40,000 | 2.42 | 4.34 |
| III | [6-128][6-64][4-32] | 100,000 | 2.24 | 2.14 |
| IV | [6-128][6-64][4-32] | 200,000 | 2.17 | 2.01 |
| V | [6-128][6-64][4-32] | 400,000 | 2.16 | 1.97 |

## 4 Conclusion

In this work, the framework of the state of the art physics-informed neural network (PINN) is explored to predict the transient mixed flow in the Wiggert benchmark. The proposed model is validated by comprison with experimental datas and numerical results. The results have shown that PINN has excellent fitting effect in velocity, but can only predict trends in water depth. According to the Frequency principle, DNN has limitaions on simulation in the high-frequency range, thus making the proposed model difficult to accurately capture water hammer vibrations. Meanwhile, a sensitivity analysis was performed to assess the impact of hyperparameter selection. Overall, physics-based data-driven method is mesh-free and computationally efficient, able to effectively capture the trends in water depth, pressure and flowrate changes. As an alternative model for urban stromwater networks, it has infinite potential. Further research will be conducted on the method's ability to capture high-frequency data and to improve the solver's solution accuracy.

**Theme:** Emerging concepts and solutions in modelling methods
**IAHR Thematic Priority Area:** [TPA-4] Digital Transformation
https://doi.org/10.3850/iahr-hic2483430201-303

# A Hybrid Model of Bin-Based and Lagrangian Super-Droplet Method to Simulate the Evolution of Cloud Droplets

**Yan Diran[1], Huang Hao[2], Chen Guoxin[1]**

[1] Department of Hydraulic Engineering, Tsinghua University, Beijing 100084, China
[2] Xingjian College, Tsinghua University, Beijing 100084, China

*Corresponding author: litiejian@tsinghua.edu.cn*

## 1 Introduction

It has been discussed extensively but remains many questions how droplet size spectrum (DSP) develops and finally evolves into rainfall in warm clouds. Collision-coalescence is proven a major mechanism of droplet growth and DSP development. Statistical parameterized methods seem too imprecise and empirical for DSP simulation despite their practicability in some specific estimations, while direct Lagrangian simulations through Computational Fluid Dynamics (CFD) face difficulty in extending their application to larger atmospheric scales with sparse droplets. A more balanced method is to solve the Kinetic Collection Equation (KCE), which is an ordinary differential equation that numerical models are necessary for an approximate solution. This article introduces a new model for the calculation of KCE.

## 2 Methods

The bin-based method (BM) and the Lagrangian super-particle method (LSM) are the two most popular methods for the approximate solution of KCE. BM is to divide the droplet size into several bins and calculate the gain and loss of droplet concentration in each bin. LSM aims to trace the growth of droplet groups called simulating particles (SIPs) without their positional information. Their performance for the evolution of small or big droplets is listed in Table 1.

Table 8 Evaluation of the two methods for small or big droplets

| Evaluation of methods | BM | LSM |
|---|---|---|
| For small droplets | Relatively accurate solution can be obtained with specially divided bins and numerical integration | Too many SIPs causes lengthy computation, or too few SIPs causes an oscillatory DSP |
| For big droplets | Difficult to divide bins, resulting in lengthy computation or program failure | Better adapted to large kernels and can reflect real concentration fluctuations |

To make use of the advantages while overcoming the shortcomings of both methods, we create a hybrid model (HM) that applies BM to small droplets and LSM to big ones, with a radius of 20 μm as the threshold. In BM, the bins are equally divided by volume, and the volume at the right endpoint represents the bin for an accurate result; the method by Shima et al. (2009) [1] is adopted in LSM. We have created the following treatments to connect the two different methods:

- The mechanism of new SIPs emerging;
- The algorithm for the collision of small and big droplets, which results in the decrease of concentration of small droplets and growth of big ones;
- The controlling of mass conservation;

- A parallel computing program realized by Python.

## 3 Results and Discussion

The Golovin kernel with its analytic solution [2] is used to compare the results of HM. We validate the stability of our model by changing its 4 variables: bin length, time step, the threshold of small and big droplets, and computing bulk that affects the number of SIPs. The resulting DSP is the average of 50 simulations and the simulations last for 1 hour. DSP including big droplets is drawn by moving average with selective window lengths, and the cumulative distributions of mass are also calculated to evaluate the accuracy and water conservation. We have also changed 3 parameters in the Golovin kernel and compared the results with a classical MFM method by Bott (1998) [3]: kernel coefficient, initial average radius, and total water content. It is found that:

- The simulations of HM fit well with the analytical results, though there are inevitable oscillations due to the moving average. The error is not evident unless the parameters are extreme. The results of changing the time step are taken as an example in Figure 1 (a-b).
- HM is closer to the analytical DSP than MFM in most conditions and adapts to a larger kernel or water content. It also works better in water conservation. Seen in Figure 1 (c) where water content is changed.

We also explore the DSP evolution in the turbulence or gravity kernel. The real initial DSP of lognormal distribution for both continental and marine clouds is introduced, and the big droplets will leave the simulation bulk after growing over the gravity-settling radius. The results indicate that HM has great potential in the computations for real clouds.

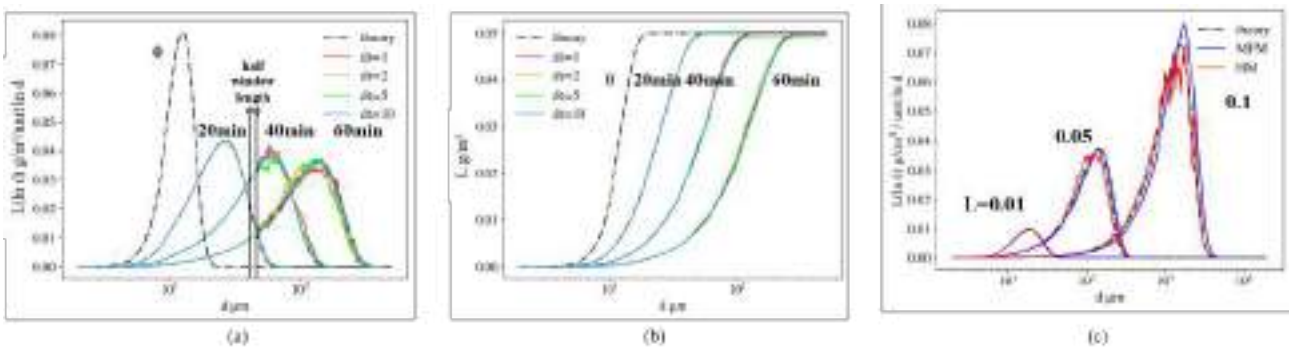


Figure 38 (a) Comparison of simulation and theoretical DSPs in 60 minutes when the time step is changed from 1 s to 10 s; (b) The cumulative curves; (c) Comparison of the resulting DSP by HM and MFM when changing the liquid water content from 0.01 to 0.1 g/m$^3$.

## 4 Conclusions

In this research, we have created a new method HM to calculate the development of DSP. Our main idea is to apply BM to small droplets and LSM on big ones, and the most important contribution is the solution of two problems: how SIPs emerge and how they interact with SDPs. The better accuracy than traditional methods can be seen from the cumulative curves that those produced by HM are really close to the theoretical ones. HM is also fast and stable enough for different parameters. We believe that HM has great potential in more complex application scenarios.

## Reference

[1] S. Shima, K. Kusano, A. Kawano, et al., The super-droplet method for the numerical dimulation of clouds and precipitation: A particle-based and probabilistic microphysics model coupled with a non-hydrostatic model, Quarterly Journal of the Royal Meteorological Society, 135.642 (2009): 1307-1320.

[2] A. M. Golovin, The solution of the coagulation equation for cloud droplets in a rising air current, Bulletin of academy of sciences. 5(1963): 783-791.

**Theme:** Emerging concepts and solutions in modelling methods
**IAHR Thematic Priority Area:** [TPA-4] Digital Transformation
https://doi.org/10.3850/iahr-hic2483430201-305

# Efficient Economic Model Predictive Control of Water Treatment Process with Learning-Based Koopman Operator

**Minghao Han[1,2], Jingshi Yao[1], Adrian Wing-Keung Law[2,3], Xunyuan Yin[1,2]**

[1] School of Chemistry, Chemical Engineering and Biotechnology, Nanyang Technological University, 62 Nanyang Drive, 637459, Singapore
[2] Environmental Process modeling Centre, Nanyang Environment and Water Research Institute (NEWRI), Nanyang Technological University, 1 CleanTech Loop, 637141, Singapore
[3] Department of Civil and Environmental Engineering, National University of Singapore, 21 Lower Kent Ridge Rd, 119077, Singapore
*Corresponding author: Adrian Wing-Keung Law*

**Abstract.** Used water treatment plays a pivotal role in advancing environmental sustainability. Economic model predictive control holds the promise of enhancing the overall operational performance of the water treatment facilities. In this study, we propose a data-driven economic predictive control approach within the Koopman modeling framework. First, we propose a deep learning-enabled input-output Koopman modeling approach, which predicts the overall economic operational cost of the water treatment processes based on input data and available outputs that are directly linked to the operational costs. Subsequently, by leveraging this learned input-output Koopman model, a convex economic predictive control scheme is developed. The resulting predictive control problem can be efficiently solved by leveraging quadratic programming solvers, and complex non-convex optimization problems are bypassed. The proposed method is applied to a benchmark water treatment configuration, and the results show that it significantly improves the overall economic operational performance. Additionally, the computational efficiency of the proposed method is significantly enhanced as compared to benchmark control solutions.

**Keywords:** economic model predictive control, Koopman operator, learning-based modeling and control, water treatment process.

## 1 Introduction

In this work, we aim to propose a Koopman-based economic predictive control framework, which is designed to alleviate the prohibitive computational burden associated with the existing non-convex EMPC frameworks to facilitate the efficient and economic operation of WWTPs. The contributions of this work are threefold:

- We propose a learning-based input-output Koopman modelling approach to predict future economic performance indices of the WWTP without requiring full-state information of the process. A

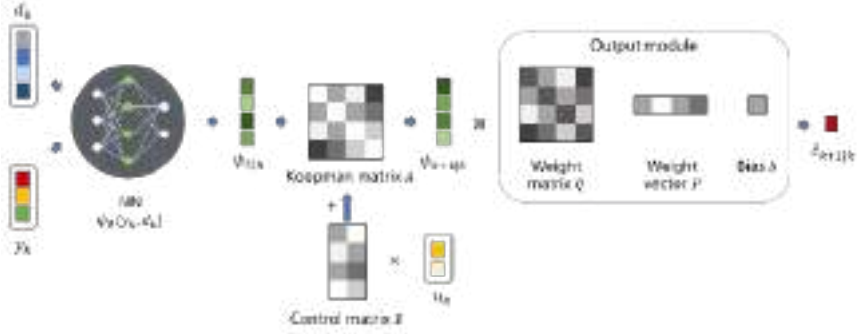


Figure 39 The proposed DIOKO model structure.

- data-driven convex economic predictive control scheme is developed for the economic operation of the WWTP which exhibits highly nonlinear dynamics.
- As compared to conventional EMPC based on a nonlinear first-principles model, our proposed framework achieves an over 5600-fold improvement in computational efficiency, while simultaneously delivering overall better economic operational performance.

## 2 Methods

In this work, instead of learning the Koopman operator and developing a control method that requires full state information, we propose DIOKO to learn a model that aims to predict the future overall economic stage cost by utilizing the available measurements from the 41 state sensors, the control inputs, and known disturbances of the WWTP. The structure of the model is shown in Figure 1. Based on the established DIOKO model, a convex computationally efficient EMPC scheme is formulated.

## 3 Results

we apply the proposed Koopman-based modelling and economic predictive control method to the WWTP of which the dynamics are characterized by the BSM1 [1]. We also compare the control performance of the proposed method with two representative baselines, including the EMPC designed for WWTP based on a nonlinear first-principles model [2] and the conventional nonlinear tracking MPC.

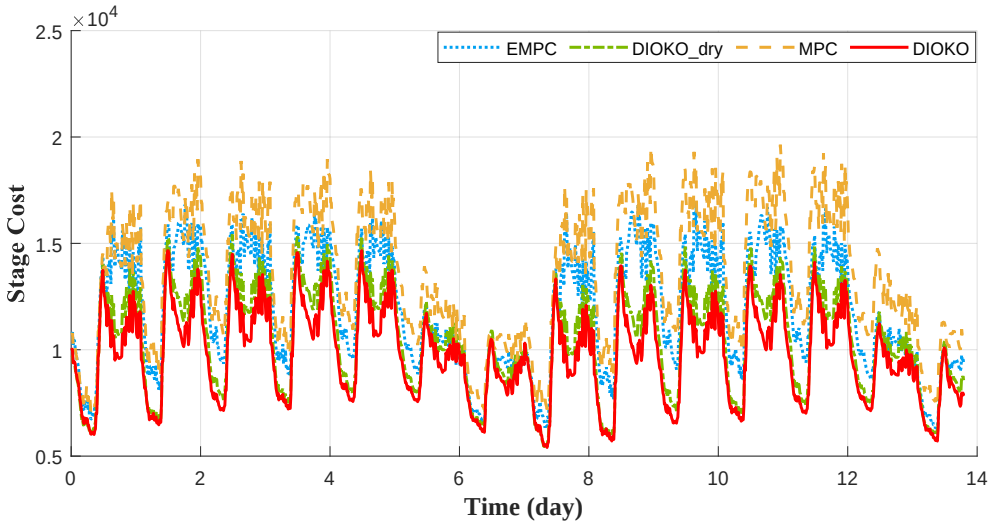


Figure 40 Trajectories of the stage cost of the proposed method and baseline methods under the dry weather condition.

In terms of the overall economic stage cost, which is computed based on the overall control index and the effluent quality, the performance provided by the proposed DIOKO EMPC is improved by 24.6% compared to the model-based baseline methods, under the dry weather condition. In terms of computational efficiency, DIOKO can solve the optimal control problem within 3 to 4 ms on average, which is approximately 5600 to 9800 times more efficient than the baseline EMPC based on the nonlinear process model, and 400 to 500 times more efficient than the MPC approach.

## Reference

[1] Jens Alex, Lorenzo Benedetti, JB Copp, KV Gernaey, Ulf Jeppsson, Ingmar Nopens, MN Pons, Leiv Rieger, Christian Rosen, JP Steyer, et al. Benchmark simulation model no. 1 (BSM1). Report by the IWA Taskgroup on benchmarking of control strategies for WWTPs, 2008.

[2] Jing Zeng and Jinfeng Liu. Economic model predictive control of wastewater treatment processes. Industrial & Engineering Chemistry Research, 54(21):5710–5721, 2015.

**Theme:** Emerging concepts and solutions in modelling methods
**IAHR Thematic Priority Area:** [TPA-4] Digital Transformation
https://doi.org/10.3850/iahr-hic2483430201-307

# An Evaluation of Different Annotation Approaches for YOLOv8 Instance Segmentation in UAV Imagery: A Case Study on the UAV-BD Dataset

**Shijun Pan, Yuki Yamada, Daichi Shimoe, Keisuke Yoshida**

Graduate School of Environmental and Life Science, Okayama University
(Tsushima-naka 3-1-1, Kita-ku, Okayama 700-8530, Japan)

*Corresponding author: p4b36znn@s.okayama-u.ac.jp*

**Abstract.** This paper presents a comprehensive analysis of the impact of distinct annotation approaches, namely bounding boxes (B-Box) and masks, on the accuracy of YOLOv8-seg, a state-of-the-art instance segmentation model, when applied to unmanned aerial vehicle (UAV) imagery. Our investigation centres on the UAV-BD dataset, a challenging and diverse dataset designed for UAV applications. Through meticulous comparisons, we assess the performance of YOLOv8-seg using mAP50 and mAP50-95 metrics under different annotation approaches, providing an understanding of the efficacy of each annotation method. Our study yields intriguing findings: while mAP50 scores exhibit comparability between bounding box and mask annotations, a distinctive divergence surfaces in the mAP50-95 metric. The mask annotation approach consistently outperforms bounding boxes, suggesting its dominance in effectively handling instances with higher IoU thresholds under all the backgrounds (i.e., sand, lawn, bush, land, step, ground and playground). The enhanced performance of mask-based annotations, particularly at higher IoU thresholds. This research provides valuable insights that can inform decision-making in digital twin applications and other domains reliant on accurate UAV-based object detection, fostering advancements in technology and application domains.

**Keywords:** Annotation Approach, Instance Segmentation, Riparian Waste Detection, UAV

## 1 Introduction

Unmanned aerial vehicle (UAV) imagery plays a pivotal role in diverse applications, ranging from surveillance to environmental monitoring. Accurate object detection and segmentation in UAV imagery are critical for extracting meaningful information and enhancing the capabilities of applications such as digital twin technology. In this context, the choice of annotation approaches significantly influences the performance of in-stance segmentation models. This paper delves into a detailed examination of the impact of different annotation methods, specifically bounding boxes (B-Box) and masks, on the accuracy of YOLOv8-seg, a cutting-edge instance segmentation model, when applied to UAV imagery. The UAV-BD dataset serves as the focal point of our investigation, providing a challenging and diverse set of scenarios that mimic real-world UAV applications. Designed to encompass various environments, including sand, lawn, bush, land, step, ground, and playground, the UAV-BD dataset reflects the complexity of UAV imagery encountered in practical scenarios. Our research adopts a meticulous comparative approach, employing mean Average Precision at IoU 50 (mAP50) and mean Average Precision between IoU 50 and 95 (mAP50-95) metrics to assess the performance of YOLOv8-seg under distinct annotation approaches. This evaluation aims to elucidate the efficacy of each annotation method and uncover their impact on the model's accuracy.

## 2 Work flow

Training UAV-BD dataset (train/valid) with mask annotations, inferring the UAV-BD dataset (test part) and getting the results derived from both the mask- and bounding-box- based standards (i.e., True Label and evaluation approach). To understand the accuracy derived from the annotation difference, the authors compared the Precision, Recall, mAP50, mAP50-95 and F1 score (IoU=0.45) between mentioned different two annotation approach (i.e., mask-based value minus bounding-box-based value) under various backgrounds.

## 3 Conclusion

As shown in the Figure 1, the findings of our study reveal intriguing nuances in the performance of YOLOv8-seg under different annotation approaches. Notably, while mAP50 scores exhibit comparability between bounding box and mask annotations, a distinct divergence emerges in the mAP50-95 metric. The mask annotation approach consistently outperforms bounding boxes, showcasing its dominance in effectively handling instances with higher IoU thresholds across various backgrounds. Considering the reasons of the evaluation-index-based difference, Figure 2 has depicted that the backgrounds in the bounding box have been trained in the model, and the bottle-based overlapping area probably have been reduced.

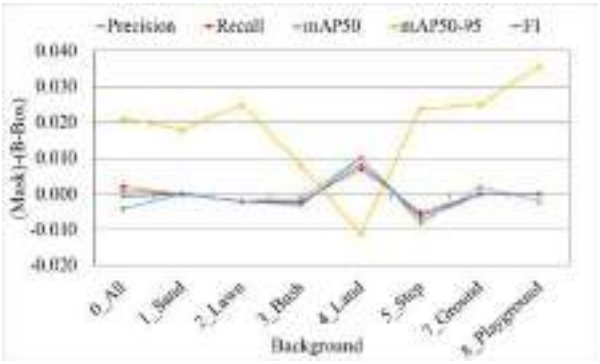


Figure 1 Comparison of the F1 score (IoU=0.45), mAP50 and mAP50-95 between the mask- and bounding-box- based standards.

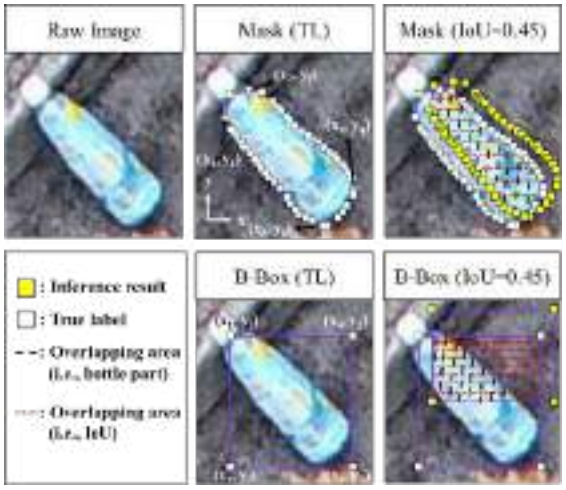


Figure 2 True Label (TL) and evaluation approach difference.

## Reference

[1] J. Wang, W. Guo, T. Pan, H. Yu, L. Duan and W. Yang, "Bottle Detection in the Wild Using Low-Altitude Unmanned Aerial Vehicles," *21st International Conference on Information Fusion (FUSION)*, Cambridge, UK, 2018, pp. 439-444, 2018. 10.23919/ICIF.2018.8455565.

**Theme:** Emerging concepts and solutions in modelling methods
**IAHR Thematic Priority Area:** [TPA-4] Digital Transformation
https://doi.org/10.3850/iahr-hic2483430201-309

# A Novel Approach to Flood Forecasting

**Agnieszka I. Olbert[1], Sogol Moradian[1]**

[1] University of Galway, Galway, Ireland

*Corresponding author: Indiana.olbert@universityofgalway.ie*

**Abstract.** Floods are one of the most severe natural disasters. An accurate flood forecasting can aid flood risk management efforts and by that reduce or even prevent flood damages. However, flood forecasting is challenging because it relies on forecasted inputs of meteorological and hydrological variables which can be subject to large uncertainties. Hydrodynamic models, if used for flood modelling, are also another source of uncertainties. Compound floods generated by coastal and fluvial drivers acting simultaneously add another layer of complexity and uncertainty. This research demonstrates a novel approach to an integrated flood forecasting system. The system combines statistical, hydrodynamic and machine learning models. In this three-model cascade the joint probability results derived from a best-fit copula function are used to force the hydrodynamic model of urban riverine-estuarine hydrological domain while the hydrodynamic model outputs are used to train and validate the machine learning model. Ultimately the machine learning model is used to forecast the states of water levels, from which the risk of flood can be determined. This research finds that the coupled statistical-hydrodynamic-ML system can be successfully used for flood forecasting.

**Keywords:** compound events, flood forecasting, flood risk management, hydrodynamic modeling, machine learning, urban floods,

## 1 Introduction

Floods are one of the most severe natural disasters that damage natural and built environments, and cause large socio-economic impacts. Flood forecasting systems are effective decision making tools that can aid flood risk management efforts and by that reduce or even prevent flood damages. However, flood forecasting is challenging because it relies on forecasted inputs of meteorological and hydrological variables which can be subject to large uncertainties. Hydrodynamic models if used for flood modeling are also another source of uncertainties and they generate numerical errors. Compound floods generated by coastal and fluvial drivers acting simultaneously add another layer of complexity and uncertainty as the compound effects of floods can be amplified and have severe consequences [1]. Both understanding the mechanisms of such complex flood events and forecasting are very challenging. In this context, the aim of this research is to demonstrate a development of an integrated flood forecasting system that combines three models: statistical, hydrodynamic and machine learning (ML) models to be used in an operational manner.

## 2 Methodology

Schematic diagram of methodology is presented in Figure 1(a). An integrated flood forecasting system developed in this research combines three models: statistical, hydrodynamic and ML models. In step one, the joint probability results are derived from a best-fit joint probability function. The joint probability curves representing the occurrence of two drivers (sea levels and river discharges) occurring simultaneously are used in step 2 to force the hydrodynamic model of riverine-coastal region. The 2-dimensional hydrodynamic model MSN_Flood is used to simulate the compound coastal-fluvial flooding over the hydrological domain [2]. The model was run for an ensemble of scenarios that represent various-impact flood events driven by combinations of coastal and fluvial drivers for a range of return period events. Such ensemble simulations provide hazard maps of various probability events. In step three, the fluvial and coastal boundary conditions of the hydrodynamic model combined with corresponding flood depths across floodplains are used to provide the

training, validation and testing data for ML algorithms. Several ML models such as Support Vector Regression (SVR), Support Vector Machine (SVM), Radial Basis Function (RBF), Linear Regression (LR), Gaussian Process Regression (GPR), Decision Tree (DT), and Artificial Neural Network (ANN) were applied in this study. Ultimately, the best performing ML model is used to forecast the states of water levels for a given set of river discharges and sea water levels upstream and downstream, respectively.

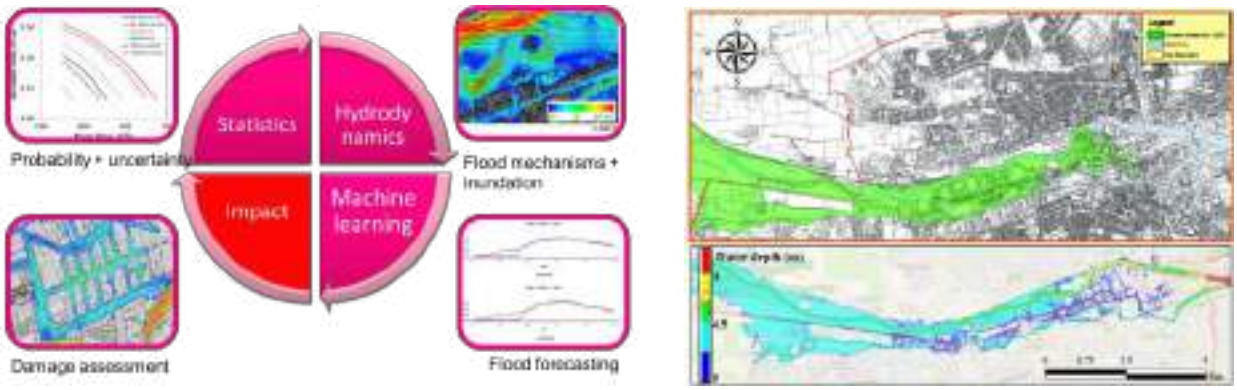


(a) (b)

Figure 41 Flood forecasting methodology (a) and ML model validation for a historical event (b).

## 3 Results

Cork City, second largest city in Ireland frequently subject to compound coastal-fluvial floods was chosen to demonstrate the three-model forecasting tool. A range of copula functions was applied to generate joint probability curves of sea water levels co-occurring with river discharges. The MSN_Flood model configured for Cork City at 2m resolution was used to simulate unsteady, non-uniform flows in the Lee River and a flood wave propagation over the Cork City floodplains. The hydrodynamic model outputs were used to train ML algorithms. Then the best ML model was chosen based on the multi-criteria decision-making technique and the 10-Fold cross validation method described in [3].

Results indicate that three ML models: RBF, ANN and DT show particularly strong performance and are suitable for forecasting of urban flooding in Cork City. In overall, the novel coupled statistical-hydrodynamic-ML system can be successfully used for flood forecasting, when the ML model is trained using the hydrodynamic model outputs for a wide spectrum of river conditions derived from the statistical analysis. An advantage of the three-model system over the traditionally used hydrodynamic model is a low computational time for forecast simulation. The ML model with built network is very efficient computationally and therefore can be used for operational forecasting, while the high-resolution hydrodynamic model suffers for high computational effort which prevents its use operationally. In overall, the novel coupled statistical-hydrodynamic-ML system can be successfully used for operational flood forecasting.

## Acknowledgements

This study has been funded by the Environmental Protection Agency (EPA), Ireland, under the EPA Research Programme 2021–2030 (project code: 2021-CCEN-CT7_1056) and the Science Foundation Ireland- National Challenge Fund (SFI-NCF), Ireland (project code: 22/NCF/DR/11286) and the Irish Research Council (IRC), Ireland (project code: GOIPD/2023/1627).

### Reference

[1] A.I. Olbert, J. Comer, S. Nash, M. Hartnett, High-resolution multi-scale modelling of coastal flooding due to tides, storm surges and river inflows. A Cork City Example, Coastal Engineering, 121 (2017) 278-296

[2] S. Moradian, A.I. Olbert, S. Gharbia, G. Iglesias, Copula-based projections of wind power: Ireland as a case study. Renewable and Sustainable Energy Reviews. 175 (2023) 113147.

[3] A.I. Olbert, S. Moradian, S. Nash, J. Comer, B. Kazmierczak, R. Falconer, M. Hartnett, Combined statistical and hydrodynamic modelling of compound flooding in coastal areas- Methodology and application. Journal of Hydrology (2023) 620 129383.

**Theme:** Emerging concepts and solutions in modelling methods
**IAHR Thematic Priority Area:** [TPA-4] Digital Transformation
https://doi.org/10.3850/iahr-hic2483430201-311

# Analysis of the Chlorophyll-*a* Concentration Distribution in Tonle Sap Lake

**YANG Yuming**[1]

[1] College of Environment, Hohai University, Nanjing 210098, China

*Correspondence to:* ***YANG Yuming*** *(2225285636@qq.com)*

*Corresponding author: corresoponding.author@email.address.com*

**Abstract.** Under the increasing impact of human activities, many lakes around the world are facing eutrophication problems. For water resource management, using MODIS remote sensing images to analyze the distribution of chlorophyll-a in lakes is a very effective method. MODIS satellite image and Ocean Color (MODIS/Terra) Level 1A image of Tonle Sap Lake（TSL）area are been analyzed，and a relationship between hydrological feature and water quality is established.

**Keywords:** Chlorophyll-A; MODIS Satellite Image; Tonle Sap Lake; Water Quality

## 1 Methodology

Tonle Sap Lake （Figure 1） is an integral part of the Mekong River, located in the northwest part of Cambodia with abundant water resources.

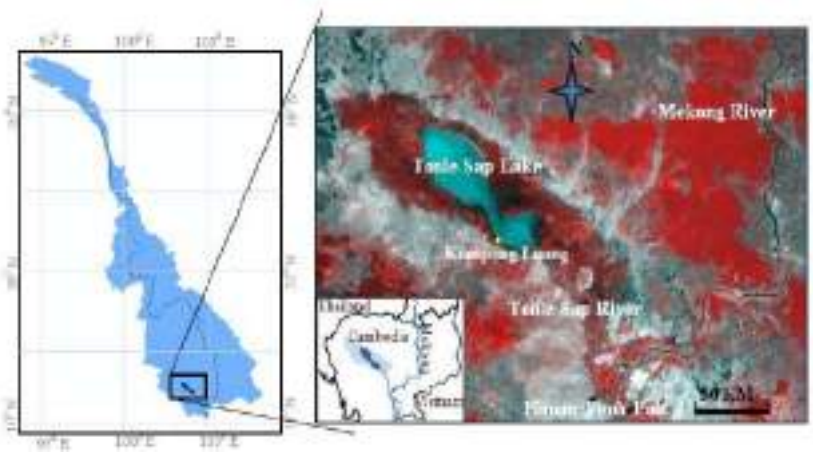


Figure1 Map of location of Tonle Sap Lake area

Chlorophyll a (Chl_a) is the parameter in this study for the assessment of TSL surface water quality. Chlorophyll a (Molecular formula: C55H72O5N4Mg) is a green pigment found in plants. It absorbs sunlight and converts it to sugar during photosynthesis. Chlorophyll a concentrations are an indicator of phytoplankton abundance and biomass in coastal and estuarine waters. They can be an effective measure of trophic status, potential indicators of maximum photosynthetic rate and are a commonly used measure of water quality. High levels often indicate poor water quality and low levels often suggest good conditions.

The bio-optical algorithm OC4A (Ocean Chlorophyll 4-Band OCTS) is applied to estimate the chlorophyll a concentration which relating the maximum of three band ratios (Rrs443/Rrs565, Rrs490/Rrs565, and Rrs520/Rrs565).

## 2 Results and discussions

December is the beginning of dry season in each year, chlorophyll a concentration in this month can represent the situation of TSL until next flood season come. Ocean Color (MODIS/Terra) Level 1A image on each December from 2002 to 2009 were collected to estimated chlorophyll a concentrations distribute in Tonle Sap Lake. SeaWIFS Data Analysis System (SeaDAS) software is used to analyze these LAC_L1 Images and the results from 2002 to 2009 are shown in Figure2.

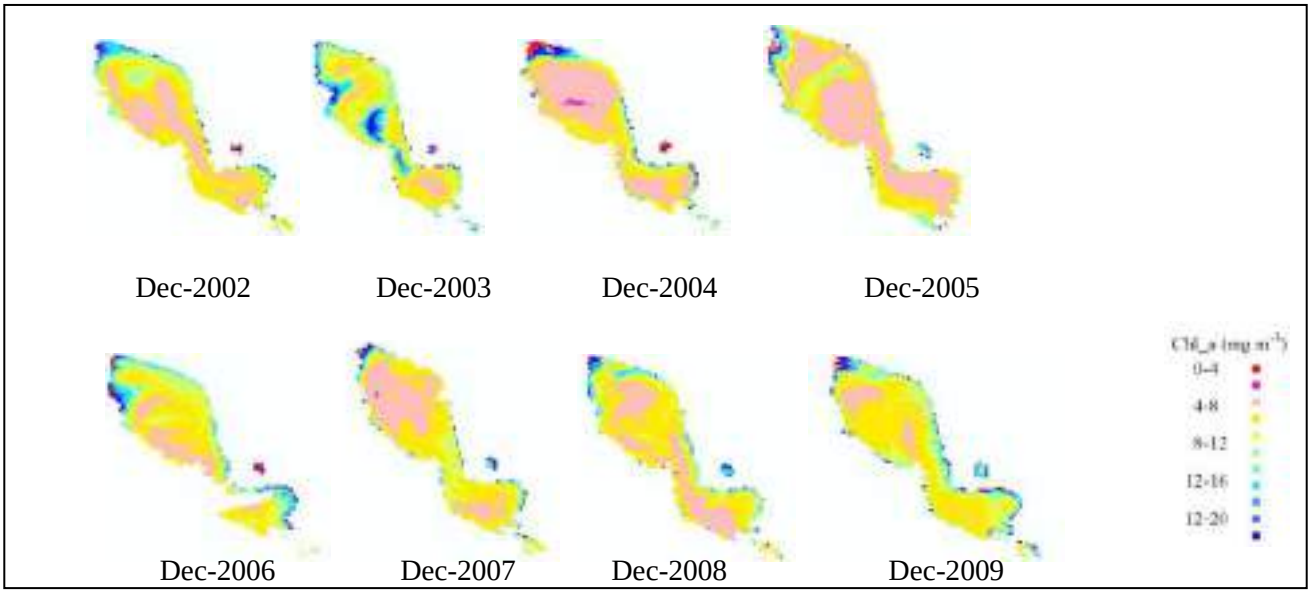


Figure 2 hl-a distribute on TSL from Dec-2002 to Dec-2009

An opposite relationship between peak flood water level (*Hmax*) in Tonle Sap Lake and chlorophyll-*a* concentration in TSL was derived: when maximum WL in TSL increases the chlorophyll-*a* concentration in TSL decreases (Figure 4).

$$Chl\_a = -9.2247 \times H_{max} + 103.84$$

$$R^2 = 0.8196 \qquad (3)$$

## 3 Conclution

Remote sensing technology support advantage in this study, especially on the water quality distribution in TSL. Chlorophyll *a* was chosen as an indicator for the water quality assessment of TSL area. Analysis results shown an opposite relation between average chlorophyll *a* concentrations of TSL water surface and peak water levels of the lake, which implies that water volume exchange between TSL and the MR has positive effect on water quality of TSL. More water volume flow into TSL from MR much better the water quality of TSL would be expected.

**Acknowledement:** Thank Jiangsu Water Conservancy Research Institute and Wu Sushu for the guidance in the process of writing the article. Thank Global Center of Excellence (GCOE) Program, Evolution of Research and Education on Integrated River Basin Management in Asian Region, University of Yamanashi.

## Reference

[1]arecki, M. and Stramski, D., 2004. An evaluation of MODIS and SeaWiFS bio-optical algorithms in the Baltic Sea, Remote Sensing of Environment 89 (3): 326–350.

[2]ooker, S.B. and Firestone, E.R., 2000. Ocean Chlorophyll-a Algorithm for SeaWIFS, OC2 and 0C4: Version 4. SeaWIFS postlaunch calibration and validation analysis, Part 3. NASA Tech. Memo. 2000-206892, vol. 11. NASA Goddard Space Flight Center, Geenbelt, Maryland: 9–23.

**Theme:** Emerging concepts and solutions in modelling methods
**IAHR Thematic Priority Area:** [TPA-4] Digital Transformation
https://doi.org/10.3850/iahr-hic2483430201-313

# Uncovering Farmers' Daily Groundwater Use Behavior for Crop Irrigation in the High Plains Aquifer

**Yao Hu[1,2], Pavel Ivanov[2], Zherui Xu[1]**

[1] Department of Geography and Spatial Sciences, University of Delaware, 125 Academy St, Newark, 19716, Delaware, U.S.
[2] Department of Civil and Environmental Engineering, University of Delaware, 127 The Green, Newark, 19716, Delaware, U.S.

*Corresponding author: yaohu@udel.edu*

**Abstract.** Accurately modeling and predicting farmers' irrigation behavior is crucial for sustainable agricultural practices and effective water resources management. However, the intricate nature of irrigation behavior, influenced by factors like bounded rationality and various environmental and socioeconomic conditions, poses significant challenges for accurate predictions. While statistical models hold promise, their effectiveness heavily relies on the available behavioral data. While accessing high quality environmental and socioeconomic data has become more feasible, obtaining irrigation behavior data at a relevant spatiotemporal scale remains challenging. Furthermore, these datasets are often noisy and prone to measurement errors. To address these data challenges in irrigation prediction, we developed a methodology framework using Deep learning-based Temporal Clustering (DTC) and Hidden Markov Models (HMMs). This framework allows us to: 1) uncover daily groundwater usage states near pumping wells where daily pumping data were collected; 2) extend predictions to regions lacking pumping observations. We applied this framework to predict daily groundwater use in the High Plains Aquifer Hydrologic Observatory Area (HPAHOA), using pumping data from dozens of wells near the Nebraska study area. Overall, our framework provides a potential solution to the common issue of data scarcity in modeling human decision-making.

**Keywords:** bounded rationality, data scarcity, groundwater, irrigation behavior, statistical modeling, temporal clustering.

## 1 Introduction

Incorporating human factors into physics-based modeling of groundwater systems represents a crucial step toward a more comprehensive understanding of groundwater dynamics[1]. This approach requires the integration of models that simulate not only the physical aspects of aquifers, but also decision-making processes of individuals and organizations involved in groundwater management. One of the central challenges is modeling of human behaviors, which often diverge from the perfect rationality assumed in classical economics. Such behaviors are characterized by high non-linearity, rendering them difficult to predict. To address this complexity, modern data-driven modeling techniques, such as machine learning (ML) models, can leverage time series data of human behaviors. However, behavioral data is often rare, complex, and unstructured, which makes extracting meaningful insights challenging. Our study confronts this primary obstacle in the modeling of daily groundwater irrigation: the scarcity of direct observations of farmers' daily irrigation practices. By focusing on predicting these practices, we aim to fill a critical gap and contribute to more informed groundwater management strategies.

## 2 Material and Methods

**Case Study Site.** The High Plains Aquifer (HPA), the largest aquifer in the U.S. covers a large area of about 174,000 square miles in parts of eight states. Over 170,000 wells are pumping groundwater from this aquifer to irrigate 500,000 km$^2$ of farmland. In this study, we chose part of the HPA, the High Plains Aquifer Hydrologic Observatory Area (HPAHOA) as the study region (Figure 42), as the area has experienced dramatic increase of pumping wells for crop irrigation between 1960 - 2000, with 18,000 wells in Nebraska and roughly 4,000 wells in Colorado and Kansas up to date. Water conflicts among the three states have arisen from the intensive groundwater pumping that has led to groundwater declining and streamflow depletion. We acquired

daily pumping data from multiple wells for 2015 and 2016 near the Nebraska study area (Figure 42). Following data quality assessment, we selected the records from 18 wells during July to September irrigation period for both years. Additionally, we retrieved daily climate data from the Global Historical Climatology Network daily (GHCNd), and daily crop and diesel prices.

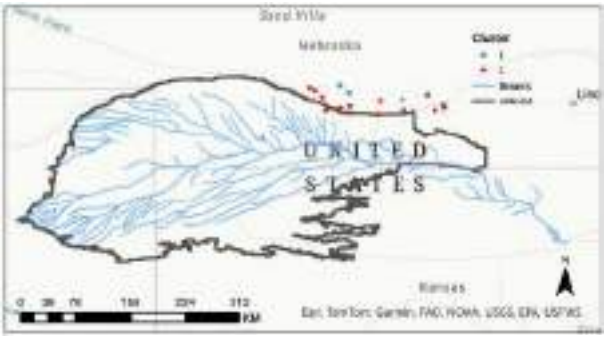


*Figure 42. Map of High Plains Aquifer Hydrologic Observatory Area (HPAHOA), U.S., showing two distinct clusters of irrigation wells (blue and red dots: Clusters 1 and 2 wells). The blue lines represent the stream network, with the black outline delineating the boundary of the HPAHOA.*

**Well Clustering**. In this study, we used a deep learning-based temporal clustering framework known as Deep Temporal Clustering[2](DTC), as the DTC can efficiently extract the spatiotemporal features from time-series data, allowing the input sequences to be more separable into distinct clusters. We applied the DTC framework to identify groups of wells with similar irrigation dynamics.

**States of Irrigation Depth**. Given that measurements of irrigation depth are prone to errors, we chose not to predict their exact actual daily values. Instead, we predicted these values as discrete, hidden states. we first determined these hidden states from the irrigation depth measurements. We then constructed a first-order Hidden Markov Model (HMM). This model predicts the state of irrigation depth for day *D+1* based exclusively on the state of day *D*, disregarding the influence of prior time steps.

## 3 Results and Discussion

**Well Clustering.** We identified two clusters of irrigation wells based on their recorded daily pumping depths (Figure 42). While analysing various physical and economic factors that can affect irrigation decisions, we noticed that daily wheat prices exclusively affected Cluster 1. In contrast, the irrigation decisions in Cluster 2 were affected by daily diesel prices, minimum temperature, and soybean prices, in addition to wheat prices. This finding further confirms the existence of two distinct clusters exhibiting different irrigation behaviors, despite the geographic proximity of some wells.

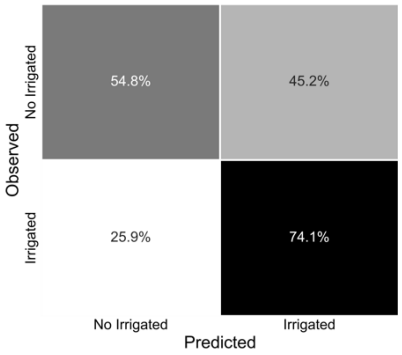


*Figure 43. Confusion matrix of irrigation events with 'Irrigated' and 'No Irrigated' denoting the model's predictions against the observed*

**Occurrence and States of Irrigation.** Considering the various factors that can influence irrigation decisions in Cluster 2, we accurately predicted the occurrence of daily irrigation events 74.1% of the time, with an overall accuracy of 65.8%, as shown in Figure 43. Furthermore, we classified irrigation into three states base on depth for all events and calculated the transition probabilities between these states (Figure 44). The results indicate a high likelihood of continuity in irrigation behavior; there is 77% chance of no irrigation occurring the following day if there was no irrigation on a given day. Conversely, if there was medium or large irrigation on the previous day, the probabilities of large irrigation the next day are 93% and 78%, respectively.

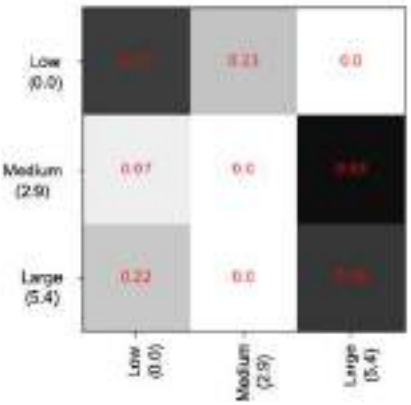


*Figure 44. Transition probabilities between three discrete states of irrigation depth: Low (0.0 mm), Medium (2.9 mm) and Large (5.4 mm).*

## 4 Conclusion

In this study, utilizing limited irrigation data from pumping wells, we identified two clusters of wells with similar irrigation dynamics and pinpointed the variables that can influence daily irrigation decision-making. With such information, we developed models to predict both the occurrence of irrigation events and the transition probabilities between different states of these events on a daily scale, which explains the intricacies of daily irrigation decision-making and enables us to scale up the predictive model from individual wells to predict daily irrigation practices across the HPAHOA.

## Reference

[1] Elshall, A. S., ... & Chun, G. (2020). Groundwater sustainability: A review of the interactions between science and policy. *Environmental Research Letters*, *15*(9), 093004.

[2] Sai Madiraju, N., Sadat, S. M., Fisher, D. & Karimabadi, H. Deep temporal clustering: Fully unsupervised learning of time-domain features. arXiv e-prints arXiv–1802 (2018).

**Theme:** Emerging concepts and solutions in modelling methods
**IAHR Thematic Priority Area:** [TPA-4] Digital Transformation
https://doi.org/10.3850/iahr-hic2483430201-315

# Graph-Based Neural Network for Contaminant Transport Modeling from Multiple Sources in Heterogenous Aquifers

**Min Pang[1,2], Erhu Du[1], Chunmiao Zheng[3]**

[1] The National Key Laboratory of Water Disaster Prevention, Hohai University, Nanjing, China
[2] College of Hydrology and Water Resources, Hohai University, Nanjing, China
[3] Eastern Institute of Technology, Ningbo, China

Corresponding author: pangmin@hhu.edu.cn

**Abstract.** Contaminant transport modeling in heterogeneous aquifers from multiple sources presents a complex and challenging problem in groundwater management. Traditional modeling approaches often encounter difficulties in capturing the intricacies of contaminant dispersion, limitations in available data, and the substantial computational demands. In this work, we propose a new deep learning method, known as the attention-based graph neural network (aGNN), to model contaminant transport with limited monitoring data. In four case studies involving varying monitoring networks in heterogeneous aquifers, aGNN is shown to outperform LSTM (long short-term memory) and CNN (convolutional neural network) based methods in multistep predictions. Furthermore, explanatory analysis based on aGNN quantifies the influence of each contaminant source, aligning with a physics-based model and achieving high $R^2$ values. The key advantage of aGNN is its ability to achieve high predictive accuracy across multiple scenarios while significantly reducing computational demands. Overall, our findings demonstrate that aGNN is an efficient and robust tool for nonlinear spatiotemporal learning in contaminant transport within the subsurface, offering promising applications in groundwater management.

**Keywords:** groundwater contamination, contaminant transport modeling, source attribution, deep learning, graph neural network

## 1 Introduction

Anthropogenic contamination has become a pressing issue jeopardizing the long-term sustainability of groundwater resources. Effective management of groundwater quality necessitates a thorough comprehension of the intricate links among contamination sources, pathways, and receptors within the system. (Soriano et al., 2021). While traditional approaches rely on physics-based models to simulate groundwater contamination dynamics (Gorelick and Zheng, 2015), employing large-scale physics-based models require lengthy simulation time, especially for multi-scenario evaluations, making studies computationally intensive and time-consuming (Pang and Shoemaker, 2023; Xia and Shoemaker, 2021). Recent advancements in data science and information technology have spurred the application of deep learning (DL) in complex modeling (Reichstein et al., 2019; Shen, 2018). DL techniques, notably LSTM and CNN showed high accuracy and efficiency. In this study, we propose a noval DL model, aGNN designed for multi-process contaminant transport modelling. We compare the performance of aGNN with CNN-based, LSTM-based methods for the task of spatial prediction over multiple steps, aiming to evaluate their effectiveness. Additionally, we employ an explainable AI technique to analyze the contributions of different factors to predictions and assess the time efficiency of aGNN in comparison to physics-based models. Our findings from various perspectives underscore the potential of attention-based graph models as promising tools for contamination modeling, with implications for policymakers involved in groundwater pollution management.

## 2 Methodology

The architecture of aGNN comprises five modules: input module, graph embedding module, encoder module, decoder module, and output module. Within the input module, there are two components: the encoder input and decoder input, both integrated into the spatiotemporal graph framework. Each of the encoder and decoder modules consists of two layers of a graph convolution network (GCN) enhanced with attention mechanisms. This network offers distinct advantages: firstly, the attention mechanism dynamically prioritizes relevant input elements, facilitating flexible learning of interrelations, and secondly, GCN effectively captures the graph's topological connections, producing predictions of target sequences, depicting the movement of contaminants.

## 3 Results

In the evaluation of temporal variations in modeling accuracy, Fig.1 illustrates that ConvLSTM consistently underperforms compared to other algorithms in multi-step prediction. Although DCRNN yields significantly smaller values, these values exhibit temporal variability. Conversely, aGNN can leverage the self-attention mechanism to dynamically adjust temporal weights based on time series input. Consequently, the values of aGNNs are lower, especially for predictions in the near future.

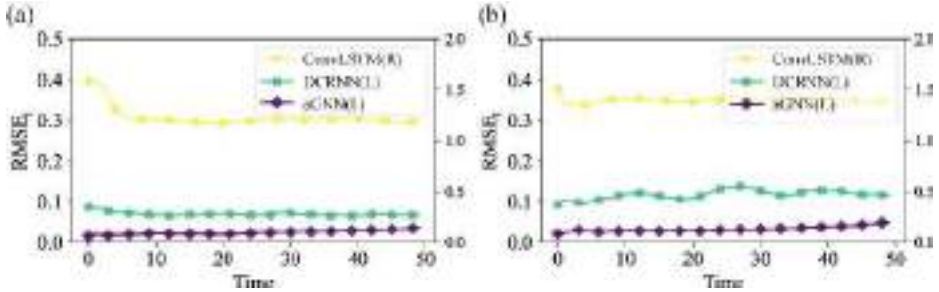


Figure 45 The temporal variations in modeling accuracy of three algorithms (a) Case A (b) Case B

Moreover, aGNN facilitates the attribution analysis of contaminant sources. Leveraging the SHAP method, the interpretations provided by aGNN establish connections between drivers (i.e., individual contaminant sources) and outcomes (i.e., induced contaminant concentration) aligning with the physical understanding of the contaminant transport process. The performance of aGNN underscores its exceptional accuracy and efficiency as a surrogate for numerical simulation models i.e., MODFLOW and MT3DMS in analyzing contaminant source attribution. It achieves an R2 value exceeding 96% and reduces the computational load of the physics-based model by 90%.

## Reference

[1] Gorelick, S.M., Zheng, C., 2015. Global change and the groundwater management challenge. Water Resour. Res. 51, 3031–3051. https://doi.org/10.1002/2014WR016825

[2] Pang, M., Shoemaker, C.A., 2023. Comparison of parallel optimization algorithms on computationally expensive groundwater remediation designs. Sci. Total Environ. 857, 159544. https://doi.org/10.1016/j.scitotenv.2022.159544

[3] Reichstein, M., Camps-valls, G., Stevens, B., Jung, M., Denzler, J., Carvalhais, N., 2019. Deep learning and process understanding for data-driven Earth system science. Nature 566, 196–204. https://doi.org/10.1038/s41586-019-0912-1

[4] Shen, C., 2018. A Transdisciplinary Review of Deep Learning Research and Its Relevance for Water Resources Scientists. Water Resour. Res. 54, 8558–8593. https://doi.org/10.1029/2018WR022643

[5] Soriano, M.A., Siegel, H.G., Johnson, N.P., Gutchess, K.M., Xiong, B., Li, Y., Clark, C.J., Plata, D.L., Deziel, N.C., Saiers, J.E., 2021. Assessment of groundwater well vulnerability to contamination through physics-informed machine learning. Environ. Res. Lett. 16, 084013. https://doi.org/10.1088/1748-9326/ac10e0

[6] Xia, W., Shoemaker, C.A., 2021. Improving the speed of global parallel optimization on PDE models with processor affinity scheduling. Comput. Civ. Infrastruct. Eng. 1–21. https://doi.org/10.1111/mice.12737

**Theme:** Emerging concepts and solutions in modelling methods
**IAHR Thematic Priority Area:** [TPA-4] Digital Transformation
https://doi.org/10.3850/iahr-hic2483430201-317

# Construction and Application of Monitoring and Early Warning Platform for Flash Floods in Hainan Province

**Xiaolei Zhang[1], Jinsong Zhou[2], Ronghua liu[1], Jiaxin Wang[1]**

[1] China Institute of Water Resources and Hydropower Research, 100038, Beijing, China
[2] Water Department of Hainan Province, 571126, Haikou, China

*Corresponding author: zhangxl@iwhr.com*

**Abstract.** Combined with advanced flash flood disaster prevention concepts and theoretical and technological advances in meteorology, hydrology and information technology, the overall framework of flash flood disaster monitoring, forecasting and early warning platform in Hainan Province was proposed, the overall framework, main functions and applications of the platform were designed, the application ways of big data on flash flood disaster investigation and evaluation were sorted out, and a multi-stage progressive flash flood disaster forecasting and early warning system and forecast were proposed The early warning model provides strong support for flash flood disaster prevention in Hainan Province.

**Keywords:** flash flood; monitoring and warning; platform

## 1 Technical Framework

The provincial flash flood disaster monitoring and early warning platform was built in Hainan Province in 2021 on the principle of emergency first. The system is built from three aspects, i.e. data, models and business, including flash flood disaster prevention data integration and sharing, geographic information services through "one map" for flash flood disaster prevention, real-time weather forewarning service and social publishing support for flash flood disasters, functional maturation of flash flood disaster monitoring and early warning system, and multi-stage forecasting and early warning system construction for flash flood disasters.

Figure 46 System framework Figure 2 Main functions of the system

## 2 System Functions and Features

(1) Flash flood disaster survey and evaluation results have been fully integrated and shared through the system, taking two main lines, i.e. "basin" and "administrative region", into account, thus achieving the general information integration, sharing and application of flash flood disaster

prevention of flash flood disasters. Flash floods can be warned early based on villages and basins, supporting the scientific prevention, commanding and decision-making;
(2) Except for the access to flash flood, hydrology, weather, real-time rain condition and water regimen, and forecasting data, the system has integrated the real-time monitoring data for large, medium-sized and small reservoirs, as well as the information flow for reservoir video and image stations in combination with the actual needs for reservoir management and protection in Hainan Province. It is able to fully master the real-time data on rain condition, water regimen and disasters of provincial medium or small rivers and reservoir projects, improving the management services of flash flood disaster prevention;
(3) Data is monitored three times a day through the access to the 1km refine grid-based weather forecast data, achieving the 24h early warning for flash flood disasters and weather risks throughout the province, which is released to the masses, enhancing the consciousness of flash flood disaster prevention in the whole province;
(4) The supervision management module is the focus of the system, enabling the classified management, abnormal station screening and platform operation monitoring of the accessed stations.

## 3 Platform Application

From May 15, 2022, 252 meteorologic early warnings have been cumulatively made based on the monitoring and early warning platform for flash floods in Hainan Province. Flash flood disaster survey and evaluation results of Hainan have been integrated, with the access to the 1km grid-based 24h rainfall forecasting data pushed by the Hainan Meteorological Service, and integrative validation of 999 automatic rainfall stations, 281 riverway water level stations, 14 riverway hydrological stations and 1118 reservoir hydrological stations in Hainan Province. 295 town- and village-based plans submitted by cities and counties have been collected, and the information of staff on duty in cities and counties has been updated, providing reliable data support and early warning basis for early warning of flash floods.


Figure 3 Meteorologic early warning based on this system

## Reference

[1]Guo L. Ding L.Q., Sun DY, et al. Key techniques of flash flood disaster prevention in China [J]. SHUILI XUEBAO,2018,49(09):1123-1136.
[2] Liu R.H, Liu Q., Zhang X.L., et al. System design and application of national flash flood disaster monitoringand warning platfrom[J]. China Water,2016(12):24-26.

**Theme:** Emerging concepts and solutions in modelling methods
**IAHR Thematic Priority Area:** [TPA-4] Digital Transformation
https://doi.org/10.3850/iahr-hic2483430201-319

# Research on Remote Joint Control Technology of Plant-Network-River Integration

**Min Lele[12],Tian Leqi[12],Li Hongwei[12],ZhaoLiang[12],Sun Yutian[12],Lu Zongren[12]**

（1.Shanghai Investigation Design&Research Institute Co.,Ltd.,Shanghai200335,China)
2.Three Gorges Smart Water Technology Co., Ltd., Shanghai 200050, China)

*Corresponding author:tianleqi@qq.com*

**Abstract.**Urban drainage control system is one of the key factors to ensure urban drainage transportation.The distribution of sewage plants, pipe network facilities ( storage tanks, intercepting wells, box culverts, etc. ), drainage and transportation lifting facilities ( integrated pumping stations, lifting pumping stations, etc. ), river gates and other facilities is relatively dispersed. The inter-plant joint scheduling system under emergency conditions has not been established,The efficiency expansion space of sewage pipe network, pumping station and sewage treatment plant is large.This paper studies the remote joint control technology of plant-network-river integration, designs a new SCADA system, remote joint control scheduling algorithm and control logic method of automatic control system.PLC is used to intuitively reflect the operation status of field equipment, and remote joint operation is realized through communication, which reduces the number of post operators and greatly improves the safety, reliability and economy of drainage equipment operation.

**Keywords：** Drainage; Remote control; Factory network river; SCADA

## 1 Introduction

In the sewage treatment system, the sewage pipe network, pumping station and other facilities in the basin of each sewage treatment plant are mostly in a relatively independent state, and the inter-plant joint scheduling system under emergency conditions has not been established. The efficiency expansion space of sewage pipe network, pumping station and sewage treatment plant is large[1].Therefore, it is imperative to carry out the research on the management system and technology of the integrated remote joint control of plant-network-rive in order to comprehensively solve the new SCADA system applying cloud platform + edge computing, remote joint control scheduling algorithm and control logic method of automatic control system.

## 2 Material and methods

The system is mainly composed of ground monitoring industrial computer, PLC control cabinet and field control box, detection sensor and video monitoring. According to the liquid level of the sewage plant, pumping station and peak valley power supply time,under the condition of unattended on-site, the pump can be turned on and off in an optimal way, which not only ensures safety but also achieves the purpose of energy saving[2].

## 3 Results and discussion

The centralized control system is an information system deployed to the large-screen display hardware. It plays an important role in providing monitoring information display and plant station control. It can macroscopically display the comprehensive operation situation of each plant station, intuitively show the construction results of drainage management, highlight the operation management ability and operation results of the enterprise, and have an excellent sense of use and viewing experience.

The sewage dispatcher starts the mature model to deploy and debug on the centralized control system, predicts the user 's drainage volume, analyzes and simulates the hydraulic model of the drainage pipe network, and optimize the pump group of the sewage pump station to obtain the optimal pump opening scheme. Rationally allocate the influent flow and water quality of each sewage plant, and formulate daily scheduling plans.According to the various monitoring data prompts of the centralized control center, the sewage dispatcher judges whether to adjust and control the sewage pump group according to the plan.

## 4 Conclusion

This paper establishes a set of intelligent joint control system applicable to the integrated management and control of plants, stations, networks and rivers, implements the integrated water control concept of "plants, stations, networks, rivers and lakes" for the Yangtze River protection, solves the current bottleneck of "monitoring but not control" in the water industry, and exerts the collaborative efficiency of decentralized water facilities,and effectively improves the effect of engineering measures such as water environment management, quality improvement and efficiency improvement in the Yangtze River protection.

## Reference

[1] Xu Kewei, Wang Jia, Li Huaibo, et al. Research on the construction of intelligent urban drainage pipe network information system, intelligent environmental protection,2023,9(2):102-105.

[2] Xu Deliang. Design and Application of Remote Automatic Control System for Underground Main Drainage in Iron Mine,2021,22(5):204-206.

**Theme:** Emerging concepts and solutions in modelling methods
**IAHR Thematic Priority Area:** [TPA-4] Digital Transformation
https://doi.org/10.3850/iahr-hic2483430201-321

# Hydrodynamic Modelling of Solute Transport Past Rigid Vegetation on the Graphics Processing Unit

**Georges Kesserwani[1,*], Xitong Sun[1], and Virginia Stovin[1]**

[1] Dept. of Civil and Structural Engineering, University of Sheffield, Sheffield, UK

*Corresponding author: g.kesserwani@sheffield.ac.uk*

**Abstract.** A practical approach to predict solute transport and mixing in environmental shallow flows is proposed using second-order discontinuous Galerkin (DG2) simulations of the two-dimensional (2D) shallow water equations (SWE) and of the advection-diffusion equation (ADE). Calibrated DG2-SWE simulations are used based on increased Manning's coefficients, $n_M$, to ensure physically acceptable ranges for fields required for the DG2-ADE simulations, i.e. the turbulent diffusivity, $D_t$, and turbulent kinetic energy, TKE, fields. The approach is successfully applied to simulate measured (temporal) concentration profiles and longitudinal (spatial) dispersion coefficients, $D_x$, from experiments involving flow past cylinder array under laminar, transitional, and low-turbulence regimes.

**Keywords:** Calibrated hydrodynamic simulations, Flow wakes past cylinders, High-resolution modelling, Solute transport, Laboratory experiments.

## 1 Introduction

In slow, quasi-steady, and uniform flow, the computation of solute transport requires addressing two steps [1]. First, the computation of the (time-averaged) components of the velocity field, and (m $s^{-1}$), and turbulent diffusivity field, ($m^2$ $s^{-1}$); and, second, the computation of the concentration fields by solving the ADE based on the computed , , and fields. Practically, these steps are still faced with many challenges [2]. The first step is hindered by the memory and runtime computational costs associated with the use of viscous turbulent flow simulators at a grid resolution near the turbulence-length scale. Hence, such simulators entail impractical costs even for a small area. For instance, the computation of , and maps over a 1 $m^2$ area for flows past thin cylinder(s), of diameter $d$ between 4 mm and 8 mm representing emergent vegetation [1], needs a resolution $\leq 0.005d$ [3]; that is, needs applying a turbulent flow simulator on a grid with more than 1 billion elements, which entails high graphics processing unit memory and days of runtime. This challenge can be addressed using DG2-SWE simulations at $0.25d$ grid resolution to efficiently produce accurate enough and maps [4]. The second step, in the scope of depth-integrated SWE simulations, is hindered by the lack of an implicit approach for the evaluation and calibration of , , and fields to meet acceptable ranges [2]. Moreover, the discretization of the advective fluxes, although requires high-order solvers [2], can fall short in preserving the positivity of the concentration fields due to knock-on effects from slope limiters that are inevitable for practical applications including thin cylinders acting as singularities.

## 2 Material and methods

Calibrated DG2-SWE simulations, with artificially increased $n_M$, were achieved to generate valid , , and fields for use to make DG2-ADE simulations supported by treatments for preserving positivity and robustness around singularities. The simulations were specific to reproduce experiments of flows in a 15 m long and 0.3 m wide flume fitted with randomly distributed cylinders [5]. The experiments covered laminar, transitional, and turbulent regimes. The turbulent regime used $d$ = 8 mm and cylinder density $\Phi = 0.027$ ($Re_d = 450$) with an $n_M$ =0.054, whereas $d$ = 4 mm and $\Phi = 0.005$ ($Re_d$ = 53 and 250) for the other two cases with an $n_M$ =0.045. The solute transport was generated by a pulse of dye, 4 m from four equidistant fluorometers at a distance of $x$ = 0, 2.5, 5 and 7.5 m with $\Phi = 0.005$ and $x$ = 0, 3, 6 and 9 m with $\Phi = 0.027$. Temporal concentration profiles were recorded and used to derive $D_x$ [5].

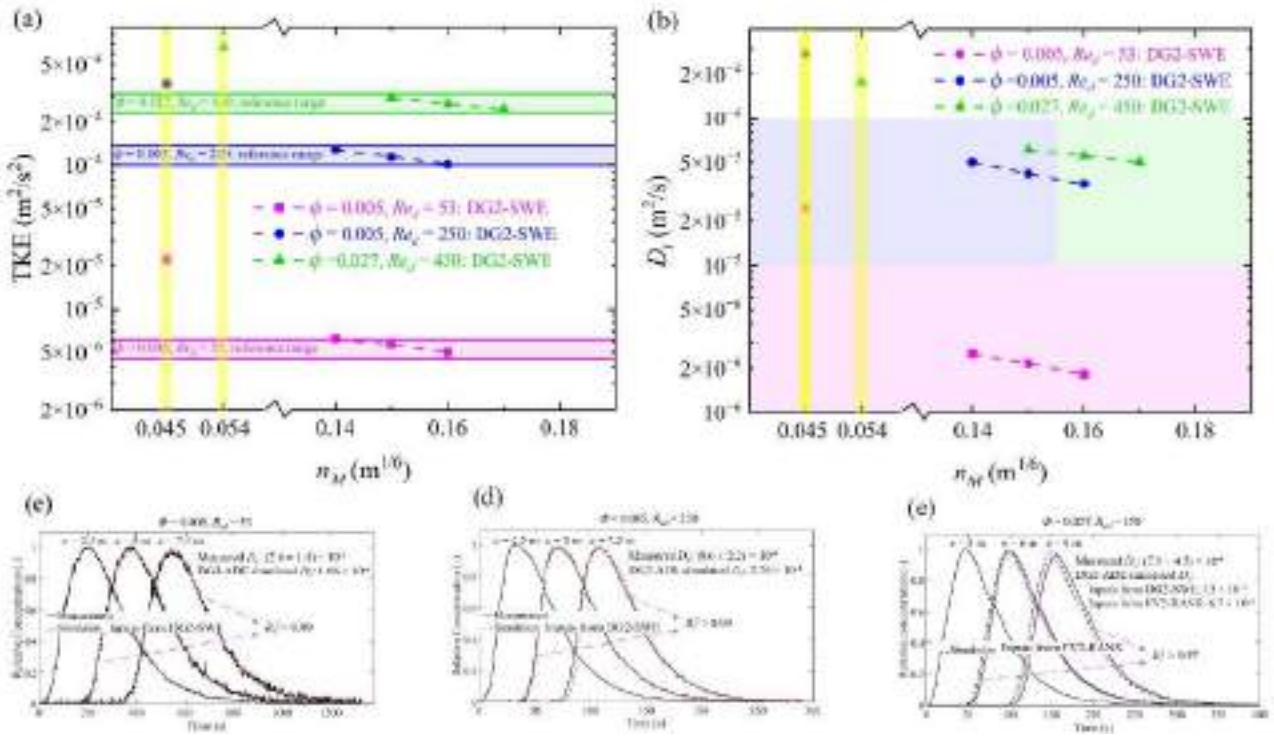


**Figure 1.** Calibrated DG2-SWE simulations, (a) and (b); and DG2-ADE simulations, (c)-(e).

## 3 Results, discussion, and conclusions

As seen in Fig. 1 (a) and (b), calibrated DG2-SWE simulations must use $n_M$ = {0.14, 0.15, 0.16} the case with $\Phi = 0.005$ and and $n_M$ = {0.15, 0.16, 0.17} for the case with $\Phi = 0.027$ to ensure valid , , and fields that are in valid ranges [6]. For the common value of $n_M$=0.15, the DG2-ADE simulation results are shown in Fig. 1 (c)-(e) for the three flow cases: $Re_d$ = 53, $Re_d$ = 250, and $Re_d$ = 450. The DG2-ADE predicted profiles are in good agreement with the measured profiles and the predicted $D_x$ has the same order of magnitude as the measured ones, both of which confirming the robustness of the proposed approach in simulating transport and mixing processes in shallow environments.

## Reference

[1] Stovin, V.R., Sonnenwald, F., Golzar, M. and Guymer, I., 2022. The impact of cylinder diameter distribution on longitudinal and transverse dispersion within random cylinder arrays. *Water Resources Research*, **58**(4), p.e2021WR030396.

[2] Mignot, Emmanuel, Nicolas Riviere, and Benjamin Dewals. Formulations and Diffusivity Coefficients of the 2D Depth-Averaged Advection-Diffusion Models: A Literature Review." *Water Resources Research* **59**, no. 12 (2023): e2023WR035053.

[3] Qu, L., Norberg, C., Davidson, L., Peng, S.H. and Wang, F., 2013. Quantitative numerical analysis of flow past a circular cylinder at Reynolds number between 50 and 200. *Journal of Fluids and Structures*, **39**, pp.347-370.

[4] Sun, Xitong, Georges Kesserwani, Mohammad Kazem Sharifian, and Virginia Stovin. Simulation of laminar to transitional wakes past cylinders with a discontinuous Galerkin inviscid shallow water model. *Journal of Hydraulic Research* **61**, no. 5 (2023): 631-650.

[5] Sonnenwald, F., Stovin, V. and Guymer, I., 2019. A stem spacing-based non-dimensional model for predicting longitudinal dispersion in low-density emergent vegetation. *Acta Geophysica*, **67**(3), pp.943-949.

[6] Tanino, Yukie, and Heidi M. Nepf. "Lateral dispersion in random cylinder arrays at high Reynolds number." *Journal of Fluid Mechanics* **600** (2008): 339-371.

**Theme:** Emerging concepts and solutions in modelling methods
**IAHR Thematic Priority Area:** [TPA-4] Digital Transformation
https://doi.org/10.3850/iahr-hic2483430201-323

# HPC Performance Tests of TELEMAC-2D on the Brague River Flood of October 2015

**Emmanuel Ah-woane[1], Thibaut Davarend[1], Florian Cordier[2], Zied Amama[2,3], Boris Basic[2], Arkadii Sochinskii[1], Mohamed Assaba[4], Samer Majdalani[5], Roger Moussa[6], Morgan Abily[7] and Olivier Delestre[8,3,1]**

[1] Polytech'Lab, Université Côte d'Azur, Sophia-Antipolis, UPR UniCA 7494, France
[2] EDF R&D LNHE-Laboratoire National d'Hydraulique et Environnement, Chatou, 78400, France
[3] Laboratoire d'Hydraulique Saint-Venant, Ecole des Ponts ParisTech – EDF R&D, Chatou, 78400, France
[4] Hydrologist and Expert for the Aix-en-Provence Court of Appeal, BET ELMA CONSEIL, Nice, 06100, France
[5] HSM, CNRS, IRD, Univ Montpellier, Montpellier, 34093, France
[6] LISAH, INRAE, IRD, Montpellier SupAgro, Univ Montpellier, Montpellier, 34060, France
[7] Université Côte d'Azur, CNRS, Observatoire de la Côte d'Azur, IRD, Géoazur, Nice, 06000, France
[8] LJAD, Université Côte d'Azur, CNRS, Nice, 06000, France

*Corresponding author: olivier.delestre@univ-cotedazur.fr*

**Abstract.** The Brague river often encounters flash floods, resulting in consequent damages. The cities of Biot and Antibes were particularly affected in October 2015. This flood event was previously studied both using hydrological and hydraulic approaches, such as 2D hydraulic modelling tools (Basilisk, HEC-RAS and TELEMAC-2D) and the FEV approach. Here, we propose to restart from a previous existing numerical model built with TELEMAC-2D, which simulates the flood event of 2015 in the downstream area of the Brague river, based on a 2D approach on an unstructured mesh. The objective of this work is to check the HPC performance of TELEMAC-2D on this study case by considering different levels of mesh resolutions.

**Keywords:** Domain decomposition, Flash floods, HPC, Hydraulic modelling, MPI, TELEMAC-2D

## 1 The Brague study case

The lower part of the Brague catchment is interesting in terms of hydraulic study due to its wide floodplain (figure 1a). The area was impacted by a severe flash flood in October 2015. A previous TELEMAC-2D model has been developed with a coarse mesh to study this specific event [1]. This work proposes an assessment of the HPC performance of TELEMAC-2D on the Brague floodplain case study. A finite elements method is used on unstructured triangular meshes. Four meshes resolutions are considered: 1 m mesh (5,177,909 nodes/10,263,426 elements; see figure 1b), 2 m mesh (1,299,558 nodes/2,553,485 elements), 4 m mesh (328,047 nodes/633,931 elements), and 8 m mesh (89,419 nodes/168,793 elements). A digital terrain model of 1 m resolution (from IGN, [2]) is used, and has been modified at the culverts locations (A8 highway) to allow the water to flow. The bottom roughness is spatialized based on the Strickler friction law. Buildings are represented by holes in the mesh. The time step is 0.1 s for the 1 m mesh and is multiplied by 2 for each increased mesh resolution (respectively 0.2-0.4-0.8 s for 2-4-8 m meshes), in order to keep a similar CFL through the different models.

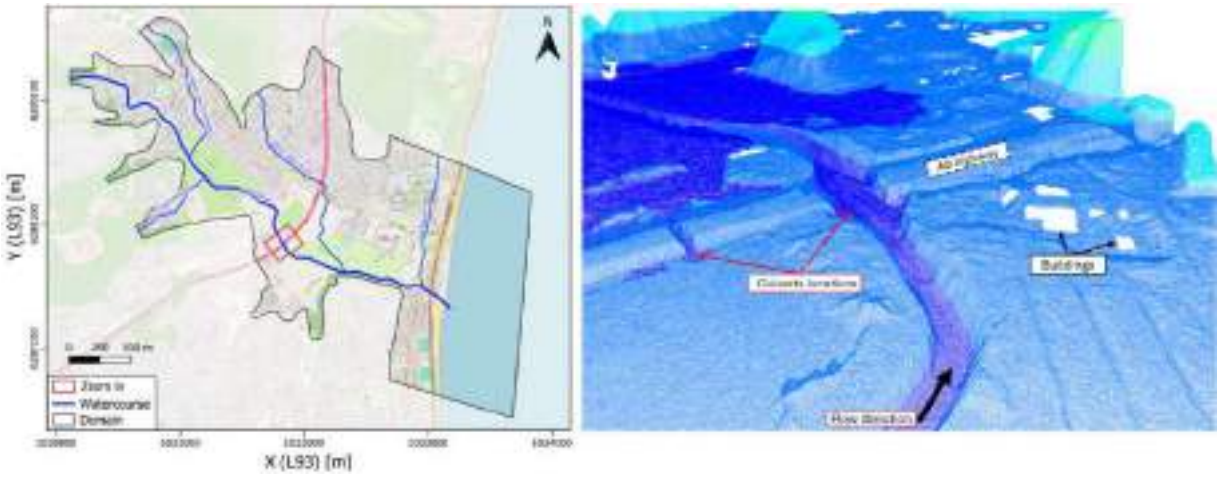


Figure 1 (a) The Brague study domain and its four tributaries, (b) zoom on part of the 1 m resolution mesh with topographic layout.

## 2 Preliminary results

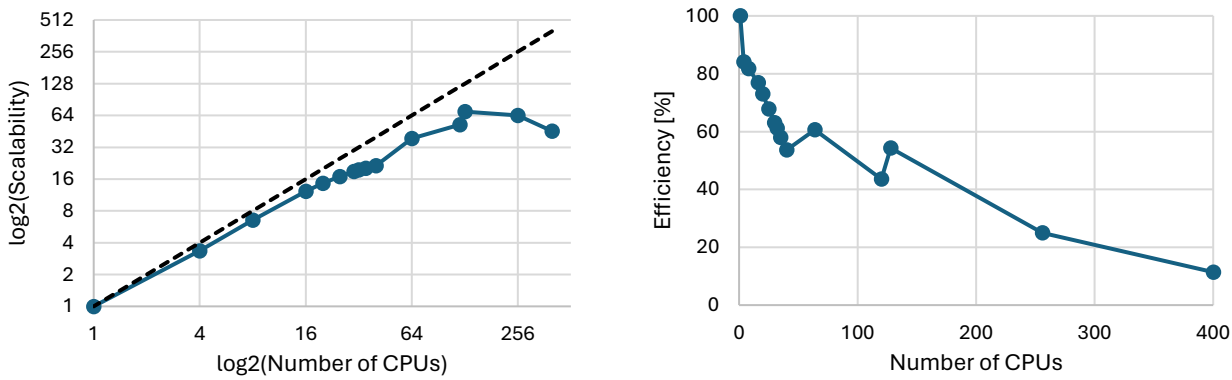


Figure 2 (a) Scalability and (b) efficiency for parallel processing of the 4 m resolution mesh for different number of CPUs. The dashed line corresponds to the ideal case identity.

The preliminary result of scalability (figure 2a), based on 4 m resolution mesh, shows a good performance of parallel processing from 1 to 128 CPUs, with a nearly linear progression. The scalability is below the ideal case though, which falls in agreement with theory. From 128 CPUs, the performance starts to collapse. The efficiency of parallel processing decreases rapidly, from 84% with 4 CPUs to 54% with 40 CPUs, compared to 1 CPU. At 400 CPUs, efficiency falls by up to 11% (figure 2b). Other results (different meshes, different metrics, etc.) will be presented later at the conference and in the extended article.

### Acknowledgements

The authors are grateful to the OPAL infrastructure and the Université Côte d'Azur's Center for High-Performance Computing for providing resources and support, financed by the UCAJEDI Investments in the Future project (ANR-15-IDEX-01) managed by the National Research Agency.

### Reference

[1] Cordier, F., Davarend, T., Ah-Woane, E., Amama, Z., Sochinskii, A., Majdalani, S., Moussa, R., Assaba, M., & Delestre, O. (2023). Simulation of the Brague flood of october 2015 in southeast of France. Conference Simhydro 2023, Chatou - France. Preprint available from https://easychair.org/publications/preprint_download/C2t5

[2] IGN (2018). RGE ALTI version 2.0. Descriptif de Contenu, 38, https://geoservices.ign.fr/sites/default/files/2021-07/DC_RGEALTI_2-0.pdf

**Theme:** Emerging concepts and solutions in modelling methods
**IAHR Thematic Priority Area:** [TPA-4] Digital Transformation
https://doi.org/10.3850/iahr-hic2483430201-325

# SERGHEI-GW: An Efficient High-Performance Variably-Saturated Groundwater Model

**Na Zheng[1], Zhi Li[1,*], Daniel Caviedes-Voullième [2,3], Mario Morales-Hernández [4,5]**

[1] College of Civil Engineering, Tongji University, Shanghai, China
[2] Simulation and Data Lab Terrestrial Systems, Forschungszentrum Jülich, Forschungszentrum Jülich, Jülich, Germany
[3] Institute of Bio- and Geosciences: Agrosphere (IBG-3), Forschungszentrum Jülich, Germany
[4] Fluid Mechanics, I3A, Universidad de Zaragoza, Zaragoza, Spain
[5] Oak Ridge National Laboratory, Oak Ridge, USA

** Corresponding author: zli90@tongji.edu.cn*

**Abstract**. Groundwater is vital for water security and aquatic ecosystems. Numerical simulation of groundwater flow, especially variably-saturated groundwater flow, is computational expensive due to the nonlinearity of the governing equations. High-performance computing (HPC) enhances the computational efficiency of traditional groundwater models. We propose an efficient variably-saturated groundwater model, named SERGHEI-GW, that solves the 3D Richards equation. SERGHEI-GW is developed based on the SERGHEI model system and under the Kokkos parallelization framework, which allows flexible model deployment on GPUs and CPUs without modifying the source code. The proposed groundwater model could be potentially coupled with SERGHEI shallow water module for catchment-scale surface-subsurface flow simulation. We present the model formulations and the testing results against existing benchmark problems and groundwater models. Notably, on a single desktop GPU, the computational efficiency of SERGHEI-GW exceeds serial CPU execution by over 200 times. SERGHEI-GW offers researchers a reliable, fast, and adaptable tool for simulating variably-saturated groundwater flow. Relevant for rapidly modeling complex hydrological processes and responding to extreme events induced by global climate change.

**Keywords:** Groundwater model, High-performance computing, Kokkos, Richards solver

## 1 Introduction

Groundwater plays a pivotal role in the hydrological cycle, and the application of the Richards equation is commonplace for simulating variably-saturated groundwater processes[1,2]. However, challenges arise due to the inherent nonlinearity of the equation and the interplay of nonlinear parameters representing soil properties, hindering the attainment of accurate solutions[3]. Moreover, when investigating catchment-scale hydrological processes, the time required for solving the Richards equation can be prohibitively extensive.

High-performance computing (HPC) has significantly enhanced the computational efficiency of traditional hydrological models, potentially enabling the use of large-scale, high-resolution, multi-domain, and multi-process hydrological simulations for hydrological research[4]. To enable flexible switching between various HPC platforms, we use the Kokkos system employed in SERGHEI to construct our variably-saturated groundwater model. The Simulation Environment for Geomorphology, Hydrodynamics, and Ecohydrology in Integrated form (SERGHEI)[5] is an open-source multi-physics model framework for environmental, hydrological, and earth system simulations, continually evolving. Its surface hydrology solver, released as SERGHEI-SWE, has demonstrated satisfactory results.

In this paper, we propose an efficient high-performance variably-saturated groundwater model named SERGHEI-GW. The model uses both iterative and non-iterative methods to solve the three-

dimensional (3D) Richards equation, enhancing flexibility in the solution process. The application of the 3D Richards equation overcomes limitations associated with the existing one-dimensional (1D) representation of the unsaturated zone, thereby improving the model's accuracy, especially in the presence of strong lateral flow. Additionally, the integration of the Kokkos system allows the SERGHEI-GW model to be flexibly employed on both CPU-based and GPU-based HPC platforms, ensuring good portability and scalability.

The accuracy and efficiency of SERGHEI-GW are validated through three numerical cases. Furthermore, we integrate SERGHEI-GW with SERGHEI-SWE to explore more efficient simulations of surface-groundwater interactions, resulting in promising preliminary results.

## 2 Methodology

In this paper, groundwater hydrological processes are reliably simulated by employing the 3D Richards equation. Soil properties are characterized using the Mualem-van Genutchen (VG) model [6,7]. For numerical solution methods, we use both an iterative approach, the modified Picard (MP) scheme[8], and a non-iterative method, the predictor-corrector (PC) scheme[9,10]. This dual scheme strategy enables the groundwater flow solver to operate flexibly across various solution modes.

Utilizing the Kokkos framework facilitates flexible execution of SERGHEI-GW model across both CPU and GPU platforms. In Section 4, we conduct comparative analyses of computational time between CPU and GPU implementations using the same study cases to demonstrate disparities in computational efficiency.

## 3 Study Cases

In this section, we describe the three benchmarks used in this paper and verify the SERGHEI-GW model through calculation results. Case 1 and Case 2 involve solely groundwater simulation, while Case 3 encompasses both surface water and groundwater calculations. Case 1 involves a 1D infiltration problem from Warrick et al. (1985)[11]. The simulation duration is 46800s, during which a fixed pressure head of 0m is maintained on the top boundary, while the other boundaries are impermeable. The simulated water content results at 3.25h, 6.5h and 13h are compared with the analytical solution in Figure 1(a). Case 2 is a 1D free drainage experiment from Abeele (1984) [12]. The domain size setting and soil properties are identical to Case 1. At the beginning of the simulation, the soil is fully saturated and the bottom of the domain is set at 0m. Figure 1(b) illustrates the simulated water content results at 1 day, 4 days, 20 days, and 100 days. The reference data is obtained from the experiment. Case 3 is a 2D superslab with three difference soil types[13]. The domain size is 400m in x-direction and 5m in z-direction. The simulation time is 12h, experiencing rainfall at an intensity of 50 mm/h during the initial three hours. The simulated saturation results are compared with some widely used models (ParFlow, CATHY, HGS, Cast3M) in Figure 1(c).

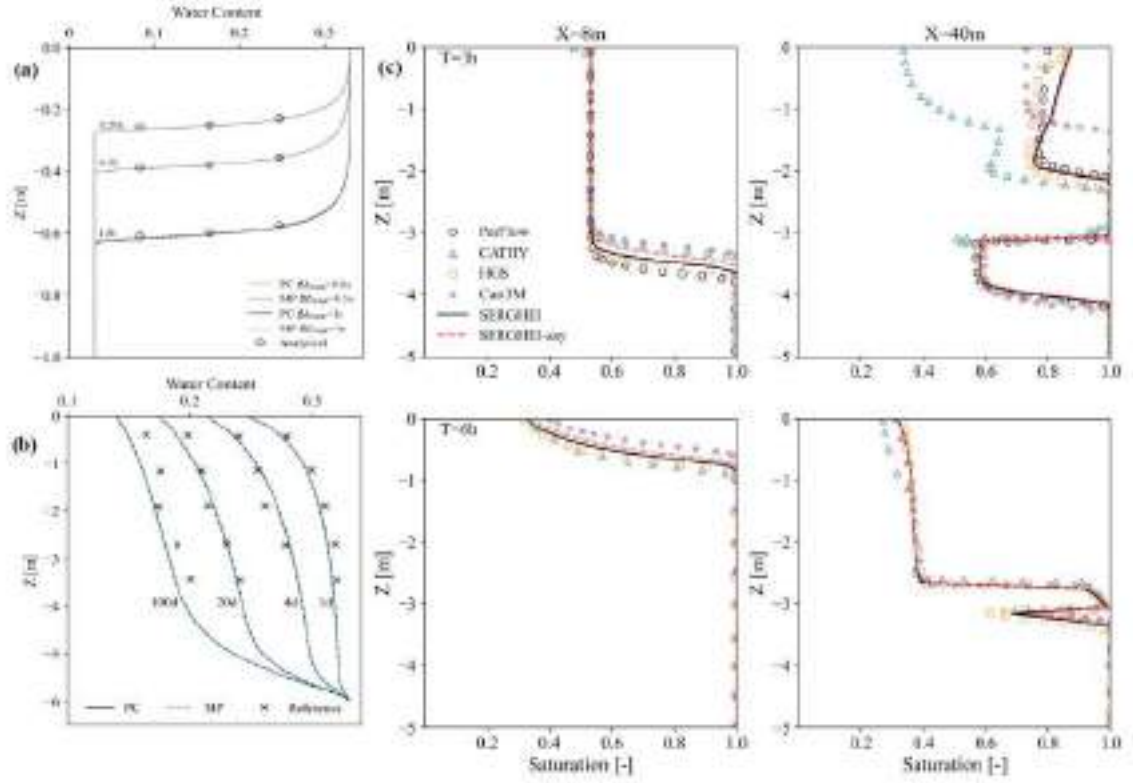


**Figure 1.** The simulated results.

## 4 Results and Discussion

As shown in the Figure 1 that across different study cases, the SERGHEI-GW model consistently produces the simulated water content or saturation that align well with analytical solutions, experimental results, and other widely used hydrological models. Notably, in Case 1 and Case 2, both the PC and MP methods exhibit negligible differences.

Regarding computational efficiency, the effectiveness of GPU acceleration increase becomes increasingly evident as simulation scale grows. The computational times for Case 3 are 44369s and 445s when performed on a Intel Core i9-12900K CPU(3.2 GHz, 16 cores, 24 threads) and an Nvidia RTX A5000 GPU (24 GB memory, 768 GB/s bandwidth, 8192 CUDA cores), respectively. This highlights the crucial role of high-performance computing, particularly for large-scale hydrological simulation.

## 5 Conclusion

The SERGHEI-GW model provides a reliable, fast, and flexible approach for simulating and calculating groundwater processes. The integration of the Kokkos framework supports continuous updates and functional enhancements of the SERGHEI-GW model. Across the three study cases presented in this paper, comparisons of computational times demonstrate a significant improvement in simulation speed through the use of GPUs. This result holds support for the simulation of large-scale and long-term hydrological processes.

Furthermore, the combination of SERGHEI-GW with SERGHEI-SWE expands the model's application scenarios. This integration provides a new approach for comprehensively simulating the hydrological cycle, as well as water resources management and risk assessment.

In conclusion, the SERGHEI-GW model represents an effective tool for simulating and calculating groundwater dynamics within the hydrological cycle, leveraging high-performance computing methods.

## Acknowledgments

This study is supported by the Fundamental Research Funds for the Central Universities (China).

## References

[1] Gleeson, T., Wada, Y., Bierkens, M. et al., 2012, Water balance of global aquifers revealed by groundwater footprint. Nature, 488, 197–200.

[2] Gunduz, O. and Aral, M. M., 2005, River networks and groundwater flow: a simultaneous solution of a coupled system, Journal of Hydrology, 301, 216–234.

[3] Lehmann, F. and Ackerer, P., 1998, Comparison of Iterative Methods for Improved Solutions of the Fluid Flow Equation in Partially Saturated Porous Media, Transport in Porous Media, 31, 275–292.

[4] Le, P. V., Kumar, P., Valocchi, A. J., and Dang, H.-V., 2015, GPU-based high-performance computing for integrated surface–sub-surface flow modeling, Environmental Modelling Software, 73, 1–13.

[5] Caviedes-Voullieme, D., Morales-Hernandez, M., Norman, M. R., Oezgen-Xian, I., 2023, SERGHEI (SERGHEI-SWE) v1.0: a performance-portable high-performance parallel-computing shallow-water solver for hydrology and environmental hydraulics, Geoscientific Model Development, 16, 977–1008.

[6] Mualem, Y., 1976. A new model for predicting the hydraulic conductivity of unsaturated porous media. Water Resources Research, 12, 513–522.

[7] Van Genuchten, M., 1980. A closed-form equation for predicting the hydraulic conductivity of unsaturated soils. Soil Science Society of America Journal, 44, 892–898.

[8] Celia, M.A., Bouloutas, E.T., Zarba, R.L., 1990. A general mass-conservative numerical solution for the unsaturated flow equation. Water Resources Research, 26, 1483–1496.

[9] Kirkland, M.R., Hills, R.G., Wierenga, P.J., 1992. Algorithms for solving richards' equation for variably saturated soils. Water Resources Research, 28, 2049–2058.

[10] Li, Z., Ozgen-Xian, I., and Maina, F. Z., 2021: A mass-conservative predictor-corrector solution to the 1D Richards equation with adaptive time control, Journal of Hydrology, 592, 125809.

[10] Warrick, A.W., Lomen, D.O., Yates, S.R., 1985. A generalized solution to infiltration. Soil Science Society of America Journal, 49, 34–38.

[12] Abeele, W. V., 1984, Hydraulic testing of crushed Bandelier Tuff. United States, https://www.osti.gov/biblio/60528.

[13] Kollet, S., Sulis, M., Maxwell, R. M., Paniconi, C., Putti, M., Bertoldi, G., Coon, E. T., Cordano, E., Endrizzi, S., Kikinzon, E., Mouche, E., Mügler, C., Park, Y.-J., Refsgaard, J. C., Stisen, S., and Sudicky, E.: The integrated hydrologic model intercomparison project, IHMIP2: A second set of benchmark results to diagnose integrated hydrology and feedbacks, Water Resources Research, 53, 867–890.

**Theme:** Emerging concepts and solutions in modelling methods
**IAHR Thematic Priority Area:** [TPA-4] Digital Transformation
https://doi.org/10.3850/iahr-hic2483430201-329

# Efficient Leakage Detection in Pressurized Looped Pipelines

**PAN Bin[1], DUAN Huanfeng[2], CHE Tongchuan[1], KERAMAT Alireza[1], WANG Manli[1]**
[1] Department of Civil and Environment Engineering, The Hong Kong Polytechnic University, Hung Hom, Kowloon, 999077 Hong Kong SAR, PR China.

*Corresponding author: hf.duan@polyu.edu.hk*

**Abstract.** The forward-backward transient analysis is capable of converting the transient-based defect detection procedure from a traditional inverse analysis into a forward problem analysis which does not rely on optimization. While the forward-backward transient analysis has been adapted for identifying defects in tree-shape pipe networks in our previous research, due to the complex multiple wave travel path characteristics of the looped pipe networks, its application to looped pipe networks remains challenging. To address this, it is essential to understand the transient behavior within each primary pipe loop of the pipe network to facilitate the continuation of the transient analysis in such systems. This paper focuses on refining the forward-backward transient analysis to enhance leak detection capabilities in looped pipe networks. The key strategy is to use additional pressure and discharge sensors to transfer a looped pipe system into an equivalent tree-shaped configuration. Then by using calculation order, the intact pipes can be gradually excluded, leading to the identification of the compromised pipe. The newly proposed algorithm for defect detection in looped pipe networks shows a significant step forward for the development of forward-backward transient analysis and transient research.

**Keywords:** Leakage detection, transient-based method, time domain analysis, forward-backward transient analysis

## 1 Introduction

The transient-based defect detection mainly relies on optimization, which usually suffers from the influence of local minima and maxima[1]. Besides, the huge amount of computational burden in solving an inverse problem may often go beyond practical availability[2]. Recently, the forward-backward transient analysis has been proposed and can identify the defective pipe without performing any optimization procedure. However, currently, it can only be used for breaking pipe identification in tree-shape pipe networks[3], which constrains the application of the forward-backward transient analysis in practice.

To further develop this method, this paper tries to expand the forward-backward transient analysis to encompass looped pipe networks, and principles of sensor layout for conducting the forward-backward transient analysis in looped pipe systems are proposed and validated by numerical cases. The findings as well as the recommendations for the forward-backward transient analysis are summarized at the end of this paper.

## 2 Methodology

The proposed forward-backward transient analysis reshapes the Method of Characteristics (MOC) calculation from progressing in time to advancing in space. The application procedure of the forward-backward transient analysis in a looped pipe network is to use measured pressure and discharge signals to convert a looped pipe network to a pipe network with only branched structures so that the forward-backward transient analysis can analyze the transient in each pipeline until the defective pipe is found.

## 3 Numerical Validation

To show this, a synthetic looped pipe network (as shown in Fig.1(a)) consisting of 21 pipes, four primary loops, 12 branched junctions, five outlets (B, C, D, E, F), and one inlet (e.g., A) is used to validate this newly proposed method. In this pipe network, once the time histories of the head and discharge rate are measured at nodes A-

E and the inlet boundaries of Pipes (6), (7), (10), and (20), the pipeline system can be converted into a tree-shape pipeline as shown in Fig.1(b). In validation, a leak with the leak effective area of 1.96e-4 $m^2$ is set at pipe 5, and is 60 m away from Junction [2]. The injected transient wave for leak detection purposes is triggered by the fast closure of the valve at node C. According to the typology structure of Fig.1(a), the calculation order is determined as: [6]-[7]-[8]-[5]-[11]-[12]-[10]-[3]-[1]-[2]-[9]-[4]. The results show that once the forward-backward transient analysis is calculated across the defective pipeline (e.g., Pipe 5), discrepancy emerges as shown in Figure 2 (c) and (d), and the leak is in the pipeline where the leak-induced wavefront (which is not physical and is caused by the intact pipe assumption) arrives at the junction earlier (e.g., Fig.1(d)).

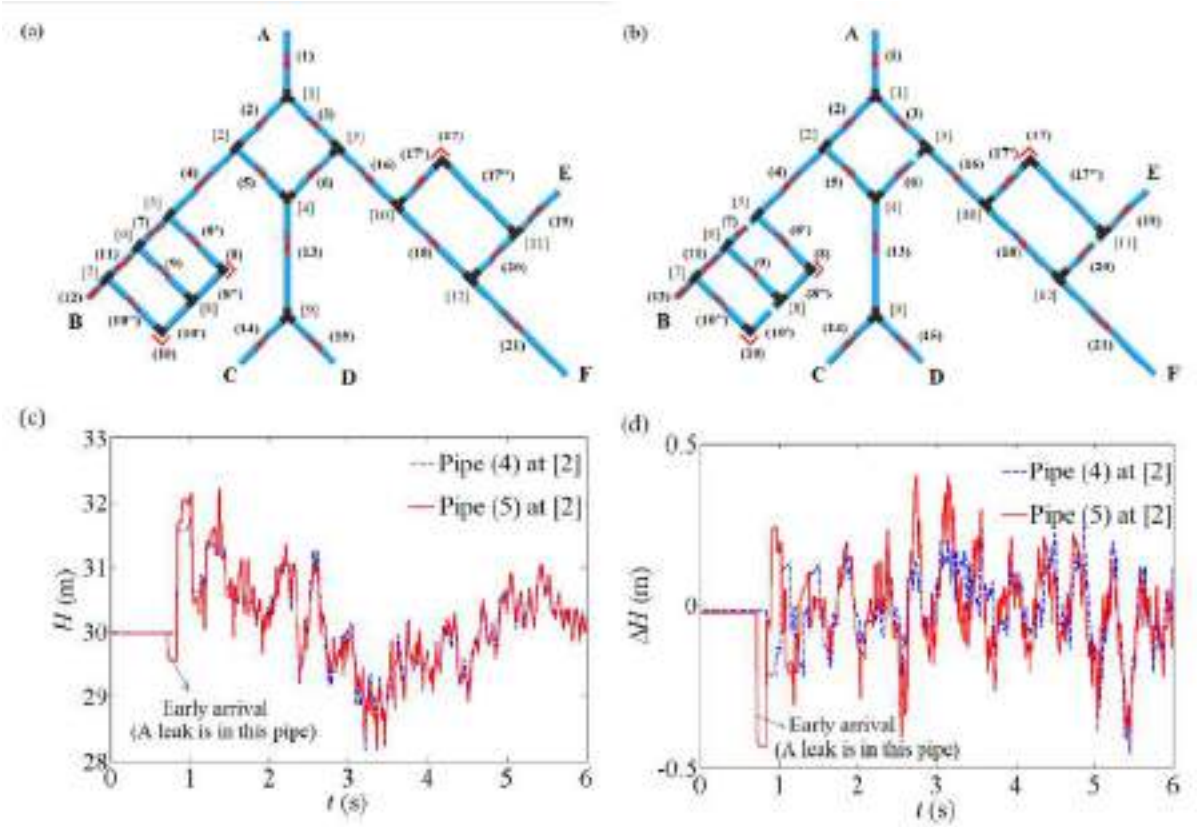


Figure 1 (a) the synthetic looped pipe network; (b) its equivalent tree-shape pipe network by using sensors; (c) the full obtained signals at [2]; (d) the leak-induced pressure signals at [2]

## 4 Conclusions

This paper successfully advances the application of the forward-backward transient analysis for leaky pipe identification in looped pipe networks. The main idea is to use the measured pressure and discharge data to transform looped structures into equivalent branched structures, thereby enabling the application of forward-backward transient analysis across the entire pipe system. Future research should delve into assessing the influence of noise on the accuracy of forward-backward transient analysis.

## Reference

[1] G.A. Nash, B.W. Karney, Efficient inverse transient analysis in series pipe systems, Journal of Hydraulic Engineering, 125 (1999) 761-764.

[2] H.-F. Duan, B. Pan, M. Wang, L. Chen, F. Zheng, Y. Zhang, State-of-the-art review on the transient flow modeling and utilization for urban water supply system (UWSS) management, Journal of Water Supply: Research and Technology-Aqua, (2020).

[3] B. Pan, H.F. Duan, A. Keramat, S. Meniconi, B. Brunone, Efficient Pipe Burst Detection in Tree-Shape Water Distribution Networks Using Forward-Backward Transient Analysis, Water Resources Research, 58 (2022) e2022WR033465.

**Theme:** Emerging concepts and solutions in modelling methods
**IAHR Thematic Priority Area:** [TPA-4] Digital Transformation
https://doi.org/10.3850/iahr-hic2483430201-331

# Advancing Environmental Simulation through SERGHEI: Novel Approaches in Hydrodynamic Modeling

**Mario Morales-Hernández[1], Sergio Martínez-Aranda[1], Pablo Vallés[1], Jose Segovia-Burillo[1], Pilar Brufau[1], Pilar García-Navarro[1]**

[1] Fluid Mechanics, I3A-Universidad de Zaragoza, Calle María de Luna, 3, Edif. Torres Quevedo, Zaragoza, 50018, Spain

*Corresponding author: mmorales@unizar.es*

**Abstract.** In the realm of environmental science, accurate simulation of hydrodynamic phenomena is essential. The SERGHEI framework stands out for its innovative modules that improve modeling of hydrological, environmental, and geomorphological processes. Our study introduces three new modules - Lagrangian Particle Tracking (LPT), Advection-Diffusion-Equation (ADE), and Sediment Transport (ST) - to enhance SERGHEI's capabilities. SERGHEI, an open-source toolkit for high-performance computing, is designed for performance portability and leverages CPU and GPU parallel processing, with the code available at https://gitlab.com/serghei-model/serghei. The LPT module enhances modeling precision by tracking particles in fluid flows, useful for analyzing debris movement during floods. The ADE module expands SERGHEI's capabilities to simulate pollutant diffusion and nutrient distribution, crucial for assessing environmental impacts. Lastly, the ST module enables the simulation of sediment movement, to simulate erosion control and habitat preservation. Despite these advancements, integrating these modules poses computational challenges, which our research addresses through optimization techniques to maintain high efficiency.

**Keywords:** lagrangian transport, high performance computing, hydrodynamic modeling, sediment transport, SERGHEI

## 1 Introduction

The continuous development of computational hydrodynamics has led to a period where intricate environmental occurrences can be replicated with unparalleled precision using large temporal and spatial scales combined with high resolution numerical models. SERGHEI [1] is at the forefront of this progress. This work presents three innovative components that have been incorporated into the SERGHEI framework: Lagrangian Particle Tracking (LPT), Advection-Diffusion-Equation (ADE), and Sediment Transport (ST). These components greatly improve the framework's ability to simulate complex natural processes in a more unified, thorough, and detailed manner.

## 2 The SERGHEI framework

SERGHEI, the Simulation Environment for Geomorphology, Hydrodynamics, and Ecohydrology in Integrated form, is an open-source, multidimensional simulation tool designed for hydrological, environmental, and geomorphological flows. Developed using C++ and Kokkos to ensure performance portability across a variety of High-Performance Computing (HPC) systems, SERGHEI incorporates highly parallel algorithms that are optimized for both Central Processing Units (CPUs) and Graphics Processing Units (GPUs) using MPI, OpenMP, and CUDA (HIP has been tested already it is still experimental). The source code for SERGHEI can be accessed at https://gitlab.com/serghei-model/serghei.

### 2.1 LPT module

The LPT module utilizes the current Eulerian velocity field every time step to perform a Lagrangian movement of the particles across the grid cells. This ensures an accurate handling of particles moving through wet/dry fronts, a critical issue in 2D flood numerical models. It also includes a random walk algorithm to realistically mimic turbulence effects on particle movement, which requires generating random numbers, a computationally intensive task that could affect simulation speed.

### 2.2 ADE module

The ADE solver in SERGHEI is capable of handling multiple scalars, providing versatility to the framework. Each additional scalar has the potential to increase the computational workload, a challenge that has been tackled through optimized algorithm design. Furthermore, the diffusion term in the ADE solver utilizes a sub-step explicit approach, which although accurate, can slow down computations.

### 2.3 ST module

The ST module uses the ADE module and incorporates new source terms that accounts for erosion/deposition processes. Similar terms are also incorporated in the momentum and mass equations in order to accurate model these phenomena [2]. This implementation poses unique challenges due to its involvement in altering bed evolution, flow characteristics, and incorporating equations for sediment transport species.

## 3 Results and discussion

A sensitivity analysis on the number of tracked particles and the turbulence model has been carried out (see Table 1) to strike a balance between simulation accuracy and computational efficiency on the LPT module.

Table 9 Computational times and overhead (in parenthesis) for different cases in the LPT module

| | 0 particles | $10^5$ particles | 5 x$10^5$ particles | $10^6$ particles |
|---|---|---|---|---|
| No turbulence | 60.5 s (-) | 79.8 s (1.32) | 143.0 s (2.36) | 222.7 s (3.68) |
| Turbulence | 60.5 s (-) | 92.0 s (1.52) | 210.5 s (3.47) | 367.4 s (6.07) |

Additionally, other simulations have been conducted to assess the impact of this diffusion term on the overall computational load in the ADE module, as well as on the additional computational requirements and communication overhead introduced by the ST module. We evaluate how these factors influence the scalability, efficiency, and load distribution of simulations, especially in large-scale environmental investigations.

## 4 Conclusions

The recent components in the SERGHEI framework greatly improve its capabilities in simulating complex environmental cases. Our research tackles these obstacles directly, presenting approaches to enhance performance and carrying out thorough examinations to grasp the consequences of these advanced characteristics on computational effectiveness, scalability, and load balancing.

## References

[1] D. Caviedes-Voullieme, M. Morales-Hernández, M. R. Norman, and I. Ozgen-Xian, "SERGHEI (SERGHEI-SWE) v1.0: a performance-portable high-performance parallel-computing shallow-water solver for hydrology and environmental hydraulics," Geosci. model dev., vol. 16, pp. 977-1008, 2023. J.

[2] J. Fernández-Pato, S. Martínez-Aranda, and P. García-Navarro, "A 2D finite volume simulation tool to enable the assessment of combined hydrological and morphodynamical processes in mountain catchments," Advances in water resources, vol. 141, p. 103617, 2020.

**Theme:** Emerging concepts and solutions in modelling methods
**IAHR Thematic Priority Area:** [TPA-4] Digital Transformation
https://doi.org/10.3850/iahr-hic2483430201-333

# Consideration of XAI In Inflow Prediction Model Using Convolutional Neural Network for Multiple Dams

**Kenta Hakoishi [1], Masayuki Hitokoto[1], Shingo Zenkoji [1], Ryota Nishiguchi[2]**

[1] R&D Center, NIPPON KOEI Co., Ltd. 2304 Inarihara, Tsukuba-shi, Ibaraki 300-1259, Japan
[2] Watershed & Water Management Operations, NIPPON KOEI Co., Ltd. 5-4 Kojimach, Chiyoda-ku, Tokyo 102-8539, Japan

*Corresponding author: hakoishi-kn@n-koei.jp*

**Abstract.** In this study, we developed the dam inflow prediction model using a 2D-CNN, taking the reanalysis precipitation from the Japan Meteorological Agency as the input condition. We applied XAI technology to visualize which input data influence the prediction results. The objective areas are the Haji Dam basin in the Gonokawa river system and the Nomura Dam basin in the Hijikawa river system in Japan. As the results of the case study, we could confirm that the degree of influence of each input data was reasonable in the sense of the rainfall-runoff mechanism.

**Keywords:** Convolutional Neural Network, Explainable AI, Runoff analysis, Dam inflow prediction

## 1 Introduction

With the advancement of AI technology, the application of technology in the analysis of dam outflows, including inflow prediction, has been actively pursued. As a case study, Hitokoto[1] improved the accuracy by applying a fully connected neural network model called Multi-Layer Perceptron (MLP) with data augmentation using previous floods, virtual floods, and conceptual models for training. Nishiguchi[2] confirmed the superiority of convolutional neural network (CNN) through a comparison of accuracy. However, a significant issue arises with the "AI black box problem." where it becomes difficult for humans to understand the internal processes. Based on this background, there has been a growing interest in Explainable AI (XAI) technologies in recent years, aiming to enhance the interpretability of AI prediction results. Therefore, in this study, in addition to the Haji Dam, we used the Nomura Dam and its watershed data to develop a prediction model and confirmed the validity of the prediction model (Figure 47).

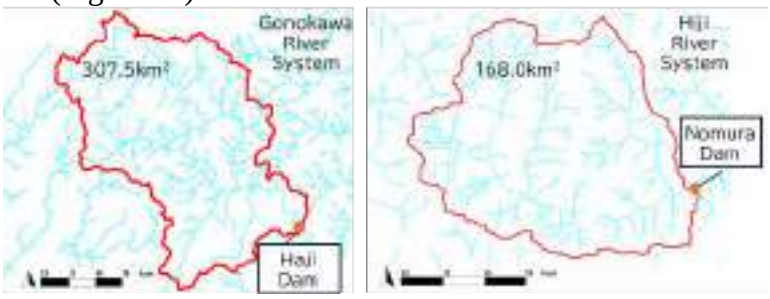


Figure 47 Location map of the dam basin.

## 2 Methodology

We developed the inflow prediction model using a 2D-CNN. The input data is the reanalysis precipitation for each watershed, and the data consist of three axes (X, Y, and time). The data in the time axis were structed of different time-averaged precipitations for each mesh. Next, we validated the prediction model using SHAP, which is one of the major XAI methods. SHAP is a method of

calculating the contribution of input data to output values using Shapley values. The influence of input for the prediction was visualized using XAI and verified at three time points: at the beginning of rising limb, at the peak time, and at the falling limb of the flood.

## 3 Results

We evaluated the RMSE of the inflow prediction model, and two cases with the representative accuracy were selected for analysis. The three lagtime rainfall of verification we conducted were as follows.

- Peak discharge:Most recent lagtime.
- Rising limb:Approximate nearest lagtime.
- Falling limb:A few hours ago.

The results demonstrated that the predictions were not coincidental, but rather reasonable predictions based on the pattern of rainfall.

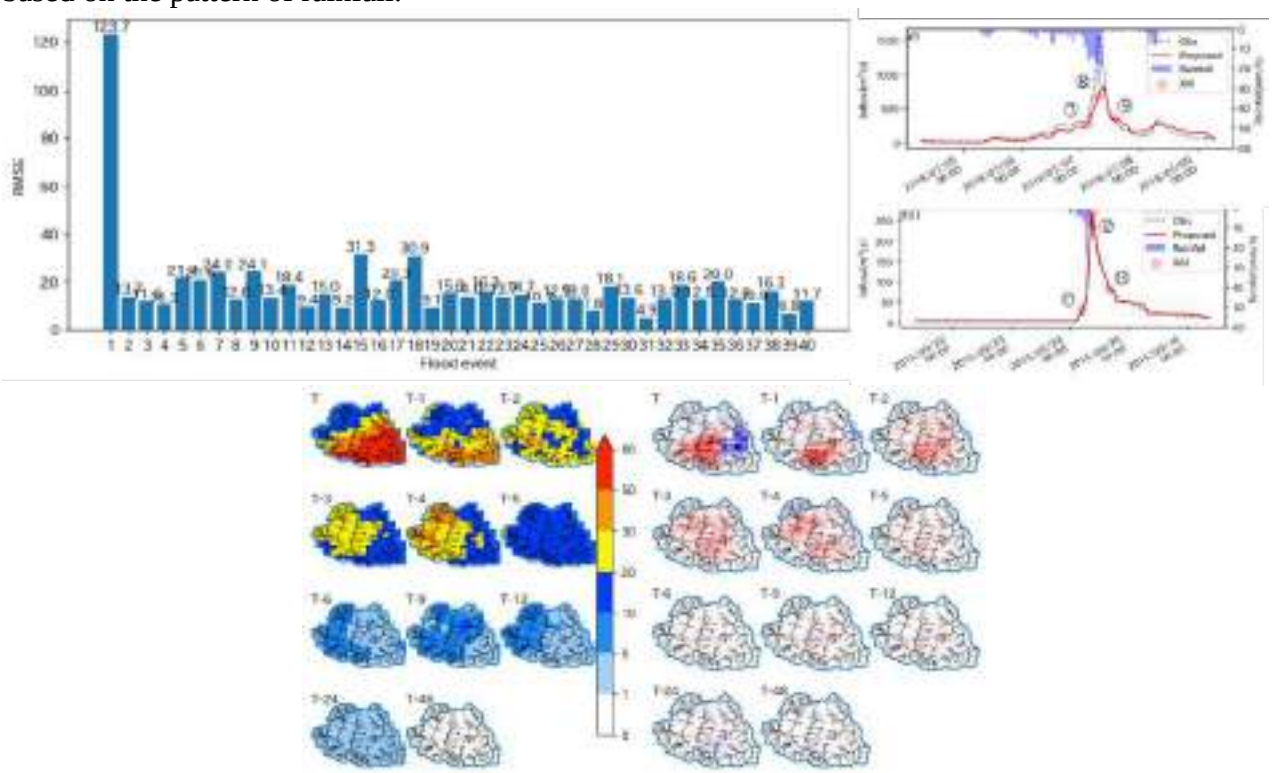

### 3.1 Conclusions

The impact of input rainfall visualized by XAI is consistent with hydrological interpretation, suggesting that AI's flood analysis is likely to accurately reflect hydrological mechanisms. Such analysis can help support the reliability of prediction models by AI. Moving forward, we would like to select the most relevant inputs based on the results of SHAP, develop a model and verify whether the accuracy improves.

### Reference

[1] Hitokoto,M., Araki,T., Hakoishi,K.,Endo,Y., Proposal for data augmentation method for dam inflow prediction using deep learning - improvement of applicability for unprecedented scale runoff -, Advances in river engineering, 2022, vol.28, pp.67-72.

[2] Nishiguchi,R., Zenkoji,S., Takagi,Y., Hitokoto,M., Impact of spatio-temporal distribution of rainfall in runoff analysis using cnn, Advances in river engineering, 2023, vol.29, pp.31-36.

[3] Hakoishi,K.,Hitokoto,M.,Zenkoji,S.,Nishiguchi,R., Consideration of XAI in Inflow Prediction Model Using Convolutional Neural Network., Artificial Intelligence and Data Science, 2023, vol.4-3, pp.539-546.

**Theme:** Emerging concepts and solutions in modelling methods
**IAHR Thematic Priority Area:** [TPA-4] Digital Transformation
https://doi.org/10.3850/iahr-hic2483430201-335

# Joint Intelligent Scheduling of Flood Control in Small and Medium Rivers Based on Hydroinformatic Model

**Gu Zhenghua[1], Zhang Jiayi[1], Yan Haowei[1], Sheng Jiaoying[1], He Baojie[1], Zhou Tong[1]**

[1] College of Civil Engineering and Architecture, Zhejiang University, Hangzhou 310058, China

*Corresponding author: WISE@zju.edu.cn*

**Abstract.** In order to reduce the flood damage from small and medium rivers, Joint Intelligent Scheduling Mode for Flood Control of Small and Medium Rivers Based on Hydroinformatic Model (JISMFCSMR-HiM) is presented, which is composed of flood control scheduling decision model, flood control scheduling simulation model, operational forecasting model, scheduling scheme intervention module and scheduling plan base, etc. The index system of joint intelligent flood control for small and medium rivers based on Pressure-State-Response (PSR) model and the simulation model of flood control for small and medium rivers based on SWMM are established. Taking Tunxi River Basin in Anhui Province of China as an example, a demonstration system for joint intelligent scheduling of flood control in small and medium rivers is developed. The application results show that JISMFCSMR-HiM provides an effective way to realize joint intelligent scheduling decision of flood control in small and medium rivers, and significantly improves the reliability, resilience, intelligence and real-time of scheduling.

**Keywords:** decision model; flood control; hydroinformatic model; simulation model; small and medium rivers

## 1 Introduction

- The joint intelligent scheduling mode for flood control of small and medium rivers refers to the dynamic joint scheduling of the flood control engineering system in the small and medium river basins on the basis of the short-term flood forecast and operational forecast, so as to realize the flood control safety and the improvement of profit and benefit in the river basins.
- Compared with the one of large river basins, the flood disaster system of small and medium river basins has more disaster factors, more complex disaster environment and more fragile disaster bearing body. How to realize the rapid and dynamic joint scheduling of reservoir groups with multi-objective and multi-constrained conditions, so as to minimize the influence of the flood in small and medium rivers, is a key problem that must be solved in the flood prevention and control of small and medium rivers.
- The development of flood control mode of river basins has experienced four stages: rule scheduling (i.e. empirical scheduling), simulation scheduling, optimization scheduling and intelligent scheduling. Compared with the first three stages, the development time of intelligent scheduling mode is not long, and the corresponding theoretical technology is not mature. The hydroinformatic model (HiM) proposed by Zhenghua Gu has been successfully applied to some practical problems such as the intelligent operation of the sluices in tidal river networks and the intelligent allocation of regional water resources[1-3]. On the basis of HiM, the intelligent scheduling theory for flood control of small and medium rivers is presented in this paper, which can also be used to large river basins.

## 2 Material and methods

### 2.1 Material

Tunxi Basin is located in the south Anhui Province of China, with a catchment area of 2696.76km$^2$. There are one large reservoir of Yuetan, one medium reservoir of Dongfanghong, and 47 small reservoirs in the basin. The rainfall data from nine precipitation stations of Wucheng, Shimen, Tunxi, Shangxikou, Rucun, Yixian, Yanqian, Xiuning and Chengcun and the evaporation and flow data from Tunxi hydrologic station were selected during 2014 to 2017.

### 2.2 General framework

The joint intelligent scheduling framework for flood control of small and medium rivers based on hydroinformatic model is shown in Figure 1, which is composed of flood control scheduling decision model, flood control scheduling simulation model, operational forecasting model, scheduling scheme intervention module and scheduling plan base. Before the scheduling system is started, some scheduling schemes are simulated by scheduling simulation model, and the initial structured plan base for scheduling decision model learning is obtained by combining the existing planning and scheduling experience. After the system is enabled, scheduling information is first imported, and a preliminary scheduling scheme is formed by the trained scheduling decision model according to the scheduling information. Then the scheduling scheme is simulated and tested by the scheduling simulation model. When the simulation result reaches the desired goal, the scheduling scheme is the one that can be issued. At this time, it is necessary to modify the scheduling scheme with the help of the intervention module, and then test the scheduling simulation model until a scheduling scheme that can meet the scheduling objective is obtained. The scheduling scheme can be added to the scheduling plan base for the refinement training of the scheduling decision model in the future. After the final scheduling scheme is issued, the job forecast model carries out the flood forecast, combines the real-time monitoring data to generate scheduling information again, and activates the scheduling system again, thus forming a rolling. On the one hand, this kind of scheduling system can ensure the safety and reliability of scheduling; on the other hand, with the repeated use of scheduling system, the knowledge of pre-plan base will become better and better, and with the enhancement of system learning ability, the number of times that the system needs to intervene will gradually decrease, thus reflecting an intelligent feature.

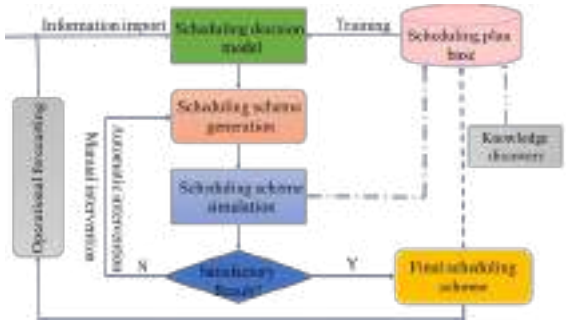


Figure 48 Joint intelligent scheduling framework for flood control of small and medium rivers based on hydroinformatic model

### 2.3 Methods

- The "Pressure-State-Response" model (abbreviated as PSR) was adopted to construct the index system of joint intelligent scheduling for flood control in Tunxi Basin;
- Using SWMM to establish the simulation model of joint intelligent scheduling for flood control of small and medium rivers;
- BP neural network was used to establish the decision model of joint intelligent scheduling for flood control of small and medium rivers.

## 3 Results and discussion

- According to JISMFCSMR-HiM, the joint intelligent scheduling for flood control in Tunxi Basin was developed by integrating the above models. GoLang and GF 2.0 were adopted to construct the back-end service. The front-end were constructed through HTML5, CSS and JavaScript. They were developed by using IntelliJ IDEA tools. MySQL 8.0 was used as the storage database.
- The measured hydrological data from June 4 to 16, 2017 was used to test JISMFCSMR-HiM. The measured main flood peak occurred at 18:00 on June 13, 2017 at Tunxi hydrologic station, and the peak flow was 1733m$^3$/s. Static scheduling and intelligent scheduling schemes were shown in Figure 2. For static scheduling, the occurrence time of the main flood peak was 20:00 on June 13, 2017, and the peak flow was 1465m$^3$/s; For intelligent scheduling, the occurrence time of the main flood peak was 23:00 on June 13, 2017, and the peak flow was 1380m$^3$/s. It can be concluded that intelligent scheduling plays a significant role in delaying the peak time of the main flood peak and reducing the main peak flow. The maximum reservoir water level of Dongfanghong reached to 296.20m for intelligent scheduling and 289.54m for static scheduling, and the maximum reservoir water level of Yuetan reached to 170.20m and 169.18m respectively. The reservoir water level of Dongfanghong and Yuetan after intelligent scheduling all added in comparison with that after static scheduling (Figure 3).

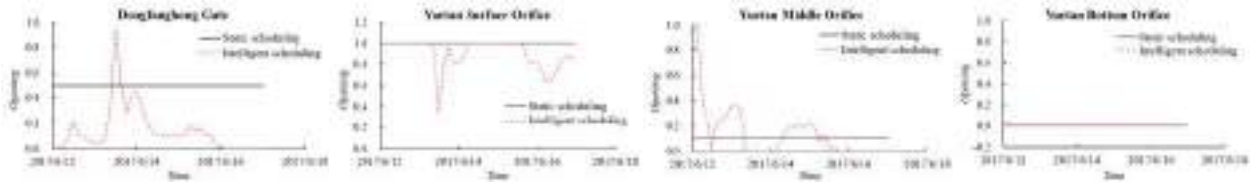

Figure 2 The schemes of static scheduling and intelligent scheduling

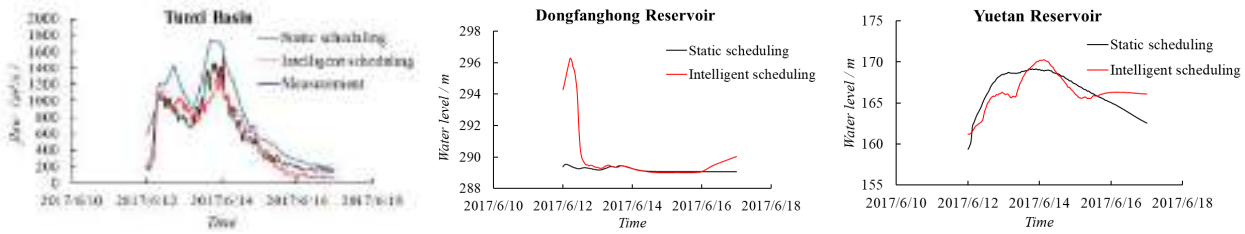


Figure 3 Water regimen changes under different scheduling schemes

## 4 Conclusions

The established JISMFCSMR-HiM improves the benefits of reservoirs, reduces the downstream flood control pressure, and shows the performances of reliability, intelligence and real-time operation.

## Reference

[1] Z.H. Gu, Study on intelligent operation aided decision making model of sluices in river networks, Journal of Zhejiang University (Engineering Science). 40.5 (2006) 822-826.

[2] Z.H. Gu, X.M. Cao, W. Liu, A hydroinformatic model and its application to river networks control, 9th International Conference on Hydroinformatics (HIC 2010). Tianjin, CHINA.

[3] G.L. Liu, Z.H. Gu, S.K. Zhao, *eta1*., Research on intelligent allocation of regional water resources based on data-driven approach, Hydro-Science and Engineering. 5 (2015) 38-45.

**Theme:** Emerging concepts and solutions in modelling methods
**IAHR Thematic Priority Area:** [TPA-4] Digital Transformation
https://doi.org/10.3850/iahr-hic2483430201-338

# Joint Modeling Research of Causal Analysis and Transformer for Multi-Sensor Cross-Temporal Granularity Water Demand Forecasting

**Wenhong Wu[1,2], Yunkai Kang[1,2], Yuexia Xu[3]**

[1] School of Information Engineering, North China University of Water Resources and Electric Power, Zhengzhou, 450046, China
[2] Henan Province Water Distribution Network Intelligent Management Engineering Research Center, Zhengzhou, 450046, China
[3] Zhengzhou Water Supply Investment Holdings Co., Ltd. Zhengzhou, 450046, China

*Corresponding author: kykinfdarksoul@gmail.com*

**Abstract.** Accurately predicting water demand is pivotal in optimizing strategies for multiple water sources. In response to challenges, including the suboptimal accuracy observed in existing prediction models, the complexity of achieving precise predictions across diverse time scales and sensors. This study introduces the Ensemble Empirical Mode Decomposition Granger causality test Attention Transformer Network (EGATN) model, which combines the advantages of traditional statistical methods with deep learning models. Experimental results demonstrate that compared to baseline models, the proposed model improves MAPE metrics by 2.12%, 4.33%, and 6.32% at forecasting granularities of 15 minutes, 45 minutes, and 90 minutes, respectively. The model achieves an R2 score of 0.97, indicating outstanding predictive accuracy, generalization, and exceptional explanatory power for the target variable. This research exhibits significant potential applications in predictive tasks within smart water management systems.

**Keywords:** Granger Causality Test, Graph Neural Networks, Transformer, Water Demand Prediction.

## 1 Introduction

Deep learning-based methods can effectively address the shortcomings of traditional methods in solving nonlinear forecasting problems, thereby becoming increasingly pre-ferred by researchers [1]. These methods mainly focus on analyz-ing the temporal autocorrelation within individual series, a practice that significantly diverges from the reality of multiple sensors contributing to complex multivariate time series in real water supply networks. To further enhance the accuracy of the model, some researchers have introduced spatial correlation based on the sensor spatial distribution, adopting a combination of CNNs and RNNs to extract spatio-temporal features from the data [2]. Overall, despite the good predictive results achieved by existing methods, the following challenges still need to be overcome:

Existing models that analyze spatiotemporal data often treat spatial and temporal relationships as separate entities. This separation can lead to significant information loss, subsequently diminishing the accuracy of the model's predictions. Furthermore, the spatial relationships between sensors might not always be apparent or accessible, complicating the model's learning process. Consequently, there is a pressing need for innovative graph-building techniques that can facilitate adequate information flow among sensor nodes without relying on predefined spatial relationships.

.

## 2 Methodology

Addressing these challenges, this paper presents a novel approach called the EEMD Granger causality test Attention Transformer Network (EGATN) to overcome the challenge of water demand forecasting. Different from other methods, this model imposes no specific constraints on data input and offers the following contributions:

We utilize EEMD–Granger causality testing to integrate additional temporal information within a fixed time dimension, circumventing the need for model stacking inherent in traditional approaches and facilitating a deeper investigation into the causal interplay among sensor networks [3]. By incorporating causal spatiotemporal embeddings into the Transformer architecture, we have refined positional encoding, enabling the EGATN model to synchronize the treatment of spatiotemporal relationships among water demand sensors [4].

## 3 Results

Through rigorous performance comparisons with baseline models, this approach ultimately demonstrates its superiority and stability across different prediction spans, outperforming other models in terms of prediction accuracy and generalization capabilities (As shown in Table 1).

Table 1 Results of comparative experiments

| Model | 15min | | | | 60min | | | | 90min | | | |
|---|---|---|---|---|---|---|---|---|---|---|---|---|
| | MAE | RMSE | MAPE | | MAE | RMSE | MAPE | | MAE | RMSE | MAPE | |
| ARIMA | 274.63 | 489 | 24.01% | 0.78 | 458.36 | 769.68 | 36.78% | 0.74 | 685.98 | 1284.34 | 48.69% | 0.72 |
| STGCN | 204.45 | 350.68 | 12.42% | 0.83 | 295.36 | 423.65 | 17.65% | 0.84 | 320.87 | 440.84 | 17.89% | 0.84 |
| ASTGCN | 149.69 | 330.36 | 9.08% | 0.94 | 250.34 | 396.51 | 14.80% | 0.92 | 300.88 | 423.56 | 16.86% | 0.90 |
| DCRNN | 150.73 | 327.21 | 8.95% | 0.92 | 260.85 | 401.35 | 16.24% | 0.85 | 340.88 | 450.08 | 19.63% | 0.85 |
| GNNLSTM | 120.89 | 298.93 | 13.26% | 0.94 | 263.45 | 398.24 | 15.98% | 0.88 | 311.25 | 424.54 | 14.01% | 0.92 |
| GraphWaveNet | 123.04 | 270.85 | 8.63% | 0.94 | 258.36 | 411.98 | 15.01% | 0.91 | 329.84 | 448.01 | 17.68% | 0.89 |
| EGATN | 92.29 | 190.48 | 4.01% | 0.97 | 218.63 | 298.64 | 14.16% | 0.96 | 222.45 | 302.27 | 13.13% | 0.94 |

## 4 Discussion

The research findings indicate that the fusion architecture of graph neural networks and Transformers can be applied to the field of intelligent water management prediction tasks, especially in conditions where sensor spatial relationships are unclear, data exhibits non-linearity and periodicity, and multiple granular prediction results are required. However, it is worth noting that as the number of sensors increases, the efficiency of constructing the graph structure using the EEMD-Granger causality test may decrease, requiring more efficient multiprocessing program design to improve graph construction efficiency. In future work, further exploration of the application of Transformer structures in water demand forecasting tasks will be pursued, along with additional training data to expand and validate the model in practical scenarios.

## Reference

[1] Mu, L.; Zheng, F.F.; Tao, R.L.; Zhang, Q.Z.; Kapelan, Z. Hourly and daily urban water demand predictions using a long short-term memory based model. J. Water Resour. Plan. Manag. 2020, 146, 05020017.

[2] Hu, P.; Tong, J.; Wang, J.C.; Yang, Y.; Turci, L.D. A hybrid model based on CNN and Bi-LSTM for urban water demand predic-tion. In Proceedings of the 2019 IEEE Congress on Evolutionary Computation, Wellington, New Zealand, 10–13 June 2019.

[3] Xu, Mingxing, Wenrui Dai, Chunmiao Liu, Xing Gao, Weiyao Lin, Guo-Jun Qi, and Hongkai Xiong. 2021. Spatial-Temporal Transformer Networks for Traffic Flow Forecasting. arXiv. http://arxiv.org/abs/2001.02908.

[4] Xu, M.; Dai, W.; Liu, C.; Gao, X.; Lin, W.; Qi, G.; Xiong, H. Spatial-Temporal Transformer Networks for Traffic Flow Forecasting. arXiv 2021, http://arxiv.org/abs/2001.02908.

**Theme:** Emerging concepts and solutions in modelling methods
**IAHR Thematic Priority Area:** [TPA-4] Digital Transformation
https://doi.org/10.3850/iahr-hic2483430201-340

# A Physics-Informed Neural Network Based on Hydrological Model Framework

**Zhaoxi Li[1], Tiejian Li[1], Chen Chen[2], Weidong Li[1], Jiaye Li[2]**

[1] Department of Hydraulic Engineering, Tsinghua University, Beijing 100084, China
[2] School of Environment and Civil Engineering, Dongguan University of Technology, Dongguan, 523808, China

*Corresponding author: litiejian@tsinghua.edu.cn*

## 1 Introduction

Slope runoff constitutes the initial phase of the hydrological processes within a watershed, serving as the foundational input for downstream phenomena such as channel flood routing. While traditional physical models have garnered substantial acclaim for their capacity to explain and forecast changes within watershed states [1], their performance depends heavily on the influence of existing physical information related to watershed. Furthermore, the calibration of parameters within these classical models exhibits marked inefficiency. With the development of technology, data-driven artificial intelligence model has become a tool for scientific prediction of the earth system. Nevertheless, despite their exceptional prowess in model fitting, these data-driven methodologies often fall short of providing substantive physical interpretations [2][3]. In this context, the physics-informed neural network model emerges as a synergistic integration, melding the merits of both traditional and modern paradigms, thereby invigorating the research of watershed hydrological processes [4]. Herein, we introduce a novel framework termed the Runoff Process Wrapped Recurrent Neural Network (R-RNN). This innovative framework anchors itself upon the slope runoff model, infused with a physical mechanism at its core, and ingeniously incorporates Ordinary Differential Equations (ODEs) within its iterative schema. By transmuting the parameters of the physical model into learnable neural network parameters, not only is the model's performance significantly enhanced, but a comprehensive consideration is also accorded to the responses elicited by each sub-module within the runoff process. This approach heralds a new era in the modelling of hydrological processes, promising improved accuracy and a deeper understanding of the underlying physical phenomena.

## 2 Methods

The model is designed as a mechanism model that mainly describes the infiltration excess runoff (Figure 1a), and the model mainly includes sub-modules such as canopy interception, surface over-infiltration runoff and soil water outflow. The water balance equation is applied to three water storage modules to generate ODE equation describing the water dynamics of each module[5]:

$$\begin{cases} \dfrac{\partial \mathrm{S_{can}}}{\partial \mathrm{t}} = \mathrm{P} - \mathrm{P_n} - \mathrm{E_{can}} \\ \dfrac{\partial \mathrm{W_u}}{\partial \mathrm{t}} = \mathrm{A}(\mathrm{q_{zu}} - \mathrm{q_{zd}} - \mathrm{E_u}) - \mathrm{Q_{gu}} \\ \dfrac{\partial \mathrm{W_d}}{\partial \mathrm{t}} = \mathrm{A q_{zd}} - \mathrm{Q_{gd}} \end{cases} \tag{1}$$

R-RNN disassembled the runoff model into four blocks, and added a block for exchanging surface soil water and bottom soil water on the basis of the original three reservoirs (Figure 1b). The input variables of R-RNN are meteorological and hydrological data, such as precipitation (*P*), evaporation ($E_p$) and leaf area index (*LAI*), and topographic data, such as slope projection area (*A*), slope (*S*) and slope projection length ($L_0$). Similar to classical recurrent neural networks (RNN), the connections between R-RNN neurons are represented using explicit discrete forms of states (i.e., state variable and flux variable), and the structural parameters of classical RNNs are replaced by physically meaningful parameters (i.e., $h_u$, $h_d$ et al.,) that are difficult to obtain in the runoff model. Through the continuous updating of state variables (i.e., , , ), the iteration of R-RNN with time step is realized, and the fitting result of R-RNN is always water conservation under the constraint of Eq. (1). The essence of R-RNN is to use the relationship between the network architecture of RNN and the numerical methods of ordinary differential equations to solve the problems involving system dynamics.

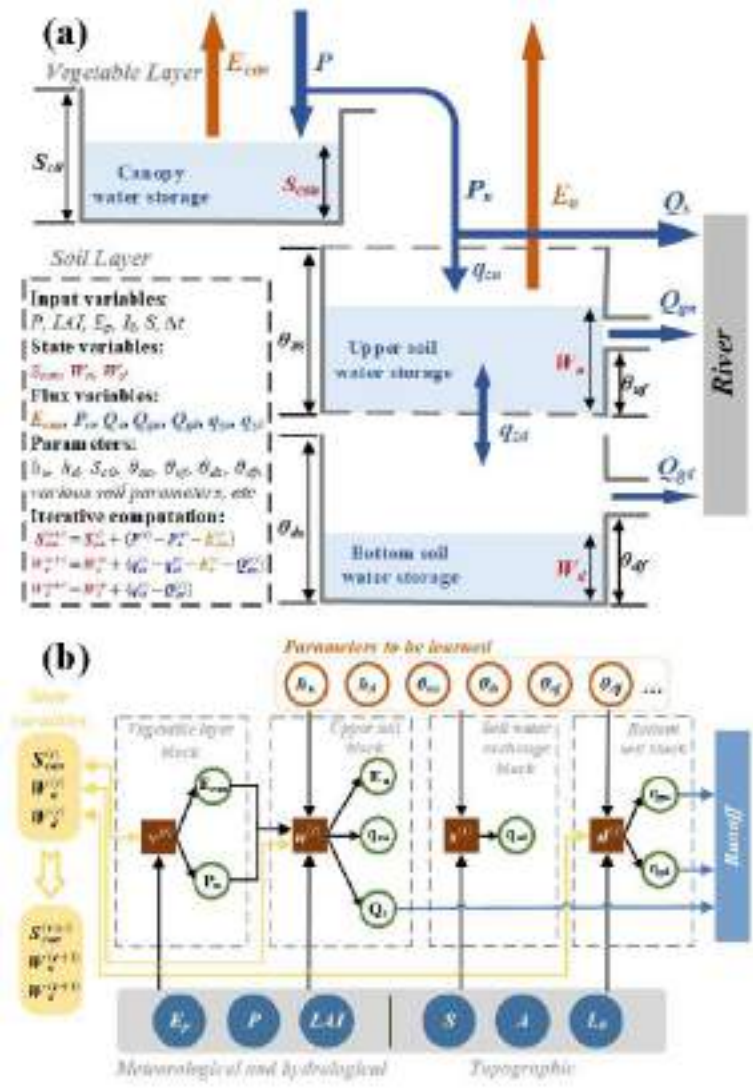


Figure 49 (a) Schematic diagram of runoff model, which shows the connection relationship among three reservoirs. The model parameters are mainly divided into four categories, including input variables, state variables, flow variables and unknown parameters. (b) R-RNN structure shows the logical relationship between different blocks and the transfer process of parameters. Where $v^{(t)}$, $u^{(t)}$, $s^{(t)}$ and $d^{(t)}$ are the states of different blocks of the model at time t.

## Reference

[1] Eyring, V., Cox, P. M., Flato, G. M., Gleckler, P. J., Abramowitz, G., Caldwell, P., ... & Williamson, M. S. (2019). Taking climate model evaluation to the next level. Nature Climate Change, 9(2), 102-110.

[2] Hulbert, C., Rouet-Leduc, B., Johnson, P. A., Ren, C. X., Rivière, J., Bolton, D. C., & Marone, C. (2019). Similarity of fast and slow earthquakes illuminated by machine learning. Nature Geoscience, 12(1), 69-74.

[3] Ebert-Uphoff, I., Samarasinghe, S., & Barnes, E. (2019). Thoughtfully using artificial intelligence in Earth science. Eos, 100(10.1029).

[4] Jiang, S., Zheng, Y., & Solomatine, D. (2020). Improving AI system awareness of geoscience knowledge: Symbiotic integration of physical approaches and deep learning. Geophysical Research Letters, 47(13), e2020GL088229.

[5] Li T. (2008). Mechanism and Simulation of River Basin Sediment Dynamics. (Doctoral dissertation, TsingHua University).

**Theme:** Complex water systems, remote sensing and control
**IAHR Thematic Priority Area:** [TPA-4] Digital Transformation
https://doi.org/10.3850/iahr-hic2483430201-343

# Chiare, Fresche et Dolci Acque: Model-Based Investment Planning of Tuscany's Regional Water Supply System

**Claudio Arena[1], Marcella Cannarozzo[1] Andrea Cappelli[2], Oberdan Cei[3], Giorgio Gullotti[1], Lorenzo Maresca[2]**

[1] Dipartimento di Ingegneria – Università degli Studi di Palermo, Palermo, 90143, Italy
[2] Area Pianificazione e Controllo, Autorità Idrica Toscana, Firenze, 50122, Italy
[3] Ingegnerie Toscane S.r.l., Firenze, 50134, Italy

* *Corresponding author: claudio.arena@unipa.it*

**Abstract.** The abstract introduces ongoing activities undertaken by the Tuscan Water Authority (Autorità Idrica Toscana) on modelling the regional water supply systems to increase the ability to evaluate and justify investments aimed at interconnecting existing systems, substituting resources with others of better quality or with smaller energy footprint. The systems have been modelled with Aquator, a commercial software for the simulation of water resources systems, and now features, among other things, over 400 supply sources, 600 demand centres, 150 water treatment works. While the model is still incomplete in the northernmost part of the region, example evaluations of some projects in the southern areas have been performed to show the benefits of system's modelling.

**Keywords:** Complex water systems, Investment evaluation, Investment planning, Simulation models of water resources systems.

## 1 Introduction

Although many of the waters supplying Tuscany are still clear, cool and fresh (*Chiare, fresche et dolci acque*, as in the onset of one of Petrarch's most famous poems), Tuscany's systems for civil water supply are faced by many challenges related to changing patterns of water availability from surface and groundwater resources, water quality issues, seasonal peak demands for touristic activities, increased environmental concerns on the energy footprint of water supply. All these issues have motivated the Tuscan Water Authority (Autorità Idrica Toscana, also AIT in the following) to develop a masterplan of strategic infrastructures to improve water supply in Tuscany. As water service is operated by seven different utilities over the region, AIT also has the role of coordinating investments to connect areas operated by different utilities. The need for a system's perspective on water investments, together with the complexity of the schemes, has motivated the choice to support planning decisions through modelling of the different supply systems over the region and of the various proposed projects. Presently, water resources systems in Tuscany have prominently a local extent, in that the region has traditionally been a water-rich area, mainly supplied by spring and groundwater from the Appennines. While local systems are still the obvious solution for small towns in impervious areas, it is starting to become questionable whether more centralized options may be a better choice for larger towns and cities, substituting small water resources with others from large reservoirs, with expected benefits from the standpoint of operation costs, water quality, and reduction of the energy footprint of the supply service. Another motivation for modelling comes from the recent national legislation [1] that requires that projects be evaluated according to the triple-bottom-line principles of sustainability, in which the economic aspects must be supported by a complete cost-benefit analysis of the investments.

## 2 Material and methods

As a modelling tool a software from the class of generic simulation models for water resources system [2] was selected, namely Hydro-Logic® Aquator. The methodology adopted to obtain the water supply schemes has required a considerable simplification and conceptualization work based on GIS-techniques. Conceptualization consists in transforming the highly detailed survey of the water supply and distribution system available for the whole region into the arc-node concept of Aquator (figure 1): the model now features, among other things, over 400 supply sources, 600 demand centres and 150 water treatment works.


Figure 1 Water supply systems of the seven Tuscan utilities modelled with Aquator (different colours indicate the areas operated by different water utilities) and summary of the number of components.

## 3 Results and conclusions

Although data from the northernmost utility are still lacking, the model has been used to evaluate two investments in the southern part of the region. This exercise has shown how the simulation model is able to highlight aspects of project performance, for instance in terms of trade-off between improved water quality by substitution of highly hard groundwaters with softer surface waters and an increase of the energy footprint of service, that could be overlooked without supporting evaluation through a simulation model. These aspects must be taken in due account, together with investment costs, in a full economic appraisal of the projects.

## Reference

[1] Italian Government, 2022, Inter-ministerial Decree 350/2022 - Reform M2C4-R.4.1. Available at https://trasparenza.mit.gov.it/moduli/downloadFile.php?file=oggetto_allegati/2318944490O__OM_INFR.GABINETTO.REG_DECRETI%28R%29.0000350.25-10-2022.pdf

[2] Sulis A. and Sechi G.M., 2013, Comparison of generic simulation models for water resource systems. Environmental Modeling and Software 40, pp 214–225.

**Theme:** Complex water systems, remote sensing and control
**IAHR Thematic Priority Area:** [TPA-4] Digital Transformation
https://doi.org/10.3850/iahr-hic2483430201-345

# Optimal Sequence of Replacements in the Renovation of Water Distribution Networks

**Vesipa Riccardo*, Avarzamani Mohsen**

Department of Environment, Land and Infrastructure Engineering, Politecnico di Torino, C.so Duca degli Abruzzi 24, 10129 Torino, Italy

** Corresponding author: riccardo.vesipa@polito.it*

**Abstract**. Aging components within WDNs pose a major concern due to their susceptibility to leakages. One possible strategy to addressing this issue is to replace a large part (up to 20%) of the conduit in the network (i.e., to perform a network renovation). However, the replacement of conduits cannot be performed all at once, rather it requires the progressive and sequential replacement of conduits. It is expected that different sequences of conduits replacement will have different effects on the WDN dynamics. This study explores the existence of an optimal sequences of pipe replacement, that minimizes disturbances to users.

**Keywords**: Renovation, Leakages, Optimization, Genetic Algorithms, Modelling, EPANet.

## 1 Overview

WDNs are aging, and investment for replacement of conduits are widespread. Usually 10%-20% of the total length of the WDN is selected to be replaced. Clearly, the conduits selected for replacement cannot be replaced all at once. The WDN undergoes the progressive replacement of one conduit at a time (called sequence of replacements). This sequence of replacements can last weeks, and can affect the users. Different sequences of replacements can affect users to a different extent. In this picture, the scientific questions that is addressed is “Is there an optimal sequence of replacements in the renovation of water distribution networks?”

## 2 Metodology

The study of optimal sequence of operations is a topic mainly studied in transportation engineering (e.g., progressive implementation of bus lanes, see [1]). Here an algorithm used in that context is applied to hydraulic engineering and WDN modelling. This is done to determine the most favorable sequence of replacements to be implemented. More in details, the methodology followed was:

- Step 1 - to develop a list of all replacements to be performed in the WDN with the corresponding duration. The typical replacement of one pipe consists in: (a) preliminary works for the installation of the new pipe; (b) the disconnection of the old pipe; and (c) the connection of the new pipe (different diameter and roughness, less leakages);
- Step 2 - to automatically obtain a sequence of operation (in calendar days) for the operations listed in (i);
- Step 3 - to model the hydraulics of this evolving system. This was done: (a) modelling the hydraulic effect of the operations listed in Steps 1 and Step 2 automatically building EPANET models of the evolving WDN with an EPANET’s MATLAB Toolkit;
- Step 4 - to assess the effect of the sequence of replacements on the network. This was done with scalars that measure the disturbance to users. Such scalars are statistics of pressure reductions, or demand deficit. The statistics were obtained from the pressure and demand time-series obtained with the hydraulic models of Step 3;
- Step 5- To use an optimization algorithm (that automatically repeats Steps 2-4) to find a sequence of replacements that minimizes (the scalars that measure) the disturbance to users.

The procedure was applied to C-Town, a city-model widely used and made up of about 400 pipes.

## 3 Results and Conclusions

The adopted algorithm found sequences of replacements of conduits that were progressively less impacting to users. The algorithm was capable of finding sequences so that dangerous events for the network (e.g., emptying of tanks were avoided).

## References

[1] Bayrak, M., Guler, S.I., and Schonfeld, P., 2021, Implementation sequence optimization for dedicated bus lane projects. *Transportation Research Record*, vol **2675**(10), pp 1184-1195

**Theme:** Complex water systems, remote sensing and control
**IAHR Thematic Priority Area:** [TPA-4] Digital Transformation
https://doi.org/10.3850/iahr-hic2483430201-347

# Evaluation of Segment Anything Model for Riparian Land Cover Classification from Aerial Imagery

**Keisuke Yoshida[1], Shijun Pan[1], Takashi Kojima[2]**

[1] Graduate School of Environmental and Life Science, Okayama University
(Tsushima-naka 3-1-1, Kita-ku, Okayama 700-8530, Japan)
[2] TOKEN C. E. E. Consultants Co., Ltd

*Corresponding author: yoshida.k@okayama-u.ac.jp*

**Abstract.** Riparian land cover classification (LCC) is an important task for environmental monitoring and management, as it provides information on the state and characteristics of riparian zones, which are the transitional areas between terrestrial and aquatic ecosystems. However, LCC is challenging due to the high diversity and complexity of riparian vegetation and land use. In this paper, we evaluate the performance of Segment Anything Model (SAM), a recently proposed deep learning model for general image segmentation, for riparian LCC from aerial imagery. SAM can produce high quality object masks from input prompts such as points or boxes, and can generate masks for all objects in an image without fine-tuning. The authors compared SAM with the results derived from the DeepLabV3+ model trained by the dataset collected in Japan. Our experiments showed that SAM achieved competitive or superior results compared to other models, and can segment various riparian land cover types with high accuracy and consistency. The authors concluded that SAM is a promising tool for riparian LCC from aerial imagery, and suggest some directions for future research combining with the other model.

**Keywords:** DeepLabV3+, Land Cover Classification, Segment Anything Model, UAV

## 1 Introduction

Recent years, imagery derived from unmanned aerial vehicle (UAV) become an important tool for environmental monitoring. LCC mapping based on the UAV imagery is an efficient and critical approach for environmental researchers to collect the information on the specific location, especially the riparian area that are difficult for on-site survey. In this context, the authors evaluated SAM (segment anything model, a state-of-the-art segment model)-assisted results with DeepLabV3+ model [1] on classifying the land cover of the same locations.

## 2 Work flow

The authors trained the DeepLabV3+ model using land cover dataset (train/valid) that include cropped ortho-photo and responding masks, and inferred the ortho-photo from 3 selected locations (with TL) using trained DeepLabV3+ model. SAM segmented ortho-photo at the same mentioned locations, and derived from the segmented mapping the authors re-classified the land cover, namely SAM-assisted LCC Results. As the final step shown in the Figure 1, comparing the LCC Results derived from DeepLabV3+ and SAM-assisted with TL, respectively.

## 3 Conclusion

As depicted in the Figure 2, the findings of this research reveal that the performance shown in CM (i.e., Low-Vegetation/Ground, High-Vegetation and Water) of SAM-assisted Results is better than DeepLabV3+ LCC Results. The collaboration of these mentioned approach is in the consideration for the future research.

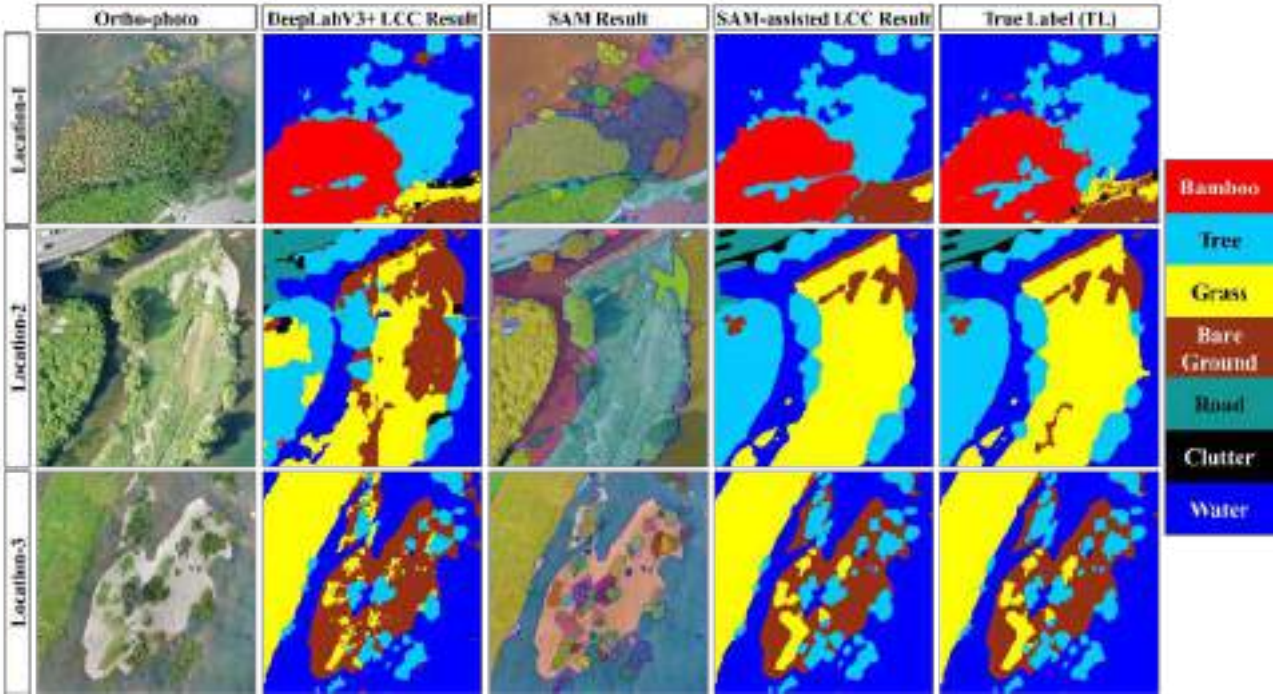


Figure 1 DeepLabV3+ and SAM-assisted LCC Results-based Comparison with Ortho-photo and TL of 3 locations.

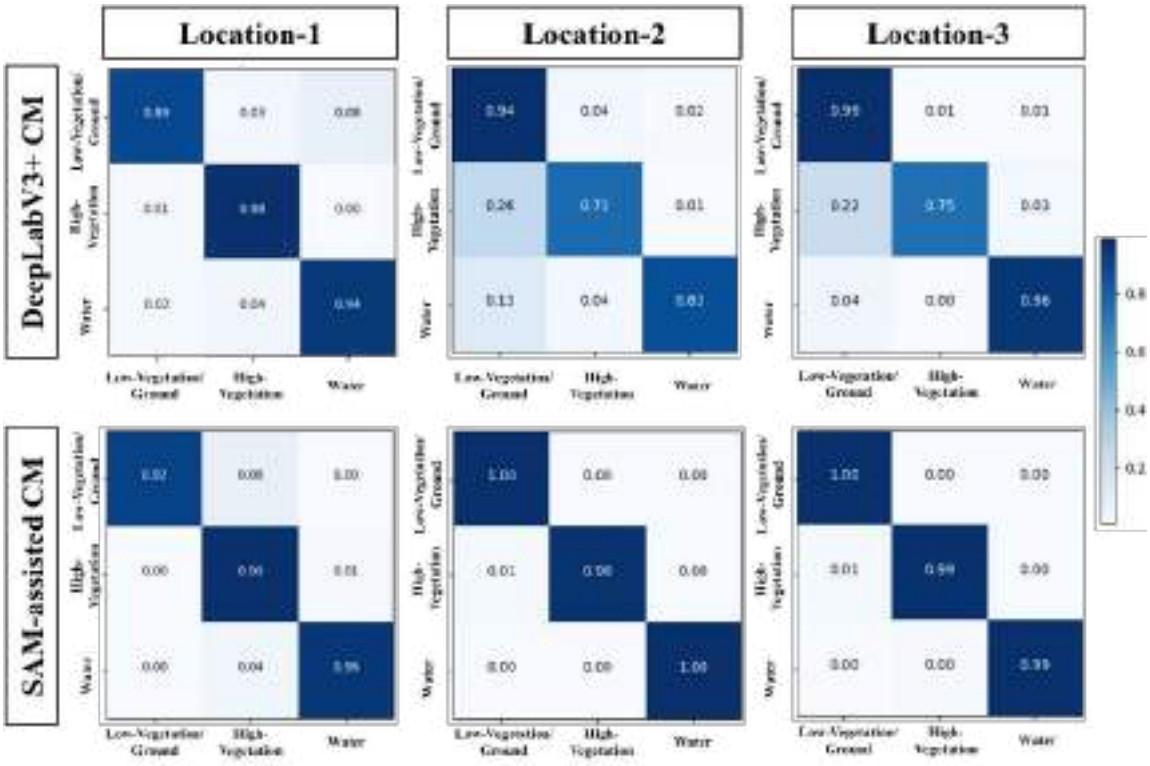


Figure 2 DeepLabV3+ and SAM-assisted LCC Confusion Matrix (CM) of 3 locations.

## Reference

[1] Yoshida, Keisuke, et al. "Airborne LiDAR-assisted deep learning methodology for riparian land cover classification using aerial photographs and its application for flood modelling." *Journal of Hydroinformatics* 24.1 (2022): 179-201. 10.2166/hydro.2022.134

**Theme:** Complex water systems, remote sensing and control
**IAHR Thematic Priority Area:** [TPA-4] Digital Transformation
https://doi.org/10.3850/iahr-hic2483430201-349

# Research on the Application of High-Resolution Remote Sensing Satellites in River and Lake Health Assessment and Supervision

**Yuxuan Chen[1,2], Guoqing Liu[1,2], Ziwu Fan[1,2,*], Chang Yang[1,2], Yang Liu[1,2]**

[1] Nanjing Hydraulic Research Institute, Nanjing 210029, China
[2] Key Laboratory of Taihu Basin Water Resources Research and Management of Ministry of Water Resources, Nanjing 210029, China

**Corresponding author: zwFan@nhri.cn*

**Abstract.** Following the comprehensive implementation of the river and lake chief system in China in 2016, the focus on protecting and restoring the health of rivers and lakes has escalated to become a central issue in water management. However, the processes for evaluating and supervising aquatic health face considerable challenges, such as high costs, inefficiencies, and regulatory obstacles, which hinder the ability to assess water bodies in real time. Guided by the 'Guidelines for Health Evaluation of Rivers and Lakes (Trial)', this paper investigates the dynamic evaluation and monitoring of river and lake health using high-resolution remote sensing satellites, covering four primary criteria: basin, water, biology, and social services It introduced a novel remote sensing interpretation method for specific health assessment indicators of rivers and lakes, thereby creating a dynamic assessment framework based on high-resolution remote sensing imagery. The research enhances the development of digital twin systems for evaluating and managing the health of rivers and lakes, providing crucial decision support for intelligent assessment.

**Keywords:** high-resolution remote sensing, indicator system, remote sensing interpretation, river and lake health

## 1 Introduction

China is characterized by its diverse geographical landscapes and climatic variations, supporting a substantial population and positioning it as the nation confronted with the most multifaceted water-related scenarios globally. The acceleration of economic and social growth has intensified the utilization of water resources[1], leading to the degradation or destruction of river and lake ecosystems, thereby threatening the sustainable development of the economy and society.

Understanding the concept of river and lake health is a significant challenge for countries aiming for sustainable development. Since the 1990s, researchers have engaged in defining and discussing the concept of river and lake ecosystem health[2]. Since the comprehensive implementation of China's river chief and lake chief systems in 2016, the preservation and restoration of river and lake health have increasingly become crucial and central tasks in their management. Following this, the Department of River and Lake Management of the Ministry of Water Resources released the 'Guidelines for Health Evaluation of Rivers and Lakes (Trial)' on August, 2020[3], and initiated pilot evaluations in Lhasa River[4]. However, challenges such as high evaluation costs, low efficiency, and difficulties in supervision arise due to the convenient yet problematic selection and assessment of certain indicators. These challenges make it difficult to obtain real-time insights into the condition of rivers and lakes.

## 2 Material and Methods

Addressing the identified challenges, this study initiates with a comprehensive analysis of the global research landscape and advancements in remote sensing satellite interpretation technology. analyzes the utilization and challenges of high-resolution remote sensing in evaluating the health of rivers and

lakes. It also assessed the viability of using remote sensing technology to gauge various health indicators of these aquatic systems.

Building upon this foundational analysis, the research focuses on Wangyu River and Taihu Lake as a case study, employing dynamic monitoring data sourced from satellite, aerial, terrestrial, and manual observations. The study develops an automated interpretation methodology for crucial elements pertinent to the health assessment of rivers and lakes, such as water bodies, shorelines, vegetation, structural features, and cyanobacteria populations. This methodology facilitates the dynamic assessment of individual indicators as well as the comprehensive health of aquatic systems.

## 3 Results and Discussion

The research findings are summarized as follows:

- A novel remote sensing interpretation approach for specific health assessment indicators of rivers and lakes was introduced. This approach facilitates the automatic extraction of information regarding water bodies, shorelines, vegetation, structures, and cyanobacteria, offering algorithmic support for the periodic and dynamic evaluation of river and lake health using high-quality remote sensing imagery.
- A dynamic assessment framework for river and lake health based on high- resolution remote sensing images has been established, which clarified 19 indices for rivers and 20 indices for lakes. This framework serves as a theoretical foundation for overseeing the entire process of river and lake management.

This paper demonstrated the effectiveness of using high-resolution remote sensing satellite technology for evaluating the health of rivers and lakes, especially when analyzing indicators across extensive river and lake areas, significantly enhancing the accuracy and efficiency of assessments and monitoring. The current research primarily utilizes high-resolution spectral remote sensing imagery. Future plans involve exploring the application of various high-resolution, hyperspectral, and both active and passive radar remote sensing data, aiming to implement a multidimensional comprehensive evaluation of river and lake health, to thoroughly monitor the ecological system status of rivers and lakes, and to improve the improve the prediction and simulation capabilities of digital twin river and lake health evaluation and management.

## 4 Conclusions

Conducting assessments of river and lake health utilizing high-resolution remote sensing satellite technology holds critical importance for the prompt identification of environmental concerns, the expedited analysis of underlying causes, and the provision of accurate feedback regarding the true health status of rivers and lakes. This approach is of practical significance as it informs and guides the designated national river and lake custodians, along with relevant regulatory bodies, in fulfilling their duties related to the management and conservation of these vital water resources.

## Reference

[1] Su, Y., Fan, Z., et al., Assessing lake health in China: Challenges due to multiple coexisting standards. Journal of Hydrology: Regional Studies, 46 (2023): 101351.

[2] Lackey, R.T., Values, Policy, and Ecosystem Health: Options for resolving the many ecological policy issues we face depend on the concept of ecosystem health, but ecosystem health is based on controversial, value-based assumptions that masquerade as science. BioScience, 2001. 51(6): p. 437-443.

[3] Mimislry of Water Resources of the People's Republic of China (2020, August). Notice from the River Chief Office of the Ministry of Water Resources on the issuance of the ‘Guide on Health Assessment of Rivers and Lakes (Trial)’. http://www.mwr.gov.cn/ztpd/gzzt/hzz/zydt/202008/t20200820_1433359.html.

[4] Zhang, Z., Li, Y., et al., Assessment of river health based on a novel multidimensional similarity cloud model in the Lhasa River, Qinghai-Tibet Plateau. Journal of Hydrology, 603 (2021): 127100.

**Theme:** Complex water systems, remote sensing and control
**IAHR Thematic Priority Area:** [TPA-4] Digital Transformation
https://doi.org/10.3850/iahr-hic2483430201-351

# Research on Multi-Source Rainfall Fusion Method of Commercial Microwave Link Based on Bayesian

**Zirun Ye[1,2,3], Xiangbing Kong[2,3], Kai Guo[2,3,4], Xin Zheng[4]**

[1] School of Water Conservancy and Transportation, Zhengzhou University, Zhengzhou, 450001, China
[2] Yellow River Institute of Hydraulic Research, Zhengzhou, 450003, China
[3] Key Laboratory of and Water Soil Conservation on Loess Plateau, Ministry of Water Resources, Zhengzhou, 450003, China
[4] The National Key Laboratory of Water Disaster Prevention, Hohai University, Nanjing, 210098, China

*Corresponding author: kongxb_whu@foxmail.com*

**Abstract.** In view of the existing problems of errors in wireless microwave links and sparse and uneven distribution of surface rain stations, in order to meet the needs of refined and accurate hydrometeorological monitoring, a Bayesian method was adopted to build a rainfall fusion model based on wireless microwave data and rainfall observation data of rain stations in Gothenburg, Sweden, and to study the multi-source rainfall fusion method. The results show that the Bayesian method improves the effect of radio microwave rainfall inversion; At the same time, the fusion effect is related to the type of rainfall. The fusion accuracy of heavy rain is higher than that of light rain.

**Keywords:** Commercial microwave link, Rainfall fusion, Bayesian

## 1 Introduction

In the context of global warming and frequent extreme weather events, natural disasters such as rainstorms and floods pose a great threat to human life and development. Strengthening rainfall monitoring ability is an inevitable requirement for the refined development of rainfall, and plays a vital role in improving flood warning and response ability and water resource utilization research. Based on the commercial microwave link data in Gothenburg, Sweden, this study uses Bayesian method to integrate the wireless microwave link with the precipitation data of the rainfall station. Firstly, the multi-source precipitation data needed to construct the model was obtained. The trend surface method is used to interpolate the microwave link data to obtain the plane precipitation data, and the Bayesian method is used to fuse the data to obtain the precipitation data with high precision.

## 2 Method

Bayesian fusion method first builds prior distribution based on the existing forecast data, and then introduces new precipitation observation data to modify the preliminary estimate, thus obtaining the posterior condition distribution and realizing the accurate inference of the real rainfall. In this process, the paper combines the wireless microwave link data with the traditional rain station data, and uses the observation results of the rain station as the prior knowledge to further calculate the likelihood of the rainfall estimation corresponding to the microwave link data[3-4]. Through this method, the accuracy and reliability of rainfall prediction can be effectively improved. The root-mean-square error RMSE, mean absolute error MAE and correlation coefficient CC deterministic coefficient COD were selected as performance evaluation indexes to verify the robustness of the model.

## 3 Result and Conlusion

The trend surface method is used to interpolate the microwave data, and the results are evaluated with the rain station data. Bayesian method fuses microwave inversion interpolation data and rain station

data. The evaluation indicators of fusion results of 4 rainfall events are shown in Table 1, and the comparison results are shown in Figure 1.

Table 10 Average result accuracy table

| | Rainfall time | RMSE/mm | MAE/mm | CC | COD |
|---|---|---|---|---|---|
| Microwave interpolation | 5. 30 5:20-14:50 | 2.238 | 1.676 | 0.771 | 0.242 |
| | 5.31 1:40-9:40 | 1.783 | 1.461 | 0.82 | 0.503 |
| | 7.16 4:40-17:30 | 2.039 | 2.465 | 0.803 | 0.491 |
| | 10.2 3:30-19:00 | 1.736 | 1.275 | 0.831 | 0.529 |
| Bayesian fusion method | 5. 30 5:20-14:50 | 1.418 | 1.741 | 0.791 | 0.620 |
| | 5.31 1:40-9:40 | 1.119 | 0.92 | 0.851 | 0.707 |
| | 7.16 4:40-17:30 | 1.47 | 0.985 | 0.823 | 0.659 |
| | 10.2 3:30-19:00 | 0.998 | 0.838 | 0.882 | 0.749 |

As can be seen from Figure 1 and Table 1, Bayesian fusion method can also accurately reflect the start and end time of rainfall, and the trend is consistent. Compared with microwave interpolation, Bayesian fusion method has higher correlation with rainfall process and smaller error. As a light rain, the fusion effect of the first rain is slightly poor, because the microwave signal has limited ability to monitor the light rain, and the rain decay value of the light rain is not obvious, and it is easy to make errors in the process of removing the basic attenuation and distinguishing the dry and wet periods. In medium and large rainfall, the CC value of Bayesian fusion method is above 0.82, the COD value is above 0.65, and the MAE value is below 1, so the fusion effect is better. In summary, Bayesian fusion method can improve the accuracy of rainfall, and the fusion effect is related to the rainfall type. The accuracy of light rain is slightly lower, while that of heavy rain is higher.

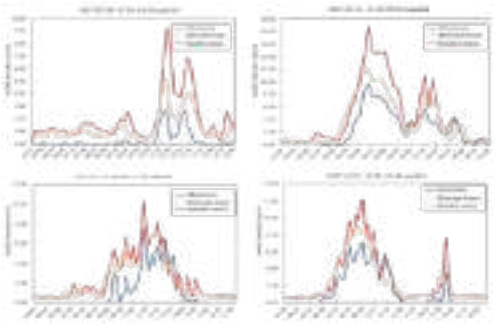

Figure 50 Comparison of rainfall observed by fusion rainfall and surface rainfall measuring station.

## Reference

[1] Guo X, Li W B, Du L, Jia D B and Liu T X 2022 Characteristics and influence factors for the hydrogen and oxygen isotopic of precipitation in Inner Mongolia China Environmental Science 42(03) pp 1088-1096.

[2] Ye Z R, Kong X B, Guo K and Wang Y N 2024 Comparative study of spatial interpolation methods for retrieving rainfall based on commercial microwave link *Journal of China Hydrology* 44(1) pp 50-56.

[3] Zhou T L, Chen M, Yang, C G and Nie Z Q 2020 Data fusion using Bayesian theory and reinforcement learning method. Science China-Information Sciences 63(7), pp 170209.

[4] Ma Y, Sun X., Chen H., Hong Y., and Zhang Y 2021 A two-stage blending approach for merging multiple satellite precipitation estimates and rain gauge observations: an experiment in the northeastern Tibetan Plateau, Hydrology and Earth System Sciences., 25(1),pp 359–374.

**Theme:** Complex water systems, remote sensing and control
**IAHR Thematic Priority Area:** [TPA-4] Digital Transformation
https://doi.org/10.3850/iahr-hic2483430201-353

# Uncertainties Due to Diverse Attributes and Models in Rainfall Retrieval based on Commercial Microwave Links

**Bin Lian[1,2], Zhongcheng Wei[3,4], Lili Huang[1,2] and Jijun Zhao[3,4]**

[1] School of Water Conservancy and Hydroelectric Power, Hebei University of Engineering, Handan, 056038, China
[2] Hebei Key Laboratory of Intelligent Water Conservancy, Handan, 056038, China
[3] School of Information and Electrical Engineering, Hebei University of Engineering, Handan, 056038, China
[4] Hebei Key Laboratory of Security & Protection Information Sensing and Processing, Handan, 056038, China

*Corresponding author: Jijun Zhao.zjijun@hebeu.edu.cn*

**Abstract.** Commercial Microwave Links (CMLs) are becoming effective methods for measuring rainfall, but there are numerous uncertainties that affect the performance of CML-based rainfall measurement. This paper first introduces the theoretical background, and then the uncertainties are categorized into two types: attribute uncertainty and model uncertainty. Furthermore, we utilize two open-source datasets to validate and discuss the impact of key parameters such as rain characteristics, sampling rate, and frequency on the performance of CML-based rainfall retrieval. The findings indicate that the time-frequency feature significantly varies with different rain characteristics. The sampling rate directly influences the selection of parameter values in the models for CML data processing, with a higher sampling rate being preferred due to its superior capability to capture the real-time variability of CML time series. Frequencies between 20 GHz and 35 GHz are found to be more suitable for rainfall retrieval using the ITU power law model.

**Keywords:** Commercial microwave link, power-law model, rainfall measurement, uncertainty analysis

## 1 Uncertainties analysis in rainfall retrieval based on CML

The uncertainties induced by atmosphere and different parameters of the link or model significantly affect the performance of CML-based rainfall measurement [1, 2]. The uncertainties can be broadly categorized into two main aspects, as detailed in **Table 1**.

**Table 1** Uncertainties classification of rainfall measurement based on CML

| Type | | Contents |
|---|---|---|
| Attribute uncertainty | link attributes | frequency, length, polarization, sampling rate, quantization level, sampling strategy (maximum/minimum RSL, average RSL) |
| | environmental attributes | temperature, water vapor, air pressure, fog, dew, wind, time of day, time of year, multi-path propagation |
| | rainfall attributes | DSD, rain types (convective/stratiform), spatial rainfall variability |
| Model uncertainty | wet/dry classification | time-spectrum series analysis model, assisted by other rainfall measurement model, machine learning model |
| | baseline determination | constant baseline model, dynamic baseline model |
| | WAA compensation | constant WAA model, time-dependent WAA model, rainfall intensity-dependent WAA model |
| | path-average rain rate estimation | ITU power law model, DSD-based model, data-driven model |
| | rainfall mapping | spatial interpolation model, tomography reconstruction model |

## 2 Validation and discussion

Two open-source datasets from Prague and Melbourne respectively, are employed to analyze the uncertainties in rainfall measurement based on CML.

### 2.1 Rain characteristics

Rain characteristics, such rainfall types, rainfall intensity and spatial rainfall varieties, are significantly important for rainfall measurement [3]. The rainfall patterns in different areas or environments are not only different in time domain but also in their frequency domain.

### 2.2 Sampling rate

**Figure 1** demonstrates that a higher sampling rate, such as 1 min in the Prague dataset, can capture the nuanced variability of the CML time series more effectively compared to the 15 min sampling rate in the Melbourne dataset, thereby enhancing the accuracy of wet/dry classification based on CML attenuation data.

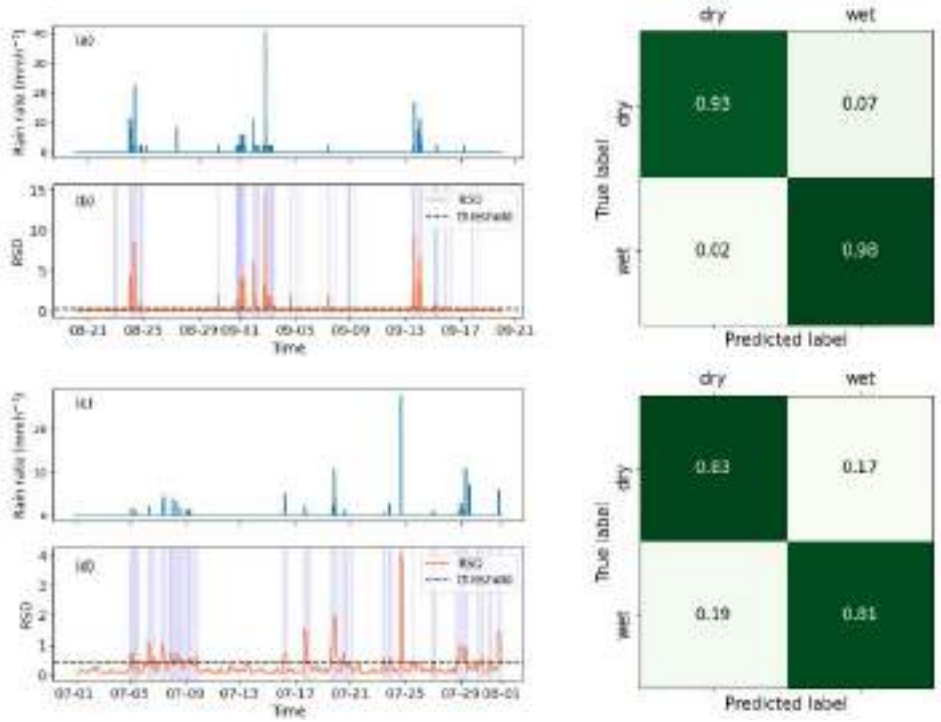


**Figure 1.** The performance of wet/dry classification from the Prague dataset (a), (b) and the Melbourne dataset (c) (d), with the normalized confusion matrices displayed in their respective right locations.

## References

[1] C. Han, G. Zhang, B. Ji, J. Huo, and H. Messer, "On the Potential of Using Emerging Microwave Links for City Rainfall Monitoring," IEEE Communications Magazine, vol. 61, no. 11, pp. 174–180, Nov. 2023, doi: 10.1109/MCOM.001.2200975.

[2] A. Špačková, M. Fencl, and V. Bareš, "Evaluation of error components in rainfall retrieval from collocated commercial microwave links," Atmos Meas Tech, vol. 16, no. 16, pp. 3865–3879, Aug. 2023, doi: 10.5194/amt-16-3865-2023.

[3] K. Pu, X. Liu, X. Sun, and S. Li, "Error Analysis of Rainfall Inversion Based on Commercial Microwave Links With A – R Relationship Considering the Rainfall Features," IEEE Transactions on Geoscience and Remote Sensing, vol. 61, pp. 1–12, 2023, doi: 10.1109/TGRS.2023.3253949.

**Theme:** Complex water systems, remote sensing and control
**IAHR Thematic Priority Area:** [TPA-4] Digital Transformation
https://doi.org/10.3850/iahr-hic2483430201-355

# The Interchangeability of the Cross-Platform Data in the Deep Learning-based Land Cover Classification Methodology

**Keisuke Yoshida [1], Shijun Pan [1], Satoshi Nishiyama [1], Takashi Kojima [2]**

[1] Graduate School of Environmental and Life Science, Okayama University
(Tsushima-naka 3-1-1, Kita-ku, Okayama 700-8530, Japan)
[2] TOKEN C. E. E. Consultants Co., Ltd

*Corresponding author: yoshida.k@okayama-u.ac.jp*

**Abstract.** This study employs a validated airborne Light Detection and Ranging (LiDAR) bathymetry system (ALB) and a UAV-borne Green LiDAR System (GLS) for cross-platform analysis of land cover classification (LCC). Furthermore, the study aims to visualize LiDAR data using high-contrast colour scales and improve the accuracy of land cover classification methods through image fusion techniques. If high-resolution aerial imagery is available, it needs to be downscaled to match the resolution of the low-resolution point clouds. The interchangeability of cross-platform data was assessed by comparing the interchangeability, which measures the absolute difference in overall accuracy (OA) or macro-F1 by comparing the cross-platform inter prediction. It is important to note that relying solely on aerial photographs is inadequate for achieving precise labelling, particularly under limited sunlight conditions that can result in misclassification. In such cases, LiDAR plays a crucial role in facilitating target recognition.

**Keywords:** Airborne LiDAR Bathymetry, Cross-platform, Deep Learning, Green LiDAR System, Riverine Land Cover Classification

## 1 Introduction

If the data collected by different platforms, the impacts on the LCC mapping results derived by this operation has not been demonstrated yet. To observe the impact of cross-platform on LCC in this study as most as possible, the resolution and data styles (i.e., digital imagery, LiDAR) of ALB [1] and GLS in mutual-prediction are chosen as same. On the other side, because of the data limitation, instead of totally same season, the similar season-related ALB and GLS dataset are selected. Eventually, the comparisons in this research obtained from cross-platform mutual-predictions can facilitate understanding of cross-platform data features, and determine a reasonable method to retain the robustness using deep learning method with cross-platform data in LCC mapping producing.

## 2 Data processing

Figure 1 depicts the processing of producing imagery input data for this study [2]. It includes three types of data, i.e., LR-DI (low-resolution digital images derived from high-resolution digital images), LiDAR-I (images derived from LiDAR-based point cloud using a high-contrast color bar), and Image Fusion (images created by superimposing the above images).

## 3 Work flow

To extract features from the input RGB-based imagery (i.e., LR-DI, LiDAR-I, Image Fusion), the processing of training and inference is represented as following: 1. Trimming the raw data from cross-platform input dataset with preprocessing module to attain imagery-based input data (320 pixel × 320 pixel), then training the input data with DeepLabV3+ model to achieve trained model; 2. Predicting the imagery-based input data with trained model. To end with attaining the results (i.e., OA and

Macro-F1 from mutual-prediction, separately); 3. Comparing the averaged and absolute difference value for confirming interchangeability of cross-platform dataset.

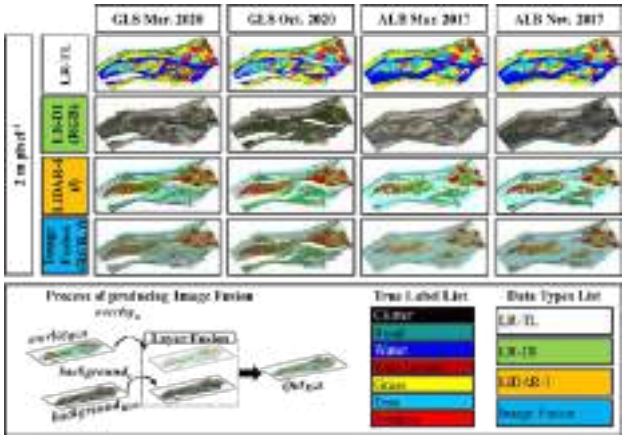


Figure 51 2 m pixel$^{-1}$ Imagery-based input (LR-TL, LR-DI, LiDAR-I, Image Fusion), Image Fusion processing, True Label List and Data Types.

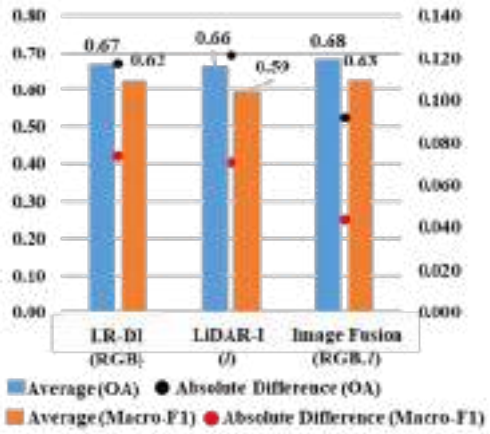


Figure 2 Comparison of data style-based averaged 2m pixel$^{-1}$ resolution cross-platform interchangeability; Left vertical axis: the reference of OA and Macro-F1 value; Right vertical axis: the reference of Absolute Difference value.

## 4 Conclusion

This study used the cross-platform LiDAR and photograph to prove the interchangeability between the data derived from different platforms in the term of performing LCC. Compared with LR-DI and LiDAR-I, Image Fusion approach improved the performance of cross-platform LCC. And all the approaches have the results of over 0.65 OA and around 0.6 Macro-F1 shown in Figure 2. To put it another way, to some content, cross-platform data can be used for inter-predicting each other. Noteworthy, digital imagery solely is not sufficient for producing TL mapping under multiple weather conditions because of the sensitive camera senor in the different weathers. Responsibly, at that moment, LiDAR becomes a considerable reference in assisting to recognize the targets.

## Reference

[1] Yoshida, K., Pan, S., Taniguchi, J., Nishiyama, S., Kojima, T., & Islam, T. Airborne LiDAR-assisted deep learning methodology for riparian land cover classification using aerial photographs and its application for flood model-ling. *Journal of Hydroinformatics 24 (1)*, 179–201, 2022.

[2] PAN, S., YOSHIDA, K., KOJIMA, T., & NISHIYAMA, S. (2022). Drone-LiDAR-assisted Image Fusion methodology for Deep Learning-based Land Cover Classification. *Artificial Intelligence and Data Science*, *3*(3), 15-25.

**Theme:** Complex water systems, remote sensing and control
**IAHR Thematic Priority Area:** [TPA-4] Digital Transformation
https://doi.org/10.3850/iahr-hic2483430201-357

# Urbanization-Induced Drought Modification: Example over the Yangtze River Basin, China

**Xiang Zhang [1], Yu Song [1]**

[1] National Engineering Research Center of Geographic Information System, School of Geography and Information Engineering, China University of Geosciences, Wuhan, 430074, China.

*Corresponding author: zhangxiang76@cug.edu.cn*

**Abstract.** This paper proposed a multi-source precipitation data fusion and downscaling method named Generate high Resolution, Accurate, Seamless data using Point-Surface fusion (GRASPS). The advantages of currently several satellite/model data were fully integrated to generate a more accurate precipitation dataset at daily and 1 km scale covering the Wuhan Urban Agglomeration, including the Integrated Multi-satellitE Retrievals for Global Precipitation Measurement (IMERG) from the Global Precipitation Measurement (GPM) mission, Tropical Rainfall Measuring Mission (TRMM) Multi-satellite Precipitation Analysis (TMPA), Precipitation Estimation from Remotely Sensed Information using Artificial Neural Networks - Climate Data Record (PERSIANN-CDR). The Pearson Correlation Coefficient reached 0.77, while Root Mean Squared Error, Mean Absolute Error and Bias were reduced to 6.08 mm, 2.20 mm and -0.13 mm, respectively, under the validation of precipitation at 36 ground gauges. Compared to previous studies, this research has successfully improved the spatial resolution of precipitation dataset to 1 km and more importantly, the accuracy of extreme precipitation was specifically corrected, resulting in an accuracy increase from 76.92% to 91.67%.

**Keywords:** fusion, ground data, random forest

## 1 Introduction

Precipitation plays a vital role in the Earth's water cycle and hydrology, meteorology, and agriculture research. However, previous studies are mainly concentrated in large-scale areas such as river basins or countries, and most of their spatial resolutions are up to 0.05°. Meanwhile, the correction accuracy varies depending on the ground gauge coverage and temporal scale. To solve these key issues, this study proposed a GRASPS method (Generate high Resolution, Accurate, Seamless data using Point-Surface fusion) to generate 3H precipitation data.

## 2 Study Area and Data

In this study, we selected a typical 30 million population urban area, i.e., Wuhan Urban Agglomeration (WUA) as our study area. Three types of data were selected for precipitation fusion in this study, including multiple satellite precipitation products, precipitation related data (i.e., cloud cover data, vegetation cover data and terrain data) and ground gauge precipitation data. Three widely used satellite precipitation products were selected, i.e., IMERG, TMPA and Precipitation Estimation from Remotely Sensed Information using Artificial Neural Networks - Climate Data Record (PERSIANN-CDR). Digital Elevation Model (DEM), Normalized Difference Vegetation Index (NDVI) and cloud cover data in the study area are also selected as alternative variables to represent the potentially spatial heterogeneity of precipitation.

## 3 Methods

The overall method process is divided into three steps: (a) Data collection and preprocessing; (b) GRASPS method execution; (c) Accuracy verification and sensitivity test. Firstly, the selected data is collected and necessary preprocessing (resampling, cropping, extraction, and dataset segmentation,

etc.) is performed. Based on that, the downscaling model is trained and the data downscaling fusion is carried out, then the optimal model is obtained by cross-validation in the training process. After that, the trained model and the generated downscaling dataset are evaluated from various aspects using a variety of evaluation indicators.

## 4 Results and Discussion

To quantitatively evaluate the accuracy of proposed method, the trained model was used to fuse the previously validated inputs. The results of four evaluation indicators (PCC, RMSE, MAE and BIAS) are shown in FIG. 1.

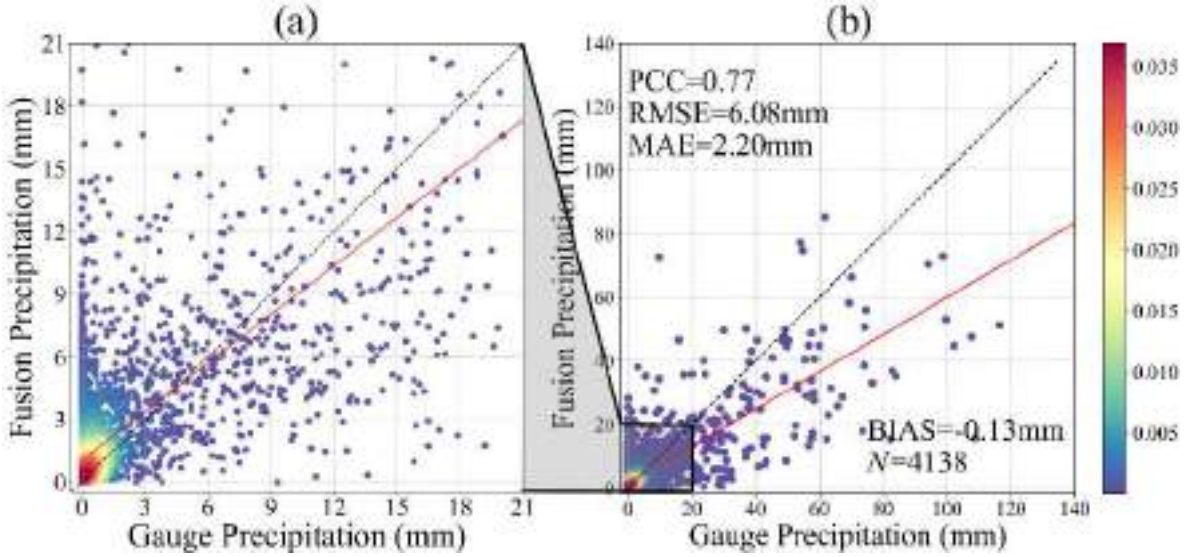


Fig. 1. Scatter plots and evaluation indicators of daily fusion precipitation data and daily ground gauge precipitation data in 2019. X-axis and Y-axis represent precipitation at ground gauges and fusion precipitation, respectively.

## 5 Conclusions

In this study, GRASPS, as a downscaling fusion correction method for multi-source precipitation data based on RF, is proposed. GRASPS firstly conducted the spatial downscaling of three kinds of satellite precipitation data (IMERG, TMPA and PERSIANN-CDR) and cloud data. Then temporal data is added for fusion, and the gauge precipitation data is used for correction. Finally, the aimed 3H precipitation dataset with high spatial resolution (1 km), high precision (Overall PCC up to 0.77 while RMSE and MAE lower to 6.08 and 2.20 mm) and spatio-temporal continuity (daily and spatial seamless) was generated in WUA in 2019. Compared with the original satellite precipitation datasets, the 3H dataset generated in this study combines their advantages and corrects their original precipitation errors. The obtained results showed a high degree of similarity with the site interpolation data. Based on the validation of 36 ground gauges, the index of PCC, RMSE and MAE demonstrated significant improvements at different spatial and temporal scales. It also shows excellent performance in different land covers, especially in urban areas.

## Reference

[1] Zhang X, Song Y, Nam W H, et al. Data fusion of satellite imagery and downscaling for generating highly fine-scale precipitation[J]. Journal of Hydrology, 2024, 631: 130665.

**Theme:** Complex water systems, remote sensing and control
**IAHR Thematic Priority Area:** [TPA-4] Digital Transformation
https://doi.org/10.3850/iahr-hic2483430201-359

# A Performance Evaluation of CA-Markov and CA-ANN in Land Use Land Cover Prediction

**Ajisha S[1], Manjula R[2]**

[1] National Institute of Technology, Tiruchirappalli 620015, India
[2] National Institute of Technology, Tiruchirappalli 620015, India

*Corresponding author: ajishaphd@gmail.com*

**Abstract.** The monitoring and management of environmental parameters depends substantially on Land Use Land Cover (LULC) prediction. Multiple frameworks have been created to forecast future LULC, with CA-Markov and CA-ANN being the most well-liked models by researchers. The purpose of this study is to compare and contrast these two model's performances in terms of LULC prediction features, including their pros and cons as well. This study uses the Cellular Automata (CA)-Markov model and the CA-ANN (Artificial Neural Network) model to anticipate and assess the future LULC of the Noyyal River Basin (36,000 sq.km), TamilNadu, India. Both models give equivalent results which shows that, the Noyyal basin experiences rapid urbanization between the years 2031 and 2041, with a drop in the area used for agriculture, water bodies, and forests and an increase in the area used for barren land and urban areas. Also, area difference is also observed in some of the predicted classes for both models. The kappa value for predicted LULC using CA-Markov and CA-ANN models is 0.832 and 0.739 respectively.

**Keywords:** Artificial Neural Network, CA-Markov, Cellular Automata, Landsat, LULC prediction, Noyyal Basin

## 1 Introduction

Land use refers to how much human intervention alters the natural land cover [1] and Land cover refers to the category of the land based on what is present on its surface and immediate sub-surface [2]. Urbanization is one of the major factors of land use change. People migrate to cities for economic growth, innovation, and to escape poverty. The World Bank projects metropolitan populations to reach 6 billion by 2045, growing 1.5 times [3]. But changes in LULC have negative impact in environment and ecosystem. Hence, prediction of LULC change is essential to monitor and protect the environment.

### 1.1 Model Description

Many models are used to analyze the LULC change, however, comparing the models within the same research region will provide light on each model's benefits and efficiency. This study evaluates CA-Markov and CA-ANN model performance on LULC prediction in Noyyal basin.
Owing to its open structure and its ability to combine with other models the spatio-temporal elements CA models are used well used for LULC prediction in recent years [4]. CA model with a transition probability matrix is used to predict LULC. Considering the right magnitude of change for a particular time generated by Markov chain and the right direction of change produced by the cellular automata analysis, the CA-Markov method has been developed [5].

### 1.2 Methodology

2001, 2011 and 2021 LULC maps were generated using the Landsat images of 30m resolution. The imagery of same seasons and cloud cover with less than 2% cloud cover are selected. Landsat images were preprocess and its quality was enhanced. Support Vector machine- Supervised Learning

technique to produce the classified LULC maps with 6 classes as Water body, Forest, Vegetation, Agricultural area, Builtup area, and Barren land. DEM, proximity from road, slope, and proximity from the river were considered as the auxiliary data. Using Euclidean distance method, the proximity from the parameters was calculated. The initial prediction was done to obtain 2021 LULC map which is validated with already available LULC map. Then the LULC map for 2030 and 2040 was generated.

## 2 Results

Results show that the trend in LULC change from one class to other (positive or negative) is predicted same by both the models. However, the area changes numerically differ with some variation. Both models give equivalent results which shows that, the Noyyal basin experiences rapid urbanization between the years 2031 and 2041, with a drop in the area used for agriculture, water bodies, and forests and an increase in the area used for barren land and urban areas. However, area difference in predicted LULC for 2031 between the two models were: Water body – 0.163 $km^2$; Forest land – 32.681 $km^2$; Vegetation- 180.08 $km^2$; Agricultural area- 75.871 $km^2$; Builtup area- 111.297 $km^2$; Barren land- 25.423 $km^2$. The kappa value for LULC forecast using CA-Markov approach is 0.832, and for the CA-ANN method is 0.739.

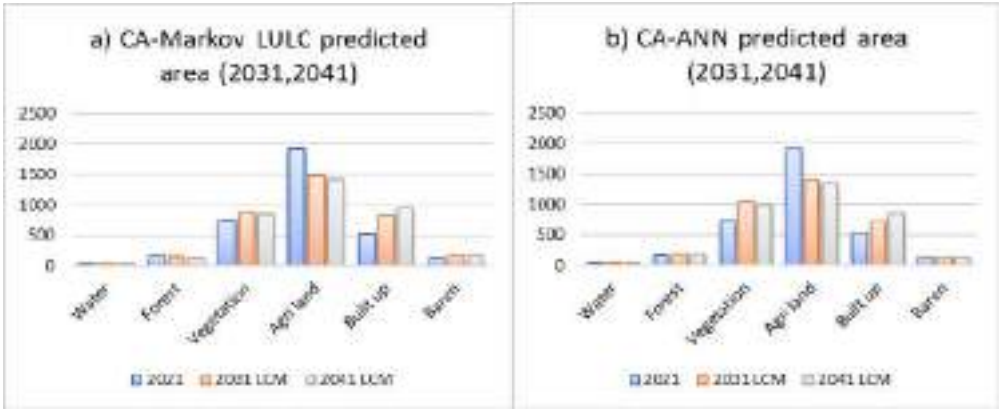


Figure 52 Comparison of predicted and actual area

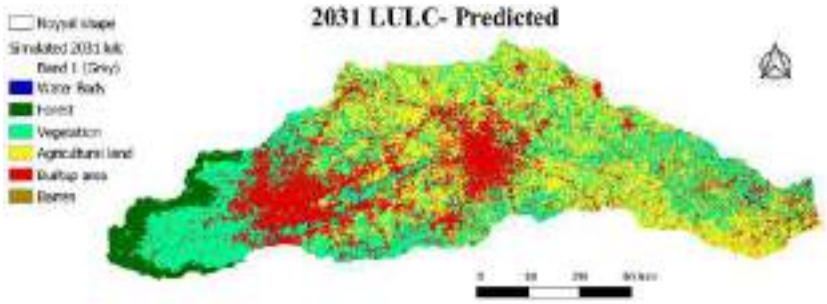


Figure 53 LULC predicted 2031 – CA Markov

## Reference

[1] Ebenezer B, Geophery KA, Jonathan AQ-B, Emmanuel AD, Land-use change and sediment yield studies in Ghana: review (2018) J Geogr Reg Plan 11:122–133.
[2] Wang SW, Munkhnasan L, Lee W-K, Land use and land cover change detection and prediction in Bhutan's high altitude city of Thimphu, using cellular automata and Markov chain. (2021) Environ Chall 2:100017.
[3] World Bank report on urban development –overwiew.
[4] M.H Saputra and H.S. Lee, Prediction of Land Use and Land Cover Changes for North Sumatra, Indonesia, Using an ArtificialNeural-Network-Based Cellular Automaton, Sustainability 2019, 11, 3024
[5] Sarkar A, Chouhan P, Dynamic simulation of urban expansion based on cellular automata and markov chain model: a case study in Siliguri Metropolitan Area. (2019) West Bengal Model Earth Syst Environ 5:1723–1732.

**Theme:** Complex water systems, remote sensing and control
**IAHR Thematic Priority Area:** [TPA-4] Digital Transformation
https://doi.org/10.3850/iahr-hic2483430201-361

# Integration of Remote Sensing and On-Site Hydro-Meteorological Data in Real-time Monitoring for Smart Irrigation

**Chih Chao Ho[1,*], Ming xing Li[1], Jian Cheng Liao[1], Shih Wei Chiang[2], Tsu Chiang Lei[1]**

[1] Construction and Disaster Prevention Research Center, Feng Chia University, No. 100, Wenhua Rd., Xitun Dist., Taichung City,407, Taiwan, China
[2] Agricultural Engineering Research Center, No. 18, Hejiang Rd., Zhongli Dist., Taoyuan City, **320030**, Taiwan, China

*Corresponding author: zz0813@gmail.com*

**Abstract.**
Taiwan is actively implementing smart irrigation technology to manage water scarcity and reduce its impact on society and the environment. By using automated water gates and monitoring hydro-meteorological conditions, soil moisture, and water storage in field, irrigation schedules and quantities are adjusted based on climate variations. This precise, "on-demand supply" approach aims to increase water use efficiency and enhance the stability of regional water supplies.
Despite advancements, challenges persist, such as the high costs of field sensor deployment and labor-intensive surveys needed for assessing irrigation zones. These hurdles limit the ability to gather real-time data on irrigation areas and water demand, which is critical for optimizing smart irrigation practices.
To address these challenges, the study utilizes satellite imagery for its broad coverage, frequent updates, and multispectral data to accurately identify current rice cultivation areas. This satellite data is integrated with real-time hydro-meteorological information, soil types, water conveyance efficiency, crop growth stages, and crop coefficients to calculate irrigation needs in agricultural regions, providing crucial real-time data for effective smart irrigation management.
The research introduces innovative models for analyzing rice cultivation and estimating real-time irrigation water usage. The overall architecture is shown as Figure 1, and the approach is described as follows.
1. Rice Crop Interpretation Model
The rice crop interpretation model employs Sentinel-2 multispectral imagery, SCL products, maps of cultivated fields, and rice cultivation surveys data to accurately determine rice-growing areas. To enhance the precision of crop identification, an uncertainty decision analysis approach is employed, strengthening the outcomes of decision trees, neural networks, and logistic regression.
2.Irrigation Water Demand Estimation Model
The TaiCropWat model estimates irrigation water demand by combining real-time hydro-meteorological data, crop data such as planting location and field size, and environmental factors like soil texture and canal water loss. This model calculates crop evapotranspiration and field water requirements for each growth stage.
The study used satellite imagery from 2021 to classify first crop rice and estimate irrigation water needs in the Hsinchu area. The imagery was collected on February 4, March 16, March 26, April 5, May 15, and June 14. Classification accuracies ranged from 92.15% to 98.78%, with Kappa coefficients from 0.82 to 0.97. The lowest classification accuracy was on February 4 due to the coarse spatial resolution and smaller size of rice seedlings during early transplanting.
Using data on rice cultivation areas and growth periods for the first crop rice—covering the nursery, field preparation, and main crop stages from February 6 to July 10—the study incorporated hydro-

meteorological, crop, and environmental data into the TaiCropWat model. This simulation provided crop evapotranspiration and field water requirements for each stage of crop growth. Results showed field leakage of 1,507 mm, effective rainfall of 430.13 mm, crop evapotranspiration of 362 mm, and field water requirements of 1,608.85 mm.

The study demonstrates the feasibility of replacing traditional manual surveys with satellite remote sensing. The findings indicate that, except for the initial stage of crop growth (February), accuracy consistently exceeds 90%, enabling efficient and rapid acquisition of the actual rice cultivation area. Furthermore, utilizing the TaiCropWat model allows us to account for variations in field water storage due to rainfall and estimate the water required for crops. This approach provides crucial insights for smart irrigation and effectively addresses past challenges, such as the substantial costs associated with sensor installation and subsequent maintenance issues.

In conclusion, this study, integrating satellite remote sensing and the TaiCropWat model, paves the way for precision agriculture in Taiwan. Through the application of these technologies, stakeholders can more accurately assess irrigation needs, optimize water resource management strategies, enhance agricultural productivity, and simultaneously reduce resource consumption and environmental impact.

**Keywords:** Satellite, Uncertainty Rice Crop Interpretation, Irrigation Water Demand Estimation

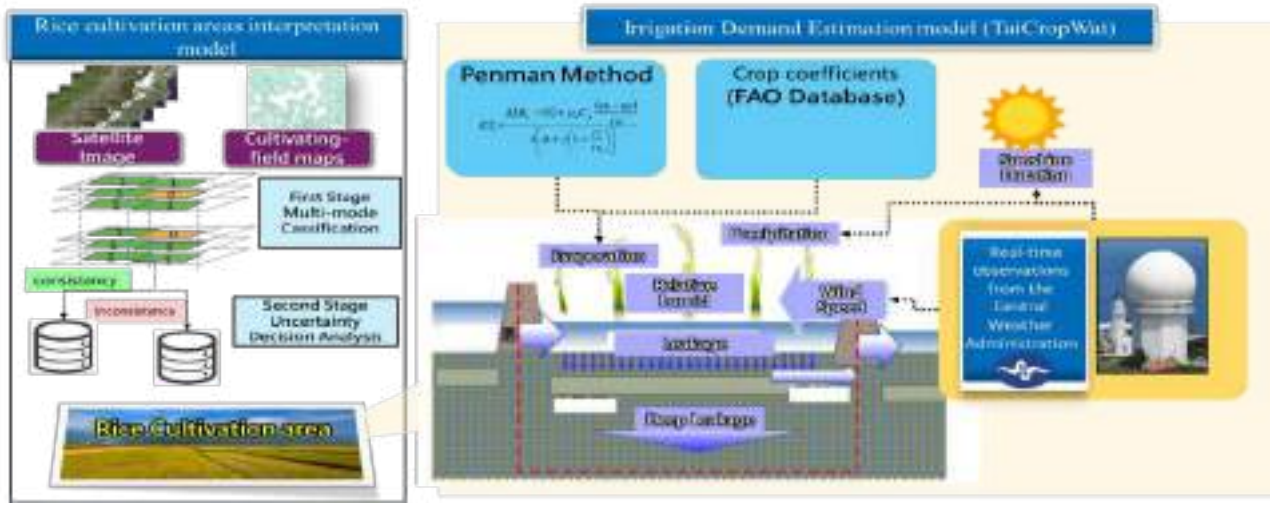


Fig. 1. Research Methodology Framework

## Reference

[1] Yang, M. D., Tseng, H. H., Hsu, Y. C., Yang, C. Y., Lai, M. H., & Wu, D. H. (2021). A UAV open dataset of rice paddies for deep learning practice. Remote Sensing, 13(7), 1358.

[2] Yang, M. D., Tseng, H. H., Hsu, Y. C., & Tsai, H. P. (2020). Semantic segmentation using deep learning with vegetation indices for rice lodging identification in multi-date UAV visible images. Remote Sensing, 12(4), 633.

[3] Allen, R.G., & Pruitt, W.O. (1991). FAO-24 Reference Evapo- transpiration Factors. Journal of Irrigation and Drainage Engineering. 117(5), 758-773.

[4] El Hajj, M., Bégué, A., Guillaume, S., & Martiné, J. F. (2009). Integrating SPOT-5 time series, crop growth modeling and expert knowledge for monitoring agricultural practices -The case of sugarcane harvest on Reunion Island. Remote Sensing of Environment, 113(10), 2052-2061.

[5] Lei, T. C., Wan, S., & Chou, T.Y. (2008). The Comparison of PCA and Discrete Rough Set for Feature Extraction of Remote Sensing Image Classification -A Case Study on Rice Classification, Taiwan. Computational Geosciences, 12, 1-14.

[6] Yang, M. D., Huang, K. S., Kuo, Y. H., Tsai, H. P., & Lin, L. M. (2017). Spatial and spectral hybrid image classification for rice lodging assessment through UAV imagery. Remote Sensing, 9(6), 583.

**Theme:** Complex water systems, remote sensing and control
**IAHR Thematic Priority Area:** [TPA-4] Digital Transformation
https://doi.org/10.3850/iahr-hic2483430201-363

# Dynamic Change Analysis of Human-induced Soil Erosion in the Fenhe River Basin from 2020 to 2023

**Kai Guo[1,2,3], Xiangbing Kong[1,2,*], Yuzhong Wen[4], Huashi Guo[4], Yinan Wang[1,2], Chunjing Zhao[1,2], Jintao Zhao[1,2]**

[1] Yellow River Institute of Hydraulic Research, Zhengzhou, 450003, China
[2] Key Laboratory of Water and Soil Conservation in the Loess Plateau, MWR, Zhengzhou, 450003, China
[3] The National Key Laboratory of Water Disaster Prevention, Hohai University, Nanjing 210098, China
[4] Huzhu County Water Resources Bureau, Huzhu, 632126, China

*Corresponding author: guokai@hhu.edu.cn; kongxb@foxmail.com*

**Abstract:** Uncontrolled human-induced soil erosion can cause land resource degradation, damage to ecosystem service functions, and is also one of the main causes of floods, landslides, and debris flows. Using high-resolution remote sensing images, a ResNeXt AttU-Net deep learning model was designed to conduct automatic interpretation experiments on human-induced soil erosion patches in the typical watershed of the Fenhe River. Combined with human-computer interaction interpretation and preliminary judgment of compliance with prevention and control responsibilities, the human-induced soil erosion areas in the Fenhe River Basin from 2020 to 2023 were interpreted and extracted. Based on topography, administrative regions, socioeconomic factors, and other factors, the distribution and dynamic changes of soil erosion were analyzed. The results showed that the interpretation accuracy of human-induced soil erosion based on the ResNeXt AttU-Net deep learning model exceeded 80%. The more developed the regional economy, the more serious the human-induced soil erosion, among which the economic development zone had the most concentrated and severe human-induced soil erosion. The serious human-induced soil erosion in the Fenhe River basin mainly occurred in hilly areas, and the project types were mainly open-pit coal mines, processing and manufacturing projects, industrial park projects, and open-pit non-metallic mines. The number and area of human-induced soil erosion patches in the Fenhe River basin showed a downward trend, and remote sensing monitoring projects for human-induced soil erosion played an important role. The article provides a solution for accurately grasping the situation of regional anthropogenic soil erosion, providing a reference basis for the scientific management, systematic governance, and policy formulation of anthropogenic soil erosion in the Fenhe River Basin.

**Keywords:** Deep learning, Human-induced soil erosion, Remote sensing interpretation, Soil and water conservation, Supervision

- A ResNeXt AttU-Net model, which considers aggregating residuals and employing an attention module, has been designed for the extraction of human-induced disturbance patches, achieving an interpretation accuracy of over 80% for human-induced soil erosion.

Table 1 Comparison of the Precision of Human-induced Disturbance Change Detection Results

| Evaluating Indicator | Precision | Recall | Omission | F1 |
|---|---|---|---|---|
| FCN | 0.528 | 0.637 | 0.363 | 0.577 |
| SegNet | 0.539 | 0.641 | 0.359 | 0.586 |
| U-Net | 0.557 | 0.664 | 0.336 | 0.606 |
| Siam U-Net | 0.683 | 0.742 | 0.258 | 0.711 |
| ResX-Att-UNet | 0.838 | 0.906 | 0.094 | 0.871 |

- The severity of human-induced soil erosion exhibits a positive correlation with the relative level of regional economic development. The more developed the regional economy, the more serious the human-induced soil erosion, among which the economic development zone had the most concentrated and severe human-induced soil erosion.

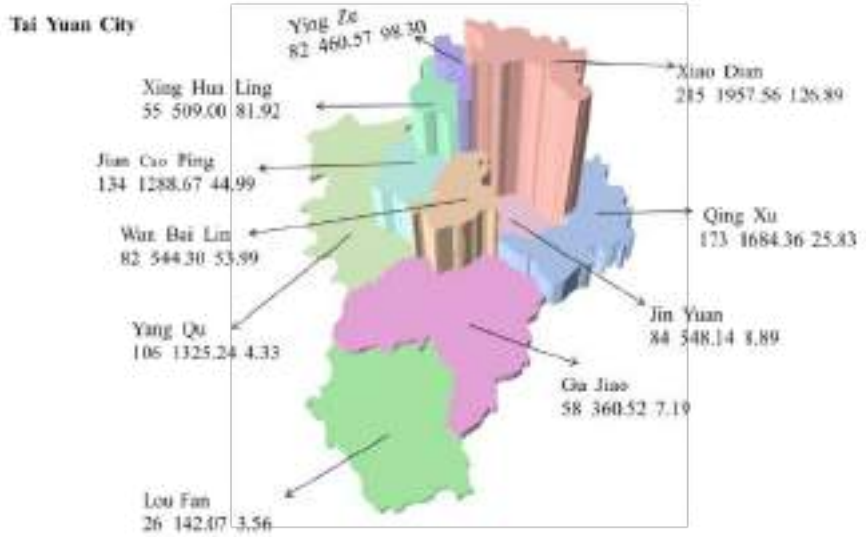


Figure 1 Analysis of the Number, Area, and GDP of Human-induced Soil Erosion Spots in Taiyuan City(Each county was represented by three numerical values, respectively indicating: the number of human-induced soil erosion spots, the area of human-induced soil erosion spots (unit:$hm^2$), and the revised GDP (unit: Billion RMB)).

- The remote sensing monitoring project for soil erosion based on high-resolution remote sensing images has played a significant role in effectively curbing violations of soil and water conservation regulations and enhancing public awareness of soil and water conservation laws, resulting in a declining trend in the number and area of man-made soil erosion spots in the Fenhe River Basin year by year.

Table 5 Statistical Table of Annual Human-induced Soil Erosion in the Fenhe River Basin

Area Unit: $hm^2$

| Types of violations | 2020 | | 2021 | | 2022 | | 2023 | | Total | |
|---|---|---|---|---|---|---|---|---|---|---|
| | Count | Area | Count | Area | Count | Area | Count | Area | Count | Area |
| Construction without approval | 1654 | 13290 | 670 | 3838 | 340 | 1899 | 250 | 1147 | 2914 | 20174 |
| Exceeding the scope of responsibility for prevention and control | 18 | 238 | 13 | 402 | 9 | 129 | 12 | 201 | 52 | 971 |
| Abandon without approval | 18 | 158 | 14 | 88 | 3 | 57 | | | 35 | 303 |
| Putting into production before acceptance | | | 4 | 35 | 1 | 29 | | | 5 | 64 |
| Change before approval | 3 | 77 | 1 | 1 | | | | | 4 | 79 |
| Change of construction site | | | 1 | 13 | | | | | 1 | 13 |
| Summary | 1693 | 13764 | 703 | 4377 | 353 | 2114 | 262 | 1349 | 3011 | 21603 |

**Theme:** Complex water systems, remote sensing and control
**IAHR Thematic Priority Area:** [TPA-4] Digital Transformation
https://doi.org/10.3850/iahr-hic2483430201-365

# Analysis of the Temporal and Spatial Evolution of NDVI and Its Correlation with Soil Moisture Content in Extreme Arid Areas: A Case Study of the Kekeya Irrigation District in Turpan

**Pengbo Zhao[1,2*], Weiwei Xu[1,2], Mei Ma[1,2], Xin Li[3]**

[1] Institute of Water Resource Science in Turpan , Turpan 838000, China; frederickarry@163.com
[2] Institute of Karez Research in Turpan, Turpan 838000, China; frederickarry@163.com
[3] Center for Water Resources Management in Turpan, Turpan 838000, China; lixin_00668@163.com

*Corresponding author: Pengbo Zhao. frederickarry@163.com*

**Abstract:** With the continuous development of remote sensing and soil moisture monitoring technologies, new technical have been provided for the allocation and regulation of agricultural water resources, facilitating the exploration of the spatiotemporal evolution of NDVI (Normalized Difference Vegetation Index) in extremely arid regions and its correlation with soil moisture content. We selected the Kekeya Irrigation District in Turpan, Xinjiang as the study area, and conducted an analysis of the spatiotemporal evolution of NDVI and the correlation between soil moisture content in different soil layers, based on Landsat 8 remote sensing images and long-term soil moisture monitoring data. The trend analysis method and Grey Relational Analysis method were employed for this analysis. The results show that NDVI exhibits a negative correlation trend from March to October, with grape crops showing the most significant trend. The ranking of soil moisture content influencing NDVI changes varies with soil depth, with the order being: 60 cm > 20 cm > 10 cm > 40 cm. By integrating remote sensing imagery with soil moisture monitoring instruments, information technology means can further enhance the management level of irrigation districts, providing reference for water resource conservation in irrigation districts.

**Keywords:** hyper-arid zone; remote sensing technology; Normalized Difference Vegetation Index; Grey System Theory

## 1 Introduction

With the escalating global climate change and intensified human activities, the issue of water scarcity is becoming increasingly severe. Soil moisture, as a vital component of water resources, holds significant importance in maintaining ecological balance and ensuring agricultural production. In Xinjiang, there is relatively little interannual variation in vegetation cover and meteorological factors, showing an overall stable trend, but significant intra-annual variations [1].

Utilizing methods such as trend analysis and Grey Relational Analysis, the study investigates the spatiotemporal evolution characteristics of NDVI and its relationship with soil moisture in the Kekeya irrigation area, a region prone to extreme drought. The aim is to provide theoretical references and technical support for vegetation protection and water resource utilization efficiency monitoring in the study area.

## 2 Methods

Based on Landsat 8 data from March to October 2023, this study employs a univariate linear regression method to calculate the trend of each pixel over eight months. A regression slope (R > 0) indicates an increasing trend in NDVI, while (R < 0) suggests a decreasing trend in NDVI.

$$Slope = \frac{n\sum_{i=1}^{n}(i \times NDVI_i) - \sum_{i=1}^{n} i \times \sum_{i=1}^{n} NDVI_i}{n\sum_{i=1}^{n} i^2 - (\sum_{i=1}^{n} i)^2} \quad (1)$$

Grey Relational Analysis is an uncertainty analysis method. It identifies the factors with the most significant influence on the target factor by calculating the primary relationships between the target factor and corresponding factors. By quantifying the degree of relationship between them, it quantitatively illustrates the interrelationship between changing factors and corresponding factors.

## 3 Results

From a temporal perspective, the analysis reveals an increasing trend in vegetation NDVI from March to September, with a maximum growth rate of NDVI exceeding 70%. During the period from May to September, the fluctuation in NDVI is relatively minor, likely attributable to continuous agricultural irrigation. However, a declining trend in NDVI is observed starting from October, coinciding with the practice of burying grapevine branches in the soil for winter insulation. We conducted univariate linear regression analysis on the data, revealing a negative trend in the variation of NDVI from March to October in the study area. The slopes in the crop-growing areas were consistently less than 0, indicating a decreasing trend. The influence of soil moisture content on NDVI changes varies depending on the soil depth, with the ranking as follows: 60 cm > 20 cm > 10 cm > 40 cm. The results indicate a higher correlation between soil at a depth of 60 cm and NDVI. As shown in **Fig. 1.**

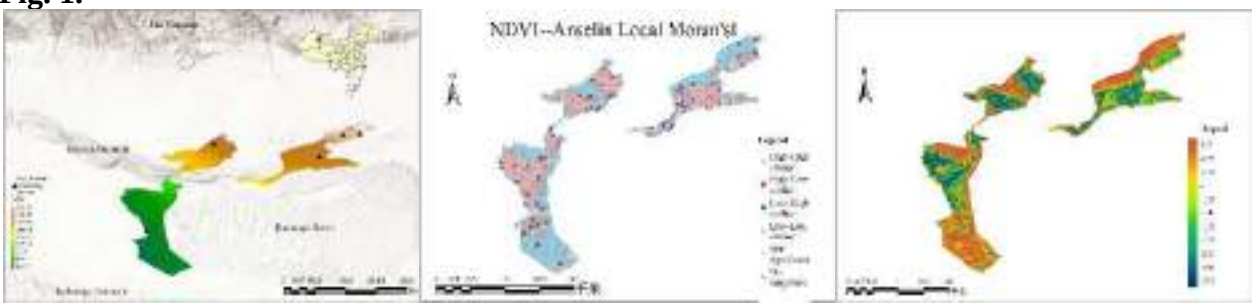


**Fig. 2.** Location of the Kekeya Irrigation District（a）; Spatial cluster distribution(b); Univariate linear regression analysis(c)

## 4 Conclusions

(1) Due to the influence of Huoyan Mountains, there are significant differences between the northern and southern regions in terms of temperature and vegetation coverage. The southern basin accumulates higher temperatures, resulting in better sugar accumulation in melon and fruit crops, but water resources are relatively scarce. The northern basin, located near the Tianshan Mountains, benefits from snow melting in the Tianshan, leading to relatively abundant water resources, albeit with temperature changes lagging behind. Spatially, temperatures are lower in the northern region of Huoyan Mountains compared to the southern region, while NDVI distribution is primarily concentrated in large areas of grape crops with significant changes.

(2) There exists a significant relationship between NDVI and soil moisture, showing sensitivity to changes in soil moisture. In terms of influence, the correlation between deeper soil layers and NDVI is stronger, likely closely related to evapotranspiration in the study area, with crops demonstrating significant absorption of moisture from deeper soil layers.

## Reference

[1] Ci, H., & Zhang, Q. (2017). Spatio-temporal Patterns of NDVI Variations and Possible Relations with Climate Changes in Xinjiang Province. Journal of Geo-information Science, 19(5), 662-671. https://doi.org/10.3724/SP.J.1047.2017.00662

**Theme:** Complex water systems, remote sensing and control
**IAHR Thematic Priority Area:** [TPA-4] Digital Transformation
https://doi.org/10.3850/iahr-hic2483430201-367

# Dynamic changes and influencing factors of soil and water erosion in the Pearl River Basin in the past decade

**Xiaolin Liu[1,2], Xiaolei Zeng[1,2], Juan Wang[1,2], Yandong Shi[1,2]**

[1] Soil and Water Conservation Monitoring Center of Pearl River Basin, Pearl River Water Resources Commission of the Ministry of Water Resource, Guangzhou Guangdong 510611, China
[2] Pearl River Hydraulic Research Institute, Peard River;Water Resources Commission of the Ministry of Water Resources, Guangzhou Guangdong 510611, China

*Corresponding author: wangjuan6231@163.com*

**Abstract.** The Pearl River Basin is an ecological barrier for the economic development of the Pearl River Delta, with complex inducements for soil erosion within the basin. Based on the Chinese Soil Loss Equation (CSLE), this article analyzes the changes in soil erosion intensity, area, distribution, and influencing factors in the Pearl River Basin from 2011 to 2023. The results indicate that during this period, the area of soil erosion in the Pearl River Basin has significantly decreased, and the intensity of soil erosion has also notably decreased. From 2011 to 2022, the land use area of forests and construction land has increased, and the vegetation condition has improved. The annual area of comprehensive soil erosion control has generally shown an increasing trend. Through quantitative analysis of the influencing factors of soil erosion changes, this study provides data support and theoretical basis for scientific soil and water conservation.

**Keywords:** soil and water erosion; erosion intensity; dynamic change; influencing factor; Pearl River Basin

## 1 Introduction

The soil erosion in the Pearl River Basin is serious, and the problem of soil erosion within the basin is complex and variable due to differences in the natural environment and policies of the region [1,2]. With the implementation of control measures, the soil erosion situation has gradually improved [3], but there is still a lack of quantitative research on the influencing factors of erosion changes.

## 2 Material and Methods

This paper analyzes the dynamic changes in soil erosion in the Pearl River Basin based on the soil erosion results of 2011 and 2023. Quantitative analysis is conducted from the perspectives of land use, vegetation coverage, and annual changes in newly implemented governance measures in 2011 and 2022, using the Vegetation coverage index data (spatial resolution of 250m) provided by National Tibetan Plateau / Third Pole Environment Data Center, the China Land Cover Dataset form National Cryosphere Desert Data Center (spatial resolution of 30m), the Statistical data on comprehensive management of soil erosion form Ministry of Water Resources of the People's Republic of China.

## 3 Results and Discussion

### 3.1 Analysis of Soil and Water Loss Characteristics

In 2023, Guangxi Zhuang Autonomous Region had the largest area of soil erosion in the Pearl River Basin, followed by Yunnan and Guizhou. The soil erosion is mainly distributed in the upper and middle reaches of the North and South Panjiang River and Yujiang River. Compared with 2011, the area of soil erosion has decreased by 20.75%, showing an overall trend of gradually decreasing from high intensity to low intensity.

Table 11 Statistics of Soil and Water Erosion Changes in the Pearl River Basin in 2011 and 2023

| Year | Soil erosion area at different intensity levels (km²) | | | | | | Total land area occupied (%) |
|---|---|---|---|---|---|---|---|
| | Total | Light | Moderate | Severe | Very Severe | Extremely Severe | |
| 2011 | 96367 | 43296 | 28480 | 13737 | 7902 | 2952 | 21.83 |
| 2023 | 76368 | 55701 | 11079 | 5101 | 3042 | 1445 | 17.30 |
| Changes | -19999 | 12405 | -17401 | -8636 | -4860 | -1507 | -4.53 |
| Change amplitude | -20.75 | 28.65 | -61.10 | -62.87 | -61.50 | -51.05 | — |

## 3.2 Analysis of Factors Influencing Soil and Water Loss

From 2011 to 2022, the forested land and land for construction in the Pearl River Basin saw the largest increase, both exceeding 2,000 square kilometers. The increase in forested land and land for construction was attributed to the concept of "ecological priority and green development" as well as policy support. The increase in the area of high-coverage vegetation and the decrease in the area of medium-low coverage indicate an overall improvement in vegetation conditions. In addition, the annual increase in the comprehensive treatment area of soil erosion has also improved the level of comprehensive treatment of soil erosion.

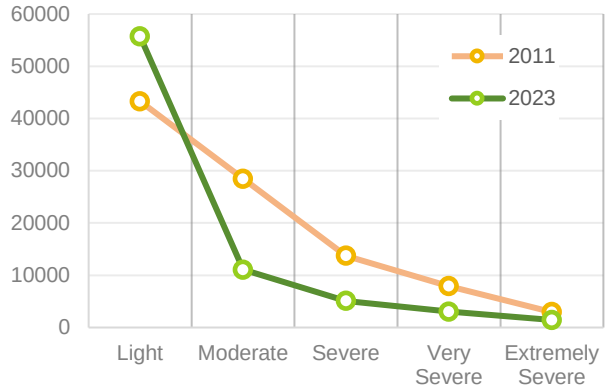


Figure 54 Soil erosion area at different intensity levels

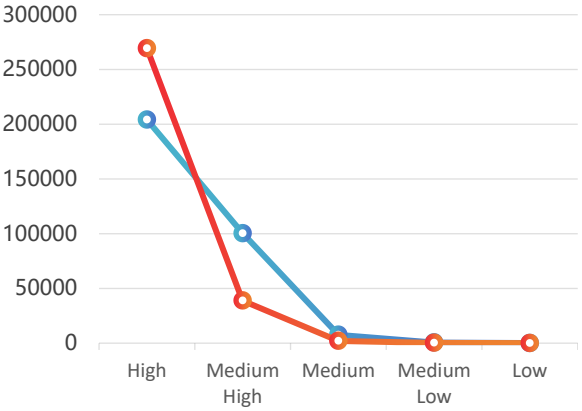


Figure 55 Vegetation coverage area of each level

## 4 Conclusions

The area of soil erosion in the Pearl River Basin has decreased significantly, and the change in soil erosion is showing a trend of gradually decreasing from high intensity to low intensity. Due to urban expansion and related policy factors, the area of forestland and construction land within the basin has increased, resulting in an overall improvement in vegetation conditions. The soil water and soil conservation capacity in the basin has continuously improved, and both the area and intensity of soil erosion have shown a dual downward trend, gradually demonstrating the effectiveness of treatment.

## Reference

[1] Xie, B., & Yang, D. (1993). The status and control of soil erosion in the upstream and midstream areas of the Nanpanjiang and Beipanjiang rivers. People's Pearl River, (04), 34-35.

[2] Wang w, Chen S M, Zhu L, et al. Research on the sensitivity assessment of soil erosion by AHP method:A case study in the Northeast of Ordos Basin[C]//E3S Web of Conferences. EDP Sciences, 2020, 194:e04020.

[3] Liu, X., Wang, J., Jin, P., & others. (2022). Spatial distribution and dynamic changes of soil erosion in the Pearl River Basin. In Proceedings of the 2022 China Water Conservancy Academic Conference (Vol. 2, pp. 542-548). China Water Conservancy Society.

**Theme:** Complex water systems, remote sensing and control
**IAHR Thematic Priority Area:** [TPA-4] Digital Transformation
https://doi.org/10.3850/iahr-hic2483430201-369

# Research on the Leakage Identification of Embankment Dams Based on UAV With Infrared Thermal Imaging

**Po Li[1,2], Lei Tang[2], Shenghang Zhang[2]**

[1] Tianjin University School of Civil Engineering, Tianjin 300350, China
[2] Nanjing Hydraulic Research Institute, Nanjing 210029, China

*Corresponding author: ltang@nhri.cn*

**Abstract.** Timely and accurate identification of leakage is vital for ensuring the safe operation of embankment projects. However, few studies have considered utilizing information related to the temperature field anomalies on dam surfaces obtained through infrared thermal imaging in the leakage detection process. In this context, to explore the feasibility and characteristics of infrared thermal imaging in detecting leakage in embankment dams under natural environmental conditions, this study fully considered the correlation between leakage and temperature, and on-site inspection tests were conducted for dam leakage detection based on infrared thermal imaging. By studying the coupling theory of the seepage and temperature fields, a numerical simulation study was designed to investigate the effects of water–air temperature difference and seepage channel permeability coefficient on the surface temperature field of a downstream dam. The results showed that the infrared images captured by the imager on board our UAV could vividly and intuitively present temperature anomalies caused by the leakage. The temperature development law and infrared image characteristics of the leakage outlet of the earthen dam were consistent with the numerical simulation results. A temperature difference rate index was proposed using model calculations to characterize the degree of the anomaly in the temperature field on the surface of small reservoirs, providing a scientific basis for leakage detection based on infrared thermal imaging using unmanned aerial vehicle platforms.

**Keywords:** Leakage, Embankment dam, UAV, Infrared thermal imaging, Temperature difference rate

## 1 Introduction

Embankment dams, such as earthen and rockfill dams, have a long linear shape and can store a large amount of water, and leakage is the most common type of hazard observed in such dams [1]. Due to the characteristics of spatiotemporal randomness, concealment, and subtle initial magnitude of the leakage, the time frame between the onset of leakage and dam failure is short, placing extremely high requirements on leakage risk mitigation methods [2–4]. Several engineering cases have shown that if leakage is not detected in a timely manner, it can cause serious damage to the dam body, even leading to dam failure [5,6]. In 1976, the collapse of the Teton Reservoir in the United States caused significant personnel and property losses [7], indicating that the rapid detection of leakage is vital for ensuring the safe operation and long-term service of embankment projects [8,9].

## 2 Method

An unmanned aerial vehicle (UAV) equipped with infrared thermal imagers was deployed in this work to detect possible leakages in earthen and rockfill dams, while fully considering the correlation between leakage and temperature. Through leakage calculations using infrared imaging models, the impact of various working conditions on the temperature field in leakage areas on the downstream dam surface during leakage development was analyzed, and the characteristics of the infrared images of these leakage areas under various working conditions were revealed.

## 3 Results

When there is leakage water on the surface of the embankment dam, the difference in the specific heat capacities between the water and the dam medium will be significant, leading to an abnormal temperature distribution at this location. The temperature at the outlet area of the leakage channel is lower than that of the surrounding normal dam body. The infrared thermal image shows a dark blue low-temperature area, which is the leakage area found in this inspection. The highest temperature on the dam surface is close to the temperature of the reservoir water, whereas the lowest temperature is slightly higher than the reservoir water temperature. This is due to the thermal conduction between the dam surface and the atmosphere, whereby a thermal balance is maintained between the dam surface temperature and the atmosphere. However, due to the thermal convection between the reservoir surface and inside of the dam body, the water temperature at the leakage outlet slightly increases. In addition, the infrared thermal imaging of the embankment dam surface is affected by surface covering, such as vegetation and stones, or uneven shallow factors such as dam surface pits. The emissivity of the dam surface is uneven, resulting in an uneven temperature field, as captured by the infrared thermal imaging instrument, causing temperature fluctuations along the characteristic lines. However, the thermal changes along the four characteristic lines in the entire thermal image show a trend of first decreasing and then increasing, with the lowest temperature being at the leakage outlet point.

## 4 Conclusions

The temperature in the region of the leakage outflow point in the exercise site under airborne infrared thermography inspection was lower than that of the surrounding normal dam body, and the IRT map appeared to show a dark blue low-temperature region. The emissivity of the dam surface was not uniform, which made the temperatures along the characteristic feature lines to oscillate; nevertheless, the overall infrared thermogram of the thermal changes along the four feature lines showed a trend of decreasing and then increasing, with the temperature being lowest at the seepage outflow point. It is feasible to use airborne infrared thermal imaging to detect dam leakage.

## References

[1] Su HZ, Zhou RL. Research progress and prospect of earth-rockfill dam leakage detection modes and method. Advances in Science and Technology of Water Resources 2022;42(1):1-10+39. (in Chinese)
[2] Zhang SH, Tang L, Jia Y, Wang YL. Properties of composite phase transition material and its application in underwater emergency plugging test. Journal of Building Materials 2020;23(6):1496-503. (in Chinese)
[3] Chen SS, Zhong QM, Shen GZ. Numerical modeling of earthen dam breach due to piping failure. Water Sci Eng 2019;12(3):169-78. https://doi.org/10.1016/j.wse.2019.08.001.
[4] Fang CG, Jia YM, Zhou XW, Wu CY. Co-relationship between conductivity and geo-technical parameters of Yaodi dike of the Hanjiang river. Journal of Hydraulic Engineering 2003;34(6):119-23+128. (in Chinese)
[5] Xu LQ, Zhang GC, Ma ZK. Development of comprehensive geophysical prospecting technology for hidden danger detection of earth rock dams. Progress in Geophysics 2022;37(4):1769-79. (in Chinese)
[6] Ma LP, Hou JM, Zhang DW, Xia JQ, Li BY, Ni LZ. Study on 2-D numerical simulation coupling with breach evolution in flood propagation. Journal of Hydraulic Engineering 2019;50(10):1253-67. (in Chinese)
[7] Penman ADM. The Teton Dam failure. Eng Geol 1987;24(1-4):257-9. https://doi.org/10.1016/0013-7952(87)90065-2.
[8] Turkmen S. Treatment of the seepage problems at the Kalecik Dam (Turkey). Eng Geol 2003;68(3):159-69. https://doi.org/10.1016/S0013-7952(02)00225-9.
[9] Unal B, Eren M, Yalcin MG. Investigation of leakage at Ataturk dam and hydroelectric power plant by means of hydrometric measurements. Eng Geol 2007;93(1-2):45-63. https://doi.org/10.1016/j.enggeo.2007.02.006.

**Theme:** Complex water systems, remote sensing and control
**IAHR Thematic Priority Area:** [TPA-4] Digital Transformation
https://doi.org/10.3850/iahr-hic2483430201-371

# Application and promotion of unmanned aerial vehicle intelligent inspection system in Panjiakou Reservoir

**Hou Haohua[1] Liu Bingchao[1] Xie Min[2]**

[1]The Water Diversion Project Management Bureau of the Haihe River Water Resources Commission of the Ministry of Water Resources, Tianjin and 300392, China
[2]China Academy of Water Resources and Hydropower Research, Beijing and 100080, China

*Corresponding author: Liu Bingchao.898802678@qq.com*

**Abstract.** Panjiakou Reservoir is the leading reservoir of the Luan River Diversion Project and the largest controlled flood control project on the main stream of the Luan River. It plays an important role in flood control, water supply, power generation, and ecology. In the new development stage, the construction of smart water conservancy has become one of the significant signs of promoting high-quality water conservancy development. Panjiakou Reservoir has closely followed the work deployment of the Ministry of Water Resources and innovatively built a drone intelligent inspection system, opening up a new mode of water conservancy supervision and effectively improving the efficiency of river and lake governance. This article focuses on analyzing the working mechanism and regulatory methods of the unmanned aerial vehicle (UAV) intelligent inspection system. After deployment in the Panjiakou Reservoir, the UAV inspection is used to obtain the surrounding impact of the reservoir, combined with neural network image recognition technology, to dynamically monitor the "four chaos" problem and quickly and intuitively grasp the reservoir situation. Based on the application situation, combined with practical work and new requirements for smart water conservancy construction, suggestions for further application and promotion of unmanned aerial vehicle intelligent inspection in the supervision of Panjiakou Reservoir are proposed.

**Keyword：** drones; intelligent inspection; Panjiakou Reservoir; intelligent water conservancy

## 1 Background of unmanned aerial vehicle intelligent inspection construction

The Ministry of Water Resources deeply implements the spirit of General Secretary Xi Jinping's important exposition on water management, promotes the construction of intelligent water conservancy, and takes it as one of the most significant signs of high-quality development of water conservancy. Panjiakou Reservoir closely followed the deployment of the Ministry of Water Resources, innovatively built a drone intelligent inspection system, opened up a new mode of water conservancy supervision, and effectively improved the efficiency of river and lake management.

## 2 Construction of intelligent inspection by drones

The construction of UAV intelligent inspection system is mainly aimed at the monitoring of the "four chaotic", water law enforcement and other regulatory issues, combined with the regularization of flood control inspection needs, the construction of a set of UAV intelligent inspection system, to achieve the Panjiakou Reservoir throughout the reservoir area of the river remote monitoring function. The construction of digital scene base map and "one map" is mainly to collect and organize satellite remote sensing image data of Luanhe River Basin, establish a phase of satellite image digital scene as the data base map, and use the image data captured in the first phase of the UAV Intelligent Patrol System as the basis for interpreting the regulatory problems of Panjiakou Reservoir, which can be superimposed on the later aerial photography images of the UAV to carry out a multi-phase data comparison and analysis. Comparison and analysis of data; construction of "one map" for Panjiakou

Reservoir supervision based on historical images, basic data of the reservoir, supervision data and "four chaotic" problems.

## 3 Application of intelligent inspection by drones

Intelligent inspection by UAV can not only plan the inspection route according to the arrangement characteristics of the reservoir regulatory elements and inspection requirements, but also realize the compound obstacle avoidance of the UAV to realize the full coverage of the inspection parts. It can also quickly process the image data collected by the drone.

## 4 Work suggestions

For the next development of drone intelligent inspection, one is to improve the system construction and accelerate the development of the "drone intelligent inspection management methods". Second, if we improve the accuracy of data analysis. Third, we should take the initiative to serve the construction of the digital twin project, and give full play to the advantages of UAV intelligent inspection technology.

## Reference

[1]Xu Haofeng, Fu Liwen, Liu Bingchao, et al. A Brief Discussion on the Application of Unmanned Aerial Vehicle Intelligent Inspection Technology in Panjiakou and Daheiting Reservoirs [C]//Chinese Water Conservancy Society. Proceedings of the 2022 China Water Conservancy Academic Conference (Volume 4). The Water Diversion Project Management Bureau of the Haihe Water Conservancy Commission of the Ministry of Water Resources;, 2022:5. DOI: 10.26914/c.cnkihy.2022.059383.

**Theme:** Complex water systems, remote sensing and control
**IAHR Thematic Priority Area:** [TPA-4] Digital Transformation
https://doi.org/10.3850/iahr-hic2483430201-373

# Geochemical Investigation of High Water Salinity at Wadi Aday Well Field: A Case Study from Oman

**Ali Al-Maktoumi[1], Osman Abdalla[2], Azizallah Izady[1], Rahma Al-Mahrouqi[1], Rasha Al-Saadi[1], Al-Mamari Al-Mamari[1], Amira Al-Rajhi[1]**

[1]Water Research Center, Sultan Qaboos University, Muscat, AlKhoud 123, Oman
[2]Earth Science Department, College of Science, Sultan Qaboos University, Muscat, AlKhoud 123, Oman

*Corresponding author: ali4530@squ.edu.om*

**Abstract.** Groundwater play an important role in public water supply in Oman. There are several wellfields operated by the concerned authority "Nama Water". Those wellfields experienced challenges that affected their water supply in both quality and quantity. This study explores causes of water quality deterioration in Wadi Aday wellfield which is located in Muscat Governorate, Oman. Wadi Aday wellfield has recently experienced an increase in groundwater salinity and the causes are still undetected. Therefore, it is crucial to understand the origin and the mechanisms of water salinization for better management and sustainable water supply. Water samples were collected from the wellfield (Nama wells) and wells scattered upstream and downstream of the catchment (agricultural and private wells. Detailed analysis of the results shows that the dominant ions of the water collected from Nama wells are $Cl^-$ , $SO_4^{2-}$, and $Na^+$. The $Ca^{++}$ is present in a reasonable variable amount. The prevailing processes that contribute to the excess of these ions can be attributed to the following factors: Minerals' dissolution, evaporation, soil profile leaching, and scarce Recharge. The dissolution of minerals as the weathering of the rocks forming the aquifers is the main source of ions in the groundwater of the Wadi Aday.

**Keywords**: Aquifer, GIS, Groundwater salinity, Isotopes, Oman

## 1 Introduction

The salinization of groundwater especially in semiarid regions is one of the main challenges and of strategic importance since it places limitations on the use of the water for urban water supply and agricultural use. For the effective management of groundwater resources, especially in arid and semiarid regions, policies depend on understanding the sources and mechanism of groundwater system salinization [2]. To manage the Wadi Aday wellfield, under conditions of accelerating degradation, it is crucial to understand the mechanisms of the salinization. This presented work aims to characterize the chemistry and isotopic composition of groundwater for the Wadi Aday wellfield (Fig. 1) to understand the origin and mechanism of salinization.

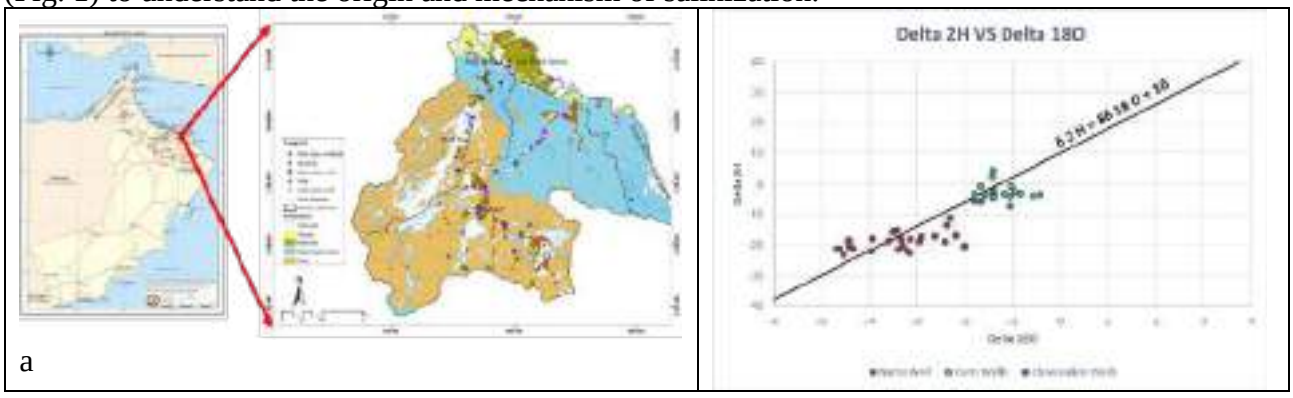


a

Figure. 1: (a) The location of the Wadi Aday wellfield, (b) The plot of $\delta^{18}O$ vs $\delta^{2}H$ for the water samples

## 2 Methodology

Water samples were collected and analysed from the wellfield and from scattered upstream and downstream wells. The collected data and information along with the laboratory measurement results will be gridded in GIS. Finally, hydrological, the hydrogeochemical and isotopes [3, 4] data will then be integrated to develop a groundwater flow and solute-transport model.

## 3 Results and discussion

For Nama wells, the EC reads 2550-2790 µS/cm but for private and public wells ranges from 914-3010 µS/cm. These values suggest moderate to high EC (Brackish water) which could be linked to the presence of dissolved salts and minerals. The TDS measurements showed values between 584.96 and 1926.4 mg/L. This range signifies the presence of dissolved solids in the water and also would suggest rock-water interaction and mineral dissolution along with evaporation effects and leaching from the soil profile which emphasizes direct infiltration. The data shows that the dominant ions of the water collected from Nama wells are Cl-, SO42-, and Na+. The Ca++ is also present in a reasonable variable amount. The prevailing processes that contribute to the excess of these ions can be attributed to the following factors: Minerals' dissolution, Evaporation, Soil profile leaching, and Scarce Recharge. The natural groundwater recharge is the main drive of aquifers' renewability and quality maintenance. The analytical results of the groundwater Isotopes show that two groups of water with slightly distinguished features have been revealed (Fig 1b). The first group comprises the depleted samples with negatively signed isotopes and is exclusively formed from Nama water samples. The second group samples are less depleted values close to 0‰ that can be described as water atmospheric interaction and distinguish between the shallow water from deeper groundwater.

## 4 Conclusion

Water quality deterioration in the study area found to be affected by various factors and processes. The prevailing processes that contribute to the excess of these ions can be attributed to the following factors: Minerals' dissolution, evaporation, soil profile leaching, and scarce Recharge. The dissolution of minerals as the weathering of the rocks forming the aquifers is the main source of ions in the groundwater of the Wadi Aday. The isotopic signature of the Nama wells is quite different from that of the farm and observation wells. Nama wells show lighter and depleted isotopes while the farms and observation wells are heavier and enriched. This could be attributed to: Infiltration from the wadi bed, leak from the public network, evaporation form the stream bed and shallow subsurface and formation under humid climatic conditions prevailed in the past.

## 5 Acknowledgement

Authors acknowledge support of Sultan Qaboos University and Nama Water through the project CR/DVC/WRC/23/01. Support of DR/RG/17 is highly appreciated.

## Reference

[1] J. Christopher, E.P. Gold Sophia, Ediacaran–Cambrian Sirab Formation of the Al Huqf region, Sultanate of Oman. GeoArabia, 2012, 17 (1): 49–98. doi: https://doi.org/10.2113/geoarabia170149

[2] I. Clark (2015) Groundwater geochemistry and isotopes. Taylor & Francis, London.

[3] T. Javed, , N. Ahmad, & , S.R. Ahmad. Coupling hydrogeochemistry and stable isotopes (δ2H, δ18O and δ13C) to identify factors affecting arsenic enrichment of surface water and groundwater in Precambrian sedimentary rocks, eastern salt range, Punjab, Pakistan. Environ Geochem Health, 2023, 45, 6643–6673. https://doi.org/10.1007/s10653-023-01635-3

[4] Nganje, T.N., Hursthouse, A.S., Edet, A. et al. Hydrochemistry of surface water and groundwater in the shale bedrock, Cross River Basin and Niger Delta Region, Nigeria. Appl Water Sci, 2017, 7, 961–985. https://doi.org/10.1007/s13201-015-0308-9

**Theme:** Big-data, knowledge, and water data management
**IAHR Thematic Priority Area:** [TPA-4] Digital Transformation
https://doi.org/10.3850/iahr-hic2483430201-375

# Enhancing Forecasting Through Data-Driven Models: A Comparative Analysis

**Daniele Dalla Torre[1], Andrea Menapace[1], Maurizio Righetti[1]**

[1] Free University of Bolzano, Via Università 3, 39100 Bolzano, Italy

*Corresponding author: daniele.dallatorre@unibz.it*

**Abstract:** The performance of data-driven models is strongly affected by the data quality used and by the methods selected. The primary objective of this contribution is to assess the efficacy of data-driven methodology as forecast tools in water related applications (e.g. streamflow or network leakages forecast) employing various meteorological data types, including ground stations and reanalysis data. The second aim is to examine the impact of bias correction applied to the meteorological datasets on models' performance, to elucidate the outcomes of different data-driven approaches to a specific problem utilizing the distinct inputs. Results unveil interesting outcomes in forecasts through the integration of bias correction techniques. The study underscores the nuanced contributions of ground stations and reanalysis datasets used as forecasting data in tackling water management challenges. By presenting the outcomes of different data-driven approaches, the research provides valuable insights into the strengths and weaknesses associated with each model, thereby guiding the selection of an optimal tailored approach to specific forecasting requirements.

**Keywords:** big-data; data-driven models; hydrology; hydraulics; sustainability; weather forecast

## 1 Introduction

Physical problems in the water field are commonly solved directly by integrating the complexity of the system using mathematical representations of the different modules composing the system itself [1,2]. These complexities depend on the topic analysed (e.g., floods prediction [3]), the type of model chosen (e.g., lumped or distributed [4]), and the assumptions of the modelled equations [5,6]. On the other hand, data-driven models have been investigated in literature as an alternative approach [7,8], with the identification of different machine learning algorithms depending on the study. The presented contribution is based on the short-term forecasting approach, feasible for different studies, such as energy [9], flood prediction [10], or water demand [11]. Specifically, streamflow forecasting using data-driven models is proven capable of managing the problem complexities [12]. These kinds of models rely completely on data, so the features selection, the quantity, and the quality of the data set influence them a lot the outcomes [6,13]. The physical models are surrogated by data-driven models.

The research focuses on South Tyrol in Italy, which has a mountain climate, characterized by precipitation mainly as snow in winter and convective rainstorms in summer and autumn. Passirio and Senales streams are the analyzed basins. Val Passiria, as the Passirio stream basin, covers an area of 410 $km^2$, ranging from 360 to 3430 m.a.s.l., with the Passirio stream yearly mean flow rate of 2.04 $m^3/s$. Rio Senales, leading to the Vernago Lake, has a yearly mean flow rate of 1.02 $m^3/s$. Its related basin covers 48 $km^2$ with elevation ranging from 1770 and 3485 m.a.s.l. and it is called Val Senales. Precipitation, temperature and streamflow are the three datasets used as input for the simulations. The data have been checked and for both the basins under investigation, the data have been set. The ground weather station data of precipitation, temperature and flow rate are collected from the Province of Bolzano OpenData provider [14]. Reanalysis ERA5-Land are provided by the European Centre for Medium-Range Weather Forecasts (ECMWF) [15].

Bias correction methods used in this contribution are commonly used algorithms, previously reviewed [16–18] and chosen as feasible for the application on precipitation and temperature.
The data-driven models used in the simulations are two: Feed Forward (FF) [19] and Support Vector Regression (SVR) [20,21]. The metrics used to evaluate all the phases of the chain are the Mean Absolute Percentage Error (MAPE) and the R-squared (R2).
The simulations of this contribution are 4: [1] Training/Testing using ground station data [1a] *TR1*: **with** the lags of **streamflow** as input; [1b] *TR2*: **without** lags of **streamflow** as input; [2] Validation [2a] *V1*: testing using **raw** ERA5-Land data; [2b] *V2*: testing using **unbiased** ERA5-Land data.

Table 12 Performance of the simulations using FF and SVR for Passirio and Senales basins

| *Simulation* | | *TR1* | | *TR2* | | *V1* | | *V2* | |
|---|---|---|---|---|---|---|---|---|---|
| Metrics | | MAPE | R2 | MAPE | R2 | MAPE | R2 | MAPE | R2 |
| **Passirio** | FF | 17.84 | 0.81 | 18.13 | 0.84 | 33.59 | 0.85 | 25.31 | 0.81 |
| | SVR | 11.32 | 0.80 | 12.18 | 0.85 | 24.82 | 0.87 | 19.07 | 0.80 |
| **Senales** | FF | 21.69 | 0.65 | 43.81 | 0.67 | 22.93 | 0.93 | 20.02 | 0.90 |
| | SVR | 19.57 | 0.72 | 38.05 | 0.69 | 20.96 | 0.93 | 17.98 | 0.91 |

This contribution findings emphasize the necessity of investigating different data-driven models and forcings to understand and justify their results. It is indeed easy to get lost in the complexity of the problem, even more so in Alpine regions such as South Tyrol, where it is crucial the meteorological component. Bias correction is an important step forward to better results in this latter component, but its importance is lower if the uncertainties of the data-driven models are high. Further analysis, taking into account other variables or case-specific information could help in this direction. Nevertheless, the approach in this contribution is promising and it needs to be well investigated.

## Acknowledgment

This research was funded by funded by the European Union - Next Generation EU within the framework of the PRIN 2022 project Hybrid Transient-machine learning approach for "ANomaly DEtection and classification in water transmission Mains (TANDEM)", grant number 6477.

## Reference

[1] Bertaglia G, Ioriatti M, Valiani A, Dumbser M, Caleffi V. Numerical methods for hydraulic transients in visco-elastic pipes. Journal of Fluids and Structures 2018;81:230–54. https://doi.org/10.1016/j.jfluidstructs.2018.05.004.
[2] Ocio D, Beskeen T, Smart K. Fully distributed hydrological modelling for catchment-wide hydrological data verification. Hydrology Research 2019;50:1520–34. https://doi.org/10.2166/nh.2019.006.
[3] Neal J, Villanueva I, Wright N, Willis T, Fewtrell T, Bates P. How much physical complexity is needed to model flood inundation? Hydrological Processes 2012;26:2264–82. https://doi.org/10.1002/hyp.8339.
[4] Khakbaz B, Imam B, Hsu K, Sorooshian S. From lumped to distributed via semi-distributed: Calibration strategies for semi-distributed hydrologic models. Journal of Hydrology 2012;418–419:61–77. https://doi.org/10.1016/j.jhydrol.2009.02.021.
[5] Arkesteijn L, Pande S. On hydrological model complexity, its geometrical interpretations and prediction uncertainty. Water Resources Research 2013;49:7048–63. https://doi.org/10.1002/wrcr.20529.
[6] Yew Gan T, Dlamini EM, Biftu GF. Effects of model complexity and structure, data quality, and objective functions on hydrologic modeling. Journal of Hydrology 1997;192:81–103. https://doi.org/10.1016/S0022-1694(96)03114-9.
[7] Elshorbagy A, Corzo G, Srinivasulu S, Solomatine DP. Experimental investigation of the predictive capabilities of data driven modeling techniques in hydrology - Part 1: Concepts and methodology. Hydrology and Earth System Sciences 2010;14:1931–41. https://doi.org/10.5194/hess-14-1931-2010.
[8] Solomatine DP, Ostfeld A. Data-driven modelling: some past experiences and new approaches. Journal of Hydroinformatics 2008;10:3–22. https://doi.org/10.2166/hydro.2008.015.

[9] Potential applications of subseasonal-to-seasonal (S2S) predictions - White - 2017 - Meteorological Applications - Wiley Online Library n.d. https://rmets.onlinelibrary.wiley.com/doi/full/10.1002/met.1654 (accessed March 31, 2024).
[10] Arduino G, Reggiani P, Todini E. Recent advances in flood forecasting and flood risk assessment. Hydrology and Earth System Sciences 2005;9:280–4. https://doi.org/10.5194/hess-9-280-2005.
[11] Zanfei A, Brentan BM, Menapace A, Righetti M. A short-term water demand forecasting model using multivariate long short-term memory with meteorological data. Journal of Hydroinformatics 2022;24:1053–65. https://doi.org/10.2166/hydro.2022.055.
[12] Oyebode OK, Otieno FAO, Adeyemo J. Review of three data- driven modelling techniques for hydrological modelling and forecasting 2014.
[13] Chen H, Chen J, Ding J. Data Evaluation and Enhancement for Quality Improvement of Machine Learning. IEEE Transactions on Reliability 2021;70:831–47. https://doi.org/10.1109/TR.2021.3070863.
[14] Portale OpenData Bolzano n.d. https://data.civis.bz.it/ (accessed March 31, 2024).
[15] Copernicus Climate Change Service E. ERA5-Land hourly data from 2001 to present 2019. https://doi.org/10.24381/CDS.E2161BAC.
[16] Teutschbein C, Seibert J. Bias correction of regional climate model simulations for hydrological climate-change impact studies: Review and evaluation of different methods. Journal of Hydrology 2012;456–457:12–29. https://doi.org/10.1016/j.jhydrol.2012.05.052.
[17] Beck HE, Wood EF, McVicar TR, Zambrano-Bigiarini M, Alvarez-Garreton C, Baez-Villanueva OM, et al. Bias Correction of Global High-Resolution Precipitation Climatologies Using Streamflow Observations from 9372 Catchments. Journal of Climate 2020;33:1299–315. https://doi.org/10.1175/JCLI-D-19-0332.1.
[18] Cannon AJ. Multivariate quantile mapping bias correction: an N-dimensional probability density function transform for climate model simulations of multiple variables. Clim Dyn 2018;50:31–49. https://doi.org/10.1007/s00382-017-3580-6.
[19] Sadler I, Reimann N, Sambell K. Feedforward practices: a systematic review of the literature. Assessment & Evaluation in Higher Education 2023;48:305–20. https://doi.org/10.1080/02602938.2022.2073434.
[20] Raghavendra. N S, Deka PC. Support vector machine applications in the field of hydrology: A review. Applied Soft Computing 2014;19:372–86. https://doi.org/10.1016/j.asoc.2014.02.002.
[21] Dalla Torre D, Lombardi A, Menapace A, Zanfei A, Righetti M. Exploring the feasibility of Support Vector Machine for short-term hydrological forecasting in South Tyrol: challenges and prospects. Discov Appl Sci 2024;6:154. https://doi.org/10.1007/s42452-024-05819-z.

**Theme:** Big-data, knowledge, and water data management
**IAHR Thematic Priority Area:** [TPA-4] Digital Transformation
https://doi.org/10.3850/iahr-hic2483430201-378

# A Machine Learning Application for The Development of Groundwater Vulnerability Studies

**Gómez-Escalonilla V[1], Martínez-Santos P[1*], De la Hera-Portillo A[2], Díaz-Alcaide S[1], Montero González E[1], Martín-Loeches M[3]**

[1] Universidad Complutense de Madrid. C/Jose Antonio Novais 2, 28040 Madrid, Spain
[2] Instituto Geológico y Minero de España CSIC. C/Ríos Rosas 23, 28003 Madrid, Spain
[3] Universidad de Alcalá. Av. de León, 4A, 28805 Alcalá de Henares, Madrid

** Corresponding author: pemartin@ucm.es*

**Abstract.** Groundwater vulnerability is a manifold concept that ultimately represents the ease with which groundwater can get contaminated by human activities. The result of groundwater vulnerability studies is typically presented in map form, as vulnerability stems from the combination of a series of spatially distributed variables, including depth to the water table, soil type, lithology, and land use, among others. Multiple approaches to determine groundwater vulnerability have been developed over the years. These mostly include GIS-based methods and numerical methods. While information is often lacking to perform numerical modelling, GIS approaches typically suffer from two major issues, namely, the reliance on static variables and coefficients, and the dependence on aprioristic knowledge, without necessarily implying actual validation. The advent of machine learning techniques could represent a major breakthrough in groundwater vulnerability studies by providing a validation-based method to update coefficients and explanatory variables in each given case. This research aims to improve upon the classic DRASTIC approach by combining what is actually known about groundwater contamination in a given aquifer with artificial intelligence approaches. A large number of machine learning algorithms from different families was trained on groundwater monitoring data for a series of aquifers in central Spain. This served the purpose of identifying which of the DRASTIC explanatory variables (depth to the water table, recharge, aquifer media, soil type, topography, impact of the vadose zone, hydraulic conductivity, land use) were more relevant in each part of the study region. Furthermore, machine learning was used to adjust the weight of each coefficient to render a calibrated representation of groundwater vulnerability in the study region. Overall, tree-based algorithms are observed to outperform other supervised classification approaches on a regular basis. This is likely attributable to the conditional logic underlying tree algorithms, which is akin to that behind DRASTIC. Certain ensemble methods are also adept at depicting groundwater vulnerability. This approach is versatile enough to cater to other classic vulnerability methods and can be readily exported to other settings.

**Keywords:** groundwater vulnerability, DRASTIC, nitrate, monitoring, GIS, Duero, Spain

## 1 Introduction

Groundwater vulnerability ultimately represents how likely pollutants are to reach the saturated zone of an aquifer based on a series of intrinsic physical and chemical features. Different approaches have been developed to estimate groundwater vulnerability, including index-based, statistical, and process-based methods. The DRASTIC method, originally developed by [1] is perhaps the most widely accepted one. DRASTIC stands for a series of factors that theoretically control groundwater vulnerability to contamination, including depth to the water table, recharge, aquifer media, soil, slope, hydraulic conductivity, and the effect of the vadose zone. While widely accepted, the DRASTIC method presents some shortcomings, including its reliance on static weights and coefficients. The purpose of this research is to provide a machine learning method to compute these based on known contamination values. The method is illustrated through its application to the Duero basin, central Spain.

## 2 Methods

All DRASTIC variables plus land use were compiled into a QGIS database. All eight variables were subsequently reclassified based on DRASTIC's original categories, then the weight of each layer was left for supervised classifiers to optimize. We used the MLMapper 2.0 software for this purpose. MLMapper is a QGIS plugin developed by the authors whose original aim is to develop predictive maps of a target variable (groundwater vulnerability), based on a series of spatially-distributed explanatory variables (the DRASTIC parameters), and a dataset of ground truth examples [2]. MLMapper 2.0 uses an array of supervised classification algorithms from the Scikit Learn toolbox [3]. These include Support Vector Machines, Linear Support Vector Machines, Nu-support Vector Classifier, Logistic Regression, Ridge Classifier, K-Neighbor Classification, Linear Discriminant Analysis, Gaussian Naïve Bayes classification, Multilayer Perceptron Neural Network, Perceptron, Quadratic Discriminant Analysis, Gaussian Process Classifier, Stochastic Gradient Descent Linear Classifier, Passive Aggressive Classifier, Decision Tree Classifier, Random Forest Classifier, Gradient Boosting Classification, Ada-Boost Classifier, and Extra-Trees Classifier. Furthermore, this software uses a number of common machine learning procedures such as collinearity checks, parameter fitting, cross validation and recursive feature elimination. It also enables the user to pick one or several among a set of scoring metrics.

## 3 Results

While the application of this tool is still ongoing, the available results suggest that machine learning classifiers are adept at optimizing DRASTIC's original weighting system. The way in which weights and coefficients can be updated on a case-by-case basis appears particularly promising. Overall, tree-based algorithms are observed to outperform other supervised classification approaches on a regular basis, which is consistent with most predictive mapping studies in the groundwater literature.

## 4 Conclusions

Contamination poses a major threat to aquifers worldwide. Advances in those techniques used to estimate groundwater vulnerability are perceived as a major aid in managing this problem. Traditional approaches suffered from shortcomings such as the reliance on static variables and coefficients. However, machine learning techniques may contribute to overcome these limitations based on the establishment of self-validated correlations between the physical and chemical variables that explain groundwater contamination and actual contamination data. This research demonstrates the ability of machine learning algorithms to update coefficients on a case-by-case basis, as well as to optimally incorporate site-specific considerations to vulnerability studies.

## References

[1] L. Aller L, J.H. Lehr, R. Petty, T. Bennett (1987). DRASTIC—A Standardized System to Evaluate Groundwater Pollution Potential Using Hydrogeologic Setting. Journal of the Geological Society of India, 29, 23-37.

[2] V. Gómez-Escalonilla, P. Martínez-Santos, M. Martín-Loeches (2022). Preprocessing approaches in machine-learning-based groundwater potential mapping: an application to the Koulikoro and Bamako regions, Mali. Hydrology and Earth System Sciences, 26(2), 221-243

[3] F. Pedregosa, G. Varoquaux, A. Gramfort, V. Michel, B. Thirion, O. Grisel, M. Blondel, P. Prettenhofer, R. Weiss, V. Dubourg, J. Vanderplas, A. Passos, D. Cournapeau, M. Brucher, M. Perrot, E. Duchesnay (2011). Scikit-learn: Machine learning in Python. Mach Learn Python. 12:2825–2830.

**Theme:** Big-data, knowledge, and water data management
**IAHR Thematic Priority Area:** [TPA-4] Digital Transformation
https://doi.org/10.3850/iahr-hic2483430201-380

# Data Correction Framework for Precipitation Events – Towards A Semi-Automated Data Correction for Classical and Low-Cost Sensor Data

**Karen Schulz[1], Andre Niemann[1], Thorsten Mietzel[2]**

[1] Institute of Hydraulic Engineering and Water Resources Management University Duisburg-Essen, Berliner Platz 6-8, 45127 Essen, Germany
[2] Department of Urban Water and Waste Management University Duisburg-Essen, Universitaetsstrasse 2, 45141 Essen, Germany

*Corresponding author: karen.schulz@uni-due.de*

**Abstract.** Classical rain gauge networks are too sparsely distributed to accurately capture the high spatial and temporal variability of precipitation. Small-scale usable and inexpensive sensors (low-cost sensors) make a contribution for a more detailed recording at the expense of a poorer data quality. We therefore suggest a framework to correct precipitation data recorded by rain gauges in real-time. Precipitation is highly unbalanced and has a right skew. But extreme events are no less important. We present analyses for common ML (machine learning) models with adjustments to unbalanced data and compare them to baseline and statistical models. It was found that error correction for classical sensors is only possible in a rudimentary way by correcting missing values in this type of setup. In the low-cost data correction, errors were reduced by 32 % to 55 % in comparison to baseline models results. We propose using a hybrid approach to account for the unbalanced precipitation using either preprocessing or model training methods in combination with postprocessing of model results.

**Keywords:** Data correction, imbalanced regression, low-cost, machine learning, precipitation, rain gauge

## 1 Introduction

In order to integrate the increasing number of low-cost sensor data into existing hydrological monitoring networks, its data has to be judged and qualified [1]. Only few studies on the error correction of low-cost rain gauges exist, which are mostly limited to statistical methods. Precipitation has a unbalanced distribution. Adjustments during pre- and postprocessing and adjustments in model training can be made for the under-explored task of unbalanced regression [2, 3]. The aim of this work is to test ML methods against simpler methods for real-time error correction of rain gauges using multiple data sources. State-of-the-art approaches from the different fields that take into account the unbalanced data are compared for the first time in a single setup for low-cost sensor data.

## 2 Material

The classical sensor data set contains 28 stations operated by the water management association EGLV [4]. It has a time series of 10 years and manually, expert-based corrected ground truth data. The low-cost data set includes 13 stations of a network from the provider Netatmo [5]. Nearby classical sensors of EGLV serve as ground truth. For each station, neighboring sensors in the network are used as features. Additional features are derived from a remote environmental parameter station as well as RADOLAN radar data of 5 x 5 km around the sensors of the German Weather Service [6].

## 3 Methods

Error correction is carried out as second part of a 2-phase data qualification. In the first part, a perfect error detection is carried out for this research work. Our framework for the automatic correction of

rain gauge data for real-time scenarios consists of 4 steps. In the first step, features are generated. Based on that, the data can be preprocessed for example using undersampling. This step is an optional adjustment. In the third step, a ML error correction model is trained using optionally modified weights for model losses. For example, the root function can be used as weighting function of the observations. Finally, postprocessing model results can incorporate adjustments of the evaluation metric. We use the $MSE$ (mean-squared error) with a weighting of the evaluation results through the root and indicator function. Models are compared with a baseline that only corrects missing values.

## 4 Results

Our analyses show that only a correction of missing values should be made for classical sensor data in a setup like this. Apparently the sensor stations's distance is too large to adjust values with already high initial data quality even more precisely. Table 1 shows results of the low-cost data set. The statistical regionalization approach always outperforms the baseline. The plain RF is the simplest best model for the $MSE$ and $MSE_{root}$. The RF with undersampling is best for precipitation of at least 1.25 mm/5min. It is strongly biased towards high precipitation due to its strongly modified distribution. Regarding rain events, the more complex adjustment of RF using root weights performs best and only slightly outperforms a regular RF approach.

Table 1 Evaluation of error correction methods on low-cost rain gauge data set

| Model | $MSE$ (n=67 K) | $MSE_{root}$ (n=67 K) | $MSE \geq 1.25$ ($n_{\geq 1.25}$=409) | $MSE_{event}$ ($n_{event}$=2 K) |
|---|---|---|---|---|
| Baseline | 0.05 | 0.15 | 2.48 | 0.39 |
| Statistical mean-imputation in space | 0.04 | 0.13 | 2.21 | 0.31 |
| Random forest | **0.03** | **0.09** | 1.97 | 0.22 |
| Undersampling + random forest | 0.13 | 0.14 | **1.17** | 0.38 |
| Random forest & root weights | 0.03 | 0.10 | 1.97 | **0.21** |

## 5 Discussion

The found superiority of ML methods for quality considerations of low-cost sensor data is in line with other results in the same field. The low-cost sensors have a limitation regarding the ground truth which we want to eliminate in future studies. They have an average distance of approximately 1.7 km to the ground truth sensors.

## 6 Conclusions

As the ever-increasing data volume requires the automation of quality assurance, we developed a framework for real-time error correction of rain gauges. It includes methods for assessing model accuracy. Low-cost sensor data correction using ML can outperform baseline and statistical models. Depending on the application, the desired correction quality is already achieved or requires additional modifications. In the future, larger networks should be investigated to examine the generalizability of the station-specific models and to draw conclusions on model selection on a larger scale.

## References

[1] C. Hahn et al., "Observations from Personal Weather Stations—EUMETNET Interests and Experience," Climate, vol. 10, no. 12, p. 192, 2022.
[2] R. P. Ribeiro and N. Moniz, "Imbalanced regression and extreme value prediction," Mach Learn, vol. 109, 9-10, pp. 1803–1835, 2020.
[3] B. Krawczyk, "Learning from imbalanced data: open challenges and future directions," Prog Artif Intell, vol. 5, no. 4, pp. 221–232, 2016.
[4] EGLV - EMSCHERGENOSSENSCHAFT und LIPPEVERBAND. Available: https://www.eglv.de/ (accessed: Dec. 12 2023).
[5] Netatmo, same home, just smarter. Available: https://www.netatmo.com/de-de (accessed: Dec. 12 2023).

[6] "DWD Climate Data Center (CDC): Station data & recent 5-minute RADOLAN grids of precipitation depth (binary),"

**Theme:** Big-data, knowledge, and water data management
**IAHR Thematic Priority Area:** [TPA-4] Digital Transformation
https://doi.org/10.3850/iahr-hic2483430201-383

# A Multivariate Methodology for Water Demand Imputation in Smart Water Distribution Systems

**Andrea Menapace[1], Ariele Zanfei[2]**

[1] Faculty of Engineering, Free University of Bozen-Bolzano, Bolzano, Piazza Domenicani 3, 39100, Italy
[2] AIAQUA S.r.l., Bolzano, Via Alessandro Volta 1, 39100, Italy

*Corresponding author: andrea.menapace@unibz.it*

**Abstract.** Advancing the management of water distribution networks is considered a current priority for the sustainable management of the urban water cycle. However, this means increasing the complexity of the operational and planning decision-making tools, which are forced to handle an ever-increasing amount of data from the network of smart sensors with which modern systems are equipped. Thus, the goal of the proposed work is the need for proper preprocessing tools and, in particular, the critical role of a filling strategy. In particular, univariate and multivariate approaches are investigated along with different inputs and various algorithms. A real test case is used to carry out the proposed analysis, which consists of the water demand of four districts of the Italian city of Trento. The results highlight the importance of adopting a proper imputation strategy for processing the stream of water demand data to guarantee a reliable feed in the integrated management systems of smart water grids.

**Keywords:** Big Data, Imputation, K-Nearest Neighbours, Water Demand, Water Distribution Networks

## 1 Introduction

In an era defined by rapid technological advancements, the real-time management of big data has emerged as a pivotal factor in augmenting the efficiency and efficacy of smart water distribution networks [1]. The escalating complexity of these systems underscores the need for a comprehensive approach to data management, ensuring that the wealth of information collected is aptly harnessed for hydraulic behaviour simulations, water demand prediction, and system diagnostics, thereby bolstering decision-making processes [2,3]. In this context, gap filling strategies within the data management pipeline assume a paramount role, despite being an area scarcely addressed in existing literature. While existing research predominantly focuses on comparing various univariate imputation algorithms and their impact on water demand prediction [4], the present study seeks to broaden this perspective by investigating different imputation techniques tailored to effectively fill gaps in water data. To this end, our study adopts two distinct approaches: a univariate method, which relies solely on information derived from the demand time series itself, and a multivariate approach that capitalises on the relationships with other exogenous variables, such as demand from other District Metered Areas (DMAs), calendar data, and weather parameters. Furthermore, we explore different combinations of inputs, including time series lags, calendar variables, and weather data (e.g., temperature and precipitation). Finally, our analysis encompasses a diverse range of K-Nearest Neighbors (KNN) configurations, alongside a comparison with simple univariate benchmarks and Kalman Filtering coupled with time series Model Decomposition. Through this comprehensive investigation, we aim to shed light on the most effective strategies for gap-filling in water data, thus contributing to the advancement of data-driven approaches in water management.

## 2 Methodology

This study involves three well-known imputation algorithms: (i) linear interpolation as a benchmark method, (ii) time series decomposition model coupled with the Kalman filter suitable to handle time series with seasonality, and (iii) the flexible machine learning K-Nearest Neighbor (KNN). On the basis of these three methods, both univariate and multivariate approaches are tested along with different combinations of inputs, including time series lags, calendar variables, and other time series, e.g., weather data and other DMAs demand.

## 3 Case study

The time series of the water demand for 4 DMAs of Trento city is analysed. In addition, the climate information of the Laste weather station is collected to allow the analysis of the impact of exogenous variables in the imputation process.

## 4 Results

The principal findings are summarised as follows. Short periods of missing data do not present significant challenges, as any method is capable of effectively addressing these gaps. However, simple univariate techniques exhibit limitations in managing missing data, showing very rough results in some conditions, e.g. time series with significant seasonality. On the contrary, the multivariate approach, particularly advantageous when dealing with datasets consisting of many time series with some relevant inter-dependence, demonstrates greater robustness in imputing missing values. Specifically, the multivariate approach consistently yields more resilient outcomes across various gap sizes. Additionally, incorporating temporal lags of the demand time series itself alongside exogenous information significantly enhances imputation accuracy due to the models' capability to retrieve more information from the data in terms of autocorrelation of itself and intra-dependence with other correlated variables. Furthermore, the study underscores K-Nearest Neighbors (KNN) as a flexible and optimal algorithm for addressing this specific problem.

## 5 Conclusion

In conclusion, leveraging data plays a critical role in the effective management of smart water distribution systems. However, the continuous flow of data in such systems is susceptible to various types of failures, such as meter malfunctions, transmission system errors, and database inconsistencies. Therefore, proper preprocessing is essential to ensure the reliability and accuracy of the data. Imputation emerges as a crucial step in the data preparation process, facilitating the seamless integration of real-time simulations, predictions, and detection tools for continuous and reliable real-time operations. Specifically, a multivariate approach is recommended, particularly for addressing long gaps, as it has the capability to leverage the dependence between missing and regularly recorded variables. By addressing gaps in the time series of drinking water demand data, we can support the enhancement of the efficiency and effectiveness of water distribution systems, ultimately contributing to improved water resource management and sustainability.

## Reference

[1] Rousso, B. Z., Lambert, M., & Gong, J., Smart water networks: A systematic review of applications using high-frequency pressure and acoustic sensors in real water distribution systems, Journal of Cleaner Production, (2003), 137193.

[2] Zanfei, A., Menapace, A., Brentan, B. M., & Righetti, M., How does missing data imputation affect the forecasting of urban water demand?, Journal of Water Resources Planning and Management, (2022),148(11), 04022060.

[3] Giudicianni, C., Herrera, M., di Nardo, A., Carravetta, A., Ramos, H. M., & Adeyeye, K., Zero-net energy management for the monitoring and control of dynamically-partitioned smart water systems, Journal of Cleaner Production, (2020), 252, 119745.

[4] Menapace, A., Zanfei, A., Felicetti, M., Avesani, D., Righetti, M., & Gargano, R., Burst detection in water distribution systems: The issue of dataset collection, (2020), Applied Sciences, 10(22), 8219.

**Theme:** Big-data, knowledge, and water data management
**IAHR Thematic Priority Area:** [TPA-4] Digital Transformation
https://doi.org/10.3850/iahr-hic2483430201-385

# Supervised Learning for CCTV Image Prediction

**Jongyun Byun[1], Jinwook Lee[2], Hyeon-Joon Kim[1], Jongjin Baik[1], Changhyun Jun[1*]**

[1] Department of Civil and Environmental Engineering, Chung-Ang University, Seoul 06974, Republic of Korea
[2] Department of Civil and Environmental Engineering, University of Hawai'i at Manoa, Honolulu, HI, 96822, USA

*Corresponding author: cjun@cau.ac.kr*

**Abstract.** Accurate rainfall forecasting is pivotal for managing environmental vulnerabilities in complex terrain. As urban areas evolve, understanding and predicting rainfall patterns become imperative for effective hydrological planning and risk mitigation. In the era of the Internet of Things (IoT), leveraging non-traditional data sources has become increasingly attractive for enhancing the spatiotemporal resolution of existing observation network. This trend is notably evident in the field of rainfall observation and recent endeavors include innovative approaches to estimate rainfall by harnessing CCTV image. Our methodology involves the application of CCTV image collected from ground observation site and intends to predict the CCTV image at a specific time point based on the preceding group of CCTV images resolving the data insufficiency. The overall output data for the model utilized rain streaks extracted from original CCTV data. K-Nearest Neighbor (K-NN) algorithm was employed to effectively separate the background and foreground. We developed a supervised learning model by constructing an encoder-decoder network based on the convolutional autoencoder architecture. This network is designed to extract the inherent characteristics of CCTV image and its rain streak and to minimize the loss between result from image prediction model and CCTV image collected in a single frame.

**Keywords:** CCTV, Convolutional Autoencoder, Supervised Learning

## 1 Introduction

Vital for water resource administration, hydrological inquiries, and global change assessments, accurate precipitation data are indispensable. In the epoch of the Internet of Things (IoT), leveraging non-traditional sources is enticing for augmenting the spatiotemporal scope of established observation networks [1]. This trend has been particularly noticeable in recent years, notably in the domain of rainfall observation. It is particularly evident in the field of rainfall observation, where recent endeavors involve innovative approaches to estimate rainfall through the analysis of CCTV image. In the scope of this research, we probed a supervised learning model, fashioning an encoder-decoder network structured on autoencoder architecture to extract the inherent characteristics of CCTV image and its rain streak.

## 2 Methodology

Our methodology involves the application of supervised learning algorithm to predict the CCTV image in a single frame along the vertical direction. To extract and combine the extracted feature maps from ten different location in a single frame of CCTV data, we developed a deep neural network by constructing an encoder-decoder network based on the convolutional autoencoder. To accurately extract and handle the characteristics of the ongoing rain streaks, it was necessary to separate only the rain streaks from the original CCTV data. The methodology adopted in this study involved implementing a model tailored to extract rain streaks from raw images through the application of the K-Nearest Neighbor (K-NN) algorithm.

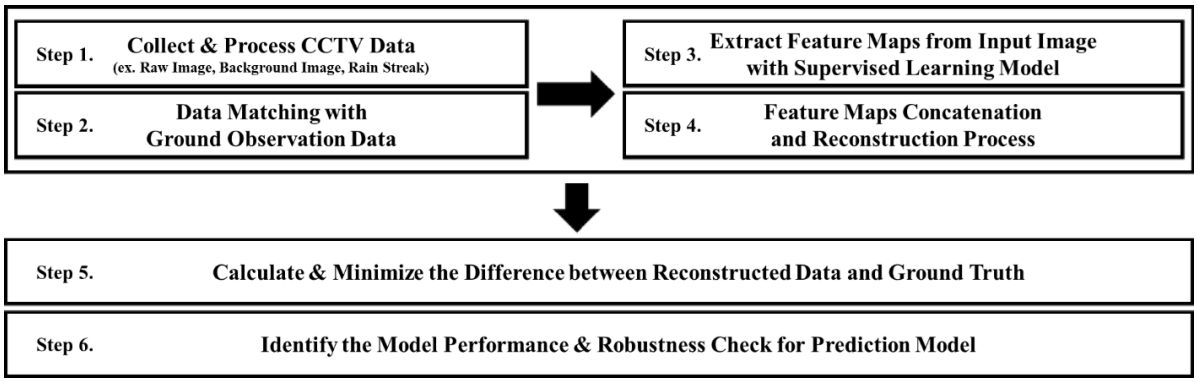


Figure 56 Flow chart of supervised learning for CCTV image prediction model

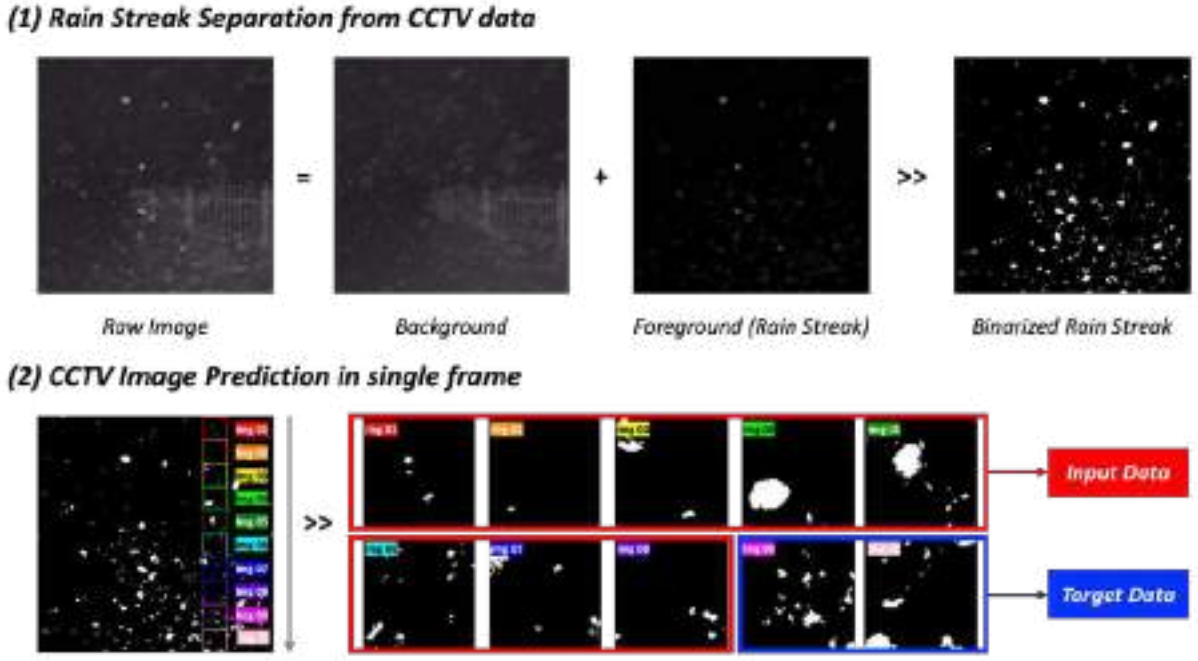


Figure 2 Subprocess in supervised learning model for CCTV image prediction in single frame

Ten images in single frame were divided along the predominant vertical direction corresponding to the typical progression of rain streaks. The model was trained using the top 8 images as input data and the bottom 2 images as target data. Subsequently, image prediction was conducted based on the direction of rain streaks within the CCTV data.

## 3 Results

Using a convolutional autoencoder, we extracted feature maps of raw data and background images from CCTV images during rainfall. The rain streaks, extracted through the K-Nearest Neighbor (KNN) algorithm, were set as the target, resulting in a model designed to predict only rain streaks from the original image. An enhancement in the capability to capture and separate rain streaks was observed compared to the conventional KNN method. It is assessed that the improved performance is applicable in a wide range of environments, especially in scenarios where the precise location of rain particles is unclear in CCTV videos during rainfall.

## Reference

[1] Amale, O., & Patil, R. (2019, March). IOT Based rainfall monitoring system using WSN enabled architecture. In 2019 3rd International Conference on Computing Methodologies and Communication (ICCMC) (pp. 789-791). IEEE.

**Theme:** Big-data, knowledge, and water data management
**IAHR Thematic Priority Area:** [TPA-4] Digital Transformation
https://doi.org/10.3850/iahr-hic2483430201-387

# Multi-sensor-based Solution for Reservoir Rainwater Monitoring and Dam Safety Monitoring

**Heliang Liu**

Hi-Target Satellite Navigation Technology Co., LTD. Guangzhou 511400, China

*Corresponding author: hb151@126.com*

**Abstract.** This paper proposes an intelligent water monitoring system for reservoir safety management. The system leverages real-time sensor data to monitor reservoir water levels and dam stability, enabling early warning and improved decision-making for reservoir safety. Traditional inspection methods are time-consuming and limited in scope, highlighting the need for a comprehensive multi-sensor-based approach. The system integrates various sensors, communication technologies, and geographical information systems to provide a reliable and accurate assessment of reservoir health. This paper also explores sensor selection considerations for optimal system implementation.

**Keywords:** Monitoring sensor; Reservoir safety; Sensor-based monitoring

## 1 Introduction

This paper proposes a multi-sensor-based system for reservoir rainwater monitoring and dam safety monitoring to improve reservoir safety management. The system leverages various sensors, communication technologies, and a geographical information system to provide real-time data for reservoir water levels and dam stability, enabling early warning and informed decision-making.

## 2 Method

The system uses a variety of sensors to monitor different aspects of the reservoir and dam, including GNSS for dam surface deformation monitoring, osmosometers for seepage monitoring, water level meters for water level monitoring, and rain gauges for rainfall monitoring. The system also sets thresholds for various monitoring points. If the sensor data falls outside the set thresholds, an early warning is triggered. To construct such a system, the first step involves setting up a cloud platform built upon location-based services.

In terms of content, the platform consists of several components: an information collection and transmission system, a computer network system, a system operating environment, a database system, a security assurance system, and a business application system. Internally, this platform can encapsulate foundational business operations and supporting services, while externally it provides Web API services. This setup facilitates functional expansion for business platforms as well as data service by third-party applications.

In terms of function, this platform encompasses a suite of business support services that include public services, warning systems, engineering management, data querying, and report generation. It visually presents these business functionalities through a Web interface, providing corresponding operations, data retrieval, spatial and data visualization, as well as data analysis features.

In terms of data access, by building a unified access standard and interface protocol, it can not only meet the needs of access and management of existing devices but also the needs of applications and upgrading of future devices. At this stage, it can access the following sensor: GNSS surface displacement monitoring device, seepage flow meter, water weir meter, water level meter, rain meter, AI-enabled HD video receiver, dam opening sensor, stroke switch, foundation InSAR, crack sensor,

inclination sensor, acceleration sensor, termite monitor, fixed inclinometer, pressure sensor, current meter and water quality monitor..

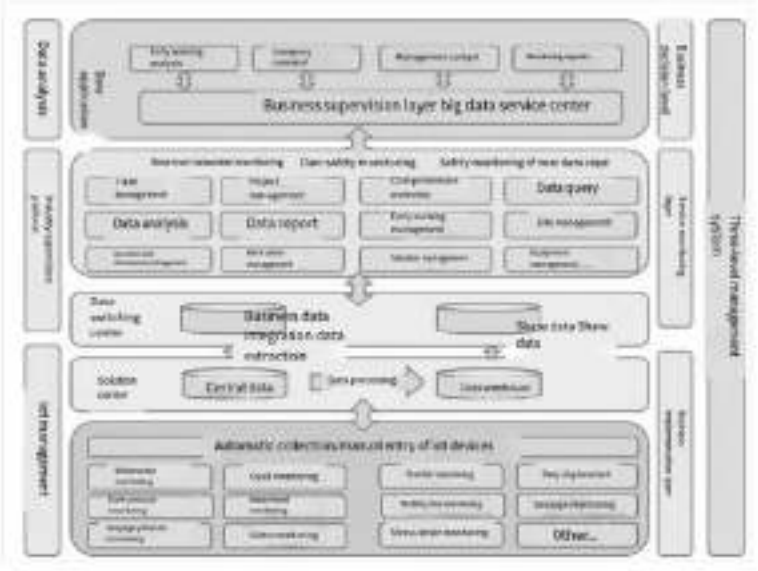


Figure 57 Multi-sensor-based rainwater monitoring and dam safety monitoring system architecture

## 3 Results

The paper presents a case study of a dam that successfully used the proposed system to monitor its safety during an earthquake. The monitoring data showed no significant changes in dam body displacement, dam foundation displacement, displacement near the dam bank slope, groundwater level, or reservoir water level before or after the earthquake. This indicates that the dam remained stable throughout the event. This paper selects a reservoir in western China as a case study, which is located in a high-altitude area. The reservoir has been equipped with a GNSS reference station and 20 surface deformation monitoring points on the dam body, dam foundation, and near-dam slopes, as well as 28 groundwater level monitoring points and one reservoir water level monitoring point. The class 1, 2 and 3 warning thresholds are set according to the requirements of reservoir management department and the project implementation experience.At 1:45 on January 8, 2022, a magnitude 6.9 earthquake occurred here, with a focal depth of 10 kilometers and an epicenter about 100 kilometers away from the monitoring point of the reservoir dam, which has a high possibility of causing disasters. The reservoir management department made accurate analysis of the displacement monitoring data and water level monitoring data of the dam body, dam foundation and slope near the dam before and after the earthquake, and made accurate assessments and judgment on the safety situation of the reservoir. It has effectively improved the level of reservoir safety management and effectively avoided social panic.

## 4 Conclusion

The paper concludes that the multi-sensor-based system is an effective tool for reservoir rainwater monitoring and dam safety monitoring. The system can provide real-time data that can be used to improve the management of reservoirs and dams and reduce the risk of accidents. The paper concludes that the proposed sensor-based intelligent water monitoring system is an effective solution for improving reservoir safety management by providing real-time data and early warning

## Reference

[1] Earthquake Emergency Response Report of a county in Qinghai.

**Theme:** Big-data, knowledge, and water data management
**IAHR Thematic Priority Area:** [TPA-4] Digital Transformation
https://doi.org/10.3850/iahr-hic2483430201-389

# Digital Twinning of Irrigation Infrastructure to Enhance the Root Cause Analysis of Water Balance Anomalies in Open Water Channels

**Samuel Hutchinson[1], Joseph H.A. Guillaume[1], Philipp Braun[1]**

[1] Fenner School of Environment and Society and Institute for Water Futures
The Australian National University, Canberra 2601, Australia
[2] Research School of Engineering,
The Australian National University, Canberra 2601, Australia

*Corresponding author: samuel.hutchinson@anu.edu.au*

**Abstract.** Operators of irrigation networks face increased demand to verify and improve network performance, including closure of the water balance. Infrastructure automation initiatives not only bring performance improvements to the network, but also add value to capital investments through opportunity to analyse live telemetry data. This research investigates the potential for reducing the uncertainty of fault recognition and root cause analyses of water balance anomalies, harnessing infrastructural data and expertise available from the Murrumbidgee irrigation area of NSW, Australia. Extending methodology in the literature for generating leakage alarms from telemetered irrigation infrastructure [1], [2], this work explores the patterns discernible in the data impacting the water balance of key equipment in an operational network. Building upon this exploration, this work reports on a case study demonstrating the key contextual information provided from a digital twin of open water channel weir regulators as part of analyses of water balance anomalies throughout an irrigation season.

This work contributes a methodology of incorporating information into a conceptual model for the behaviour of system components of the channel and demonstrates its integration into the process of root cause analysis of water balance anomalies. The process involves the continual refinement of a conceptual model by iteratively mapping functions and components of the systems in the irrigation network. These components are described using a process inspired by the unified modelling language (UML), an established engineering principle providing a framework for describing behavioural and structural relationships [3]. Figure 1 illustrates a snapshot of the digital twinning process of a regulator using this language. The information within the available operational data is mapped to the functional components of the regulator. Since many of the high level behaviours of channel components are shared across the network they are first described at an abstract level. Collaboration with irrigation operators yields expert knowledge about the behaviours of the specific components in the field leading to the detailing of information, such as previous and potential failures of systems, in a more concrete and site specific way. The intended pathway of knowledge generation is by expansion out from the core regulator node. As new information is gained, the map is refined with additional components and levels of abstraction. This UML concept provides a toolkit for situational awareness in the process of root cause analysis as it facilitates hypothesis generation as analysts use the map to navigate potential faults and lump observations through correlation analysis.

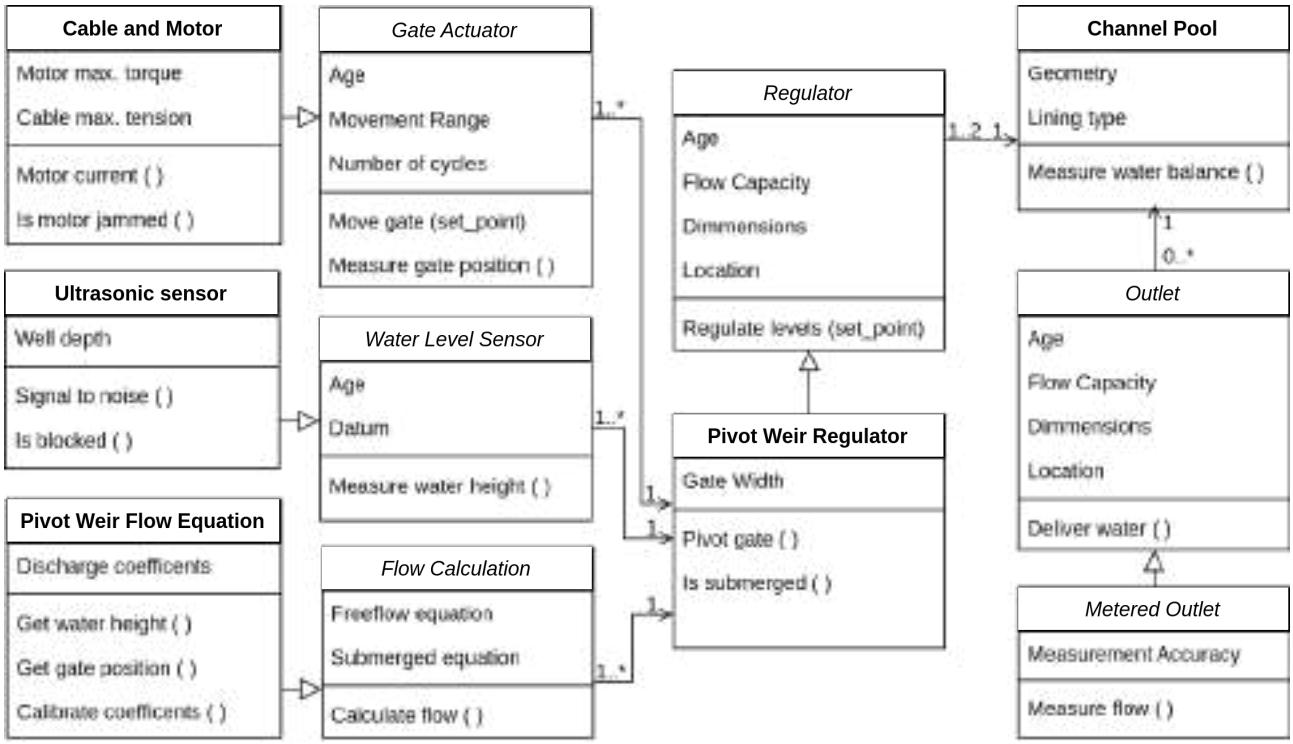


Figure 58: An example of building up understanding of the functionality of a regulator. The central object is the regulator itself, an abstract component (notated with italics) which has high level functions and properties. These are more concretely defined when more is known about the type of regulator (notated in **bold**). Additional features of the regulator's behaviour come from describing its components. Functions and properties are associated with characteristic behaviours such as the type of failure modes and patterns in the data. In this notation 1..* → 1 is UML shorthand for "many to one", 0..* → 1 is "any to one", and 1..2 → 1 is "one or two to one".

To demonstrate the digital twinning process, sites were monitored across the the 2021-2022 irrigation season in the open water channels at Murrumbidgee Irrigation. The sites had Rubicon™ FlumeGate™ regulators, a type of sharp crested pivot weir. A water balance anomaly detection algorithm (Measure water balance) was used to identify particular regulators of interest throughout the operational irrigation season. Anomalies were localised by searching for equal but opposite water balance disturbances in adjacent pools. Specific anomalies that met a magnitude threshold were identified for case study. For each of these sites, the digital twinning process was initiated, building up information using the specific components in the field. Using the UML map as a guide, examination of the magnitude of the water balance anomaly and patterns in available data yielded correlations that were used to answer hypotheses based on assumptions of the digital twin of the regulator. Figure 2 illustrates an example how gate tip submergence is one of one of the correlations identified. In a submerged condition (Is submerged), when the gate tip is below the downstream water level, the Freeflow equation for a pivot weir leads to a flow over-estimate manifesting as a water balance anomaly. Using an alternate Submerged equation suggested by Nikou, Ziaei and Safavi [4] leads to better flow calculation however requires additional coefficients to be estimated or measured (Calibrate coefficients). The actioning approach in this case involves notating the data quality issue of submergence and a further annotation of the UML map.

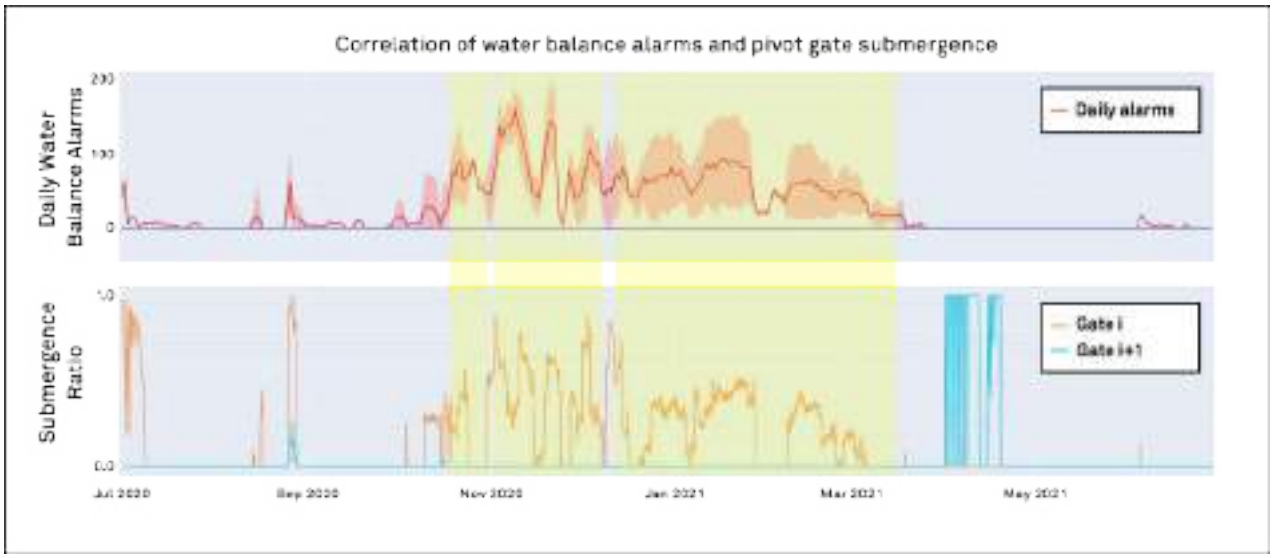


Figure 59: Correlations between water balance alarms and gate tip submergence for a pool in the 2020-2021 season. The daily alarms are shown with an uncertainty (red shaded area) based on documented measurement tolerances of sensors in the field. Periods of water balance anomalies that met a threshold equivalent to >=10 megalitres per day were selected for root cause analysis (denoted in the yellow bands). The submergence is measured as a ratio of the head of upstream and downstream sides of the gate with respect to the gate tip position. Gate i is the gate at the top of the regulator pool and Gate i+1 is at the end of the pool. In this situation the submergence of the gate at the top of the pool results in an over estimate of flow into the pool water balance which never translated to a real change in volume and appearing as a leakage.

A further contribution of this work is a discussion on the value added to the understanding of the irrigation network by digital twinning functional components of the infrastructure. This is exemplified through a demonstration of how feeding back root cause analysis information can be used to assess components of the network for early warning signs of asset degradation. For example, water balance anomalies that correlate to gate flow magnitude which build up over the period of a season links to deteriorating gate tip surface due to diverging of modelled and actual discharge coefficients. This work serves to highlight the importance of further harnessing the information of the rapidly expanding telemetry from infrastructure to ensure the management processes are resilient against changing relationships with our natural waterways in the context of climate change. The authors thank Murrumbidgee Irrigation Ltd for their collaboration and access to data from operational infrastructure for this project.

**Keywords**: digital twinning, root cause analyses, water balance anomalies

## Reference

[1] N. Bedjaoui and E. Weyer, “Algorithms for leak detection, estimation, isolation and localization in open water channels,” Control Eng. Pract., vol. 19, no. 6, Art. no. 6, 2011, doi: 10.1016/j.conengprac.2010.06.008.

[2] Y. Lami, “Distributed approach for fault diagnosis in open complex systems,” Université Grenoble Alpes, France, 2022.

[3] H. Koç, A. M. Erdoğan, Y. Barjakly, and S. Peker, “UML Diagrams in Software Engineering Research: A Systematic Literature Review,” in The 7th International Management Information Systems Conference, MDPI, Mar. 2021, p. 13. doi: 10.3390/proceedings2021074013.

[4] N. S. R. Nikou, A. N. Ziaei, and K. Safavi, “Closure to ‘Extraction of the Flow Rate Equation under Free and Submerged Flow Conditions in Pivot Weirs with Different Side Contractions’ by N. Sheikh Rezazadeh Nikou, M. J. Monem, and K. Safavi,” J. Irrig. Drain. Eng., vol. 144, no. 4, Art. no. 4, 2018, doi: 10.1061/(asce)ir.1943-4774.0001247. (1)

**Theme:** Big-data, knowledge, and water data management
**IAHR Thematic Priority Area:** [TPA-4] Digital Transformation
https://doi.org/10.3850/iahr-hic2483430201-392

# Hydro30 V2: A Refined Global Drainage Network Dataset Derived From 30-Meter Resolution

**Tiejian Li[1,2], Jiaye Li[3], Zhaoxiang Jiang[2], Li Zhang[4], Yu Fu[3]**

[1] State Key Laboratory of Hydroscience and Engineering, Tsinghua University, Beijing 100084, China
2 Department of Hydraulic Engineering, Tsinghua University, Beijing 100084, China
[3] School of Environment and Civil Engineering, Dongguan University of Technology, Dongguan 523808, China
4. North China Electric Power University, Beijing 102206, China

*Corresponding author: litiejian@tsinghua.edu.cn*

**Abstract.** The topology and geometry of drainage networks with high resolution and precision is essential to geomorphological research, water resource management and hydrological simulations. This study proposes a refined dataset of drainage networks from up-to-date 30-meter resolution DEMs. Following a previous Hydro30 dataset, we name this refined one as Hydro30 V2, develop it for higher precision in planar shapes and geometry parameters, with a reach-by-reach codification system and a Horton-Strahler order-based hierarchical data pyramid, aiming at the global scale. We first comprehensively compared the global 30-meter DEM data from different sources, and selected the latest and most appropriate DEM as the data source for drainage network extraction. Then, we produce the Hydro30 V2 by using a high-efficient drainage network extraction software developed by our team, which is based on the D8 method and least-cost search algorithm, and integrates improvements including depression breaching, channel head identification and known river data strengthening. Finally, after coding each river reach with a binary-tree based method and building a data pyramid, the Tsinghua Hydro30 V2 are being continuously produced to cover the whole globe, while provided for free access.

**Keywords:** digital elevation model, drainage network, Hydro30

## 1. RELATED WORK

In the past, datasets of rivers, e.g., the Hydro1k, have limited resolution, coverage, and water channel density. HydroSHEDS is the first dataset that offers comprehensive data on water channels, watersheds, and supplementary information including flow directions, but its first version (Wickel, Lehner; 2008) has limited coverage (up to 60N and 56S in latitude), resolution (varying from 3 second to 5 minutes) and contemporaneity (made in 2007). A higher density river centerline dataset GRWL (Allen, Pavelsky, 2018) focuses on reproducing river width at the resolution of 30 meters on global extent using LandSAT-8. However, it does not yield either a hierarchical arrangement of rivers from headwater to estuary or flow directions of water channels. HydroROUT (Bernhard etc; 2013) maintains a spatial hierarchy of rivers; however, as it shares a similar data source with HydroSHEDS version 1, its extent needs improving.

## 2. MATERIALS AND METHODS

We apply the method proposed by Bai (2015) and Li (2020), with binary tree sorting and least cost search on the 2-D DEM image. We sort pixels based upon their elevations, store them in balance binary search tree, and store the ranking of each raster in accordance with its elevation. The flow path comes from the steepest possible descent by following the max difference of ranks between

neighboring pixels. After removing spurs and vectorizing, we successfully extract channels from DEM data. Supplementary information, such as flow directions and watershed area, is produced and provided with river reaches.

We compared different DEM sources including the 30-meter ASTER GDEM, the ALOS 12.5-meter resampled DEM, and the bare land FABDEM. We also used known river lines from the Open Street Map to strengthen the results in flat and city areas.

## 3. RESULTS AND DISCUSSION

The extracted water channels are more accurate, cover more area and have higher resolution than those in previous datasets of water channels. The centerlines of water channels are clearly depicted even though some of them bend repetitively in a small area. Compared to the previous datasets, we add rivers of higher levels to our dataset, thanks to the improved algorithms and DEM data.

The whole dataset are being produced continuously and can be accessed via https://www.hydro30.civil.tsinghua.edu.cn.

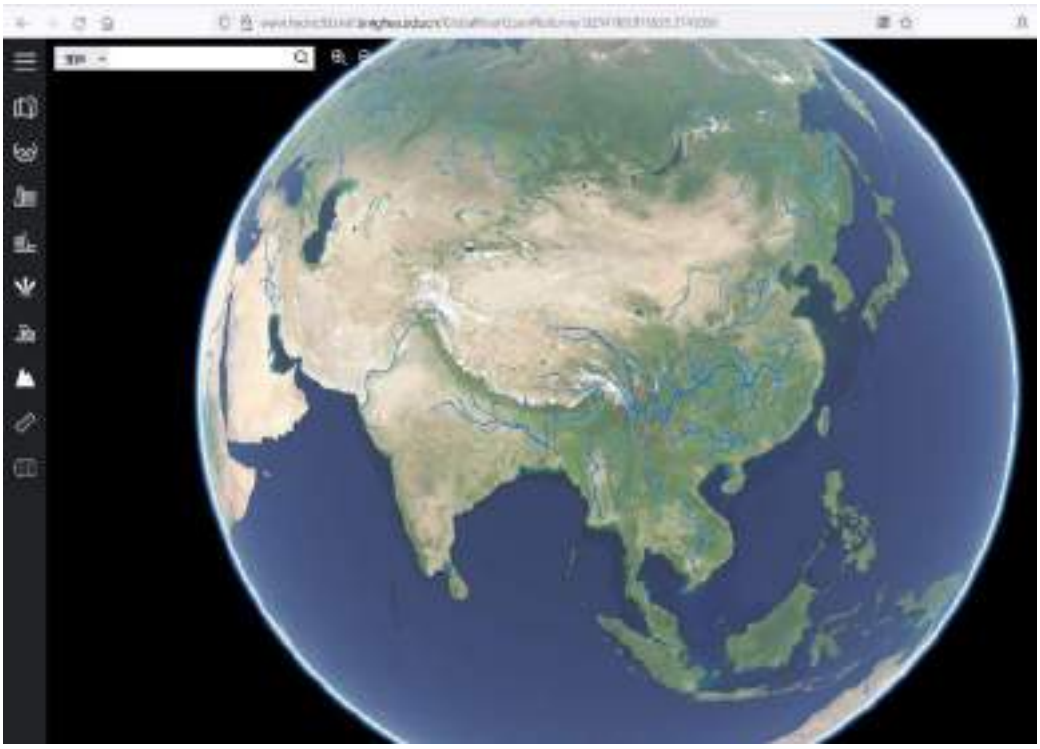

Figure 60 The Hydro30 website

## Reference

[1] Bai R, Li T J, Huang Y F, Li J Y, et al. An efficient and comprehensive method for drainage network extraction from DEM with billions of pixels using a size-balanced binary search tree. Geomorphology, 2015, 238:56-67.

[2] Allen G H, Pavelsky T M.Global extent of rivers and streams. Science, 2018, 361(6402).

[3] Bernhard L, Günther G. Global river hydrography and network routing: baseline data and new approaches to study the world's large river system. Hydrological Processes, 2013, 27(15):2171-2186.

[4] Li J Y, Li T J, Zhang L, Bellie S, Fu X D, Huang Y F, Bai R. A D8-compatible high-efficient channel head recognition method. Environmental Modelling & Software, 2020, 104624.

[5] Wu T, Li J Y, Li T J, Bellie S, Zhang G, Wang G Q. High-efficient extraction of drainage networks from digital elevation models constrained by enhanced flow enforcement from known river maps. Geomorphology, 2019. 340:184-201.

**Theme:** Big-data, knowledge, and water data management
**IAHR Thematic Priority Area:** [TPA-4] Digital Transformation
https://doi.org/10.3850/iahr-hic2483430201-394

# Preliminary Statistical Analysis of a Large Hydraulic and Hydrological Dataset for Mudflows and Debris Flows Events in The South Tyrol Region (Italy)

**Anna Prati1*, Andrea Menapace1, Michele Larcher1**

[1] Free University of Bozen-Bolzano, Faculty of Engineering, University Square 3, Bozen, 39100 (Italy)

*Corresponding author: anna.prati@unibz.it*

**Abstract.** The study focuses on the South Tyrol region, investigating factors influencing debris flow triggering and empirically calculating rainfall thresholds for event occurrence. Through a comprehensive analysis of debris flow events since 1960, cataloging geological and rainfall data, the study is preliminary but innovative step towards a better understanding and therefore mitigation of the risks associated with these phenomena. The main result of this work consists indeed of specific thresholds curves that establish which intensities and durations of rainfall events may cause the triggering of a debris flow.

**Keywords:** data analysis, debris flow, trigger thresholds

## 1 Introduction

The consequences of climate change on our atmosphere include an increase not only in the frequency but also in the intensity of heavy-to-extreme precipitation events all over the world. While the effects of these short but very intense precipitations are relatively limited on large river basins, they can have an extremely severe impact on smaller basins. The possibility to activate debris flows is strictly connected to the presence of rainfall events that have short duration and high intensity which are quite common in the Alps. The literature has so far highlighted that debris flows triggering is mainly connected to three general factors: the slope and the saturation of the terrain, as well as the intensity of the rainfall events [1].

This study investigates the influence of different factors on the triggering of debris flow events in this alpine region. In addition, the rainfall thresholds were empirically calculated both for the lower critical limit and the upper limit in the case of occurrence or not of debris flow events [2]. Each event has been catalogued by defining the geology of the terrain and the rainfall events recorded in that area prior to and after the debris flow; eventually, the debris flow events have been clustered based on the geography of the region and on the altitude at which the debris flow occurred.

The debris flows analyzed for this study have all been triggered within the borders of the Province of Bolzano, an alpine area in Northern Italy. 677 debris flows that have been taken place after 2014 have been used for the analysis presented hereafter. From this year on the rain measurements are collected with a time resolution of 5 minutes instead of 60 minutes, thus allowing to evaluate the intensity of very intense, but short, rainfall events.

## 2 Debris flow trigger thresholds

The most important goal of this work is to first associate each debris flow event with the rainfall event that triggered it and then investigate the intensity and duration of this rainfall event. The ultimate purpose of this analysis is to identify some sort of thresholds that can help understand the features of the rainfall events able to trigger a debris flow. The analysis of the intensities and

durations of the rainfall events that were able to trigger a debris flow has initially been done on the entire dataset and for ten of the most active catchments of the entire region.

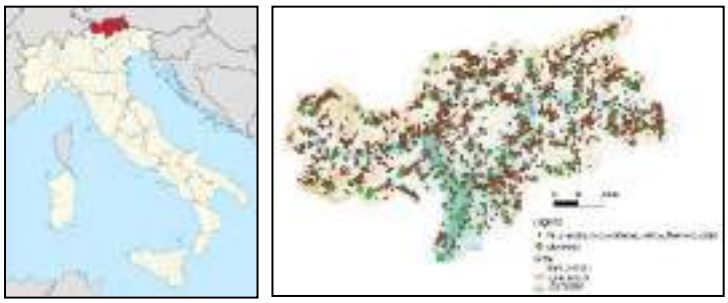

Figure 1 Location of the Alto Adige Province (left), of the location of the rainfall measurement stations and of the analysed debris flows (right).

## 3 Conclusion

A first attempt at classifying the debris flow events based on the intensity of the rainfall event that triggered it and on the volume of displaced did not reveal clear clusters among the data.
A second and deeper analysis of the rain data has instead allowed to identify the limits of the area on the plot of the intensity of the rain events versus their duration, which contains rainfall events that did trigger a debris flow. This analysis proved that the limits evaluated using the entire database differ from the ones evaluated for each of the 10 most active catchments, thus proving that these thresholds might have a strong component dependent on the geomorphological features of the catchment itself.

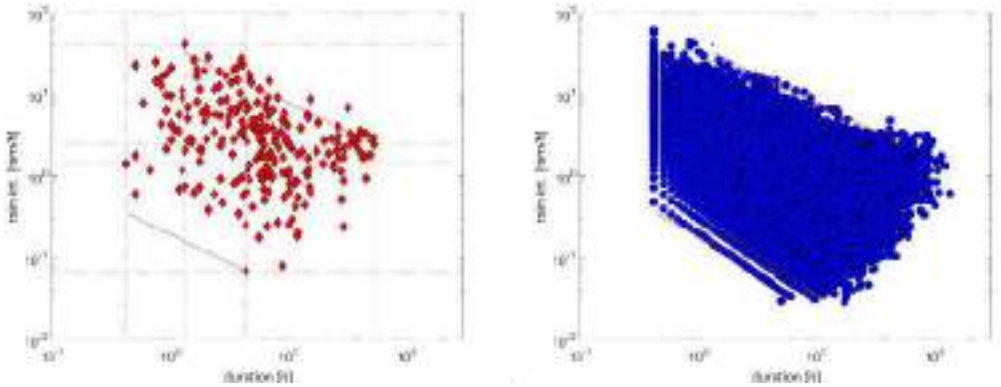

Figure 2 Example of the thresholds for the entire debris flow database: upper and lower thresholds plotted on the rain data that produced a debris flow (left) and that did not produce a debris flow (right).

## Reference

[1] Destro, E., Marra, F., Nikolopoulos, E. I., Zoccatelli, D., Creutin, J. D., and Borga, M. 2017. Spatial estimation of debris flows-triggering rainfall and its dependence on rainfall return period. Geomorphology, 278, 269-279.

[2] Deganutti, A. 2000. Rain fall and debris-flow occurrence in the Moscardo basin (Italian Alps). In Second International Conference on Debris-flow Hazard Mitigation: Mechanics, Prediction, and Assessment, (pp. 67-72). AA Balkema, 2000..

**Theme:** Big-data, knowledge, and water data management
**IAHR Thematic Priority Area:** [TPA-4] Digital Transformation
https://doi.org/10.3850/iahr-hic2483430201-396

# A River Entity Coding System for Object-Oriented Digital Twins of River Basins

**Jiaye Li[1], Tiejian Li[2*], Xuhong Fang[3], Chen Chen[1], Zhihui Du[4]**

[1] School of Environment and Civil Engineering, Dongguan University of Technology, Dongguan 523808, China
[2] State Key Laboratory of Hydroscience and Engineering, Tsinghua University, Beijing 100084, China
[3] School of Computer Science and Technology, Dongguan University of Technology, Dongguan 523808, China
[4] Zhongguancun Industry & Information Research Institute of Two-Dimensional Code Technology, Beijing 100080, China

*Corresponding author: litiejian@tsinghua.edu.cn*

**Abstract.** Aiming at resolving and delineating the composition of river basins, this paper chooses the philosophy of using drainage networks to represent intricate river basins, and proposes a unified coding system to identify each river reach in drainage networks over the whole globe, which would be a key technique in building an objected-oriented digital twin of river basins. The proposed river entity coding system (RECS) is based on the IDCode coding system following international standards. Each RECS code consists of a head starting with MA.1002, and the standard and extended domains. An open platform was developed to display the global drainage networks and demonstrate the use of RECS, where each river reach, as well as related information, can be queried and then shared through RECS QR codes. We believe that RECS is an efficient approach in building object-oriented digital twins of river basins, which will be further used in a variety of information systems in the water conservancy industry.

**Keywords:** Drainage networks, River entity, Unified coding system, Digital twins, QR codes

## 1 Introduction

In the wake of an escalating demand for efficient, detailed, and visually intuitive river basin management, the concept of digital twins [1] has garnered considerable attention within the water conservancy sector. [2] This paper confronts the challenge of encapsulating the complexity of river basins through the foundational use of drainage networks, proposing a comprehensive coding system that uniquely identifies individual river segments on a global scale. This pivotal advancement serves as the underpinning for the creation of object-oriented digital twins of river basins.

## 2 Material and methods

The River Entity Coding System (RECS) is a crucial component of the well-known IDCode framework, initiated with the prefix "MA.1002". As shown in Figure 1, this coding system is meticulously structured, comprising standard and extended domains. The standard domain employs a binary-tree model [3] to assign a unique code to each river, which likes DNA in biology. Such a system simplifies the global recognition and categorization of river basins, mirroring the natural division of river systems.

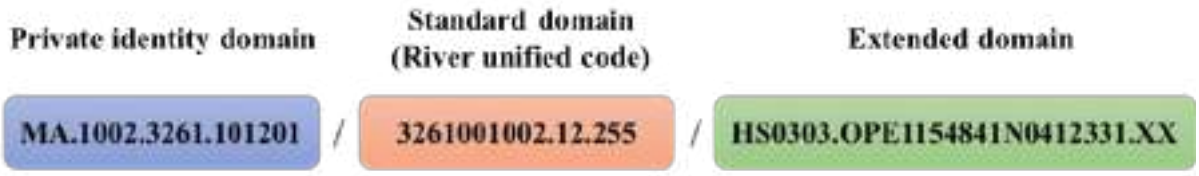


Figure 61 River entity coding system representation

The extended section of RECS enriches each river segment with additional data, linking rivers to the global tapestry of water basins. It includes comprehensive details such as the water's properties, environmental significance, and the socioeconomic impact of the rivers. These insights are invaluable for understanding the role of rivers within their ecosystems and the effects of human activities on these vital waterways. RECS is designed to integrate seamlessly with other coding systems, which is essential for data sharing and collaborative efforts among various countries and regions. Moreover, its flexible nature ensures that it can evolve with advancements in hydrological science and technology, maintaining its foundational principles.

## 3 Results and discussion

We produced a dataset of global drainage network with the RECS by using a high-efficient drainage network extraction algorithm [4] and channel head identification algorithm [5]. By integrating these areas of expertise, we create a complex but efficient system that reveals the finer details of river sections and broadens our comprehension of worldwide water networks. The system is complemented by a carefully curated, universally accessible platform that maps and effectively showcases RECS applications via a user-centric interface. This platform secures straightforward access to river segments and their encompassing data, including affiliations with hydrological or meteorological stations and reservoirs (website: https://eslab.dgut.edu.cn/GlobalRiverOpenPlatform/). All this information can be quickly accessed and shared through RECS QR codes.

## 4 Conclusions

The RECS, aligning with international coding standards, offers a robust framework for representing river systems within digital twins. It ensures accurate identification and nuanced characterization of river segments, strengthening global connectivity and comprehension. The accompanying open platform demonstrates the practical application of RECS, promising to enhance data accessibility and decision-making in hydrological management. Moreover, the potential integration of RECS into diverse information systems signals a watershed moment for the advancement of water conservancy technologies.

## Reference

[1] Mihai S, Yaqoob M, Hung D V, et al. Digital twins: A survey on enabling technologies, challenges, trends and future prospects. IEEE Communications Surveys & Tutorials, 2022, 24(4): 2255-2291.

[2] Li X, Luo J, Li Y, et al. Application of effective water-energy management based on digital twins technology in sustainable cities construction. Sustainable Cities and Society, 2022, 87: 104241.

[3] Li, T., Wang, G., Chen, J., A modified binary tree codification of drainage networks to support complex hydrological models, Computers and Geosciences, 2010, 36(11): 1427-1435.

[4] Bai R, Li T, Huang Y, et al. An efficient and comprehensive method for drainage network extraction from DEM with billions of pixels using a size-balanced binary search tree. Geomorphology, 2015, 238: 56-67.

[5] Li J Y, Li T J, Zhang L, Bellie S, Fu X D, Huang Y F, Bai R. A D8-compatible high-efficient channel head recognition method. Environmental Modelling & Software, 2020, 104624.

**Theme:** Big-data, knowledge, and water data management
**IAHR Thematic Priority Area:** [TPA-4] Digital Transformation
https://doi.org/10.3850/iahr-hic2483430201-398

# The Study on Marine Multi-Element Datasets Integration Based on Element Decomposition

**Yingxiang Hong[1], Yazhen Wang[1], Xuan Wang[1*]**

[1] School of Marine Science and Technology, Tianjin University, Tianjin, 300072, China

** Corresponding author: xuanwang@tju.edu.cn*

**Abstract.** The marine environment plays a crucial role in analyzing ocean dynamics, including ocean circulation, eddies, and waves. Currently, this information is primarily obtained from reanalysis products and satellite observations. While marine reanalysis products offer multi-element and multidimensional analysis with coordinated matching of dynamic and thermal forces, their accuracy is not as precise as observational data. Conversely, remote sensing datasets are extensively used for their real-time and high precision, but they only provide information on sea surface height anomaly (SSHA) and sea surface temperature (SST). Therefore, it is necessary to integrate information from both products into a new data system. This study investigates the internal structure of various marine environmental elements and introduces a straightforward statistical and dimension transformation approach to assimilate different datasets and reconstruct a new spatial-temporal marine dataset. The results indicate that the assimilated dataset can provide information with more comprehensive elements, while maintaining accuracy comparable to satellite observation.

**Keywords:** Marine elements, Marine dataset, Remote sensing, Data assimilation

## 1 Introduction

Elements are crucial components that define the properties of seawater and are essential for studying marine temperature-salinity profiles, eddies, and other phenomena. The primary source of marine element information are reanalysis products and satellite observations.

Previous studies have utilized a variety of reanalysis products in ocean circulation research. Marine reanalysis products can provide the computation of various important ocean elements and facilitate detailed analysis of ocean phenomena at high resolution. However, their accuracy in describing the ocean's motion state and physical-chemical properties is not as precise as observational data.

Satellite observations data are also frequently utilized in oceanography research to forecast various elements and study different marine phenomena. Although satellite observations datasets can provide real-time and highly precis data sets, they are limited in the types of elements that can be observed.

To address the limitation, it is essential to integrate the strengths and weaknesses of these two different datasets, utilize the reanalysis products to supplement missing elements and take advantage of the near real-time nature of satellite observations data.

A straightforward statistical and dimension transformation method has been conducted to generate a new spatial-temporal marine dataset which takes the area of the Pacific Northwest as example. A more comprehensive range of elements has been included with the accuracy comparable to satellite observation.

## 2 Data and Methodology

### 2.1 Study area and data collection

Two variables are provided from the oceanographic satellite data (SSH and SST). More comprehensive variables are available from the ocean reanalysis product (HYCOM) including SSH, SST, SSS, SSU and SSV.

### 2.2 Methodology

Assuming that the inner relationships among different marine elements remain consistent as long as the datasets are reliable and accurately reflect real ocean phenomena, we can use the structure inferred from the reanalysis datasets to extrapolate satellite-observed elements to unobserved variables through Eq.(1-3).

$$Y_{all} = f(Y_{obs}^{sat}) \tag{1}$$

$$Z_t = X_{all-t}^{a}(X_{obs-t}^{a})^{\mathrm{T}}\left(X_{obs-t}^{a}X_{obs-t}^{a\ \mathrm{T}}\right)^{-1} \tag{2}$$

$$Z = \frac{1}{T}\sum_{t=1}^{T} Z_t \tag{3}$$

$f(\cdot)$ □ $Z$

where, $Y_{all} = (y_1, y_2, ...y_n)$ is the data for all the marine elements; $Y_{obs}^{sat} = (y_1^{obs}, y_2^{obs}, ..., y_m^{obs})$ is the satellite data for observed elements, namely SSH and SST data in this study; f is the transfer function or operator; $X_{all}^{a} = (x_1, x_2, ...x_n)$ is the reanalysis data for all the marine elements; $X_{obs}^{a} = (x_1, x_2, ..., x_m)$ is the subset from the same reanalysis datasets but only for the elements observed, it indicates SSH and SST here.

In this way the operator can be estimated and the satellite data can be updated for all the elements including SSH, SST, SSS, SSU and SSV based on the Eq.(1).

## 3. Results

When comparing the reconstructed dataset with the reanalysis data, Table 1 presents the statistical expressions of RMSE and RE for each variable.

Table 1 RMSE and RE of reconstructed variable compared with the reanalysis product.

| Variable | RMSE | RE |
|---|---|---|
| SSH(m) | 0.093 | 0.001340 |
| SST(℃) | 0.457 | 0.153295 |
| SSS(‰) | 0.224 | 0.001345 |
| U(m/s) | 0.197 | 0.015687 |
| V(m/s) | 0.175 | 0.111334 |

## 4. Conclusions

When compared to reanalysis data, the reconstructed results demonstrate similar accuracy when satellite observation is considered as the reference point. This means we can generate a dataset with comprehensive elements and comparable effectiveness to reanalysis data, while also maintaining the timeliness of satellite observation. The proposed method provides a simple approach and valuable insights for integrating diverse marine science datasets.

**Theme:** Big-data, knowledge, and water data management
**IAHR Thematic Priority Area:** [TPA-4] Digital Transformation
https://doi.org/10.3850/iahr-hic2483430201-400

# Identification Of Critical Thresholds of Flow States in Mountainous Small and Medium-Sized Rivers

**Xiaoyan Zhai[1,2], Ronghua Liu[1,2], Liang Guo[1,2], Zhaohui Li[1,2]**

[1] China Institute of Water Resources and Hydropower Research, Beijing 100038, China
[2] Research Center on Flood and Drought Disaster Reduction of the Ministry of Water Resources, Beijing 100038, China

**Abstract.** The critical thresholds of flow states directly influence the morphology of river networks. Using the D8 algorithm and mean change point method, the relationship between catchment drainage area threshold and river source density is established, and the critical threshold between overland flow and streamflow is determined. A total of 2859 small and medium-sized rivers in mountainous regions across China are selected for case study. Results showed that a power function relationship with the form of $y=kx^a$ was determined between catchment drainage area thresholds and corresponding river source densities for all the rivers. The values of coefficient $k$ for all the rivers ranged from 2.39 and 878.39 with an average value of 352.76, which tended to gradually increase from north to south and from west to east in China. The values of power $a$ ranged from -1.1 and -0.9 for 96% of the rivers. The critical threshold between overland flow and streamflow was determined as 0.375 km$^2$, 0.5 km$^2$ and >0.5 km$^2$, respectively for 37.39%, 60.30% and 2.30% of the rivers. This study is expected to provide references for the extraction of digital river networks and the analysis of unit hydrographs.

**Keywords:** Catchment drainage area threshold; Flow state; Mean change point method; Small and medium-sized rivers

## 1 Introduction

The critical thresholds of flow states directly influence the morphology of river networks, and further act on the calculation of runoff confluence processes. The purpose of this study is to establish the relationship between catchment drainage area threshold and river source density, and identify the critical threshold of flow states in mountainous small and medium-sized rivers in China. This study is expected to provide references for the extraction of digital river networks and the analysis of unit hydrographs.

## 2 Material and Methods

### 2.1 Study area and data sources

Referring to the “Code for China River” (SL249-2012), a total of 2859 small and medium-sized rivers with an average drainage areas of approximately 1600 km$^2$ in mountainous regions across China are selected for case study. Approximately 82% of the total rivers have drainage areas ranging from 100 km$^2$ to 2500 km$^2$. The average slope of the river basins ranges from 0.06° to 61.46°, 95% of which have an average slope greater than 5°. The river length ranges from 32.6 km to 1225.1 km. The collected data include DEM (Digital Elevation Model, grid: 25m × 25m) and DOM (Digital Orthophoto Map, 0.8m), both of which are obtained from the National Geomatics Center of China (http://ngcc.sbsm.gov.cn/article/en/), and are used for river network extraction and accuracy comparison.

### 2.2 Methodology

Based on DEM and DOM data, the D8 algorithm is used to extract river network, and the mean change point method is used to establish the relationship between catchment drainage area critical

threshold and river source density. The critical threshold of drainage area is determined ranging from 0.0625 $km^2$ to 4 $km^2$, and the corresponding number of river sources under each critical threshold is extracted. The relationship between catchment drainage area critical threshold and river source density can be established, and the grids with drainage areas no less than the threshold is marked as river channel. The flow forms can be divided into overland flow and streamflow, which can be determined as a change point on the power function relationship where the river source density decreases rapidly to slowly. The change point, i.e., the optimal critical threshold, can be used to extract river network, which is compared with the manually extracted river network based on 2.5m resolution DOM data to determine the accuracy of the critical threshold.

## 3 Results and Discussion

A power function relationship with the form of $y=kx^a$ is determined between catchment drainage area thresholds ($x$) and river source densities ($y$) for all the rivers, with the determination coefficients great than 0.97 for 97% of total rivers. The values of coefficient $k$ for all the rivers range from 2.39 and 878.39, the values of power $a$ range from -1.1 to -0.9 for 96% of total rivers, and thus the power function relationship can be approximated as an inverse proportional function. A greater value of $k$ indicates a denser river network, and vice versa. Overall, the values of $k$ tend to gradually increase from north to south and from west to east in China. The average relationship is expressed as $y = 352.76x^{-0.974}$ for all the selected rivers across China, with the determination coefficient being 0.9997. The average values of coefficient $k$ for all the 132 national flash flood disaster forecasting and warning zones range from 223.50 and 530.49.

The critical thresholds between overland flow and streamflow are determined as 0.375 $km^2$, 0.5 $km^2$ and >0.5 $km^2$, respectively for 37.39%, 60.30% and 2.30% of all the rivers. Compared with the river networks manually extracted using digital orthophoto map with a spatial resolution of 0.8m (Figures 1 and 2), the absolute relative errors of drainage densities are less than 3%.

Figure 62 DOM map of Gongqu river basin

Figure 2 Comparison of river networks

## 4 Conclusions

With catchment drainage area thresholds ranging from 0.0625 $km^2$ to 4 $km^2$, a power function relationship was established between catchment drainage area threshold and river source density for 2859 small and medium-sized rivers. The critical threshold between overland flow and streamflow was considered as a change point on the relationship where the river source density decreased rapidly to slowly, which was determined as 0.375 $km^2$, 0.5 $km^2$ and >0.5 $km^2$, respectively for 37.39%, 60.30% and 2.30% of the rivers. Compared with the river networks manually extracted using DOM with a spatial resolution of 0.8m, the absolute relative errors of drainage densities were less than 3%.

## Reference

[1] Ministry of Water Resources of the People's Republic of China. Code for China River. SL 249-2012. 2012.

**Theme:** Big-data, knowledge, and water data management
**IAHR Thematic Priority Area:** [TPA-4] Digital Transformation
https://doi.org/10.3850/iahr-hic2483430201-402

# Analysis Of Spatial and Temporal Characteristics of Water Quality in Miho-River, Korea

**Eunju Lee, and Sewoong Chung**

[1] Environmental engineering, Chungbuk National University, Cheongju, 28644, Korea

*Corresponding author: schung@chungbuk.ac.kr*

**Abstract.** Water quality management in the Miho River, a major tributary of the Geum River in Korea, is crucial due to significant contamination from various sources. This study employs spatiotemporal analysis to assess water pollution, revealing elevated Biochemical Oxygen Demand (BOD) levels in the Miho River compared to its tributaries. Principal Component Analysis (PCA) identifies clusters reflecting seasonal variations and pollutant influences, guiding effective water quality management policies.

**Keywords:** Clustering analysis, Miho-River, Principal component analysis, Spatiotemporal analysis

The Miho River, the largest and most contaminated tributary of the Geum River in Korea, significantly influences the flow rate and water quality of the Geum River. Predominant sources of water pollution include agricultural paddy and farm fields, livestock manures, and industrial wastewaters [1, 2]. This study employs spatiotemporal data analysis, incorporating correlation analysis among multiple water quality variables and principal component analysis (PCA) with clustering in terms of space and variables, to delineate water pollution issues in the Miho River. The primary objective of this research is to inform water quality management policies and measures for the river.

Over the past decade (2013-2022), water quality data was gathered from 10 monitoring stations in the Miho River and 18 stations in 12 tributaries. The water quality variables used were Water Temperature (Temp), Biochemical Oxygen Demand (BOD), Total Organic Carbon (TOC), Chemical Oxygen Demand (COD), Total Phosphorus (TP), Total Nitrogen (TN), and Chlorophyll-a (Chl-a). These data were collected through the Water environmental information system [3].

Descriptive statistics, spearman correlation analysis, and PCA were conducted for analysis of characteristics in Miho-River. PCA, extracting principal components with eigenvalues exceeding 1.0 [4], and was analysed using FactoMineR package and psych package from R [5, 6].

Spatiotemporal water quality analysis revealed that BOD in the Miho River surpassed that of its tributaries. The tributaries exhibited the highest BOD levels in the following sequence: Musim stream, Han stream, Seoknam stream, and Byeongcheon stream. BOD pollution in the Miho River was more pronounced downstream than at upstream stations. To assess changes in water quality over time, the analysis was conducted by segregating into irrigation (April 1 to September 30) versus non-irrigation periods (October 1 to March 31) and flood season (June 21 to September 20) versus non-flood season (September 21 to June 20). Results indicated higher pollution levels of BOD, COD, TOC, and TP during the irrigation period and flood season compared to the non-irrigation period and non-flood season. The flood season exhibited higher concentrations, likely due to inflow from non-point pollution.

Correlation analysis revealed a strong positive correlation (Fig 1) among BOD, TOC, and Chl-a. As a result of PCA, identified a cluster formed by TP, TOC, and BOD, significantly influencing the positive direction of the first principal component axis. Clusters with similar irrigation periods and flood seasons were observed, with the Miho River forming clusters in the positive direction of the

first principal component axis and tributaries forming clusters in the negative direction (Fig 2). Given elevated pollution levels during the flood season and irrigation period, managing non-point pollution sources from the agricultural sector becomes imperative during these periods.

Moreover, the higher water pollution in the Miho River than in its tributaries, coupled with a strong correlation between BOD and Chl-a, suggests a high internal organic matter load due to primary production in the river. Consequently, improving flow rate and reducing nutrient load are crucial for controlling algal growth in the river.

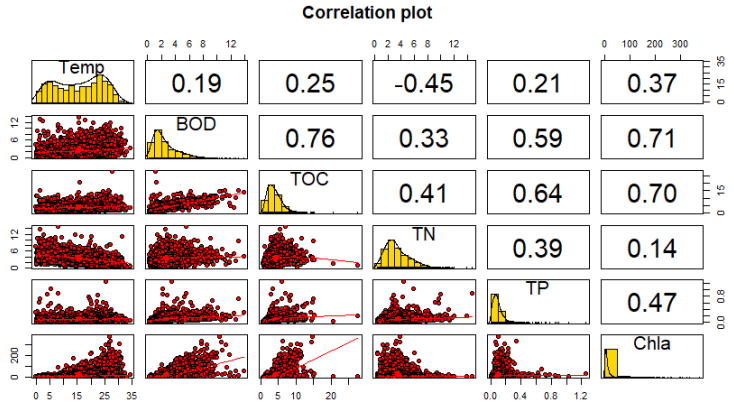


Figure 63. Correlation matrix of measured variables

(a) Flood season (b) Irrigation season

**Figure 2.** The bi-plot of PCA results

## Acknowledgments

This work was supported by the Korea Environmental Industry & Technology Institute (KEITI) through the Aquatic Ecosystem Conservation Research Program, funded by Korea Ministry of Environment (MOE) (Grant number 2021003030004).

## Reference

[1] Song, Y.H., Lee, Y.H., Lee, J.G., Park, Y.K., and Kim, K.E., 2021, Policy analysis and response measures to improve Miho Stream water quality, Daejeon Sejong research institute

[2] Committee for Management of Geum River, 2021, A study of the investigation and improvement on the water quality deteriorating area of Mihocheon

[3] Ministry of environmental (ME). (2013-2022). Water Environment information system (WEIS), http://water.nier.go.kr/

[4] Box, G.E.P. and Cox, D.R., 1964, An analysis of transformations, Journal of the Royal statistical Society, Series B (Methodological), 26(2), pp 211-252

[5] Le, S., Josse, J. and Husson, F., 2008, FactoMineR: An R Package for Multivariate Analysis. Journal of Statistical Software, 25(1), pp 1-18.

[6] Revell, W., 2019, psych: Procedures for Personality and Psychological Research, https://CRAN.R-project.org/package=psych

**Theme:** Big-data, knowledge, and water data management
**IAHR Thematic Priority Area:** [TPA-4] Digital Transformation
https://doi.org/10.3850/iahr-hic2483430201-404

# Research on the Prediction of Yellow River Runoff and Sediment Based on Deep Learning Framework

**WU Dan1,2, LIU Qixing1,2**

1 Yellow River Institute of Hydraulic Research, YRCC, Zhengzhou 450003,China
2 Henan Engineering Research Center of Smart Water Conservancy, Zhengzhou 450003,China

*Corresponding author: LIU Qixing 1012633702@qq.com*

**Abstract.** This study utilizes deep learning (DP) technology based on big data to deeply mine data in the Yellow River water and sediment data warehouse, and further studies the machine learning modeling theory and method for runoff and sediment prediction based on deep learning framework.

**Keywords:** x

## 1 Introduction:

The water and sediment data warehouse in this study contains a variety of massive data. There is a deep and close relationship between some physical distributions of hydrological information. The use of deep learning theory and key technologies for runoff and sediment prediction is of great significance to explore the change trend of runoff and sediment and forecast floods in sediment transport areas. Therefore, "learning" useful information from historical experience and sample data and establishing an intelligent model for runoff and sediment prediction based on the deep learning framework has become one of the key problems in analyzing the change law of runoff and sediment for hydrological prediction.

## 2 Material and methods

Based on deep learning frameworks such as Tensorflow, Caffe, Torch, PyTorch, etc., a variety of training algorithms such as DBN, RNN, XGBoost and other network structures are used to describe the internal rules of data, compare the prediction levels of different models, and build a multi-base high-dimensional machine learning model that comprehensively considers empirical risk and confidence risk.

## 3 Results and discussion

Our research findings include:(1)The hyperparameter optimization of the neural network model is studied through the grid search function and cross validation function, the value of the hyperparameter of the model is determined, the compression and acceleration method of the neural network is studied, and the weighted pruning and dynamic reasoning methods are used to build the network slimming model to optimize the network structure of the model.(2)Using long short-term memory network (LSTM) and deep belief network (DBN) algorithm, an intelligent runoff prediction model for typical basins in the main sediment-producing areas of the Yellow River was designed and constructed. The Nash efficiency coefficient of the model in the test set of Wuding River Basin and Kuye River Basin was more than 0.75. The runoff prediction results of the two basins basically reflected the fluctuation process of floods, and the flood frequency and peak shape were in good agreement.(3)Based on the data warehouse of water and sediment in the typical basins of the main sediment-producing areas from 2002 to 2019 and the extreme gradient boosting tree (XGBoost) algorithm, the intelligent prediction model of sediment transport in the typical basins of the main sediment-producing areas of

the Yellow River was constructed to calculate the sediment transport in the typical basins of the main sediment-producing areas of the Yellow River under different rainfall scenarios and vegetation conditions in 2019. The average relative percentage error of the model in the validation data sets of the typical basins of the main sediment-producing areas of the Yellow River was generally within 20%.

## 4 Conclusions

One important reason why data-driven machine learning technology is not widely used in the field of hydrology and water resources is that deep neural network is a black box model, and the internal operation mechanism is not yet understood. Therefore, in the future, it is necessary to analyze the evolution law of the input key elements of hydrology and meteorology in the water cycle system of the basin, and digitize the driving forces of natural changes and human activities. In this way, in the process of applying artificial intelligence technology to the study of water and sediment changes in the Yellow River basin, the reasons for the selection of deep network are explained and understood, and the structural parameters suitable for the machine learning model are found to reflect the hydrological propagation and hydraulic process, so as to improve the accuracy and feasibility of scientific research.

## Reference

[1] Liu Xiaoyan, Gao Yunfei, Wang Lue, et al. Change of sediment environment in the main sand-producing areas of the Yellow River in the last 100 years [J]. Yellow River,2016,38(5):1-5.

[2] XIA Runliang, Liu Qixing, Li Tao, Liu Xiaoyan, GAO Yunfei, Wu Dan. Prediction of uncontrolled Yellow River runoff based on ensemble learning [J]. Chinese Journal of Basic and Engineering Sciences, 2019,28(03):740-749. (in Chinese)

[3] RUI Xiaofang. On hydrological model of watershed [J]. Advances in Water Resources and Hydropower Science and Technology,2017,37(4):1-7.

[4] HUANG Yihua. Research Progress of Big Data Machine learning system [J]. Big Data,2015,1(1):28-47.

[5] LEI Xiaoyun, Zhang Lixia, Liang Xinping. Research on annual runoff prediction model based on BPneural network based on MATLAB toolbox: taking Wulastai River in Tacheng Area as an example [J]. Journal of Hydrology,2008,28(1):43-46.

[6] Wu Dan, XIA Runliang, Li Tao, Liu Qixing. Research on key technologies of constructing data warehouse of water and sediment change in Yellow River [J]. Yellow River of People,2022,44(10):159-162.

[7] Badrzadeh H, Sarukkalige R, Jayawardena A W. Hourly runoff forecasting for flood risk management: Application of various computational intelligence models[J].Journal of Hydrology, 2015, 529:1633-1643.

[8] Wang W C, Chau K W, Qiu L, et al. Improving forecasting accuracy of medium and long-term runoff using artificial neural network based on EEMD decomposition.[J].Environmental Research,2015,139:46-54.

[9] Su H D, Jia Y W, Ni G H, et al. Application of machine learning in runoff prediction [J]. China Rural Water Resources and Hydropower,2018(6).

[10] Wang Fuqiang. Research on Medium and long term hydrological prediction and its application in plain flood resource utilization [D]. Dalian University of Technology,2008.

[11] Shi Jianwei, Jiang Shijun, Liu Qixing. Research on runoff prediction model based on LSTM and XGBoost algorithm [J]. Zhihuai,2020(08):29-31.

**Theme:** Big-data, knowledge, and water data management
**IAHR Thematic Priority Area:** [TPA-4] Digital Transformation
https://doi.org/10.3850/iahr-hic2483430201-406

# Current Practices, Gaps and Opportunities in Data Utilization in Water Utility Industry

**Ishara Rakith Perera[1], Joby Boxall[1], Vanessa Speight[1], Scott Young[2], Graeme Moore[2]**

[1] The University of Sheffield, Sheffield S10 2TN, United Kingdom
[2] Scottish Water, Edinburgh EH10 6XH, United Kingdom

*Corresponding author: isharatck@gmail.com*

**Abstract.** Water utility companies collect vast amounts of diverse data types, employing them for regulatory reporting, operational decisions, and strategic planning. The data undergoes intermediary steps from raw collection to insights extraction, which is crucial for informed decision-making. Current practices often involve fragmented data silos, leading to inefficiencies and missed opportunities in data utilization across business applications. This paper identifies key data types in managing water distribution networks (WDNs), categorizing them into static asset, time-series, customer, work management, external, and financial data. A graphical mapping approach is used to connect raw data to applications, enhancing understanding of data usability and identifying underutilized but potent datasets. A critical ranking of intermediary analysis layers highlights high-potential options, including adopting machine learning techniques (especially deep learning) alongside deterministic models for improved decision making. Leveraging less common data types (like asset-specific data) in tandem with traditional datasets shows promise for decision support in WDN management. We expect our attempt to structuralize and understand the usage/ opportunities of data in WDNs can expose new avenues that can be leveraged by advanced analytics tools to further strengthen the water industry's effort to shift from reacting to failures to proactive root cause identification for tackling challenges around WDNs.

**Keywords:** Data to insights, Efficient data utilization, Information systems, Water utilities

## 1 Introduction

Many current data utilization practices in the water distribution industry do not fully leverage available data, despite significant financial resources being invested in developing state-of-the-art data acquisition, transmission, and storage facilities and infrastructure [1]. This inherent issue acts as a bottleneck, impeding the transformation of raw data into actionable insights for making well-informed decisions to its fullest potential [2]. To address this, this study focuses on identifying the key types of data collected and utilized in the management and operation of water distribution networks (WDN) and provides a broad-level categorization of the data into static asset, time-series, customer management, work management, external, and financial data. This categorization lays the groundwork for a more unified and systematic approach to data utilization. This is followed by mapping data to business cases through the identification of middle analysis layers, which serve as intermediary layers where significant improvements can be made to increase data utilization efficiency and improve potential insights about the network.

## 2 Method

Data collected from water distribution systems, are used in a multitude of ways to achieve various business applications in practice. Some of these business applications include (but are not limited to) tasks such as background leakage detection/localization, burst detection/localization, water quality management, pressure management, pipe replacement, network expansion, and energy optimization. In the process of unravelling all potential opportunities for improvements and identifying prevailing gaps, it is essential to have a clear understanding of the intermediary steps involved in the process of

going from data to business applications. Typically, the raw data are put through a number of intermediate analysis layers before they can be readily utilized in the above business applications. These intermediate layer analyses depend on the types of business applications they are intended for. For instance, the burst detection and localization business process can be achieved by some of the following intermediary processes, sometimes in isolation or at times in combination of multiple methods together. They include: (i) Pressure data analysis, (ii) Hydraulic modelling and simulations, (iii) DMA inlet flow monitoring, (iv) Real-time transient analysis & (v) Acoustic signal processing. An in-depth analysis by way of performing a comprehensive mapping of data -> intermediate analyses -> business applications enables a much clearer identification of the gaps as well as opportunities pertaining to where further improvements can be made in both data utilization and adoption of more efficient methods and tools for analysing the data to serve specific business purposes.

## 3 Results

An extraction of the graphical mapping is presented in Figure 1 as an example for a selected business application. Similar mappings are conducted for all business applications. This illustration provides detailed information about the specific data types that connect to the various intermediate analysis layers. One advantage of such a mapping on a broader scale, is that it reveals crucial information such as the most frequently used data types, rarely used data types, the reliance of specific data types for certain business applications, as well as data and analysis methods with great potential for use but are typically underutilized.

Figure 64 Example of a data to business cases mapping, for a selected business application

## 4 Conclusion

It is noted that, besides utilizing deterministic modelling tools, there is significant potential in harnessing the power of machine learning algorithms for assisting various business applications. We also uncover substantial opportunities to utilize data types not typically included in traditional data-driven techniques, such as various asset-specific data, for making operational decisions around WDNs. This potential can be realized when these data types are used in conjunction with commonly used data like pressure, flow, and water quality.

## References

[1] J. Sirkiä, T. Laakso, S. Ahopelto, O. Ylijoki, J. Porras, and R. Vahala, “Data utilization at finnish water and wastewater utilities: Current practices vs. state of the art,” *Utilities Policy*, vol. 45, pp. 69–75, Apr. 2017, doi: 10.1016/j.jup.2017.02.002.

[2] K. Thompson and R. Kadiyala, “Leveraging Big Data to Improve Water System Operations,” *Procedia Engineering*, vol. 89, pp. 467–472, Jan. 2014, doi: 10.1016/j.proeng.2014.11.235.

**Theme:** Big-data, knowledge, and water data management
**IAHR Thematic Priority Area:** [TPA-4] Digital Transformation
https://doi.org/10.3850/iahr-hic2483430201-408

# Predicting Urban Stormwater Quality in Data-Deficient Areas: Enhancing Deep Tunnel Systems with Machine Learning Techniques

**Haibin Yan[1], David Zhu[1,2]**

[1] University of Alberta, Department of Civil and Environmental Engineering, Edmonton, T6G 1H9, Canada
[2] Ningbo University, School of Civil and Environmental Engineering, Ningbo, 315211, China

*Corresponding author: dzhu@ualberta.ca*

**Abstract.** Deep tunnel systems are designed to mitigate the risk of flooding and corresponding pollution in urban areas. Predictive modeling can enhance the functionality of deep tunnel systems. Machine learning is an effective predicting tool in data-deficient areas. By integrating data from different catchments, the model performance can be enhanced. Consideration of catchment characteristics can improve the model's generalization capacity. The pseudo-labeling learning can elevate the model's predictive ability.

**Keywords:** Data-deficient, Deep tunnel, Machine learning, Prediction model, Semi-supervised learning, Urban stormwater quality

## 1 Introduction

Deep tunnel systems can store and convey excess stormwater, reducing flooding and pollution risks in urban areas. However, accurate prediction of stormwater quality within these systems are limited by data deficiencies (Zhu et al., 2022). Machine learning models offer a simpler alternative to process-driven models, but their predictive power relies heavily on the quantity and quality of available training data (Zhi et al., 2021). Given the scarcity of comprehensive water quality datasets in many urban catchments, semi-supervised machine learning holds promise as a solution to this challenge (van Engelen and Hoos et al., 2020). This research aims to leverage semi-supervised machine learning to develop a framework for predicting urban stormwater quality in data-deficient areas, potentially enhancing the effectiveness of deep tunnel systems in managing stormwater pollution.

## 2 Material and methods

In this study, four catchments in Calgary, Canada were examined over two ice-free seasons from 2018 to 2019, with weather stations monitoring rainfall and autosamplers collecting 57 composite water samples during rainfall events. A Random Forest (RF) model was developed to predict event mean concentrations (EMC) for total suspended solids (TSS), total nitrogen (TN), and total phosphorus (TP). The base RF model (RF-B) used single catchment rainfall data as input, optimized via genetic algorithm with RMSE assessing training performance. Additional models were developed: RF-R, which included data from three other catchments but only used rainfall as input, and RF-RC, which incorporated catchment characteristics as well. The semi-supervised RF model (RF-Semi), shown in Figure 1, expanded the training dataset using pseudo-labels generated from high-confidence predictions across 27 unique RF-RC models. These pseudo-labels were created by averaging the predictions of samples with low coefficient of variation (CV), enhancing the model's training dataset.

## 3 Results and discussion

To evaluate the performance of RF models, the NSE are shown in Figure 2. RF-B demonstrated a good fit for TSS during training with an NSE of 0.90 but performed poorly on the testing dataset. For

TN and TP, the performance was similarly inconsistent with negative or low NSE scores in testing, suggesting issues with model overfitting. The RF-R model showed improved test results for TSS and TP compared to RF-B, indicating enhanced prediction capabilities. However, TN predictions remained weak. The RF-RC model showed slight improvements in TSS and TP predictions over RF-R, indicating that additional catchment data can aid model performance. However, TN continued to pose challenges. The RF-Semi model yielded the best performance across all parameters, with the highest NSE values in testing datasets, particularly for TSS and TP. This model's use of pseudo-labels likely contributed to its improved ability to generalize and predict unseen data more accurately. Despite its success, TN predictions in the testing dataset were still negative.

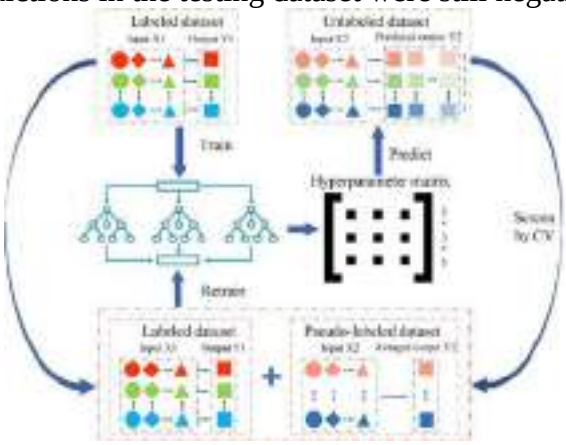


Figure 1 Flowchart of semi-supervised random forest model

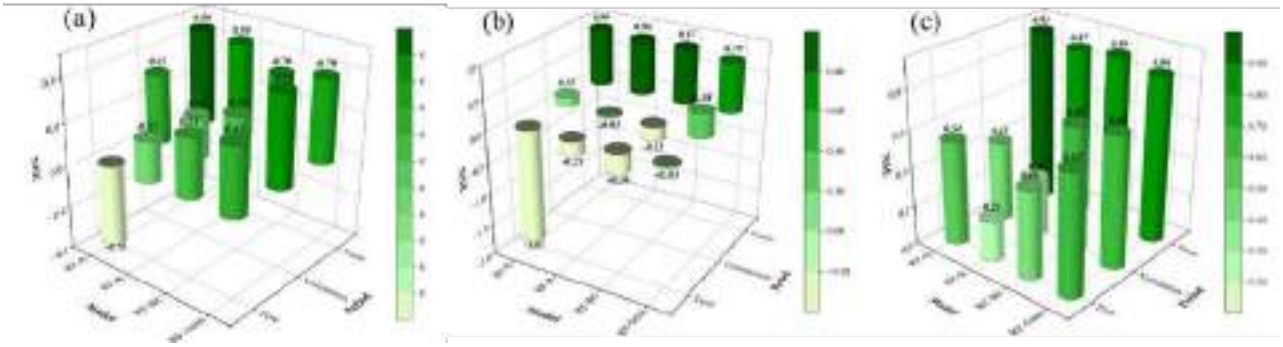


Figure 2 NSE of RF for (a) TSS; (b) TN; (c) TP

## 4 Conclusions

Machine learning is an effective tool for predicting EMCs of TSS and TP. Relying on limited data and features may lead to overfitting, which affects its predictive effectiveness. By integrating data from different catchments, the model performance can be improved. Consideration of catchment characteristics, which can be directly linked to water quality, can improve the model's capacity for generalization. Semi supervised model can enrich the training dataset, and this semi-supervised machine learning approach can further improve the model's predictive ability. This approach potentially enhances the effectiveness of deep tunnel systems in managing stormwater pollution.

## Reference

[1] Van Engelen, J.E., Hoos, H.H., 2020. A survey on semi-supervised learning. Mach. Learn. 109, 373–440.
[2] Zhi, W., Feng, D., Tsai, W.-P., Sterle, G., Harpold, A., Shen, C., Li, L., 2021. From hydrometeorology to river water quality: can a deep learning model predict dissolved oxygen at the continental scale? Environ. Sci. Technol. 55, 2357–2368.
[3] Zhu, M., Wang, J., Yang, X., Zhang, Y., Zhang, L., Ren, H., Wu, B., Ye, L., 2022. A review of the application of machine learning in water quality evaluation. Eco-Environ. Health.

**Theme:** Big-data, knowledge, and water data management
**IAHR Thematic Priority Area:** [TPA-4] Digital Transformation
https://doi.org/10.3850/iahr-hic2483430201-410

# Hydraulic Characteristics of Stepped Dropshafts

**Shangtuo Qian[1], Fei Ma[1], Weichen Ren[2], Jianhua Wu[1], Hui Xu[1]**

[1] Hohai University, Nanjing 210098, China
[2] China Institute of Water Resources and Hydropower Research, Beijing 100048, China

*Corresponding author: qshttc@163.com*

**Abstract.** Dropshafts are an important part of deep tunnel storage and drainage systems, which need to operate safely and efficiently under high head and high flow conditions. For the deep tunnel storage and drainage systems in China, we have designed a stepped shaft, which mainly consists of a central ventilation pipe with air holes and a succession of spiral steps. A series of studies were carried out on the hydraulic characteristics of stepped dropshafts, demonstrating their advantages over traditional dropshaft designs. The flow classification was made and the expressions for predicting the thresholds of the flow regimes were established. The shock wave characteristics were clarified and the expression for the maximum overflow capacity was established. Expressions for the outflow residual energy and ventilation characteristics were also established, and the main influencing factors and their specific roles were clarified. The conclusions support the engineering application of stepped dropshafts and suggest further structural optimization.

**Keywords:** Deep tunnel storage and drainage system; Energy dissipation; Flow regime; Overflow capacity; Stepped dropshaft; Ventilation.

## 1 Intrudction

The deep tunnel storage and drainage system has been applied as an effective engineering tool to solve urban stormwater problems. The system mainly consists of dropshafts, underground tunnels, and lift pumping stations, in which the dropshafts collect surface runoff and convey it to the underground tunnels. The dropshafts need to operate safely and efficiently under conditions of high head and high flow rate, and are susceptible to problems such as water fluctuation and choke, cavitation erosion, high-energy flow impingement and scouring, and poor ventilation.

The stepped dropshaft was developed specifically for the deep tunnel storage and drainage systems[1]. It essentially consists of a central ventilation pipe with air holes and a succession of spiral steps (see Figure 1). The water flows down the steps, and the dragged air is exchanged with the atmosphere through the ventilation pipe. Compared with the conventional dropshaft types, the stepped dropshaft has high energy dissipation rate and low cavitation risk, large overflow capacity and smooth ventilation performance, stable overall flow pattern, and limited vibration caused by water-air interaction. However, the hydraulic characteristics of stepped dropshafts need to be studied in depth, and the applicability of existing conclusions for traditional stepped spillways needs to be verified. In particular, there is a limited understanding of the nonuniform flow discharge distribution along the width direction under the influence of centrifugal force. For this reason, we have carried out a systematic study of the hydraulic characteristics of stepped dropshafts, to develop an in-depth understanding and provide a basis for engineering applications.

## 2 Result and discussion

Depending on whether the step cavities are filled with backwater or not, the flow regimes in the stepped dropshaft can be classified into three types: nappe, transition and skimming, which occur sequentially with increasing flow (see Fig. 1). In the nappe flow regime, the water flow falls down step by step and there is a cavity beneath the falling water. Energy dissipation in the nappe flow

regime is mainly caused by the impact of the falling water flow and the step surface, the breakup of the water flow, the mixing of the falling water and the backwater, and the hydraulic jump. In the skimming flow regime, the main flow skims along the step tips, step cavity is completely filled with a strong vortex, and the water flow energy dissipation is mainly caused by the impact of the water flow on the step surface and the vortex to increase the turbulence of the water flow. The transitional flow regime is between the above two flow regimes and shows obvious instability and fluctuation. The theoretical equations are established based on the two phenomena of cavity filling and main flow parallel to the bottom slope, and the thresholds of each flow regime are derived by considering the uneven distribution of the water flow discharge along the width direction[2]. It is observed that the centrifugal force of the water flow forms shock waves, and expressions are established for their characteristic parameters, which can also tell us the maximum flow rate of the stepped dropshaft with the limitation that the shock wave peak touches the upper step bottom.

The outflow residual energy of the stepped dropshaft is used to characterize its energy dissipation. The concept of energy dissipation area is proposed for the two-dimensional stepped spillway, considering that the energy of the water flow is mainly dissipated by turbulence of the vortex. Based on it, the concept of dissipation volume in combination with the stepped dropshaft geometry is proposed, and the expression of the outflow residual energy applicable to the stepped shaft is established [3]. On the other hand, the air flow field inside the stepped dropshaft is revealed, and the ventilation pipe mainly plays the role of discharging the gas dragged by the water flow, and then the expressions of the air inflow and outflow volume are established.

## 3 Conclusion

The results have demonstrated the hydraulic characteristics and advantages of stepped shafts, as well as elucidated the undesirable flow patterns, to support the practical application. In order to further improve the characteristics of the stepped dropshaft and to control the undesirable flow, we have also carried out a number of geometry optimization researches, and the recommendations for geometry optimization and the outlook for the future have been concluded.

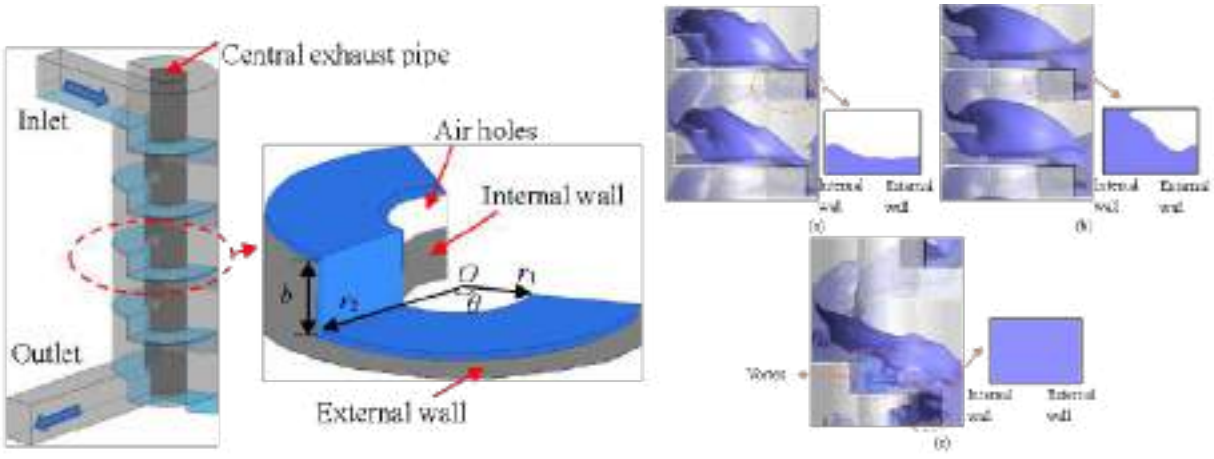


Figure 65 Geometry and flow regimes of stepped dropshaft: (a) nappe flow, (b) transitional flow, (c) skimming flow

## Reference

[1] Ren, W., Wu, J., Ma, F., & Qian, S. (2021). Hydraulic performance of helical-step dropshaft. *Water Science and Technology*, *84*(4), 954-965.

[2] Qian, S., Wu, J., Xu, H., & Ma, F. (2022). Transition flow occurrence on stepped channels. *Journal of Hydraulic Research*, *60*(3), 487-495.

[3] Wu, J., Qian, S., Wang, Y., & Zhou, Y. (2020). Residual energy on ski-jump-step and stepped spillways with various step configurations. *Journal of Hydraulic Engineering*, *146*(4), 06020002.

**Theme:** Big-data, knowledge, and water data management
**IAHR Thematic Priority Area:** [TPA-4] Digital Transformation
https://doi.org/10.3850/iahr-hic2483430201-412

# Air-Water Flow Features along Deep-Tunnel system

**Nian Ye[1], Yiyi Ma[1]**
[1] College of civil engineering and architecture, Zhejiang University, Hangzhou 310058, China

**Abstract:** This study investigated the air-water flow characteristics along the tunnel under the effects of air entrainment by the upstream dropshaft under various downstream water levels and inflow rates. The air-water flow appearance was recorded and the pressure fluctuations along the tunnel were measured. Observed from the experiments, there are four flow patterns as the downstream water level increased, accompanied with different ways of air release. The most significant pressure fluctuations were observed at the air release points under all the experimental conditions. This study can contribute to a better understanding of the operation processes of a deep tunnel system.

**Keywords**: air entrainment, air-water two phase flow, deep tunnel system, dropshaft, pressure

## 1 Introduction

The dropshaft, which is part of the deep tunnel system, usually reaches dozens of meters and can entrain large amount of air into the system[1]. The air can be transported to the downstream tunnel by flowing water and different patterns of air-water flow is then formed there. Previous studies on air-water interactions in drainage pipes were most conducted with air pockets formed by manual air injection or sudden rise of water level[2–4]. There have been few studies on the air-water flow features under the effect of continuous air intake by the upstream dropshaft, which is close to real-world situations. This study experimentally investigated the air-water flow characteristics along the tunnel under the effects of air entrainment by the upstream dropshaft through a large-scale physical model.

## 2 Experiments

The physical model of the dropshaft-tunnel system in this study is sketched in Fig. 1(a). It consists of a horizontal tunnel, three plunging dropshafts of different drop heights, an inlet pipe, and a downstream tank. The pipeline system was made of 15-mm-thick Plexiglas. The horizontal tunnel was 14 m long and had an inner diameter D = 0.3 m. The end of the tunnel was connected to the water tank of 1.5 m × 1.5 m × 1.5 m for downstream water level control (see Fig. 1b). The three dropshafts had the same inner diameter of Ds = 0.3 m, numbered #1, #2 and #3, respectively. The drop heights were $H_1$ = 2.0 m, $H_2$ = 3.0 m and $H_3$ = 5.8 m. The inlet pipe had a diameter of 0.2 m and fed water to dropshaft #3. The relative drop of the plunging dropshaft #3 was $H_3$/Ds = 19.3.

## 3 Results

The air-water flow patterns along the tunnel can be divided into four regimes, as shown in Fig. 2. The pressure fluctuation intensity measuring by the standard deviation of pressure data is presented in Fig. 3.

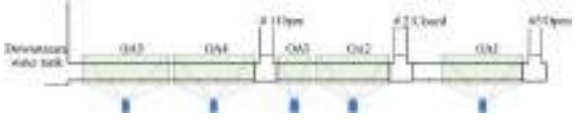

(b)

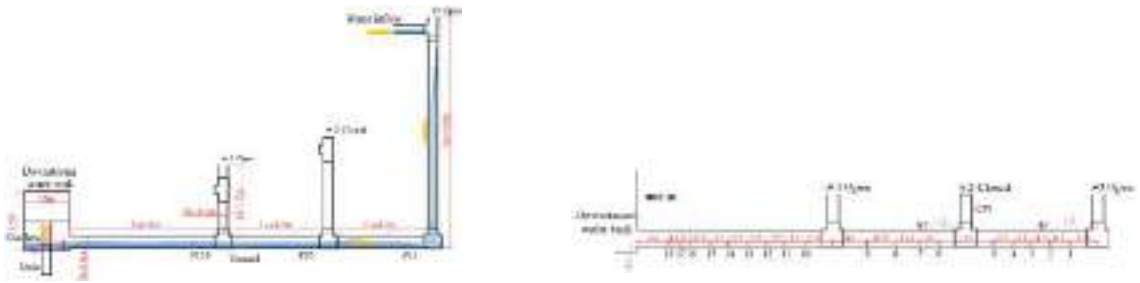

(a) (c)

**Fig. 1.** (a) Schematic of the experimental setup, (b) sensor arrangement, (c) watch windows for air-water flow patterns along the tunnel.

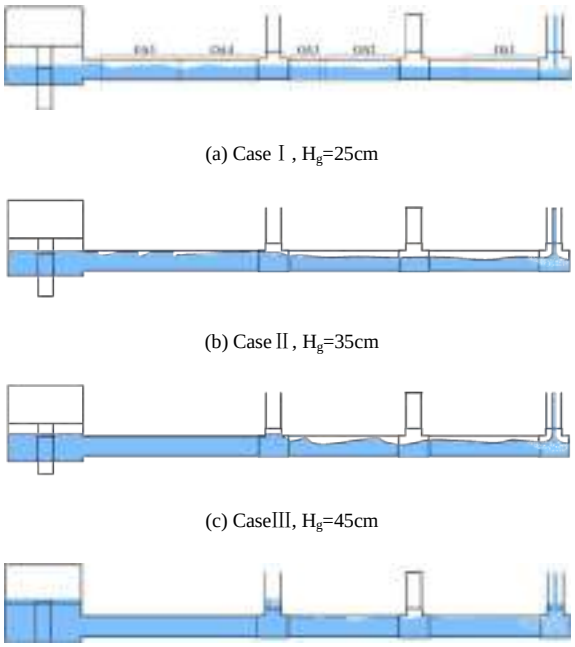

(a) Case Ⅰ, $H_g$=25cm

(b) Case Ⅱ, $H_g$=35cm

(c) CaseⅢ, $H_g$=45cm

(d) CaseⅣ, $H_g$=80cm

**Fig. 2**. Development of air-water flow patterns along the horizontal tunnel under different downstream gate heights (water flow rate $Q^*$ =0.09).

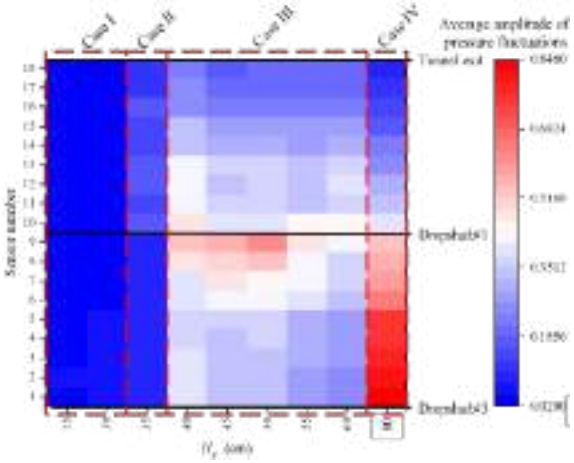

**Fig. 3.** Average amplitude of pressure fluctuation along the horizontal tunnel under different downstream water levels (water flow rate Q* =0.09).

## 4 Conclusions

In this study, the air-water flow patterns and pressure fluctuations along a horizontal tunnel downstream of a dropshaft were investigated by a large-sized physical model. Four air-water flow patterns can be observed. Based on the analysis of the pressure data, it indicates that the movement of air pockets and the associated air-water interactions are the primary causes of intense pressure fluctuations within the tunnel. Adequate attention should be paid as it is likely to cause operation problems to deep tunnel systems.

**Reference**

[1] Liu J, Huang B, Zhu D Z. Jet Impinging in Plunging Dropshafts of Medium Height[J]. Journal of Hydraulic Engineering, American Society of Civil Engineers, 2022, 148(12): 04022028.

[2] Yang Q, Yang Q. Experimental investigation on the hazard of geyser created by an entrapped air release in baffle-drop shafts[J]. Scientific Reports, Nature Publishing Group, 2023, 13(1): 7953.

[3] Wang X, Qian S, Chen H. Experimental Study on Geysers Induced by the Release of Trapped Air in Storage Tunnel Systems[J]. Applied Sciences-Basel, Basel: Mdpi, 2019, 9(24): 5326.

[4] Cong J, Chan S N, Lee J H W. Geyser Formation by Release of Entrapped Air from Horizontal Pipe into Vertical Shaft[J]. Journal of Hydraulic Engineering, American Society of Civil Engineers, 2017, 143(9): 04017039.

**Theme:** Big-data, knowledge, and water data management
**IAHR Thematic Priority Area:** [TPA-4] Digital Transformation
https://doi.org/10.3850/iahr-hic2483430201-414

# Water Slug in Dropshaft of Deep Tunnel Drainage Systems

**Qingzhi Hou[1,2], Youxu Song[1]**

[1] State Key Laboratory of Hydraulic Engineering Intelligent Construction and Operation, Tianjin University, Tianjin 300350, China
[2] School of Civil and Transportation Engineering, Qinghai Minzu University, Xining 810007, China

Corresponding to: qhou@tju.edu.cn

**Abstract.** Deep tunnel drainage systems have been widely used in many majority cities in the world to solve the urban waterlogging problems. During the rapid filling process of deep tunnels, entrapped air pockets occur due to complex water-air interaction, which are continuously compressed by surrounding water and carry a high pressure. When the compressed air pocket travels to a dropshaft of the deep tunnel, the sudden pressure release propels the water slug ending with a blowing-out of air-water mixture and causing a pressure oscillation harmful to the tunnel system. This phenomenon is known as geysering. To study the water slug characteristics and its influencing factors, the mechanisms of liquid shedding from the tail of the water slug plays a vital role. In this paper, the mass shedding rate of the water slug in the dropshaft with a dead-end orifice of different sizes is studied experimentally and numerically. The results show that the numerical simulations are in good agreement with the experimental data. When the aperture ratio is greater than 0.3, it has no effect on the slug mass shedding rate.

**Keywords:** Geysering, mass shedding rate, physical experiment, slug flow, three-dimensional CFD model

## 1 Introduction

Deep tunnel drainage systems have been widely used in many cities in the world to solve the urban waterlogging problems. During the rapid filling process of deep tunnels, entrapped air pockets often occur due to water-air interaction, which are continuously compressed by surrounding water and carry a high pressure. When the compressed air pocket travels to a dropshaft of the deep tunnel, the sudden pressure release propels the water slug ending with a blowing-out of air-water mixture and causing a pressure oscillation harmful to the tunnel system. This phenomenon is known as geysering. Cong *et al.* [1] confirmed that geysering in the dropshapt of the deep tunnel drainage system is similar to slug flow but not to Taylor bubble. In numerical modeling of the geyser, different mass shedding rates are usually taken. However, it has been verified that slug mass shedding rate plays a critical role when simulating slug travelling in pipelines [2, 3]. Fan *et al.* [4] studied the effects of inclination angle, gravity and pipe roughness on slug mass shedding rate. To further study the effect of the size of the orifice at the end of the drop shaft, numerical simulations and physical experiments are conducted.

## 2 Methodology

The vector form of incompressible Navier-Stokes equations with VOF model used herein are expressed as:

$$\nabla \cdot \vec{u} = 0 \tag{1}$$

$$\frac{\partial \vec{u}}{\partial t} + \vec{u} \cdot \nabla \vec{u} = \vec{f} - \frac{1}{\rho}\nabla p + \nu \nabla^2 \vec{u} + \frac{\vec{F}}{\rho} \tag{2}$$

where $\vec{u}$ is velocity vector, $p$ is pressure, $\vec{f}$ is the external force per unit volume, $\nu$ is the kinematic viscosity, and $\vec{F} = -\sigma\big(\nabla \cdot (\nabla\alpha/|\nabla\alpha|)\big)\nabla\alpha$ is the interface-force-source term, and $\sigma$ is the surface tension. The RNG $k-\varepsilon$ model is used for turbulence. The PISO algorithm is used to solve the governing equations.

The slug mass shedding rate can be defined as the reciprocal of slug maximum travelling distance (before breaking) [4]:

$$L_l = L_0 - L(t) = \beta s \tag{3}$$

where $L_l$ is the accumulated slug loss length, $L_0$ is the initial slug length, $L(t)$ is the slug length in motion, $\beta$ is the slug mass shedding rate, and $s$ is the slug's travelling distance.

## 3 Results

The experimental test rig is shown in Fig. 1. The air tank provides gas with different driving pressures $p_0$ of 0.5 bar, 1.0 bar, 1.5 bar and 2.0 bar. There are five initial slug lengths $L_0$ of 0.6 m, 0.7 m, 0.75 m, 1.0 m and 1.5 m, and five different sizes of orifice $D_0$ of 0 mm, 5 mm, 10 mm, 15 mm and 50 mm. The slug motion captured in the experiment is shown in Fig. 2. The calculated slug mass shedding rate of different cases are shown in Table 1.

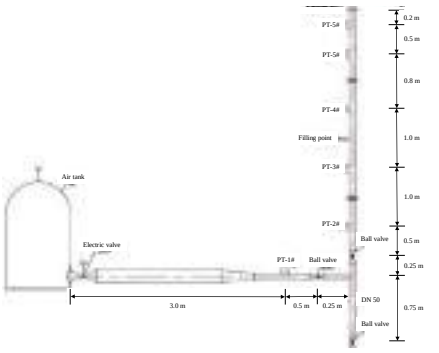


**Figure 1.** Schematic diagram of the experimental test rig

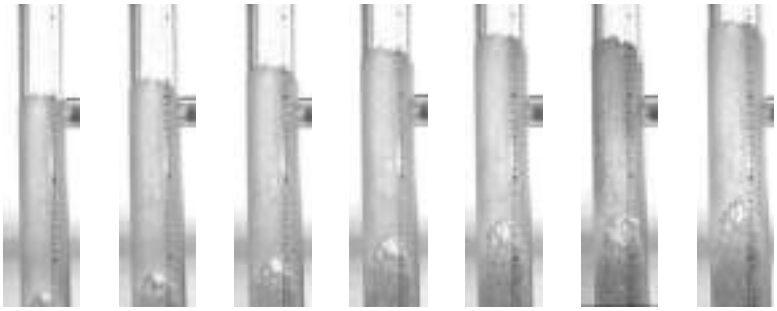


**Figure 2.** Flow regime at different time for the case of $p_0$ = 0.5 bar, $L_0$ = 0.6 m, and $D_0$ = 50 mm

**Table 1.** Slug mass shedding rate of different cases (exp = experiment, sim = simulation)

| Case no. | type | $p_0$ (bar) | $L_0$ (m) | $D_0$ (mm) | $\beta$ | Case no. | type | $p_0$ (bar) | $L_0$ (m) | $D_0$ (mm) | $\beta$ |
|---|---|---|---|---|---|---|---|---|---|---|---|
| 1 | exp | 1.0 | 0.6 | 50 | 0.173 | 10 | sim | 1.0 | 1.0 | 5 | 0.159 |
| 2 | exp | 1.0 | 0.7 | 50 | 0.177 | 11 | sim | 1.5 | 1.0 | 5 | 0.150 |
| 3 | exp | 0.5 | 0.6 | 50 | 0.171 | 12 | sim | 2.0 | 1.0 | 5 | 0.151 |
| 4 | exp | 0.5 | 0.7 | 50 | 0.177 | 13 | sim | 2.0 | 1.5 | 5 | 0.151 |
| 5 | exp | 0.75 | 0.6 | 50 | 0.169 | 14 | sim | 1.0 | 1.0 | 10 | 0.183 |
| 6 | exp | 0.75 | 0.7 | 50 | 0.171 | 15 | sim | 1.5 | 1.0 | 10 | 0.171 |
| 7 | sim | 1.0 | 0.6 | 50 | 0.176 | 16 | sim | 2.0 | 1.0 | 10 | 0.171 |
| 8 | sim | 2.0 | 1.5 | 0 | 0.133 | 17 | sim | 2.0 | 1.5 | 10 | 0.171 |
| 9 | sim | 2.0 | 0.75 | 0 | 0.133 | 18 | sim | 2.0 | 1.0 | 15 | 0.176 |

## 4 Conclusions

Through physical experiment and numerical simulation, the mass shedding rate of the water slug in dropshafts with different sizes of end orifice is studied. The three-dimensional CFD model is validated through physical experiments. The results show that the simulation data are in good agreement with the experimental data. When the aperture ratio is greater than 0.3, it has no effect on the slug mass shedding rate. When the aperture ratio is less than 0.3, the slug mass shedding rate increases with the increase of aperture ratio. This study provides an empirical reference for the value of mass shedding rate of water slugs in the dropshaft of deep tunnel drainage systems.

## Reference

[1] J. Cong, S. N. Chan, J. H. W. Lee, Geyser formation by release of entrapped air from horizontal pipe into vertical shaft, J. Hydraul. Eng. 143(9) (2017) 04017039.

[2] O. E. Coronado-Hernandez, V. S. Fuertes-Miquel, P. L. Iglesis-Rey, F. J. Martinez-Solano, Rigid water column model for simulating the emptying process in a pipeline using pressurized air, J. Hydraul. Eng. 144(4) (2018) 06018004.

[3] Q. Hou, S. Li, A. S. Tijsseling, J. Laanearu, Discussion of rigid water column model for simulating the emptying process in a pipeline using pressurized air, J. Hydraul. Eng. 146(3) (2020) 07020001.

[4] H. Fan, Q. Hou, A. S. Tijsseling, X. Sun, J. Lian. Mass shedding rate of an isolated high-speed slug propagating in a pipeline, Eng. Appl. Comp. Fluid. 18(1) (2024) 2303372.

[5] J.L. He, Q. Hou, X. Yang, H.F. Duan, L. Lin. Isolated slug traveling in a voided line and impacting at an end orifice. Phys. Fluids 36 (2024) 027105.

**Theme:** Big-data, knowledge, and water data management
**IAHR Thematic Priority Area:** [TPA-4] Digital Transformation
https://doi.org/10.3850/iahr-hic2483430201-416

# Research on the Mechanism of Water-Air Coupling in Plunging Dropshafts

**Jiachun Liu[1], Biao Huang, David Z. Zhu**

*School of Civil & Environmental Engineering and Geography Science, Ningbo University, Ningbo, Zhejiang, China*

*Corresponding author:* liujiachun@nbu.edu.cn.

**Abstract.** A dropshaft is a critical component in urban deep tunnel systems, designed to channel surface runoff downward effectively. A physical model study was conducted on jet impingement in a plunging dropshaft with different drop heights of 3.38 m and 1.88 m. Horizontal jets impinging on the shaft wall and falling jets impinging on the pool were investigated, and it was found that the impingement pressure on the shaft wall was dominated by the incoming flow rate, and that the average pressure on the shaft wall could be reasonably predicted, taking into account the rebound flow. The impinging pressure at the bottom of the shaft depends mainly on the velocity of the falling jet reaching the pool. The average value can be well estimated using the annular flow and bouncing jet assumptions.

**Keywords:** dropshaft; deep tunnel systems; rebound flow; impinging pressure

## 1 Methodology

A plunging flow dropshaft model was built. The vertical dropshaft was composed of plexiglass pipes of diameter $D_s$ = 0.36 m, connected with a horizontal approaching pipe of diameter $D_1$ = 0.26 m and length $L_1$ = 3.0 m, and a downstream outlet pipe of diameter $D_2$ = 0.36 m and length $L_2$ = 2.5 m. There was a 0.1 m diameter air vent at the top and a plunging pool with 0.1 m depth at the bottom of the dropshaft. A jet gate was used to control the approaching flow depth $h_0$, and no air was brought in. The downstream flow was directed to a chamber connected with a 0.3 m diameter downspout and an air vent of a diameter of 0.1 m.

### 1.1 Horizontal impingement on the shaft wall

The maximum impinging pressure on the shaft wall is about 1.4-3.8 times the mean value, which can be partly attributed to turbulence and air-water interactions. In addition, negative pressures exist near the impinging area due to airflow induced by drag, which results in alternating positive and negative pressure distribution that may cause safety concerns.

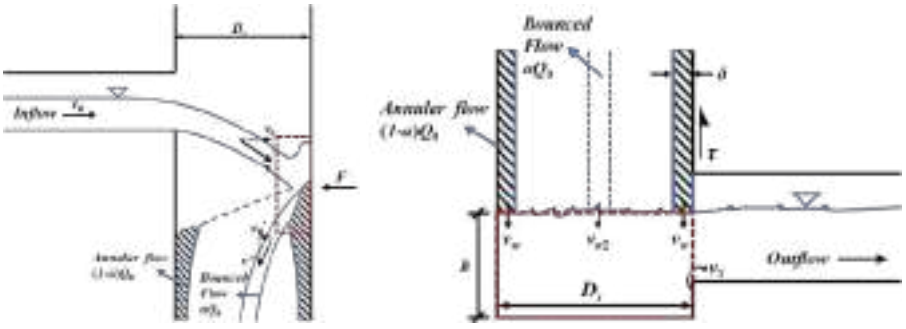


Figure 1 Jet impingement in the dropshaft: (a) horizontal jet impact on the shaft wall; (b) falling jet impact on the plunging pool

### 1.2 Plunging impingement on the shaft bottom

The impinging pressure on the shaft bottom is mainly determined by the velocity of the falling jet when it reaches the pool, which is associated with the water flow rate and the drop height. If the terminal flow velocity is not reached, the jet velocity increases with the increase of the flow rate and the drop height; whereas if the terminal flow velocity is reached, the jet velocity increases with the increase of the drop height. The estimation by assuming annular flow and bounced jet compares well with experimental results, indicating that the simplified model can be used to evaluate the impinging pressure at the shaft bottom to determine whether it is necessary to take structural safety protection measures.

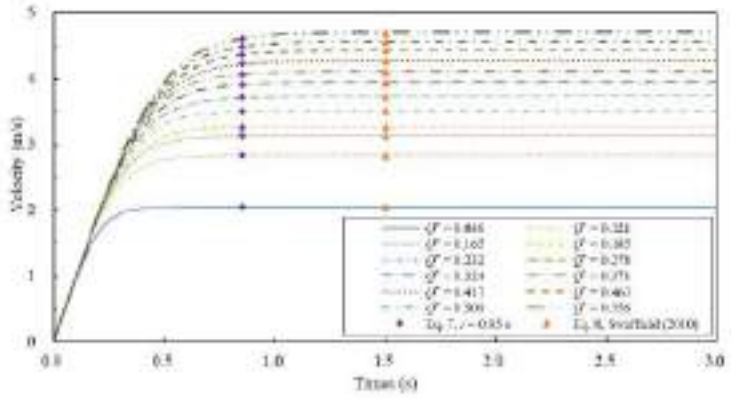

Figure 2 Calculated velocities of the falling annular flow at different flow rates

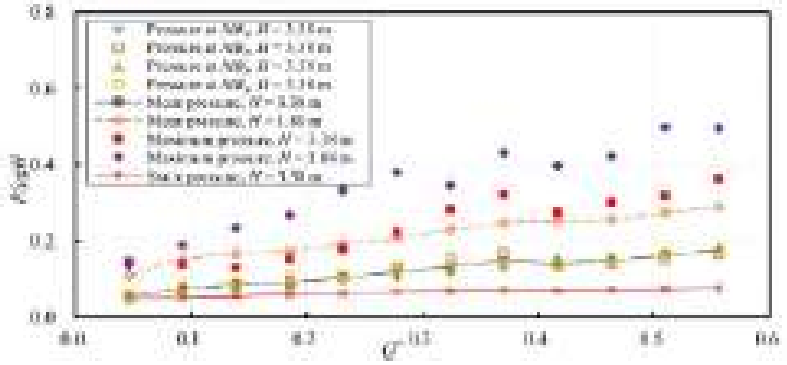

Figure 3 Measured pressure with different drop height

## 2 Conclusions

The impinging pressure on the shaft wall was mainly dominated by the incoming flow velocity, and the mean pressure on the shaft wall can be reasonably well predicted when considering the bounced flow. The impinging pressure at the shaft bottom was primarily determined by the velocity at which the falling jet reached the pool. The mean value can be well estimated using the annular flow and bounced jet assumption. The pulsation intensity increased with an increase in drop height or flow rate, which could be alleviated by a plunging pool with a larger depth.

## Reference

[1] Adriana Camino, G., Zhu, D. Z., and Rajaratnam, N. (2015). “Flow observations in tall plunging flow dropshafts.” J. Hydraul. Eng., 141(1), 06014020.

[2] Ma, Y., Zhu, D. Z., and Rajaratnam, N. (2016). “Air entrainment in a tall plunging flow dropshaft.” J. Hydraul. Eng., 142(10), 04016038.

[3] Rajaratnam, N., Mainali, A., and Hsung, C. Y. (1997). “Observations on flow in vertical dropshafts in urban drainage systems.” J. Environ. Eng., 123(5), 486-491.

**Theme:** Big-data, knowledge, and water data management
**IAHR Thematic Priority Area:** [TPA-4] Digital Transformation
https://doi.org/10.3850/iahr-hic2483430201-418

# Smart Monitoring in Deep Tunnels for Urban Drainage

**Biao Huang[1], Jiachun Liu[1], David Z. Zhu[1,2]**

[1] Institute of Hydraulics and Ocean Engineering, Ningbo University, Ningbo 315211, China
[2] Department of Civil and Environmental Engineering, University of Alberta, Edmonton T6G 2H5, Canada

*Corresponding author: huangbiao@nbu.edu.cn*

**Abstract.** Deep tunnel drainage systems are effective for managing stormwater and preventing flooding, particularly in densely populated areas. This study introduces a novel smart monitoring approach that enhances the operation of such underground systems. Utilizing real-time data on water levels and discharges, the analysis facilitates the early identification and diagnosis of operational anomalies within the deep tunnels. The method integrates fundamental hydraulic principles to analyze the hydraulic performance and sediment deposition. A series of controlled experiments were conducted to validate the effectiveness of the smart monitoring technology. Results indicate substantial improvements in the detection of abnormal flow conditions when compared to conventional methods. The implementation of this smart monitoring approach not only provides early warnings but also significantly boosts the resilience of urban drainage infrastructures.

**Keywords:** deep tunnel; drainage performance graph; smart monitoring; sediment deposition; urban drainage

## 1 Introduction

Smart monitoring refers to the integration of advanced technologies and data-driven approaches into the management and operation of engineering systems. For deep tunnel drainage systems, it aims to improve the efficiency, sustainability, and resilience in the face of challenges such as climate change and urbanization. The primary goal is to manage stormwater and wastewater effectively while minimizing flooding, pollution, and environmental impacts. Smart monitoring has become one of the most efficacious techniques for sewer management, enabling real-time status of the system to be ascertained. This technique typically involves the utilization of flow rate and water level sensors to measure the quantity of water that flows through the sewer system (Bertrand-Krajewski et al., 2021). The data collected can then be analyzed and used to identify any potential problems or areas of concern in the system. The unexpected changes in the system that may be indicative of a problem can be forewarned, thus costly emergency issues can be avoided.

Basic hydraulics play a crucial role in the context of smart urban drainage systems, of which the knowledge is essential to interpret the monitoring data and develop accurate models that predict how the drainage system will respond under different conditions (Yang et al. 2024). For quasi-steady flow in deep tunnels, the relationship between discharge and water level can be easily estimated as a drainage performance graph (DPG). This study delves into the utilization of the DPG technique in conjunction with flow monitoring data. Laboratory experiments were executed within a sewer test rig system, introducing sediment depositions characterized by varying spatial distributions across an array of flow rates and outlet controls. The findings reveal a notable uniformity in the energy losses induced by comparable sediment accumulations at distinct locations. A curve-fitting approach was employed to quantitatively assess the deposition height within the pipe.

## 2 Drainage Performance Graph

For steady gradually varied flow, the relationship between the discharge and the upstream and downstream water levels is non-linear, which can be described by the backwater differential equation.

A unique discharge corresponds to each specific combination of downstream and upstream depths (Yen and Gonzalez-Castro 1994). Identification of a single upstream water elevation within the transition range can be made feasible by incorporating pressurized flow into the DPG (Zimmer et al. 2013).

For a deep tunnel with sediment bed, it essentially transforms the circular cross-section of the pipe into a specific one, altering the original roughness. Drainage performance graphs can be constructed. When combined with monitored flow data, curve fitting techniques can be employed to determine the bed height.

## 3 Results and Discussion

A laboratory study was conducted to investigate the hydraulic characteristics of sewer flow in the presence of various sediment depositions. Investigations primarily focused on continuous deposition and localized deposits, considering different flow rates, deposition heights, lengths, locations, and outlet controls. DPGs were constructed for sewers with sediment beds. When combined with monitored flow data, curve fitting techniques were employed to determine the bed height, a method that was validated in the present study. For cases of localized deposits, this approach also permits the construction of DPGs, although the diagnostic analysis requires monitoring data that meet specific requirements.

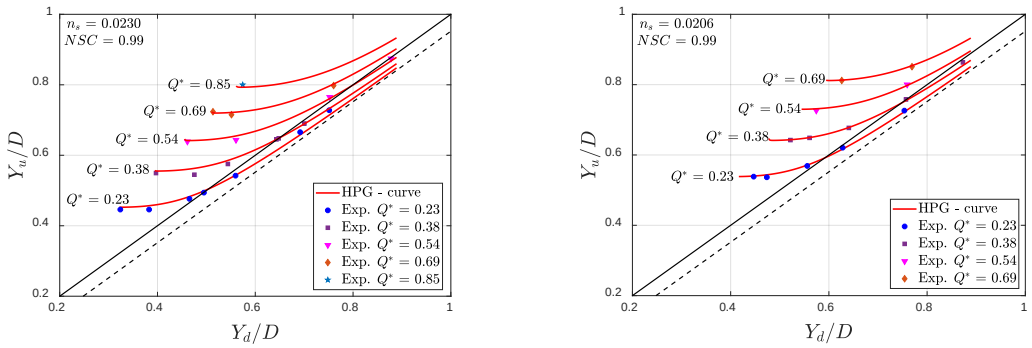


Figure 1 Diagnosis of sediment bed height based on DPG: (a) $h/D$ = 0.11; (b) $h/D$ = 0.22.

The performance of the prediction method was evaluated under laboratory-controlled conditions, with results shown in Fig. 1. The DPG proved successful in delineating the correlation between discharge and the water levels both upstream and downstream across varying conditions of bed deposition. Specifically, with multiple assumptions, for a bed height of $h$ = 20.0 mm, the method achieved a near-perfect Nash-Sutcliffe coefficient (NSC) of 0.99, indicating a strong goodness of fit, as seen in Fig. 1a. The analysis for a bed height of $h$ = 40.0 mm also yielded a highly satisfactory NSC of 0.99, as illustrated in Fig. 1b.

## Final Remarks

The proposed DPG method, when integrated with online monitoring, can be used to detect operational abnormalities in urban deep drainage tunnels. Future research may focus on managing sediment accumulation through smart monitoring techniques.

## References

[1] Bertrand-Krajewski, J. L., Clemens-Meyer, F., & Lepot, M. (2021). Metrology in urban drainage and stormwater management: Plug and pray. IWA Publishing.

[2] Yen, B. C., & Gonzalez-Castro, J. A. (1994). Determination of Boneyard Creek flow capacity by hydraulic performance graph. WRC Research Report No. 219, Univ. of Illinois, Urbana, IL.

[3] Zimmer, A., Schmidt, A., Ostfeld, A., & Minsker, B. (2013). New method for the offline solution of pressurized and supercritical flows. Journal of Hydraulic Engineering, 139(9), 935-948.

[4] Yang, Z., Huang, B., & Zhu, D. Z. (2024). Flow in Sewers with Bottom Obstacles. Journal of Hydraulic Engineering, 150(4): 04024011.

**Theme:** Environmental, Marine and Coastal Hydroinformatic
**IAHR Thematic Priority Area:** [TPA-2] Water for the Energy Transition Food Security and Nature
https://doi.org/10.3850/iahr-hic2483430201-420

# The Response Pattern of the Bed Volume of the Yangtze Estuary Southern Branch to the Reduction of Sediment Inflow

**JIAO Jian[1], DING Lei[1], DOU Xiping[1], YANG Xiaoyu[1], WANG Yifei[1]**

[1] Nanjing Hydraulic Research Institute, Port and Navigation Channel Sediment Transport Lab., MOT, Nanjing 210029, China

*Corresponding author: jjiao@nhri.cn*

**Abstract.** In recent years, the sediment load in the middle and lower reaches of the Yangtze River decrease continuously. Its effect on river bed erosion has gradually been reflected in the Yangtze Estuary. However, there is a lack of quantitative research on the variation characteristics of riverbed volume in the Yangtze Estuary. Furthermore, the spatiotemporal response to the decrease in sediment load is not clear. The discharge and sediment concentration of Datong Station and Xuliujing Station of the Yangtze River are analyzed. The time-dependent characteristics of river bed volume under different elevations were analyzed. The relationship between riverbed volume at different elevations and upstream sediment discharge was established. The results show that the annual sediment transport volume of Datong Station from 2003 to 2020 is significantly reduced compared to the period before the completion of the Three Gorges Project, which has a direct and significant impact on the sediment concentration of the Xuliujing Station during the flood season. The riverbed below 0m in the South Branch of the Yangtze Estuary is in a state of scouring and the riverbed scour rate has increased significantly after 2003. Among them, the erosion of the deep groove below -10m contributes the most. The riverbed volume of the main ebb channel in the South Branch has a significant correlation with the average incoming sediment volume of Datong in the previous year. Therefore, the decrease in sediment flux mainly caused the increase in the volume of the ebb channel bed in the Yangtze Estuary. Furthermore, the effect has a hysteresis of about one year.

**Keywords:** Discharge and Sediment Load Changes, Hysteresis, River Bed Volume, Response Law, South Branch of the Yangtze Estuary

## 1 Introduction

The Yangtze Estuary, as China's largest estuary, plays a crucial role in the sediment dynamics and morphological adjustments of the estuarine section. The reduction in sediment inflow from upstream, due to soil and water conservation efforts, reservoir regulation, increased water usage, and climate change, has led to a significant impact on the estuarine projects and the ecological environment. This study focuses on the Southern Branch of the Yangtze Estuary, which is less affected by engineering activities, to understand the response pattern of the bed volume to the reduction in sediment inflow.

## 2 Study Area

The Southern Branch stretches from Xuliujing to Wusongkou, with a length of 70.5 km. It is divided into upper and lower sections by Qiyakou, with the upper section being a bifurcated river type and the lower section a multi-channel river type. The study area includes 12 different periods of underwater cross-sections from 1978 to 2018 (Fig.1 ).

## 3 Analysis of Sediment Discharge Changes Upstream

Datong Station, the last permanent hydrological station on the main stream of the Yangtze River, shows a clear three-stage change in sediment discharge since the completion of the Three Gorges Project in 2003. The sediment discharge has significantly decreased, with an average annual sediment

discharge of 132 million tons from 2003 to 2020. The sediment concentration at Xuliujing Station also shows a clear response relationship with the sediment discharge at Datong Station, with a significant decrease in sediment concentration during the flood season post-2003.

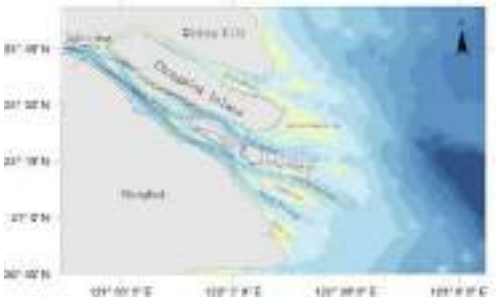

Figure 66 Study area and section layout diagram

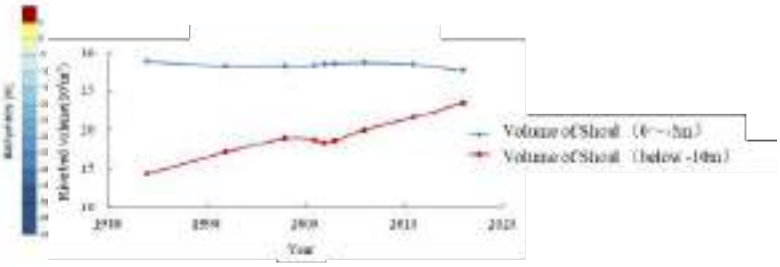

Figure 67 Volume of shoals and channels

## 4 Analysis of Riverbed Volume Changes in the South Branch of the Yangtze Estuary

The riverbed volume below 0m from Xuliujing to Zhongyang Shoal section was statistically analyzed, showing an overall state of scouring from 1984 to 2016. The volume increased by approximately 10 billion cubic meters over 22 years, with a significant increase observed after 2003. The volume change trend of shoals (0 to -5m) was significantly different from that of deep channels (below -10m), with the latter showing a clear increasing trend(Fig.2 ).

## 5 Spatial and Temporal Response Relationship of Riverbed Volume to Sediment Load Changes

The study establishes the relationship between the sediment load of Datong Station and the changes in riverbed volume of the South Branch river section. A clear correlation was found between the sediment load and the riverbed volume, with the best correlation observed with the average sediment discharge of Datong Station in the previous year (Fig.3 ). This indicates that the impact of sediment load reduction on the riverbed volume has a hysteresis of about one year.

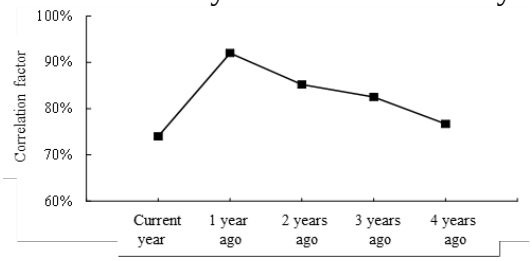


Figure 68 Trend of sediment load relationship in the past 5 years

## 6 Conclusion

The study provides a comprehensive analysis of the response pattern of the bed volume of the Southern Branch of the Yangtze Estuary to the reduction in sediment inflow. The results highlight the significant increase in the scouring rate of the riverbed below 0m post-2003, with the main ebb channels being the most affected. The findings are crucial for understanding the sediment dynamics in the Yangtze Estuary and for the management of estuarine projects.

## Reference

[1] Syvitski J P M, Vorosmarty C J, Kettner A J, et al. Impact of humans on the flux of terrestrial sediment to the global coastal ocean[J]. Science, 2005, 308: 376-380.

[2] ZHAO Yifei., ZOU Xiqing, LIU Qing, et al. Assessing natural and anthropogenic influences on water discharge and sediment load in the Yangtze River, China[J]. Science of The Total Environment, 2017: 607-608.

[3] DOU Xiping, JIAO Jian, CHU Ao, et al. Review of hydro-sediment change and tendency in Yangtze estuary[J]. The Ocean Engineering, 2020,38(4):2-10. (in Chinese)

**Theme:** Environmental, Marine and Coastal Hydroinformatic
**IAHR Thematic Priority Area:** [TPA-2] Water for the Energy Transition Food Security and Nature
https://doi.org/10.3850/iahr-hic2483430201-422

# Development about Engineering Solution of Integrated Real-time Observation Systems for Coastal Erosion Management[1]

**Pengfei Liu[1,2], Changyi Yang[1,2] , Yusheng Zhuo[1,2] , Baojiang Zhou[1,2] , Runjie Miao[1,2]**

CCCC First Harbor Consultants Co Ltd., Tianjin 300222, China
Tianjin Municipal Key Laboratory of Geotechnics and Structure of Coastal and Offshore Engineering, Tianjin 300222, China

*Changyi Yang: yangchangyi@ccccltd.cn*

**Abstract.** Coastal erosion presents a dynamic and complex challenge, necessitating advanced monitoring and management strategies. This paper research advancements in engineering solution of Integrated Real-time Observation Systems (IROS), focusing on their application in coastal erosion prediction and protection. IROS are adept at collecting, processing, and analyzing multifaceted data from nearshore environments, including tidal levels, currents, wave dynamics, sediment transport, meteorological conditions, and topographical changes. Integrating diverse data sets can enhance the accuracy of coastal erosion predictions, providing a solid scientific basis for decision-making in coastal management.

## 1 Background

The currently widely applied integrated marine observation systems primarily focus on the oceans and large marine areas [1]. However, among these observation methods, the locations for field observations are mostly far from the coast, and satellite remote sensing data are limited by resolution. On the other hand, results obtained from remote sensing also need to be verified through ground truth measurements.

For specific engineering applications related to coastal protection, the focus is mainly on localized coastal sections, characterized by relatively smaller scales. In such engineering projects, there is a need for more cost-effective, broad-applicable, and observationally rich field methods combined with open-source data. Thus, integrated observation systems usually rely mainly on field observations, supplemented by satellite remote sensing.

## 2 Integrated Observation Systems for Coastal Protection

### 2.1 Existing observation methods

Core observation contents for coastal protection include but are not limited to the following aspects: tidal levels, currents, sediment, waves, topography, and seabed sediments. In field observations or remote sensing, it is common to integrate multiple observation objectives into a single platform, vessel, or satellite for simultaneous measurement.

### 2.2 Integrated real-time observation methods.

In engineering applications, the main characteristics is focus on smaller-scale coastal erosion, meanwhile, relatively high requirements for the accuracy of measurement data. Based on the existing observation methods, a combination of field measurements and open data observation systems can be used, which is IROS, with open-source data from satellite or buoy far offshore, and field measurements for areas of engineering interest. The field measurement combines buoy and

*Funding: This work was supported by the Tianjin Municipal Transportation Science and Technology Project: Research on Key Technologies for Coastal Smart Channel (2024-A03)*

underwater observations station, specifically, the buoy could provide power support for underwater sensors while receiving the data collected from the seabed, which is then transmitted from the buoy.

## 3 Data processing and Real-time Mathematical Models

### 3.1 Data Processing and Integration.

Quality control: Initial data quality check, including identifying and correcting errors, removing outliers, and filling in missing values to ensure data accuracy and reliability.
Calibration and validation: Standardized methods and tools are used for data calibration to ensure comparability across different sources and times.
Formatting: Data is converted into a uniform format for storage, sharing, and analysis.
Data fusion: Data from different sources is combined, using models and algorithms to address inconsistencies among the data. For example, combining satellite data with buoy data to provide more comprehensive monitoring of the marine environment.

### 3.2 Real-time Mathematical Models

Common hydrodynamic mathematical models are based on the Saint-Venant equations, while wave models mostly used the SWAN model, which based on wave equations and spectral methods. Ideally, if all observational results are to be applied for model validation, it would be best to couple multiple models during the computation process, which requires high-performance computing and considerable time to obtain results. The SED model [2], which utilizes sediment dynamics principles for material transport, can be applied to simulate the deposition of suspended sediments.
After calibrating the numerical model with on-site measurement data, subsequent real-time data is also used to correct deviations in the model's predictions. The main indicators are tidal levels, currents, and waves. At the same time, the results of the terrain observed by the ship-based survey are used to verify the indicators of sediment erosion and deposition. In the engineering sea area, when there are other abnormal conditions, such as construction, typhoons, storm surges, etc., the frequency of observations and model verification indicators are increased.
Based on real-time observation data, mathematical models can be continuously validated to approximate actual measurements, thus obtaining an integrated real-time data model for analysing and studying coastal protection trends. The application of these technologies enables IROS to provide strong technical support for predicting and protecting against coastal erosion, offering a reliable decision-making foundation for coastal management.

## 3 Summary

In summary, the application of IROS in coastal erosion management demonstrates its powerful capability in collecting, processing, and analysing various aspects of coastal environmental data. Based on the results of the multi-index coupled model, it is possible to gain a clearer understanding of the characteristics of sediment erosion and deposition changes and the dynamic factors in the engineering sea area. By integrating existing technologies and applying new ones, it significantly improves the accuracy of predicting coastal erosion trends and rates, provides scientific evidence for coastal management decisions, and thus promotes the protection and sustainable management of coastal environments.

## Reference

[1] Révelard, A., Tintoré, J., Verron, J., Bahurel, P., Barth, J. A., Belbéoch, M., Benveniste, J., Bonnefond, P. (2022). Ocean Integration: The Needs and Challenges of Effective Coordination Within the Ocean Observing System. Frontiers in Marine Science, 8, Article 737671.
[2] Zhu, F., Chen, L., & Qin, J. (2024). Study on Sediment Transport Characteristics under Wave-Current Coupling in Qinzhou Bay. Port, Waterway and Offshore Engineering, (01), 8-12+19. https://doi.org/10.16403/j.cnki.ggjs20240102

**Theme:** Environmental, Marine and Coastal Hydroinformatic
**IAHR Thematic Priority Area:** [TPA-2] Water for the Energy Transition Food Security and Nature
https://doi.org/10.3850/iahr-hic2483430201-424

# Fuzzy Uncertainty Analysis of Coastal Aquifer Under Seawater Intrusion

**Mohammadali Geranmehr[1], Domenico Bau[2]**

[1,2] Department of Civil and Structural Engineering, University of Sheffield, Sheffield, S1 3JD, UK

*Corresponding author: mgeranmehr@gmail.com*

**Abstract.** The coastal aquifer system is highly susceptible to seawater intrusion, and numerical simulation of this phenomenon is a reliable approach for sustainable management. This paper presents a fuzzy uncertainty analysis of the Henry Problem, a well-known benchmark case for studying saltwater intrusion in coastal aquifers. Fuzzy functions are employed to capture the inherent uncertainty associated with input parameters, and the uncertainty in saltwater intrusion is calculated, using a simulation-optimisation tool. The optimization tool will calculate the minimum and maximum possible values of total saltwater, considering uncertain input parameters. The preliminary results for Henry's problem show that small uncertainties in input parameters could significantly affect seawater intrusion.

**Keywords:** Coastal aquifer, fuzzy theory, optimisation, seawater intrusion, simulation, uncertainty

## 1 Introduction

Seawater intrusion simulation is typically based on solving two coupled partial differential equations, including density-dependent flow and solute-transport. Lack of field data which yields a weak calibration model, as well as inherent uncertainty in some values will provide unsure results. Uncertainty analysis of the seawater intrusion model is a helpful tool to determine the effect of uncertainty on input parameters to output values [1,2,3]. Fuzzy set theory is a powerful tool to handle uncertainty in different systems, especially when there is no historical data [4]. In this study, a fuzzy uncertainty analysis model is presented for simulating seawater intrusion in coastal aquifers. The proposed model is based on using an optimization algorithm to find the system's maximum and minimum possible values for output parameters. The decision variables are the system's input parameters, and the constraints are the minimum and maximum possible values for decision variables.

## 2 Henry's Problem

The Henry problem is a well-known model in groundwater science that simplifies how saltwater can intrude into coastal aquifers. It's named after Henry, who proposed it in 1964. The model imagines a vertical slice of land by the coast with a specific type of soil and water movement. Herein, the standard settings for the model's variables are based on literature [5].

## 3 Methodology

The fuzzy uncertainty analysis of seawater intrusion in Henry's problem is briefly as follows:

- Define fuzzy functions for uncertain input parameters.
- Select α-cut between zero and one.
- Use a simulation-optimization model two times to minimize and maximize the total dissolved mass (TDM) of salt in the aquifer.

As depicted in Figure 1, porosity, molecular diffusion, hydraulic conductivity, inflow, and seawater concentration, are five uncertain parameters. Based on the original Henry's problem, the crisp values of these parameters are respectively equal to 0.35, 0.57024 ($m^2$/day), 864 (m/day), 5.702 ($m^3$/day/m),

and 35 (kg/m$^3$). The simulation model is SEAWAT, and the optimization is based on using an off-the-shelf Genetic Algorithm.

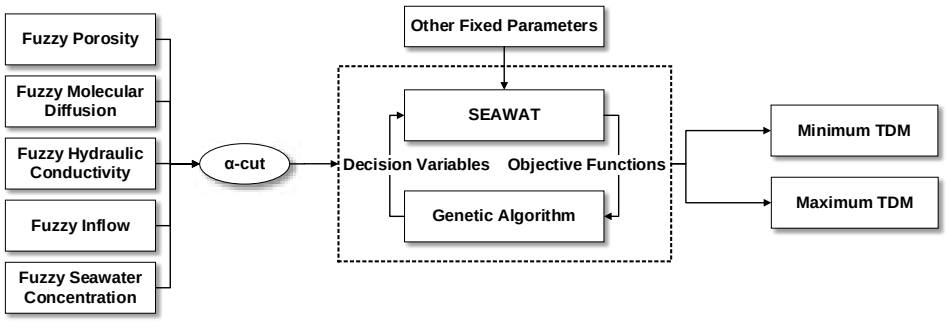


Figure 1. Flowchart for uncertainty analysis

## 4 Results and Discussion

The concentration values for two different uncertainty analysis models of Henry's problem are presented in Figures 2a and 2b for 10% and 20% uncertainty in input parameters. In this study, the alpha-cut is considered equal to one. Results show that ±5% and ±10% uncertainty could affect the TDM to the range of -10.6% to 11.4% and, -20.6% to 23.5% respectively. This means that only small uncertainties in input parameters could result in significant uncertainty in saltwater intrusion.

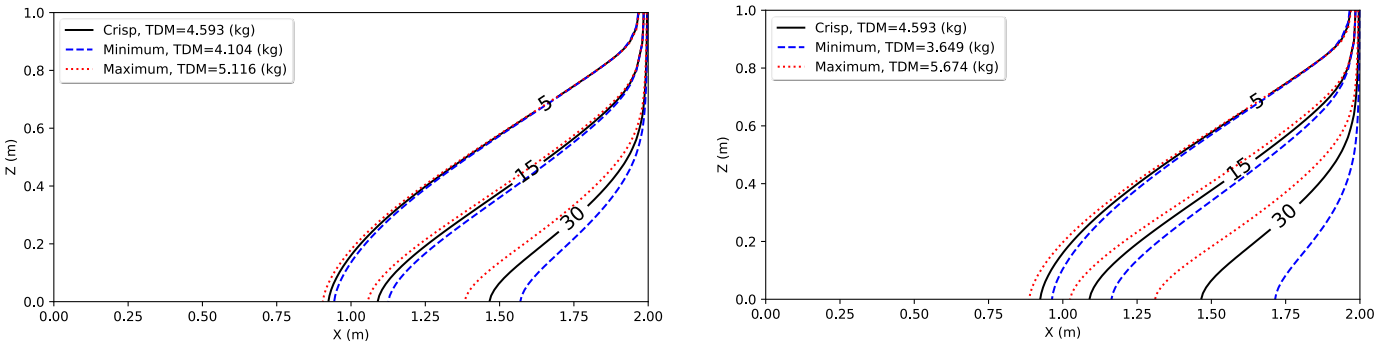


(a) (b)

Figure 2. Uncertainty analysis results for Henry's problem, a) 5% uncertainty and b) 10% uncertainty

## 5 Conclusion

A fuzzy-based uncertainty analysis model for seawater intrusion simulation is presented in this study. The proposed model uses an optimisation tool to find the minimum and maximum possible output values based on uncertainty in input parameters. The application of the model investigated Henry's problem, which shows that even minor uncertainties in input parameters could lead to considerable uncertainty in saltwater intrusion. This study will expand to complex and real-world case studies to explore the effect of uncertainty on seawater intrusion.

## Reference

[1] M. Rajabi, and B. Ataie-Ashtiani, Sampling efficiency in Monte Carlo based uncertainty propagation strategies: Application in seawater intrusion simulations. Advances in Water Resources, 2014. 67: p.46-64.
[2] M. Riva, A. Guadagnini, and A. Dell'Oca, Probabilistic assessment of seawater intrusion under multiple sources of uncertainty. Advances in Water Resources, 2015. 75: p. 93-104.
[3] B., Koohbor, Uncertainty analysis for seawater intrusion in fractured coastal aquifers: Effects of fracture location, aperture, density and hydrodynamic parameters. Journal of Hydrology, 2019. 571: p. 159-177.
[4] M. Geranmehr, K. Asghari, and M.R. Chamani, Uncertainty analysis of water distribution networks using type-2 fuzzy sets and parallel genetic algorithm. Urban Water Journal, 2019. 16(3): p.193-204.
[5] W. Guo, and C.D. Langevin, User's guide to SEAWAT; a computer program for simulation of three-dimensional variable-density ground-water flow, in Open-File Report. 2002.

**Theme:** Environmental, Marine and Coastal Hydroinformatic
**IAHR Thematic Priority Area:** [TPA-2] Water for the Energy Transition Food Security and Nature
https://doi.org/10.3850/iahr-hic2483430201-426

# Mechanisms Underlying the Formation of Parallel Tidal Channels in Estuarine and Coastal Areas

**Zeng Zhou**[1]

[1] Jiangsu Key Laboratory of Coastal Ocean Resources Development and Environment Security, Hohai University, Nanjing 210024, China

*Corresponding author: zeng.zhou@hhu.edu.cn*

**Abstract.** Tidal channel systems arising from morphodynamic interactions exhibit a suite of diverse morphological configurations. A prevalent type is represented by linear dendritic channels formed by single-thread streams aligned roughly parallel or subparallel to each other in the cross-shore direction. We conducted an analysis of more than 200 parallel tidal channels from different locations worldwide and found that the angle between individual parallel branches and the parent stream, from which they develop, largely falls within the range of 80-100º. We employed numerical modeling to shed light on the underlying mechanisms governing their formation, revealing that alongshore uniformity in bed topography and the strength of tidal currents condition the alignment of parallel channels. Straight and shore-normal parallel branches tend to form where the bed profile changes sharply around the mean sea level, while linearly sloping profiles lead to oblique parallel branches.

**Keywords:** morphodynamic modeling, parallel tidal channels, tidal flats

## 1 Introduction

Tidal channels are prevalent and distinct geomorphological features present in estuarine and coastal environments[1]. They are found across a wide range of scales, spanning from small mudflat runnels and marsh creeks to larger estuarine and deltaic distributary channels. Understanding the mechanisms underlying tidal channel formation and evolution is crucial for comprehending the overall functioning of tidal ecosystems and managing their conservation effectively, as they provide the physical ground for a number of vital ecomorphodynamic processes, including tide propagation, sediment transport, nutrient exchange, and habitat provision[2].

Worldwide, tidal channel systems exhibit various planform morphologies, including dendritic, distributary, braided, interconnected, and parallel channels[3]. Among these, complex dendritic channel network systems have been extensively studied, with a focus on their remarkable tree-like morphology and associated scaling properties. In contrast, parallel channel systems that are prevalent in many coastal and estuarine environments worldwide, have received comparably little attention. Compared to complex branching and meandering tidal channel systems, we observe that the geomorphology of parallel channel systems differs notably in several aspects. First and foremost, these systems commonly develop on open-coast tidal flats or along the flanks of major tidal channels, with individual branches being similar in size and nearly parallel to each other. Second, the dimensions of individual parallel branches, including width, length, and depth, are significantly smaller than those of the parent channel from which they originate. This study aims to gain deeper understanding on the processes driving the formation of these parallel channel systems.

## 2 Methods

This study conducted comprehensive morphological analyses of a number of parallel channels selected from sites worldwide, encompassing diverse geomorphological settings, including estuaries, lagoons, and open coasts. Moreover, to gain deeper insights into the physical processes underlying

parallel channel inception, we performed morphodynamic simulations to disentangle the influence of alongshore tidal currents and bed topography.

## 3 Results

The simulation was conducted on an initial bed surface where the upper platform has a slope of 0.08% and the transition point between the upper platform and the lower bank has an elevation of -3m. In Fig.1, $\alpha_C$ and $\beta_C$ are the connecting channel angles and overall channel angles, respectively. $\alpha_F$ and $\beta_F$ are the flow angles measured at the roots and at the middle of the channel branches. Fig. 1 shows that the flood flow angle is smaller than ebb flow angle, and the ebb flow is close to 90°. It indicates that the flood currents provide a stronger contribution on generating channel branches with small angles, while the direction of ebb currents is heavily influenced by gravity, resulting in a more perpendicular trend with the shorelines.

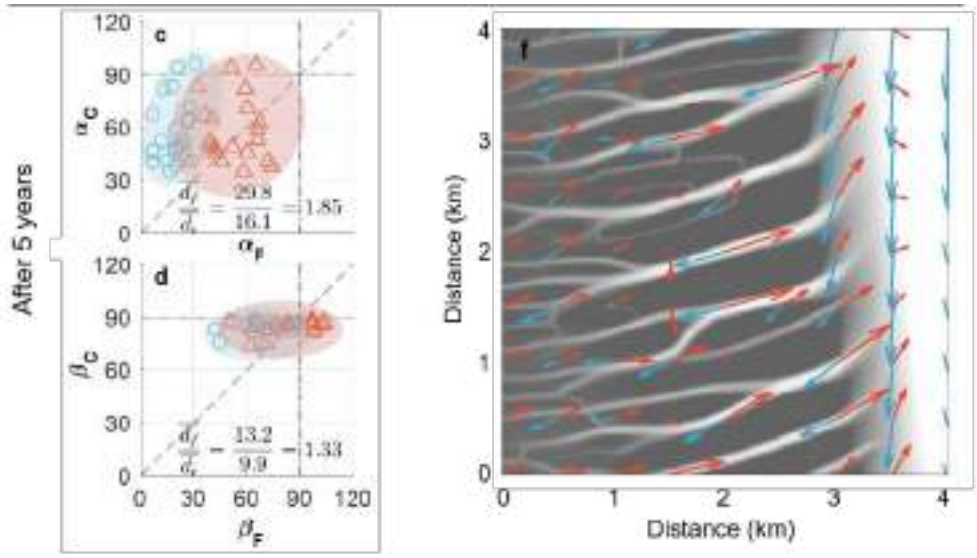


Figure 69 Channel angle and flow direction during flood and ebb phases after 5 years

## 4 Conclusions

We investigate the mechanisms by which alongshore tidal currents generate cross-shore parallel tidal channels. Through analysis of a large number of satellite imagery from coastal regions worldwide, we find that parallel channel branches often intersect shorelines or parent channels at near 90° angles, distinct from typical dendric tidal or fluvial channel networks. Numerical simulations demonstrate that this characteristic channel orientation arises from the abrupt turning of alongshore currents at the interface where a sudden change in bed elevation occurs. Our results bear significant ramifications for the understanding and management of valuable tidal ecosystems.

## Reference

[1] Perillo, G.M.E., Geomorphology of Tidal Courses and Depressions, in Coastal Wetlands: An Integrated Ecosystem Approach, G.M.E. Perillo, et al., Editors. 2019, Elsevier. p. 221-261.
[2] Hughes, Z.J., Tidal Channels on Tidal Flats and Marshes, in Principles of Tidal Sedimentology. 2012. p. 269-300.
[3] Eisma, D., et al., Intertidal deposits: river mouths, tidal flats, and coastal lagoons. 1 ed. 1998: CRC press. 544.

**Theme:** Environmental, Marine and Coastal Hydroinformatic
**IAHR Thematic Priority Area:** [TPA-2] Water for the Energy Transition Food Security and Nature
https://doi.org/10.3850/iahr-hic2483430201-428

# Effects of Offshore Artificial Islands on Beach Evolution Processes, Hongtang Bay, Sanya as an Example

**Wang Yanhong[1], Gao Lu[1,2]**

[1] River and Coastal Engineering Department, Nanjing Hydraulic Research Institute, No. 34 Hujuguan Road, Nanjing, 210013, China
[2] Haikou Marine Center of the Ministry of Natural Resources，No. 79 Qiongshan Avenue, Haikou, 570100, China

*Wang Yanhong: yhwang@nhri.cn*

**Abstract.** Offshore artificial islands are one way to develop and utilize coastal areas. Since the early 1990s, more than 30 artificial islands of various sizes and purposes have been constructed off the coast of China, with most of them located along the sandy shoreline. In most cases, sandy coasts are erosive. The construction of offshore artificial islands also plays a significant role in mitigating coastal erosion. However, the alteration of the wave field due to artificial islands will inevitably impact the erosion and deposition patterns of sandy coasts. Taking the offshore artificial island of Hongtang Bay, Sanya as an example, the paper analyzes the changes in shoreline erosion and deposition before and after the implementation of the artificial island and its dynamic mechanism.

**Keywords:** Artificial Island, Beach Evolution, Coastal Erosion

## 1 Introduction

The Hongtang Bay located on the south end of Hainan Island, China, extends 19 km in length, face to the South China Sea. The bay has different coastal types, including long beaches backed by high dune systems and fronted by beach rocks, and rocky headlands extend no more than 1 km to the sea.An elliptic artificial island covering about 4 $km^2$, extending about 3km alongshore and 2 km cross-shore, was planned to be 0.7~2.6 km from the shore of the bay, with water depth between 9m and 15m, partly constructed between May. 2016 to July 2017.

## 2 Research methods

Based on the measured tidal levels, tidal currents, waves, and sediment data, an analysis of the characteristics of the dynamic sediment environment in the project area is conducted. The satellite remote sensing images from various periods since 1969 and sea charts since 1939 have been collected. The seabed landform maps before and after the construction have been measured. Regular measurements of the fixed beach profiles were conducted before and after the construction of the artificial island from 2016 to 2022. The variations in sedimentation and erosion on the seabed and beach were compared and analyzed to understand the dynamic mechanisms associated with the artificial island project.

## 3 Results

The results indicate that the tidal current is weak in the project area, and wave action is the dominant force in erosion and deposition processes. In the decades before the project, the seabed and the beach remained relatively stable, with very little variation in erosion and deposition. After the implementation of the artificial island located approximately 700 meters offshore, with a water depth ranging between 9 and 11 meters, measuring about 2 km in length and 1 km in width. The shoreline

erosion and deposition have been significantly altered. According to the comparison of water boundary lines in satellite remote sensing images and fixed profile measurements since the construction of the artificial island in 2016, the changes in the shoreline have been primarily concentrated around the artificial island, affecting approximately 6km of shoreline on both sides. These changes include a 2.1 km silting section sheltered by the artificial island, a 2.1 km scouring section on the west side, and a 2.0 km scouring section on the east side of the sheltered section. The average sedimentation range of the silting section is approximately 20 meters towards the sea, with a maximum sedimentation depth of about 40 meters, mainly concentrated in the section above -2 meters, forming a beach berm with an elevation of about 2.5 meters.~3.0 meters. The erosion on the west side retreated by an average of 5 meters. The erosion section, approximately 2.0 km on the eastern side of the sheltered area, has retreated by an average of about 6 m.

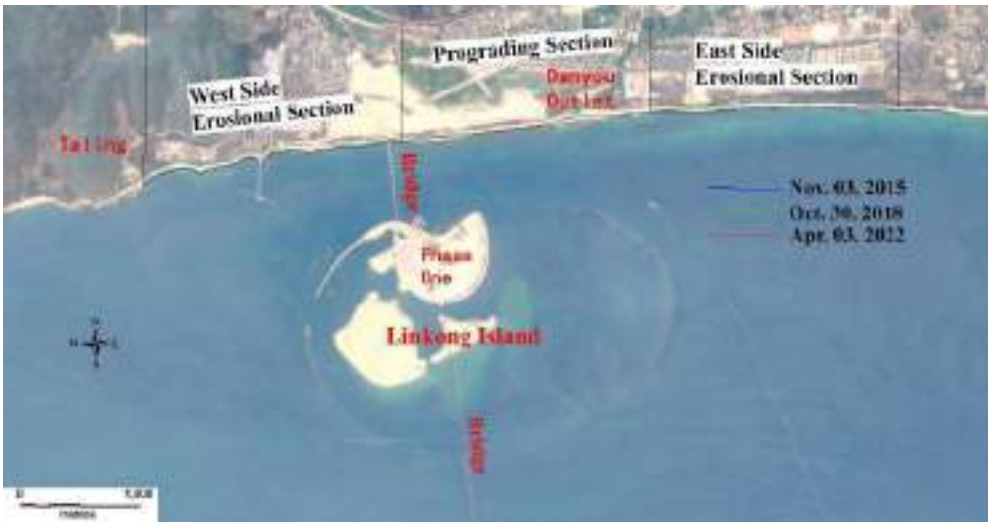


Figure 1 Shoreline change between 2015 and 2022 before and after construction of the island

## 4 Discussion

In the project area, the beach rock has formed a good protective cover for the shoreline, and erosion gradually slows down as the area of beach rock exposure increases. Since the construction of the artificial island, its influence has mainly been within a radius of about 6 km on both sides of the island. After 2019, the erosion and deposition of the beach have noticeably slowed down, and the rate of change in erosion and deposition has been very gradual. The reasons are as follows: First, the beach rocks on the west side of the artificial island cover a fully developed area, enhancing the protection of the beach rocks on the rear beach after beach erosion. This slows down the intensity of further erosion of the beach. Secondly, on the east side of the artificial island shelter area, a sand barrier (groin) with a length of approximately 60 meters was constructed in 2019. This barrier partially intercepts the transport of longshore sand transportation from east to west. With changes in shoreline morphology, the shoreline tends to align more parallel to the normal wave crest line. Consequently, the coastal sand transport capacity decreases gradually, and shoreline adjustment also exhibits a slowing trend over time. Under the influence of the aforementioned factors, shoreline erosion and deposition due to artificial islands in 2019 generally slowed down significantly.

## Reference

[1] He W H, et. Observation report on tidal currents and sediment in Sanya Hongtang Bay[R], South China Sea Institute of Oceanography, Chinese Academy of Sciences, 2016.5

[2] Zhao Hongjun, Song Liqin. Wave Mathematical Model Report in Sanya New Airport Artificial Island[R], Hohai University, 2016.6

**Theme:** Environmental, Marine and Coastal Hydroinformatic
**IAHR Thematic Priority Area:** [TPA-2] Water for the Energy Transition Food Security and Nature
https://doi.org/10.3850/iahr-hic2483430201-430

# CE-QUAL-W2 Hydrodynamic and Water Quality Simulation Capabilities in Support of Water Management

**Zhonglong Zhang**

Department of Civil & Environmental Engineering, Portland State University, Portland, OR, USA

*Email: zz3@pdx.edu*

**Abstract:** CE-QUAL-W2 (referred to as W2 henceforth) is a two-dimensional (2D) longitudinal/vertical hydrodynamic and water quality model. A typical model grid is shown in Figure 1. W2 has undergone continuous development and use since its release in 1986. It has been successfully applied to hundreds of rivers, lakes, and reservoirs in the United States and around the world. W2 is considered the model of choice for various aspects of water quality, water resources management, and reservoir operations. The latest version, 5.0, and previous versions of the W2 model can be freely accessed and downloaded from the PSU and U.S. Army Corps of Engineers websites. The user manuals include the model theory, fundamental equations, and application guidelines. W2 requires multiple inputs to establish boundary conditions (inflow, outflow, point and non-point source flows), meteorological forcing data, and model parameters. A set of pre- and post-processing tools is available and has been used to directly support model setup, calibration, and result visualization.

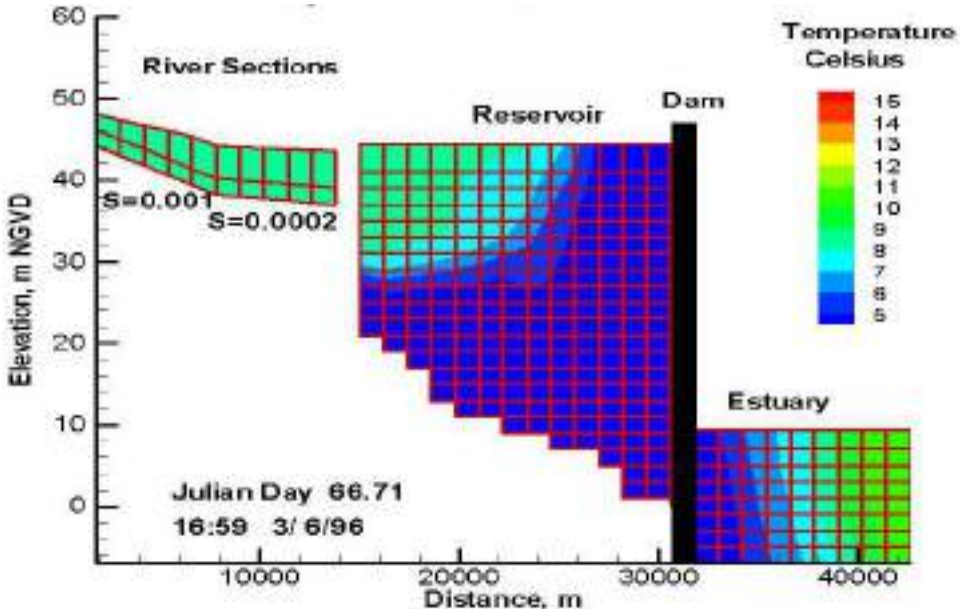


Figure 1. A representation of W2 model computational grid.

The W2 model has the capability to simulate entire river basins comprising rivers and interconnected lakes, reservoirs, and/or estuaries. In W2, the laterally-averaged 2D continuity and momentum equations governing surface water hydrodynamics are solved numerically using finite difference methods. Additionally, the model solves the 2D advection-diffusion equations for water temperature and other water quality constituents at longitudinal segments and vertical layers within water bodies. A prominent feature of the model is its ability to compute the 2D velocity field for surface water systems and generate detailed outputs for flow and water quality constituents at any longitudinal, vertical, and temporal point.

W2 Version 5.0 possesses the capability to forecast water surface, velocity, temperature, and many water quality constituents. The water quality constituents simulated by the model are outlined in Table 1. W2 incorporates zero-order and first-order methods as well as sediment diagenesis simulation to quantify sediment oxygen demand and sediment-water fluxes of nutrients.

Table 1. List of water quality constituents simulated by W2 Version 5.0.

| Water quality constituent | Water quality constituent |
|---|---|
| temperature | alkalinity |
| # of generic constituents (contaminants) | silica species |
| # of inorganic suspended solids | labile dissolved organic matter |
| conservative tracer(s) | (LDOM/LDOC/LDON/LDOP) |
| water age or hydraulic residence time | refractory dissolved organic matter |
| coliform bacteria(s) | (RDOM/RDOC/RDON/RDOP) |
| nitrogen gases | labile particulate organic matter |
| dissolved gas pressure | (LPOM/LPOC/LPON/LPOP) |
| hydrogen sulfide | refractory particulate organic matter |
| sulfate | (RPOM/RPOC/RPON/RPOP) |
| methene | # of phytoplankton groups |
| two Fe species | # of epiphyton/periphyton groups |
| two Mn species | # of CBOD/CBODN/CBODP groups |
| bioavailable phosphorus | # of zooplankton groups |
| ammonium | # of macrophyte groups |
| nitrate-nitrite | four of algae toxins |
| dissolved oxygen | three Hg species for the water column |
| inorganic carbon | two Hg species for the sediment |

W2 is a hydrodynamic and water-quality model recommended by the United States Environmental Protection Agency (EPA) for comprehensive surface water quality studies. It has served as a management tool for conducting thermal and water quality investigations, assessing direct and indirect impacts from various stressors, updating reservoir operation manuals, and supporting environmental impact statement studies. Below are three example applications demonstrating the utilization of W2 Version 5.0.

- Temperature simulations
- Eutrophication and Dissolved Oxygen simulations
- Hg simulations

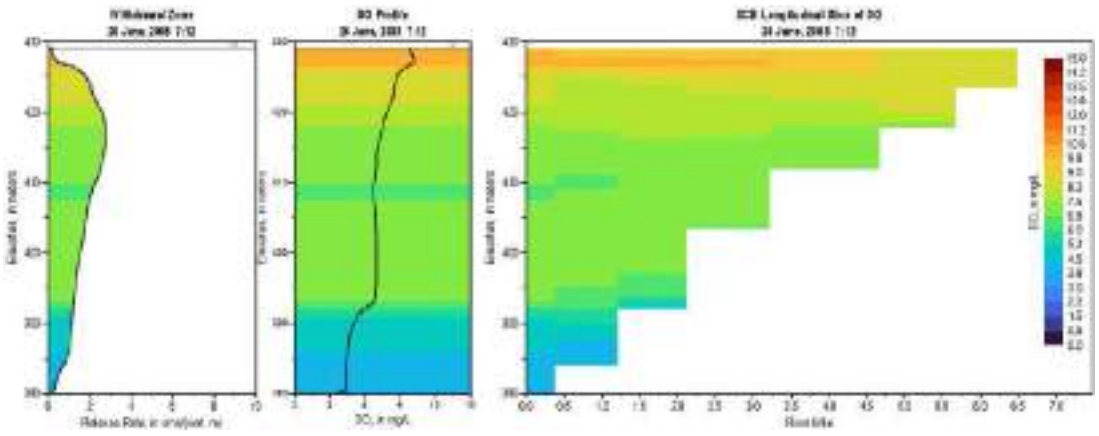

Figure 2. Modeled withdrawal flow, profile, and longitudinal animations of dissolved oxygen.

**Keywords:** CE-QUAL-W2, Modeling, Water management, Water quality

**Theme:** Environmental, Marine and Coastal Hydroinformatic
**IAHR Thematic Priority Area:** [TPA-2] Water for the Energy Transition Food Security and Nature
https://doi.org/10.3850/iahr-hic2483430201-432

# Whether to Treat the Rural Sewage or Not? A Decision-Making Approach by System Dynamics Model and Environmental Capacity

**Xingxiang Zhang [1], Jiping Jiang [2], Xiao Hu [2], Guangshan Zhang [1]**

[1] College of Resource and Environment, Qingdao Engineering Research Center for Rural Environment, Qingdao Agricultural University, Qingdao 266109, PR China
[2] School of Environmental Science and Engineering, Southern University of Science and Technology, Shenzhen, 518055, China

*Corresponding author: Jiping jiang. jiangjp@sustech.edu.cn*

**Abstract.** This study constructed a WRECC-SD coupled model to address the necessity and focal points of sewage treatment in rural areas. The model comprehensively incorporates changes in agriculture, animal husbandry, industrial production, and population dynamics. It calculates the water consumption and wastewater discharge data for these sectors and determines the necessity and focus of rural wastewater management through the ratio of total water demand and water supply capacity, as well as the ratio of total pollutant emissions and environmental capacity. The results of the study found that both the water resources and water environment ratios in Liuyang County are overloaded in 2040, and measures need to be taken to manage the current situation. Among them, agricultural water use, COD emission from farming, and industrial ammonia nitrogen emission can be the focus of treatment. The findings of this study will aid relevant decision-makers in making more precise and comprehensive assessments concerning wastewater management in rural areas.

**Keywords:** Rural wastewater, Governance decisions, Water resources, Water environment, Carrying ratio

## 1 Introduction

China, as the largest developing country in the world, faces significant regional disparities, funding shortages, and technological insufficiencies in sewage treatment efforts in rural areas [1], hindering the progress of sewage treatment in rural China. Currently, most studies focus on selecting sewage treatment technologies rather than addressing the necessity and focus points of governance decisions [2]. In reality, the coverage of sewage treatment facilities in rural China is limited, and progress in this area lags behind that of developed countries. In this context, the benefits of technical optimization at the planning level are relatively small, whereas decision-making on the necessity and focal points of governance at the policy level can help government and other decision-makers quickly and effectively carry out rural sewage treatment work.

## 2 Method

Our developed WRECC-SD model first includes four state variables: population size, agricultural scale, farming scale, and industrial scale. The following figure illustrates the overall analysis process flow of the study. The constructed WRECC-SDM consists of three subsystems and strives to approximate the real-world situation by incorporating data and conditional constraints.

## 3 Results

Under the baseline (BA) scenario, the simulated water carrying ratio for Liuyang County in 2040 is calculated at 1.226. A ratio exceeding 1 indicates that Liuyang County presently grapples with water resource overload, where its indigenous water supply falls short of meeting local developmental demands, necessitating alternative measures to mitigate local water resource

tensions. Examining the proportions of each state variable in water demand (50%), it is apparent that agricultural water usage maintains a high proportion.The carrying ratio of water quality elements comprises two factors: WECR-COD and WECR-$NH_3$-N. The emissions of the two pollutants in 2040 are 63927 t and 6560 t, respectively. However, the simulated data under the BA scenario far exceeds these environmental capacities, indicating that Liuyang County's current water environmental carrying ratio is in a severely overloaded state. Regarding pollutant emissions from various industries, the livestock industry exhibits a significant and rapidly increasing amount of COD emissions, while industrial emissions and $NH_3$-N losses from farmland account for a considerable proportion .

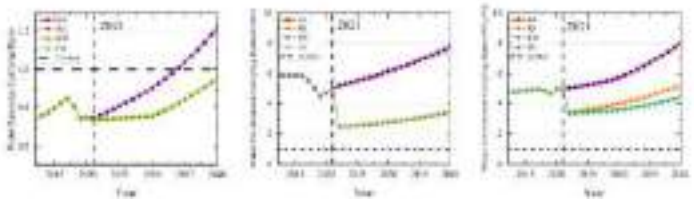

Figure 1 Trends in the carrying capacity of water quantity and quality elements

This study defines four development scenarios: baseline (BA), pollution reduction (RE), water-saving (RW), and integrated development (DE).The alterations in water resource carrying ratios under the BA, RE, RW, and DE scenarios are depicted in Figure 1. In 2040, the specific values are 1.226, 1.226, 0.963, and 0.963, respectively. Figure 1 illustrates the changes in water environment carrying ratios (WECR) under the BA, RE, RW, and DE scenarios.

## 4 Conclusions

1. Under the baseline scenario, the Water Resources Carrying Ratio in Liuyang County is 0.79, ,the projected WRCR for the medium to long term (2040) is 1.226. The Water Environment Carrying Ratios for COD and $NH_3$-N are 7.7429 and 8.0118 respectively, indicating a severe overload.

2. Analyzing the proportion of each state variable in water demand reveals that agricultural water usage has a higher proportion, while industrial water usage shows the fastest growth. Examining pollutant emissions in various industries, the livestock industry has a significant and rapidly increasing COD emission, while industrial emissions and ammonia nitrogen ($NH_3$-N) from farmland erosion have higher proportions.

3. Data analysis under different scenarios indicates that in the RW scenario, measures such as improving agricultural and industrial water use efficiency can partially alleviate the issue of high water resource carrying ratios in Liuyang County. In the RE scenario, raising emission standards can alleviate the current overload of Water Environment Carrying Ratios in Liuyang County, but it cannot completely solve the problem.

## Reference

[1] P. Cheng, Q. Jin, H. Jiang, M. Hua, Z. Ye, Efficiency assessment of rural domestic sewage treatment facilities by a slacked-based DEA model, Journal of Cleaner Production, 267 (2020) 122111.

[2] J. Jiang, X. Hu, Y. Gu, W. Wang, Z. Bi, C. Yao, X. Liang, Q. Wen, M. Luo, Y. Zheng, X. Xia, Suitability evaluation of rural sewage treatment facilities in China considering lifcycle environmental impacts and regional differences, Journal of Environmental Management, 344 (2023) 118516.

**Theme:** Environmental, Marine and Coastal Hydroinformatic
**IAHR Thematic Priority Area:** [TPA-2] Water for the Energy Transition Food Security and Nature
https://doi.org/10.3850/iahr-hic2483430201-434

# Assessing the Combined Risk of Fire and Flood on A National Scale for Sweden

**Fainaz Inamdeen[1], Magnus Larson[2]**

[1] Water Resources Engineering, Lund University, Lund 22100, Sweden

*Corresponding author: fainaz.inamdeen@tvrl.lth.se*

**Abstract.** Floods and wildfires are two critical hazards that impose substantial direct and indirect costs to society, including the resource needs of rescue services. Their occurrence is strongly linked to meteorological conditions, playing a fundamental role in hazard development and assessment. These hazards are notably distinguishable due to opposing weather requirements, wet conditions for floods and dry conditions for wildfires. However, certain regions are exposed to the convergence of these hazards simultaneously or in temporal proximity, demanding different levels of resources and mitigation strategies. Consequently, there is a vital need for a comprehensive combined risk assessment to enhance the effectiveness of rescue services to face such risks. This study presents an analysis for the combined risk of wildfires and floods on a national scale in Sweden over an 11-year period based on daily values on the Fire Weather Index (FWI) and river flow data, taken as proxies for the occurrence of fire and flood, respectively. The present study employed different methods to assess the joint occurrence of fire and floods including simultaneous plots of FWI and flow time series, scatter plots with risk categorization, and index plots combining standardized FWI and flow, offering both qualitative and quantitative insights into combined risk assessment.

**Keywords:** Combined risk, Fire weather Index, Flood risk, Flow, Rescue service, Wildfire risk

## 1 Background

Methods for risk assessment involving several hazards that may occur simultaneously have been developed during the latest decades [1-3]. Such methods may range from purely qualitative approaches, where applications will involve elements of subjective judgement, to quantitative approaches resulting in index values that yield firm estimates related to the impact of interest [2]. The quantitative approaches require more elaborate methods to normalize and combine the descriptors representing the different hazards, as well as data to validate the approach [4].

In this study, the joint occurrences of the two hazards wildfire and flood were investigated for the entire country of Sweden. As a descriptor for wildfire, the Fire Weather Index (FWI) was employed, whereas the flow was taken to represent flooding. Although using quantities that have a clear correlation with fire and flood, this was a rather schematic approach that did not attempt to resolve the details of the specific hazard and its impacts. An underlying aim of the present study is to estimate the resource needs for rescue services to deal with multiple hazards in a planning perspective, not to address specific events in space at short time scales. Thus, the overall objective of the present paper is to assess the combined risk for wildfire and flood on a country-wide scale, which will provide useful information for rescue services in dealing with these hazards.

## 2 Results and Discussion

Although the analysis encompassed eight locations, the study only presents the results for a few locations that illustrate the main characteristics relevant to the key discussion. Analysis of the time series was conducted to explore the temporal fluctuations in FWI and flow over an 11-year period. The analysis indicated distinct regional differences in the behavior of FWI and flow values across the country. FWI values typically peak during the summer regardless of location, indicating a higher

likelihood of wildfires by encompassing warmer and drier conditions. Conversely, flow variations exhibit significant temporal shifts from north to south. In the north, peak river flows occur during late spring due to snow melt, thus creating a scenario where both hazards could occur in temporal proximity. In the south, peak flows emerge during winter when wildfires are less likely, yet warm summer temperatures can lead to intense rainfalls [5,6], presenting the potential for concurrent hazards. Figure 1 shows annual average of daily FWI and flow for Vidsel and Ljungby, located in the north and south of Sweden, respectively.

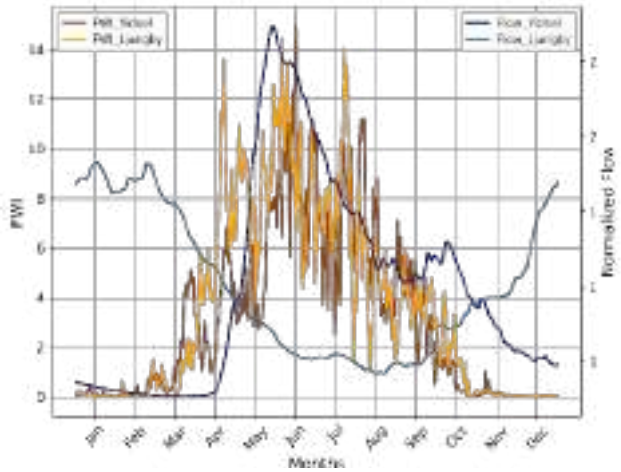


Figure 1. Annual average of daily FWI and flow for the locations Vidsel and Ljungby; flow values are normalized by the mean flow.

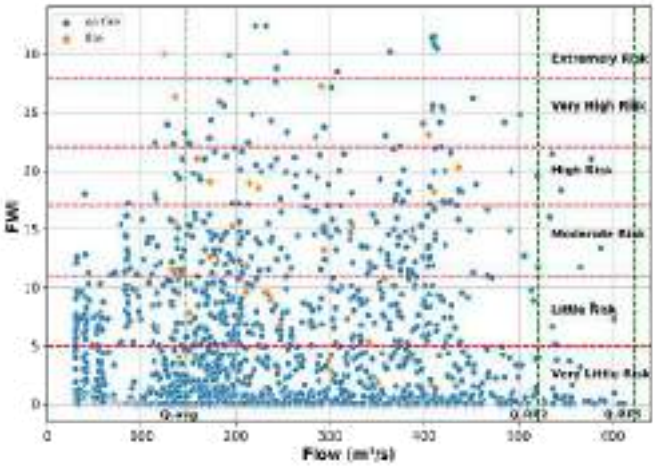


Figure 2. The characteristics of FWI and flow at location Vidsel for the same day.

The scatter plots with risk categorization were developed for the study locations to visualize concurrent characteristics of FWI and flow for period of interest. The risk categorization were marked on the plots based on wildfire risk classes defined by MSB [7] and on flows with specific return periods. Furthermore, days of actual wildfire occurrences are marked with orange color points. As an example, the scatter plot classification for Vidsel is shown in figure 2, indicating that there were few, but significant, instances in the past where both FWI and flow were high during the same day. An approach was also explored to develop an index called Extreme Index (EI) by integrating wildfire and flood risks that could aid rescue services in collectively assessing threats and resource needs in a particular environment.

## References

[1] N. Johansson, C. P. Eriksson, and M. Mcnamee, Review of multi-hazard indices: Focus on methods applicable for a Swedish context, 2021.
[2] M. S. Kappes, M. Keiler, K. von Elverfeldt, and T. J. N. h. Glade, Challenges of analyzing multi-hazard risk: a review, vol. 64, pp. 1925-1958, 2012.
[3] A. Tilloy, B. D. Malamud, H. Winter, and A. J. E.-S. R. Joly-Laugel, A review of quantification methodologies for multi-hazard interrelationships, vol. 196, p. 102881, 2019.
[4] T. Lung, C. Lavalle, R. Hiederer, A. Dosio, and L. M. J. G. E. C. Bouwer, A multi-hazard regional level impact assessment for Europe combining indicators of climatic and non-climatic change, vol. 23, no. 2, pp. 522-536, 2013.
[5] A. Eklund, J. A. Mårtensson, S. Bergström, E. Björck, J. Dahné, L. Lindström, D. Nordborg, J. Olsson, L. Simonsson and E. Sjökvist, Sveriges framtida klimat: Underlag till Dricksvattenutredningen. SMHI, 2015.
[6] P. Lind and E. Kjellström, Temperature and precipitation changes in Sweden; a wide range of model-based projections for the 21st century. SMHI, 2008.
[7] J. Sjöström and A. Granström, Skogsbränder och gräsbränder i Sverige: Trender och mönster under senare decennier, ed, 2020.

**Theme:** Environmental, Marine and Coastal Hydroinformatic
**IAHR Thematic Priority Area:** [TPA-2] Water for the Energy Transition Food Security and Nature
https://doi.org/10.3850/iahr-hic2483430201-436

# The Impacts of The Bi-Modal Temporal Variability of Storms on The Urban Flood Behavior

**Gwangseob Kim[1], Sunghwan Lee[1], Jin Moon[1]**

[1] Department of Civil Engineering, Kyungpook National University, Daegu, Korea

*Corresponding author: kimgs@knu.ac.kr*

**Abstract.** This study aimed to calculate and analyze the impacts of different bi-modal temporal distribution characteristics of heavy rainfall on urban floods. The manhole overflow quantity in the target urban basin was computed using the EPA-SWMM model and the inundation behavior was estimated using the two-dimensional flood model (FLO-2D). The bi-modal extreme rainfall events were produced using a rainfall time distribution model using the truncated Laplace function for different storm durations and return periods such as such as 1 to 3-hours and 20-year, 50-year, 80-year, 100-year respectively. The inundation model was validated using the inundation trace map of a urban basin in the Chunan city. The total overflow amount for same quantity and different time distribution rainfall events showed considerable differences. Furthermore, the inundation behaviors also were related to the temporal characteristics of storms such as the temporal location of storm peak and quantitative ratio of bi-modal distribution etc. Results demonstrated that the consideration of temporal distribution characteristics of extreme rainfall events is essential to understand the accurate inundation behavior in urban drainage basins.

**Keywords:** Bi-modal, Impacts of temporal variability of storms, Rainfall time distribution, Urban flood

## 1 Introduction

Urban flood inundation has gained significant international attention in recent years because of the regional effects of climate change, which results in increasingly frequent intense storms. In order to precisely represent the temporal distribution properties of the input rainfall data needed for urban flood simulation and analysis, numerous studies have been carried out [1,2,3,5]. The urban flood inundation impacts associated with the time distribution characteristics of heavy storms were analyzed using unimodal HUFF quartile approach [4]. The impacts of bi-modal time distribution characteristics of heavy storm on urban floods are analyzed as follows.

- Bi-modal storm distribution scenarios generation
- Analysis of the impacts of temporal variability of storms on the urban flood inundation

Table 13 The EPA-SWMM-model-simulated 3-hr total overflow results with bimodal peak scenarios

| 2 peaks quartile | Return period(yr) | Quantitative ratio of each peak (%) 0-100 | 10-90 | 20-80 | 30-70 | 40-60 | 50-50 | Avg. ($m^3$) | Min. ($m^3$) | Max. ($m^3$) |
|---|---|---|---|---|---|---|---|---|---|---|
| 1-3 | 20 | 35.5 | 28.2 | 21.3 | 17.3 | 14.1 | 8.0 | 17.8 | 8.0 | 35.5 |
| | 50 | 127.2 | 113.1 | 96.3 | 76.6 | 57.6 | 34.6 | 75.7 | 34.6 | 127.2 |
| | 80 | 193.2 | 166.2 | 147.3 | 118.3 | 87.9 | 54.9 | 114.9 | 54.9 | 193.2 |
| | 100 | 221.2 | 197.7 | 171.5 | 138.4 | 105.3 | 67.7 | 136.1 | 67.7 | 221.2 |
| 2-3 | 20 | 35.5 | 28.5 | 23.3 | 20.5 | 16.7 | 12.6 | 20.3 | 12.6 | 35.5 |
| | 50 | 127.2 | 115.4 | 101.5 | 85.0 | 72.2 | 57.6 | 86.3 | 57.6 | 127.2 |
| | 80 | 193.2 | 171.7 | 155.5 | 133.3 | 115.1 | 93.3 | 133.8 | 93.3 | 193.2 |
| | 100 | 221.2 | 201.4 | 180.6 | 156.7 | 133.4 | 110.6 | 156.6 | 110.6 | 221.2 |
| 4-3 | 20 | 35.5 | 17.5 | 10.8 | 14.4 | 24.8 | 38.0 | 21.1 | 10.8 | 38.0 |
| | 50 | 127.2 | 99.5 | 78.5 | 75.5 | 86.4 | 110.1 | 90.0 | 75.5 | 127.2 |

| | | | | | | | | | |
|---|---|---|---|---|---|---|---|---|---|
| 80 | 193.2 | 154.5 | 137.2 | 127.3 | 137.3 | 159.8 | 143.2 | 127.3 | 193.2 |
| 100 | 221.2 | 186.1 | 164.6 | 156.8 | 164.5 | 187.8 | 171.9 | 156.8 | 221.2 |

## 2 Results

Table 1 demonstrates the sample EPA-SWMM-model-simulated 3-hr total overflow results with bi-modal peak scenarios using the truncated Laplace function. It shows that despite the same amount of rainfall, there was almost three times difference in overflow. Boxplots (Fig. 1) of the simulated total manhole overflow provide a visual summary of the results of 348 different rainfall scenarios reflecting the temporal characteristics of rainfall events such as the quantitative ratio of each peak and the locations of 1st and 2nd storm peaks. The bi-modal rainfall scenarios consisted of six quantitative ratio of different peaks(0–100%), twelve different combinations of bi-modal peak quartile (1–4th, …, 4-1st ) and five different return periods (10, 20, 50, 80, and 100-year) Results show that, even with the same amount of rainfall, the manhole overflow volume and the inundation area vary significantly based on variations in the time distribution features of storms. Thus, a precise understanding of the rainfall–runoff response and the inundation behavior in urban environments requires taking into account the temporal distribution characteristics of heavy rainfall events. Results demonstrate that when rainfall forecasts with both amount and temporal distribution features are provided, it may be possible to implement suitable flooding mitigation measures in urban drainage basins.

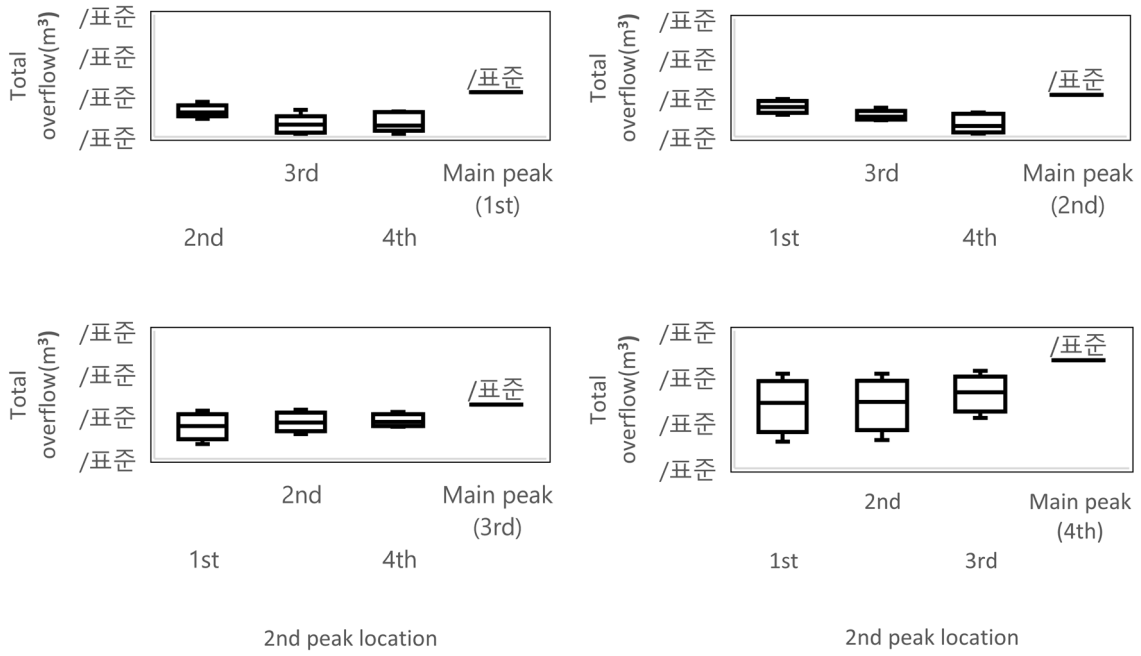


Figure 70 Boxplots of the simulated total manhole overflow of 348 different rainfall scenarios

## 3 Acknowledgments

This research was supported by a grant (RS-2022-ND634021(2022-MOIS61-002)) for the Development Risk Prediction Technology of Storm and Flood for Climate Change based on Artificial Intelligence funded by Ministry of Interior and Safety (MOIS, Korea)

## Reference

[1] F.A. Huff, Time Distribution of Rainfall in Heavy Storm. Water Resour. Res., Vol. 3, No. 4, (1967) 1007-1019.
[2] F.A. Huff, Urban Hydrology Review. Bull. Am. Meteorol. Soc. Vol. 67, No. 6, (1986) 703-712.
[3] S. Choi, K.W. Joo, H.J. Shin, J.H. Heo, Improvement of Huff's Method Considering Severe Rainstorm Events. J. Korea Water Resour. Asso., Vol. 47, No 11, (2014) 985-996.
[4] T. Li, G.W. Lee, G. Kim, Case Study of Urban Flood Inundation—Impact of Temporal Variability in Rainfall Events. Water 21 (2021) 1-17.

[5] H. Cho, G. Kim, Development of a Rainfall Time Distribution Considering Characteristics of Temporal Variability of Extreme Rainfall Events. J. Korean Soc. Hazard Mitig. Vol. 15, No. 4, (2015) 23-29.

**Theme:** Environmental, Marine and Coastal Hydroinformatic
**IAHR Thematic Priority Area:** [TPA-2] Water for the Energy Transition Food Security and Nature
https://doi.org/10.3850/iahr-hic2483430201-439

# Laboratory Investigation on Spatial Distribution of Wave Overtopping Volumes Over a Composite Seawall with a Berm

**Shudi Dong[1,2], Md Salauddin[3*], Yize Zhang[1], Yanming Yu[1], Siyuan Hong[1] and Yongming Zheng[1]**

[1] PowerChina Huadong Engineering Corporation Limited, Hangzhou 311122, China
[2] College of Harbor, Coastal and Offshore Engineering, Hohai University, Nanjing 210098, China
[2] School of Civil Engineering, University College Dublin, Dublin 4, Ireland

*Corresponding author: md.salauddin@ucd.ie*

**Abstract.** An accurate prediction of the spatial distribution of overtopping volumes is crucial for the reliable assessment of the safety of coastal regions in response to potential wave overtopping hazards in a rapidly changing climate. Here, for the first time, we present a comprehensive suite of laboratory-scale physical modelling experiments to investigate the spatial distribution of overtopping volumes behind a composite seawall with a berm placed on a seaward slope. Test results show that the spatial distribution of overtopping water can be described with an exponential function of the distance x behind the seawall crest. A new empirical equation is proposed to estimate the spatial distribution of overtopped water behind a berm composite seawall, subjected to regular wave attack.

**Keywords:** Berm; Climate Change, Composite Seawall; Hazard-zone, Spatial Distribution.

## 1 Introduction

Over the past 30 years, there has been a considerable increase in studying the spatial distribution of overtopping volumes on coastal protections [1-3]. Nevertheless, the vast majority of spatial distribution data has been analysed for wave overtopping on either simply vertical or sloping structures without a berm in place. There is a clear knowledge gap on the shape of spatial distribution over composite structures with a berm due to a lack of field and laboratory research. The purpose of this study is to develop/advance our understanding of the spatial distribution of overtopping volumes over a berm composite seawall with different upper and lower slope angles by collecting novel physical modelling datasets and then developing empirical prediction tools for predicting such processes. The shape of spatial distribution and landward travel distance of overtopping water behind seawalls are given special attention. For the first time, an empirical equation is developed to predict the spatial distribution of overtopped water on a vertical breakwater with a berm.

## 2 Experimental set-up

Small-scale laboratory tests were carried out in a two-dimensional wave flume (35m × 0.8m × 1.0m), equipped with a piston-type wave generator and an active absorption system. The model seawall was constructed with upper and lower slopes with different slope angles and a berm. In each test case, regular waves were generated under swell and storm conditions. The tests were designed at a length scale of 1:40. Two sets of wave gauges (three in each set) were placed close to the wave paddle and model seawall, respectively, to determine the incident and reflected wave characteristics. The inshore wave conditions were calibrated in the 'bare' flume without the structure in place, adopting the techniques as proposed in recently performed similar small-scale wave flume investigations [4-5].

## 3 Results and Discussions

By plotting measured overtopping volume in each chamber against the distance from the seawall, it is found that the spatial distribution of overtopping wave in each test overall follows an exponential

function. Hence, the exponential function is applied, and the shape of spatial distribution is determined by an empirical parameter *k*. Figure 1 illustrates that the measured *k* from each test increases with the increase of $R_c/L$. Overtopping water distributes further landward as relative freeboard ($R_c/L$) decreases. Figure 1 also shows that *k* follows an exponential function of $R_c/L$. This exponential function can be empirically derived and presented as Eq.1 with the RMSE (Root Mean Square Error) of 0.51.

$$k = 0.7\exp(22 \times R_c/L) \quad (1)$$

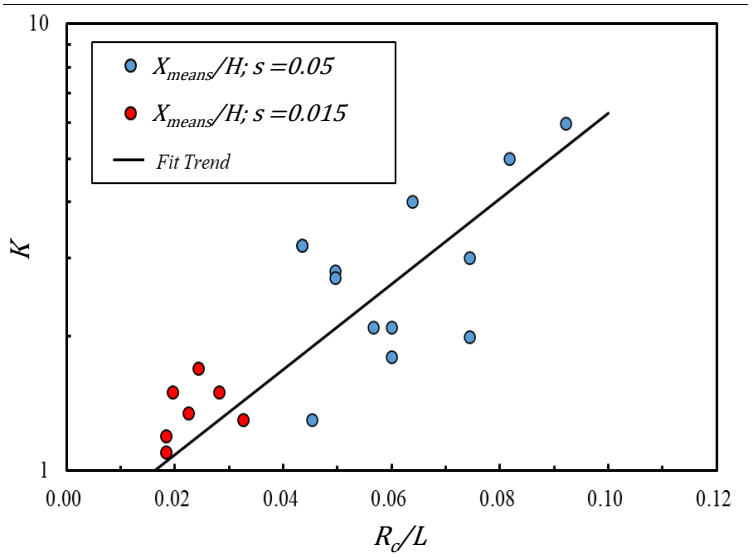


Figure 1. The relationship between spatial parameter *k* on the berm composite seawall and relative freeboard ($R_c/L$)

Furthermore, a new equation (Eq. 2) predicting the spatial distribution of overtopping water behind the berm composite seawall tested in this study is developed incorporating Eq.1 into the original equation suggested by Andersen et al. [6] for smooth sloping seawalls. The new empirical equation is then validated by comparing the predicted travel distance of 99.5% overtopping water behind the structure with values measured from physical modelling experiments within this study. Good agreements are reached between measurements and predicted values of travel distance of overtopped water.

$$\frac{q_{passing}}{q_{total}} = exp\left(-0.7 \cdot exp\left(22 \times \frac{R_c}{L}\right) \cdot \frac{max(x/\cos\beta - 2.7 \cdot h_{level} \cdot s^{0.15},\ 0)}{H}\right) \quad (2)$$

## 4 Conclusions

This paper presents the analysis of spatial wave overtopping volumes at a composite seawall with a berm under regular wave attack. The results of this experimental study showed that the berm's influence in mitigating wave overtopping volumes varies with its geometrical configurations, showcasing that the different widths and heights of the berm lead to different overtopping volumes. Additionally, it was reported that the spatial distribution of overtopping water behind the composite seawall may alter with the influence of various structural configurations. Further validation of the proposed equation considering the different geometrical configurations of berms and seawalls would be albeit desirable, in particularly under irregular wave conditions.

## 5 References

[1] T. Bruce, T. Pullen, W. Allsop, J. Pearson, How far back from a seawall is safe?, Int. Conf. on Coastlines, structures and breakwaters 2005, 166–175.
[2] T. Pullen, W. Allsop, T. Bruce, Wave Overtopping at Vertical Seawalls: Field and Laboratory Measurements of Spatial Distributions, In Proc. of the Coastal Engineering Conference, 2007, 4702–4713.
[3] S. Dong, S. Abolfathi, M. Salauddin, J. Pearson, Spatial distribution of wave-by-wave overtopping at vertical seawalls, Coastal Engineering Proc., structures.17, 2020 doi:10.9753/icce.v36v.structures.17.
[4] S. Dong, S. Abolfathi, M. Salauddin, J. Pearson, Spatial Distribution of Wave-by-Wave Overtopping behind Vertical Seawall with Recurve Retrofitting, Ocean Engineering (238), 2021, 109674.
[5] M. Salauddin, J.J. O'Sullivan, S. Abolfathi, Z. Peng, S. Dong, J.M. Pearson, New insights in the probability distributions of wave-by-wave overtopping volumes at vertical breakwaters, Sci. Reps. 12(1), 2022, 16228.
[6] T.L. Andersen, H.F. Burcharth, F.X., Gironella, Single wave overtopping volumes and their travel distance for rubble mound breakwaters. Coastal Structures Conference, 2009, 1241–1252.

**Theme:** Environmental, Marine and Coastal Hydroinformatic
**IAHR Thematic Priority Area:** [TPA-2] Water for the Energy Transition Food Security and Nature
https://doi.org/10.3850/iahr-hic2483430201-441

# Algal Organic Matter Transformation and Removal by Ozone Oxidation and Ion Exchange: Implications for Selective Nitrate and Phosphate Recovery from Algae Filtrate

**Ji Wu [1], Xiaoyu Wang [1], Chen Xie [1], Ziwu Fan [1],**

[1] Key Laboratory of Taihu Basin Water Resources Management, Ministry of Water Resources, Nanjing Hydraulic Research Institute, Nanjing, 210029, China

*Corresponding author: zwfan@nhri.cn*

**Abstract.** Harmful algal blooms have become a major threat to freshwater systems. Various algae separation methods have been used to suppress algal biomass, and this has resulted in the generation of a large amount of algae residues and highly concentrated algae filtrate due to the rupture of algal cells. In this study, the efficacy of combined ozonation and ion-exchange processes for algae filtrate treatment was evaluated. Diverse approaches were used to characterize variation in the functional groups and conformations of algal organic matter in algae filtrate during the ozonation process at the molecular scale. The chromophores and fluorophores were destroyed via ozone oxidation within 5 min. The organic nitrogen in algae filtrate was effectively oxidized to $NO_3$--N, which resulted in a continuous increase in inorganic nitrogen. In the post-oxidation treatment, the nano-scale $La(OH)_3$-loaded resin could achieve near 100% phosphate removal, and this was maintained during five successive adsorption-desorption cycles; the $NO_3$--N removal performance was enhanced with resin containing a triethylamine group. Overall, combined ozonation and ion-exchange processes could be used to effectively treat algae filtrate and promote selective nitrate and phosphate recovery; our findings also demonstrate the high potential for this approach to treat algae-laden water. (max 200 words).

**Keywords:** Algal organic matter, algae filtrate, ozone oxidation, two-dimensional correlation spectroscopy, phosphate recovery

## 1 Introduction

Harmful algal blooms have become a major threat to freshwater systems. Various algae separation methods have been used to suppress algal biomass, and this has resulted in the generation of a large amount of algae residues and highly concentrated algae filtrate due to the rupture of algal cells. Many studies have concluded that oxidation treatment is effective for controlling algae and the degradation of AOM[1]. Various algae-derived pollutants, such as microcystins (MCs), polysaccharides, peptides, odor compounds, and other algal inclusions, are effectively degraded during the ozonation process. High quantities of nitrogen and phosphorus in oxidized algae filtrate should be reduced to an acceptable level before the filtrate is discharged into aquatic environments to prevent algal blooms. Moreover, nitrogen and phosphorus are important nutrients and nonrenewable resources. The removal and recovery of these nutrients from wastewater are thus critically important, especially phosphorus, which will be exhausted in the near future[2]. Therefore, the relative benefits of AOM control vs. degradation by-product recovery require consideration. Anion exchange is considered an effective approach for the removal of nitrate and phosphate from wastewater due to its high selectivity and reusability. But the concept of ozone oxidation and ion exchange has thus received increased attention.

The aim of this study was to explore the efficiency of combined ozone oxidation and ion exchange processes for the disposal of algae filtrate, as well as the selective recovery of nitrate and phosphate. The characteristics of AOM structure and conformation in algae filtrate during the ozonation process

were revealed by HP-SEC, EEM-PARAFAC, as well as 2DCoS, hetero-2DCoS, and moving window two-dimensional (MW2D) correlation analyses of UV, synchronous fluorescence (SF), and Fourier transform infrared spectroscopy (FTIR) spectra. Moreover, nitrate and phosphate in oxidized algae filtrate were recovered by four types of resins, and their reusability during five adsorption-desorption cycles was evaluated.

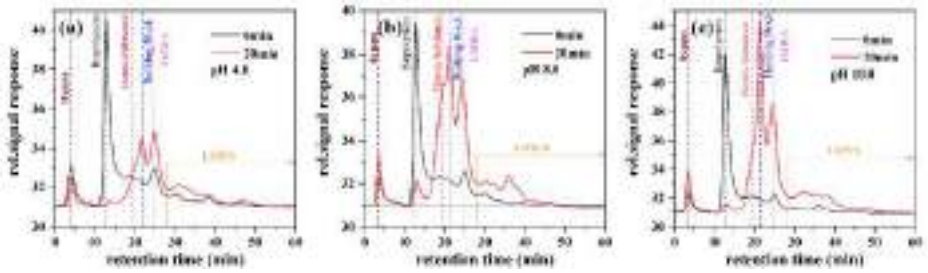

Figure 71 SEC chromatograms of AOM in algae filtrate before and after ozone oxidation: (a) initial pH 4.0, (b) initial pH 8.0, and (c) initial pH 10.0

In this study, the combined processes of ozone oxidation and ion exchange were used for algae filtrate treatment and further selective recovery of nitrate and phosphate. Multiple methods were used to analyze variation in molecular structure and the resulting degradation products. Carboxyl, aromatic, and phenolic groups were the basic units of chromophores and fluorophores. The portion of DIN increased gradually during the ozonation process. The final concentration of MCs was far lower than the drinking water threshold of 1.0 μg/L. In the post-oxidation treatment, the nano-scale $La(OH)_3$-loaded resin could achieve near 100% phosphate removal, and this was maintained during five successive adsorption-desorption cycles; the $NO_3$--N removal performance was enhanced using resin containing a triethylamine group. All these results demonstrated that combined ozonation and ion-exchange processes can potentially be used to treat algae filtrate. Overall, this study provides new insights into the disposal of algae filtrate, as well as the prevention, control, and remediation of AOM in algae-laden surface waters.

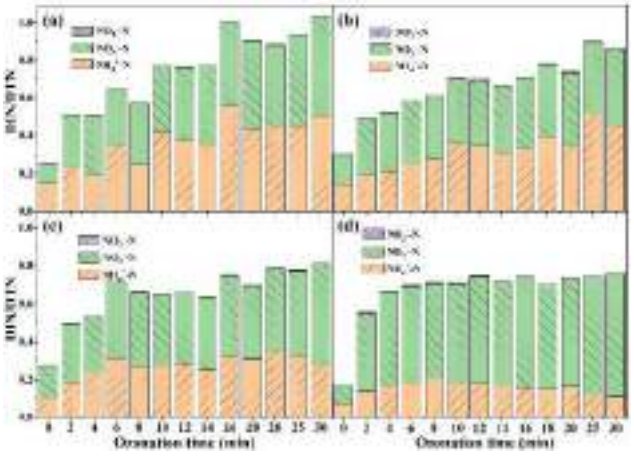

Figure 2 Portions of different forms of nitrogen accounting for DTN during the ozonation process: (a) pH 4.0, (b) pH 6.0, (c) pH 8.0, and (d) pH 10.0

## Reference

[1] Guo, K., Wang, Z., Wu, J., Li, W., Liu, B., Yue, Q., Gao, Y. and Gao, B. 2023. Insights into the Mechanism of Coagulation Pretreatment for Membrane Fouling Control from the Perspective of Organic Removal Based on a Sensitive SEC-DAD-FLD-OCD/OND Method. ACS ES&T Engineering 3(6), 851-861.

[2] Lin, B., Zhang, Y., Shen, F., Zhang, L., Wang, D., Tang, X., Zhou, Y., Nie, X., Lv, L., Zhang, W., Hua, M. and Pan, B. 2020a. New insights into the fractionation of effluent organic matter on diagnosis of key composition affecting advanced phosphate removal by Zr-based nanocomposite. Water Research 186, 116299.

**Theme:** Environmental, Marine and Coastal Hydroinformatic
**IAHR Thematic Priority Area:** [TPA-2] Water for the Energy Transition Food Security and Nature
https://doi.org/10.3850/iahr-hic2483430201-443

# Evaluation of River Health in Chongming Island, Shanghai

**Yifan Ding[1], Dacheng Chen[2], Xin Zhang[1], Yulin Chen[1], Ning Yang[1], Yaqi Dai[3]**

[1] Shanghai Municipal Engineering Design Institute, Shanghai 200092, China
[2] Shanghai Scientific Technology Development Branch of Arcplus Group, Shanghai 200041, China
[3] Shanghai Water Engineering Design and Research Institute, Shanghai 200061, China

*Corresponding author: zhangxin@smedi.com*

**Abstract.** Chongming Island is the world's largest estuarine alluvial island and the third-largest island in China. An indicator system for evaluating the health of the rivers in Chongming Island was established and applied. The methodology includes the selection of indicators, the determination of index weight and grading standard, and the River Health Index (RHI) scoring. The data were collected by various means, including literature survey, remote sensing interpretation, biological survey and satisfaction questionnaire. The results indicate that the RHI of the selected rivers range from 55.05 to 73.15, with the health status grades of "sub-healthy" and "healthy". At the criterion level, the average scores of water resources and water quality indicators were the highest, while biological indicators were the lowest, indicating that the water environment quality of Chongming Island is relatively good, but the integrity of the intrinsic biological system is still far from the ideal state, and biological indicators are the most important factors affecting the health of rivers in Chongming Island. The findings are of relevance to other areas of the plain river network.

**Keywords:** Chongming Island, Biological Survey, Ecological Security, Remote Sensing Interpretation, River Health Index, Social Service Function.

## 1 Introduction

Chongming Island is the largest estuarine alluvial island in China, accounting for approximately 20% of the total land area of Shanghai. It is planned to be a world-class ecological island. A meticulous and comprehensive assessment of the condition of the island's rivers is of paramount importance.

## 2 Materials and Methods

The study employs a district and county administrative unit as the primary unit of analysis, with small and medium-sized rivers serving as the unit of observation. A total of eight rivers were selected for study, and an index system for evaluating the health of the rivers in Chongming Island was constructed. The system comprises four guideline layers and 14 indicators, as illustrated in Figure 1. The indicator weights and evaluation standard levels were determined. The health of rivers and lakes is categorised into five levels: excellent (score 80~100), healthy (score 60~80), sub-healthy (score 40~60), unhealthy (score 20~40), and pathological (score 0~20).

## 3 Data and Results

Data were collected by various means, including literature survey, remote sensing interpretation, biological survey and satisfaction questionnaire. The results of this survey and evaluation indicate that the health evaluation scores of the study rivers range from 55.05 to 73.15, with the health status grades of "sub-healthy" and "healthy". The results show that the water environment quality of Chongming Island is relatively good, but the integrity of the inherent biological system is still far from the ideal state, and the biological indicators are the most important factors, showed in Figure 2.

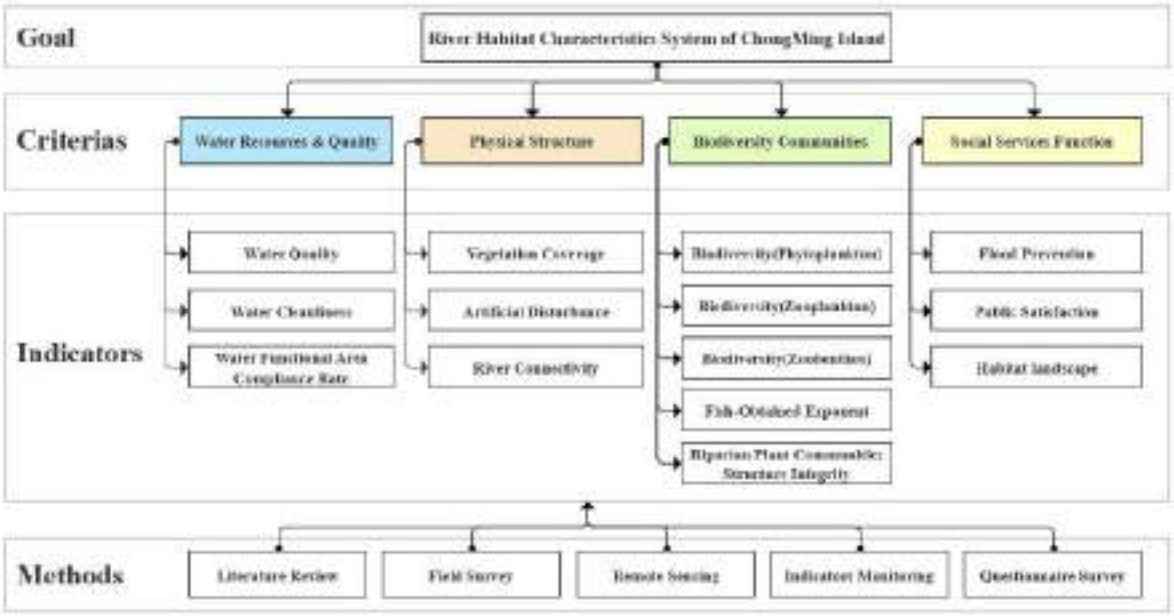


Figure 72. River health evaluation index (RHI) system for the Chongming rivers

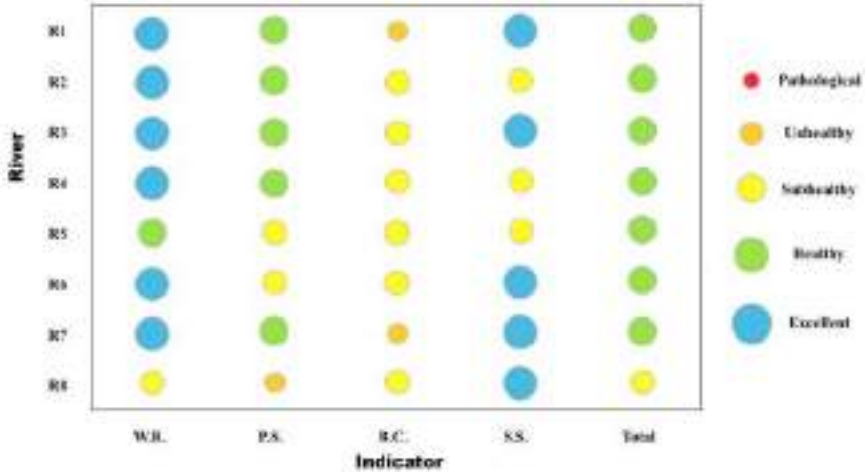


Figure 73. RHI scores of each river

## 4 Discussion

This study found that the rivers on Chongming Island generally have a low level of artificial disturbance in the riparian zone. However, the vegetation condition is poor, indicating that the conflict between residents and enterprises who built illegal structures to encroach on the river channel in the previous period has been alleviated. Nevertheless, the ecological restoration of the river has not been completed, and it is generally in the trend of improvement. It is not yet at a healthy level.

## Reference

[1] Xi H, Li T, Yuan Y, Chen Q, Wen Z. River Ecosystem Health Assessment Based on Fuzzy Logic and Harmony Degree Evaluation in a Human-Dominated River Basin. Ecosyst. Health Sustain.2023;9:Article 0041.

[2] Ding, Y., Tang, D., Dai, H. et al. Human-Water Harmony Index: A New Approach to Assess the Human Water Relationship. Water Resour Manage 28, 1061–1077 (2014).

[3] Peng, B., Shi, B., Wang, Y.P. et al. Establishment and application of ecological health evaluation system for urban and rural rivers in Yangtze Estuary. Anthropocene Coasts 6, 9 (2023)

**Theme:** Environmental, Marine and Coastal Hydroinformatic
**IAHR Thematic Priority Area:** [TPA-2] Water for the Energy Transition Food Security and Nature
https://doi.org/10.3850/iahr-hic2483430201-445

# A Case Study on Ming Lake for Intelligent Management

**Xiaoyu Wang[1], Chen Xie[1], Ziwu Fan[1]**

[1] Nanjing Hydraulic Research Institute, Nanjing 210029, China

*Corresponding author: zwfan@nhri.cn*

**Abstract.** In accordance with the requirements of "demand-driven, application-first, digital empowerment, enhancement of capabilities", the main line of digitalization, networking, intelligence, the construction of digital twins lake prototypes, to help the construction of happy rivers and lakes in Ming lake, the formation of replicable, scalable solutions for river and lake governance management and care. Focus on Lake Ming Basin to comprehensively improve the arithmetic: strengthen the information infrastructure construction, enhance the perception, transmission, computing capacity; focus on the five major data sets to improve the arithmetic: upgrade the multi-level data base plate, improve data standardization and display effect; focus on intelligent decision-making construction core algorithm: construction of professional and knowledge models, enhance the core algorithm decision-making support capacity; focus on happy river and lake to provide four pre support: construction of five business modules To improve the level of intelligent governance and management.

**Keywords:** digital twin; happy rivers and lakes; intelligent management and protection; Ming Lake

## 1 Project Description

Based on the current construction needs, the project aims at "flood control and safety, high-quality water resources, healthy water ecology, livable water environment and advanced water culture", adheres to the holistic nature of Ming Lake and the systematic nature of the watershed, and enhances the ecological protection and management capability of Ming Lake through the implementation of systematic management, improvement of management and care capacity, and development of the watershed, and promotes the economic development of the watershed and the improvement of residents' living standard. The goal is to improve the ecological protection of Ming Lake through the implementation of systematic governance, improvement of management capacity and development of the basin, enhance the ecological value of Ming Lake, boost the economic development of the basin and improve the standard of living of the residents, and promote the river and lake management system to be "famous and responsible" and "capable and effective", so as to create the first national model of a happy lake in a city and play an exemplary leading role in the construction of the national happy river and lake. It has played a leading role in demonstrating the construction of happy rivers and lakes, exploring the construction path of happy rivers and lakes, and arriving at a set of replicable and generalizable experience in the construction of happy rivers and lakes.

The construction of Lake Ming digital watershed comprehensively integrates the core results of three aspects of system governance, management and care capacity enhancement, and development of watersheds, and takes the lead in exploring the digital twin watershed construction program, and establishes the "four pre" business system of flood control, water ecosystem regulation, and river and lake inspection, which is an important practice for the implementation of the long-term management and care mechanism of rivers and lakes, and also practicing the path of high-quality development of water conservancy.

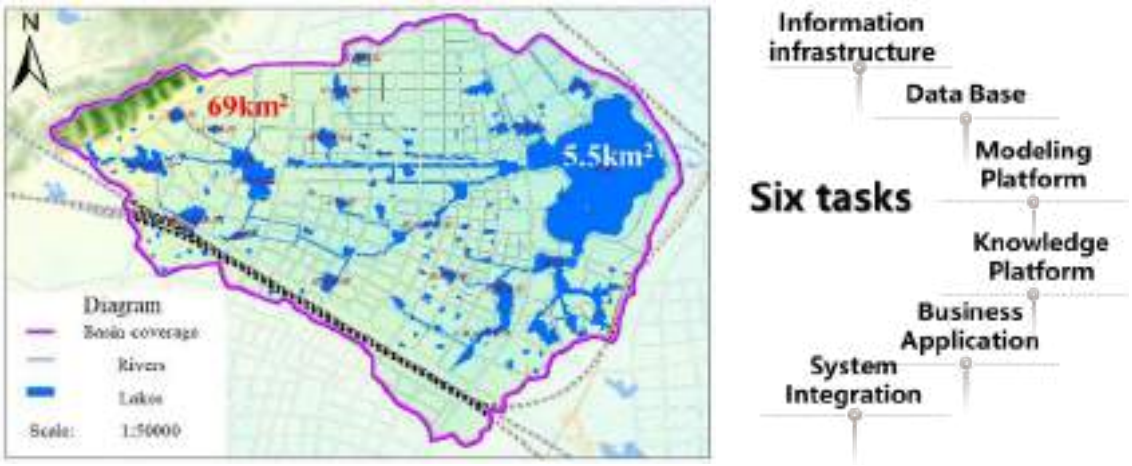


Figure 74 The Ming Lake basin and six tasks of the digital watershed system of Ming Lake

## 2 Digital Watershed System of Ming Lake

The digital watershed Ming Lake adopts diversified basic base maps, with three-dimensional twin base plates and eagle-eye videos, and comprehensively demonstrates the construction results of five aspects of happy rivers and lakes by extracting core perceptual and operational information.

Figure 2 The Digital watershed system of Ming Lake

Figure 3 The flood preview scenario

**Theme:** Environmental, Marine and Coastal Hydroinformatic
**IAHR Thematic Priority Area:** [TPA-2] Water for the Energy Transition Food Security and Nature
https://doi.org/10.3850/iahr-hic2483430201-447

# Analysis of Periphytic Algae Community Structure and the Correlation with Environmental Factors in Xuhong River

**YANG Yuming**[1]

[1] College of Environment, Hohai University, Nanjing 210098, China

*Correspondence to: YANG Yuming (2225285636@qq.com)*

**Abstract**：Periphytic algae in rivers are widely used to evaluate the impact of human disturbance on aquatic ecosystems. The community of periphytic algae and water quality were investigated from September 2021 to August 2022 in Xuhong River. Relationship between the characteristics of periphytic algae community and water environmental factors was discussed. The results showed that 58 species of algae were detected in Xuhong River, belonging to 42 genera of 3 phyla. The average density of periphytic algae was 1.17×106 cells/cm2, the average diversity index was 1.64, and the evenness index was 0.65. The density of algae was very significantly correlated with water temperature, dissolved oxygen, ammonia nitrogen and total phosphorus in the river. There was a significant positive correlation between the diversity of periphytic algae and permanganate index, and a very significant correlation with turbidity. Furthermore, the permanganate index content was the key factor to promote the succession of periphytic algae community structure.

**Key words**: algae; correlation analysis; environmental factor; Xuhong Rive

## 1. Materials and methods

### 1.1 Monitoring sections

As a typical hydrodynamic system, river ecosystem has complex multi-dimensional structure[1]. However, river ecosystems affected by human activities are degraded in recent years[2-4]. Xuhong River is mainly for water diversion and has flood control, drainage, drinking water, irrigation, shipping, ecological environment and so on. Based on the periphytic algae in Xuhong River, this paper analyzes its structure and correlation with environmental factors to provide reference for the restoration and protection of river ecosystem [5]. Five monitoring sections have been settled up along the river. The monitoring time is September 2020, January 2021, April 2021 and August 2021, representing autumn, winter, spring and summer respectively.

### 1.2 Samples Collection

For each monitoring section, Seth transparency plate measures the transparency(SD), and YSI(the portable multi-function water quality analysis instrument) measures water temperature (WT), dissolved oxygen (DO), electrical conductivity (Cond) and pH. According to the width of the river, the monitoring sections mix collected surface water samples on its left, middle and right side respectively. Then, total nitrogen (TN), total phosphorus (TP), hypertonic acid index ($COD_{Mn}$) and ammonia nitrogen ($NH_4^+$-N) within 24 hours were determined. The algae in Xuhong River was monitored according to “The River Water Ecology Monitoring Code” of DB 32/T[6].

## 2. Results and Analysis

### 2.1 The diversity of periphytic algae

Algae in each section of Xuhong River in each season was calculated by using the Shannon-wiener diversity index (H'). The results showed that its average value in each section of Xuhong River is 1.64 (0.76-2.25), in which the diversity of algae in the upper reaches is lower， middle and lower

reaches is higher. The seasonal variation of the Shannon-wiener diversity index of algae showed that the diversity of algae in spring was significantly lower than that in other seasons（$P<0.05$）.

### 2.2 Correlation Analysis between Environmental factors and Aquatic organisms

Nine environmental factors were selected to analyze the correlation with the diversity index of algae. Environmental factors include total nitrogen, total phosphorus, permanganate index, ammonia nitrogen, water temperature, pH, dissolved oxygen, turbidity and electrical conductivity. The results of Spearman correlation analysis (Table1) revealed that three environmental factors were extremely significantly negatively correlated with the density of algae in Xuhong River. According to the results, the species and abundance of cyanobacteria and Chlorophyta, which are more adaptable to the environment with high nutrient content, gradually increase, which leads to the increase of algae diversity. Therefore, the content of permanganate index is the key factor to promote the succession of algae community structure in Xuhong River.

Tab.1 Spearman correlation analysis of various environmental factors and aquatic organisms in Xuhong River

| | Temperature | pH | DO | EC | Turbidity | $COD_{Mn}$ | $NH_3$-N | TN | TP |
|---|---|---|---|---|---|---|---|---|---|
| **Density of periphytic algae** | -0.714** | 0.506* | 0.621** | -0.366 | -0.468* | -0.483* | -.661** | -0.368 | -0.627** |
| **Diversity of periphytic algae** | 0.141 | -0.337 | 0.092 | -0.173 | -0.561* | 0.461* | 0.379 | 0.351 | 0.337 |

## 3 Conclusions

A total of 58 species of algae in 3 phyla were identified in Xuhonghe River, and the dominant species were Cyclotella meneghiniana, Carriformis and Curvularia expandata. According to the analysis of the Shannon-Wiener diversity index, the periphytic algae is 1.64 (0.76-2.25), which the diversity level of algae is not high as a whole. The content of permanganate index is the key factor to promote the succession of algae community structure in Xuhong River.

## Reference

[1] WANG Lixin,LIU Huamin,LIU Yu-hong, et al.Introduction to the concept, foundation and focuses of riverscape Ecology[J].Wetland Science,2014,12(02):228-234.

[2] ZHANG Shuilong, FENG Ping. River monitoring program based on ecology concepts[J].The adminstration and technique of environmental monitoring,2005(05):12-14+26.

[3] CAI Qinghua, TANG Tao, LIU Jiankang. Several research hotspots in river ecology[J]. Chinese journal of applied ecology, 2003(09): 1573-1577

[4] WU Yuyu, HE Yong, SHAO Yong, et al. Macroinvertebrate community structure and water quality biological evaluation in rivers entering Taihu lake[J]. The Adminstration and Technique of Environmental Monitoring,2023, 35(01): 26-31.

[5] Jiangsu Provincial Market Supervision Administration. Code for river water ecology monitoring: DB 32/T 4178-2021 [S]. Beijing: China Standards Press, 2021.

**Theme:** Environmental, Marine and Coastal Hydroinformatic
**IAHR Thematic Priority Area:** [TPA-2] Water for the Energy Transition Food Security and Nature
https://doi.org/10.3850/iahr-hic2483430201-449

# Analysis of Lake Change and North-South Boundary in China from 2000 to 2020

**Zhiwen Yang[1,2], Jia Chen[3], Lingkui Meng[3], Penghui Ma[1,2], Bingjie Liang[1,2], Yumiao Fan[1,2], Jian Yang[1,2], Changji Song[1,2], Ming Jing[1,2]**

[1] Yellow River Institute of Hydraulic Research, Yellow River Conservancy Commission, Zhengzhou 450003, China;
[2] Henan Engineering Research Center of Rural Water Environment Improvement, Zhengzhou 450003, China;
[3] School of Remote Sensing and Information Engineering, Wuhan University, Wuhan 430079, China

*Corresponding author: 13983013364@163.com*

**Abstract.** As one of the important water resources, Lake has both ecological and social functions, and is an indispensable component of the Earth's environmental system. The dynamic monitoring of lakes is very necessary to study the regional hydrological characteristics. Based on GEE platform, this paper extracts and analyzes the long-term changes of lakes in China by using surface water data set and lake data set. First, lake masks of different ages are generated from the lake data set. Secondly, use mask to extract the monthly lake data in China, and then carry out data cleaning on the lake data. Finally, the lake change trend of the whole country and every province is analyzed, and the correlation of lake change among every province is calculated. Thus, the north-south boundary of the hydrological difference of lakes in China is obtained. The findings are as follows: 1) the lake area in China showed a trend of first decreasing and then increasing, which was a trough in 2012. 2) most of the lakes in the northern provinces showed the trend of first rising, then falling, then rising, while most of the lakes in the southern provinces showed the trend of first falling, then rising or smooth trend of change. In addition, there are some western provinces have been rising. 3) on the large spatial scale, the north of Shandong, Henan, Shaanxi and Gansu is the northern region, while the south of Jiangsu, Anhui, Hubei and Sichuan is the southern region. The changes of lakes in the north and the south show obvious spatial heterogeneity. The study in this paper is of great significance to reveal the changes and spatial distribution of lakes in China, and even to the study of hydrological regional boundaries in China.

**Keywords:** Correlation analysis, GEE, Lake changes, Surface water, Spatial heterogeneity, the North-south boundary

## 1 Introduction

Water resources represent one of Earth's most crucial natural assets, serving as the foundation for the sustenance of all living organisms and forming an integral component of the ecosystem. Among these water bodies, lakes emerge as significant entities, not only constituting vital elements of water resources but also fulfilling diverse ecological roles. Statistical records indicate that China boasts abundant lake resources, encompassing 2670 natural lakes spanning over 1 km2 in area throughout the year, totaling 80700 km2, with a markedly uneven spatial distribution.

Currently, there exists a considerable body of research dedicated to the analysis of lake changes on a large scale. Most studies analyze regional changes in lake area annually or within a period of time, and some also consider the impact of certain driving factors. Given the vast spatial expanse of lake distribution in China, the variations in lake dynamics across different regions exhibit pronounced spatiotemporal heterogeneity. This article not only scrutinizes the long-term change patterns of China's lakes but also employs the method of lake change correlation analysis to explore the north-

south boundary of lakes based on this heterogeneity. Moreover, the hydrological boundary zone between the northern and southern regions of China is delineated from the perspective of disparities in lake dynamics.

## 2 Method

The overarching objective is to construct a multi-year comprehensive lake mask utilizing the existing China Lakes Dataset. This mask will then be applied to buffer the Global Surface Water Dataset, ensuring coverage of national lake bodies for the entire period. Subsequently, the lake area will be screened and the correlation of lake changes across the country will be computed.

Firstly, the data from the China Lakes Dataset are merged to generate a comprehensive lake mask. Subsequently, the Monthly Water History data from the Global Surface Water Dataset are buffered individually, facilitating the acquisition of complete monthly national lake data. Due to limitations in early Landsat imaging technology, resulting in significant data gaps within the Chinese region, only data from 2000 onwards are utilized in this study.

However, during the extraction of monthly national lake data, certain outliers may be observed, particularly during winter months. Therefore, it is imperative to clean the lake area data by eliminating zero values, followed by outlier detection and removal procedures. Subsequently, the lakes are categorized by province, and the changing trends of lake areas in both the entire country and each province are statistically analyzed. Additionally, the lake data for each province are organized into arrays. As zero values and outliers are removed, gaps may arise in the lake area sequences, leading to inconsistencies in the months with missing data across provinces. Consequently, when calculating the correlation of lake changes, the intersection of corresponding months with valid data in the sequences is obtained. The correlation of lake area change trends is then computed using the corresponding data. Finally, the northern and southern boundary zones of Chinese lakes are delineated based on the distinct distributions of lake change correlations.

## 3 Conclusion

This article delves into the spatiotemporal dynamics of China's lakes, aiming to delineate the northern and southern regions of China's lakes and characterize the hydrological disparities between them. Initially, leveraging the China Lakes Dataset and the Global Surface Water Dataset, national monthly lake data was acquired via buffer analysis on the Google Earth Engine (GEE) platform, with Chinese administrative divisions overlaid to derive the lake area for each province. Subsequently, data cleaning procedures were employed to eliminate outliers, ensuring the integrity of the dataset. The processed data was then utilized to analyze the changing trends in lake area at both the national and provincial levels. Through the calculation of correlations between changes in lake area data series, insights into the regional variations in China's lakes were garnered.

The study uncovered that the delineation of north-south boundaries of China's lakes closely aligns with traditional geographical demarcations. In the northern region, most lake areas exhibit an increasing trend, or undergo an initial decline followed by a subsequent increase, with fluctuation points concentrated around 2012. However, areas near the sea, such as Tianjin and Shandong, demonstrate a negative or weak correlation with other provinces, indicating distinct hydrological dynamics. Conversely, the southern region presents a more complex picture, with no consistent fluctuation trend observed, leading to weaker correlations among lake changes across most regions.

Regarding nationwide changes in lake area, provinces with larger lake areas exhibit stronger correlations, with relatively consistent trends among them. These findings hold significant implications for hydrogeographic zoning studies in China. Additionally, further research can be advanced through refining geographical partitioning methods and incorporating additional data sources, thereby enhancing the accuracy and reliability of the results.

**Aknowledgements**

The study was supported by Special Basic Research Fund for Central Public Research Institutes (HKY-JBYW-2024-09).

**Theme:** Hydroinfomatics for extreme hydrological events and resilience improvement
**IAHR Thematic Priority Area:** [TPA-3] Improving Resilience against Water Hazards and Disasters
https://doi.org/10.3850/iahr-hic2483430201-452

# How and Where Flash Flood Hazards Come from?

**Changzhi LI[1], Dongya SUN[1], Bingshun HE[1]**

[1] China Institute of Water Resources and Hydropower Research, South Road, Yuyuantan, Haidian District, Beijing, 100038, China

*Corresponding author: lichangzhi@iwhr.com*

Flash floods are usually triggered by rainstorm and characterized by rapid abrupt rising and falling. In the past years, much attention has been paid to early warning system to delivery early warnings on flash flood disasters for local people. However, it is critical for the early warning system to identify how and where flash flood hazards come from in a timely way, then deliver warnings for those threatened by flash flood. Based on the recent typical flash flood disaster events in China, this study aims to find out the sources of flash flood hazards at catchment scale through early warning system. Generally, the countermeasures for identifying flash flood hazard sources include the following three categories.

First of all, hydrometeorological monitoring networks, widely used in flash flood disaster mitigation, need more refined performance. Ideally, a monitoring network should have powerful capacities of catching information on spatial and temporal rainstorm, flood stages at spots of interest, and some hidden dangers that may potentially magnify disasters if they are triggered. Typically, hidden dangers come from debris, bridge and culverts, small reservoirs or pounds, and riverside landslides. However, the acts are not exactly true for the following reasons. The first one is about time interval of rainfall record and sliding. Currently, the rain gages for flash flood monitoring can send rainfall depth to an early warning system each 5 minutes, but the comparison between the real rainfall and rainfall threshold are commonly conducted each hour at an hourly clock time, which may trigger flash flood early warning. Therefore, a very strong rainstorm within 60 minutes crossing an hourly clock time may be heavily cut off and averaged, and probably lead to neglecting a real rainfall depth exceeding the threshold of 60 minutes, then missing early warning delivery in a timely way. Therefore, a sliding time method is necessary for rainfall depth comparing rainfall threshold. The real rainfall records in Liulin flash flood event indicates that the differences between sliding rainfall depth and non-sliding rainfall depth are too significant to be ignored; another case is the flash flood event in Fuyang District, which has rainfall-runoff duration of about 40 minutes, much less than one hour. Hence, sliding is necessary for rainfall accumulation in a smaller time interval. The second one is about hidden factors which may significantly magnify disasters. A study on flash flood disaster mode has been conducted in which a mode consists of hazard, process and destroy manner, and eight modes are proposed as: (i) rainstorm-flood-inundating, (ii) rainstorm-flood-blocking-choking, (iii) rainstorm-flood-break-rushing, (iv) rainstorm-flood - (upper break lower blocking) - (rushing, choking and inundating), (v)rainstorm-flood-silting-rushing, (vi) rainstorm-flood-silting-rechannelling-inundating, (vii) rainstorm-flood-silting-sediment covering, (viii) rainstorm-flood- (upper break lower blocking) - silting-rushing and blocking. In these modes, small bridges, culverts, and movable stones, bamboos, and debris are usually found as factors which may drastically magnify disasters. Therefore, much attention should be paid to capturing the real situations about these factors and take proper actions during flash flood event. The third one is some real existing areas where there are no facilities for rainfall and flood monitoring, typically, the upper reach areas, no residents. This is very common in mountainous river basins where there is no rain gage in the upper reach areas, but rainstorms occur frequently, and towns or villages are usually located in the lower reach areas.

Secondly, hydrodynamical simulation are powerful approaches to predicate flash flood risk. Flood numeric simulation has the advantages of acquiring the information of rainfall-runoff, flood routing, debris flow, and failure of water-related structures, typically, the mixed scenarios of these situations, from which, the key information can be obtained on inundated area, water/debris depth, flow velocity, and energy. These outputs are remarkably helpful for local people to raise awareness and to take correct actions in case of flash flood disasters. Much attention should be paid to the following issues in order to get flash flood information by hydrodynamical simulation. First, rainfall amount and its timing spatial distribution. In many cases, rainfall is the most upper boundary conditions for flash flood simulation, in which a reliable rainfall process is crucially important, whether meteorologically predicated or rain-gage measured. Especially, capturing the rainfall peaking time and intensive rainfall location is a difficult but essential important point in flash flood modelling. A case in point is the Liulin flash flood event, flood process was simulated according to the rainfall process of two intervals (1 hour and 10 minutes) at Liulindian Gage, and the results indicate that, with same rainfall amount, the flood peak discharge of a rainstorm with 10-minute interval is 13% higher than that with 1-hour interval. In fact, the rainfall process with 1-hour interval has more homogenization than that with 10-minute interval, which reduces the flood peak discharge to a certain extent. Second, terrain data is another important factor that plays vital important role in flash flood modelling. However, the best available open terrain data, with spatial resolution of 12m, generally cannot meet the requirements of flash flood simulation. At least, river channels are needed to be excavated along villages and towns based on the terrain data. Third, more detailed information on terrain data are also needed to simulate flash floods in various scenarios. As mentioned before, some structures, such small bridges, culverts, are prone to be blocked by movable stones, bamboos, or debris; moreover, structure failures may lead to significant losses of life and property. A quintessential example is the Wangzongdian-Haigouzhai flash flood event in Zhengzhou 7.20 Extreme Rainstorm Disaster. Therefore, the sizes of these structures are necessary for flash flood risk analysis.

Thirdly and the last one, experiences from historic flash flood disaster events, including local or similar areas disaster events are also important ways to find out flash flood hazard. In words of water digitalization, it is Knowledge Base of flash floods. The main sources for this base include the following aspects. The first is rainstorm-flood retrospective analysis. Commonly, retrospective analysis needs to be performed for each flash flood event to find out the reasons, available measures to improve response actions in similar cases in the future. This analysis on typical flash flood events indicates that the sources of flash flood disaster mainly include rainstorm within a very short duration, such as 1 hour, 3 hours, bridge and culvert prone to blocking, sediment silting or scour, and debris flow, etc. Second, flood marks. They are natural marks or artificial inscriptions left on buildings or banks along rivers that mark the highest flood level, and make the public intuitively feel the harm of floods, further play the role of publicity, education and warning, help the public to strengthen the awareness of flood disaster risk, improve the self-rescue capability. Typically, after 2023 Catastrophic Floods, Beijing has set up many flood marks in ways of engraving and filling, spray printing, stainless steel plate or bronze plate, stone pillar, etc.; moreover, QR Code technology has also been used on flood mark with purpose of providing more detailed information. Finally, remote sensing interpretation technology can contribute much to identify occupation of flood passage area. For a specific region, flood awareness of local people is always deceasing after disaster, on the contrary, occupation to flood passage area become more and more, and remote sensing technology is one of the practical means to find out the occupation to flood passage area in a timely way.

**Keywords:** Countermeasures, Flash flood, Hazard source

**Theme:** Hydroinfomatics for extreme hydrological events and resilience improvement
**IAHR Thematic Priority Area:** [TPA-3] Improving Resilience against Water Hazards and Disasters
https://doi.org/10.3850/iahr-hic2483430201-454

# Regionalization of Flash Floods in the Hengduan Mountains, China, with Graph Neural Network Methods

**Yifan Li[1, 2], Chendi Zhang[1], Shunyu Yao[3,4], Guotao Zhang[1]**

[1] Key Laboratory of Land Surface Pattern and Simulation, Institute of Geographic Sciences and Natural Resources Research, CAS, Beijing 100101, China
[2] College of Resources and Environment, University of Chinese Academy of Sciences, Beijing 100049, China
[3] China Institute of Water Resources and Hydropower Research, Beijing 100038, China
[4] Research Center on Flood and Drought Disaster Reduction of the Ministry of Water Resources, Beijing 100038, China
*Corresponding author: zhangchendi@igsnrr.ac.cn*

**Abstract.** The geomorphology, meteorology and underlying surface conditions of the Hengduan Mountains region are complicated. And this region is seriously threatened by flash flood disasters. Flash flood regionalization contributes significantly to quantifying the spatial heterogeneity of disaster-inducing factors of flash floods. In this study, we applied three state-of-the-art unsupervised graph neural network (GNN) methods, which considered both the attribute characteristics and spatial topology structure of the input data, to establish the regionalization of flash floods at raster-scale in the Hengduan Mountains. Our research provides a scientific basis for flood control and disaster reduction in southwest mountainous areas.
**Keywords:** Disaster-inducing factors, flash floods, graph neural network, regionalization, the Hengduan Mountains

## 1 Introduction

Flash floods are devastating natural disasters that have a significant impact on the economic and social development of mountainous regions in China. In the past two decades, flash floods have accounted for 66.4% of flood-related casualties in China [1]. The Hengduan Mountains region is seriously threatened by flash flood disasters, surpassing the national average. With the background of global climate change [2], it is anticipated that the frequency and magnitude of flash flood disasters in the Hengduan Mountains will increase in the future. With increasingly severe and frequent flash flood disasters, the need for accurate forecast and early warnings for flash flood disasters, and effective disaster prevention and reduction facilities is also growing. However, these are limited by the lack of advanced monitoring equipment for hydrology and rainfall. Flash flood regionalization, an important means of flash flood research, contributes significantly to quantifying the spatial heterogeneity of flash flood disasters and their influencing factors, provides insights to the formation mechanism of flash floods, and offers estimates for the key hydrological parameters related to flash floods in ungauged regions. Clustering is the typical method used for flash flood regionalization, with various traditional clustering methods [3] and machine learning techniques [4]. However, these approaches have not fully considered the spatial topology structure of input geographical data and hence, the spatial interactions among the input data cannot be reflected in the regionalization.

This study aims to establish flash flood regionalization in the Hengduan Mountains, incorporating the spatial topology of flash flood factors and revealing distribution patterns. Three state-of-the-art unsupervised GNN methods (Dink-Net, DGI, and DMoN) were applied to establish raster-scale regionalization results, which were compared with non-spatial methods like K-means and SOFM. These GNN methods offer advantages in integrating large-scale data with spatial information, enhancing clustering performance and scalability.

## 2 Study Area and Data

The Hengduan Mountains region is situated at the junction of the first and second topographic ladder, specifically at the southeastern margin of the Qinghai-Tibet Plateau. Encompassing the western portion of Sichuan Province, the southeastern portion of Tibet Autonomous Region, the northern portion of Yunnan Province, and portions of Qinghai and Gansu, the region spans a total area of about 420,000 $km^2$.

The selection of influencing factors for flash floods has a direct impact on the regionalization result of flash floods. Based on previous research in the study area, we selected 18 key disaster-inducing factors for this study, covering topographic and geomorphologic factors (DEM, slope, Aspect, Relief, topographic wetness index(TWI), stream power index (SPI), drainage network, fault, and geomorphic type); climate and meteorological indicators (annual mean temperature, annual mean rainfall, annual mean potential evapotranspiration, and multiple extreme rainfall factors with different statistical characteristics); and underlying surface factors (NDVI, vegetation type, soil type, soil texture, soil **depth, and soil gravel content).**

## 3 Methods

After pre-processing the topographic and geomorphologic factors, climate and meteorological indicators, and underlying surface factors, the graph data is constructed. The graph data is then classified into regional units using the deep graph clustering methods, as well as using the traditional clustering analysis method. The clustering quality index (CQI) is calculated to determine the optimal number of regionalizations for all methods. All the regionalization results are evaluated based on both the Davies-Bouldin Index (DBI) and the spatial distribution of historical flash flood disasters. The fragment polygons with an area smaller than 200 $km^2$ are merged into the adjacent large polygons by the Eliminate tool in ArcGIS 10.8 before the final regionalization of flash floods was achieved.

## 4 Results

The regionalization results obtained from the three GNN methods matched better with the spatial distribution of historical flash flood disasters, compared with regionalization results obtained from traditional results. Among the three GNN methods, Dink-Net had the smallest DBI value, showed the regionalization closest to the distribution of historical flash floods, and required the least computation time. Based on CQI value, the region is divided into14 regionalization subunits based on Dink-Net method. The result showed that the flash flood disaster frequently occurred in regionalization subunit 3, 10 and 14. In subunit 3 and subunit 10, annual mean temperature, annual mean rainfall, and altitude were the main influencing factors. In subunit 14, the influence of slope and hypsography were also important, in addition to the above factors.

## 5 Conclusion

This research verified the effectiveness of GNN methods in geographical regionalization. Average rainfall, average temperature, altitude, slope, and topographic height difference are important factors influencing the zoning of mountain flood.

## Reference

[1] MINISTRY OF WATER RESOURCES OF CHINA. 2021 Bulletin of Flood and Drought Disasters in China [R]. Beijing: Ministry of Water Resources of China, Beijing, 2022.

[2] HIRABAYASHI Y, MAHENDRAN R, KOIRALA S, et al. Global flood risk under climate change [J]. Nature Climate Change, 2013, 3(9): 816-21.

[3] ZHANG R, CHEN Y, ZHANG X, et al. Mapping homogeneous regions for flash floods using machine learning: A case study in Jiangxi province, China [J]. International Journal of Applied Earth Observation and Geoinformation, 2022, 108: 102717.

[4] EKMEKCIOĞLU Ö, KOC K, ÖZGER M, IŞIK Z. Exploring the additional value of class imbalance distributions on interpretable flash flood susceptibility prediction in the Black Warrior River basin, Alabama, United States [J]. Journal of Hydrology, 2022, 610: 127877.

**Theme:** Hydroinfomatics for extreme hydrological events and resilience improvement
**IAHR Thematic Priority Area:** [TPA-3] Improving Resilience against Water Hazards and Disasters
https://doi.org/10.3850/iahr-hic2483430201-457

# Dynamic Analysis of Flash Flood Risk Warning Considering Soil Moisture Variability and Risk Factors

**Xiaoyan Zhai[1,2], Ronghua Liu[1,2], Chaoxing Sun[1,2], Xiaolei Zhang[1,2], Qi Liu[1,2]**

[1] China Institute of Water Resources and Hydropower Research, Beijing 100038, China
[2] Research Center on Flood and Drought Disaster Reduction of the Ministry of Water Resources, Beijing 100038, China

*Corresponding author: Liurh@iwhr.com*

**Abstract.** Flash flood disaster induced by heavy rainfall with short duration is regarded as one of the most devastating natural hazards in China. The current flash flood disaster risk warning methods usually neglect the effects of dynamic variations of soil moisture and underlying conditions, resulting in low accuracy of early-warning and frequent occurrences of false alarms. To address this issue, this study combines the real-time dynamic simulation of soil moisture and multi-factor risk assessment, and proposes the flash flood dynamic risk warning model that comprehensively considers soil moisture variability, flash flood hazard, exposure and vulnerability. The accuracy and lead time of the proposed model are assessed taking the historical flash flood disaster events in Guangdong province as an example. Results showed that the flash flood dynamic risk warning model can accurately simulate the hourly variability of soil moisture at catchment scale in the flood season with the determination coefficient greater than 0.90. The warning accuracy of the model was high with a lead time of 24 hours, as the occurrences of three flash flood disaster events were exactly forecasted by the model, which were within the very high and high possibility warning ranges.

**Keywords:** Dynamic risk warning; Flash flood disaster; Multi-factor risk assessment; Soil moisture variability

## 1 Introduction

Flash flood disaster induced by heavy rainfall with short duration is regarded as one of the most devastating natural hazards in China, which is characterized by sudden onset, fast rising and declining processes, and pose great challenges for flash flood disaster prevention and control. The timely and accurate forecasting and warning of flash floods at catchment scale provides information supports and references for personal evacuation and lifesaving. The current flash flood disaster risk warning methods characterized by long lead time and wide coverage, has been widely used to remind the public for travel alert. However, the method usually neglects the effects of dynamic variations of soil moisture and underlying conditions, resulting in low accuracy of early-warning and frequent occurrences of false alarms. In this study, a flash flood dynamic risk warning model is proposed, which comprehensively considers soil moisture variability, flash flood hazard, exposure and vulnerability.

## 2 Flash flood dynamic risk warning model

The design rainfalls with various return periods are determined as the benchmarks for rainfall thresholds at different warning levels. Specifically, four warning levels are divided, including low, medium, high and very high possibility levels, and the corresponding benchmarks are rainfalls with 2-year, 5-year, 20-year and 50-year return periods. Based on the benchmarks for rainfall thresholds, the flash flood dynamic risk warning model is constructed through combining the real-time dynamic simulation of soil moisture and multi-factor risk assessment. The flash flood rainfall threshold with various warning levels can be dynamically determined and are compared with the forecasted rainfall in the future 24 hours. If the forecasted rainfall amount exceeds the rainfall threshold at certain

warning levels, the corresponding risk warning information is considered to be issued. Compared with the static flash flood warning model, this model can improve the warning levels for catchments with high risks and soil moistures.

## 3 Study area and data sources

Flash flood disasters occur frequently in Guangdong province, China, which is selected for case study. The data sets for flash flood dynamic risk warning are collected including geographical information system (GIS) data, flash flood disaster evaluation and assessment data, historical flash flood disaster events, soil moisture observations, rainfall observations and forecasted 24h rainfall data.

## 4 Results and Discussion

Based on CNFF model, a total of 152 model units are constructed for the dynamic soil moisture simulation at catchment scale with an average area of 1322 $km^2$. The determination coefficients between the simulated and observed soil moisture processes are greater than 0.90 for most stations. Thus, CNFF mode can well reflect the dynamic variability of soil moisture in Guangdong province.

The flash flood risk levels at catchment scale are determined on basis of the multi-factor risk assessment. The ratios of small catchments with high, medium and low risk levels are 9.07%, 33.50% and 57.43%, respectively. The flash flood risk warning levels are considered to be increased for small catchments with high risk levels.

The occurrences of three flash flood disaster events are exactly forecasted by the flash flood dynamic risk warning model. Specifically, the disaster event on June 13, 2019 is forecasted to be within the medium possibility warning range, and the disaster event on May 21, 2020 is forecasted to be within the very high possibility warning range. While the disaster event on May 18, 2019 is forecasted to have no warning. Because the forecasted 24h rainfall with a total amount of 8 mm is much lower than the observed rainfall with a total amount of 103 mm during six hours. Thus, the warning accuracy of the model is high with a lead time of 24 hours. It should be noted that the accuracy of the flash flood dynamic risk warning model is significantly affected by to the quality of forecasted rainfall data, which should be further improved in further studies.

## 5 Conclusions

In this study, the flash flood dynamic risk warning model is proposed that comprehensively considers soil moisture variability, flash flood hazard, exposure and vulnerability. The model could accurately simulate the hourly variability of soil moisture at catchment scale in Guangdong province, the flash flood risk levels were identified at catchment scale, and the flash flood risk warning accuracy was high with a lead time of 24 hours.

## 6 Acknowledgements

This study was supported by the National Natural Science Foundation of China (No.42171047).

## Reference

[1] L. Guo, L.Q. Ding, D.Y. Sun, C.J. Liu, B.S. He, R.H. Liu. Key techniques of flash flood disaster prevention in China. Journal of Hydraulic Engineering. 49(2018) 1123-1136.

[2] X.Y. Zhai, Y.Y. Zhang, Y.Q. Zhang, L. Guo, R.H. Liu, Simulating flash flood hydrographs and behavior metrics across China: implications for flash flood management. Sci. Total Environ. 763 (2021) 142977.

[3] S. Lei, Y.W. Liu, Risk early warning research of progressive-type mountain torrent disaster and practice. Water Resources and Power. 38 (2020) 87–90.

[4] H. Xu, Y. Cao, Z.Y. Zeng, A method of flash flood risk early warning based on FFPI. Journal of Catastrophology. 35 (2020) 90–95.

[5] B.W. Liu, H.H. Li, J. Hu, Study on the precipitation rainfall at the meteorological risk pre-alarm for Yunnan's Chuxiong prefecture. Yunnan Geographic Environment Research. 31 (2019) 6–12.

**Theme:** Hydroinfomatics for extreme hydrological events and resilience improvement
**IAHR Thematic Priority Area:** [TPA-3] Improving Resilience against Water Hazards and Disasters
https://doi.org/10.3850/iahr-hic2483430201-459

# Real Time Modelling for Flash Floods Decision Support Systems: Needs and Gaps

**Philippe Gourbesville**[1,2]

[1] Institute of Water Resources and Hydropower Research, China
[2] Université Côte d'Azur, Polytech Lab, 930 route des Colles,06903 Sophia Antipolis, France
Corresponding author: philippe.gourbesville@unice.fr

**Abstract.** The mitigation of flash flood events impacts requests to have an accurate understanding of processes and an efficient strategy based on a good preparedness. Within the crisis management procedure, the time is a key variable: most of the events are characterized by a very sudden and short duration and consequently, reaction time from rescue teams must be as reduced as possible. Within this context, Decision Supports Systems must integrate modeling tools that are able to operate in real time and to deliver the expected results within the timeframe of the event itself. These requirements do not fit with most of the Hydroinformatic models that have been developed for an engineering use focused on design or assessment tasks. The analysis of various DSSs currently deployed mainly in Europe and in Asia has allowed to identify needed improvements to match the expectation of the flood managers and other first responders' teams. Efforts should be focused on multiple model approaches, cloud computing and spatial information rendering.

**Keywords:** Cloud computing, Decision Support Systems, Flash floods, Multi model approach, Real-time, Spatial information.

## 1 Context

The mitigation of flash flood events impacts requests to have an accurate understanding of processes and an efficient strategy based on a good preparedness. Within the crisis management procedure, the time is a key variable: most of the events are characterized by a very sudden and short duration. Consequently, reaction time from rescue teams must be as reduced as possible. Within this context, Decision Supports Systems (DSSs) must integrate modeling tools that are able to operate in real time and to deliver the expected results within the timeframe of the event itself. These requirements do not fit with most of the Hydroinformatic models that have been developed for an engineering use focused on design or assessment tasks. The development of efficient flash flood warning systems requests to choose, to adapt and to tune the models able to produce the requested information for the flood managers and the first responders' teams.

## 2 Methodology

Identification of needs was achieved by a review of major flood warning systems in Europe and in Asia countries applied for different scales:

- National Flash Flood disaster prevention platform used in China (https://weather.cma.cn/) [1];
- VigieCrues - French national modelling architecture for flood forecasting (https://www.vigicrues.gouv.fr);
- Länderübergreifendes Hochwasser PortalLHP – German national center for flood monitoring (https://www.hochwasserzentralen.de);
- Tokyo Metropolitan Flood Control Integrated Information System (https://www.kasen-suibo.metro.tokyo.lg.jp/im/uryosuii/tsim0102g_en.html)
- AquaVar – Decision Support System used by Nice Metropolis in France [2], [3].

## 3 Results and discussion

The analysis has identified three key areas: simplification of orchestration tasks, optimization of computing tasks and improved rendering processes especially for spatial information.

### 3.1 Multiple models approach

The time constraint requests to mobilize models able to produce in limited time realistic estimations for hydrographs. This operational constraint imposes frequently to combine various models to achieve the production of expected forecasts. Obviously, the initial point is defined by the availability of an estimation of the precipitation event's intensity at the relevant spatial scale (resolution of 5 $km^2$ or lower). This information must be available continuously not less than two to one hour ahead. The production of this spatial forecast can be based on meteorological model outputs, radar images and field observations. The implementation of an efficient procedure for data production, collection and synthesis is essential and determines the quality of the full warming procedure. The meteorological analysis of the on-going event must help to identify the magnitude of the precipitations and to assess its frequency. Recurrent events request responses that are well known and frequently implemented by the field teams. However, exceptional conditions such as large convective cells or combination of several convective cells, must be identified as early as possible. The extreme conditions – return period higher than 100 years – are associated to physical processes like intense runoff and sediment transport that are not commonly faced by the first responders and flood managers. During those extreme events, additional processes like landslides are involved and can greatly generate complex conditions for rescue teams. The early identification of the rainfall intensity is a major input for the modelling strategy targeting hydrographs and inundation maps production. In fact, data driven and conceptual models frequently used for events with higher frequency are not able to generate consistent results as the extreme conditions are not included within their knowledgebase or training data. Added value of distributed deterministic hydrologic models has been demonstrated in numerous cases to produce meaningful hydrographs for extreme events. The experience gained over the last recent events [4], [5], has demonstrated the robustness of the approach and its efficiency to deliver estimations that can be used as a first estimation of the processes. The modelling approach within the warning systems must combine multiple models - data driven, conceptual and deterministic – to ensure the expected quality of forecasts. The difficulty to address extreme conditions suggests simulating such conditions with deterministic approaches and to use the results as training inputs for data driven models. The procedure can potentially improve the performance of the system but obviously request an easier way for models' integration within the DSS platforms and standards on data formats and exchange procedures.

### 3.2 Cloud computing solution

The production of forecasts based on multiple model approach requests important computational resources. At the same time, field observation data are increasing and are enriched continuously with new devices like water focused satellites. The cloud architecture is offering storing facilities and computational power that can be mobilized on demand. In addition, the solution can be accessed remotely through web interface standards and offers efficient security environment. The cloud approach is obviously the target environment for the early warning systems especially dedicated for flash floods. However, a relevant deployment within the cloud environment requests to address the data format, the orchestration of modules and the rendering of spatial information. Standards are lacking in those three key sectors and initiatives must be taken quickly to ensure a smooth integration within the existing cloud environments: OpenMI [6] is a potential answer for efficient orchestration and WaterML 2.0 OGC standard [7] is a format that could be extended to models' outputs.

### 3.3 Spatial information rendering

The data management procedures involved within the preprocessing and the post processing processes are now frequently the most challenging bottlenecks for the implementation and

deployment for real-time operation of the modelling systems. In fact, the constraint can be easily understood by the used data formats that are currently used by most of tools were not designed with the objective of real-time operation. For this reason, formats remain heavy and lengthy by mobilizing heavy computational power and writing process within the storing devices. The spatial information is frequently addressed with GIS tools that are mobilizing databases and displaying routines. In such environments, representation of dynamic processes like inundation propagation requests to display attributes of pixels over time. The frequently used format netCDF (Network Common Data Form) allows to handle array-oriented scientific data and is mobilized to generate inundation maps in a pixel-based approach. The lack of efficient data format and the systematic use of pixel-based approach are two major constraints that are deeply affecting the development of real-time modelling. Innovative data formats able to handle large spatial datasets and dynamic processes are deeply needed. The current formats [8] such as GRIB (Gridded Binary), BUFR (Binary Universal Form for the Representation of meteorogical data), HDF5 (Hierarchical Data Format 5, [9]), netCDF4 (last evolution of the netCDF format, [10]) and Zarr (file format designed to store large arrays of data) are not providing the requested performance even if they are offering potential improvements such as HDF5. In addition, the needed formats must be compliant with the WaterML 2.0 OGC standard [7] that is the standard information model for water observations.

## 4 Conclusions

The performed analysis has identified three areas where efforts must be concentrated. The lack of efforts in those areas contributes to restrain the efficiency of the early warning systems addressing the flash flood issues. Efforts must be engaged to produce unified and consolidated approaches that can ensure the production of the needed tools and standard procedures to improve efficiency of systems and improve resiliency of exposed populations.

## References

[1] Liu, C., Guo, L., Ye, L., Zhang, S., Zhao, Y. and Song, T., 2018. A review of advances in China's flash flood early-warning system. *Natural hazards*, *92*, pp.619-634.

[2] Gourbesville, P., Tallé, H.A. and Ghulami, M., 2022. AquaVar: High Performance Computing for Real Time Water Management.

[3] Gourbesville, P., Tallé, H.A., Ghulami, M., Andres, L. and Gaetano, M., 2022. Challenges for Realtime DSS: Experience from Aquavar System. In Advances in Hydroinformatics: Models for Complex and Global Water Issues—Practices and Expectations (pp. 719-735). Singapore: Springer Nature Singapore.

[4] Pons, F., Bonnifait, L., Criado, D., Payrastre, O., Billaud, F., Brigode, P., Fouchier, C., Gourbesville, P., Kuss, D., Le Nouveau, N. and Martin, O., 2022, May. Towards a hydrological consensus about the 2nd-3rd October 2020 ALEX storm event in the French" Alpes Maritimes" region. In EGU General Assembly Conference Abstracts (pp. EGU22-7913).

[5] Liu, C., Ma, Q., Zhang, X., Li, C., Li, Q., Gourbesville, P., Guo, L. and Ding, L., 2022. Identification and quantitative analysis of flash flood risks for small catchments in China: A new operational modelling approach. LHB, 108(1), p.2019561.

[6] Harpham, Q.K., Hughes, A. and Moore, R.V., 2019. Introductory overview: The OpenMI 2.0 standard for integrating numerical models. *Environmental Modelling & Software*, *122*, p.104549.

[7] Grellet, S. and van Der Schaaf, H., 2024, January. Integrating new OGC Standards-SensorThings API and WaterML2. 0-Water Quality Interoperability experiment. In *Concept Note for Capacity Building on Hydrological Data Exchange, standardization, and Interoperability in Region VI*.

[8] Ambatipudi, S., & Byna, S. (2022). A comparison of hdf5, zarr, and netcdf4 in performing common i/o operations. *arXiv preprint arXiv:2207.09503*.

[9] Folk, M., Heber, G., Koziol, Q., Pourmal, E., & Robinson, D. (2011, March). An overview of the HDF5 technology suite and its applications. In *Proceedings of the EDBT/ICDT 2011 workshop on array databases* (pp. 36-47).

[10] Lee, C., Yang, M., & Aydt, R. (2008). NetCDF-4 performance report. *URL: https://support. hdfgroup. org/pubs/papers/2008-06 netcdf4 perf report. pdf*.

**Theme:** Hydroinfomatics for extreme hydrological events and resilience improvement
**IAHR Thematic Priority Area:** [TPA-3] Improving Resilience against Water Hazards and Disasters
https://doi.org/10.3850/iahr-hic2483430201-462

# Driving Factors and Refined Risk Identification Framework of Flash Flood Disasters in China

**Xiaolei Zhang[1], Ronghua liu[1], Rong Zhou [2], Ruihua Qin [3]**

[1]China Institute of Water Resources and Hydropower Research, 100038, Beijing, China
[2] China Renewable Energy Engineering Institute, 100013, Beijing, China
[3]Xi'an University of Architecture and Technology, 710399, Xi'an, China

*Corresponding author: zhangxl@iwhr.com*

**Abstract.** Mountain flash flood disasters are regarded as one of the most serious natural disasters worldwide, characterized by their acute spontaneity, swift escalation, immense destructive force, and high propensity for inflicting substantial casualties. Thus, for effective management and mitigation, it is crucial to identify potential high risk areas, and to adopt effective approaches. Located on the southeast coast of China, Fujian Province features a landscape dominated by continuous hills, with upland areas accounting for 90% of its territory, significantly surpassing the national average of 66.7%. Fujian Province presents complex terrain structures, frequent occurrences of heavy rainstorms, and densely populated areas. Mountain flash floods in Fujian have led to massive economic losses and considerable loss of life. This paper focuses on exploring the driving factors behind mountain flash flood disasters in Fujian Province, aiming to identify high-risk zones.

**Keywords:** flash flood; risk; driving factors

## 1 Introduction

Climate change has altered hydrometeorological patterns. Flash flood disaster, as a kind of sudden flood disaster, has higher destructive power in a short time. In China, high frequency and high death toll account for 70% of the flood disaster losses. In order to mitigate and respond to extreme disaster events, it is urgent to select the driving factors affecting disasters, and develop reliable modeling techniques to identify the risk regionalization of flash flood disasters.

## 2 Objectives

This project reveals the risks of flash flood disasters by analyzing the relationship between the disaster environment, rainfall, human activities and other aspects of flash flood disasters in Fujian province, so as to identify potential risk areas and provide solid foundation for early warning decision-making.

## 3 Methods

According to the characteristics of rainfall, underlying surface and human activities in Fujian Province, a total of 54 alternative indicators were obtained such as rainfall characteristics, underlying surface characteristics. Principal component analysis was used to reduce the dimension of 54 alternative indicators and 10 main indicators were obtained. It includes the elevation of villages, distance between villages and rivers, short duration heavy rainfall in small watershed, topography, confluence time, flood peak modulus, wading projects, housing types, current flood control capacity, monitoring and warning facilities.

According to the risk theory, the index system of flash flood disaster risk analysis is constructed by integrating the above indexes, and the index system is constructed and analyzed from three dimensions of risk, exposure and vulnerability.

## 4 Results

The high risk areas are mainly concentrated in coastal areas with high typhoon frequency and inland mountainous areas with high rainstorm value. Meanwhile, through comparative analysis of historical flash flood disasters in Fujian Province, 80% of historical flash flood disasters fell in high-risk and medium-risk areas. The occurrence density of flash flood disaster in high-risk areas is 3 times than that in low-risk areas.

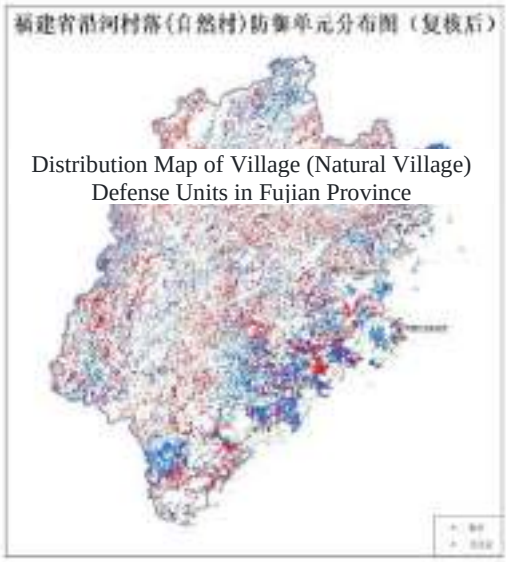


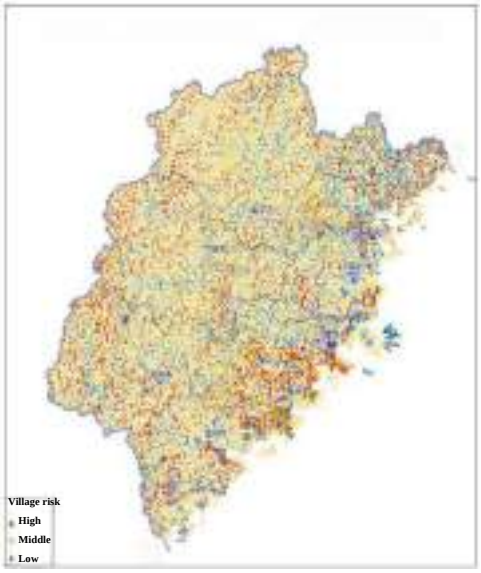


Figure 1 Distribution Map of Coastal Village (Natural Village) Defense Units in Fujian Province

Figure 2 Risk level distribution map of administrative villages in Fujian province

## 5 Conclusion

(1) Flash flood risk identification based on small watershed can reflect the response of flash flood disaster to short-term heavy rainfall, the underlying surface and human activities. The risk assessment method based on watersheds has a certain physical mechanism.

(2) The evaluation results show that flash flood disaster prone area in Fujian Province is concentrated in the coastal area affected by typhoon rainstorm and the high value area of severe convective rainstorm in inland mountainous area. The frequency of flash flood disaster is affected by both natural environment and human activities.

(3) Through the verification of historical flash flood disaster data, the risk identification results are reliable, and risk assessment model can reflect the risks more accurately, which can provide reliable support for flash flood disaster prevention and accurate forecast and early warning.

## Reference

[1] Cheng Dong, Liu Ronghua, Zhai Xiaoyan, et al. Real-time dynamic analysis of flash flood warning indicators based on Chinese mountain hydrological models [J]. Journal of China Institute of Water Resources and Hydropower Research, 2023, 21(5): 444-454.

[2] Zhang Xiaolei, Liu Qi, Liu Ronghua, et al. Exploration and Design of a List-based Management Model for Hazardous Areas Affected by Mountain Torrent Disasters [J].China Flood and Drought Management, 2022, 32(11): 48-53.

**Theme:** Hydroinfomatics for extreme hydrological events and resilience improvement
**IAHR Thematic Priority Area:** [TPA-3] Improving Resilience against Water Hazards and Disasters
https://doi.org/10.3850/iahr-hic2483430201-464

# National Mountain Flood Disaster Supplementary Survey and Evaluation of Key Cities and Towns Results Review Rules Discussion

**Xie min [1] Dou yan hong [1] Zhang xiao lei [1]**

China Institute of Water Resources and Hydropower Research, Bei Jing, 100038, China

*Corresponding author: Dou yan hong, xiemin@iwhr.com*

**Abstract.** In order to fully grasp the underlying surface conditions of small watersheds in hilly areas,the country has launched a supplementary investigation and evaluation of flash flood disasters, and on the basis of the first round of villages along rivers, new key urban market towns have been added.This paper expounds the contents of supplementary investigation and evaluation of key cities and towns，introduces in detail the principles, contents and rules of national results audit, and discusses the rationality of new early warning indicators,the scientificity of related stations, the professional audit rules of dangerous areas and resettlement sites on the basis of formal audit of data quality,which effectively improves the quality of results and greatly improves the application value of results. To lay a solid foundation for the transformation of mountain flood disaster prevention from "having" to "good".

**Keyword:** flash flood disaster; investigation and evaluation; audit rule; quality control

## 1 Introduction

In order to fully grasp the conditions of the sub-basin in small watersheds in hilly areas, the country has launched a supplementary survey and evaluation of flash floods. On the basis of the first round of surveys and evaluations, new key cities and towns were added. Its main work content is to investigate in detail the latitude and longitude, elevation of the house foundation, gate address, personnel, housing type, etc. of each residential building in the key cities and market towns. Measurement of river control sections, comprehensive evaluation of the current flood control capacity of key cities and towns, calculation of the inundation range of floods of 5, 10, 20, 50 and 100 years, etc., and determination of flash flood hazard levels in different regions.

## 2 Audit Principles

The main principle of the review of the results is that the national flash flood prevention and control project team is responsible for reviewing and compiling the work at the national level, which focuses on evaluating the reliability, completeness, standardization, consistency and reasonableness of the data at the macro level, and requires that the rate of reviewing and passing the review be more than 95 per cent.

## 3 Audit Content

The main elements to be reviewed are data, data catalogs,data content, attribute fields, data formats, file formats, and other elements. And the reasonableness of the data, values, quantities and densities are reviewed.

## 4 Audit Rules

The rules for this audit are divided into a formal audit and a professional audit.
Formal audit focuses on data reliability, completeness and standardization, and found that the number of tasks is missing, the catalog is missing, the content does not conform to the template, the table

duplicates the primary key, the column type does not match, and so on, more than 20 kinds of common error-prone problems.

The professional audit focused on data consistency and reasonableness. The first audit analyzes and evaluates the representativeness of cities and towns to avoid centralized distribution in some watersheds. Then, the key contents such as population and households, static warning indicators, hazardous areas and resettlement sites, automatic monitoring stations, etc. were audited. Finally, it produces a statistical form for the audit and a distribution map of the reported data.

## 5 Conclusions

The result data of the National Supplementary Survey and Evaluation of Flash Flood Disasters in Key Cities and Market Towns are highly specialized, with large data volume, diverse types and complex topological relationships. The national flash flood prevention and control project team, in accordance with the audit rules introduced in this paper, based on the data warehouse data audit method combining automatic software audit and manual interpretation, utilized ETL technology to effectively identify problems in the data, realized the data quality control objectives, effectively supplemented the national flash flood survey and evaluation results database, and provided reliable data support for the prevention and control of flash floods.

## Reference

[1] Guo Liang, Ding Liuqian, Kuang Shangfu, Key technology and application of investigation and evaluation of flash flood disaster in China, [J]. China Flood Control and Drought Management, 2018.

[2] Huang Xianlong, Chu Minghua, Shi Jinsong, An analysis of investigation and evaluation of flash flood disaster in China, [J]. China Flood Control and Drought Management, 2015.

[3] Zhu Xisong, Xiao Biao, A preliminary study on dynamic management and hierarchical management of flash flood hazardous areas in Sichuan Province, [J]. China Flood Control and Drought Management, 2021.

[4] He Bingshun, Supporting Fine Management with Hazardous Area Classification and Winning Preventive Initiatives with Progressive Early Warning China Water Resources News/2023 Key Technologies and Applications for Investigation and Evaluation of Flash Flood Disasters in China

**Theme:** Hydroinfomatics for extreme hydrological events and resilience improvement
**IAHR Thematic Priority Area:** [TPA-3] Improving Resilience against Water Hazards and Disasters
https://doi.org/10.3850/iahr-hic2483430201-466

# A Framework for Merging Precipitation Retrievals and Gauge-based Observations Based on A Novel Concept Namely Virtual Gauges

**Yanhong Dou**[1]

[1] China Institute of Water Resources and Hydropower Research, Beijing 100038, China

*Corresponding author: douyh@iwhr.com*

**Abstract.** The merging of multi-source precipitation retrievals (PRs) and gauge-based observations (GO) provides a new opportunity for precipitation field estimation. However, the uncertainties associated with PRs may become relatively more evident when the gauge network better captures the spatial distribution of the rainfall fields. To dynamically balance the utilisation of PRs, we propose a merging framework based on a novel concept; namely, the virtual gauge, where the grid cells utilising PRs are regarded as virtual gauges, and the framework is henceforth referred to as VG. The main steps were as follows: i) determine the locations of virtual gauges from multi-source PRs, ii) estimate rainfall at virtual gauges using a basic merging method, and iii) spatially interpolate using both actual and virtual gauges. Accordingly, the case study employed random forest (RF) and inverse distance weight (IDW) as the basic merging and interpolation methods of VG. Evaluation using real world data over a region where nearly each 0.1◦ grid cell contains a ground gauge indicates that VG improves around 7–11% over its basic methods and improves around 32–240% over its inputting PRs. VG performed better and was more stable than the basic methods under various gauge densities, rainfall intensities, and rainfall distributions.

**Keywords:** Precipitation merging; Gauge density; Rainfall field distribution; Virtual gauges; Multi-source precipitation products

## 1 Introduction

Accurate monitoring of precipitation fields remains challenging owing to their large spatial heterogeneity. In general, there are two approaches to estimating precipitation. One is via gauge-based observations (GO), which is known as the direct measurement approach. The other is via grid precipitation retrieval (PRs) based on radar, satellites, numerical weather models, and crowd-sourced models; known as indirect estimation approaches. GO is accurate at the point scale, but maximum or minimum rainfall can be missed. Indirect estimation approaches make it possible to obtain the locations of maximum and minimum rainfall, but there are still multiple errors and uncertainties in the rainfall estimations of PRs [1], particularly in PRs which can be obtained in real-time or near real-time. Hence, merging the two mainstream approaches of precipitation estimation is significant. Based on the advantages and disadvantages of GO and PRs, two types of merging principles can be considered. They are: i) to correct rainfall estimations of PRs using GO as a reference and ii) to supplement the spatial distribution information of rainfall fields interpolated by GO using PRs. In recent years, efforts have been made to derive grid rainfall estimations by merging GO and PRs following the first type of merging principle.

## 2 Methodology

As shown in Fig. 1b, when estimating rainfall fields by spatial interpolation using ground gauges, the theoretical range of rainfall estimation located at the grid cell ($x$) without gauges can be approximated as:

$$\widehat{P_x} \in [P_{min}, P_{max}]$$

where

$$P_{min} = \min\left(P_{G_1}, P_{G_2}, \ldots\right)$$
$$P_{max} = \max\left(P_{G_1}, P_{G_2}, \ldots\right)$$

$\widehat{P_x}$ indicates the estimated rainfall located in grid cell $x$. $P_{G_i}$ indicates the rainfall measured by $G_i$. $G_i$ indicates the ground gauge within a certain distance from the grid cell $x$. However, as shown in Fig. 1, rainfall in a number of grid cells is heavier than $P_{max}$ or lighter than $P_{min}$, resulting in the loss of spatial information of the rainfall field by spatial interpolation using only actual gauges. After adding the virtual gauges, spatial information was supplemented.

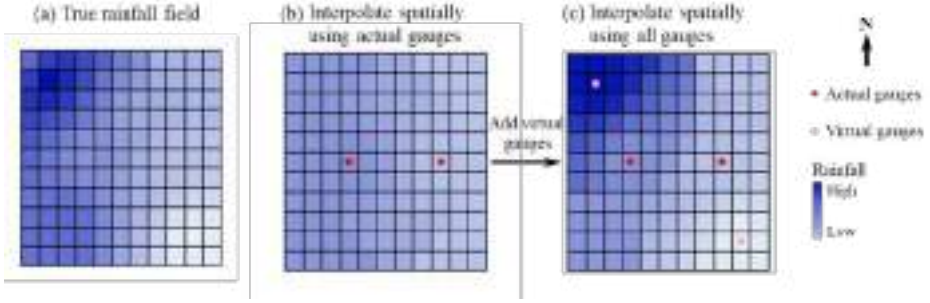


Fig. 1. Schematic diagram of the effect of the virtual gauges.

The main steps of the proposed VG are i) dividing the study area into multiple sub-areas; ii) for each sub-area, determine the locations of virtual gauges from the spatial comparison between the rainfall fields estimated by multiple PRs and GO; iii) estimating rainfall located at virtual gauges by grid-by-grid merging methods; and iv) spatial interpolation using both actual gauges and virtual gauges.

## 3 Results

The VG and RF were forced by ten actual gauges and eight sources of PRs, while the corresponding ten actual gauges were employed to force the IDW. Rainfall estimations can be divided into three echelons according to their overall performance. VG, RF, and IDW were the first echelons with significantly better performance than pure PRs, benefiting from the consideration of GO. GSMaP-N, GSMaP-GN, IMERG-E, and IMERG-L are the second echelon, with a $\overline{CC}$ from 0.39 to 0.41 and an $\overline{RMSE}$ from 8.64 mm to 9.19 mm. The performances of the timeliest PRs (namely PERSIANN-CCS, ECMWF, JMA, and NCEP) are the worst, with a $\overline{CC}$ from 0.18 to 0.26 and an $\overline{RMSE}$ from 9.24 mm to 10.67 mm. Among the first echelon, RF and IDW perform similarly with a $\overline{CC}$ of 0.56 and 0.54, respectively, and an $\overline{RMSE}$ of 6.40 mm and 6.38 mm, respectively. VG is better than RF and IDW in terms of both $\overline{CC}$ and $\overline{RMSE}$. The $\overline{CC}$ of VG was 0.60, which improved by 7.1% and 11.1% over that of RF and IDW, respectively. The $\overline{RMSE}$ of VG was 5.89 mm, which improved by 8.0% and 7.7% compared to RF and IDW, respectively. Virtual gauges were added daily. During the study period, the number of virtual gauges varied from 1 to 27, averaging 10.82 virtual gauges for each day which is approximately equal to the number of actual gauges.

## 4 Conclusions

This paper proposes a framework (VG) for merging rainfall estimation of multi-source PRs and GO based on a novel concept, namely, the virtual gauge. VG was assessed over a region where almost all 0.1° grid cells contained a ground gauge. VG improves around 7–11% over its basic methods and improves around 32–240% over its inputting PRs. In the proposed VG, PRs can perform positively under various densities of gauge networks and various the ability of gauge networks to capture the heterogeneity of rainfall fields.

## Reference

[1] Tang, G., Clark, M.P., Michael, S., Ma, Z., Hong, Y., Tian, Y., Huffman, G.J., Adler, R.F., Tang, L., Sapiano, M., Maggioni, V., Wu, H.. Have satellite precipitation products improved over last two decades ? A comprehensive comparison of GPM IMERG with nine satellite and reanalysis datasets. Remote Sens. Environ. (2020)240.

**Theme:** Hydroinfomatics for extreme hydrological events and resilience improvement
**IAHR Thematic Priority Area:** [TPA-3] Improving Resilience against Water Hazards and Disasters
https://doi.org/10.3850/iahr-hic2483430201-468

# A Transformer-Based Convolution Neural Network Framework For Building Change Detection From High-Resolution Remote-Sensing Images

**Han Wang[1], Shunyu Yao[1], Qing Li[1], Tao Sun[1], Changjun Liu[1]**

[1] China Institute of Water Resources and Hydropower Research, Beijing 100038, China

*Corresponding author: Han Wang (wanghan@iwhr.com)*

**Abstract.** With the rapid advances in monitoring technology, remote-sensing images have become gradually available with a dramatic improvement in both quality and resolution, which can significantly contribute to natural disaster analysis such as flash floods, drought, water and soil erosion, etc., strongly influenced by human activities. However, the accuracy and efficiency in detecting anthropogenic influence remain challenging due to the complex, interdependent abundance of feature details within these high-quality images. Therefore, this study proposes a new, change detection framework to enhance the capability of capturing both local features and their long-range spatiotemporal relationships in context by renovating the Vision Transformer (ViT) structure and incorporating it with convolution neural networks (CNNs). The model framework is then trained by thousands of remote sensing images and the performance is finally evaluated by comparing to several widely used networks.

**Keywords:** change detection; convolutional neural networks (CNN); remote-sensing image with high resolution; self-attention mechanism; Vision Transformer (ViT)

## 1 Introduction

The occurrence and severity of natural disasters are strongly linked to climate change and human activities [1]. Climate change alters the characteristics of these hazards while human infrastructure can amplify or reduce their potential risk. Enhancing supervision is an effective approach to reducing anthropogenic influence by promptly identifying and monitoring these behaviours. With advancements in remote sensing technology, real-time monitoring over targeted regions with high resolutions can be achieved without manual inspection efforts. By using monitoring images, changes in human infrastructure can be detected along with risky behaviours. The methods proposed and widely applied for several decades to identify changes in objects based on images and typically involve preprocessing input images by normalizing them to mitigate variations in illumination and colours, where image features are extracted and changes can be detected by calculating pixel differences. However, simple normalization is insufficient to effectively mitigate disturbances like illumination and sensor noises during collection. These basic steps fail to extract the deep semantic features embedded within the images because they focus more on detecting pixel or regional-level changes or differences. In this study, we propose a new, hybrid CNN-ViT framework named ResNet18+Transformer for detecting changes from high-resolution remote sensing images. This model framework incorporates the Vision Transformer into CNN and renovates the layer structure to leverage the advantages of ViT in capturing global features and CNN's expertise in local features. To train the model, the data of remote-sensing image samples from Shandong Province and Anhui Province of China with a resolution of 2 metres are used and the performance of the model is evaluated by five widely-used metrics (Overall Accuracy, F1-Score, IoU, Precision and Recall) and further compared to several advanced deep learning models.

## 2 Method

The overall architecture consists of three main components of the framework, i.e., Initial feature extraction, Transformer-based network development, and Prediction head construction. The first step of the modelling framework is to extract the features from two images to be compared, using a pre-tained ResNet-18 network. By implementing this, the two images ( $\text{Image}^1$ and $\text{Image}^2$ ) are transformed into certain corresponding feature tensors, e.g., $\text{Feature}^1$ and $\text{Feature}^2$ with the size of $H \times W \times C$ (height × width × number of channels) where the superscript number indicates different images. The second step is to construct the new, transformer-based network for extracting deep features from these tensors. ( $\text{Feature}^1$ and $\text{Feature}^2$ ) by taking the context into account. This step incorporates the self-attention mechanism to carry out context-aware feature transformation and employs a Semantic Tokenizer to downsample the image features. It generates the sequences $\text{Tokens}^1$ and $\text{Tokens}^2$ with the size of $L \times C$. Then the sequences from two images are merged into one single sequence with the length of $2L$. The merged sequence is fed to a Transformer encoder, where multiple-layer self-attention mechanism and feedforward neural networks are applied to generate a new sequence $\text{Tokens}_{\text{new}}$ where the context information is fully involved. Then the new sequence is split back into two, i.e., $\text{Tokens}^1_{new}$ and $\text{Tokens}^2_{\text{new}}$ of $\text{Image}^1$ and $\text{Image}^2$. which are mapped to the decoded, context-aware image features $\text{Feature}^1_{\text{new}}$ and $\text{Feature}^2_{\text{new}}$ by using a Transformer Decoder. The last step is to build the prediction head for converting the context-aware features $\text{Tokens}^1_{new}$ and $\text{Tokens}^2_{\text{new}}$ to the change mask which can be used to represent the changing area in the images.

## 3 Results

The training of the proposed network model framework is took in the module of image cropping to segment the remote-sensing image samples with the size of 256 × 256, which have manually marked change regions on them. In this case, we utilized the stochastic gradient descent (SGD) algorithm for iterative learning, with the following settings: an initial learning rate of 0.01, maximum epochs of 200, linear decay for learning rate decay, every ‘step_size’ epochs for learning rate decay step, and a learning rate decay rate of 0.1. The training process was conducted on an NVIDIA GeForce RTX 4090. The overall accuracy of the model on the training, validation, and test sets is 0.99269, 0.98779, and 0.98764, respectively.To further evaluate the performance of the proposed modelling structure, we selected several advanced deep learning models which were applied to image pattern recognition to detect changes, including one convolution-based model, i.e., the bitemporal-FCN, and three attention-based models, i.e., the STANet-BAM, the STANet-PAM, and the SNUNet . The proposed model outperforms both the convolution-based model and attention-based models in terms of Overall Accuracy, F1-score, and IoU since it combines the great capability of CNN on image feature extraction, and the ability to obtain global semantic information from the attention mechanism. It presents a significant improvement in the balance between identifying the positive samples and avoiding false positives in complex image change detection.

## 4 Conclusion

This paper proposes a new deep learning model called the ResNet18+Transformer model by combining a renovated Transformer and CNN to detect the changes from remote-sensing images with high resolution. The developed architecture of the model outperforms the other convention and attention-based models. Future research in the change detection model is expected to increase the resistance to strong illumination reflections and apparent colour changes.

## Reference

[1] Gill, J.C., Malamud, B.D. Anthropogenic processes, natural hazards, and interactions in a multi-hazard framework. Earth-Sci. Rev. 2017, 166, 246–269.

**Theme:** Hydroinfomatics for extreme hydrological events and resilience improvement
**IAHR Thematic Priority Area:** [TPA-3] Improving Resilience against Water Hazards and Disasters
https://doi.org/10.3850/iahr-hic2483430201-470

# Application Research of Video Flow Measurement Technology

**Guomin Lyu[1,2], Linrui Shi[1,2], Nan Qiao[1,2], Xiao Liu[1,2], Shunfu Zhang[1,2], Qiang Ma[1,2], Qiyi Zhang[1,2]**

[1] China Institute of Water Resources and Hydropower Research, No. 1 Fuxing Road, Haidian District, Beijing 100038, China
[2] Research Center on Flood & Drought Disaster Reduction of the Ministry of Water Resources, No. 1 Fuxing Road, Haidian District, Beijing 100038, China

*Corresponding author: lugm@iwhr.com*

**Abstract.** This study aims to explore the applicability of multiple image-based flow measurement methods under specific conditions. It comprehensively investigates the results of three mainstream image-based flow measurement methods—Space Time Image Velocimetry (STIV), Large Scale Particle Image Velocimetry (LSPIV), and Optical Tracking Velocimetry (OTV)—in open channel conditions to deeply evaluate the applicability and accuracy of each method under specific conditions. The research results show that all three image-based flow measurement algorithms can effectively identify surface flow velocities. Among them, the method with the highest precision in average relative error in surface flow velocity is OTV, with an error of 2.34%, followed by the STIV method with an average relative error of 4.69%, and finally the LSPIV method with an average relative error of 10.13%. Through the in-depth exploration in this study, theoretical and practical support is provided for optimizing image-based flow measurement technology, offering valuable insights for the application of image-based flow measurement technology, and advancing the further application and development of image-based flow measurement technology in engineering practice and scientific research.

**Keywords:** Image velocity measurement,LSPIV,OTV,STIV,Water monitoring

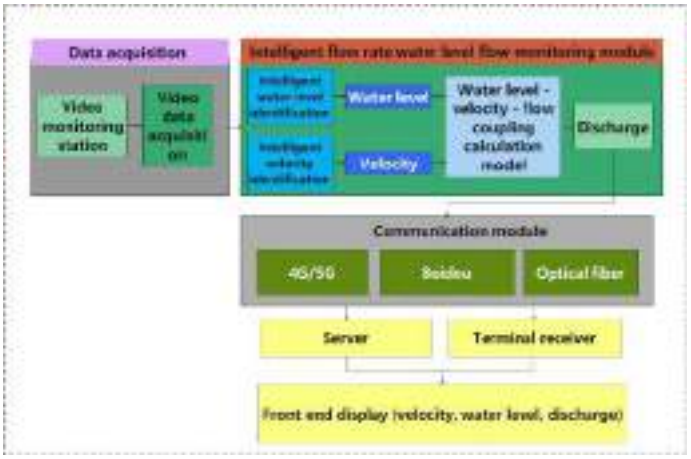


Figure 1. The technical flow chart

This study selects and analyzes the flow measurement accuracy and applicability of the STIV, LSPIV, and OTV image-based flow measurement methods under the same working conditions. STIV and LSPIV are evolved from the Particle Image Velocimetry (PIV) algorithm, which is an indirect method used to convert images of free surface fluid flow captured by video recordings. They utilize image processing and analysis techniques to estimate flow velocities. On the other hand, OTV employs a motion target detection algorithm, which separates the changing areas or moving objects from the background image in a sequence of pictures. The technical flow chart is shown in Figure 1.

In order to reduce experimental errors caused by external environmental factors and thoroughly validate the accuracy of each image-based flow measurement method, environments with standard river channels, good lighting conditions, minimal to no wind, and abundant tracer particles were selected whenever possible. The experimental cross-section for this study was sourced from the "PtClaix_test_data" dataset in Fudaa-lspiv (https://riverhydraulics.inrae.fr/en/tools/measurement-software/fudaa-lspiv-2/). This dataset includes longitudinal section data, current water level values, and coordinates of calibration points (GRPs), providing all the necessary information for image-based velocity measurements. The camera at this site was installed above the water surface downstream of the comparison section, positioned at a fixed angle to capture upstream flow, with a frame rate of 30 frames per second and an image resolution of 1280x720 pixels. During this period, the river channel contained a sufficient amount of tracer particles and surface ripples, allowing for the accurate depiction of local water flow dynamics. The image below shows the flow velocities at each starting point, with the left bank designated as the starting point zero.

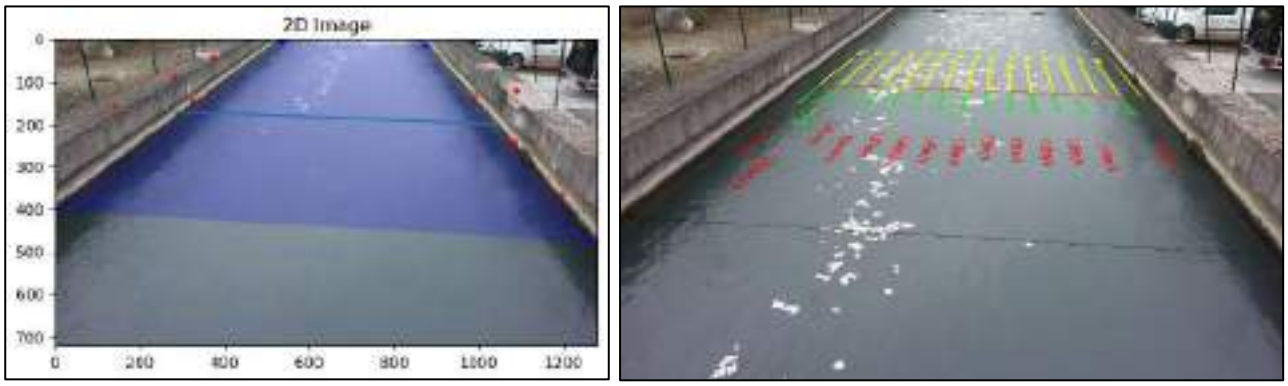


(a) (b)

Figure 2. Original and orthorectified images with search lines: (a) original; (b) result image.

Based on the image analysis method of flow velocity identification, the surface velocity in the flow direction is estimated by analyzing the video taken from the bank slope, as shown in Figure 1a. First, search lines or velocity measurement lines of constant physical length are usually set on the original image, parallel to the direction of the water flow, at a certain interval, as shown in Figure 1b. Next, a spatiotemporal image (STI) is generated for each search line by superimposing the distribution of sequential image intensities over time along the search lines. As a result, the STI displays a tilt pattern indicating the flow direction to the surface at the location of the search line.

Starting from 1 meter from the left bank at the comparison section, a flow measurement point was set every 0.5 meters for each of the three image-based flow measurement algorithms. The surface flow velocity was calculated at these points, with distances from the left bank of 1.0m, 1.5m, 2.0m, ..., 6.0m, totaling 10 sets of data. The flow measurement results indicated that compared to the actual measurements, the STIV method had the smallest overall error of 0.02 m/s at 3.5m, and the largest error of 0.27 m/s at 1.5m. The average absolute error between STIV and the actual measurements was 0.06 m/s, with an average relative error of 4.69%;the LSPIV method had the overall minimum error was 0.018 m/s at 5.5m, and the maximum error was 0.37 m/s at 1m;The average absolute error between LSPIV and the actual measurements was 0.13 m/s, with an average relative error of 10.15%; the OTV method had the overall minimum error was 0.0 m/s at 1.5m, and the maximum error was 0.12 m/s at 3.5m,the average absolute error between OTV and the actual measurements was 0.03 m/s, with an average relative error of 2.34%.

**Theme:** Hydroinfomatics for extreme hydrological events and resilience improvement
**IAHR Thematic Priority Area:** [TPA-3] Improving Resilience against Water Hazards and Disasters
https://doi.org/10.3850/iahr-hic2483430201-472

# Identifying Influential Conditioning Factors of Design Rainfall-Flood Response and Constructing Design Flood Prediction Models for Mountainous Catchments

**Wang Xuemei[1,2], Liu Ronghua[1,2], Zhai Xiaoyan[1,2], Guo Liang[1,2]**

[1] China Institute of Water Resources and Hydropower Research, Beijing 100038, China
[2] Research Center on Flood and Drought Disaster Reduction of the Ministry of Water Resources, Beijing 100038, China

*Corresponding author: liurh@iwhr.com*

**Abstract.** Design flood provides powerful technical supports for carrying out flash flood prevention and control in mountainous catchments. Based on China National Flash Flood Disasters Investigation and Evaluation, the design flood peak discharge data of 6,914 villages (recurrence interval ranging from 5 to 100 years) in Jiangxi Province, China were collected. Fourteen design flood conditioning factors, combined with Random Forest algorithm, were used to develop design flood regression prediction model for Jiangxi Province. Results showed that model showed satisfactory regression prediction capacity, with *rRMSE* ranging from 0.248 to 0.254, and $R^2$ ranging from 0.932 to 0.936 for different recurrence intervals.Catchment area was of the greatest influence on prediction results, followed by 6-hour rainfall, altitude, average slope and other conditioning factors. The study is of great significance for evaluating design flash flood.

**Keywords:** design flood; mountainous catchment; random forest algorithm; terrain and underlying surface characteristic; rainfall characteristic

## 1 Introduction

Characterized by extremely sudden onset, rapid flood response, and highly concentrated flood energy, flash floods are recognized as the main flood disasters causing grave losses of life and property [1-2]. Design flood is an important reference for formulating flash flood management strategies, and obtaining reasonable and reliable design flood results has always been the focus of flash flood research.

Machine learning algorithms are providing new insights for flash flood analysis and study. Riazi [3] et al. used radial basis function (RBF), and three hybrid models to delineate flood susceptibility areas at Goorganrood watershed, Iran. Zhou [4] et al. proposed an integrated model incorporating Xinanjiang conceptual model (XAJ) and Monotone Composite Quantile Regression Neural Network (MCQRNN) to carry out multi-step-ahead flood probability density forecasts.

Jiangxi Province is located in the southeast of rainy area in China, frequently suffering from flash flood disasters. In our study, a regression prediction model, based on Random Forest algorithm, for design flood analysis in Jiangxi Province are developed, aiming to provide powerful references for improving local capacity of flash flood management and control.

## 2 Data

The collected data included design flood data, geographic information data and design rainfall data, among which geographic information data and design rainfall data were used to extract catchment characteristics. Design flood data included design flood peak discharge of 6,914 villages in mountainous regions of Jiangxi province with recurrence interval ranging from 5 to 100 years. Geographic information data, including digital elevation model (DEM, 1:50,000), water system

(1:100,000), etc. Design rainfall data (25 m×25 m) including rainfall statistical parameters and design rainfall amount for 1-hour, 3-hour, 6-hour and 24-hour rainfall.

## 3 Method

Fourteen catchment characteristic indices, i.e. area, altitude, average slope, length of the longest flow path, slope of the longest flow path, shape coefficient, average velocity coefficient, average infiltration rate, average 3-hour rainfall, average 6-hour rainfall, concentration of 3-hour design rainfall process, concentration of 6-hour design rainfall process, extreme ratio of 3-hour design rainfall and extreme ratio of 6-hour design rainfall, were selected as design flood conditioning factors to describe the hydrometeorological characteristics of village watershed[5-6], including terrain and underlying surface characteristic indices and design rainfall characteristic indices.

Random forest algorithm (RF) was used to develop the regression prediction model (RF model) for design flood. 80% and 20% sample data were determined as training set and test set, respectively. Training set was used with GridsearchCV algorithm for model hyperparameter optimization, and test set was used for model accuracy evaluation with relative root mean square error (rRMSE) and coefficient of determination (R2).

## 4 Result

The prediction accuracy for design flood of Jiangxi Province was shown in Table 1. *rRMSE* ranged from 0.248 to 0.254, and $R^2$ ranged from 0.932 to 0.936, indicating that the developed RF model can provide satisfactory explanation for design flood analysis in Jiangxi Province. For different recurrence intervals, RF model provided competitive performances.

Table 1 Evaluation indices for design flood model

| Recurrence interval (year) | *rRMSE* | $R^2$ |
|---|---|---|
| 5 | 0.254 | 0.936 |
| 10 | 0.252 | 0.935 |
| 20 | 0.249 | 0.934 |
| 50 | 0.249 | 0.932 |
| 100 | 0.248 | 0.933 |

Using “feature_importance” module built into sklearn library of python, the importance of fourteen conditioning factors were obtained. Conditioning factors’ importance for different recurrence intervals showed great consistency, and the importance of catchment area was obviously stronger than other factors, followed by average 6-hour rainfall, altitude, average slope and other factors.

## References

[1] J. Ritter, M. Berenguer, C. Corral, et al. ReAFFIRM: real-time assessment of flash flood impacts-a regional high-resolution method, Environ. Int. 136 (2020) 105375.
[2] X.M. Wang, X.Y. Zhai, Y.Y. Zhang, et al. Evaluating flash flood simulation capability with respect to rainfall temporal variability in a small mountainous catchment, J. Geogr. Sci. 33(2023) 2530-2548.
[3] M. Riazi, K. Khosravi, K. Shahedi, et al. Enhancing flood susceptibility modeling using multi-temporal SAR images, CHIRPS data, and hybrid machine learning algorithms, Sci. Total Environ. 871 (2023) 162066.
[4] Y.L. Zhou, Z. Cui, K.L. Lin, et al. Short-term flood probability density forecasting using a conceptual hydrological model with machine learning techniques, J. Hydrol. 604 (2022) 127255.
[5] M.H. Ma, Z. Gang, B.S. He, et al. XGBoost-based method for flash flood risk assessment. J. Hydrol. 598 (2021) 126382.
[6] N.M. Gharakhanlou, L. Perez. Flood susceptible prediction through the use of geospatial variables and machine learning methods, J. Hydrol. 617 (2023) 129121.

**Theme:** Hydroinfomatics for extreme hydrological events and resilience improvement
**IAHR Thematic Priority Area:** [TPA-3] Improving Resilience against Water Hazards and Disasters
https://doi.org/10.3850/iahr-hic2483430201-474

# Flash Flood Disaster Risk Evaluation Based on Geographic Detector and Interval Number Ranking Method

**Xiao Liua,b, Ronghua Liua,b*, Xiaolei Zhanga,b, Qi Liua,b**

[a] China Institute of Water Resources and Hydropower Research, No.1 Fuxing Road, Haidian District, Beijing 100038, China
[b] Research Center on Flood & Flash flood Disaster Reduction of the Ministry of Water Resources, No.1 Fuxing Road, Haidian District, Beijing 100038, China

*Ronghua Liu: liurh@iwhr.com*

**Abstract.**
Flash flood disaster is one of the natural disasters that have a significant impact on human beings，causing enormous damage to the national economy and people's lives and properties. Conducting a risk assessment of flash floods is an effective way to defend against them，and an accurate assessment of flash flood risk can provide strong technical support for flash flood prevention and decision-making. This study analyzed the driving forces of flash flood disaster-causing factors in Heilongjiang Province. 9 types of driving factors related to flash floods in Heilongjiang Province were selected, and the degree of influence of each driving factor on flash floods was quantitatively analyzed, and the driving force analysis of the driving factors of flash floods in Heilongjiang Province was carried out by using the geographic probe model. The uncertainty method is introduced, this paper using Statistical-based interval weight determination of evaluation index method and Interval number sorting method based on two-dimensional information to establish flash flood risk evaluation model. On this basis, it was applied in Heilongjiang province of China to evaluate and rank the risk of flash flood in 6 regions. The ranking result was: Bayan ≻ Shuangcheng ≻ Boli ≻ Suibin ≻ Hailun ≻ Yian. The results show that the evaluation method based on interval number can better deal with the uncertainty in reality.

**Keywords:** Flash flood; advantage degree function; ranking; flash flood risk evaluation

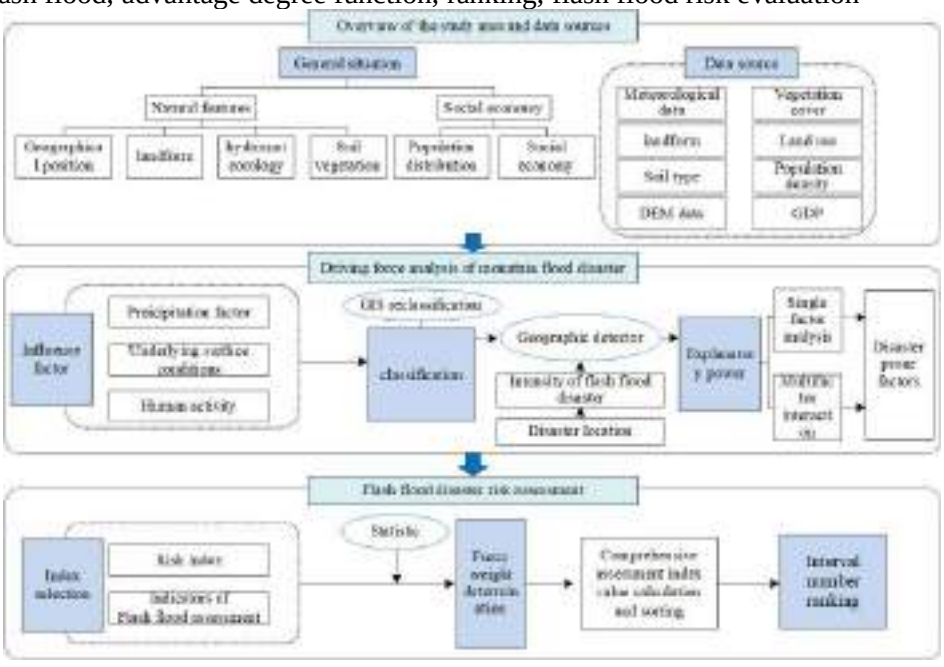


Figure 1 Technical roadmap


Figure 2 Evaluation indexs

Table 1 The comprehensive evaluation interval values $\tilde{z}_i$

| Area | Bayan | Shuangcheng | Boli | Suibin | Hailun | Yian |
|---|---|---|---|---|---|---|
| $z_i^*$ | [0.528,0.836] | [0.584,0.644] | [0.494,0.604] | [0.331,0.511] | [0.461,0.517] | [0.419,0.546] |

In this paper, 9 kinds of disaster factors were selected, including rainfall, elevation, slope, landform, soil, NDVI, land use, population density and GDP, and the driving force analysis of flash flood disaster factors in Shaanxi Province was carried out by using geographical detector model. The results showed that the flash flood disaster in Shaanxi Province was affected by various driving factors, and the rainfall factor had the greatest impact on the flash flood disaster in Heilongjiang Province, followed by elevation and soil type. In Heilongjiang province, population density, rainfall and landform have a great impact on the flash flood disaster. It shows that rainfall factor is the direct factor and stimulating condition of inducing flash flood, topography is the material basis and potential condition of flash flood, and unreasonable human activities aggravate the harm degree of flash flood. The explanatory power of the interaction of two factors in each region is greater than that of a single one, indicating that the combined action of multiple factors on flash flood disasters will strengthen the occurrence and risk degree of flash flood disasters.

On this basis, it was applied in Heilongjiang province of China to evaluate and rank the risk of flash flood in 6 regions. Evaluation indicators includes Risk of hazard factors, Vulnerability of the environment, Exposure of the disaster-bearing body and Disaster prevention and mitigration capability. Finally, the area with the highest risk of flash flood is Bayan and the area with the lowest risk is Yian.

Risk analysis is an effective technical tool for studying uncertain systems.Agricultural flash flood disaster phenomenon is extremely complex, involving many factors and with high degree of uncertainty. Therefore, it is urgent to apply the risk theory to the study of agricultural flash flood disaster.It is of great significance for risk management of agricultural flash flood disaster to make full use of modern scientific and technological achievements, apply risk quantification and risk evaluation techniques to study agricultural flash flood disaster, so as to effectively improve the credibility and reliability of risk grade evaluation results..

**Theme:** Hydroinfomatics for extreme hydrological events and resilience improvement
**IAHR Thematic Priority Area:** [TPA-3] Improving Resilience against Water Hazards and Disasters
https://doi.org/10.3850/iahr-hic2483430201-476

# Simulation Study of Super-Standard Flood Evolution Based on Flow3D

**Honghua Li[1], Jingshan Yu[1], Shugao Xu[1]**

[1] Beijing Key Laboratory of Urban Hydrological Cycle and Sponge City Technology, College of Water Sciences, Beijing Normal University, Xinjiekouwai Street 19, Beijing 100875, China

*Corresponding author: jingshan@bnu.edu.cn*

**Abstract.** Simulation of flood evolution beyond standard has always been one of the important means to study flood prevention and mitigation countermeasures, and flow3d is a classical CFD fluid dynamics model, which has very efficient ability to describe the three-dimensional change process of hydrodynamics. In this study, we selected the Muwen River Basin in Shandong Province to carry out a simulation study on the evolution of super-standard floods, focusing on the identification of risky riverbanks and embankments, and carried out three-dimensional hydrodynamic simulation studies, aiming to provide reliable and effective countermeasures for the prevention of over-standard floods.

**Keywords:** 3D hydrodynamic simulation, Flood beyond the standard, Flood evolution simulation, Risk riverbank, Risk embankment, FLOW3D

## 1. Introduction

Due to the high computational power required for simulating river flow dynamics, it is often not possible to directly simulate three-dimensional flood and water-logging process of the entire basin. A case study explores the use of high-precision CFD models combined with digital twin foundation layer construction technology, to simulate excessive flood processes, analyze the impact of hydrodynamic changes on riverbed and embankment erosion, optimize flood control engineering renovation measures, and provide scientific suggestions for dam scheduling and defense plans.

## 2. Material and methods

To use the hydrological frequency chart search method and the hydrological analogy method to obtain the inflow boundary condition, and involve four physical models of “gravity and non-inertial reference frame”, “density evaluation”, “viscosity and turbulence”, and “shallow water” from the flow-3d hydrodynamic model. To establish the digital twin base we used a geographic mapping RTK measuring instrument, the riverbed and embankment terrain data was fitted and repaired, and utilized drone aerial surveys to assist in engineering data exploration, and established a three-dimensional gate and dam engineering data component, gradient solutions and terrain restoration were performed on the riverbed bottom elevation.

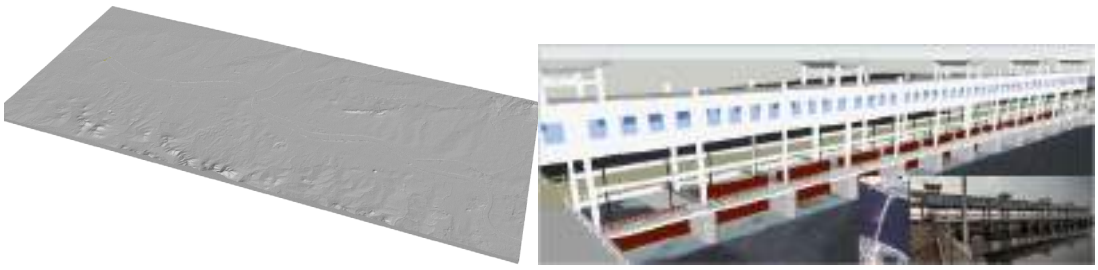

Figure 1 Digital Twin Base in the Muwen River Basin

Based on once in a thousand year flood disaster scenario, the simulation calculation analysis is carried out to identify the main overflow outlets and potential breaches, and conduct elevation analysis on weak embankments. Design a rubber dam scheduling plan, simulate and analyze the flood peak process and flood evolution law, and propose suggestions for adjusting the rubber dam scheduling plan.

## 3. Results and Discussions

The results show that the risk of the left bank embankment is slightly higher than that of the right bank embankment. The gradient of embankment construction near the overflow outlet decreased rapidly, and during the process of flood rise, it failed to constrain the downward flow of the flood, leading to the development of nearby overflow and a certain degree of farmland inundation.

Figure 2 Muwen River Main Stream Overflow Flood Area (Red Box Area)

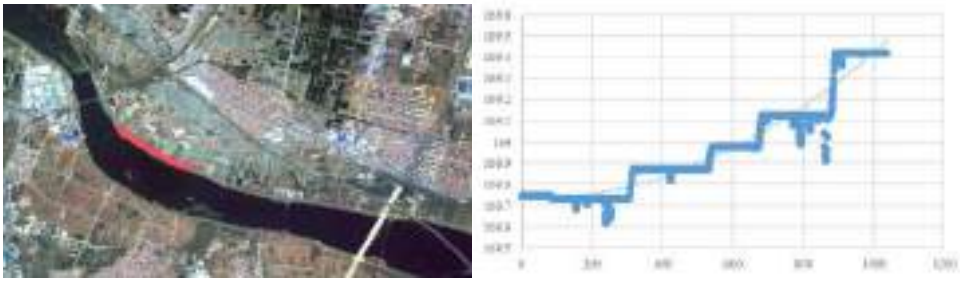

Figure 3 Analysis of the elevation of the right bank overflow embankment above the mouth of the Sima River

## 4. Conclusions

4.1 Simulation analysis and suggestions for rubber dam scheduling plan

Considering the requirements for safe operation, by rasing 1 #~3 # rubber dams, Taigang Rubber Dam, Mount Taishan Paper Rubber Dam height by 0.5m in normal and dry years, the flood peak can be moderately blocked from descending at a very fast speed, the 4 # rubber dam is mainly controls mountain floods so it's only suitable for dam collapse operation. In addition, the discharge flow of Fangxia River and Sima River is relatively large. It is recommended to add two rubber dams before Fangxia River and Sima River enter the main stream. In case of 24-hour rainstorm forecast with a frequency of more than 2-year return period, to release rubber dams in advance. By appropriately intercepting and storing floods in the middle and upper reaches before the upstream flood peak descends, it has a certain alleviating effect on the initial flood discharge in the downstream.


Figure 4 Distribution map of rubber dam location

4.2 Suggestions for reinforcement of embankments

It is recommended to increase the height of embankments and reinforce the erosion resistance of dam bodies in areas prone to flooding. Key river embankment pile sections should be upgraded to improve the flood control level of the project, and the flood control standards for overflow dams and rubber dams should be raised to effectively enhance the flood resistance capacity beyond the standard.

## Acknowledgments

This study was supported by 2021 Jinan Water Science and Technology Project (Project No. JNSWKJ202101).

## Reference

[1] Yilin Jun. P-III curve hydrological frequency calculation program (method). [EB/OL]. (2023-11-10).[2024-02-26]. https://zhuanlan.zhihu.com/p/666136627

[2] High precision computational fluid dynamics (CFD) software - FLOW-3D product introduction. [EB/OL]. (2021-01-26).[2024-02-26]. http://www.uninsim.com/article-113.html

[3] FLOW-3D® Version 2023R1 Users Manual (2023). FLOW-3D [Computer software]. Santa Fe, NM: Flow Science, Inc. [EB/OL]. [2024-02-26]. https://www.flow3d.com
[4] Licheng Wang, et al. Application of FLOW-3D in Water Conservancy Engineering[M]. First edition. Zhengzhou:Yellow River Water Conservancy Publishing House Co., Ltd. 2020.

**Theme:** Hydroinfomatics for extreme hydrological events and resilience improvement
**IAHR Thematic Priority Area:** [TPA-3] Improving Resilience against Water Hazards and Disasters
https://doi.org/10.3850/iahr-hic2483430201-479

# Research and Application of Key Technology of National Flash Flood Forecasting and Early Warning Platform in China

**Liu Ronghua[1,2], Liu Qi[1,2], Tian Jiyang[1,2], Zhang Xiaolei[1,2], Zhai Xiaoyan[1,2], Sun Chaoxing[1,2], Wang Xuemei[1,2]**

[1] China Institute of Water Resources and Hydropower Research, Beijing 100038, China
[2] Research Center on Flood and Drought Disaster Reduction of the Ministry of Water Resources, Beijing 100038, China

*Corresponding author: liurh@iwhr.com*

**Abstract.** National Flash Flood Forecasting and Early Warning platform in China is constructed considering the nationwide demand for large-scale, refined, and highly timely flash flood disaster warnings. Breakthroughs in several key technologies have been achieved, such as the method for super-large-scale high-frequency real-time information processing and the dynamic integration framework for flash flood risk warning models. The platform has been successfully applied in provincial flash flood risk warning business throughout China and provide risk warning information services for multiple industries, such as power and railways, playing a crucial role in flash flood prevention and defense. This article provides a detailed description of the functions, key technologies and applications of the national platform.

**Keywords:** flash flood, forecasting, early warning, national platform

## 1 Functions

The construction of National Flash Flood Forecasting and Early Warning Platform started in 2014[1], which has been serving as a powerful tool for the Ministry of Water Resources to comprehensively evaluate national situation of flash flood disaster prevention and control[2].

The functions of the platform mainly include four aspects, i.e. rainfall monitoring and forecasting, multi-stage flash flood warning, duty reminder and consultation management.

## 2 Key technologies

The key technologies of platform construction mainly include five aspects[3-6].

- Flood analysis for small watershed lacking data. China Flash Flood hydrological Model (CNFF) was developed coupled with calculation database, parameter database and knowledge database. A algorithm database of distributed hydrological model was established as well, covering six types of hydrological processes.
- Model construction for large-scale flash flood simulation. A dynamic integration framework of model algorithms was proposed. An intelligent modeling tool based on depth-first traversal of tree data structure was constructed for very large-scale model construction.
- High-performance heterogeneous parallel flood simulation. A multi-scale and multi-process hierarchical coupled parallel computing framework for flood simulation was constructed. Two kinds of scheduling model algorithms with least resource consumption were established for given resource, fastest speed and given time.
- Abnormal rainfall station screening system. A progressive abnormal rainfall station screening platform was constructed based on improved Graebs criteria, peripheral station analysis, radar-assisted calibration and other technologies.

- Flash flood disaster early warning system. A multistage progressive flash flood disaster dynamic early warning system was developed, with meteorological early warning, approaching forecast and warning as well as real-time monitoring early warning included.

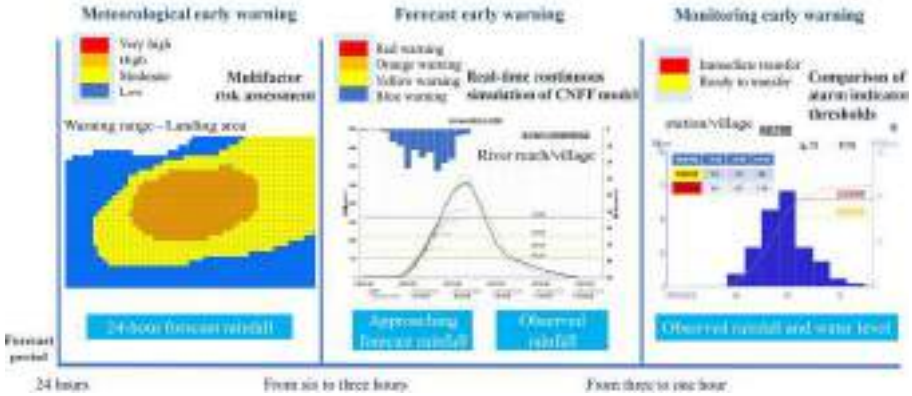


Figure 1 Multistage early warning system of National Flash Flood Forecasting and Early Warning Platform

## 3 Applications

Since 2015, a total of 1,091 national flash flood disaster meteorological warnings have been issued, 289 of which have been issued by China Central Television (CCTV). In 2023, flash flood risk caused by "Dusuri" and "Haikui" typhoon was successfully forecasted in advance and provied strong supports for the Ministry of Water Resources to carry out flash flood disaster prevention deployment. Besides, as applied to the review and investigation analysis of 16 major flash flood disaster events such as "Zhengzhou July 20 event" in 2021 and "Datong August 18 event" in 2022, the platform has realized the rapid grasp of disaster situation, and the recurrence analysis of flash flood disasters.

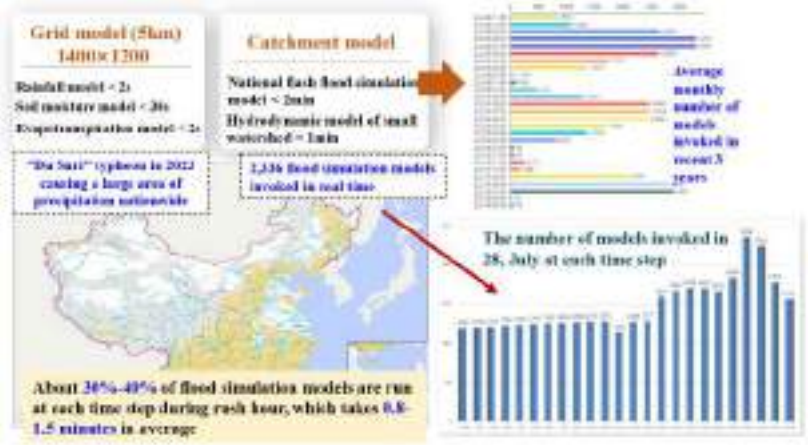


Figure 2 The operation efficiency of National Flash Flood Forecasting and Early Warning Platform

## References

[1] R.H. Liu, Q. Liu, X.L. Zhang, et al. Design and application of national mountain flood monitoring and prewarning platform, China Water. Resour. 21 (2016) 24-26. (in Chinese)
[2] H.X. Liu, J.X. Lu, Q.M. Shang, et al. National flash flood disaster prevention in China in 2023, China Flood & Drought Manage. 33(2023) 5-8. (in Chinese)
[3] R.H. Liu, Y.Y. Zhou, L. Guo, et al. Research progress on early warning of flash flood disasters in the United States, China Flood & Drought Manage. 30(2020) 141-148. (in Chinese)
[4] J.J. Gourley, Y. Hong, Z.L. Flamig, et al. A unified flash flood database across the United States, B. Am. Meteorol. Soc. 94(2013) 799-805.
[5] S.M. Martinaitis, K.A. Wilson, N. Yussouf, et al. A path toward short-term probabilistic flash flood prediction, B. Am. Meteorol. Soc. 104(2023) E585-E605.
[6] M. Špitalar, J.J. Gourley, C. Lutoff, et al. Analysis of flash flood parameters and human impacts in the US from 2006 to 2012, J. Hydrol. 519(2014) 863-870.

**Theme:** Hydroinfomatics for extreme hydrological events and resilience improvement
**IAHR Thematic Priority Area:** [TPA-3] Improving Resilience against Water Hazards and Disasters
https://doi.org/10.3850/iahr-hic2483430201-481

# A Dynamic Real-time Heuristic Evacuation Pathfinding Algorithm for Flood Avoidance

**Xin Huang[1], Youcan Feng[2], Donghe Ma[3], Lin Tian[1]**

[1]College of Water Conservancy and Environmental Engineering, Changchun Institute of Technology, Changchun, Jilin Province, China
[2]College of New Energy and Environment, Jilin University, Changchun, Jilin Province, China
[3]Changchun Municipal Engineering Design and Research Institute, Changchun, Jilin Province, China

*Youcan Feng：youcan_feng@jlu.edu.cn*

*Lin Tian：tianlin@ccit.edu.cn*

**Abstract.** Floods are a serious global threat, causing large numbers of casualties and economic losses. Evacuation routes with high accessibility and low exposure are essential to reduce flood risk. However, finding effective routes in the dynamics of floods is a challenge. In this study, a fully distributed real-time heuristic flood avoidance evacuation route search algorithm (RHEPFA) is proposed based on dynamic flood forecasting from the Anuga 2D hydrodynamic model with the aim of dynamically avoiding flood hazards and ensuring safe arrival at designated helters.RHEPFA takes into account dam failure floods, weather extremes, topography, and population mobilization rates. Compared to Dijkstra's algorithm and the ACO algorithm, RHEPFA improves the ccessibility of flood protection paths by a factor of 5 and maintains more than 90% path availability in rural flooded areas. It can effectively aid evacuation in extensive flood scenarios.The real-time paths provided by RHEPFA will play a crucial role in future flood control strategies.

**Keywords:** Anuga; Flood Avoidance; Flood Propagation; Heuristic Algorithm; Hydrodynamic Model.

## 1 Introduction

With the increase in extreme precipitation events globally, the frequency and severity of flooding has risen[1], resulting in huge losses and highlighting the urgent need for preventive measures to mitigate dam failure or catastrophic flood damage. The limited effectiveness of traditional engineering solutions has driven a shift towards non-engineering strategies such as evacuation plans. In the past, traditional flood avoidance path planning algorithms, which are planned prior to flooding, acted as early warning trip planners[2], identifying the least time-consuming paths prior to departure. However, these algorithms lack the ability to dynamically modify the evacuation routes based on the latest forecasts of flood propagation at each stage. This limitation may lead to unnecessary detours or life-threatening route failures[3]. Considering the destructive nature of flood waves, it is proposed to develop a real-time routing algorithm capable of dynamically adapting routes based on flood propagation, taking into account realistic factors such as obstacle avoidance and sloping terrain. To fulfill this need, we propose the new Real-time Heuristic Evacuation Pathfinding Algorithm for Flood Avoidance (RHEPFA) to provide such analysis.

## 2 Methods

Evaluation pathfinding algorithms are integrated into an Emergency Flood Response System (EFRS) that includes dam failure calculations and two-dimensional inundation modeling. The system activates the hydrodynamic model to predict the flood propagation after detecting the signal of a dam failure or an external flood event; at the same time, the system activates the pathfinding algorithm, where the pathfinding algorithm is developed based on heuristic algorithms, which uses the water depth, slope, flow velocity, crowd movement speed, and minimum distance from the floodwater as algorithmic operating rules, and analyzes the evacuation routes in real time, using the new inundation maps generated at each step. As a result, evacuees can start using the optimal route determined by the latest flood forecast without having to wait for the completion of the hydrodynamic simulation.

## 3 Results & conclusion

The RHEPFA algorithm can be dynamically driven by real-time inundation forecasts rather than relying on time-specific static inundation range forecasts. The RHEPFA algorithm fully dominates in performance comparisons with static paths consisting of the static ACO algorithm and the Dijkstra algorithm.The RHEPFA algorithm has the advantage of static paths. In terms of reachability, it is consistently five times better than the two static search algorithms, with the RHEPFA algorithm's reachability approaching 95%. The dynamic global planning based flood avoidance algorithm also has a significant performance advantage over the Dijkstra algorithm, which maintains a reachability of about 85%, a computation time more than 10 times that of the RHEPFA algorithm, and a path that is generally smaller than the RHEPFA algorithm when avoiding floods and detours that have to occur. Dijkstra dynamic flood avoidance algorithm. This study proposes a dynamic real-time flood avoidance algorithm that integrates reservoir breaching and two-dimensional hydrodynamic modeling into the flood avoidance algorithm. The results show that the algorithm has higher effectiveness in path selection compared to other algorithms. The algorithm provides higher effectiveness in path selection compared to other algorithms and shows significant advantages in terms of adaptation to various environments and ease of operation. In particular, the paths provided by the algorithm represent the best dynamic flood avoidance paths available, with short detour lengths and real-time dynamic search capabilities. The flood avoidance path can be adjusted in real time by navigating and receiving location feedback to guide people to avoid floods. It is also capable of navigating in areas that have not been explored beforehand.

## 4 References

This work was kindly supported by the Scientific Research Program of The Education Department of Jilin Province of China (JJKH20231179KJ) and the Natural Science Foundation of Jilin Province of China (YZDJ202201ZYTS492).

## Reference

[1] MERZ B, BLöSCHL G, VOROGUSHYN S, et al. Causes, impacts and patterns of disastrous river floods [J]. Nature Reviews Earth & Environment, 2021, 2(9): 592-609.

[2] LI G, DENG Y. Crowd Dynamics Analysis Using a Bio-inspired Model [Z]. 2021 IEEE Asia-Pacific Conference on Image Processing, Electronics and Computers (IPEC). 2021: 931-4.10.1109/ipec51340.2021.9421275

[3] HE M, CHEN C, ZHENG F, et al. An efficient dynamic route optimization for urban flooding evacuation based on Cellular Automata [J]. Computers, Environment and Urban Systems, 2021, 87.

**Theme:** Hydroinfomatics for extreme hydrological events and resilience improvement
**IAHR Thematic Priority Area:** [TPA-3] Improving Resilience against Water Hazards and Disasters
https://doi.org/10.3850/iahr-hic2483430201-483

# Hydrologic-Hydrodynamic Modelling for An Early Signal of Flash Flooding in Mountainous Ungauged Areas

**Mingfu Guan[1*], Kaihua Guo[1]**

[1] Department of Civil Engineering, the University of Hong Kong, Hong Kong SAR, China
[2] School of Geography, East China Normal University

*Corresponding author: Dr. Mingfu Guan: mfguan@hku.hk*

**Abstract.** Flash flooding is particularly devastating due to its nature of sudden onset, high flow velocities and short duration. Identifying early signals for a flash flood, particularly in ungauged mountainous regions, is crucial to mitigate their impacts. To address this, our study proposes an approach based on a flash flood hazard index, utilizing gridded flood hydrodynamic modeling. To demonstrate the effectiveness of our methodology, we applied it to the 2022 Datong flash flooding event. This flash flood was triggered by a heavy rainfall event with an intensity exceeding 34 mm/h, resulting in 25 fatalities and 6 missing individuals (data as of August 21, 2022). Initially, we conducted two-dimensional hydrodynamic modeling of the flash flooding induced by the rainfall across the entire Datong basin. The modeled inundation was then compared to observed flood extents, revealing a general agreement. However, it should be noted that uncertainties exist due to limited data availability in ungauged mountainous areas. Subsequently, the modeled flood hydrodynamics were utilized to derive a Flash Flood Vulnerability Index (FFVI), which can serve as an early warning signal for emergency response purposes. The study offers a valuable and reliable approach for predicting and mitigating flash floods.

**Keywords:** Emergency response, Flash flooding, Mountainous ungauged areas, Numerical simulation

## 1 Introduction

In mountainous areas, flash flooding is particularly devastating due to its nature of sudden onset, high flow velocities and short duration[1]. Identifying early signals for a flash flood is crucial to mitigate their impacts. Over the past few decades, various flash flood prediction models have been developed, including rainfall-threshold methods[2], hydrology-based models[3], sophisticated hydro-morphodynamic models[4], and emerging machine-learning based models. However, it is recognized that these methods may lead to significant uncertainties in flash flood warnings due to the complexity of a real-world flash flood event. Here are significant challenges that need to be addressed to enhance the accuracy and reliability of these models. The hydrodynamic model has demonstrated the ability to not only predict flood discharge but also model inundation areas. In this study, we propose a hydrologic-hydrodynamic modelling-based approach to identify the early signals of flash flooding in mountainous ungauged areas.

## 2 Study area and methodology

A heavy rainfall hit Datong County, Xining City, Qinghai Province, China, triggering a severe flash flood and mudslides on August 17th, 2022, which was used as a case study to verify the capability of the proposed method. Figure 1 shows bed terrain data of the study mountainous catchment. This study used a flood model based on two-dimensional shallow water equations for rainfall-induced surface water and river flood modelling at the catchment-scale[4]. A Flash Flood Vulnerability Index (FFVI) based on exposure, susceptibility and resilience to flash flooding is developed. FFVI is computed by categorising the indicators to the factors to which they belong (exposure (E), susceptibility (S) and resilience (R)) as shown in Equation (1)

$$\mathrm{FFVI} = \frac{E \times S}{R} \tag{1}$$

Factors selected for exposure(E) is the distance from riverbank. For susceptibility(S), the flood hazard is applied which is assessed by the Grid-level hazard mapping method developed by Guan et al.(2023)[5]. It is calculated by the distributed simulation water depth and velocity. Resilience(R) factors include building area ratio and population. And all factors are normalized.

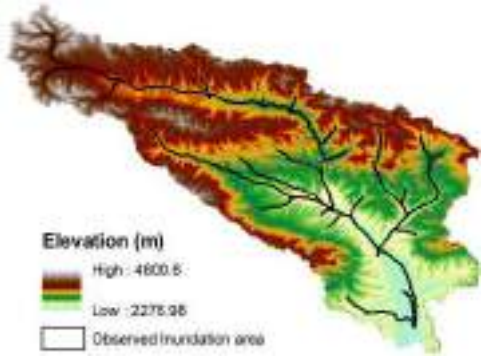


Figure 1. Bed terrain data of the study catchment and observed inundation area.

## 3 Results and conclusion

Based on the comparison between simulated results and the observed data, as depicted in Figure 2(a), the inundation is well reproduced by the model. Thus, it can be regarded as a valuable tool for flash flooding simulation. The FFVI method has been developed to decrease the uncertainties arising from limited data availability in ungauged mountainous regions, which combines detailed hydrodynamic simulation results with other socioeconomic data. The distribution of FFVI is presented in Figure 2(b). It can serve as an effective means to detect early indications of flash flooding. in ungauged mountainous areas.

(a) (b)

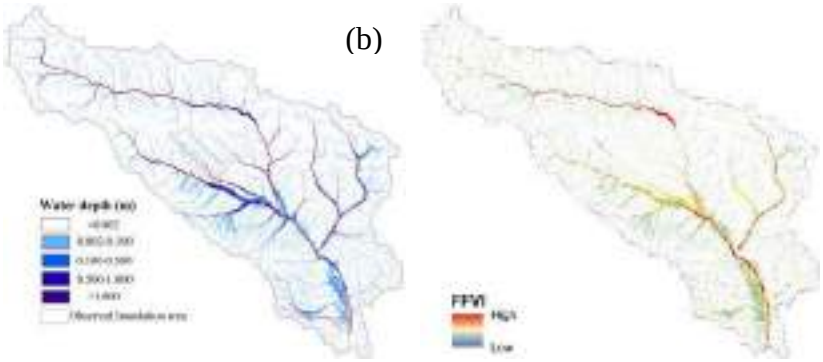


Figure 2. Comparison of the simulated and observed inundation area(a) and FFVI distribution (b).

Reference

[1] Gao, D., Yin, J., Wang, D., Yang, Y., Lu, Y., and Chen, R.: Modelling and validation of flash flood inundation in drylands, Journal of Geographical Sciences, 34, 185-200, 2024.

[2] Young, A., Bhattacharya, B., and Zevenbergen, C.: A rainfall threshold-based approach to early warnings in urban data-scarce regions: A case study of pluvial flooding in Alexandria, Egypt, Journal of Flood Risk Management, 14, e12702, 2021.

[3] Molina, J.-L., Espejo, F., Zazo, S., Molina, M.-C., Hamitouche, M., and García-Aróstegui, J.-L.: HydroPredicT_Extreme: A probabilistic method for the prediction of extremal high-flow hydrological events, Journal of Hydrology, 610, 127929, 2022.

[4] Guo, K., Guan, M., Yan, H., and Xia, X.: A spatially distributed hydrodynamic model framework for urban flood hydrological and hydraulic processes involving drainage flow quantification, Journal of Hydrology, 130135, 2023.

[5] Guan, M., Guo, K., Yan, H., and Wright, N.: Bottom-up multilevel flood hazard mapping by integrated inundation modelling in data scarce cities, Journal of Hydrology, 129114, 2023.

**Theme:** Hydroinfomatics for extreme hydrological events and resilience improvement
**IAHR Thematic Priority Area:** [TPA-3] Improving Resilience against Water Hazards and Disasters
https://doi.org/10.3850/iahr-hic2483430201-485

# Three-Dimensional Simulation and Analysis of Urban Waterlogging Based on Numerical Modeling: Maling River Urban Watershed Case Study

**Mei Chao[1,2]，Zhang Kehan[1]，Liu Jiahong[1,2*]，Wang Jia[1,2]，Song Tianxu[1,2]，Li Yulong[1,3]**

[1] State Key Laboratory of Simulation and Regulation of Water Cycle in River Basin, China Institute of Water Resources and Hydropower Research, Beijing 100038, China
[2] Key Laboratory of River Basin Digital Twinning of Ministry of Water Resources (Preparation), Beijing 100038, China
[3] Hebei Key Laboratory of Intelligent Water Conservancy, Hebei University of Engineering, Handan 056038, China

*Jiahong Liu (J H. Liu): liujh@iwhr.com*

**Abstract.** Urban governance globally faces the problem of urban waterlogging, which results in significant economic losses and casualties, arousing widespread concern for society as a whole. As a typical representative of information technology, digital twin technology plays an important role in various industries and is widely implemented in urban waterlogging prevention and control decision-making, that is, emergency management and decision support. To analyze urban waterlogging, this study considers the Maling River watershed, a highly urbanized watershed in Suqian City, China, for a case study. Data on urban waterlogging monitoring, elevation, land use, and drainage systems were collected. A numerical model of urban waterlogging was constructed by coupling hydrology with one- and two-dimensional hydrodynamic modules. A three-dimensional simulation base was then constructed, which included buildings, roads, green spaces, and water surfaces. Urban waterlogging under extreme rainstorm conditions was simulated using the constructed numerical model based on the Cesium platform. The combined numerical modeling results and urban three-dimensional simulation base was used to achieve three-dimensional visualization simulation and analysis of urban waterlogging processes. The results indicate that the simulation method constructed in this study could achieve inversion and three-dimensional visualization of historical waterlogging processes.

**Keywords:** digital twin; numerical modeling; three-dimensional simulation; urban waterlogging

## 1 Introduction

Urban waterlogging has become one of the most widespread natural disasters and has received significant attention globally from researchers, managers, and technicians. A generalized digital twin includes comprehensive technical schemes such as data dynamic perception, numerical modeling, and three-dimensional (3D) imaging. This study reports on the numerical modeling and 3D simulation of urban waterlogging in the form of a case study. A numerical model of urban waterlogging was constructed utilizing several modules and thereafter combined with 3D simulation. Visualization and digital twin simulations of the urban waterlogging process were performed.

## 2 Materials and methods

The study area, namely the Maling River urban watershed, is located in Suqian City, Jiangsu Province, China, and has an artificial drainage area of 11.6 km$^2$. The Maling River is a drainage channel in old Suqian City with a width in the range of 8—15 m. The surfaces surrounding the Maling River comprise a high proportion of impervious surfaces such as buildings and roads, with a low natural

rainwater infiltration rate, leading to frequent waterlogging and inundation during the flood season wherein heavy rainfall conditions occur.
The storm water management model (SWMM), which is widely used in urban drainage modeling, was employed to construct the urban drainage system model in this study. The Horton equation and nonlinear reservoir method were used to simulate urban surface runoff. To better model the surface inundation process, the TELEMAC-2D module was coupled with the SWMM to comprehensively simulate urban waterlogging.
The validated model was used to simulate actual extreme rainfall events, namely the rainstorms that occurred on July 21, 2012 in Beijing (BJ 721) and July 20, 2021 in Zhengzhou (ZZ 720).

The Cesium platform was used to develop an urban inundation digital twin inference system. The numerical modeling results of the urban waterlogging case study were used to construct a 3D visualization system and superimpose it on a city digital base. The water depth and flow velocity were rendered in the system, and the results were displayed in the 3D landscape.

## 3 The 3D simulation and deduction analysis of urban waterlogging

Fig. 1 shows the 3D simulation results of urban waterlogging under the BJ 721 and ZZ 720 rainfall events. The numerical simulation results, when overlaid with the 3D digital city base, present a better image of the evolution process and inundation area of urban waterlogging in the city. Water surface results mainly show the real evolutionary process of urban waterlogging, whereas the water depth mainly reveals the state of urban waterlogging in the city.

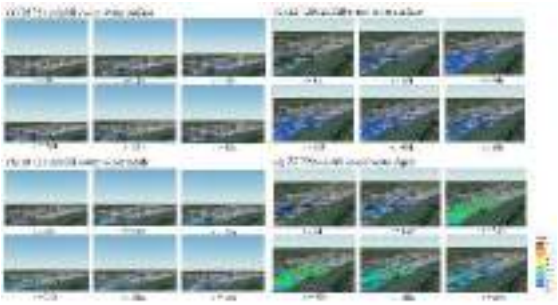

Figure 1 The 3D simulation and deduction of urban waterlogging under the BJ 721 and ZZ 720 rainfall events

As shown in Fig. 1, compared with the 2D urban waterlogging modeling results, the 3D simulation view is mainly oriented toward the low-lying areas in the east and southeast, and the water flows along the main road beside the Maling River to the east and southeast during the simulation process. As rainfall progresses, the inundated area and water depth increase, reaching a maximum at the end of the rainfall period. As the deduction process progresses, a trend of water regression can be observed. In contrast to the BJ 721 rainfall event, the trend of water regression for the ZZ 720 rainfall event is more obvious.
Fig. 2 shows a detailed image of the 3D simulation effect of urban waterlogging, exhibiting more clearly and intuitively the evolution process of urban waterlogging and indicating that the flow of waterlogging mainly evolves along the road under extreme rainfall conditions.

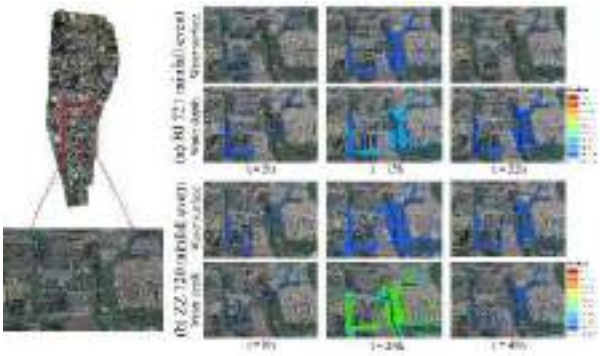

Figure 2 Detailed image of 3D simulation of urban waterlogging

## 4 Acknowledgments

This study is supported by the National key research and development program (No. 2021YFC30001404 & No. 2022YFC3090600), open research fund of Key Laboratory of River Basin Digital Twinning of Ministry of Water Resources (No. Z0202042022).

**Theme:** Hydroinfomatics for extreme hydrological events and resilience improvement
**IAHR Thematic Priority Area:** [TPA-3] Improving Resilience against Water Hazards and Disasters
https://doi.org/10.3850/iahr-hic2483430201-488

# Fast Simulation of Urban Pluvial Floods Using a Deep Convolutional Neural Network Model

**Yaoxing Liao[1], Zhaoli Wang [1,2], Xiaohong Chen[3], Chengguang Lai[1,2]**

[1] School of Civil Engineering and Transportation, State Key Laboratory of Subtropical Building Science, South China University of Technology, Guangzhou 510641, China;
[2] Pazhou Lab, Guangzhou 510335, China;
[3] Center for Water Resources and Environment, Sun Yat-sen University, Guangzhou 510275, China.

*Corresponding author: School of Civil Engineering and Transportation, South China University of Technology, Guangzhou 510641, China. E-mail address: laichg@scut.edu.cn (C. Lai).*

**Abstract.** Rapid prediction of urban floods is crucial for disaster prevention and mitigation. However, physics-based models often demand significant computational time, making them less suitable for time-sensitive scenarios. This study explores a deep learning (DL) approach employing convolutional neural network (CNN) combined with physics-based model for fast urban flood prediction. The results indicate that: 1) The inundation water depths predicted by the CNN model closely match those predicted by the physics-based model, with average PCC, MAE, and RMSE metrics during a test rainstorm reaching 0.983, 0.020 m, and 0.086 m, respectively. 2) The CNN model accurately reproduces the trend of water depth in each grid cell over time. 3) The predictive performance of the CNN model surpasses that of extreme gradient boosting (XGBoost) model, followed by multi-objective random forest (MORF) model and K-nearest neighbor (KNN) model. 4) The computation speed of the CNN model is extremely fast, and is 600 times faster than that of the physics-based model. The CNN model serves as a powerful surrogate model for rapid simulation of urban pluvial floods, offering a reference for the utilization of DL in early warning and mitigation of urban flood disasters.

**Keywords:** convolutional neural network; deep learning; fast simulation; urban pluvial flood

## 1 Introduction

Floods are major natural disasters with impacts globally, characterized by their rapid and frequent occurrence, resulting in significant losses. Real-time urban flood warning and forecasting systems, capable of accurately and rapidly simulating urban flood processes, are becoming more and more important. Models based on hydrodynamic mechanisms have been widely applied in flood simulation, but they often require a significant amount of computational time.

To address the problem of computationally slow physics-based models, machine learning (ML) and deep learning (DL) techniques have attracted great attention [1]. Many traditional ML models such as support vector machine (SVM) models, random forest (RF) models, and gradient boosting decision tree (GBDT) models were utilized for fast simulation of flood inundation [2]. Relative to the traditional MLs, some latest DL approaches can automatically discover the desired features of original data, hence improving the performance of these approaches.

Currently, most studies have mainly focused on predicting the maximum flood inundation depth but not its dynamic evolutionary process. This study aims to construct a predictive model that uses CNN model to fast simulate the dynamic process of urban pluvial flood inundation.

## 2 Material and methods

The Chebei River Basin (CRB) is a highly urbanized region located in Guangzhou City, China, with an area of about 74 km². The CRB often suffers from pluvial flood disaster due to heavy rainstorm.

In this study, we generate a rainstorm-inundation database using a physics-based coupled model (SWMM+LISFLOOD-FP). Subsequently, a CNN model is developed to predict the spatial and

temporal evolution of rainstorm inundation. Finally, we compare the effectiveness of the CNN model with that of the coupled model and three other classical machine learning (ML) models.

## 3 Results and discussion

The spatial water depth predictions of the CNN model and the coupled model are compared. These results show that the spatial inundation depths predicted using the CNN model were close to those of the coupled model, and the water depth differences between them are small. The average PCC value of the CNN model reaches 0.983 and the average MAE value is 0.020 m, indicating a satisfactory prediction effect. Figure 1 illustrates the results of inundation predictions for a 50a rainstorm.

As for simulation time, the CNN model can complete the calculation of spatial inundation depth and its evolution over the study area within 12s. The CNN model can offer a reference for the utilization of DL in early warning and mitigation of urban flood disasters.

Figure 1. The simulated inundation water depth predicted using the CNN model (left) and the coupled model (right) under 50a test rainstorm scenarios (t=2.0h).

## 4 Conclusions

Combining the advantages of hydrological-hydrodynamic models and CNN models, we propose a fast prediction method for spatio-temporal variation of urban pluvial flood, and discuss the prediction performance of the CNN model by comparing it with a physics-based coupled model and three other classic ML models. The results show that in terms of accuracy, the developed CNN model shows satisfactory results in predicting the spatial and temporal changes of inundation and its predicted water depths correlate well with those of the physics-based coupled model.

## Reference

[1] Kabir, S., et al., 2020. A deep convolutional neural network model for rapid prediction of fluvial flood inundation. J. Hydrol., 590: 125481.

[2] Hou, J., et al., 2021. Rapid forecasting of urban flood inundation using multiple machine learning models. Nat. Hazard., 108(2): 2335-2356.

**Theme:** Hydroinfomatics for extreme hydrological events and resilience improvement
**IAHR Thematic Priority Area:** [TPA-3] Improving Resilience against Water Hazards and Disasters
https://doi.org/10.3850/iahr-hic2483430201-490

# Mining and Forecasting of Rainstorm Disaster Chain based on Knowledge Map

**Jing Huang[1,2], Xingyan Wu[2], Huimin Wang[3]**

[1] Hohai University, Nanjing 211100, China
[2] The National Key Laboratory of Water Disaster Prevention, Nanjing 210024, China
[3] Tianjin University, Tianjin 300072, China

*Corresponding author: j_huang@hhu.edu.cm*

**Abstract.** In order to understand the evolution process of the rainstorm disaster chain and predict the secondary disasters and their impacts, it is necessary to develop disaster chain mining and prediction methods. Taking Pearl River Delta region as a study area, a knowledge graph for rainstorm disaster chains is constructed firstly, and rainstorm disaster chains are mined based on link coupling of knowledge graph. Rainstorm secondary disasters and their impacts in '8.29 Shenzhen Rainstorm' event are predicted based on Bayesian networks. The research results indicate that: a) The constructed knowledge graph for rainstorm disaster chains comprehensively depicts the rainstorm disasters and their impacts. b) The rainstorm disaster chain mining method based on link coupling reveals the evolutionary mechanism of the rainstorm disaster chain by coupling multiple independent events. c) The proposed Bayesian network prediction model for rainstorm disaster chains can effectively forecast secondary disasters and the impacts of disaster situations in the rainstorm disaster chain. The framework of rainstorm disaster chain mining and forecasting based on knowledge map can improve the accuracy and reliability of the model, enhancing the emergency response capability of rainstorm disaster chains.

**Keywords:** Bayesian network; knowledge graph; probability prediction; rainstorm disaster chain mining

## 1 Introduction

In recent years, extreme rainstorm events in urbanized areas of China have been increasing due to climate change and rapid urbanization. These rainstorms not only trigger secondary derivative disasters like landslides and urban flooding but also severely impact urban infrastructure, public services, and personal and property safety. This phenomenon, referred to as a rainstorm disaster chain, occurs when rainstorms directly or indirectly trigger a sequence of secondary and derivative disasters. However, predicting and controlling its evolution and development presents significant challenges. Knowledge graphs have been utilized in representing and mining various disaster chains [1], including geological disaster chains, drought disaster chains, and typhoon disaster chains. Bayesian networks can predict the entire process of disaster chains through probabilistic inference by quantifying the likelihood of causal relationships between nodes [2], essential for effective disaster mitigation through broken chain management.

## 2 Methods

### 2.1 Rainstorm disaster chains mining method based on knowledge graph

In this paper, a knowledge graph for rainstorm disaster chains is constructed, incorporating the impact on vulnerable entities into the conceptual layer of the rainstorm disaster chain ontology model. The concept of rainstorm disaster events (Con) is categorized into two types: natural disasters and the impacts on affected entities. Natural disasters include 13 categories such as flood disasters, typhoon disasters, rainstorm disasters, wind disasters, etc., while the impacts on affected entities include 9 categories such as casualties, property damage, destruction of buildings and structures, damage to transportation facilities and equipment, etc. Based on the rainstorm disaster chain ontology, entity

information of rainstorm disaster events is extracted through Natural Language Processing [3]. We then employ a graph database (Neo4j) to store and visualize rainstorm disaster chain events.
A rainstorm disaster chain mining method based on link coupling is proposed. Entities with similar descriptions, whether natural disasters or the impacts on affected entities, are generalized into certain conceptual types. Merge event nodes belonging to the same conceptual type, and duplicate edges are removed to achieve link coupling of rainstorm disaster chains.

### 2.2 Rainstorm Disaster Chain Prediction Model Based on Bayesian Networks

Rainstorm disaster chain prediction calculates the probabilities of secondary disasters or impacts on sub-nodes under different states, given evidence of the primary disaster parent node states. Bayesian networks are constructed from the mined structure of the rainstorm disaster chain, and their topological structure is determined. Using the conditional probability information in the Bayesian network, the probabilities of event nodes in the rainstorm disaster chain are predicted.

## 3 Study area and results

### 3.1 Study area and data

The Pearl River Delta (PRD) region in southern Guangdong Province, China. We collect 588 disaster chain records from 2007 to 2021 across all cities in the PRD.

### 3.2 Results

#### 3.2.1 Rainstorm disaster chain in PRD

The rainstorm disaster chains in PRD can be categorized into the following five types:

- Natural disaster: Such as typhoons leading to rainstorms, heavy rain causing floods.
- Urban lifeline disruption: Such as impact on transportation by typhoons and floods.
- Equipment and building accidents: Involving damage to drainage pumps leading to internal flooding and the collapse of makeshift buildings at construction sites due to rainstorms.
- Casualty: Caused by collapsed buildings, landslides, and debris flow.
- Potential impacts on production and life: Such as fluctuations in agricultural product prices and impacts on tourism due to transportation disruption by rainstorms.

#### 3.2.2 Rainstorm disaster chain prediction for the '8.29 Shenzhen Rainstorm' event

For the severe rainstorm event in Shenzhen from August 29th to 31st, 2018, the rainfall intensity, duration, wind force, and other node states are set as evidence information for input, the most probable consequences, including landslide, severe internal flooding, severe transportation interruption, and building collapse, are predicted accurately during the early stages.

## 4 Conclusion

This paper constructs a rainstorm disaster chain ontology framework that includes the impact on vulnerable entities, mining the complete rainstorm disaster chain. The proposed knowledge graph-based prediction model enhances prediction accuracy and reliability.

## Reference

[1] H. Wang, W. Du, J. Liu, J. Wang, C. Mei, Derivation and transmission analysis of urban flood disaster chain based on knowledge graph, Advances in Water Science, 35(2): 185-196.
[2] J. Wang, X. Gu, T. Huang, Using Bayesian networks in analyzing powerful earthquake disaster chains, Nat Hazards, 68(2): 509-527.
[3] W.Kong, Q. Dai, S. Gao, X. You, H. Wang, J. Huang, L. Mao, A method for constructing a knowledge graph of flood-type Natech disaster events based on text mining, Jiangsu Province, 2022, CN114860960B.

**Theme:** Hydroinfomatics for extreme hydrological events and resilience improvement
**IAHR Thematic Priority Area:** [TPA-3] Improving Resilience against Water Hazards and Disasters
https://doi.org/10.3850/iahr-hic2483430201-492

# Characteristics and Adaptive Structure of Urban Flood Governance Network: The "7.20" Flood Event in Zhengzhou, China

**Wang Dandan[1], Liu Gaofeng[1], Wang Huimin[1], Huang Jing[1], Wang Yixin[1]**

[1]Business School, Hohai University, Nanjing, China

*Corresponding author: gaofengliu@hhu.edu.cn*

**Abstract.** Cooperative actors and their interactions are crucial to improve the efficiency of urban flood governance. Combined with the theory of Complex Adaptive System and the Social Network, this study explores a new adaptive structure of urban flood governance, trying to solve the problem of efficiency of emergency cooperation. Conducted via the Social network analysis, examining the density and centrality of urban flood disaster governance network, and identifies the importance of actors and how to play a role. The Exponential Random Graph Model is used to simulate the urban flood adaptive network, revealing the promotion effect of network endogeneity and interaction on the formation of adaptive networks. A study is carried out on the 720 flood in Zhengzhou to reveal the flexible adjustment trend and adaptive governance process. The results suggest that the network endogeneity and interactivity will influence the development of adaptive networks. Networks that are endogenous and highly interactive are more likely to form close collaborative relationships and information flows that are conducive to adaptive network. By establishing network committees or collaborative alliance to improve the participatory process of actors, can create reliable and effective adaptive response patterns for urban flood disasters.

**Keywords:** Urban flood; Complex Adaptive System; Governance network; ERGM; the 7.20 extraordinary flood in Zhengzhou

## 1 Introduction

This study attempts to establish the exponential random graph model to analyze the urban flood governance network.

- First point: Define the flood governance through the concept of social network, and analyze the overall structure of governance network and the role of core actors by quantifying the status and connection strength of governance actors;
- Second point: Focus on the interactions of actors in the governance network, consider two different adaptive behavior rules, build an adaptive network for urban flood management, and analyze the factors affecting the formation and evolution of the adaptive network.

## 2 Method

Adaptive governance can learn from the concepts of node adaptability and network dynamics in Complex Adaptive System theory (CAS) to better understand network structure and dynamic behavior (Kellogg et al, 2018). Based on the concept of complex adaptive systems, Chou proposed that resilient cities improve flood management capabilities, considering various risks and uncertainties (Qiu, 2018). Nevertheless, current research on the adaptation principle into urban flood management is lagging behind (Henstra et al, 2020). Therefore, this study combines the CAS theory with the Social Network Analysis (SNA) method to apply in flood risk scenario (Figure 1). This research framework considers the influence of the network's endogenous dependence structure and interactive organization cooperation on the formation and persistence of the network, and studies the linkage relationship between actors and the formed network structure.

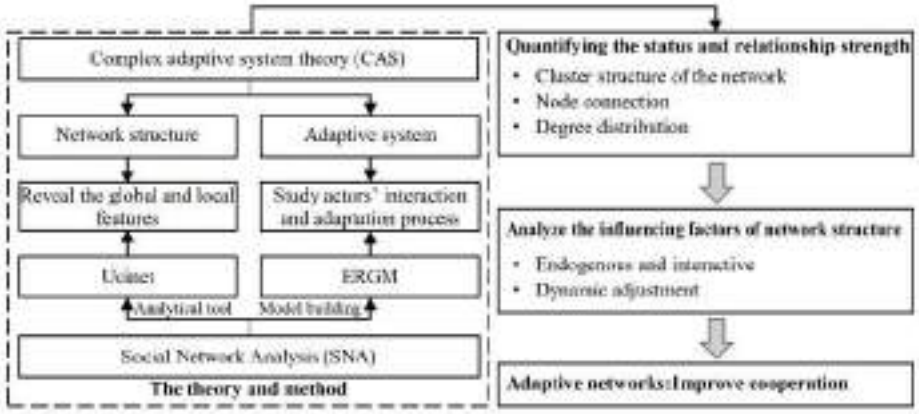


Figure 75 The framework of urban flood adaptive network structure analysis

## 3 Results

By contrast, two models are constructed to analyze the change of network structure by considering the different connection rules of endogeneity and interactivity. Compared with benchmark model 01, the endogeneity and interactivity in model 02 and model 03 show a higher level of significance, respectively, indicating high density and high information exchange efficiency in the network. For urban flood adaptive management, it shows that each actor can respond to emergency situations brought more quickly and coordinate rescue and post-disaster repair under its own rules.

Table 14 Estimated values of coefficients and statistical test results for models 01-03

| | Model 01 | Model 02 | | Model 03 | |
|---|---|---|---|---|---|
| | edges | edges | gwesp.fixed.0.2 | edges | mutual |
| Estimated value (standard error) | -1.414 *** (0.027) | -7.277 *** (1.155) | 5.094 *** (0.921) | -4.345 *** (0.067) | 2.569 *** (0.280) |
| AIC | 8547.985 | 8496.316 | | 2588.240 | |
| BIC | 8555.050 | 8510.446 | | 2603.756 | |
| Log-Likelihood | -4272.993 | -4246.158 | | -1292.120 | |

*** p<0.001; **p<0.01; *p<0.058

## 4 Conclusion

By revealing the network characteristics of urban flood management, this study can help practitioners in urban flood management better understand their unique roles and responsibilities, as well as the importance of cross-level collaboration, which is an essential foundation for effective urban flood management and well-functioning networks. Besides, the findings (e.g., the need for more balanced, decentralized decision-making and collaboration across levels) provide a new way of thinking for actors to better collaborate on current management practices. For policy makers to make out the pros and cons of the current organization, and the future challenges and opportunities of cooperation, can promote cooperation more effective, to cope with the challenge of complex risk.

## Reference

[1] Kellogg, Wendy A., and Aritree Samanta. "Network structure and adaptive capacity in watershed governance." Journal of environmental planning and management 61.1 (2018): 25-48.

[2] Qiu, Baoxing. "Resilient urban design methods and principles based on the complex adaptive system theory." Landscape Architecture Frontiers 6.4 (2018): 42-47.

[3] Henstra, Daniel, Jason Thistlethwaite, and Shanaya Vanhooren. "The governance of climate change adaptation: stormwater management policy and practice." Journal of environmental planning and management 63.6 (2020): 1077-1096.

**Theme:** Hydroinfomatics for extreme hydrological events and resilience improvement
**IAHR Thematic Priority Area:** [TPA-3] Improving Resilience against Water Hazards and Disasters
https://doi.org/10.3850/iahr-hic2483430201-494

# Dynamic Impact Assessment of Urban Floods on the Compound Spatial Network of Buildings-Roads-Emergency Service Facilities

**Yawen Zang [1] , Jing Huang [1,3] , Huimin Wang [1,2,3]**

[1] Institute of Management Science, Hohai University, Nanjing, 211100, China
[2] College of Management and Economy, Tianjin University, Tianjin, 300072, China
[3] The National Key Laboratory of Water Disaster Prevention, Nanjing, 210098, China

*Corresponding author: hmwang@hhu.edu.cn*

**Abstract.** There are complex interactions among urban spatial elements in rainstorm scenarios. Road interruptions may cause isolation between partially submerged buildings and emergency service facilities, thereby affecting the recovery capability of flooded buildings and the accessibility of emergency service facilities. This study constructed a compound spatial network of urban buildings-roads-emergency service facilities, and analyzed the complex impacts of dynamic floods on building risk, road risk, and emergency service accessibility. Firstly, a refined flood risk assessment at the building scale was carried out in combination with flood inundation, flood loss, population, vulnerable areas, underground buildings, and life facilities. Secondly, betweenness centrality indicator in complex networks was used to calculate road traffic capacity and collapse threshold, and the accessibility of emergency service facilities is calculated based on road traffic capacity. Finally, the interaction and feedback relationships between building flood risk and emergency service accessibility were analyzed. The results show that: (1) building flood risk analysis reveals that floods have a significant impact on residential and commercial losses, and high-risk flood areas are mainly concentrated in the central region of study area. (2) The road network has a collapse threshold when t=3h, and the fluctuating state of emergency service accessibility is significantly influenced by road traffic capacity. (3) Roads act as "bridges" connecting buildings and emergency service facilities, leading to the redistribution of building flood risk and emergency service accessibility, presenting complex dynamic changes. Additionally, submerged roads also affect the accessibility of emergency service facilities around flooded buildings, reducing the recovery capacity of flooded buildings, and exhibiting significant heterogeneity characteristics. Future research should consider the complex impacts of floods on urban elements in order to better manage dynamic flood risk.

**Keywords:** Dynamic assessment, Compound spatial network, Building flood risk, Road risk, Emergency service accessibility, Complex impacts

## 1 Structure

This paper aims to establish a compound spatial network of buildings-roads-emergency service facilities to evaluate the impact of dynamic impacts of time-varying dynamic floods on the interaction and dynamic changes between these spatial elements. Therefore, the main objectives are:

- First point: to calculate the vulnerability of different building land use types, and to carry out refined flood risk assessment with buildings as a unit considering water depth, building vulnerability, population density and the distribution of vulnerability areas, underground buildings, and lifeline facilities.
- Second point: to evaluate the collapse threshold and dynamic traffic capacity of road network using complex network indicator, and to calculate the accessibility of emergency service facilities based on road traffic capacity and building flood comprehensive risk
- Third point: to evaluate and discuss the interaction between building risk, road risk and emergency service accessibility and its dynamic change characteristics over time.

## 2 Method

This study considered road network as the foundation of urban compound spatial network, shaping the spatial structure of city under heavy rainfall scenarios. Firstly, the research abstracted road intersections and ramps during different rainfall periods as a set of points $V_P^T = \left\{v_1^t, v_2^t, ..., v_p^t\right\}$. The road segments connecting these intersections were abstracted as a set of edges $L_P^T = \left\{l_1^t, l_2^t, ..., l_m^t\right\}$. Additionally, taking into account the impact of heavy rainfall on the vehicle speed of roads $e^t$, we used the travel time $\tau$ required for road segments connecting road intersection $v_i, v_j$ at time *t* as the weight of network edges, constructing an adjacency matrix $\left\{A_{ij}^t\right\}$, forming a dynamic weighted undirected graph $G(V_p^T, L_P^T)$ that changes over time.This study extracted the centroids of flooded buildings and emergency service facilities, using the comprehensive risk values of water depth, building flood vulnerability, population density, and vulnerable areas, underground buildings, lifeline facilities at different time periods, as well as the capabilities of emergency service facilities as weights, to form sets of dynamic nodes $V_D^T = \left\{v_1^t, v_2^t, ..., v_d^t\right\}, V_F^T = \left\{v_1^t, v_2^t, ..., v_f^t\right\}$. It then identified the nearest road intersections to these nodes at different time periods, connecting them to form a set of edges $L_D^T = \left\{l_1^t, l_2^t, ..., l_n^t\right\}, L_F^T = \left\{l_1^t, l_2^t, ..., l_n^t\right\}$, thus creating a dynamic and weighted compound spatial network of urban buildings-roads-emergency service facilities $G(V_P \cup V_D \cup V_F, L_P \cup L_D \cup L_F)$.

## 3 Results

Emergency services need to consider the real-time changing building flood risk. In this paper, building flood risk at Level I-III was categorized as low-risk areas, while Level IV-V was considered high-risk areas. Regions with an accessibility of 0 were regarded as inaccessible areas, with Level I-II being low-accessible areas, and Level III-V being high-accessible areas. The combination of building flood risk and emergency service accessibility is referred to as building flood risk and emergency service accessibility indicator (BEI), resulting in six categories: low-risk and inaccessible (LI), low-risk and low-accessible (LL), low-risk and high-accessible (LH), high-risk and inaccessible (HI), high-risk and low-accessible (HL), high-risk and high-accessible (HH). It is evident that as rainfall duration increases, LI, HH show an increasing trend, while LL exhibit a fluctuating trend, LH show a growing trend. At t=1h, building flood risk is relatively low with high accessibility, so as to LH, HH account for 70% of the total flooded buildings. At t=2h-6h, high-risk areas significantly increase, the impact of floods on roads has intensified leading to a gradual increase in HI, while HL show a fluctuating trend. From t=2h to 5h, the proportion of LH is the highest. At t=6h, LL are the most numerous, LH significantly decrease, and HL noticeably increase.

## 4 Conclusions

The study found that: (1) Analyzing at the building scale revealed that due to the concentration and centralization of residential and commercial properties, floods have a significant impact on the losses of these building types. High-risk areas for building flood risk are mainly concentrated in the central region of study area. (2) As the rainfall duration increases, road traffic capacity continuously decreases. Due to the impact of road traffic capacity, the fluctuation of emergency accessibility is pronounced. (3) Roads, as "bridges," connect buildings with emergency service facilities, leading to a complex dynamic redistribution of building flood risk and emergency service accessibility levels.

## Reference

[1] Li, Z., He, W., Cheng, M., Hu, J., Yang, G., Zhang, H., 2023. SinoLC-1: the first 1-meter resolution national-scale land-cover map of China created with the deep learning framework and open-access data. Earth Syst. Sci. Data Discuss. [preprint] in review. https://doi.org/10.5194/essd-2023-87.

**Theme:** Hydroinfomatics for extreme hydrological events and resilience improvement
**IAHR Thematic Priority Area:** [TPA-3] Improving Resilience against Water Hazards and Disasters
https://doi.org/10.3850/iahr-hic2483430201-496

# Groundwater Response to Future Droughts Under Climate Change in A Coastal Region

**Jun Zhang[1,*], Laura E. Condon[2]**

[1] Key Laboratory of VGE of Ministry of Education, Nanjing Normal University, Nanjing, China
[2] Department of Hydrology and Atmospheric Sciences, The University of Arizona, Tucson, United States

*Corresponding author: jun.zhang@njnu.edu.cn*

**Abstract.** Drought is a widespread hazard globally and is associated with great uncertainty under climate change. Previous studies on future drought scenarios have mainly focused on the atmospheric aspect, but few have considered the buffer function of groundwater for droughts. Using a severe drought occurred in the 1960s as a baseline event, this study examined the overall hydrological responses to droughts under climate change in the northeastern coast of the United States. Based on the atmospheric forcing of the drought in the past (1960s) and future scenarios (2020s, 2040s and 2090s) with ParFlow-CLM. Results show that more precipitation is expected in the future and less snow pack may reduce the streamflow in spring. Groundwater storage recharged by precipitation was found to increase in the future and more importantly the contribution of groundwater to streamflow was shown to be more significant in dry periods. Increasing groundwater storage and varying groundwater contribution in different time periods will further influence the hydrological performance of the system such as the runoff ratio. In this study, groundwater has been demonstrated to be an important source for mitigating the effects of drought and has the capacity to enhance the resilience of the hydrological system to the drought.

**Keywords:** Climate change, Drought, Groundwater, ParFlow-CLM

## 1 Introduction

Drought is one of the world's most catastrophic hazards globally, historically costing billions of dollars and affecting millions of people in the past. Global warming may not cause droughts but the droughts are expected to be quicker and more intense [1]. Research into the evolution of droughts and regional hydrological responses in the future is critical to mitigate the impacts of potential droughts. The process of drought propagation has been demonstrated in detail, but how the hydrological system attempts to mitigate the effects of droughts is still poorly understood. In this study, we take the 1960s drought as a baseline drought event and explore the hydrological responses in the future[2]. The physically based hydrological model ParFlow-CLM allows the simulation of hydrological processes from the canopy to the bedrock and is employed to simulate the hydrological processes especially the groundwater reactions to droughts. A comprehensive insight into the groundwater responses to historical drought and future droughts under pseudo-global warming is expected from this study.

## 2 Method

A coastal region in the Northeast of the US is selected for comprehensive hydrological simulations in historical and future scenarios by ParFlow-CLM. We simulated the hydrological response to historical and future droughts using an integrated model ParFlow-CLM [3]. The domain is simulated in hourly 1km-resolution for each scenario. The subsurface of the domain in this study is 392m deep and is divided into ten layers. Before conducting transient simulations we first perform a model spin-up, allowing the groundwater reach an equilibrium state and serves as the model initial condition. To

assess the model performance, we compared the simulated daily streamflow with 321 USGS stream gauges and WTD with long-term observations from datasets in the 1960s.

## 3 Results

The simulated streamflow in the 1960s was compared with the daily observations at 321 USGS stream gauges. All 321 gauges were evaluated by the Spearman's Rho and the Absolute relative Bias. The results illustrate that the Spearman's Rho of most of the gauges is greater than 0.5 and the Absolute relative Bias of almost all gauges is less than 1.

The subsurface storage simulated in this study includes soil moisture at the top two-meter soil and the deep groundwater at a depth of 392m, which is missing in the previous study [2]. From the results, the increase of subsurface storage in top two-meter layers is mainly found in the mountains, while the increase of deep groundwater is also observed near the coast. The results show that subsurface storage can increase over time, with the largest amount of water in the subsurface in 2090s. The increase in subsurface water in the second half is more significant than in the first half. Fluctuations are also expected for all the scenarios, in particular a decrease in almost every spring. In 1960s, 2020s and 2040s, the baseflow ratio in dry years is generally larger than that in moderate years, demonstrating that groundwater contributes more to the streamflow during droughts. This trend is less pronounced in 2090s, which is probably because the dry years in 2090s are much less severe in other scenarios. Figure 1(b) presents the difference in streamflow versus the difference in baseflow ratio by future scenarios minus 1960s. As streamflow decreases in the future, groundwater tries to contribute more to make up this deficit.

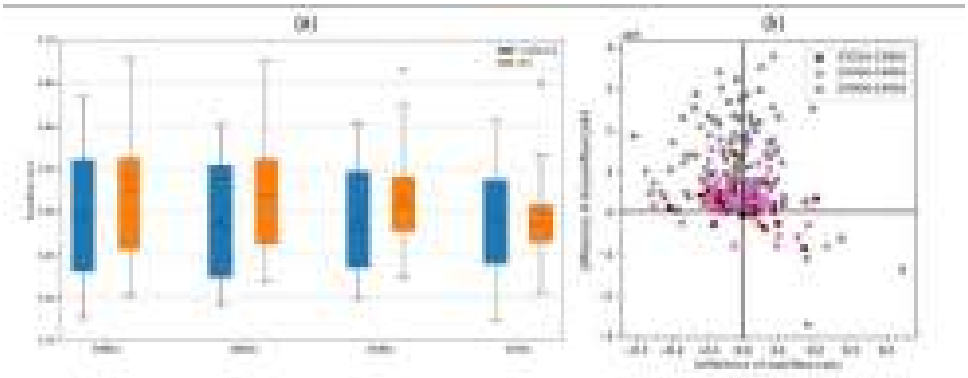

Figure 1 (a) baseflow ratio in moderate and dry years in four scenarios, (b) the difference of streamflow against baseflow ratio between future scenarios and 1960s

## 4 Conclusion

This study investigates the hydrological responses to the historical drought (1960s) and future droughts (2020s, 2040s, 2090s) under climate change in a coastal region. With higher precipitation, the domain is expected to receive more water and produce more streamflow. We also show that subsurface storage is likely to increase with greater precipitation in the future. This long-term increase in storage can provide an important buffer to future droughts. This delivers an important message that groundwater is an essential water resources in drought assessment and management in the future.

## References

[1] K. E. Trenberth et al., Global warming and changes in drought, Nat. Clim. Chang. 4 (2014), 17–22.
[2] Z. Xue and P. Ullrich, A Retrospective and Prospective Examination of the 1960s U.S. Northeast Drought, Earth's Future, 9 (2021).
[3] S. J. Kollet and R. M. Maxwell, Capturing the influence of groundwater dynamics on land surface processes using an integrated, distributed watershed model," Water Resour. Res. 44 (2008) 1–18.

**Theme:** Hydroinfomatics for extreme hydrological events and resilience improvement
**IAHR Thematic Priority Area:** [TPA-3] Improving Resilience against Water Hazards and Disasters
https://doi.org/10.3850/iahr-hic2483430201-498

# Evolution Characteristics of Drought-Flood Abrupt Alternation Events in The Yangtze River Basin, China

**Wuxia Bi[1,2,*], Cheng Zhang[1,2], Dawei Zhang[1,2], Fan Wang[1,2], Weiqi Wang[1,2], Wenqing Lin[1,2]**

[1] State Key Laboratory of Simulation and Regulation of Water Cycle in River Basin, China Institute of Water Resources and Hydropower Research, Beijing 100038, China
[2] Research Center on Flood & Drought Disaster Prevention and Reduction of the Ministry of Water Resources, Beijing 100038, China

*Corresponding author: biwx@iwhr.com*

**Abstract.** In recent years, compound extreme events have increasingly occurred globally. A new type of compound extreme event, drought-flood abrupt alternation (DFAA), has been reported multiple times, especially in China. According to our previous study, DFAA events in China mainly occurred in the southeastern part. As the third largest watershed in the world, Yangtze River Basin, has strategic significance for China's socio-economic development. The DFAA events normally have negative effects on the agricultural production, eco-environment, etc. Therefore, this study explored the evolution characteristics of DFAA events in the Yangtze River Basin, which can help quantitively estimate the impact of climate change on one of the important grain bases in China. The results show that the occurrence of DFAA events has increased in the past 60 years, and the average annual area proportion covered by DFAA events has a statistically significant ($P < 0.05$) increasing trend in the Yangtze River Basin. The possible targeted regulation measures were proposed as well.

**Keywords:** compound extreme event, daily scale, multi-indicators, Yangtze River Basin

## 1 Introduction

Compound extreme events, the combination of multiple drivers and/or hazards that contributes to societal or environmental risk, has been increasing in recent years [1]. Drought-flood abrupt alternation (DFAA), a new kind of compound extreme event, has attracted more and more attention in recent years, especially in China. Several studies show that DFAA had negative superposition effects on agriculture, economy, and so on [2]. Therefore, it is of great significance to study the DFAA events in improving determination method and quantitively analyzing the evolution characteristics.
This study proposed an improved determination method of DFAA events, and analyzed the spatiotemporal evolution characteristics of DFAA events in the Yangtze River Basin in the past 60 years. The findings could provide a scientific reference for local targeted measures making.

## 2 Material and methods

We proposed a daily-scale determination method of DFAA, which considers multiple indicators including the meteorological and agricultural aspects.

$$\mathrm{DFAA}_L = \begin{cases} \sum_{j-i}^{j} P_{d,l1} = 0, W_{d,l1,m} = \dfrac{\theta_{d,l1,m}}{F_c} \times 100,\ j-i \le m \le j \\ \sum_{j}^{j+n-1} P_{f,l2} \end{cases} \quad (1)$$

Where, $\mathrm{DFAA}_L$ is the level of the DFAA event; $i$ is the duration of drought period (days); $j$ is the day beginning to rain; $P_{d,l1}$ is the amount of effective precipitation; $W_{d,l1,m}$ is the relative soil moisture on day $m$ (%); $\theta_{d,l1,m}$ is the soil moisture on day on day $m$ (%); $i$ is consecutive rainy days; $P_{f,l2}$ is the total amount of precipitation from day $j$ to day $j+n-1$ (mm). $\mathrm{DFAA}_L$ is determined by the drought level $l1$ and the flood level $l2$.

This study mainly analyzed the frequency and spatial coverage of DFAA events in the Yangtze River Basin. According to our proposed method, the data used in this study contains daily precipitation data, soil moisture data, soil field capacity, and land cover.

## 3 Results and discussion

The frequency of DFAA events during 1961 to 2018 in the Yangtze River Basin decreased in the order of light level > moderate level > severe level, with highest count of DFAA events of 28 times, 15 times, and 6 times, respectively (Fig. 2). The DFAA events mainly occurred in the middle and lower reaches, and occurred in summer. The average annual area proportion covered by DFAA events has a statistically significant increasing trend ($P < 0.05$), with an increasing rate of 0.646%/10a. Our findings are basically consistent with previous studies.

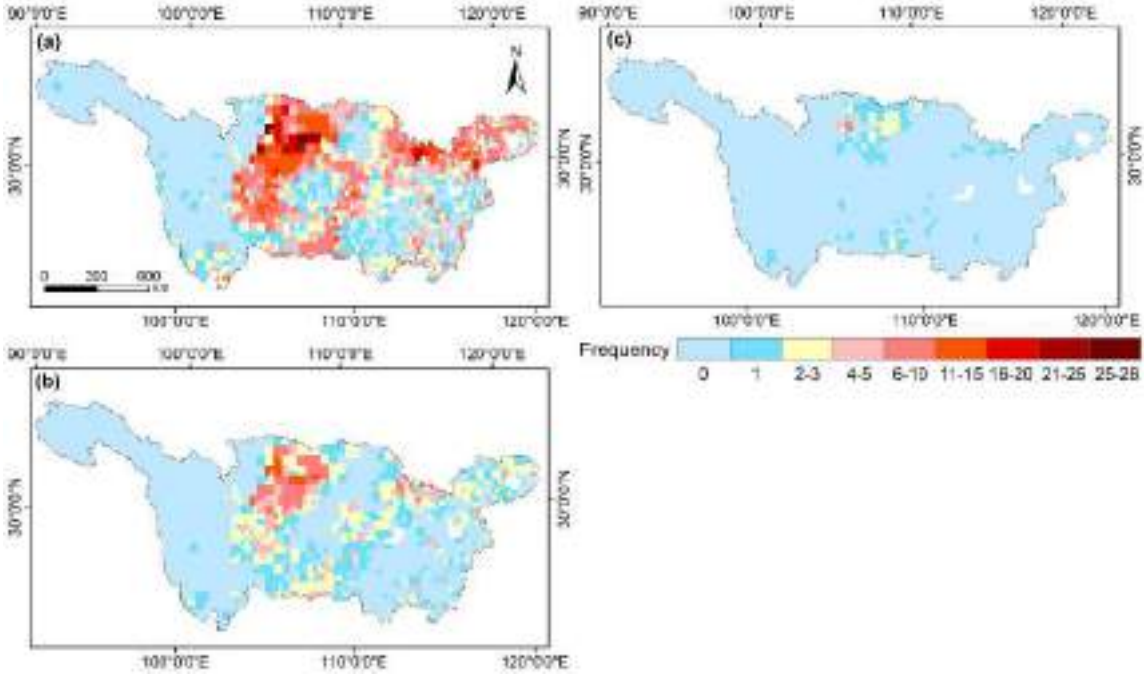


Figure 1 Frequency of drought-flood abrupt alternation (DFAA) events from 1961 to 2018 in the Yangtze River Basin. (a) in light level, (b) in moderate level, (c) in severe level in ten river basins.

## 4 Conclusions

Based on our proposed DFAA determination method, we found that i) The frequency of DFAA events decreased in the order of: light level > moderate level > severe level, and summer > autumn > spring > winter; and ii) The average annual area proportion covered by DFAA events increased by 0.646%/10a.

## Reference

[1] IPCC, Climate Change 2021: The Physical Science Basis. Contribution of Working Group I to the Sixth Assessment Report of the Intergovernmental Panel on Climate Change, Cambridge University Press, New York, 2021.

[2] W. Shi, S. Huang, K. Zhang, B. Liu, D. Liu, Q. Huang, W. Fang, Z. Han, L. Chao, Quantifying the superimposed effects of drought-flood abrupt alternation stress on vegetation dynamics of the Wei River Basin in China, J. Hydrol. 612 (2022) 128105.

**Theme:** Hydroinfomatics for extreme hydrological events and resilience improvement
**IAHR Thematic Priority Area:** [TPA-3] Improving Resilience against Water Hazards and Disasters
https://doi.org/10.3850/iahr-hic2483430201-500

# Urbanization-Induced Drought Modification: Example Over the Yangtze River Basin, China

**Xiang Zhang [1, 2], Shuzhe Huang [2]**

[1] National Engineering Research Center of Geographic Information System, School of Geography and Information Engineering, China University of Geosciences, Wuhan, 430074, China.
[2] State Key Laboratory of Information Engineering in Surveying, Mapping, and Remote Sensing (LIESMARS), Wuhan University, Wuhan 430079, China

*Corresponding author: zhangxiang76@cug.edu.cn*

**Abstract.** The 21st century witnessed unprecedented development in Chinese cities and rapid urbanization has exerted substantial effects on regional environmental and climate change. While increased precipitation and temperature extremes have been widely observed under urbanization, whether increasing urbanization enhances or mitigates drought evolution is still unknown. By applying a series of trend analysis, nonstationary frequency analysis, and spatial characteristics analysis, this study investigates urbanization effects and contributions on drought development, taking the rapidly developing Yangtze River Basin (YRB) as an example. Results indicate that urbanization leads to exacerbation of drought at three major urban agglomerations in YRB, which accounts for 46.62% of total variations for Standardized Precipitation Evapotranspiration Index (SPEI). Considering nonstationary features, urbanization appears to mitigate extreme drought conditions (1.14%) while drought duration and severity are increased (9.02%) and enhanced (9.12%) under 50-year return period over YRB, respectively. From the spatial perspective, area of urbanizing region in a drought event also indicates a significant increasing trend during 1981 to 2018. These findings further confirm that urbanization appears to be a notable local factor that leads to the modifications of regional drought development. The results are expected to provide implications for mitigating drought impacts and making related policy.

**Keywords:** Drought; Urbanization effect; Yangtze River Basin

## 1 Introduction

As one of the most devastating disasters, drought has led to tremendous losses and has become one of the biggest challenges to the sustainable development goal at global scale. However, it is still unclear that what changes the urbanization process will bring to drought. In other words, does the drought exhibit higher (or lower) magnitude and longer (or shorter) duration under urbanization is still unknown. Here we attempt to fill the research gaps by answering the following key questions: (1) How does the trend patterns of meteorological drought change in different urbanization periods? (2) To what extent has the urbanization modified drought characteristics (e.g., duration, severity, extreme)? (3) How is the extent of the drought events related to the urbanization?

## 2 Study Area and Data

Yangtze River Basin (YRB), as the third largest river basin in the world, has contributed greatly to the development of economy and climate change in China. In recent decades, the variations of drought characteristics and hydrological cycle were accelerated due to the intensification of human activities (e.g., urbanization process) and climate change. Considering the demand of spatial and temporal resolution, the Climate Hazards Group InfraRed Precipitation with Station (CHIRPS), a satellite-based quantitative precipitation estimate product, was applied with a 0.05° resolution from 1981 to

2018. In addition, we collected air temperature data from the China Meteorological Forcing Dataset (CMFD), ranging from 1981 to 2018 with a spatial resolution of 0.1°.

## 3 Methods

We propose a framework that combines trend analysis, frequency analysis, and spatial analysis to study the urbanization effects on drought from spatial and temporal perspectives. The challenges include eliminating the confounders from other factors (e.g., topography, climate change) and considering the nonstationary feature under changing environment. Entire methodology can be divided into four parts: (a) Data collection and preprocessing; (b) Trend analysis for various drought series; (c) Stationary and nonstationary frequency analysis; (d) Spatial characteristics analysis for drought events. Based on the analysis above, the framework can finally help the investigation of urbanization effects on drought development.

## 4 Results and Discussion

Based on the analysis above, the study period (1981-2018) was first divided into a relatively weak urbanization (pre-2000) and a rapid urbanization part (post-2000). Trend analysis was conducted for the drought characteristics for all grids in the study region.

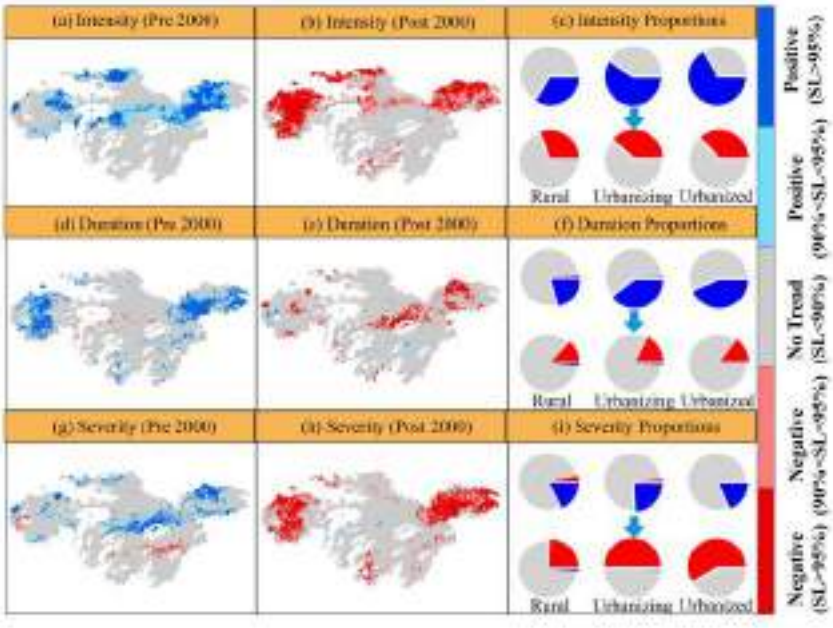


Fig. 1. Trend analysis for drought intensity, duration and severity in pre-2000 and post-2000 periods.

## 5 Conclusions

Significant and non-uniform changes were identified in the drought patterns for different urbanization periods. Considering the nonstationary nature of drought, the results from frequency analysis again confirm that the urbanization process significantly modified the drought characteristics. Examining the variations in proportions of rural, urbanizing, and urbanized areas in the drought events, it was found that the proportion of the urbanizing regions showed a significant upward trend in all three urban agglomerations. The findings above further provided evidence that urbanization appears to be one notable local factor that led to the modifications of drought development.

## Reference

[1] Huang S, Zhang X, Yang L, et al. Urbanization-induced drought modification: example over the Yangtze River Basin, China[J]. Urban Climate, 2022, 44: 101231.

**Theme:** Hydroinfomatics for extreme hydrological events and resilience improvement
**IAHR Thematic Priority Area:** [[TPA-3] Improving Resilience against Water Hazards and Disasters
https://doi.org/10.3850/iahr-hic2483430201-502

# A Novel Fusion Method for Generating Surface Soil Moisture Data With High Accuracy, High Spatial Resolution, and High Spatio-Temporal Continuity

**Xiang Zhang [1, 2], Shuzhe Huang [2], Tailai Huang [1]**

[1] National Engineering Research Center of Geographic Information System, School of Geography and Information Engineering, China University of Geosciences, Wuhan, 430074, China.
[2] State Key Laboratory of Information Engineering in Surveying, Mapping, and Remote Sensing (LIESMARS), Wuhan University, Wuhan 430079, China

*Corresponding author: zhangxiang76@cug.edu.cn*

**Abstract.** Surface soil moisture (SSM) has considerable impact in land-atmosphere exchanges of water and energy. However, due to the inherent deficiencies of remotely sensed data (e.g., cloud contamination), none of the current algorithms alone can provide daily and seamless SSM at field scale (i.e., 30 m). To explore this research gap, we proposed a novel SSM fusion framework of Generating high Resolution, Accurate, Seamless data using Point-Surface fusion (GRASPS) based on multiple remotely sensed, reanalysis, and in-situ datasets. First, 30 m seamless continuous SSM correlated variables (land surface temperature, NDVI, Albedo) were generated by enhanced spatial and temporal adaptive reflectance fusion model (ESTARFM). Then, downscaled auxiliary variables and other background variables were input into a deep learning model to produce 30 m daily and seamless SSM. The average Pearson correlation coefficient (PCC), root mean squared error (RMSE), unbiased RMSE (ubRMSE), Bias, and mean absolute error (MAE) over all validation sites for the downscaled SSM achieved 0.78, 0.048 m^3 m^(-3), 0.033 m^3 m^(-3), -0.001 m^3 m^(-3), and 0.041 m^3 m^(-3), respectively. After bias correction, the RMSE, ubRMSE, Bias, and MAE at validation sites further decreased by 13%, 7%, 22%, and 18%, respectively.

**Keywords:** Deep learning, Point-surface data fusion, Surface soil moisture

## 1 Introduction

Surface soil moisture (SSM) has been identified as an “Essential Climate Variable” in the Global Climate Observing System. It is one of the most significant land surface variables and plays a critical role in monitoring and understanding global environment and climate change. Generally speaking, the current point-wise (ground sensor network) and surface-based (satellite or airborne) approaches have diverse while also complementary capabilities in SSM monitoring/estimation. The main objective of this study is to propose a complete and advanced SSM downscaling framework by applying point-surface data fusion method through a deep learning approach. We design this method to generate field scale (30 m) spatio-temporally continuous (daily) SSM at a relatively high accuracy (e.g., high correlation coefficients, low RMSE). The proposed method will shed light on the generation of 3H SSM data, which is expected to provide much better basis for understanding environmental changes and supporting hydrological applications at finer spatial scale.

## 2 Study Area and Data

The study area is located in Petzenkirchen, Austria (48º9’N, 15º9’E), covering an area of about 400 ha. A soil moisture network obtained from the International Soil Moisture Network (ISMN), is operated here in an agricultural catchment named Hydrological Open Air Laboratory (HOAL). In this study, a total of three categories of datasets were adopted for generating 30 m spatio-temporally

continuous soil moisture (Table 1). Specifically, the data sets contained: (1) remotely sensed products including Landsat 8, MOD11A1, MOD09GA; (2) model-based products including SMAP Level-4 SSM and the ERA-5 reanalysis product; (3) ISMN in-situ soil moisture measurements.

## 3 Methods

The proposed framework of Generating high Resolution, Accurate, Seamless data using Point-Surface fusion (GRASPS) is illustrated in Fig. 2. There are four steps to generate 3H SSM data: (1) Data collection and preprocessing; (2) Generation of 30 m seamless LST and surface reflectance; (3) Deep learning based SSM downscaling; (4) Pixel classification based bias correction.

## 4 Results and Discussion

DBN was adopted to downscale SSM at 30 m by fitting a total of seven SSM related predictor variables. The average PCC, RMSE, ubRMSE, Bias, and MAE were 0.78, 0.048 $m^3m^{-3}$, 0.033 $m^3m^{-3}$, -0.001 $m^3m^{-3}$, and 0.041 $m^3m^{-3}$, respectively. Results indicated that the RMSE, ubRMSE, Bias, and MAE of the downscaled SSM at the validation sites after the bias correction were improved by 13%, 7%, 22%, and 18%, respectively. Further spatial and temporal analysis of downscaled SSM in comparison with ERA-5 SSM and SMAP SSM exhibited that our GRASPS-SSM can better capture the local SSM dynamics and represent more detailed spatial characteristics. Moreover, the comparative analysis confirmed the effectiveness of the deep learning algorithms and the combinations of the input variables in the GRASPS framework.

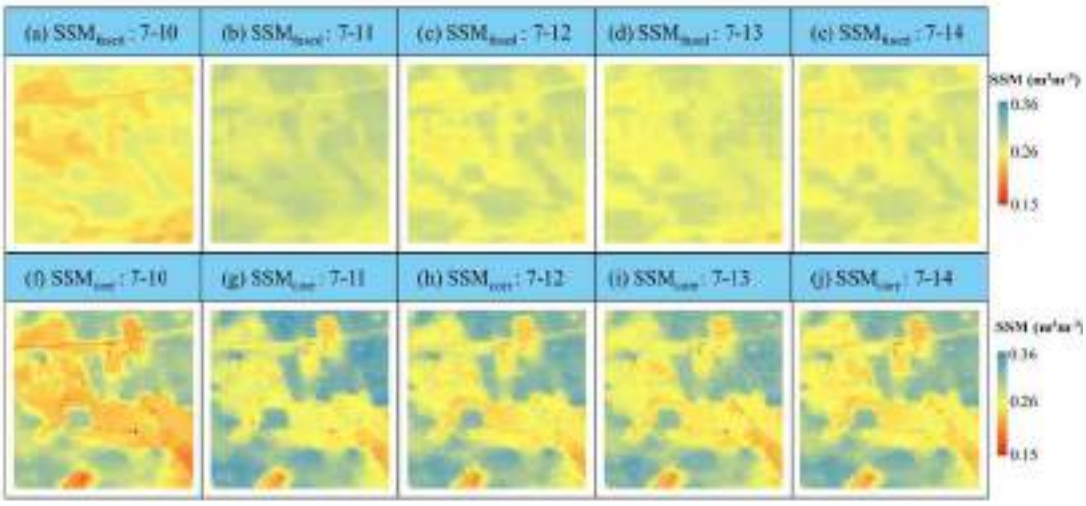


Fig. 1. Spatial distributions of corrected and downscaled SSM for 5 consecutive days in June, 2017. The unit for SSM is m^3 m^(-3).

## 5 Conclusions

In this study, an integrated methodology (GRASPS), inspired by point-surface data fusion and deep learning, was proposed along with fusion of multisource remotely sensed, model-based, and in-situ ground data sets. GRASPS was designed to generate 3H (i.e., high spatial resolution, high accuracy, high spatial-temporal continuity) SSM data and it was evaluated in a densely distributed soil moisture sensor network (HOAL network) located in Petzenkirchen, Austria.

## Reference

[1] Huang S, Zhang X, Chen N, et al. A novel fusion method for generating surface soil moisture data with high accuracy, high spatial resolution, and high spatio-temporal Continuity[J]. Water Resources Research, 2022, 58(5): e2021WR030827.

**Theme:** Digital transformation of urban water systems
**IAHR Thematic Priority Area:** [TPA-4] Digital Transformation
https://doi.org/10.3850/iahr-hic2483430201-504

# Asset Management Support Indicator to Drive Technical Decisions in Real Water Distribution Systems

**Orazio Giustolisi[1], Gabriele Freni[2], Giovanni Bruno[3], Franz Bruno[3], Luigi Berardi[4] and Gianfredi Mazzolani[5]**

[1] DICATECH, Politecnico di Bari, Bari, 70125, Italy orazio.giustolisi@poliba.it
[2] Università di Enna "Kore", Enna, 94100, Italy
[3] COGEN S.p.A, Enna, 94100, Italy
[4] INGEO, Università "G. d'Annunzio" di Chieti Pescara, Pescara, 65127, Italy
[5] Acquedotto Pugliese S.p.A., Bari, 70121, Italy

**Abstract**. Water Performance Indicators, WPIs, were originally conceived to measure the effectiveness in managing water distribution networks, WDN, to deliver safe, reliable, and affordable water services to the customers; they are currently used to support ex-ante and ex post evaluation of water providers by national regulation agencies worldwide. On this premises, they are being used by water companies also to drive the allocation of investments among different WDNs or different portions of the same WDN. Nonetheless, not all WPIs are adequate to support asset management activities aimed at leakage reduction and the selection of a wrong indicators might conduct to misleading conclusions and inefficient investments. The novel Asset Management Support Indicator, AMSI, is here presents to provide insight into the most efficient course of actions in WDNs. Differently from other WPIs reported in literature, AMSI is consistent with WDN hydraulics and exploits the opportunities from advanced hydraulic modelling and digital transformation. AMSI is demonstrated and discussed using real WDNs managed by the water utility of the province of Enna in Sicily. It is shown that AMSI is scalable and can effectively support technical decisions about the leakage control strategy, i.e. pipeline replacement and active leakage detection/localization versus pressure control, thus maximizing the efficiency of investments of a water utility.

**Keywords**: Asset Management, Digital Transition, Digital Water, Leakage Management, Water Distribution Networks, Water Performance Indicators, KPIs in Water Losses

## 1 Introduction

This paper presents a novel WPI for leakage management named Asset Management Support Indicator (AMSI) [1], which is characterized by several novelties. AMSI was developed from the advanced hydraulic modelling of pressurized water systems; therefore, it is physically based and not empirical. As such, AMSI meets the needs of WDNs digitalization by allowing the use of data collection and hydraulic modelling to drive investments rationally and efficiently.

## 2 AMSI for the rationality of investment path decisions

The aim is here to show the capability of AMSI to support the rationality of investments of pipe replacement and active leakage detection versus pressure control to reduce the density of water losses [2]. Figure 1 shows $D_{s\text{-}leak}$ versus $P_{s\text{-}ref}$ for several values of AMSI, from 0.2 to 5 assuming $\alpha = 1$ and the relevance of AMSI reporting $D_{s\text{-}leak}$ both in $m^3/d/km$ and in L/s/km. The term "system" is used here to refer to a portion of the pressurized water system under analysis.

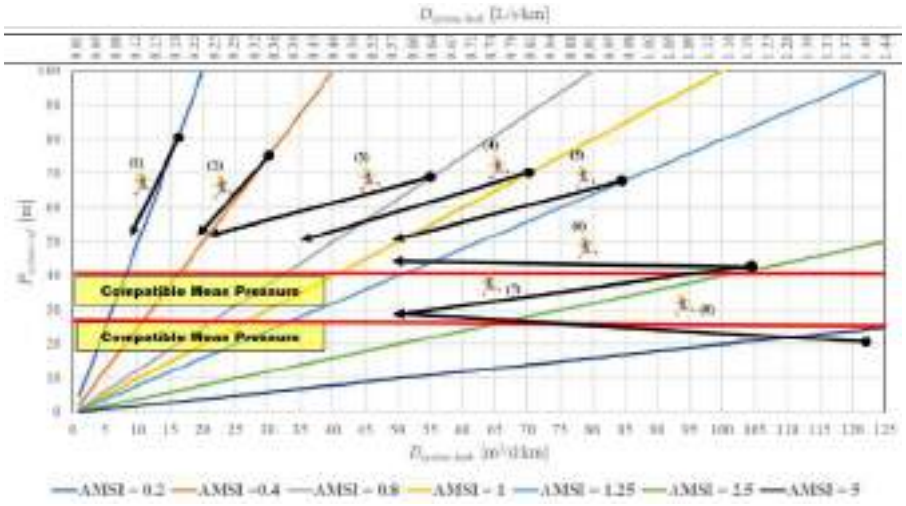


**Figure 1**. Diagram to support investments for leakage management.

Figure 1 reports eight arrows from (1) to (8) representing different investment paths. Furthermore, for explanatory purposes, two possible levels of "compatible mean pressure" of the system at 40 m and 25 m are indicated in the graph. It is a relevant concept to understanding the actual unavoidable density of water losses in the system. In fact, WDNs are quite different as management history, terrain altimetry, building heights, presence of local private tanks with pumping, minimum pressure required by service charters, etc. Therefore, each consumption centre and DMA may be characterized by the lowest mean pressure that can be compatible with the minimum pressure required for a correct service to customers. Arrows (1) and (2) represent the investment paths in non-deteriorated systems, AMSI = 0.2 and 0.4, where the density of water losses is generally low, and the pressure control activity is the best cost/benefit investment path to reduce $D_{s\text{-}leak}$. Arrows (3), (4) and (5) represent investment paths in systems characterized by medium deterioration–and high pressure in the examples. The arrows represent the paths of pressure control with reduction of the $P_{s\text{-}ref}$, associated to the reduction of AMSI due to pipes replacement and/or active leakage detection activities. Arrows (6), (7) and (8) represent investment paths in systems characterized by high deterioration. They are also generally distinguished by a low pressure because of the deterioration itself, i.e., hydraulically speaking, because of the high value of the linear leakage outflow, as shown in Figure 1. The investment path is here constrained by the technical situation, and the pressure control is not applicable unless there are pressure reduction margins with respect to the compatible mean pressure, as for arrow (7). Then, pipe replacement plans and/or active leakage detection are required to decrease AMSI, and although these activities are more expensive and riskier (also more uncertain) than pressure control, they represent the only possible choice to reduce water losses. The investment path of the arrow (7) shows the possibility to reduce pressure along with AMSI. It depends on the starting level of reference pressure with respect to the compatible one. Finally, the path (8) shows the case of a system where pipe replacement allows to increase the reference pressure which starts below the minimum level for a correct service.

**References**

[1] Giustolisi, O., Digital Transition, Digital Twin and Digital Water: History, Concepts and Overview for the application to Aqueducts. Digital Water: Knowledge Application & Hydroinformatics, 1(1), 1-25, (2024).

[2] Giustolisi, O., Mazzolani, G., Berardi, L., & Laucelli, D.B., From Advanced Hydraulic Modelling to Performance Indicator for the Efficiency of Investments in Leakage Management of Pressurized Water Systems. Water Research, submitted for pubblication, (2024).

**Theme:** Digital transformation of urban water systems
**IAHR Thematic Priority Area:** [TPA-4] Digital Transformation
https://doi.org/10.3850/iahr-hic2483430201-506

# Improving the Knowledge of Real WDNs by Building Geometric Model

**Francesco Gino Ciliberti[1], Luigi Berardi[1], Daniele Biagio Laucelli[2], Gabriele Freni[3], Antonietta Simone[1] and Stefania Piazza[3]**

[1] INGEO, Università "G. d'Annunzio" of Chieti-Pescara, Pescara, Viale Pindaro 42, Pescara 65127, Italy
[2] DICATECH, Politecnico di Bari, Via E. Orabona 4, Bari, 70125, Italy
[3] School of Engineering and Architecture, University of Enna "Kore", Cittadella Universitaria, Enna (Italy)

*Corresponding author: luigi.berardi@unich.it*

**Abstract.** The construction of a reliable geometric model for WDNs entails the first necessary step in this direction for many reasons: it represents the physical domain where WDN hydraulics takes place; it is essential to provide a consistent representation of the corresponding *digital twin* called by *digital water services*; it represents a structured platform to integrate information from the field and from *digital transition tools*, as well as to gain system knowledge. This contribution addresses the pressing need of many water providers to give value to all data stored into the water utilities' database, integrating information coming from recent infrastructure surveys and monitoring campaigns, as well as the daily first-hand knowledge of the operators. The resulting methodology was developed based on the authors' experience on many real WDNs where the digital transition process has just begun.

**Keywords:** Asset Management, Digital Transformation, Digital Water, Hydraulic Model, Geometric Model, Water Distribution Networks

## 1 Introduction

The *digital transformation* in the sector of water distribution networks (WDNs) management involves the application of digital technologies and methodologies to improve the efficiency of technical decision-making [1]. The concepts of Digital Twin (DT) and Digital Water Services (DWSs*)* [2][3] have been introduced in recent years in the WDN sector to support such transition. The *geometric model* is meant as the spatial representation of WDN physical layer, encompassing crucial information about WDN layout of the DT, including the connectivity among pipes, hydraulic devices, diameter of pipelines, georeferenced position of consumers and related properties, and elevation of each system feature. Therefore the geometric model is mandatory to the implementation of the WDN *digital twin*, acting as an essential pre-requisite for implementing the whole set of actions involved in the WDN management workflow at different time scale, at short-term (operational), medium-term (tactical) and long-term (strategic) horizon.

## 2 Structured methodology to support the building of the WDN geometric model

This contribution presents a structured methodology to support the building of the geometric model combining data from infrastructure surveys and information from water utilities databases. The procedure, whose steps are detailed in Figure 1, starts from data contained in the water providers' database, e.g., on GIS platforms, and addresses common issues encountered when using data from network survey, which are generally not suited for hydraulic modelling.
The first part (leftmost in Figure 1) of the procedure focuses on identifying all potential connectivity flaws within WDN layout, specifically detecting the portions of the network that are connected to

*water sources* from those that are non-connected due to representation errors. Accomplishing such step should pursue the maximum interaction with water operators who daily work on such peculiar systems. This phase is iterative and can be assisted by advanced tools, possibility embedded into DWSs, as they help the identification of possible mistakes for water utilities' operators to review. The result of this phase is a *connected geometric model* since all elements are connected to some *water sources*, i.e. reservoirs, tanks, or pumps, as reported in Figure 2 for a real WDN.

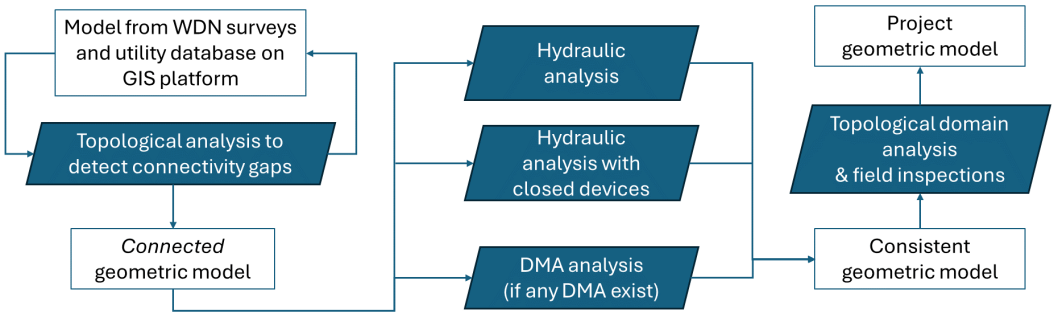


Figure 76 Methodology to build the geometric model

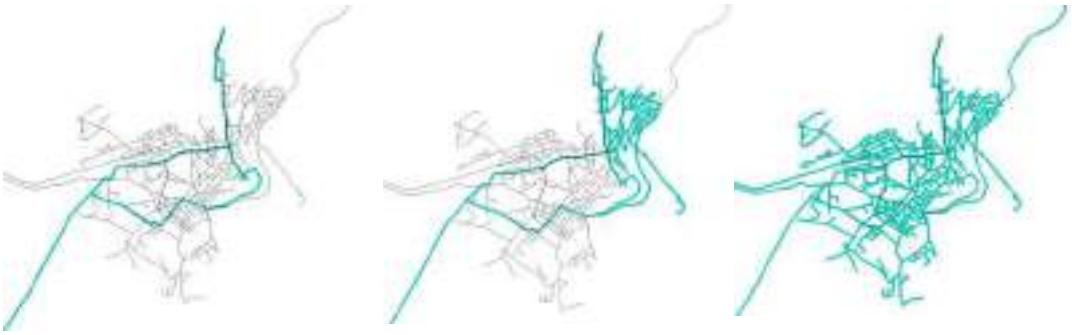

Figure 2 Iterative topological analysis: pipes connected to water sources (cyan); WDN layout from water utilities' database (black).

The second part (middle in Figure 1) turns into the implementation of devices on the geometric model. Such process starts from inserting closed gates, as they might change the flow paths in the network. As soon as devices are inserted in the model, further gaps may be found using advanced hydraulic modelling and tools for the automatic identification of DMAs. Additional inconsistencies or knowledge gaps, deserving further investigations or field inspections, can be identified from analyses combining results from the developing hydraulic model with asset information.
In the third part (rightmost in Figure 1) of the procedure, the analysis of the topological domain [4] of WDN based on the analysis of the shortest paths can be useful to detect possible inconsistencies related to the properties of the main flow paths along WDN.

## References

[1] O.Giustolisi, "Digital transition, digital twin and digital water: history, concepts and overview for the application to aqueducts".*Digital Water*, vol. 1, no. 1, 2023, doi: 10.1080/28375807.2024.2313975.
[2] P. Conejos Fuertes, F. Martinez Alzamora, M. Hervás Carot, and J. C. Alonso Campos, "Building and exploiting a Digital Twin for the management of drinking water distribution networks", *Urban Water J.*, vol. 18, no. 8, pp. 704-713, 2020.
[3] F.G. Ciliberti, L. Berardi, D.B. Laucelli, A.D. Ariza, L.V. Enriquez, O. Giustolisi "From digital twin paradigm to digital water services" *Journal of Hydroinformatics*, 25(6) (2023) 2444–2445
[4] O. Giustolisi, L. Ridolfi, and A. Simone, "Embedding the intrinsic relevance of vertices in network analysis: the case of centrality metrics," *Sci. Rep.*, vol. 10, no. 1, Dec. 2020, doi: 10.1038/s41598-020-60151-x.

**Theme:** Digital transformation of urban water systems
**IAHR Thematic Priority Area:** [TPA-4] Digital Transformation
https://doi.org/10.3850/iahr-hic2483430201-508

# Water Distribution System Operational Optimization Using a Nonlinear Model Predictive Control Framework

**Ernesto Arandia[1], Lu Xing[1*], Jim Uber[2], and Ehsan Shafiee[3]**

[1] Decision Intelligence Solution Group, Xylem Inc.

*Corresponding author: lu.xing@xylem.com*

**Abstract.** This paper aims to create a network monitoring and management system that optimizes energy cost through real-time demand forecasts and control. The proposed system is based on a digital twin of the distribution system that integrates the real-time SCADA data and a nonlinear model predictive control (NMPC) optimization framework that determines pumping operations and storage levels to minimize energy costs. The proposed framework is applied to optimize the annual operation of the Southern Nevada Water Authority. The results show that the optimized control can lead to a 10% to 20% reduction in energy costs.

**Keywords:** Dynamic water network optimization, nonlinear predictive control, operation optimization

## 1 Introduction

Water utilities are major energy consumers, often accounting for 30-40 percent of total energy consumption for municipal governments [1]. Improving network operation is one of the most important energy saving measures. However, dynamic optimization problems involving real-world water networks present several challenges, including the large scale of the networks, the nonlinearity of the relationships among physical quantities, and the discrete nature of operation decisions. Due to the above challenges, previous studies are mostly based on heuristic methods, and applications are restricted to small-scale networks, synthetic data, and limited optimization horizons [2].

## 2 Method

This paper proposes the application of a nonlinear model predictive control (NMPC) strategy within an integrating framework for planning and scheduling real-time water distribution system operations. Model predictive control refers to a class of algorithms that make explicit use of a process model to optimize the future predicted behaviour of a system. The NMPC strategy has been identified as a powerful approach for the adaptive management of water distribution systems due to its capability of incorporating disturbance forecasts into real-time optimal control problems.

The proposed framework discretizes the system operations into hourly increments and implements the rolling horizon optimization strategy. The rolling horizon strategy grants the optimizer a foresight to make optimal operation decisions for the coming day, with only the first time point of the optimal control sequence applied online. For each hour, we formulate an optimization model that reduces pump energy consumption cost over the horizon of 24 hours while meeting all system demands and operational requirements. Then, optimal control settings prescribed for the next hour are implemented, and optimization is run for the next 24 hours. The process is repeated for each hour until terminated. Figure 1 summarizes the rolling horizon strategy.

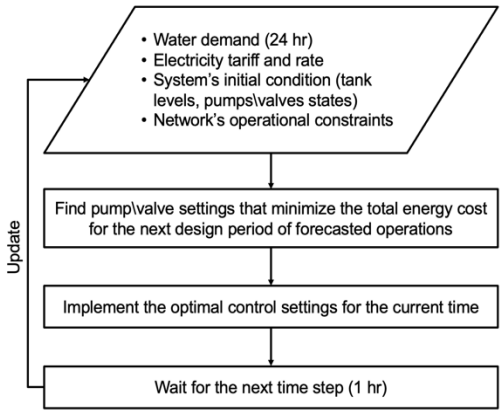


**Figure 1.** Rolling horizon optimization framework.

Within the proposed framework, the scaling problem is addressed through a combination of network skeletonization and the use of a large-scale NLP solver that can handle millions of variables efficiently. The nonlinearities are explicitly expressed through hydraulic relationships for all the types of network components involved [3]. A disjoint representation is introduced to reduce the nonlinearity and uncertainties related to valves and pump facilities. The discrete decisions are handled by decomposing the optimization problem into a primary or master problem that solves the network first, and a secondary problem that solves the pump facilities using results from the primary problem.

## 3 Results

The proposed framework implements a 1-year energy optimization proof-of-concept analysis for the Southern Nevada Water Authority (SNWA). The calendar year of 2022 was selected as the time window to demonstrate the solution, and the following subtasks were completed: 1) compile historic SCADA and billing records for 2022, 2) implement energy optimization framework based on a digital twin hydraulic model, 3) compare optimized and historical metrics for system behavior. Figure 2 summarizes the monthly cost reduction between historic and optimized system behaviors. The total reduction in energy costs over the 1-year period is estimated at $2.57 million dollars, with most of the savings being incurred during the summer months of June to September. Based on the results, it is recommended that using the rolling horizon optimization framework moving forward to dictate pumping schedule and operations can save SNWA a significant sum of energy consumption and cost.


**Figure 2.** Monthly cost reduction summary.

## References

[1] Copeland C, Carter NT. Energy-water nexus: The water sector's energy use.

[2] Castelletti A, Ficchì A, Cominola A, Segovia P, Giuliani M, Wu W, Lucia S, Ocampo-Martinez C, De Schutter B, Maestre JM. Model Predictive Control of water resources systems: A review and research agenda. Annual Reviews in Control. 2023 Apr 11.

[3] Arandia E, James U. A Nonliner Model Predictive Control Framework for Dynamic Water Network Optimization. *2nd International Joint Conference on Water Distribution Systems Analysis & Computing and Control in the Water Industry*. 2022.

**Theme:** Digital transformation of urban water systems
**IAHR Thematic Priority Area:** [TPA-4] Digital Transformation
https://doi.org/10.3850/iahr-hic2483430201-510

# Assessing Mixing in Service Reservoirs To Protect Drinking Water Quality

**Killian Gleeson[1], Stewart Husband[1], John Gaffney[2], Sebastian O'Shea[2], Arthur Costa Lopes[2], Joby Boxall[1]**

[1] The Department of Civil and Structural Engineering, University of Sheffield, Sheffield, S1 3JD, United Kingdom.
[2] Siemens UK, Manchester, M20 2UR, United Kingdom.

*Corresponding author: k.gleeson@sheffield.ac.uk*

**Abstract.** Service reservoirs (SRs), or tanks, are critical components of drinking water distribution systems that operate to balance supply and demand. To achieve this they may retain large volumes of water for significant periods of time. SRs are hence a potential source of water quality issues due to the kinetic reactions and interactions that occur during the period water is resident within them. In particular, inadequate mixing can cause the formation of dead zones with prolonged stagnation increasing water age and reducing disinfectant residual, thereby increasing microbial activity and contamination risks. We propose and demonstrate a novel way to assess how well a SR is performing in terms of mixing, by comparing the difference between idealised well mixed and operationally estimated values of residence times. The greater the difference in these values the further from well mixed the performance of the SR is and the greater the potential for impacts on water quality.

**Keywords:** Cross correlation, service reservoirs, time series data, water quality sensors.

## 1 Introduction

Efficient mixing within service reservoirs (SRs) is vital to maintaining water quality, by preserving disinfection residuals and eliminating the development of dead zones. Though computational fluid dynamics (CFD) can be employed to assess SR mixing characteristics [1], it is both time-consuming and expensive. Therefore, there is a need to develop alternative approaches to proactively assess the performance of SRs. This research presents a novel approach that combines data from water quality, flow and level sensors to determine SR mixing characteristics.

## 2 Method

Assuming a SR is acting as a perfectly well mixed reactor, its idealised residence time can be estimated from area, level and flow data. Recent work by Gleeson et al [2] showed how travel time in distribution systems can be estimated using cross-correlation between water quality sensors. Applying this approach to data from the inlet and outlet of SRs provides an estimate of the operational residence time of SRs. In the original work the method was applied to chlorine data, here we show that this is also possible using the more robust parameter conductivity for SR residence time. This operational measure will be dominated by the passage of the majority of the water; for a poorly mixed SR this will be the water that 'short circuits' through the reservoir and will be less than the idealised well mixed residence time.

## 3 Results

The novel approach is demonstrated for multiple SRs from an operating UK drinking water distribution system showing a range of performance and successfully identifying assets with inadequate mixing characteristics. Figure 1 shows the idealised residence times for 10 SRs alongside

the operational residence time for 6 SRs. The operational approach requires inlet and outlet water quality sensor data that was unavailable for four of the featured SRs. Higher idealised residence time is directly associated with increasing risk of deterioration in water quality. SR J was found to have the highest idealised residence time of 90 hours, and an operational residence time of only 5 hours, suggesting extreme short circuiting. Inspection of discreet samples collected for regulatory purposes, also analysed using flow cytometry, for this SR shows the highest average total cell count indicating increased bacteriological activity. Figure 2 plots the correlation of idealised versus operational residence times for six SRs, further identifying F and C (after J) as those with high level of water quality risk due to both their high residence times and their lower relative operational residence time (represented by distance from the green dotted line), indicating poor mixing performance.

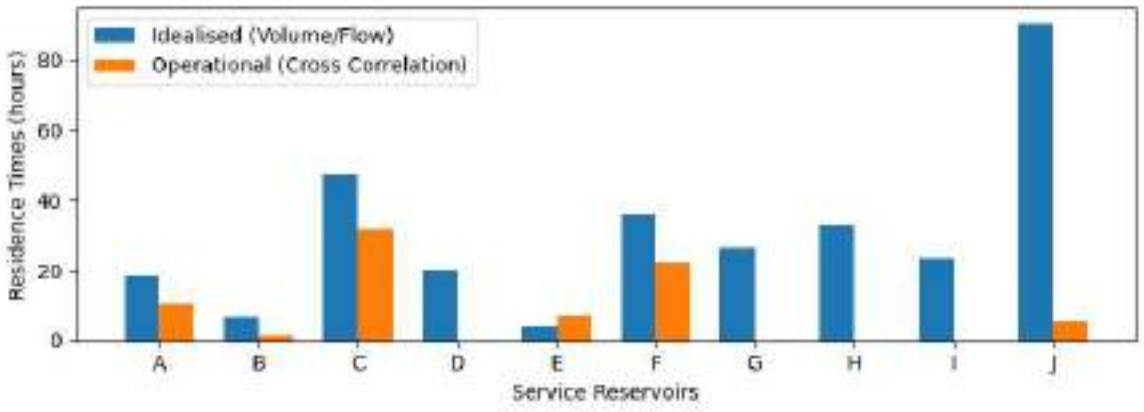


Figure 77 Idealised and operational residence times for ten service reservoirs.

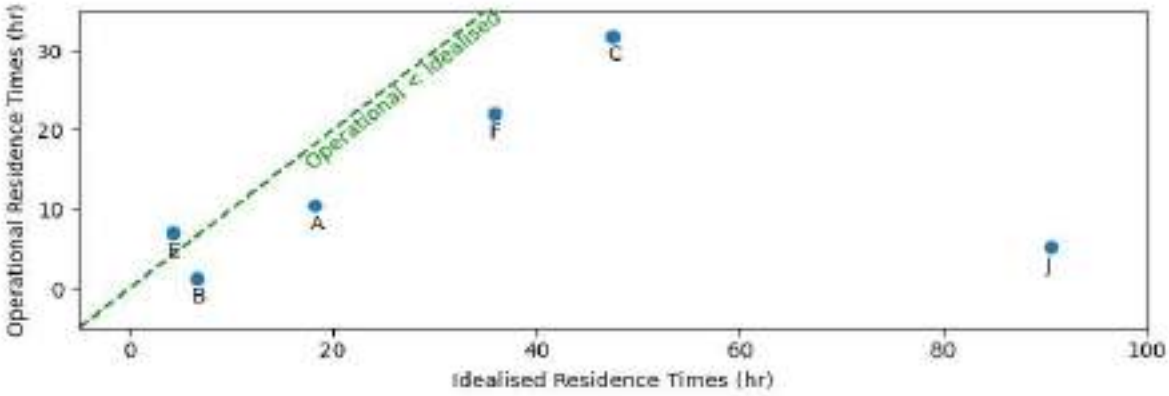


Figure 2 Scatter plot of idealised versus operational residence times for six service reservoirs.

## 4 Conclusion

The work provides evidence of the value of continuous water quality monitoring at SR inlets and outlets and highlights how water quality data can be combined with hydraulic data to derive actionable insights. The methodology provides an understanding of the mixing characteristics within SRs without the need for complex, time consuming CFD or other analysis. This approach facilitates a move away from conventional time-based maintenance regimes to a more proactive approach, enabling poorly performing SRs to be identified sooner and therefore safeguarding water quality.

## Reference

[1] Zhang, Lee, Khoo, Peng, Zhong, Kang, and Ba. Shape Effect on Mixing and Age Distributions in Service Reservoirs. Journal AWWA 2014; 106(11). doi: 10.5942/jawwa.2014.106.0094.

[2] Gleeson, Husband, Gaffney, Boxall, A data quality assessment framework for drinking water distribution system water quality time series datasets, AQUA - Water Infrastructure, Ecosystems and Society 2023; 72 (3): 329–347. doi: https://doi.org/10.2166/aqua.2023.228

**Theme:** Digital transformation of urban water systems
**IAHR Thematic Priority Area:** [TPA-4] Digital Transformation
https://doi.org/10.3850/iahr-hic2483430201-512

# The Application of Machine Learning in the Systemic Decision Process Development for Water Supply Pipe Replacement Performance in Thailand

**Manatsawee Nawik[1], Suwatthana Chitthaladakorn[2], Sitang Pilailar[2]**

[1] Metropolitan Waterworks Authority, 400 Phachachuen Rd., Thoongsong hong, Laksri, Bangkok, THAILAND.
[2] Kasetsart University, 50 Ngamwongwan Rd, Khwaeng Lat Yao, Khet Chatuchak, Bangkok, THAILAND.

*Corresponding author: manatsawee.n@mwa.co.th, mnsv.nawik@gmail.com*

**Abstract.** This study aims to identify the optimal algorithm for enhancing the systematic decision-making process in pipe management within specified investment constraints, utilizing risk assessment and asset valuation. The objective is to implement this refined approach by applying it to the field datasets of MWA, thereby examining the correlation between prediction results and the corresponding action plan. The findings highlight the Random Forest regression model and the Random Forest classification model as the most effective algorithms for predicting RI and allocating measures to specific areas. In conclusion, the comparison reveals that MWA's action plan surpasses the necessary in terms of pipe management within the defined budget constraints.

**Keywords:** Area Characteristic Index; Infrastructure Value Index; Machine learning; Pipe replacement; Risk Index; Systemic decision process

## 1 Introduction

Many metropolitan areas have a variety of water supply infrastructures to serve all activities of urban community life. Generally, the lifetime of a pipe is designed to be approximately 50 years. However, it can be deteriorated and disturbed by severe operation conditions, e.g., temperature, vibration, chemical, material properties, and land use. Pipe replacement is the first priority measure to decrease the water loss caused by pipe breaks in the water supply system.

However, the productiveness of this policy cannot be achieved perfectly due to the technique of deteriorated pipe selection and economic reasons. Nawik et al. (2023) investigated the Area Characteristic Index and risk and value-based analysis to create the risk and asset value-oriented pipe management guideline matrix. In this study, the machine learning algorithms will improve the decision matrix. The objective of the proposed works is to explore the appropriate regression model for the risk analysis and classification model for pipe management and to implement this advanced decision process in the case study area of the Metropolitan Waterworks Authority (MWA) of Thailand to determine the consistency between the MWA's pipe replacement plan and the prediction results.

## 2 Material and Methods

The three regression models—the multi-regression model, the gradient-boosting regression model, and the random forest regression model—are the algorithms that were used by many researchers in the various research fields (Cai et al., 2020; Kadam et al., 2019; Kumar et al., 2020; Liu et al., 2020; Zhang et al., 2022) will be assessed to predict the Risk Index (RI) for finding out the length of high-risk pipes, while the asset valuation will be estimated using Infrastructure Value Index (IVI) (Alegre et al., 2014). Its performance will be evaluated using its accuracy: R-square, Mean Square Error (MSE), Root Mean Square Error (RMSE) and Mean Absolute Error (MAE).

Moreover, several pieces of evidence associated with the classification model were reported in the literature (Charbuty et al., 2021; Felton et al., 2019; Jadhav et al., 2016; Lalian et al., 2022; Xia et al., 2022). In this study, three classification models are used: the decision tree model, the random forest model, and the support vector machine (SVM) with a Gaussian radial basis function (RBF) kernel model. These models will be used to test and train with synthetic datasets and evaluated using the confusion matrix. Finally, the classification model will allocate the four different measures to each area and compare them with MWA's action plan.

## 3 Results and Discussion

The results indicate that the random forest model outperformed in predicting the RI, achieving an impressive R-square of 0.9968, MSE of 0.00038, RMSE of 0.0195, and MAE of 0.0065. Notably, the random forest classification model exhibited superior performance with a precision of 0.90 and recall of 0.95, making it the preferred algorithm for assigning measures. However, a notable disparity exists between the action plan and the predictions, highlighting the inefficiency of the previous pipe management system. For instance, while DMA 540903 was initially planned for the replacement of approximately 23,000 meters of pipes, the model predicted a K measure for this DMA, suggesting that pipe replacement might not be necessary in this particular area.

## 4 Conclusion

Machine learning is the contemporary tool for solving not only the complex problem in widely fields but also the engineering challenges. Pipe replacement management can be improved by using random forest regression model and classification model in the decision process. The comparison between prediction and action plan presents the impropriated action plan. It can result in the adjustment of the action plan in the future for the productive management of MWA.

## References

[1] Alegre, H., Vitorino, D. and Coelho, S. J. P. E. (2014). Infrastructure value index: a powerful modelling tool for combined long-term planning of linear and vertical assets. 89, 1428-1436.

[2 Cai, J., Xu, K., Zhu, Y., Hu, F. and Li, L. J. A. e. (2020). Prediction and analysis of net ecosystem carbon exchange based on gradient boosting regression and random forest. 262, 114566.

[3] Charbuty, B., Abdulazeez, A. J. J. o. A. S. and Trends, T. (2021). Classification based on decision tree algorithm for machine learning. 2(01), 20-28.

[4] Felton, B. R., O'Neil, G. L., Robertson, M.-M., Fitch, G. M. and Goodall, J. L. J. W. (2019). Using random forest classification and nationally available geospatial data to screen for wetlands over large geographic regions. 11(6), 1158.

[5] Jadhav, S. D., Channe, H. J. I. J. o. S. and Research. (2016). Comparative study of K-NN, naive Bayes and decision tree classification techniques. 5(1), 1842-1845.

[6] Kadam, A., Wagh, V., Muley, A., Umrikar, B., Sankhua, R. J. M. E. S. and Environment. (2019). Prediction of water quality index using artificial neural network and multiple linear regression modelling approach in Shivganga River basin, India. 5, 951-962.

[7] Kumar, V., Vardhan, H., Murthy, C. S. J. G. and Geoengineering. (2020). Multiple regression model for prediction of rock properties using acoustic frequency during core drilling operations. 15(4), 297-312.

[8] Lalian, V. U., Bekti, R. D., Pratiwi, N., Sutanta, E. and Pradnyana, I. W. J. (2022). Analysis of Consumer Satisfaction Levels with GoRide Services Using the Support Vector Machine (SVM) Classification Method. Paper presented at the 2022 IEEE 8th Information Technology International Seminar (ITIS).

[9] Liu, D., Fan, Z., Fu, Q., Li, M., Faiz, M. A., Ali, S., et al. (2020). Random forest regression evaluation model of regional flood disaster resilience based on the whale optimization algorithm. 250, 119468.

[10] Nawik, M., Pilailar, S. and Chittaladakorn, S. J. A. W. S. (2023). Effect of DMA characteristics on risk and asset analysis of the Metropolitan Waterworks Authority pipe network. 5(5), e1354.

[11] Xia, D., Tang, H., Sun, S., Tang, C. and Zhang, B. J. R. S. (2022). Landslide susceptibility mapping based on the germinal center optimization algorithm and support vector classification. 14(11), 2707.

[12] Zhang, W., Zhang, R., Wu, C., Goh, A. T. and Wang, L. J. U. S. (2022). Assessment of basal heave stability for braced excavations in anisotropic clay using extreme gradient boosting and random forest regression. 7(2), 233-241.

**Theme:** Digital transformation of urban water systems
**IAHR Thematic Priority Area:** [TPA-4] Digital Transformation
https://doi.org/10.3850/iahr-hic2483430201-515

# Domain Analysis to Identify the Main Hydraulic Pathways in Wdns to Support Asset Management

**Antonietta Simone[1], Luigi Berardi[1], Daniele B. Laucelli[2], Orazio Giustolisi[2]**

[1] University "G. D'Annunzio" of Chieti Pescara, Viale Pindaro, 42, Pescara, 65127, Italy
[2] Technical University of Bari, Via E. Orabona, 4, Bari, 70125, Italy

*Corresponding author: danielebiagio.laucelli@poliba.it*

**Abstract**. Water distribution networks management is a complex technical-scientific problem with a large socioeconomic impact. In recent years this problem has been addressed in a more efficient way using new approaches based on complex network theory, which allows to conceptualize water networks as graphs, composed of nodes and links, studying their behavior from a topological point of view, before using physically based hydraulic modelling. This work proposes using relevance-tailored edge betweenness to perform a topological domain analysis for real water distribution networks, identifying the shortest paths along which the main water volumes move within the pipes. The strategy is tested on an urban network characterized by multiple sources, comparing the analysis for subnetworks to the entire system one**.**

**Keywords:** digital water service, topological domain analysis, water distribution networks

## 1 Introduction

Water Distribution Networks (WDNs) are composite systems (water pumping, storing, supplying, etc.) whose management is increasingly complex for several reasons, ranging from social aspects (e.g., the ever-increasing expansion of urban centres), asset management issues (e.g., age and conditions of working elements), knowledge of the geometric model (e.g., connectivity problems) and the hydraulic model (e.g., pressure regime), presence and functioning of hydraulic devices (e.g., flow and pressure meters, isolation valves, etc.), and so on. Therefore, it is not always easy to immediately use a complete hydraulic analysis of the system to be managed. For this reason, it could be useful to have alternative tools and approaches, which allow for preliminary analysis of the network, constituting initial support for subsequent WDN management activities, e.g., monitoring, functional improvement, calibration, etc. The Complex Network Theory (CNT) is proving useful in defining innovative tools and approaches for the analysis and management of complex systems. The present work uses a tailored centrality metric to perform a topological domain analysis of real WDNs: the relevance-based edge betweenness, proposed in [1] to classify the predominant role that some pipes assume within the network, thus identifying the network elements along which the main information propagates, corresponding with the shortest paths along which the main volumes of water move. This way it is possible to define the emerging hydraulic behaviour of WDNs even before the hydraulic analysis, allowing to recognize the most important pipes for the network, for consequent management-related activities, such as calibration of the hydraulic model, districtualization, pipes rehabilitation planning, etc. The topological domain analysis here presented is conducted using the digital water service *DigitalWaterDomain_Analyzer* [2], which allows the visualization of the variability of the metric in GIS environment.

## 2 Method

The formulation of the Edge Betweenness tailored to WDNs [1] to embed the information about the intrinsic relevance of the nodes through the function $f(R_s, R_t)$ here used is the following,

$$EB(l) = \sum_{s \neq t \in N} f(R_s, R_t) \frac{\sigma_{s,t}(l)}{\sigma_{s,t}} \quad (1)$$

where $N$ is the number of nodes of the network, $\sigma_{s,t}(l)$ and $\sigma_{s,t}$ are the number of shortest paths traversing the link $l$ and the total number of all shortest paths, respectively, for all the couples of nodes $s$ and $t$ of the network, while $R_s$ and $R_t$ are the intrinsic relevance of node $s$ and $t$, respectively.

## 3 Results

The topological domain analysis is here proposed for the real WDN of Nicosia, city located in Sicily (Italy), whose hydraulic simulation model is composed of 2170 pipes and 2084 nodes. Four reservoirs of different size and volume, provides the water supply to the customers. The studied network is topologically connected, but the water utility operates a few closed valves to divide it in four subnetworks, each one referring to its own reservoirs, and hydraulically separated. This operating condition, which is common to many WDNs characterized by more than one source of supply, suggested analysing the topological domain of the network by considering both the entire system and the different subnetworks individually. The investigation of the domain analysis results in both situations highlighted the most important mains of the network, as related to the management scheme adopted by the water utility. The analysis here assumes the intrinsic relevance in Eq. (1) as equal to the customers demand for each node and to the sum of demands for each reservoir (i.e., source nodes). The function $f(R_s,R_t) = (R_s+R_t)/2$ is used during the analysis. The domain analysis performed separately for the four subnetworks is summarized in Figure 1.

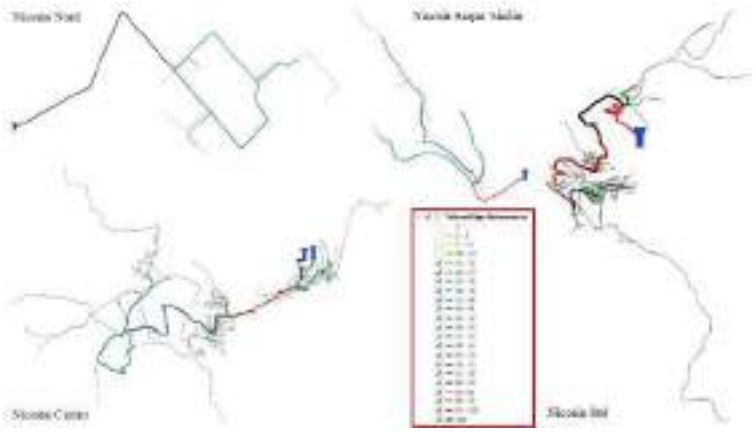

Figure 1. Domain analysis of the four subnetworks of the Nicosia WDN.

## 4 Conclusions

The topological domain analysis performed using the relevance-based edge betweenness allowed to achieve a topological screening of the system and identify the pipes that most influence the hydraulic operation of the network. The results showed that the analysis by subnetworks is more informative than the analysis of the complete network because the former allows to better identify the hierarchies between pipelines within the system, without the relevance of the most important nodes to "mask" the significant pipes within the less important network parts.

## References

[1] O. Giustolisi, L. Ridolfi, A. Simone, Embedding the intrinsic relevance of vertices in network analysis: the case of centrality metrics, Sci. Rep., 10, (2020) 3297.

[2] F.G. Ciliberti, L. Berardi, D.B. Laucelli, A.D. Ariza, L.V. Enriquez, O. Giustolisi, From digital twin paradigm to digital water services, J. Hydroinformatics, 25 (2023) 2444-2459.

**Theme:** Digital transformation of urban water systems
**IAHR Thematic Priority Area:** [TPA-4] Digital Transformation
https://doi.org/10.3850/iahr-hic2483430201-517

# Evaluating the Impact of Rainfall Variability on Urban Flood Saturation: A Case Study in Ha Noi

**Ha Minh Do[1,2,3,*], Gerald Corzo Perez[1,2], Chris Zevenbergen[1,2]**

[1] Department of Coastal and Urban risk & resilience, IHE – Delft, Westvest 7, 2611 AX. Delft, The Netherlands
[2] Faculty of Civil Engineering and geosciences, TuDelft, Stevinweg 1, 2628 CN, Delft, The Netherlands.
[3] Faculty of urban infrastructure and environment engineering, Hanoi Architectural University, Km10, Nguyen Trai, Thanh Xuan, Ha Noi, Viet Nam.

* *Corresponding author: h.do@un-ihe.org.*

**Abstract**. Traditional models for predicting flood risk often overlook rainfall events' spatial and temporal variability, focusing instead on aggregate patterns represented through time series. This research challenges this approach by examining the impact of spatially and temporally varied rainfall, including differences due to urban microclimates and convection rainfall, on urban flooding dynamics. Utilizing a hydraulic model, we investigate the sensitivity of drainage systems and flood scenarios to rainfall variability across spatiotemporal scales. Our findings reveal that a delay of 29 minutes in rainfall onset can reduce the flooded area by 6% and the rate of flood expansion by 21.1%. This study underscores the critical need for flood risk assessments to incorporate spatiotemporal rainfall variability, offering stakeholders vital insights for prioritizing flood management strategies with a nuanced understanding of initial flooding locations and pre-saturation periods in urban drainage systems.

**Keywords:** Delayed rainfall timing, spatiotemporal flood, urban flood.

## 1 Introduction

Flood in urban area recently focus on the spatial distribution[1–6]. However, accumulating time, the water volume and the sequential pattern of flow saturation in different city parts can pose a high level of danger to citizens [7,8]. Therefore, flood evolution in time during the flood event is needed to understand comprehensively.

Moreover, rainfall movement has significantly impacted on the location and time of flow saturation in drainage system such as in hydrographs, especially in flash flood situations[9–12]. Under the storm movement effects, these were changes in peak discharge and velocity which, in turn, have implications in storage capacity designs[13]. Since the storm movements caused the changes in different areas, it is crucial to explore the sensitivities in hydrological response under this circumstance. In addition, as a foundation of nature-based solution, assessing the sensitivity of rainfall movement is essential for optimizing the design and placement for flood mitigation measurements.

This research aims to assess the spatiotemporal sensitivity of hydraulic responses in drainage system under rainfall variability, which is comprised by variety of consequential precipitation datasets.

## 2 Material and methods

Hydraulic model in Do Lo, Yen Nghia, Ha Dong, Ha Noi, Viet Nam was adopted from previous research [14]. Geographic information and drainage system were included. Induce rainfall patterns were collected from 2 actual historical precipitation events.

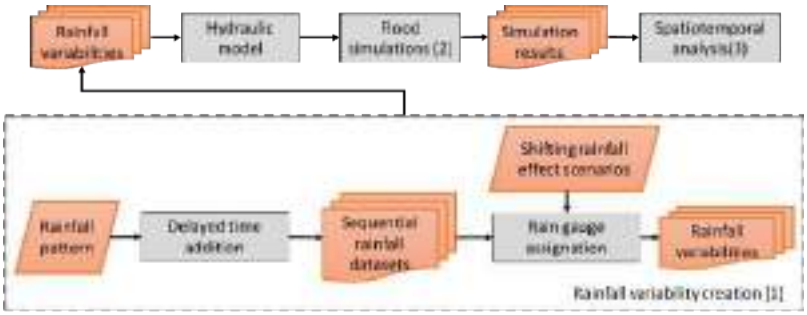


*Figure 78. Research scheme*

Research was conducted followed 3 steps showed in Figure 1. Rainfall variabilities were created based on sequential rainfall datasets and two shifting rainfall effect scenarios on three synthetic rain gauges. Delayed time ($\Delta_t$) between sequential rainfall patterns ranged from – 1440 to 1440 minutes.Two shifting rainfall effect scenarios were considered with different rainfall area rain gauges. Spatiotemporal analysis interpreted SWMM results using python package namely swmm_api [15] adopted from previous research[14].

## 3 Results and discussion

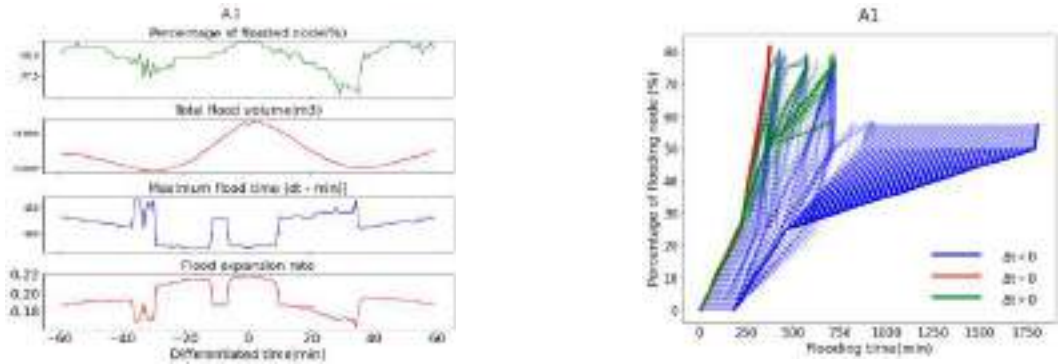


*Figure 79. Rain gage sensitivity assessment scenarios 1 (a) Percentage of flooded node, Total flood volume, Maximum flood time, and Flood Expansion Rate (b) Temporal sensitivity of flood evolution*

From both scenarios, effective and meaningful delayed time was in range from -500 to 500 mins. Uniform rainfall ($\Delta_t$ =0) is the worst case of flood. In scenario 1, flood impacts reduced approximately 6% percentage of flooded nodes, 1151 $m^3$ total flood volume (3.67%) with 29 minutes of delayed rainfall (Figure 4). In scenario 2, with 32 mins of delayed rainfall, flood effects reduce 6% in percentage of flooded node, 1045 $m^3$(3.34%) in total flood volume.

## 4 Conclusion

This research presented a methodology that can be used to quantify the sensitivity of spatial rainfall variability and its impacts in floods. Besides, delayed rainfall timing is not only the basic uncertainty assessment, but also a tool to explore the flood interventions to control the maximum flood in the future(e.g. nature-based solution). The optimal delayed rainfall – resulting runoff could be defined through the combined proposed rainfall generation and the flood spatiotemporal analysis.

## References

[1] Agonafir C, Lakhankar T, Khanbilvardi R, Krakauer N, Radell D, Devineni N (2023) A review of recent advances in urban flood research. Water Secur 19, 100141.

[2] Mishra A, Mukherjee S, Merz B, Singh VP, Wright DB, Villarini G, Paul S, Kumar DN, Khedun CP, Niyogi D, Schumann G, Stedinger JR (2022) An Overview of Flood Concepts, Challenges, and Future Directions. J Hydrol Eng 27, 1–30.
[3] Afsari R, Nadizadeh Shorabeh S, Kouhnavard M, Homaee M, Arsanjani JJ (2022) A Spatial Decision Support Approach for Flood Vulnerability Analysis in Urban Areas: A Case Study of Tehran. ISPRS Int J Geo-Information 11, 380.
[4] Levin N, Phinn S (2022) Assessing the 2022 Flood Impacts in Queensland Combining Daytime and Nighttime Optical and Imaging Radar Data. Remote Sens 14,.
[5] Zhou R, Zheng H, Liu Y, Xie G, Wan W (2022) Flood impacts on urban road connectivity in southern China. Sci Rep 12, 1–17.
[6] Wijaya OT, Yang TH, Hsu HM, Gourbesville P (2023) A rapid flood inundation model for urban flood analyses. MethodsX 10, 102202.
[7] Dong B, Xia J, Li Q, Zhou M (2022) Risk assessment for people and vehicles in an extreme urban flood: Case study of the “7.20” flood event in Zhengzhou, China. Int J Disaster Risk Reduct 80,.
[8] Arrighi C, Oumeraci H, Castelli F (2017) Hydrodynamics of pedestrians’ instability in floodwaters. Hydrol Earth Syst Sci 21, 515–531.
[9] Liu Y, Huang Y, Liu Y, Li K, Li M (2021) The impact of rainfall movement direction on urban runoff cannot be ignored in urban hydrologic management. Water (Switzerland) 13, 1–12.
[10] Seo Y, Schmidt AR (2012) The effect of rainstorm movement on urban drainage network runoff hydrographs. Hydrol Process 26, 3830–3841.
[11] Sigaroodi SK, Chen Q (2016) Effects and consideration of storm movement in rainfall-runoff modelling at the basin scale. Hydrol Earth Syst Sci 20, 5063–5071.
[12] Ghomash SK Bin, Bachmann D, Caviedes-Voullième D, Hinz C (2022) Impact of Rainfall Movement on Flash Flood Response: A Synthetic Study of a Semi-Arid Mountainous Catchment. Water (Switzerland) 14, 1–25.
[13] Mrowiec M, Ociepa E, Malmur R (2019) Influence of Dynamic Properties of Rainfall on Urban Drainage Infrastructure. In New Trends in Urban Drainage Modelling Springer International Publishing, pp. 419–423.
[14] Do Minh H, Corzo Perez GA, Barreto W, Zevenbergen C (2023) A Spatiotemporal hydrological response of extreme urban floods in Ha Noi – Vietnam. In EGU General Assembly 2023, Vienna, Austria, 24-28 Apr 2023, EGU23 - 6891, Vienna, Austria.
[15] Pichler M (2022) swmm_api: API for reading, manipulating and running SWMM-Projects with python (0.3).

**Theme:** Digital transformation of urban water systems
**IAHR Thematic Priority Area:** [TPA-4] Digital Transformation
https://doi.org/10.3850/iahr-hic2483430201-520

# Utilizing Smartphone-derived Photogrammetry 3D Model for AI-based Riparian Crack Segmentation and Measurement

**Shijun Pan, Keisuke Yoshida, Satoshi Nishiyama**

Graduate School of Environmental and Life Science, Okayama University
(Tsushima-naka 3-1-1, Kita-ku, Okayama 700-8530, Japan)

*Corresponding author: p4b36znn@s.okayama-u.ac.jp*

**Abstract.** In this paper, the authors present a simple free methodology that harnesses the potential of smartphone-derived photogrammetry 3D models for the AI-driven segmentation and quantification of riparian cracks. The approach the authors propose leverages the YOLOv7-seg model to precisely delineate cracks, employing photogrammetry techniques to construct an orthophoto, subsequently enabling the extraction and accurate measurement of crack dimensions. This research underscores the fact that the proposed methodology yields outcomes in both the detection and measurement aspects of riparian cracks. This investigation carries profound implications for the realm of environmental oversight and administration, as it heralds an innovative approach toward the identification and amelioration of issues pertaining to cracks in riparian asphalt surfaces. Through the rigorous analysis of this approach, not only crack detection and measurement but also holds promise for wider applications in the field of environmental assessment. It extends the boundaries of AI-driven methodologies in the context of environmental preservation.

**Keywords:** Instance Segmentation, Riparian Crack Detection, River Monitoring, Smartphone

## 1 Introduction

The monitoring of cracks along river banks is a vital aspect of the evaluation of the environmental stabilization of riparian areas. Recently, promising progress has been made in riverbank crack monitoring by using Unmanned Aerial Vehicle (UAV) platforms for artificial intelligence tasks such as instance segmentation [1]. However, high accurate instance segmentation using closer distance has not been thoroughly verified and evaluated. To address this gap, the authors collected several angle-fixed videos along the targeted river bank for selecting the suitable one, and this video was used to be inferred by the You Only Look Once version 7 (YOLOv7) instance segmentation model specifically tailored for crack segmentation, referred to as YOLOv7-seg. In this research, the authors generated a work flow that the asphalt-paved cracks can be extracted and size-measured automatically, and by a free version 3D model processing software, the video-derived frames can be transformed to an orthophoto, which these results can be important data accumulation for the construction ecosystem digital-twin in the future.

## 2 Work flow

A systematic process for measuring crack size using various technologies and methods is outlined in the workflow shown in the Figure 1. It starts with the acquisition of videos using a smart phone with a fixed camera angle of 45°. These video are then processed by Video2Eachframe.py to be analyzed by YOLOv7-seg Inference. Simultaneously, the images are used to create a 3D texture mesh, which is further refined by photogrammetry using 3DF Zephyr. Orthophoto is used along with measurement programming to facilitate accurate crack size measurements. The final result provides detailed cracked measurements.

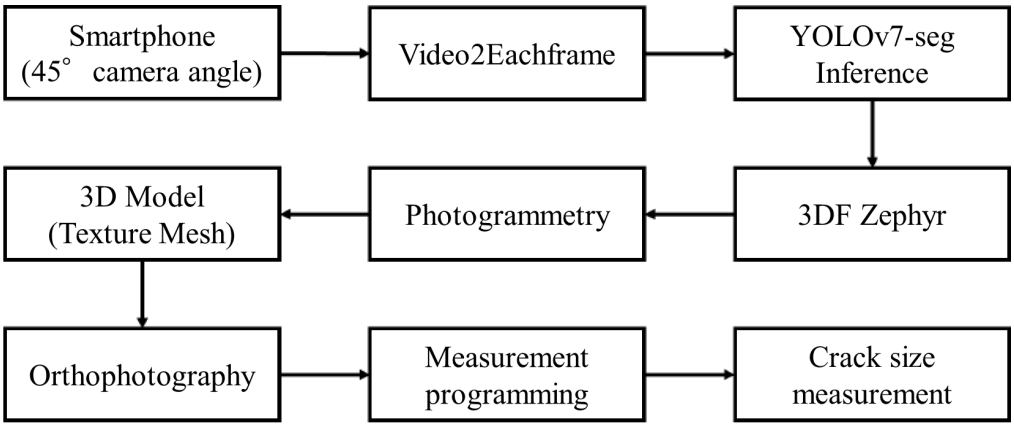


Figure 80 Process of the data collection and the workflow .

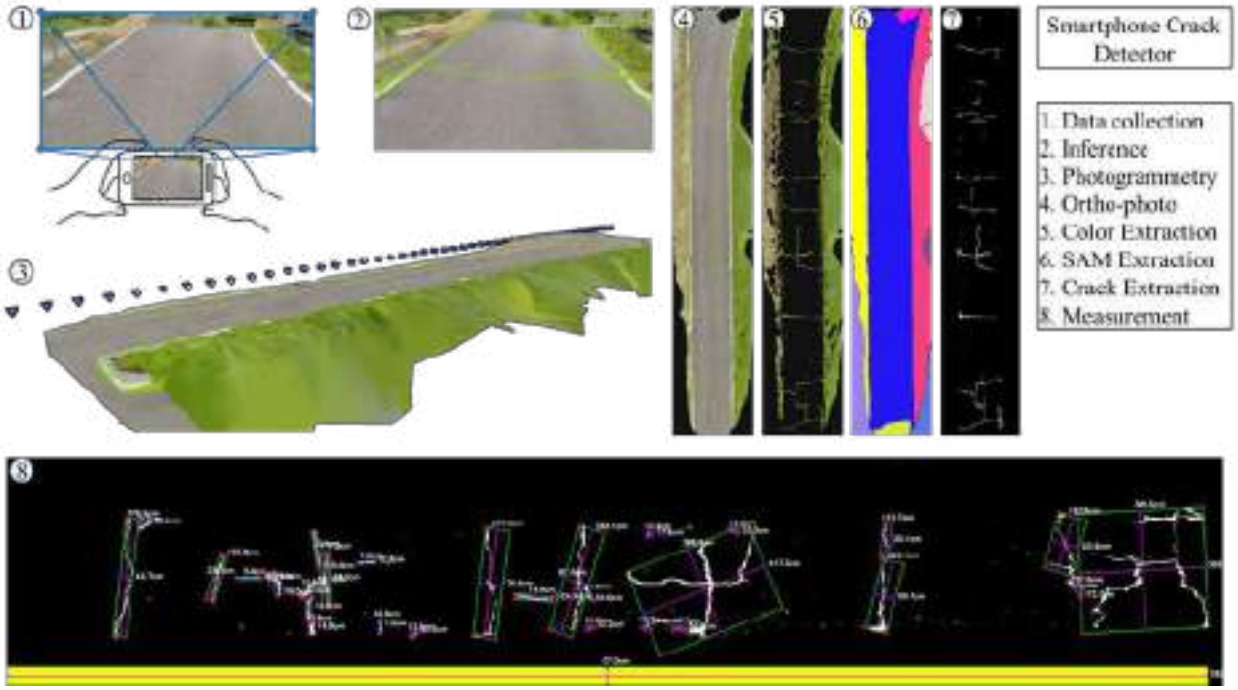


Figure 2 Process of the crack size measurement

## 3 Conclusion

As shown in Figure 2, this study has extracted the cracks with the detailed information from the video after the mentioned process. In this process, orthophoto ensures accurate surface representation, while measurement programming facilitates precise crack size determination. This comprehensive approach yields detailed measurements, enhancing our understanding of cracks and aiding in maintenance and safety assessments.

## Reference

[1] Shijun, P. A. N., YOSHIDA, K., & NISHIYAMA, S. Detection and Segmentation of Riparian Asphalt Paved Cracks Using Drone and Computer Vision Algorithms. *Intelligence, Informatics and Infrastructure*, *4*(2), 35-49. 2023

**Theme:** Digital transformation of urban water systems
**IAHR Thematic Priority Area:** [TPA-4] Digital Transformation
https://doi.org/10.3850/iahr-hic2483430201-522

# Integrating Data-Driven and Hydraulic Modelling with Acoustic Sensor Information for Improved Leak Location in Water Distribution Networks

**Ignasius Axel Hutomo[1*], Ioana Popescu[2], Leonardo Alfonso[3]**

[1,2,3] IHE Delft Institute for Water Education, Delft, Netherlands, Delft, 2611 AX, Netherlands

** Corresponding author: axelhutomo@gmail.com*

**Abstract**. Despite ongoing research and practical efforts, water losses in water distribution networks remain alarmingly high, impacting water quantity and quality. Traditionally, water utilities have employed separate approaches using acoustic sensors and hydraulic models to address leaks. However, the integration of these methods and their potential for mutual improvement have not been thoroughly studied. This research proposes a novel approach to improve leak location accuracy by integrating acoustic sensor data and hydraulic modelling within a machine learning framework, using data from an actual use case. Results show that by combining selected acoustic statistical data in time and frequency domains, and various hydraulic features from physical modelling as inputs, a 94% accuracy in the leak location of leaks above 1 L/s can be achieved. This represents a substantial improvement relative to the accuracy achieved by the acoustic methods alone (84%) or by the hydraulic modelling data alone (64%).

**Keywords:** Acoustic Sensor, Artificial Neural Network, Hydraulic Model, Leakage, Water Distribution Networks.

## 1 Introduction

Several researchers have processed and analysed acoustic file data to classify leakage incidents in the water network using machine learning approach [1], [2], [3]. However, as reviewed by Fan, further development should focus on study cases that rely on the actual event and not only in an experimental setting [4]. This is substantiated by Bykerk and Valls, who comprehensively review studies analysing acoustic information and include a test in a real District Metered Area (DMA) in Sydney without any hydraulic modelling analysis [5].

Only Saqib et al., (2017) proposes an integration between acoustic information and hydraulic modelling. They approach this integration by introducing an initial screening of leaks based on pressure data generated with EPANET, followed by a simulation of leak vibrations using the acoustic sound propagation mathematical model which developed by Brennan et al. [6]. The drawbacks of the study is that a theoretical network is modelled, and that no real acoustic data is analysed.

This is the gap this paper aims to address. In particular, the extent to which the combination of these two data sources can improve the overall performance of the leak location method is therefore an open question. We propose a novel method that integrates hydraulic modelling-generated data with real acoustic sensor information to improve leak location in a real DMA of a WDN in a city in Eastern Europe. The framework to make this integration is a data-driven model, specifically an Artificial Neural Networks (ANN).

## 2 Methods

This study adopts a systematic and sequential methodology, encompassing three distinct steps: data preparation, ANN model building, and experimental setup, described in detail below.

## 2.1 Data Preparation

This step is intended to prepare the acoustic and hydraulic data for training and applying the ANN model. On the acoustic side, four variables are extracted from the noise logger file, namely Mean-Time Domain, Peak-Time Domain, Peak-Frequency Domain, and Kurtosis-Frequency Domain. Conversely, on the hydraulic side, a leakage scenario is simulated at a location where the noise logger is deployed, with leak rates ranging from 0.125 to 5 L/s. In this leakage modeling process, several variables are taken into consideration, including pressure and velocity.

## 2.2 ANN Model Building for Predicting Leak Occurrence

The second phase of the methodology consist of the construction of the ANN for the purpose of predicting leak occurrence based on binary classification (leak/no leak). Selected acoustic and hydraulic properties are the set of independent variables from which the target (output's dependent variable) is the leak / no leak condition.

The dataset preparation process is automated using Python scripting language in conjunction with various packages, including NumPy, Pandas, SciPy, TensorFlow, Keras, and SciKit Learn. From the data ratio perspective, 80% of the data is used as a training set, while the rest is used as a testing set. The input layers are formed by sets of acoustic and hydraulic features; two hidden layers are used, each consisting of eight nodes, to calculate the relation weight among features. Finally, the output layer consists of one layer with a single node. The hidden layers are activated using the rectified linear unit (ReLU) activation function, and the output is activated using a sigmoid function. Since the leakage determination is a binary classification problem, the Binary Cross Entropy method was used as the loss function. Adam's optimiser [7] was employed to optimise the forward and backpropagation to reduce error.

## 2.3 Experimental Setup

The final phase of this research involves training and evaluating the performance and applicability of the ANN in accurately classifying leak and non-leak incidents within WDNs, utilizing various feature inputs as presented in Table 1. In each experiment, different sets of acoustic and hydraulic attributes (and their combinations) are used. Note that the hydraulic attributes include the incremental variation of leak rate.

**Table 1.** Experiments using Different Input Data Features for ANN Leakage Classification

| Experiment ID | Input Attribute | | | Output Attribute |
|---|---|---|---|---|
| | Acoustic Data Input | Hydraulic Data Input | Combined Data Input | |
| A - 1 | Mean – TD<br>Peak – TD<br>Kurtosis – FD | Pressure at leak | Mean – TD<br>Peak – TD<br>Kurtosis – FD<br>Pressure at leak | Leak /<br>no leak |
| A – 2 | Mean – TD<br>Peak – TD<br>Kurtosis – FD | Delta pressure at leak | Mean – TD<br>Peak – TD<br>Kurtosis – FD<br>Delta pressure at leak | Leak /<br>no leak |
| A – 3 | Mean – TD<br>Peak – TD<br>Kurtosis – FD | Pressure at leak<br>Delta pressure at leak | Mean – TD<br>Peak – TD<br>Kurtosis – FD<br>Pressure at leak<br>Delta pressure at leak | Leak /<br>no leak |
| A – 4 | Mean – TD<br>Peak – TD<br>Kurtosis – FD | Pressure at leak<br>Delta pressure at leak<br>Upstream velocity<br>Downstream velocity | Mean – TD<br>Peak – TD<br>Kurtosis – FD<br>Pressure at leak<br>Delta pressure at leak<br>Upstream velocity<br>Downstream velocity | Leak /<br>no leak |

| | | | | |
|---|---|---|---|---|
| B – 1 | Mean – TD<br>Peak – FD<br>Kurtosis – FD | Pressure at leak | Mean – TD<br>Peak – FD<br>Kurtosis – FD<br>Pressure at leak | Leak /<br>no leak |
| B – 2 | Mean – TD<br>Peak – FD<br>Kurtosis – FD | Delta pressure at leak | Mean – TD<br>Peak – FD<br>Kurtosis – FD<br>Delta pressure at leak | Leak /<br>no leak |
| B – 3 | Mean – TD<br>Peak – FD<br>Kurtosis – FD | Pressure at leak<br>Delta pressure at leak | Mean – TD<br>Peak – FD<br>Kurtosis – FD<br>Pressure at leak<br>Delta pressure at leak | Leak /<br>no leak |
| B - 4 | Mean – TD<br>Peak – FD<br>Kurtosis – FD | Pressure at leak<br>Delta pressure at leak<br>Upstream velocity<br>Downstream velocity | Mean – TD<br>Peak – FD<br>Kurtosis – FD<br>Pressure at leak<br>Delta pressure at leak<br>Upstream velocity<br>Downstream velocity | Leak /<br>no leak |

# 3 Results

## 3.1 Features Selection

On the acoustic data input, four variables have been explored: Mean–TD, Peak–TD, Peak–FD, and Kurtosis–FD. Previous research has shown that these variables strongly relate to a leak signal in WDN [3], [4], [8]. While on the hydraulic data input, pressure, delta pressure, and velocity have been selected. Table 2 provides a detailed overview of the multicollinearity analysis of input features in experiments using the Variance Influence Factors (VIF). It is observed that employing these features individually leads to a substantial reduction in the value of VIF, signifying a decreased level of dependency.

**Table 2.** Multicollinearity Analysis of Input Features in Experiments using VIF

| | | Experiment ID | | | | | | | |
|---|---|---|---|---|---|---|---|---|---|
| Input Variables Feature | | **A-1** | **A-2** | **A-3** | **A-4** | **B-1** | **B-2** | **B-3** | **B-4** |
| | **Mean -TD** | 1.03 | 1.02 | 1.04 | 1.04 | 1.03 | 1.00 | 1.04 | 1.04 |
| | **Peak -TD** | 1.67 | 1.50 | 1.85 | 2.10 | - | - | - | - |
| | **Peak – FD** | - | - | - | - | 1.23 | 1.12 | 1.25 | 1.37 |
| | **Kurtosis – FD** | 1.15 | 1.14 | 1.15 | 1.26 | 1.08 | 1.11 | 1.11 | 1.24 |
| | **Pressure wo Leak** | - | - | - | - | - | - | - | - |
| | **Pressure w leak** | 1.51 | - | 1.61 | 2.3 | 1.19 | - | 1.40 | 2.21 |
| | **Delta Pressure** | - | 1.36 | 1.45 | 2.4 | - | 1.13 | 1.33 | 2.41 |
| | **Velocity Upstream** | - | - | - | 3.08 | - | - | - | 3.13 |
| | **Velocity Downstream** | - | - | - | 2.02 | - | - | - | 1.91 |

## 3.2 ANN Performance for Different Input Features

ANN models were trained and tested using the inputs in Table 1 as independent variables and the output leak / no leak as the dependent variable. The confusion matrix summary as seen in Figure 1 shows that the use of different feature sets and their impact on the model's performance underscored the importance of feature selection and representation in achieving accurate classification results. Based on the experiment result, it can be conluded that a combination of acoustic features including Mean-Time Domain (Mean-TD), Peak-Time Domain (Peak-TD), and Kurtosis-Frequency Domain (Kurtosis-FD) is considered alongside hydraulic features such as pressure at leak and delta pressure at leak gives better performance compared to others input combinations.

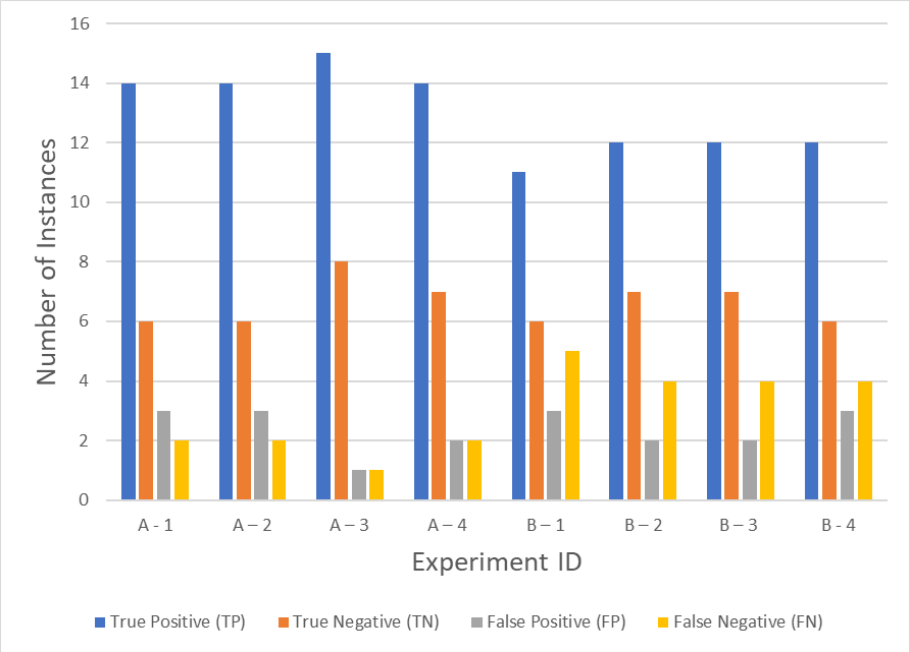


**Figure 1.** Summary of the confusion matrices from all experiments with combined input

## 4 Conclusion

In conclusion, our analysis of the confusion matrix from multiple experiments revealed variations in the model's performance across different conditions. The consistent TP and TN values across similar experiments indicated stability in the model's classification ability, while discrepancies in FP and FN values highlighted areas where the model could benefit from further improvement. The use of different feature sets and their impact on the model's performance underscored the importance of feature selection and representation in achieving accurate classification results.

References

[1] S. El-Zahab, A. Asaad, E. Mohammed Abdelkader, and T. Zayed, "Development of a clustering-based model for enhancing acoustic leak detection," *Can. J. Civ. Eng.*, vol. 46, no. 4, pp. 278–286, Apr. 2019, doi: 10.1139/cjce-2018-0229.

[2] Y. Jin, W. Yumei, and L. Ping, "Approximate entropy-based leak detection using artificial neural network in water distribution pipelines," in *2010 11th International Conference on Control Automation Robotics & Vision*, Dec. 2010, pp. 1029–1034. doi: 10.1109/ICARCV.2010.5707291.

[3] S. Li, Y. Song, and G. Zhou, "Leak detection of water distribution pipeline subject to failure of socket joint based on acoustic emission and pattern recognition," *Measurement*, vol. 115, pp. 39–44, Feb. 2018, doi: 10.1016/j.measurement.2017.10.021.

[4] H. Fan, S. Tariq, and T. Zayed, "Acoustic leak detection approaches for water pipelines," *Autom. Constr.*, vol. 138, p. 104226, Jun. 2022, doi: 10.1016/j.autcon.2022.104226.

[5] L. Bykerk and J. Valls Miro, "Detection of Water Leaks in Suburban Distribution Mains with Lift and Shift Vibro-Acoustic Sensors," *Vibration*, vol. 5, no. 2, Art. no. 2, Jun. 2022, doi: 10.3390/vibration5020021.

[6] M. Brennan, F. Lima, F. Almeida, P. Joseph, and A. Paschoalini, "A virtual pipe rig for testing acoustic leak detection correlators: Proof of concept," *Appl. Acoust.*, vol. 102, pp. 137–145, Jan. 2016, doi: 10.1016/j.apacoust.2015.09.015.

[7] D. P. Kingma and J. Ba, "Adam: A Method for Stochastic Optimization." arXiv, Jan. 29, 2017. Accessed: Jul. 13, 2023. [Online]. Available: http://arxiv.org/abs/1412.6980

[8] I. A. Tijani, S. Abdelmageed, A. Fares, K. H. Fan, Z. Y. Hu, and T. Zayed, "Improving the leak detection efficiency in water distribution networks using noise loggers," *Sci. Total Environ.*, vol. 821, p. 153530, May 2022, doi: 10.1016/j.scitotenv.2022.153530.

**Theme:** Digital transformation of urban water systems
**IAHR Thematic Priority Area:** [TPA-4] Digital Transformation
https://doi.org/10.3850/iahr-hic2483430201-526

# Automatic Detection of Water Consumption Temporal Patterns in A Residential Area in Northen Italy

**Francesco Viola[1], Elena Cristiano[1], Roberto Deidda[1]**

[1] Dipartimento di Ingegneria Civile, Ambientale e Architettura, Università degli Studi di Cagliari, Via Marengo 2, 90123 Cagliari, Italy

*Corresponding author: viola@unica.it*

**Abstract.** One of the main challenges for the city development is to ensure a sustainable water resource management for the water supply system. A clear identification of the urban water consumption patterns supports policy and decision makers in managing the water resources, satisfying the total demand and, at the same time, reducing losses and identifying potential leakages or other issues in the distribution network. High resolution smart meters have widely shown to be an efficient tool to measure in pipe water consumption. The collected data can be used to identify water demand patterns at different temporal and spatial scales, reaching the end-uses level. Water demand patterns at building level can be influenced by multiple factors, such as socio-demographic aspects, seasonality and house characteristics. The presence of a garden that requires summer irrigation strongly alters the daily average pattern. In this framework, we present an innovative approach to automatically detect the presence of garden irrigation, identifying daily average water consumption patterns with and without it. The proposed methodology has been applied in a residential area in Northen Italy, where 23 smart meters have recorded data at 1 min resolution for two years. Results show that the proposed approach can easily distinguish between days with and without garden irrigation and provides an average normalized water demand pattern for both situations, which can help decision makers and water managers to correctly regulate the pressure regimes in the distribution network.

**Keywords:** domestic water use, smart meter data, water consumption pattern

## 1 Introduction

To provide an effective support to the policy makers and water managers, it is important not only to identifying the most relevant influencing factors of water consumption, but also to evaluate how they modify their temporal patterns. Although it is well known that the presence of an irrigated garden is one of the most influencing factors [1] the actual changes in the water consumption patterns are still poorly investigated. In this context, we aim to provide an automatic approach to identify the signature of irrigation for domestic garden irrigation in water consumption patterns. Data collected from 23 smart meters, installed in a residential area in the Northern Italy by the Blue Gold company, for two years (2019-2020) at 1-minute temporal resolution, have been used to validate the proposed approach. The work is structured as follows. First, we introduce the case study and the available data from the smart meters, then we present the methodology developed to automatically identify the domestic water consumption patterns, highlighting days with and without garden irrigations. Results are then illustrated comparing the average consumption patterns with and without irrigation. Finally, we summarize the main conclusions and suggest possible research pathways.

## 2 Case study

To investigate and classify the domestic water consumption patterns, the Municipality of Carpiano (Italy) has been chosen as case study. Carpiano is a small village, located in the north of Italy, in the province of Milan, with about 4000 inhabitants and a surface of 17 $km^2$. The residential areas are spread in an historical agricultural area, where 23 buildings with multiple apartments connected to

the water supply network of Carpiano have been monitored during 2019-2020. Specifically, water consumption of each building was recorded by smart meters produced by the Blue Gold company. Locations of the 23 measuring sites.
The installed smart meters ensure a continuous monitoring of the system, with collection and transmission of data at 1 minute resolution.

## 3 Automatic detection of water consumption patterns

In this work we used normalized cumulative daily water consumption curves for describing temporal pattern. These curves have been then analyzed to classify the water consumption patterns, applying criteria to select whether the days are characterized by garden irrigation or not. In this work, two main assumptions have been considered to define the selection criteria, mainly related to nocturne or unexpected high gradient in the cumulative normalized curve, which corresponds to a temporary increase in the water consumption, likely caused by irrigation.

## 4 Results

Results showed how the proposed approach can automatically classify the daily water consumption patterns, separating days with and without irrigation. Focusing only on the days without irrigation, the average normalized daily water consumption pattern is aligned with the patterns available in the literature, with peaks at 8:00 in the morning, at lunch time, around 13:00, and in the evening around 20:00, and lower consumption during the night. No significant differences have been observed among average water consumption patterns recorded in different seasons. Days characterized by garden irrigation, on the other hand, present quite different water consumption patterns, with high seasonal peaks during the night and early morning, between 23:00 and 5:00.

## Reference

[1] Cominola, A., Preiss, L., Thyer, M., Maier, H.R., Prevos, P., Stewart, R.A. and Castelletti, A. 2023. The determinants of household water consumption: A review and assessment framework for research and practice. npj Clean Water 6(1), 11.

ISBN: 978-90-834302-0-1
ISSN: 3007-2174

Hosted by:

IAHR International Association for Hydro-Environment Engineering and Research
AIRH
Hosted by Spain Water and IWHR, China

IWA

Organized by:

IWHR